

SUMMARY OF
SIGNIFICANT
RESULTS IN—

Mineral resources
Water resources
Engineering geology
and hydrology
Regional geology
Principles and
processes
Laboratory and
field methods
Topographic surveys
and mapping
Management of
resources on
public lands
Land information
and analysis
Investigations in
other countries

LIST OF—

Investigations in
progress

GEOLOGICAL SURVEY RESEARCH, FISCAL YEAR 1981



GEOLOGICAL SURVEY PROFESSIONAL PAPER 1375

GEOLOGICAL SURVEY RESEARCH, FISCAL YEAR 1981

GEOLOGICAL SURVEY PROFESSIONAL PAPER 1375

*A summary of recent significant scientific
and economic results accompanied by a
list of geologic, hydrologic, and cartographic
investigations in progress*



UNITED STATES GOVERNMENT PRINTING OFFICE, WASHINGTON, D.C.: 1984

UNITED STATES DEPARTMENT OF THE INTERIOR

WILLIAM P. CLARK, *Secretary*

GEOLOGICAL SURVEY

Dallas L. Peck, *Director*

Library of Congress catalog-card No. 68-46150

**For sale by the Distribution Branch, U.S. Geological Survey,
604 South Pickett Street, Alexandria, VA 22304**

CONTENTS

	Page		Page
Abbreviations	V	Geologic and hydrologic principles, processes, and techniques—Continued	
SI units and inch-pound system equivalents	VII	Chemical, physical, and biological characteristics of water	184
Mineral-resource investigations	1	Relation between surface water and ground water	190
United States and world mineral-resource assessments	1	Limnology and potamology	192
Mineral-resource assessments—land areas	2	New hydrologic instruments and techniques	194
Geologic studies of mining districts and mineral-bearing regions	5	Analytical methods	198
Geochemical and geophysical techniques in resource assessments	10	Environmental geochemistry	198
Resource information and analysis	12	Geology and hydrology applied to natural hazards	201
Sedimentary mineral resources	12	Earthquake studies	201
Mineral-fuel investigations	15	Volcanic hazards	215
Coal resources	15	Engineering geology	218
Oil and gas resources	24	Landslide hazards	219
Oil shale resources	33	Reactor hazards research program	222
Nuclear-fuel resources	33	Hydrologic aspects of coal- and mineral-resource development	223
Geothermal resources	45	Hydrologic effects of volcanism	229
Regional geologic investigations	47	Geology related to national security	231
New England	47	Relation of radioactive waste to the geologic environment	232
Appalachian Highlands and the Coastal Plains	49	Relation of radioactive waste to the hydrologic environment	233
Central region	53	Floods	235
Rocky Mountains and the Great Plains	54	Effects of pollutants on water quality	236
Basin and Range region	63	Land subsidence	239
Pacific coast region	67	Hazards information and warnings	240
Alaska	75	Astrogeology	242
Water-resource investigations	82	Planetary studies	242
Northeastern region	83	Lunar investigations	248
Southeastern region	89	Remote sensing and advanced techniques	249
Central region	92	Earth Resources Observation Systems Office	249
Western region	96	Applications to geologic studies	259
Special water-resource programs	99	Applications to hydrologic studies	263
Marine geology and coastal hydrology	110	Land use and environmental impact	265
Coastal and marine geology	110	Long range planning	265
Estuarine and coastal hydrology	122	Environmental impact studies	265
Management of natural resources on Federal and Indian lands	125	International activities in the earth sciences	267
Classification and evaluation of mineral lands	125	Technical assistance	271
Waterpower classification—preservation of resource sites	127	Participant training	272
Management of mineral leases on Federal and Indian lands	127	Topical resource studies	272
Management of oil and gas leases on the Outer Continental Shelf	128	Scientific cooperation and research	273
Cooperation with other Federal agencies	129	International commissions and representation	276
Geologic and hydrologic principles, processes, and techniques	130	International hydrological program and related activities	278
Geophysics	130	Summary of selected activities by country or region	280
Geochemistry, mineralogy, and petrology	136	Cartographic and geographic research	292
Geothermal systems	152	Automated spatial data handling	292
Sedimentology	159	Cartographic and geographic studies	295
Climate	162	Remote sensing and space technology research	301
Ground-water hydrology	165	Radar studies	304
Surface-water hydrology	170	Systems and techniques research and development	307
Paleontology	176	Associated activities	311
Plant ecology	183		

	Page		Page
Computer resources and technology	312	U.S. Geological Survey publications—Continued	
Microcomputers.....	312	How to obtain publications.....	316
Teleconferencing and office automation.....	312	References cited.....	318
Information management technology.....	312	Investigations in progress.....	329
Array processing.....	312	Indexes.....	377
U.S. Geological Survey publications	314	Subject index.....	377
Publications program.....	314	Investigator index.....	416
Publications issued.....	315		

ILLUSTRATIONS

	Page
FIGURE 1. Index map of the conterminous United States showing areal subdivisions used in the discussion of water resources	82

TABLES

	Page
TABLE 1. Mineral production, value, and royalty for FY 1981	127
2. OCS oil and gas lease sales for FY 1981.....	129
3. Technical assistance provided by the USGS to other countries during FY 1981.....	267
4. Technical and administrative documents issued during FY 1981 as a result of USGS technical and scientific cooperation programs.....	271

ABBREVIATIONS

A.....angstrom
 AAPG.....American Association of Petroleum Geologists
 ABAG.....Association of Bay Area Governments
 ac.....alternating current
 A.D.....anno Domini
 ADP.....automatic data processing
 AESOP.....Automatic Surface Observation Platforms
 AGID.....Association of Geoscientists for International Development
 AGWAT.....Ministry of Agriculture and Water
 AID.....Agency for International Development
 AIDJEX.....Arctic Ice Dynamics Joint Experiment
 AMRAP.....Alaska Mineral Resource Assessment Program
 ANCSA.....Alaska Native Claims Settlement Act
 AOCS.....Atlantic Outer Continental Shelf
 APD.....antiphase domain
 ARPA.....Advanced Research Projects Agency
 ASL.....Albuquerque Seismological Laboratory
 ASRO.....Advanced Seismological Research Observatories
 atm.....atmosphere

 b.....barn (area)
 bbl.....barrel
 BIA.....Bureau of Indian Affairs
 BLM.....Bureau of Land Management
 BOD.....biochemical oxygen demand
 B.P.....before present
 Btu.....British thermal unit
 b.y.....billion years

 °C.....degrees Celsius
 CAI.....color alteration index
 cal.....calorie
 CAM.....Cartographic Automatic Mapping
 CARETS.....Central Atlantic Regional Ecological Test Site project
 CCD.....Computer Center Division
 CCOP.....U.N. Committee for Coordination of Joint Prospecting for Mineral Resources in Asian Off-shore Areas
 CCT.....computer-compatible tape
 C/DCP.....convertible data-collection platforms
 CDP.....common depth point
 CENTO.....Central Treaty Organization
 CFRUC.....Colorado Front Range Urban Corridor Project
 cfs.....cubic feet per second
 CGIS.....Canada Geographic Information System
 cgs.....centimeter-gram-second
 Ci.....curie
 cm.....centimeter
 COD.....chemical oxygen demand
 COGEO DATA.....Committee on storage, automatic processing, and retrieval of geologic data
 COM.....computer-oriented microform
 COST.....Continental Off-shore Stratigraphic Test Group
 cps.....counts per second
 CPU.....central processing unit
 CRIB.....Computerized Resource Information Bank
 CUSMAP.....Continental United States Mineral Assessment Program
 CV.....characteristic value

 d.....day
 D.....Darcy
 db.....decibel
 DBMS.....Data Base Management System
 dc.....direct current
 DCAP.....Digital Cartographic Applications Program
 DCASS.....Digital Cartographic Software System
 DCDB.....Digital Cartographic Data Base
 DCS.....data-collection system
 DDES.....Digital Data Editing System
 DEM.....Digital Elevation Model
 DEROCs.....Development of Energy Resources of the Outer Continental Shelf

DLG.....Digital Line Graph
 DMA.....Defense Mapping Agency
 DO.....dissolved oxygen
 DOD.....Department of Defense
 DOE.....Department of Energy
 DOI.....Department of the Interior
 DSDP.....Deep Sea Drilling Project
 dyn.....dyne

 EDC.....EROS Data Center
 Eh.....oxidation reduction potential
 EIS.....environmental impact statement
 EM.....electromagnetic (soundings)
 EMRIA.....Energy Mineral Rehabilitation Inventory and Analysis
 emu.....electromagnetic unit
 EPA.....Environmental Protection Agency
 EROS.....Earth Resources Observation System
 ERTS.....Earth Resources Technology Satellite
 ESCAP.....Economic and Social Commission for Asia and the Pacific Committee on Natural Resources
 eV.....electronvolt

 FAA.....Federal Aviation Administration
 FAO.....Food and Agriculture Organization
 ft.....foot
 FLD.....Fraunhofer line discriminator
 FY.....fiscal year
 FWS.....Fish and Wildlife Service

 g.....gram
 Ga.....billion years
 GHz.....gigahertz
 GIPSY.....General Information Processing System
 GIRAS.....Geographic Information Research and Analysis System
 G.M.T.....Greenwich mean time
 GNIS.....Geographic Names Information System
 GOES.....Geostationary Operational Environmental Satellite
 GPa.....gigapascal
 GPM-2.....Gestalt Photo Mapper II
 GRASP.....Geologic Retrieval and Synopsis Program

 h.....hour
 h.....height
 H.....Henry
 ha.....hectare
 HFU.....heat-flow unit
 HIPLEX.....High Plains Cooperative Program
 hm.....hectometer
 HUD.....Department of Housing and Urban Development
 Hz.....hertz

 IAH.....International Association of Hydrogeologists
 IAHS.....International Association of Hydrological Scientists
 ICAT.....Inorganic Chemical Analysis Team
 IDB.....Inter-American Development Bank
 IDIMS.....Interactive Display Image Manipulation System
 IDOE.....International Decade of Ocean Exploration
 IGCP.....International Geological Correlation Program
 IGU.....International Geophysical Union
 IHD.....International Hydrological Decade
 IHP.....International Hydrological Program
 IMW.....International Map of the World
 in.....inch
 IR.....infrared
 ISAM.....Index Sequential Access Method
 ISO.....International Standardization Organization
 IUGS.....International Union of Geologic Sciences

 J.....joule
 JECAR.....Joint Commission of Economic Cooperation
 JPL.....Jet Propulsion Laboratory

JTU.....Jackson turbidity unit

 K.....kelvin
 kbar.....kilobar
 KCLA.....Known Coal Leasing Area
 KeV.....kiloelectronvolt
 kg.....kilogram
 KGRA.....Known Geothermal Resources Area
 KGS.....Known Geologic Structure
 kHz.....kilohertz
 km.....kilometer
 kn.....knot
 KRCRA.....Known Recoverable Coal Resource Area
 KREEP.....potassium-rare-earth element-phosphorus
 kWh.....kilowatt-hour

 l.....liter
 lb.....pound
 LARS.....Laboratory for Application of Remote Sensing
 lat.....latitude
 LMF.....lithic matrix fragments
 long.....longitude

 m.....meter
 M.....magnitude (earthquake)
 mb.....magnitude from body waves
 M_L.....Richter magnitude
 M_s.....magnitude from surface waves
 mcal.....millicalorie
 mD.....millidarcy
 m/d.....meters per day
 MEF.....maximum evident flood
 Mg.....megagram
 mg.....milligram
 mGal.....milligal
 Mgal/d.....million gallons per day
 mi.....mile
 min.....minute
 ml.....milliliter
 mm.....millimeter
 MM.....Modified Mercalli intensity
 MN.....meganewton
 mo.....month
 mol.....mole
 MPa.....megapascal
 MPN.....most probable number
 ms.....milliseconds
 MSS.....multispectral scanner
 Mt.....megaton
 mV.....millivolt
 MW.....megawatt
 MWe.....megawatts electrical
 m.y.....million years
 μ.....micron
 μ cal.....microcalorie
 μ e.....microequivalents per liter
 μ g.....microgram
 μ Gal.....microgal
 μ l.....microliter
 μ m.....micrometer
 μ mho.....micromho
 μ rad.....microradian
 μ strain/yr.....engineering shear

 NAS.....National Academy of Science
 NASA.....National Aeronautics and Space Administration
 NASQAN.....National Stream Quality Accounting Network
 NAWDEX.....National Water Data Exchange
 NCRDS.....National Coal Resources Data System
 NEIS.....National Earthquake Information Service
 NEPA.....National Environmental Policy Act
 ng.....nanogram
 NGSDC.....National Geophysical and Solar-Terrestrial Data Center
 NGVD.....National Geodetic Vertical Datum

VI

NLCR.....nonlinear complex resistivity
 nm.....nanometer
 NMAS.....National Map Accuracy Standards
 NOAA.....National Oceanic and Atmospheric Administration
 NOS.....National Ocean Survey
 NPRA.....Naval Petroleum Reserve in Alaska
 NRA.....National Resources Agency
 NRA.....Nuclear Regulatory Agency
 NSF.....National Science Foundation
 nt.....nanotesla
 NTIS.....National Technical Information Service
 NTMS.....National Topographic Map Service
 NTS.....Nevada Test Site
 NURE.....National Uranium Resource Evaluation
 NWS.....National Weather Service

OAS.....Organization of American States
 OCS.....Outer Continental Shelf
 OE.....Oersted
 ohm-m.....ohm-meter
 ORNL.....Oak Ridge National Laboratory
 OWDC.....Office of Water-Data Coordination
 Ω.....ohm

PAIGH.....Pan American Institute of Geography and
 History

PCB.....polychlorinated biphenyls
 pCi.....picrourie
 ppb.....part per billion
 ppm.....part per million
 psi.....pounds per square inch
 PSRV.....pseudorelative velocity

R.....range
 rad.....radian
 RASA.....Regional Aquifer Systems Analysis
 RASS.....Rock Analysis Storage System
 RBV.....return beam vidicon
 REE.....rare-earth element
 RF.....radio frequency
 rms.....root mean square
 rmse.....root mean square error
 R/V.....research vessel

s.....second
 SFBR.....San Francisco Bay Region Environment and
 Resources Planning Study

SIP.....strongly implicit procedure
 SLAR.....side-looking airborne radar
 SMS.....Synchronous Meteorological Satellite
 SOM.....Space Oblique Mercator
 SP.....self potential
 SRO.....Seismic Research Observatory

t.....tonne
 T.....Tesla
 TEM.....transmission electron microscopy
 TIU.....thermal-inertia unit
 TL.....thermoluminescence
 TVA.....Tennessee Valley Authority

UNDP.....United Nations Development Program
 UNESCO.....United Nations Educational, Scientific, and
 Cultural Organization

USAID.....U.S. Agency for International Development
 USBM.....U.S. Bureau of Mines
 USDA.....U.S. Department of Agriculture
 USFS.....U.S. Forest Service
 USGS.....U.S. Geological Survey
 USPHS.....U.S. Public Health Service
 U.S.S.R.....Union of Soviet Socialist Republics
 UTM.....Universal Transverse Mercator

V.....volt
 VDETS.....Voice Data Entry Terminal System
 VES.....vertical electric soundings
 VHRR.....very high resolution radiometer
 VLF.....very low frequency
 V_p.....velocity of P-waves

W.....watt
 WATSTORE.....National Water Data Storage and
 Retrieval System

WHO.....World Health Organization
 wk.....week
 WMO.....World Meteorological Organization
 WRC.....Water Resources Council
 WRD.....Water Resources Division
 WRDD.....Water Resources Development Department
 wt.....weight
 WWSSN.....Worldwide Standardized Seismograph
 Network

yr.....year

SI UNITS AND INCH-POUND SYSTEM EQUIVALENTS

[SI, International System of Units, a modernized metric system of measurement. All values have been rounded to four significant digits except 0.01 bar, which is the exact equivalent of 1 kPa. Use of hectare (ha) as an alternative name for square hectometer (hm²) is restricted to measurement of land or water areas. Use of liter (L) as a special name for cubic decimeter (dm³) is restricted to the measurement of liquids and gases; no prefix other than milli should be used with liter. Metric ton (t) as a name for megagram (Mg) should be restricted to commercial usage, and no prefixes should be used with it. Note that the style of meter² rather than square meter has been used for convenience in finding units in this table. Where the units are spelled out in text, Survey style is to use square meter]

SI unit	Inch-Pound equivalent		SI unit	Inch-Pound equivalent		
Length			Volume per unit time (includes flow)—Continued			
millimeter (mm)	=	0.039 37	inch (in)	decimeter ³ per second (dm ³ /s)	= 15.85	gallons per minute (gal/min)
meter (m)	=	3.281	feet (ft)		= 543.4	barrels per day (bbl/d) (petroleum, 1 bbl = 42 gal)
	=	1.094	yards (yd)			
kilometer (km)	=	0.621 4	mile (mi)	meter ³ per second (m ³ /s)	= 35.31	feet ³ per second (ft ³ /s)
	=	0.540 0	mile, nautical (nmi)		= 15 850	gallons per minute (gal/min)
Area			Mass			
centimeter ² (cm ²)	=	0.155 0	inch ² (in ²)	gram (g)	= 0.035 27	ounce avoirdupois (oz avdp)
meter ² (m ²)	=	10.76	feet ² (ft ²)	kilogram (kg)	= 2.205	pounds avoirdupois (lb avdp)
	=	1.196	yards ² (yd ²)			
	=	0.000 247 1	acre	megagram (Mg)	= 1.102	tons, short (2 000 lb)
hectometer ² (hm ²)	=	2.471	acres		= 0.984 2	ton, long (2 240 lb)
	=	0.003 861	section (640 acres or 1 mi ²)			
kilometer ² (km ²)	=	0.386 1	mile ² (mi ²)	Mass per unit volume (includes density)		
Volume			Pressure			
centimeter ³ (cm ³)	=	0.061 02	inch ³ (in ³)	kilopascal (kPa)	= 0.145 0	pound-force per inch ² (lbf/in ²)
decimeter ³ (dm ³)	=	61.02	inches ³ (in ³)		= 0.009 869	atmosphere, standard (atm)
	=	2.113	pints (pt)		= 0.01	bar
	=	1.057	quarts (qt)		= 0.296 1	inch of mercury at 60° F (in Hg)
	=	0.264 2	gallon (gal)	Temperature		
	=	0.035 31	foot ³ (ft ³)	temp kelvin (K)	= [temp deg Fahrenheit (°F)+ 459.67]/1.8	
meter ³ (m ³)	=	35.31	feet ³ (ft ³)	temp deg Celsius (°C)	= [temp deg Fahrenheit (°F)- 32]/1.8	
	=	1.308	yards ³ (yd ³)			
	=	264.2	gallons (gal)			
	=	6.290	barrels (bbl) (petroleum, 1 bbl = 42 gal)			
	=	0.000 810 7	acre-foot (acre-ft)			
hectometer ³ (hm ³)	=	810.7	acre-feet (acre-ft)			
kilometer ³ (km ³)	=	0.239 9	mile ³ (mi ³)			
Volume per unit time (includes flow)						
decimeter ³ per second (dm ³ /s)	=	0.035 31	foot ³ per second (ft ³ /s)			
	=	2.119	feet ³ per minute (ft ³ /min)			

Any use of trade names and trademarks in this publication is for descriptive purposes only and does not constitute endorsement by the U.S. Geological Survey.

MINERAL-RESOURCE INVESTIGATIONS

UNITED STATES AND WORLD MINERAL-RESOURCE ASSESSMENTS

A new genetic model for sedimentary manganese deposits

Most of the world's major manganese deposits are sedimentary accumulations in shallow marine rocks. During review of the world literature on manganese deposits, W. F. Cannon and E. R. Force have found that there is a striking affinity of manganese accumulations and basal marine transgressive units. A temporal correspondence also is suggested between manganese deposits and ocean anoxic events, or, at least, between very widespread black shales and manganese accumulations. Manganiferous beds are believed to be lateral facies equivalents to marine black shales. Manganese is highly soluble in anoxic water within black shale basins but is less soluble in oxidized water. Manganese deposits form where manganese-rich anoxic water from deeper parts of basins wells up onto shelves and becomes oxidized in wave-mixed zones, thus depositing manganese.

Hydraulic concentration of heavy minerals in Pleistocene glacial lake delta sands

Studies of Pleistocene glacial lake deltas by E. R. Force and B. D. Stone have shown that foreset beds in these deltas have huge volumes of sand (6 billion t in one delta complex; B. D. Stone and E. R. Force, 1980), and the potential resources of ilmenite, rutile, and other economic heavy minerals in the deltas are significant. The deltas consist predominantly of sandy, dipping foreset strata always unconformably overlain by gravely horizontal fluvial topset beds. In Connecticut, Force and Stone found that the foresets include a number of deposits which appear to represent delta lobes and channel fills that are separated by unconformities. Foreset sands are mostly planar laminated or ripple laminated. Directional sedimentary structures show complex patterns.

In these deltas, deposits that have lithologies with unimodal grain sizes are sorted. Heavy-mineral concentrations average 4 percent or more in foresets of some deltas. Further, there is an orderly distribution of average grain sizes of different heavy minerals relative to grain size of the whole sample. Thus, sorting and structures indicate high-energy deposition. Paradoxically, these sequences are probably the result of turbidity currents, in this case, continuous currents of cold sediment-laden water that plunge down the foreset slope. Rarity of "typical" turbidite features is due to the absence of a

head or a tail of these continuous turbidity currents. Mineralogy of nearby coeval deltas can be markedly different and corresponds to contrasts in local bedrock. Dispersal patterns in plan view and vertical section can readily be determined from detrital mineralogy.

Niobium and tantalum world resource picture

G. P. Landis has collected data on the known world tantalum supply and on major deposits of niobium. No significant domestic deposit of either strategic metal is known; all consumption must come from imports. Niobium is in abundant supply in Brazilian carbonatite complexes (Araza). Major sources of tantalum depend upon foreign investment capital and the political environment.

Peat in Maine and Alaska

Peat deposits in and near Piscataquis and Somerset Counties and northeastern Aroostook County, Maine, were investigated by C. C. Cameron (USGS) and M. K. Mullen (Maine Geological Survey) for their estimated potential as peat resources suitable for energy, horticultural, and agricultural uses. Resources in these peat deposits occupy a total of 5,774 ha and will yield 23,670,000 short t of air-dried peat. Laboratory analyses show that 69 percent of the 48 deposits containing potential peat resources have an ash content below 6 percent and a Btu range of 9,118 to 10,627. Twenty-one percent have an ash content of 6 to 11 percent and a Btu range of 8,978 to 9,445. Eight percent have ash content ranging from 11 to 16 percent and Btu from 8,368 to 9,199. Ash content in the remaining 2 percent is 22 percent on the dry basis and Btu is 8,185. Almost all the resources may be classed as moss (fibric) peat and reed-sedge (humic) peat.

Two areas in the Susitna Valley, about 97 km northwest of Anchorage, Alaska, were mapped for peat resources by C. C. Cameron (USGS), T. J. Malterer (Minnesota Dept. of Natural Resources), and S. E. Rawlinson and S. B. Haedy (Geological and Geophysical Surveys, Alaska). These areas contain an estimated 5.6 million t of air-dried peat of commercial quality; ash content is less than 25 percent on the dry basis and Btu is roughly around 8,000.

Low-grade chromite resources

Chromite, the only ore of chromium, occurs almost exclusively in mafic-ultramafic rocks and their weathering producers. However, not all kinds of mafic-ultramafic

rocks are favorable hosts for possible low-grade chromite deposits. For instance, chromium-bearing basalts are not favorable because they commonly contain less than 0.3 percent Cr_2O_3 , and chromite is almost always less than 50 μm in diameter, if it is present at all. Chromite-bearing ultramafic rocks in stratiform and alpine complexes tend to be either ore grade, greater than 25 percent chromite, or very low grade, less than 2 percent chromite; intermediate rocks are scarce. In most complexes, large tonnages exist only in the less than 2 percent chromite group and the composition of the chromite may be unsuitable for metallurgical use. Some nickel laterite districts contain more than 100 million t of material with 2.0 percent to 5.5 percent Cr_2O_3 , and hence, chromium could be a byproduct of nickel mining in these districts. In addition, some chrome sand placers may contain tens to hundreds of millions of tons of material between 2 and 5 percent Cr_2O_3 .

MINERAL-RESOURCE ASSESSMENTS—LAND AREAS

Geochemistry and resource potential of the Selway-Bitterroot Wilderness

Geochemical studies of stream sediment, stream-sediment concentrate, and rock samples from the Selway-Bitterroot Wilderness, Idaho and Mont., combined with geologic mapping, revealed no areas of significant mineral occurrences or potential. Three large epizonal Eocene plutons within the wilderness have been identified by B. W. Coxe as potential source or host plutons for granite molybdenite-type mineralization. Analyses of magnetic and nonmagnetic heavy-mineral concentrates show strong positive anomalies of both molybdenum and tin within these plutons; however, geologic mapping in the area shows no signs of mineralization. Other anomalies are few and weak. The rock samples throughout the wilderness exhibited very low background values for most of the trace elements, regardless of rock type.

Molybdenum-silver anomalies, Ten Mile West RARE II Roadless Area, Idaho

Geochemical analyses of stream-sediment and rock samples taken in the Ten Mile West Roadless Area, Boise and Elmore Counties, Idaho, show pronounced molybdenum and silver anomalies in a northwest-trending belt that crosses the roadless area. The mineralized anomalies are chiefly along the downthrown side of a regional fault and, as such, mark the continuation of a mineralized belt southeast of the roadless area described by Kiilsgaard and others (1970).

Regional geochemical exploration in Alaska

Preliminary reconnaissance data indicate that the known copper and zinc stratiform volcanogenic sulfide belt found in the Ambler River and Survey Pass quadrangles extends eastward along the southern flank of the Brooks Range into the Wiseman quadrangle. A northeast trend mineralized in Cu, Zn, Pb, As, Sb, W, U, and Ba encompasses the Doonerak Anticline and appears to extend into the Philip Smith Mountains quadrangle.

Mineralogical and geochemical analyses of heavy-mineral concentrate stream samples collected from streams draining Yukon Upland-type rocks west of the Hayes glacier near the western border of the Mount Hayes $1^\circ \times 3^\circ$ quadrangle, Alaska, have indicated mineralized rock. R. B. Tripp, G. C. Curtin, and D. L. Huston reported that pyrite, chalcopyrite, pyrrhotite, arsenopyrite, galena, sphalerite, gold, and sheelite have been identified in the concentrates. A rock sample collected from the area was coarsely pulverized, panned down with a gold pan, and fractionated by using bromoform and an electromagnet. The resulting heavy-mineral sample was found to contain chalcopyrite, bornite, pyrite, arsenopyrite, and gold.

A sample of galena containing significant amounts of tin, bismuth, and silver was found in a previously unreported mineralized zone in the Yukon Upland metamorphic terrane near Miller Creek, 20 km west of Central, Alaska. R. B. Tripp, D. E. Detra, and J. M. Nishi (1982) reported that the zone, which is about 0.6 m thick and traceable for about 6 m, contains crystalline pods and stringers of galena associated with cerussite, mimetite, and iron oxides. Other sites in the Miller Creek area are characterized by irregularly shaped sulfide zones as wide as 6 m in diameter with finely disseminated grains and crystals of arsenopyrite and some pyrite.

Preliminary reconnaissance data indicate possible occurrences of copper, molybdenum, and tungsten minerals in an area predominately underlain by Cretaceous-age intrusive rocks just south of the Tlikakila River on the eastern boundary of the Lake Clark quadrangle. The minerals identified in heavy-mineral concentrates of stream-sediment samples from this area are chalcopyrite, arsenopyrite, pyrite, malachite, scheelite, and powellite.

D. E. Detra and R. L. Detterman reported that geochemical reconnaissance studies and geologic mapping in the Bristol Bay, Ugashik, and Karluk quadrangles have resulted in the delineation of two possible metallic mineral occurrences. One area of interest is located on an unnamed mountain to the northeast of Mother Goose Lake, between Volcano and Wondering Creeks,

and surrounds the Red Porphyry copper deposit identified by Bear Creek Mining Company. The streams draining this first area were found to contain gold and silver anomalies with associated less significant lead, copper, and tungsten values. The second area of interest is in the area surrounding the Mike Prospect at Painter Creek Pass near the south-central region of the Ugashik quadrangle where streams were found to contain anomalous concentrations of Mo, Cu, Zn, Pb, As, and Ag.

H. D. King, K. D. Duttweiler, and W. D. Johnson reported that preliminary results of geochemical studies in the Bendeleden quadrangle, Seward Peninsula, Alaska, show the presence of an area geochemically anomalous in copper, lead, and zinc that is in the headwaters of the Nuikluk River extending eastward to Pargon Creek, east of Mount Bendelben. Base-metal mineralization in this general area has been previously noted (Hudson, 1977).

Mineral production from counties in the Charlotte 1° × 2° quadrangle, North and South Carolina

Preliminary results of a study of mineral commodity production from the 31 counties that are entirely or partially within the boundaries of the Charlotte (North and South Carolina) quadrangle show that construction materials are the dominant mineral product in counties with the highest cumulative mineral production values over the past 80 years. Crushed and dimension stone contribute more than 80 percent of the cumulative constant dollar value of 5 of the leading 10 counties, and sand and gravel comprises 97 percent of another county's value. Leading the 31 counties in mineral production value is Mitchell County, N.C., whose feldspar and mica production was gained from parts of the county outside the Charlotte quadrangle boundaries. Other commodities that contributed a significant portion of the leading counties' values were lithium minerals and iron ore.

Preliminary resource appraisal in the southern Snake Range, Nevada

Preliminary appraisal of the mineral-resource potential of the Wheeler Peak and Highland Ridge Further Planning Areas indicates that favorable areas are in the lower plate of the Snake Range décollement and that rocks in the upper plate have low potential. The Pioche Shale, Pole Canyon Limestone, and granitic rocks, which contain known mineral deposits within and adjacent to the study areas, are the most favorable host rocks.

Geologic and mineral-resource studies, Glacier Peak Wilderness Area, Washington

Geologic mapping by A. B. Ford, W. H. Nelson, R. A. Loney, and R. A. Sonnevil confirms general results of early studies (personal comm., Univ. Wash., Misch) that a crystalline complex of medium-rank schist and gneiss forms the core of the northern Cascade Range in the Glacier Peak Wilderness Area, Washington. The crystalline terrane is juxtaposed on the west, along the strike-slip Straight Creek fault, by a terrane of blueschist-facies metagraywacke and metabasalt. Approximately 30 mapped plutons in the area range in age from possible pre-Cretaceous to late Tertiary. Preliminary K-Ar age determinations by R. J. Fleck indicate that plutonism in the Snowking Mountain area was as young as about 15 m.y. No significant resource potential is apparent in the youngest plutons. The major resource potentials are for copper and molybdenum porphyry-type deposits associated with somewhat older plutons (about 20 m.y.) related to Cloudy Pass batholith.

Mineral resources of the Mt. Henry RARE II Study Area, Lincoln County, Montana

R. E. Van Loenen, D. F. Siems, and G. A. Wadsworth, USGS, and Martin Conyac, USBM, report that geologic and geochemical studies of the Mt. Henry Wilderness Study Area have indicated a low potential for strata-bound copper and silver mineralization within the Ravalli Group strata of the Belt Supergroup of Precambrian age. Fault structures north and south of the area have recorded mineral production; however, these related structures within the area have little or no potential. No mines or prospects are located within the study area.

Mineral resource potential of the Marble Platform, Coconino County, Arizona

The mineral resource potential of the Marble Platform west of the Colorado River and north of 36°30' N. in Coconino County, Arizona, has been rated as very low by A. L. Bush, USGS, and M. E. Lane, USBM. The only commodity considered to have any potential is construction aggregate; it occurs as gravel, cobbles, and boulders of the Kaibab Limestone in thick pediment gravels and could be mined from the Kaibab Limestone itself. The limestone is not near the surface over most of the area studied. A single occurrence of uranium with associated vanadium and copper is in a small remnant of the Shinarump Member of the Chinle Formation. The conglomerate has been eroded from the rest of the study area, and the deposit has been mined out.

Resource appraisal completed for Wallace 1° × 2° quadrangle, Montana and Idaho

The CUSMAP resource appraisal for the Wallace 1° × 2° quadrangle has recently been completed by the appraisal team of J. E. Harrison, D. L. Leach, M. D. Kleinkopf, E. R. Cressman, C. L. Long, L. C. Rowan, and J. A. Domenico. The area is typical of the highly mineralized ground characteristic of much of western Montana and northern Idaho. Seven types of ore deposits—placer gold, stratabound copper-silver, Sullivan-type stratabound lead-zinc-silver, porphyry molybdenum-tungsten, platinum-group metals, epithermal silver, and base and precious metal mesothermal veins—are known or possible in the quadrangle. Geologic, geochemical, geophysical, remote sensing, and isotope data were collected to help evaluate the area for metallic resources. The team designed a system that allows the user to follow the trail of data, assumptions, and rationale. The reconnaissance data do not have sufficient detail to pinpoint ore deposits, but they do identify subareas of the quadrangle that are diagnostic or suggestive of presence of ore deposits. Several of the subareas appear to have few or no prospects in them, so the appraisal maps should be useful for mineral exploration as well as for land-use classification.

Geochemical anomalies of tin and tungsten in north-central New Hampshire

Analysis of the nonmagnetic fraction of heavy-mineral concentrates of stream sediments collected in 1980 in north-central New Hampshire has revealed two strongly anomalous patterns of tin and tungsten that could possibly be of economic significance. The anomalous patterns are largely spatially separate, although some overlap is present. The tin pattern is homogeneous and correlates spatially with granitic rocks of the White Mountain Plutonic-Volcanic Suite of Mesozoic age. Cassiterite has been identified in some of the heavy-mineral samples from the SW. one-fourth of the Lewiston 1° × 2° map of the area. The anomalies appear to relate to volcanic rocks and sediments that contain appreciable amounts of volcanic debris. Limited geological investigations so far have failed to locate any obvious bedrock sources of the two metals.

Geophysical studies in the Sherbrooke and Lewiston 1° × 2° quadrangles, Vermont, New Hampshire, and Maine

Gravity surveying by W. A. Bothner (University of New Hampshire), who was assisted by R. E. Bracken (USGS), M. J. Carnese, and T. B. Gage (University of New Hampshire), has been completed for the Sherbrooke and Lewiston quadrangles, Vermont, New

Hampshire, and Maine (and included White Mountain Wilderness Area).

Preliminary results indicate that the character of felsic intrusions of the New Hampshire Plutonic Suite of Devonian age changes from southwest to northeast across the high to low metamorphic transition (middle to upper crust) in west-central Maine. Those intrusions within the sillimanite plateau of central New England are thin, subhorizontal, semiconcordant sheets seldom thicker than 3 km, while those to the northeast of the transition are more discordant and thicker. Mafic intrusions of both mid-Paleozoic and Mesozoic age are considerably thicker (5 km or more).

Detailed study of Mohawk Mountain geochemical anomaly

A single regional geochemical anomaly, mapped at a scale of 1:250,000, at the southeast end of the northern Mohawk Mountains, New York, was found by R. H. Eppinger, at a scale of 1:24,000, to consist of four separate geochemical terranes that are separated by faults. Common to all are high concentrations of copper, molybdenum, and lead. The four separate terranes are characterized by tungsten, thorium, tin, and tungsten-bismuth. They probably reflect potential for at least two distinct types of mineral deposits: a grissen, skarn, or vein type rich in tungsten, and a zoned, porphyry or base-metal vein system.

Mineral resource potential, RARE II Study Areas, southwest New Mexico and east Arizona

J. C. Ratte, R. A. Martin, J. R. Hassemer, J. P. Briggs, and M. E. Lane report that mineral resource appraisals of the Hells Hole and Lower San Francisco Wilderness Study Areas (RARE II) indicate a low to moderately high potential for base- and precious-metal resources related to silicic subvolcanic intrusive centers in both areas. The Hells Hole volcanic center was active from about 27 m.y. ago to about 18 m.y. ago, culminating in the eruption of highly evolved high-silica rhyolite. Weak gold, silver, copper, molybdenum, and other metal anomalies warrant further exploration in the Hells Hole area.

The main target for mineral exploration in the Lower San Francisco area is the partially exhumed 26 to 28-m.y.-old dacitic Goat Basin volcanic cone. In its eroded out center, propylitically altered rocks are cut by small silicified and pyritized rhyolite dikes having sniffs of copper and molybdenum (200 ppm copper in one sample; 70 ppm molybdenum in another, out of about 20 samples analyzed). A 100-gamma aeromagnetic low over the Goat Basin volcanic cone shows a low magnetic susceptibility at depth, indicating a possible enlarge-

ment of the rhyolite or other intrusive rock which could be mineralized. Nineteen-m.y.-old high-silica rhyolite in this area also is weakly mineralized with gold and silver, and the rhyolite center is expressed also as a magnetic low that is contiguous with the magnetic low of the Goat Basin volcano.

GEOLOGIC STUDIES OF MINING DISTRICTS AND MINERAL-BEARING REGIONS

Origin of manganese deposits in Franciscan rocks of the Yolla Bolly terrane, California

Geologic mapping by M. C. Blake, Jr., and A. S. Jayko, combined with geochemical data, indicates that the manganese chert deposits of the Yolla Bolly terrane (Franciscan assemblage) in northern California probably formed in a tectonic setting similar to the present Gulf of California. The cherts were deposited within a deep-sea fan system consisting largely of quartz-feldspathic graywacke of latest Jurassic to Early Cretaceous age. Subsequently, the sedimentary rocks were intruded by sills of diabase and quartz keratophyre which remobilized the sedimentary manganese within the chert to form small ore bodies. Following this, all of the rocks were involved in a subduction or collision event that metamorphosed them to the blueschist facies and further modified the manganese minerals.

Genesis of sulfide ores in the Duluth Complex

Work in the Duluth Complex by M. P. Foose has resulted in the identification of two distinct sequences of rock. The lower sequence is a sulfide-bearing intrusive composed of heterogeneous lithologies that include magnetite, troctolites, anorthosites, and hornfels which lack lateral continuity. The sequence over the sulfide-bearing zone is composed of sulfide-free rocks that show laterally continuous cyclic repetitions of the crystallization sequence, plagioclase and plagioclase plus olivine. Cryptic variations associated with these cycles show both upward enrichments and depletions in nickel. These variations probably result from a combination of repeated injections of new magmas and from changes in pressure within the magma. Depletion of nickel is the expected trend of normal fractional crystallization; upward nickel enrichment patterns may be due to pressure unloading in the magma chamber. The abrupt contact between the sulfide-bearing and sulfide-free rocks indicates that a distinct sulfur-rich magmatic event occurred and was subsequently followed by successive

injections of sulfide-free liquids. The recognition of this early sulfide-rich magmatic event does not support suggestions that the sulfide ores formed as a result of sulfur contamination from the country rock.

Gold in the Gold Basin-Lost Basin districts, Mohave County, Arizona

Gold mineralization in the Gold Basin-Lost Basin districts is being studied jointly by T. G. Theodore, W. N. Blair, J. T. Nash, E. H. McKee, and J. C. Antweiler. Known gold occurrences are associated with the quartz-carbonate-galena-chalcopyrite stages of quartz-feldspar veins, presumably emplaced episodically during Proterozoic Y and Late Cretaceous time. Gold is also found disseminated in small episyenitic alteration pipes or in veins caught up along a regionally extensive Miocene detachment fault. Hydrothermal micas from the veins give K-Ar ages of 822, 712, 69, 68, and 65 m.y., and from the pipes, 128 and 129 m.y.; primary mica from a peraluminous two-mica monzogranite gives an age of 72 m.y. Biotite from a Proterozoic X gneissic granodiorite in the central part of the Gold Basin district gives an age of 86 m.y., most probably reflecting a closely underlying lobe of two-mica monzogranite. Most occurrences of gold in the veins probably result from the remobilization of metals during Late Cretaceous time and redeposition during galena- and ferroan-carbonate-bearing stages of the veins. Temperatures probably were in the range 300-335° C during the onset of mineralization at the gold-bearing pipes and veins, and pressures were probably in the range 500 to 700 bars at the pipes, on the basis of fluid-inclusion relations and comparisons with experimentally studied systems. Most fluids are moderately saline (6-14 weight percent NaCl equivalent), non-boiling, and the fluids also contain abundant carbon dioxide and, in places, fluorite. Fluorite-bearing veins are especially concentrated in the area of the exposed two-mica monzogranite and in the southeastern part of the Gold Basin district. In native-gold samples from 20 mines in the Gold Basin district and 48 veins in the Lost Basin district, silver content ranges from 6 to 50 weight percent, and copper from 0.01 to 0.5 weight percent. Metal zonation and possible relation to a porphyry-copper system can be inferred from some of these chemical data. The differences in the composition of placer gold studied in 24 occurrences in the Lost Basin district from that of nearby lode sources suggest that other sources contributed gold to the placers, or that locally derived grains were enriched by oxidation and weathering of the lodes. All rocks in the general areas of oxide facies, iron formation, and quartz tourmalinite of Proterozoic X age should be evaluated carefully as potential indicators of gold-bearing exhalative systems.

Studies of the root zone of the Ajo porphyry copper system

Abundant mineral-rich inclusions occur in primary interstitial quartz in the Cornelia quartz monzonite at Ajo, Ariz. The pluton has been recognized as the root zone of the Ajo porphyry copper deposit (Gilluly, 1946) and the inclusions are believed to represent trapped samples of the hydrothermal fluid that formed the deposit (Cox and others, 1981). Detailed mapping of the pluton by D. P. Cox (USGS) and Eijun Ohta (Japan Geological Survey) has established a large amoeba-shaped body of fine aplitic-textured porphyry within the pluton. This phase, first recognized by Wadsworth (1968), is believed to represent pressure quenching of magma and may be related to boiling of contained fluids and separation of the highly saline brine trapped in the inclusions.

Tourmaline-rich rocks as possible indicators of massive sulfides

C. E. Brown and R. A. Ayuso (1982) have analyzed tourmaline from metasedimentary rocks in St. Lawrence County, New York, that contain as much as 30 percent tourmaline. Tourmalines in these rocks are magnesian rich like those in genetically related tourmalinites found at the Sullivan Mine in British Columbia and massive sulfide deposits in Maine and Vermont, thus implying the possibility of similar deposits here.

The B chromite zone of the Stillwater Complex, Montana

B. R. Lipin and P. J. Loferski reported that the B chromite is the third thickest chromite zone in the Archean stratiform Stillwater Complex, Montana. At the west fork of the Stillwater River, the B chromite ranges from about 0.3 to 7 m in thickness over a strike length of almost 600 m, and it contains from 2 to 15 distinct chromite layers that range from 1 to 2 grains thick (about 1 mm) to 0.3 m thick. Cr_2O_3 in chromite varies along strike from 42 to 52 percent, with the lower values in rocks with pyroxene and plagioclase and the higher values generally in rocks with olivine. This indicates subsolidus reequilibration. Compared with accessory chromite, segregated chromite is generally lower in $\text{Cr}/(\text{Cr}+\text{Al})$ and $\text{Fe}^{3+}/(\text{Cr}+\text{Al}+\text{Fe}^{3+})$, and slightly higher in $\text{Mg}/(\text{Mg}+\text{Fe}^{2+})$. Much of the chromite is anisotropic; however, X-ray diffraction analysis did not reveal any deviation from cubic symmetry. The anisotropy might be caused by an impurity in the chromite that creates a slight distortion of the lattice to produce a deviation from cubic symmetry that is too slight to be detected by X-ray diffraction. Multiphase silicate inclusions are nearly ubiquitous in the West Fork B chromite. Phases include amphibole, pyroxene, phlogopite, biotite,

serpentine, talc, and sulfides. The shape and arrangement of the inclusions are variable. Some have negative crystal shapes, others are rounded, irregular or ragged, and some have protrusions into the chromite. They occur variously as a single large central inclusion, as a ring around the core, or scattered throughout chromite grains. Some inclusions may be trapped melt and may provide information as to the composition of the original Stillwater Complex magma. The total thickness of magma from which the West Fork B chromite crystallized was 370 to 480 m, on the basis of a chromitite thickness of 37 to 48 cm and a minimum Cr_2O_3 enrichment factor of 1,000 in chromite compared to the magma.

Large hydrothermal systems studied in Carolina slate belt

About 40 large bodies of very aluminous rock are known within the volcanic rocks of the Carolina slate belt. Characterized by kaolinite, sericite, andalusite, pyrophyllite, topaz, rutile, diaspore, and locally much disseminated sulfide, these deposits have formed by intense hydrothermal alteration of mostly andesitic eruptive rocks; several are presently mined for andalusite and pyrophyllite. Although no metallic ores have been identified, copper, molybdenum, bismuth, arsenic, and tin are locally present in minor amounts, especially in those systems with extensive peripheral zones of silicification. Gold has been mined at three aluminous deposits and may be associated with a few more. The regional geologic setting and the detailed geology of several of these hydrothermal systems is being studied by R. G. Schmidt and T. L. Klein, who are seeking evidence that these systems may include significant metallic sulfide deposits. Analogous deposits in other regions selected to help understand those in the Carolinas include deposits at Mount Pleasant in New Brunswick, Canada, scattered porphyry copper deposits in the North and South American Cordillera, and deposits in Southeast Asia. The Kounrad and some other deposits in Kazakhstan, U.S.S.R., are major porphyry copper systems where abundant andalusite and pyrophyllite closely associated with the ore zone have formed by hydrothermal action, and there is extensive peripheral silicification. Comparisons with Kazakh ore bodies suggest that some Carolina deposits are variations of porphyry-type systems and that alteration mineral zonation is a potential tool to identify the part of a greater system represented by the surface exposures.

Ages of mineralization at the Buckingham molybdenum deposit, Nevada

Collaborative studies by T. G. Theodore and E. H. McKee have established that protracted igneous activity occurred in the general area of the Buckingham por-

phyry molybdenum stockwork system. This stockwork system, in the northeastern part of the Battle Mountain mining district, is hosted mostly by composite monzogranite bodies of Late Cretaceous age and by the Upper Cambrian Harmony Formation. As defined by drilling during 1981, the system is elongate in an east-west direction, and surface projection of the system measures approximately 2,500 by 700 m. However, the system has been extended tectonically by significant postmineral faulting, some of whose dislocations began near the final stages of magmatic activity associated with the development of the molybdenum system. Emplacement of the molybdenum-related magmas apparently inflated the surrounding country rock in such a way that some rocks, including copper-rich skarns comprising the Copper basin orebody, slid off the top of the overall mineralized system. The Buckingham deposit was further disrupted by significant faults that are mostly younger than 35 m.y.

The Buckingham porphyry system is centered on numerous small leucocratic, hornblende-biotite monzogranite bodies that are typified by intensely silicated domains containing quartz with or without pyrite and with or without molybdenite stockwork veins. The well-developed stockworks extend laterally about 300 m from some of the large intrusive masses, and the stockworks are associated with both potassic and sericitic alteration assemblages. The stockworks extend into the open pit of the Copper basin porphyry deposit which occurs at the eastern margin of the molybdenum-mineralized rocks. Geochronologic studies include K-Ar age determinations on 10 mineral separates and 1 whole rock from the Buckingham-Copper basin areas. Four rocks from within the surface projection of the outer limit of intense quartz stockworks that surround the molybdenum system yield K-Ar ages ranging from about 60 to 70 m.y. Two of these ages are from hydrothermal white mica, one is from primary biotite, and the other (70.3 m.y.) is from an intermineral granite aplite which cuts the quartz-molybdenite stockworks and which contains some disseminated molybdenite. However, all of these ages are probably reset. Replicate age determinations on white mica from a mineralized dike near the eastern end of the molybdenum system yield ages of 86 and 88 m.y. Therefore, it is assumed that the bulk of the molybdenum was introduced approximately 90 m.y. ago. Five other ages from different intrusive masses in the Buckingham-Copper basin areas are in the 35.4 to 39.3 m.y. interval, generally the same age as the copper mineralization established at Copper Canyon, which is about 15 km to the south. This group of ages also includes two age determinations of primary biotite from essentially unmineralized rhyolite which crops out near the Buckingham porphyry molybdenum system. These age relations suggest that a complex

sequence of Late Cretaceous intrusive events was involved in the evolution of the igneous hydrothermal system(s) in the Buckingham-Copper basin areas. Apparently, the bulk of the molybdenum was introduced about 90 m.y. ago. There finally was a resurgence of intrusive activity in the area during the Oligocene, about 35 to 39 m.y. ago. Mineralization associated with this Oligocene event includes mostly base and precious metals along veins.

Ore genesis processes at Gilman-Leadville

G. P. Landis, in a continuing study of the ore-forming processes at Gilman, Colo., has extended the study to include the mineral deposits of the Leadville district and surrounding mineral deposits in the Leadville dolomite of the central Colorado mineral belt (e.g., Sherman, Alps Gulch, Hock Hocking, Continental Chief, Russia, Peerless, Sacramento, Dyer, and Mineral Park mines). In the central Leadville district, the only mineralization examined is that accessible through the Blackcloud mine. Gilman appears to be but one part of the mineralization history of the area, with other factors represented in the Leadville area. Sulfur isotope data on sulfide minerals and barite and oxygen isotope analyses of barite define two sources for sulfur in the Leadville mineralization: a sedimentary evaporitic sulfate sulfur (present in Sherman-type barite-galena-sphalerite ores) and a postmagmatic hydrothermal sulfur (observed in the Blackcloud mine, the Leadville-type mineralization). Fluid inclusion data and sulfur isotope fractionation data from sulfide minerals indicate temperatures of 250 to <400° C. The Sherman-type mineralization appears to predate the later Leadville-type ores in the district. In the mineral paragenesis at the Sherman mine, early white barite contains sedimentary-sulfate sulfur, whereas late golden barite is much more depleted in ³⁴S and is comprised of sulfate formed by the meteoric water oxidation of reduced aqueous sulfur. Gilman may be a superposition of both mineralizing events.

Gold veins of the Granite District, Chaffee and Lake Counties, Colorado

The fissure gold veins in the Granite District are currently (1982) being studied as a part of the mineral resource appraisal of the Buffalo Peaks Wilderness Area. As in many other old mining districts of Colorado the early production figures are largely estimates, and in the Granite District the lode gold production was valued at about \$2 million (about 100,000 troy ounces). Most of the production was in the 1860's and 1930's, and the ore chiefly came from the veins on Yankee Blade Hill and those to the north in the vicinity of the Belle of Granite mine. Within the district older Precambrian biotite gneiss and migmatite ore are intruded by synkinematic adamellite and two-feldspar granite. The

metamorphic gneisses comprise a dismembered synclinal fold, about 4.5 km across, with an axial plane that strikes N. 50°-55° E. The nearly vertical limbs of the fold are discontinuous and the granite magma penetrated the keel of the fold. The fold axis plunges 45° to 50° N. 55° E., and the faulted keel of the fold shows closure to the west near Granite.

The biotite gneiss is highly foliated, locally migmatized, and contains as much as 50 percent quartz, 25-30 percent biotite, and 5-10 percent fibrolitic sillimanite. Stretched quartz pebbles are locally present and the gneiss is clearly of sedimentary origin.

The fissure veins occur in swarms and are chiefly confined to the gneiss, not the granite, and preferentially follow the foliation in the gneiss by striking N. 60°-70° E. Some veins can be traced along strike for 2,200 m, although pinch-outs are common locally. Some veins have abundant gouge, others are brecciated, and quartz veining is common. Both argillic and sericitic wall rock alteration of the gneiss is observed. The mineralogy is simple, chiefly early pyrite and gold and very minor amounts of later chalcopyrite, galena, and sphalerite. The veins are oxidized to depths of 60 m, and in the oxidized zone the gold is coarser grained and more unevenly distributed than in the nonweathered veins at depth. Most of the past production came from the oxidized zone.

A few thin scattered rhyolite dikes cut the gneiss nearly parallel to the foliation. The dikes are of probable Laramide or mid-Tertiary age. Most dikes are less than 2 m thick and have locally been faulted-out along the veins; the Two Bit mine extension exemplifies this. Some pyritized dike fragments have been observed in the mine dumps of the district, although dike outcrops were absent.

There are two hypotheses for the origin of the gold veins: (1) magmatic-hydrothermal origin from a silicic magma source, and (2) reconcentration of gold derived from Precambrian metasedimentary rocks by Laramide hydrothermal fluids. The absence of a Laramide or mid-Tertiary pluton in the district, the paucity of sulfides other than pyrite, and the essential confinement of the gold veins to Precambrian gneiss all are indicative of a hydrothermally mobilized gold deposit derived from Precambrian metasedimentary rocks.

Molybdenum mineralization model for central Idaho

Mapping by D. A. Seeland in the White Cloud Peaks area of central Idaho has shown that the Castle Peak molybdenum discovery is directly related to the physical and chemical character of the host rock. Previous studies in the area assigned the host rock of the Castle Peak deposit to the Pennsylvanian-Permian Wood River Formation. However, thin argillites and other

lithologic characteristics, together with physical continuity with paleontologically dated rocks, suggest that the rocks containing the deposit are Mississippian in age.

The molybdenum mineralization occurs on the northeast margin of the White Cloud stock in quartz and quartz-feldspar veins in brittle siliceous Mississippian quartzite. In contrast, the remainder of the stock is bordered by unmineralized calcareous sandstones of the Pennsylvanian-Permian Wood River Formation which have been metamorphosed to a wollastonite-rich calc-silicate granofels on the margin of the stock.

This association of molybdenum mineralization with siliceous Mississippian quartzites intruded by Upper Cretaceous granitic rocks should be a valuable exploration guide elsewhere in central Idaho.

Copper and uranium in sediments shed from the ancestral Rocky Mountains

Geologic mapping and stratigraphic and mineral resource studies of Pennsylvanian-Permian red-bed sequences in the northern Sangre de Cristo Mountains by D. A. Lindsey, S. J. Ashe, and R. F. Clark show that stratiform copper-uranium deposits there occur in gray strata (reduced diagenetic facies) immediately below the red-gray boundary and in lenses of shale, siltstone, and limestone (shallow marine-lagoonal facies) containing abundant fossil plant trash and marine invertebrates. These facies are part of an assemblage deposited on fan deltas east of the San Luis-Uncompahgre highland during Middle Pennsylvanian time. The fan-delta deposits are part of a coarsening-upward sequence of facies that comprise the Minturn Formation of Pennsylvanian age and the Sangre de Cristo Formation of Pennsylvanian-Permian age, and that range, from bottom to top, from turbidite (fan-delta slope), through fan-delta facies, through braided alluvial-plain (lower fan) facies, to proximal alluvial-fan facies. The emergent part (in Pennsylvanian time) of this sequence has been oxidized to red beds by ground water, but the submergent part has remained mostly reduced gray beds; copper and uranium occur below this red-gray (oxidized-reduced) boundary. Inasmuch as similar sequences of Pennsylvanian and Permian strata were deposited elsewhere around the highlands of the ancestral Rocky Mountains, copper and uranium can be expected to occur in the same setting as that of the northern Sangre de Cristo Mountains.

Recycled gold, interior Alaska

Warren Yeend reported that it seems increasingly clear that gold has been recycled through continental deposits of Tertiary age prior to its incorporation in the

recent placers throughout much of interior Alaska. Yeend panned gold from several suspected Tertiary conglomerates within the so-called Tintina fault zone of the Circle quadrangle. Although gold has been reported from Tertiary rocks in neighboring quadrangles (Mertie, 1938), none has been listed from Tertiary rocks of the Circle quadrangle.

Tertiary(?) clastic rocks in the Circle quadrangle seem to be restricted to the Tintina fault zone, although it seems probable that when initially deposited they covered areas beyond the fault zone. If so, they most likely were a source for much of the gold that now occurs in Holocene alluvium and has supplied the Circle district placer miners with a gold resource for over 80 years.

Within the Healy quadrangle, Yeend panned gold from the Lignite Creek Formation-Nenana Gravel contact of Tertiary age near the area where the main highway to Fairbanks crosses Panguingue Creek. In the Mt. Hayes quadrangle, directly east of the Healy quadrangle, gold is present in conglomerates of early Tertiary(?) age (Yeend, 1981).

Origin of Kuroko ore deposits of Japan

The isotopic composition of lead was investigated in and around Kuroko deposits of the Hokuroku Basin by M. H. Delevaux and B. R. Doe (USGS), and by Udo Fehn (University of Rochester). Although the ore leads of these deposits were found to occupy a narrow isotopic range, each ore deposit has a characteristic isotopic composition. Within a given ore deposit, black ore (Pb-Zn rich) has a uniform isotopic composition but is significantly higher in radiogenic lead than yellow ore (Cu-rich). The differences between ore types are, however, smaller than those between ore deposits. The volcanic host rocks are, in general, lower in radiogenic lead than are the ores, whereas the deeper, older formations, in particular the Sasahata Formation and the Paleozoic basement, have more radiogenic lead than do the ores.

On the basis of the isotopic distribution, Delevaux, Doe, and Fehn conclude that a major part of the lead in the Kuroko deposits was derived from igneous, probably volcanic rocks with an uncertain but significant contribution coming from the underlying pre-Nishikurozawa Formations. The ore fluids reached the Sasahata Formation and most likely also the Paleozoic basement. Each ore deposit within the basin was formed by a local hydrothermal system. The difference in isotopic composition between yellow ore and black ore reflects a shift in the proportions coming from the two major sources due to the temperature evolution of the hydrothermal system. The yellow ore seems to have a greater igneous rock lead component than does the black ore.

Mineralization in North Carolina RARE II Areas

W. R. Griffitts, J. W. Whitlow, D. F. Siems, and K. A. Duttweiler made geochemical and heavy mineral studies at the Lost Cove and Harpers Creek RARE II Areas, N.C. They found unexpectedly high values of niobium and beryllium, which indicates that the mineralization in the areas is more complex than had been suspected. The niobium- and beryllium-rich areas overlap the previously known area of uranium mineralization. Fluorite and galena were found in pitchblende veinlets within the RARE II areas, and columbite and thorite were found just outside the areas. In addition, Theodore Botinelly identified florencite ($\text{CeAl}_3(\text{PO}_4)_2(\text{OH})_6$) at a thorium prospect a few miles south of the RARE II boundary.

Age of mineralization, Mogollon mining district, Catron County, New Mexico

A potassium feldspar (adularia?) concentrate from mineralized quartz-vein materials off the dump of the Last Chance Mine in the Mogollon mining district has given a K-Ar age of 17.5 ± 0.6 m.y. Two analyses of the feldspar concentrate, which contained some quartz, have 9.67 and 9.63 percent K_2O . The 17.5 m.y. age is significant in two respects: in dating mineralization in the Mogollon mining district and in enhancing the mineral-resource potential of other areas where mineralization is associated with rhyolites of that age, as along the Mogollon Mountains front and in the area between Mogollon and Steeple Rock, N. Mex., and Morenci, Ariz.

Mine studies, Lake City, Colorado

Field studies of vein deposits surrounding the Lake City caldera were made by A. R. Kirk, Patty Billings, and R. F. Sanford during the summer of 1981.

Greater emphasis was placed on the two operating mines in the Lake City district, the Golden Wonder and the Gladiator. Although these deposits do not contain uranium, both are of interest in determining the distribution of uranium in the Lake City ores. The Gladiator, a silver-gold deposit, is located immediately adjacent to the Golden Fleece, a known uranium occurrence. The Golden Wonder is a gold-telluride deposit, as is the Golden Fleece. Comparison of these deposits to the Golden Fleece may serve to further delineate conditions for uranium deposition and zoning patterns in the Lake City area.

The Golden Wonder deposit was identified as a fossil hot-springs system developed in a rhyolite dome-flow complex. The rhyolite shows characteristic sinter deposits, acid-sulfate alteration, and hydrothermal

alteration and brecciation. Pebble dikes are common. Alteration minerals include kaolinite, dickite, illite, alunite, and possible smectites. Preliminary studies of the minor element chemistry of the altered rhyolite by energy-dispersive X-ray fluorescence indicate that yttrium, an element usually considered to be immobile, may be mobile during extreme acid-sulfate alteration. Zirconium and niobium, however, appear to be immobile. Rubidium is commonly depleted in the most altered rhyolite, but may be enriched in or near the vein. Lead seems to increase near the veins and may be useful as a "pathfinder" element.

The vein material itself can be divided into two major types—a pyrite-marcasite episode and a fine-grained silica episode. The pyrite-marcasite episode appears to be older. Locally, at least, it may be prealteration. Tetrahedrite and other sulfosalts are also associated with this episode, and commonly line vein cavities into which the second suite of vein minerals was deposited.

The second type of vein material is a fine-grained silica which is economically important because it carries finely disseminated gold tellurides. The silica is cherty and commonly shows crossbeds, soft-sediment deformation features, and intraunit breccias. Pods of kaolinite and alunite may also be present, as well as sphalerite, galena, tetrahedrite, and other complex sulfosalts. This chert was probably deposited as a sediment in underground ponds and fissures by the hot springs waters.

Veins themselves appear to be en-echelon features controlled by the intersection of a northeast-trending joint and shear set with vertical flow foliation of the rhyolite. High-grade pockets appear to be relatively shallow, but this does not rule out the possibility of a disseminated gold deposit at depth.

Cesium concentrations in caldera complex, Nevada and Oregon

Geochemical analysis of caldera-fill sediments within the McDermitt caldera complex indicate a major resource of cesium is present. Cesium contents up to 0.09 percent, reported by R. E. Mays, are present in tuffs altered to analcime and clinoptilolite. Cesium contents of unaltered rhyolites within the McDermitt complex are among the highest known. Hydrothermal and diagenetic alteration of these rhyolites released cesium that was subsequently concentrated in zeolites.

GEOCHEMICAL AND GEOPHYSICAL TECHNIQUES IN RESOURCE ASSESSMENTS

Geochemical mapping of the southern Coast Ranges of California

Geochemical mapping of the southern Coast Ranges of California by J. M. McNeal, W. R. Miller, J. M.

Motooka, and D. E. Detra using stream-sediment samples and heavy-mineral concentrates shows trends of occurrence of trace metals that relate to geologic units, uranium deposits, and to human contamination. The occurrence of chromium, copper, and nickel is closely related to Mesozoic ultrabasic rocks, molybdenum to middle Miocene marine rocks, zirconium to Mesozoic granitic rocks, and lead to urban areas.

Trace-element geochemistry of the West Shasta District, California

Preliminary results of geochemical investigations of supergene alteration associated with the massive sulfide deposits of the West Shasta district, Shasta County, Calif., indicate that small-scale variations in the gossans are sufficiently large to mask patterns related to zoning of the district or the sulfide bodies, according to data accumulated by R. F. Sanzolone and J. A. Domenico. Transported oxides along fractures near sulfide bodies show similar patterns, but R. N. Leinz and D. F. Siems report that elements normally associated with felsic rocks show a significant increase toward the Mule Mountain stock.

Probable monazite in South Carolina

Spectrographic analyses of heavy-mineral concentrates collected in Chester and Fairfield Counties, S.C., by Henry Bell show unusual values for rare-earth elements. This suggests that monazite and other thorium and rare-earth minerals not previously reported from this area may be present.

Uranium in spring water and bryophytes at Basin Creek in central Idaho

Mosses (bryophytes) in uranium-bearing spring waters coming from arkosic sediments at Basin Creek (near Stanley, Idaho) concentrate uranium (and other metals) from the water. H. T. Shacklette and J. A. Erdman suggest that these mosses, at least in this area, are more reliable indicators of uranium occurrence than the spring waters, which fluctuate widely in metal content.

Geochemical investigation of a molybdenum-tin anomaly in southwestern Utah

J. D. Tucker, W. R. Miller, J. M. Motooka, and A. E. Hubert made a detailed geochemical survey using bed-rock samples from an area with a known molybdenum-tin anomaly in the southern Wah Wah Mountains in southwestern Utah. The geochemical patterns found in this survey are similar to those around porphyry-type molybdenum deposits and suggest the known molybdenum-tin anomaly may be related to a porphyry-type molybdenum mineralization at depth.

Geochemical exploration by analyses of fecal material from herbivorous mammals

Keith Robinson reported favorably on the possibility of using fecal material (scat) of herbivorous land mammals as a geochemical sample material. Moose, deer, and jack rabbits establish territorial areas of a few square miles at certain times of the year, and, if environmental conditions permit, live on a relatively well-balanced diet of plants. Analyses of moose scat collected from the McCarthy quadrangle, Alaska, show that some elements (Mn, Ag, B, Cd, Cu, Ni, Sr, and Zn) are enhanced by an order of magnitude in moose scat samples, compared to willow and stream sediment samples. Moose scat collected near the Kennicott copper mines, Alaska, showed high copper and an association of copper, silver, and barium that is characteristic of the copper deposits in the area. Samples of deer scat collected from an area containing known uranium-bearing magnetite in the Warwick Mountains, N.Y., contained significantly higher uranium than samples from an unmineralized area at Waywanda State Park, N.J.

Crown Point uranium mineralization trend, New Mexico

B. D. Smith, in geophysical studies of the Crown Point uranium mineralization trend near Gallup, N. Mex., reported that ground geophysical surveys (electrical and electromagnetic) have defined shallow (60 m deep) zones of high resistivity that are associated with deep (600 m) uranium mineralization. Deep time and frequency domain electromagnetic soundings appear to define a pipe-like electrically anomalous section above the uranium mineralization that extends to a depth of at least 300 m. Interpretation of high resolution airborne magnetic data suggests zones of basement structure, 2,700 m deep, some of which correlate with known uranium mineralization. On the basis of this geophysical data and a limited amount of drill hole data, Smith believes that the basement structures have directly or indirectly perturbed the paleosedimentation. This, in turn, has created favorable areas for the concentration of uranium ore deposits. The electrical surveys suggest that the "disturbed" paleosedimentary features may have persisted through geologic time to strata above the mineralization.

Anomalous electrical conductors as indicators of potential mineralization

D. B. Hoover reports that audio-magnetotelluric soundings in the Ryan Hill, N. Mex., study area have identified a conductive region at several hundred meters depth where the geology and geochemistry suggest that

a base-metal sulfide system is present. In the Sheep Hole, Calif., study area, the presence of very conductive sediments on the margin of Dale, Bristol, and Cadiz Lakes suggests the presence of significant quantities of saline deposits below the lakes.

Magnetic provinces, tectonostratigraphic terranes, and resource guides, Lake Clark quadrangle, Alaska

Interpretation of the aeromagnetic map (scale 1:250,000) of the Lake Clark quadrangle, Alaska, by J. E. Case and W. H. Nelson indicates correlations between tectonostratigraphic terranes, as defined by Jones and others (1981), and patterns of magnetic anomalies. These terranes, in turn, may be characterized by distinctive suites of mineral deposits, prospects, or "shows," as evidenced by geochemical anomalies found in stream-sediment samples.

The two main tectonostratigraphic terranes are the Deformed Upper Mesozoic Flysch terrane in the western part of the quadrangle and the Peninsular terrane (mainly the Alaska Range batholith portion of that terrane) in the eastern part of the quadrangle. Both terranes trend about northeast across the quadrangle.

Three magnetic provinces have been identified: (1) A northwest area characterized by a flat, nearly featureless magnetic field except where small isolated plutons are interpreted from isolated magnetic anomalies. (2) A northeast-trending central magnetic province characterized by a mixture of magnetic anomalies—a nearly featureless field over the flysch unit; positive and negative anomalies associated with plutons of Late Cretaceous and (or) early Tertiary age; positive and negative anomalies over calc-alkaline volcanic rocks of Tertiary age; and positive anomalies over a belt of Paleozoic (probably Silurian) mafic metavolcanic rocks, limestone, and volcanogenic sedimentary rocks, which is probably a small allochthonous terrane with respect to the Deformed Mesozoic Flysch terrane. (3) A southeastern magnetic province of high-amplitude highs and lows over the Jurassic, Cretaceous, and middle Tertiary plutons and Tertiary volcanic rocks of the Alaska-Aleutian Range batholith (Reed and Lanphere, 1973) and roof pendants of Mesozoic and Paleozoic(?) age within the batholith.

The northwestern and central magnetic provinces are characterized by geochemical anomalies of gold, tin, and tungsten, and by the scarcity or absence of anomalies of zinc, molybdenum, copper, and thorium. Furthermore, lead and arsenic anomalies are rare in the northwestern province. In contrast, geochemical anomalies of tin and gold are rare in the southeastern province, but copper, molybdenum, thorium, and arsenic anomalies are relatively common.

RESOURCE INFORMATION AND ANALYSIS

The Resource Information and Analysis Program is designed to assist the decision-making process for national mineral and fuels policy as well as USGS resource programs. This is done by improving methods for accessing and locating mineral and fuel resources and for the storage, retrieval, manipulation, and display of commodity information for mineral-resource evaluation and prediction. Highlights of this program for fiscal year 1981 follow; they represent progress since the last report.

Data collection and processing

A new microprocessor-based utility, the Single User Data System (SUDS), was successfully field tested with an Apple II microcomputer. A wide variety of features is available to the user for analysis and display of field data. A graphics package was implemented on MULTICS that allows the user to construct fence diagrams.

Scientists using the Minerals Data System (MDS, formerly CRIB) continued to collect, enter, and verify deposit data through State cooperative programs and through the commodity program. Increased activity was initiated on commodity-specific data records and on international deposit data. MDS activities continued to support CUSMAP and Wilderness Program research. Metal data were encoded for South Dakota and for the Wallace 2° quadrangle (Idaho-Montana).

Mineral resource analysis

The stages of the mineral supply process, from exploration and development to mining and beneficiation, were examined in relation to the geologic properties of resources, including location and depth of the orebody, grain size and mineralogy, and grade and tonnage. It was shown that in the long term, increases in real prices of metals are likely because the cost of the supply process is dependent on the geologic properties of the specific mineral deposit.

New grade-tonnage, or contained-metal, models were constructed for epithermal precious-metal vein districts, disseminated gold deposits, and for fluorine deficient porphyry molybdenum deposits. A new district containing epithermal precious-metal deposits was identified in the resource assessment of the Medford 1° × 2° quadrangle, Ore.

A method was developed to aid the government in estimating the net benefits, in terms of its recovery of expected net economic value, of performing various levels of exploration of mineral tracts prior to leasing

and making such information available to potential bidders. The method demonstrates that the optimal data-collection program should use an area-by-area approach and that the value of information depends on: (1) the expected degree of lease competition; (2) the degree of bidders' risk aversion; (3) output price stability; (4) unique factors that determine economic rents, grade, ore thickness, proximity to markets, extraction costs, and (5) the spatial correlation characteristics of point measurements.

Resource estimates were made of the twelve most productive copper deposits in the United States, those deposits that have contributed 95 percent of the copper produced since 1845. The production-grade method was used to estimate the remaining minable copper at specified future average mining grades.

A new method was introduced to use assay data from boreholes of the Stillwater Complex, Mont., in order to describe the distribution of contained critical commodities. This method mimics the electric log displays recovered from petroleum drill holes.

SEDIMENTARY MINERAL RESOURCES

Phosphate resources in the U.S.

Concern about phosphate resources in the U.S. has led to a reevaluation of resources of this vital agricultural mineral (J. B. Cathcart, R. P. Sheldon, and R. A. Gulbrandsen, 1981). Their data clearly indicate that resources of phosphate in the Atlantic Coastal Plain district and the northwest phosphate district are sufficient to supply domestic demands for the foreseeable future.

Metals in black shales

Field and laboratory studies by J. S. Leventhal and R. C. Kepferle were combined to establish relations between the sedimentology and geochemistry of uranium and other metals. Uranium and molybdenum contents of 50 to 100 ppm occur in Upper Devonian shales in Tennessee and in newly identified areas in Kentucky and Indiana. These high values, found in organic-rich sediments, are restricted to certain stratigraphic units and specific parts of the Appalachian basin. Higher uranium contents were observed in some phosphate-rich units in Indiana. Other metals, such as copper, nickel, and vanadium are associated with organic matter in the shale. Pyrite contents of 5 to 10 percent are present with associated arsenic, zinc, and mercury.

The source of the uranium and other metals was probably extensive beds of volcanic ash on land (represented in the shales only as thin beds). Abundant organic mate-

rial of terrestrial origin and low rates of deposition of clastic detritus were the two primary factors responsible for the high uranium content of the shale. An estimate of the quantity of subeconomic uranium occurring in a shale unit containing 50 ppm uranium, which is 60 ft thick and covers an area of 61 hectares, is 16,000 t. Similar quantities of V, Mo, Cu, Ni, and Zn are present also. These elements could be removed from the shale by some combination of retorting, for oil and gas, and leaching, for the organic and sulfide portions of the shale.

New data from the Devonian black shales of the Appalachian basin and Cambrian Alum shale of Sweden are used by J. S. Leventhal as distinct prototypes to examine the enrichment controls for metals. These samples are contrasted with the Permian Kupferschiefer of central Europe. Major controls are relatively low sedimentation rate and relatively high input of organic matter and metals. Organic carbon and sulfide-sulfur relationships can be used by analogy with the Holocene Black Sea to establish the presence of an H_2S -laden water column for these ancient shales.

Trace-element abundances are closely related to organic carbon (uranium and molybdenum) and (or) sulfide sulfur (arsenic and mercury) in the Devonian shales. Somewhat different element association patterns are present in the Alum shale. For the Devonian shales, the type of organic matter is also a control for the uranium. In particular, terrestrially derived organic matter is a specific control and residence site of the uranium. Trace-element/organic and trace-element/sulfide ratios vary by less than a factor of 2, whereas the sedimentation rate varies by more than an order of magnitude in Appalachian basin samples. Uranium and organic-carbon contents of individual stratigraphic units from various parts of the basin show an inverse relation to the thickness of the unit.

The source of the uranium and certain trace elements is in part related to leaching of volcanic ash (near its source, on land), as demonstrated by increased contents of metals in samples stratigraphically above ash beds, as compared to those below the ash. These black shales are important because: (1) they can be the host for (Kupferschiefer type) or the source of (metamorphic type) higher grade mineralization, and (2) their high organic content can provide a source of energy for mining and milling metals of the black shale itself when higher grade metal deposits, without such associated energy sources, become uneconomic.

Bentonite in the Gulf Coastal Plain

The Gulf Coastal Plain produces approximately 11 percent of the bentonite for the U.S. Texas is the biggest producer, followed by Mississippi and Alabama.

According to J. W. Hosterman, the best commercial grade bentonite is from the Upper Cretaceous Ripley Formation (Alabama), Eutaw Formation (Mississippi), and the Eocene Clairborne and Jackson Groups (Texas). Lower quality bentonite is found in the Miocene Catahoula Sandstone and Fleming Formation and the Paleocene Midway Group. The bentonite occurs as lens-shaped, massively-bedded bodies 1 to 6 m thick, associated with gravel, sand, silt, and limestone or marl. The minable deposits are approximately 135 to 1,000 m by 225 to 1,200 m, with less than 10 m overburden. The best commercial grade bentonite averages more than 96 percent clay, of which 90 to 100 percent is smectite. Quartz is the major nonclay mineral and illite and kaolinite are present in very low amounts.

Continental evaporites in Owens Lake, California

Following the abnormally wet 1969-70 winter, Owens River flood waters partially dissolved the surface salt layers of the normally-dry Owens Lake, southeast Calif. In 1970-71, saline minerals recrystallized as the lake desiccated. During 1970-71, G. I. Smith and I. Friedman collected samples of the brines, and periodically between 1970 and 1977 they collected samples and cores of the undissolved and recrystallizing salts. Mineral compositions of the salts were monitored, as were the isotopic deuterium/hydrogen (D/H) ratios of the hydrous saline minerals and interstitial brines; seasonal changes in all three variables were observed. The D/H values of the 1970-71 salts and brines initially differed greatly from those of the older undissolved salt layers, but over the years, their values slowly converged.

Observed mineral changes in the recrystallizing layer were chiefly results of seasonal variation in the temperature of the near-surface salts. Winter cooling produced 10-hydrate minerals, natron and mirabilite, and summer warming caused them to recrystallize as trona and burkeite. Once formed, halite did not dissolve seasonally. Each summer, the expelled water of hydration mixed with the interstitial brines, producing a brine that was compositionally the same but isotopically different from that of the previous year. The following winter, after the lake brine had been modified isotopically by several months of evaporation, it was incorporated into these new hydrated salts that were mineralogically the same but isotopically different from the previous winter's salts. With time, the isotopic compositions of the new salts and brines evolved toward the isotopic composition of the brines and undissolved salts in the deeper saline layers, which probably attained their isotopic makeup by the same seasonal diagenetic process during the first decade after crystallization early this century.

Marine evaporites in southwestern Utah

Detailed geologic mapping in the Beaver Dam Mountains of southwestern Utah, by L. F. Hintze and his co-workers, has revealed extensive beds of gypsum in the

Permian Toroweap Formation throughout the range. These deposits appear to be a potentially important resource of gypsum, which is primarily used in the manufacture of dry-wall panels used in building construction.

MINERAL-FUEL INVESTIGATIONS

COAL RESOURCES

FIELD INVESTIGATIONS

The Coal Resources Investigations Program of the Geologic Division classifies the Nation's remaining coal resources into resource and reserve base categories based on geographic and geologic distribution and physical and chemical characteristics. As part of this effort, personnel in the Division in 1981 mapped and assessed coal-bearing lands in Alabama, Arkansas, Colorado, Florida, Georgia, Idaho, Maryland, Mississippi, Montana, New Mexico, North Dakota, Pennsylvania, Tennessee, Utah, Virginia, West Virginia, and Wyoming. Included in these field investigations were studies conducted on the following Indian Reservations: Blackfoot and Fort Peck, Mont.; Wind River, Wyo.; and Alamo-Navaho and Cañoncito, N. Mex. About 15,400 m of rotary and core drilling was completed in coal basins of the Rocky Mountains, the Great Plains, and the Colorado Plateau, in coordination with the geological investigations to assess the quantity and quality of buried coal and to provide stratigraphic information. More than 800 channel and bench samples of coal beds were collected for chemical and physical analyses from 13 States, in cooperation with two State Geological Surveys and the Conservation Division.

Geologic studies of coal-bearing strata were conducted for the U.S. Forest Service (USFS), Department of Agriculture, under its Roadless Area Resource Evaluation II Program in the following areas: Allegheny Front-Hickory Creek and Clarion River, Pa.; Devil's Fork, Va.; Cheat Mountain, W.V.; Burden Falls and Lusk Creek, Ill.; and Sipsy, Ala. Similar studies were undertaken in the Beaver Creek, Ky., and Garden of the Gods, Ill., Wilderness Areas, also for the USFS.

COMPUTERIZATION OF THE NATION'S COAL RESOURCES

The National Coal Resources Data System (NCRDS) continues to grow in size and use under the direction of M. D. Carter, M. A. Carey, S. S. Crowley, and K. K. Krohn. During 1981, approximately 30,000 records of coal resources, stratigraphy, and chemical analyses were added to the system; these additions raised the total to nearly 200,000 entries. The data base includes 40,000 coal-resource tonnage records and 55,000 records of USBM proximate and ultimate analyses that are largely reported by coal bed on a State and county basis. The NCRDS contains 8,000 geodetically located

records of proximate, ultimate, major-, and trace-element analyses and associated data provided by the USGS coal geochemical program. In addition, the NCRDS contains 50,000 stratigraphic and drill hole records. The NCRDS has cooperative agreements with 18 State Geological Surveys for the collection, correlation, transmission, entry, retrieval, manipulation, and display of drill hole, chemical analyses, and other relevant coal-resources-related data.

COAL OCCURRENCES OF NORTH AMERICA AND ADJACENT AREAS

More than 1,000 coal occurrences exist on the North American continent and its adjacent islands, according to G. H. Wood, Jr. About 370 are in Canada, 430 in the United States, 130 in Mexico, and 130 in Central America, Greenland, Iceland, and the Caribbean Islands. An occurrence is a locality, area, or region where coal has been found at the surface or was discovered by drilling; occurrences may be as small as a single outcrop or a single drill hole, or as large as an entire coal field.

Coal underlies about 3,880,000 km² of the studied area. More than 6.6 trillion t are estimated to be contained in the coal-bearing areas, of which more than 99 percent is in the conterminous United States, in mainland Canada, and in adjacent Arctic islands. This estimate includes all beds of anthracite and bituminous coal thicker than 35.6 cm and all beds of subbituminous coal and lignite thicker than 76.2 cm that extend from the surface to a maximum depth of 1,800 m; in several coal fields the estimate includes coal beds extending to a depth of 4,500 m.

The coal resources are concentrated, in decreasing order of tonnage, in the following areas: Wyoming, Alberta, North Dakota, Montana, Colorado, and the Appalachian coal field of the Eastern United States, each containing more than 360 billion t. Of the estimated 6.6 trillion t resource of coal, about 2.5 trillion t is classed as identified and 2.5 trillion t as hypothetical. Another 1.45 trillion t is classed as onshore speculative and 145 billion t as offshore speculative.

EASTERN COAL

The Mississippian-Pennsylvanian boundary

Lithostratigraphic and biostratigraphic studies in northwestern Georgia by T. J. Crawford, W. H. Gillespie, and T. W. Henry indicate that the Mississippian-Pennsylvanian systemic boundary is conformable.

Detailed studies of fossil plants and marine invertebrates do not reveal a significant hiatus.

Physical and biostratigraphic studies of Upper Mississippian and Lower Pennsylvanian rocks of southwestern Virginia by K. J. Englund, W. H. Gillespie, P. L. Johnson, and H. W. Pfefferkorn have demonstrated that well-known coal-bearing facies in Lower Pennsylvanian rocks extend stratigraphically into Upper Mississippian rocks of the faulted and folded Appalachians. Preliminary investigations show that coal deposits in these Upper Mississippian rocks are of minable thicknesses and possess characteristics that are desirable for in-situ gasification, such as steeply-dipping beds, structural confinement of beds, and lack of active mining operations.

Northern Black Warrior Basin, Alabama

S. P. Schweinfurth measured sections along the Pennsylvanian escarpment at the northern side of the Black Warrior Basin, Ala., westward from Isbell to near Halltown, a distance of about 40 km. He indicated that the stratigraphy of the basal 120 to 180 m of the Pennsylvanian remains fairly constant across that distance. The stratigraphic section in this area appears to lack coal beds, which previously had been reported. The lower 60 m, consisting of rocks assigned to the Parkwood Formation, contain many beds bearing marine invertebrate fossils, but marine fossils have not been found in the upper 100 to 120 m of strata assigned to the lower part of the Pottsville Formation.

Schweinfurth's mapping in the northwestern part of the Haleyville 1-degree quadrangle established the existence of many normal faults, which in general strike northwest-southeast and are downthrown to the southwest on an average of about 30 m. The frequency and the relatively uniform spacing and geometry of these faults suggest that some systematic tectonic activity controlled deformation of the basement and overlying rocks in this part of the basin.

Paleoecology of a Mesozoic rift lake

The existence of a Triassic lake ("Fossil Lake Danville") has been confirmed by E. I. Robbins. The lake was present in the Dan River-Danville Basin of North Carolina and Virginia in tilted fault-block basins of the Newark rift system (Robbins, 1981; unpub. data, 1982). It had three stages of "maximum development" as shown by lakebed and lakeshore deposits preserved in the Cow Branch Formation as used by Thayer (1970). The rocks contain pollen, spores, bacteria, algae, zooplankton, and aquatic worms. Aquatic insects, fish, aquatic lizards, and phytosaurs were previously iden-

tified by Olsen and others (1978). The pollen and spores indicate a middle and late Carnian (Late Triassic) age and were collected throughout 1,500 m of black shale, siltstone, carbonaceous shale, and coal beds. The plant communities of the valley floor, wetlands, flood plains, talus slopes, and horst uplands consisted of bryophytes, lycopods, horsetails, ferns, seed ferns, voltzialean gymnosperms, cycads, and conifers.

Thick semianthracite beds are widespread in the lower member of the Cow Branch, which suggests that extensive swamps filled in the earliest lake stage. Coal beds from the middle and youngest lake stages, preserved in the upper member of the Cow Branch, are irregularly distributed. The patchy distribution, coupled with field mapping and sediment analyses by Thayer (1970), suggests that the preserved wetland vegetation was confined to river deltas and lake embayments.

Biological, mineralogical, and biochemical evidence suggests that all lake stages were alkaline, the two youngest of which were strongly alkaline, and that the lakes were anoxic at depth. The (proto)crocodyl-conchostracan-ostracod assemblage is similar to that in other alkaline lakes, such as ancient Lake Uinta in Colorado and Utah, and modern Lake Malawi at the borders of Malawi, Mozambique, and Tanzania. Hematite and pyrite are in most black-colored rocks in the stratigraphic section, occurrences which are analogous to some of the deep basins in the alkaline Red Sea. A pale blue amphibole similar to sodium-bearing riebeckite has been identified in rocks assigned to the youngest lake stage. Amorphous algal tissues, pollen and spores, and cuticle are degraded, which is typical where lipids in tissues are saponified in alkaline reagents; even lignified wood cells are degraded in the youngest lakebed deposits. Pyrite and wurtzite in laminated lake-bottom rocks suggest that the bottom waters of the lake were anoxic.

Origin of the Fire Clay parting in eastern Kentucky

The Fire Clay parting is a kaolinitic claystone 8-10 cm thick, found within the Hazard No. 4 coal bed of the Breathitt Formation in eastern Kentucky. It is of wide lateral extent, covering at least 2,000 km², and has sharp contacts with the enclosing benches of coal. It is hard, fine grained, and breaks with a conchoidal fracture; hence, it has been called a flint clay by miners. Its volcanic origin was recognized by Seiders (1965).

B. F. Bohor and D. M. Triplehorn collected samples from several outcrops of the Fire Clay parting in the Hazard No. 4 coal bed in Pike and Perry Counties in eastern Kentucky; the samples were analyzed by X-ray diffraction and scanning electron microscopy. These analytical techniques confirmed the volcanic origin of

the parting. Mineralogically, the parting is an altered volcanic tuff completely changed by diagenesis (Bohor and Triplehorn, 1981). Its origin as an air-fall volcanic ash means that this parting can be used as an isochronous marker horizon even though the source is unknown.

Confirmation of this parting as volcanic in origin may lead to important advances in stratigraphic correlations, both locally and intercontinentally. Paleogeographic reconstructions based on plate tectonics show the North American and European continents in juxtaposition during the Pennsylvanian Period. The Fire Clay and similar partings in coal beds of the Appalachian basin may correlate with tonsteins (partings in coal beds) in England and Europe formed during the same period by volcanoes on the European continent.

Coal resources in Tazewell County, Virginia

A resource estimate for Tazewell County, Va., by K. J. Englund, N. K. Teaford, and P. L. Johnson demonstrates the existence of 2,060 million t of coal. This estimate, based on recent 1:24,000-scale mapping supported by several hundred core holes drilled by mining companies, is about three times the amount of resources previously reported for the county by Brown and others (1952).

GULF COAST LIGNITE

Stratigraphic framework and distribution of lignite along Wilcox outcrop belt, Mississippi

The Paleocene-lower Eocene Wilcox Group of Mississippi is part of a continuous belt of lignite-bearing rocks that spans eight States from Georgia to Texas in the Mississippi Embayment. A geologic analysis by C. R. Meissner, Jr., B. S. Hackman, and J. C. Ossi, who used drill-hole and measured-section data, showed thickening of the Wilcox from north to south. The upper part of the unit is absent in northern Mississippi either because of nondeposition, erosional beveling, or onlap of the overlying Claiborne Group, or because of a combination of these geologic events. Other stratigraphic studies show the cyclic nature of deposition of the unconsolidated sands, silts, clays, and thin lignite beds comprising the Wilcox Group. Most major formation contacts are marked by erosional unconformities reflecting transgressions and regressions of the seas. As the sand content increases in the stratigraphic column, the lignite beds disappear or decrease in number.

Vertical and horizontal distribution of lignite 0.75 m or more thick and up to 75 m deep indicates that most

areas contain two or more beds. Most lignite along the Wilcox outcrop belt in Mississippi is in discontinuous beds that are as much as 5 km wide and 15 km long.

WESTERN COAL

Coal deposition in the southwestern Williston Basin, North Dakota

During the summer of 1981, the Fort Union Formation was investigated by R. M. Flores, E. S. Belt, and P. Warwick in a belt 80 km long along the Little Missouri River in the southwest part of the Williston Basin, N. Dak. Special emphasis was placed on the environments of deposition and their relation to accumulation of coal. A total of 225 measured stratigraphic sections supplemented by published drill-hole data were used to construct three-dimensional cross-section panels from which facies sequences, relationships, and associations were determined. The Ludlow Member of the Fort Union Formation, a largely delta-plain sequence, contains brackish marine tongues of the Cannonball Member. This sequence contains thin to thick laterally discontinuous coal beds, some as thick as 4.5 m. The thin coals formed in interdistributary swamps and the thick coals formed in subdelta swamps. The Tongue River Member of the Fort Union Formation, which overlies the Ludlow Member, consists of coastal-plain fluvial facies and thin to thick laterally continuous coal beds, some as thick as 7.6 m. The thick, continuous coal beds accumulated in poorly drained swamps of large floodbasins between major river channels. Continuous drainage into these floodbasins culminated in deposition of preserved thick peat accumulation and in the provision of limited accumulation of thin, discontinuous peat deposits. The coastal-plain peat deposits of the Tongue River Member in the southwest part of the Williston Basin are downflow equivalents to the trunk-tributary fluvial deposits of the lower part of the Tongue River Member in the Powder River Basin.

Volcanic episodes in Montana coal bed

Volcanic eruptions were frequent during early Paleocene time in an area not far from the Bull Mountain coal field of central Montana. C. W. Connor reports that the aptly named Big Dirty coal comprises one or two 3- to 4-m-thick sequences of coal, tuffaceous coal, and carbonaceous tuff densely interlayered with altered volcanic ash and crystal tuff (Connor, 1982). Earlier investigators noted the many partings but did not recognize their volcanic origin. The crystal tuff layers, some as thick as 0.3 m, consist largely of fine- to coarse-grained sanidine euhedra. J. K. Griffith assisted in tracing the Big Dirty around the coal field.

The nearest identified areas of early Tertiary volcanism lie in an arc from southwest to northwest, 150 to 185 km from the center of the Bull Mountain Basin. During development of coal swamps after Big Dirty time there apparently was little volcanic activity, as demonstrated by the absence of crystal tuffs in the coal beds in the 450 m of Fort Union rocks above the Big Dirty bed. Some coal beds have a few thin, altered ash partings. As an example, the Mammoth coal bed in contrast to the Big Dirty has three persistent altered volcanic ash partings, each less than 1 cm thick.

Coal-bed correlation in the Powder River Basin, Montana

A series of recently measured stratigraphic sections combined with an analysis of geophysical logs has resulted in a new interpretation of a part of the stratigraphic framework of the Powder River Basin in southeastern Montana. The new interpretation indicates that Knoblock coal bed has been incorrectly correlated between the Birney and the Broadus 1-degree by 1/2-degree quadrangles. Marguerite McLellan and L. R. Hasche extended correlations eastward from the stratigraphic section established by W. C. Culbertson in the Birney quadrangle and determined that the Knoblock coal bed of the eastern part of that quadrangle is not correlative with the so-called Knoblock of the Broadus quadrangle. They concluded that the Knoblock of the Birney quadrangle is correlative with either coal bed A or the lower part of the Sawyer coal bed of the Broadus quadrangle. These corrected correlations suggest that the nomenclature and correlations of other coal beds in the Tongue River Member of the Fort Union Formation in southeastern Montana should be reexamined and corrected.

A thick coal deposit in the Powder River Basin, Wyoming

A routine survey of gamma-ray logs of oil and gas wells in the central part of the Powder River Basin, made by B. H. Kent, indicated the presence of a large, discrete coal deposit about 48 km west of Gillette, Wyo. The deposit, elongate to the northwest, lies virtually flat just east of the structural trough of the basin and about 340 m below the present level of the Powder River. As outlined, the deposit underlies an area of about 2,500 km² and consists of a single bed of coal as thick as 55 m that has an average thickness of 30 m. The coal is presumed to be subbituminous and to have an average weight of 1.13 million short t of coal per square-mile-foot. Frances Pierce made a geostatistical Kriging analysis of the deposit and estimated the deposit to contain 102 billion t at a 95 percent level with confidence limits of ± 4 percent.

The regional stratigraphic framework, as reconstructed to include the coal deposit, indicates that several coal beds merge locally to form this single bed and that the depositional center for this thick deposit is the westernmost of several major depositional centers where very thick beds of peat were deposited during basin filling in late Paleocene time. These major depositional centers are progressively offset north or south across the east flank of the basin as they migrated westward during late Paleocene time. This developing pattern is currently being used to guide exploration for other centers.

Coal in the Cow Creek Butte area, Little Snake River field, Wyoming

A large deposit of coal occurs in the lower part of the Almond Formation, of Late Cretaceous age, in the southern part of the Little Snake River coal field, Carbon County, Wyo. Extensive geologic mapping by C. S. V. Barclay and J. G. Honey was followed in 1981 by drilling and by chemical analyses of coal samples as part of a cooperative project between the Conservation and Geologic Divisions. The deposit under investigation lies in the Cow Creek Butte area in the southeastern part of the Baggs 15-minute quadrangle; it contains 660 million t of demonstrated coal resources in the Almond Formation. Analyses indicate that the principal beds, at least 1.3 m thick, are subbituminous A in rank and average 5.5 percent ash and 0.7 percent sulfur. The heat value averages 10,500 Btu's per pound.

Coal correlation in the Carbondale quadrangle, Colorado

Coal zones and, to a lesser extent, coal beds within the Carbondale quadrangle, Colo., were correlated and interpreted by Margaret Ellis, V. L. Freeman, and J. R. Donnell, who used stratigraphic sections measured by J. R. Donnell, E. R. Landis, and Walter Hallgarth; electric logs from oil, gas, and coal exploration drilling programs; and private data from several sources. The coal beds are assigned three zones, each of which lies above a major sandstone unit in the Upper Cretaceous Mesa-verde Formation. The zones, from oldest to youngest, are the Wheeler coal zone (Fender and Murray, 1978), South Canyon group (Collins, 1976), and Coal Ridge group (Collins, 1976). The Wheeler is the most persistent, correlatable, and economic of the zones, whereas the Coal Ridge group is the most erratic. In the western part of the quadrangle the coal zones coalesce and are not individually recognized. The eastern boundaries of the coal zones correspond to the strand lines proposed by Zapp and Cobban (1960).

Stratigraphic relations in Upper Cretaceous rocks of the Chaco area, New Mexico

Stratigraphic studies in the Chaco Culture National Historical Park by J. W. Mytton show intertonguing of the Upper Cretaceous Menefee Formation and the overlying Cliff House Sandstone. Coastal Plain deposits of the Menefee, which include coal and carbonaceous shale, lens out laterally into marine sandstones of the Cliff House, identified as lower and upper shoreface deposits. Three distinct lower shoreface sandstone tongues of the Cliff House are in the area, and reconnaissance to the southeast indicates their continuation throughout Chacra Mesa into the Chaco Mesa 1-degree by 1/2-degree quadrangle. The lowermost of these sandstone tongues forms the imposing cliffs above the Anasazi ruins in the park.

INDIAN RESERVATIONS

Coal in the northeastern part of the Crow Indian Reservation, Montana

The northeastern part of the Crow Indian Reservation is about 420 km² and is located on the northwest flank of the Powder River Basin in southeastern Montana. Three economically important coal beds, in ascending order, are the Robinson, McKay, and the Rosebud, located in the slightly northeast-dipping strata of the Tongue River Member of the Paleocene Fort Union Formation. Information from drill holes and field investigations in 1981 by L. N. Robinson and A. J. Zdzinski shows 20 northeast- or east-trending normal faults. The faults range from 1.2 to 4.8 km in length and displace the coal-bearing strata vertically as much as 90 m.

Samples collected from the three major coal beds and analyzed on an as-received basis have an average heating value of 4,640 kcal/kg, an average sulfur content of about 1 percent, an average ash content of about 11 percent, and a moisture content of about 25 percent.

Lignite deposits in the Fort Peck Indian Reservation, Montana

A study to delineate and appraise coal deposits in the Fort Peck Indian Reservation, northeastern Montana, was begun in 1978 by H. H. Arndt and J. K. Hardie. Previous investigations indicated that potentially recoverable lignite was preserved at widely scattered localities within a 2,600 km² area underlain by the lower Tertiary Fort Union Formation in the eastern part of the reservation. The relation of these known coal deposits to each other and to other unknown coal deposits was little understood. An extensive coal exploratory drilling program, during which 98 exploratory

holes and core holes were drilled in the eastern part of the Fort Peck Reservation, was completed in 1980 and was followed by detailed and reconnaissance geologic mapping in 1981. Study of information derived from the exploratory drilling and geologic mapping has shown that the coal-bearing sequence includes at least 10 beds of lignite ranging from 1 to 4 m in thickness. Several potentially economic lignite deposits covering widespread areas in the eastern part of the Fort Peck Reservation have also been delineated.

Coal resource assessment of the Wind River Indian Reservation, Wyoming

Detailed mapping, drilling, and examination of the logs of oil and gas wells in the Wind River Indian Reservation by J. E. Windolph, Jr., N. L. Hickling, and R. C. Warlow, indicate that coal occurs in the Mowry Shale and Frontier, Mesaverde, Meeteetse, Fort Union, and Wind River Formations of Cretaceous and Tertiary age. Most of the coal is of subbituminous rank, although several samples from outcrops of the Frontier and Mesaverde coals are of bituminous rank. One sample obtained from a development gas well at a depth of 2,100 m in the Meeteetse Formation also is of bituminous rank.

Coal beds in the Mowry, Fort Union, and Wind River are thin and impure, but seven beds in the Frontier, Mesaverde, and Meeteetse range from 0.8 to 6 m in thickness. These thicker coal beds are estimated to contain 4.8 billion t to a depth of 2,000 m and an additional 0.6 billion t of coal between 2,000 and 4,000 m. The deepest coal bed lies 4,500 m below the surface.

Frontier and Mesaverde coal beds were deposited in near-shore deltaic environments subjected to transgressive and regressive movements of the sea. During Meeteetse time sedimentation was controlled and influenced by an uplift paralleling the Owl Creek Mountains and by rapid subsidence along the central axes of the present basin; the Meeteetse Formation is as thick as 1,200 m. The formation contains more than 100 coal beds, most of which were not included in the resource estimates because of insufficient data points. In the deeper part of the basin these beds have a cumulative thickness of more than 50 m. Major unconformities developed at the beginning of Lance, Fort Union, and Indian Meadows times.

Volcanic activity was intermittent and the stratigraphic section contains many tonsteins, ash beds, bentonites, and tuffaceous beds. A mafic dike 3 km long is conspicuous near Winkleman Dome.

Structurally, the coal-bearing formations are principally in a large, complexly deformed synclinal trough plunging to the southeast. The northeastern limbs of

many component synclines dip steeply, are locally overturned, and are cut by faults. Another large synclinal trough is completely concealed beneath unconformably overlying rocks of Indian Meadows age. Drilling indicates that this later trough contains coal beds in the Mesaverde Formation at depths greater than 2,000 m.

Coal resources in the Ramah Indian Reservation, New Mexico

Coal resources of the Ramah Reservation, N. Mex., are in 12 identified Upper Cretaceous beds or zones in the basal part of the Crevasse Canyon Formation, in the middle part of the Gallup Sandstone, and in the member near Carthage of the sandstone of Tres Hermanos, according to D. E. Ward and W. J. Mapel. The thickest coal beds and the only ones that have potential for development are in the lower 6 m of the middle coal-bearing part of the Gallup Sandstone in a 5-7 km wide belt that extends for at least 10 km southeastward across the west-central part of the reservation. Coal beds at this stratigraphic level have an aggregate thickness of 1-2 m within the reservation. Coal beds in the middle part of the Gallup Sandstone coalesce at the western edge of the reservation to form a single bed 2.2 m thick. A preliminary coal resource estimate indicates that about 30 million t of bituminous coal are contained in beds more than 36 cm thick within the reservation.

Deposition between Gallup, N. Mex., and the reservation was controlled, in general, by a uniform climate, base level, and availability of eroded source material. The sedimentary sequence along the depositional strike is as a result generally similar. Geologists have measured many stratigraphic sections along the depositional strike; these sections provide a depositional model that can be used to determine where coal might be expected in the reservation.

Coal resources in the Alamo Band Navajo Indian Reservation, New Mexico

Geologic studies and coal resource assessment of the Alamo Band Navajo Indian Reservation in Socorro County have been cooperatively conducted by the New Mexico Bureau of Mines and Mineral Resources and the U.S. Geological Survey. J. C. Osburn, of the New Mexico Bureau, reports that the demonstrated coal resources of the reservation total about 31 million t of high volatile A bituminous coal; about 65 percent is under less than 45 m of overburden.

PALEOBOTANY

Peat petrology and aspects of coal formation in the Everglades, Florida

As part of a comprehensive study of the peat deposits in the southern Everglades and mangrove forests of south Florida, C. C. Silber studied the peat petrography in regional cross sections to identify plant species, interpret the environments of deposition, and describe any trends in degradation from plant to peat that comprise the initial processes in the formation of coal.

The four regionally dominant plant species in the Everglades are red mangrove (*Rhizophora mangle*) and black mangrove (*Avicennia nitida*) in the tidal zone, water lily (*Nymphaea odorata* spp.) in freshwater sloughs, and sawgrass (*Mariscus jamaicensis* Crantz.) in freshwater marshes. The investigator prepared 255 thin sections, 10 to 20 mm thick, by standard botanical methods from 171 samples taken at intervals of 10 to 15 cm in 22 cores that ranged from 0.3 to 1.2 m long, 14 of them from freshwater peat and 8 from saline or brackish peat. Because the same plant species predominate throughout these sections, it is suggested that the environments of deposition during the approximately 5,000 yr represented in the peat were like those of today.

Four aspects of the peat, as seen in thin section, suggest transformation toward coal. The first three, breakdown of plant materials (such as thinning of cell walls and digestion of tissues by bacteria and fungi), change in shape of the plant remains (such as the flattening of round to oval rootlets), and reduction of space within and between plant fragments, result in compaction. The last aspect is change of color, which includes both discrete blackening and gradational darkening.

Point-counting of constituents of the peat, from the ground surface to the base of the peat, including space between fragments of tissue, reveals an overall trend of increase in degradation of plant tissues, an increase in flattening of tissues, a decrease of porosity, and an increase of dark color. There is, however, considerable variation of each aspect both within and between cores.

Intertonguing of the Blackhawk Formation and Star Point Sandstone, Wasatch Plateau, Utah

Intertonguing of the lowermost part of the coal-bearing Blackhawk Formation and the uppermost part of the marginal marine Star Point Sandstone, both of Late Cretaceous age, has been mapped in the central and southern parts of the Wasatch Plateau by J. D. Sanchez, L. F. Blanchard, T. L. Brown, W. J. Muldoon, W. E. Marley, and R. F. Flores. The intertonguing relation caused a progressive steplike southwestern offset

of the Blackhawk coal beds. The tongues of the Star Point Sandstone represent episodic northeasterly paleo-shoreline transgressions of the Upper Cretaceous epeiric seaway. The development of these sandstone tongues affected the geometry, lateral continuity, and thickness of the associated Blackhawk coal beds.

Mapping and exploration of potentially economic coal beds and sandstone tongues in the lowermost part of the Blackhawk Formation will help identify the location of thicker coal beds. Knowledge of coal bed distribution can assist the exploration geologist in determining a coal bed's geometry. Analysis of economic coal beds associated with the marginal marine sandstone tongues shows that such coal beds trend parallel to the paleo-shoreline and may be thicker to the landward side of the sandstone tongues. Delineation of such coal beds, in conjunction with current exploration and development of Blackhawk coal beds in the study area, is a primary target of drilling programs.

Coal resources of the Cañoncito Indian Reservation, New Mexico

Coal resources of the Cañoncito Indian Reservation, located about 50 km west of Albuquerque, N. Mex., were studied by Annabel Olson and estimated to be about 100 million t. The coal beds are of Cretaceous age and are in the Gibson Coal Member of the Crevasse Canyon Formation and possibly in the Menefee Formation. The reservation is partly in the San Juan Basin on the west and the Rio Grande trough on the east. The San Ysidro monocline and associated faults, down to the east, form the boundary and have a combined structural relief of more than 610 m. In the Rio Puerco fault zone, incomplete stratigraphic sections of coal-bearing rocks have been preserved in downfaulted blocks. As a result of the faulting and a cover of soil, alluvium, colluvium, and wind-blown deposits, a complete sequence of Cretaceous rocks does not crop out, the facies changes in the coal-bearing sequence, and associated rocks are not readily apparent.

Coal deposits and associated strata in the southern part of the San Juan Basin record the existence of an oscillating shoreline of the Cretaceous epicontinental sea. In the reservation the sea lay to the northeast and the shoreline trended northwest. The Dalton Sandstone Member of the Crevasse Canyon Formation and the Point Lookout Sandstone both record a retreat of the shoreline. Landward, plants that were predecessors of coal accumulated in low, swampy areas, and fluvial sand, silt, and mud were deposited. Each of these lithologies is preserved in the Gibson Coal Member of the Crevasse Canyon Formation and the Menefee Formation.

COAL GEOCHEMISTRY

Peat from the Everglades: a study of the origin of coal and natural gas

Three cores of peat from the Everglades, each about 1 m long and representing accumulation over a period of about 5,000 yr, have been studied in detail by I. A. Breger, P. G. Hatcher, J. L. Zelibor, M. R. Krasnow, and J. C. Chandler to ascertain the fate of each major plant chemical constituent during the early stages of coalification. The following conclusions were reached: (1) the methoxyl content of the peat is constant to a depth of about 40 cm, this fact indicating the stability of lignin; and (2) there is no clear relation between humic acid and humin. Chemical analyses do not indicate whether the humic acid condenses to form humin, whether the humin breaks down to form humic acid, or whether the humic acid and humin are derived, in part or totally, from different sources.

Microbiological studies with methanogenic bacteria in the laboratory have shown that the rate of evolution of methane from several areas of the Everglades ranges from 2 to 13 millimoles CH_4/g of peat per day. Cellulose isolated from the peat has been shown by nuclear magnetic-resonance studies to contain, as an impurity, an insoluble paraffinic component. This latter material has been found to be a general component of humic substances and is currently under study to establish its origin.

The origin of primary pyrite in coal by bacterial diagenesis of organic sulfur

In previously reported studies of sulfur distribution in Everglades peat, Z. S. Altschuler, M. M. Schnepfe, and C. C. Silber (1980) reported a consistent regional relationship in which pyrite is generated at the expense of the ester-sulfate content of the organic matter. They attributed this to the bacterial reduction of ester-sulfate to H_2S during the degradation of organic matter by heterotrophic anaerobes. Further studies during 1981 revealed a more specific linkage of the reduction of ester-sulfate to dissimilatory respiration by sulfur-reducing bacteria incident to their biodegradation of the peat, rather than to general bacterial or chemical hydrolysis of ester-sulfate. This conclusion is derived from the investigation of mangrove peat cores in which pyrite accumulates at shallow depth and declines at greater depth. In such cases, the ester-sulfate content remains inversely related, declining where pyrite accumulates and increasing again at greater depth.

These findings of generation of pyrite across a major swamp by the conversion of organic oxy-sulfur compounds afford an explanation of the primary genesis of pyrite in coal and organic-rich sediments and suggest

that the residual organic sulfur in coal is largely carbon-bonded and highly-reduced sulfur. This paragenesis also provides an explanation for the preferred tissue-bound association of framboidal pyrite in peats and recent sediments.

Solid-state ^{13}C nuclear magnetic resonance studies of coalified logs

P. G. Hatcher, I. A. Breger, N. M. Szeverenyi, and G. E. Maciel (Colorado State University) have examined coalified logs ranging from Pennsylvanian to Miocene by solid-state ^{13}C nuclear magnetic resonance (NMR) by using the technique of cross polarization and magic-angle spinning. Samples of exhumed logs of Holocene age were also examined by using this technique. NMR spectra of these logs were obtained at the Colorado State University as part of a USGS grant to G. E. Maciel and at the National Bureau of Standards by W. L. Earl. The results of this study indicate that coalification of wood to the rank of high volatile bituminous coal involves at least three major changes in its chemical composition. The first change involves hydrolysis and removal of cellulose with concomitant concentration of lignin. The second change involves chemical alteration of lignin, whereby methoxyl groups and C_3 side-chains are lost and the lignin becomes depleted in hydrogen. Lignitic coalified wood, a product of these two changes, is formed directly from the lignin. The third change is the conversion of lignitic coalified wood to high-volatile bituminous coalified wood via the loss of oxygen functional groups. Soluble, oxygen-rich humic acids are formed as products of these chemical changes and are mobilized and transported from the coal, thereby providing an effective mechanism for the removal of oxygen during this stage of coalification. This mechanism for coalification contradicts current interpretations which suggest that humic acids are intermediate reactants in the formation of coal.

Authigenic quartz in coal

A cathodoluminescence (CL) investigation of quartz in the Upper Freeport coal bed, conducted by L. F. Ruppert and C. B. Cecil, has shown that most of this quartz is authigenic in origin and not detrital. Quartz derived from igneous, metamorphic, and hydrothermal sources luminesces in the visible range of light, whereas authigenic quartz does not; as a consequence, cathodoluminescence can be used to determine the origin of quartz in coal. A scanning electron microscope and an electron microprobe, both equipped with cathodoluminescence detectors, were used to examine quartz from various lithotypes in polished blocks of the Upper Freeport coal bed and in standard ASTM pellets

prepared from float-sink separates from bench samples. More than 80 percent of the quartz in both mineral-rich bands and vitrinite-rich bands in the polished blocks did not exhibit cathodoluminescence. In the float-sink separates, 100 percent of the quartz examined in the light specific-gravity fraction (1.275 float) and 60 percent of the quartz in the heavy specific-gravity fraction (1.800 sink), which included shale-parting material, did not luminesce. In contrast, more than 90 percent of the quartz in a sample of shale directly overlying the coal bed did luminesce. These results indicate that most of the quartz in the Upper Freeport coal bed is, therefore, authigenic in origin. The authigenic quartz is believed to be crystallized from amorphous silica originally contained in plant matter. Determination of the origin of minerals such as quartz is essential to the successful prediction of coal-quality variations as related to quartz in resource assessment.

The origin of carbonate minerals in the Upper Freeport coal bed

Calcium carbonate in the Upper Freeport coal bed in west-central Pennsylvania was deposited in at least two and perhaps three or four stages. On the basis of isotope and other data, C. B. Cecil, E. C. Spiker, and F. T. Dulong have postulated that the first stage of carbonate genesis was associated with carbon dioxide production resulting from bacterial sulfate reduction. The earliest carbonate tends to be isotopically light, about $\delta^{13}\text{C}$ 10 o/oo, and occurs as finely disseminated particles within macerals. A second stage of carbonate formation was associated with methanogenesis. The second-stage carbonate tends to be isotopically heavy ($\delta^{13}\text{C}+8$ to $+24$ o/oo), and occurs mainly on cleat surfaces and as cleat filling. On the basis of both carbon and carbon isotope values, it is thought that a third possible stage of carbonate genesis may have been associated with coalification. Carbonate derived from coalification would have carbon isotope values similar to carbonate generated during bacterial sulfate reduction. Preliminary oxygen isotope values, also determined in this study, suggest temperatures of formation for the carbonate containing isotopically light carbon consistent with early carbonate from sulfate reduction and late carbonate from coalification. On the basis of available data, Cecil and his associates believe that the carbonate minerals in the Upper Freeport coal were derived directly from processes operating within the coal bed and not from external sources.

Tonsteins in the C coal bed, Emery coal field, Utah

D. M. Triplehorn and B. F. Bohor studied the tonsteins (kaolinitic partings in coal) in the C coal bed of the Ferron Sandstone Member of the Mancos Shale in

the Emery coal field in central Utah. Previously, Ryer and others (1980) had shown the existence of these tonsteins and had proven them to be volcanic in origin. These authors also had determined how these isochronous markers could be used to demonstrate the development of the ancestral swamps and to divide the coal bed into time-equivalent sequences useful in guiding sampling for coal quality and trace elements.

Triplehorn and Bohor (1981) found that diagenetic alteration in the coal bed of the glassy volcanic ash to clay minerals was a function of bed thickness as well as chemical conditions in the sedimentary environment. Thin beds of tuff (less than 15 cm thick) in this coal bed are altered to kaolinite throughout, whereas thick tuff beds (greater than 15 cm in the C coal) were altered to kaolinite in their upper and lower parts but are a mixture of kaolinite and smectite in their central part. This relation suggests that mineralogical changes during diagenesis were controlled by water flushing, a function of bed thickness. Thus, the mineralogy of thin altered tuffs in coal beds can be used as an indicator of the conditions in the sedimentary environment (paleosalinity). Conversely, the mineralogy of thick, altered tuff beds has more complex origins.

Analyses of samples from the Vermillion Creek coal bed, Sweetwater County, Wyoming

R. W. Stanton, J. A. Minkin, and T. A. Moore analyzed samples from three drill cores of the Vermillion Creek coal bed and associated stratigraphic units in Sweetwater County that were obtained as part of a field investigation conducted by H. W. Roehler. On the basis of maceral and chemical composition and megascopic differences, 26 samples were grouped into facies and correlated between cores. Analyses consisted of determinations of maceral compositions, vitrinite reflectances, chemical compositions determined through use of the electron microprobe, densities, and ash and sulfur contents.

The samples of the Vermillion Creek coal bed contain an average 81 percent vitrinite, 7 percent exinite, 1 percent inertite, and 11 percent mineral matter, on a whole coal basis. This coal bed has an unusually high content of gelocollinite and desmocollinite, submacerals of the vitrinite group. The principal exinite maceral is resinite.

The average organic-sulfur content of the Vermillion Creek coal bed is 4.3 weight percent, which was confirmed by electron-microprobe analyses of selected samples. This is the highest organic-sulfur content reported for any freshwater coal bed in the United States.

Variations in the densities of Vermillion Creek coal samples were determined to be primarily a function of their ash content. The average ash content of the coal samples is 15 weight percent, which corresponds to a density of approximately 1.47 g/cm³.

Formation of the Vermillion Creek peat occurred in a lacustrine environment. Interstitial waters in the peat had an above-neutral pH and contained high concentrations of reducible carbonate and sulfate ions; interbedded calcite and the high organic and pyritic sulfur contents of the coal samples demonstrate this.

Chemical composition of gulf coast lignites

The chemical composition of 116 gulf coast lignite samples has been determined; the determinations were made for 10 oxides and 29 trace elements, as well as proximate analysis, ultimate analysis, heat values, forms of sulfur, and ash deformation temperatures. The lignite beds range from Paleocene to Upper Eocene; 23 samples are from the Wilcox Group in Texas, 15 from the Calvert Bluff Formation of Plummer (1933) in Texas, 31 from the Wilcox Group in Arkansas, 20 from the Claiborne Group in Tennessee, 6 from the Wilcox Group and 1 from the Claiborne Group in Mississippi, 9 from the Naheola Formation of the Midway Group in Alabama, and 8 from the Tuscahoma Formation of the Wilcox Group in Alabama.

The lignite samples contain from 4 to 5 times the concentrations of boron, manganese, and niobium found in Appalachian bituminous coal samples, whereas the concentration of other elements is similar to those found in bituminous coal. The geometric means for major and minor oxides in lignite ash indicate that SiO₂ is higher in the lignite beds from the northern part of the gulf coast embayment; Fe₂O₃ and K₂O are higher in its eastern part, and TiO₂ is higher in its western part (Oman and others, 1982). There is a notable increase in moisture from the western part of the embayment to the eastern part. The heat values are higher in the Texas lignites and decrease eastward.

Use of Mössbauer spectroscopy to identify iron-sulfide minerals in coal

The responsive emission spectra from gamma-ray irradiation of iron-bearing minerals indicate the valence and lattice orientation of their contained ⁵⁷Fe ions in a technique known as Mössbauer spectroscopy. B. J. Evans, R. G. Johnson, F. E. Senftle, C. B. Cecil, and F. T. Dulong (1982) investigated the potential of using the technique to identify the iron sulfide minerals contained in coal, mainly pyrite and marcasite, and also of measuring the relative amounts of these two minerals in any given coal. Evans and his colleagues first obtained the spectra of 18 pyrite and 12 marcasite specimens, all collected from inorganic rocks or mineral deposits, and determined that the spectral ranges of each mineral, where pure, were sufficiently distinctive to permit positive identification. The spectral ranges were

broader, however, where the mineral lattices contained other elements such as arsenic.

This study was followed by examination of the spectra of mechanical mixtures of pyrite and marcasite to establish the quantitative and qualitative accuracy of Mössbauer analysis. Although the spectra are distinct, they do require least-squares computer fittings to obtain the final data, which are limited to accuracies ranging from ± 5 to ± 15 percent as compared to the spectra of the pure phases.

Results from testing coals with Mössbauer spectroscopy will be useful in establishing the geochemical environments that prevailed during the deposition of these minerals in the original peat swamps or in the resulting coals.

OIL AND GAS RESOURCES

ALASKA

Hydrocarbon potential of Norton basin, Alaska

From regional geology and patterns of seismic reflection, mainly nonmarine rocks were interpreted by M. A. Fisher, W. W. Patton, Jr., and M. L. Holmes to lie at depth in the Norton basin. Condensate and gas are considered the most likely hydrocarbons to have been generated from such rocks. Basement rocks were nested and deformed about 50 m.y. before the basin began to develop, so they are not likely to contain source rocks for hydrocarbons. Potential source rocks probably are present only in the basin fill, and they make up only 10 percent of the total basin volume.

Preliminary results from gravity modeling suggest that the Earth's crust thinned as the Norton basin formed. Thus, heat flow through the basin may have been higher than the average heat flow through continental areas and may have caused hydrocarbon generation.

Time and degree of thermal maturity of rock units in NPRA

The North Slope of Alaska, which contains some of the largest oil reserves in the United States, lies on the southern flank of a ridge system that rifted during Early Cretaceous time to form the Canada basin on the north and to deepen the east-west-trending Colville trough on the south. The Barrow arch, the southern flank of the rifted ridge, forms a regional high between the Canada basin and the Colville trough. The arch, which trends west-northwest, has been a focus for migrating oil from Early Cretaceous through Cenozoic time. Previous work identified at least two types of oils

associated with the arch and several probable source-rock units for at least one of these two oils. Even though potential source-rock units occur in the Colville trough and in places drape over the Barrow arch, the time and geographic locale of oil generation remain in doubt.

Temperature-sensitive analytical data and observed temperatures were used by L. B. Magoon and G. E. Claypool to determine the threshold of oil and gas generation, and Lopatin's method was used to determine the time of maturity for source-rock units penetrated in the Inigok No. 1 well. Vitrinite reflectance, gas wetness (percent C_2-C_4/C_1-C_4), and present subsurface temperatures were compared along two regional cross sections: a north-south cross section from the Barrow arch to the Colville trough and a west-east cross section from the South Barrow gas field through the Kuparuk and Prudhoe Bay oil fields to the western edge of the Wildlife Range. These three types of data are in general agreement for comparable thermal history along the two cross sections. However, where uplift has occurred, high vitrinite reflectance and associated high gas-wetness values are present at much shallower depths than would be expected from present subsurface temperatures. Thermal maturity data also suggest that oil and gas in the Barrow oil field have undergone long-distance migration, because organic matter in shales for some distance from the field is thermally immature.

In the Inigok No. 1 well, good agreement was found between temperature-sensitive analytical data and present temperatures for the onset of oil generation and for the wet-gas preservation deadline. This agreement suggests that the sedimentary rocks encountered in the well are near maximum depth of burial and never were more deeply buried. Using time-temperature index (TTI) values that correspond to the measured vitrinite values in conjunction with burial curves of selected stratigraphic horizons, the investigators calculated the geothermal gradients that prevailed during geologic time for the Inigok locality. The observed vitrinite reflectance versus depth-age profile requires lower geothermal gradients (28°C/km) during the Tertiary, and higher geothermal gradients (50°C/km) throughout the late Paleozoic and prior to the Early Cretaceous. The time of the decrease in thermal gradient coincides with the time of rifting.

GREAT PLAINS AND ROCKY MOUNTAIN BASINS

Diagenesis and gas generation in Gammon Shale, northern Great Plains

Investigations by D. L. Gautier (1982) indicated that important aspects of the early diagenetic history of the gas-bearing Upper Cretaceous Gammon Shale can be

interpreted from mineralogic, textural, and isotopic data from authigenic carbonates. The consistent relations between volume percent siderite and $\delta^{18}\text{O}$ in siderite concretionary cements suggest that time and (or) relative depth and, in some cases, approximate actual depth of concretion formation can be estimated. These estimates give the minimum depth for depletion of sulfate dissolved in pore water and for onset of methane generation. Minimum depths were controlled largely by sedimentation rate and therefore varied from place to place and with time during Gammon deposition. In regions of or during times of relatively rapid sediment accumulation, large quantities of reactive, metabolizable organic matter became available for methane generation. In contrast, where and when sediment accumulated slowly, siderite precipitation and methane generation did not begin until long after deposition and after significant sediment compaction. In these sediments, much, if not most, available metabolizable organic matter was consumed by aerobic oxidation and sulfate-reducing bacteria and thus was not available for methane generation.

Effect of clay on gas production data from Gammon Shale, Williston basin

D. L. Gautier, H. C. Starkey, and K. I. Takahashi found that in the Upper Cretaceous Gammon Shale, a hydrocarbon source bed and gas reservoir rock in North Dakota, variations in cation exchange capacity, clay hydration, and sensitivity to drilling muds are due to differences in mixed-layer illite-smectite clay content. These differences may affect drill-log response and give adverse production information without influencing gas production capacity. Therefore, possible producing zones may have been overlooked during exploration, and resources estimates that are too low may have been made.

Geochemical prospecting over Bell Creek oil field, Powder River Basin

Investigations by M. C. Dalziel and T. J. Donovan suggested that petroleum microseepage is a cause of chemical and isotopic changes in surface and near-surface rocks and soils. The reducing environment brought about by the presence of hydrocarbons induces reduction and mobilization of iron and manganese. These elements, essential for plant growth, are assimilated in the reduced divalent state and are found in anomalously high concentrations in pine needles and sage leaves overlying the Bell Creek oil field, a large stratigraphic trap in the Powder River Basin of southeastern Montana.

Reduction of hydrated iron oxides and (or) hematite to form magnetite is also a consequence of petroleum

microseepage. High-wave-number magnetic anomalies at Bell Creek field are interpreted to reflect increased amounts of diagenetic magnetite in near-surface rocks. Correlation between these preliminary biogeochemical and aeromagnetic studies suggested that changes in transition-element chemistry attributed to petroleum microseepage in surface rocks and soils also may be a useful indicator of oil fields.

Geochemistry of oils from Pennsylvanian and Lower Permian Minnelusa Formation, Powder River Basin

Oil was sampled from the upper member of the Minnelusa Formation in the Raven Creek, Dillinger Ranch, and Reno oil fields (Wyoming) and from the middle member of the Minnelusa in the Buck Creek, Leimser, Lance Creek, Red Bird, Pine Lodge, and Indian Creek oil fields (Wyoming and South Dakota). A preliminary evaluation of the geochemical data—such as weight-percent organic carbon, $\delta^{34}\text{S}$, $\delta^{13}\text{C}$, thermal analysis, and distribution of gasoline-range hydrocarbons—gathered from these oil samples suggested to R. T. Ryder and J. L. Clayton that the Minnelusa oil in all but one of the fields was derived from a Paleozoic source. At present, however, it cannot be determined whether the Minnelusa oil was derived from Pennsylvanian black shale in the middle member of the Minnelusa Formation, from a more distant black shale in the Phosphoria Formation, or from both sources. Oil extracts from Minnelusa and Phosphoria black shales are geochemically similar to one another and to the Minnelusa oil and thus do not help resolve the problem. The oil sample from the Lance Creek field is significantly different from oil samples in the other eight fields and is attributed to a Cretaceous source.

Sedimentologic and diagenetic history of reservoirs in Niobrara Formation, Denver Basin

The Niobrara Formation, which is a target of hydrocarbon exploration from Colorado northward to the Canadian border, was studied in the Denver Basin by R. M. Pollastro, P. A. Scholle, and M. A. Arthur. Along the eastern flank of the Denver Basin, biogenic gas is found in thermally immature strata at depths of 270 to 850 m. Westward and deeper into the basin, however, the rocks are thermally mature and were capable of generating oil at time of maximum burial. Minor amounts of oil have been produced from fractured carbonate rocks in those areas.

Porosity and isotopic composition of the chinks are consistently related to burial depth (or paleoburial depth) and thermal history. Initial porosities of 60 percent or more were reduced to approximately 25 percent with 1 km of burial depth and to less than 10 percent

with 2 km or more of burial depth. Whole-rock oxygen isotopic values reflect these changes.

The compositions of bentonite beds and insoluble residues from the chinks also reflect progressive transformation with increased burial depth and porosity loss. Although the starting composition of mixed-layer illite smectite clay (I/S) in chalk residues is highly variable, its expandability range is increasingly more limited with greater burial. A systematic increase in illite-type layers in I/S of bentonites, as well as the transformation from random to ordered I/S, was noted in more deeply buried samples. A regularly interstratified chlorite-smectite (Ch/S) is also formed in aluminous bentonites at elevated temperatures and pressures during deep-burial conditions ($>100^{\circ}\text{C}$). The occurrence of ordered I/S and Ch/S in bentonites can be used as relative geothermometers, which, in several cases, indicate that strata in the Denver Basin in the past were either more deeply buried and (or) were subjected to paleogeothermal gradients higher than those of the present.

Origin of natural gases in San Juan Basin

Large resources of mainly nonassociated natural gas (0.65 trillion m^3) are present in the central part of the San Juan Basin, a roughly circular, asymmetric structural depression situated in northwestern New Mexico and southwestern Colorado. The major producing intervals are stratigraphic traps in the Cretaceous Dakota Sandstone, Mesaverde Group, and Pictured Cliffs Sandstone. Lesser amounts of oil and (or) gas are produced from Pennsylvanian, Jurassic, and Cretaceous rocks along the southern and western flanks of the basin.

The chemical and isotopic composition of natural gas was tabulated by D. D. Rice from 73 producing intervals throughout the basin. The gases generally tend to become isotopically heavier ($\delta^{13}\text{C}_1$ values range from -49 to -31 ‰) and chemically drier ($\text{C}_1/\text{C}_{1-5}$ values range from 0.75 to 0.99) with increasing depth. These changes are related to the extent of thermal cracking processes, which are controlled by temperature and depth of burial. With increasing levels of maturation, the organic matter in the source rocks becomes increasingly depleted in ^{12}C . Also, the content of C_{2+} hydrocarbons first increases with the generation of fluid hydrocarbons and then decreases as heavier hydrocarbons are destroyed by thermal cracking processes.

In addition to their general variation with depth, the gases become isotopically heavier and chemically drier regionally in a northeast direction. This regional variation is interpreted to be the result of greater burial depths and higher levels of maturity toward the northeast in the past. This maturation is reflected by changes in the rank of coal beds in the Upper Cretaceous

Fruitland Formation, which directly overlies the Pictured Cliffs Sandstone. The rank of coals increases from high-volatile B bituminous to medium-volatile bituminous northward across the basin.

Gas in the Upper Cretaceous Gallup Sandstone in the southern part of the San Juan basin is associated with oil and is isotopically lighter and chemically wetter than nonassociated gas at comparable levels of maturation. The presence of oil and the composition of the gas suggest the probable existence of source rocks containing sapropelic organic matter in the Gallup Sandstone. The lack of oil in the central part of the basin suggests that Cretaceous source rocks contain primarily humic organic matter there.

WESTERN OVERTHRUST BELT

Oil and gas resources of Western Overthrust Belt

The Western Overthrust Belt has now been recognized as the most promising oil and gas exploration frontier in the onshore United States, according to R. B. Powers. Since 1975, more than 20 new fields were discovered in the Wyoming-Utah-Idaho segment of the thrust belt, at least eight of which are of giant size (>100 million bbl of oil or >1 trillion ft^3 of gas). The three new small fields that were discovered in the Montana segment in 1980-81 indicate a smaller but still promising resource potential there. The Sevier segment in central Utah experienced a considerable increase in wildcat drilling activity, including a small wildcat discovery in the Middle Jurassic Entrada Sandstone. The southern Arizona-southwestern New Mexico segment has had a slight increase in drilling and seismic activity, but no discoveries have yet been made.

Middle Paleozoic history interpretation as an aid to Western Overthrust Belt petroleum exploration

The Middle Devonian to Late Mississippian history of the Western Overthrust Belt region has been studied by C. A. Sandberg, R. C. Gutschick, F. G. Poole, and W. J. Sando, USGS, and J. G. Johnson (Oregon State University) and interpreted to consist primarily of two eustatic (transgressive-regressive marine) cycles. The interpretation was made by using a series of thickness, lithofacies, and paleogeographic maps, the intervals or horizons of which are dated mainly by conodonts. The conodont zonation includes 28 high-resolution Upper Devonian conodont zones (all but one having a timespan of ~ 0.5 m.y.) and 10 moderate-resolution Mississippian zones (each having a timespan of ~ 1.5 or ~ 3 m.y.). A Middle to Late Devonian eustatic cycle, which lasted

~17 m.y., comprises a sequence of 12 numbered events. This cycle was followed by event 13, an episode of continental stability, and event 14, the incipient highland phase of Antler orogeny. An Early to Late Mississippian eustatic cycle, which lasted ~19.5 m.y., comprises a sequence of 6 additional numbered events. These 20 eustatic and epeirogenic events for the Western Overthrust Belt are comparable to a similar sequence of events that was used by Sandberg (1980) to date the Antler orogeny, which is farther west. Knowledge of the geologic history of the Western Overthrust Belt and adjacent regions is an aid in identifying source rocks and conduit beds and in locating petroleum reservoirs. Moreover, the late Mesozoic Sevier thrust system is so close and subparallel to the late Early Mississippian shelf edge that changes in facies and competence of Mississippian rocks near this shelf edge may have helped control the location of later thrusting.

Facies control of porosity in Mississippian gas reservoirs, northwestern Montana

The Mississippian Madison Group is a gas reservoir in the northwestern Montana segment of the Western Overthrust Belt and is a correlative of Mississippian carbonate rocks, which are major gas producers in the Canadian foothills. In northwestern Montana, three facies were recognized by K. M. Nichols in the upper 125 m of the Madison, an upward-shoaling carbonate shelf sequence that is unconformably overlain by Jurassic strata. Economically significant porosity occurs within a crinoidal grainstone in the upper part of the Madison and is controlled by eogenetic secondary dolomitization.

The dolomitized crinoidal grainstone unit (facies C), which is the lowest of three facies recognized in the upper part of the Madison Group, overlies lagoonal limestone that forms most of the group. The upward transition from limestone to dolomite commonly takes place in the lower part of facies C. Facies C is massively bedded and exhibits large-scale cross stratification suggestive of its origin as a subaqueous dune field. Measured vuggy, intergranular, and intercrystalline porosity in facies C is as high as 18 percent in surface samples. The thickness of facies C ranges from 25 to 75 m and is inversely proportional to the thickness of overlying facies B, with which facies C intertongues.

The two higher facies, facies B and A, reflect the upward transition from an open-platform to a restricted-platform environment. Facies B ranges in thickness from 25 to 75 m and is a nonporous, dolomitized mudstone and wackestone sequence generally containing some 1-m-thick interbeds of porous dolomitized grainstone. This sequence is capped by <10 m of intertidal

rocks of facies A, which is thin bedded, partly algal laminated micritic dolomite.

Locally, facies A and part of facies B have been cut out by pre-Jurassic folding and erosion. However, all lateral thickness changes in facies C reflect its intertonguing with facies B. Although original facies patterns are greatly telescoped by thrusting, facies C is thickest in a northeast-southwest trend that passes through the Blackleaf gasfield.

New structural interpretation as an aid to petroleum exploration of Snowcrest Range area, southwestern Montana

A preliminary synthesis of the tectonics, thermal maturation, and petroleum potential of the southwestern Montana segment of the Western Overthrust Belt, by W. J. Perry, Jr., R. T. Ryder, and E. K. Maughan (1981), hypothesized a major northeast-trending sub-Snowcrest Range thrust as the root zone of the Greenhorn-Snowcrest thrust system. This inferred thrust was then tested by closely constrained gravity modeling by D. M. Kulik on the basis of data from the Clover Divide area. Best-fit models showed that this thrust dips about 20° northwestward with about 17 km of northwest-to-southeast displacement. Work with D. M. Kulik resulted in a major reinterpretation of the regional geology: the Greenhorn-Snowcrest thrust system is chiefly responsible for the yoked Blacktail-Snowcrest uplift and Ruby synclorium. Preliminary reinterpretation of available paleontological data by D. J. Nichols helped date this Laramide thrusting event as Late Cretaceous (middle Campanian to Maastrichtian). Preliminary isotopic dating (Rb/Sr) by Z. E. Peterman indicated that 2.7- to 3.0-b.y.-old crystalline rocks are involved in the hanging wall of this major thrust 9 km east-northeast of Lima, Mont. At least 800 km³ of Cretaceous rocks and ~400 km³ of Cambrian through Triassic rocks probably extend northwestward under the lip of the sub-Snowcrest Range thrust, perhaps markedly affecting the oil and gas potential of the area.

Interpretation of upper Paleozoic lineaments as an aid to petroleum exploration in southwestern Montana

Two major upper Paleozoic lineaments that may have important implications for oil and gas exploration were recognized by E. K. Maughan in the southwestern Montana segment of the Western Overthrust Belt. The Greenhorn lineament trends north-northeast from near Bannock Pass on the Idaho State line southwest of Lima, Mont., to the vicinity of White Sulphur Springs, Mont. This lineament coincides for part of its course with the Greenhorn and Snowcrest thrust faults and

terminates at approximately normal-trending structures of the Lewis and Clark line. The Musselshell lineament trends east-southeast as a possible continuation of the Lewis and Clark line from western into south-central Montana. It coincides in part with the east-southeast trending course of the Musselshell River and seems to die out in the vicinity of Billings and Hardin, Mont. The two lineaments mark the western and northern boundaries of a platform called the Beartooth shelf (Peterson, 1981), a part of the Wyoming shelf that was uplifted slightly more than adjacent parts of the Wyoming shelf to the south.

Troughs that trend parallel to the lineaments are called the Snowcrest trough west of the Greenhorn lineament and the Big Snowy trough north of the Musselshell lineament. As much as 300 m of the Upper Mississippian Big Snowy Group occurs in these troughs, but correlative strata on the platform are present mainly as thin remnants of the basal Kibbey Formation and more locally as remnants of the Otter and Heath Formations. As much as 300 m of Lower Pennsylvanian rocks of the Amsden Group fill the troughs and correlative strata onlap the platform as a blanket of mudstone and limestone generally <40 m thick. The relations of Upper Mississippian and Lower Pennsylvanian rocks indicate that most vertical movement between platform and troughs occurred contemporaneously with deposition of Pennsylvanian sediments. Dying-upward normal faults in Pennsylvanian and Permian rocks, observed by W. J. Perry, Jr., within the Snowcrest trough, and lesser differences in thickness of Permian rocks between troughs and shelf suggest diminishing subsidence of the troughs in latest Paleozoic time. Petroleum source rocks, migration paths, seals, and reservoirs have been affected by these structural movements. Later thrusting along the Greenhorn lineament, expressed as a sub-Snowcrest Range thrust fault, and related structures may have produced traps for oil accumulation in southwestern Montana (Perry and others, 1981). Fluvial and nearshore littoral sands deposited adjacent to the Musselshell lineament provide oil reservoirs in the Lower Pennsylvanian Tyler Formation of central Montana.

Interpretation of Cretaceous stratigraphy as an aid to petroleum exploration between Moxa arch and Overthrust belt, southwestern Wyoming

The Upper Cretaceous Frontier Formation crops out on the northern flank of the Uinta Mountains, near the south end of the Moxa arch, and in the eastern part of the western Overthrust belt, about 40 km west of the crest of the arch. By use of logs and cores from boreholes, investigators have also recognized the formation

in the subsurface of the region. The strata in the Frontier Formation of southwestern Wyoming, as described by E. A. Merewether, are mostly clastic and were deposited in marine and continental environments during late Cretaceous (Cenomanian, Turonian, and Coniacian) time. Molluscan fossils from the marine beds were identified by W. A. Cobban. The Frontier conformably overlies the Mowry Shale or the Aspen Shale of Early Cretaceous age and is conformably overlain by the Hilliard Shale of Late Cretaceous age. The Frontier thickens northward along the Moxa arch from ~60 m near the Uinta Mountains to >300 m near La Barge and westward from the arch to >600 m in the Overthrust Belt.

In the eastern part of the southwestern Wyoming segment of the Western Overthrust Belt, the outcropping Frontier is composed of the following conformable members (Myers, 1977), from oldest to youngest: Chalk Creek of Hale, 1960 (dominantly nonmarine beds), Coalville of Hale, 1960 (marine sandstone and shale), Allen Hollow Shale of Hale, 1960 (marine shale), Oyster Ridge Sandstone (largely marine sandstone), and Dry Hollow of Hale, 1960 (mainly nonmarine rocks). The Chalk Creek, Coalville, Allen Hollow Shale, and Oyster Ridge Members are of Cenomanian to middle Turonian age. The Dry Hollow Member is probably late Turonian to early Coniacian. At outcrops near the Uinta Mountains, the Frontier locally includes a thin basal marine shale, probably of Cenomanian age, which is disconformably overlain in the upper part of the formation by nearshore marine and nonmarine strata of middle and late Turonian age. The basal unit thickens northward along the Moxa arch, reflecting a progressive northward decrease in the amount of truncation by an uplift centered in the Uinta Mountains area during late early Turonian time.

In southwestern Wyoming, the upper part of the Frontier Formation includes nonmarine and nearshore-marine beds that are of middle and late Turonian age at outcrops near the Uinta Mountains and of middle Turonian to early Coniacian age in boreholes on the Moxa arch. The strata at the two localities are about the same age and are represented in the western Overthrust belt by nonmarine and nearshore-marine rocks of Turonian and early Coniacian age in the Dry Hollow Member of the Frontier.

MIDCONTINENT

Study of diurnal variations as an aid to helium-survey prospecting for small oil fields in Kansas

Helium surveys by A. A. Roberts and K. I. Cunningham over 6 oil fields in Trego County, Kans., indicated diurnal variations in soil-gas helium concentra-

tions. These fields are small (80 to 240 ha), result from stratigraphic traps along the eastern flank of the Central Cambridge arch in the Salina basin, and produce oil from the Lansing, Kansas City, and Marmaton Groups of Middle and Late Pennsylvanian age and the Arbuckle Group of Late Cambrian and Early Ordovician age. The surveys were run using a 0.16 km spacing for the sampling grid. Soil-gas samples were taken at 0.5 m depth through a stainless steel probe and subsequently analyzed on a field-portable mass spectrometer capable of 10 ppb precision. A permanent probe was located at the approximate center of the survey area and sampled an average of three times daily to quantitatively determine the diurnal variation of helium in the soil gas. A linear regression analysis of helium concentration on time of day revealed a strong correlation (coefficient of determination = 0.77). This regular decrease in helium concentration has tentatively been attributed to the fact that the soil was significantly wetter in the mornings because of large amounts of dew that dried out during the day. The moist soil would be less permeable than the dry soil and would act as a cap under which helium could accumulate from the upward flux. A simple algorithm to correct for this diurnal variation was developed and applied to these data. A very large helium anomaly was observed over the most prolific oil fields in the area, and moderate anomalies were observed over two of the other fields. However, no significantly high levels of helium were observed over the other fields. Thus, it appears that helium surveys can be of some use in locating very small stratigraphic traps.

Comparative organic geochemistry of Middle Pennsylvanian shale and coal

Midcontinent Middle Pennsylvanian organic-rich rocks include coal (33-76 percent organic carbon); dark-gray to grayish-black marine shales (1-8 percent organic carbon); and laminated, phosphatic black shale (4-28 percent organic carbon). Organic matter in these rocks came mostly from peat swamps. This origin was determined by J. R. Hatch and J. S. Leventhal through similarities between coal and shale in organic petrography, hydrogen (H) and oxygen (O) indices (Rock-Eval pyrolysis), pyrolysis-gas chromatographic analyses, and gas-chromatographic analyses of saturated-hydrocarbon fractions of chloroform extracts. A halocline, resulting from the river waters that transported the dissolved- and fine-particulate organic matter from the extensive swamps, may have been the principle mechanism for restricting circulation in the shale-depositing environments.

Because some organic geochemical properties vary significantly within and between coal and shale

samples, inferred differences in dissolved oxygen contents of deposition and diagenetic waters and degree of thermal maturation are reflected. For shales with comparable thermal maturities, less dissolved oxygen results in higher organic carbon, P, U, Se, Mo, V, Ni, Ag, and Cr contents, H indices, saturate/aromatic and NSO/asphaltene ratios in chloroform extracts, and lower O indices, pristane/phytane ratios, and organic-carbon $\delta^{13}\text{C}$ values (more negative by 1-2 per mil). The H and O indices of coals resemble those of shales deposited under the most anoxic conditions. In contrast, saturate/aromatic, NSO/asphaltene and pristane/phytane ratios in coal extracts, trace-element and minor-element contents, and organic carbon $\delta^{13}\text{C}$ values of coals resemble shales deposited under relatively oxic conditions. With increased degree of thermal maturity, H and O indices decrease in both coals and shales; total bitumen/organic carbon and pristane/phytane ratios increase in shales but decrease in coals; and saturate/aromatic ratios increase significantly only in shales that were subject to anoxic diagenesis. Black phosphatic shales contain extractable organic matter that is most similar to Middle Pennsylvanian Cherokee Group crude oils from northeastern Oklahoma and southeastern Kansas.

GULF OF MEXICO AND FLORIDA

Petroleum potential of Maritime Boundary region, Gulf of Mexico

A study of the geologic framework, petroleum and mineral resource potential, and geologic hazards of the Maritime Boundary region in the Gulf of Mexico was conducted by R. B. Powers, R. G. Martin, and R. Q. Foote, in response to a U.S. Senate request. The principal findings were that favorable conditions exist for the occurrence of significant quantities of oil and gas in parts of the study area and that exploitation of these resources should be feasible within the next 20 to 30 yr.

Petroleum source rocks found in South Florida basin

Source-rock studies of pre-Punta Gorda Anhydrite (lowermost Cretaceous) rocks were conducted for the deep (3,660 to 5,700 m) part of the South Florida basin by J. G. Palacas and T. A. Daws (USGS), and A. W. Applegate (Florida Bureau of Geology) (1981). Organic-carbon and Rock-Eval pyrolysis analyses of drill-cutting samples from seven widely spaced boreholes indicated that fair to good potential petroleum source rocks occur in the upper part of the Lower Cretaceous (late Coalhulan age) Pumpkin Bay Formation and in parts of the Lehigh Acres Formation (Trinity 'F' of

Exxon Company, USA). Oil potential is rated generally poor for pre-upper Pumpkin Bay rocks. Potential for gas, although seemingly also unfavorable, cannot be eliminated because of an apparently good gas show in a production test in carbonate rocks of the Upper Jurassic? Wood River Formation at a depth of 4,785 m.

EASTERN OVERTHRUST BELT

Potential gas resources of southern Blue Ridge province

The basic geologic framework of the Appalachian orogen, as interpreted from seismic reflection studies by L. D. Harris, consists of a low-angle megathrust fault system that stretches from the Appalachian Plateau to the Continental Shelf. Crystalline rocks of the Blue Ridge and Piedmont provinces were thrust westward by this system; as a result, a large segment of sedimentary rocks of the Valley and Ridge province was buried. Thus, large areas with unsuspected and untested resource potential occur in the subsurface beneath the crystalline thrust sheet (Harris and others, 1981). Because regional thermal patterns, which have a direct bearing on the maturity levels of organic matter in sedimentary rocks, existed prior to thrusting, westward movement of thrust sheets disrupted and telescoped that pattern by placing thermally more mature rocks over less mature western sedimentary rocks. Palimpsestic reconstruction of the original thermal pattern in the southern Appalachians emphasized that rocks with possible commercial gas potential may extend eastward for about 80 km beneath crystalline rocks of Blue Ridge and Piedmont provinces.

Fracture-blanket reservoir with high gas potential in Pine Mountain thrust sheet, Virginia

Since the late 1940's, gas has been produced from thin-skinned fracture systems associated with the Devonian shale sequence in and adjacent to the north-eastern part of the Pine Mountain thrust sheet in Virginia. Contrary to the older concept that the Devonian shale sequence was both a source and reservoir for the gas, modern well-completion practices demonstrated to L. D. Harris that the Devonian shale sequence is only the source and that the Lower Mississippian Berea Sandstone at the top of the shale sequence is the reservoir. The existence of a regional compound joint or fracture system within the Berea, apparently produced during movement of the Pine Mountain thrust sheet, is emphasized by the fact that the volume of gas after well completion is independent of local anticlines or synclines. Thus, the Berea appears to be a fractured-

blanket reservoir, so that the probability is high that anywhere it is penetrated by a drill hole and the well is properly treated, commercial production may be expected. The exploration success in the Pine Mountain thrust sheet suggests that thin-skinned deformations characteristically produce widespread fracture porosity in tight sandstone beds that can be readily exploited. Perhaps this exploration rationale could be applied to other parts of the Eastern Overthrust belt as well as to other thrust Belts.

Regional metamorphism of organic matter in Devonian shale of Appalachian basin

Organic matter in black shales of Middle to Late Devonian age in the Appalachian basin shows regional variation that is due primarily to differences in burial and temperature history. Alternative interpretations involving major differences in the original chemical composition of the organic-matter source were satisfactorily eliminated on the basis of thermal-alteration experiments conducted by G. E. Claypool, C. N. Threlkeld, C. M. Lubeck, A. H. Love, USGS, and R. E. Sweeney, Global Geochemistry. In these experiments, black shales containing the least altered organic matter were subjected to progressively increasing degrees of intensity and duration of heating, with chemical characterization of the organic products and residual reactants being made at intermediate states. All of the regional changes observed in the Devonian black shales (hydrocarbon geochemistry, carbon isotopic composition, elemental composition, maceral proportions) were reproduced experimentally, thus obviating the alternative interpretation of major regional differences in the original composition of organic matter deposited within Devonian black shales.

ATLANTIC CONTINENTAL SHELF

Thermal maturation study in Georges Bank basin, North Atlantic margin

The time-temperature burial relations that influenced organic maturation processes in Upper Triassic to Lower Jurassic rift-basin sediments and the Middle Jurassic carbonate-shelf, reef, and clastic-delta facies of the North Atlantic Georges Bank basin are believed to have been regionally influenced by a large residual subsidence due to tectonics associated with contractions and cooling of a thinned lithosphere and crust. Also, localized zones of high heat flow may have occurred during the rifting process. Relict heat from both sources may have influenced the principal zone of oil formation (PZOF) in the Georges Bank basin, according to R. E.

Miller, R. E. Mattick, and H. E. Lerch. Plots of specific temperature-sensitive inter-compound ratios of isomeric groups for light hydrocarbons that elute chromatographically in the cyclohexane through methylcyclohexane range, along with plots of the molecular ratio of *n*-hexane to methylcyclohexane, were found to be consistent with the temperature-sensitive saturated hydrocarbon-to-organic-carbon ratios. These ratios suggest that the threshold of intense oil generation in the depocenter of the basin begins at a depth of ~2.8 km with the PZOF occurring from 3.5 to 4.5 km. Correlation of temperature-sensitive maturation parameters with the time-temperature burial model proposed by Arthur (1982) suggests that the lower Abenaki, Mohican, and upper Iroquois Formations (Canadian offshore nomenclature) are the most favorable exploration targets in the Georges Bank basin.

Evolution of humic substances in mid-Atlantic OCS and slope sediments

Geochemical studies of humic substances in mid-Atlantic OCS and slope surface sediments suggested to D. M. Schultz, R. E. Miller, and E. C. Spiker that a natural progression from fulvic acid to humic acid to types of unsaturated protokerogens may constitute a significant evolutionary pathway for humic substances. Because elemental compositions, atomic and stable carbon isotopic ratios, and infrared spectra were similar for each humic acid isolated from different shelf locations, derivation from similar organic source materials was suggested. The hydrogen-rich nature (H/C 1.33 to 1.36) and aliphatic character, coupled with stable carbon isotopic values in the -22.4 per mil range, indicate that the fulvic and humic acids probably are of predominantly marine origin. Protokerogens were found to have stable carbon isotopic ratios that were isotopically lighter (-25.2 per mil) than the fulvic and humic acid isolates. This difference is believed to be evidence for a progression of humic and fulvic acids to types of unsaturated protokerogens.

NEW EXPLORATION TECHNIQUES

Conodont study as an aid to petroleum exploration of Upper Devonian rocks

Study of multielement taxa of the conodont Family Icriodontidae in Europe and North America by C. A. Sandberg (USGS) and Roland Dreesen (University of Leuven, Belgium) (1982) has revealed three phylogenetic lineages: A *Pelekysgnathus*-*Icriodus* lineage that evolved from *Pelekysgnathus* n. sp. through *P.*

planus and *P. inclinatus* to "*Icriodus*" *cornutus*, "*I.*" *chojnicensis*, "*I.*" *raymondi*, "*I.*" *pectinatus*, and "*I.*" *costatus*; a true *Icriodus* lineage that evolved from *I.* aff. *I. symmetricus* and gave rise to *I. symmetricus*, *I. alternatus*, *I.* cf. *I. alternatus*, *I. iowaensis*, and several new species; and an *Antognathus* lineage that apparently evolved through *A. mowitzaensis*. A fourth lineage of apparent *Icriodus* homeomorphs may represent the earliest gondolellids or eotaphrids. The icriodontids occur mainly in shallow-water marine biofacies that are devoid of zonally significant, mainly deep-water or off-shore conodonts of the standard zonation. Knowledge of their ranges and distribution provides a zonal scheme and paleoecologic analysis for petroleum-producing Upper Devonian shallow-water platform-carbonate formations that hitherto have been unzonable.

Calculations of global rate of burial of Cretaceous organic carbon and oceanic stable carbon as an aid to source-rock studies

During the Cretaceous, significant amounts of organic carbon were buried in both shallow epicontinental seas and in deeper marine environments. Times of enhanced burial of organic carbon worldwide were: the Aptian-Albian, the Cenomanian-Turonian, and, to a lesser extent, the Coniacian-Santonian. Modeling of $\delta^{13}\text{C}$ fluctuations and calculation of average global accumulation rates of organic carbon, on the basis of DSDP data and independent analyses, agree very closely and suggested to M. A. Arthur and P. A. Scholle that rates of organic-carbon burial during the Aptian-Albian were more than 6 to 9 times that of the present. The $\delta^{13}\text{C}$ values can be used for stratigraphic correlation and for evaluation of source-bed potential in frontier areas that have adequate geologic-oceanographic models. Some of the $\delta^{13}\text{C}$ fluctuations have been shown to be global events.

The times of enhanced organic-carbon burial do not appear to be related to increased overall oceanic fertility (availability of phosphate). Major marine phosphorite deposits are not significantly correlated with global oceanic anoxic events. This lack of correlation suggests that the Cretaceous organic-carbon burial episodes are not, in general, due to increased organic productivity, with the possible exception of the Cenomanian-Turonian event, which lasted less than 2 m.y. and may have resulted from increased rates of oceanic overturn and increased surface fertility. The increased rates of burial of organic carbon are most likely due to enhanced preservation under increased oxygen deficits in deeper water masses. Episodes of increased organic-carbon burial are usually correlated with high sea-level stands and warm, favorable global climates.

Carbonate submarine fans: better petroleum reservoirs than carbonate-debris aprons

Facies models for clastic submarine fans have existed and have been well documented for a number of years. In contrast, carbonate mass-transport deposits rarely develop systematic facies sequences that resemble clastic-fan models (Cook and Egbert, 1981a). Carbonate mass-transport sediment is common along the margins of carbonate basins throughout the geologic column. These deposits, however, typically form randomly distributed debris-flow aprons, which often make up millions of cubic meters of debris transported tens of kilometers basinward during a single event, thin-bedded turbidites, and isolated blocks that collectively show little, if any, systematic facies sequences. Descriptions of complete carbonate submarine-fan systems are rare. One exception is in a well-exposed carbonate-continental margin sequence that prograded seaward during the Paleozoic in the Western United States (Cook and Egbert, 1981a, 1981b). This 1,500-m-thick sequence changes progressively upward from thin-bedded turbidites (basin plain and outer-fan fringe), to thickening upward calcarenite sheets (outer-fan lobes), to thinning-upward braided channel conglomerates (mid-fan distributary channels), to entrenched boulder-bearing conglomerates (inner-fan feeder channels), to slope facies. According to H. E. Cook, the predictability of favorable petroleum reservoirs should be better in carbonate fans than in carbonate-debris aprons. As exploration extends to deeper water deposits, it will become important to understand the geologic conditions that favored development of carbonate fans over development of carbonate-debris aprons and to determine when and where these conditions prevailed in the geologic past.

Detection of geopressured zones by seismic-reflection method

Detection of geopressured zones may be possible through detailed processing of multichannel seismic-reflection data from suspected areas. A seismic line was shot over a known geopressured area, as determined by well information, in the Gulf of Mexico. After detailed processing of the multichannel seismic-reflection data, a distinct velocity inversion was noted by D. J. Taylor and R. Q. Foote on the stacking velocity analysis for seismic data at the same depth as the over-pressured zone in the well. If an over-pressured zone is thick enough and within the resolution of the seismic data, the same seismic technique could be used to determine the extent and magnitude of that over-pressured zone.

RESOURCE STUDIES

World oil and gas resources of small fields and unconventional deposits

Conventional oil and gas fields have been exploited for more than a century. Although remaining resources of oil and gas are large, their geographic distribution and other constraints on their use are leading to a careful examination of alternative sources. The following summary of world oil and gas resources in small fields and unconventional deposits was made by R. F. Meyer:

Oil (in bbl)	
Small fields -----	100
Heavy oil (reserves in known fields) -----	15
Heavy oil (resource in deposits (tar sands)) -----	745
Undiscovered heavy-oil resources -----	300
Shale oil -----	190
Total -----	1,350
Natural gas (in trillion ft ³)	
Geopressured reservoirs -----	2,500
Lakes -----	20
Shallow Japanese-type brines -----	100
Shale rich in organic matter -----	1,000
Tight sands -----	2,000
Occluded in coal -----	3,000
Hydrates in permafrost -----	500
Underground coal gasification -----	13,000
Total -----	22,120

Conterminous United States offshore oil and gas resource assessments

Detailed geologic and oil and gas resource studies of deep-water (>3,650 m) areas in the Gulf of Mexico and southern California borderlands were made by J. G. Vedder, R. G. Martin, R. Q. Foote, and E. W. Scott. These two reports represent the first such attempts to analyze the geology and estimate resources in such deep-water, frontier areas. The USGS is the first organization to publish findings of this type, which will provide the Department of State with information useful for discussions with other maritime-boundary countries.

Probabilistic and statistical resource appraisal methodology

Probabilistic and statistical methodology was developed by R. A. Crovelli for assessing the quantity of undiscovered oil or gas in a province. Mathematical formulas and computer algorithms were derived by using probability theory to obtain subjective probabilistic estimates of oil, nonassociated gas, associated-dissolved

gas, total gas, and petroleum resources in two or more provinces by Monte Carlo simulation techniques. Both conditional and unconditional probability distributions were derived for each assessed resource. A series of computer programs and graphics routines were written on the basis of the computer algorithms. Statistical methodology was developed to describe finding rates by using decline curve models. Hyperbolic and exponential decline curves fit to historic data by regression analysis displayed good finding-rate projection capability.

All of the developed methodology was applied in making estimates of undiscovered recoverable conventional resources of oil and gas in the United States, which was divided into 137 provinces. The methodology was also used in the World Energy Resources Program to make foreign assessments.

A modified play-analysis methodology was developed by R. R. Charpentier for the assessment of unconventional natural-gas resources of the Devonian shale in the Appalachian basin.

OIL-SHALE RESOURCES

Oil-shale core drilling in Uinta basin, Utah

Two oil-shale core holes were drilled during the winter of 1981-82 in the eastern Uinta basin, Utah, by the Conservation, Water Resources, and Geologic Divisions. R. W. Scott, Jr., and M. P. Pantea supervised the drilling operations for the USGS.

The Red Wash-1 core hole (RW-1) is located in sec. 1, T. 9 S., R. 22 E., Uintah County, Utah, and lies nearly in the depositional center of the oil-shale sequence. In the RW-1 hole the overburden to the top of the Mahogany zone in the Parachute Creek Member of the Green River Formation is 792.7 m; the zone is 40.5 m thick and averages 83 l of oil per ton.

The Coyote Wash-1 drill hole (CW-1) is located in sec. 22, T. 9 S., R. 23 E., Uintah County, Utah. In CW-1 the overburden to the top of the Mahogany zone is 669.2 m; the zone is 39.0 m thick and averages 91 l of oil per ton.

Both holes penetrated the Birdsnest aquifer of the Parachute Creek Member of the Green River Formation; this aquifer produced water at rates varying from 2270 to 3400 l per min. Analyses of water samples from RW-1 and CW-1 show the waters to be primarily sodium carbonate brines. Both core holes were cased from the surface to a point below the Birdsnest zone for the purpose of hydrologic monitoring.

Complete results including lithologic descriptions, water analyses, and Fischer assay data for RW-1 and CW-1 are available as USGS open-file reports 82-965 and 82-966, respectively.

NUCLEAR-FUEL RESOURCES

In FY 1981 USGS nuclear-fuel studies continued with the primary objective of achieving the most comprehensive understanding of the habitats of uranium and thorium and the processes that form deposits in various specific geologic environments in the United States and world. Known deposits occur in a variety of rock types within sedimentary, igneous, and metamorphic geologic settings. The programmatic approach to the understanding of habitat involves geologic, geochemical, and geophysical studies within known uranium and thorium districts. In addition to habitat studies, a major part of the uranium-thorium program involves the development of guides to uranium and thorium exploration as well as methods of determining uranium and thorium favorability and resource estimation using approaches based on geologic-genetic models and data from habitat studies.

Geochemical characteristics of uranium-enriched volcanic rocks

The average uranium concentration for rhyolites and dacites in the Western U.S. is 6.5 ppm. Most of the volcanic terranes containing uranium mineralization (25 ppm) appear to be part of the calc-alkaline suite.

Correlation coefficients between uranium and other elements from a study by K. J. Wenrich of 1,352 unmineralized silicic volcanic rocks from the Western U.S. showed significant correlations at the 99 percent confidence limit (positive or negative, as indicated) in decreasing order of strength, with Th, Be, Rb, Cs, Ta, -V, Nb, -Ba, -Eu, Si, -Sr, -Ca, Yb, -Sc, -Fe, -Co, Pb, Lu, K, and -Mg. Those elements showing positive correlations with uranium are essentially the incompatible elements that are normally concentrated in late stage silicic rocks by magmatic processes. In contrast, those elements which commonly are strongly enriched with uranium in mineralized volcanic rocks are: Ag, As, B, Ce, Cr, Cu, Mo, Ni, Sr, and V; this enrichment appears to occur in rocks containing more than 25 ppm uranium. The similarity between this element assemblage and that for epithermal ore deposits, as well as that for modern hot springs, suggests that the secondary processes concentrating the uranium above 25 ppm are hydrothermal in nature.

Data from uranium-enriched rocks shows that secondary enrichment, in addition to enrichment produced by magmatic processes, appears to create uranium concentrations above approximately 25 ppm. Thus, there appears to be two geochemical processes controlling the uranium concentration in silicic volcanic rocks: (1) magmatic processes such as partial melting or fractional

crystallization, which produce whole-rock uranium concentrations up to approximately 25 ppm, and (2) post-magmatic processes, which can produce whole-rock uranium concentrations in excess of 25 ppm.

Volcano-tectonic evolution of the Date Creek Basin uranium area in western Arizona

According to J. K. Otton, severe crustal extension, characterized by close-spaced listric normal faulting, fault block rotation, and formation of a regional detachment surface, appears to have begun in western Arizona in late Oligocene time. This extension was accompanied by calc-alkalic volcanism with lavas ranging in composition from basaltic andesite to rhyolite. A peculiar alkali rhyolite was generally the first eruptive unit. These volcanic rocks and intertonguing alluvial-lacustrine sedimentary rocks were deposited during extension as suggested by the progressively shallower dips upwards through the section. Older, variably dipping volcanic and sedimentary rocks are overlain with slight to moderate angular discordance by a sequence of sedimentary and volcanic rocks with generally gentle dips. The age of this unconformity seems best placed at 24 to 21 m.y. Rocks above the unconformity are cut by rather widely spaced high-angle normal faults. The alluvial-lacustrine rocks show a growth-fault relation to the normal faults. Debris shed from rising arches west of the Date Creek Basin dominates facies on the west and southwest side. Major uranium deposits developed in the lacustrine facies of these basinal sediments. Volcanism associated with these rocks includes basalts, basaltic andesites and, again, alkali rhyolites very similar to the older alkali rhyolites. Significant normal faulting ceased about 10 m.y. ago. Basaltic volcanism persisted to about 6 m.y. ago (Suneson and Lucchitta, written commun., 1981).

Resistivity investigations of Tertiary basins of western Arizona

Resistivity soundings in the Date Creek basin of western Arizona show that fine-grained lacustrine sediments have apparent resistivities less than 30 ohm-m. J. K. Otton reports that uranium mineralized lakebeds at the Anderson mine show resistivities less than 5 ohm-m and that resistivity variations on profiles across the basin closely reflect facies variations in the section seen in drill hole data along the trace of the profiles. The basin-basement interface can be traced in the profiles and its position is in good agreement with basement intercepts in drill holes. Profiles constructed from soundings in Sacramento Valley and the Big Sandy basin near Wikieup suggest that those basins are 1.5 to

2 km deep and that significant sections of potentially mineralized lacustrine rocks are present.

Uranium in the San Mateo Mountains, New Mexico

C. S. Bromfield and C. T. Pierson made a preliminary study of the geology of uranium occurrences in volcanic rocks of the San Mateo Mountains of west-central New Mexico. About 28 km² were mapped. In this area Paleozoic carbonate rocks are overlain by Oligocene volcanic flows, breccias, and welded ash-flow tuffs ranging from mafic to silicic in composition. Uranium occurs in at least three environments: (1) as pitchblende associated with a quartz-flourite pipe cutting Paleozoic rocks near the volcanic contact; (2) associated with opaline silica along and near fractures in a latitic flow; and, (3) in a silicified and hematized zone near the top of a silicic tuff. Uranium in this zone may have been leached from an overlying riebeckite rhyolite which also contains anomalous amounts of uranium.

Uranium in granites, southwest Colorado

Research by J. D. Collier in the Florida Mountain area of the Needle Mountains mining district, southwestern Colo., suggests that uranium vein deposits formed in Proterozoic granitic rocks by hydrothermal processes initiated during the intrusion of the 9-10-m.y.-old Chicago basin stock. The Eolus and Trimble Granites of Middle Proterozoic age are believed to have been the source of uranium, and trace-element evidence suggests that initial uranium enrichment was the result of repeated partial melting and extensive fractional crystallization. Radiographic techniques indicate that uranium is located primarily in refractory accessory minerals in early, more mafic granitic rocks, but occurs mostly in uranium-rich minerals such as uranorthite and uraninite in more felsic, highly differentiated units. Radiographic evidence also suggests that these uranium-rich minerals were later destroyed by hydrothermal alteration, liberating uranium for concentration in the vein systems.

Hydrothermal convection was initiated by intrusion of the late Miocene granite and rhyolite porphyries of the Chicago basin stock. Uranium was probably leached from large breccia zones within the Proterozoic granites and possibly transported as a fluoride complex. Pitchblende was deposited from oxidizing, paragenetically early fluids at approximately 300° C. The pitchblende-depositing fluids were rich in CO₂ and either boiled or effervesced CO₂. Uranium was precipitated as a result of increase in pH and (or) reduction produced by boiling or effervescence.

Uranium occurrences with base and precious metals in Excelsior Mountains, Nevada

According to J. K. Felmlee, uranium occurrences in the Excelsior Mountains at the northwest edge of Teels Marsh, Nev., are spatially and genetically associated with the granite of Silver Moon of Stewart, Kleinhampl, Speed, Johannesen, and Dohrenwend (written comm., 1981). Uranium occurs with base and precious metals, including lead, zinc, gold, silver, copper, and molybdenum, in quartz veins and breccia zones in or near the granite in amounts of 0.0075 to 7.6 percent in selected hand samples. Only secondary uranium minerals, including beta-uranophane, were identified.

The granite of Silver Moon is a muscovite- and biotite-bearing granite of probable Cretaceous age. Compared with the biotite- and hornblende-bearing granite of Whisky Flat, which it intrudes, the Silver Moon has more SiO₂ and Na₂O, and less Al₂O₃, Fe₂O₃, MgO, CaO, TiO₂, and loss on ignition as reflected in a greater quantity of quartz, lesser amounts of a more sodic plagioclase, lesser amounts of biotite and sphene, and an absence of hornblende. The quartz veins and breccia matrix material in the granite of Silver Moon and in adjacent contact metamorphosed calcareous sedimentary rocks of the Dunlap Formation are thought to have been formed from magmatic-hydrothermal solutions by aqueous partitioning during the late stages of granite crystallization.

Studies of the Schwartzwalder mine, Jefferson County, Colorado

The Schwartzwalder uranium deposit of the Colorado Front Range is structurally controlled and was formed from ascending hydrothermal fluids, according to new studies by A. K. Wallace and Cotter Corporation geologists. Conduits and spaces for transportation and precipitation of uranium were provided by the steep, westerly dipping, north-trending Illinois fault and by easterly dipping horsetail fractures in the hanging wall of the Illinois fault, which opened during Laramide uplift. The open spaces occur only at the intersections of these fractures with a transition zone of rocks, called the "Schwartz" rocks, which are between the calc-silicate gneisses and the mica schists of the Idaho Springs Formation of former usage (now abandoned by U.S. Geological Survey) of Early Proterozoic age.

The uranium deposits of the Schwartzwalder extend for more than 800 m vertically. Post-ore movement on the Illinois fault has produced 150 m of normal displacement, which obscures the true depth of mineralization. Recent core drilling at the mine has revealed a diminution of ore grade along the main Illinois vein, which may indicate the lower limit of the deposit.

Ore emplacement in the Schwartzwalder mine, Jefferson County, Colorado

Current geologic studies of the Schwartzwalder mine have resulted in new interpretations of ore emplacement. The steeply dipping Illinois fault created a conduit of great depth and small horizontal dimensions, which favored fluid transport and uranium deposition. Fracturing and brecciation occurred repeatedly, at least twice before uranium deposition, and several times afterwards. Intergrown pitchblende and coffinite filled interstices between early-formed breccia fragments; subsequent brecciation fragmented these uranium minerals. Adularia and Ca-Mg-Fe carbonates were deposited as gangue between all stages of breccia. Graded bedding of breccia fragments is common, which suggest fluidization. Wallrock alteration produced carbonatization of mafic minerals, strong potassium enrichment, and sodium depletion. Filling temperatures of fluid inclusions in late-stage amethyst and calcite are approximately 120° C and 150° C, respectively, and probably are minimum temperature estimates for vein formation. Freezing studies indicate salinities of about 10 weight percent NaCl equivalent. It is likely that ore was deposited from an ascending carbonate-dominated hydrothermal fluid. Heat, and perhaps some chemical components, may have been provided by nearby, contemporaneous mafic intrusive bodies. Current studies of light stable isotopes should produce more knowledge of the source of the fluids.

Oligocene volcanic rock—a source of epigenetic uranium in central Colorado

The lower Oligocene Wall Mountain Tuff appears to have been a major source of uranium for the deposits in the Tallahassee Creek uranium area in central Colorado, according to K. A. Dickinson and F. A. Hills. The original uranium content of the rhyolitic Wall Mountain Tuff probably was 10 ppm, and that of the leached tuff about 6 ppm. This suggests a uranium loss of 4 µg/g of leached tuff. In the Tallahassee Creek area, the Wall Mountain overlies a major uranium host rock, the upper Eocene Echo Park Alluvium, and underlies another major host rock, the lower Oligocene Tallahassee Creek Conglomerate. The Wall Mountain was deposited over a low-relief erosional surface from Castle Rock to the northern end of the Wet Mountain Valley. In this area, uranium occurrences are common in host rocks that apparently were overlain by Wall Mountain Tuff, such as the Fountain Formation of Middle and Late Pennsylvanian and Early Permian age, the Morrison Formation of Late Jurassic age, the Dakota Sandstone of Cretaceous age, and the Dawson Arkose of Late Cretaceous to early Tertiary age.

Other Oligocene volcanic rocks such as the tuff of Stirrup Ranch and the Thorn Ranch Tuff also may have yielded a significant amount of uranium, but they have a more limited geographic distribution. The Oligocene Badger Creek Tuff is leached to a greater degree in the Castle Rock gulch paleovalley than in the Salida-Waugh Mountain paleovalley.

The original uranium content of the samples is estimated from vitropheric samples, or a minimal original uranium concentration was estimated from the thorium to uranium ratio of the least leached samples. The high thorium to uranium ratios suggest a greater degree of leaching. The thorium to uranium ratio may be a better measure of uranium leaching than is the weathered appearance of the rock.

Geologic studies of the Ranger uranium deposits, Northern Territory Australia

With the cooperation of Ranger Uranium Mining, about 25 selected drill cores from Ranger I No. 1 and No. 3 orebodies have been logged and sampled, and a number of detailed geochemical studies are being made by J. T. Nash and David Frishman. In both orebodies, oxidized and reduced uranium minerals occur chiefly in quartzose schists that have highly variable amounts of muscovite, sericite and chlorite. Retrogressive metamorphism is pervasive in the vicinity of orebodies where biotite and garnet are altered to chlorite, and feldspars to white mica or chlorite. Oxidized uranium minerals, associated with earthy iron oxides, occur from the surface to a depth of about 60 m. Below the oxidized zone, uranium occurs chiefly as uraninite and pitchblende disseminated through thick sections of quartz-chlorite-muscovite schist, and has no apparent association with graphite or sulfides. In fact, graphite is rare and sulfides are generally low in abundance (less than 0.5 percent). Higher ore grades occur in disrupted zones a few centimeters thick and in some quartz-chlorite veinlike zones of uncertain origin. Uranium correlates strongly with chlorite, but not all the many ages of chlorite have associated uranium. At least five textural varieties of chlorite that represent at least three ages, and large variation in Mg-Fe-Al content, are recognized. Uranium is not common in carbonate rocks and seems to occur only in disrupted zones that have chlorite, talc, or serpentine alteration. Chloritization and silicification are more widespread and intense in the No. 1 orebody than in the No. 3. In both orebodies, hematite occurs tens to hundreds of meters below the weathered zone, in both altered and largely unaltered rocks, with and without uranium.

Uranium in Archean migmatites, northern Michigan

Archean granitoids of the Southern complex (informal usage) in northern Michigan comprise large areas with anomalous uranium accumulations of 10 to 50 ppm. Recently, these granitoids have received attention as possible source rocks for a variety of potential uranium accumulations in younger rocks, for example, the carbonaceous black shales flanking the domes of the Southern complex and the Proterozoic unconformity-type deposits related to the 1.1 b.y. Jacobsville unconformity. The source-rock potential of this area is being examined by M. A. Hoffman as part of a thesis at Michigan Technological University on the mineralogy and history of uranium in the granitic members of the complex. A 36 m section of a drill core from a 2.56 b.y. migmatite zone near Republic, Michigan, averages 20 ppm uranium and 19 ppm thorium. Optical and SEM observation indicates that the major uranium-bearing minerals in this interval are brannerite and niobian-anatase. Textural evidence implies a two-stage mobility for uranium: Stage I, incomplete alteration of niobian (1-2 percent Nb_2O_5) ilmenite to brannerite + pyrite, followed by Stage II, low-temperature hydrothermal alteration of ilmenite + brannerite to anatase (0.5-5 percent Nb_2O_5), also an incomplete reaction. Fission-track maps show that anatase contains only minor uranium when compared to brannerite; this suggests that Stage II represents a uranium loss. Textures support a post-Penokean (1.9 b.y.) formation of anatase. The nature and timing of uranium loss from these granitoids near Republic does not preclude their being source rocks for post-Penokean deposits.

Geochronology of a xenotime-monzite gneiss, southern New York

U-Th-Pb isotope analyses of zircons from migmatite and granite at an outcrop in the Hudson Highlands of New York, by J. N. Aleinikoff, indicate an age of about 1,015 m.y., which reflects the time of the Grenville orogeny. Xenotime and monazite from the same outcrop, however, radiate a well-defined age of about 950 m.y., evidently reflecting a final thermal pulse. Apparently detrital, zircons are probably about 1,600 m.y. old, consistent with provenance ages of zircons from other metasedimentary rocks of Grenville age.

Electromagnetic geophysics of Jacobsville Basin, northern Michigan

A combined airborne electromagnetic and magnetic survey was conducted during the spring of 1980 along the contact of the Jacobsville Sandstone in the western

Upper Peninsula of Michigan and interpreted by P. S. Ensign, Michigan Technological University. A total of 318 lines, spaced from 0.2 to 0.4 km, were flown by Geotrex Limited, using the Barringer Mark V INPUT electromagnetic system. The conductivity contrast between the Jacobsville and older adjacent rocks has permitted more accurate mapping of the contact, most of which is hidden by up to 100 m of overburden. In addition, the EM data were used to approximate the size, depth, and dip of several bedrock conductors. The sub-Jacobsville unconformity has been considered to be a possible site for uranium ore deposition, and several promising locations are suggested. One is near the south end of Lake Gogebic, where the Jacobsville overlies conductors in the Michigamme Formation, and another is about 40 km northeast of L'Anse, where the Jacobsville overlies Archean granite.

Proterozoic quartzite and conglomerate of central Idaho

Quartzite and conglomerate in the Lowell-Elk City and Salmon-Cobalt areas of east-central Idaho have been appraised by F. A. Hills for their potential for uranium deposits of the Precambrian quartz-pebble type. Quartzite and conglomerate of the Lowell-Elk City area occur as highly metamorphosed and deformed layers in schist of the Clearwater orogenic zone and are probably 1,600 to 1,800 m.y. old. No placer concentrations of radioactive minerals were found, and none of the characteristics of the Precambrian quartz-pebble-uranium environment (such as placer concentrations of pyrite) were noted. Quartzite of the Salmon-Cobalt area is less metamorphosed and deformed, and possibly younger than quartzite of the Lowell-Elk City area. It is generally fine grained to silty and interbedded with mudstone. No placer concentrations of radioactive minerals or of pyrite were found. Quartzites of both areas appear to be too young to contain appreciable detrital uraninite and were probably deposited in deep-water or ensimatic environments, which are thought to be unsuitable for placer uraninite deposits.

Silver Plume Granite—a possible source of uranium, Tallahassee Creek deposits

High concentrations of thorium, lanthanum, and cerium discovered by F. A. Hills in Middle Proterozoic Silver Plume Granite suggest that the actinides and light lanthanides were enriched abnormally by magmatic processes that formed granite in areas adjoining Tallahassee Creek, Fremont and Teller Counties, Colo. However, no such enrichment is found in the Early Pro-

terozoic Boulder Creek Granodiorite. Although uranium presently does not appear to be significantly enriched in sampled outcrops of the Silver Plume Granite, a large part of the original uranium content of Silver Plume may have been removed by oxidizing ground waters, leaving behind mainly the uranium bound in resistate minerals such as zircon and monazite.

Lead isotopic compositions of the acid leachate from barren shale and sandstone associated with the Hansen uranium deposit (Tallahassee Creek area) indicate that (1) the predominant source of acid-soluble lead is 1,410 m.y. old (Silver Plume age); (2) the source of the lead is characterized by a thorium-uranium ratio around 1 (this ratio in the source may apply to soluble minerals only and may exclude thorium and uranium in resistate minerals); and, (3) at the time of sediment deposition, a paleohydrologic system existed that was capable of transporting Silver Plume lead and, therefore, Silver Plume uranium to the Hansen deposit.

Although a significant contribution of uranium from Tertiary volcanic rocks is probable, it appears also probable that some of the uranium in deposits of the Tallahassee Creek area was derived from the Silver Plume Granite.

Thorium and rare-earth veins associated with alkalic rocks in New Mexico

A number of thorium and rare-earth veins are found on the southwest flank of Laughlin Peak in Colfax County, N. Mex. These veins, which have been traced for as much as 550 m, are found over an area of about 12 km². According to M. H. Staatz, thorium content of the veins ranges from 30 to 24,200 ppm and rare-earth content from 147 to 19,030 ppm. The majority of the veins are richer in yttrium-group than in cerium-group rare earths. Thorium and rare earths are found in the minerals brockite, xenotime, and crandallite. The veins are associated with alkalic rocks. Phonolite, trachytes, trachyandesites, and tephrites occur in the area. The phonolites have a high thorium and rare-earth content, and the vein fluids were probably derived from the magma of these rocks.

Central Idaho paleodrainage history and implications for uranium exploration

Studies by D. A. Seeland suggest that the complex depositional and drainage history of the Sawtooth Valley of central Idaho may provide guides for uranium exploration in the area. In pre-Eocene time, the present Sawtooth valley contained the northern part of the

south-flowing Big Wood River drainage system. In the Eocene, eruption of the Challis Volcanics blocked the valley near Galena Summit. A large lake formed and overflowed northward into the Middle Fork of the Salmon near Cape Horn. The lake was eventually filled with sediment and the subsequent drainage of the valley continued to be northward into the Middle Fork until Pleistocene time when glaciers of Bull Lake time dammed the valley northwest of Stanley. Another lake formed and eventually overflowed eastward across a divide east of Stanley.

This history has implications for uranium exploration in the area. First, the postulated drainage, volcanic, and topographic history of the Sawtooth Valley should have resulted in sedimentary environments favorable for the development and preservation of uranium deposits in the fluvial and lacustrine valley fill. The Sawtooth batholith on the west side of the Sawtooth Valley is enriched in uranium and is a possible source rock. Second, the nearby Stanley uranium district, now downstream east of Stanley, but upstream in Eocene time, has uranium in Eocene carbonaceous sandstones along valleys now buried beneath the Challis volcanics. These streams would have flowed southward into the present Big Wood River drainage. Potential uranium host-sediments of streams draining at least two areas of uranium-bearing granites (the Sawtooth batholith and upstream from the Stanley uranium district) now lie beneath rocks and sediment varying in age from Eocene to Pleistocene both in the Sawtooth Valley and southward down the Big Wood River drainage.

Pre-Oligocene valleys as guides for uranium and hydrocarbon accumulation

Maps of the pre-Oligocene surface in eastern Wyoming by Macke and Denson (1981), and by DeGraw (1969) in western Nebraska were used by D. A. Seeland to prepare an Oligocene stream map of the Hartville uplift—High Plains area east of the Laramie Range. Northward flowing Eocene streams seem to have crossed the Laramie Range and continued flowing northward into the southern Powder River Basin. Oligocene streams are postulated to have followed the same valleys across the range. However, a change in the regional slope from northward to eastward caused the Oligocene streams to flow eastward after crossing the Laramie Range. Uranium mineralization has been recently discovered in the coarse fluvial sandstone of the White River Group of Oligocene age at two locations in Wyoming and one near Crawford, Nebr. All three of these mineralized areas lie in the same major

Oligocene valley which is inferred to extend from the Granite Mountains 560 km eastward into western Nebraska. Other uranium deposits are likely along this and other Oligocene valleys in eastern Wyoming and western Nebraska.

The coarse fluvial sandstones deposited in these valleys have additional economic significance; first, as hydrocarbon reservoir rocks (Goolsby and Miller, 1982) and, second, as a conduit that allows uraniumiferous ground water to enter underlying host rocks as in Weld County, Colo. The position of the interfluves can also guide hydrocarbon exploration. The Bedtick field on the southern margin of the Powder River Basin produces hydrocarbons from Mesozoic rocks where they have an angular relationship with the overlying impermeable Oligocene overbank silts and clays of the interfluve rocks (Goolsby and Miller, 1982).

Westwater Canyon Sandstone Member of Morrison Formation

According to C. E. Turner-Peterson, three distinct fluvial stratigraphic units can be recognized within the uranium-bearing Westwater Canyon Sandstone Member of the Morrison Formation along the west side of the San Juan Basin in New Mexico. Two of the fluvial stratigraphic units (lower and upper) persist to the east and can be recognized as far east as Laguna. The middle fluvial package is as thick as the lower and upper on the west side of the basin but thins rapidly to the east; fluvial sandstones cannot be recognized in this interval east of the Gallup area.

Cross-bedding studies show that streams of the lower stratigraphic unit flowed east-northeasterly, whereas streams of the middle and upper stratigraphic units flowed generally easterly and southeasterly. Volcanic pebbles are present in abundance only in the middle package. Isopach maps of each separate stratigraphic unit, together with maximum pebble-size data, show that major fluvial axes shifted through time. North-easterly flowing streams of the lower fluvial package had two distinct lobes. One lobe, centered near Thoreau, apparently traversed the area of the present-day Zuni uplift, and the other lobe was centered northwest of the Gallup sag, near Asaayi Lake. The easterly and southeasterly flowing streams of the middle and upper fluvial stratigraphic units dropped their coarsest bed-load material just east of the Defiance uplift as they entered the basin from the west. Farther east, the middle unit changes facies rapidly and loses its fluvial character. The upper stratigraphic unit maintains its fluvial character, but the fact that contours for maximum pebble size for this interval widen considerably in an eastward direction suggests a more constant energy level as the streams traversed the basin.

Results of these studies are not compatible with the concept of one fan emanating from the southwest, as has been proposed by previous workers. Separating the Westwater Canyon Sandstone Member into discrete stratigraphic units and treating them individually eliminates the need to have streams enter from the southwest, "turn," and then flow southeasterly in the vicinity of the mineral belt. Both northeast and southeast paleocurrent directions occur in the Westwater Canyon, but in different parts of the member.

Depositional cycles in the Chinle Formation

Time correlations based on sediment cycles observed in outcrops of the Upper Triassic Chinle Formation were extended by R. D. Lupe into southeast Utah and northeast Arizona from an adjacent area to the north. In southeast Utah and northeast Arizona, the Chinle is characterized by three fining-upward, fluvial-lacustrine cycles. The fining-upward character of each depositional cycle and the succession of environments progresses upward from fluvial sediments through lacustrine to soil. This indicates a decrease in the depositional system's sediment transport energy. Generally, each overlying cycle was found to be finer grained than the one below it. Rock units deposited during cycle 1 include the Monitor Butte Member, Moss Back Member, and part of either the Petrified Forest or Owl Rock Members, depending on clay composition. Units deposited during cycle 2 are the Capitol Reef and Black Ledge beds (equivalent), the remainder of the Petrified Forest or Owl Rock, and the lower part of the Church Rock Members. Cycle 3 includes the Hite Bed and that part of the overlying Church Rock Member.

San Juan Basin drilling project, McKinley County, New Mexico

The principal objective of the Mariano Lake-Lake Valley drilling project under the direction of A. R. Kirk, A. C. Huffman, and R. S. Zech, was to provide core samples and geophysical logs for petrologic, sedimentologic, geophysical, and geochemical studies of the Upper Jurassic Morrison Formation. Other objectives included the following: stratigraphic and coal studies of Upper Cretaceous rocks; hydrologic and water monitoring of well no. 2; control for a proposed seismic study of the same geographic area; and development of water wells by the Navajo Tribal Water and Sanitation Department. The general drilling plan called for most holes to be rotary drilled into the Upper Cretaceous Dakota Sandstone and then cored into or through the Recapture Shale Member of the Morrison Formation. The following suite of geophysical logs was included in

the general drilling project: natural gamma, self potential, neutron-neutron porosity, resistance, resistivity, temperature, deviation, gamma-gamma density, caliper, magnetic susceptibility, gamma ray spectrometer (KUT), induced polarization, conductivity, and high resolution 4-arm digital dipmeter.

A total of 28,529 ft were drilled with 4,208 ft of core recovered. Four holes (3, 4, 7, 7A) encountered uranium mineralization; all but hole no. 1 penetrated coal beds in Upper Cretaceous rocks; two holes (9 and 10) produced artesian flows of water admixed with oil from the Upper Cretaceous Point Lookout Sandstone.

The core was described in the field, taped, boxed, and shipped to the USGS Core Library in Denver where it was frozen, split, and reboxed. A split of the core has been archived for reference and future study. Cores 1, 3, 6, and 7 were sampled by J. S. Leventhal for geochemistry, L. J. Schmitt for petrography, Paula Hansley for heavy minerals, R. L. Reynolds for paleomagnetism, and C. G. Whitney for clay mineralogy.

Origin of uranium deposits, Smith Lake district, New Mexico

Uranium deposits in the Smith Lake uranium district, N. Mex., occur on the chemically reduced side of a regional reduction-oxidation (redox) interface. This spatial association led previous workers to conclude that uranium mineralization in the district resulted from late Tertiary redox redistribution of uranium from preexisting primary (tabular) uranium deposits. Detailed geochemical studies integrated with petrologic investigations of two of the uranium deposits in the Smith Lake district, by N. S. Fishman and R. L. Reynolds, however, indicate that both deposits are primary (tabular), not redistributed, orebodies. The orebodies are geochemically similar and have uranium contents correlating positively with those of organic carbon. The organic carbon occurs as an amorphous organic material that partly impregnates the host rock and that was introduced as a soluble organic species into the host early in the diagenetic history. The organic material localized and concentrated the uranium to form uranium orebodies that also contain high concentrations of vanadium, primarily as vanadiferous chlorite, and of sulfur as pyrite and marcasite. Chlorite, pyrite, and marcasite are all intimately associated or mixed with uraniferous organic material. Precipitation of post-ore calcite in the ore zone of one of the deposits lowered the transmissivity of the host beds, thereby contributing to the preservation of that orebody. Preservation of the other deposit may be related to nearby Laramide structures that perhaps retarded or diverted oxidizing waters.

Reevaluation of Jurassic-Cretaceous contacts and uranium anomalies, Chama Basin, New Mexico

Surface and subsurface evaluation of the contact between Dakota Sandstone and Burro Canyon Formation in the Chama basin, N. Mex., by J. L. Ridgley, indicates the presence of an extensive basal fluvial sandstone interval in the Dakota Sandstone. This sandstone interval has been included by Saucier (1974) in the Burro Canyon Formation in his isopach studies. Three samples submitted for palynomorph evaluation, from mudstone and carbonaceous horizons in this basal sandstone, yielded palynomorphs indicative of the Dakota Sandstone. This redefinition of the base of the Dakota drops the position of the pre-Dakota unconformity and places some uranium ore reserves in the Dakota. These particular ore resources occur in this basal fluvial sandstone.

Surface and subsurface evaluation of the contact between the Burro Canyon and Morrison Formations contact indicates that this contact is also an unconformity. The unconformity is gently undulatory; basal sandstones of the Burro Canyon rest on mudstone or sandstone of the Brushy Basin Shale Member of the Morrison Formation.

Subsurface studies of radioactive anomalies in the southeast part of the Chama Basin show that these anomalies occur in sandstones in the upper Brushy Basin Shale member, in the Burro Canyon Formation and in the Dakota Sandstone. Major radioactive anomalies occur in the Burro Canyon, in the basal fluvial Dakota Sandstone, and in the interbedded sandstone-shale sequence of the Dakota that immediately overlies the basal fluvial sandstone.

Thrust fault uranium in overthrust and disturbed belts, Montana

Preliminary studies by H. W. Dodge, Jr., in southwest and west-central Montana show significant uranium anomalies, surface and subsurface, in the Lower Cretaceous Kootenai and Blackleaf Formations. These formations consist of fluvial sandstone and conglomerate, with interfluvial swamp and lacustrine siltstone and mudstone. These formations are equivalent to the Cloverly Formation of western and central Wyoming and the Lakota and Fall River Formations of the Black Hills region.

Uranium anomalies occur in sandstones and associated sediments in footwall blocks which are at least partially overridden by Paleozoic thrust slabs. In the southwestern Montana overthrust belt, these anomalies are only seen in rather deep subsurface gamma logs. In west-central Montana, surface anomalies are found at, or close to, the contact of the disturbed belt and easterly directed thrust sheets.

Uranium potential of the Kootznahoo Formation, Zerembo Island area, Alaska

According to K. A. Dickinson and J. A. Campbell, the lower Tertiary Kootznahoo Formation in the Zerembo Island area of southeastern Alaska is potentially an excellent host rock for uranium. It includes permeable sandstone and conglomerate beds together with suitable reductants. Carbonaceous fragments are common in some of the sandstone and conglomerate beds, and pyrite is present in a coal bed. Slight epigenetic uranium enrichment is present in some of the conglomerate and sandstone beds and possibly in the coal bed. Epigenetic enrichment is believed to have occurred in samples that contain over 10 ppm uranium. In these samples, no significant correlation was found between uranium and titanium or zirconium, the latter two elements being common in heavy minerals. Samples containing less than 10 ppm show a significant positive correlation between zirconium and uranium and between titanium and uranium, and the uranium appears to be carried in the heavy minerals.

Developing regional setting, copper-uranium prospects, Uinta Basin, Utah

Copper-uranium prospects in the upper Eocene Uinta Formation of the central Uinta Basin, Utah, occur in fluvial sandstone that was deposited in and adjacent to ancient Lake Uinta during its waning stages. Reconnaissance mapping by L. C. Craig, assisted by Mark Larson and G. A. Miller, shows that some thin, lacustrine limestone beds extend as much as 50 km into the dominantly fluvial facies. The distribution of the limestone beds indicates that the lake margin migrated widely during these late stages. These areally extensive limestone beds, in addition to widespread mappable tuff beds, should provide a regional framework for constructing the geologic setting of the metalliferous deposits in the poorly known central part of the basin.

The Middle Jurassic vanadium-uranium belt in western Colorado

Preliminary results of studies by M. W. Green, C. T. Pierson, and H. C. Granger in the Entrada vanadium-uranium belt, which extends from Durango northward to Meeker in western Colorado, indicate that the Pony Express Limestone Member of the Wanakah Formation in the Durango, Graysill, and Barlow Creek areas contains a lower lacustrine sandstone facies presently included in the underlying Entrada Sandstone. The stratigraphic and sedimentologic relationships in the Placerville/Slick Rock area indicate a possible lateral time equivalency between the siltstone units of the lower Wanakah and Summerville Formations at Slick

Rock and limestone of the Pony Express at Placerville. No major depositional breaks or erosional hiatuses were noted between the base of the Pony Express Member of the Wanakah Formation and the top of the Morrison Formation in the region of the vanadium-uranium belt; however, rapid changes in sedimentary depositional regime and resultant lateral and vertical lithofacies are common in this interval. The dominant lithofacies and environments of deposition include limestone (lacustrine), sandstone (eolian, fluvial, and lacustrine), and siltstone (floodplain and lacustrine). The lower parts of the sequence also locally contain bedded chert and gypsum deposited in association with arid lacustrine units and eolian dune environments. The upper part of the sequence, including the Morrison Formation, is dominated by sedimentary rocks deposited in floodplain, lacustrine, and medium- to high-energy fluvial environments. This indicates that conditions during deposition of the sequence changed progressively from arid evaporative climates to more humid climates.

Vanadium-uranium deposits in the underlying Entrada Sandstone occur in proximity to the base and western depositional margin of the Pony Express throughout the mineral belt. Vanadium-uranium deposits occur in zones or thin bands which are suspended approximately parallel to the Entrada-Pony Express contact within texturally uniform eolian, lacustrine, and low-energy fluvial sandstone bodies of the Entrada a few meters below the contact. Mineralization probably followed or was contemporaneous with the bleaching of the Entrada beneath the Pony Express, possibly caused by the infiltration of organic-rich fluids derived from decayed algal growths and other vegetal matter in the Pony Express. The suspended stratigraphic position and planar-tabular geometry of ore deposits suggest that mineralization occurred at paleo-fluid interfaces which existed between ground-water fluids derived from the Pony Express and fluids of a different composition contained within the Entrada. No other controlling mechanism for the emplacement of ore deposits is apparent in the Entrada sequence.

Fossil Ridge, Colorado, uranium studies

In the Fossil Ridge area, the middle facies of the Leadville Limestone was noted by R. S. Zech to be unusually pure limestone, rather than dolomitic. At the nearby Pitch mine, this facies is dolomitic and serves as a host for uranium that occurs along fractures. The potential for uranium accumulation in this facies in the Fossil Ridge area is diminished because the limestone tends to deform rather than fracture. However, the great structural complexity of the area increases the potential for uranium mineralization in other units,

including the upper (dolomitic) Leadville Limestone, Manitou Formation, and Fremont Limestone.

Shifting margin of the Cretaceous sea in the San Juan Basin

Geologic mapping in the Tohatchi NW quadrangle by R. E. Thaden has shown a major early regression of the Cretaceous sea from the southwest margin of the San Juan basin, as demonstrated by the presence of great thicknesses of the continental fluvial Torrivio Member of Molenaar, 1973, of the Gallup Sandstone that extends north and east beyond the Tohatchi NW quadrangle, and the virtual absence, except as thin beds and isolated lenses, of the marine facies of the Gallup Sandstone, which occurs in the southwest corner of the quadrangle. The next transgression only reached near the south border of the quadrangle, as is indicated by the six or more shoreface sandstone bodies that occur there in the Mulatto Tongue of the Mancos Shale. These sandstone bodies shingle upsection to the south and probably merge with the overlying progradational Dalton Sandstone member of the Crevasse Canyon Formation. Neither the Mulatto nor the Dalton is present southwest of the quadrangle. Later shifts in the shoreline of the Cretaceous sea in this area have been documented previously.

Application of genetic-geologic models for uranium resource estimates

Work by W. I. Finch, H. C. Granger, and R. B. McCammon has led to the development of genetic-geologic models designed to evaluate the favorability for undiscovered uranium resources. A systematic matrix of all known geologic characteristics of a given type of uranium deposit and their corresponding genetic aspects constitutes a provisional genetic-geologic model. The initial provisional model was built for the tabular humate-related uranium deposits in the San Juan Basin, and it consisted of about 140 variables arranged in 11 genetic stages. For application in the unexplored part of the basin, research on this provisional model reduced the final working model to about 20 variables in only three of the genetic stages. The chief criteria used to identify an essential variable was based on the requirement of regional variability of the data needed to establish the presence or absence of that variable. The essential genetic stages in the working model are host-rock deposition, host-rock preparation for uranium mineralization, and favorable conditions for transport of both uranium and humate. All other genetic stages were proven to have been favorable over the entire basin. Data sets have been completed for use in the working model by using geologic decision analysis. This data-based analysis method will weight the favorability for a given cell of ground to contain

uranium deposits. By combining this favorability with grade-tonnage data for deposits in the known mineral belt by an extension of the geologic decision analysis, the undiscovered uranium resources will be estimated.

Geologic decision analysis in the San Juan Basin, New Mexico

Preliminary estimates of uranium resources have been made through geologic decision analysis for the deeper, largely unexplored parts of the San Juan basin in northwest New Mexico. According to R. B. McCammon, the estimates are the result of large-scale integration of geologic data within a logical framework of a genetic-geologic model representing tabular humate uranium deposits in the Grants Mineral Belt. Favorability of occurrence of this type of deposit is based on subtle areal variations in total thickness, net sandstone thickness, average sandstone thickness, number of sandstone/mudstone alternations, sandstone to mudstone ratio, color, grain size, sorting, and composition within the Westwater Canyon Sandstone member of the Upper Jurassic Morrison Formation. Potential resource estimates within favorable areas were derived from statistical correlation with areas of similar favorability containing known uranium resources. McCammon and associates have estimated the potential uranium resources in the unexplored East Chaco Canyon area to be comparable with the discovered uranium resources in the Gallup-Crown Point area. Geologic decision analysis has provided a quantitative approach to potential resource estimation.

Enhancement of data from helium soil gas surveys

According to G. M. Reimer, the concentration of helium in soil varies as a function of meteorologic parameters. On a daily basis, helium variations are a function of air and soil temperature. Often, the daily variations are of the same magnitude as the range of concentrations found from a field survey. A new approach, developed by Reimer, to evaluating and correcting the helium data from field surveys adjusts for the daily air and soil temperature variations. Permanent collecting stations are established in a field area, and gas samples are withdrawn several times a day while the survey is being conducted. The daily changes in helium concentration are regular and predictable. Hence, corrections can be made by comparing the concentration and time of collection of the unknown sample to the equivalent time and concentration of the samples collected from the permanent probe. This improvement in data processing enhances field data that previously were considered uninterpretable.

Uranium contents of igneous zircons and granitic rocks

According to J. S. Stuckless and George VanTrump, Jr., concentration data for igneous zircons (Stuckless and VanTrump, 1982a) and granitic rocks (Stuckless and VanTrump, 1982b) of the contiguous United States show that bulk uranium values for zircons and uranium and thorium contents (and ratios involving these elements in granitic rocks) follow log-normal distributions. Means and standard deviations of values examined are in the following table:

Variable	Number	Mean	Standard deviation	
Whole-rocks				
U (ppm) -----	2507	3.54	+4.58	-2.00
Th (ppm) -----	2492	16.76	+22.47	-9.60
Th/U -----	2484	4.73	+5.97	-2.64
Th/K -----	2250	5.00	+5.98	-2.72
K/U -----	2266	0.95	+1.18	-0.53
K -----	2280	3.52	+1.02	-1.02
Zircons				
U (ppm) -----	963	636	+934	-378
Th (ppm) -----	304	312	+615	-207
Th/U -----	302	0.41	+0.45	-0.21

The areal distribution of anomalous values (which were arbitrarily chosen as those more than one standard deviation greater than the mean) does not uniquely define known uranium mining districts. Anomalously uraniumiferous zircons are common around the Colorado Plateau, within central Wyoming, near the Midnight mine in Washington State, and near the Marysvale district of Utah, but are also common in the east-central Sierra Nevada Mountains of California, the region of northwestern Michigan-northern Wisconsin, east and northern New England, and the inner piedmont of Georgia. Anomalously large thorium-uranium ratios are found in granitic rocks associated with the sandstone deposits of central Wyoming, but are absent near other deposits of this type. Anomalously large uranium concentrations occur sporadically throughout the United States.

The concentration of uranium in igneous zircons and granitic rocks is probably controlled by a number of variables; therefore, these concentration data, without supplemental information, seem to be of little use as a tool for exploration or resource assessment. Examination of the variations in thorium-uranium ratios for a few specific granites suggests that variability may be caused by late-stage magmatic or secondary processes that can be associated with ore-forming processes. Therefore, highly variable uranium concentrations or thorium-uranium ratios may be useful in the search for uranium deposits. If uranium content of zircons is to be used as an exploration tool, it will be necessary to first identify and quantify the variables that control these values so that each data point can be compared to an appropriate normal value.

Uranium, carbon, and sulfur in roll-type uranium deposits in Wyoming

Work by J. S. Leventhal and E. S. Santos shows that organic carbon, sulfide sulfur, and uranium are inter-related in sandstone roll-type uranium deposits.

Organic carbon, sulfide sulfur, and uranium content in samples from the Highland uranium mine, Powder River Basin, Wyoming, are presented. These data show strong statistical correlation between organic carbon and sulfur and uranium and sulfur, but not between uranium and organic carbon. This is interpreted to mean that sulfide is the concentrating agent for the uranium in this roll-type deposit. However, organic carbon (possibly introduced) is the energy source for sulfate-reducing bacteria.

Petrographic investigations of primary uranium ore, Ambrosia Lake district, New Mexico

In the Ambrosia Lake district, N. Mex., petrographic work by J. D. Webster on primary uranium ores has shown that organic material was introduced into the host Morrison Formation sandstones before introduction of uranium but that the uranium was absorbed onto the organic material while it was still plastic. Preliminary isotopic work confirms the time of mineralization as early in the history of the Upper Jurassic host rock.

Age of uranium mineralization of the Churchrock mine, New Mexico

The low concentrations of vanadium and lead in ore-grade host rocks from the Churchrock mine in New Mexico, together with a considerable degree of disequilibrium in high-grade samples, suggests to E. S. Santos that this is a very young redistributed uranium deposit which was probably derived from a preexisting redistributed uranium deposit.

Uraniferous opal, Virgin Valley, Nevada: conditions of formation

Studies by R. A. Zielinski have shown that uraniferous, fluorescent opal, which occurs in tuffaceous sedimentary rocks at Virgin Valley, Nev., records the temperature and composition of uranium-rich solutions as well as the time of uranium-silica coprecipitation. Results have been integrated with previous geologic and geochronologic data for the area to produce a model for uranium mobility that may be used to explore for uranium deposits in similar geologic settings. Uraniferous opal occurs as replacements of diatomite, or silicic air-fall ash layers, in tuffaceous lakebeds of the Miocene Virgin Valley Formation of Merriam (1907). Fission-track radiography shows uranium to be homo-

geneously dispersed throughout the opal structure. This finding suggests coprecipitation of dissolved uranium and silica gel. Fluid inclusions preserved within opal replacements of diatomite have homogenization temperatures in the epithermal range and are of low salinity. Four samples of opal from one locality all have uranium-lead apparent ages which suggest uraniferous opal precipitation in late Pliocene time. These ages correspond to a period of local, normal faulting, and high-angle faults may have served as vertical conduits for transport of deep, thermal ground water to shallower levels. Lateral migration of rising solutions occurred at intersections of faults with permeable strata. Silica and some uranium were dissolved from silica-rich host strata of 5 to 20 ppm original uranium content and reprecipitated as the solutions cooled. The model predicts that in similar geologic settings, ore-grade concentrations of uranium will occur in permeable strata that intersect high-angle faults and that contain uranium source rocks as well as efficient reductant traps for uranium. In the absence of sufficient quantities of reductant materials, uranium will be flushed from the system or will accumulate in low-grade disseminated hosts such as uraniferous opal.

Tuffaceous sediments as source rocks for uranium: a case study in Wyoming

Fine-grained tuffaceous sediments of the Oligocene White River Formation have been evaluated as a possible source of uranium for the sedimentary uranium deposits of Wyoming. The evaluation, by R. A. Zielinski, is based upon a model in which volcanic glass is considered to be a major source of uranium and thorium and in which uranium and silica are released during alteration of glass to montmorillonite. The evaluation scheme is applicable to other tuffaceous sediments in similar geologic settings. The average uranium and thorium contents of glass separates and glassy air-fall ashes of the White River Formation are 8 and 22.4 ppm, respectively, and these values approximate the average composition of glass deposited in Wyoming basins in Oligocene time. Comparison of these values with the uranium and thorium concentrations in montmorillonite separates indicates little change in thorium concentrations but reductions in uranium concentrations which average 3.3 ppm. In spite of the apparent major removal of uranium during alteration of glass to montmorillonite, whole-rock samples of tuffaceous siltstones have a calculated average uranium loss of only 0.7 ppm because of generally small amounts of clay alteration. This conclusion is supported by additional comparisons between glassy ash and partially altered vitric siltstones; the latter corrected for mixing of altered glass

and uranium- and thorium-poor primary and detrital materials. The original volume of the White River Formation is adequate to generate economically significant amounts of mobile uranium, even with such modest losses. Uranium and silica which are mobilized during glass alteration can coprecipitate as uraniferous secondary silica in areas where solutions become silica saturated. These precipitates indicate pathways of ancient, uranium-rich solutions in tuffaceous rocks. Exploration efforts in the White River Formation and underlying units should concentrate on areas where such pathways intercept reducing environments. Intercepts of this type are present at some uranium deposits in the study area, and this lends support to a tuffaceous source-rock model.

Redistributed uranium as indicator of incipient rock/water interaction

Fission track radiography of variably altered/welded/fractured ash-flow tuffs, Yucca Mountain, Nevada Test Site, by R. A. Zielinski, indicates intergranular-scale redistribution of uranium that is not evident from bulk chemical data. Redistributed uranium is adsorbed on secondary oxides of iron and manganese that line fractures, coat ferromagnesian minerals and fill cavities of partially welded pumice. Redistributed uranium is most evident in obviously zeolitized samples, but is also present in petrographically fresh, densely welded tuffs. The component of whole-rock uranium associated with hydrous secondary phases is interpreted as the uranium mobilized by an aqueous phase during or after ash-flow emplacement. Attempts will be made in the future to quantify this component by selective leaching of host oxides.

Formation of a tabular vanadium-uranium deposit at a solution interface

Studies were conducted by M. B. Goldhaber, in collaboration with H. R. Northrup and C. G. Whitney, on the clay mineralogy and clay stable isotopy (oxygen and hydrogen isotopes) of the Tony-M vanadium-uranium deposit hosted by the Upper Jurassic Morrison Formation in Utah. The data reveal a complex clay mineralogy. Within the underlying Tidwell unit of the Morrison, (of Peterson, 1980) interstratified chlorite-smectite formed during early postdepositional times as a result of the evaporative nature of this unit. Within the ore zone, an unusual vanadium-bearing chlorite phase formed which is a major host for vanadium in the deposit. Stratigraphically above ore, kaolinite is the typical phase found in Morrison sandstones. The isotopic data demonstrate that the vanadium-chlorite was formed at and below the interface between two fluids; the lower one was a brine and the upper one,

which carried the ore constituents to the deposit site, was flowing meteoric water. The data also demonstrate that the lower (brine) fluid was formed in a shallow evaporative basin. The Tidwell unit is, in part, just such an evaporative basin and is therefore the likely source of the brine. Authigenic clays in the Tidwell unit are of the appropriate isotopic composition to have formed from this brine.

Quartz behavior in vanadium-uranium deposits

In 1980, H. C. Granger and C. G. Warren outlined the problems related both to replacement of quartz by clays within the ore layers of Colorado Plateau-type vanadium-uranium deposits and to seemingly simultaneous precipitation of overgrowths in the enclosing rocks. They noted the apparent requirements of a non-conventional explanation for dissolution in the presence of solutions that seemingly should have been saturated relative to quartz. Further extensive research into the problem has resulted in the tentative explanation that follows.

Vanadium-uranium ores were formed in the reaction zone between a humic-enriched meteoric solution and a brine. In the humic solution, aluminum hydroxides are transported principally as humic complexes, which equilibrate with soluble alumina and aluminum hydroxide adsorbed on quartz grain surfaces. This adsorbed aluminum-hydroxide greatly depresses quartz solubility from about 6 ppm SiO_2 in pure water to as little as 0.5 ppm in an aluminum-bearing solution. The effect can be reversed, however, by reactions that consume aluminum. During formation of clay minerals in the ore zone, the aluminum-hydroxide is stripped from quartz surfaces, leaving that quartz free to dissolve normally. Outside the ore zone, where clays are not forming, aluminum-hydroxides depress the quartz solubility to a very low value. The concentration difference motivates the dissolved silica to diffuse from the ore zone, where concentrations can be in the order of 6 ppm SiO_2 , to regions outside the ore, where concentrations of dissolved silica are much lower. Petrographic and related studies suggest that considerable secondary, ore-stage quartz was deposited in the adjacent host rock on the humic-rich side of the ore layer, but the evidence is less conclusive on the brine side.

Vanadium reduction in vanadium-uranium deposits

A part of the hypothesis by H. C. Granger and C. G. Warren concerning the geochemical genesis of Uravan Belt vanadium-uranium deposits is that the vanadium was introduced in solution as reduced species rather than having been concentrated by reduction. Extensive

review of the literature has disclosed the revealing fact that geologists have frequently written about the capacity of both organic matter and H_2S to reduce vanadium to V^{+++} , but the chemists have never shown that this is possible at low temperatures.

In aqueous solution at low temperature, vanadium (IV) apparently doesn't react with H_2S between pH 1 and 4; solid $VO(OH)(HS)$ or $VO(HS)_2$ are formed at pH 4 to 8; and above pH 8, a soluble yellow sulfide complex (thiovanadate?) forms. H_2S and vanadyl sulfate react at $300^\circ C$ to yield patronite, VS_4 , a vanadium (IV) sulfide. This reaction illustrates the difficulty in reducing vanadium (IV) by means of sulfur species.

Several published reports indicate that vanadium (V) is reduced and forms vanadium (IV)-humate and -fulvate complexes in the presence of humic and fulvic acids. Granger and Warren's experiments show that certain pure organic reagents (similar to reduced forms of humic materials) in the presence of H_2S can preserve either vanadium (III) or vanadium (IV) in the form of blue or yellow soluble complexes. Over an observation period of months, these colors remain unchanged, a fact that indicates a fixed oxidation state, but no further reduction. Laboratory results such as these suggest that unoxidized humates are capable of carrying vanadium (III) or vanadium (IV) without changing either oxidation state.

These data place considerable doubt on geologists' claims that low temperature solutions of H_2S and organic matter can reduce vanadium to vanadium (III).

Two-mica granite geochronology, tectonic space, and uranium content

Two-mica granite in New England is known to be emplaced during the Hercynian, Acadian, and probably the Oliverian orogenies (local usage), or the entire Caledonian-Hercynian time, which may have spanned as much as 175 m.y., according to E. L. Boudette (USGS) and J. B. Lyons (Dartmouth College). Intervals of two-mica granite production appear to have occurred at about 445 m.y., 385 m.y., 330 m.y., and 270 m.y. These granites are formed in strike belts in the tectonic grain of the Caledonian-Hercynian orogen, but a progression of increasing age of granite east-to-west is no longer apparent. Granite of the 270 m.y.- and 385 m.y.-age groups appears in the Massabesic terrane of the Avalonian tectono-stratigraphic zone, which is adjacent to and parallels the coast. Granite of the 330 m.y.-age group (Sunapee belt) is medial in the Gander tectono-stratigraphic zone, and granite of the 385 m.y.-age group (Barre belt) occurs in the west, just east of the Ottawaquechee ophiolitic melange (Iapetus suture). The Barre belt is distinctive because it occurs west of an enormous tectonic dislocation, which is prob-

ably an extension of the Brevard zone of the southern Appalachians. This dislocation appears to be part of a segmented thrust fault passed subsequently into trans-current motion.

Total uranium in the 385 m.y.-old granite is the lowest, less than 5 ppm. The 270-m.y.-old rocks are intermediate with 5 to 12 ppm uranium, and the 330-m.y.-old group is 12 ppm or more. Incomplete Pb-U-Th isotope systematics in zircons of the granite groups suggest that there may be an inverse relationship between uranium content and a direct relationship with thorium content in zircon and the total rock. Approximate uranium content in zircon in the three age groups is as follows: group 1, 385 m.y. ago, 3,050 ppm uranium, 385 ppm thorium; group 2, 330 m.y. ago, 2,300 ppm uranium, 620 ppm thorium; and group 3, 270 m.y. ago, 3,800 ppm uranium, 500 ppm thorium. The isotope systematics and zircon morphology suggest that each of the groups had a different anatectic history.

To date, uranium deposits are known only in the 330 m.y. age group rocks in New Hampshire and Maine. The protolith of the 330 m.y. age group is not presently established, but possibilities are either Lower Devonian age cyclic turbidite (metashale) of the Seboomook Formation or an unnamed, undated apparently older carbonaceous, sulfidic black metashale unit with some scattered stratabound Cu-Pb-Zn occurrences. It is possible that these later rocks, in particular, were once enriched in uranium. Vitrac and others (1981) have interpreted lead isotope data from Hercynian-age granitic rocks in the Avalonian zone of New England to indicate an influence from fluid circulation during orogenic events in a continental crust in the Appalachians that exceeds an ultimate age of 3 billion yrs.

GEOTHERMAL RESOURCES

Low-temperature geothermal resources in the United States—1981

M. J. Reed reported that the first quantitative assessment of the low-temperature (less than $90^\circ C$) geothermal resources within the United States was nearly completed in 1981. Quantitative estimates were made for the accessible resource base (energy in the ground), the resource (energy available at the surface), and beneficial heat (energy used in an application) for both identified and undiscovered low-temperature geothermal systems. A new methodology was developed to determine the recovery of energy from large-area systems and to calculate the beneficial heat. Low-temperature systems were identified in all regions of the country. The greatest number of systems are in the Western U.S., but the largest systems, which contain the most energy, are in the Central U.S.

Geothermal drilling at Newberry Volcano, Oregon

E. A. Sammel reported that drilling of a 7.6-cm geothermal test hole in the caldera of Newberry Volcano, Ore., was completed in September of 1981. The total depth of the hole was 932 m, and the temperature at the bottom of the hole was 265° C. The bottom few meters of the hole was in permeable rock from which steam was produced in a 20-hour flow test. Nearly continuous core was recovered from the hole. The information gained from this highly successful research drilling added considerably to an understanding and evaluation of geothermal potential of Newberry Volcano. The results at Newberry may also have wide application in assessment of the geothermal potential of the Cascade Range, adjacent to Newberry on the west.

Magnetotelluric study of the Cascade Range

W. D. Stanley completed magnetotelluric (MT) studies at two volcanic centers in the Cascade Range of the Pacific Northwest. The first of these is Medicine Lake Volcano, east of Mt. Shasta in northern California, and the second is Newberry Volcano in central Oregon. The study of these volcanic centers was part of a regional study of most of the Cascade Range. The MT data suggest a four-layer electrical structure, with a surface layer of high resistivity rocks, a second layer of

more conductive material, a third, relatively thick layer of resistive rocks interpreted to be nonvolcanic upper crust, and finally, a conductive layer interpreted to be lower crustal rocks containing small amounts of free water or partial melt. The second layer in most of the regional survey, and in particular in the area of Newberry and Medicine Lake Volcanoes, is thought to consist of volcanic rocks with a greater concentration of alteration products than the more resistive and younger shallower volcanics. The bottom of the second layer is generally at about 2 to 4 km, and the depth to the top of the fourth layer, interpreted to be lower crustal rocks, is typically 15 to 20 km. At both Medicine Lake Volcano and Newberry Volcano the MT data indicate a structural high at the top of the third layer. Relief of about 2 to 3 km exists on this surface beneath the volcanoes. This structure is also suggested by gravity and seismic data for Medicine Lake Volcano and by the gravity data for Newberry Volcano. The MT data suggest that these structural highs contain little, if any magma, although locally molten zones isolated vertically or horizontally could be present. The resistivity of the second layer suggests a relatively great degree of hydrothermal alteration. A geothermal test well which encountered high temperatures at a depth of 1 km in Newberry Crater was drilled approximately at the center of the structural high outlined by the MT soundings.

REGIONAL GEOLOGIC INVESTIGATIONS

NEW ENGLAND

Recurrent movements on faults north of Boston

In northeastern Massachusetts some regional faults that have minimum strike displacements of several kilometers exhibit the superimposed effects of several episodes of movement, according to A. F. Shride. These effects are reflected in styles of cataclasis ranging from ductile mylonitization to brittle brecciation. The oldest large scale faulting is pre-Silurian; the youngest is post-Triassic. Smaller faults are perhaps much younger still.

High kames trace fractures in late Wisconsinan ice in southeastern Massachusetts

A belt of 20 isolated high-standing hills, composed of glacial meltwater sediments and informally known as high kames, has been mapped in southeastern Massachusetts by J. D. Peper and B. D. Stone as part of a compilation of the Quaternary geologic map of Massachusetts. This belt appears to delimit an area in which englacial and supraglacial sediments were deposited in ice channels along the intersections of radial and transverse crevasses within stagnant ice marginal to the retreating edge of the late Wisconsinan Narraganset Bay-Cape Cod Bay Ice Lobe. The belt of kames is about 20 km wide and extends from the vicinity of Providence, R.I., north-northeastward for about 50 km into the eastern part of the Taunton River valley. The belt is parallel to the coastal moraines to the south. The kames are grouped in three lines with 5 km spacing. Individual kames, 0.5 to 2.0 km long, are composed of fluvial sediments at the surface, and many have deltaic foreset and bottomset beds at depth. The tops of the hills stand several to tens of meters above surrounding younger deposits. Most kames have ice contact slopes on all sides, and normal faults and open or recumbent folds formed during collapse. The linear map pattern of the kames within the belt and topographic elements within many individual kames define a rectilinear pattern of transverse north-northeast and radial south-southeast trends due to accumulation of the deposits in ice fractures.

Glacial deposits of the Shetucket River Basin, eastern Connecticut

J. P. Schafer has highlighted the importance of ice-marginal lakes in producing a detailed record of the retreat of the last ice sheet by compilation of the Shetucket River Basin section for the glacial geologic map of Connecticut. The relatively broad valley of the

Shetucket and the lower Natchaug River in the 13-km-long South Windham-Willimantic-Mansfield Center area contains deposits of at least 8 successive lakes. Each lake was dammed by the next older deposit, sometimes including detached bodies of dead ice. The initial blockage of the valley probably occurred at a bedrock narrows just downstream. Each lake was in contact with a marginal zone of dead ice so that the heads of the successive lake deposits record successive positions of the ice margin. In contrast, the stratified glacial deposits along most south-draining stream segments in this basin show much more widely spaced ice-contact heads, as far as 5 to 15 km apart. Although lake deposits are common in such valleys, drainage conditions during their deposition did not produce topographic separation of successive deposits. Instead, they merged into one another. In such areas, retreatal positions are better recorded by small upland deposits which are generally ponded against divides.

Late Wisconsinan stratigraphy along the terminal moraine, northern New Jersey

Detailed surficial mapping and coring of part of the late Wisconsinan terminal moraine, promoraine deltas and subaqueous fans, and varves in the glacial Lake Passaic Basin of northern New Jersey, show proximal to distal relationships of surface and subsurface stratigraphic units that were deposited during the glacial maximum. A core from the crest of the moraine in Madison, studied by B. D. Stone (USGS), M. J. Pavich (USGS), and G. E. Reimer (Rutgers University), contains from top to bottom: deltaic sand, homogeneous compact till (10 m thick), and interbedded lacustrine clay, silt, and sand, and thin till beds. The entire moraine sequence is apparently stratigraphically equivalent to lake-bottom beds that underlie the Great Swamp Basin south of the moraine. These beds include a 19-m thick section of more than 600 varves, which consist of regularly laminated clay and fine silt couplets that average 3.1 cm thick. X-radiographs of varves obtained by J. C. Liddicoat (Lamont-Doherty Geological Observatory) reveal discrete, locally graded microlaminations within the silt layers of the varve couplets. These microlaminations probably resulted from deposition by individual meltwater density underflows on the lake bottom. Oriented paleomagnetic samples analyzed by Liddicoat show normal polarity and also show apparent paleosecular variation of less than 10° over a sampling interval of tens of varves.

Juxtaposed terranes in northern New Hampshire: possible extension of Brevard zone

Geologic mapping by R. H. Moench, L. J. Cox, A. R. Pyke, and Viki Lawrence in the Second Connecticut Lake quadrangle, northern New Hampshire, has delineated a south-facing lower Paleozoic sequence of rusty-weathering euxinic melange, succeeded by interbedded turbiditic quartzite and pelitic schist (Albee Formation), and then by complexly interstratified Middle Ordovician subaqueous mafic and felsic metavolcanic rocks and black phyllite (Dixville Formation). The Middle Ordovician assemblage is exposed in an area of about 25 km² that includes Magalloway Mountain, previously mapped as Albee Formation. It comprises a large doubly plunging basinlike feature and locally shows evidence of sulfide mineralization. The Albee and subjacent melange strike east-west. They represent the westernmost known extent of a south-facing sequence of ophiolite, melange, and abyssal flysch mapped by Boudette (unpub. data, 1982) and Boudette and Boone (1976) to the east in Maine. Together with underlying Precambrian rocks (Chain Lakes massif) and overlying Ordovician, Silurian, and Lower Devonian metavolcanic and metasedimentary rocks, the entire assemblage comprises a major crustal block that extends nearly to the New England coast.

In the Second Connecticut Lake quadrangle, rocks of the southeastern block are truncated on the northwest by a major northeast-trending fault zone. Northwest of the fault is a very different terrain of metamorphosed volcanics, hypabyssal intrusives, and sedimentary rocks traditionally considered to be Silurian to Early Devonian, but on the basis of no conclusive evidence. These rocks appear to be preserved in fault slices, each of which is internally structurally complex. The volcanics are host to one known major massive sulfide deposit (Ledge Ridge) and elsewhere show evidence of premetamorphic mineralization. From regional geologic relationships shown on Williams' (1978) map of the Appalachian orogen, the fault zone may be the northeast continuation of the Brevard zone, a major terrain boundary in the southern Appalachians. Reed, Bryant, and Myers (1970) interpret the Brevard as a zone of major combined left-slip thrust faulting. Regardless of its origin, the possibility that the Brevard extends into this part of New England should provide new focus for research. It raises the possibility, for example, that the width of the orogen has been approximately doubled by left-slip faulting on a feature analogous to the San Andreas fault. The remarkable similarity of probable Precambrian diamictites of the Chain Lakes massif in Maine and the Sykesville Formation in Maryland (Boudette, unpub. data, 1982; Hopson, 1964) provides a

measure of about 900 km of possible left-slip displacement. Assuming a high but reasonable rate of 10 cm/yr displacement, 900 km of relative movement would have taken 9 million yr. Based on geologic relationships, this may have occurred mainly in Early Devonian time.

Analysis of faulted glacial pavement in southeastern New York

In the lower Hudson River valley, faulted glacial pavement (20,000–16,000 yr old) spatially associated with late brittle faults is being reexamined by N. M. Ratcliffe to determine if tectonic or nontectonic origin is applicable. Seven new and three previously identified exposures (Oliver and others, 1970) have been studied. Analysis of these faults suggests that all the reported instances may have formed from ice wedging acting on brittly fractured rocks. Structures suitable for the operation of ice wedging, such as open cracks, shallow dipping lift off floors, and wedge-shaped blocks, are present. Although not proven, the available data suggest that postglacial faults reported from the southern Hudson River valley are nontectonic in origin.

Exotic terranes in the New England Appalachians

Reexamination of the tectonic relations of the New England segment of the Appalachian orogen in light of accreted and exotic terranes indicates that the concept may be applicable. The coastal belt of Massachusetts, Rhode Island, and Maine, or "Avalonia," may have been accreted in latest Acadian or early Alleghenian time, as indicated by its stratigraphy, lack of Acadian deformation, and by paleomagnetic data. This Avalonian terrane is itself composite, consisting of subterraces. It is bounded inboard by high angle faults such as the Clinton-Newbury fault; its contact against the Meguma terrane (offshore and in Canada) is probably also high angle faults. The Carboniferous basins may have evolved on Avalonia through oblique-slip faulting. Inboard of Avalonia is the Merrimack terrane, now largely underlain by Silurian-Devonian rocks. The western margin of this terrane was welded to the Taconian North America in pre-Late Silurian time, but large pieces of this terrane in southern New England may have been removed immediately after the Acadian deformation. The Taconian North American craton margin must be eastward of the present Bronson Hill gneiss domes; in northern Maine it runs from just south of Chain Lakes massif (Jim Pond-Boil Mountain ophiolite) northeast toward the Elmtree ophiolite in northern New Brunswick. This line has excellent gravity and aeromagnetic expressions. The distribution of

ophiolites, age and nature of basement rocks, blueschist terranes, trench melange, island arcs, and continental margin facies tend to support this demarcation. Except for the classic thrust allochthons, such as the Taconic allochthon, the only likely exotic terrane that might be assigned to the Taconian subduction-induced deformation is the Chain Lakes massif itself, which might be a piece of the basement of the opposite shore of Iapetus Ocean and which may be the basement of the Merrimack terrane.

Fault definition and seismicity in the Ramapo seismic zone

Fault mapping in southeastern New York State by L. M. Hall, H. Helenek, and N. M. Ratcliffe has further defined the distribution of brittle (Triassic-like) faults and more ductile features in the Ramapo (N.Y.-N.J.) seismic zone. In Westchester County, Hall has determined that Mesozoic brittle faults trend north-northwest nearly normal to the northeast seismic trends of nodal planes available from fault plane solutions. No evidence for reactivation of northeast-trending structures has been found.

Faults in Pleistocene sediments at trace of Ramapo fault

A trench dug near the ancient shoreline of glacial Lake Passaic (10,000-12,000 yr old) revealed numerous faults in Pleistocene deltaic deposits along the updip projection of the Ramapo fault, as determined from core drilling in bedrock. Numerous southeast dipping, vertical, and northwest dipping high-angle faults show predominant reverse movement with throws up to 2 cm. Analysis of the faults by B. M. Stone and N. M. Ratcliffe indicates that the numerous faults terminate downward against bedding and are thus intrastatal. The faults appear to be compaction, syndepositional faults rather than tectonic in origin.

Seismo-tectonic model for Ramapo seismic zone, New York and New Jersey

A seismo-tectonic model developed by N. M. Ratcliffe for the Ramapo seismic zone and lower Hudson River valley area suggests that current seismicity here is controlled by the structure of Middle Proterozoic basement gneiss. Where this basement forms shallow level thrust sheets or is deeply buried, no seismicity occurs; where highly faulted basement rocks are exposed near the surface, recurrent earthquakes do occur.

APPALACHIAN HIGHLANDS AND THE COASTAL PLAINS

Geology of the Piedmont between the Brevard and Towaliga fault zones, central Georgia

The high-grade metamorphic terrane of the Georgia Piedmont between the Brevard and Towaliga fault zones in the Atlanta and Griffin quadrangles is composed of three groups of stratified metasedimentary and metavolcanic rocks that crop out in two major, refolded synforms separated by a complex antiformal area that shows numerous fold interference patterns. The synforms are interpreted by M. W. Higgins and R. L. Atkins as reclined second-generation folds that have folded first-generation fold nappes and have been modified by three subsequent fold generations. The first and second fold generations are separated by an angular unconformity that regional extrapolation indicates may be roughly equivalent to the Taconic unconformity. The three stratigraphic groups, the Atlanta Group, the "Griffin group," and the "La Grange group" are related by common units, the most distinctive of which are a gondite (spessartine quartzite) and a closely associated, finely laminated impure marble. The marble, an ortho-quartzite, and a distinctive amphibolite unit tie the three groups to the "Opelika group" in the Alabama Piedmont. The stratified rocks have been intruded by six major granitic bodies and numerous smaller plutons. Four of the six major bodies are of batholithic size. The largest has contact aureoles in which mafic rocks have been thermally altered, epidotized, and subjected to copper mineralization. Three swarms of northeast-trending mafic dikes in the Griffin quadrangle are younger than the granites and all deformation but are older than northwest-trending Mesozoic diabase dikes.

Cambrian paleogeographic features of the central Virginia Piedmont

Geologic mapping by Louis Pavlides indicates that much of the central Virginia volcanic-plutonic belt of Cambrian age(?) has been thrust westward concomitant with the destruction, by thrusting, of an associated back-arc basin that was adjacent to the west of the volcanic-plutonic belt. During the destruction of the back-arc basin, tectonically disrupted ocean-floor and associated basin-floor volcanics were deposited as debris in front of the advancing thrusts to form the olistostromal melange zones that now contain blocks and boulders of serpentinite, metagabbro, and amphibolite. Several imbricated melange zones now represent the remnants of the back-arc basin. The easternmost melange zone, that closest to the Chopawamsic

Formation (volcanic) of the central Virginia volcanic-plutonic belt, contains felsic and mafic metavolcanic fragments of the Chopawamsic Formation. These were apparently shed from the Chopawamsic as it was being thrust westward and accumulated as olistoliths in the easternmost melange zone.

The west border of the melange terrane is in thrust contact with a unit of calcareous to noncalcareous siltstone and schist that includes the Everona Limestone of early Paleozoic age and which as a unit discontinuously overlies the Catoctin Formation of Late Proterozoic age. This siltstone-, schist-, and limestone-bearing unit probably formed as a thin deposit upon the eastern margin of Cambrian North America, which was bordered here by the Catoctin Formation and the subjacent rocks of the Blue Ridge province.

Successively outboard (eastward) from the "Blue Ridge massif" continental margin of North America, therefore, were the back-arc basin and the island arc now represented by the metamorphosed rocks of the central Virginia volcanic-plutonic belt. Presumably outboard from the arc in the ocean (Iapetus?) proper to east, there was a trench and an associated westward-dipping subduction zone (Pavrides, 1981).

The trench and back-arc basin along the Cambrian margin of eastern North America were destroyed by thrusting prior to about 440 m.y. ago. This whole-rock Rb/Sr isotopic age was obtained by J. G. Arth for the Ellisville pluton that intrudes and thermally metamorphoses rocks of the melange zone. Thus, this deformational event is a Taconic event, although some of the thrusting may have started earlier.

Studies of depth of weathering on Atlantic Coastal Plain formations

Investigations by J. P. Owens in 1981 included studies of the depth of weathering on surfaces of different ages in the Cape Fear area. The relative depth of weathering and the type of mineral assemblages produced have been used earlier as an age indicator in the Chesapeake Bay area.

One of the main minerals used to determine the age of weathering in the Chesapeake Bay area is gibbsite, the amount of which generally increases with age. Surfaces of comparable age between Chesapeake Bay and Cape Fear revealed that the Cape Fear surfaces were notably deficient in gibbsite in all cases.

Two possible explanations for this phenomenon are that (1) the original detrital minerals necessary to produce gibbsite (mainly feldspar) were absent or present in very small amounts in the surface sands of Cape Fear as compared with the surface sands of the Chesapeake Bay area, or (2) the surface sands of the Cape Fear area were stripped extensively postdepositionally. The latter

interpretation is favored. The stripping of the near-surface sands in Cape Fear appears to be related to the formation of widespread surface depressions, "Carolina bays," found on nearly all of the surfaces in the area. One theory explaining the formation of these bays is deflation, which would provide the mechanism for the removal of the upper gibbsite-bearing soil profiles over a wide area.

Effects of Pleistocene glaciation on development of New River terraces, Virginia

Mapping by H. H. Mills along a 100-km reach of the New River in southwestern Virginia shows that unpaired river terraces are more abundant below 12 m and above 30 m. Weathering characteristics, including color, grain-size distribution, and heavy-mineral content, suggest a post-Wisconsinan age for the lower terraces. Terraces that are more than 30 m above river level are hypothesized to have formed during the Sangamon, a time of relative stream stability that came to an end with the onset of the Wisconsinan and more rapid downcutting.

Structures in the Roanoke recess area, Virginia and West Virginia

A geologic map of Giles County and adjacent areas in southwestern Virginia and southeastern West Virginia is currently being compiled by R. C. McDowell from published and unpublished reports and other data and is being supplemented by field mapping. The study area is along the western side of the Valley and Ridge province just south of the Roanoke recess (or Virginia promontory), which marks the boundary between the central and southern Appalachians. Preliminary results show the presence of previously unrecognized topographic and structural features of central Appalachian trend within the area of dominant southern Appalachian structures. The origin of these features, as well as the deep-seated Giles County seismic zone, which also has a central Appalachian trend, is unknown; it is hypothesized that they may represent structures of central Appalachian origin that have been affected by younger southern Appalachian deformation.

An Avalonian terrane in the Charlotte 2° quadrangle, North and South Carolina Piedmont

The three eastern lithotectonic belts in the Charlotte 2° quadrangle are, from east to west, the Carolina slate belt, the Charlotte belt, and the Kings Mountain belt. On the basis of petrographic, fossil, and isotopic evidence, these lithotectonic belts appear to be segments of an Avalonian terrane, perhaps an island-arc-basin complex, according to D. J. Milton, J. W. Horton,

Jr., and Richard Goldsmith. In the Carolina slate belt, rhyolitic lavas and tuffs of the Upper Proterozoic Uwharrie Formation are overlain by low-grade, fine-grained clastic sediments (apparently deep water turbidites) and volcanic rocks (largely subaqueous tuffs) of the Lower Cambrian Albemarle Group. Major-element and trace-element studies of the volcanics suggest an island-arc complex, but heavy mineral suites in the siltstones indicate contributions from a continental source. The Charlotte belt is dominated by plutonic rocks and is probably an island-arc core complex. An early igneous complex of ultramafic and gabbroic (ophiolitic?) to granodioritic and tonalitic composition, including some metavolcanic and hypabyssal rocks, is intruded by Silurian to Devonian gabbro, syenite, and granite, and by Pennsylvanian to Permian granite. The Kings Mountain belt consists largely of low- to medium-grade metavolcanic and metasedimentary rocks characterized by marble, quartzite, and quartz-pebble conglomerate, as well as aluminous schists, and is interpreted as a nearer-shore facies than the Carolina slate belt. Apparent correlatives of the principal intrusive units of the Charlotte belt also occur in the Kings Mountain belt.

Supracrustal rocks of the three belts could be age-equivalent or the overall structure could be anticlinorial, having one or both outer belts unconformable on the Charlotte belt. The boundary between the Charlotte belt and the Carolina slate belt is a zone of strong shearing, but probably not one of regional-scale displacement. This structure, known as the Gold Hill shear zone, contains major polymetallic sulfide and gold deposits. No evidence is available as to whether the Avalonian belts are, or are not, allochthonous. The boundary of the Kings Mountain and the Charlotte belts with the Inner Piedmont to the west is, however, characterized by repeated faulting along the Kings Mountain shear zone and along the more brittle Eufola fault zone. Both zones are metamorphic as well as structural discontinuities. A narrow zone of spodumene pegmatite dikes, containing the largest developed reserve of lithium in the world, is located in the Inner Piedmont within a few hundred meters of the Kings Mountain shear zone.

The Inner Piedmont belt consists of polydeformed, medium- to high-grade gneisses and schists intruded by lower Paleozoic synkinematic granites. Foliation is characteristically gently dipping, in contrast to the steep dips in the adjacent Kings Mountain and Charlotte belts. The Inner Piedmont is separated from the stacked thrust slices of the Blue Ridge province by the Brevard zone, a complex of ductile and brittle faults. The Inner Piedmont, like the Blue Ridge, is probably allochthonous; seismic profiling by Harris and others (1981) suggests a series of thrust plates above a master

thrust at a depth of 6 to 15 km. A single occurrence of charnockite within the Inner Piedmont suggests Grenville basement within the stack. A few similarities in lithology between the western part of the Kings Mountain belt and zones within the Inner Piedmont belt (including the "Chauga belt") suggest that the Inner Piedmont rocks may be, in part, at least derived from the Avalonian terrane.

A high Taconic slice in the Pennsylvania Piedmont

While mapping in 1981 in low-grade phyllites of the South Valley Hills (SVH) in the Piedmont west of Philadelphia, P. T. Lyttle recognized a tectonic slice of Taconic-like rocks that contain phyllonite zones. Along their northern contact, the phyllites are thrust over, and perhaps included as slivers in, the Conestoga Limestone of Cambrian to Ordovician(?) age. Along their southern contact, the phyllites lie structurally beneath the Peach Bottom Slate, Peters Creek Schist, oligoclase-mica schist of the Wissahickon Formation, and Proterozoic gneisses of the West Chester anticline. Serpentinite bodies along and south of this southern fault zone are absent to the north. The SVH phyllites are greenish-gray to silver-gray rocks that weather to a dark olive green and contain zones of abundant white-weathering albite porphyroblasts and large magnetite octahedra in a fine-grained chlorite-sericite-quartz matrix. The albites commonly are zoned; their rims are free of inclusions, but their cores have streams of inclusions that show rotation of an early foliation. In the SVH, these inclusions represent the same metamorphic grade as the matrix, whereas 65 km southwest, along strike in Carroll County, Md., the inclusions may preserve evidence of an earlier, slightly higher grade of metamorphism than that recorded by the surrounding matrix. All these characteristics suggest similarities to some of the units of the high Taconic slices of Vermont and Massachusetts (Dorset, Greylocke, and Everett slices). In Pennsylvania, the Taconic-like rocks of the Hamburg Klippe consist largely of Lower Ordovician rocks. The SVH phyllites may consist largely of Cambrian and older rocks like those of the higher Taconic slices and, therefore, may be a suite of allochthonous Taconic rocks in the Maryland-Pennsylvania Piedmont.

Soil chronosequences and ^{10}Be isotopic dating in mid-Atlantic States

M. J. Pavich and H. W. Markewich have demonstrated that characteristics of soils in chronosequences can be qualified and used to approximate ages of Quaternary surfaces on Coastal Plain sediments. ^{10}Be in soils has been analyzed by Louis Brown, Department of Terrestrial Magnetism, Carnegie Institute. Analyses of

^{10}Be , a cosmogenic isotope of half life 1.5 m.y., from four soils in a chronosequence show that ^{10}Be accumulation fits a simple line function.

Stratigraphy and structure of the Chesapeake Group in Virginia and Maryland

During fiscal year 1981, W. L. Newell, Lucy McCartan, and R. L. Jacobson measured detailed stratigraphic sections of the Chesapeake Group in Virginia and southern Maryland. From these sections, extensive photomosaics of river bluffs, well logs, and bridge borings, cross-sections that correlate classically zoned fossiliferous units with nonfossiliferous, near-shore shelf and terrestrial facies have been compiled. The fossiliferous and nonfossiliferous units are interpreted to show a repeating history of transgressive and regressive events.

The lithostratigraphic framework indicates that the Chesapeake Group consists of two major sequences separated by an angular unconformity. The lower sequence includes the Calvert, Choptank, and St. Marys Formations of Miocene age. The upper sequence includes the Eastover and Yorktown Formations of late Miocene and Pliocene ages respectively. Regional mapping indicates that the lower sequence was deposited in the Salisbury embayment to the east, whereas, the upper sequence was deposited in the Albemarle embayment to the southeast. The southward shift of the depocenter indicates uplift of the southern Maryland and northern Virginia area during subsidence of the Albemarle embayment.

On the local scale the data show that the faunal zones are laterally discontinuous, that the upper zones of the Choptank Formation are facies of the St. Marys Formation, and that, in all units, facies change systematically across hinge lines and troughs, which are underlain by subsurface faults thought to be controlled by sub-Coastal Plain tectonics.

Polydeformed rocks in the Lowndesville shear zone, South Carolina and Georgia

Studies by A. E. Nelson show that deformed fabrics in rocks of the Lowndesville shear zone range from mesoscopic to microscopic in size; they include folds, mylonitic deformation, and cleavages, as well as a variety of fabrics attributed to both ductile and brittle deformation. Generally, deformation intensity seems to grade from less deformed Inner Piedmont rocks, showing minor crush breccia zones to highly deformed phylonites of the Kings Mountain belt. The shear zone boundaries appear to be gradational.

The ductile and brittle fabrics suggest the following deformational history: ductile deformation was domi-

nant in most of the shear zone with localized concomitant brittle deformation; folding of mylonitic foliation formed some rootless isoclinal folds; late stage ductile deformation was associated with development of penetrative cleavage; a stage of folding produced late north-northeast trending folds and associated slip cleavage; one or more periods of fracturing occurred during and after the mylonite formation, as well as some seismic faulting of unspecified age, to form minor pseudotachylytes.

Correlation of aeromagnetic patterns with major lithotectonic units in the southern Appalachian Mountains

According to A. E. Nelson, aeromagnetic patterns over three major lithotectonic units (the Valley and Ridge rocks, the Great Smoky thrust sheet, and the Hayesville thrust sheet and associated Helen belt), which underlie parts of the Greenville and Knoxville 2° quadrangles in the southern Appalachian Mountains, show that most magnetic anomalies over the Great Smoky thrust sheet and the Valley and Ridge rocks have long wavelengths with low amplitudes that reflect deeply buried magnetic source rocks in the Middle Proterozoic(?) basement. Anomalies in the Hayesville thrust sheet and Helen belt usually have short wavelengths with higher amplitudes that represent source rocks at or near the surface. An aeromagnetic lineament, the Clingman lineament, crosses parts of the Valley and Ridge rocks and the Great Smoky thrust sheet and separates magnetic gradients originating in magnetic source rocks in the basement that have N.15E. trends on its northwest side from gradients with a N.45E. trend on its southeast side. The Clingman lineament represents a major discontinuity in the Middle Proterozoic(?) basement.

Lower Jurassic igneous rocks in the Culpeper Basin, northern Virginia

Remanent magnetization determined in 78 cores from six diabase sills, four diabase dikes, and three basalt flows in the Culpeper Basin shows directional consistency within each site and between sites, according to B. D. Leavy (USGS), and C. A. Raymond, B. B. Ellwood, and Lisa Chaves (University of Georgia). Calculated pole positions plot on the polar wander path for North America at about 200 m.y., but yield pole positions intermediate to those of the 175–190 m.y. paleopoles previously calculated in the Hartford Basin. Thus they estimate an age of 180–185 m.y. for the igneous rocks of the Culpeper Basin.

Preliminary dating of the same suite of igneous rocks by J. F. Sutter (USGS) indicates whole rock $^{40}\text{Ar}/^{39}\text{Ar}$ plateau ages of about 197 ± 4 m.y. The ages from dikes and sills are highly concordant and consistent with a

very small margin of error for the apparent age. This is consistent with the tight grouping of paleomagnetic pole positions; however, the $^{40}\text{Ar}/^{39}\text{Ar}$ age data suggest that pole position and the age of igneous rocks in the Culpeper Basin are about 195 m.y. old.

Emplacement of these igneous rocks through continental crust accompanied the early Jurassic rifting event that preceded the opening of the central Atlantic Ocean to the east.

Amino-acid dating of fossil shells in the Atlantic Coastal Plain

Age estimates for Pleistocene formations determined from amino-acid ratios in mollusks were compared with relative and absolute age estimates for the same units determined from U-series coral dates, biostratigraphy (mainly mollusks and ostracodes), magnetic stratigraphy, and lithostratigraphy. Pleistocene units at numerous localities in the Southeastern United States Coastal Plain were studied by Lucy McCartan, J. P. Owens, B. W. Blackwelder, and B. J. Szabo (USGS), D. F. Belknap (University of Southern Florida), J. F. Wehmiller (University of Delaware), Nivat Kriausakul (University of Texas), R. M. Mitterer (University of Texas), and J. C. Liddicoat (Lamont-Doherty Geological Observatory). There is fair to good correspondence and reproducibility of age estimates determined from D/L ratios of leucine and those determined from the ratio isoleucine/alliosoleucine in samples from the test area between New Bern, N.C., and Charleston, S.C. In addition, there is good agreement of the amino-acid ages with U-series coral ages in some areas. However, amino-acid ratios from the Socastee Formation at Myrtle Beach, S.C., almost completely overlap the ratios from the Wando Formation at Charleston, 170 km to the south. The Socastee contains 200,000-yr-old corals, and the Wando has yielded several coral ages of about 90,000 yr. Hence, the amino-acid data appear to suggest that the two formations represent a coeval unit, whereas the coral dates suggest two temporally distinct units. One interpretation of the amino-acid data, which would resolve the discrepancy, is that a steep temperature gradient caused the overlap in the amino-acid ratios; that is, the D-enantiomer production was retarded at Myrtle Beach by cooler temperatures during the two glacial periods subsequent to deposition of the Socastee Formation.

Geology of Tertiary sediments near the Cooke fault, Charleston, South Carolina

Tertiary Coastal Plain sediments located 25 km northwest of Charleston, S.C., near Cooke Crossroads, Dorchester County, have been studied through the use of cuttings, cores, and geophysical logs from water wells

and stratigraphic test holes. Fossils studied by J. E. Hazel, L. M. Bybell, and L. E. Edwards indicate that the units are of late Paleocene, early Eocene, middle Eocene, late Eocene, and late Oligocene age. According to G. S. Gohn and E. M. Lemon, these units vary considerably in thickness and are separated by unconformities with as much as 60 m of relief. The Cooke fault, located about 1 km southeast of Cooke Crossroads, was identified on seismic profiles. It is a northeast-trending, northwest-dipping reverse fault that deforms reflectors correlated with Coastal Plain units as young as Paleocene. The distribution and thickness of lower Eocene and younger beds, shown by the drill-hole data, are not affected by faulting. Rather, the Eocene and Oligocene units dip to the northeast and thicken in that direction. In addition, middle Eocene limestones present on the seismically defined upblock of the fault are not present on the seismically defined downblock. From these data, it is concluded that the rate of post-Paleocene movement on the Cooke fault was not large enough to control or localize Eocene and Oligocene erosion and deposition and that the effects of Cenozoic movement on faults in the Charleston area may be subtle and difficult to detect in the Cenozoic Coastal Plain.

CENTRAL REGION

Supracrustal stratigraphy and geochemistry, northern Wisconsin

A shallow-water sedimentary rock sequence underlies the Quinnesec Formation and overlies the basement Dunbar gneiss in the Florence Southeast quadrangle in northeastern Wisconsin. This sedimentary sequence, metamorphosed to amphibolite grade, includes quartzite, marble, calc-silicate rocks, biotite schist, and meta-arkose. Stromatolites are present in some carbonate units. K. J. Schultz and P. K. Sims tentatively correlate this sequence with basal units of the Marquette Range Supergroup, thus establishing an Early Proterozoic age for the Quinnesec Formation.

Newly recognized gneiss dome, northeastern Wisconsin

The Dunbar gneiss dome is a newly recognized feature of the Proterozoic crystalline terrane of northeast Wisconsin, delineated during geologic mapping by P. K. Sims and K. J. Schulz in 1982. The dome is 20 km by 30 km across, trends northwest, and has a structural relief greater than 1 km. The core of the dome is composed of complexly deformed and metamorphosed biotite gneiss, foliated megacrystic granite, and foliated gray tonalite. It is unconformably mantled by less deformed metavolcanic rocks of the Quinnesec Formation

and, locally, by quartzite, meta-arkose, marble, calc-silicate rock, and biotite, hornblende, and pyroxene-bearing schist. These rocks dip steeply and face stratigraphically outward, as indicated by pillow structures in the lavas. Metamorphic zoning is concentric, having amphibolite facies in the core and in the inner part of the mantle and greenschist facies in the outer part. Many small bodies of compositionally diverse granitoid rocks are in the inner part of the mantle. The core is interpreted as a window exposing part of an extensive terrane of Early Proterozoic (about 1,860 m.y.) age that was dynamothermally metamorphosed prior to diapirism. The Early Proterozoic crystalline sequence is inferred to underlie northern Wisconsin, but evidently is absent in northern Michigan.

Lake Superior Basin geology and tectonics

A memoir on the geologic and tectonic history of the Lake Superior Basin was completed (Wold and Hinze, unpub. data, 1982). Twenty papers on the geology and geophysics of the Lake Superior Basin present an integrated multidisciplinary approach in which each geologic discipline built upon the results of previous studies and has led to the acceptance of the theory that the Lake Superior Basin is a surface manifestation of a major crustal rift. However, caution must be used in extending the Lake Superior Basin model to the entire Midcontinent Rift System because of the many variations possible in tectonism, igneous activity, and the effect of subsequent deformation along the length of the rift.

ROCKY MOUNTAINS AND THE GREAT PLAINS

IGNEOUS ROCKS

Geology of the Anaconda-Pintlar Wilderness Study Area, Montana

Mapping by C. A. Wallace, J. M. O'Neill, D. J. Lidke, and D. A. Lopez shows that rocks exposed in the Anaconda-Pintlar Wilderness Study Area in southwestern Montana consist of two major types: (1) sedimentary rocks of Proterozoic and Paleozoic age, which are exposed over much of the central and northwestern parts of the area, and (2) Cretaceous to Tertiary granodioritic to granitic plutonic rocks, which occupy much of the remaining part of the area. The sedimentary rocks are present as a series of stacked thrust plates that show older-over-younger as well as younger-over-older thrust relations. The thrust plates have been folded and intruded by the plutons. Intrusion of plutons in the

southwestern part of the area was commonly accompanied by high-grade synkinematic metamorphism. Sedimentary rocks adjacent to plutons in the northeastern part of the area generally show only contact metamorphic effects. During the Tertiary, sediments were shed from the area and are now preserved in the Big Hole Valley to the south. The Anaconda-Pintlar range apparently was raised to its present elevation in late Tertiary and early Quaternary time along northeast-trending, high-angle faults.

Mapping at the eastern edge of the Idaho batholith, Montana

Geologic mapping in the southwestern part of the Sapphire Mountains resulted in delineation of part of the eastern edge of the Idaho batholith. In that area, mapping by S. E. Zarske and C. A. Wallace has separated two granodiorite bodies and an augen gneiss, which is of uncertain relation to the granodiorite plutons. Prominent high-rank metamorphic borders formed around the plutons in thrust-faulted rocks of the Missoula Group. These metamorphic rocks are characterized by lit-par-lit injection of leucocratic granitoid rock and by ptygmatic folding that has cross-cutting relations to disharmonic folds in the metasedimentary rocks. Although detailed analysis of these relations is lacking, it appears that more than one event of folding was associated with intrusion of the Idaho batholith and that there may have been several plutonic events that characterize this easternmost part of the batholith.

Pyroxenite stocks mapped in the same general region by C. A. Wallace and D. C. Ferris may postdate intrusion of the Idaho batholith. Pyroxenites are associated with leucosyenite, hornblende syenite, and hornblendite dikes and pods. The pyroxenite stocks may be related to a linear, east-trending body of quartz diorite and tonalite that is about 0.5 km wide and 4 km long. This quartz diorite stock and the pyroxenite stocks are the only major east-west oriented plutons in the Sapphire Mountains, and are thus a regional petrologic and structural anomaly.

Geology of the Bitterroot lobe of the Idaho batholith

Mapping by M. I. Toth, M. D. Bradley, Lawrence Garmenzy, D. S. Hovorka, K. I. Lund, M. E. Koesterer, W. E. Motzer, R. R. Reid, and W. R. Greenwood in the Bitterroot lobe of the Idaho batholith has determined the plutonic history of the lobe. Cretaceous foliated hornblende-biotite tonalite and quartz diorite form the western border of the lobe and occur along the northeastern border as isolated plutons. Cretaceous to Tertiary foliated biotite granodiorite to monzogranite forms the major part of the lobe and intruded the

tonalite on the west, southwest, and north. Complex migmatite terrane generally separates tonalite from granodiorite to monzogranite plutons and involves septae of Proterozoic metasedimentary rocks. Large, Eocene subalkalic epizonal plutons intruded the Proterozoic metasedimentary rocks and all the earlier phases of the Bitterroot lobe on the northern, southwestern, and southern sides. Possible related rhyolitic to andesitic tuff and flow deposits are preserved in two places in downdropped fault blocks and locally overlie parts of an epizonal pluton on the south side of the Bitterroot lobe.

Studies in Wheeler Peak, Latir Peak, and Columbine-Hondo area, New Mexico

Geologic mapping by J. C. Reed, Jr., and P. W. Lipman (USGS), and J. R. Robertson (New Mexico Bureau of Mines) reveals that Precambrian rocks in the core of the Laramide Sangre de Cristo uplift have been invaded by batholith bodies of granitic rocks and swarms of associated dikes of middle Tertiary age. The Questa caldera represents a major eruptive center fed by the intrusive system. The intrusive rocks were emplaced during early stages of extension along the Rio Grande rift. Listric faults rotate welded tuff erupted from the caldera by as much as 90°; Tertiary intrusive bodies occupy space provided by movement along some of the fault zones. Major molybdenum orebodies are associated with granitic intrusions along the south wall of the Questa caldera.

Tectonic framework of Chief Joseph plutonic complex, southwest Montana

The Chief Joseph plutonic complex is an east-trending, linear belt of foliated granitic plutons and associated high-grade metamorphic host rocks, and of younger, nonfoliated intrusive rocks northwest of the Big Hole Basin in southwest Montana. The complex is about 70 km long and about 40 km wide and is along a major east-trending shear zone that is the southern boundary of the Grasshopper thrust plate. The shear zone appears to reflect recurrent movements along a basement fault zone that also controlled the location of magmatic intrusion. Studies by N. R. Desmarais showed that the plutonic complex was emplaced in three major episodes of magmatism that span late Cretaceous to middle Tertiary time.

The earliest magmatic episode, in the Late Cretaceous (about 80 m.y. ago), slightly overlapped and followed high-grade metamorphism and isoclinal folding accompanied by the development of axial planar foliation in the host rocks. The granitic rocks are regionally foliated

concordantly with the axial planar foliation in the host rocks. This foliation in the granitic rocks seems clearly to be a result of regional deformation associated with thrusting and not the result of igneous processes in the individual plutons, because structures associated with thrusting in the host rocks of the upper plate can be traced through a transition zone into isoclinally folded plastic structures in the lower plate.

The second magmatic episode was in the Eocene (about 50 m.y. ago), when the emplacement of shallow epigenetic plutons accompanied regional uplift. These plutons are broken both by east-trending faults, parallel to the major shear zone, and by northeast-trending faults that break the older east-trending fault system. Uplift continued along the northeast-trending fault zones, and in the mid-Tertiary emplacement of rhyolitic to latitic dikes of the third magmatic episode occurred along the northeast-trending fault zones, accompanied by the eruption of related tuffs and breccias.

STRATIGRAPHY

Age of Colorado Plateau margin, central Arizona

Miocene and Pliocene(?) volcanism, in concert with extensive erosion and normal faulting, has sculptured the Colorado Plateau margin in central Arizona. Mapping by G. E. Ulrich in the West Clear Creek region of the eastern Verde Valley and southwestern margin of the Plateau supported the conclusion of Peirce and others (1979) that the elevated plateau margin existed before middle Miocene time.

A structural lowering from east to west of approximately 680 m has been determined along the 40-km course of West Clear Creek. About 380 m of this structural relief is accounted for by normal faulting and 300 m accounted for by westward dip of the Permian sedimentary rocks. A prominent fault (the Cash Tank fault), 18 km east of the present plateau rim, separates, on its upthrown east side, an area of thin basaltic cover typical of the plateau in this region from a large volcanic pile over 450 m thick to the west. These volcanic rocks are mainly basaltic with abundant pyroclastic material but also include minor andesite and dacitic to rhyolitic ash flows. Near the bottom of the pile, a late Miocene age of 10.6 ± 0.3 m.y. for a basalt has been reported by Peirce and others (1979).

A broad paleovalley west of the Cash Tank fault and about 10 km wide and 400 m deep was carved at or inside the plateau margin before volcanic infilling. The basal deposits in this valley are coarse conglomerates

derived mostly from the Permian rocks of the valley walls.

Thus the high-standing Colorado Plateau rim and west-facing escarpment in this area existed as early as late Miocene and, in view of the extensive tectonic and erosional record that preceded volcanism, probably existed well before that time.

Details of Chinle stratigraphy in northwest New Mexico

New insights into the stratigraphy of the Upper Triassic Chinle Formation of northwest New Mexico came from study by J. F. Robertson of electric logs from deep drill holes. The Chinle Formation consists of lenticular red-bed deposits from fluvial channels, flood plains, and continental basin fill. The Owl Rock Member, containing beds of cherty limestone near or at the top of the Chinle, and the distinctive buff arkosic Sonsela Sandstone Bed in the middle of the Petrified Forest Member are generally useful as stratigraphic marker beds in a sequence of beds otherwise deposited discontinuously. Correlations between the well-studied area around Mesa Gigante, 42 km west of Albuquerque, and the area near Grants have been rendered difficult by an intervening gap 68 km wide, where the Chinle Formation is buried beneath younger Jurassic to Tertiary rocks. In addition, an unconformity at the top of the Chinle gradually cuts out the Owl Rock Member eastward from Gallup so that it does not appear in drill holes east of Grants and is lost as a marker.

Drill-hole data in the covered interval indicate that significant changes take place in the lithologic character of the Chinle from west to east. Eastward from its prominent exposures north of Grants, the Sonsela Sandstone Bed thins drastically, then pinches out abruptly. Its termination is accompanied by thickening of the Chinle Formation as a whole, however, and a corresponding decrease in the ratio of sandstone to shale and mudstone. A similar change occurs on the east side of the San Juan Basin, beginning with exposures at the margin of the Nacimiento Uplift. Southwestward and westward from the uplift, the Chinle Formation thickens in the subsurface while sandstone and conglomerate beds in its lower part become finer grained, thinner, and include more mudstone and shale. The convergency of sedimentary trends from east and west outlines a depositional basin whose sediments, fining basinward, indicate derivation from at least two separate source areas. The Sonsela Sandstone Bed appears to have originated to the southwest as a large fan lobe deposited by streams that dropped most of their coarse load near the margin of the basin.

Distribution of Pearlette family volcanic ash marker beds

G. A. Izett and R. E. Wilcox completed compilation of a map that shows the known distribution of four important ash-bed stratigraphic markers in the upper Pliocene and Pleistocene deposits of the Great Plains, Rocky Mountains, Basin and Range provinces, and parts of California, Louisiana, and Saskatchewan, Canada (G. A. Izett and R. E. Wilcox, unpub. data, 1982). Formerly known as Pearlette ash beds, they are named for their respective source-area rock units in the Yellowstone National Park region: members A and B of the Lava Creek ash (0.62 m.y. age), Mesa Falls ash (1.27 m.y.), and Huckleberry Ridge ash (2.02 m.y.). A text accompanying the map describes the history of research on the Pearlette beds, their isotopic ages, and their distinguishing characteristics. A list of the localities by State and county is keyed to the map.

Influence of storms and paleotectonism on shelf sedimentation in Montana, South Dakota, and Wyoming

Studies by D. D. Rice indicate that the Upper Cretaceous Mosby Sandstone Member of the Belle Fourche Shale and Turner Sandy Member of the Carlile Shale occupy the shallow western shelf of a north-trending epicontinental seaway of the northern Great Plains. The Mosby and Turner are composed of thin units (average 1.5 m) of very fine grained sandstone interbedded with shale. The base of each bed is a planar to undulating erosional surface, and the top is gradational with the overlying shale. The dominant sedimentary structure is hummocky cross stratification. Characteristics of the sandstone units suggest deposition by storm waves on ancestral topographic highs that were episodically uplifted. The upward sequence of sedimentary structures within a single bed indicates decreasing energy levels and deposition during waning stages of a storm. Sediments in the Mosby, which form a widespread lobe in central Montana, were transported by the interaction of waves and southward-flowing, semipermanent current as far as 1,100 km from the strandline during fair-weather conditions. The sand was later concentrated on the central Montana uplift by storm waves and distributed into discontinuous bodies of limited extent (several square kilometers). In contrast, sand in the Turner was emplaced by storm-surge runoff currents as far as 350 km from the strandline. Sole marks indicate a north-northeastward flow that is opposite to direction of flow during fair-weather conditions. The sandstones occur on the flanks of the Black Hills uplift as laterally continuous bodies.

Iridium anomaly at Cretaceous-Tertiary boundary, New Mexico

The Cretaceous-Tertiary boundary in marine rocks is recognized by an abrupt change in microfossil content. At several localities in the world an anomalously high iridium concentration has been found at this horizon. It is postulated that the iridium anomaly originated from debris generated by the impact of a large extraterrestrial object.

Search for a similar iridium anomaly was undertaken in the nonmarine rocks of the Raton basin of New Mexico by an interdisciplinary team consisting of C. L. Pillmore and R. H. Tschudy (USGS), J. E. Fassett (Minerals Management Service), and C. J. Orth, J. S. Gilmore, and J. D. Knight (Los Alamos National Laboratory). In the Raton basin, deposition was apparently continuous across the Cretaceous-Tertiary boundary. In these rocks the boundary is identified by an easily recognizable change in the pollen content of the rocks. Several species that characterize the Late Cretaceous of the Western Interior abruptly disappear. This palynological boundary was identified by Tschudy from core material, and when these rocks were then tested for iridium content by C. J. Orth and others at the Los Alamos Laboratory, they found that an anomalously high iridium concentration was present at this boundary. This coincident occurrence of iridium at the palynological boundary has been narrowed to a 2-cm interval. The iridium anomaly at the Cretaceous-Tertiary boundary in both marine and nonmarine rocks invites speculation regarding a cause-effect relationship for the apparent widespread biotic extinctions at the end of the Cretaceous.

Late Cretaceous orogenic pulses in north-central Utah

Three pulses of uplift indicated by westward-thickening conglomerate tongues occurred during deposition of the Frontier Formation in its westernmost exposures in the Parleys Canyon syncline, 20 km east of Salt Lake City, according to mapping by Bruce Bryant. Pollen identified by D. J. Nichols and megafossils identified by W. A. Cobban (E. A. Merewether and C. M. Molenaar, written commun., 1979) date these uplifts, which must have occurred not far west or northwest of the original depositional site of the Frontier. The first pulse, in late Cenomanian or early Turonian time, produced a tongue of conglomerate that extended as far east as East Canyon Creek; the second, in late Turonian or early Coniacian time, caused an hiatus in the deposition of the Frontier and spread conglomerate 30 km farther east to the Coalville area (Trexler, 1966; Ryer, 1976); the third occurred in the middle Coniacian and produced a conglomerate tongue intermediate in extent between the

two earlier ones. These conglomerates thicken westward rapidly so that about 2,000 m of the 3,500-m thickness of the Frontier Formation is composed of conglomerate in its westernmost exposures. The conglomerates contain mostly rounded clasts of sandstone and lesser amounts of limestone derived from Mesozoic and late Paleozoic rocks. Average clast size is 0.1 to 0.3 m, but a few are as much 1 m in diameter.

Final withdrawal of the sea from north-central Utah and deposition of the Henefer Formation and the Echo Canyon Conglomerate in the Coalville area occurred in the late Coniacian or Santonian.

Although these conglomerates only demonstrate uplift to the west, it is likely that uplift accompanied episodes of movement on thrust faults in the Sevier orogenic belt.

Precambrian rift filling beneath Colorado plains

A thick sequence of graywacke, slate, and chert in the Precambrian basement beneath the plains of southeastern Colorado was identified by Ogden Tweto. The sequence was named the Las Animas Formation and assigned a Late Proterozoic age (Ogden Tweto, 1982). The Las Animas occupies a west-trending belt about 130 km long and as much as 50 km wide, as established from borehole data. It is evidently a deepwater fill in a rift that cut an older Precambrian terrane consisting of gneisses and a granite of 1,300-1,400 m.y. age. The formation closely resembles the Tillman Metasedimentary Group of Ham and others (1964) of the Wichita Mountains province in Oklahoma. The two units also share the same age brackets. Like the Las Animas, the Tillman has been interpreted as a rift deposit. The two units probably represent responses in different areas to the same tectonic event.

Relation of Bishop Conglomerate to Browns Park Formation in eastern Uinta Mountains, Colorado and Utah

Mapping by P. D. Rowley and W. R. Hansen demonstrated that in the eastern Uinta Mountains region the Miocene Browns Park Formation rests directly on the Oligocene Bishop Conglomerate in places where post-Bishop subsidence had lowered the Bishop to the Browns Park depositional level. In these places the Bishop has been called the basal conglomerate of the Browns Park, but elsewhere the Browns Park fills paleovalleys eroded into the Bishop substrate or into the Gilbert Peak erosion surface under the Bishop. Mid-Tertiary collapse of the eastern Uinta Mountains began after Bishop time, but preceded and accompanied deposition of the Browns Park. Further regional warping followed deposition of the Browns Park Formation.

Subsidence along the eastern Uinta crestline was as much as 1,600 m. Gravitational displacement along the Uinta fault reached 800 m, down to the south.

Spokane Formation (Belt Supergroup), northwest Montana

The relation of the Spokane Formation (Belt Supergroup) in its type area to equivalent(?) strata to the west and northwest in the main part of Belt terrane remains elusive. Walcott defined the formation in 1899 for red beds in the Spokane Hills, west of Helena, Mont. Detailed examination by J. J. Connor of the Spokane in and near its type area in the Helena Embayment from 1979 to 1981, however, suggested that the formation as mapped in the Rogers Pass area west of the Hoadley thrust bears little resemblance to the formation in its type area, which is only about 50 km to the southeast.

In its type area, the formation ranges from about 1,200 m to about 1,500 m in thickness. It thickens to the west, toward Helena. West of the Hoadley thrust, the formation is less than 500 m thick. In the embayment, the formation consists of five informal units. West of the Hoadley thrust, it has at most three informal units, only the upper two of which bear any resemblance to units east of the Hoadley. In the embayment, the formation is dominantly siltstone and argillaceous siltstone with a few calcareous sandstones near the base. West of the Hoadley thrust the formation contains up to 25 percent vitreous quartzite in its central part.

A red siltstone in the upper part of the formation in the embayment has been tentatively identified west of the Hoadley where it apparently thins to nothing, further westward. The lower half of the formation in the embayment, which is spectacularly exposed in Little Prickly Pear Creek north of Helena, has not been identified west of the Hoadley.

The Hoadley thrust may have up to 70 km of translation on it (Mudge and Earhart, 1980), and the rapid change in the Spokane across this thrust is presumably due to structural telescoping of lateral facies. The cause of the changes, however, is less relevant to terminology than the fact that changes occur. The provisional recognition of only the uppermost beds of the formation west of the Hoadley thrust, together with the marked changes in lithology and thickness, suggests that in a future paper the name Spokane may be formally restricted to the Helena Embayment.

Stratigraphic relations of the Arapien Shale, central Utah

Previous workers in central Utah have suggested that the Arapien Shale of Middle Jurassic age rests directly on the Navajo Sandstone of Jurassic and Triassic(?) age. Recent fieldwork in Red Canyon, near Nephi, by I. J.

Witkind indicated, however, that a sequence of siltstone, sandstone, and carbonate beds, possibly representing the lower and middle parts of the Twin Creek Limestone of Middle Jurassic age, separates the Arapien from the Navajo.

This sector of central Utah is dominated by the southern Wasatch Mountains, an allochthonous plate emplaced along the Charleston-Nebo thrust fault. The plate is a huge, overturned, almost recumbent anticline; consequently, younger strata underlie older beds, and all beds are overturned. In the following discussion the beds are described in their inverted sequence.

In Red Canyon the Navajo Sandstone is underlain by a series of beds tentatively correlated with five members of the Twin Creek Limestone. In descending (and inverted) order, these are the Gypsum Spring, Slide-rock, Rich, Boundary Ridge, and Walton Canyon(?) Members. The beds tentatively identified as Walton Canyon are directly underlain by the lowermost member of the Arapien, the Twelvemile Canyon Member, a most unusual unit perhaps best visualized as an intrusive sedimentary body. The Twelvemile Canyon Member, throughout central Utah, has been intensely deformed by its contained salt, and in turn has locally intruded and deformed the overlying strata to form fan-shaped diapiric folds. It is uncertain whether the contact between the Twelvemile Canyon Member and the Walton Canyon(?) Member, in the Red Canyon area, is depositional or intrusive. In places, the Walton Canyon(?) beds are tilted vertically; in a few localities they are overturned (thus, oddly, bringing them right-side up). These attitudes imply that the Twelvemile Canyon Member has intruded and bowed up the Walton Canyon(?) strata. It is possible that the Twelvemile Canyon Member originally was in depositional contact with the Walton Canyon(?). Subsequent episodes of salt diapirism may have forced the Twelvemile Canyon Member to bow up and fold back the limestone beds of the Walton Canyon(?).

Exploratory drilling by Placid Oil Company in the Sevier-Juab Valley area has demonstrated that Twin Creek beds (Leeds Creek(?) Member of the Twin Creek Limestone) correlative with the Twelvemile Canyon Member are underlain by a thick sequence of dominantly carbonate strata (D. A. Sprinkel, Placid Oil Co., oral comm., 1981). Sprinkel correlates this carbonate sequence with the Gypsum Springs-Walton Canyon interval of the Twin Creek and notes that these carbonate beds rest on the Navajo Sandstone.

Witkind believes that the Twelvemile Canyon Member of the Arapien Shale is separated from the Navajo Sandstone by the Gypsum Spring-Walton Canyon sequence throughout much of the Sanpete-Sevier Valley area of central Utah.

Stratigraphy of the Lower Belt Supergroup, Glacier National Park, Montana

Stratigraphic studies in the Belt Supergroup of Glacier National Park, by R. L. Earhart, indicated marked facies changes over relatively short distances. For the most part, the units reflect deposition near the margin of the Proterozoic Belt basin. The lower Belt rocks in the eastern part of the park were mostly deposited in a supratidal to intertidal environment. Those in the western part were deposited in an intertidal to subtidal environment. The Altyn Formation, a carbonate unit in the eastern part, grades westward into argillite, siltite, and minor carbonate rocks of the Prichard Formation. The lower part of the Greyson Formation grades westward into thin-bedded green-to-gray argillite and siltite.

A series of thrust faults in the western part of the park are localized in the central part of a salient formed by the trace of the Lewis thrust fault. The thrusts appear to be closely related in time to translation on the Lewis thrust.

SURFICIAL GEOLOGY

Fission-track ages and structure in clinker

The baked and fused rocks that make up the clinker produced by burning of coal beds are also generally marked by slumping, which is always in the direction of the free face. The direction of propagation of the burn is into the outcrop and away from the free face. Thus the direction of propagation is easily inferred if the direction of slumping can be discovered. Small-scale structures in major slump blocks were found to indicate the direction of the slumping. D. A. Coates and E. R. Verbeek developed a method of determining extension direction within slump blocks by the use of stereographic plots showing orientation of faults that bear striations going directly down-dip and orientation of tilted bedding. Because extension is an element of the total slump movement, it is toward the free face and so allows inference of direction of burn propagation. Burning directions at multiple localities in a limited area form a pattern delineating individual ancient fires.

Paleomagnetic directions in clinker collected in Montana by D. A. Coates (USGS), A. H. Jones and J. W. Geissman (Colorado School of Mines), and E. L. Heffern (Bureau of Land Management) have shown magnetic reversals, confirming fission-track ages that place burning as old as the Brunhes and Matuyama magnetic reversals.

Fission-track ages of a boulder of sandstone clinker in a high terrace gravel above the Yellowstone River west

of Miles City, Mont., put a maximum age of the gravel of 4.0 m.y., which is consistent with a proposed Pliocene age of the gravel.

Pinedale deglaciation in the North Fork of the Flathead Valley, Montana

Airphoto analysis and field mapping by P. E. Carrara and R. G. McGimsey along the North Fork of the Flathead River on the western side of Glacier National Park reveal the following chronology during the last major glaciation. The entire region was overrun by the Cordilleran ice lobe whose southern margin lay in the Flathead Lake region of northwest Montana, about 100 km to the south. At this time the valley of the North Fork of the Flathead River lay under at least 1,000 m of ice, as suggested by numerous meltwater channels lying across the broad divides between drainages along the west side of the Livingston Range and by glacially striated boulders on the summit of Huckleberry Mountain. After retreat of the Cordilleran ice lobe from the North Fork of the Flathead Valley, large (15–30 km) valley glaciers continued to flow from the Livingston Range westward into the eastern edge of the Flathead Valley. Evidence of this phase consists of broad U-shaped troughs gouged into the Flathead Valley along the tributary streams and of dead-ice features at points where the glaciers emerged from the high-walled upper segments of the tributary valleys. The lack of well-defined moraines upvalley suggests that retreat of these valley glaciers was rapid.

Scattered high-level terrace remnants along Nowood Creek, Bighorn Basin, Wyoming

During the 1981 field season, R. M. Barker, assisted by R. L. Vincent, was able to identify several small but significant high-level terrace remnants associated with the drainage of Nowood Creek, a tributary of the Bighorn River in Wyoming. Nowood Creek receives water from several tributaries descending the Bighorn Mountains from the east, and its lower terraces are easily distinguished from Bighorn River terraces by an abundance of clasts from Paleozoic and older source rocks in the Bighorn Mountains. Identification of terrace remnants as related to Nowood Creek depends on this abundance of Bighorn Mountain lithologies.

Scattered high-level terrace remnants occur at elevations 110 to 225 m above present stream level. One remnant caps North Butte, a peak 15 km west of present Nowood Creek that constitutes the highest elevation in the intricately dissected badlands of The Honeycombs. The coarser constituents of the high terrace remnants, like those of the lower terraces, are clearly derived from

Bighorn Mountain rocks. The remnants so far discovered along Nowood Creek are too scattered and discontinuous to permit detailed reconstruction of a fluvial chronology.

Volcanic ash on Missouri River-Yellowstone River drainage divide, Montana

Field mapping by R. B. Colton and petrography by R. E. Wilcox contributed to a study of 4.3 m of water-laid volcanic ash underlain by 30 m of sand and gravel and overlain by 6.7 m of sand and gravel. The deposit is on the drainage divide between the Yellowstone and Missouri Rivers, 32 km south of Circle, Mont. N. D. Briggs determined that the zircons in the ash yielded a fission-track age of 7.1 ± 1.4 m.y.

The ash deposit is at an altitude of 1,060 m, which is 410 m above the present Yellowstone River. If one assumes a steady rate of southeastward migration and downcutting of the Yellowstone River during the last several million years, a plot of altitude versus time indicates that primary river terrace sand and gravel deposits at altitudes lower than 732 m are Pleistocene, those between altitudes of 762 m and 945 m are Pliocene, and those at altitudes higher than 945 m are Miocene. The range of ± 1.4 m.y. for the fission-track date indicates that the range of altitude of the Pliocene-Pleistocene boundary is ± 30 m and the range of altitude of the Miocene-Pliocene boundary is ± 60 m. The estimates of altitudes of primary terrace gravel deposits of specific ages apply only to deposits in the Circle-Fallon-Terry area. Altitude ranges of correlative terrace deposits upstream and downstream along the Yellowstone River differ.

STRUCTURAL GEOLOGY

Complex thrusting in Snake River Range, Idaho

The St. John thrust sheet and the overlying Elk thrust sheet are principal components of the Idaho-Wyoming thrust belt. Mapping by D. W. Moore and S. S. Oriol showed that the Elk thrust sheet is cut by at least six thrust slices on Mount Baird in easternmost Idaho. Overthrusting is toward the east, along fault surfaces that strike northward, and involves major stratigraphic offsets. The St. John thrust places Ordovician Bighorn Dolomite and other Paleozoic units on units ranging from the Mississippian Mission Canyon Limestone to the Triassic(?) and Jurassic(?) Nugget Sandstone. The Elk thrust places Cambrian Gros Ventre Formation on Mission Canyon Limestone. The thrust slices repeat parts of the upper Paleozoic sequence, which in

places is isoclinally folded. The fact that higher slices cut lower slices indicates that back-limb thrusts are younger with increasing distance from the main fault. The Mississippian Lodgepole Limestone in one slice is intruded by two andesitic sills, 3 and 10 m thick, which have some associated mineralization.

Deformation of Precambrian rocks along Jemez zone, New Mexico

Studies by J. C. Reed, Jr., showed that plutonic and supercrustal rocks of presumed Early Proterozoic age in the Wheeler Peak area near Taos, N. Mex., exhibit intense cataclastic foliation and lineation and partial or complete recrystallization to phyllonite and mylonite gneiss in a 5- to 10-km-wide zone. The date of this deformation is presumed to be Proterozoic, as diabase dikes of probable early Paleozoic age are undeformed. Although much disrupted by both Laramide and mid-Tertiary deformation, the zone of cataclastic rocks lies along the inferred trend of the Jemez zone, a zone of crustal weakness of inferred Precambrian ancestry, but along which exposed Precambrian rocks have not previously been examined in detail.

Libby thrust belt, northwestern Montana

Tectonic shortening from west to east across the Libby thrust belt in the northwest corner of Montana is greater than previously suspected. Detailed mapping in the west by E. R. Cressman and in the east by R. E. Van Loenen was connected by 1:250,000-scale mapping by J. E. Harrison. A western facies of Belt rocks has been juxtaposed against an eastern facies across a zone of thrusts that is about 25 km wide. Pronounced facies changes occur in all Belt rocks from the Prichard through the Helena-Wallace Formations, a stratigraphic thickness of about 7,600 m. The gradual facies changes characteristic of most formations in most Belt terranes contrast with these abrupt changes, which suggests that the Libby thrust belt represents a tectonic shortening of many tens of kilometers.

Mechanics of joints in the Piceance Creek Basin, Colorado

E. R. Verbeek and M. A. Grout have additional evidence that joint spacings in the Piceance Creek Basin are dependent on layer thickness and lithology of sedimentary rocks. Consistent relations exist in the Piceance Creek Basin and beyond. In the oil shales of the Green River Formation, evidence suggests a long history of clastic-dike intrusion that spans diagenesis and fracture of the oil shales. In the deltaic sands of the Uinta Formation, penecontemporaneous slump blocks contain several sets of joints formed within delta sands

under minimal superincumbent load before the blocks slumped from the delta front.

Monocline southwest of Cedar Creek anticline, Montana

Mapping by R. B. Colton (USGS) and Susan Vuke (Montana Bureau of Mines and Geology) delineated a monocline or fault 8 km southwest of and parallel to the west edge of the Cedar Creek anticline in eastern Montana. The structure, which extends northwestward 60 km from the Montana-South Dakota border to a few kilometers north of Plevna, is marked by a belt of disturbed strata that is about 1 km across and strongly defined. Within the disturbed belt, strata belonging to the Fort Union and Hell Creek Formations dip southwest 10° to 15° , but in areas to the southwest and northwest the strata are nearly horizontal. Colton and Vuke infer that a fault at depth caused the monocline at the surface.

Reserve graben, southwestern New Mexico and eastern Arizona

A study of fault trends in the vicinity of the Reserve graben by J. C. Ratté clarified relations between the graben and the Jemez and Morenci lineaments. The northeast-trending Reserve graben, about 50 km wide, lies between the Blue Range in eastern Arizona near Beaverhead and the northwest flanks of the Mogollon Mountains north of Mogollon, N. Mex. Approximately 1,000 m of stratigraphic throw exists between the Blue Range and the deepest part of the graben at the San Francisco River. The dominant trend of faults within the graben between Morenci, Ariz., and Reserve, N. Mex., is N. 25° to 30° E. Northeast from Reserve, the trend projects along the east edge of the Quaternary Bandera basalt field to an acute intersection with the Jemez lineament between Grants, N. Mex., and Mount Taylor. To the south, the Reserve trend intersects acutely with the projected east-northeast trend of the Morenci lineament. In the Morenci area, however, east-northeast faults are greatly subordinate to north-northeast faults of the Reserve trend. Also in the Morenci area, Precambrian granitic gneisses with north-northeast fabric are intruded by 55- to 60-m.y.-old mineralized quartz monzonite plutons that have a strong north-northeast trend.

Thus, compilations of fault trends in the Reserve-Morenci area seem to indicate that the Reserve graben and the Morenci lineament represent two largely separate structural zones and that the Reserve trend is probably the younger and somewhat stronger structure and could be the southwest extension of a slightly reoriented Jemez lineament.

Thrust faults in the Highland Mountains, Montana

Preliminary results of mapping of Belt Supergroup rocks in the southern part of the Highland Mountains by J. M. O'Neill suggest the presence of at least three thrust plates. The lower plate consists of the lower Belt LaHood Formation, Prichard Formation, and Chamberlain Shale, which probably have not been transported far from their original site of deposition. The middle plate consists of lower Belt argillites, siltites, and middle Belt carbonate rocks and contains tectonic slices of quartzites tentatively correlated with upper Belt Missoula Group rocks. The uppermost thrust plate consists of complexly deformed Paleozoic rocks. Mullion structure, slickensides, and the axes of folds contained in these rocks indicate right reverse slip along major faults; tectonic transport was directed to the east-southeast.

Young faulting, southwestern Wyoming and adjacent Utah

Ground inspection by D. D. Dickey and A. B. Gibbons of about 100 lineaments seen on high-altitude air-photographs indicated about 50 young faults in southwestern Wyoming and adjacent Utah. The faults show a clear spatial association with the valley of Bear River, which they locally help to define. Most of the faults are on the east side of the valley, with the most distant (Rock Creek fault) about 12 km from the valley. Rock Creek fault and the fault at the west edge of the Crawford Mountains have total displacements of more than 100 m, but most of the young faults have displacements of less than 2 m over a length of a few kilometers. The area has low seismicity and plots of earthquake epicenters cannot be identified with specific young faults.

Assignment of faults to the geologically young categories was based mainly on offset of surfaces or materials developed in the current geomorphic cycle. Gastropod shells collected by Dickey and A. J. Crone from alluvium offset by the very young looking Whitney Canyon fault were submitted to G. H. Miller of the University of Colorado for amino acid age determination, yielding ages of 2,000 and 7,000 yr. Age estimates for three faults, including the Whitney Canyon fault, based on the relation between fault-scarp height and slope (Bucknam and Anderson, 1979), all were in the range of 100,000 yr.

The study area is within the Middle Rocky Mountain physiographic province about 30 to 40 km east of the boundary of the Basin and Range province. Descriptions of the geometry of these young faults at depth have not been published, leaving it unclear whether steep Rocky Mountain-type faults or listric Basin and

Range-type faults are developing in the transition zone between the two provinces.

MINERAL RESOURCES

Potential petroleum traps in Pennsylvanian rocks, northeastern New Mexico

Mapping of the southern Sangre de Cristo Mountains, N. Mex., and biostratigraphic analyses of outcropping Pennsylvanian and Lower Permian rocks by E. H. Baltz and D. A. Myers indicate that these marine and mixed marine-nonmarine rocks are absent at the southeast margin of the mountains southwest of Las Vegas because of angular unconformity with overlying non-marine Permian rocks. However, the mainly marine rocks thicken northward, and near Mora, about 45 km north of the wedgeout, they are more than 2,050 m thick. Most of the thickening takes place within the Sandia Formation (Morrowan and Atokan), which contains thick units of dark-gray shale and interbedded sandstones and arkosic conglomerates.

The Sandia is overlain by the Porvenir Formation (Des Moinesian). At the south, the Porvenir is mainly limestone and calcareous shale and contains bioherms and biostromal banks. Northward this facies grades into shales that contain sandy limestone, some oolite, and thick units of sandstone and arkosic conglomerate. The Porvenir is overlain, with local unconformity, by the Alamitos Formation (Des Moinesian through Virgilian and, locally Wolfcampian). The Alamitos consists of gray, greenish-gray, and red shale and interbedded limestone, sandy limestone, and thick conglomeratic arkoses deposited as marine and nonmarine units.

East-west variations in thickness of all the Pennsylvanian units occur because of syndepositional tectonic activity of three northerly trending Paleozoic uplifts and intervening basins that correspond closely with Cenozoic anticlines and synclines. This correspondence of ancient and present structures in outcrop areas suggests that updip wedgeouts of some Pennsylvanian stratigraphic units occur in the subsurface of the west limb of the Las Vegas basin east of the mountains. Therefore, stratigraphic traps may be present in lithofacies where potential petroleum source beds and reservoir beds are closely associated. The possibility of traps is enhanced by Cenozoic thrust faults that may have displaced Precambrian basement rocks as much as 1 to 2 km eastward across Pennsylvanian rocks on the west limb of the Las Vegas basin.

TECTONICS

Direction of post-Oligocene klippen movement, Markagunt Plateau, Utah

Klippen-like features as much as 0.6 km² in area consisting largely of volcanoclastic units were reported in the 1970's in the northern and central Markagunt Plateau by students and faculty of Kent State University, Ohio, and interpreted as gravity slide blocks (Judy, 1974; Iivari, 1979). These features appear similar to many allochthonous block relations reported throughout the Great Basin. Such allochthonous block remnants exposed northeast of Brian Head Peak in the Cedar Breaks, Panguitch Lake, and Red Creek Reservoir quadrangles, Iron County, Utah, are composed of Needles Range Formation (Oligocene) and Isom Formation late Oligocene or earliest Miocene tuffs, and younger volcanoclastic and related alluvial and eolian epiclastic units. Speculations on origin and mode of emplacement of such blocks generally relate them to downslope movements on inclined fault block components or on flanks of domal structures resulting from igneous intrusion.

In the Sydney Peaks area, 4 to 5 km northeast of Brian Head Peak, E. G. Sable identified several fairly well exposed block remnants which comprise an estimated 100 m of normal section consisting of units field-identified as Needles Range Formation tuff, conglomerate of unknown affinity with clasts of volcanic rock, quartz chert, quartzite, minor limestone, and overlying Baldhills Tuff Member of the Isom Formation. The Isom Formation remnants discordantly overlie about 70 m of younger (latest Oligocene or earliest Miocene), flat-lying Narrows Tuff Member of the Leach Canyon Formation. The intervening surface, dipping from a few degrees to about 25 degrees northeast to north and subparallel to the overlying beds, is marked by prominent striations trending N. 35° E. to N. 45° E. Slickenside smoothness and chattermarks(?) tentatively suggest northeastward movement. These striation trends serve to modify previous speculations of easterly movement on tilted fault block surfaces (Judy, 1974; Iivari, 1979). If the units have been correctly identified, then northeastward movement of older onto younger units seems at least locally established. A glacial origin for the striations is possible but is not considered likely. Mapping also tentatively suggests that multiple gravity sliding may have taken place and that movement may have preceded at least some of the major horst-and-graben structure that characterizes much of the area.

BASIN AND RANGE REGION

MINERAL-RESOURCE STUDIES

Age of vanadiferous shales in central Nevada

Age-diagnostic conodonts have been obtained from a vanadiferous mudstone unit in the Woodruff Formation in the southern Fish Creek Range in southern Eureka County, Nev. (loc. 1). C. A. Sandberg identified late Late Devonian conodonts in Woodruff samples collected by F. G. Poole and G. N. Green during their detailed stratigraphic and structural studies. The Woodruff Formation is an allochthonous eugeosynclinal sequence that was considered by previous workers to be Ordovician to Mississippian locally. Regional and local studies suggest that the Woodruff here is an exotic block that was emplaced during Mississippian tectonic activity.

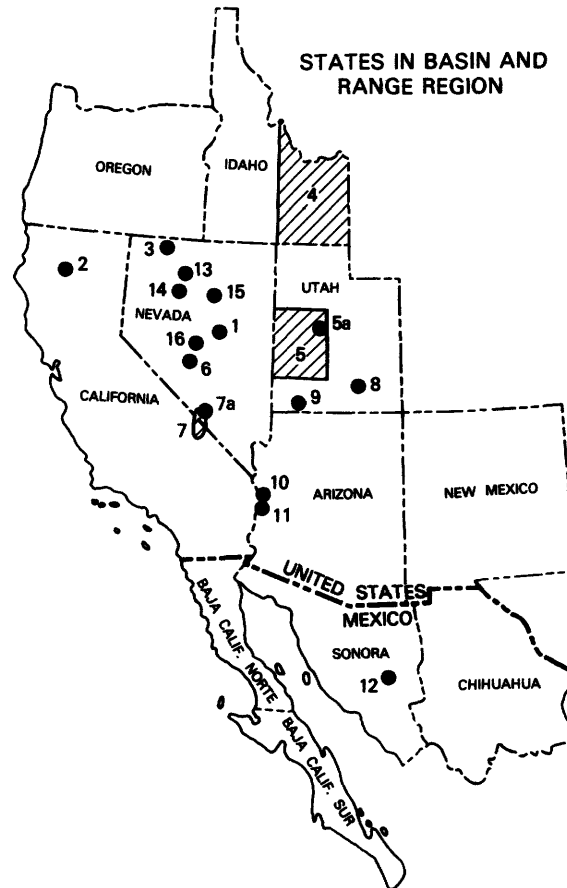
STRATIGRAPHIC AND STRUCTURAL STUDIES

Comparison of Bouguer anomaly and isostatic residual maps of Nevada

H. W. Oliver, R. W. Saltus, D. R. Mabey, and T. G. Hildenbrand generated an isostatic residual map of Nevada from a Bouguer gravity map by removing the gravity effect of a single-layer crustal model assuming perfect Airy-type local compensation. Parameters used were $T = 25$ km, $\rho = 2.67$ g/cm³, and $\Delta\rho = 0.49$ g/cm³. After removing the effect of isostasy, the lowest residual gravity value in Nevada is -68 mGal over the Silent Canyon and northern Timber Mountain calderas in southern Nevada. The highest residual gravity is about $+30$ mGals over Precambrian rocks in northeastern Nevada. The "butterfly anomaly" of Eaton and others (1978), which is a 90 mGal regional gravity low between 37 and 40 degrees north latitude in central Nevada, was reduced to an amplitude of 30 mGal by the isostatic reduction. Thus, the residual map indicates that the Bouguer anomaly map was strongly influenced by isostasy.

Permian and Triassic tectonic events in northern California and adjacent Nevada

Field studies and refined radiolarian and molluscan dating of Permian and Triassic rocks of the East Klamath terrane in the Shasta Lake area of northern California (loc. 2) and of the Bilk Creek terrane near Quinn River Crossing in northwestern Nevada (loc. 3) by N. J. Silberling and D. L. Jones place constraints on interpretations of the tectonic history of the region. Rocks of both terranes have been interpreted to be parts



of a volcanic arc termed "Sonoma," whose supposed collision with North America in Early Triassic time resulted in thrust emplacement of the Golconda allochthon during the Sonoma orogeny in northern Nevada. In both terranes, however, the youngest Paleozoic rocks are bedded cherts of Permian age, which are disconformably overlain by Middle(?) Triassic chert and mudstone. In the dated sections, volcanic rocks of those ages are poorly represented. Thus, during the time of supposed collision, these terranes record neither deformation nor volcanism, and their relation to Golconda thrusting is questionable.

Pleistocene alluvial-gravel deposition in eastern Idaho

Widespread gravel deposits in eastern Idaho (loc. 4) provide a key datum for Quaternary fault studies. Soils, carbonate coatings on stones, carbon-14 dating, and relations to local glacial deposits indicate that well-washed, clast-supported gravels are of late Pleistocene and older ages. K. L. Pierce and W. E. Scott concluded that these gravels were deposited under conditions with much greater runoff than present; a shorter more intense snowmelt runoff may have been responsible for vigorous streamflow in areas where streams seldom

flow at present. In the Holocene, deposition was limited to rubbly deposits at fan heads below steep mountain valleys and to fine-grained sediment along axial drainages.

Regional relations of Wah Wah-Frisco thrust fault in western Utah

According to H. T. Morris, regional geologic studies centered in the Richfield and Delta 2-degree quadrangles in Beaver, Juab, and Millard Counties, Utah (loc. 5), indicate that the Wah Wah-Frisco thrust sheet is locally the youngest overthrust plate of the Sevier orogenic belt. The thrust sheet overrides and conceals transcurrent faults, such as the Leamington tear fault (loc. 5a), that cut the older thrust sheets located farther east. The Wah Wah-Frisco plate also is characterized by the distinctive Pilot Shale-Joana Limestone-Chainman Shale sequence, chiefly of Mississippian age, whereas the age-equivalent rocks of its lower plate consist of a grossly dissimilar sequence of limestone, arenaceous limestone, and sandstone.

Inferred pre-Oligocene strike-slip fault zone in central Nevada

Paleozoic eugeosynclinal facies belts are reported by F. G. Poole to be offset as much as 20 km in a left-lateral sense in northern Nye County, Nev. (loc. 6), between the San Antonio Mountains and the southern Toiyabe and Toiyabe Ranges and within the southern Monitor and Hot Creek Ranges. Tertiary volcanic rocks as old as Oligocene(?) are not offset by the lineament. Although sparsely exposed, areal distribution and lithology of the Paleozoic rocks indicate significant offset across the lineament. The inferred left-lateral fault zone trends about N. 75° W., and is nearly parallel to the west-trending Pancake Range and Warm Springs lineaments postulated by Ekren and others (1976). These lineaments were inferred by them to be deep-seated crustal features.

Geologic and tectonic history of the southern Great Basin and Amargosa drainage system in southwestern Nevada

W. J. Carr reported that a better understanding has been achieved of the geologic history of the Amargosa drainage system in southern Nye County, Nev. (loc. 7), as a result of studies in cooperation with J. W. Hillhouse, W. C. Swadley, D. L. Hoover (USGS), and R. L. Hay (University of California at Berkeley). As a consequence of work in the Amargosa Valley and Tecopa basin in eastern Inyo County, Calif., several important conclusions were reached: (1) the Amargosa Valley was probably a closed basin containing lakes and ponds during the period from about 4 to 2 m.y. ago; (2) the

Amargosa Lake may have spilled into the Tecopa basin through a basalt dam near Eagle Mountain approximately 2.5 m.y. ago; (3) time of lake-sediment deposition apparently did not overlap significantly between the Tecopa and Amargosa basins; (4) a lake in the Tecopa basin spilled into Death Valley and the Amargosa River system became through-going and integrated about 500,000 yr ago, probably as the indirect result of continuing tectonic activity in Death Valley; (5) only minor faulting and tectonic adjustment have occurred in the Amargosa Valley since about 2.5 m.y. ago; (6) no faulting of consequence has occurred in the Tecopa basin since about 500,000 yr ago; and (7) some regional tilting (about 20 ft/mi) to the south or southeast appears to have occurred in Quaternary time.

Trenching and mapping in Crater Flat in southern Nye County (loc. 7a) confirmed the relative maturity of faults on the east side of the valley and exposed basalt ash in one fault. This ash had its source nearby in basaltic centers 1.1 m.y. old. The ash serves to date the enclosing alluvial unit, shows that the faulting and volcanism were synchronous and that the fault last moved 1.1 m.y. ago.

Seismicity data being collected and analyzed by A. M. Rogers and W. J. Carr from a 50-station seismic net in the southern Great Basin indicates that small, relatively shallow earthquakes are occurring fairly continuously on the northeast-trending Rock Valley fault system in a zone between the Funeral Mountains in California and Frenchman Flat in Nevada. A similar area of activity on northeast-trending faults is in the area north of Scotty's Castle along the California-Nevada State line. This contrasts with much of the activity elsewhere in the southern Great Basin, which tends to be quite sporadic with respect to both time and location. The continuous nature of the seismicity in these zones and its distribution with respect to the faults, regional stress field, and the thick Paleozoic carbonate aquifer in the region suggest that hydrologic stimulation of these faults may be occurring.

Traveltime anomalies to seismic stations in the network were obtained from nuclear explosions and distant earthquakes, the latter study being conducted in cooperation with H. M. Iyer and M. E. Monfort. Results from both energy sources are generally similar in that crustal velocities increase slightly west-northwestward across the Nevada Test Site (NTS); this velocity gradient parallels a zone of slightly higher tectonic flux called the Death Valley-Pancake Range belt.

Faults with northwest trends, including the important Death Valley-Furnace Creek system, have remained virtually inactive seismically, despite obvious evidence of young faulting in Death Valley. A crude analysis of the rate of uplift on the Black Mountains

front in Death Valley, when compared with estimates of the age of the last major earthquake there, suggests considerable potential exists for a large earthquake on the Death Valley fault.

A tentative volcano-tectonic history for Crater Flat has been interpreted from a variety of data, including detailed gravity analysis in cooperation with D. B. Snyder. The data support the concept of at least two caldera sources beneath Crater Flat for the Crater Flat Tuff, now known to consist of three members.

Study of the chronology and petrology of basalts in the southern Great Basin in cooperation with B. M. Crowe and D. T. Vaniman (Los Alamos National Laboratory) has demonstrated cyclic or pulslike eruptive episodes in basalts ranging from about 10 to 0.3 m.y. old. Significant results of this work are as follows: (1) petrologic data suggest the rate of basaltic magma rise in the NTS region has been relatively slow, on the order of $0.1\text{--}0.5\text{ m/s}^{-1}$; (2) fairly quantitative estimates of the amount of magma erupted in Quaternary fields indicate magma volumes ranging from about $7.8 \times 10^6\text{ m}^3$ to $1.0 \times 10^8\text{ m}^3$; (3) lithic fragments in scoria show that erupted wallrock ranges from about 0.009 to 0.060 percent by volume of erupted material and that the fragments were derived mostly from depths less than about 200 m.

The rate of Pliocene to Quaternary basaltic eruptions in the NTS (Death Valley-Pancake Range) basalt belt appears to be increasing, but the volume has been decreasing.

Tectonics reflected in sediments of the Morrison Formation in south-central Utah

According to Fred Peterson (1982), the Salt Wash Member of the Morrison Formation of Late Jurassic age in eastern Garfield County, Utah (loc. 8), consists of an alluvial complex deposited primarily by braided streams with minor contributions by meandering streams. Paleoslope directions and progressive downslope decrease in fluvial energy regimes are indicated by crossbedding dip vectors, facies distribution, and progressive downslope changes in maximum pebble size and stratification ratios (SR = planar crossbedding/planar crossbedding plus horizontal laminations measured in detailed sections). Salt Wash streams flowed predominately northeast during deposition of most of the member. Slight but significant contemporaneous structural deformation, as indicated primarily by thickness and facies variations, played an important role in determining local variations in the regional sedimentologic framework. Locally, in some of the downwarped areas, the percent of horizontal laminations is higher and thus the stratification ratio is lower than regional

trends. This suggests that subsidence locally lowered stream gradients below their equilibrium profiles, causing greater than normal amounts of flooding, thus increasing the amount of horizontal laminations in fluvial deposits and decreasing the stratification ratios. The fact that vector magnitudes (or consistency factors) derived from trough crossbedding in the braided-stream sandstone beds also tend to be low in downwarped areas suggests greater sinuosity of the braid channels in areas of active subsidence. Thin lenticular lacustrine deposits of carbon-bearing mudstone, a rare lithology in the Salt Wash, are intercalated between some of the fluvial sandstones and occur only in some of the downwarped areas. They reflect a slight shift in sedimentologic processes that favored ponding in some of the synclines when fluvial energy regimes were low.

Interpretation of compound crossbedding in the Navajo and Entrada Sandstones of southwestern Utah

Using graphical techniques to model the migration of a variety of superimposed and intersecting dunes, D. M. Rubin and R. E. Hunter predicted the three-dimensional geometry of structures that such dunes should deposit. They subsequently observed many of the modeled structures in the eolian Navajo Sandstone of Late Triassic(?) and Jurassic age and Entrada Sandstone of Middle Jurassic age in southwestern Utah (loc. 9). The structures included compound crossbeds deposited by trains of two- or three-dimensional dunes migrating down or along the lee slope of larger primary dunes and compound crossbeds with scallop-shaped lower bounding surfaces deposited by trains of scour pits that migrated rapidly along the troughs of primary dunes. Preliminary observations in the Navajo Sandstone suggest that the superimposed dunes and scour pits generally migrated clockwise with respect to the migration direction of the primary dunes, a pattern inferred to be a result of the obliquity of the dunes to the direction of flow. In addition, the migration direction of primary dunes rotated from generally southeastward in the lower part of the Navajo to generally southwestward in the upper part. A clockwise rotation in the resultant regional wind direction is suspected to be the cause of their change in migration direction and may also have contributed to their oblique orientation.

Tertiary stratigraphy, intrusion, and structure in the Mohave Mountains in west-central Arizona

J. E. Pike, J. K. Nakata (USGS), and V. L. Hansen (University of Montana at Missoula) reported that Tertiary volcanic and sedimentary rocks of the Mohave Mountains, Mohave County, Ariz. (loc. 10), are divisible

into three sequences: (1) an older early Miocene unit of mafic and silicic flows, pyroclastic and sedimentary rocks; (2) a middle unit of similar rock types that are dominantly sedimentary rocks; and (3) a younger unit that consists principally of fanglomerate and thin silicic and basaltic flows. The middle and youngest units probably are middle Miocene in age. Except for the uppermost layer (Peach Springs Tuff of Young and Brennan, 1974) of the oldest unit, individual strata have little lateral continuity, and lithologies vary with locality. The oldest unit is complicated further by repeated, locally voluminous intrusive rocks. The oldest unit lies unconformably on Precambrian gneiss along the western flank of the range. Where contact relations are exposed, the middle unit is separated from the overlying and underlying sequences by angular unconformities.

Swarms of pre-Tertiary and Tertiary dikes intrude the Precambrian crystalline rocks of the Mohave Mountains. The volcanic sequences and dike swarm record repeated magmatism and apparent northeast-southwest crustal extension that was related to Oligocene and Miocene regional low-angle detachment faulting described by Davis and others (1980), Carr (1981), and Rehrig (1981).

Radiometric ages from the Mohave Mountains are too few to establish the timing of intrusive, eruptive, and tectonic events. However, two K-Ar age determinations from the Mohave Mountains and a small number from nearby ranges suggest that mafic volcanism and fault-induced deformation occurred between 21 and 18 m.y. ago. Renewed faulting, volcanism, and rapid sedimentation followed silicic intrusion of the oldest unit, possibly before deposition of the Peach Springs Tuff of Young and Brennan (1974), about 18 m.y. ago.

Reconnaissance in several adjacent ranges and detailed mapping in a portion of the Turtle Mountains indicate that similar sequences are present regionally, although only a few ash flows, such as the Peach Springs Tuff, may be correlated regionally. Related crystalline terranes of widely separated ranges may be identified from correlation of the Tertiary dike swarms; dike swarms of the Mohave and Whipple Mountains are similar and may be part of the same dike complex.

Origin of folding of Tertiary low-angle fault surfaces in southeastern California and western Arizona

The lower Colorado River trough (loc. 11) in eastern San Bernardino County, Calif., southwestern Mohave and northwestern Yuma Counties, Ariz., is a detachment-fault terrane in which tectonic denudation by low-angle detachment faulting has removed 4 to 7 km of rock. Detachment faults have been warped into two sets of folds that have approximately perpendicular

axes. J. E. Spencer (1982) suggested that application of principles of mechanics to simple models of the denudation process provides an explanation for the origin of these folds. Folds whose axes parallel the northeasterly to easterly direction of allochthon transport can be explained as resulting from deviatoric stresses generated in autochthonous rocks by tectonic denudation and consequent elastic decompression and expansion. The amount of denudation is modeled as increasing linearly in the direction of displacement of allochthonous rocks. Greater isostatic uplift in areas of greater denudation causes flexure of autochthonous rock masses. Stresses generated by flexure may have played an important role in producing the north- to northwest-trending folds.

Newly discovered Paleozoic section in central Sonora, Mexico

According to F. G. Poole, J. H. Stewart, and A. K. Armstrong, a nearly complete section of Paleozoic miogeoclinal and cratonic-platform carbonate rocks with subordinate sandstone, siltstone, and shale occur in the vicinity of Cerro El Pollo in the Sierra Agua Verde (loc. 12). Total thickness of the Paleozoic section was estimated to be as much as 6,000 m. The Cambrian rocks are similar to coeval rocks in the Caborca area in northwestern Sonora and in southeastern California and southwestern Nevada, and the Ordovician to Pennsylvanian rocks have similarities to coeval rocks in Nevada and southeastern California as well as in southern New Mexico. The Sierra Agua Verde section is an important control point for establishing facies and thickness trends of these shallow marine rocks on the southwest margin of Paleozoic North America.

IGNEOUS ROCKS

Permian plutons in north-central Nevada

R. W. Kistler, D. E. Lee, and A. C. Robinson have identified relatively small, isolated plutons in north-central Nevada that yield a Rb-Sr whole-rock isochron of 270 m.y. The plutons occur in the Sonoma Range in southeastern Humboldt County (loc. 13), East Range in eastern Pershing County (loc. 14), Cortez Mountains in northern Eureka County (loc. 15), and northern Toquima Range in northern Nye County (loc. 16). Most of these plutons intruded rocks of the "ocean-floor terrane" of R. C. Speed (1977a) that are bounded on the west by a Paleozoic "island-arc terrane" and on the east by the Golconda thrust. The plutons were probably sub-volcanic. Detrital hornblendes in the Permian Mina Formation of Speed (1977b) in west-central Nevada have maximum K-Ar ages of 268 m.y. The source for these

hornblendes could be the volcanic rocks that were associated with the Permian plutons.

PACIFIC COAST REGION

CALIFORNIA

Comagmatic granitoid sequence, Sierra Nevada

Compilation of a plutonic map, additional geologic mapping, and reconnaissance Sr isotope studies by D. A. John and A. C. Robinson in the Walker Lake 1° by 2° quadrangle, Calif. and Nev., indicated the presence of a very large (approximately 2,000 km²) comagmatic granitoid sequence of Late Cretaceous age centered on Sonora Pass. The sequence consists of two major units: an inner potassium feldspar megacryst-bearing unit, which is the granodiorite of Topaz Lake (also referred to as the Sonora Pass pluton in older literature), and an equigranular outer unit containing euhedral mafic minerals, which concentrically wraps around the Topaz Lake pluton on its north, west, and south sides. The outer unit has a six-point whole-rock Rb-Sr isochron of about 89 m.y.; initial Sr ratios of the two units are identical. This granitoid sequence is similar to the well-described Tuolumne Intrusive Suite centered about 65 km southeast of Sonora Pass, which also has a similar age (about 88 m.y.) and a similar initial Sr ratio. However, the Sonora pass sequence is about three times as large as the Tuolumne Intrusive Suite, and is elongated in a north-northeast-south-southwest direction unlike the Tuolumne Intrusive Suite and most other granitoid sequences in the central Sierra Nevada, which are elongated in a northwest-southeast direction.

Amount of offset of Salinian block remains equivocal

Synthesis of data on granitic and metamorphic rocks of the Salinian block by D. C. Ross has shown that some basement units and gross structural trends in the central Salinian block are comparable to similar rocks and structures in the Sierra Nevada tail area. Such data suggest that these basement features have been offset some 300 km by movement on the San Andreas fault zone. However, use of the 300 km reconstruction shows that other parts of the Salinian block, notably some of the northern granitic exposures and the southeastern part, do not match comparable rocks across the San Andreas fault. Thus, a 300 km offset on the San Andreas fault zone only partially (and possibly fortuitously) satisfies basement unit reconstruction, and the Salinian block as a whole may have a longer and more complex history of movement.

Geometry of a thrust fault in northern California

Interpretations by R. C. Jachens of gravity and aeromagnetic data from the Condrey Mountain, Marble Mountains, and Orleans Mountain Wilderness areas in Northern California yielded information on the geometry of the major thrust fault that lies at the base of the western Paleozoic and Triassic belt. In the north, the western Paleozoic and Triassic belt is thrust over the Condrey Mountain Schist, and to the south it is thrust over the western Jurassic belt. The rocks that make up the western Paleozoic and Triassic belt are typically much more dense (by +0.1 to 0.3 g/cm³) and more magnetic than rocks contained in the western Jurassic belt and the Condrey Mountain Schist. Two- and three-dimensional models of the gravity and magnetic data suggested that the Condrey Mountain Schist and the western Jurassic belt are connected at depth and that the western Paleozoic and Triassic belt is a thin plate that overlies both. This plate is typically less than 5 km thick and attains a maximum thickness of approximately 8 km beneath the Marble Mountains. The basal thrust fault dips gently at angles of less than 30 degrees. Gravity modeling of the Wooley Creek batholith, which intrudes the western Paleozoic and Triassic belt, yielded a thickness of 2 to 3 km for the plate, although the steep regional eastward dip of the intrusive contact indicated that the pluton should extend deeper. These data suggested that the Wooley Creek batholith was detached during thrusting of the western Paleozoic and Triassic belt over the western Jurassic belt.

Structures in the offshore Eel River Basin

Preliminary interpretation of marine seismic reflection data collected by S. H. Clarke, M. E. Field, B. D. Edwards, J. V. Gardner, and W. C. Richmond showed that major structures in the offshore Eel River basin parallel the trend of the basin axis approximately northwest near the south end of the basin swinging to a near northerly orientation toward the north. Folds involving Pliocene and younger strata on the marginal plateaus, located above the Continental Slope and seaward of the basin axis, and on the adjacent Continental Slope are expressed in the seafloor and are cut by high-angle reverse faults having dip separations that are predominantly west-side down. That the folds are characteristically broadly symmetrical or asymmetrical with east-dipping axial planes reflects a principal compression stress from the west, the result of Quaternary underthrusting. Some folds of the marginal plateaus appear to be associated with shale flowage and diapirism, and some of the marginal ridges are piercement structures.

Samples from the exposed cores of these structures are typically sheared, dewatered clays containing lower and middle Pliocene foraminifera. Numerous unconformities occur in the sedimentary section. The deep structural depression landward of the uplifted marginal plateaus is filled by upper Tertiary and Quaternary hemipelagic sediment and turbidites having an aggregate thickness of about 3,500 m.

Synthesis and analysis of accreted terranes in the Sierra Nevada

Stratigraphic, structural, and tectonic studies and analyses in the Kings River RARE II project area by W. J. Nokleberg and J. C. Moore revealed that the wall rocks of the Sierra Nevada batholith in this region constitute two distinct accreted tectonostratigraphic terranes. The eastern Goddard terrane consists of a suite of Andean-type arc metavolcanic rocks of intermediate composition that were erupted in the Triassic or Jurassic. The western Kings terrane consists of a suite of metamorphosed quartzite, limestone, shale, and silicic tuff that was deposited under marine conditions in the Late Triassic or Early Jurassic. Both sequences were intensely deformed during right-lateral strike-slip displacement that resulted in juxtaposition of the two terranes against each other. Intrusion of granitic plutons occurred during migration as evidenced by schistose and locally mylonitic zones in various plutons bordering the wall rocks. Younger nonschistose plutonic rocks of Early Cretaceous age weld the two terranes together.

Progress in correlation and age determination of late Cenozoic tephra

Correlations of volcanic ashes and tuffs from several localities in California and western Nevada have been made on the basis of field and laboratory studies. These correlations have provided information to several workers studying diverse problems in the field such as crustal deformation, climatic studies, and correlation of marine and continental faunal chronologies. These studies were conducted by A. M. Sarna-Wojcicki, C. E. Meyer, M. J. Woodward, J. L. Slate, and Jose Rivera, in cooperation with S. A. Matheson, S. D. Morrison, and K. R. Lajoie of the USGS, and J. O. Davis, of the Desert Research Institute, Reno, Nev.

An ash bed found in new road cuts in Santa Clara Valley, central California, in deformed and faulted alluvium of the Santa Clara Formation, has been identified as the Rockland ash by electron-probe and energy-dispersive X-ray fluorescence analyses of the volcanic glass. Recognition of this ash bed, previously dated as 0.45 m.y. by fission-track analyses on zircons, made it

possible to correlate the Santa Clara Formation south-east of the San Francisco Bay area with a member of the Santa Clara Formation that contains the same ash bed, part of a fault-bounded block situated along the San Andreas fault near the town of Woodside, west of San Francisco Bay.

An ash bed exposed in ancient lake beds of Mohawk Valley, northeastern California, was also correlated with the Rockland ash bed, thus dating the lake beds at 0.45 m.y. Another ash, identified as the Dibekulewe ash bed, was found in the same area but its age relative to the Rockland ash could not be deduced on the basis of local stratigraphy. However, the Rockland and Dibekulewe ash layers have been identified in stratigraphic context near Mexican Dam, south of Carson City, western Nevada, where the Rockland ash layer overlies the Dibekulewe ash layer (Davis, 1978). The Dibekulewe ash bed has also been identified from an exposure near Oreanna, in west-central Nevada. At this locality, the ash bed is stratigraphically above the Lava Creek ash bed, the latter dated elsewhere at 0.6 m.y. (Naeser and others, 1973). Thus, age of the Dibekulewe ash bed is between 0.45 and 0.6 m.y.

An ash layer obtained from a core sample in south San Joaquin Valley north of Wasco, Calif., was identified as the Lava Creek ash, on the basis of X-ray fluorescence analysis of the glass. Similarity coefficients between the ash from the San Joaquin Valley and Lava Creek ash samples are very high, 0.98, where 1.00 represents identity. The Lava Creek ash appears to define the end of a major pluvial period in the Western United States. At two sites where it was identified (one in west-central Nevada, the other in southeastern California), the ash is at or near the top of a sequence of pluvial lake beds that are overlain by alluvium. A similar situation is found in the southern San Joaquin Valley, where the Lava Creek ash overlies the lacustrine Corcoran Clay Member of the Tulare or Turlock Lake Formation and is overlain by alluvium. These relations suggest that the Corcoran Clay Member itself may have been formed during a pluvial period.

The Lava Creek ash bed (0.6 m.y.) was found and identified in marine silts and sands near the base of the San Pedro Formation, near Ventura in southern California. In addition to the diagnostic chemical fingerprints of the Lava Creek ash bed, its identification was supported by the presence of the Bishop ash bed (0.73 m.y., Dalrymple, 1980) in the underlying Santa Barbara Formation and by an amino-acid age estimate (0.2 m.y., Lajoie and others, 1982) on fossil mollusks obtained near the top of the San Pedro Formation, stratigraphically above the Lava Creek ash bed. This identification documented for the first time the presence of Lava Creek ash bed in a marine section and permits correlation of mid-Pleistocene marine and continental chronologies.

An ash layer in Pleistocene Lake Tecopa beds of southeastern California (stratigraphically below the Lava Creek ash bed), previously correlated with the Huckleberry Ridge ash bed of the Yellowstone area of Wyoming and Idaho, was dated at 1.58 ± 0.08 m.y. by the fission-track method on zircons. This age is somewhat younger than ages reported by others (1.6 to 2.0 m.y., Naeser and others, 1973) for the Huckleberry Ridge ash bed. The discrepancy in ages can be attributed to one or more of the following factors: (1) the fission-track age on the ash in the Tecopa lake beds is too young, owing to analytical error; (2) the ages of the Huckleberry Ridge ash (K-Ar and fission-track) are incorrect owing to contamination or analytical error; or (3) there are two, or possibly several ashes that are attributed to the Huckleberry Ridge ash, the ashes having differences in ages of several tens of thousands to several hundreds of thousands of years.

Electron-probe analysis of glass and pumice shards obtained from an ash layer from a core drilled about 100 km southwest of Cape Mendocino, northwestern California (DSDP site 173), matched well with that of an ash bed in the marine Rio Dell Formation of the Wildcat Group exposed north of the Cape. The Rio Dell Formation in this area is unconformably overlain by the Hookton Formation of Ogle (1953); the latter contains the Rockland ash bed. Ages assigned to the Rio Dell ash bed by others on the basis of K-Ar analyses, magnetostratigraphy, and biostratigraphy range widely from about 1.2 m.y. to 2.3 m.y. The new data correlate the on-land marine section and associated magnetostratigraphy and biostratigraphy with the worldwide deep-ocean chronology and support an age closer to about 1.2 m.y.

Results of energy-dispersive X-ray fluorescence and electron-probe analysis of volcanic glass indicated that an ash bed in the marine Eel River Formation of the Wildcat Group, underlying the Rio Dell Formation, was correlative with the Putah Tuff Member of the continental Tehama Formation in southwestern Sacramento Valley, dated by others at 3.4 m.y. by the K-Ar method (Miller, 1966). This correlation established the contemporaneity of the marine Eel River Formation with the continental Tehama Formation.

In addition, the Putah Tuff Member was identified in the subsurface of the Sacramento Valley near Orland from a borehole sample obtained at about 440 m below the surface. Another tuff, about 10 m higher in the same borehole, was identified as the Nomlaki Tuff Member of the Tehama Formation, dated by others at 3.4 m.y. by the K-Ar method (Evernden and others, 1964), an age identical to that obtained on the Putah Tuff Member. Exposures of the Putah Tuff Member are restricted to the southwestern flank of the Sacramento Valley; exposures of the Nomlaki Tuff Member to the northwest-

ern and northeastern flanks. Identification of the two tuffs in stratigraphic proximity within the core established for the first time their relative ages and supported their similar radiometric ages.

Stratigraphy and sedimentology of the Hornbrook Formation

Reconnaissance geologic investigations by T. H. Nilsen of the Upper Cretaceous Hornbrook Formation in southern Oregon and northern California revealed a stratigraphic sequence that in ascending order consists of fluvial conglomerate, shallow-marine sandstone, and deep-marine turbidite sandstone and shale. The sequence rests unconformably on crystalline basement rocks of the Klamath Mountains and is overlain unconformably by Eocene volcanic rocks of the Cascade Mountains. Present interest in reservoir- and source-rock potential of the Hornbrook Formation has stimulated detailed mapping and stratigraphic subdivision. A single, very thick turbidite extends across the California-Oregon border and appears to represent a useful, correlatable marker bed. Sedimentologic, lithostratigraphic, and biostratigraphic data tentatively permit subdivision of the Hornbrook into six stratigraphic members.

New ages for Franciscan rocks of Hull Mountain areas, northern California

R. J. McLaughlin, C. D. Blome, and H. N. Ohlin reported that metachert from the Franciscan assemblage near Hull Mountain in northern California contains a radiolarian fauna of Aptian or Albian age that is much younger than radiolarian faunas of Tithonian to Valanginian age previously found in chert from this same Franciscan terrane. Mollusk fossils of Cenomanian age have previously been reported by M. C. Blake and D. L. Jones (1974) from stratigraphically higher argillite and metasandstone of the Hull Mountain terrane. However, the relation between the Upper Jurassic and Lower Cretaceous radiolarian-bearing strata and overlying Upper Cretaceous mollusk-bearing strata has not been studied in detail. The paleontologic confirmation of the presence of chert of Aptian or Albian age fills a large part of the age gap between the previously dated rocks. The new data suggest that there probably is no large depositional or tectonic hiatus between the Lower and Upper Cretaceous parts of the Hull Mountain terrane.

The upper part of the Hull Mountain section is intruded by diabase (92 to 95 m.y. or younger) that is metamorphosed with the wall rocks to blueschist-grade actinolite \pm pumpellyite \pm lawsonite. Lawsonite in the wallrocks was formed cogenetically with an early foliation and was deformed (bent) by a later deformational event.

Crystalline rocks near Frazier Mountain, western Transverse Ranges

Crystalline rocks in the western Transverse Ranges south of the San Andreas fault and west of the San Gabriel fault were examined and compared by R. E. Powell and V. A. Frizzell, Jr., with similar rocks in the eastern Transverse Ranges. Mesozoic and Mesozoic(?) batholithic rocks of several lithologies, chiefly one- and two-mica monzogranite with apparent K-Ar ages of 58 to 72 m.y., intrude three distinct groups of country rock. Large parts of Frazier and Alamo Mountains are composed of 1,655-m.y.-old granodioritic augen gneiss which intrudes pelitic schist and gneiss on the south flank of Alamo Mountain and along Mutau Creek. This U-Th date was determined by L. T. Silver. Granulitic gneiss, retrograded to amphibolite facies, crops out extensively to the east of the augen and pelitic gneiss where it has incorporated augen gneiss and has cross-cut the contact between augen and pelitic gneiss. Locally, the contact between granulitic and augen gneiss has been deformed to a steep nearly north-striking mylonite zone. These lithologic units and sequencing relations are equivalent to those of the San Gabriel terrane of Powell (1981) in the eastern Transverse Ranges.

In antiforms in the west half of Frazier Mountain, the augen and retrograded granulitic gneiss overlie quartzite and pelitic granofels along an apparent structural contact marked by discontinuous mylonite. The quartzite and granofels are similar in outcrop and hand specimen to part of the Joshua Tree terrane of Powell (1981) in the eastern Transverse Ranges. On Mt. Pinos northwest of Frazier Mountain and on Cobblestone Mountain south of Alamo Mountain, the interlayered marble, calc-silicate rock, and pelitic schist that occur as inclusions within Mesozoic(?) batholithic rocks have affinities to part of the Placerita Formation of Miller (1934) in the San Gabriel Mountain. The prebatholithic boundary between these metasedimentary rocks and the San Gabriel terrane is lost in the intrusive rocks and is further obscured by postintrusive cataclasis and high-angle faulting. On the north flank of Mt. Pinos, the deformed Mesozoic(?) granitic rocks containing meta-sedimentary septa are thrust over Pelona Schist.

Franciscan mélangé in central northern California

Extensive mapping, structural and petrographic studies, and paleontologic dating by R. J. McLaughlin, M. C. Blake, Jr., and D. L. Jones indicated that the Franciscan assemblage in central northern California is a collage of numerous subterrane of coherent but folded and broken rocks that are interleaved with mélangé mainly of tectonic origin. Fossils in the

coherent subterrane and mélangé show that much tectonic mixing occurred after the Late Cretaceous (Campanian).

The distinctive "101" mélangé along the southwest side of the central terrane contains abundant knockers of high-grade garnet-bearing blueschist, amphibolite, and eclogite, together with the well-studied type III metabasalt, metagraywacke, and metachert slabs of the Ward Creek and Warm Springs Creek areas. Minor pink-to-gray foraminiferal middle Cretaceous Laytonville-type limestone is also present. Mélangé intercalated with coherent subterrane to the northeast contains few high-grade knockers and no Laytonville-type limestone but does contain abundant blocks derived from adjacent coherent subterrane.

Among the coherent subterrane are the following: (1) slabs of sandstone interbedded with chert, basaltic flows, and intrusive rocks metamorphosed to lawsonite grade that probably are derived from the eastern (Yolla Bolly) terrane of the Franciscan assemblage; (2) slabs and lenses of ophiolitic rocks and the Great Valley sequence derived from the upper plate of the Coast Range thrust; and (3) slabs of basalt overlain by an unusual Upper Jurassic to Upper Cretaceous chert and sandstone sequence (Golden Gate Bridge, Nicasio, and The Geysers localities).

These geologic data, combined with paleomagnetic results, indicated that formation and accretion of the mélangé and coherent subterrane is a consequence of complex interplay between large-scale northward transport from low paleolatitudes between Late Cretaceous (Cenomanian) and early Miocene time, clockwise rotations, and oblique convergence.

The Yolla Bolly triple junction revisited

Additional mapping and petrologic-geochronologic studies by M. C. Blake, Jr., in the complicated triple junction between the Coast Ranges, Great Valley, and Klamath Mountains suggested an even more complex history than was previously considered (Blake and Jones, 1977). The present boundary between the Franciscan rocks and those of the Klamath Mountains and Great Valley sequence is a west-dipping, high-angle reverse fault which probably formed in late Cenozoic time. This fault has deformed a series of imbricate low-angle thrust faults within the Great Valley sequence and its basal ophiolite. The Coast Range thrust is probably the basal thrust of this system. The highest thrust emplaced the entire Klamath Mountains above the Great Valley sequence. On the basis of work in southwest Oregon, the timing of this thrusting is probably earliest Tertiary.

Quaternary floodplain deposits of the lower San Joaquin River

B. F. Atwater and W. R. Lettis reported that, between the Tuolumne River and Suisun Bay, Calif., the floodplain of the San Joaquin River underwent four major episodes of aggradation during the past 40,000 yr. Three predictable episodes correlate with times of high sea level, one Holocene and two others about 30,000 and 40,000 yr ago. The levels of all of these floodplains, however, lie below the level of a floodplain that was built of glacial outwash and presumably correlates with the late Wisconsinan low stand of the sea. The high floodplain, like the glacial-outwash fans of the northeastern San Joaquin Valley, probably records exceptionally great sediment loads of glacial or immediately postglacial times.

Glacially induced alluvial dams for Tulare Lake, California

It is widely believed that tectonic subsidence maintained a large Tulare Lake through most of late Quaternary time. Recent auger drilling by B. F. Atwater and W. R. Lettis, however, revealed that lakes have alternated with throughgoing streams during the past 100,000 yr and that each Tulare Lake probably resulted from renewal of an alluvial dam. Each major dam probably consists of glacial- and (or) deglacial-age deposits of the Kings River fan. Material for radiocarbon dating has been collected that should clarify the timing of both alluvial-fan deposition in the San Joaquin Valley and glaciation in the Sierra Nevada.

Late Quaternary tilting in the northeastern San Joaquin Valley, California

On the Tuolumne River alluvial fan, the top of the Turlock Lake Formation (approx. 600,000 yr old) extends from the Sierra Nevada foothills where it forms a widespread, dissected terrace, to the central part of the San Joaquin Valley where it is marked by an exceptionally strong soil beneath 20 to 40 m of younger alluvial-fan deposits. Relief on the terrace remnants suggests local folding or faulting along the boundary zone between the uplifting Sierra Nevada and the subsiding San Joaquin Valley. The overall profile of the top of the Turlock Lake Formation, however, approximates a straight line. B. F. Atwater and W. R. Lettis inferred from the profile that the structural boundary between the Sierra Nevada and the northeastern San Joaquin Valley has functioned like a fulcrum during the past 600,000 yr.

Valley-margin faults of the western San Joaquin Valley

Investigations by W. R. Lettis demonstrated that Quaternary deposits are displaced by three fault systems along the western valley margin and in the adjacent foothills of the Diablo Range, Calif. The Ortigalita fault at the eastern margin of the central Diablo Range exhibits primarily lateral displacement. Upper Miocene volcanic rocks and Pliocene and Pleistocene alluvium extending across the fault with no vertical displacement indicate that the postulated uplift of the central Diablo Range relative to the foothills along the fault ceased prior to the late Miocene. The San Joaquin fault at the foothill-valley border vertically displaces middle to upper Pleistocene geomorphic surfaces from 0 to 140 m; lateral displacement is not evident. The O'Neill fault system is a zone of reverse faults between the Ortigalita and San Joaquin fault. The system has vertical displacement ranging from 0 to 100 m on individual fault segments; no lateral displacement was observed. Displacement of Holocene alluvium was evident only along the Ortigalita fault.

WASHINGTON**Early Tertiary crustal extension in northeastern Washington**

Geologic mapping in and near the Republic graben within the Colville Indian Reservation, Wash., by B. F. Atwater, R. W. Holder, F. J. Moye, and C. D. Rinehart has revealed dike swarms of rhyolite and dacite near the bounding faults of the graben. The dike swarms are so voluminous that accommodation by the host rocks locally requires as much as 4 km of crustal extension. Judging from K-Ar ages of the dike rocks and associated volcanic rocks, the investigators concluded that the episode of extension began about 52 million yr ago and lasted no more than 5 million yr.

Redistribution of the Mount St. Helens ash with time

Stratigraphy, thickness, and grain size of the ash layer formed by the May 18, 1980, eruption of Mount St. Helens have been studied by Susan Shipley to monitor changes that took place as a consequence of erosion and redeposition within the first 18 months following the eruption. At many downwind locations, the original three-fold and two-fold stratigraphy has been little modified since initial deposition, except for compaction of as much as 45 percent over the May 18, 1980, thicknesses. At other localities, the ash lobe axis has been

shifted as a consequence of reworking by wind. In several small basins, a considerable thickening of the May 18 air-fall layer has been observed, a consequence of local reworking. At such sites, the original air-fall stratigraphy is preserved beneath a massive, poorly-stratified layer of reworked ash.

Thickness of Quaternary sediments, central Puget lowland

Subsurface data from water wells, marine- and land-based seismic surveys, and test borings compiled by Fred Pessl, Jr., S. A. Safioles, and J. C. Yount for the Port Townsend 1:100,000-scale quadrangle, Wash., delineate a northwest-southeast elongated basin centered between Whidbey and Camano Islands that contains Quaternary sediments more than 1,000 m thick. Steep east-west oriented isopachous gradients south of Port Townsend and south of San Juan and Fidalgo Islands are similarly oriented, as are previously mapped bedrock structures (Whetten, J. T., and others, 1981 personal commun.), and may define the steep margins of fault-bounded depositional basins.

Outwash terraces along the Cowlitz River

D. P. Dethier (USGS) and John Bethel (University of Washington) identified six distinct outwash terraces ranging from early(?) to latest Pleistocene along the Cowlitz River near Toledo, Wash. Terrace deposits of the Hayden Creek, Wingate Hill, and older Evans Creek glaciations can be traced upstream to moraines or to ice limits inferred from the extent of till. Terrace surfaces converge downstream, and in most places they can be distinguished by topography and weathering characteristics. This sequence of Cowlitz River terraces is probably the best-preserved record of Alpine glacial events in the Pacific Northwest.

Chemical characteristics of selected rivers, western Washington, 1961-1980

D. P. Dethier summarized the general chemistry of 23 rivers in western Washington for the years 1961-80 and reported that dilute concentrations and neutral pH levels were the dominant characteristics. Calcium and sodium were the dominant cations and bicarbonate the dominant anion. Silicon levels were higher than calcium concentrations in most cases. Relatively high levels of calcium and sulfate in waters draining the Olympic Mountains suggest contributions from the dissolution of calcite and gypsum in altered volcanic bedrock. Locally elevated chlorite levels are apparently associated with areas of marine sedimentary bedrock.

Mineralogy of volcanoclastic sands associated with Glacier Peak

S. A. Safioles and D. P. Dethier reported that volcanoclastic sands containing dacitic lithic fragments and microlites are associated with flowage deposits from Glacier Peak and occur 75 to 145 km from this volcanic mountain in the Skagit and Stillaguamish River valleys. The sands record deposition of volcanically derived sediments during intervals of volcanic activity about 1,800, 4,800, and 10,350 yr ago.

Tectonostratigraphic terranes in northeastern Washington

K. F. Fox, Jr., reported that the contact between the North American craton, as it existed in the Jurassic, and the tectonostratigraphic terranes flanking the craton on the west follows the Kootenay arc northward from the vicinity of Hunters, Wash. ($48^{\circ}7'N$, $118^{\circ}12'W$), to the International Boundary near Northport, Wash. ($49^{\circ}N$, $117^{\circ}30'W$). Recent map compilations by F. K. Miller and R. G. Yates (1976) showed that in Washington the sedimentary rocks of the craton consist of miogeoclinal Precambrian rocks of the Belt Supergroup and Deer Trail Group, overlain by Cambrian to Mississippian shelf deposits. The numerous tectonostratigraphic terranes to the west form two groups, an eastern and western, in mutual contact at the north-northwest-trending Pasayten fault, which crosses the International Boundary at about $120^{\circ}30'$ west longitude. The geology of rocks near this fault is being studied by V. R. Todd. Farther east, the eastern group of tectonostratigraphic terranes are well exposed within the Okanogan 2° quadrangle.

Fox, C. D. Rinehart and B. F. Atwater have found evidence of an east-trending tectonic contact (suture?) at about $48^{\circ}30'$ north latitude, which juxtaposes two of the more extensive tectonostratigraphic terranes of the eastern group. The contact itself, except for isolated remnants, has been obliterated by later plutonism and metamorphism. The pre-Cretaceous rocks of the northern terrane, here called the Oroville terrane, consist of thick eugeosynclinal marine deposits of the upper Paleozoic Anarchist Group, unconformably overlain by Permian or Triassic marine basalt of the Kobau Formation, and Jurassic marine basalt of the Rosslund Group. The southern terrane, here termed the Incheilium terrane, consists of thick, bathyal marine turbidites of the Covada Complex. Fossils from the eastern part of the Covada Complex are Ordovician, according to Snook and others (1981). The Covada Complex is unusual in that it contains voluminous potassium-feldspar-bearing arkose derived through erosion of an as yet unidentified granitic source. At its western margin, the Incheilium

terrane is overlain by Triassic marine carbonate rocks and lavas of the Cave Mountain Formation similar, but not quite identical, to Permian or Triassic rocks overlying the Oroville terrane.

If, as seems likely, these Permian and (or) Triassic rocks are parts of a once coextensive deposit, the Oroville and Inchelium terranes were joined to form the nucleus of the eastern group by Late Triassic time. This super terrane was evidently joined to the craton during the Mesozoic. More precisely, the absence of depositional overlap of the marine volcanics of Late Triassic to Early Jurassic(?) age onto the craton suggests that the Oroville-Inchelium super terrane docked to the craton after Early Jurassic. Overlap of terrane boundaries by dated plutonic and metamorphic rocks indicates that all major tectonostratigraphic terranes of the eastern group were in place by latest Cretaceous time.

Timing and nature of tectonic events in northwest Olympic Peninsula

Geologic mapping and stratigraphic studies by P. D. Snively, Jr., indicated that the Tertiary rocks along the north flank of the Olympic Mountains and beneath the Strait of Juan de Fuca were subjected to episodic periods of north-south compression. These tectonic events are evidenced by northward-dipping thrust faults and olistostromal units derived from the uplifted fault-blocks.

The earliest period of north-south compression was during the late middle to early late Eocene, when the Crescent and Striped Peak north-dipping thrust faults had their major movements. Olistostromal blocks and conglomerate derived from volcanic rocks of the Crescent Formation in the upper plate of the Striped Peak thrust were transported southward into the Juan de Fuca deep marginal basin and now form mappable stratigraphic units in the upper middle to lower upper Eocene Aldwell Formation. Upper Eocene sedimentary rocks overlap the Crescent and Striped Peak thrusts; only minor movements have occurred along these thrust faults in post-late Eocene time.

A period of middle late Eocene faulting uplifted the pre-Tertiary terrane along the San Juan and Leech River faults on southern Vancouver Island. Sediments eroded from these fault scarps were transported southward into the Juan de Fuca basin and formed thick clastic wedges (debris flows) and channels of conglomerate and sandstone in the Hoko River and Lyre Formations of late Eocene age.

Middle Oligocene thrust faulting on the narrow Vancouver Island shelf uplifted shallow-water marine strata of late Eocene age, which, in turn, were transported southward by gravity sliding into the basin. This ancient submarine landslide deposit, the Jansen Creek

Member of the Makah Formation, is more than 250 m thick and extends for more than 12 km along the south coast of the Strait of Juan de Fuca. This olistostromal unit, which consists of blocks up to 100 m in length of basaltic sandstone and conglomerate that contain shallow-water mollusks of late Eocene age, is interbedded with bathyal siltstone and sandstone strata of middle Oligocene age.

Renewed faulting on the Vancouver shelf occurred in latest Oligocene time, and blocks of mollusk-bearing shallow-water marine sandstone and conglomerate derived from fault scarps were transported southward in broad channels. These conglomerates form thick lenticular units in the bathyal siltstone strata of the upper Oligocene Pysht Formation. The deep marginal Juan de Fuca basin shoaled during the early Miocene as coarse clastic debris derived from the uplifted Vancouver terrane filled the basin, culminating in coal-bearing continental deposits.

North-trending sandstone dikes, which are common in the lower Eocene to upper Miocene sequence, lend support to north-south compression during this period, as they were interpreted as having been injected along fractures perpendicular to the direction of minimum compressional (east-west) stress.

The episodic periods of north-south compressive tectonics along the north side of the Olympic Peninsula and in the Strait of Juan de Fuca were interpreted as resulting from the buttress effect of Vancouver Island to a northward moving Washington-Oregon Coast Range Tertiary terrane. This northward motion of the Washington-Oregon terrane was inferred to have been driven by either the strongly oblique convergence of the Farallon plate or intermittent coupling between the northward moving Farallon plate and the Washington-Oregon terrane.

A major period of northeastward directed convergence between the Farallon plate and newly accreted Washington and Oregon Coast Range terrane occurred in late middle Miocene time. The regional unconformity at the base of upper Miocene strata and the upper Oligocene to upper middle Miocene mélange and broken formations exposed along the west side of the Olympic Peninsula (Hoh assemblage) provide a geologic record of this period of plate convergence. Interpretation of seismic-reflection profiles indicated that subduction of the Farallon plate continued on the continental margin of Oregon and Washington from late Miocene through late(?) Pleistocene time, as evidenced by landward and seaward verging thrust faults and associated anticlines that involve strata of these ages on the Continental Shelf and Slope.

Molybdenum and tungsten mineralization in northern Washington

During recent mapping for the geologic framework programs, F. K. Miller and T. G. Theodore encountered significant amounts of molybdenum mineralization and geochemical indications of tungsten mineralization in and around two small granodiorite stocks in the Harvey Creek and Noisy Creek drainages in Pend Oreille County, Wash. Another pluton of the same rock type also has yielded anomalous amounts of molybdenum in a single stream-sediment sample about 14 km to the east.

All the mineralization appears to be associated with muscovite-biotite granodiorite of Cretaceous age that crops out in at least five noncontiguous plutons of about 0.2 km² to about 35 km² in area. Molybdenum mineralization occurs primarily in a small stock, the Harvey Creek body, which is cut by many quartz veins from less than one millimeter to several centimeters in width. The pluton inferred to be responsible for the single anomalous molybdenum value in a stream-sediment sample, the Boulder Mountain body, has not yet been examined beyond the mapping of its areal extent.

Tungsten mineralization is indicated only by stream-sediment anomalies; apparently it is associated with a pluton of composition similar to those of the Boulder Mountain and Harvey Creek bodies. The pluton with associated tungsten mineralization, the Hall Mountain body, is about 3 km northwest of the Harvey Creek body. The Hall Mountain pluton intrudes carbonate rocks of the Wallace Formation of Middle Proterozoic age for at least 1.2 km along strike. A thin veneer of glacial material and slope wash covers the contact zone, which presumably is the site of the tungsten mineralization. Gold and silver anomalies have been detected in stream-sediment samples from drainages east and northeast of the Hall Mountain body; the anomalies may be related to that pluton. Each of the three bodies mentioned above and two others are separate plutons of a single plutonic type referred to as the granodiorite of Hall Mountain.

The combination of abundant quartz veins, widespread but locally intense alteration, and sparsely but widely distributed molybdenite in the Harvey Creek body and nearby host rocks warranted detailed exploration of the stock. Fluid-inclusion studies by Theodore suggested that the major part of the molybdenum system has not been removed by erosion. Anomalous concentrations of tungsten and locally anomalous molybdenum values from panned stream-sediment samples taken in streams draining the Hall Mountain body suggested that parts of that pluton and the carbonate rocks near it are attractive targets for shallow-depth exploration.

The anomalous molybdenum content in the panned stream-sediment sample from the Boulder Mountain

body and the abundant quartz veins in parts of that body suggested that mineralization may be fairly widespread throughout the plutonic type, although the detailed work required to verify the economic potential has not been conducted. At least two occurrences of tungsten-molybdenum mineralization associated with the granodiorite of Reeder Creek, about 25 km south-east of the Hall Mountain body, have not yet been examined by Miller and Theodore. The granodiorite of Reeder Creek is similar and possibly genetically related to the granodiorite of Hall Mountain. The repeated association of tungsten-molybdenum mineralization with this rock type qualifies it as an attractive exploration target.

Stratigraphy of Tertiary volcanic rocks, Cascade Range

Recent geologic mapping in the Snoqualmie Pass 1:100,000 quadrangle, west-central Washington, by R. W. Tabor, V. A. Frizzell, and D. B. Booth has revealed a twofold sequence of middle and younger Tertiary volcanic rocks that are probably equivalent to parts of the classic sequence of the Ohanapecosh-Stevens Ridge, and Fifes Peak Formations in Rainier National Park described by Fiske, Hopson, and Waters (1963).

In the western part of the quadrangle, in the vicinity of the Green and Cedar Rivers, a thick pile of well-bedded, highly altered pyroclastic rocks of mostly andesitic composition conformably overlies the upper Puget Group of probable late Eocene age. To the east, the pyroclastics overlie, with angular unconformity, the Naches Formation, a Puget Group time equivalent. Flow rocks of andesite and basalt are common in the lower part of this pile of altered pyroclastics. A dacite ash-flow tuff, well up in the pile, is 32 m.y. old, on the basis of zircon fission-track ages. These rocks appeared to correlate with the Ohanapecosh Formation in the Mount Rainier area to the south (Vance, 1982).

Overlying the unit equivalent to the Ohanapecosh, and separated from it by a probable unconformity, is a sequence of porphyritic andesitic lavas and interbedded mudflow breccias. On the basis of lithology, these rocks correlate with the Fifes Peak Formation. The dacitic Stevens Ridge Formation, which occurs between the Ohanapecosh and the Fifes Peak elsewhere, is missing in the Cedar and Green River areas, although thin, dacitic ash-flow tuffs below the andesite flow unit may be equivalent to the Stevens Ridge.

The volcanic sequence in the Snoqualmie Pass quadrangle is folded into broad synclines separated by west-northwest trending faults that are subparallel to a major fault in the White River area that has downdropped to the south rocks continuous with the Ohanapecosh-Fifes Peak sequence.

The Pasayten fault, a major tectonic boundary in north-central Washington

Mapping in the Doe Mountain 15' quadrangle in north-central Washington in 1981 by V. A. Todd revealed that the Pasayten fault, a major structural boundary between the Jurassic-Cretaceous rocks of the Methow Graben and the Cretaceous(?) crystalline rocks of the Okanogan Highlands, has had at least two periods of activity. The earlier of the two periods was accompanied by mylonitization of the western margin of a zoned trondhjemitic batholith which lies northeast of the fault (part of the Okanogan crystalline complex), and the later period by brittle deformation localized in the eugeosynclinal rocks of the Methow Graben west of the fault. Prebatholithic inclusions of miogeoclinal(?) sedimentary rocks east of the fault have been metamorphosed to high grade, whereas the marine sedimentary and volcanic rocks of the Methow Graben are essentially unmetamorphosed. The Pasayten fault, therefore, must have a net displacement of regional extent but the direction(s) of slip were not yet determined.

ALASKA

STATEWIDE

Alaska Mineral Resource Assessment Program

The goals of the Alaska Mineral Resource Assessment Program (AMRAP) are (1) to provide mineral resource information to Congress, the administration, and the public for land-use decisions, particularly in regard to the mandate of the Alaska National Interests Lands Conservation Act (ANILCA); (2) to provide geological information to the mineral industry, natives of Alaska and other private and public users concerned with exploration and development; (3) to provide comprehensive mineral resource information to help guide national mineral policy; and (4) to increase the limited knowledge of Alaska's mineral resources.

AMRAP functions at four levels. Level I produces statewide summaries of the State's mineral resources. Compilation at this level continued during 1982 and is based on past and present investigations by the USGS and other agencies and organizations. Level II studies identify areas of mineral resource potential, with favorable areas shown on maps at 1:1,000,000 scale, and present some measure of the probable size and grade of undiscovered deposits. One study, in southeastern Alaska, continued at this level in 1982. Level II reports incorporate findings of Level III work, which addresses 1:250,000-scale quadrangles (approximately 1.8 million ha each) and includes geologic mapping, aeromagnetic

and other geophysical analysis, geochemical sampling, grade and tonnage modeling, and topical studies. The main thrust of AMRAP at present is Level III; it uses interdisciplinary teams for each quadrangle. Fieldwork was conducted in 16 quadrangles and final reports were in preparation for 14 additional quadrangles in 1982. Level IV investigations focus on (1) individual mineral deposits or mining districts to determine their size, nature, and origin, and (2) topical studies that can provide answers to major stratigraphic, structural, paleontologic, and petrologic problems and aid in interpreting the geologic setting and character of mineral deposits. Thirty-seven Level IV investigations were undertaken in 1982.

ANILCA calls for mineral resource assessment of all public land in Alaska, and the USGS, through AMRAP, has the lead role in this endeavor. This act affects the selection of areas, and in some instances projects, and enlarges the program to consider mineral fuels. Six USGS projects that focus on various aspects of mineral fuels were active in 1982.

ANILCA activities

Members of the USGS headquartered in Alaska, California, Colorado, and elsewhere were engaged in numerous projects that contributed to reports or data-gathering requirements of various sections of ANILCA. The first of the annual reports mandated by Section 1011 was published as Geological Survey Circular 884. That report, prepared with the cooperation of other Federal agencies and relying heavily on AMRAP, summarizes public information about activities and findings of these agencies that relate to energy, nonfuel, and critical and strategic mineral resources of the State.

Tectonostratigraphic terrane studies

The Alaska fragments project, work being conducted by D. L. Jones, N. J. Silberling, J. W. Miller, and P. J. Coney, commenced in 1976 with detailed studies of the Chulitna terrane of south-central Alaska. This study was the first application in Alaska of detailed radiolarian biostratigraphy and resulted in (1) recognition of Upper Devonian ophiolites overlying Upper Jurassic cherts and argillites, and (2) complete revision of Devonian through Cretaceous stratigraphy. Results were published in Professional Papers 1121-A and 1121-B (Jones and others, 1980; Nichols and Silberling, 1979.) The scope was then expanded to include the entire central Alaska Range from Farewell on the west to Windy Pass on the east. A reconnaissance geologic map of this region is in preparation as an open-file map; a summary of results was published in 1982 (Jones and others, 1982).

Eleven discrete terranes characterize the central Alaska Range, including fragments of continental margins, oceanic seamounts, deep marine basins with pelagic sediments, and deep basins with flysch. Time of accretion of these disparate terranes was late Early to Late Cretaceous. A preliminary terrane map of the entire State was released in open file in 1981 (Jones and others, 1981). This map shows the distribution and character of more than 50 Alaskan terranes. A revised edition is in preparation and will be published on the new North American base map at a scale of 1:250,000. This will constitute sheet A of a 5-sheet series of terrane maps that will cover the entire cordillera of North America.

In 1981 project studies were extended northward, in collaboration with Robert Chapman, into the Rampart district (Tozitna terrane). These studies were continued in 1982 with additional investigations along the southeastern margin of the Brooks Range (Angayucham terrane). This latter area will be the main focus for 1983 field operations. Approximately 110 chert samples were collected in 1982, and these will provide new biostratigraphic data needed to unravel the complex internal stratigraphy of these oceanic terranes.

NORTHERN ALASKA

Depth and temperature of permafrost on the Alaskan Arctic Slope

The only way to determine the depth of permafrost is to monitor the return to equilibrium of temperatures in boreholes that penetrate it. Such measurements are under way by A. H. Lachenbruch, J. H. Sass, L. A. Lawver, M. C. Brewer, and T. H. Moses, Jr., in 25 wells on the Alaskan Arctic Slope. Twenty-one of these wells are in the National Petroleum Reserve and four are in the foothills to the east. Near-equilibrium results indicate that permafrost thickness in the Reserve generally ranges between 200 and 400 m (compared to more than 600 m at Prudhoe Bay); there are large local variations and no conspicuous regional trends. By contrast, the long-term mean temperature of the ground surface (one factor determining permafrost depth) varies systematically from north to south in a pattern modified by regional topography. The observed variations in permafrost temperature and depth cannot result primarily from effects of surface bodies of water or regional variations in heat flow; they are consistent, however, with expectable variations in the thermal conductivity of the sediments. It remains to be determined by conductivity measurements whether certain sites with anomalously high local gradients have anomalously high heat flow. If

so, this might indicate upwelling of interstitial fluids in the underlying basin sediments.

Permafrost, heat flow, and the geothermal regime at Prudhoe Bay

Temperature measurements made through permafrost in the oil field at Prudhoe Bay, combined with laboratory measurements of the thermal conductivity of drill cuttings, permit an evaluation of in situ thermal properties and an understanding of the general factors that control the geothermal regime. A sharp drop in temperature gradient at approximately 600 m represents a contrast in thermal conductivity caused by the downward change from interstitial ice to interstitial water at the base of permafrost under near steady-state conditions. Interpretation of the gradient contrast in terms of a simple model for the conductivity of an aggregate yields the mean ice content (approximately 39 percent) and thermal conductivities for the frozen and thawed sections (8.1 and 7.4 mcal/cm sec degrees C, respectively). These results, obtained by A. H. Lachenbruch, J. H. Sass, B. V. Marshall, and T. H. Moses, Jr., yield a heat flow of approximately 1.3 HFU, which is similar to other values on the Alaskan Arctic coast; the anomalously deep permafrost is a result of the anomalously high conductivity of the siliceous ice-rich sediments. Curvature in the upper 160 m of the temperature profiles represents a warming of about 1.8 degrees C of the mean surface temperature and a net accumulation of 5.6 kcal/cm² by the solid Earth surface during the last 100 yr or so. Rising sea level and thawing ice cliffs probably caused the shoreline to advance tens of kilometers in the last 20,000 yr, inundating a part of the continental shelf that is now the target of intensive oil exploration. A simple conduction model suggests that this recently inundated region is underlain by near-melting ice-rich permafrost to depths of 300 to 500 m; its presence is important to seismic interpretations in oil exploration and to engineering considerations in oil production. With confirmation of the permafrost configuration by offshore drilling, heat-conduction models can yield reliable new information of the chronology of arctic shorelines.

Desert conditions in northern Alaska during the last glaciation

Fossil sand wedges of late Wisconsin age have been identified on the Alaskan Arctic Coastal Plain by L. D. Carter, D. M. Hopkins, and J. P. Galloway. Sand wedges are not forming today in Alaska, but are forming in the driest parts of the ice-free areas of Antarctica where eolian sand moving across a vegetation-free surface drops into open thermal-contraction cracks.

The fossil sand wedges are as much as 3 m wide and 7 m deep and occur over a broad area northeast of a large, stabilized sand sea that occupies more than 7,000 km² (Carter, 1981). Bedding attitudes in the dunes and dune ridge orientations indicate that the sand-moving winds were easterly to northeasterly. The sand wedges evidently developed as some of the wind-driven sand dropped into thermal-contraction cracks as it moved west across the coastal plain. Radiocarbon dating of sparse herbaceous plant remains shows that the dunes were active during late Wisconsin time.

Downwind of the dunes is a broad belt of eolian silt. Fossils of mammoth, horse, and bison are common in this area, but no radiocarbon dates on these animals are less than 28,000 yr B.P., and few organic remains have been found in deposits of this area that are between 28,000 and 14,500 yr old.

This part of the Arctic Coastal Plain between 28,000 and 14,500 yr ago was evidently a dry, wind-swept desert that was nearly devoid of vegetation and large mammals. The remainder of the coastal plain and of the foothills probably was similarly barren, and steppe-tundra vegetation and large mammals may not have persisted into late Wisconsin time throughout this region.

Maturity of upper Paleozoic surface rocks related to Cretaceous heating event

Samples of black shale collected by W. P. Brosge, H. N. Reiser, J. T. Dutro, Jr., and R. L. Detterman during several years of work in the eastern and central Brooks Range have been analyzed in order to judge their quality as source rocks for hydrocarbons. Data from 78 samples of upper Paleozoic and 40 samples of Mesozoic rocks show that most of the rocks are supra-mature. The Jurassic and Cretaceous shales contain sufficient organic material of the right type to have been source rocks for oil and gas. The youngest Devonian and Mississippian shales also contain sufficient organic material to have been source rocks, but they contain kerogen that probably would have yielded gas rather than oil. The lower Upper Devonian and Permian shales contain organic material that is insufficient and of the wrong kind to have yielded oil or gas. The geographic and stratigraphic distribution of paleotemperatures indicated by the reflectance of vitrinite, correlated with temperatures indicated by the alteration of conodonts in the same area, suggests that in the central Brooks Range the maximum heating was not related to depth of stratigraphic or tectonic burial but to distance north of the Cretaceous heating center in the metamorphosed core of the Brooks Range.

The Kanayut Conglomerate: one of North America's most extensive ancient fluvial deposits

Fieldwork in 1981 by T. H. Nilsen and T. E. Moore in the Husky Mountains and Mulgrave Hills of northwestern Alaska revealed the presence of a nonmarine unit above the Noatak Sandstone and below the Kayak Shale that they consider to be the Kanayut Conglomerate. The Kanayut, the fluvial part of a major Upper Devonian and Lower Mississippian(?) deltaic complex, was distinguished from the adjacent units by the presence of fining-upward cycles of conglomerate, sandstone and shale, intervals of red and brown shale with paleosols and plant fossils, highly indurated silica-cemented sandstone and conglomerate, and many channelized beds. The maximum thickness of the Kanayut measured is 240 m; the maximum clast size is 3 cm. Recognition of the Kanayut near the Chukchi Sea shows that its fluvial deposits once covered an area at least 900 km long and 100 km wide in northern Alaska.

EAST-CENTRAL ALASKA

Glacial studies in the Yukon-Tanana Upland

In the summer of 1982, F. R. Weber, assisted by H. L. Foster and Ann Byrd, completed field examination of the glacial deposits near Glacier Mountain and other alpine areas in the northeastern part of the Yukon-Tanana Upland. A major terrace system on the Seventymile River and on the Fortymile River was related to outwash of the second oldest recognizable glaciation. A thin tephra layer was found in several excavations near the Seventymile River, further confirming a northern extent of the White River ash (Weber, 1982).

Studies were also completed in the Charley River area for setting up a glacial type section representative of the entire upland. Organic-rich samples for pollen studies were collected from poorly consolidated sediments underlying the oldest moraine, in the hope that they might represent a continuous sequence from Tertiary to Quaternary. A continuous collection was made by T. A. Ager in the Mount Harper glacial lake sediments to help establish a pollen flora sequence from Sangamon(?) to late Wisconsin time.

Recycled gold in interior Alaska

It seems increasingly clear that gold has been recycled through Tertiary continental deposits prior to its incorporation in the recent placers throughout much of interior Alaska. Gold was panned from several suspected Tertiary conglomerates in the so-called Tintina

fault zone of the Circle quadrangle during fieldwork in 1981 by W. E. Yeend and co-workers. Although gold has been reported from Tertiary rocks in neighboring quadrangles (Mertie, 1938), none has been listed from Tertiary rocks of the Circle quadrangle. Tertiary(?) clastic rocks in the Circle quadrangle seem to be restricted to the Tintina fault zone, although it seems probable that when initially deposited they covered areas beyond the fault zone. If so, they most likely were a source for much of the gold that now occurs in the recent alluvium and has supplied the Circle district placer miners with a gold resource for over 80 yr. In the Healy quadrangle, directly west of the Mount Hayes quadrangle, gold was panned from the contact of the Lignite Creek Formation of middle Miocene age and the Nenana Gravel of Late Miocene and Early Pliocene age near the area where the main highway to Fairbanks crosses Panguingue Creek. In the Mount Hayes quadrangle, gold is present in conglomerates of early Tertiary(?) age (Yeend, 1981). Therefore, it seems likely that at least some gold in Holocene deposits in these quadrangles has been reworked from the Tertiary clastic rocks.

Radiolaria indicate Carboniferous and Triassic ages for chert in the Circle Volcanics, Circle quadrangle

Radiolaria-bearing chert samples were collected by H. L. Foster, G. W. Cushing, F. R. Weber, and Jo Laird from cherts interlayered in both the Circle Volcanics (Mertie, 1937) and the mafic igneous rocks of the Crazy Mountains, in the Little Crazy Mountains, and along the Yukon River in the Circle quadrangle, east-central Alaska. The Radiolaria were identified by D. L. Jones, B. L. Murchey, and C. D. Blome.

Chert along the Yukon is interlayered with fine-grained basalt and underlain by gabbro; it contains Radiolaria of latest Late Mississippian or Early Pennsylvanian age. In the east Crazy Mountains, an east-trending band of chert beds, probably part of the Circle Volcanics, yields Late Mississippian and latest Late Mississippian or Early Pennsylvanian Radiolaria. To the north of this band, chert in contact with gabbro and basalt contains late Triassic radiolarians. In the Little Crazy Mountains, both Carboniferous and Middle to Late Triassic Radiolaria occur in chert interlayered in gabbro and basalt.

In the field, cherts of different ages and the mafic igneous rocks with which they are associated cannot be distinguished on lithologic characteristics and, at present, the cherts and basalts of different ages are not mapped separately. Because of the poor exposures and scarcity of fossils in the Circle quadrangle, identification of radiolarians from chert is of major significance in deciphering the geologic relations and history. The

radiolarians from the Circle Volcanics indicate a terrane that includes at least two widely separated times of chert deposition, Carboniferous and Triassic. This information will aid in correlation with similar-appearing chert and mafic igneous rocks to the west.

WEST-CENTRAL ALASKA

New evidence for strike-slip displacement on the Kaltag fault

A potassium-argon age of 112 m.y. (Early Cretaceous) was obtained from a biotite mineral separate from the granite pluton in the southwestern part of the Kaiyuh Mountains. The age is of interest because it suggests that the pluton may represent the southern end of the Melozitna pluton, offset approximately 160 km to the west along the Kaltag fault. The Melozitna pluton, located north of and apparently cut off by the fault, has yielded a potassium-argon age of 111 m.y. and is compositionally similar to the Kaiyuh Mountains pluton (Patton and Hoare, 1968; Chapman and Patton, 1978). Both plutons intrude lithologically similar metamorphic complexes. A previous estimate of 130 km of strike-slip movement along this segment of the Kaltag fault is based on right-lateral separation of the southeastern margin of the Yukon-Koyukuk basin (Patton and Hoare, 1968). North of the fault this margin lies along the Melozitna River valley, a short distance west of the Melozitna pluton; south of the fault it appears to lie between the Kaiyuh Mountains and the Yukon River.

SOUTHERN ALASKA

Evolution of sedimentary systems during the Mesozoic and Cenozoic Eras, southern Alaska

The evolution of sedimentary systems during the Mesozoic and Cenozoic Eras in southern Alaska can be divided into six episodes, each representing a tectonic cycle that is presently recorded, with varying degrees of clarity, as a plutonic belt containing related sedimentary rocks that are bounded by unconformities or faults. These six episodes or tectonic cycles, which are sequential but in places overlap, occurred during the (1) Permian(?) through Early Jurassic, (2) Early Jurassic into Early Cretaceous, (3) late Early Jurassic into early Late(?) Cretaceous, (4) Late Cretaceous, (5) early Cenozoic, and (6) late Cenozoic, according to L. B. Magoon and C. E. Kirschner.

Each tectonic cycle began with magmatism and volcanism that constructed a magmatic arc with a backarc and a forearc basin, outerarc ridge, shelf, slope, trench,

and abyssal plain. Uplift and erosion dissected the magmatic arc and outerarc ridge, and sediment filled the arc basins, slope, and trench and then spilled onto the abyssal plain. Throughout the cycle, tectonism, magmatism, and sedimentation were ongoing at varying intensities, each cycle or episode affecting the previous cycle. This evolution can be traced in the composition of the plutonic bodies, conglomerates, and sandstones. Thus, southern Alaska has evolved from a young continental and oceanic crust to mature continental crust by magmatism, sedimentation, and accretion.

Paleomagnetic data suggest that much of southern Alaska south of the Denali fault evolved as one or more terranes or plates in southerly latitudes in Permian(?) time that were accreted to the North American continental terranes by early Cenozoic time. The temporal and spatial relations of these terranes throughout geologic time in relation to the tectonic cycles is intricate and complicated. The Alaska-Aleutian Range volcanoplutonic arc and the associated Queen Charlotte transition zone transform-fault system have dominated the depositional and structural pattern in southern Alaska since early Cenozoic time.

SOUTHWESTERN ALASKA

Offset of Tertiary arcs on the Alaska Peninsula

Geologic mapping and potassium-argon dating by R. L. Detterman, F. H. Wilson, J. E. Case, and Nora Shew in the Ugashik and western part of the Karluk quadrangles have shown that the Eocene and Oligocene volcanic arc continues into these quadrangles from the south in the Chignik and Sutwik Island quadrangles. Surface exposures of the arc extend northward to approximately 57°30'N., or midway through the Ugashik quadrangle, but none are observed north of that point. Subsurface drill-hole data (Brockway and others, 1975) indicate continuation of the arc, possibly offset to the northwest of the northernmost known surface exposures.

In the extreme northern part of the Ugashik and Karluk quadrangles, volcanic rocks again become important. These volcanic rocks are as yet undated; however, they may be related to the Katmai late Tertiary volcanic centers.

Like the early Tertiary volcanic arc, the present-day Aleutian arc is also offset to the northwest in the northern part of the Ugashik and Karluk quadrangles. No major offset of the Mesozoic rocks is indicated through the offset zone; this fact suggests a change in the Tertiary tectonic regime in the area of the offset.

SOUTHEASTERN ALASKA

Burnt Island Conglomerate (Upper Triassic) on Screen Islands

The Burnt Island Conglomerate (Muffler, 1967) is an important unit in the Upper Triassic section in Keku Strait. This distinctive unit had not been recognized previously in other Triassic localities. Recent detailed mapping, fossil determinations, and evaluation of tectonic setting support correlation of rocks on the Screen Islands in Clarence Strait with the type Burnt Island Conglomerate.

Fieldwork by S. M. Karl on the Screen Islands shows that the conglomerate is associated with calcarenite, calcisiltite, silty limestone, and calcareous lithic sandstone. It is a well-bedded, poorly sorted, bimodal chert, volcanic, and limestone cobble conglomerate, with a matrix of medium- to coarse-grained calcarenite and calcareous lithic sandstone. The composition of clasts suggests a local source effectively isolated from terrigenous influence. Limestone clasts in the conglomerate contain Permian fossils. Ammonites and conodonts in the sandstone and limestones overlying and intercalated with the conglomerate are Late Triassic (late Carnian to early Norian) in ages.

Recognition of this unit on the Screen Islands extends the known area of Burnt Island Conglomerate some 100 km southeast of the type area and establishes the presence of the unit in the Clarence Strait fault zone, a wide pre-middle Tertiary structural feature that includes blocks as old as Silurian(?) and as young as Early Cretaceous.

New fossils from Taku terrane suggest Permian metallogenic province

The Taku terrane is one of several major tectonostratigraphic terranes in southeastern Alaska (Berg and others, 1978) and is host to numerous undated vein and stratabound massive sulfide deposits (Berg, 1979). For most of its extent, it is fault bounded on the west by Upper Jurassic and Cretaceous flysch and volcanic rocks of the Gravina-Nutzotin belt, which separates the Taku from the Alexander terrane. On the east the Taku is bounded by the metamorphic and plutonic complex of the Tracy Arm terrane. Although grossly dissimilar in its geologic and structural history from adjoining terranes, the Taku is difficult to characterize stratigraphically. Its heterogeneous rocks are complexly deformed, pervasively metamorphosed, and sparsely fossiliferous.

In 1980 and 1981, collections of Permian conodonts and brachiopods and Triassic mollusks were made from the Taku terrane by H. C. Berg, N. J. Silberling, D. L. Jones, and P. J. Coney (Silberling and others, 1981).

Conodonts from marble intercalated with phyllite and felsic metatuff near Coon Cove include *Neogondolella idahoensis* (Youngquist, Hawley, and Miller) and *Hindeodus* sp. of Leonardian (late Early Permian) Age. Poorly preserved Permian brachiopods from this locality are assigned to *Stenocisma* sp. and *Neospirifer?* sp. About 4.5 km south of Coon Cove, ammonites and fragments of halobiid bivalves (probably *Daonella*) are preserved as crushed molds in small concretions in foliated limestone and slate. The ammonites include *Lobites* cf. *L. pacianus* McLearn, *Joannites* sp., and *Meginoceras?* sp., diagnostic of a late Ladinian (latest Middle Triassic) Age.

Although the stratigraphy of the Taku terrane is still imperfectly known, these age determinations reinforce the pronounced stratigraphic differences between the Taku and the Annette terranes as portrayed by Berg and others (1978). Briefly stated, in the Annette terrane, Upper Triassic strata, ranging from early Norian to middle Norian in age, rest unconformably on Devonian and older metamorphic and plutonic rocks; strata correlative with those at the two fossil localities in the Taku terrane are not represented. The fact that faunally dated Middle Triassic rocks are not known elsewhere in southeastern Alaska further distinguishes the Taku terrane.

The new fossil discoveries also have potentially significant metallogenic implications for the stratabound mineral deposits in the Taku terrane. Many of these deposits are localized in rusty-weathered quartz-muscovite-calcite-pyrite schist similar to the felsic metatuff intercalated with the Permian marble near Coon Cove. The original age of these metamorphosed syngenetic deposits and host rocks is unknown, but the similarity in lithology suggests that it may be Permian. If so, many of the numerous stratabound massive sulfide deposits in the Taku terrane may be parts of a heretofore unrecognized metamorphosed and structurally dismembered Permian metallogenic province that stretches from Ketchikan to Juneau.

Mineral assemblages and compositional variations, Barrovian metamorphic sequence, near Juneau

A regional metamorphic terrane containing mineral assemblages reflecting conditions of metamorphism that range from those of the pumpellyite-prehnite facies to those of the upper amphibolite facies is exposed along the west margin of the Coast plutonic-metamorphic complex in southeastern Alaska. It is well exposed near Juneau, where Forbes (1959) documented the first appearance of the Barrovian index minerals biotite, garnet, staurolite, kyanite, and sillimanite in a transect along Blackerby Ridge. More recently, moderately to steeply northeast-dipping mineral isograds have been

mapped over a broad area from Taku Inlet to Berners Bay (Ford and Brew, 1973, 1977; Brew and Ford, 1977). The existence and character of the sequence are important in understanding the evolution of the Coast plutonic-metamorphic complex, which is the major geologic entity in the western cordillera of North America.

Studies by G. R. Himmelberg, A. B. Ford, and D. A. Brew show that the metamorphic belt consists dominantly of intermixed pelitic and semipelitic sedimentary rocks and mafic volcanic and intrusive rocks. Impure calcareous metasediments, quartzite, and quartz dioritic and granodioritic orthogneiss are also present. Seven equilibrium pelitic mineral assemblages have been identified; two each in the biotite, garnet, and sillimanite zones, and one in the kyanite zone.

Biotite in 26 samples and garnet in 19 samples have been chemically analyzed with the electron microprobe analyzer. In the lower biotite zone the biotites are green, whereas all others are brown or reddish brown. Biotite shows a range in $100 \text{ Mg}/(\text{Mg}+\text{Fe}+\text{Mn})$ of 30.9 to 71.6; however, there is no correlation between this ratio and metamorphic grade. Retention of the biotite compositional differences on a scale of millimeters indicates that intergrain metamorphic diffusion has been restricted to a scale of millimeters or less.

Garnet compositional variation is complex, both in individual crystals and between crystals of different specimens. Most garnets are zoned. In the garnet, staurolite, and part of the kyanite zone, garnet cores are generally lower in iron and magnesium and enriched in manganese relative to the margins, a well established pattern generally considered as "normal." In the higher grade rocks, garnet is most commonly reversely zoned; that is, the rims are generally enriched in manganese and lower in iron and magnesium relative to the cores.

Temperatures of equilibration have been calculated from the distribution of iron and magnesium between garnet and biotite in 19 specimens by using the empirical calibration of Thompson (1976) and the experimental calibration of Ferry and Spear (1978). The temperature range, calculated by Thompson calibration, is from approximately 495° C in the lower garnet zone to 690° C in the sillimanite zone; the range is from 495° to 750° C if calculated by Ferry and Spear calibration.

Granitic rocks and migmatites in the Coast plutonic complex near Petersburg

A variety of plutonic rocks dominates the western part of the Coast plutonic complex (CPC). The most outstanding of these is the CPC sill, a foliated tonalite mass hundreds of kilometers long (Brew and Morrell, 1980; Brew and Ford, 1981). In the project area, the sill shows

both magmatic and metamorphic features and is considered to be synkinematic with Eocene metamorphism and deformation that primarily affected rocks to the west. Preliminary information suggests that the CPC sill may locally "grade" into the cross-cutting unfoli-

ated granodiorite that forms the backbone of the Coast Mountains. Complicated migmatites have resulted from the intrusion of country rock, first by the CPC sill rocks and later by representatives of the unfoliated suite.

WATER-RESOURCE INVESTIGATIONS

The mission of the USGS's Water Resources Division (fig. 1) is to provide, interpret, and apply the hydrologic information needed for the optimum utilization and management of the Nation's water resources. This is accomplished, in large part, through cooperative programs with other Federal, State, and local agencies. The USGS also cooperates with the Department of State in providing scientific and technical assistance to international agencies.

The USGS conducts systematic investigations, surveys and research on the occurrence, quality, quantity, distribution, use, movement, and value of the Nation's water resources. This work includes (1) investigations of floods and droughts and their magnitudes, frequencies, and relations to climate and physiographic factors; (2) evaluations of available waters in river basins and ground-water provinces, including assessments of water requirements for industrial, domestic, and agricultural purposes; (3) determination of the chemical, physical,

and biological characteristics of surface and ground water and the relation of water quality and suspended-sediment load to various parts of the hydrologic cycle; and (4) studies of the interrelation of water supply with climate, topography, vegetation, soils, and urbanization.

One of the USGS's most important activities is disseminating water data and the results of investigations and research by means of reports, maps, computerized information services, and other forms of public releases.

The USGS coordinates the activities of Federal agencies in the acquisition of water data for streams, lakes, reservoirs, estuaries, and ground waters, maintains a national network, conducts special water-data-acquisition activities, and maintains a central catalog of water information for use by Federal agencies and other interested parties.

Supportive basic and problem-oriented research is conducted in hydraulics, hydrology, and related fields of science to improve the scientific bases for investigations



FIGURE 1.—Index map of the conterminous United States showing areal subdivisions used in the discussion of water resources.

and measurement techniques, and to provide sufficient information about hydrologic systems so that quantitative predictions of their responses to stress can be made.

During FY 1981, data on streamflow were collected at 7,543 continuous-record discharge stations, at 1,188 lake- and reservoir-level sites, and at 8,993 partial-record streamflow stations. More than 13,000 maps of flood-prone areas in all States and Puerto Rico have been completed to date. Studies of the quality of surface water were expanded; the USGS analyzed surface water at 10,037 water-quality stations in the United States. Constituents and properties measured include selected major cations and anions, specific conductance or dissolved solids, and pH. Other constituents measured as needed include trace elements, phosphorous and nitrogen compounds, detergents, pesticides, radioactivity, phenols, BOD, and coliform bacteria. Water-temperature records were collected at most of the water-quality stations. Sediment data were obtained at 4,197 locations.

Annually, about 500 USGS scientists report participation in areal water-resource studies and research on hydrologic principles, processes, and techniques. There were 1,304 active water-resource projects in FY 1981; 369 of the studies were classified as research projects. Of the water-resource studies, 85 were related to urban hydrology problems, 182 were energy related projects, and 62 were related to water use.

In FY 1981, 725 areal appraisal studies were carried out. Maximum and average areas of the studies were about 1.5×10^6 km² and 0.058×10^6 km², respectively. Total areal appraisal funding was \$49.8 million. Ground-water studies have been made or are currently in progress in all areas of the Nation. Measurements of ground-water levels were made in about 17,000 wells, and periodic measurements in connection with investigations of ground water were made in many thousands of other wells. Quality of ground water was studied at 12,076 sites in the United States. Studies of saline-water aquifers, particularly as a medium for disposal of waste products, are becoming increasingly important, as are hydrologic principles and analytic and predictive methodologies for determining the flow of pollutants in ground-water systems. Land subsidence caused by ground-water depletion, the possibilities for induced ground-water recharge, and the practicality of subsurface disposal of wastes are under investigation. Ground-water supplies for energy development and the effects of coal-mining activities on both ground- and surface-water resources are being intensively studied. FY 1981 saw the continuation of an intensive program designed to monitor and to evaluate hydrologic effects of the Mount St. Helens volcanic eruptions.

The use of computers in research studies of hydrologic systems, in expanding data-storage systems, and

in quantifying many aspects of water-resource studies continued to increase during FY 1981. Daily streamflow records for about 20,445 sites were stored on magnetic tape, and data on about 815,000 wells and springs have been entered in a new automated system for storage and retrieval of ground-water data. Digital-computer techniques are used to some extent in almost all of the research projects, and new techniques and programs are being developed continually.

NORTHEASTERN REGION

Water-quality activities in the northeastern region are shifting strongly toward assessing ground-water contamination rather than surface-water contamination, although selected river reaches are being comprehensively assessed. Evaluating the impact of atmospheric deposition continues to be a strong element and will continue to be from all indications.

Emphasis on ground-water contamination and atmospheric deposition in the Northeast may be directly related to the high concentration of people and industry and the consequent waste products. Most ground-water investigations involve assessing contamination from landfills, which commonly contain complex mixtures of exotic organic compounds.

The Appalachian and New England corridors are impacted by atmospheric deposition of solids and liquids transported by winds from both west and south. The direct impact is subtle and difficult to measure. Therefore, analyzing the deposition itself constitutes the major effort. Delineation of acid-prone areas and studies of processes that control impacts are in progress and are highly dependent on surficial geology.

Streamflow from Virginia to Maine was significantly below normal from January to March 1981. In January, the Delaware River Basin Commission declared a drought emergency and ordered reduced diversions, minimum design flows, and restrictions on nonessential water use. Reservoir levels in northern New Jersey were at or near record lows. Streamflow and reservoir levels recovered slightly in February, but by the end of March had decreased to nearly the record lows of January. Flows did not return to near normal range until May.

Ironically, the most severe flooding in the Northeast during 1981 occurred in August in northern Maine, where two periods of extremely heavy rain caused local flooding in the Caribou area, with damage estimated at \$4 million. The monthly mean flow of the St. John River at Fort Kent was the highest for August in 55 years of record.

Two-dimensional and three-dimensional digital modeling of aquifers in Indiana, New York, Pennsylvania, and Maryland was used to assess the flow systems and

aquifer characteristics of selected aquifers, which are important to the water resources of these areas.

Studies that evaluated potential water-well yields from selected aquifers were completed in Minnesota, Pennsylvania, and New York. In each of these investigations, water quality also was evaluated to provide additional information on the availability of additional water supplies.

The drought of fall 1980 continued to intensify in much of the Northeast, and, during 1981, water supplies in many areas remained critically low. One measure of the severity of the drought is the quantity of water in storage in the three reservoirs constructed by New York City in the Delaware River basin. Under provisions of a decree of the Supreme Court, the city is allowed to divert out of the basin an average of 3×10^6 m³/d. Compensating releases from the reservoirs are required for the benefit of downstream riparians. The releases are intended to maintain a minimum flow downstream at the USGS gaging station at Montague, N.J., of 49.6 m³/s, with higher seasonal flows stipulated during the summer.

On January 2, 1981, storage in the reservoirs was 3.4×10^8 m³, 33 percent of capacity and lower than at any time since January 1, 1966, when storage declined to 2.3×10^8 m³ during the worst drought of record in this area. Storage continued to decline until early February, when a minimum of 2.6×10^8 m³ was reached.

Because of the precarious situation, the quantity of water New York City was allowed to divert was appreciably curtailed; as a further conservation measure, the quantity required to be released for maintaining downstream flows was also reduced. By mid-January, the city's allowable diversion had been reduced in several steps from 3×10^6 m³/d to 2×10^6 m³/d, and the flow at Montague gaging station was targeted between 31 m³/s and 45 m³/s, with New Jersey diversions through the Delaware and Raritan Canal curtailed from an allowable 3.8×10^6 m³/d to 2.3×10^6 m³/d.

Water-supply conditions improved during February and for the next 3 months, after which withdrawals again exceeded inflow. At the end of December, the water in storage totaled about 5.4×10^8 m³, a distinct improvement during the year, but still far below the average of roughly 8.7×10^8 m³ in recent years.

DELAWARE

Unconfined aquifer mapped in southeastern Sussex County

J. M. Denver reported that the altitude of the base of the unconfined aquifer ranges from 9 m to more than 53 m below the NGVD of 1929. The deepest section ex-

tends from Indian River Bay to Selbyville and coincides with the subcrop area of a confined Miocene aquifer. Saturated thickness is greatest in the same area.

Geologic, geophysical, and drillers' logs were used to prepare five geologic sections and a configuration map of the base of the unconfined aquifer. A map of the saturated thickness was prepared by subtracting the altitude of the base of the aquifer from the altitude of the water table. Clay and silt layers within the aquifer were not included in the saturated thickness.

INDIANA

Ground-water resources of a glacial-outwash aquifer in Johnson and Morgan Counties

An unconfined glacial-outwash aquifer was studied by Z. C. Bailey and T. E. Imbrigiotta. Test drilling along the White River south of Indianapolis defined the 228-km² areal extent and the thickness of that segment of the sand and gravel. Saturated thickness of the aquifer, calculated from fall 1980 water levels, is as much as 30 m. Average hydraulic conductivity of the sand and gravel, estimated by specific-capacity tests, is 104 m/d. Observation of water levels and stream stage indicated that tributaries draining into the White River lose water to the ground-water system and recharge the aquifer with runoff from the bedrock and till uplands surrounding the outwash. Some recharge also enters the aquifer through areas where till interbeds with thinning outwash, but most recharge is direct precipitation. A two-dimensional digital ground-water flow model, calibrated to autumn 1980 water levels, was used to study the steady-state flow system of the outwash aquifer. Sensitivity analyses were made to test calibrated values of aquifer characteristics. A maximum pumpage simulation of 61 wells pumped 5 m³/s, reduced streamflow in the White River by 30 percent, and resulted in a maximum areal drawdown of about 8 m.

Chemical analyses of ground-water samples indicated a calcium bicarbonate water type with near-neutral pH, high alkalinity, very high hardness, and oxidizing redox conditions. National Drinking Water Regulations were exceeded for iron in 15 percent of the analyses and those for manganese in 49 percent. Temperature and dissolved organic carbon concentration varied seasonally. Dissolved organic carbon, manganese, and aluminum concentrations varied with differing boundary material, till, or bedrock.

Hydrologic and chemical evaluation of the ground-water resources of northwestern Elkhart County

A 3-year study defining the general flow and quality of water in the outwash aquifer system in northwestern Elkhart County, Ind., has been completed by T. E.

Imbriotta and Angel Martin, Jr. The saturated thickness of the primarily sand and gravel unconsolidated deposits averages 55 m and ranges from 25 to 150 m. Regional ground-water flow is toward the St. Joseph River. A ground-water flow model was used to simulate pumpings of 0.8×10^6 m³/s, 1.1×10^6 m³/s, and 2.2×10^6 m³/s at a proposed well-field site at the Elkhart Municipal Airport. The model-generated water-level maps indicated that only for the 2.2×10^6 m³/s simulated pumping could even a small part of the total flow into the pumping center come from the Himco landfill area.

The general ground-water quality was characterized by near neutral pH (7–8), average hardness greater than 200 mg/L as calcium carbonate, alkalinity greater than 150 mg/L as calcium carbonate, and a calcium bicarbonate water type. Eight volatile organic compounds were detected in samples from an industrial park area in east Elkhart. Concentrations of dissolved solids, HCO₃⁻, Br, Cl, SO₄⁻², NH₄⁺, Ca, Mg, Mn, K, Na, and dissolved organic carbon in the Himco landfill leachate were at least five times background concentrations. Bromide concentrations, the best indicator of the leachate, showed that the plume extended between 950 and 1,700 m downgradient from the landfill and was moving to lower horizons in the shallow aquifer as it moved downgradient.

Ground-water availability in the outwash aquifer, Marion County

A two-dimensional digital model of the outwash aquifer along the White River and Fall Creek was calibrated to conditions of October 1980 by B. S. Smith. The outwash aquifer is the principal ground-water resource in central Indiana, supplying 38 million m³ of water to industrial, commercial, and municipal users in 1980. Pumpage accounted for 29 percent of the total steady-state water budget of the aquifer.

Areal recharge to the aquifer was simulated at 62 million m³/yr, or 48 percent of the total recharge. Boundary flux from confined aquifers of the till plain flanking the outwash aquifer accounted for 41 percent of the total recharge; and leakage from the White River and Fall and Eagle Creeks induced by pumping accounted for 11 percent.

Steady-state pumpage experiments indicate that additional pumpage of 88 million m³/yr could be sustained without causing unacceptable water-level declines or streamflow reductions under normal conditions. However, streamflow reductions were near the 7-day, 10-year low flows recorded on the White River and Fall Creek with this additional pumpage. Additional withdrawals of 102 million m³/yr, when simulated, caused streamflow reductions in excess of the 7-day, 10-year low flows.

MARYLAND

Newly discovered paleochannels on the Delmarva Peninsula

Test drilling by L. J. Bachman of the USGS and J. M. Wilson of the Maryland Geological Survey has revealed two paleochannel segments incised in Miocene sediments and filled with the sediments of the Pensauken Formation. The channels are in the central Delmarva Peninsula near the towns of Ridgely and Harmony in Carolina County. There is a possible third paleochannel segment near the village of Barclay in Queen Annes County. The paleochannel segments seem to be aligned with previously described segments to the south and east (Mack, Webb, and Gardner, 1971; Weigle, 1972). They seem to range from 400 to 800 m wide in the Ridgely and Harmony areas, and the maximum thickness of the channel fill ranges from 24 to 27 m. Test drilling did not reveal the maximum width of the segment at Barclay, but the maximum thickness is 18 m.

The channel fill is a medium to coarse silty tan to orange feldspathic sand with some gravel layers. Pumping tests in other segments of the paleochannel have revealed transmissivities as high as 5,340 m²/d (Mack and Thomas, 1972), one of the highest values in Maryland. These newly discovered paleochannel segments may also have the potential for a large-scale shallow water source for agricultural, industrial, and municipal users.

MASSACHUSETTS

Ground-water assessment in the Connecticut Valley lowlands

Nine mud rotary test wells drilled in Hadley and Sunderland, Mass., penetrated 30.5 to 92.4 m of unconsolidated sediments, according to B. P. Hansen. The lithology, in general, consisted of a surface deposit of 3.05 to 9.14 m of alluvial fine sand to gravel, with some silt, underlain by lacustrine clay to very fine sand. A thin discontinuous layer of till overlies Triassic bedrock. Geophysical logs and samples indicate that the clay fraction of the lacustrine deposits decreases toward the bottom of the sequence. Depths to bedrock were generally less than shown on bedrock contour maps, which were based on geophysical surveys and scant well information. Deep bedrock channels are much narrower or more discontinuous than previously suspected.

Evaluation of the Mattapoissett aquifer

As part of a statewide plan to protect ground-water quality and avoid competition and overdevelopment, the Massachusetts Water Resources Commission and

the USGS have selected the Mattapoissett aquifer for resource evaluation and digital analysis to demonstrate the hydrologic interdependence between well fields, streams, and land use. The aquifer, composed of glacial deposits of gravel and medium to fine sand, is typical of the many small aquifers that sustain public supplies in New England. In order to gather data to develop and calibrate a digital model, the USGS has installed 24 observation wells and 3 gaging stations, participated in aquifer tests to determine hydraulic properties, and conducted seismic refraction surveys of the bedrock surface. Preliminary analyses by J. C. Olimpio and Virginia deLima indicate that ground-water and surface-water quality is good throughout the valley; however, iron and manganese are typically high for the region, and occasional periods of salt-water intrusion into the southern part of the aquifer have been reported.

MICHIGAN

Water resources in Sleeping Bear Dunes National Lakeshore

A. H. Handy and J. R. Stark studied the water resources of the water-rich 24,585 ha Sleeping Bear Dunes National Lakeshore. The park contains more than 100 km of Lake Michigan shoreline, 16 inland lakes, and 4 streams. In addition, aquifers in glacial deposits contain an abundance of water at depths ranging from 100 feet to land surface.

Chemical quality of ground water and surface water is excellent; mean concentration of dissolved solids is 172 mg/L in ground water and 283 mg/L in surface water. None of 11 trace metals for which analyses were made exceeded EPA drinking water standards, and all samples were free of chlorophenoxyacid herbicides, organochlorine insecticides, polychlorinated naphthalenes, and polychlorinated biphenyls.

Water in Van Buren County

Water resources of Van Buren County, Mich., were studied by F. R. Twenter and T. R. Cummings to determine their quantity and quality, especially as related to agricultural practices, land use, industrial and municipal water use, and contamination. Forty sites on streams have been established and 30 wells installed to measure streamflow and water levels and to collect water samples for determining quality.

Most water supplies are from glacial aquifers. The deposits, 30 to 180 m thick, yield water of good quality in many places. Dissolved-solids concentration in most samples was less than 300 mg/L. In places, primarily in heavily irrigated and fertilized areas, problems arise

because of insufficient supplies, interference between wells, and contamination of both ground water and surface water. Near South Haven, glacial deposits as thick as 150 m consist mostly of clay and yield little or no water to wells. The municipal water supply is taken from Lake Michigan.

MINNESOTA

Appraisal of surficial aquifers

A ground-water appraisal of surficial outwash aquifers in Carlton, Kanabec, and Pine Counties is being completed by C. F. Myette. The aquifers cover about 1,500 km² and generally consist of fine sand. However, narrow channels (less than 2 km) of medium to very coarse sand, greater than 30 m thick, have been defined. Transmissivities range from less than 60 m²/d to greater than 2,000 m²/d, and potential well yields range from less than 1 to greater than 125 L/s. Depth to water is generally less than 6 m, and annual water-level fluctuations are less than 1.5 m.

Chemical analyses of water samples indicate that the ground water is a calcium bicarbonate type. Regionally, pH ranges from 6.3 to 8.4, specific conductance ranges from 65 to 850 μ mhos/cm, and dissolved solids range from 60 to 600 mg/L. Selected samples for dissolved radon-222 and dissolved radium-226 showed that concentrations ranged from 10 to 600 pCi/L of radon-222, while concentrations of radium-226 were all less than 0.1 pCi/L.

Water-quality appraisal of sand-plain aquifers

A regional investigation of water quality conditions that have resulted from contamination from nonpoint sources in the surficial sand-plain aquifers in Hubbard, Morrison, Otter Tail, and Wadena Counties is being conducted by C. F. Myette. Preliminary results indicate that concentrations of dissolved chloride and nitrite plus nitrate as nitrogen differ from place to place throughout the area but generally do not vary significantly with time. Exceptions have been noted in two local areas in west-central Minnesota where slight annual increases (1964-1981) in nitrite plus nitrate as nitrogen were detected. Most seasonal and annual variations in chemical concentrations coincide with seasonal water-level fluctuations. Results of sampling for pesticide analyses in November 1980 (3 months after application) showed no residuals of either the triazine group of herbicides or the orthophosphate group of insecticides. Residuals of simazine (0.1 mg/L) and atrazine (0.2 mg/L) were found.

Analyses of samples from nested wells near an experimental agricultural plot showed little vertical mixing of applied chemicals near the plot (150 m downgradient). High concentrations of nitrite plus nitrate (10 to 30 mg/L) were found near the water table and low concentrations (0.01 to 0.1 mg/L) were found near the base of the aquifer.

Water-level changes in major aquifers of the Twin Cities metropolitan area

M. E. Schoenberg reported that, although a cone of depression persists in the Mount Simon-Hinckley aquifer in the Twin Cities metropolitan area, water levels rose as much as 20 m during 1971-80. During the same period, water levels in the Prairie du Chien-Jordan aquifer were relatively stable regionally, but fluctuated through a range of 1 to 3 m locally. Patterns of seasonal water-level change in 1980 differed from those in 1971 for both aquifers. In the Mount Simon-Hinckley aquifer, seasonal changes from winter to summer were more areally extensive and of greater magnitude in 1980 than in 1971. In the Prairie du Chien-Jordan aquifer, the seasonal changes were less areally extensive and of smaller magnitude in 1980 than in 1971. These analyses generally suggest that (1) total annual pumpage from the Mount Simon-Hinckley aquifer decreased during 1971-80, and (2) the seasonal component of pumpage has increased in the Mount Simon-Hinckley aquifer from 1971-80 and decreased in the Prairie du Chien-Jordan aquifer.

NEW YORK

Potential supplement to New York City water supply

Ground-water resources in western Long Island are being considered for redevelopment as an emergency or supplemental source of water in Brooklyn and Queens. Ground water was a major source of public-water supply in Brooklyn and Queens until deterioration in quality from intrusion of salty ground water caused cessation of pumping in Kings County in 1947 and in southwest Queens County in 1974.

According to H. T. Buxton, this investigation was designed to ascertain (1) if the present ground-water quality justifies redevelopment of these resources, and (2) if so, what pumpage, either continuous or periodic, can be sustained without jeopardizing quality.

Ground-water levels were monitored and have recovered to near the levels of 1903. Chloride and nitrate were utilized as indicators of contamination from saltwater intrusion and surface sources. The data indicate that

the upper glacial aquifer in both counties has been contaminated with nitrate and chloride. However, the degree of contamination decreases eastward. The upper glacial aquifer shows indications of recovery from the severe saltwater intrusion induced during heavy pumping, but chloride contamination and remnants of past saltwater intrusion are still dominant in inland areas. Some contamination of deeper aquifers from surface sources is evident and is attributed to downward migration through areas of good hydraulic connection between aquifers.

Some potable water is available in the Jameco, Magothy and Lloyd aquifers; however, a precise estimate of the quantity available is undetermined.

Evaluation of ground-water resources in the Montauk area, Long Island

Fresh ground water in the Montauk area occurs as thin lenses floating on salinewater in the upper glacial aquifer, according to K. R. Prince. A preliminary cross-sectional flow model was developed to aid in accessing the freshwater resources. Location of the freshwater/salinewater interface was estimated on the basis of the Ghyben-Herzberg relationship, and sensitivity to various hydrologic parameters was tested. Model simulations show the interface location to be most dependent upon the location and characteristics of a clay unit anticipated at approximately 40 m below mean sea level.

Eight test wells were drilled to determine gross lithology and to locate the freshwater/salinewater interface. Results were in general agreement with preliminary model simulations, as freshwater occurs at thicknesses no greater than 40 m. Furthermore, the maximum thickness of freshwater tends to coincide with the contact between the upper glacial aquifer and the underlying Gardiners Clay unit.

Geophysical logs reveal extensive till near sea level. Because this till is low in hydraulic conductivity, differences are created in head potential of as much as 9.4 m over a vertical distance of 24.3 m. Ground water, formerly presumed to be perched, is actually part of the main flow system, but its movement through the system is being greatly impeded by the till. The till unit may also be acting as a confining layer to the main ground-water body, thereby tending to exacerbate saltwater upconing at some public-supply wells.

Synoptic study of snowpack chemistry

After an evaluation of snowpack chemistry and distribution throughout New York in 1981, R. V. Allen, N. E. Peters, and C. R. Barnes report that accumulation and storage of acids in the snowpack was at a maximum

in the southwestern Adirondack region. specific conductance, pH, and chloride concentration were measured for snowpack samples taken during four periods from approximately 90 sites. Areas of lowest pH included the Adirondack, Catskill, and southwestern regions. Relations between specific conductance and pH indicate an absence of acid-neutralizing materials in the snowpacks of remote watersheds. With increasing local development, samples show an increase in pH and contributions of neutralizing materials.

PENNSYLVANIA

Numerical-model evaluation of ground-water resources in the lower Susquehanna River basin

J. M. Gerhart and G. J. Lazorchick (Susquehanna River Basin Commission) report that a quasi-three-dimensional model of regional unconfined ground-water flow was used to evaluate the ground-water resources of the 9,044-km² lower Susquehanna River basin in Pennsylvania and Maryland. Steady-state and transient calibrations were used to determine the regional hydrologic characteristics of the various secondary permeability lithologies present. Hydraulic conductivities range from 0.02 to 53.04 m/d; specific yields range from 0.006 to 0.035; and stream leakage coefficients range from 0.02 to 13.11 m/d. Simulation of a uniform withdrawal of 25.4 mm of ground water showed that carbonate rocks are the most productive aquifers. Simulation of a hypothetical withdrawal scheme in which ground water was withdrawn until average annual ground-water flow to streams was halved resulted in a yield potential of 3.4 million m³/d for the lower basin. Under this scheme, the greatest yield potential is in the Cumberland Valley carbonate rocks, about 730 m³/d/km²; the least is in the Triassic conglomerate rocks, about 145 m³/d/km².

Appraisal of aquifers

J. H. Williams and D. A. Eckhardt report that glacial outwash and carbonate rocks are the most productive aquifers in Columbia County and surrounding areas. Estimated median yield for the aquifers, based on specific capacity, water-bearing zone, and water-level data, is about 12 L/s. The median yield for interbedded carbonate rocks and shale is estimated to be 6.3 L/s. Clastic aquifers, including shale and interbedded sandstone and shale, have the lowest median yield, 0.6 L/s.

Geophysical logs, including wellbore fluid-velocity tests, indicate that water occurs in the bedrock aquifers in discrete water-bearing zones, most within 100 m of

land surface. Drawdown data recorded for observation wells during pumping tests are erratic because of the variable secondary permeability, but the data indicate a directional hydraulic behavior along strike. Water quality is generally good, although local contamination problems exist.

WISCONSIN

Deep test wells

Three deep test wells were drilled in southwestern Wisconsin, according to P. J. Emmons. The wells, which penetrate Paleozoic sections to the top of the Precambrian crystalline basement rocks, were drilled to provide hydrologic and geologic information on the Cambrian-Ordovician aquifer system. Geophysical logs were made and aquifer tests using inflatable packers were conducted on each of the wells. Water-quality samples were collected from each interval where packers were set.

Potentiometric heads in the packer intervals in the 388-m-deep Red Mound School test well ranged from 60.3 to 131.5 m below land surface, and the specific capacities ranged from 2.3×10^{-3} to 4.1×10^{-5} m²/s. Water from each of the packer intervals was of a calcium-magnesium bicarbonate type. Heads in the 193-m-deep Stoddard test well ranged from 3.2 m below to 5.9 m above land surface. The specific capacities of the packer interval ranged from 5.0×10^{-5} to 3.2×10^{-3} m²/s. The water from each of the zones was a calcium-magnesium bicarbonate type. The Bagley test well, which is 435 m deep, has potentiometric heads ranging from 18.7 m above to 2.7 m below land surface. Specific capacities ranged from 8.1×10^{-6} to 5.9×10^{-2} m²/s in the packer intervals. With increasing depth, the water quality changes from a calcium bicarbonate and sulfate type through a calcium-magnesium bicarbonate type to a calcium-sodium sulfate and chloride type.

Ground-water-level fluctuations

G. L. Patterson analyzed historical ground-water-level data by using Pearson Type III statistical analyses to determine the frequency of occurrence of extreme high and low water levels. Preliminary results show that the 10 percent, 20 percent, and 50 percent probability of exceedance levels for both high and low water levels in five water-table wells vary only about 0.06 to 0.14 m from month to month. Only wells having at least 20 years of measurements were used. Similar results were obtained by using seasonal rather than monthly data.

SOUTHEASTERN REGION

Drought continued to plague the Southeastern United States during fiscal year 1981. The year ended with no relief in sight. Streamflow, which was deficient at the beginning of the year, continued to decline. Low flows of record were established for many streams with each succeeding month. Water-supply reservoirs, especially the smaller ones, were nearly dry and many communities were taking emergency measures to assure even a minimal water supply. Power generation at major hydroelectric plants was greatly reduced owing to lack of water. Navigation was halted on the Apalachicola-Chattahoochee Rivers owing to low stage, and navigation on other major river systems was impaired.

Declines in ground-water levels paralleled those of streamflow. Recharge to most aquifers was so slight during the so-called wet season that ground-water levels showed nothing more than a slight leveling off before they continued to decline. Ground-water use for irrigation increased in proportion to the severity of the drought. In the Mississippi alluvial plain of northern Arkansas, there was a 22 percent increase in the amount of irrigation water applied to rice and an 80 percent increase in that applied to cotton and soybeans. Ground-water levels, as a result, declined at 5 to 10 times the average rate. Similar impacts on ground-water levels were reported for other major irrigation areas such as the Yazoo Delta of Mississippi, southwestern Georgia, and central Florida.

The Cienaga Tiburones, a below sea level reclaimed swamp, is a prime area for rice production, which is being promoted by the Commonwealth of Puerto Rico. At present, however, seawater moves into the area through subsurface conduits in a limestone ridge that lies between the swamp and the sea. Studies presently underway indicate that the conduits can be located and the hydrogeology of the area is such that the seawater inflow can be controlled.

In Florida, as in most coastal areas, a reliable source of freshwater and saltwater encroachment into freshwater aquifers is of constant concern. A feasibility study of injection of freshwater into brackish water aquifers and later recovery of the freshwater is underway in Miami, Fla. Digital models are being used to analyze the relation of recovery efficiency to hydrologic conditions. At St. Petersburg, Fla., tertiary-treated sewage effluent is being injected in brackish water aquifers for disposal and possible future recovery for irrigation.

The origin and distribution of salty water along the Florida gulf coast is being investigated through geochemical studies in the Manasota and lower Peace basins and through a modeling study of the intercon-

nection of the Floridan aquifer and Tampa Bay. Ship channels being dredged in Tampa Bay are cutting into the top of the Floridan aquifer, an action that possibly will affect the freshwater-saltwater interface.

A counterpoint to the dominant concern for freshwater in Florida is a study of the Loxahatchee River estuary in southeastern Florida. Here a study to determine the relation of growth and type of vegetation and fouling organisms to salinity, bed material, and season of year is being completed.

The Coastal Plain aquifers in Georgia and other Southeastern States were a major area of study by teams from Georgia, South Carolina, Alabama, Florida, and the Regional Aquifer Systems Analysis projects. A model of the Tertiary limestone aquifer was constructed and calibrated for the Dougherty Plain, a major area of irrigation in southwest Georgia. The existing model of the Tertiary limestone aquifer at Savannah, Ga., was expanded and redesigned. Information from this model was incorporated in a model, constructed by RASA personnel, of the Tertiary limestone system that includes southeastern Georgia, northeastern Florida, and southern South Carolina.

Preliminary evaluation of the water chemistry of the Cretaceous aquifers in the southwestern Coastal Plain indicate high iron (15 mg/L) in the Columbus, Miss., area, high boron (8 mg/L) and high fluoride (10 mg/L) in coastal South Carolina.

Surface-water studies were not neglected in Georgia. A streamflow model developed for the Chattahoochee River in Georgia was applied to stage-hydrograph flood data for several sites in Kentucky. Results indicate that the model may be feasible for use at sites with hysteric or loop stage-discharge problems. Another study determined the probable magnitude of average standard error due to time-sampling bias for statistics of monthly minimum flows computed for streamflow stations. Also, in Georgia, regional storage requirements for utilization of as much as 60 percent of the mean average flow of streams were computed and compiled into draft storage diagrams.

In North Carolina, water quality in streams and rivers was once again a major item of study. Water-quality variability, pollution loads, and long-term water-quality trends of the Cape Fear River were investigated. A long-term study of the effects of channel excavation in the Black River near Dunn, N.C., is drawing to a close. Data collected before, during, and after construction document changes in water quality, streamflow, and ground-water levels.

Flow in a regulated reach of the Alabama River in central Alabama was modeled using a one-dimensional open-channel flow simulator. The model successfully tracked steep transients and computed negative flow

extending up major tributaries. In another modeling study, data from five small basins in contrasting hydrologic settings in mined and unmined basins in the Warrior coal field were used to develop a precipitation-runoff model.

Chloride-monitor wells in the Chicot aquifer of southwestern Louisiana show little indication of lateral salt-water encroachment in the coastal area. Locally, however, in isolated inland areas, increases in chloride have been observed. The increases are attributed to saltwater moving through openings in the confining bed separating the freshwater sands from underlying saltwater sands.

A study of the hydrogeology of lignite beds in three areas of northwestern Louisiana indicates that considerable dewatering of aquifers overlying or underlying the lignite beds may be required. High concentrations of iron, manganese, or chloride in the water from the different aquifers to be dewatered may cause disposal problems.

Researchers at the Gulf Coast Hydroscience Center reported on a variety of studies ranging from determining the precision of specific ion electrodes for the measurement of chloride and bromide in water to experiments involving vertical velocity profile in stratified open-channel flow and the evaluation of selected one-dimensional stream water-quality models. Samples from a massive "shale" formation from the geopressed zone of the northern Gulf of Mexico Basin were subjected to a number of physical and chemical analyses which gave unexpected results. In a companion study, methods were developed to use selected isotope as natural tracers in the aquifers of geopressed systems.

The newly established Hydrologic Instrument Facility has under development or is testing a variety of new equipment, including a Hydrologic Data Acquisition System that will provide universal instrumentation support, automatic field data collectors, and a rather prosaic but welcome lightweight tagline and tagline reel.

MULTISTATE STUDIES

Potentiometric surface of the Tertiary limestone aquifer system, Southeastern United States

The Tertiary limestone aquifer system of the Southeastern United States is a sequence of carbonate rocks referred to as the Floridan aquifer in Florida and is the principal artesian aquifer in Georgia, Alabama, and South Carolina. Currently, about 10 million m³ of water are pumped daily from this aquifer system. The potentiometric surface of the upper part of the aquifer system was mapped on the basis of water levels or artesian

pressures measured in more than 2,700 wells during a 12-day period in May 1980.

In about three-quarters of the area of aquifer occurrence, the potentiometric surface is largely unchanged from predevelopment conditions. In the remaining quarter of the area, the heavy withdrawal of water from the aquifer has produced areally extensive cones of depression. The two major areas of water-level decline are (1) a strip paralleling the Atlantic Ocean shoreline, including coastal Georgia and adjacent South Carolina and northeast Florida, and (2) west-central Florida to the east and south of Tampa Bay.

Geologic and hydrologic effects of Late Cretaceous and Cenozoic faulting of the Coastal Plain near the Savannah River, Georgia and South Carolina

Geologic and hydrologic investigations by R. E. Faye and D. C. Prowell have defined stratigraphic and hydraulic anomalies suggestive of faulting within Coastal Plain sediment near the Savannah River in Barnwell County, S.C., and Burke County, Ga. Site-specific investigations of subsurface geology indicate that hydraulic anomalies such as abrupt changes in potentiometric head and aquifer transmissivity, as well as relatively large discharges of ground water to the Savannah River, probably were caused by faulting of Triassic rocks and overlying Upper Cretaceous and Cenozoic Coastal Plain strata. Vertical offsets of sedimentary horizons of about 200 m were observed, and the thickness of the basal Coastal Plain aquifer across the fault was reduced from about 200 to about 55 m.

Other anomalous potentiometric and geologic data along a northeast-trending line between Statesboro, Ga., and Fairfax, S.C., suggest the possibility of similar faulting in correlative geologic units.

ARKANSAS

Effects of 1980 drought on ground-water levels in the Mississippi alluvial plain

In a recent analysis of the effects of the 1980 drought on water use for crop irrigation in the intensely farmed Mississippi alluvial plain of northern Arkansas, A. H. Ludwig noted that precipitation for 1980 was 201 mm below normal, and in some areas of the alluvial plain there was no measurable precipitation during the entire summer of 1980. In addition, maximum daily temperatures during the summer of 1980 remained above 38° C for more than 100 consecutive days.

Because of the deficient precipitation and soil moisture, there was a 22 percent increase in the amount of

irrigation water applied to rice as opposed to that applied during normal years of precipitation and an 80 percent increase in the amount of irrigation applied to cotton and soybeans as opposed to that applied during normal years of precipitation. The increased withdrawals of ground water in 1980 for crop irrigation were reflected by the lowering of ground-water levels (Edds, 1981) between March 1980 and March 1981. Declines in water levels in the alluvial aquifer, the principal source of irrigation water, ranged from 0.61 to 1.83 m. Water levels in the Sparta Sand, a supplementary-source aquifer for irrigation, declined as much as 3.05 m. The water-level changes in both aquifers between 1980 and 1981 represent a decline rate of 5 to 10 times greater than the long-term average rate.

FLORIDA

Hydrogeologic framework defined for the Sarasota-Port Charlotte area

A hydrogeologic study of the Sarasota-Port Charlotte area is nearing completion. According to R. M. Wolansky, the hydrogeologic framework consists of the surficial aquifer, intermediate aquifers (Tamiami-upper Hawthorn and lower Hawthorn-Tampa aquifers) and confining beds, Floridan aquifer, and basal confining bed (or base of the Floridan aquifer).

A water budget for the Sarasota-Port Charlotte area shows that with an average annual rainfall of 1295 mm/yr minus an evapotranspiration of 965 mm/yr and streamflow of 315 mm/yr, 15 mm/yr of recharge to the surficial aquifer remain. Combined pumpage from the aquifers is 35.8 mm/yr, and pumpage returned to the surficial aquifer is 27 mm/yr. Ground-water inflow to the aquifers is 54 mm/yr, and ground-water outflow is 61 mm/yr.

A preliminary quasi-three-dimensional model has been applied to the study area to check the reasonableness of the hydrogeologic framework defined and of aquifer parameters. The model was considered calibrated when the final head matrix was within plus or minus 1.5 of the starting head.

GEORGIA

Variability of average annual rainfall and average annual runoff

R. F. Carter and H. R. Stiles computed the quantity and variability of average annual rainfall and average annual runoff for the period 1941-70 for areas in Georgia. Average annual rainfall was as much as

1930 mm in northeast Georgia, but elsewhere was within about 10 percent of the statewide average of 1270 mm. Annual average runoff was as much as 1120 mm in the northeast but varied as much as 50 percent from the statewide average of 380 mm in other parts of the State. Runoff varied from 58 percent of the rainfall in the north to 24 percent of the rainfall in the south. Runoff also varied from year to year, but was more variable in the south than in the north. The standard deviation of the average annual runoff was as much as 67 percent of the mean for some stream gages in the south and was as little as 19 percent of the mean for some stream gages in the north.

Potentiometric surfaces and ground-water withdrawals from aquifers in southern Georgia

Potentiometric surfaces of the Clayton aquifer of southwest Georgia for predevelopment years 1950-56 and March 1981 were mapped by J. S. Clarke and R. E. Faye. Declines in the potentiometric surface of the Clayton aquifer were widespread throughout southwest Georgia and in the Albany area. The decline exceeded 55 m during the period 1892-1981.

Potentiometric surfaces of the Barnwell aquifer of east-central Georgia for predevelopment and November 1981 were mapped by H. R. Vincent. Declines in the potentiometric surface of the Barnwell aquifer were minimal over most of the study area, but declines in excess of 9 m were recorded in parts of Toombs, Tattnall, Bulloch, and Candler Counties.

Ground-water withdrawals in southwest Georgia over the period 1950-80 were analyzed by Rebekah Brooks and J. S. Clarke. They found that ground-water use increased 229 percent in Americus and 238 percent in Albany. During 1980, 0.38 m³/s was pumped from the Providence aquifer and 0.87 m³/s was pumped from the Clayton aquifer for municipal, industrial, and agricultural supplies.

LOUISIANA

Regional geohydrology of the northern Louisiana salt-dome basin

In FY 1981, hydrologic data were analyzed from a test-drilling program that was completed in FY 1980. A total of 16 observation wells at five test-drilling sites were completed as part of a Department of Energy study to determine if conditions are suitable for developing a high-level waste repository in salt domes in the northern Louisiana salt-dome basin. The test wells were drilled to depths as great as 910 m, and observation wells were completed in the Sparta Sand and Wilcox-Carrizo aquifers of Tertiary age and in the aquifers in

the Cretaceous Nacatoch Sand and rocks of Austin age. In the northern Louisiana salt-dome basin, the saline part of the Wilcox-Carrizo aquifer and aquifers in the Nacatoch Sand and rocks of Austin age are used for the disposal of industrial waste, principally oil-field brines, by injection wells.

Injection wells make the study of the regional hydrology of the northern Louisiana salt-dome basin difficult. According to G. N. Ryals, the drilling program provided an indication that injection wells have modified the flow system. For example, at one of the test-drilling sites located about 5 km south of Arcadia, La., two wells are screened in the Wilcox-Carrizo aquifer. The water level in the well screened in the upper part of the aquifer is about 55 m above the NGVD of 1929, which is consistent with other regional values. The water level in the well screened in the lower part of the aquifer is about 83 m above NGVD. An injection well, located about 3 km from the site, is screened in the same interval in the lower part of the aquifer. The water level in the upper well is probably not yet responding to the stress of increased pressure caused by the injection of fluids because of the retarding effect of an intervening clay bed.

VIRGINIA

Hydrogeology of the Culpeper basin

Inclusions and thin horizontal seams of fibrous gypsum (selenite) were present as fillings in fractures and bedding plane partings in core samples from a 168-m-deep well drilled in siltstone near the eastern border of the Triassic-Jurassic Culpeper basin in northern Virginia, according to Chester Zenone. The gypsum was observed in core samples from depths of about 140 m to the bottom of the well; vugs and open fractures above the 140 m depth probably resulted from solution of the gypsum (Posner and Zenone, 1982). The presence of gypsum in the siltstone had been postulated to explain the highly-mineralized, calcium sulfate type water produced from wells deeper than about 152 m, but had not been observed previously in cuttings from wells completed by air-rotary drilling methods.

CENTRAL REGION

Hydrologic activities in the central region during 1981 continued to emphasize studies related to energy development. Intensive hydrologic investigations related to coal mining continued in Colorado, Montana,

and Oklahoma; similar studies related to oil shale development continued in Wyoming. Hydrologic studies of small basins that are representative of potential coal-mining areas were given continual attention. Results of these studies are expected to be applied to leasing decisions, environmental impact statements, mining-plan formulations, and specifications for reclamation of mining areas.

Studies of regional aquifer systems continued in the High Plains of Colorado, Kansas, Nebraska, New Mexico, Oklahoma, South Dakota, Texas, and Wyoming that are underlain by the Tertiary Ogallala aquifer and associated deposits; in the southwestern alluvial basins in New Mexico and adjacent parts of Colorado and Texas; and in parts of Arkansas, Colorado, Kansas, Missouri, Nebraska, New Mexico, Oklahoma, South Dakota, and Texas that are underlain by carbonate aquifers. A study of the aquifers underlying the west gulf coast and the Mississippi Embayment in parts of Arkansas, Kentucky, Louisiana, Mississippi, Missouri, Tennessee, and Texas was started. In these areas, aquifer-system boundaries and characteristics are being studied intensively to determine storage capacity, natural discharge, withdrawals, sources and volumes of recharge, anticipated yields of wells, and effects of well yields on supplies and water quality. The studies also determine the history of ground-water development and the effects of future development on the aquifers under various assumptions as to rates and points of withdrawals. Mathematical models of the flow systems in the High Plains and southwestern alluvial basins are being prepared. The study of the regional aquifer system underlying the northern Great Plains in parts of Montana, North Dakota, South Dakota, and Wyoming has been completed and final reports are being prepared.

More detailed studies of the regional aquifer systems in the individual States have been completed in Montana (northern Great Plains), Nebraska (High Plains), Oklahoma (High Plains), and South Dakota (northern Great Plains). A study to determine the ground-water flow patterns in the carbonate aquifers in northeastern Missouri is continuing.

Surface-water activities continued to be an important part of the regional program. A study of flood hydrology of foothill streams continued in Colorado. Studies of channel geometry of streams in Colorado, Texas, and Wyoming were started or continued. Extensive studies of floods in Montana, including the effects of urbanization on flood peaks at Missoula and updated techniques for estimating magnitude and frequency of floods throughout the State, were completed. Transmission of "real time" surface-water data using data-collection platforms and an orbiting satellite started in Colorado and Texas during 1981.

Studies to determine the relations between surface water and ground water increased in the central region during 1981. These relations were studied in the Big Blue and Little Blue River basins in Gage and Jefferson Counties, Nebraska; in the Arkansas River basin in Finney and Kearny Counties, Kansas; along the North Canadian River in Oklahoma; and in the upstream parts of the Brazos River and Red River basins in Texas. Digital-computer models were used in the latter three studies to simulate the effects of possible management alternatives for these stream-aquifer systems.

Increasing demands for ground water have resulted in increased efforts to locate aquifers containing water suitable for irrigator and municipal supplies in the northeastern part of the central region. Significant aquifers have been delineated in Towner County, North Dakota, and Aurora, Davison, Hanson, Hughes, and Jerauld Counties, South Dakota.

The effects of acid rain on lakes, a potential national problem, continued to be studied in Colorado with emphasis on the flat Tops Wilderness Area. The nutrient primary-productivity study of Lake Koccanusu, Montana and British Columbia, was completed. A study to determine water-quality changes in small reservoirs in northeastern Montana has been started.

Principal studies related to water contamination were concentrated in Kansas and Oklahoma where the effects of discharge from abandoned lead and zinc mines on the quality of both ground and surface water are being investigated. Additional water-contamination studies were completed in Montana (ground water) and started or continued in Colorado (ground water), Montana (surface water), New Mexico (surface water), and Oklahoma (ground and surface water).

Central region research activities continued to be varied and complex. The toxicity of leachate from spent oil shale on alga is being investigated. Definition of the components of humic acids and spectrographic techniques have been improved. Sediment research continued in several areas: studies of bedload in Wyoming, and studies of large-scale bedforms, discharge needed for channel-width maintenance, sediment transport and effective discharge, and morphologic changes in channels, as related to streamflow changes in the Platte River basin in Nebraska, Colorado, and Wyoming. Numerous advances in borehole geophysics included theoretical methods for interpreting shear and compressional waves in fluid-filled boreholes; development of an improved heat-pulse flowmeter, an improved borehole-acoustic televiewer, and a prototype compensated-neutron porosity probe; use of borehole data to calibrate surface-resistivity measurements; use of borehole geophysics to characterize hydraulic properties of fractured rocks; and development of computer programs to

calculate hydraulic-conductivity distributions and estimate radioisotope concentrations in rocks penetrated by a borehole.

MULTISTATE STUDIES

Hydrochemistry of the Lower Cretaceous aquifers of the northern Great Plains, Montana, Wyoming, North Dakota, and South Dakota

The hydrochemistry of the Lower Cretaceous aquifers of the northern Great Plains has been studied at a reconnaissance level as part of the assessment of bedrock ground-water supplies. K. D. Peter mapped hydrochemical facies by using the relative proportions of the principal ions and identified factors controlling the hydrochemistry. Calcium bicarbonate facies, indicating recharge by recent meteoric water and water-mineral interactions, predominate near the outcrop areas in central Montana, the Black Hills, and part of eastern Wyoming. Sodium chloride facies in the Dakota-Newcastle-Muddy aquifer, but not the underlying Inyan Kara aquifer, indicate leakage of water from overlying marine shales to the Dakota-Newcastle-Muddy aquifer in southeastern Montana and northwestern South Dakota. The facies is sodium chloride in both aquifer systems in areas where there is upward leakage from Paleozoic aquifers containing water more saline than that in the Lower Cretaceous aquifers. These areas are in the Powder River Basin, northern Williston Basin, and part of south-central Montana. In eastern North Dakota, leakage of water from Paleozoic aquifers produces a sodium calcium chloride sulfate facies in the Inyan Kara. In central South Dakota, leakage of relatively fresher water from Paleozoic aquifers to the Inyan Kara aquifer generally produces a sodium sulfate facies or, further east, a calcium magnesium sulfate facies. Leakage from the Inyan Kara and possible Paleozoic aquifers to the Dakota-Newcastle-Muddy aquifer in southeastern South Dakota also produces a calcium magnesium sulfate facies. In northeastern South Dakota, the lower part of the Dakota also has a calcium magnesium sulfate facies due to leakage, but the upper part of the Dakota has a sodium sulfate chloride bicarbonate facies because mixing has decreased the effect of the leaking water on the hydrochemistry.

COLORADO

Ground water in Raton basin, Las Animas County

A. L. Geldon studied ground-water occurrence and quality, ground-water/surface-water relations, and the

impact of coal mining on the hydrologic system in the Raton basin. The basin is an asymmetrical trough filled with more than 4,900 m of Cretaceous to Holocene sedimentary rocks that are intruded by numerous stocks, dikes, and sills.

Virtually all the sedimentary formations transmit water, but intrusive rocks generally are barriers to flow. The Cheyenne-Dakota aquifer is moderately permeable, but the water commonly is a calcium sulfate type, and the aquifer generally is too deep to be economically developed. Cretaceous shales between the Dakota and Trinidad Sandstones yield excessively mineralized sulfate sodium chloride type water from confined sandstone and limestone layers and near-surface fractured and weathered zones. The Trinidad Sandstone generally contains potable calcium sodium bicarbonate type water, but has minimal specific capacity and is drained in outcrop areas. The coal-bearing Vermejo Formation and overlying Raton Formation yield less than 3 L/s to wells from arkosic sandstone and coal. The water is most commonly a sodium bicarbonate or a bicarbonate sulfate type. Yields and quality are best at the top of the Raton Formation, which receives recharge from the overlying Poison Canyon Formation. The Poison Canyon Formation and overlying Cuchara Formation commonly yield less than 0.5 L/s to wells in extensively dissected terrain around the Spanish Peaks, but as much as 5 L/s to wells north of the peaks. Water generally moves horizontally in sandstone layers and vertically through fractures in confining shale layers. The ground water is typically a calcium bicarbonate type with minimal dissolved solids, but excessively mineralized sodium chloride water surrounded by an aureole of sodium bicarbonate water occurs in the axial region of the basin. Holocene alluvium, as thick as 15 m in stream valleys, is saturated 0.3 to 6 m above bedrock; it yields as much as 30 L/s to wells. Water from the bedrock and mine discharge seeping into valley alluvium alter the quality of alluvial and surface water in river systems.

Ground water flows towards the structural axis of the basin. In small drainages, water collecting in alluvium from bedrock springs, mine discharge, precipitation, and storm runoff flows downgradient, issuing intermittently where bedrock is near the surface or where dikes cross the stream channel. Depth to water is less than 30 m in stream valleys, in the axial region of the basin, and at the Raton-Poison Canyon contact; depth to water is 30 to 120 m beneath drainage divides. Water levels in deep bedrock wells generally are isolated from seasonal climatic fluctuation, but shallow wells may become dry during droughts. Coal mining lowers the potentiometric surface, adds dissolved solids to ground and surface water, and increases sediment in rivers.

MISSOURI

Ground-water flow patterns in northeastern Missouri

According to J. L. Imes, the ground-water flow system in the Cambrian-Ordovician aquifer of northeastern Missouri has previously been poorly understood. Speculation regarding the movement of deep ground water has proceeded along two paths: (1) The northwest to southeast regional flow was assumed to discharge along the length of the Missouri River. This idea was supported by some early potentiometric maps of the area. (2) Freshwater entering the large outcrop zone around the St. Francois Mountains flowed northward under the Missouri River to meet the regional flow of saline ground water from the northwest, thus accounting for the presence of a saltwater-freshwater transition zone in northern Audrain County.

The construction of more detailed potentiometric maps and the results of modeling studies in this area show that an eight-county region immediately north of the Missouri River acts as a quasi-independent local freshwater flow system. Water enters this area by vertical leakage from the overlying Mississippian limestones and infiltration recharges where the aquifer outcrops atop the Lincoln fold; water discharges along the Missouri River. Potentiometric divides have developed that keep regional saline water from flowing through this region, resulting in the saltwater-freshwater interface. Part of the regional water discharges in Chariton and southern Howard Counties. The remainder flows eastward around the Lincoln fold.

MONTANA

Water-resource investigations of the Lake Creek valley, northwestern Montana

The potential effects on the water resources of the Lake Creek valley as a result of mining activities on Mt. Vernon were the subject of a study by G. W. Levings, R. F. Ferreira, and J. H. Lambing. During the 2-year study, 53 private wells were inventoried and water samples were collected from 24 of them. Ten small-diameter test holes, ranging in depth from 4 to 57 m, were drilled for observation of water levels and collection of water-quality samples. Water samples for determination of physical, chemical, and biological characteristics were collected from Bull, Savage, and Schoolhouse Lakes during the summers of 1980 and 1981.

The concentration of dissolved solids in water samples ranged from 27 to 289 mg/L for wells, from 25

to 58 mg/L for streams, and from 27 to 159 mg/L for lakes. Although all lakes had near-anaerobic bottom conditions, the water quality was not detrimental to most recreational uses. However, further nutrient enrichment from possible real estate and recreational developments could result in nuisance algal conditions and summer or winter fishkills.

NEBRASKA

Geohydrology of the High Plains aquifer system in Nebraska

The geohydrology of the High Plains aquifer system in Nebraska was evaluated by R. A. Pettijohn and H. H. Chen as part of a regional study of the High Plains aquifer. This aquifer system underlies about 80 percent of the State and is the principal source of water for irrigation in Nebraska. Preliminary results indicate that the saturated thickness of the aquifer system exceeds 60 m in 66 percent of the study area. Approximately 4.95 trillion m³ of water are stored in the aquifer system.

Hydraulic conductivity of the aquifer system varies from less than 7.6 m/d in fine grain Tertiary deposits in western Nebraska to more than 91 m/d in Quaternary sands along the Republican River valley in south-central Nebraska. The average hydraulic conductivity is about 15 m/d. Specific yield ranges from 10 to 20 percent and averages 16 percent.

The number of registered irrigation wells in the High Plains area of Nebraska exceeded 63,500 by 1980. Forty-two percent of the land area overlying the High Plains aquifer system is cropland and 29 percent of the cropland was irrigated during 1980. The volume of water pumped during 1980 to irrigate 2,181,000 ha of cropland was about 10.6 billion m³, or an application rate of approximately 1.2 m/ha.

NORTH DAKOTA

Extension of Spiritwood aquifer system through North Dakota into Canada

Results of test drilling show that an extensive buried glacial-drift aquifer complex underlies about 800 km² of Towner County, North Dakota. A study by P. G. Randich indicates that the aquifer extends from the Devils Lake area north through Towner County into Canada near Hansboro, North Dakota. Saturated thicknesses of sand and gravel deposits indicate that in places potential yields to wells completed in the aquifer will be as much as 90 L/s. Water quality generally meets drinking-water standards established by the EPA.

OKLAHOMA

Geohydrology of the Roubidoux aquifer, northeastern Oklahoma

Withdrawal of ground water from the Roubidoux aquifer has developed a cone of depression with an area of about 1,000 km² and a depth of about 200 m, according to R. W. Fairchild. Although the deepest part of the depression is in Oklahoma, its shape is influenced by pumpage in adjacent Kansas and Missouri. Water levels near the center of the cone appear to have stabilized, but the cone appears to be widening.

Water in the Roubidoux aquifer is potentially subject to contamination from water in abandoned zinc mines about 150 m above the aquifer. In most of northeastern Oklahoma, the Chattanooga Shale serves as an impermeable layer between the Boone Formation and the underlying rocks. In the mine area, however, the Chattanooga Shale is absent and the head in the Boone aquifer is about 360 m higher than in the Roubidoux aquifer. Consequently, the head differential may cause the highly mineralized mine water to flow downward into the Roubidoux aquifer.

Analyses of water from the Roubidoux aquifer show that dissolved-solids concentrations ranged from 140 to 1,170 mg/L and averaged about 380 mg/L. Dissolved-iron concentration of 20,000 µg/L occurred in water from one well, suggesting that the water may have been affected by mine water. Of 13 samples analyzed for radiocativity, the gross alpha radiation ranged from 16 to 57 pCi/L; the source of the radioactivity is unknown.

SOUTH DAKOTA

Large yields from glacial aquifers in Aurora and Jerauld Counties

More than 1 billion m³ of slightly saline water is stored beneath an area of 800 km² in five major glacial aquifers, according to a study of Aurora and Jerauld Counties in southeastern South Dakota by L. J. Hamilton. Hamilton estimates that wells yielding as much as 0.1 m³/s can be constructed within the 150 km² area of the aquifers where the transmissivity of the sand and gravel exceeds 1,000 m²/d. Pumping does not significantly affect water levels of the glacial aquifers. Draw-down generally was less than 1 m in observation wells located less than 2 km from 22 irrigation wells that pumped nearly 3 million m³ of water from three of the aquifers during 1979.

Outwash-channel aquifer in central South Dakota

L. J. Hamilton reports that a 50-km long buried channel, filled with as much as 30 m of outwash sand and

gravel, was found beneath about 200 km² of western Hughes County in central South Dakota. This extensive glacial aquifer, called the Gray Goose aquifer, was discovered through a comprehensive program of well canvassing and test drilling in cooperation with the South Dakota State Geological Survey. Water levels in the aquifer range from 15 m below land surface at Oahe Reservoir on the Missouri River to 75 m below land surface 30 km east of the reservoir.

Water from the aquifer varies in quality. Water from one well had a specific conductance of 1,150 μ mhos/cm and a hardness of 380 mg/L, but another well 5 km away yielded water with a specific conductance of 5,000 μ mhos/cm and a hardness of 3,400 mg/L.

Aquifers in south-central South Dakota

Five glacial and three bedrock aquifers were mapped in an appraisal by D. S. Hansen of the water resources of Hanson and Davison Counties, south-central South Dakota. The glacial aquifers contain about 1 billion m³ of water in storage and the bedrock aquifers contain about 13 billion m³ of water in storage.

The Floyd aquifer, a shallow glacial sand and gravel aquifer in Hanson County, averages 12 m in thickness and may yield as much as 0.06 m³/s to wells. The Niobrara aquifer, a fractured Cretaceous chalk in Davison County, ranges from 6 to 37 m in thickness and may yield as much as 0.06 m³/s to wells. Water from the aquifers is used for irrigation. The water from both the Floyd and Niobrara aquifers is a sodium calcium sulfate type. Average dissolved-solids concentrations are 1,500 mg/L in water from the Floyd aquifer and 1,700 mg/L in water from the Niobrara aquifer.

WESTERN REGION

The water year 1981 in the western region was characterized by an absence of extreme hydrologic events. Local flooding occurred at a number of places, but there were no major or regional floods. In contrast, streamflow was deficient in the summer of 1981 in a broad band that included most of Oregon, southern Idaho, and the northern third of California and Nevada. The situation had not developed into a major regional drought. The water levels in 21 of 24 reservoirs throughout the region were at or above normal levels at the end of September 1981.

The national program for RASA continued to play a major role in the Water Resources Division program in

FY 1981. Four RASA projects were active in the western region: the Southwestern Alluvial Basins RASA Project (Arizona, with small adjacent parts of California, Nevada, and New Mexico); the Central Valley Aquifer Project (California); the Great Basin RASA Project (Nevada and Utah); and the Snake River Plain RASA Project (Idaho).

Major accomplishments of the Southwestern and Great Basin Projects were the classification of the many ground-water basins of each study area into a few generic types, so that generic models with wide transfer value can be developed.

In the Central Valley Project, geochemical studies resulted in identifying mineral controls on the quality of shallow ground water and isolating sources of nitrates. A technique of texture mapping, based on computer analysis of well logs, was developed. The resulting texture maps are useful as guides for siting of wells and waste-disposal facilities. The two-dimensional ground-water model for the Central Valley was completed and calibrated. Calibration runs of the model pointed out significant errors in the datum elevations used in many water-level measurements.

Among the major accomplishments of the Snake River Plain Project were mapping the thickness of the basalt aquifer, estimating irrigation water use and ground-water recharge, and development of a ground-water model of the regional aquifer system. The basalt aquifer of the Snake River Group was found to range in thickness from less than 600 m to about 1,800 m, on the basis of surface-resistivity profiles, regional gravity models, and interpretation of drillers' logs.

Quality of ground water is an increasingly important concern and is therefore becoming a greater component of the USGS' Federal-State Cooperative Program of water resources investigations. A recently completed study of the San Juan Islands, Wash., found that 11 percent of the wells sampled had chloride concentrations indicating seawater intrusion, and 12 percent had occurrences of coliform bacteria. Another project is underway to determine the feasibility of injecting treated wastewater for ground-water recharge in the baylands at Palo Alto, Calif. Injection-well tests showed a slight improvement of well specific capacity during testing and no evidence of clogging. The improvement of specific capacity is believed to be the result of dissolution by injection water of calcite in the aquifer.

Columbia Glacier, near Valdez, Alaska, underwent a record rate of retreat during 1981 and released increased numbers of icebergs into the important oil shipping lanes of Prince William Sound. The front of the glacier had retreated about 450 m between mid-June and mid-October, at least 200 m more than in any previously observed year since 1899. A team of USGS glaciologists

had predicted in 1980 that the glacier's rate of retreat would accelerate during the next two to three years; these observations appear to bear out that prediction, which is based on a model that relates calving to water depth. Prior to 1981, the glacier's terminus was on or near a moraine shoal that restricts calving of icebergs. Because of that year's rapid glacial retreat, however, the terminus now faces much deeper water, a condition that could lead to an even more drastic rate of retreat and breakup. Once drastic retreat is underway, the glacier is expected to recede, with possible short-period interruptions, for 30 to 50 years. Such a retreat will reduce the glacier's length by almost half, from about 66 km to 34 km.

Studies of the effects of the May 18, 1980, eruption of Mount St. Helens continued in 1981. Resurveys of stream-channel cross sections and field observations in the Toutle River basin indicate that large volumes of the material emplaced in headwater areas by the eruption have been transported to downstream areas. Individual downvalley reaches exhibited multiple episodes of scour and fill, in a complex response to induced sediment. However, a net trend toward channel aggradation in downstream reaches appears to exist. Large volumes of material, particularly from debris avalanche deposits in the North Fork basin, still remain readily available for transport to downstream reaches.

Studies of gases from Mount St. Helens show that the water (steam) in the volcano is derived from dehydration of metamorphic rocks in the basement below the volcano. Although water is the dominant (85 percent) gas in the unsaturated zone of the volcano, it is at low pressure and has a very low discharge rate. The rate is so low that water in the clouds above the volcano is almost entirely meteoric water. The steam is at much too low a pressure to cause an eruption. The explosive gas is CO_2 from very deep (mantle) sources.

As a result of the catastrophic eruption of Mount St. Helens, assessment of baseline conditions and potential hydrologic hazards was begun at several other volcanoes in the western region. Those included in the program are Lassen Peak and Mount Shasta (California); Mount Hood and Three Sisters (Oregon); Mount Baker and Mount Rainier (Washington); and Mount Spurr (Alaska). Stream channels were surveyed and water-quality data collected, and aerial photography was obtained to develop photogrammetric information on channel cross sections for potential use in flood-routing models.

A 932-m diamond core hole was drilled into the caldera of Newberry Volcano near Bend, Oreg., as part of the Geothermal Research Program. A maximum temperature of 265° C, the highest temperature yet recorded in a drill hole in the Pacific Northwest, was

measured at the bottom of the hole. The high geothermal gradient suggests that a potent heat source underlies the crater at relatively shallow depth in the Earth's crust. These findings offer the first positive evidence that geothermal resources suitable for electric power generation may underlie volcanoes in the U.S. Cascade Range at shallow depths.

Studies of the hydrodynamics, chemistry, and ecology of the San Francisco Bay estuarine system continued to produce interesting and significant results. An intensive survey of the distribution, species composition, and productivity of phytoplankton and zooplankton in the bay, based on data collected between 1975 and 1979, demonstrated that plankton dynamics to northern San Francisco Bay, a partially mixed estuary, clearly are related to discharge through the Sacramento River. During the severe drought of 1976-77, plankton biomass was lower than in previous and subsequent years of normal river discharge. Both abundance and species composition of plankton changed during the drought. These results suggest that further diversions of freshwater from the estuary will reduce primary production and food resources for fisheries.

Significant trends in western region programs of the Water Resources Division are a greater emphasis on water-quality studies, ground-water models, and network-design analyses. Water-quality studies are increasingly concerned with toxic wastes as a source of ground-water contamination and nonpoint sources of pollution of streams, lakes, and estuaries. As water management becomes more sophisticated, often involving conjunctive use of surface and ground waters, model studies are in greater demand to assist the managers in evaluating alternative plans. In the present period of scarce resources, both fiscal and personnel, network design studies that seek improvement in the cost-effectiveness of data collection programs are being undertaken.

IDAHO

Ground-water conditions in the Michaud Flats area, Fort Hall Indian Reservation

N. D. Jacobson reports that ground water occurs under both confined and unconfined conditions in the Michaud Flats area. Productive artesian wells are completed in the pediment gravel, basalt flows of the Big Hole Basalt and Starlight Formation, and sand and gravel of the Sunbeam Formation. A few shallow domestic wells are completed in a water-table aquifer in the Michaud Gravel.

Two chemical industries are located in the study area. One is a complex that produces dry and liquid fertilizers from phosphate ore and manufactures gypsum and phosphoric acid. The other is a plant that produces elemental phosphorus. These industries are the largest users of ground water in the area and, together, pumped about 8.9×10^6 m³ in 1980.

Historically, high levels of arsenic and other minor elements were observed in water sampled from several wells completed in the water-table aquifer. During this study, concentrations of arsenic and other minor elements in most wells and springs were within drinking-water standards. The concentration of arsenic exceeded the standard in only one well.

Ground-water-quality assessment, southern Elmore and northern Owyhee Counties

In a study undertaken to relate current ground-water quality to hydrogeologic and cultural environments, D. J. Parliman collected water-quality and well-construction data for 92 wells completed in aquifers in 5 major geologic units.

Results indicate that the chemistry of the water is affected by mixing between hot water (more than 40° C) that migrates upward from great depths along faults and cold water (less than 20° C) that occurs in near-surface aquifers at relatively shallow depths. Sodium, potassium, and bicarbonate are the principal ions in the hot water, whereas the cold water is characteristically calcium magnesium bicarbonate dominated. Warm waters, having temperatures between 20° and 40° C, generally reflect the degree of mixing between the hot and cold waters.

Locally, some waters contain concentrations of dissolved solids, sulfate, nitrite plus nitrate, fluoride, arsenic, iron, manganese, or selenium that exceed limits established by the EPA or exceed tolerance thresholds for irrigation and livestock uses. Where long-term water-quality data are available, some waters show an increase in concentration of dissolved solids, sulfate, nitrite plus nitrate, chloride, or total phosphorus that may indicate contamination from land-surface sources.

Ground-water trends

In a study analyzing hydrographs from wells and determining possible causes for water-level trends, R. E. Lewis reports that 359 wells had net long-term (10 years) water-level changes between -13.0 and +7.3 m. About 18 percent of the wells showed long-term rises in water levels; the remainder showed long-term declines. Nine wells showed net declines of more than 6.1 m but only one showed a net rise of more than 6.1 m.

NEVADA

Ground water in Kyle and Lee Canyons, Spring Mountains, southern Nevada

Rocks in the study area consist of faulted and fractured carbonate bedrock of Paleozoic age, and unconsolidated to consolidated alluvium of Quaternary age that partly fills each of the canyons, according to R. W. Plume. Part of the alluvium of Kyle Canyon is saturated throughout the year. It receives inflow from carbonate rocks in upper parts of the canyon and loses outflow to carbonate rocks in lower parts of the canyon. The entire Kyle Canyon watershed receives an estimated 6 hm³ of recharge per year, mostly from spring snowmelt. During 1980, the alluvial fill of Kyle Canyon received slightly more than 4 hm³ of recharge derived from snowmelt on the canyon floor and inflow from carbonate rocks. Estimated discharge from the alluvium in 1980 (underflow at the canyon mouth and outflow to carbonate rocks) was slightly less than 4 hm³. Recharge to the carbonate rocks in Lee Canyon watershed is estimated at 4.2 hm³/yr. The alluvium of Lee Canyon apparently remains unsaturated. Data suggest that septic-system effluent may have affected ground-water quality in both canyons. If so, the effects are slight and the ground water easily meets established water-quality standards.

Water budget for Washoe Valley near Reno, Nevada

Within the 218-km² Washoe Valley, the estimated system yield of 34 hm³/yr, which is composed of surface water and ground water, moves toward Washoe Lake, where more than two-thirds (27 hm³/yr) evaporates from the lake surface. F. E. Arteaga has concluded that ground-water recharge of 7.4 hm³/yr is distributed approximately as follows: 1.2 hm³/yr is derived from the Virginia Range and 6.2 hm³/yr comes from the Carson Range. The water budget was computed both from a precipitation-yield relation developed in an earlier study and from a water budget derived from lake-level data for Washoe Lake. The lake-surface evaporation was computed with the Penman equation, which was found to be in agreement with both the Radiation and Blaney-Criddle techniques.

OREGON

Precipitation quality in Salem

During an urban storm-water reconnaissance study in Salem, Oreg., precipitation samples were collected

weekly by T. L. Miller who used a wet-dry sampler so that the samples would contain minimal dry fallout. Samples collected between February and December 1981 ranged in pH from 4.0 to 5.8, with a medium value of 4.6. Specific conductance at 25° C ranged from 7 to 59 $\mu\text{mhos/cm}$, with a median of 12 $\mu\text{mhos/cm}$. Total lead in the precipitation samples was found to be from 4 to 60 $\mu\text{g/L}$ and had a median value of 11 $\mu\text{g/L}$. Preliminary results indicate that there may be some seasonal trend to pH values which generally were higher in summer and early fall.

Declining ground-water levels in northeastern Oregon

Declining ground-water levels have been documented in a basalt aquifer in northeastern Oregon. According to P. A. Davies, water-level measurements made by the Oregon Water Resources Department and the USGS indicate annual declines in excess of 3 m per year over nearly 40 km² in Umatilla and Morrow Counties. Lesser declines are occurring throughout an area of extensive irrigation development. According to Davies, deepening of wells during the last 15 years has revealed variation in head within the aquifer. Some of the more severe long-term decline rates have been accentuated by the penetration of zones of low head deep in the basalt.

Background-water quality in Three sisters area

D. D. Harris reports that samples have been collected to document the water quality of the Three Sisters area as a part of "other volcano" studies in Oregon. The data are intended to provide background information as a basis for evaluating effects of volcanic activity in the event of any future eruptions.

The pH of seven lakes in the area ranged from 6.5 to 8.2. Specific conductance of the lake water ranged from 4 to 44 $\mu\text{mhos/cm}$ at 25° C. Streams draining the mountains had pH ranging from 6.8 to 7.9 and specific conductance ranging from 9 to 83 $\mu\text{mhos/cm}$ at 25° C.

WASHINGTON

Declining ground-water levels in east-central Washington

Withdrawals of ground water by irrigation wells in east-central Washington have caused water levels in parts of the area to decline more than 30 m, according to a study by D. R. Cline. Pumpage in nearby Adams, Lincoln, eastern Grant, and northern Franklin Counties quadrupled from 137 hm³ to 477 hm³ in the 10-year period from 1967 to 1977, and the increase was even greater by 1981.

Many new wells have been drilled in the Wanapum Basalt and underlying Grande Ronde Basalt of the Columbia River Basalt Group, and other wells were deepened. Few wells were deeper than 300 m in 1967, but several were more than 600 m deep by 1981. Water levels in the Grande Ronde Basalt, locally exceeding 60 m in depth, commonly are lower than those in the Wanapum Basalt. With shifting patterns of pumping and changing depths of wells, water level declines have shifted also. In the area of heaviest pumping, in southern Adams County, water levels declined as much as 41 m in the Wanapum Basalt and 46 m in the Wanapum and Grande Ronde Basalts from spring 1968 to spring 1981; the rate of decline has been increasing during this interval.

Occurrence and quality of ground water in selected islands, San Juan County

The four largest islands in San Juan County (San Juan, Lopez, Orcas, and Shaw) are experiencing water-quality deterioration from sea-water intrusion and bacterial contamination. According to primary investigators K. J. Whiteman, D. Molenaar, and G. C. Bortleson, 11 percent of the 275 wells sampled in September 1981 had chloride concentrations at levels indicating sea-water intrusion, and coliform bacteria were found at 12 percent of the 170 sites tested. Most residents obtain water from wells tapping either glacial drift materials or fractured bedrock; wells in both aquifers are experiencing water-quality problems.

Most of the wells are drilled into bedrock that has been subjected to deformation, and water is produced from joint and fracture systems; specific capacities are characteristically low. Wells drilled into glacial drift in the northern part of Lopez Island have higher specific capacities; however, heavy pumping from these deposits correlates with sea-water contamination of the ground-water supply. Estimated ground-water pumpage on the four islands was 832,700 m³.

SPECIAL WATER-RESOURCE PROGRAMS

DATA COORDINATION, ACQUISITION, AND STORAGE

OFFICE OF WATER DATA COORDINATION

At the outset of FY 1981, a joint meeting (14th) of the Interagency Advisory Committee on Water Data

(IACWD) and the Advisory Committee on Water Data for Public Use (ACWDPU) was held. Also, the 15th meeting of the IACWD was held. Publications by the Office of Water Data Coordination (OWDC) included several chapters of the "National Handbook of Recommended Methods for Water Data Acquisition" and Volume IV of the "Index to Water Data Activities in the Coal Provinces of the United States." In addition, the annual updating of the "Catalog of Information on Water Data" was completed. A strong recommendation was made at the joint meeting of the two Advisory Committees to strengthen and improve coordination of water-data acquisition activities.

The IACWD met September 17-18, 1981, in Charleston, South Carolina. All agencies described their water-data requirements and changes anticipated in the near future. Most data needs continue from earlier years, but diminished manpower and budget will impact data collection in FY 1982. Automated data collection and telemetry to provide real-time data were prominent among emerging needs of the agencies. Acid precipitation information and a variety of water-quality data needs, such as nonpoint source stream load, mining impact, toxic waste, and ground-water-quality data requirements, were frequently reported. All needs will be enumerated in the Federal Plan for FY 1982-83.

Volume IV of the 5-volume series of the "Index to Water Data Activities in Coal Provinces of the United States, Northern Great Plains, and Rocky Mountain Provinces" was published. In the "National Handbook of Recommended Methods for Water Data Acquisition" series, Chapter 2, Ground Water, was published. Other chapters were updated and reprinted as follows: Chapter 3, Sediment, Chapter 5, Chemical Quality, and Chapter 7, Basin Characteristics. Chapter 9, Snow and Ice, was updated. Chapters to be printed in FY 1982 include Chapter 1, Surface Water, Chapter 6, Soil Water, and Chapter 8, Evaporation and Transpiration. Remaining chapters to be published are Chapter 4, Biology and Microbiology, Chapter 11, Water Use, and Chapter 12, Data Handling. There has been some discussion of a 13th chapter on automated data collection.

The "Catalog of Information on Water Data," a computer file of OWDC and the National Water Data Exchange (NAWDEX), was updated by the annual solicitation of data in the spring and summer of 1981 and by computer interface with the Geological Survey's WATSTORE file on surface-water quantity and the Environmental Protection Agency's STORET file on water quality.

OWDC's file of digitized traces of hydrologic units was used experimentally to map individual States. The hydrologic unit code system was accepted by the Geological Survey's Data Standards Committees.

NATIONAL WATER DATA EXCHANGE

NAWDEX is a national confederation of water-oriented organizations whose purpose is to improve access to water data. It has continued to grow and as of December 1981, the membership, which is voluntary, had increased to 216 organizations.

The national water-data indexing program, operated by NAWDEX in cooperation with the USGS Office of Water Data Coordination, continued to expand. By the end of 1981, over 750 organizations had been registered in the computerized Water Data Sources Directory (WDSD), which identifies organizations that are sources of water data or other services and products pertinent to water-data studies and investigations. In addition, the directory gives the locations within these organizations from which data or services can be obtained, types of data or services available, and the geographic areas in which water data are collected. Also, nearly 400,000 sites for which water data are available from over 400 organizations have been indexed in the computerized Master Water Data Index (MWDI), which identifies individual sites for which water data are available, the location of those sites, organizations collecting the data, hydrologic disciplines represented by the data, periods of record for which data are available, and the major parameters for which data are available. Automated indexing interfaces between the MWDI, the Texas Natural Resources Information System (TNRIS), WATSTORE of the USGS, and the Storage and Retrieval System (STORET) of the EPA were continued in operation during the year.

During 1981, the MWDI was redesigned to include the indexing of selected meteorological data stored in water-data files of NAWDEX members, the indexing of data stored in the Unit Values File of the USGS WATSTORE systems, and many other features which improve the index's utility and efficiency. New systems were also introduced for producing site-location maps and many other graphic products from the Index. The NAWDEX data bases continued to be used to produce a variety of information products including State-level printed indexes and special-subject indexes and listings.

The NAWDEX Program Office continued to coordinate direct access to the data files of NAWDEX, the USGS WATSTORE system, and EPA's STORET system by outside organizations. By the end of 1981, 72 organizations had been provided access at 144 locations, nationwide.

NAWDEX services and products are available through a nationwide network of 64 Assistance Centers in 45 States and Puerto Rico. These centers, with the NAWDEX Program Office located at the USGS National Center in Reston, Va., provide a variety of services to assist users of water data in identifying, locating, and

acquiring needed data. Most of the centers have direct access to the WATSTORE system of the USGS, and they provide referral services to many data systems and services available through NAWDEX members. The Program Office in Reston also has direct access to the STORET system of EPA and, upon request, can provide data from this system.

WATER-DATA STORAGE SYSTEM

The National Water Data Storage and Retrieval System (WATSTORE) is a large-scale computerized system developed to process and disseminate water-resource data collected by the USGS. Representative WATSTORE products are computer-printed tables and graphs, statistical analyses, digital plots, and data in machine-readable form. The computer system consists of a central computer located in Reston, Va., and remote terminal facilities in nearly every State.

The Station Header File contains identifying information for all sites for which data are stored in the Daily Values, Water-Quality, Peak Flow, and Unit Values Files of WATSTORE. Nearly 290,000 sites are now indexed in the Station Header File.

Geologic and well-inventory data are stored for wells, springs, and other sources of ground water in the Ground-Water Site-Inventory File. This file continues to grow and currently contains data for nearly 815,000 sites.

The National Water Use Data System collects, stores, and disseminates data about water used in the United States. The data are classified by the following functional-use categories: agricultural, commercial, domestic, industrial, irrigational, mining, fossil-fuel power, geothermal power, hydroelectric power, nuclear power, sewage treatment, and water supply. The Water-Use File, containing summary data about the withdrawal, return, and use of water throughout the Nation, became part of WATSTORE in 1980. Information from this file can be used to make projections of future water requirements.

A project to test the feasibility of distributed information processing for the Water Resources Division was completed. Minicomputer systems were installed and evaluated in two district offices and one regional research office. Approval was obtained for the distributed information system and requests for proposals were solicited to vendors.

URBAN WATER PROGRAM

The objective of the USGS Urban Water Program is to provide generalized relations for estimating (1) hydro-

logic changes due to urbanization and (2) hydrologic conditions under urbanization. To fully meet these objectives, the USGS, in cooperation with EPA, is continuing development of a consistent and accessible urban-hydrology data base.

Rainfall-runoff and runoff-quality model for urban watersheds

A rainfall-runoff and a runoff-quality model for urban watersheds have been developed by W. M. Alley and P. E. Smith. The two models are separate computer programs that can be linked together with direct access files or can be applied separately.

The rainfall-runoff model provides short-time-interval simulations of storm-runoff events and a daily soil-moisture accounting between events. A drainage basin is represented as a set of overland-flow, channel, and reservoir segments that jointly describe the drainage features of the basin. Kinematic wave theory is used for routing flows over contributing overland-flow areas and through the channel network. The model provides a choice of three methods for solving the kinematic wave equations. These include a method of characteristics and implicit and explicit finite-difference methods. A means of avoiding kinematic shock problems in the method of characteristics has been developed.

The runoff-quality model is structured very similarly to the rainfall-runoff model. It provides short-time-interval simulations of the quality of storm-runoff events and a daily accounting of the accumulation and washoff of water-quality constituents on impervious areas of the watershed between events. The model considers, separately, constituents in impervious-area runoff, pervious-area runoff, and precipitation. The model can be applied on either a lumped-parameter or distributed-parameter basis. For distributed-parameter simulations, constituent transport through channel segments is modeled by using a Lagrangian method.

Urban stormwater data management system

A data management system (Doyle and Lorens, 1981) was developed to store, update, and retrieve data collected in urban stormwater studies jointly conducted by the USGS and EPA in 11 cities in the United States. The principal investigators were W. H. Doyle, Jr., and J. A. Lorens. The data management system is used to retrieve and combine data from USGS data files for use in rainfall-runoff-quality models and for data computations such as the determination of storm loads. The system is based on the data management aspect of the Statistical Analysis System (SAS) and was used to create all the data files in the data base. SAS (Barr and others, 1979) is used for storage and retrieval of basin

physiographic, land-use, and environmental-practices inventory data. Also, storm-event water-quality characteristics are stored in the data base. The advantages of using SAS to create and manage a data base are many; it is simple, easy to use, contains a comprehensive statistical package, and can be used to modify files very easily.

Data base system development has progressed rapidly during the last two decades, and the data management system concepts used in this study reflect the advancements made in computer technology during this era. Urban stormwater data is, however, just one application for which the system can be used.

Trace-metal partitioning in suspended sediments from urban stormwater runoff

J. F. Rinella has developed a method to separate suspended sediments into particle-size classes. This method is based on fall velocities in quiescent native water. It will aid in predicting the transport of trace metals associated with suspended sediments. Particle-size classes with fall diameters finer than 62, 31, 16, 8, and 4 μm have been analyzed for trace metals. Analyses of eight stormwater samples indicated that the concentrations ($\mu\text{g/g}$) of chromium, copper, lead, and nickel associated with the finer than 4- μm particle-size class were about twice those associated with the finer than 62- μm particle-size class. With the exception of manganese being constant from one size class to another, no consistent trends were observed for the other metals (cadmium, cobalt, and zinc) that were analyzed.

Effects of stormwater detention on water quality near Glen Ellyn, Illinois

According to R. G. Striegl, water-quality data collected at a 4.5 ha urban lake (Lake Ellyn at Glen Ellyn, Ill.) during 35 rainfall, snowmelt, and low-flow periods in 1980 and 1981 indicate reductions in suspended sediment, copper, iron, lead, and zinc loads of 90 percent and greater that may be attributed to detention storage in the lake. Chloride, sodium, and total dissolved solids concentrations in the lake inflows and outflows exhibit annual peaks in February corresponding with road salting and snowmelt runoff. Inflow concentrations of these constituents sharply decline because of road washoff by spring rains. Outflow concentrations cycle annually with low concentrations appearing around October. Annual low and peak concentrations are less extreme in the lake outflows than in the inflows because of solute diffusion in the lake.

Size analyses of inflowing suspended sediments and lake bottom sediments indicate that greater than 75 percent of the sediments transported into the lake

are less than 62 microns in size. An estimated 3,800 m^3 of sediments have been deposited in the lake since it was last dredged in 1970. According to the Northeastern Illinois Planning Commission, mean concentrations of heavy metals from three lake sediment samples are: 4.8 mg/kg Cd, 45 mg/kg Cr, 130 mg/kg Cu, 20,100 mg/kg Fe, 1,090 mg/kg Pb, and 470 mg/kg Zn. Dissolved-ion and metals concentrations from soil water samples collected by the author from two locations at points 1, 2, and 3 m below the lake bottom indicate no contaminant leakage from the lake into the unsaturated zone.

Contamination of Jones Falls in Baltimore, Maryland

As part of the Nationwide Urban Runoff Program in Baltimore, Maryland, in cooperation with the State of Maryland Regional Planning Council, B. G. Katz and G. T. Fisher have been sampling streamwater and stormwater runoff from three small urban catchments during base flow and storms from Jones Falls near its mouth. The high-density residential catchments range in size from 4.2 to 6.9 ha, and the drainage area for varied land uses in the Jones Falls watershed is approximately 140 km^2 . On the basis of data from analyses of over 350 samples of stormwater runoff and streamflow collected during base flow, Katz and Fisher report high concentrations of total organic nitrogen (1 to 55 mg/L), total phosphorous (0.2 to 85 mg/L), total lead (<20 to 30,000 $\mu\text{g/L}$), and high numbers of coliform bacteria (10^6 to 10^7 colonies per 100 mL) in stormwater entering Jones Falls from small urban catchments. The fecal coliform bacteria content in Jones Falls during base flow and storm periods (10^5 to 10^7 colonies per 100 mL) is considerably higher than State standards for body-contact water recreation (log mean of 200 colonies per 100 mL in 5 or more samples over a 30 day period). During storms, large quantities of organic nitrogen, phosphorus, iron, and lead are being transported by Jones Falls to the inner harbor, a revitalized and newly renovated area of downtown Baltimore. Sewage effluent, runoff from impervious areas, and other urban wastes are contributing to the contamination of Jones Falls in the Baltimore area.

Quality of runoff from small watersheds in the Twin Cities metropolitan area, Minnesota

A study of runoff from selected watersheds in the Twin Cities metropolitan area has been completed by R. G. Brown, M. A. Ayers, and G. A. Payne. Study results indicate that nonpoint-source pollution from the runoff is widespread and a serious problem. Flow-weighted mean annual concentrations of total suspended solids, total phosphorus, and fecal coliform exceed standards set by the Minnesota Pollution Control

Agency. Flow-weighted mean annual concentrations of metals and chloride exceed U.S. Environmental Protection Agency standards. Analysis of loading data shows that 67 to 94 percent of the 1980 annual loading in urban storm-sewered watersheds and 50 to 76 percent of the loading in main stem urban and rural watersheds occurred during snowmelt. Results of load modeling indicate that median annual loads of phosphorus, nitrogen, total suspended solids, lead, and chloride are significantly related to land use and basin characteristics. Percentage of watershed in wetlands was found to be a particularly important basin characteristic in controlling both urban and rural nonpoint-source pollution. The results of regression modeling show that the loss of wetlands resulting from urban or agricultural development probably will lead to increased loading. Atmospheric-deposition data indicate that nitrogen, phosphorus, and lead from wetfall and dryfall contributed significantly to nonpoint-source pollution in the metropolitan area in 1980.

Quality and quantity of urban stormwater runoff to recharge basins, Long Island, New York

The urban-runoff program on Long Island, N.Y., determines the source, type, quantity, and fate of pollutants in urban stormwater runoff, and quantifies their impact on the ground-water reservoir, which has been designated a sole-source aquifer for 2.8 million residents of the island. The principal investigators in this project are H. F. H. Ku and D. L. Simmons.

Over 2,000 recharge basins on Long Island collect stormwater runoff and return it to the ground-water reservoir. Five recharge basins representing different land-use types (highway, low-density residential, medium-density residential, shopping center, and strip commercial) were selected for study. Forty storm events have been sampled to collect data on the quantity and quality of precipitation, stormwater inflow into the basins, and amounts of stormwater reaching the water table beneath the basins.

Analysis of a limited number of storm events indicates that urban stormwater contains bacteria on the order of 10^4 to 10^5 MPN/100 ml (total coliform) and that the bacteria are principally of nonhuman origin. Ground water beneath the recharge basins following a storm event commonly shows less than 3.0 MPN/100 ml (total coliform). This fact suggests that the unsaturated zone acts as a filter for bacteria.

Stormwater runoff from the highway land-use area contains concentrations of chromium and lead up to 65 and 3,300 $\mu\text{g/L}$, respectively. Analyses indicate that these concentrations are generally reduced by an order of magnitude as the water moves through the unsaturated zone.

Chloride concentrations of up to 670 mg/L have been found in stormwater. This occurs mainly at the highway and shopping center sites during the winter months, following road deicing activities. Total nitrogen in stormwater ranges up to 37 mg/L, although concentrations of less than 10 mg/L are more common. The largest contributors to the nitrogen load are thought to be the large number of domestic cats and dogs on the island and the application of fertilizer to lawns. Neither chloride nor nitrogen is appreciably reduced during infiltration.

The organic pollutants benzene, toluene, and 1,1,1-trichloroethane were found in both stormwater and ground water in concentrations less than 5 $\mu\text{g/L}$.

WATER USE

A nationwide tabulation of 1980 water-use data was completed in 1981. The data will be the basis for a USGS Circular detailing the estimated use of water in the United States in 1980. This report is the latest in the USGS 5-year report series on water use.

The National Water-Use Information Program had 49 States and Puerto Rico cooperating in the program by mid-1981. About 26 States have entered some water-use data in the National Water-Use Data System, and all 1980 water-use data will be entered into the system in 1982.

The design of computer software for a State Water-Use Data System (SWUDS) was initiated and will be available in 1982 to States from the National Water-Use Information Program Office in Reston, Va. The system will be installed at the State level and will facilitate the storage and retrieval of water-use data on a site-specific basis. The SWUDS will provide for aggregation and subsequent input of data in the National Water-Use Data System (NWUDS). This should provide the much needed continuity between State water-use data files, avoid considerable duplication of efforts in developing State data systems, and strengthen the cooperative approach to collecting, storing, and retrieving water-use information.

An assessment of water-use information needs and applications was completed for the Missouri River basin. The purpose of the study was to assess the type of water-use information needed (and used) by a cross section of information user groups in the Missouri River basin. It appears that the NWUDS, in cooperation with the States, generally would be capable of meeting specifically determined and perceived needs within the Missouri River Basin Commission water resources community. Awareness of the NWUDS' capabilities to meet water-use information needs is very limited. It is essential that a concerted effort be made by Federal and

State agencies to standardize techniques for data collecting and reporting of various categories of water-use information.

A method for estimating water use in thermoelectric power generation is being developed. The method uses data elements, such as power generation, generating capacity, type of plant, type of cooling, and other plant design characteristics, to estimate water use. Additional methods are being developed to document statistical sampling techniques, indirect measurement methods, and remote sensing techniques. This information is needed for all functional-use categories to provide reliable and uniform water-use data.

Irrigation water use on the Snake River Plain in southern Idaho

As part of the Snake River Plain RASA study, power company records for about 7,800 ground-water and 600 surface-water pumping plants were compiled and are being used to estimate pumpage for irrigation on the Snake River Plain. Field tests were run on 83 irrigation wells and 11 river pumping plants to develop an estimate of discharge per unit of power consumed. Horsepower, type of distribution system, and total lift were taken into account. Annual power consumption was then used to estimate the volume of water pumped in 1980. According to B. B. Bigelow, in 1980, about 617 hm³ of water were withdrawn from the Snake River between King Hill and Weiser.

For the purpose of estimating quantities of recharge to the ground-water system, L. C. Kjelstrom defined inflow-outflow elements of the surface-water irrigation-distribution system, including quantified gains and losses in 15 reaches of the Snake River in water year 1980. Kjelstrom made water-budget analyses and assumed that the residuals in the budgets represented evapotranspiration (consumptive use) of irrigation water. In water years 1934-80, average annual evapotranspiration of irrigation water was estimated to be 800 m³/hm² on the eastern Snake River Plain and 750 m³/hm² on the western plain.

Ground-water use in Minneapolis-St. Paul area, Minnesota

Ground-water use from 1880 to 1979 in the Minneapolis-St. Paul metropolitan area has been studied by M. A. Horn. Ground-water use increased from 1 million m³/yr in 1880 to a peak in the early 1970's of 275 million m³/yr and decreased in the late 1970's to 266 million m³/yr. Although ground-water use by self-supplied industry has historically been the largest of all use categories, such industrial use declined from 162 million m³/yr in the late 1960's to 106 million m³/yr in the late 1970's. During this period, municipal use in-

creased to 122 million m³/yr. Although use for irrigation of crops increased dramatically during the 1970's, this still accounts for only 9 percent of all ground water used in the area. One aquifer, the Prairie du Chien-Jordan, is the source of 80 percent of all ground water used in the area. On the basis of an analysis of monthly pumpage for 2 years, average summer pumpage is 43 percent greater than winter pumpage in a normal year and 53 percent greater in a dry year.

Water use in Montana

Information on the amounts of water used in Montana for industrial purposes, public water supplies, and electric-power generation was collected in 1981 as part of a cooperative program between the USGS and the Montana Department of Natural Resources and Conservation. According to Charles Parrett, a comprehensive mail and telephone survey was made to collect the data; all known users in each category were contacted. The collected data, along with estimates of data accuracy, are being compiled and computerized.

Water use in Wisconsin in 1979

Users withdrew about 8,140 hm³ of water (excluding that used for hydroelectric power) during 1979 in Wisconsin, according to C. L. Lawrence and B. R. Ellefson. Of that amount, about 6,430 hm³ (79 percent) was for thermoelectric powerplant cooling. The next largest single use was 490 hm³ for process water at pulp and paper industries. Cities and villages pumped 750 hm³, which was about equally divided between surface-water and ground-water sources. Ninety-four percent of these municipalities used ground water; however, because several large population centers, located on the shore of Lakes Michigan, Superior, and Winnebago, pumped water from those lakes, the actual withdrawals from surface-water and ground-water sources were similar.

NATIONAL WATER-QUALITY PROGRAMS

National Stream Quality Accounting Network

Operation of the National Stream Quality Accounting Network (NASQAN), the national program the USGS for uniformly measuring the quality of the major rivers of the United States, continued at its full complement of 516 stations during FY 1981. An extensive list of water-quality characteristics is measured on a continuous, monthly, bimonthly, or quarterly basis at all sites.

Locations of NASQAN stations are based on hydrologic accounting units, which are subdivisions of river basins in the United States that were developed by the USGS' OWDC in conjunction with the U.S. Water Resources Council. The council's hydrologic subdivisions include 21 regions, 222 subregions, and 352 accounting units. There is usually at least one NASQAN station in each accounting unit; the station generally is near the most downstream location in the unit. Some complex units contain multiple stations.

Two subnetworks are operated at selected NASQAN sites. These are the Pesticide Subnetwork and the Radiochemical Subnetwork. The Pesticide Subnetwork, operated cooperatively by the USGS and the EPA during FY 1981, consists of 152 stations at which water is sampled quarterly and bottom (streambed) material is sampled semiannually. The list of pesticide residues being monitored presently is under review for possible expansion in order to observe the effects of pesticides being applied currently and the residual effects of persistent pesticides applied during prior years. The Radiochemical Subnetwork consists of 52 stations that are monitored semiannually under high- and low-flow conditions for general levels of radioactivity and specific radionuclides.

Data for NASQAN sites are published annually in USGS water-data reports, and summaries of national patterns of water quality that are developed through analysis of NASQAN data are described in periodic special network reports. The data also are available through the USGS computerized hydrologic data system, WATSTORE, and through STORET, the data system operated by EPA. Public access to these data can be facilitated through the use of NAWDEX, which is operated by the USGS. NASQAN data are used by many State, Federal, and Private organizations and have been summarized in annual reports of the President's Council on Environmental Quality since 1975.

An active program is underway to implement methods for use in analyzing NASQAN data for evidence of persistent changes with time, or trends, in the quality of the Nation's rivers. A report summarizing trends and long-term calculated annual loads of water-quality characteristics is expected to be published in FY 1982. The design of the NASQAN program is undergoing an intensive review to determine whether the original goals of the program are being achieved, and whether the information derived from operation of the network satisfies the need for a general assessment of the Nation's water quality. Network size, water-quality characteristics measured, and sampling frequency are being evaluated to determine the most efficient and cost-effective way to obtain the data required to make regional and national assessments of water quality.

National Hydrologic Bench-Mark Network

The Hydrologic Bench-Mark Network, started in 1958, consists of 57 stations in 39 States. The stations are located in stream basins having a wide variety of climate and topography that are expected to be minimally affected by population growth and its attendant impacts on natural resources. Water-quality samples are collected at 52 sites on a monthly, bimonthly, quarterly, semiannual, or annual basis, depending upon the station and particular group of constituents. A report summarizing the data collected to date is expected to be published in FY 1983, and, like the NASQAN program, the bench-mark program is being reviewed as a means of determining its future direction.

ATMOSPHERIC DEPOSITION PROGRAM

During FY 1981, the USGS continued to be active in the development of the Federal interagency National Acid Precipitation Assessment Plan. R. J. Pickering continued his assistance to the Department of the Interior in coordination of programming and budgeting by Interior bureaus that are participating in the 10-year research program. Departmental leadership in atmospheric deposition activities was placed in the office of the Assistant Secretary—Energy and Minerals.

The USGS is acting for the Department of the Interior as lead agency for atmospheric deposition monitoring. In this capacity, R. J. Pickering chairs an interagency Task Group on Deposition Monitoring that is part of the Interagency Task Force on Acid Precipitation. The task group is charged with designing and implementing a National Trends Network and a U.S. component of a Global Trends Network for monitoring the composition of atmospheric deposition. The task group is also responsible for conducting research on methods and equipment for monitoring dry deposition, a component not being satisfactorily sampled at the present time. W. L. Bradford and B. A. Malo of the Quality of Water Branch are guiding planning efforts in these areas for the USGS.

Operation of selected monitoring sites and coordination of the National Trends Network, as a whole, constitute a major component of the USGS atmospheric deposition program. Other components of the program include participation with the EPA in the identification of areas in the United States that are sensitive to acid precipitation and monitoring by the USGS of selected lakes, streams, and ground-water bodies in those sensitive areas to detect changes in water quality that might be the result of atmospheric deposition. Research projects investigating the geochemical processes through

which atmospheric deposition affects water quality are being coordinated by O. P. Bricker.

During FY 1981, the USGS continued to provide quality assurance for analytical work of the Central Analytical Laboratory of the National Atmospheric Deposition Program. Several monitoring sites in the Program, which is conducted by the Department of Agriculture's agricultural experiment stations, are operated by the USGS through its Federal and State cooperative program. L. J. Schroeder and B. A. Malo reported that the Central Analytical Laboratory continued to perform in an exemplary manner during the year.

Reviews of several years of small-stream water-quality data for possible effects of acid precipitation, conducted in Pennsylvania by J. R. Ritter and A. E. Brown and in New York by N. E. Peters, R. A. Schroeder, and D. E. Troutman, failed to demonstrate any clear pattern of change during the 10- to 15-year period studied. A review of data by the same three investigators from New York's 9-station deposition monitoring network for the period 1965-78 suggested that the pH of bulk precipitation decreased slightly in the western part of the State and increased slightly in the eastern part. Concentrations of sulfate and nitrate in precipitation increased slightly throughout the State during the same period.

R. J. Pickering has continued to provide technical advice to Department of Interior representatives involved in development of a bilateral agreement on transboundary air pollution with Canada. Several negotiating meetings of U.S. and Canadian personnel were held during the year and some progress was made in drafting the agreement. The technical basis for the agreement will be a series of reports on the present state of knowledge of transboundary air pollution, and acid rain in particular, that are being prepared by bilateral work groups.

REGIONAL AQUIFER-SYSTEM ANALYSIS PROGRAM

The following new regional aquifer studies were initiated in FY 1981: (1) a study of consolidated rock aquifers of the central Midwest; (2) a study of alluvial aquifers of the Great Basin; and (3) a study of the unconsolidated aquifers of the Mississippi Embayment region. Investigations continued in nine ongoing projects in the following areas: the Snake River Plain, the Atlantic Coastal Plain, the Southeastern Coastal Plain, the Ogallala Aquifer of the High Plains, the unconsolidated deposits of the California Central Valley, the aquifers of the northern Great Plains, the sandstone aquifers of the northern Midwest, the carbonate

aquifers of the Southeast, and the alluvial basins of the Southwest.

Calibration of flow simulation models has been completed for the northern Great Plains and California Central Valley projects and final reports are in preparation. In addition, numerous other reports on aspects of geology, hydrology, and ground-water quality have been published by the ongoing studies.

Stressed flow system in the Tertiary limestone aquifer system

As part of the Regional Aquifer System Analysis Program, R. E. Krause has modeled ground-water flow in the Tertiary limestone aquifer system in southeast Georgia, northeast Florida, and southern South Carolina. According to Krause, unstressed flow in this prolific carbonate aquifer system over most of the area can be divided into and modeled as two discrete water-bearing zones. Modeling the ground-water flow under stressed conditions (1980 pumpage data) indicates, however, that an additional water-bearing zone underlying the two zones of the aquifer is part of the stressed flow system in southeast Georgia and northeast Florida. This lower zone consists mainly of cavernous dolomitic limestone and dolomite of Early Cretaceous to Paleocene age that lies 600 to 650 m below land surface. The zone contains connate water that ranges from brackish in northeast Florida to as salty as seawater near Brunswick, on the Georgia coast. Under unstressed equilibrium conditions, the lower zone contributed almost no water to the overlying layers, but withdrawal of 21 m³/s (1980 data) from the upper zones has induced leakage across semiconfining beds, disrupting the freshwater-saltwater interface. According to the model, an estimated 7 m³/s of the water pumped from the overlying freshwater zone is being replaced by brackish to salty water from the lower zone, contaminating parts of the aquifer system near the large pumping centers.

Central Midwest RASA Study

Sedimentary rocks of Paleozoic and Mesozoic age in the central Midwest are commonly water bearing. Regional-flow patterns based on new project maps indicate that slightly saline and saline waters flow generally east-to-west from Colorado and Nebraska to meet freshwater that flows outward from the Ozark area of southern Missouri, northern Arkansas, southeastern Kansas, and northeastern Oklahoma.

Maps of dissolved-solids concentrations prepared by D. C. Signor show a transition zone of mixed fresh and saline waters. The 10 to 40 mile wide transition zone extends from central Missouri through southeastern

Kansas, northeastern Oklahoma, and into the Boston Mountains of Arkansas. Two regional aquifers exist in the Ozark area. The major aquifer, the lower Ozark aquifer, is found in rocks of Ordovician and Cambrian age. A less productive and also less used regional aquifer, the upper Ozark aquifer, is found in rocks of Mississippian age. The two aquifers are separated by thin shales at most locations.

In the past, extensive coal, lead, and zinc mining has been undertaken in Missouri, northeastern Oklahoma, and southeastern Kansas. Ground- and surface-water contamination problems related to past mining are now appearing. The most notable example, identified by the EPA as one of the sites most in need of remedial efforts, is the contamination of Tar Creek in northeastern Oklahoma. At this site, water from the upper Ozark aquifer, which is contaminated from previous mining, is now entering Tar Creek as base flow.

High Plains aquifer study

According to J. S. Havens, the High Plains aquifer in Oklahoma is part of a regional aquifer system extending from South Dakota to Texas and New Mexico. The principal aquifer, the Ogallala Formation of Tertiary age, is hydraulically connected with other unconsolidated deposits, principally of Quaternary age. During 1978, the USGS began a 5-year study of the High Plains aquifer to provide hydrologic information to evaluate the aquifer and to develop predictive computer models of it. According to a recently released report, bedrock slopes generally from west to east and is composed of rocks of Permian, Triassic, Jurassic, and Cretaceous age (Havens, 1982a). Altitudes of the base were determined from published and unpublished data.

A second report showing the 1980 water table in the aquifer indicates that the water table sloped generally from west to east at an average rate of 2.65 m/km and that the altitude of the water table ranged from about 1,417 to about 610 m (Havens, 1982b).

A third report describes the predevelopment water table in the aquifer (Havens, 1982c). The slope and altitude of the water table generally were similar to the 1980 values; locally, altitudes of areas not yet subject to intensive irrigation pumpage were higher. Predevelopment data were taken from published and unpublished records.

Northern Midwest (Minnesota) RASA Study

The St. Peter and Prairie du Chien–Jordan aquifers in extreme southeastern Minnesota contain ground-water mounds as high as 30 m above the regional potentiometric surface. According to D. G. Woodward, the

mounds occur where the Decorah-Platteville–Glenwood confining bed has been removed by erosion and the aquifers are overlain by thin drift that is only about 7 m thick. The resulting head distribution produces a radial-flow pattern away from the mounds and diverts the regional west-to-east movement of ground water to the south and west instead of toward the Mississippi River. Because the basal St. Peter confining bed, which is as much as 25 m thick in the Twin Cities Basin, is not present in southeastern and south-central Minnesota, the St. Peter and Prairie du Chien–Jordan aquifers in this area probably constitute a single aquifer. Therefore, the ground-water mounds in the St. Peter are readily transmitted vertically to the underlying Prairie du Chien–Jordan aquifer.

Geologic mapping on the Snake River Plain in southern Idaho

As part of the Snake River Plain RASA study, R. L. Whitehead and G. F. Lindholm mapped the thickness of the basalts of the Snake River Group. The mapping is considered to be a first approximation of the basalt thickness and is based on about 700 km of surface-resistivity profiles, regional-gravity models, and interpretation of drillers' logs. Under most of the plain, the basalt is less than 600 m thick, but it reaches a maximum of about 1,800 m in the central part of the eastern plain. Geologic data obtained from a 342-m-deep test hole near Wendell, Id., at the western edge of the eastern plain, were used as a control for interpretation of the resistivity soundings. At this site, the base of the basalt is underlain by sediments of the Banbury Basalt of the Idaho Group of Tertiary age.

Montana RASA Study

The Montana part of the northern Great Plains Regional Aquifer System Analysis included canvassing about 1,650 wells and drilling 16 test wells in data-poor areas of Montana, according to W. R. Hotchkiss. In addition, seepage along the Tongue, Powder, and Red-water Rivers (Dodge and Levings, 1980; Druse and others, 1981) documented base surface flow in the area. Creation of a comprehensive data base for 21 stratigraphic (aquifer) units above the Madison Group, publication of a selective annotated bibliography (Levings and others, 1981), and extensive data reports completed the initial project results.

Interpretation of the geologic framework from geophysical logs of 2,037 wells (Feltis and others, 1981) led to completion of maps covering the eastern two-thirds of the State; the maps describe the configuration of the top, feet of sand, and thickness of the most area aquifers—the Fox Hills–lower Hell Creek, Judith River,

Eagle, Dakota, Lakota, and Swift aquifers. Interpretation of existing hydrologic data, well-cavass data (Levings, 1981a), and data from selected oil-well drill-stem tests (Levings, 1981b) led to construction of potentiometric-surface maps. The potentiometric-surface maps indicate that ground water flows generally eastward at gradients ranging from 1.14 to 3.32 m/km for the Fox Hills-lower Hell Creek, Judith River, Eagle, and Lakota aquifers. The gradient is apparently less for the Dakota and Swift aquifers. Interpretation of geochemical data were used to prepare maps and descriptions of geochemical facies changes along the ground-water flow paths in the Tertiary aquifers of Montana and North Dakota.

Data from the Judith Basin, Montana, (Levings and Dodge, 1981) were used to construct a quasi-three-dimensional digital-flow model of the Kootenai and adjacent aquifers. Calibrated transmissivities of the Kootenai ranged from 13 to 33.4 m²/d. A broader three-dimensional digital-flow model of the Upper Cretaceous and Tertiary aquifers in the Powder River, Bull Mountains, and western Williston basins generally reproduced hydraulic heads in all aquifers.

Piezometers in deep test well in northeast Illinois

As part of a RASA study, three piezometers have been installed in a test well located at Illinois Beach State Park in northeastern Lake County, Ill. According to M. G. Sherrill, project chief for the Illinois part of this Cambrian-Ordovician RASA study, piezometers were installed in three water-producing zones in this 1,042 m well: (1) at 690 m below land surface in the deep part of the Elmhurst-Mount Simon aquifer; (2) at 514 m in the upper part of the Elmhurst-Mount Simon aquifer; and (3) at 367 m in the Ironton-Galesville aquifer. (Aquifer names follow the usage of the Illinois State Geological Survey.) An early water-level reading in December 1981 indicated that the Ironton-Galesville aquifer, with a depth to water of 67.1 m below land surface, has the lowest hydraulic head of the three tested zones. Depth to water is 65.0 m and 50.4 m for the upper Elmhurst-Mount Simon and deep Elmhurst-Mount Simon aquifer, respectively.

Southeastern Sand Aquifer Study

M. E. Davis, A. K. Sparkes, and B. S. Peacock report that a test well was drilled near Melvin, Ala., to a depth of 630 m as a part of the Southeastern Sand Aquifer Study (RASA). The purpose was to investigate the water-bearing characteristics of the Paleocene Nanafalia Formation and to determine the chemical quality of the water. The well was cased to a depth of 536 m below land surface and screened from 536 to 542 m.

A calculated transmissivity value of 385 m²/d for a selected sand bed in the Nanafalia was determined from a 24-hour aquifer-recovery test. The chemical analysis indicates that the water is of the sodium bicarbonate type, and is soft, basic, and low in iron. The chloride content is 73 mg/L. The static water level on January 17, 1981, was 33.26 m below land surface. The water level indicates that there is no effect from nearby faulting.

According to Davis, Sparkes, and Peacock, this aquifer has a higher transmissivity than shallower aquifers now used and could be used as a water supply in the area. Drought conditions and declining water levels in shallower aquifers have heightened interest in other sources of water for municipal supplies.

Southwest Alluvial Basins RASA Study

T. W. Anderson reports that the 72 basins in the 218,000-km² area of the Southwest Alluvial Basins Study can be grouped into three broad categories: the river-dominated basins, the desert basins, and the multiple source-sink basins. The mechanisms that control ground-water flow and the responses of the systems to stress are similar among basins in each category. Field data and model results indicate irrigation water applied in excess probably is returning to the regional system in a few basins. Data indicate that the transit time of the water through an 80-m unsaturated zone in one basin was 20 to 25 years. Surface-geophysical techniques were used at selected sites to supplement available borehole data in defining the location, extent, and shape of the fine-grained unit. Definition of the fine-grained unit, which typically occurs in the alluvial material filling the basins, is essential for adequate simulation of the ground-water systems because of the effects of the unit on the areal and vertical patterns of hydraulic conductivity and storage characteristics. The fine-grained unit also influences the water-quality characteristics and is related to the potential subsidence hazard of an area.

Upper Cretaceous units in the southeastern Virginia Coastal Plain

J. F. Harsh and A. A. Meng report that Upper Cretaceous deposits were found to extend into the subsurface Coastal Plain of southeast Virginia. Extensive investigations, through the use of geophysical log correlations, drillers' logs, and previous reports have verified that the sediments extend further than previously thought. Correlation of sediments was based upon characteristic electric log response and drillers' records which indicate that the sediments are limey clays and silts and very fine sands.

Deep test well in Maryland

A test well drilled at Cambridge, Md., for the Northern Atlantic Coastal Plain RASA project penetrated 1006 m of unconsolidated Tertiary and Cretaceous sediments and bottomed in quartz-monzonite gneiss, according to Henry Trapp, Jr., and L. L. Knobel. Drilled primarily to determine the ground-water salinity gradient, the well provided water samples squeezed from 20 cores and produced from 6 screened or perforated zones. The transition from fresh to salty ground water is indicated by samples containing 140 mg/L chloride at 804 m, 440 mg/L at 820 m, and 27,800 mg/L at 969 m below land surface.

A temperature log run to a depth of 922 m by W. S. McClung of Virginia Polytechnic Institute and State University showed a maximum temperature of 41.9° C and a mean temperature gradient of 27.5° C/km. Heads calculated by P. P. Leahy indicated an upward component of flow for the zones tested (432 to 979 m in depth), which include parts of both the freshwater and the saltwater zones.

Analysis of fresh and saline ground water in the New Jersey Coastal Plain and Continental Shelf

Study by Harold Meisler and P. P. Leahy indicates that a shallow wedge of relatively fresh ground water extending seaward for more than 90 km from the New Jersey coast is underlain by saltwater that extends westward beneath much of the Coastal Plain of New Jersey. A digital cross-sectional model was designed to test the hypothesis that this salinity distribution is a result of eustatic sea-level changes during the late Pleistocene. The model simulates both convective flow and hydrodynamic dispersion of a varying density fluid in a highly anisotropic medium. Model results show that sea-level changes can produce the present salinity distribution in the Coastal Plain of New Jersey and Continental Shelf and that the aquifer system is not in equilibrium at present. Saline water is moving slowly westward in response to the present relatively high sea level.

MARINE GEOLOGY AND COASTAL HYDROLOGY

COASTAL AND MARINE GEOLOGY

SEA-FLOOR MINERAL AND WATER RESOURCES

The recovery of metalliferous fragments in sampling a sea-floor area of suspected hydrothermal activity 400 km west of Astoria, Oreg., provided the highlight of 1981 marine geologic activities. Indicative of rich ores, the fragments offer an inducement for further exploration to determine the size of the deposit from which they came and whether or not similar deposits exist nearby. Discovery of the fragments confirms the concepts that led to their recovery and also increases incentive to learn more about sea-floor conditions and processes that will help in understanding resource distribution and place constraints on resource development, both on land and offshore. Pertinent research by the USGS included studies of seamounts, manganese nodules, and deep-sea fans, and reports on the geologic framework of the continental margins.

Geology and mineral deposits of the Juan de Fuca Ridge off Oregon

W. R. Normark, with his knowledge gained from submersible studies of hydrothermal vents on the East Pacific Rise near Mexico, was able to help define areas of probable polymetallic sulfide occurrence along the Juan de Fuca Ridge, 400 km west of Oreg. He then led a September 1981 cruise of the USGS Research Vessel *S. P. Lee* that succeeded in recovering 10 kg of sulfides that had formed around one of five hydrothermal vents photographed near the southern end of the ridge. During the cruise, Normark and his team also obtained a large collection of fresh basalts and successfully sampled the hydrothermal vent waters of the Juan de Fuca Ridge crest.

David Clague made analyses of the polymetallic sulfides and the basalts, some of which contained cognate xenoliths. The sulfide samples consisted of sphalerite, wurtzite, pyrite, marcasite, cubanite-chalcopyrite, galena, amorphous silica, barite, and anhydrite. Microprobe analyses of the zinc sulfide phases showed that cadmium and iron were concentrated in wurtzite cores and were generally less abundant in sphalerite. Some very low iron sphalerites, however, had a high cadmium content.

The samples of basalt from the Juan de Fuca Ridge have generally constant compositions and almost identical strontium isotope ratios. The contained xenoliths are thought to represent partly crystallized wall rock of the magma chamber that underlies the axis of the ridge.

Petrology of Loihi Seamount, Hawaii

David Clague, J. G. Moore, and W. R. Normark undertook extensive sampling of Loihi Seamount, a submarine volcano that lies southeast of the Island of Hawaii and is the youngest eruptive center of the Hawaiian Emperor volcanic chain. The recovered samples of lava were mostly tholeiitic but included some alkalic basalt. The thickness of palagonite on the glassy rims of the alkalic pillow fragments indicates ages that exceed those of the tholeiites, a discovery that requires changes in present concepts of hot-spot models and magmatic evolution at Hawaiian volcanoes.

Geochemistry of sea-floor minerals and sediments

The distribution of Pacific deep ocean manganese nodules relates closely to the sediments with which they are associated. As shown on maps by D. Z. Piper and T. R. Swint, nodules are most abundant in regions of pelagic clay and are absent where carbonate sediments are present, except in a small area of the central South Pacific. Piper and J. R. Blueford have noted a further relation between nodule coverage and sedimentation rates within a 1,000 km² area of the equatorial North Pacific. In an analogous survey of marine phosphorite deposits, Piper and W. C. Burnett (Florida State University) have been able to distinguish depositional environments by using rare earth and other minor elements which substitute in lattices of the phosphate minerals.

Growth and development of the upper and middle Laurentian fan

Analyzing seismic data from two separate areas of the deep sea Laurentian fan off eastern Canada, W. R. Normark (USGS) and D. J. W. Piper (Geological Survey of Canada) were able to distinguish a complex pattern of

fan growth and sedimentation. On the upper slopes, erosion and mass wasting have produced a gullied terrane that feeds three large fan valleys. Erosion and fill sequences of the valleys bound undisturbed bedded deposits of the lower slopes and upper fan. Previous authors had misidentified these deposits as large slide blocks. Within the transition from leveed valley to depositional lobe on the middle part of the fan, Normark and Piper attribute the features to rapid deposition at the mouth of one of the major valleys, by either lobe aggradation or debris flows, and a consequent pronounced eastward deflection of turbidity current flows. The deflection, in turn, has produced a sharp bend in the western levee as it has continued to grow across the fan.

Destin Dome and the west Florida Shelf

The Destin Dome, a large, west-northwest-trending anticlinal structure off northwest Florida, attracted widespread attention during a Department of the Interior OCS lease sale in 1973 with spirited bidding for 32 tracts on its eastern flank. Later, nine dry holes were drilled, seven of them into a structural high in Upper Cretaceous strata. Structural crests of Jurassic and Lower Cretaceous strata were known but lay to the west beneath an area that was withheld from leasing because of use as a Department of Defense bombing range.

M. M. Ball examined a network of 1,280 km of common-depth-point (CDP) seismic data that includes line ties to the dry wells of the Destin Dome, to eight onshore wildcat wells drilled north of Tampa, Fla., and to the regional multichannel net of the University of Texas. The sections confirm features indicating Late Cretaceous and Cenozoic structural growth of the salt-related Destin Dome and Jurassic to Early Cretaceous growth of a salt pillow which lies 30 km to the south. Numerous low relief anticlines overlie basement highs elsewhere beneath the west Florida Shelf.

Petroleum geology of the U. S. Mid-Atlantic Slope

R. E. Mattick identified petroleum plays of three basic types beneath the Mid-Atlantic Upper Continental Slope in an area where the Department of the Interior held a lease sale during December 1981: (1) a Jurassic "backreef" carbonate and sandstone play, (2) an Upper Jurassic-lowermost Cretaceous "reef" play on the margin of a buried paleoshelf, and (3) a Lower Cretaceous sandstone play. At the sale, industry interest, as expressed by high bids, seemed concentrated on the Jurassic backreef play, especially in the southern part of the basin where structural relief on the top of the Jurassic beds is greatest. Within this play, basinal shales over which the Jurassic carbonate bank pro-

graded may have charged potential reservoirs that are sealed updip by impermeable rocks of the reef facies.

CONTINENTAL MARGIN STRUCTURAL FRAMEWORKS

The continental margins of the United States provide a diversity of geologic environments, some possessing known or prospective resource potentials, others having few or no potentials but offering insights to the discovery of resources elsewhere. The majority lie in the intervening gray areas. The areas of accessible sand and gravel deposits off the Northeastern States that are of interest to the onshore construction industry and the deep sedimentary basins of the continental shelves that are being explored and exploited by the petroleum industry exemplify areas of known or prospective resource potentials. The margin along the south side of the Alaska Peninsula, where active tectonism and associated volcanic and geothermal activity are altering the subsurface and redistributing its mineral components offers insights into new discoveries.

Decoupling within the Aleutian subduction zone

Roland von Huene applied results of his research on the Japan and Middle America trenches to interpret tectonism associated with the Aleutian Trench and concluded that overpressured pore fluids exert an important control at all three convergent margins. Direct observations of pore pressures within holes drilled into the flanks of the Japan and Middle America trenches substantiate the classic model of Hubbert and Rubey (1959) that is based on the static effects of vertical loading and predicts an appreciable rise of pore pressures in response to tectonic thickening by overthrusting. The high pore pressures can literally "float" the upper plate of a subduction zone and cause a high degree of decoupling, which explains the lack of strong earthquakes despite large thrust displacements along the front of the zone.

Aleutian Ridge tectonics, petrology, and sedimentation

The Aleutian Ridge consists geomorphically of two provinces: the west-trending, flat-topped Aleutian Island Arc, which rises 4,000 m above the adjacent sea floor, and a 30 to 90 km wide forearc province that includes a broad forearc basin, the Aleutian Terrace, and the landward slope of the Aleutian Trench. T. L. Vallier and D. W. Scholl group the upper crustal rocks of the two provinces into a three-tiered chronostratigraphic sequence: a lower series of mostly Eocene volcanic rocks, a

middle series of Oligocene through lower middle Miocene strata that include large volumes of sedimentary beds, and an upper series of middle Miocene to Holocene deposits that are dominantly sedimentary but include upper Cenozoic eruptive masses of the arc's modern volcanic centers.

Except for the landward trench slope, the ridge's upper crustal framework is a massive antiform with a core of lower series rocks produced by voluminous submarine volcanism prior to about 35 m.y. ago. The base of this mostly igneous massif is at least 200–250 km wide and extends from the landward trench slope northward beneath the forearc basin and adjacent geanticlinal mass of the island arc to the abyssal floor of the Bering Sea. The upper Eocene and lower Oligocene(?) igneous rocks have calc-alkaline and tholeiitic differentiation trends similar to those of lavas now being erupted along the island arc. Flank activity practically ceased after the Eocene, and except for a pulse in early middle Miocene time, summit arc activity was subdued. In Oligocene through early Neogene time denudational debris from the regionally elevated and volcanically dying crestal area accumulated on the submerged (or submerging) flanks and basal regions to form the middle series. The post-middle Miocene history of the ridge's crestal area attests to the dominance of extensional collapse and erosional destruction over continuing but localized volcanic buildup. Erosion carved a wave-base summit platform across the arc, and was accompanied by the deposition of basinal sequences of upper series beds in summit grabens and possible subsidence of large areas of the arc's sloping geanticlinal flanks. In the more deeply submerged forearc area, relative uplift of the seaward part of the igneous basement framed the structural basin to the Aleutian Terrace, permitting 3–5 km of upper series deposition. Concurrently, a mass of trench deposits of mostly Alaskan origin was accreted to the lower part of the adjacent trench slope.

Basically, the Aleutian Ridge (arc + forearc) has had a two-part history of early Tertiary growth and subsequent destructional and deformational modification, a formative sequence that can be linked to a major late Eocene change in the plate tectonic setting along the northern rim of the Pacific basin. Because of dominant erosion and deformation during the second stage, Oligocene and younger sediments that are potential habitats for petroleum blanket the ridge's igneous framework. Petroleum is most likely to occur in the thick (3–5 km) and only slightly deformed basinal sections of upper series beds that underlie the Aleutian Terrace and fill summit grabens. Tertiary sandstone and siltstone beds associated with these sections are little altered and exhibit favorable porosity, permeability, and organic contents.

Structure of the Navarin and Anadyr Basins, Bering Sea

Continuing analyses of geophysical data collected during a 1980 cruise to the Bering Sea have helped clarify structures of the underlying Navarin and Anadyr Basins and the extension of the Koryak Range of eastern Siberia which separates them. In their interpretation of the data, M. S. Marlow and A. K. Cooper found anomalies indicating the probable presence of hydrocarbons within both basins. For example, special processing (stack-slant transformation) of one sonobouy record from the Navarin Basin by Gary Boucher discloses a section that is 12 to 13 km in thickness. The gravity data, however, provide only modest anomalies in this part of the basin, and thereby suggest a shallow mantle that would favor high heat flow and generation of hydrocarbons.

Tectonic framework, continental margin of southwestern Washington

P. D. Snively, Jr., and H. C. Wagner interpret the tectonic framework of the southwestern Washington continental margin to consist of two tectonostratigraphic terranes overlying the subducted Farallon plate. A low eastward dipping thrust fault forming the interface between these two terranes reaches the sea floor several kilometers west of the coastline. East of this thrust fault, Miocene(?) oceanic crust overlain by a melange of upper Oligocene and middle Miocene deposits is inferred to have been thrust beneath lower to middle Eocene oceanic crust, which constitutes the Crescent Formation of coastal Washington and consists of ridge basalt and associated oceanic islands. Hydrocarbon seeps and the small quantities of oil produced near the Washington coast probably were generated in the Neogene sediments of the underthrust plate.

Geophysical studies, U.S. Atlantic Coastal Plain and continental margin

Integrating data from drill holes with that of magnetic, gravity, and seismic reflection surveys, K. D. Klitgord, W. P. Dillon, and Peter Popenoe delineated upper Triassic and Jurassic structures, including Triassic grabens and zones of Triassic sediment accumulation, beneath the coastal plain sediments of the Charleston region, S.C. They used magnetic anomaly patterns and a reconstruction of the Jurassic continental margin to locate Paleozoic zones of weakness, such as transform faults. A combination of magnetic and seismic-reflection data permitted delineation of the landward edge of the Blake Plateau basin and Carolina Trough, two Mesozoic basins which are separated by a

large offset at the Blake Spur fracture zone. The resulting tectonic map provided a base for identifying old zones of weakness that could be rejuvenated and cause earthquakes in the Charleston region.

In comparable studies of the Georges Bank Basin off New England, Klitgord, J. S. Schlee, and Karl Hine (1982) have delineated basement structures that include a series of down-stepping half grabens on the landward side of the basin axis and a zone of seaward-dipping reflectors merging into oceanic crust on the outer side. Seaward edges of the Long Island, Gulf of Maine, and LeHave platforms are bounded by the grabens which produce lineated magnetic anomalies consisting of lows over the depressed blocks and highs along their margins. The largest horizontal offset in the platform edges is at the juncture of the Gulf of Maine and LeHave platforms; the offset is extended as far seaward as the Yarmouth arch by a broad transitional block-faulted zone between the Georges Bank Basin and the LeHave platforms. Zones of sedimentary ridges and salt diapirs off the Scotian margin were traced southwestward into a series of buried benches located just seaward of the Jurassic shelf edge beneath Georges Bank.

Depositional sequences and stratigraphic gaps of the U.S. Atlantic margin

C. W. Poag and J. S. Schlee correlated seismic reflection profiles with deep stratigraphic test wells to deduce a series of depositional sequences that can be traced through the three major sedimentary basins of the submerged U.S. Atlantic margin. These sequences are bounded in large part by unconformities whose stratigraphic positions are similar to those predicted by the Vail model of relative coastal onlap and eustatic sea-level change (Vail and others, 1977). The Mesozoic depositional sequences nearly match the supercycles of the Vail model, but the Cenozoic record indicates marked variability among the basins. There is little doubt that these depositional sequences are the product of sea-level fluctuations modulated by changing rates of deposition and variable rates of basin subsidence.

Offshore stratigraphy of Georges Bank Basin

Using drill hole data and samples collected from research submersibles, C. W. Poag made a stratigraphic analysis of a multichannel seismic profile across the Georges Bank Basin. Here Cretaceous and Cenozoic units of dominantly siliciclastic marine and nonmarine deposits overlie Triassic(?) and Jurassic evaporites and shallow marine carbonates. The lithologies, unconformities, and paleoenvironmental cycles of the sequence re-

semble those of the Scotian Basin on the Canadian margin to the immediate north.

Geologic history of Cape Hatteras

At present, Cape Hatteras extends seaward almost to the Continental Slope and continues to build eastward through sediment prograding at the merge point of north-flowing Gulf Stream and south-flowing shelf currents. On the basis of a stratigraphic analysis of seismic reflection data, Peter Popenoe concludes that events leading to this buildup began in the Eocene when sea levels were high and the Gulf Stream transgressed onto the shelf to the approximate present position of the shoreline between Cape Fear and Cape Hatteras. Construction of a Florida-Hatteras shelf along the present coastline at this time included deposition of a thick mound of winnowed carbonate sediments (Castle Hayne Formation) on the lee side of the Cape Fear Arch. The deposition terminated eastward along a steep, straight, northeast-trending slope.

Low sea levels of the late Oligocene and early Miocene and a prominent bathymetric buildup on the northern Blake Plateau (the Late Cretaceous, pre-Gulf Stream shelf of the area) caused an offshore deflection of the Gulf Stream south of Cape Fear. This deflection of the Gulf Stream allowed accumulation of a thick, uniform sequence of upper Oligocene and lower Miocene sediments across the northern Blake Plateau.

With return of high sea levels in the middle Miocene, the Gulf Stream again transgressed landward, the result being the construction of a shelf just inshore of the present shelf. This middle Miocene shelf ended in a large northeast-trending ridge of drifting sediments that underlie and form the southern margin of present Cape Hatteras; the shelf also bounded an embayment to the north which was 50 km wide and 250 m deep. The cape continued to build in Pliocene and Pleistocene time as prograding sediments delivered by shelf currents from the Chesapeake Bay area to the north filled the deep embayment behind the ridge of drifting sediments from the south.

Freshwater beneath the Carolina Continental Shelf

In vibracores recovered by S. R. Riggs (East Carolina University) from Onslow Bay off North Carolina, F. T. Manheim, C. Lane, and P. C. Bowker found that interstitial waters became fresher with depth, reaching near-potable levels at depths of 4 to 5 m below the sea floor within 30 km of shore. They attribute the occurrences to Pleistocene freshwater recharge within sediments of the shelf area. The offshore interstitial freshwater can be

expected to buffer shoreward intrusion of sulphate-bearing seawater and therefore constitutes a factor to be considered in future mining of phosphate deposits beneath the Bay.

In contrast to Onslow Bay, Manheim, Lane, and Bowker measured increasing chlorinity with depth in the interstitial waters of sediments that overlie diapirs within the continental slope off South Carolina. Here, in studies performed jointly with J. D. Grow, D. Peeler, and Page Valentine, they attribute the salinity change to upward diffusion of salt dissolved from the underlying diapirs.

Late Paleogene watermass fluctuations along east coast continental margin

Quantitative analyses of *Globigerinoides* populations by R. E. Hall (USGS) and studies on the carbon and oxygen isotopes of these foraminifers by D. F. Williams (University of South Carolina) have been used to ascertain watermass structures in the western North Atlantic during late Oligocene time. The results suggest three to four watermass fluctuations, and, for a site on the Blake Plateau, the pulses of *Globigerinoides* correlate well with the global sea-level curve which Vail and others (1977) have derived for upper Oligocene and lowest Miocene strata.

Geology and evolution of the Blake Escarpment

The Blake Escarpment, a 4,000 m high sea-floor cliff, forms the seaward boundary of the Blake Plateau east of Florida. Deep-penetration CDP seismic profiles indicate apparent termination of nearly horizontal Blake Plateau strata at the escarpment. They also provide indications of a subbottom bench that extends seaward beyond the foot of the escarpment. These features led W. P. Dillon and his associates to conclude, preliminarily, that deep-sea erosion probably formed the bench and face of the escarpment. GLORIA sidescan sonar records showed a rough, stepped cliff face that also suggested outcropping strata that have been eroded differentially. To observe and sample these old strata directly, Dillon's team then undertook a series of 10 dives in the research submersible *Alvin*. The dives were made along the transect of three good quality seismic profiles and extended from the *Alvin*'s maximum dive depth of 4,000 m to the top of the escarpment. On the basis of nanofossils from samples that were collected, P. C. Valentine determined ages of Valanginian to Albian, almost the entire Lower Cretaceous section. From thin section examination of the samples, E. A. Shinn (USGS) and Michael Arthur (University of South Carolina) concluded that the Lower Cretaceous rocks formed in a shallow carbonate platform environment. Fragments of

rudists, which N. F. Sohl dates as Albian and possibly Cenomanian, may be representative of the organisms which formed an apparent reef identified in seismic profiles. Evidence of active erosion by currents included observations of undercut blocks that had collapsed, differentially eroded outcrops and sand ripples, and measurements of current velocities of as much as 2 knots during dives. On the basis of observed pitting, the lack of talus at the base of the escarpment, and the location of the outcrops below the carbonate compensation depth, C. K. Paull (Scripps Institution of Oceanography) suggested a need to consider an important role for chemical weathering. A. C. Newmaun (University of North Carolina) by noting that an extensive cover of encrusting organisms implies biologic breakdown and that this too may be significant, led to the ongoing controversy concerning the relative importance of mechanical, chemical, and biologic processes.

Surface structures of the southwest Florida shelf

On the basis of examination of high resolution seismic data, C. W. Holmes suggests existence of a Miocene(?) karstic platform beneath much of the modern southwestern Florida shelf and slope south of 26° N. A lens of upper Tertiary and Quaternary sediments covering the platform thickens from the central shelf to a maximum of 150 m at the shelf-slope break and then thins against a ridgelike outcrop of the Miocene(?) platform on the upper slope. An 8-km-wide north-trending double-reef complex on the central shelf separates the post-Miocene sediment lens from a shoreward zone where the Miocene(?) platform has no more than a thin veneer of biogenic sand.

A second double-reef complex overlies the thickest post-Miocene section at the shelf-slope break. The lower reef of this set forms a well developed 40 m scarp; the upper is distinguished by a low-amplitude ridge for most of its length. Beneath this reef complex, two stratigraphic units are identifiable within the Tertiary and Quaternary lens: (1) a lower unit of unknown age which is continuous beneath the shelf-slope break and onlaps the Miocene(?) ledge of the central shelf, and (2) an upper unit which consists of sediments from shelf edge and pelagic sources and at its lowermost exposures on the upper slopes has an accordianlike morphology that may be attributed to downslope creep.

A Miocene(?) ridge with a surficial phosphorite deposit trends north-south at depths of 400 to 510 m along the west-facing continental slope that bounds the Florida shelf. The ridge is buried in the Florida Straits region. The younger reefs along the shelf-slope break and still younger reefs on the central shelf are also being covered by more recent material. Present reef growth

and associated sedimentation continue to extend the shelf to the south and west.

Oil and gas potential of the Gulf of Mexico Maritime Boundary region

The Maritime Boundary region encompasses a part of the Gulf of Mexico where jurisdiction over natural resources by adjacent coastal countries has not yet been established. Within it, R. G. Martin and R. Q. Foote distinguished six areas for assessment of the geologic framework and resource potentials for oil and gas. The areas cover a total of about 153,000 km² and contain an estimated sediment volume of 784,000 km³. Water depths range from a minimum of 30 m on the Continental Shelf off the Rio Grande to a maximum of about 3,740 m in the deep abyssal plain of the west-central Gulf; more than 75 percent of the region has depths exceeding 3,000 m.

A variety of evidence favors the occurrence of crude oil and natural gas in the Maritime Boundary region. The Perdido fold belt, a system of broad linear folds beneath the deep Gulf Basin at the foot of the continental slope off southernmost Texas, appears to have the most attractive potentials. Structures in the Sigsbee Knolls salt-diapir belt that fall within the region rank a close second. The Abyssal Gulf Basin assessment area probably has the largest estimated volumes of oil and gas resources as a result of its extent (91 percent of the region) and sediment volume (93 percent of the total region); it lacks discrete structures of major size, but contains many broad, low-relief structural closures and numerous attractive stratigraphic traps. The Campeche Escarpment, Rio Grande margin, and Sigsbee Escarpment assessment areas were determined to have successively less petroleum potential because of generally unfavorable geological aspects.

Estimates of the in-place petroleum resources for the Maritime Boundary region range from 2.24 to 21.99 billion barrels of crude oil and from 5.48 to 44.4 trillion ft³ of natural gas. Estimates of ultimately recoverable resources were not made because there is a lack of present knowledge about reservoir properties, economics, and technology needed to develop these deep-water areas. Exploitation of deep-water resources, however, is expected to be technically possible within the next 20 to 30 yr.

Caribbean tectonostratigraphic terranes

J. E. Case, R. G. Martin (USGS), and T. L. Holcombe (U.S. Naval Ocean Research and Development Activity) interpret the Caribbean region to be a complex of more than 100 geologic terranes, many of which are allochthonous with respect to cratonic North and South

America and therefore are tectonostratigraphic terranes as defined by Jones and others (1981). Neogene volcanic and seismic belts are genetically related to northeastward underthrusting of the Cocos and northern Nazca plates beneath Middle America and to westward underthrusting of the North and South American plates beneath the Lesser Antilles deformed belts. The north and south borders of the Caribbean plate are wide plate-boundary zones, characterized by complex left-lateral and thrust faults on the south. Many, perhaps most, Tertiary sedimentary basins in both northern and southern plate-boundary zones are complex pull-apart basins of the strike-slip transform systems. Although they are far from complete and well-documented, the published paleomagnetic data suggest major northward and eastward translations and clockwise rotations since Cretaceous time for individual terranes in the southern plate-boundary zone and major northward and eastward translations and counterclockwise rotations for the Cayman Trough–Puerto Rico Trench transform systems. Available paleomagnetic data for the Chortis block of Middle America suggest extremely complex Cretaceous and post-Cretaceous translations and rotations.

SEA-FLOOR CONDITIONS AND PROCESSES

Much recent USGS research on the surficial geology of the Continental Shelf and Slope has emphasized the applied objectives of identifying and evaluating hazards that must be considered in managing OCS oil and gas activities. In conducting the research, however, the USGS scientists have maintained a variety of other goals, some of which have general and scientific interest. Among results of studies in 1981, described below, were several that provided further grounds for changing our concepts of the relief of the Continental Slope from a relatively simple, smooth surface incised by a few large canyons and intervening nearly straight furrows to a complex of canyons, tributary valleys, and subordinate relief comparable to that of fluvial systems on land. Observations of sediment movement and associated sea-floor relief require that we continue to modify our beliefs concerning ways that material reaches the base of the Continental Slope.

Slope stabilities, Georges Bank and Baltimore Canyon areas, Atlantic continental margin

Slope stabilities have attracted special interest in the Georges Bank and Baltimore Canyon areas off the Northeastern United States because prospects of finding petroleum within sediments of the underlying basins are greatest beneath the dissected Continental

Slope. To aid in evaluating hazards associated with potentially unstable slopes, J. S. Booth and his associates have compared surficial geologic processes and conditions of the two areas. They conclude that although differences exist, both areas are generally stable with respect to mass movement and have sediments that tend to be overconsolidated. Of the two areas, the Baltimore Canyon slopes tend to have lower safety factors for slope failure and to have sediment that is closer to being normally consolidated. The dominant sediment in both areas is an inorganic silty clay of medium to high plasticity. Analyses of piston cores recovered from apparent mass-movement scarps at two sites on the Georges Bank slope indicate probable removal of approximately 10 m and 35 m of overburden. Similar locales were not cored in the Baltimore Canyon region; however, clasts found in cores on the lower slope and rise provide evidence of past mass movement in the area.

In detailed studies of the Baltimore Canyon area, H. W. Olsen, B. A. McGregor, J. S. Booth, A. P. Cardinell, and T. L. Rice (1982) examined 31 sites in terms of an infinite-slope stability model which utilizes geotechnical profiles based on information obtained from piston cores together with sea-floor gradients interpreted from bathymetric and geophysical data. The majority of the sites had overconsolidated sediments and offered relatively high safety factors (2.0 or more) for both drained and undrained conditions. About one-third of the sites, however, had underconsolidated materials. Among these, low safety factors for undrained conditions (1.0 or less) were obtained for five sites where sea-floor gradients amounted to 15 degrees or more. Four of these five sites were on valley walls, and one was on an intervalley ridge.

Submarine canyon dynamics

Through operation of a midrange sidescan system (SEAMARK I) on a cooperative USGS-Lamont-Doherty Observatory cruise, complemented by use of the Deep Sea Research Vehicle (DSRV) *Alvin* to observe and sample features identified on the sidescan images, B. A. McGregor obtained much added detail on the micro-physiography of the Continental Slope and rise in the vicinity of Wilmington Canyon, east of Delaware. The added detail is essential to interpreting dynamics of the canyons which are fed here by dendritic tributary drainage systems that extend over the entire slope and are strikingly similar to fluvial systems on land. The canyons display channel morphologies ranging from a straight downslope trend to one of tight meanders and an apparent flood plain. The canyons have flat floors, which, however, do not represent infill and apparently flush sediment episodically.

Geologic processes of the east coast Continental Shelf

During July 1981, J. M. Robb, J. C. Hampson, Jr., and J. R. Kirby (1982) used the DSRV *Alvin* to make four dives into an area of Tertiary outcrops on the lower Atlantic Continental Slope between Lindenkohl and South Toms Canyons off New Jersey. Here the team noted 10-m-high talus blocks at the base of slopes, cliffs, and steep valley walls having as much as 40 m relief. The observers also noted clastic dikes, joint-controlled cliff surfaces and valley shapes, and sets of parallel furrows that are 4 to 12 m deep, are spaced 20 to 50 m apart, and probably eroded into the Eocene calcareous claystone at the mouth of Berkeley Canyon. At some places, the smaller scale topography of the lower slopes appeared fresh; some planar surfaces were unscoured or un bored by organism, and some talus fragments on the upper rise had a recent appearance. A thin cover of fine flocky sediment on horizontal surface implies current activity that is either energy deficient or intermittent. Even so, canyon and valley thalwegs should still be treated with caution if considered for construction sites.

Mass movement, Atlantic Continental Slope off New England

D. W. O'Leary and K. M. Scanlon conducted and interpreted high resolution seismic profiling and midrange sidescan sonar surveys that provided evidence for a complex history of mass wasting along the Atlantic Continental Slope between 70° and 71°30' west longitude, south of New England. Between canyons, the slope surfaces conform generally to the underlying sediment layering and typically have smooth, relatively low relief. Downslope the surfaces are offset to successively lower stratigraphic levels along scarps. The scarps, bound polygonal areas from 10 to 30 m deep, indent (scallop) the slope and at places converge upslope to form arcuate rubble-filled amphitheatres. The scarp-bounded polygonal areas may be "slide scars." Elsewhere, slide debris that issues from arcuate reentrants in the scarps form tear-shaped bodies that are 1 to 3 km long and less than 1 km wide. *Alvin* and Atlantic Canyons have broad bordering cirques and amphitheatres that probably are mass-wasting features also. The cirques lack associated relief features that may be attributed to detached or collapsed debris; however, the morphology of the adjacent continental rise provides evidence indicating abundant slide-flow debris.

The Lydonia Canyon experiment—preliminary results

Lydonia Canyon and the adjacent shelf's slope on the southern flank of Georges Bank were selected for detailed study and continuing measurements of circulation and sediment movement from November 1980 to

July 1982. On the basis of their observations and preliminary examination of early records from an array of moored instruments, Bradford Butman, M. H. Bothner, M. A. Noble, D. C. Twichell, and J. A. Moody report that in the canyon axis, average current speeds (computed from data records having a 7.5 minute sampling interval) measured 5 m above bottom (mab) from November 1980 to April 1981, were 13 cm/s (stand. dev. 10, max. 60) at 282 m water depth, 16 cm/s (stand. dev. 9, max. 54) at 600 m, and 8 cm/s (stand. dev. 4, max. 26) at 1,380 m. On the slope, average current speed 5 mab was 18 cm/s (stand. dev. 9, max. 51) at 250 m. Mean Eulerian flow in the canyon head was downcanyon at approximately 3 cm/s 5 mab but was upcanyon at approximately 2 cm/s 50 mab. No significant net near-bottom flow was observed deeper in the canyon axis at 600 or 1,380 m. However, typical near-bottom net Eulerian cross-canyon currents of 1 to 3 cm/s were recorded at all stations. Sediment traps 5 mab in the canyon axis collected 10, 4, and 0.7 cm³/(cm²/yr) at 282, 600, and 1,380 m, respectively. On the slope, a trap 5 mab at 250 m collected 0.3 cm³/(cm²/yr). In the canyon axis the surficial sediments are primarily sand (75 percent) at the head (300 m); they become finer downcanyon at 1,500 m (80 percent mud). Small ripples were observed at 300 m, whereas larger ripples and sand waves were found at 600 m; the bottom was tranquil at 1,100 m. The observations to date suggest reworking of the surficial sediments in the canyon axis to depths of at least 100 m.

Importance of mass sediment transport in continental margin processes

J. M. Coleman and D. B. Prior of Louisiana State University have shown that landslide processes may move much larger volumes of shallow water sediments from major deltas into deep water than originally thought. With L. E. Garrison (USGS), they concluded that in late Pleistocene and Holocene times alone, about 12,000 km³ of sediment have been moved from the shelf fronting the Mississippi Delta into the deep Gulf of Mexico; this sediment accounts for at least 15 percent of the total volume of the Mississippi fan. Furthermore, landslide processes can move extremely large volumes of material in a surprisingly short time. For example, correlation of seismic reflectors and C-14 dating of borehole samples in the region west of the present Mississippi Delta indicates that the Mississippi trough was formed by the removal of nearly 2,000 km³ of shelf deposits in the 7,000-yr interval between 27,000 and 20,000 years B.P. Within so short a time, density currents and fluvial processes were unlikely mechanisms for eroding to depths exceeding 1,200 m when sea level was only 100 to 150 m below present. The most reasonable answer, a

retrograde landsliding process, is supported by intensive industrial studies showing the lowermost canyon fill to be dominantly slump-deposited.

Subaqueous avalanching, Carmel Canyon, California

During field experiments on subaqueous avalanching in the head of Carmel Submarine Canyon west of Monterey, Calif., J. R. Dinger, R. J. Anima, and D. W. Hirschaut discovered that inversely graded beds develop within a remarkably short distance below the start of grain flow (<2 m). Entrainment of surficial material by the flows, which form when the sand slopes oversteepen, is negligible. When used with other environmental indicators, the character of the deposits should be a significant help in identifying comparable ancient deposits. The observed grain-flow process may also apply to evidence of large-scale subaqueous grain-flow recorded in deep-water deposits.

Bottom stresses and sediment transport, central California continental shelf

During 1981, D. A. Cacchione, D. E. Drake, and their associates completed field measurements of bottom currents, bottom pressures and temperatures, and the distribution of both bottom and suspended sediment in a continental shelf region that had been selected to serve as a control for studies of sediment transport off central California (U.S. Geol. Survey, 1980, p. 156). Initial interpretation of the GEOPROBE, shipboard sampling, and current-meter data indicate that most modern sediment from the Russian River has been transported northward. Here, fine sand and coarser components are confined to the steeper inner shelf where water depths are 50 m or less, and medium silt and finer sizes accumulate along the middle shelf where water depths range from 50 m to about 100 m. Most surficial sediment of the outer shelf from the Russian River mouth northward to Point Arena consists of relict sands. D. A. Klise and J. W. Gardner have compiled detailed bottom sediment textural and mineralogical maps that define the sedimentary provinces in this area.

Bottom-current data and bottom-stress estimates (calculated from GEOPROBE velocity measurements) indicate a dominant poleward (northwesterly) flow near the sea floor (bottom to about 30 m above the sea floor), even during the spring-summer upwelling period when north-northwest winds are common. This northwesterly flow accounts for most sediment distribution. Occasionally, the bottom flow reverses equatorward (southerly) under strong northwesterly winds stresses. These southerly bursts transport a small amount of modern sediment toward the San Francisco area; the result is a

thin, diffuse modern sediment cover on the shelf between the Russian River and Point Reyes.

W. B. Grant and A. S. Williams of the Woods Hole Oceanographic Institution have used specially constructed bottom tripods containing high-resolution acoustic current meters to measure the turbulent (Reynolds) stresses at the sea floor. On the basis of their measurements and the GEOPROBE measurements of bottom velocities taken concurrently, Cacchione, Drake, Grant, and Williams developed a well-defined estimate of the bottom friction (bottom stress) caused by waves and currents on the shelf. The measurements have shown that recent theoretical estimates of combined stresses (waves and currents) are reasonably accurate and that formulation of a model for shelf bottom stresses is feasible.

Sediment failure of November 1980, Klamath River Delta, northern California

On the basis of data obtained after a 1980 earthquake, M. E. Field and his co-workers (unpub. data, 1982) were able to identify and delineate a complex zone of sediment failure that the shock caused on the Klamath River Delta off northern California. The earthquake ($M_L=6.5$; $M_s=7.2$) took place off Eureka, Calif., on November 8 and initiated extensive sediment failure on sea-floor slopes of less than 25 percent. The affected zone was continuous for a distance of about 20 km.

Sediment deposition on the Pacific continental margin

Rivers and other major sediment sources of the Northwestern United States and the Gulf of Alaska feed directly onto swell- and storm-dominated shelves. M. W. Field and B. D. Edwards note that on narrow unprotected shelves, the sediment has a short residence time in submarine deltaic deposits prior to remobilization and dispersion to outermost-shelf and upper-slope environments. Prograding sequences of shelf-edge sedimentary deposits which form in these environments commonly have a high preservation potential. On broad or protected shelves, however, sediments deposited on prodeltas have a longer life expectancy and only small amounts escape to the shelf edge. Large magnitude earthquakes and local uplift trigger failure of rapidly accumulating organic-rich muds on the Gulf of Alaska and northern California continental margins. Repeated failures over long intervals produce unique sedimentary packages that have potential for becoming both source beds and stratigraphic traps for hydrocarbons.

Geotechnical properties and sedimentary processes of the Alaskan OCS

Geologic processes operating within the diverse environments of the broad areas of the Continental Shelf off Alaska have produced sediments characterized by a variety of geotechnical properties. Knowledge of the range of properties and their relations to the processes is rudimentary at best, and therefore to improve it, M. A. Hampton and H. J. Lee have chosen three contrasting environments for detailed studies: (1) northeast Gulf of Alaska, (2) the Shelikof Strait between Kodiak Island and the Alaska Peninsula, and (3) Norton Sound off northwest Alaska.

Within the northeast Gulf of Alaska, the sediment is primarily a glacial-marine rock flour which has relatively high densities and low plasticities. Preliminary cyclic loading tests indicate a high level of strength degradation during repeated loading—a reaction that may contribute to the abundance of observed landslides in this area of high seismicity and frequent storm waves.

In the Shelikof Strait, the sea-floor sediment grades uniformly down current from muddy sand to mud. Geotechnical properties, with decreasing strength and increasing plasticity and compressibility as grain sizes become finer, reflect this trend. Trends of repeated-loading (earthquake) test data remain inconclusive.

In Norton Sound, in situ penetration resistance in areas of gas charged sediment is low relative to that in widespread areas of normal prodelta deposition. Depositional ridges in the northern part of the Sound, as compared to adjacent swales, have high penetration resistance extending down to a basal gravel unit beneath both features.

Postglacial sediments of the northern Bering Sea

G. R. Hess completed preparation of maps and reports delineating the distribution, depicting thicknesses, and evaluating hazards of extensive areas of postglacial sediments within the northern Bering Sea. The central Chirikov Basin (a western subdivision of the Norton Basin) has a large deposit of these postglacial materials. The Chirikov Basin also has large, deep, filled fluvial channels of a major drainage system that existed during periods of lowered sea level.

Sea-floor hazards of the Navarin Basin, northern Bering Sea

About 5,000 km of high resolution seismic data and 105 sea-floor sediment samples collected during 1981 on a second cruise to the Navarin Basin in the northern

Bering Sea provided added support for the earlier conclusion of P. R. Carlson and H. A. Karl (U.S. Geol. Survey, 1981, p. 126) that gas-charged sediments constitute the region's geologic hazard of greatest concern. Seismic reflection anomalies indicating gas-charged sediments are most numerous on records from the northern half of the Navarin province. These anomalies also indicate that the gas-charged sediments may be as shallow as 15 m beneath the sediment-water interface. According to K. A. Kvenvolden and T. M. Vogel, the dominance of methane in subsamples from gravity cores indicates a biogenic origin for the gas. Other mapped evidence of geohazards in the Navarin Basin province included the effects of submarine slides and slumps at many places on the Continental Slope, shallow faults near the shelf edge, and fields of large sand waves in the heads of three great submarine canyons. While contouring bathymetric data to make a preliminary base map of the Navarin continental margin, J. A. Fischer and P. R. Carlson identified two large previously unknown submarine canyon systems.

Northwestern insular shelf, Puerto Rico

In mapping sediment types on the insular shelf of the Anasco-Camuy area, northwestern Puerto Rico, J. V. A. Trumbull, K. A. Grove, and O. H. Pilkey found that sediments derived from erosion of island rocks dominate some mostly nearshore areas but sediments composed entirely or in large part of biogenic grains cover most of the shelf. Rivers bring predominately silicate sands and muds to the shelf where waves and currents of the shelf then transport them short distances. By mostly in-place growth, a wide variety of organisms, among which algae are particularly important, create sources for carbonate grains of mud, sand, and gravel sizes. Shelf processes of the area have also produced intimate admixtures of the land and biogenically derived sediments. High-resolution profiles of the shelf sediments provide little evidence for recent tectonism despite the proximity of structures associated with the Mona Submarine Canyon and Puerto Rico Trench.

NEARSHORE AND COASTAL STUDIES

Resident time of flood sediment on insular shelf

The narrow high-energy insular shelf off the north coast of Puerto Rico is a natural laboratory for the study of shelf geologic processes because sediments there are in equilibrium with present processes rather than those of the past, as is true of most continental shelves. Here, J. V. A. Trumbull, K. A. Grove, and O. H.

Pilkey conducted repeated surveys of the great volumes of river mud and sand dumped on the shelf by the Rio de la Plata during Hurricanes David and Frederick in late 1979. They found that immediately after the floods, mud covered much of the shelf area near the river mouth in water depths of 5 to 55 m. A month later, all mud except that in topographic depressions had vanished seaward. Seven months after the flood, hardly a trace of river mud was found even in topographic depressions, and the normal distribution of biogenic and river-derived sand prevailed.

Evidence for a major pre-Wisconsin glacial event in New England

R. N. Oldale (USGS) and D. M. Eskenasy (Woods Hole Oceanographic Institution) propose a major pre-Wisconsin glacial event to account for the lower till on Nantucket Island, Mass. The till lies below fossiliferous marine beds of oxygen-isotope stage 5 (Sangamonian) age, and therefore is considered to be Illinoian in age, but on very tenuous evidence. The till, correlated to the lower till of New England, supports the view that the New England upper and lower tills represent two glaciations. The pre-Wisconsin lower till in New England may correlate with older tills elsewhere in the Northeastern United States and southeastern Canada that are considered to be early Wisconsin or older in age.

Giant involutions in the upper Wisconsin drift of Nantucket Island

R. N. Oldale has investigated pot-shaped involutions formed in the uppermost part of upper Wisconsin outwash on Nantucket Island. The giant involutions are roughly circular in plan and semicircular to bulbous in section. They range up to several meters in diameter and several meters deep. Cores consist of periglacial eolian silty sand and the involutions deform the adjacent and underlying outwash. Oldale speculates that the involutions are the result of collapse as ice (discontinuous ground ice or blocks of river ice) or snow, buried at shallow depths within the outwash, slowly melted away when the late Wisconsin climate warmed. The giant involutions may or may not be evidence of permafrost in southern New England during the Wisconsin glaciation.

Modern sedimentary environments and geologic history, Rhode Island inner shelf

The inner Continental Shelf to the south of Narragansett Bay, R.I., has a broad central depression bordered by shallow, irregular sea floor on the north and east and by a discontinuous curvilinear ridge on the south and west. Within this area, H. J. Knebel, S. W. Needell, and

C. J. O'Hara distinguish four sedimentary environments, each of which has a characteristic sea-floor relief that produces a recognizable pattern on sidescan sonar records. (1) Sea-floor exposures of crystalline rocks at isolated nearshore locations (water depths < 32 m) have pronounced irregular relief that produces blotchy patches. (2) Morainal deposits of a discontinuous offshore ridge to the north and east of Block Island have a hummocky relief and a cover of lag gravels and boulders that yield a predominantly black, strongly reflective pattern. (3) Bottoms around bedrock outcrops, on the flanks of morainal ridges, and atop bathymetric highs produce a mosaic of light and dark patches and lineations ascribable to areas of coarse sediments and mega-ripples that either have no detectable relief or form slight depressions (dark) and are surrounded by finer grained sea-floor sediments (light). (4) The smooth floor of the broad, central depression, where a peripheral belt of silty sand provides moderate tonality, and a central core of modern sandy silt that extends 16 km southward from West Passage, Narragansett Bay, produce practically no shading on the records. These four environments represent the sedimentation range from erosional or nondepositional (bedrock and morainal) through mixed (textural patchiness) to depositional (featureless sea floor).

In a related study, Needell, O'Hara, and Knebel have used recent closely spaced, high-resolution seismic reflection profiles (580 km) and sidescan sonographs (580 km) to make detailed geologic and shallow structure maps of Rhode Island Sound from eastern Narragansett Bay to Block Island and to gain information on the stratigraphic framework and late Mesozoic and Cenozoic history of the inner Continental Shelf off southern Rhode Island. The deepest observed acoustic reflector is a major erosional unconformity of late Tertiary to early Pleistocene age that defines a broad, fluvial, east-west oriented lowland. The lowland is bounded to the north by crystalline and consolidated sedimentary rocks of mostly pre-Mesozoic age and to the south by a deeply eroded cuesta composed of Coastal Plain and Continental Shelf rocks of Late Cretaceous and Tertiary age. Paleodrainage consisted of streams flowing generally southward over the crystalline bedrock and northward down the steep scarp of the cuesta, all tributary to a larger river that flowed westward to Block Island Sound. Massive to well stratified glacial drift overlies the erosional unconformity and is inferred to be mostly of late Wisconsin age and to correlate with till and proglacial outwash found elsewhere in southern New England. Following deglaciation of the inner shelf, streams from the retreating ice sheet cut into the glacial drift and older deposits and flowed south and southwestward to a major stream that drained westward to Block Island Sound.

In another study of the late Tertiary and Quaternary history of the region to the west, Needell and R. S. Lewis concluded that following deglaciation of the inner shelf and prior to the Holocene rise of sea level, Block Island Sound was the site of a proglacial lake which formed behind moraines to the south and drained through a water gap between Long Island and Block Island. The lake received water from streams that flowed southeast across the western side of the sound as well as from southwest- and west-flowing streams from the region to the east of Block Island. As the sea level rose, the stream valleys were partly filled by fluvial, freshwater peat, estuarine, and saltmarsh peat deposits as thick as 20 m. Transgressing seas eroded the shoreline and bottom and deposited marine sediments. Tidal currents continue to erode the sea floor in the western half of Block Island Sound.

In their study of Block Island Sound, Needell and Lewis traced the previously identified New Shoreham fault an additional 10 km northwestward, from the earlier landward limit of 16 km to 11 km south of Rhode Island. The fault, observed only within the offshore coastal plain strata, has a vertical offset of 15 m and, insofar as determined, does not affect submerged coastal plain surfaces. Needell and Lewis concluded that the fault became active after deposition of the Upper Cretaceous and lower Tertiary strata and that movement ceased prior to Pleistocene deposition of glacial drift.

Upper Quaternary stratigraphy of a south Texas barrier island complex

G. L. Shideler, D. E. Owen, T. M. Cronin, R. M. Flores, and C. W. Keighin used 7 cores, which are nearly continuous to depths of 60 m, well logs, and about 75 km of high resolution seismic reflection profiles to determine the upper Pleistocene to Holocene stratigraphic section and history of an area that includes southern Mustang Island, northern Laguna Madre, southern Corpus Christi Bay, and the adjacent Texas mainland. The Pleistocene-Holocene boundary is an unconformity of considerable relief. The thickness of the Holocene sediments therefore varies from 0 m on the mainland (Encinal Peninsula-Oso Bayshores) where the Pleistocene Beaumont Formation crops out, to 36 m within a pre-Holocene channel beneath southern Mustang Island. Within the late Pleistocene and Holocene interval, the Nueces River system underwent several episodes of channeling and valley infilling caused by glacio-eustatic changes of sea level. The oldest observed channeling appears to reflect a Wisconsin low stand of sea level. Younger channeling occurring within the Holocene section suggests discontinuous transgression with one or more minor stillstand or regressive

phases. The modern Mustang Island barrier apparently began to develop about 8,500 yr B.P.

Ostracode death assemblages (virtually all extant species) of the cores allowed recognition of five paleosalinity regimes/paleoenvironments: (1) limnic (0 to 0.5 ppt) freshwater/fluvial environment of freshwater and bay taxa; (2) oligohaline (0.5 to 5 ppt) upper-bay environment of freshwater and bay taxa; (3) mesohaline (5 to 18 ppt) mid-bay environment of bay taxa; (4) polyhaline (16 to 30 ppt) lower bay/inlet environment of mixed bay and marine taxa; and (5) euhaline (30 to 36 ppt) sublittoral environment of marine taxa. Vertical changes in ostracode assemblages of the cores indicate fluctuations in water salinity and depth that appear to reflect transgressive-regressive events of the glacio-eustatic record.

Lithologically, the cored section consists predominantly of alternate mud and sand layers and a few layers of molluscan shell gravel. The mud layers are multicolored and variably consolidated. Textural and petrographic characteristics of the sand units suggest the presence of at least two genetically distinct sand facies. Very fine grained sands having a low detrital matrix content (trace to 5 percent) represent barrier/strandplain deposits such as those that compose modern Mustang Island and the Pleistocene Ingleside sand body. In contrast, medium-grained sands having a relatively high detrital matrix content (average of 10 percent) appear to represent fluvial deposits of the ancestral Nueces River system. The detrital matrix of these sand facies appears to have come from the disaggregation of fine-grained rock fragments, as indicated by evidence of fragment deformation. The framework grains of the sand facies consist of a wide variety of components that include monocrystalline and polycrystalline quartz, orthoclase, microcline, plagioclase, and rock fragments (chert, limestone, siltstone, shale, and sandstone). Quartz ranges from 58 to 92 percent, feldspar from 1 to 22 percent, and rock fragments from 2 to 36 percent. The barrier/strandplain sand facies generally contains more quartz and less rock fragments than the fluvial sand facies. Cementing agents of both sand facies are rare. Observed calcite appears to be both allochthonous and authigenic. Varying amounts of gypsum and halite probably are late precipitates of pore-water evaporation that occurred during coring operations.

Rapidly migrating sand ridges and pulses of foreshore accretion

A. H. Sallenger, Jr., and B. M. Richmond measured sand ridges that had heights of less than 10 cm, had shore-normal lengths exceeding 10 m, and lay in the swash zone of a coarse-sand, high-energy beach on the California coast. These ridges formed in the seaward

part of the swash zone and migrated landward at rates of as much as 0.9 m/min. Migration was caused mostly by erosion on the seaward flank of each ridge and lesser amounts of accretion on the landward flank; thus, the ridges became smaller during migration. Migration of successive ridges resulted in pulses of net accretion in the upper swash zone. The time between pulses, which equaled the period of migration from the lower to the upper swash zone, was about 15 min. These small-scale ridges are similar, in some respects, to large-scale swash bars (ridge-and-runnel systems). Both features migrate landward through the swash zone and cause pulses of foreshore accretion. However, the accretionary pulses of the large-scale bars (or ridges) have periods of migration on the order of weeks, whereas those of the small-scale ridges described here are on the order of minutes.

Inner shelf textural and bathymetric irregularities, Monterey Bay, California

Using a small research vessel having a side-scan sonar system, R. E. Hunter, Jr., J. R. Dingle, R. J. Anima, and B. M. Richmond have surveyed the inner shelf of southern Monterey Bay during various seasons. This area is characterized in part by elongate patches of relatively coarse sand that trend parallel to the shore and lie as much as a meter below the surrounding finer grained sand. The coarse sand contains symmetrical ripples that are spread as much as a meter apart and must be products of storm waves. Changes in the pattern of the patches during the period of monitoring evidently occurred during winter storms. These unusual patches are restricted to a part of Monterey Bay where sand is mined commercially from the beach; it is not known whether or not a relation exists between mining and the unusual patches.

Pre-Flandrian sand sheet within Morro Bay, California

On the basis of underwater stratigraphic sampling within Morro Bay, Calif., and investigations of pre-Flandrian dune deposits adjacent to the Bay, R. L. Phillips and R. J. Anima confirmed preservation of pre-Flandrian subaerial dune deposits within the bay-fill stratigraphy. The subaerial sand sheet consists of oxidized and partially cemented large-scale crossbeds which are exposed underwater at depths of 3.6 to 5.6 m along the flanks of the main channel within the bay. They rest on older estuarine accretionary bank and tidal flat deposits. Identification of this stratigraphic horizon provides a datum to determine possible rates of coastal uplift and amounts of Holocene sedimentation since sea level reached its present position.

The temporal scale of disturbance in estuarine benthic communities

F. H. Nichols examined data on long-term (multiyear) patterns in estuarine benthos and concluded that year to year variations in species composition and abundance are commonly greater than seasonal variations. The variations include large fluctuations in the abundance of the numerically dominant species, which results in major shifts in dominance among species, and the apparent disappearance of other species. Large fluctuations over periods of several years, suggestive of instability, reflect the combined effects of varying recruitment patterns and intermittent natural or man-induced disturbances of the physical/chemical environment. The implications of such patterns are that within a habitat (for example, intertidal mudflat) the community is routinely in the process of recovery from a previous disturbance and that appreciation of community structure during any given year requires knowledge of the developmental history of that community. The few continuous records of more than 5 years, on the other hand, demonstrate the cyclic nature of structural variations and thus provide support for the view that in general estuarine benthic communities are highly resilient.

ESTUARINE AND COASTAL HYDROLOGY

Riverine-estuarine process

The U.S. Geological Survey is presently conducting a comprehensive interdisciplinary study of the San Francisco Bay estuarine system. The broad goals of this study are to understand processes and rates by which water, solutes, sediments, and organisms interact and to develop and verify conceptual and numerical models of these interactions. Evaluation of these interactions requires a basic understanding of the water circulation and mixing. Quantification of important sources, sinks of various chemical and biological constituents, and determination of the relative importance of river inflow, wind, and tides as transport and mixing mechanisms has begun. The data-collection program is carefully designed to provide data required for development of conceptual and numerical models. Near-monthly surveys of hydrographic properties in the main channels have been extended to include coverage in the broad shoal areas, where current meters are used to measure long-term circulations in the bay system. Recently, the USGS initiated collaboration with the National Ocean Survey/National Oceanographic and Atmospheric Administration in a systematic current-measurement program that is expected to increase the data base of the USGS hydrodynamic observations.

The Lagrangian residual circulation is being studied

whereby the tidal circulation is first computed in a conventional Eulerian way, then the Lagrangian residual circulation is determined by a method similar to the method of markers and cells. Application of this approach, by R. T. Cheng, to south San Francisco Bay (South Bay), Calif., shows that estimation of the Lagrangian residual circulation from Eulerian data may lead to unacceptable error, particularly in a tidal estuary where the tidal excursion is of the same order magnitude as the length scale of the basin.

Selected physical processes in the subtidal time range were studied by R. A. Walters who used sea-level and current-meter data from south San Francisco Bay. These data were filtered by a low-pass digital filter that removed tidal period variations; the data then were subjected to an empirical orthogonal function analysis. For the sea-level data, there is one dominant empirical mode that is correlated with nonlocal coastal forcing. A small amount of the variance is associated with local wind set-up. For the current-meter data, there are two dominant empirical modes that correlate with local wind forcing and tidal forcing over the spring neap cycle. In general, South Bay is dominated by wind and tidal forcing on the residual currents during the summer.

Continuing analysis of sea level- and current-meter data for the northern portion of San Francisco Bay shows a variety of phenomena related to nonlocal coastal forcing and local nonlinear tidal forcing. The northern reach is a partially mixed estuary that responds to low frequency forcing in a different manner than South Bay does. The low-frequency variations in sea level are dominated by nonlocal variations in the coastal sea level and also show a smaller influence of tidally induced fortnightly sea-level variations. The low frequency currents demonstrate a gravitational circulation which is modified by wave drift and changes in eddy viscosity over a spring neap-tidal cycle and by changes in freshwater outflow. Transients in freshwater outflow induce internal oscillations that last two to four days.

The USGS's understanding of estuarine and riverine processes has been improved by the simultaneous and continuous measurement of several physical, chemical, and biological parameters (salinity, temperature, turbidity, chlorophyll fluorescence, dissolved oxygen, pH, pCO₂, nitrate, nitrite, ammonia, phosphate, and silicate) both laterally and with depth. L. E. Schemel, D. D. Harmon, and others see broad estuarywide variations in these parameters as well as large variations occurring over short lateral distances of 100 m or less and to depths of a few meters. Many of these variations could not be adequately described by conventional discrete-sample and analysis techniques.

J. E. Cloern found that reduced freshwater inflow during the drought of 1976-77 had a significant impact on

the biomass and species composition of phytoplankton in the northern San Francisco Bay estuary. During subsequent years of "normal" hydrologic conditions, the estuary experienced spring and summer blooms of diatoms. Population growth of diatoms appeared to be a consequence of two interacting factors: (1) physical accumulation of dense suspended particles (including diatoms) by estuarine circulation, and (2) location of this suspended-particle maximum adjacent to shallow areas where light availability permitted cell division. During 1976 and 1977, river discharge was so low that the suspended-particle maximum was located upstream, away from the productive shallows. Population growth of diatoms did not occur, and the phytoplankton community was dominated year-round by relatively small numbers of microflagellates. The loss of diatom productivity during periods of low freshwater inflow may have important trophic-dynamic implications.

Numerical simulation experiments by D. H. Peterson, USGS, and John Festa, National Oceanographic and Atmospheric Administration, of simple light-driven phytoplankton productivity models suggest that, in some partially- to well-mixed estuaries having adequate light penetration (moderate suspended particulate matter concentrations and shallow depths), it may be a relative advantage for phytoplankton to sink. Species that sink may increase their concentration and form a phytoplankton maximum in a similar mechanical way which maintains the turbidity maximum but does not necessarily maintain it in the same location. In estuaries, or during extended periods of severe light attenuation, however, sinking species may have more difficulty in maintaining their population than nonsinking species. Field observations from San Francisco Bay appear to follow these numerical results. A related complication which needs to be considered is phytoplankton shade adaptation.

Saltwater movement in the coastal areas

An analysis of the records from chloride-monitor wells in the Chicot aquifer of southwestern Louisiana shows that there is little indication of saltwater encroachment in the coastal area; however, some inland saltwater mounds are growing, according to studies concluded by D. J. Nyman.

Chloride concentrations in the "upper sand unit" of the Chicot aquifer southeast of Lake Charles, increased about 20 mg/L per year from 1963, when records began, until 1975. Water levels in the area leveled off around 1972, following a period of declines averaging about 0.3 m per year.

Local occurrences of saltwater in isolated inland areas have resulted from openings in aquitards separating overlying freshwater sands from underlying saltwater

sands in combination with upward gradients caused by pumping from the upper aquifers. An occurrence of this nature has been mapped in the "500-foot" sand of the Lake Charles industrial area, where chlorides increased 20 mg/L per year from 1970 to 1976 following water-level declines of about 2.4 m/yr from 1967 to 1970. Recently, chloride concentrations have been decreasing and water levels have been rising.

Present and future urban development in the coastal parts of the Manasota and lower Peace Basins in southwestern Florida depends largely on the availability of a satisfactory water supply. The Floridan aquifer is a regionally extensive Tertiary carbonate geohydrologic system that contains water of variable quality in the 5,400-km² area of interest. W. C. Steinkampf sampled 23 sites, the data from which show that water quality deteriorates to the south and west, grading from a fresh calcium-magnesium-bicarbonate-sulfate type water to a very saline sodium-magnesium-chloride type water downgradient. Mixing of fresh and saline waters largely accounts for observed relative dissolved-species concentrations and distributions and observed water types. The relative effect of these and additional factors on observed water quality depends on the location of the water in the flow system.

C. B. Hutchinson is evaluating the factors controlling interflow of freshwater and saltwater between the 990-km² Tampa Bay and the underlying Floridan aquifer. The study focuses on general areas in Tampa Bay where saltwater from the bay is leaking into the Floridan aquifer and where freshwater from the Floridan aquifer is leaking upward into the bay. A computer model of ground-water flow was developed to evaluate the increases in interflow between the bay and aquifer that may result from widening and deepening the shipping channels, an action proposed as part of Tampa's harbor-improvement project.

Bay-aquifer interconnection decreases from north to south. In the north, the top of the Floridan aquifer is generally less than 12 m below bay level and is separated from the bay by a 8-m-thick layer of sand and clay. In the south, the aquifer is about 100 m below bay level and is overlain by a 80-m-thick layer of sand, clay, and limestone. The potentiometric surface of the Floridan aquifer is expected to rise as much as 0.5 to 0.9 m at the eastern end of the Alafia River channel in response to a net increase of 0.6 m³/s in downward leakage of saltwater in the vicinity of the dredged ship channel. Total impact of proposed channelization upon bay-aquifer interconnection is expected to be small.

Seawater entering through subterranean conduits is the source of saltwater in the Cano Tiburones area, northern P.R. The Cano, a reclaimed swamp, includes about 2,430 hm² of prime land targeted for rice cultivation. A study by A. L. Zack to determine the feasibility

of restoring freshwater in the Cano area was begun in 1980 in cooperation with the Puerto Rico Department of Agriculture. Results indicate that ground water below the Cano does not contribute to surface salinities. The salinity of organic soils is derived from seawater springs, and their control has allowed the system to become fresher. Water from some canals can now be used for irrigation.

Growth of estuarine-fouling organisms in Loxahatchee River estuary, Florida

B. F. McPherson and W. H. Sonntag measured the monthly settlement and growth of estuarine-fouling organisms on test panels at eight locations in the Loxahatchee River estuary, southeastern Florida, in 1981. Average growth ranged from 22 g/m² dry weight in January to 684 g/m² in September and ranged from 8 to 14 percent organic material. Growth was suppressed in August by low salinities (less than 10 parts per thousand in much of the estuary) from large freshwater discharges associated with Tropical Storm Dennis on August 18. Maximum growth occurred the following month, probably because of high temperatures and high nutrient loading associated with the storm and subsequent rainfall runoff.

Barnacles were dominant on the panels, followed by hydroids, bryozoans, and colonial ascidians. Barnacles settled throughout the year, in greatest numbers (sometimes exceeding 40,000/m²) during summer. Settlement of hydroids occurred throughout the year, whereas bryozoans settled mostly during winter and ascidians during spring and summer. Serpulid polychaetes dominated at the low salinity, upstream location.

The fouling community growing under natural conditions on bridge pilings and seawalls was dominated by barnacles and bivalve mollusks. Patterns of distribution for species of barnacles correlated with patterns of salinity. The maximum biomass of the fouling community ranged from 3,684 to 7,600 g/m² dry weight, of which 5 percent was organic. The lower percentage of organic material in this older community than that on the test panels is attributed to the proportionately greater buildup of calcium carbonate shell material in the older community.

Time-of-water sampling in tidal-affected chloride monitor well in west-central Florida

During an areal study of coastal Citrus, Hernando, and Levy Counties, Fla., J. D. Fretwell observed a wide range in specific conductance values during bimonthly sampling of a well. The well, located 3.7 km from the coastline, is one of a network of wells used to monitor saltwater movement along the gulf coast. Variations appeared to be random but ranged from 612 to 9,500 μ mho. A continuous-recording monitor was placed on the well in November 1980 to define the nature of the variations in specific conductance. Specific conductance and temperature were recorded at 30-minute intervals for a 10-day period. Results of the study showed that sharp peaks in specific conductance occurred in the well shortly after high tide and returned to a base level soon thereafter. Time-of-sampling relative to the phase of the tide is critical to understanding the relation of chloride concentrations in the well to long-term movement of the saltwater-freshwater interface.

MANAGEMENT OF NATURAL RESOURCES ON FEDERAL AND INDIAN LANDS

The Conservation Division¹ of the U.S. Geological Survey is responsible for carrying out the role of classifying leasable mineral and potential water-resources development sites on Federal lands and managing the exploration and development of leasable minerals on Federal and Indian lands, including the Outer Continental Shelf. Primary functions are (1) classification and evaluation of Federal mineral lands for multiple-use management and for leasing, (2) delineation and preservation of potential public-land reservoir and water-power sites, (3) promotion of orderly exploratory development, conservation, and proper use of mineral resources on Federal lands under lease, (4) supervision of mineral operations to assure protection of the environment, the realization of a fair value from the sale of leases, and satisfactory royalty collection on mineral production, and (5) cooperation with other agencies in the management of Federal mineral and water resources.

CLASSIFICATION AND EVALUATION OF MINERAL LANDS

The Organic Act creating the USGS gave the Director the responsibility of classifying and evaluating the mineral resources of public-domain lands. There are about 9 million ha of land for which estimates of the magnitude of leasable mineral occurrences only partially have been made. Such appraisals are needed for multiple-use planning by Federal land managers and for leasing by the BLM. Estimates are based on existing data. When additional data are required, field studies and spot checks must be undertaken. Guidelines are prepared from time to time by the USGS to assure uniform executive action in the classification of leasable minerals on Federal lands.

CLASSIFIED LAND

With the passage of the Federal Land Policy and Management Act of 1976, numerous changes occurred

¹Secretarial Order No. 3071, dated January 19, 1982, established the Minerals Management Service to exercise the responsibilities of the Conservation Division, USGS.

in the classification program. For example, classification for retention of mineral rights is no longer appropriate. Also, fair market value is required for exchanges and conveyances of mineral rights.

The following classification responsibilities still remain: (1) to identify competitive leasing areas for leasable minerals, (2) to inventory leasable mineral resources, (3) to furnish the Federal land-managing agencies with adequate leasable-mineral data on Federal lands for land-use planning and multiple-use or best-use decisions, and (4) to furnish Congress and other Federal agencies leasable-mineral data on the Federal lands being considered for withdrawal by congressional or executive action.

As a result of USGS investigations, large areas of Federal land have been formally classified as mineral land. At the end of FY 1981, more than 284,223 ha of land had been formally classified and about 1,090,262 ha had been designated prospectively valuable for a leasable mineral, as shown in the following table:

Lands classified

Commodity	During FY 1981		Total at end of FY 1981	
	Formally classified (hectares)	Prospectively valuable (hectares)	Formally classified (hectares)	Prospectively valuable (hectares)
Asphalt minerals -----	0	0	0	0
Coal -----	4,306	0	9,107,765	142,040,102
Geothermal resources -----	0	4,662	0	41,866,764
Oil and gas -----	0	0	1,714	595,321,498
Oil shale -----	265,398	1,090,262	265,398	6,449,449
Phosphate -----	0	0	59,764	4,096,716
Potassium and sodium -----	14,519	0	283,574	95,303,526

Hydrology of Federal coal lands in eastern National Forest areas

The most abundant and available Federal coal reserves in the Eastern United States are found in areas in and near the National Forests. The National Forest areas in this part of the country offering the greatest potential for coal development are the Daniel Boone in Kentucky and Tennessee, Hoosier in Indiana, Jefferson in Virginia, Monongahela in West Virginia, Shawnee in Illinois, and Wayne in Ohio. David Grason has made an evaluation of the available data and references relevant

to coal mining and the water resources of these areas and has identified unfilled information needs. Three such needs common to all six National Forest areas are for (1) numerical simulation of streamflow, water-quality, and sedimentation characteristics, (2) information related to ground-water availability, movement, and quality before, during, and after mining, and (3) a hydrologic reconnaissance of all major lakes and impoundments within the prospective Federal-coal leasing area. Grason proposes that a coordinated program of investigations to fill these and other hydrologic information needs be conducted by the USGS over a 6-yr period. In this proposed program, the application of sophisticated analytical and interpretive techniques is to be preceded by a potentially more demanding effort to gather and prepare the proper hydrologic data.

KNOWN GEOLOGIC STRUCTURES OF PRODUCING OIL AND GAS FIELDS

Under the provisions of the Mineral Leasing Act of 1920, as amended, the Secretary of the Interior is authorized to grant to any qualified applicant a noncompetitive lease to prospect for oil and gas unless the Federal mineral estate is within a Known Geologic Structure (KGS) of a producing oil and gas field. Lands within a KGS must be competitively leased to the highest qualified bidder. During FY 1981, 327,786 ha of onshore Federal land were classified as KGS lands, either as a new KGS or as additions to a previously established KGS. The total area at the end of FY 1981 was over 9.2 million ha. The KGS's are summarized in the table "Known Geologic Structures for FY 1981."

KNOWN GEOTHERMAL RESOURCE AREAS

The Geothermal Steam Act of 1970 provides for development by private industry of federally owned geothermal resources through competitive and noncompetitive leasing. Those areas that are determined to be within Known Geothermal Resource Areas (KGRA's) must be leased competitively. On September 30, 1981, there were 107 KGRA's that contained 2,758,574.52 acres of public lands under lease. The results of lease sales held in FY 1981 are summarized in the table "KGRA Lease Sales in FY 1981."

KNOWN RECOVERABLE COAL RESOURCE AREAS

The Federal Coal Leasing Amendments Act of 1976 provides for the development of federally owned coal lands by private industry through competitive leasing

Known Geologic Structures (in acres) for FY 1981

	End of FY 1980 (9/30/80)	Added In FY 1981 No. of actions are in parentheses	End of FY 1981 (9/30/81)
Alabama -----	22,105	6,444(2)	28,549
Alaska -----	146,064	0	146,064
Arizona -----	7,677	0	7,677
Arkansas -----	336,895	1,280(1)	340,735
California -----	444,847	360(1)	524,983
Colorado -----	1,195,925	122,303(110)	1,135,203
Florida -----	160	0	160
Illinois -----	510	720(2)	1,230
Indiana -----	820	4,760(2)	5,580
Kansas -----	2,734,872	160(1)	2,735,032
Kentucky -----	25,551	602(2)	26,153
Louisiana -----	858,559	2(1)	858,561
Maryland -----	2,380	0	2,380
Michigan -----	73,030	120(3)	73,150
Mississippi -----	91,096	2,160(4)	93,256
Montana -----	2,550,569	80,604(68)	1,593,481
Nebraska -----	27,397	440(2)	27,837
Nevada -----	6,520	0	6,520
New Mexico -----	4,758,151	147,524(185)	4,905,675
North Dakota -----	353,856	57,726(77)	411,582
Ohio -----	243,297	16,703(6)	260,000
Oklahoma -----	3,990,068	25,515(6)	4,015,583
Pennsylvania -----	11,168	16,700(1)	27,868
South Dakota -----	21,877	7,685(7)	29,562
East Texas -----	126,863	9,601(3)	136,464
West Texas -----	46,217	0	46,217
Utah -----	1,332,664	113,944(30)	1,446,608
Virginia -----	2,120	0	2,120
West Virginia -----	83,603	0	83,603
Wyoming -----	2,436,532	194,641(249)	2,631,173
Totals -----	21,931,393	809,994	21,603,006

KGRA Lease Sales in FY 1981

Sale date (Total sales, \$)	State	Tracts offered	Acres offered	Tracts leased	Acres leased	Total accepted high bids
10/23/80	Oregon	2	4,926.46	2	2,360.00	\$ 249,617.20
12/10/80	California	1	10.26	1	10.26	45,176.11
08/26/81	New Mexico	21	31,015.63	9	13,835.36	102,251.79
09/15/81	California	28	60,862.78	21	45,097.08	6,797,885.04
09/29/81	Nevada	39	78,391.93	8	15,304.16	59,874.53
09/29/81	California	5	11,679.48	5	11,679.48	29,805.11
Total		96	186,886.54	46	88,286.34	7,284,609.78

and authorizes the Secretary of the Interior to designate Known Recoverable Coal Resource Areas (KRCRA). During FY 1981, 4,306 ha of coal land was classified KRCRA's or added to existing ones. The total at the end of FY 1981 was 9,107,765 ha.

KNOWN LEASING AREAS FOR SODIUM AND OIL SHALE

During FY 1981, known sodium leasing areas were increased by 14,519 ha, for a total of 295,464 ha. Known oil shale leasing areas were established on 265,398 ha.

WATERPOWER CLASSIFICATION— PRESERVATION OF RESOURCE SITES

Suitable sites for water-resource development are valuable natural resources. The waterpower classification program is conducted to identify, evaluate, and protect from disposal and injurious uses those Federal lands located in sites having significant potential for future development. USGS engineers review maps, aerial photographs, and streamflow records to determine potential dam and reservoir sites. Topographic, engineering, and geologic studies are made of the identified sites to determine whether or not the potential value warrants formal classification of the affected Federal lands. These resource studies provide the land-administering agencies and others with information that is basic to management decisions and effective land-use planning. Previous classifications are reviewed as additional data become available and as funds permit. If the sites are no longer considered suitable for development, revocation of the classification of the affected Federal lands is recommended. If the lands are not reserved for other purposes, they are returned to the unencumbered public domain for possible disposition or other use.

To assure consideration of potential reservoir and waterpower sites in the preparation of land-use plans, information concerning such sites was furnished to the BLM and the USFS for several planning units in the Western States and Alaska.

MANAGEMENT OF MINERAL LEASES ON FEDERAL AND INDIAN LANDS

Supervision of competitive and noncompetitive leases for the development and recovery of leasable minerals in deposits on Federal and Indian lands is a function of the USGS, delegated by the Secretary of the Interior. For leases offered competitively, the USGS advises BLM as

to the appropriateness of the high bid in determining if fair market value would be returned from the lease. Also included is the responsibility for the evaluation of mineral resources on tracts of Federal lands that are offered for exchange. The USGS function includes geologic and engineering examination of applied-for lands to determine whether or not a lease or a permit is appropriately applicable, approval of operating plans, inspection of operations to insure compliance with regulations and approved methods, and verifications of production and the collection of royalties (see table 1).

Before recommending approval of a lease or a permit, USGS engineers, geologists, and environmental scientists consider its possible effects on the environment. Of major concern are the esthetic value of scenic and historic sites, the preservation of fish and wildlife and their breeding areas, and the prevention of land erosion, flooding, air pollution, and the release of toxic chemicals and dangerous materials. Consideration also is given to the amount and kind of mining-land reclamation that will be required.

General coal lease sales for FY 1981

Coal lease sales were held in three regions during FY 1981 (see following table). The total acres sold were 50,943. Bids on 24 tracts were accepted for bonus bids totaling \$27,550,090. The highest bonus bid was \$3,150 per acre for 3,347.31 acres in the Cottonwood tract in the Uinta-SW Utah sale.

Leasing regions	Dates	Tracts	Total bonus	Total acres
Green River-Hams Fork region, Colorado-Wyoming	01/13/81	9	\$12,545,575	22,829
	01/14/81			
	04/30/81			
	10/28/81			
Southern Appalachian Alabama subregion	06/25/81 12/16/81	10	804,105	17,259
Uinta-SW Utah	07/30/81	5	14,200,410	10,855
Totals		24	27,550,090	50,943

TABLE 1.—Mineral production, value, and royalty for FY 1981
[All minerals except petroleum products; includes coal, potassium, sodium minerals, and so forth.]

Lands	Oil (tonnes)	Gas (cubic meters)	Gas liquids (liters)	Other (tonnes)	Value	Royalty
Public	19,281,193	29,658,564,143	908,574,485	96,555,416	\$ 8,018,496,726	\$ 825,957,319
Acquired	1,793,567	739,565,302	29,845,308	985,321	689,870,408	72,590,097
Indian	3,083,567	3,420,663,995	118,788,561	27,427,811	1,297,248,719	157,001,481
Military	24,099	337,720,361	31,364,667		22,129,553	3,613,758
Outer Continental Shelf	38,885,727	138,180,135,451	7,057,992		18,782,220,126	3,059,436,796
Total	63,068,153	172,336,649,252	1,095,631,013	124,968,548	28,809,965,532	4,118,599,451

Onshore oil and gas lease sales

During FY 1981, there were 19 sales of Known Geological Structure (KGS) lands, the same as the previous fiscal year. However, the increase in revenue was outstanding (\$111,678,579 compared to \$38,653,493 in fiscal year 1980). Average per acre income increased from \$384 in FY 1980 to \$1,031 in FY 1981. The number of acres sold increased to 485,886 from 399,761 the previous year. The significant increase in sales income reflects the positive efforts of Interior Department personnel to keep pace with industry's search for oil and gas. Onshore oil and gas lease sales during FY 1981 are listed in the following table:

Onshore oil and gas lease sales during FY 1981
FEDERAL LANDS

Sale date	State	Number of tracts offered	Acres offered	Number of tracts	Acres sold	Total accepted high bids
11/05/80	Wyoming	25	8,106.95	25	8,106.95	\$ 1,396,063.97
11/19/80	Montana	12	1,157.46	12	1,157.46	142,416.20
11/26/80	Miss., La., Ark.	8	626.05	8	626.05	886,924.98
12/10/80	Wyoming	36	5,523.50	36	5,523.50	428,669.24
12/16/80	N. Mex., Okla.	63	14,363.70	62	14,281.95	15,190,447.64
01/22/81	Arkansas	60	24,876.13	60	24,876.13	43,021,598.44
04/05/81	Ky., Mich., Va.	4	747.83	2	522.00	340,571.64
02/11/81	Wyoming	16	2,130.40	16	2,130.40	952,638.04
02/24/81	N. Mex., Okla.	40	7,338.85	40	7,258.83	4,472,933.74
03/11/81	Wyoming	30	4,760.50	28	3,800.50	1,321,497.11
04/09/81	Mich., Ohio, Ark., La.	19	1,147.49	19	1,147.49	140,744.92
04/21/81	N. Mex., Okla.	38	9,396.20	35	8,316.20	12,799,195.39
05/06/81	Mont., N. Dak.	13	2,188.46	13	2,188.46	952,555.86
06/10/81	Wyoming	34	6,410.97	33	5,790.41	1,917,959.61
06/23/81	N. Mex., Okla., Tex.	28	3,832.06	26	2,362.74	2,072,657.60
07/30/81	Mich., Alaska, Ky.	31	6,320.34	28	5,320.00	1,318,722.87
08/18/81	Utah	24	7,787.95	22	7,547.89	2,031,525.81
08/26/81	New Mexico	22	3,795.23	22	3,785.06	4,859,357.77
09/16/81	Wyoming	22	3,364.48	21	3,288.48	1,233,999.00
09/16/81	Kansas	2	200.00	2	200.00	7,821.20
Total		527	114,074.55	510	108,230.50	\$95,488,301.03

There were 24 sales of oil and gas leases on Indian land during FY 1981, compared to 26 in FY 1980. These sales resulted in the leasing of 485,886 acres for \$119,789,378, nearly four times greater than the revenue received during FY 1980. The following table is a summary of Indian land lease sales during FY 1981:

Onshore oil and gas lease sales during FY 1981
INDIAN LANDS

Sale date	State	Number of tracts offered	Acres offered	Number of tracts	Acres sold	Total accepted high bids
10/14/80	Oklahoma	76	3,470.50	24	1,019.58	\$ 143,015.31
10/14/80	Oklahoma	274	23,513.51	94	7,792.02	3,173,768.75
10/21/80	Wyoming	138	76,075.41	90	47,361.94	3,759,677.30
10/29/80	Oklahoma	31	2,656.38	14	1,093.88	486,150.00
12/02/80	Oklahoma	12	1,374.03	9	921.95	188,889.00
12/16/80	Montana	397	72,294.75	364	66,810.32	11,702,821.31
01/13/81	Oklahoma	20	1,711.07	20	1,711.07	1,421,927.50
01/13/81	Oklahoma	83	3,846.71	37	2,474.78	153,151.35
03/24/81	Oklahoma	308	15,917.48	113	4,462.55	714,412.88
03/25/81	Oklahoma	32	3,305.32	18	1,777.12	1,880,866.25
03/26/81	Oklahoma	516	28,392.58	227	11,229.70	23,735,984.00
03/27/81	Oklahoma	115	7,109.95	48	3,258.91	257,037.48
04/13/81	Florida	336	76,800.00	336	76,800.00	751,844.80
04/14/81	Oklahoma	95	4,681.87	61	3,084.96	397,974.78
06/24/81	Oklahoma	414	33,037.61	158	10,894.52	23,900,789.50
06/25/81						
07/09/81	Oklahoma	68	3,709.24	28	2,253.67	2,644,449.89
07/14/81	Oklahoma	84	5,815.00	35	2,213.02	248,040.23
07/15/81	Montana	500	112,878.95	268	59,903.09	2,987,797.95
07/23/81	Montana	472	61,417.52	365	49,264.07	733,856.96
07/27/81	N. Dakota	106	12,496.33	92	9,464.30	190,939.69
08/11/81	California	7	377.13	6	297.13	30,299.33
08/24/81	Wyoming	346	134,301.66	259	105,358.62	5,695,412.05
08/27/81	Oklahoma	210	12,208.73	76	4,393.42	625,332.11
09/01/81	Oklahoma	438	32,308.04	219	11,955.33	34,054,930.00
Total		5,078	729,699.77	2,961	485,885.95	\$119,879,379.42

MANAGEMENT OF OIL AND GAS LEASES ON THE OUTER CONTINENTAL SHELF

The Outer Continental Shelf (OCS) Lands Act of 1953 authorizes the Secretary of the Interior to issue oil and gas leases on a competitive basis in the submerged lands of the OCS. The functions of the USGS, delegated by the Secretary of the Interior, include (1) participation in tract selection and evaluation to insure orderly resource development, protection of the marine environment, and receipt of a fair market value, (2) review and approval or disapproval of proposed exploration plans and development and production plans, (3) inspection of operations to insure compliance with regulations and approved methods, and (4) verification of the amount and value of production and the assessment and collection of rentals and royalties.

The Outer Continental Shelf Lands Act Amendments of 1978 provided the Secretary of the Interior with policy guidance for administration of the leasing provisions of the amended Act and provided an additional enforcement tool in the form of civil penalties. The USGS administers the civil penalties that are assessable for any failure to comply with any provisions of the Act, any term of a lease, license, or permit issued under the Act, or any regulation or order under the Act. USGS

TABLE 2.—OCS oil and gas lease sales for FY 1981

[Figures for leased lands include only those not in litigation. FNPS=Fixed Net Profit Share.]

Area and date	Tracts offered	Acreage	Tracts leased	Acreage	Total bonus accepted
Gulf of Alaska 10/21/80					
Total	210	1,195,569	35	199,262	\$ 109,751,073
1/6 royalty	90	512,387	16	91,091	53,213,147
Sliding scale	32	182,182	3	17,080	579,000
FNPS	88	501,100	16	91,091	55,958,926
Western Gulf of Mexico 11/18/80					
Total	81	458,308	67	383,323	1,417,961,511
1/6 royalty	38	210,628	29	164,443	463,017,160
1/3 royalty	11	63,360	8	46,080	204,983,920
Sliding scale	10	57,600	10	57,600	533,326,280
FNPS	22	126,720	20	115,200	216,634,151
Central California 5/28/81					
Total	111	603,613	55	292,101	2,036,954,089
1/6 royalty	59	325,367	33	177,344	1,681,176,944
1/3 royalty	16	83,505	3	16,800	53,880,400
Sliding scale	36	194,741	19	97,957	301,896,745
Gulf of Alaska 6/30/81					
Total	175	996,307	1	5,693	170,496
1/6 royalty	74	421,296	1	5,693	170,496
Sliding scale	29	166,102	0	0	0
FNPS	72	409,909	0	0	0
Central and western Gulf of Mexico 7/21/81					
Total	212	1,077,914	156	799,899	2,649,628,752
1/6 royalty	188	939,674	138	696,219	2,414,892,336
FNPS	24	138,240	18	103,680	234,736,416
South Atlantic 8/4/81					
Total	285	1,622,557	47	267,580	342,766,174
1/6 royalty	104	592,091	0	0	0
1/8 royalty	85	483,921	33	187,875	329,417,000
FNPS	96	546,545	14	79,705	13,349,174
Lower Cook Inlet 9/29/81					
Total	153	858,246	13	73,157	4,405,899
1/6 royalty	104	586,998	6	33,305	3,240,075
FNPS	49	271,248	7	39,852	1,165,824

review and approval of proposed exploration plans and development and production plans also must assure compliance with the new statutory requirement to use the best available and safest technologies on all new drilling and production activities.

Outer Continental Shelf lease sales for oil and gas

Seven Outer Continental Shelf (OCS) oil and gas lease sales were held in FY 1981. Sales were held for leases in the Gulf of Mexico in November 1980 and July 1981, Lower Cook Inlet in September 1981, in the Gulf of Alaska in October 1980 and June 1981, in central California in May 1981, and in the South Atlantic in August 1981.

A summary of the results of these individual lease sales is presented in table 2. For these sales 1,227 tracts totaling 6.8 million acres were offered for lease. High

bids of \$6,561 billion were accepted on 374 tracts totaling 2 million acres that were offered for lease. For the entire Federal OCS, through FY 1981, 10,209 tracts totaling 48.03 million acres were offered for lease. High bids of \$33.78 billion were accepted on 4,197 tracts totaling 20.2 million acres.

COOPERATION WITH OTHER FEDERAL AGENCIES

The USGS acts as consultant to other Federal agencies in land-disposal cases. The USGS determines, in response to the agencies' requests, the mineral character and water-resource development potential of specific tracts of Federal land under their supervision that are proposed for sale, exchange, or other disposal. About 900 such reports were made during FY 1981.

GEOLOGIC AND HYDROLOGIC PRINCIPLES, PROCESSES, AND TECHNIQUES

GEOPHYSICS

ROCK MAGNETISM

Limits to northward drift of the Paleocene Cantwell Basin, central Alaska

The Cantwell Basin in the central Alaska Range contains continental sedimentary rocks and calcalkaline volcanic rocks that were deposited during the Paleocene. Paleomagnetic results obtained by J. W. Hillhouse and C. S. Grommé from 18 lava flows within the Teklanika Formation of Gilbert and others (1976) yield an inferred paleolatitude of 83°N. with confidence limits of 9.7°. A positive fold test suggests that the magnetic directions, which are of reversed polarity, were acquired during initial cooling of the lavas. No significant difference was found between the observed magnetic latitude of the Teklanika and the expected latitude that is calculated from coeval North American reference poles. Therefore, tectonostratigraphic terranes north of the Denali Fault have apparently undergone little or no northward drift relative to the craton since the Paleocene. Whether this constraint applies to terranes south of the fault, such as Wrangellia and the northeastern Alaska Peninsula, depends on the relationship of early Tertiary igneous rocks of the southern terranes with volcanic rocks of the Cantwell Basin. If these suites of volcanic and plutonic rocks are cogenetic, then results indicate that Wrangellia and the Peninsular terrane, which show evidence of thousands of kilometers of northward drift in post-Jurassic time, have not drifted north significantly since the Paleocene.

Paleointensity study of the Steens Mountain, Oregon polarity transition

A detailed record of a Miocene reversal of geomagnetic polarity has been recorded in a sequence of lava flows exposed on Steens Mountain, Oregon. Paleomagnetic samples have been obtained from a stratigraphic thickness of nearly 600 m of lava flows spanning this transition. Variation of geomagnetic intensity during this transition has been investigated by E. A. Mankinen

and C. S. Grommé (USGS), Michel Prévot (University of Paris), and R. S. Coe (University of California, Santa Cruz) by using the Thelliers method of paleointensity determination. Results of this study show that geomagnetic intensities below 0.1 gauss were recorded by lava flows spanning a thickness of approximately 200 m and that a minimum of 0.04 gauss was reached during part of the transition. It was also found that little variation of intensity occurred during the transition except during one period when the intensity briefly increased to 0.3 gauss. The virtual geomagnetic pole (VGP) returned to a high latitude at the same time, which therefore appears to have been an aborted attempt to reestablish the geomagnetic dipole. Normal geomagnetic intensity variations began as soon as all transitional changes in direction had been completed.

Paleomagnetic evidence for structural development of the Latir volcanic field, New Mexico

A paleomagnetic study of the Latir volcanic field was undertaken by J. T. Hagstrum, in collaboration with P. W. Lipman, to obtain information on the structural orientation of its eruptive and intrusive units and to employ the magnetic directions for an evaluation of the tectonic and igneous history of the Questa caldera and the enclosing volcanic field.

The middle Tertiary Latir volcanic field in northern New Mexico comprises intermediate-composition volcanics overlain by a regional ash-flow sheet and associated lavas of rhyolitic composition that are all cut by silicic-alkalic granitic intrusives. Deeply exposed along the eastern flank of the Rio Grande rift, the silicic extrusive and intrusive rocks all yield radiometric ages of about 23 m.y. Mineralization by hydrothermal fluids derived from the silicic magma subsequently produced base- and precious-metal fissure deposits and large low-grade molybdenite orebodies. Flow banding and eutaxitic structures within the extrusive units indicate intense structural deformation, which for the most part increases toward the Questa caldera.

Radiometric ages and paleomagnetic data indicate that an episode of pronounced extension coincided with a major pulse of igneous activity in the region 23 m.y.

ago. Eastward tilting of the volcanic units appears to have been closely followed by caldera collapse and then by resurgent doming of the caldera. Welded tuff units within the caldera were turned on end, and together with older volcanic units were incorporated into a collapse megabreccia.

The megabreccia and other nearby units were partially or entirely overprinted by a thermochemical aureole associated with the resurgent doming and attendant hydrothermal circulation. The stocks of the resurgent dome and the structurally disturbed magnetically overprinted rocks appear to have undergone no significant later tilting.

Paleomagnetic evidence for structural rotation of the Klamath Mountains, California

A new aspect of the tectonics of the eastern Klamath Mountains terrane in northern California is being developed by E. A. Mankinen, C. S. Grommé, and W. P. Irwin through use of the paleomagnetic method. Oriented cores of Permian to Jurassic volcanic and sedimentary strata were drilled in the northern part of the province where the regional trend of the formations is east-northeast. Preliminary results of the paleomagnetic measurements indicate that there has been large clockwise rotation of the Permian volcanic rocks but significantly smaller rotation of the Jurassic strata. Permian rocks also were cored in the middle part of the province where the regional trend of the formations is north-south. Preliminary work on these cores suggests that the Permian rocks in the central area have not rotated as much as those to the north. These findings seem to indicate that the eastern Klamath terrane did not rotate as a rigid block and that the arcuate distribution of the Permian rocks is the result of oroclinal bending.

The origin of reverse thermoremanent magnetism in ilmenite-hematite

Ilmenite-hematite minerals having intermediate compositions in the range between $\text{Ilm}_{46}\text{Hem}_{56}$ and $\text{Ilm}_{76}\text{Hem}_{26}$ are ferrimagnetic and can have room temperature saturation magnetizations as large as 30 emu/g and are, therefore, of interest to studies in rock magnetism and paleomagnetism. Minerals of this compositional range can also acquire a reverse thermoremanent magnetization (reverse TRM) which results when a sample that is cooled from above its Curie temperature in an applied field takes on a magnetic moment that is op-

posite in direction to that of the applied field. Reverse TRM can be shown theoretically to result from magnetic coupling of two different magnetic phases, which has been the explanation for reverse TRM in ilmenite-hematite.

G. L. Nord, Jr. (USGS), and C. A. Lawson (Princeton University) have examined both normal and reverse TRM synthetic samples by transmission electron microscopy in order to identify the second phase responsible for the reverse TRM phenomenon. Instead of a second phase, the reverse TRM samples contained a high density of 100 nm thick magnetic domains, each bounded by an antiphase boundary (APB). These domains arise from the order-disorder transition in ilmenite where iron and titanium are disordered at high temperature and become ordered into iron-rich and titanium-rich layers at low temperature. Because the low-temperature ordered phase can choose either layer as its origin, two adjacent domains with different origins can impinge and an antiphase boundary will result. For crystal chemical reasons, specifically charge balance, the antiphase domain boundary will be more likely to lie between two iron layers.

This configuration results in a thin ribbon of hematite-like structure and composition. Hematite has a higher Curie point than ilmenite and, therefore, the APB is the probable candidate for the second phase. Upon annealing, the domains coarsen and the APB area is reduced. This reduction coincides with the change-over from reverse to normal TRM, further substantiating the APB mechanism as the origin of reverse TRM.

Volcanic correlation and dating using geomagnetic secular variation

The nature of geomagnetic secular variation in the Western United States for the past 20,000 yr has been under study for several years. Comparing precise remanent magnetization directions with known portions of this secular variation curve, D. E. Champion has been able to correlate and date a number of latest Pleistocene and Holocene volcanic units in the Western United States. In the Crater Lake area of Oregon, differences in magnetization direction due to secular variation substantiate a two-part eruption history for Mount Mazama that C. R. Bacon originally determined by using stratigraphic evidence. Older episodes of volcanic activity in the area have also been recognized. The same techniques were used in Hawaii to identify a major basalt flow about 1,400 yr old that inundated the area of present-day Hilo. This flow was mapped by J. P. Lockwood.

GEOMAGNETISM

Geomagnetic observatories

R. W. Kuberry acquired 16 microprocessor-based controllers for the automation of geomagnetic observatories. One system has been installed and is operational at the Boulder, Colo., observatory and a second system is being installed at the Fresno, Calif., observatory. L. R. Wilson and co-workers M. E. Flynn, N. E. Rouillard, and D. C. Herzog have generated the necessary programs for the PDP 11/34 microcomputer to communicate with these automated observatories. All observatory data are deposited in the World Data Center in Boulder, Colo., and are added to a master data file. This master file is the source of magnetic information used in U.S. Government mapping and charting programs with an annual distribution of some 50 million copies.

Repeat magnetic surveys

Under the direction of J. D. Wood, repeat magnetic surveys were made in Alaska, Alabama, Georgia, Texas, Mississippi, North Dakota, Florida, and on four Pacific islands. The purpose of the surveys is to determine the magnetic secular changes in those areas. Both absolute and variation recordings of the magnetic field components were made at each station. These data are used in USGS magnetic chart compilation, in secular change studies, and in the development of mathematical models for a wide variety of global and regional studies in geomagnetism.

Total magnetic intensity map of the U.S.

E. B. Fabiano and N. W. Peddie (1981) published a new total magnetic intensity map for the conterminous United States at a scale of 1:5,000,000. The map is the result of an analysis of 20,000 measurements which include recent aeromagnetic surveys and the MAGSAT survey of 1979-1980. Analysis of the MAGSAT vector data demonstrated that reasonably accurate field models can be obtained from such vector data (Langel and others, 1980).

Geomagnetic models and the solar cycle effect

Component measurements of the Earth's magnetic field show a solar cycle effect (SCE) with an amplitude of 10-20 nt and a period of about 11 yr. Spherical harmonic models compiled from these data do not show a noticeable SCE in their coefficients. L. R. Alldredge explains that external sources are orthogonal to internal sources and, therefore, contribute nothing to spherical

harmonic coefficients, if a good distribution of component data is used in the compilation. This important conclusion does not follow if total field data are used in the compilation.

PETROPHYSICS

Geophysical well logs detect fractures in granite

J. J. Daniels, J. H. Scott, and G. R. Olhoeft (1981) have conducted borehole geophysical studies in granite that show neutron-neutron measurements to be useful for detecting open fractures. Resistivity measurements can be used to detect microfractures that contain only a small amount of water but provide a conduit for electric current. Felsic-porphyry regions within fractured granite are often characterized by low magnetic susceptibility values and high gamma-ray well log response values. The studies illustrate the usefulness of conventional borehole geophysical measurements for determining fractures in granite.

Interpretation of borehole geophysical data at NTS

J. J. Daniels and J. H. Scott (1981 a, b) have conducted borehole geophysical studies at the Nevada Test Site that have included hole-to-surface dc-resistivity measurements in addition to conventional in-situ physical properties measurements. Qualitative interpretation of hole-to-surface resistivity measurements made separately from four drill holes confirm the presence of near-surface anomalies that could be caused by fracture zones. The feasibility of the presence of these anomalies has been confirmed by three-dimensional numerical models. Field studies in areas other than the NTS (Utah, Wisconsin, and Illinois) indicate that these measurements could be useful for defining inhomogeneities at depths of up to 2,000 m.

NTS radioactive waste isolation

Forty-nine samples from the Calico Hills area and fifty-nine samples from the Yucca Mountain area (both areas are located in the southwest sector of the Nevada Test Site) were measured by L. A. Anderson (1981 a, b) for textural, electrical, magnetic, and acoustic properties as part of a large scale site evaluation program intended to identify suitable underground repositories for radioactive waste products. At the Calico Hills location the stratigraphic column, in descending order, consists of unaltered, altered, and calcareous argillite and is the result of fracturing, alteration, and mineral reconstitution which accompanied and followed localized doming of the Calico Hills by intrusive activity. These phenom-

ena were observed in the measured rock properties and suggest that the textural qualities of the rock make them unsuitable for radioactive waste containment. The Yucca Mountain borehole penetrated the Tiva Canyon and Topopah Spring Members of the Paintbrush Tuff, the tuffaceous beds of Calico Hills, and the Prow Pass and Bullfrog Members of the Crater Flat Tuff. Although the collective rock property data is primarily intended for use in the interpretation and calibration of borehole and surface geophysical surveys, an evaluation of the laboratory results indicates that the Topopah Spring Member in the 200–500 m interval may best provide the conditions required of a repository for radioactive waste.

Hole-to-surface resistivity mapping homogeneity in bedded salt

Jeff Daniels (1982) has completed the qualitative interpretation of hole-to-surface resistivity data from Gibson Dome, Utah, by using three different sound depths (304 m, 518 m, and 102 m), which penetrated a sequence of sandstone, shale, and evaporite. Repeating the surface measurements (at distances up to 2,000 m from the drill hole) gives an indication of variations in the geoelectric section with depth. The data generally show a uniform layered earth having a gentle dip of the geoelectric section to the northwest. A few localized anomalies may be representative of localized thickening or folding of the salt layers.

Role of water in crustal deformation

Russell Lee and S. H. Kirby, investigating the chemical effects of water and aqueous solutions on the strengths of rocks and minerals, have demonstrated that topaz is fundamentally brittle. Pam Burnley has confirmed that another hydrous mineral, tremolite, shows little or no ductility in the laboratory. They believe that hydrous minerals with greater than 1 weight percent water are brittle because of an influence of hydrogen in promoting crack growth. Mark Linker and S. H. Kirby have confirmed an anisotropy in the rheology of quartz.

APPLIED GEOPHYSICS

Effects of draping on aeromagnetic anomalies

V. J. S. Grauch and D. L. Campbell studied the effects of draping aeromagnetic data, a recourse often followed when magnetics is an added option in airborne radiometric or electromagnetic surveys. Both computer simulation and field data show that draping accentuates topographic artifacts in the resulting magnetic con-

tour map; the opposite generally has been assumed. Naive models of draped aeromagnetic maps, which incorporate procedures developed for level-flown surveys, result in magnetic-source bodies which are too shallow and whose sides are rotated towards the horizontal.

Magnetic terranes of Iron River quadrangle

E. R. King found that the aeromagnetic map of the Iron River 2° quadrangle shows two major magnetic provinces which divide the Precambrian bedrock into an older Archean and Proterozoic metamorphic complex and a younger assemblage of volcanic and clastic rocks of the Keweenawan midcontinent rift system. In the older pre-Keweenawan province the Archean gneissic terrane forms domes that are outlined by magnetically anomalous iron-rich horizons in the overlying Marquette Range Supergroup. In the Keweenawan magnetic province the north-dipping volcanic rocks produce linear magnetic anomalies that separate nearly featureless magnetic areas associated with clastic rocks both above and within the volcanic sequence. A circular anomaly associated with the Porcupine Mountains indicates a middle Keweenawan volcanic center. The lower Keweenawan volcanics have a reversed remanent magnetization that is expressed in a set of negative linear anomalies associated with the Baraga County dike swarm that cuts the pre-Keweenawan terrane in the quadrangle.

Magnetic survey of eastern North Dakota

A study by E. R. King of a recently completed magnetic survey of eastern North Dakota, together with new gravity data, shows that a conspicuous northeast-trending pattern consists of a series of alternate magnetic highs and lows that have an 80 km wavelength. Some of the highs correlate with gravity lows and are on trend with similar anomalies over Archean felsic intrusive bodies in adjacent Minnesota. Other magnetic highs, without associated gravity lows, also have the same trend as other magnetic highs in Minnesota over Archean greenstone terrane that includes sub-economic deposits of iron formation.

Aeromagnetic and gravity data over the eastern overthrust

J. D. Phillips and D. L. Daniels found that the aeromagnetic anomalies over the allochthonous Blue Ridge and Piedmont provinces of North Carolina can be separated into short wavelength components corresponding to the anomaly fields of the near-surface crystalline rocks and long-wavelength components corresponding to the anomaly fields produced by the deeper Precambrian basement. This separation permits independent

mapping of geologic structures in the overthrust sheet and in the basement. In a similar way, residual Bouguer gravity anomalies, which correspond in large part to surface geology, are separated from long-wavelength gravity anomalies produced near the base of the crust. Study of the resulting maps reveals that basement magnetic and gravity anomalies can be distinguished from near-surface anomalies over the Blue Ridge, Inner Piedmont, and Carolina Slate Belt, a fact that suggests that the major décollement extends to the east beneath much of the Piedmont. Average depths of 12 to 15 km to the Precambrian basement surface are estimated from the aeromagnetic anomalies, and an average crustal thickness of 40 km is estimated from the gravity anomalies.

Schlumberger soundings at Medicine Lake, California

Fifty deep Schlumberger electrical soundings were made in the Medicine Lake highland area, California, by R. J. Bisdorf and D. R. Schoenthaler, with maximum electrode spacings (AB/2) ranging from 2 to 7 km. The data were obtained along severely winding roads, and A. A. R. Zohdy developed the necessary mathematical formulas for correcting the field data. The resistivity survey covered an area of approximately 380 km². The sounding data were processed and automatically interpreted on an HP 9845-B desk-top computer. Ten geoelectric sections and two equal depth maps depicting the distribution of interpreted true resistivity were produced in color by using an Applicon plotter. The interpreted data showed three significant low resistivity anomalies at shallow depth (250 m) west of Medicine Lake, near Bullseye Lake, and north of Red Shale Butte. These anomalies indicate a high geothermal potential for these areas. Record high near-surface resistivities (150,000 ohm-m) were measured at one sounding approximately 1 km southwest of Indian Butte.

Schlumberger soundings in the Date Creek Basin, Arizona

Forty Schlumberger soundings were made by R. J. Bisdorf in the Date Creek Basin, Arizona. Three color geoelectrical sections (two 17.3 km and one 24 km long) were produced to map the subsurface extension of a known uranium deposit associated with fine-grained low resistivity lacustrine sediments. The sediments were mapped and their areal extent was estimated to be about 70 km². A fault with a vertical offset of about 1 km was mapped on the southern side of the basin. In the middle of the basin, two drill holes confirmed the depth to basement (about 1.5 km) as it had been estimated from the interpretation of the resistivity data.

Magnetotelluric soundings over the Colorado Plateau and Basin and Range provinces

Magnetotelluric array measurements using fluxgate magnetometers and conventional magnetotelluric measurements were made by F. C. Frischknecht, M. R. Greenhaus, and P. V. Raab along the Utah-Arizona border and extending into southeast Nevada. The purpose of the survey was to study the deep electrical structure of the Colorado Plateau-Basin and Range transition zone and to study the thrust belt to the west of it. The principal conductor seen with the array studies, as determined from surface geology, lies at a considerable distance east of the boundary between the two provinces. The vertical magnetic field due to induction is almost nil in the Basin and Range province; however, a small vertical field was recognized at the easternmost station near Mexican Hat, Utah. Collection and interpretation of conventional magnetotelluric data in southeast Nevada proved difficult because of the complexity of near-surface structures there. However, excellent data was collected along the western margin of the Colorado Plateau where low conductance in the sedimentary section provides a very good window for deep sounding.

Tensor audio magnetotellurics

A system for tensor measurements of natural audio-frequency magnetotelluric signals has been assembled by Victor Labson. The primary emphasis of the new system is on measurement of the tipper. High quality data with little scatter has been obtained with the system near the Iron Mountain deposit in the Shasta district, Calif., and over a conductive carbonaceous slate near Mariposa, Calif. The results of the Iron Mountain study are very complex and difficult to interpret, apparently due to the convoluted nature of the conductors there. Results at Mariposa are simpler and more easily understood. In general, the data corroborates scalar audio-frequency magnetics (AFMAG) measurements made there several years ago but provides more complete information on the conductive unit.

Time-domain electromagnetic sounding

In a study of time domain electromagnetic sounding methods (TDEM), F. C. Frischknecht, W. L. Anderson, and P. V. Raab found that the single loop and central loop TDEM methods have several advantages over frequency domain methods. Theory and field experience show that, for a conductive layer, the TDEM method can sound to depths which are two to three times the dimensions of the loop. Also, by use of the single loop configuration, the effects of near-surface conductivity

variations tend to be averaged and moderate variations in topography do not cause significant distortion of the sounding curves. Thus, in the presence of lateral boundaries, the TDEM method can sound to greater depths than any other existing electrical method without resorting to two and three-dimensional modeling in interpretation.

Electromagnetic modeling and inversion of controlled source data

W. L. Anderson developed several computer programs to perfect the inversion of electromagnetic (EM) field data. A new nonlinear adaptive least-squares algorithm (Anderson, 1982a) was used to enhance the inversion technique and is available for use on a VAX 11/780 computer. Several new time-domain forward and inverse solutions were programmed for central-induction (Anderson, 1981) and coincident loop (Anderson 1982b) sounding systems. A major computer conversion from the Multics EM library to the VAX was accomplished during 1981 and 1982. This effort involved approximately 500 Fortran modules.

Vertical seismic profiles help detect stratigraphic oil and gas traps

Surface and deep well seismic studies made by A. H. Balch, M. W. Lee, J. J. Miller, and R. T. Ryder indicate that certain stratigraphic oil and gas traps may be detectable by reflection amplitude anomalies. Field and model studies carried out on a Leo sand unit of the Minnelusa Formation, Powder River Basin, Wyo., show a substantial seismic reflection amplitude anomaly where the Leo is thick and productive. If these results, obtained on and adjacent to one known producing field, can be verified in the area, it would have considerable impact on seismic exploration for stratigraphic traps.

Multichannel seismic measurements in the Bahaman-Cuban collision zone

D. J. Taylor analyzed approximately 3,500 km of multichannel seismic reflection, gravity, and magnetic data to reveal the presence of five domal structures beneath water depths of 500 m in the old Bahama channel. Closure crossings span as much as 10 km. The cores of these domal structures may be salt, subducted shallow water carbonate blocks, or both. The size of the structures and their occurrence in relatively shallow water make them attractive exploration targets. The semiconsolidated sediments comprising the basin fill show extensive continuity of reflections, which probably resulted from interbedding of shallow water carbonate turbidites with pelagic oozes. Crinkling of reflections at depths of several hundreds of meters appears to be related to compaction.

Image processing laboratory developed to support uranium exploration

D. L. Sawatzky reported that the image processing laboratory was developed to support remote sensing research and that the facilities were designed to enhance geological information in digital images. Airborne data are generated by an airborne multispectral scanner, whereas satellite data (such as those from Landsat and Heat Capacity Mapping Mission) are purchased from the EROS Data Center. The main processing units are a Perkin-Elmer 3220 minicomputer and a Floating Point Systems AP-120B array processor. Peripheral devices consist of 200 megabytes of disk storage, two dual density tape drives, and a printer. Film transparencies are the chief products of the laboratory. They are generated by three film writing devices in both color and black-and-white in 25 by 25 cm size. The devices are two Optronics C-4300's and an Optronics P-1700. An in-house photographic laboratory provides for most film-handling requirements. Image data tapes are generated from aircraft scanner tapes through an analog-to-digital converter connected to a Computer Automation LSI/2-20 minicomputer. About 400 images reside in the tape library. A COMTAL Vision 1/20 is used for interactive analysis of color-ratio composite, false-color infrared, and single band images. A Tektronix graphics digitizing station is used to digitize line maps and profiles. Computer programs existing prior to the completion of the laboratory have been converted and reside in two packages: REMAPP for images enhancement and LINANL for lineament analysis. In addition, two statistical packages have been purchased: Earth Resources Laboratory Applications Software (ELAS) and Biomedical Programs (BMDP).

Interpretation of aerial radiometric data for Lake City caldera

Maps of aerial gamma-ray spectrometric data were prepared by J. A. Pitkin and J. S. Duval for the Lake City caldera and vicinity, in San Juan Mountains, Colo. High radioelement concentrations characterize more silicic ash-flow tuffs, whereas low concentrations indicate less silicic or intermediate composition volcanic and volcanoclastic rocks. Several of the more silicic Miocene intrusives are known to have uranium mineralization (Steven and others, 1977) and are associated with anomalous radioelement concentrations. Several Oligocene intrusives show common anomalous levels for all three (U, Th, K) radioelements and are mapped as rhyolites. Thus, despite the anomalous radioactivity, uranium mineralization similar to that of the Miocene intrusives has not been discussed in the literature to date. West of the caldera, a large area of anomalous potassium and slightly anomalous equivalent uranium

and equivalent thorium exists where bedrock is mapped as Oligocene volcanic and volcanoclastic rocks. Published information does not explain this observed anomaly either.

A new slim-hole gravity meter

In January 1981, the first field surveys with the new slim-hole borehole gravity meter were made in five wells in southern California by S. L. Robbins, F. G. Clutson, F. J. Martinez, and L. A. Beyer. All of the surveys were successful and the bottom hole temperatures of three of the wells were at or above 120°C.

Thermal convection in drill holes at high geothermal gradients

Studies by T. C. Urban and W. H. Diment of thermal convection in cased water-filled drill holes have been extended to environments where the thermal gradients reach 1°C/m in drill holes from 2 to 25 cm in diameter (Urban and Diment, 1980). The aspect ratios (height/radius) of the principal convective motions range largely between 6 and 12, although individual values may exceed 100. Gas in the holes produces additional complications (Diment and others, 1981). Such studies provide a basis for (1) establishing the limit to which temperature logs can be used to determine the ambient geothermal gradient and the rock type surrounding the hole, and (2) establishing the velocity of fluid motion in a hole and the effect of fluid motion on devices suspended in a hole.

New borehole geophysical tools for uranium exploration

Two new borehole measurement tools were investigated by J. H. Scott: a low-drift magnetic susceptibility probe and a gamma-ray spectrometer probe. The low-drift magnetic susceptibility probe was redesigned and tested successfully. The probe is based on a unique design concept that reduces temperature drift to less than 10 micro cgs units per hour, thus it is possible to detect anomalies of 10 micro cgs units or smaller. Anomalies of this type are frequently associated with sedimentary uranium deposits where detrital magnetite is destroyed by oxidizing ground waters. The design and performance characteristics of the probe are described by Scott and others (1981). The downhole gamma-ray spectrometer probe with a cryogenically cooled intrinsic germanium detector was tested unsuccessfully. Failure was caused by leakage in the high-vacuum chamber required for maintaining the detectors at cryogenic temperatures. The probe is being redesigned and rebuilt to correct the problem prior to future testing.

Constraints on yield strength in the oceanic lithosphere

The yield strength for the oceanic lithosphere depends on depth and age. Old oceanic lithosphere has no long-term strength below 40 cm. M. K. McNutt (USGS) and H. W. Menard (Scripps Inst. of Oceanography) compared the yield envelope deduced from field studies of sea-floor deformation with that obtained from rock deformation analyses in the laboratory and found that the oceanic crust and upper mantle appear to be weaker than laboratory extrapolations would predict. Their favored explanation for this observation is that the activation energy for ductile flow decreases at low strain rates from 125 Kcal/mole to 100 Kcal/mole.

GEOCHEMISTRY, MINERALOGY, AND PETROLOGY

EXPERIMENTAL AND THEORETICAL GEOCHEMISTRY

Three-dimensional fluorescent spectra of humic acids

Three-dimensional fluorescence spectroscopy, as described by M. C. Goldberg, E. R. Weiner, and R. L. Wershaw, allows one to examine the emission and excitation spectra of a compound over the response range 200 to 800 nm and present this data to the viewer on a single figure. By combining the excitation wavelength, emission wavelength, and emission intensity in this manner, a spectral pattern of a compound can be obtained that is unique, even though the conventional emission scan done at a single wavelength for a given material might be indistinguishable from the spectra of a number of other materials.

The technique of three-dimensional spectroscopy was used to study humic acid fractions. Florida muck samples were fractionated on a Sephadex column into four fractions. These fractions vary in molecular weight, molecular number, and composition of reactive groups. The fractions were examined by collecting a three-dimensional fluorescence spectrum in the form of a contour map. The axes were excitation wavelength, emission wavelength, and fluorescence emission intensity. The latter is presented as contour lines at 10 percent intensity intervals. The unfractionated sample had excitation peaks at 210 and 300 nm, with a single emission peak at 465 nm. As the fractions were examined, in order of elution from the Sephadex column, the spectral pattern no longer showed the single emission line at 465 nm, but different patterns emerged. The final pattern had excitation peaks at 320 and 510 nm and emission peaks at 450 and 580 nm. In addition to the fluorescence pattern, these spectra made possible the selection

of 465 nm as the proper wavelength to obtain an excitation spectrum on the unfractionated sample which should best match the absorption spectrum. Several absorption spectra were determined with the absorption maxima confirmed by ultra-violet analysis.

Xenoliths from trachybasalt, Sierra Nevada

Xenoliths discovered by F. C. W. Dodge, D. G. Fates, and L. C. Calk in an upper Tertiary trachybasalt flow remnant overlying a granodiorite pluton of the central Sierra Nevada batholith at Chinese Peak suggest a layered mafic intrusion at depth. There is a limited range of rock types at Chinese Peak but broad textural variation within types. More than half of the studied xenoliths are granular pyroxenites, ranging from seemingly undisturbed magmatic cumulates to highly strained, recrystallized tectonites; two-thirds are websterites with subequal amounts of clinopyroxene and orthopyroxene making up the remainder. Xenoliths of felted mats of fine, bladed pyroxene are reminiscent in form and texture of chrysotile serpentine and make up nearly a fifth of the assemblage. These xenoliths represent original pyroxenites that were serpentinized and then in turn dehydrated and recrystallized. Several composite samples have "recrystallized serpentine" in sharp contact with granulitic pyroxenite, a condition suggesting that these xenoliths represent fragments of metasomatized vein material. Biotite-bearing norites and two-pyroxene gabbros and diorites make up over one-third of the suite. Highly altered harzburgites and lherzolites comprise a minor fraction of the assemblage. Studies of granulitic xenoliths worldwide suggest that gabbroic layered intrusions are widespread in the lower crust, and the assemblage of xenoliths at Chinese Peak suggests chemical migration from a deep-seated intrusive complex. If this area of the Sierra Nevada is underlain by such a body, it is probably of limited extent, as a volcanic plug a few kilometers distant contains a more heterogeneous assemblage of xenoliths.

Silica solubilities in hydrothermal salt solutions

R. O. Fournier developed a general equation for calculating solubilities of quartz and amorphous silica in aqueous salt solutions,

$$\log m_{(\text{aqueous silica})} = \log K + n \log \rho F + n \log \left[1 - \frac{h \nu m_{(\text{salt})}}{55.51} \right] - \log \gamma$$

where m is molality, K the equilibrium constant for the dissolution reaction, n is the average hydration number of the aqueous silica species normalized to one molecule of SiO_2 , ρ is the solution density, F is the weight fraction

of water in the solution, h is the apparent cation hydration number of the salt, ν is the number of cations per mole of salt, and γ is the activity coefficient for aqueous silica. For NaCl solutions at 100°C, the above equation reduces to

$$\log m_{(\text{aqueous silica})} = \log K + n \log \rho F$$

Values for n and K at the desired temperature and pressure can be obtained from data on the solubility of quartz and amorphous silica in pure water.

A comparison of calculated and experimentally determined solubilities shows excellent agreement when the experiments were carried out in containers that do not react with the saline solution.

Thermodynamic properties of minerals

R. A. Robie, B. S. Hemingway, and H. T. Haselton measured the heat capacities of $\text{LiAlSi}_4\text{O}_{10}$ (petalite), $\text{Ab}_{0.25}\text{Or}_{0.75}$ (alkali-feldspar, solid solution), $\text{CaAl}_2\text{SiO}_6$ (pyroxene), $\text{CaAl}_2\text{SiO}_6$ (glass), $\text{CaFeSi}_2\text{O}_6$ (glass), Mn_3O_4 (hausmannite), Mn_2O_3 (bixbyite), Al_2SiO_5 (kyanite and andalusite), $\text{BeAl}(\text{SiO}_4)(\text{OH})$ (euclase), and an iron-rich chlorite between 5 and 375 K and also determined the standard entropies of these materials at 298.15 K. Hausmannite and bixbyite exhibit sharp lambda-type anomalies in heat capacities at 43.1 and 79.4 K, respectively, arising from the antiferromagnetic ordering of the spin moments of the manganese ions at low temperatures. Bixbyite also has a "second order" transition at 308 K, associated with the change from orthorhombic to cubic symmetry.

National Center for the Thermodynamic Data of Minerals

The National Center for the Thermodynamic Data of Minerals, established in 1976 at the Geological Survey, is a cooperating data center of the National Standard Reference Data System. J. L. Haas, Jr., G. R. Robinson, and C. S. Schafer of this center established a complete correlation of the thermodynamic and volumetric properties of 29 phases in the chemical system lime-alumina-silica-water-carbon dioxide. This led to major revisions in the available Gibbs energy data for anorthite, gehlenite, grossular, boehmite, and the calcium-aluminum clinopyroxene. The correlation was the result of evaluating almost 2,500 observations of heat capacity, relative enthalpy, entropy, enthalpies and Gibbs energies of reaction, equilibrium constants, cell potentials, molar volumes, expansivities, and compressibilities in this system to temperatures and pressures as high as 1,800 K and 40,000 bars, respectively. The investigators also established a complete correlation of the thermodynamic and volumetric properties of 10

phases in the chemical system magnesia-silica-water-carbon dioxide. This correlation was the result of evaluating over 1,000 experimental observations of various types as listed above. Internally consistent properties are now available for forsterite, enstatite polymorphs, talc, chrysotile, anthophyllite, antigorite, brucite, and magnesite.

Migration rates of brine inclusions in single crystals of NaCl

Rock-salt deposits have been considered as a possible medium for the permanent storage of high-level radioactive wastes and spent fuel. Brine inclusions present in natural salt can migrate if the temperature gradients in the vicinity of the radioactive waste are large enough. To better assess the problem, I-Ming Chou estimated the migration rates of these brine inclusions under various repository conditions. Among the existing models of the migration process, the one presented by Anthony and Cline (1971) is considered as being the most complete because it accounts for most of the phenomena known to occur in the migration process. However, application of their model is difficult because of an insufficient data base. By utilizing recent data for halite saturated brines and the model of Anthony and Cline, I-Ming Chou evaluated the effect of brine composition on the migration rate of inclusions at 50° and 100° C. Because Soret coefficients (σ) of salt in brines are not known, the Soret coefficient must be treated as a variable. To simplify the calculation, the interface kinetics are neglected. Then the isothermal maximum migration rate predicted by Anthony and Cline's model reduces to a simple linear function of σ for each brine composition. Although the estimated maximum migration rates for WIPP-A, NBT-6, and 2.41 molality $MgCl_2$ brines are of the same order of magnitude, they differ markedly from those of pure NaCl solution (except in a narrow region of σ values). At 100° C, these calculated migration rates are considerably higher than those measured experimentally. This discrepancy indicates either that the neglected interface kinetics might be an important retarding factor for the migration rates of inclusions or that the model used is deficient.

MINERALOGIC STUDIES IN CRYSTAL CHEMISTRY

Electron-diffraction patterns of manganese oxides

The diffraction patterns produced by the transmission electron microscope can be used to identify the mineral species present in microcrystalline synthetic and natural manganese oxides. Studies by C. J. Lind (1982) demonstrated that this technique will give struc-

tural information on particles with diameters substantially less than 0.1 μm , a size range in which X-ray diffraction techniques commonly fail to give useful results. The electron diffraction technique also is useful for identification of other microcrystalline minerals having d -spacings equal to, or less than 4.9 Å.

Pyroxene decomposition in kimberlites

G. L. Nord and R. H. McCallister (Purdue University) have studied the thermal history of low calcium diopsides occurring in certain kimberlites (McCallister and Nord, 1981). Twenty-six subcalcic diopside megacrysts ($Ca/(Ca+Mg)=0.280$ to 0.349 and containing approximately 10 mol percent $NaAlSi_2O_6$) from 15 kimberlite bodies in South Africa, Botswana, Tanzania, and Lesotho have been characterized by electron microprobe analysis, X-ray-precession photography, and transmission electron microscopy. Significant exsolution of pigeonite was observed only in those samples for which $Ca/(Ca+Mg)$ was less than or equal to 0.320. The exsolution microstructure consists of coherent (001) lamellae having wavelengths from 20 to 31 nm. Compositional differences between the hosts and the lamellae vary from 10 to 30 mol percent $Ca_2Si_2O_6$. These observations suggest that the exsolution reaction mechanism was spinodal decomposition and that the megacrysts were quenched at various stages of completion during this decomposition process.

Annealing experiments in evacuated silica glass tubes at 1,150° C for 128 h failed to homogenize the microstructure, whereas, homogenization was complete after annealing for 7.25 h at 5 kbar and 1,150° C. This "pressure effect" suggests that spinodal decomposition in the kimberlitic subcalcic diopside megacrysts can only occur at depths less than approximately 15 km; the cause of the effect may be due to the $NaAlSi_2O_6$ component in the pyroxene. Apparent quench temperatures for the exsolution process in the megacrysts varying from 1,250° C to 990° C suggest that decomposition must have commenced at temperatures of more than approximately 1,000° C.

These studies lead to the conclusion that spinodal decomposition of subcalcic diopside megacrysts occurred at shallow levels (< 15 km) within the kimberlite bodies and at temperatures greater than about 1,000° C.

Stability of ferrobustamite

Mineral assemblages in certain magnesium-free skarns have led to the suggestion that ferrobustamite (a pyroxenoid) of approximate composition $Ca_{0.85}Fe_{0.15}SiO_3$ might be stable at low metamorphic temperatures. Hydrothermal experiments carried out by P. E. Brown

and J. S. Huebner proved that wollastonite plus hedenbergite, not ferrobustamite, are stable below $775 \pm 5^\circ \text{C}$ at 2 kbar. Their experiments also showed that small amounts of johannsenite component ($\text{Ca}_{0.5}\text{Mn}_{0.5}\text{SiO}_3$) stabilize ferrobustamite to lower temperatures. This finding provides an explanation for some occurrences of ferrobustamite in retrograde rocks: the manganese component stabilizes the pyroxenoid to lower temperatures below which the reactions are too slow for ferrobustamite to decompose to the stable assemblage, wollastonite plus hedenbergite.

Chlorite associated with Henry Mountains uranium deposits

An unusual vanadium-bearing chlorite has been found by C. G. Whitney and Roy Northrup to be the dominant clay mineral of the uranium deposits of the Henry Mountains, Utah. The chlorite is clearly authigenic and is found in intimate association with the uranium-bearing mineral coffinite. X-ray diffraction analysis shows that the vanadium must be concentrated in the interlayer hydroxide sheet of the chlorite crystal structure. It is believed that the vanadium precipitated under highly reducing conditions with components of preexisting clays.

Silicon-bearing magnetite

Microprobe analyses by P. J. Modreski of magnetites from certain ore deposits, particularly contact-metasomatic deposits and some igneous-related hydrothermal deposits, contain 1 to 3 weight percent of SiO_2 in solid solution. Analyses of magnetite synthesized under hydrothermal conditions (P. J. Modreski and I-Ming Chou, 1981) has confirmed that magnetite is a potential indicator of temperature, pressure, oxygen fugacity, or other (possibly nonequilibrium) conditions of formation of ore deposits. Study of the silicon content of magnetite has been combined with a general study of the variation of other minor elements in this phase, including Mg, Al, Ca, Ti, V, Cr, Mn, Co, Ni, and Zn.

Characterization of mineral precipitates by electron diffraction

Electron diffraction patterns taken with the transmission electron microscope have been used by C. J. Lind (1982) to identify the mineral species present in synthetic and naturally occurring samples of manganese oxides. Structural information is obtained on single particles with diameters substantially less than $0.1 \mu\text{m}$, a size range in which X-ray diffraction techniques commonly fail to give useful results.

Diurnal periodicity in NaCl precipitation in Permian salt basins

Studies by Edwin Roedder (1982) have shown that some core samples of bedded Permian salt from the Palo Duro basin of Texas exhibit periodic fluid inclusion textures that appear to be related to diurnal cycles rather than to annual cycles, as is frequently reported in the literature of bedded salt deposits. The sodium chloride crystals, approximately 1 cm in length, apparently grew vertically from the bottom of a very shallow sea. Each day's solar evaporation at the water surface produced denser supersaturated brines which convected downward and caused a rapid growth of a 0.40 to 0.85 mm thick layer of NaCl on the salt crystals. These rapidly growing layers trapped numerous inclusions containing brine. A small amount of residual supersaturation at nightfall caused a very thin layer of clear inclusion-free salt to form. The next day the process was repeated and the finely banded crystals of sodium chloride were yielded. The process is of more than academic interest, for it proceeds only in very shallow waters. There is considerable interest in estimating the water depths during Permian salt deposition; any data on these depths can help in reconstructing the paleogeography of these salt basins.

Chemical compositions of igneous hornblende amphiboles

Electron microprobe analyses, obtained by Jane M. Hammarstrom, of hornblendes in granitoids from several calc-alkalic intrusive complexes suggest that (1) the range of compositions for a given complex reflects tectonic setting, and (2) compositions within single grains and rock units change in response to changes in intensive parameters during crystallization of the magma. Hornblendes occurring in various rocks, including gabbros and granites from the Pioneer batholith of southwestern Montana, are associated with biotite, plagioclase, sphene, magnetite, and sometimes with potassium feldspar and pyroxene. The hornblendes contain 0.7 to 1.8 atoms of Al(IV), 0 to 0.4 atoms of Al(VI), and 0.1 to 0.4 atoms of titanium per 23 oxygen formula. The $\text{Fe}/(\text{Fe}+\text{Mg})$ ratio varies from 0.3 to 0.5 and tends to increase slightly with increasing rock silica content. Other correlations with rock chemistry are poor because of hornblende heterogeneity. Hornblendes in mafic rocks have brown titanium- and aluminum-rich cores and green silicon-rich rims. Hornblendes in other rocks are green but exhibit dark and light patches, sometimes in core-rim relationship reflecting, respectively, aluminum- and silicon-rich compositions. The variations from dark to light patches are less extreme than the brown to green variations and are not related to alteration. The $\text{Fe}/(\text{Fe}+\text{Mg})$ ratio tends to decrease with decreasing aluminum and titanium. Experimental and

field studies suggest the aluminum and titanium content decreases in hornblendes as temperature decreased.

Hornblendes from representative samples of three complexes that are characterized by the presence of magmatic epidote (Rivallogegido Island, Alaska; Ecstall Pluton, British Columbia; Riggins area, Idaho) have distinctly more aluminous compositions, Al(IV) 1.3 to 1.7 atoms and Al(VI) 0.5 to 0.8 atoms, than seen in hornblendes from the Pioneer batholith. E-an Zen suggests that these epidote-bearing rocks may represent a high pressure facies of typical calc-alkalic rocks.

VOLCANIC ROCKS AND PROCESSES

HAWAIIAN VOLCANO STUDIES

The August 1981 intrusive event at Kilauea Volcano

The most notable activity of Kilauea Volcano during 1981 was the major intrusive event into the southwest rift August 10-12. About 40 million m³ of magma moved from the summit storage chambers into a dike about 18 km long, 4 km high, and up to 1 m wide. Ground deformation above the dike indicates that it dips 85 degrees to the southeast and reaches to within 250 m of the surface. Since the major magnitude 7.2 earthquake in 1975, there have been 14 intrusions at Kilauea and only 2 eruptions, nearly the reverse of the ratio of intrusions to eruptions before the 1975 earthquake. The August 1981 intrusion is the largest during the last 25 yr of geophysical monitoring of Kilauea. The tendency since 1975 for intrusions not to culminate in eruptions is apparently related to the major strain release and reduction of stress on the east and southwest rift zones of Kilauea that resulted from the 1975 earthquake. Dikes can now more easily dilate the rift zones than erupt to the surface.

Three other Kilauea intrusive events during 1981 were a south summit to the upper southwest rift intrusion on January 20, a middle southwest rift intrusion that began January 25, intensified on February 6, and continued intermittently into early June, and a small but rapid intrusion in the south caldera area on June 25. Self-potential (SP) and controlled-source electromagnetic induction (EM) surveys on Kilauea have shown marked changes related to intrusive events near the sensors.

Eruption forecasting for Kilauea

The experiment in eruption forecasting for Kilauea based on earthquake, tilt, and tidal data shows considerable promise from its first full year of trial. The results were 77 percent better than random guessing but 23 percent poorer than a perfect forecasting system. The

only time during 1981 that the forecasting estimates exceeded the long-term statistical estimates based on historical eruption frequency was a period of 6 weeks preceding the August 1981 intrusive event.

Mauna Loa Volcano

Mauna Loa Volcano continues to slowly inflate at a more or less steady rate of about 12 million m³/yr. This estimate is based on deformation data which indicate that the top of the inflating magma chamber beneath Mauna Loa is at a depth of about 5 km. Although inflation of Mauna Loa has been continuous since its last eruption in 1975, seismicity beneath Mauna Loa has remained at relatively low levels compared to the high number of earthquakes in 1974 and 1975 which preceded the July 1975 eruption.

Hawaiian earthquakes

Twenty-three earthquakes of magnitude 4 or greater occurred beneath or near the Island of Hawaii in 1981. The largest of these, a magnitude 5.3 earthquake, occurred on March 5 at 04:09:41 Hawaiian Standard Time about 30 km west of Hawaii. The total number of recorded microearthquakes exceeded 100,000 during 1981.

Depth of origin of olivine nodules, Loihi Seamount

The Loihi Seamount, an active small underwater volcano 1 km deep off the south coast of Hawaii, is particularly interesting, as it has alkali basalt flows containing olivine nodules, even though it is young. Most other such alkali basalts in Hawaii erupted late in the history of large volcanoes. Dense carbon dioxide inclusions found in the olivine nodules from alkali basalt flows over the world (Edwin Roedder, 1965) indicate the worldwide presence of a separate, immiscible, dense CO₂ phase (in effect, incipient "vesiculation") at depth. In most occurrences, these inclusions are along secondary fractures and hence tell us little about the original environment of formation of the host crystals of olivine. Edwin Roedder (1981) has shown that at least some of the CO₂ inclusions in the nodules from Loihi, however, are primary, and thus pressure estimates based on these inclusions yield the pressure-depth at which these olivines grew. These depths were found to be in the range 8 to 17 km. These data thus correlate with the seismic evidence of Klein (1982), to suggest that these olivine crystals grew in a magma chamber 8 to 17 km deep. Decrepitated (burst) inclusions in other olivines suggest that at least part of the olivine nodules crystallized at still greater depths. The inclusions also show that three fluid

phases were present simultaneously: basaltic melt, sulfide melt, and supercritical CO₂ fluid.

CENOZOIC VOLCANISM IN WESTERN UNITED STATES

Emplacement of the andesite tuff and revised stratigraphy of the Medicine Lake Volcano, California

J. M. Donnelly-Nolan finds that earlier, simpler views of Medicine Lake Volcano need to be revised. Previous workers concluded that the volcano began with an andesitic ash flow (the andesite tuff of Anderson, 1941) followed by successively more silicic andesites building the highest, steepest parts. In fact, all rock types from basalt through rhyolite are interspersed through the volcanic stratigraphy. Andesite appears to be dominant, but olivine andesites and silicic andesites erupted randomly with no consistent evolution in silica content. A complex sequence of lavas and development of a central caldera were followed, not preceded, by eruption of about 2 mi³ of the andesite tuff. The andesitic ash flow apparently erupted near the center of the caldera through the volcano's ice cap and flowed rapidly over the ice. Flooding, channel cutting, and deposition of gravels low on the flanks followed. Within the 11 by 6 km caldera, the andesite tuff occurs at only one site where evidence of fumarolic alteration indicates that the tuff probably was preserved because the ice had melted. The ash flow traveled as far as 30 km north, southwest, and east of the caldera. It is thickest in valleys and low spots, where its base is typically fine-grained and welded. It also welded against the caldera-facing sides of hills, overtopping only the lowest ones. Eruptive activity since emplacement of the andesite tuff has been dominantly bimodal as pointed out by Anderson (1941). During the last few thousand years, no andesites have erupted. Instead, basaltic lavas have alternated with dacites and rhyolites, several of the flows being only about a thousand years old.

Phenocrysts record magma mixing in Coso volcanic field, California

Pliocene volcanic rocks of the Coso volcanic field range in composition from olivine basalt to high-silica rhyolite. Field observations indicate that mixing of magmas was a common occurrence at relatively long-lived volcanic centers. Spheroidal mafic inclusions in dacitic lavas and interbanded phenocryst-poor mafic lava and porphyritic dacitic lava in flows and bombs provide examples of incomplete mingling of contrasting magmas. Sieved plagioclase and rounded, pyroxene-mantled quartz in mafic lavas and olivine in the biotite dacites show more thorough mixing. Bulk compositions suggest that mixing of basaltic and silicic magmas was

an important process in generation of intermediate-composition magmas.

Detailed electron microprobe study of phenocrysts by C. R. Bacon and S. W. Novak shows that rocks with anhydrous silica contents between about 52 and 65 percent commonly contain multiple populations of phenocrysts derived from both basaltic and silicic magmas (sodic and calcic plagioclase coexisting with forsteritic olivine and quartz). Textural evidence and zoning patterns indicate that few crystals were derived from basement rocks. Coarsely-sieved plagioclase phenocrysts typically contain inclusions of potassium-rich, silicon-rich glass that is depleted in calcium and aluminum. Rather than melted feldspar, these inclusions represent melt trapped during rapid growth of the host crystal. The coarse melt inclusions are similar in composition to groundmass glass adjacent to euhedral phenocrysts. Sudden change in heat content of magmas upon mixing would be expected to cause undercooling and result in incorporation of melt depleted in components of the growing host crystal. Finely sieved phenocrysts may have experienced reaction and partial melting as a result of mixing with higher temperature magma. The complexity of zoning and variety of phenocryst compositions within single specimens suggests multiple mixing events in some lavas. The intermediate-composition magmas were probably formed by mixing of mafic and silicic magmas in comparatively small, compositionally zoned crustal reservoirs. Though the evidence for physical mixing of magmas is compelling, mixing alone probably cannot account for all of the compositional diversity in the Pliocene part of the Coso volcanic field. Crystallization differentiation of basaltic magma, partial melting of crustal rocks, and shallow differentiation of silicic magma may also have taken place within the same magmatic systems and contributed to the complex compositional variations.

Climactic eruption of Mount Mazama and formation of Crater Lake caldera, Oregon

The climactic caldera-forming eruption of Mount Mazama about 6,800 yr ago was immediately preceded by eruption of tephra and five related rhyodacite lava flows during perhaps 200 yr, according to C. R. Bacon. The lava flows represent eruptions of at least 2 km³ from the differentiated top of a magma chamber zoned from rhyodacite downward to mafic andesite or basalt. These pre-caldera eruptions apparently resulted in sufficient depressurization of the top of the chamber for vesiculation to occur at depth, the result being Plinian eruption of rhyodacite pumice before the last of the lava flows had cooled completely. Thirty or more km³ of rhyodacite magma were erupted rapidly from an areally restricted vent area and thick deposits of air-fall pumice

and ash accumulated before the caldera began to collapse and before the ash-flow phase of the eruption began. The Wineglass Welded Tuff of Williams (1942), a welded ash-flow tuff, records sudden collapse of the eruption column as vent geometry changed during the transition from single to multiple vents. Because the lithic fragments in proximal deposits correlate with local caldera wall rock types, the investigator concluded that the following climactic ash flows came from a ring of vents. Relations on the top of the Cleetwood rhyodacite flow, youngest of the precursory lavas, show that the crust was brittle, but its interior still plastic when the caldera collapsed: rift valleys formed in the crust as the interior oozed down the caldera wall where the scalloped wall bit into the flow. The walls of the rifts cut air-fall deposits and Wineglass Welded Tuff but are partly covered by proximal ash-flow deposits, facts indicating that the caldera had begun to collapse by the time the climactic ash flows were erupted. All of the events, from emplacement of the Cleetwood flow through collapse of the caldera, took place over a short time. The ash-flow deposits represent about 13 km³ of magma, in which rhyodacite is far more abundant than andesite, and the total for the climactic eruption is about 50 km³. Reconstruction of the form of Mount Mazama at the time of the eruption on the basis of mapping of the caldera walls and rim indicates a loss of about 50 km³ attributed to formation of the caldera, an amount equivalent to the volume of magma erupted.

Miocene ash-flow tuffs, central Snake River Plain, Idaho

P. L. Williams and G. B. Dalrymple recognize that four major rhyolite ash-flow tuff units were erupted in late Miocene time and are exposed in the Cassia Mountains and Monument Hills south of the plain and in the Mount Bennett Hills north of the plain. These rocks, for which Williams and Dalrymple propose the name Cassia Group, are 300–400 m thick in the Cassia Mountains and consist of densely to moderately welded tuff sheets separated by bedded tuffs. Isotopic dating by these investigators and by Armstrong and others (1975, 1980) indicates emplacement of the tuffs occurred about 16, 12, 9.3, and 8.5 million yr ago, an age range compatible with that of the Trapper Creek flora (Axelrod, 1964) which occurs in tuffaceous beds conformably underlying the Cassia Group. All the tuffs contain small to moderate amounts of plagioclase and clinopyroxene, but from base to top of the succession they are progressively poorer in K₂O and in SiO₂ (75 to 69 percent) and correspondingly richer in femic constituents, except for the uppermost unit, which is rich in K₂O and SiO₂. The investigators infer that the lower three tuffs were erupted from the roof zone of a magma chamber that

was vertically zoned by fractionation and was progressively depleted in SiO₂ in the manner described by Smith (1979). The uppermost unit appears to have originated from a source farther east and is the single eruptive product of a small magma chamber.

Eruption rates and lava compositions, Craters of the Moon lava field, Idaho

Field, paleomagnetic, and radiocarbon studies by M. A. Kuntz, D. E. Champion, E. C. Spiker (USGS), and R. H. Lefebvre (Grand Valley State Colleges, Michigan) reveal a time-dependent relation between repose intervals and the volume (thickness times area) of lava erupted in each successive period in the Craters of the Moon lava field. The field formed in the last 15,000 yr during eight eruptive periods. Each eruptive period was probably several hundred years in duration, on the basis of paleomagnetic evidence, and eruptive periods were separated by repose intervals of several hundred to several thousand years.

The eruption rate for the eruptive periods between 15,000 and 7,600 yr ago was about 1.7 km³ per 1,000 yr; the eruption rate for the eruptive periods between about 6,600 and 2,000 yr ago was about 2.7 km³ per 1,000 yr. The increase in eruption rate coincides with a marked change in composition. Prior to 7,600 yr ago, only basalt lavas (less than 50 percent SiO₂) were erupted. After 6,600 yr ago, both basalt and hawaiite-trachyandesite (more than 50 percent SiO₂) were erupted. The eruption of more fractionated lavas was accompanied by building and partial destruction of large cinder-spatter cones; the eruption of basalt lavas was mainly from fissures and was relatively nonexplosive.

The increased eruption rate results from addition of more fractionated lavas, at a rate of about 1.0 km³ per 1,000 yr, to the basalt component, which remained fairly constant at about 1.7 km³ per 1,000 yr. Petrographic and chemical data suggest that fractionated lavas represent a mixture of basalt magma and a partial melt component from deep crustal, granulitic rocks.

Differentiation in the Springerville volcanic field, Arizona

J. C. Aubele, L. S. Crumpler, and Christopher Condit found that the Springerville, Ariz., volcanic field contains basanite, alkali basalt, hawaiite, mugearite, benmoreite, and andesite in vents and flows dating from several m.y. to less than 100,000 yr old. Two vents have produced andesite plugs within benmoreite and alkali olivine basalt cones. A number of vents produced aphyric basalt flows, generally hawaiites, that cover the topographically highest central part of the field. These may represent a fractionated product from an alkali basalt magma that resided in the upper crust. Similar

differentiated sequences have been observed in the San Francisco and Mount Taylor volcanic fields in adjacent regions of the southern Colorado Plateau margin.

PLUTONIC ROCKS AND MAGMATIC PROCESSES

The paradox of aqueous inclusions in a chondritic meteorite from Jilin, China

Aqueous inclusions, with moving bubbles, have been found by Edwin Roedder and H. E. Belkin in olivine and pyroxene crystals from chondrules in a Chinese meteorite. Lu Huanzhang, a scientist visiting the USGS fluid inclusion laboratory, from Kweiyang, P.R.C., brought with him a part of the large Jilin ("Kirin" in the older orthography) chondritic meteorite that fell in 1976. There are many silicate glass inclusions in it, as has been reported in a series of Chinese studies, but the investigators have found planes of secondary inclusions and a few possible primary inclusions, with small moving bubbles, in the olivines of rimmed and other chondrules. The inclusions are small, mainly 3–4 μm in length, and appear to be water, not CO_2 . The inclusions present a paradox: how could such fluid be trapped in the olivine of a chondrule? This trapping would require considerable pressure (and hence depth of burial) as olivine reacts with water below approximately 500° C, and there is no evidence of serpentine. Does this mean that the chondrules accumulated into a body of planetary size which was subjected to hydrothermal effects under pressure and was subsequently disaggregated? The presence of abundant glass inclusions in these same mineral grains effectively precludes such metamorphism, and all the many theories of chondrule formation involve very high temperatures and very low pressures, under which water of this density would be impossible.

These are not the first fluid inclusions to be reported from meteorites. Other than some unsubstantiated claims, previous studies have found them in crystals of feldspar and a phosphate phase from Peetz (Fieni and others, 1978) and in an Antarctic achondrite (an igneous rock; Ashwal and others, 1981), but both of these come from mineralogical environments in which liquid water would be much less anomalous than in olivine of chondrules. All this work, as well as some additional discoveries in other meteorites, is summarized by Warner and others (1982).

Cogenetic volcanic and granitic rocks of Miocene age in the Questa caldera, northern New Mexico

Large structural and topographic relief in the Sangre de Cristo Mountains of northern New Mexico, along the east margin of the Rio Grande rift zone, permits petro-

logic comparisons between Miocene rocks of the Latir volcanic field and batholithic granitic rock interpreted as representing a cogenetic subvolcanic magma chamber. Investigations by P. W. Lipman indicate that volcanism began with outpouring of calc-alkaline lavas and emplacement of mudflow breccias from several central volcanoes; it culminated with eruption of a large-volume ash-flow sheet of alkali rhyolite that extended at least 45 km from its source, now marked by the Questa caldera. Lavas erupted just prior to pyroclastic activity; associated caldera collapse became increasingly alkalic and silicic and a major volcano of comenditic rhyolite near the east margin of the subsequent caldera developed. The granitic rocks include several isolated plutons at present erosional levels, but contact geometry and gravity data indicate that they connect at shallow depth to form a composite batholith about 15 by 30 km in plan dimensions. Calc-alkaline biotite-hornblende quartz monzonite (62–64 percent SiO_2) locally grades upward into biotite granite (76 percent SiO_2) below subhorizontal roof rocks. The geometry of the plutons and nature of compositional variations indicate that the Questa caldera collapsed into the originally uppermost part of the batholith. Most of the batholithic rocks are notably less alkalic than the caldera-related rhyolitic welded tuff and lava that they intrude, but within the caldera area rhyolitic dikes, small aplitic plutons, and porphyritic alkalic margins of the main granitic mass are compositionally similar to the ash-flow tuff and related lava flows. The alkalic granite is locally characterized by sodic amphibole and pyroxene (riebeckite and aegirine) as well as by such elements as zirconium, niobium, and yttrium in high concentrations that are similar to those in volcanic rhyolites of the caldera. Accordingly, the alkalic granite and associated rhyolitic intrusions are interpreted as early phases of the subvolcanic magma chamber quenched at the time of rhyolitic volcanic activity.

The changing sequence of differentiation in the Questa magma chamber—from initial calc-alkaline for postcaldera magmatism—supports interpretations of alkalic magmatism by mechanisms related to volatile buildup. The important molybdenum mineralization at Questa is related to the postcaldera calc-alkaline activity, rather than to buildup of volatile pressures and alkalic differentiation at the time of caldera formation. The Latir volcanic field and Questa caldera offer exceptional opportunities to make comparisons between volcanic activity, subvolcanic plutonism, hydrothermal activity, and associated mineralization.

Uranium-lead isotopic ages from Sierra Nevada batholith, California

J. G. Moore (USGS) and J. H. Chen (California Institute of Technology) report that the results of 140 U-Pb

mineral ages taken from 82 granitic masses in the south-central Sierra Nevada are consistent with and extend those reported by Stern and others (1981) in the central Sierra Nevada to the north of this study area. The new results do not differentiate the five cyclic epochs of plutonism proposed by Evernden and Kistler (1970) on the basis of K-Ar dating. Triassic plutons are localized on the east side of the batholith. Jurassic plutons are isolated masses within the Cretaceous batholith and occur south and east of the Triassic plutons east of the Sierra Nevada in the western Sierra foothills, principally north of 37 degrees north latitude. Following emplacement of the Jurassic plutons no granitic intrusion occurred for 37 m.y. The Late Jurassic (148 m.y.) Independence dike swarm was intruded in a zone 350 km long and 30 km wide at the beginning of this period of no granite plutonism. The dike injection probably represents a period of crustal extension at the eastern margin of the Sierra Nevada. Intrusion of Cretaceous granitic plutons in large volume began about 120 m.y. ago in the western Sierra Nevada and migrated relatively steadily eastward to the area of the present Sierra crest at a rate of 2.7 mm/yr. This slow migration may result either from parent magma generation at successively deeper levels or from a general flattening of the subduction system. The abrupt termination of Sierran plutonism 80 m.y. ago may have resulted from an increased rate of convergence of the American and eastern Pacific plates and rapid flattening of the subduction system. U-Pb ages determined from a group of nested plutons, the Giant Forest-alaskite sequence in Sequoia National Park, indicate that the time of emplacement of the entire sequence is relatively short (1-2 m.y.) and cooling of the plutonic complex took about 3 m.y. from the margin toward the center. Comparison among isotopic ages determined by different methods such as zircon U-Pb, sphene U-Pb, hornblende K-Ar, and biotite K-Ar suggests that the zircon U-Pb ages can generally approximate the emplacement age of a pluton. However, some plutons probably contain "inherited" or "entrained" old zircons, and the zircons of some samples are disturbed by younger thermal and metamorphic events.

Geochemical, isotopic, and petrologic studies of an Archean granite, Owl Creek Mountains, Wyoming

Rb-Sr analyses by C. E. Hedge of whole-rock samples of an Archean granite from the Owl Creek Mountains, Wyoming, yield an age of 2,704 plus or minus 24 m.y. Muscovite-bearing samples yield results that indicate hydrothermal alteration at approximately 2,300 m.y. This event was sufficiently intense to cause partial

resetting of zircons. Zircons were also affected by Laramide and possibly Precambrian uplift.

Petrogenetic modeling of the granite by Q-mode factor analysis by J. S. Stuckless and A. T. Miesch (USGS) and D. B. Wenner (University of Georgia) yields a five end-member solution. The end members are interpreted to be a series of initial liquids (represented by two end members), a series of initial solids (represented by two end members), and a solid that was fractionally crystallized. The evolution of the magma may have consisted of either two distinct stages of fractional crystallization, or alternatively, the first stage may have been fractional fusion. By either interpretation, the initial liquid compositions for each sample can be correlated with whole rock $\delta^{18}\text{O}$ values. The $\delta^{18}\text{O}$ values also correlate with initial $^{87}\text{Sr}/^{86}\text{Sr}$ and $^{208}\text{Pb}/^{204}\text{Pb}$ ratios. These correlated variations reflect inhomogeneities in the protolith which may have been similar to the diverse suite of metamorphic rocks intruded by the granite. The two-stage history of the magma indicated by either interpretation of the petrogenetic model is compatible with derivation of or initial differentiation at approximately 3 kbar and near water-saturated conditions followed by differentiation at a lower pressure of perhaps 1.0 to 0.5 kbar.

The granite locally hosts subeconomic uranium deposits. Analysis of whole-rock U-Th-Pb systematics by Stuckless, I. T. Nkomo, and K. A. Butt, shows that the uranium deposits could have formed from uranium leached from other parts of the granite during early Laramide time or shortly before. Unlike other Wyoming granite with similar isotopic systematics and uranium distributions (Stuckless and Nkomo, 1978), the granite of the Owl Creek Mountains is not spatially associated with economic deposits. This lack of economic deposits is attributed to the small areal extent of the granite, the lesser amount of leaching in terms of both depth and weight loss per unit volume, and timing of leaching which apparently predates the deposition of sediments that elsewhere in Wyoming host uranium ore.

Reversal of normal role of thorium in fractional crystallization

Thorium is considered by many French geochemists to be among the most hygromagmaphile of elements where hygromagmaphile is defined as denoting strong affinity of an element for the residual liquid during fractional crystallization (Treuil and Varet, 1973). Accordingly, in plotting their correlation diagrams, Villemont and others (1982) used thorium as a reference with which to compare the behavior of all other elements. This approach seems generally reasonable so long as the thorium content of the initial liquid is in the normal low

range. George Phair has found, however, that where the thorium content of the initial liquid is above 50 ppm, the role of thorium in fractional crystallization is commonly the exact reverse of that described above. The thorium content is highest in the earliest members of the differentiating sequence and decreases progressively in the later members.

The root of the difference in behavior lies in the early crystallization of monazite from the thorium-rich liquid. On the basis of petrographic evidence, the early formation of monazite appears to correlate with the failure of sphene to crystallize. Sphene is an accessory mineral that normally accounts for the major fractions of the nonleachable-thorium content of most granitic rocks. The failure of sphene to crystallize in turn correlates with a lower than normal CaO concentration in the magma at the particular stage of magmatic differentiation. The reversal of the role of thorium is well documented on a batholithic scale in the thorium-rich Silver Plume Granite of Middle Proterozoic age in Colorado, in which the high thorium content is known to be concentrated in monazite. Thorium is present at levels as high as 125 ppm in the earliest members, mafic granodiorite and mafic quartz monzonite (minimum SiO₂ content 64 weight percent), and decreases linearly with decrease in MgO and CaO and with increase in SiO₂ in the later members. Thorium ultimately falls to levels as low as 28 ppm in the end-member granites. Where, however, the earliest member in a given complex is granite, as in the Silver Plume dike swarm that intrudes the Boulder Creek batholith, the granite may be highly enriched in thorium up to 100 ppm, the thorium content falls rapidly with small systematic decreases in CaO and MgO and increases in SiO₂ during the final states of fractional crystallization.

Petrology of alkaline intrusive rocks, western Montana

Syenites from Haines Point and Skalkaho and syenite dikes from Rainy Creek, Mont., lack modal and normative nepheline and typically contain 0–5 percent modal and normative quartz, according to T. J. Armbrustmacher. All the syenites contain anomalously high concentrations of barium, strontium, manganese, and vanadium relative to crustal averages. Pyroxenites from Skalkaho tend to be slightly quartz normative; pyroxenites from Rainy Creek tend to be slightly nepheline normative. Pyroxenites from Skalkaho contain normative diopside but no normative hypersthene or olivine; pyroxenites from Rainy Creek contain normative diopside and olivine but no normative hypersthene. Pyroxenites from both localities have trace-element abundances similar to average alkaline ultramafic rocks. Geochemical variations between different petrographic varieties of pyroxenite within the same complex

are minor. Carbonatite (sovite) from a dike at Rainy Creek contains abundant strontium and barium but low amounts of niobium and rare-earth elements. Pegmatitic mafic rocks at Skalkaho are quartz normative and tend to be subalkaline in composition.

METAMORPHIC ROCKS AND PROCESSES

Lake Ellen kimberlite, Michigan: thermobarometry of mantle inclusions

E. S. McGee and B. C. Hearn, Jr., have completed a study on the mineralogy and petrology of inclusions from a kimberlite intrusion in northern Michigan. The poorly exposed Lake Ellen kimberlite cuts Proterozoic volcanic rocks that overlie Archean basement. A post-Ordovician age is implied by abundant dolomite inclusions of probable Ordovician age. Ground magnetic surveys show a main kimberlite that is 200 m in diameter and a smaller body that is 25 by 90 m in diameter and lies 30–100 m to the northeast. Xenocrysts and megacrysts are ilmenite (abundant, 13–15 percent MgO), pyrope-almandine and chromium-pyrope (up to 9.3 percent Cr₂O₃), chromium-diopside (up to 4.5 percent Cr₂O₃), olivine (Fo 91), enstatite, and phlogopite. During intrusion the kimberlite assimilated crustal schist and granulite, and a heterogeneous upper mantle of eclogite, garnet pyroxenite, and garnet peridotite. Eclogites, up to 3 cm in size, have granoblastic equant or tabular textures and consist of jadeitic clinopyroxene (cpx) (up to 8.4 percent Na₂O, 15.3 percent Al₂O₃) + pyrope-almandine + rutile + -kyanite + -sulfide. Garnet pyroxenite contains pyrope (0.44 percent Cr₂O₃) + cpx (0.85 percent Na₂O, 0.63 percent Cr₂O₃) + Mg-Al spinel. Garnet peridotites are represented only by separate pyrope and cpx grains or by granular composite pairs of pyrope (2.5–5.5 percent Cr₂O₃) and cpx (2.1–4.8 percent Na₂O, 1.2–4.5 percent Cr₂O₃). The latter pyroxenes give Lindsley-Dixon temperatures (T) of 880–1120° C. Garnet-cpx pairs from eclogites and garnet pyroxenites give Ellis-Green T's of 900–1046 and 785–913° C, respectively. Pressures of equilibration can only be inferred. Presence of kyanite in eclogites indicates pressures (P) greater than 18–20 kbar. Projection of T's onto a 44 mw/m² continental geotherm implies pressures of 33–46 kbar for eclogites, 24–35 kbar for garnet pyroxenites, and 25–53 kbar for peridotitic garnet-cpx pairs. Pressures of one eclogite and three peridotitic pairs imply derivation from within the diamond stability field. The estimated P–T data and the presence of kimberlite in northern Michigan indicate that bedrock sources of the diamonds found in glacial deposits in the Great Lakes area could lie within the Northern United States.

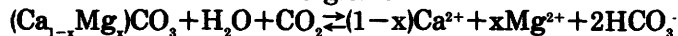
GEOCHEMISTRY OF WATER AND SEDIMENTS

Ground-water chemistry of the Aquia aquifer in southern Maryland

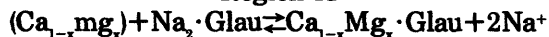
F. H. Chapelle completed a study of the ground-water chemistry of the Aquia aquifer (in the Paleocene Aquia Formation). This aquifer, in southern Maryland, occupies three regions, which are characterized by distinctly different water compositions. Region I is 43 km wide and parallels the outcrop. Water in Region I has relatively high calcium (30 mg/L), magnesium (10 mg/L), and bicarbonate (150 mg/L) concentrations. Sodium concentrations in Region I are relatively low (2 mg/L). Region II, parallel to and downgradient from Region I, is 37 km wide. Water in Region II is characterized by constant bicarbonate, increasing sodium, decreasing calcium, and decreasing magnesium concentrations. Region III is the farthest downgradient and is characterized by low calcium (2 mg/L), low magnesium (5 mg/L), high bicarbonate (300 mg/L), and high sodium (100 mg/L) concentrations.

The major mineralogic constituents of the Aquia aquifer are quartz, glauconite, and shell material. Chemical models based on this mineralogy were developed to describe changes in the water chemistry of each region. These models are:

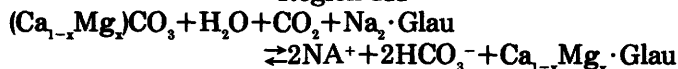
Region I



Region II



Region III



These models were verified by comparing predicted molar ratios of dissolved species to molar ratios obtained by linear regression.

Bottom-sediment chemistry of the Saw Mill River, Westchester County, New York

R. J. Rogers reported that bottom sediments in the lower 5.0 km of the Saw Mill River are enriched in copper, lead, and zinc, compared with those upstream. Enrichment factors for the three metals, calculated through the use of metal concentrations in the 1–2 mm fraction of sediment, are 3.8, 5.5, and 5.0, respectively. These findings are in good agreement with land-use patterns, as the highest concentration of industry is in the lower section of the river basin. Concentrations of As, Cd, Cr, Co, Hg, and Ni in the bottom sediments are, in

general, near or below their respective analytical detection limits, and therefore no enrichment of any of these metals is discernible.

Chlordane, dieldrin, PCB's, and DDT and (or) its metabolites DDD and DDE occur in bottom sediments throughout the river. However, preliminary data suggest that, of these organochlorine compounds, only PCB's are enriched in the downstream bottom sediments.

Geochemistry of water from Cretaceous aquifers in the Southeastern United States: Mississippi, Alabama, Georgia, and South Carolina

Preliminary evaluation of existing and new chemical data from Cretaceous aquifers in the Southeastern Coastal Plain, by Roger W. Lee, indicates several significant geochemical aspects of ground water from these aquifers:

1. Excessive iron (15 mg/L) is present in several areas down dip of the Fall Line, especially in the Columbus, Miss., area.
2. High boron (8 mg/L) is present in the deeper parts of the Cretaceous aquifers, notably in coastal South Carolina.
3. High fluoride (10 mg/L) is present, especially in South Carolina, as previously reported.
4. Unadjusted carbon-14 ages indicate freshwater as old as 35,000 yr B.P. in eastern Mississippi Cretaceous aquifers.

According to Lee, preliminary mass-transfer simulation indicates that increasing dissolved solids down the hydraulic gradient in the freshwater parts of the aquifers may be primarily due to calcite dissolution, exchange of sodium for aqueous calcium, and increasing aqueous carbon dioxide.

The freshwater boundaries in the Cretaceous aquifers are seawater or brines known to be present down dip. The nature of these interfaces is being studied by Lee, and there is good evidence that freshwater is present in deeper aquifers below shallower saline waters in Cretaceous aquifers throughout the Southeastern Coastal Plain.

Physical and chemical properties of fine-grained sediments

During a comprehensive study of fine-grained sediments from the geopressed zone of the northern Gulf of Mexico Basin, coordinated by T. F. Kraemer, a massive "shale" formation was cored and samples were subjected to a number of physical and chemical analyses that revealed basic information on the nature of this little-studied type of sediment. Nuclear magnetic

resonance and differential scanning calorimetry by A. Tice and J. Oliphant (U.S. Army Cold Regions, Research Laboratory, Hanover, N.H.) revealed the sediments to be quite dehydrated, generally having less than one monolayer of water covering the particles. Chemical analysis by F.T. Manheim showed the shale to have high chloride content. This, in combination with the low water content, indicates this shale did not undergo the classical process of compaction that results in saline water expulsion with development of several monolayers of anion-free water surrounding the clay particles. Alternatives to this theory are now being developed.

Radiometric studies of geopressed systems

T. F. Kraemer has been investigating the behavior of naturally-occurring radionuclides in geopressed systems in the northern Gulf of Mexico Basin. He has studied uranium, thorium, radium, and radon isotopes and has developed uses for these various isotopes as natural tracers to study water-rock interactions and aquifer processes. For example, Kraemer has shown that the $^{228}\text{Ra}/^{226}\text{Ra}$ ratio in brine reflects the Th-U ratio in the aquifer matrix material and can be used as an indicator of aquifer quality. He has also shown that radon segregates in a gas phase within the aquifer, and a measurement of ^{226}Ra and ^{222}Rn in produced fluids can often indicate the presence of a low (nonflowing) free-gas saturation in the aquifer.

Temperature dependence of the gas-film coefficient

R. E. Rathbun and D. Y. Tai determined the temperature dependence of the gas-film coefficient of the two-film model by using laboratory measurements of water evaporation rates. The coefficient increased 0.94 percent per °C. By using this temperature function and a wind function derived from the literature, these investigators developed an equation for predicting the gas-film coefficient for the volatilization of organic compounds from streams and rivers. Adjustments of the coefficient for different organic compounds were based on the molecular-diffusion coefficient or the molecular weight.

Determination of chloride and bromide in water

D. Y. Tai and R. E. Rathbun established the precision of specific ion electrodes for the determination of chloride and bromide in water. Ten replicates, each of 10, 25, and 125 mg/L of chloride, had relative standard deviations of 1.40, 3.80, and 2.40 percent, respectively. Ten replicates, each of 0.5, 2, and 10 mg/L of bromide, had relative standard deviations of 1.04, 2.21, and 2.28 percent, respectively. The bromide electrode generally

stabilized more rapidly than the chloride electrode. Control of the sample temperature was important in obtaining stable readings.

ISOTOPE AND NUCLEAR GEOCHEMISTRY

ISOTOPE TRACER STUDIES

Evolution of continental crust as inferred from a hafnium isotope study

Using a newly developed hafnium isotope technique, P. J. Patchett, Olavi Kouvo, C. E. Hedge, and Mitsunobu Tatsumoto measured initial $^{176}\text{Hf}/^{177}\text{Hf}$ ratios for many samples of continental crust of 3.7–0.3 b.y. age. Results are based chiefly on zircons (1 percent hafnium) and whole rocks: zircons were shown to be reliable indicators of initial hafnium when properly chosen on the basis of U-Pb studies. Pre-3.0 b.y. gneisses apparently were derived from an unfractionated mantle, but both depleted and undepleted mantle are evident as magma sources from 2.9 b.y. age to the present. Rocks representing major episodes of crustal growth at 2.8, 1.8, and 1.7 b.y. ago all show gross heterogeneity of $^{176}\text{Hf}/^{177}\text{Hf}$ reflecting magma sources from epsilon-Hf = 0 to +14, or about 60 percent of the variability of the present mantle.

The approximate epsilon-Hf = 2epsilon-Nd relationship in ancient and modern igneous rocks shows that $^{176}\text{Lu}/^{177}\text{Hf}$ fractionates in general twice as much as $^{147}\text{Sm}/^{144}\text{Nd}$ in mantle melting processes. This allows an estimation of the relative value of the unknown bulk-solid/liquid distribution coefficient for hafnium. $D_{\text{Lu}}/D_{\text{Hf}}=2.3$ holds for most mantle source regions. For garnet to be an important residual mantle phase, it must hold hafnium strongly in order to preserve the observed Hf-Nd isotopic relationship.

The ancient hafnium initials are consistent with incorporation of only a small proportion of recycled older cratons in new continental crust and with quasicontinuous, episodic growth of the continental crust with time. However, recycling of crust that is less than 150 m.y. old cannot realistically be detected by using hafnium initials. The mantle shows clearly the general positive epsilon-Hf resulting from a residual geochemical state at least back to 2.9 b.y. ago and seems to have repeatedly possessed a similar degree of heterogeneity rather than a continuously developing depletion.

Neodymium and strontium isotopes in inclusions from the Sierra Nevada

Sm-Nd and Rb-Sr systematics were examined by M. A. Domenick, R. W. Kistler, F. C. W. Dodge, and M. Tatsumoto for eight upper mantle and lower crustal

xenoliths, a xenolith-bearing trachyandesite, and a granodiorite intruded by the trachyandesite in the Sierra Nevada batholith. Isotopic heterogeneity is shown by the xenoliths: $^{143}\text{Nd}/^{144}\text{Nd}$ ranges from 0.5117 to 0.5131, and $^{87}\text{Sr}/^{86}\text{Sr}$ from 0.7031 to 0.7333. These ranges are similar to those of the plutonic rocks of the batholith. This similarity suggests that the xenoliths, believed to be representative of mantle and crustal reservoirs, may approximate the diverse source regions from which the varied granitic rocks of the batholith were derived and that the Sr-Nd isotopic correlation seen in granitic rock may not be due to simple mixing of two end-member components.

The subgranitic crust in this part of the Sierra apparently consists of metamorphosed sedimentary and igneous rocks. The mantle beneath the Sierra Nevada is isotopically heterogeneous both vertically and laterally.

Isotopic composition of uranium and thorium in crystalline rocks

J. N. Rosholt has found that the ^{238}U , ^{234}U , ^{230}Th , ^{232}Th system can reveal geochemical and physicochemical processes that cause open system behavior of uranium and its daughter products in crystalline rocks, provided the disturbance occurred within the last 0.5 m.y. To the extent that uranium-series disequilibrium is a product of rock-water interaction, its measurement may help evaluate the effective permeability of unfractured and macroscopically-fresh rocks and can be used to assess geologically recent uranium mobility in sealed fracture zones.

This radioactive decay system has been investigated in 84 silicic crystalline rocks obtained from drill cores, surface and near-surface samples in California, Wyoming, Colorado, and Illinois. Results of these analyses, displayed on ternary diagrams with apexes for ^{238}U , ^{234}U , and ^{230}Th , indicate five predominant geochemical processes that affected uranium in the rock: (1) bulk uranium leaching where ^{238}U and ^{234}U were removed with little or no fractionation; (2) preferential ^{234}U leaching by alpha-recoil displacement (^{234}U recoil loss) with lesser ^{238}U loss; (3) ^{234}U recoil loss with little or no ^{238}U loss; (4) uranium assimilation where both ^{238}U and ^{234}U were added with present-day $^{234}\text{U}/^{238}\text{U}$ activity ratios varying from 0.8 to 1.2; and (5) addition of ^{234}U and ^{230}Th by daughter emplacement processes ($^{234}\text{U} + ^{230}\text{Th}$ recoil gain). The data indicate that (1) only unfractured rock from drill cores is in radioactive equilibrium, (2) ^{234}U recoil loss and preferential ^{234}U leaching predominates in surface and near-surface rocks, and (3) $^{234}\text{U} + ^{230}\text{Th}$ recoil gain and uranium assimilation occur predominantly in drill-core samples of fractured rocks. Uranium leaching preferential, ^{234}U leaching, or ^{234}U recoil loss also occur in some unfractured rocks from drill holes. Ternary diagrams are especially useful in distinguishing between process numbers 2 and 3 and between process numbers

4 and 5, both of which are more difficult to visualize from isotopic ratios only. Independent evidence for the existence of process number 5 is important because this process affects many types of alluvial deposits and is the basis of an empirical open-system model for uranium-trend dating of Quaternary deposits (J. N. Rosholt, 1980).

The predominant process associated with incipient weathering is ^{234}U recoil loss, whereas uranium assimilation and $^{234}\text{U} + ^{230}\text{Th}$ recoil gain accompany substantial penetration of water into fractures and weathered zones. Nevertheless, $^{234}\text{U}/^{238}\text{U}$ ratios near unity may be found in significantly weathered rocks not because of undisturbed radioactive equilibrium but because these ratios represent only a transitional state in the weathering profile. Incipient weathering generally produces a relative deficiency of ^{234}U , but as weathering progresses there is also a tendency for recoil gain incorporation of ^{234}U that ultimately produces an excess of ^{234}U in intensively weathered rocks. The three parts of weathered rock that occur in the upper one meter of the basement rock in UPH-3 (Illinois deep drill hole) appear to be examples of such isotopic evolution. The samples from greater depth in the UPH-3 drill core are the closest to radioactive equilibrium for any suite of rocks included in this study, and they demonstrate that equilibrium during the last 0.5 m.y. is maintained over a substantial vertical distance in unfractured, petrographically fresh crystalline rock.

Plumbic prospecting in the northern Rocky Mountains

Bruce Doe and Maryse Delevaux determined the lead-isotope composition of 83 galenas from western Montana and Idaho. The study was designed to detect any correlation between the size of a deposit and its lead-isotopic composition. A correlation had previously been demonstrated for deposits of the southern Rocky Mountain region, where the underlying basement is of Proterozoic age. In the northern Rockies the basement is Archean in age. The new data indicate the same correlation between size and composition for this region. A number of prospects appear to have significant economic potential, including two deposits in limestone in the Dillon quadrangle. These two show lead-isotope values that may indicate the presence of a pluton at depth.

STABLE ISOTOPES

Stable isotope systematics of copper-silver occurrences in the Belt Supergroup

Stable isotope studies by R. O. Rye, J. F. Whelan, and J. E. Harrison indicate that subeconomic as well as economic copper occurrences in the Belt Supergroup de-

veloped in ancient freshwater aquifers in the marine sediments.

Subeconomic copper-silver occurrences are common throughout the Belt Supergroup. At Blacktail Mountain, near Kalispell, Mont., disseminated bornite-chalcocite occurs in the upper Spokane Formation in two of five green argillite-siltite beds in a sequence of green and purple beds representing transgressive and regressive cycles in a tidal flat environment. The $\delta^{34}\text{S}$ of disseminated barite (19.5 ± 1.5 ‰) in the barren red and green beds indicates the presence of seawater sulfate in the depositional basin. The $\delta^{13}\text{C}$ and $\delta^{18}\text{O}$ of carbonates (-6.4 ± 1.4 and 13.0 ± 0.7 ‰, respectively) and the $\delta^{34}\text{S}$ of barite and sulfides (-0.2 ± 1.0 ‰) in the mineralized beds indicate a strong influence on continental ground waters during diagenesis and later mineralization.

Ore-grade disseminated copper-silver mineralization occurs in the deltaic or beach and bar quartzites of the upper Revett Formation at Spar Lake in northwestern Montana. Diagenesis of carbonates also occurred in the presence of freshwater as indicated by their very low $\delta^{13}\text{C}$ and $\delta^{18}\text{O}$ (-13.0 ± 2.5 ‰ and 11.3 ± 0.7 ‰, respectively). However, later disseminated copper-sulfide mineralization ($\delta^{34}\text{S} = 7.5 \pm 1.5$ ‰) was from ore fluids with a large seawater sulfate component derived from the interior of the sedimentary basin.

Mineralogy and stable isotope geochemistry of hydrothermally altered rocks from the East Pacific Rise and the Mid-Atlantic Ridge

Mineralogical and isotopic variations observed in altered glassy and crystalline rocks from the East Pacific Rise and Mid-Atlantic Ridge provide information about the temperatures of alteration and seawater/rock ratios for various hydrothermal regimes within the oceanic crust. J. R. O'Neil (USGS) and D. S. Stakes (California Institute of Technology) have found that a systematic increase in alteration temperature is evident for the glassy rocks in the sequence: (1) nontronite and celadonite vesicle fillings (35°C); (2) saponite-rich pillow breccias ($130\text{--}170^\circ\text{C}$); (3) calcite-rich greenstone breccias and epidote-rich greenstone ($200\text{--}250^\circ\text{C}$). These results include the highest temperatures thus far reported for saponite formation.

The "seawater-dominated" hydrothermal alteration process that formed the saponite-rich pillow breccias is characterized by high water/rock ratios ($>50:1$), low to moderate temperatures, a seawater origin for most of the carbon in vein calcites ($\delta^{13}\text{C} = 0$) and the predominance of iron-rich saponite and calcite as secondary phases. Greenstones (chlorite-quartz-epidote) and greenstone breccias (chlorite-quartz-albite-calcite) are altered in a "rock-dominated" system with lower water/rock ratios ($50:1$ to $<1:1$), higher temperatures, and vein calcites with carbon that is principally of magmatic origin ($\delta^{13}\text{C} = -4$). The crystalline rocks (diabase,

gabbro, and metagabbro) are affected to varying degrees by pervasive high-temperature seawater interactions that commence soon after solidification and produce varying proportions of fine-grained secondary minerals including talc, smectite, chlorite, vermiculite, actinolite, and sodic plagioclase. Hydrothermal solutions, derived from alteration of the crystalline rocks, are of the appropriate temperature and isotopic composition to alter the overlying glassy rocks to the observed mineralogies as well as being the source of metal-rich deposits associated with the oceanic spreading centers.

Strontium-isotope composition of plutons in the southern Snake Range, Nevada

Six discrete plutons are exposed within $9,000\text{ km}^2$ in the southern Snake Range of eastern White Pine County, Nev. These granitoids range in age from Jurassic to Tertiary. Strontium and oxygen isotopic studies by D. E. Lee, R. W. Kistler, and A. C. Robinson (unpub. data, 1982) show initial $^{87}\text{Sr}/^{86}\text{Sr}$ ratios ranging from 0.707145 to about 0.7165, $\delta^{18}\text{O}$ values ranging from -2.6 to 13.2 per mil, and SiO_2 contents ranging from 63 to 76 weight percent. The petrologic types exposed include calc-alkalic rocks and two different types of two-mica granites. The younger granitoids were emplaced at progressively more shallow depths and generally crystallized from more evolved magmas. Each of the intrusive types present in the southern Snake Range is also present elsewhere in the eastern Great Basin, but the southern Snake Range appears to be distinguished by the grouping of all these intrusive types within a relatively small area. The timing of the igneous events described here is remarkably similar to that found in the Ruby Mountains of Elko County, Nev., about 200 km northwest of our study area, but the Ruby Mountains have been more deeply eroded than the southern Snake Range.

Negative $\delta^{18}\text{O}$ values in cataclastic plutonic rocks

In cooperation with R. F. Marvin, H. H. Mehnert, Irving Friedman, and J. D. Gleason of the Isotope Geology Branch, D. E. Lee (unpublished data, 1982) has found that four plutons tens of kilometers apart in eastern White Pine County, Nev., have been deformed or even cataclastized by postcrystallization movement along spatially related thrust faults. These plutons are located in the Young Canyon-Kious Basin area of the southern Snake Range, in the Kern Mountains, and in the Warm Springs and the Cherry Creek areas of the northern Egan Range. Deformation of these plutons has resulted in the reduction of both the $^{18}\text{O}/^{16}\text{O}$ ratios and the apparent K-Ar ages of the affected rocks. In each case, there apparently was oxygen isotope exchange between the rock and meteoric waters at about the same time as

the constituent micas were degassed by stresses resulting from movement along the thrust faults.

The Young Canyon-Kious Basin area intrusive was fragmented by postcrystallization movement along the spatially related Snake Range decollement as recently as 17–18 m.y. ago, and $\delta^{18}\text{O}$ values as low as -2.6 per mil have been determined for the cataclastic intrusive. Cataclasis and (or) deformation of the Kern Mountains and northern Egan Range intrusive rocks occurred 25–35 m.y. ago and has resulted in $\delta^{18}\text{O}$ values as low as -5.4 per mil.

A study of the relevant maps shows the same spatial relationship between intrusive rocks and regional thrust faults in other parts of the eastern Great Basin. It is important to determine which of these other plutons may also have been cut by late movement along the nearby thrust faults not only from the standpoint of the geologic history of the area but also for very practical reasons.

Where an intrusive has been decapitated by a regional thrust fault the possibility exists that any ore deposits formed in the country rock above the magma chamber may have been moved away from their "roots" by post-mineralization movement along the fault. In the area of this study, the upper plates have moved toward the east or northeast. It is possible that some of the ore deposits of the area may be found in the valley fill to the east or northeast of the plutons with which they are genetically related.

Radiometric ages of two-mica granites of northeastern Nevada

Three representatives of a unique (muscovite-phenocrystic) type of two-mica granite are exposed along a north-south trend about 225 km long in northeastern Nevada (Lee and others, 1981). This type of two-mica granite is distinguished in part by the presence of large phenocrysts of muscovite, and practically all of the biotite in the rock is present as euhedra within this muscovite. Chemical, mineralogical, and isotopic data collected by D. E. Lee, J. S. Stacey, and Lynn Fischer (unpublished data, 1982) suggest that the muscovite-phenocrystic two-mica granites crystallized from anatectic magmas formed from late Precambrian and Lower Cambrian pelitic sediments.

Near the southern part of the trend just described, three examples of a more common (equigranular) type of two-mica granite are exposed in which muscovite and biotite are present as discrete crystals. The equigranular-type two-mica granites may also have evolved through anatexis of the pelitic sediments.

A recent study (Lee and others, 1980) presents radiometric ages for zircon recovered from the muscovite-phenocrystic two-mica granite of the Kern Mountains, White Pine County, Nev. Together with previously re-

ported K-Ar and Rb-Sr age data, this new information suggests that all three of the muscovite-phenocrystic two-mica granites probably crystallized during Late Cretaceous time. The equigranular two-mica granites appear to range in age from Jurassic to Cretaceous, and possibly to Tertiary.

Lee and others (unpub. data, 1982) also present radiometric age data for zircons from the Osceola intrusive of the southern Snake Range, Nevada, and from the Notch Peak intrusive of the House Range, western Utah. Both of these calc-alkalic intrusives are Jurassic in age. This Jurassic igneous event was rather widespread in the region.

$\delta^{18}\text{O}$ and δD anomalies as earthquake precursors

δD and $\delta^{18}\text{O}$ analyses of certain ground waters in seismically active regions of California have been shown by J. R. O'Neil and C. Y. King to be sensitive indicators of changes in local hydrological regimes that precede or accompany earthquakes. For example, there was a clear-cut lowering of both the $\delta^{18}\text{O}$ and δD values of spring water at the Mission Farm Campground near San Juan Bautista about one month prior to the largest and closest event ($m = 4.8$) that occurred during a 18-month period of bimonthly analyses. Inasmuch as both isotopic ratios changed in the same direction, another ground water must have entered the system, possibly by the (temporary?) creation of a connection between two aquifers. Dramatic concurrent changes took place in the chemistry of this fluid as well. The hydrological regime at this site is undoubtedly delicate, but the isotopic anomalies observed there so far look promising for earthquake prediction.

Atmospheric carbon dioxide

Irving Friedman now has a year's record of CO_2 data at the South Pole and Mauna Loa, as well as a 6-month record at Samoa and Point Barrow, Alaska. The data show changes in $\delta^{13}\text{C}$, some of which can be correlated with seasonal (photosynthetic) changes in CO_2 abundance. Other $\delta^{13}\text{C}$ changes may be due to air mass trajectory variations.

ADVANCES IN GEOCHRONOMETRY

K-Ar ages of bentonites in the Seabee Formation, northern Alaska

M. A. Lanphere (USGS) and Irving Tailleux (NPRA) completed a geochronologic study of bentonites in Alaska that provides documentation for a point on the Cretaceous time scale. The Shale Wall Member, the lower member of the Upper Cretaceous Seabee Forma-

tion, which is present over much of north-central Alaska, is characterized by abundant interbedded bentonites that contain biotite. The Shale Wall Member contains a megafauna consisting of ammonites and pelecypods. *Inoceramus labiatus* (Schlotheim) has a worldwide distribution, and *I. labiatus* Zone is considered the basal faunal zone in the Turonian stage. *Sciponoceras subdelicatulus* from the Shale Wall Member has close affinities with ammonites from the latest Cenomanian *S. gracile* Zone of the Western Interior of the United States. Therefore, the best age assignment for the Shale Wall Member is latest Cenomanian and earliest Turonian.

K-Ar ages were measured on biotite from six bentonite beds in three different coreholes from the Umiat and Simpson areas of the National Petroleum Reserve in Alaska. The K-Ar ages range from 91.5 ± 0.9 m.y. to 93.6 ± 1.2 m.y. and indicate an age of about 92 m.y. for the highest occurrence of *Inoceramus labiatus* in the three coreholes. In order to tie the Shale Wall ages into the Late Cretaceous time scale constructed by J. D. Obradovich and W. A. Cobban (1975), a K-Ar age was measured on biotite from a bentonite within the *I. labiatus* Zone in the Marias River Shale in Montana. The age of 89.2 ± 0.7 m.y. suggests there is a real difference of about 3 m.y. in the age of the *I. labiatus* Zone in Montana and northern Alaska. If additional work in Montana supports this pattern, then the *I. labiatus* Zone may be time transgressive.

Geochronology of granites and associated uranium occurrences, Olary Province, Australia

Detailed isotopic studies by K. R. Ludwig (USGS) and J. A. Cooper (Univ. of Adelaide) of the brannerite and davidite U-Ti-Th deposits in the Olary region, south Australia, have shown that the brannerite mineralization is directly associated with a diverse and widespread suite of granitic rocks that were all intruded into Precambrian metamorphics of the Willyama series about 1,580 m.y. ago. Early Paleozoic (Delamerian) and Tertiary disturbances to the apparently fragile isotopic systems of the brannerite and davidite largely preclude their direct use as dating tools, however.

Geochronology of roll-type uranium ores of the Felder deposit, Texas

U-Pb isotope analyses by K. R. Ludwig of rollfront uranium ores from the Felder mine, south Texas, yielded an unusually well-defined $^{207}\text{Pb}/^{204}\text{Pb}$ - $^{235}\text{U}/^{204}\text{Pb}$ isochron age of 5.07 ± 0.15 m.y., despite the unconsolidated and relatively low-grade nature of the ores and strong evidence for migration of ^{238}U radioactive daughters. Apparently, fault-leached H_2S in the mine immobilized quadrivalent uranium and lead as PbS and prob-

ably was responsible for the termination of roll-front migration 5 m.y. ago.

Thermoluminescence dating of silicic volcanic rocks

Analysis by R. J. May of the thermoluminescence (TL) properties of sanidine separates from rhyolite and rhyodacite of known age shows that TL dating of young silicic volcanic rocks through the use of sanidine is feasible over the age range 500 to 175,000 yr. The method developed for dating the full range of sanidine compositions with a single age equation will require further refinement before it will be ready for routine use.

The analyzed sanidine separates ranged in K_2O content from 7.2 to 11.4 weight percent. Preliminary spectral analysis revealed significant variations in the spectral distribution of the TL emission for individual samples that correlate closely with changes in sanidine K_2O content. Samples with low K_2O content have a significantly greater proportion of the TL emission in the blue-green part of the spectrum, in the bandwidth 450-600 nm, than do those with high K_2O contents. High K_2O sanidines have most or all of their emission in the blue part, the bandwidth approximately 350-450 nm.

When the TL data are corrected for the bias in light detection imposed by the fixed, but nonlinear with wavelength, sensitivity of the photomultiplier tube, and for difference in the innate TL sensitivity of the sanidine separates themselves, the resulting normalized TL ratios for the full range of sanidine compositions as a group increase approximately linearly with age.

An age equation was derived by using TL ratios for eight samples of sanidine of known age containing more than 10 percent K_2O . This age equation was then applied to 14 samples of sanidine from domes of the Mono Craters, Calif. The TL ages for the early, porphyritic stage of volcanism range from $9,000 \pm 1,600$ yr to $49,000 \pm 3,500$ years B.P. The TL ages are consistently older than K-Ar ages measured by G. B. Dalrymple and obsidian hydration-rind ages measured by S. H. Wood. The reason for these discrepancies is not known at present.

Thermoluminescence dating of pedogenic calcium carbonate

R. J. May and M. N. Machette have shown, by experiments on two soil sequences from New Mexico, that TL dating of pedogenic calcium carbonate is feasible within the age range of about 5,000 to at least 500,000 yr.

One soil sequence, exposed in an erosional scarp near the Bernalillo County Dump west of Albuquerque, consists of four carbonate-rich paleosols that were successively buried and preserved by recurrent movement on a normal fault and a fifth carbonate horizon now forming

in the present surface soil. The second soil sequence consists of four caliche horizons developed on surfaces of varying age bordering the Rio Grande rift near Las Cruces. Independent age control for the experiment is provided by estimates of the carbonate accumulative rates (Bernalillo sequence) and uranium-trend dating (Las Cruces sequence).

A plot of the ratio NEa/AEn (where N is the natural TL, A the laboratory induced TL, Ea the laboratory radiation dose, and En the natural radiation dose) versus control age for the Bernalillo carbonates shows the TL "age" increases linearly with the control age from about 5,000 to 500,000 yr. For the exposed soils near Las Cruces, the TL ratios also increase linearly with the control ages. The plots for both sections are virtually coincident, which shows that the effect of local factors is probably minimal and that both carbonate soils from the region can be dated with a single calibrated TL curve. The precision of the method appears to be about ± 10 percent, and has an accuracy perhaps ± 25 percent. These findings constitute a significant breakthrough in methodology for determining the ages of ancient carbonate soils.

A new reversed polarity event within the Brunhes epoch

D. E. Champion, G. B. Dalrymple, and M. A. Kuntz have documented a new, brief reversed geomagnetic polarity event within the Brunhes Normal Polarity epoch. The event is recorded in two basalt lava flows sampled in five cored drill holes in the eastern Snake River Plain. The two reversed flows are overlain and underlain by flows of normal polarity. The reversed flows record a reversed direction with an inclination of -40 to -45 degrees and a declination of about 216 degrees, these data indicating that the event was a true geomagnetic reversal and not a field excursion. The reversed flows are not petrographically suitable for dating, but the flow above and the two below the reversed flows have a weighted mean age of 0.46 ± 0.05 m.y. This reversed polarity event has also been found in sea-floor magnetic anomalies and in sediment cores. On the basis of frequency of normal and reversed radiometric polarity data within the Brunhes, the duration of the event was about 0.005 to 0.01 m.y. in length.

^{210}Pb activity and pollen dating, Potomac estuary, Virginia

Comparisons by E. A. Martin of sedimentation rates obtained by ^{210}Pb and pollen analyses of 1-m cores collected throughout the Potomac estuary show a good agreement in the majority of cores that can be analyzed by both methods. Most of the discrepancy between the methods can be explained by the analytical precision of the ^{210}Pb method and by the exactness with which time

horizons can be identified and dated for the pollen method. X-radiographs of the cores and the distinctness of the pollen horizons preclude significant displacement by reworking and (or) mixing of sediments. Differences between the methods are greatest where uncertainties exist in assigning a rate by one or both methods (^{210}Pb trends and (or) possible horizon assignments). Both methods show the same relative rates, with greater sediment accumulation being more common in the upper and middle estuary and less common toward the mouth. The results indicate that geochronologic studies of estuarine sediments should be preceded by careful observation of sedimentary structures, preferably by X-radiography, to evaluate the extent of mixing of the sediments. Generally, where mixing has occurred, time horizons, whether paleontologic or isotopic, are blurred beyond precise identification. Whenever possible, two methods should be used for dating sediments because a rate, albeit erroneous, can be obtained isotopically in sediments that are mixed; accurate sedimentation rates are also difficult to determine where the time boundary is a zone rather than a horizon, where the historical record does not provide a precise data for the pollen horizon, or where scouring has removed some of the sediment above a dated pollen horizon.

^{210}Pb geochronology, Upper Klamath Lake, Oregon

E. A. Martin and C. A. Rice have calculated rates of sedimentation from analyses of ^{210}Pb activities in cores from two shallow lakes whose mean depths are 2.4 m, Upper Klamath Lake and Euwana (Klamath County, Oregon). The results indicate that they are filling at approximately 3.0 mm/yr. Average sedimentation rates for compaction-corrected cores range from 0.9 mm/yr to 8.5 mm/yr or from 0.03 g/cm²/yr to 0.38 g/cm²/yr, respectively. Plots of excess ^{210}Pb activity versus depth show a mixing layer due to biological activity and other physical mixing that ranges in thickness from 5 to 20 cm and that is found below the sediment-water interface at all coring locations. Trace-metal analyses performed to establish baseline levels of selected elements show very low concentrations of all metals measured in cores from Upper Klamath Lake (Cd, Cu, Cr, Fe, Pb, Mn, and Zn) when compared with concentrations of these metals found in other North American lacustrine environments.

GEOHERMAL SYSTEMS

Aquifer thermal-energy storage in the Franconia-Ironton-Galesville aquifer, St. Paul, Minnesota

Six rotary-drilled observation wells, two core-drilled observation wells, and two heat-injection/withdrawal

production wells have been completed for the aquifer thermal-energy storage project in St. Paul, Minn., according to R. T. Miller. Analysis of data from inflatable-packer hydraulic tests completed for the two core-drilled observation wells indicates that four distinct hydraulic zones occur in the Franconia-Ironton-Galesville aquifer (Franconia Formation, Ironton Sandstone and Galesville Sandstone of Cambrian age). Calculated values of horizontal hydraulic conductivity ranged from 0.03 to 1.22 m/d. Step-drawdown well-efficiency tests were made on the two production wells. On the basis of these tests, drawdowns of 22.25 and 48.76 m were estimated for the well bore for pumping rates of 18.93 and 37.86 L/s, respectively, for steady-state conditions.

Hypothetical energy-storage cycles were simulated for the aquifer by using a radial, nonisothermal flow and energy-transport model. Model simulations varying the injection/withdrawal rate, injection/withdrawal time, and time of storage indicate that the injection/withdrawal rate is the most sensitive model parameter with respect to efficiency of heat recovery.

Geochemistry of the Bradys Hot Springs geothermal area, Churchill County, Nevada

The geochemistry of thermal fluids produced at Bradys Hot Springs appears to be a result of evaporative concentration before deep circulation, which is followed by an increase in silica and perhaps carbonate plus bicarbonate in the deep thermal aquifer. According to A. H. Welch, the thermal fluid apparently has a maximum temperature between 143 and 169° C, as indicated by chemical geothermometers. Despite this relatively high temperature, the increase in concentration of the trace constituents barium, bromide, fluoride, and zinc is no greater than would be expected as a result of evaporative concentration. This apparent lack of significant increase limits the use of these minor constituents as indicators of thermal water in the Bradys Hot Springs area.

Geothermal test drilling at Newberry Volcano, Oregon

In a Cascade Range study under the Geothermal Research Program of the USGS, a 932 m diamond core hole was drilled into the caldera of a large Cascade Range volcano located near Bend, in west-central Oreg. (MacLeod and others, 1981). During the summer of 1981, a maximum temperature of 265° C was measured at the bottom of the hole. This is the highest temperature yet recorded in a drill hole in the Pacific Northwest, according to E. A. Sammel, the project leader.

The scientific objectives of the drilling, most of which

were accomplished, were to aid in deciphering the history of the volcano and the evolution of the caldera, to determine the characteristics of the thermal regime beneath the volcano, and to obtain core samples from which measurements of physical properties could be related to existing geophysical data. Nearly continuous core samples were obtained in the interval from 98 to 932 m.

The fluid recovered from the hole in the interval from 930 to 932 m during a 20-hour flow test was predominantly steam. Noncondensable gasses consisted of 97 percent carbon dioxide and minor amounts of methane and hydrogen sulfide.

Heat-flow at the drill site may be as high as 3 W/m², on the basis of temperature profiles and thermal conductivities measured in the hole. Chemical and isotopic analyses of the fluid and gasses are in progress, and the physical properties of the core are being studied by a number of USGS researchers. A preliminary account of the test drilling was given by Sammel (1981). Interpretive results will be published when all analyses have been completed.

Geochemistry of thermal springs in the Idaho batholith region, Idaho

Continuation of geothermal studies in Idaho focused on drainage basins in the Idaho batholith region. H. W. Young and R. E. Lewis collected water samples from 22 thermal and 5 nonthermal springs in the Boise River drainage basin. Water temperatures of the thermal springs ranged from 33° to 87° C. The thermal springs discharge water low in dissolved solids (less than 280 mg/L) and typically of a sodium carbonate type. Reservoir temperatures, estimated by using silica and sodium-potassium-calcium geothermometers, ranged from 50° to 98° C. Tritium in the thermal waters is near zero and indicates a circulation time greater than 30 yr. Stable-isotope analyses indicate that more than one hot-water reservoir supplies hot springs in the drainage basin. Depletion of stable isotopes in thermal waters relative to local nonthermal waters indicates a source of recharge from other than present-day meteoric water. Thermal-water discharge in the Boise River drainage was about 6.0×10^6 m³ in 1981; heat discharged convectively from the system was about 4.6×10^7 W.

Geothermal systems of the Cascade Range

The Cascade Range extends 1,200 km from northern California to southern British Columbia and is related to northeastward subduction of the Juan de Fuca plate beneath the North American plate. In the central and southern parts of the range, plate convergence is oblique and Quaternary volcanism is predominantly

basalt and mafic andesite; large andesite-dacite composite volcanoes and silicic dome fields occur in restricted areas of long-lived igneous activity. To the north, plate convergence is normal to the range and Quaternary volcanism consists of a line of widely spaced centers in which mafic lavas are comparatively minor. L. J. P. Muffler, C. R. Bacon, and W. A. Duffield report that several volcanoes (Lassen, Medicine Lake, Crater Lake, Newberry, South Sister) may be associated with large silicic magma chambers that could easily support major geothermal systems. Most of the Quaternary volcanoes, however, are either small basaltic shields or stratovolcanoes underlain at shallow levels by only small bodies of magma.

High-temperature geothermal systems have been identified at three of the major Quaternary volcanic centers: Meager Mountain (British Columbia), Newberry Volcano (where a recent USGS research drill hole encountered hot water at 265° C), and the Lassen region (where a large vapor-dominated system is centered in a national park and is therefore not available for development except perhaps in peripheral, hot-water zones outside the park). Fumaroles occur on most of the other Quaternary composite volcanoes, but there has not yet been sufficient drilling to determine whether exploitable geothermal reservoirs occur at depth.

Thermal manifestations away from the major volcanic centers are few and of only moderate intensity. In Oregon, warm springs are concentrated near a major fault that separates the Quaternary volcanic chain from upper Tertiary volcanic rocks to the west. To the east, a large 120° C geothermal system is being exploited for heating at Klamath Falls, Oreg., in block-faulted terrane at the margin of the Basin and Range province.

Geothermal exploration in the Cascade Range has not yet been extensive, in part because of the paucity of thermal manifestations away from the major volcanic centers. In the region of high precipitation along and just west of the Cascade Range, however, significant geothermal systems may be masked by abundant, cold ground water.

The Lassen geothermal system

L. J. P. Muffler, N. L. Nehring, A. H. Truesdell, J. M. Thompson, M. L. Clynne, and C. J. Janik reported that the Lassen region of northern California contains the most conspicuous geothermal system in the Cascade Range. Extensive manifestations of a vapor-dominated reservoir occur in Lassen Volcanic National Park (LVNP). Boiling thermal waters containing chloride and SiO₂ occur 8 km south of LVNP at Morgan Hot Springs and in a geothermal well drilled on private land in the southeast corner of LVNP. Observations all fit a model originally suggested by D. E. White of a single large

geothermal system with a central vapor-dominated reservoir surrounded by a zone of hot water discharging at lower elevations. The focus and major thermal upflow of this geothermal system is at Bumpass Hell along the contact between a 0.5-m.y.-old andesitic composite volcano and a field of dacite domes that were emplaced over the past 0.25 m.y. The most recent volcanic activity was the 1914-17 eruption at Lassen Peak.

Bumpass Hell (elevation 2,500 m) contains numerous superheated fumaroles, one of which in 1976 had a temperature of 159° C. Superheated fumaroles having temperatures of as high as 125° C in 1976 also occur in Little Hot Springs Valley at a height of 2,130 m, but steam being discharged from other fumarole areas in LVNP is either saturated or only slightly superheated. Old siliceous sinter found at Devil's Kitchen indicates discharge of hot water in the recent past at an elevation of 1,830 m. Siliceous sinter is currently being deposited at Morgan Hot Springs (elevation 1,520 m); Na-K-Ca, sulfate-water isotope, and mixing-model geothermometers indicate that the deep thermal water feeding these springs has a temperature approaching 240° C.

Recent studies of gases from the fumaroles and hot springs strongly corroborate the interpretation of the Lassen thermal features as manifestations of a single geothermal system. With increasing distance from Bumpass Hell, gases are progressively depleted in H₂S and enriched in CO₂ and N₂. These chemical changes are due to reaction of H₂S with oxygen in ground water and admixed air and to dilution with atmospheric N₂.

Stable isotope interpretation of the Lassen geothermal system

According to C. J. Janik, N. L. Nehring, and A. H. Truesdell, the deuterium and ¹⁸O content of waters of the Lassen geothermal system suggest four distinct types of water: meteoric water, deep thermal water, reservoir steam, and water from acid hot springs or drowned fumaroles. Meteoric water plots along a line defined by $\delta D = 8 \delta^{18}O + 12$. The variation in δD , ranging from -90, near Mineral, Calif., to -102 at Old Boundary Spring, is largely controlled by the local storm pattern which trends in a north-northeast direction. Steam from superheated fumaroles at Bumpass Hell and Little Hot Springs Valley and high-chloride waters from Morgan Hot Springs exhibit an oxygen isotope shift from local meteoric waters. The steam from the highest temperature fumarole at Bumpass Hell (Big Boiler) and the water from the highest chloride thermal water at Morgan (Growler) have isotopic compositions corresponding to vapor-liquid equilibrium at 237° C, which is a reasonable temperature for the geothermal system. Fluids from the acid hot springs and drowned fumaroles are mixtures of reservoir steam and

local meteoric water and plot along a line of nonequilibrium evaporation having a slope of 3.4.

On the basis of the assumption that the steam issuing from Big Boiler has the isotopic composition of reservoir steam, the calculated composition for the equilibrium deep water at 237° C is $\delta D = -95.2$ and $\delta^{18}O = -9.15$. The fact that deuterium closely approximates the average for meteoric waters near the thermal features in the Park suggests that recharge to the system is local.

Gases of the Lassen geothermal system

N. L. Nehring and L. J. P. Muffler reported that gas compositions of fumaroles and hot springs in Lassen Volcanic National Park indicate that Bumpass Hell is nearest to the center of the geothermal system. Near-surface reaction of the reservoir gas with rock and ground water, addition of air, and thermal decomposition of near-surface organic matter account for systematic changes in gas composition in directions away from Bumpass Hell. Proposed reactions for changes in gas composition are supported by geologic findings: oxidation of H_2S by ferrous iron or other metal results in deposits of sulfur; oxidation of H_2S by oxygen results in sulfate deposits; thermal decomposition of organic matter in landslide material results in high N_2/Ar ratios. Gas geothermometers predict 250–300° C for the system. Hydrocarbon analyses show an intimate relationship between the fumarolic areas of Lassen Volcanic National Park and Morgan Hot Springs.

Noble gases of the Lassen geothermal system

Superheated fumaroles at 159° and 125° C at Bumpass Hell and Little Hot Springs Valley of LVNP have the same atmospheric noble gas (ang) concentrations as water saturated with air (asw) at 5° C and 2,500 m elevation (5° C asw) but 300 times higher helium. A. H. Truesdell and Emanuel Mazor suggest that these fumaroles originated by total boiling of steam condensate equilibrated in gas contents with boiling recharge water. Total boiling may have resulted from pressure decrease following tectonic opening of conduits from the reservoir to the surface. Because lower temperature fumaroles near the center of the thermal system have higher ang/ CO_2 ratios but lower He/ CO_2 ratios, dilution with cold ground water is indicated. The fact that some fumaroles at the edges of the system (Devils Kitchen and Cold Boiling Lake) have higher He/ CO_2 ratios suggests CO_2 loss by reactions with water and reservoir rocks at lower temperatures to form $NaHCO_3$ waters.

High chloride hot springs south of LVNP (Growler and Morgan) have one three-hundredth the helium of the superheated fumaroles and the same ang relative abundances but only one twentieth the ang concentrations at 5° C asw. This suggests that these waters are mixtures of cold water and almost completely degassed thermal water resulting from 3.5 percent steam loss by Raleigh boiling.

Fumarolic incrustation at Mount St. Helens

T. E. C. Keith, T. J. Casadevall, and D. A. Johnston report that fumaroles associated with the Mount St. Helens activity occur (1) within the crater, where heat and fluids may in part be derived from magma and from crustal rocks in contact with the rising magma, and (2) as rootless fumaroles in the flowage deposits, where heat and fluids are derived locally from within the deposits. Much of the encrustation material was deposited at temperatures less than 250° C as non-crystalline yellowish films on ash particles and rock fragments and as encrustations around fumarole vents. Encrustations are mostly red, orange, yellow, and white. They begin to crystallize during cooling and dehydration immediately after deposition. Common mineral phases are sulfur, gypsum, halotrichite, and hematite. Less common phases are sal ammoniac, thenardite, glauberite, anhydrite, melanterite, alunite, and halite. Numerous unstable and poorly crystalline phases in process of dehydration and crystallization are under study. The major chemical components making up the fumarole deposits are Cl, F, H_2O , Fe, Al, Ca, Na, K, and S.

Hydrothermal systems in Montana

Manual Nathenson (1981), using the assumption that geothermometer temperatures reflect reservoir temperatures, investigated the relationship between geothermometer temperatures, spring temperatures, and spring flow in hydrothermal systems in Montana. When the data for hot springs in Montana were originally published by Robertson, Fournier, and Strong (1976), only the silica and Na-K-Ca geothermometers were available. The agreement between the geothermometers was excellent for some systems, but poor for others. Nathenson recalculated geothermometer temperatures by applying the Mg correction of Fournier and Potter (1979) to the Na-K-Ca geothermometer. Above 100° C, cation temperatures indicate equilibrium with quartz; from 30° to 100° C, cation temperatures indicate equilibrium with chalcedony.

When the excellent agreement between geothermometer temperatures was attained, Nathenson returned to calculating heat-loss models for the Montana systems.

Two end-member models for heat loss were considered: thermal water rising to the surface through a narrow conduit, with cylindrical heat-transfer, and thermal water rising to the surface up a fault, with linear heat-transfer. Nathenson's models, having reasonable values for the depth of initial upflow and being based on the assumption that the geochemical temperatures are reservoir temperatures, indicate that some of the hot springs must lose energy by heat conduction while flowing up a narrow conduit. The fact that other hot springs have a much larger heat loss suggests that the flow is upward through a fault system.

Temperature versus depth in deep drill holes in the U.S.

Marianne Guffanti and Manuel Nathenson (1981) published temperature versus depth data and calculated geothermal gradients for 91 deep drill holes in the United States. These holes were selected from the much larger compilation by Spicer (1964) of data taken by using maximum-reading thermometers. The selected subset consists of those holes that have been logged to depths generally greater than 600 m while at temperature equilibrium and that display conductive temperature gradients. Temperature gradients calculated for each hole were supplemented by recent data to produce a contoured geothermal gradient map (Guffanti and Nathenson, 1980).

Geologic mapping in Yellowstone National Park

A large-scale (1:4,800) geologic map of Upper Geyser Basin in Yellowstone National Park, Wyoming, was completed by L. J. P. Muffler, D. E. White, M. H. Beeson, and A. H. Truesdell, with assistance by A. O. Cook. The large scale shows all of the major and most of the minor thermal features, including geysers, flowing springs, vents with no surface flow, and steam vents. Hydrothermal deposits such as travertine, sinter, diatomaceous silt, hydrothermal mud, hydrothermal explosion deposits, old travertine, and old sinter along with the usual alluvial deposits, talus, glacial deposits, and rhyolite flows are differentiated.

Seismic investigations in geothermal areas

H. M. Iyer, J. R. Evans, D. A. Stauber, R. G. Daniel, Alan Rite and Mary Monfort measured teleseismic P-wave residuals in several geothermal and volcanic areas in the Western United States to obtain anomalous P-wave velocities in the crust and upper mantle that could be related to the presence of magma bodies. In the eastern Snake River Plain, P-wave velocities in the up-

per mantle were lower by 2 to 4 percent than in the surrounding region. This is interpreted as the remnant of a magma body, probably still quite hot, that existed in the region about 3 to 5 m.y. ago. In the Cascade Range, P-delay studies of Lassen Peak, Mount Hood, and Newberry Volcano do not reveal any evidence for crustal magma bodies. Magma chambers and magma conduits under these volcanoes probably have volumes below the resolution limit of the P-delay technique (5 km×5 km×5 km). Three-dimensional models of the Oregon Cascades show lower than normal velocities in the crust and upper mantle beneath the volcanoes in the whole region. High seismic wave attenuation is observed in the Roosevelt Hot Springs area, Utah.

Seismicity in the Cascades of Oregon and California

H. M. Iyer, Alan Rite, Auriel Kollman, and David Knapp continued to operate a 32-station seismic network in the Oregon Cascades during FY 1981 to help characterize this young volcanic region. Eight-station networks were also operated around Lassen Peak and Mount Shasta in California. The seismic activity in the Oregon Cascades during FY 1981 was mainly concentrated in the north with only sparse activity occurring in the central and southern parts. None of the Oregon volcanoes showed unusual swarm activity. During early 1981, a swarm of several hundred shallow earthquakes occurred near Tennant, Calif., about 30 km northeast of Mount Shasta. Seismic activity was, as usual, high in the Lassen Peak region, with the main swarm activity occurring immediately to the south of the volcano summit.

Crustal structure of Mauna Loa Volcano, Hawaii

In October 1978, the U.S. Geological Survey established a 100-km-long seismic refraction profile normal to the Kona coast of Hawaii Island. Analysis of these data together with available gravity data by J. J. Zucca and D. P. Hill showed that the oceanic crust dips about 3 degrees landward under the submerged flank of the island, increasing to 8.5 degrees under the Kona coast. Maximum vertical deflection of the base of crust from beneath the deep ocean to a point beneath the summit of Mauna Loa is about 9 km. High-velocity, high-density rocks (V_p about 7.1 km/s, density about 2.9 g/cm³) comprise the bulk of the volcanic edifice and reach to within a few kilometers of the surface beneath the north flank of Mauna Loa. The data also suggest that an elongate high-velocity, high-density body lies parallel to the Kona coast just below the surface; this body probably represents an extinct, buried rift zone.

Seismic refraction survey of the Imperial Valley, California

An extensive seismic refraction survey was conducted in the Imperial Valley region to determine the crustal structure in more detail, over a wider area, and to greater depth than was accomplished by earlier studies. A fortunate combination of new instrumentation and improved methods of analysis expedited this project.

Forty shots, ranging in yield from 1,000 to 2,000 pounds (TNT equivalent), were fired at 7 shot points. Each shot was recorded by 100 portable seismic instruments arranged in profiles and arrays with a typical instrument spacing 0.5 to 1 km. More than 1,300 recording locations were occupied and more than 3,000 usable seismograms obtained.

Five profiles crossing the Imperial Valley and bordering mesas at different azimuths are modeled. Major results reported by G. S. Fuis, D. P. Hill, and J. J. Zucca include the following:

1. All models have in common a section of sediments (modeled in one to three parts), a transition zone, a basement, and subbasement.
2. Velocity in the section of sediments increases with depth without discontinuities but often with changes in gradient.
3. The thickness of unmetamorphosed sediments ranges along the axis of the trough from 4.8 km at the U.S.-Mexico border to 3.7 km along the southwest shore of the Salton Sea.
4. In the central Imperial Valley the sediment-basement transition zone is generally 1 km thick and velocity increases from that at the base of the sediments, about 5 km/s, to an upper basement velocity of 5.65 km/s in most places. On West Mesa and in other places where the sediments thin to 2.5 km, a prominent velocity discontinuity is present above this zone, and the zone is thinner.
5. Upper basement has a velocity of 5.65 km/s in most places in the Imperial Valley, but on West Mesa its velocity is 5.9 to 6.0 km/s.
6. Several structures are seen which affect basement, transition-zone, and deeper sediments. They are (a) a scarp along the Imperial fault that decreases in height from 1 km southeast of El Centro to 0 km southwest of Brawley, (b) a structure in deeper sediments along the Brawley seismic zone north of Brawley, and (c) a scarp passing under shot point 1, ranging in height from 1 to 3.5 km. The latter scarp probably correlates with the Superstition Mountain fault northwest of shot point 1 and with a roughly north-south

trending basement bench south of shot point 1 which has no surface expression.

7. A subbasement (or intermediate layer) with a 7.2 km/s velocity is present at depths ranging from 10 km at the U.S.-Mexico border to 16 km under the southwest part of the Salton Sea.

Seismic refraction study of Mount Shasta and Medicine Lake region

During the period June through August 1981, the U.S. Geological Survey conducted a seismic refraction experiment in the region around Mount Shasta, California, including the Klamath Mountains, Cascade Range, and Modoc Plateau. The experiment consisted of 27 one- to two-ton explosions, recorded at a total of 600 instrument locations, constituting five reversed profiles. The primary objectives of the experiment were to investigate the transitions between the major geologic provinces of northern California, to look for velocity anomalies that might suggest the presence of magma chambers, and to investigate the seismically active fault zone northeast of Mount Shasta near the town of Tennant.

To date, the interpretation has centered mainly on the profile extending southeast from the town of Dorris, Calif., across Medicine Lake Highland to the town of Adin, Calif. J. J. Zucca, G. S. Fuis, and D. P. Hill reported that preliminary interpretation of this line indicates basement P-wave apparent velocities ranging from 5.7–6.1 km/s with a suggestion of slightly higher true velocities southeast of Medicine Lake Highland. Strong (midcrustal?) reflections are observed with critical distances ranging from 60 to 100 km southeast of Medicine Lake Highland. On Medicine Lake Highland a 0.35 to 0.45 s traveltime advance is observed. This advance is seen at the same stations for all the shots, indicating an anomalous region of high velocity shallow in the crust.

In addition, preliminary interpretation of an east-west profile crossing the Tennant fault zone indicates a traveltime offset of as much as 0.3 s associated with this feature.

Seismic studies between Crater Lake and Mount Hood

A refraction profile along the Oregon Cascades between Crater Lake and Mount Hood and a shallow magnitude 5.5 earthquake in southern Washington were interpreted by D. S. Leaver, W. D. Mooney and W. M. Kohler to develop a velocity model for the crust beneath the Oregon Cascades. The refraction pattern is characterized by a 3-km-thick surface layer in which velocities vary from 2.9 to 5.2 km/s, upper crustal velocities of 6.1 to 6.5 km/s between the depths of 3 and 29 km, lower crustal velocities near 7.0 km/s between the depths of 29

and 42 km, and a gradual transition between 42 and 46 km to the mantle. No significant crustal variations below the surface layers from the north end to the south end of the profile were observed. Arrivals from the earthquake are consistent with this profile and indicate average Pn velocity (mantle refraction wave) of 7.9 km/s. Arrivals from the earthquake along the west side of the Cascade Range are later than corresponding arrivals to the east; this phenomenon indicates a thickening of the crust (by as much as 10 km), a slowing of Pn velocities (by as much as 0.5 km/s), or some combination of both. No evidence was found for a crustal low-velocity zone.

These results are consistent with models based on surface-wave dispersion and indicate that the average crustal velocities within the Oregon Cascades are much higher than those of the Sierra Nevada and slightly higher than those in the northern Washington Cascades.

Geothermal energy in magma

P. L. Ward reports that review of geological, geophysical, and engineering data suggests that development of magma energy in the Western United States is scientifically feasible. Several large magma bodies exist at depths as shallow as 5 or 6 km. Seismic reflection data provide the most direct evidence of depth and shape of these bodies. Geologic data coupled with heat flow considerations imply that it took several million years for these bodies to be emplaced and that the hottest, youngest magma may well be near the tops of the bodies.

Response of ground water to rapid intrusion of magma

Theoretical and field investigations by P. T. Delaney showed that when magma invades a region of abundant ground water, rapid pressurization and flow occur. The balance of pressurization and flow depends primarily upon the thermal and hydraulic diffusivities of the host rocks and the compressibility of the rock and water; the magnitude depends upon the overall thermal expansion of water over the temperature difference between the ambient and magma conditions. The effect of water flashing to steam concentrates the expansion at a particular isotherm but does not significantly affect the pressure distribution. Assuming that the wall rocks do not deform appreciably, rocks with porosities, permeabilities, and compressibilities typical of the finer grained sandstones and siltstones can undergo pore-pressure increases greater than 50 bars. In some instances, calculated pressure increases are sufficiently great that host rocks can be expected to fail by fracture and comminution. Where a steam layer is present, host-rock failure in

the heated region does not lead to a significant drop in pore pressure, so that the driving stresses for continued failure may remain appreciable. Examples of such fractures and breccias are abundant in the San Rafael region of Utah where magma was emplaced into a Mesozoic sequence of sandstones and shales about 4 million years ago.

Preliminary heat-flow investigations of the California Cascades

A heat-flow reconnaissance of the Cascade Range in California combines results from shallow (200 m) drilling with less reliable values derived from temperature gradients measured in "holes of opportunity" and thermal conductivities of hand-sampled equivalent rock types. Although the distribution of sites is uneven (control is concentrated in the Medicine Lake, Mount Shasta, and Lassen Peak areas), the new data provide a considerable improvement over previous representations of the regional near-surface heat flow. Measurements to depths of 300 m and less show an elongate region of anomalously low heat flow (less than 30 mwm²) along the axis of the Range. There are two broad areas of zero heat flow: the northern one encompasses the Medicine Lake Highlands and the southern one is situated north of Lassen Peak. C. W. Mase, J. H. Sass, and A. H. Lachenbruch have attributed observed low heat flow that contrasts with the high heat flow expected along a magmatic arc to regional circulation of ground water. This low heat flow indicates that the surficial thermal regime of the California Cascades is dominated by convection heat transfer. The Cascades are bounded on the west by the Klamath Mountains, a region of uniformly low heat flow (approximately 40 mwm²), and on the east by the Modoc Plateau, a region of variably high heat flow (70–100 mwm²) characteristic of the Basin and Range. The paucity of data prohibits the definition of a regional heat flow for the northern Sierra Nevada to the south. Conductive heat flux from the transition zones bounding the Cascades is effectively masked by hydrothermal circulation. Although data on discharge rates and temperatures are insufficient to calculate a thermal budget, the estimated thermal discharge from springs could conceal deep conductive heat flows of 100 mwm² or more, values characteristic of other areas of Quaternary magmatic activity.

Heat flow from five wells in west-central Arizona

J. H. Sass, R. J. Munroe, and Claudia Stone reported that five holes drilled in sedimentary basins of west-central Arizona for the evaluation of their uranium potential all have primarily conductive thermal regimes as evidenced by the equilibrium temperature profiles. With some minor perturbations over short vertical dis-

tances, variations in temperature gradients correlate very well with lithologic changes and hence, variations in thermal conductivity. The conductivity of drill cuttings was combined with porosity estimates of varying uncertainties (depending on the lithology) to provide reasonably well-constrained values of thermal conductivity for each lithologic unit. These conductivities were, in turn, combined with the appropriate least-squares thermal gradients to produce estimates of heat flow. Component heat flows within individual holes generally were in good agreement, confirming that the thermal regimes are indeed conductive. The range of heat flows (1.6 to 2.2 HFU) measured within this area in these deep wells generally coincides with the range of values from a larger group (approximately 25) of shallower (approximately 100–200 m) wells in the same region.

Heat flow in the east Brawley and Glamis areas of the Salton Trough, California

C. W. Mase, J. H. Sass, C. A. Brook, and R. J. Munroe obtained thermal gradients and thermal conductivities in real time by using an in situ heat-flow technique in 15 shallow (90–150 m) wells drilled between Brawley and Glamis in the Imperial Valley, southern California. The in situ measurements were supplemented by follow-up conventional temperature logs in seven of the wells and by laboratory measurements of thermal conductivity on drill cuttings. The deltaic sedimentary material comprising the upper approximate 100 m of the Salton Trough generally is poorly sorted and high in quartz, the result of which are quite high thermal conductivities (averaging 2.0 w/m²K as opposed to 1.2 to 1.7 for typical "alluvium"). A broad heat-flow anomaly with maximum of about 200 mwm² (approximately 5 HFU) is centered between Glamis and east Brawley and is superimposed on a regional heat-flow high in excess of 100 mwm² (greater than 2.5 HFU). The heat-flow high corresponds with a gravity maximum and partially with a minimum in electrical resistivity; these correspondences suggest the presence of a hydrothermal system at depth in this area.

Pressured fractures in hot rock

The principal conduits for magma transport within rift zones of basaltic volcanoes are steeply dipping dikes, some of which feed fissure eruptions. Elastic displacements accompanying a single dike emplacement elevate the flanks of the rift relative to a central graben. Concomitant normal faulting may lower the graben, thus accentuating the topographic features of the rift. If eruption occurs, the characteristic ridge-trough-ridge displacement profile changes to a single

ridge, centered at the fissure, reversing the graben-forming displacements. To investigate this process, D. D. Pollard computed the elastic displacements and stresses in a homogeneous, two-dimensional half space driven by a pressurized crack that could breach the surface. A derivative graphical method permits one to estimate the three geometric parameters of the dike (height, inclination, and depth-to-center) and the mechanical parameter (driving pressure/rock stiffness) from a smoothly varying displacement profile. Theoretical stress states associated with dilation of a pressurized crack are used to interpret the distribution and orientation of structures (open cracks, normal faults, buckles, and thrust faults) and their role in rift formation.

Volcanic tremor and hydrothermal wedging

An empirical correlation between volcanic tremor and igneous intrusion or eruption has encouraged the use of tremor in forecasting volcanic activity, yet the origin of this seismic signal remains obscure. The discovery of tremor at Mount St. Helens that is similar to tremor at Kilauea casts doubt upon the general applicability of source mechanisms which rely on magma flow in cracks because viscosities of dacitic and basaltic magmas differ by many orders of magnitude. However, water is common to both volcanoes. Slowly moving magma wedges open the crack tip and provide a low-pressure sink for water lodged in the surrounding rock. The magma supplies heat that raises vapor pressure and drives the opening phase; pressure drops as vapor expands into the dilating crack tip and heat is transferred to the crack walls. D. D. Pollard completed a theoretical analysis of a crack subject to linear gradients in driving pressure and identified an instability in the rate of crack dilation with change in vapor pressure. The instability could excite vibration of the magma reservoir. Escape of steam from ground cracks preceding fissure eruptions in Kilauea and the steam eruptions and fumarolic activity at Mount St. Helens support this mechanism. Further evidence comes from the presence of hydrothermally altered rock in cracks above basaltic dikes.

SEDIMENTOLOGY

Sedimentology, the study of sediments and sedimentary rock, encompasses investigations of principles and processes of sedimentation and includes development of new techniques and methods of study. The USGS sedimentology studies are directed toward the solution of water-resource problems and the determination of the genesis of sediment and application of this knowledge to sedimentary rocks to gain a more precise interpretation of their depositional environments. Many USGS studies

involving sedimentology have applications to other topics such as marine, economic, and engineering geology and to regional stratigraphic and structural studies; these are presented elsewhere in this volume under their appropriate headings.

Studies of fluvial sedimentation are directed toward the solution of water-resource problems involving water-sediment mixtures. Sediment is being considered more and more as a pollutant. Inorganic and organic sediment, transported by streams to sites where deposition takes place, carries major quantities of sorbed toxic metals, pesticides, herbicides, and other organic constituents that accelerate the eutrophication of lakes and reservoirs. A knowledge of erosion processes, the movement of sediment in rivers and streams, and the deposition of sediment in stream channels and reservoirs is of great economic importance to the nation.

Bedload studies in Wyoming

The movement and storage of bedload in the East Fork River, Wyo., has been studied by R. H. Meade, R. M. Myrick, and W. W. Emmett. Most of the bedload of East Fork River is discharged during the few weeks of snowmelt runoff. It consists of coarse sand and fine gravel that move over an essentially immobile layer of coarse gravel or bedrock. The mean annual bedload discharge through the study reach is about 2,700 mg. During low-water periods, the movable bed material is stored in distinct and separated areas of channel that are centered 500 to 600 m (25 to 30 channel widths) apart. The storage areas are located in the same parts of the river from year to year, in reaches where the slope is smaller than the mean river slope. Each storage area contains an average of 2,300 to 2,700 mg of sediment. During a typical runoff season, the bulk of the stored sediment is moved downstream to the next storage area, a distance of 500 to 600 m. Because the supply of transportable material is not uniformly distributed along the stream channel, the relation of bedload transport to water discharge is markedly different from one part of the stream to another. In reaches immediately downriver of storage areas, bedload discharge at a given water discharge is greater on the rising limb of the hydrograph than it is on the falling limb. In reaches immediately upriver of storage areas, bedload discharge is greater on the falling limb of the hydrograph.

Channel change in the Big Lost River, Idaho

In a 1-year study to assess channel changes since 1917 in the Big Lost River and to estimate the probable response of the river system to planned structures (such as riprap and rock-filled gabions), R. P. Williams obtained data from five subreaches that were descriptive

of source-transport-deposition zones. Williams reports that cyclic effects of temperature, precipitation, and runoff coincide with systematic changes in hydraulic geometry. Sediment available for transport in the main channel has apparently declined since 1967. Further erosion of the channel bed is constrained because of armor-ing and channel structures. This constraint results in lateral channel shifting and bank undercutting. In the lower reaches, rising ground water adds to erosion of the streambed and flood plain. Mackay Reservoir apparently has a low sediment-trap efficiency. Field data analysis (reservoir surveys, remnant fence lines, and tree stumps) and cesium-137 dating of core samples indicate that 95 percent of the initial (1917) reservoir storage capacity still exists. Several kilometers below the reservoir, streambed elevations have fluctuated only ± 0.2 m over the long-term record. In most sub-reaches, coarse material was deposited at peak discharges and was scoured on the recession. Three sub-reaches indicate a decreased bedload rate as the velocity distribution factor increases with increased stream discharge.

An evaluation of suspended sediment and turbidity in Cow Creek, Oregon

Preliminary evidence indicates that a correlation exists between persistent turbidity and the 0.002-mm and smaller size fraction of the suspended sediment transported by Cow Creek in southwestern Oregon. The importance of this correlation, according to D. A. Curtiss, is that it could provide a quantitative assessment of the turbidity potential of a hypothetical impoundment on a stream if used in conjunction with a 0.002-mm suspended-sediment transport curve. This method of assessment utilizes a series of residual-turbidity tests that measure the turbidity of a sample over time for each different size classification of the sediments on the basis of settling velocity. The correlation from the residual-turbidity tests could be used to convert a computed discharge-weighted concentration of the clay-size material to a turbidity value.

Long-term sediment yields from Bay Creek, Pike County, Illinois

T. R. Lazaro, using multiple-regression analyses on 5 years of suspended-sediment record, defined correlations between streamflow and suspended-sediment discharge as a means of estimating long-term sediment yields for Bay Creek, a 417 km² tributary to the Mississippi River, at Nebo, Ill. The best relations, based on observed seasonal (cyclic) variations in sediment loads, were between daily suspended-sediment discharge and daily mean stream discharge, sine (T), and cosine (T); where T is equal to b times d , and b is a constant used to

convert the day of a water year to an angle in radians (one day equals $2\pi \div 365.25$) and d is the day of the water year (October 1, $d=1$; September 30, $d=365$ or 366).

Large-scale bedforms in the Platte River, Nebraska

K. D. Crowley (1981) reported that the channel of the Platte River in Nebraska, especially downstream from Grand Island, is characterized by large, periodic, and geometrically distinct bedforms called macroforms. Macroforms have dimensions commensurate with the width and depth of the channel and are emergent at all but the highest flow stages.

Macroforms are submerged and active only at highest flows. For example, in the Platte River at North Bend, Nebr., macroforms are covered only when discharge exceeds 219 m³/s. Moreover, macroforms do not move downstream at any detectable rate until they are covered with approximately 0.2 m of water. At North Bend, the average macroform was covered with 0.2 m of water for about 2 weeks during the 1980 water year, not including the period the macroforms were covered with water from ice jamming.

Estimating water discharge for channel-width maintenance

M. R. Karlinger, R. C. Mengis, J. E. Kircher, and T. R. Eschner (1981) used theoretically derived regime equations (Parker, 1978, St. Anthony Falls Hydraulic Laboratory, University of Minnesota) to estimate channel geometry response to changes in water discharge. The first Parker regime equation relates slope, depth, and particle size. The remaining equations establish dimensionless water discharge and sediment discharge as functions of particle size and hydraulic parameters. These equations comprise an algorithm that is unique in that channel cross-sectional characteristics are physically rather than statistically related to bed-material size, sediment load, channel slope, and an effective discharge.

The sediment sizes for use in the regime equations were calibrated with discharge and channel-width data from five sites along the Platte River between Cozad and Odessa, Nebr. A single calibration curve was acceptable throughout the entire reach because (1) size-distribution curves for the five sites are homogeneous, and (2) the calibrated sizes in the design curve approximate those necessary to satisfy the physical processes outlined by Parker.

Sediment transport and effective discharge

J. E. Kircher (1981) computed sediment discharge for 4 locations along the North Platte, South Platte, and the Platte Rivers between North Platte and Grand

Island, Nebr., in order to determine the effective discharge. A definition of effective discharge is the mean value of a narrow range of water discharge that transports on the average more sediment than any other water discharge.

Streamflow and sediment records from four gaging stations (North Platte River and the South Platte River at North Platte, the Platte River near Overton, and the Platte River near Grand Island) were used to compute sediment discharge and to determine the effective discharge. Total-sediment discharge was determined by three methods: (1) by summing the measured bedload and suspended-sediment discharges; (2) by using the Colby (1957) method; (3) and by using the modified Einstein method (Colby and Hembree, 1955) for all four gaging stations. These three methods were then compared and found to agree closely.

The expected values of the total-sediment discharge (mean annual total-sediment discharge for the period of record) computed by combining flow frequencies and sediment-transport relations for the three total load methods ranged from 597 to 887 Mg/d for the North Platte River at North Platte, from 307 to 370 Mg/d for the South Platte River at North Platte, from 980 to 1,120 Mg/d for the Platte River near Overton, and from 1,080 to 1,260 Mg/d for the Platte River near Grand Island.

Morphologic changes in Platte River channels

T. R. Eschner, R. F. Hadley, and K. D. Crowley (1981) reported that the channels of the Platte River in south-central Nebraska have undergone major changes in hydrologic regime and morphology since about 1860. These changes are attributed to agricultural, municipal, and industrial water use. Prior to water development in the 19th century, the Platte was a wide (≈ 2 km), shallow (1.8 to 2.4-m-deep) river characterized by bankfull spring flows and low summer flows. Comparison of surveyors' maps drawn during the 1860's with six sets of aerial photographs taken between 1938 and 1979 shows that the channels have narrowed considerably above the confluence with the Loup River. The width of the channels in 1979 ranged from 8 to 50 percent of the channel width in 1860. Below the confluence with the Loup River, the width of the river in 1979 was about 92 percent of the 1860 channel width. Width reduction has occurred by progressive encroachment of vegetation and consequent vertical and horizontal accretion on sand bars in the channel.

Sediment yields from areas affected by surface mining in Pennsylvania

L. A. Reed and R. A. Hainly measured storm runoff

and suspended-sediment yields from single land uses associated with surface mining in three basins in Pennsylvania. The highest measured sediment yields were from an unimproved haul road that was constructed by blading the top soil to the side and using the subsoil as the road bed. During the 6-month period the road was used, 6 storms produced sediment yields of 15 Mg/ha. Rainfall for the 6 storms ranged from 17 to 65 mm. Sediment yields from an improved haul road, constructed with rock fill, were only 1.3 Mg/ha during similar storms. Sediment yields from a new diversion terrace, before vegetation was established, were 9 Mg/ha, and yields below a sediment control pond having the capacity to store about 30 mm of runoff were 0.7 Mg/ha for similar storms.

Sediment transport in the Tanana River near Fairbanks, Alaska, 1977-79

To facilitate design and operation of engineering structures on the Tanana River and to regulate gravel extraction from the river near Fairbanks, the U.S. Army Corps of Engineers, Alaska district, requested that the U.S. Geological Survey collect and evaluate sediment-transport and river-hydraulic data during periods of principal runoff beginning in 1977. Investigators are R. L. Burrows, W. W. Emmett, and Bruce Parks.

Measurements of suspended-sediment and bedload-transport rates for two sites, up and downstream of in-river disturbances, indicate average annual suspended-sediment loads of 21.8 and 24 million Mg, respectively. Annual bedload is usually 1 to 1.5 percent of the suspended load, the average being 298,000 and 321,000 Mg.

Particle-size distribution for suspended sediment at the two sites (about 26 km apart) is similar. Median particle size is generally in the silt range, but at some low water discharges it is in the fine sand range.

Median particle size of bedload at the upstream site is generally in the gravel range, but at some low transport rates it is in the medium sand range. In 1977, median bedload particle size was comparable at both sites, but in 1978 the median size was markedly smaller at the downstream site. In 1979, generally coarser material was transported at both sites, but the difference in bedload particle size was even greater. At both locations and at all water discharges and all sediment-transport rates, suspended load particles are significantly smaller than bedload particles.

Runoff and sediment transport from an agricultural watershed in northern Illinois

Analysis by H. E. Allen, Jr., and J. R. Gray of stream-flow and suspended-sediment data collected on a

7.28 km² agricultural watershed near Rockford, Ill., disclosed that during a 2-year period (July, 1979 to June 1981) 2,620 Mg of suspended sediment were transported from the watershed, of which 2,440 Mg or 93.1 percent was transported during a 46.6-hour period. Mean quarterly suspended-sediment yields during the 2-year period ranged from 172 Mg/km² (April through June) to 0.74 Mg/km² (October through December). Estimates of the total sediment discharge indicated not more than 2 percent of the sediment was moving as bedload. Suspended-sediment yields during storm runoff were related to peak-water discharge with an average standard error of 58 percent.

CLIMATE

Research of the USGS Climate Program in 1981 was directed towards understanding the history of climate change. Studies documented records of past climates and determined correlation of climate change and sedimentary processes.

Quaternary reference core

Analyses of two long sediment cores from Clear Lake, Lake County, California, have revealed the longest continuous pollen record from the North American Continent. Proposed correlations of the pollen record (Adam, Sims, and Throckmorton, 1981) show that the Clear Lake record can be matched in great detail with similar pollen records from Grande Pile, France (Woillard, 1978), and Tenaghi Phillipon, Macedonia (Wijmstra, 1978), during the early part of the last glacial cycle that corresponds to deep-sea oxygen-isotope stages 5a through 5d (Shackleton and Opdyke, 1973). The detailed correlations establish that the climatic sequence common to all three sites transcends regional significance and can be used as a reference sequence for the climatic fluctuations of the last glacial cycle for a large part of the Northern Hemisphere, including North America. The sequence of five cold-warm oscillations found in the period between the end of the last interglaciation and the first full development of the North American continental ice sheet during the last glacial cycle has not been generally recognized in North American continental deposits. The Clear Lake work thus demonstrates a need for reevaluation of the transition from the last interglaciation to the early part of the last glaciation throughout North America.

Late Quaternary vegetation and climate history from western Alaska

Pollen analysis of lake-sediment cores and peat cores from northern Yukon Delta and St. Michael Island in

southern Norton Sound is being used by T. A. Ager to reconstruct a detailed history of vegetation and climate of this region during the past approximately 40,000 yr. Lacustrine-sediment cores as long as 15 m were obtained in 1978 and 1979 from ice-covered lakes within maar craters on the volcanic island of St. Michael.

The time interval of about 40,000 to 14,000 (Wisconsin glacial interval) was characterized by herb tundra vegetation and an arid, cold climate. Between 14,000 and 7,000 yr ago the regional vegetation was a shrub tundra, and the climate was moister and drier than during the full-glacial interval. Poplar trees invaded, perhaps only briefly, about 11,000 yr ago. Spruce trees began to invade the eastern Norton Sound region about 5,000 yr ago.

Diatom stratigraphy of the 15-m core from St. Michael Island is being studied by J. P. Bradbury. Preliminary zonation of diatom assemblages closely parallels the pollen zonation. Full-glacial diatom floras are characterized by low species diversity; many of the "glacial" sample assemblages include a new species of *Cyclotella*. Post 14,000-yr-old diatom assemblages are characterized by much greater species diversity and a relative abundance of temperate diatom types.

Three volcanic-ash layers have been recognized in the 15-m core from St. Michael Island. Ash I is about 16,000 yr old and is probably of local origin (Stuart Island?). Ash II is about 14,500 yr old and also appears to be of local origin. Ash III is about 4,000 to 5,000 yr old but is probably from a distant source (Alaska Peninsula?); it is an important marker horizon in western Alaska.

Lacustrine sediment cores in south-central Alaska

Preliminary investigations of lacustrine sediment cores from the Cook Inlet region of south-central Alaska by J. D. Sims, J. R. Riehle, and S. B. Bartsch-Winkler show that all five lakes studied thus far contain multiple volcanic ash layers and useful pollen records that will contribute to the reconstruction of a detailed history of regional vegetation, climate, and volcanic eruptions. Cores were obtained from Hideaway Lake (Anchorage), Upper Salamatof Lake (Kenai Peninsula), Bear Lake, and Big River Lakes (west side Cook Inlet near Mount Redoubt Volcano). An additional core was obtained from Hidden Lake (Kenai Peninsula) by J. D. Sims and M. J. Rymer.

Glacial Lake Passaic

Detailed surficial mapping and coring of part of the upper Wisconsin terminal moraine, pro-moraine deltas and subaqueous fans, and varves in the glacial Lake Passaic basin, northern New Jersey, show prox-

imal to distal relationships of surface and subsurface stratigraphic units that were deposited during the glacial maximum. A core from the crest of the moraine in Madison, studied by B. D. Stone and M. J. Pavich (USGS) and G. E. Reimer (Rutgers University) contains from top to bottom: deltaic sand, homogeneous compact till, 10-m thick, interbedded lacustrine clay, silt, and sand, and thin till beds. The entire moraine sequence is apparently stratigraphically equivalent to lake-bottom beds that underlie the Great Swamp basin south of the moraine. These beds include a 19-m thick section of more than 600 varves, which consist of regularly laminated clay and fine silt couplets that average 3.1 cm thick. X-radiographs of varves, obtained by J. C. Liddicoat (Lamont-Doherty Geological Observatory) reveal discrete, locally graded microlaminations within the silt layers of the varve couplets. These microlaminations probably resulted from deposition of individual meltwater density underflows on the lake bottom. Oriented paleomagnetic samples analyzed by Liddicoat show normal polarity and also show apparent paleosecular variation of less than 10° over a sampling interval of tens of varves.

Lake Bonneville revisited

A substantially modified history of the last two cycles of Lake Bonneville, based on stratigraphic studies by W. E. Scott, amino-acid studies by W. D. McCoy (University of Massachusetts), soil studies by R. R. Shroba, and radiocarbon ages provided by Meyer Rubin, have several significant climatic implications for the Great Basin and the central Rocky Mountains, of which, two are discussed below:

1. Either the effect of Pleistocene climate on lakes in the Great Basin or the climate itself may have differed from place to place. In particular, the chronology of the last lake cycle differs from that proposed by Benson (1978) for Lake Lahontan. From radiocarbon dates on tufa and gastropod shells, Benson infers that Lake Lahontan was at its highest level from 25,000 to 22,000 yr ago and again at 13,500 to 11,000 yr ago. In contrast, Lake Bonneville was still only at a low level until 22,000 yr ago; it was close to its maximum level by 16,000 yr ago; it was falling rapidly 13,500 yr ago; and it had receded to a very low level by 11,000 yr ago. The reality of these differences, of course, depends on the accuracy of the dates in the two basins.
2. If the last lake cycle is an accurate analogue, then older lake cycles were probably relatively brief and were broadly synchronous with major mid-latitude glaciations. However, the last two lake

cycles were separated by a long interlacustral episode that included the last interglacial as well as the early and middle Wisconsin glaciation. This inference is at odds with the early Wisconsin conditions indicated by the marine record (Shackelton and Opdyke, 1973) and by glacial sequences in the Midwestern United States (Johnson, 1976), which together imply widespread glaciation. To the extent that glacial conditions might be expected to be generally matched by lacustrine conditions in the Great Basin, the lack of persistent lakes during the Wisconsin is anomalous. Therefore, the global cooling that accompanied mid-latitude glaciations was probably not the sole cause of major rises of Lake Bonneville. More likely, other effects of glacial climates, such as the shifting and concentration of storm tracks that would alter the rate and distribution of precipitation, affected the timing and magnitude of lake fluctuations. For instance, during early and middle Wisconsin time, very low precipitation rates might not have provided sufficient runoff to maintain a high lake in the Bonneville basin, in spite of low temperatures. A subsequent increase in precipitation rate, but not necessarily to a rate greater than today's, if coupled with low temperatures would have caused the lake to rise.

Late Cenozoic sea levels

U-series dating of corals from Pleistocene marine units of the U.S. Atlantic Coastal Plain from Delaware to Georgia has been continued by B. J. Szabo. Accurate dating of these marine units is important for delineating Pleistocene sea level history. As reported by Cronin and others (1981), corals from three localities in the Norfolk Formation near Norfolk, Va., have yielded an average ^{230}Th age of 75,000 yr B.P. Additional coral samples were collected recently from three more Norfolk localities, Stetson, City Line, and Gomez pits. The dates for these corals are 73,000, 74,000, and 70,000 yr B.P., respectively. The average of the six age determinations for corals from the Norfolk is $74,000 \pm 2,000$ yr B.P. (1 sigma).

The average age of corals from three localities of the Wando Formation near Charleston, S.C. (Island Construction, Venning pits and Scanawah Island), has been reported previously to be 94,000 yr old. The $^{230}\text{Th}/^{232}\text{Th}$ activity ratios in these samples are rather low, ranging between 2 and 7, the indication being initial ^{230}Th contamination. A new sample of coral from Scanawah Island (collected by F. J. Wehmiller, Univ. of Delaware) has yielded a lower ^{230}Th age of 82,000 yr B.P. and a

higher $^{230}\text{Th}/^{232}\text{Th}$ ratio of 8. These new results necessitate an initial ^{230}Th correction of the previously analyzed Wando corals; the average age of the four corals (including the new sample) is calculated to be about $84,000 \pm 8,000$ yr B.P.

Two samples of corals of the Socastee Formation of DuBar (1971) (Johns Island and Ravenel localities near Charleston, S.C.; samples collected by R. Weems) have yielded ^{230}Th ages of 202,000 and 230,000 yr, respectively. These results and results of two other corals from Socastee-equivalent units reported previously yield an average U-series age of $202,000 \pm 17,000$ yr B.P. (1 sigma).

An average U-series age (^{234}U age) of $460,000 \pm 90,000$ yr B.P. has been reported previously for the age of the marine unit of the Canepatch Formation near Myrtle Beach, S.C. All of the coral samples analyzed from this unit before are *Septastrea* sp., whereas all of the dated corals from the younger sediments are *Astrangia* sp. *Astrangia* consists of a structure of thin plates rather difficult to clean from clay and silt that are accumulated around and within the specimen. On the contrary, *Septastrea* builds massive branches that are relatively clean. The results of the analyses indicate that there is no difference between Canepatch *Astrangia* and Canepatch *Septastrea*. The ^{230}Th is found to be in equilibrium with ^{234}U , and the $^{234}\text{U}/^{238}\text{U}$ activity ratio of the *Astrangia* sample yields the same ^{234}U age as the *Septastrea*, or about 460,000 yr B.P.

Sediment samples of the older Waccamaw and James City Formations have reversed magnetic polarity, therefore, these lower Pleistocene sediments have been deposited before about 700,000 yr ago. Preliminary results of He/U method have yielded dates for these units between 1.0 and 1.4 m.y. Coral samples from the Waccamaw near Myrtle Beach, S.C. (Calabash pit, collected by Lucy McCartan), have yielded a ^{234}U date of $>600,000$ yr B.P. Another coral from the Waccamaw near Charleston, S.C. (collected by R. E. Weems), has yielded a ^{234}U date of $>700,000$ years B.P. Two coral samples from James City Formation near James City, N.C. (collected by Lucy McCartan and J. P. Owens), have also yielded ^{234}U dates of $>700,000$ yr B.P., which are in accordance with geologic age estimates.

Late Cenozoic paleohydrology of California desert

The ages of some upper Cenozoic continental sedimentary deposits can be estimated by correlating their time of deposition with deep-sea isotopic stages, but this method requires an assumption that fluctuations in local hydrologic regimes were in phase with the growth and waning of high-latitude continental ice sheets. Evi-

dence from Searles Valley, Calif., a now-arid area east of the southern Sierra Nevada, suggests that synchronous global climatic change may be a partly correct assumption when applied to events of the past 130,000 yr but may not be correct for much of the preceding 3,000,000 yr when there was little discernible relation between the hydrologic regimes of this mid-latitude continental area and the volumes of high-latitude ice sheets.

In Searles Valley, a 930-m core hole (KM-3) that extends to bedrock, provides a 3.2 million yr record of nearly continuous deposition in a closed-basin lake that fluctuated in response to changes in regional hydrologic regimes. The lake sediments are subdivided into informal stratigraphic units that reflect a succession of distinct regional hydrologic balances. Some units indicate periods characterized by deep perennial lakes, others by repeated lake-level changes, and still others by intermediate to shallow salt lakes, salt flats, or playas.

Variations in 180 marine foraminifers are regarded by most workers as a record of isotopic changes in sea water caused by the waxing and waning of polar ice sheets (together with sea-water temperature changes). Comparison of these data with the continental hydrologic regime stages identified in KM-3 shows very few points of similarity. Study of marine and continental records representing a relatively short period of time, with the best age control and resolution of climatic events, shows the closest points of similarity in timing to be those representing the ends of the last two marine isotope glacial stages, but the responses of the continental climate are opposite. The end of the next-to-last marine glacial period about 130,000 yr ago coincides with the beginning of a period of deep lakes in Searles Valley, and the end of the last glacial period about 10,000 yr ago coincides with the beginning of a period of dry lakes. Relative to the continental record from KM-3, longer marine records also indicate more frequent climatic reversals. For example, two cores from the equatorial Pacific indicate eleven distinct glacial stages in the last 850,000 yr, whereas core KM-3 documents less than five distinct hydrologic regimes during this period. A 2-million-yr record of isotopic changes in the Atlantic Ocean also shows few similarities between the marine and continental histories. However, older marine isotopic data and the KM-3 sediments both record a major change about 3.2 million yr ago. The marine record indicates a "preglacial" global climate prior to that time; the continental record from Searles Valley indicates alluvial deposition and an absence of lakes prior to that time. It is possible that the sudden development of a lake in Searles Valley was an expression of global climate change, but other geologic evidence argues more strongly for a local geologic, nonclimatic cause of change.

GROUND-WATER HYDROLOGY

Development and application of techniques in ground-water hydrology covered a variety of geographical and subject areas during the past year. Applications of digital modeling techniques continued to be an important part of hydrologic investigations. A recently developed nonlinear least-squares regression technique was used to estimate transmissivity and leakage-rate values for a digital model of the regional aquifer system underlying the Snake River Plain. A two-dimensional finite-difference ground-water flow model was prepared for the principal artesian aquifer in the Dougherty Plain area of southwest Georgia. An automated technique was used to convert latitude and longitude coordinates of an irrigation pumpage data base to a cartesian coordinate system that was used in the model. A quasi-three-dimensional finite-difference model was used to evaluate the hydraulic connection of a surficial aquifer artesian aquifer in an area containing nine municipal well fields near Tampa, Fla. A two-layer Galerkin finite-element ground-water flow model was used to simulate the ground-water system in Eagle Valley, Nev. The possible effects of prominent fracture trace directions on transmissivity were evaluated by using a two-dimensional steady-state model in the Culpepper basin of northern Virginia.

Recharge studies, waste injection, and storage of energy in aquifers received attention during the year. Methods were developed for computing recharge to alluvial basins in New Mexico. Observation manholes were equipped to monitor the unsaturated zone beneath recharge basins on Long Island, N.Y. Near St. Petersburg, Fla., permeable zones and confining zones have been identified in the Floridan aquifer, and treated sewage was injected for a year in the lower part of the aquifer. Hydraulic zones were evaluated for potential thermal-energy storage in the Franconia-Ironton-Galesville aquifer at St. Paul, Minn.

Other studies in the year included the application of numerical Laplace transform inversion procedures to well-test analysis, documentation of rapid changes in salinity in ground water along the gulf coast in Florida, and hydrologic testing of zones of low permeability in New Mexico.

SUMMARY APPRAISALS OF THE NATION'S GROUND-WATER RESOURCES

A series of assessments, initiated in 1970, to provide broad-scale analyses of the quantity and quality of ground water in each of the Nation's 21 water-resources regions (as defined by the Water Resources Council) is

virtually complete. These assessments have demonstrated that ground water is a large, important, and manageable resource that should have a significant role in regional water development. The completed series of assessments will constitute a national ground-water compendium for the guidance of planning agencies and all others concerned with the Nation's water supply.

The analyses include appraisals of the significance of the ground-water resource to regional water supply, the quantities of ground water available, the quality of ground water, the present and potential problems associated with ground-water use, and additional information needed for planning and efficient development of ground water.

These summary appraisals are being published in the USGS Professional Paper 813 series, and the following 20 of the 21 regional appraisals are available: Bloyd, R. M., Jr., 1974, 1975; Price, Don, and Arnow, Ted, 1974; West, S. W., and Bronhurst, W. L., 1975; Thomas, A. E., and Phoenix, D. A., 1976; Baker, E. T., and Wall, J. R., 1976; Eakin, T. E., Price, Don, and Harrill, J. R., 1976; Bedinger, M. S., and Sniegocki, R. T., 1976; Sinnott, Allen, and Cushing, E. M., 1978; Weist, W. J., Jr., 1978; Reeder, H. O., 1978; Zurawski, Ann, 1978; Takasaki, K. J., 1978; Terry, J. E., Hosman, R. L., and Bryant, C. T., 1979; Cederstrom, D. J., Boswell, E. H., and Tarver, G. R., 1979; Taylor, O. J., 1978; Zenone, Chester, and Anderson, G. S., 1978; Davidson, E. S., 1979; Foxworthy, B. L., 1979; Gomez-Gomez, Fernando, and Heisel, J. E., 1980.

AQUIFER-MODEL STUDIES

Model of the regional aquifer system underlying the Snake River Plain in southern Idaho and eastern Oregon

Based on a nonlinear least-squares regression technique developed by R. L. Cooley (1977, 1979), two-dimensional models were used by S. P. Garabedian and G. D. Newton to estimate transmissivity and leakage-rate values in the regional aquifer system underlying the Snake River Plain. The values obtained are being used as initial estimates to develop three-dimensional models of the ground-water system. Hydrologic data for the 1980 water year were used to calculate recharge rates, boundary fluxes, and spring discharges. For preliminary analyses, ground-water withdrawals were estimated by using acreages obtained from irrigated-land maps and crop consumptive-use needs. Modeling results indicate a wide range in transmissivity from 400 to 350,000 m²/d in the aquifer underlying the eastern plain. These are similar to the values obtained in previous studies by Mundorff (1964) and Norvitch and others (1969). Statistical support of model-generated

parameter values is expressed in terms of correlation coefficients, error variance, and parameter standard errors.

Based upon measurements made in March 1980, a regional water-table map was prepared for the western Snake River Plain. Newton reports that map interpretation suggests that the western plain is a closed ground-water basin and the only outlet for discharge is the Snake River. There seems to be little or no underflow from the eastern to the western Snake River Plain. Newton further reports that preliminary modeling of the ground-water system underlying the western plain and basin-budget calculations suggest that the volume of water in the cold-water system is much larger than that in the underlying geothermal system. Further model analysis will be used to test this hypothesis.

Mathematical model of the Eagle Valley ground-water basin, west-central Nevada

A two-layer Galerkin finite-element model, consisting of 422 elements and 274 nodes for each layer, was used to simulate the ground-water system in Eagle Valley, Nev., according to F. E. Arteaga. Simulation modeling of equilibrium conditions represented by water levels in 1964 indicated that (1) discharge of ground water through evapotranspiration was 3.6 hm³/yr, which is in close agreement with recent findings, and (2) discharge of ground water by subsurface flow was 2.0 hm³/yr, which is less than previously computed. Additional calibration and analysis accomplished by simulating transient conditions from 1964 to 1978 indicate that evapotranspiration decreased to 2.5 hm³/yr as water levels in the western part of Eagle Valley have declined but that discharge by subsurface flow remained unchanged.

The model was used to predict water-level declines through the year 2000 under water-withdrawal rates as of 1978. This predictive simulation indicates water-level declines of as much as 46 m in the western part of the valley that would result in the suppression of evapotranspiration to a rate of 1.5 hm³/yr and a decrease of subsurface flow to the Carson River to 1.8 hm³/yr. Another predictive example includes simulation of 1978 conditions until an ultimate steady state is achieved. The model indicates net water-level declines of as much as 107 m in the western part of the valley, with evapotranspiration losses suppressed to a rate of 0.86 hm³/yr and subsurface discharge to the river decreasing from 2.0 to 0.12 hm³/yr.

Aquifer model of the Culpeper basin, Virginia

A simple two-dimensional, steady-state was developed by R. J. Lacznik to simulate ground-water flow in

a part of the Culpeper basin in northern Virginia. An anisotropy factor was assigned to transmissivities used in the model to concur with major fracture trace directions, but the effects of individual fractures are "transparent" in the generalized model. Transmissivities were averaged over the entire basin, the highest values being assigned to fractured sedimentary rocks and lowest values to an intrusive diabase complex and its thermally metamorphosed aureole. Input parameters were adjusted during model calibration until the difference between simulated and measured water levels were 30 percent or less. Differences greater than 10 percent occur near streams not simulated in the model and near no-flow boundaries at the eastern and western margins of the basin.

Appraisal of the surficial aquifers in the Pomme de Terre and Chippewa River valleys, western Minnesota

W. G. Soukup used a numerical model to simulate flow in the surficial aquifer and estimate the probable effects of development of irrigation on water levels in parts of Pope and Swift Counties, western Minnesota.

Near Appleton, model analysis indicates that water levels have declined about 1 m owing to pumping since 1973. The model results also show that if present (1981) pumping and average recharge continue, declines of 0.3 to as much as 1.2 m can be expected in some areas. Model simulation of a 3-year drought as severe as that of 1976-77 indicates that water levels generally would decline from 1 m to as much as 2.7 m. Similar declines can be expected in the area south of Cyrus, although the model indicates that water levels may decline as much as 3.7 m near till boundaries.

Numerical simulation of the alluvium and terrace aquifer along the North Canadian River from Canton Lake to Lake Overholser

Alluvium and terrace deposits of Quaternary age, which cover an area of about 1,000 km² along the North Canadian River between Canton Lake and Lake Overholser, locally yield 3×10^{-2} m³/s to wells, according to S. C. Christenson. The deposits are as thick as 30 m and consist of varying proportions of clay, silt, sand, and gravel, with sand-sized material dominating. The underlying bedrock is Permian sandstone and shale. During 1980, the amount of water stored in the aquifer was estimated to be 1.13×10^9 m³.

A digital model was used to determine the ability of the aquifer to continue to supply water for irrigation, industry, and domestic use. A block-centered, finite-difference model with 1.6-km node spacing was used to project the amount and distribution of water in the aquifer until 1993. The model-calibration criteria were aquifer discharge to the North Canadian River and the

difference between computed and measured heads. The model was calibrated by using a recharge rate of 25 mm/yr, a hydraulic conductivity of 1.4×10^{-4} m/s, and a specific yield of 0.16.

Model simulations using the 1979 pumping rate, a projected pumping rate, and double the projected pumping rate were made to 1993. With the 1979 pumping rate, the volume of water in storage would be 1.10×10^9 m³ and aquifer discharge to the stream would be about 0.30 m³/s. With the projected pumping-rate increase, the volume of water in storage would be 1.08×10^9 m³ and aquifer discharge would be about 0.20 m³/s. At double the projected pumping rate, the volume of water in storage would be 1.06×10^9 m³ and the aquifer discharge would be about 0.083 m³/s.

Modeling of well-field areas near Tampa, Florida

C. B. Hutchinson is developing a quasi-three-dimensional finite-difference model for simulation of steady-state ground-water flow in two aquifers throughout a 2,400 km² area containing nine municipal well fields. The surficial aquifer contains an unconfined water table and is coupled to the underlying Floridan aquifer by a leakage term that represents flow through a confining layer separating the two aquifers. Under the steady-state condition, all storage terms are set to zero. Utilization of the head-controlled flux condition allows both head and flow in the Floridan aquifer to vary at model-grid boundaries. The water-table elevation is constant at model-grid boundaries and at large surface-water bodies but is allowed to fluctuate elsewhere in response to changes in evapotranspiration, recharge, and leakage.

Preliminary model runs predict water-balance and water-level changes that can be expected as a result of pumping all nine well fields at annual average permitted capacities totaling 8 m³/sec with recharge varying 20 percent above and below the long-term average rate to represent wet and dry conditions. Expected drawdown, averaging less than 1.5 m in both the surficial and Floridan aquifers, is maximized under the dry recharge condition. Drawdown predicted by the quasi-three-dimensional model is greater in every well field and averages about 0.5 m more than that predicted by a two-dimensional model previously developed for the same area.

Ground-water-resource-management model of the Savannah, Georgia, area

R. B. Randolph expanded and updated the two-dimensional finite-difference ground-water-flow model of the principal artesian aquifer in the Savannah, Ga., area developed by Counts and Krause (1976). The model

area was expanded and the grid redesigned to include areas of interest previously unaffected by pumping. New and more accurate data on Tertiary limestone obtained from a Regional Aquifer Systems Analysis project and recent aquifer tests were utilized in the model. This update resulted in a better calibration not only for the new areas of interest but also for the Savannah area. The model results are presently being used to examine management alternatives in the area.

Increases in water use based on projected normal population growth were used to determine the effects on future water levels in the aquifer system. The model indicates that a 22-percent increase in water use over the next 30 yr will cause as much as 30 m of drawdown in some areas of the aquifer. This will result in heads as low as 73 m below sea level in the vicinity of Savannah.

Automated conversion of geocoded water-withdrawal information for input to a two-dimensional ground-water model

M. L. Maslia and L. R. Hayes calibrated a two-dimensional finite-difference model for the simulation of ground-water flow in southwest Georgia. Concurrently, as part of the Georgia Water Use Program, R. R. Pierce constructed an irrigation data base which supplied irrigation pumpage data for the ground-water model. The model simulations required as part of the data input site-specific information on irrigation withdrawals. This necessitated converting the latitude and longitude coordinates of the irrigation data base to the model's cartesian coordinate system. The modeling project had subdivided the project area into 2.59-km² grid block areas. The grid pattern of the model is not oriented north-south when overlaid on a 1:250,000 USGS topographic map. Therefore, it produces cell blocks which do not represent a constant change in either latitude or longitude. This presents a problem in locating irrigation pumpage systems in the correct grid block area. The solution involved three steps: (1) selection of coincidental points of latitude and longitude on USGS topographic maps and X-Y coordinates on the model grid, (2) conversion of the latitude-longitude coordinates by the use of an algorithm to Universal Transverse Mercator (UTM) coordinates, and (3) transformation of the UTM coordinates into the local ground-water model cartesian coordinate system through use of an algorithm which applied a least-squares solution technique to solve a system of linear polynomials. This resulted in an automated system which uses water-withdrawal information specified by latitude and longitude as input data and produces aggregated water withdrawals by cell-block location for a two-dimensional ground-water model.

Numerical modeling of the geohydrology of the principal artesian aquifer, Dougherty Plain, Georgia

The principal artesian aquifer in Georgia is part of the Tertiary limestone aquifer that underlies the Coastal Plain of Georgia, parts of Alabama and South Carolina, and all of Florida. In the Dougherty Plain area of southwest Georgia, pumpage from the aquifer for irrigation use has increased from about 5.7 m³/s in 1977 to about 9.2 m³/s in 1980. L. R. Hayes, M. L. Maslia, and W. C. Meeks used hydrogeologic data obtained from test drilling and from historical records to construct and calibrate a two-dimensional finite-difference model of the ground-water flow system. The model was calibrated for steady-state conditions that exist seasonally during late fall to early winter in the Dougherty Plain. The average error between simulated water levels and those measured during November 1979 was computed to be about 0.15 m, the standard deviation of the error being approximately 5. Steady-state ground-water flow calculated from the calibrated model was 56.0 m³/s. The model was then verified with a comparison of simulated and measured heads for the May 1980 potentiometric surface. Steady-state ground-water flow was simulated to be 95.2 m³/s. The model was then used to simulate the ground-water conditions during the 1980 irrigation season by conducting a transient simulation from May 15 to November 5, 1980. The model was also used to simulate the effects of a 3-year hydrologic drought and the effects of increased pumpage over a 10-year period. Results indicate that a short hydrologic drought has a more adverse effect on ground-water levels in the Dougherty Plain than does increased irrigation pumpage over a 10-year period.

Model studies of subsurface storage and recovery of freshwater, southern Florida

Digital models were used by M. L. Merritt to analyze the relation of recovery efficiency of aquifers containing brackish water in southern Florida. The study examined the feasibility of cyclic freshwater injection under various management alternatives. The analysis used an approach in which the control for sensitivity testing was a hypothetical aquifer representative of potential injection zones in southern Florida, and parameter variations in sensitivity tests represented possible variations in aquifer conditions in the area. The permeability of the aquifer determined whether buoyancy stratification could reduce recovery efficiency. Critical permeability levels became lower as resident fluid salinity increased, and recovery efficiency was optimized by both low permeability and low resident fluid density. High levels of simulated hydrodynamic dispersion led

to the lowest estimates of recovery efficiency. Advection by regional flow within the artesian injection zone could significantly affect recovery efficiency, depending upon the storage period, the volume injected, and site-specific hydraulic characteristics. Recovery efficiency was unrelated to the rate of injection or withdrawal or to the degree of penetration of permeable layers and improved with successive cycles of injection and recovery. Calculated recovery efficiency was determined to be optimum in certain tested combinations of well configurations and injection and withdrawal schedules. These configurations consisted of a central well surrounded by peripheral wells. Injection began at the central well but did not begin at peripheral wells until the injected freshwater from the central well reached them. Withdrawal was at a common rate from all wells.

RECHARGE STUDIES

Subsurface injection of highly treated sewage, St. Petersburg, Florida

The Floridan aquifer at the St. Petersburg, Fla., injection site has four permeable zones and three semiconfining beds, according to J. J. Hickey and G. G. Ehrlich. Rocks composing the aquifer range in age from middle Eocene to early Miocene. The injection zone is within the lower part of the Floridan aquifer in a dolomitized section of the Avon Park Limestone.

Subsurface injection was for one year at a mean rate of 0.15 m³/s. Volume of water injected was 4.8 × 10⁶ m³. In twelve observation wells at the site, calculated pressure buildup at the end of one year of injection ranged from less than 0.7 kPa to 16.6 kPa. Buoyant lift occurred and was probably a dominant factor in causing pressure buildup in and above the injection zone in permeable zones that had water density changes.

Nassau County Recharge Project, Long Island, New York

E. T. Oaksford reports that two observation manholes have been equipped to monitor the unsaturated zone beneath basins used to artificially recharge the ground-water reservoir with tertiary-treated sewage. A microprocessor-based data acquisition system has been installed and programmed to continuously monitor soil-moisture tension (Oaksford, 1978), temperature, soil gas, and pH, dissolved oxygen, and suspended solids in soil water collected from gravity lysimeters (Prill and others, 1979). Background data for soil-moisture tension, temperature, and soil-water chemistry have been collected since June 1980 and recharge is expected to begin in 1982. Temperatures in the unsaturated zone at a depth of 4.25 m have ranged from 6° to 16° C. Soil-

moisture tension values have fluctuated with precipitation and have ranged between -10 and -60 cm of water in the 4.25 m of instrumented soil profile.

Background soil-water samples have been collected from lysimeters installed in the unsaturated zone at depths of 0.76, 1.62, 2.50, and 3.35 m. Specific conductance of samples has ranged from 85 to 180 μmhos/cm² and dissolved organic carbon (DOC) concentrations have been low (3 to 15 mg/L). Dissolved oxygen was usually around 7 mg/L and, as a result, nitrogen, found primarily as nitrate, rarely exceeded 3 mg/L. Trace organics, insecticides, and herbicides have not been detected.

Injection of treated wastewater for ground-water recharge in the Palo Alto, Baylands, California

Field work has been completed in a study of ground-water recharge by injection of reclaimed water to alleviate saltwater contamination in the Palo Alto marsh along the San Francisco Bay, Calif. S. N. Hamlin has compiled chemical and hydraulic data to study compatibility of injection and ground water.

Straight-line mixing plots of major ion concentrations in ground water during injection indicate that ion exchange and dissolution reactions occur. Sodium data indicate slight enrichment, whereas potassium data show a slight depletion. Calcium and magnesium were removed from the water, most likely through ion exchange with sodium. Alkalinity was significantly enriched over the conservative mixing line, in agreement with calculations that predict undersaturation of calcite when saline ground water is mixed with relatively fresh injection water. This analysis explains the slight improvement in specific capacity of the monitor well during testing. No evidence of clogging was observed.

MISCELLANEOUS STUDIES

Solutions to problems of well-test analysis

A. F. Moench and Akio Ogata obtained solutions to complex problems of well-test analysis by using a simple and accurate, numerical Laplace transform inversion procedure. New solutions were obtained by combining leaky aquifer theory with the theory of partially penetrating wells and the theory of large-diameter wells. Typical type curves for these and other well-test problems were obtained.

Computing recharge to alluvial basins in New Mexico

Methods for computing ground-water recharge to southwest alluvial basins are being developed by J. D.

Dewey. Sources of recharge are flows from mountain fronts, ephemeral streams crossing alluvial fans, streams in hydraulic connection with the aquifer, and direct infiltration from precipitation.

The multiple-regression equation used to calculate mountain-front runoff was derived by using selected mountain-stream basin characteristics. The calculated average annual mountain-front recharge for the Albuquerque-Belen basin was about 3,400 L/s.

The recharge model used for distributing recharge along ephemeral channels uses infiltration coefficients and the annual frequency distribution of flow from a gaged stream. For ungaged streams, a precipitation-frequency distribution was used to simulate discharge for nearby gaged streams. The model gave an average recharge of 510 L/s for the Rio Salado, 620 L/s for the Rio Puerco, and 311 L/s for Abo Wash.

Streams hydraulically connected to the alluvial aquifer were evaluated by one or more of the following methods: water budget, winter low-flow seepage runs, and infiltration between gages. The calculated average recharge from the Jemez River was about 990 L/s.

Precipitation infiltrates directly into permeable rocks. The direct recharge estimates were based on a water budget using precipitation, soil moisture, vegetation type, elevation, and temperature.

Hydrologic testing of low-permeability zones in southeastern New Mexico at the Waste Isolation Pilot Plant

Increased attention is being directed toward the investigation of low-permeability zones in relation to the storage and disposal of hazardous wastes. Shut-in tests, slug tests, and pressure-slug tests were applied by K. F. Dennehy and P. A. Davis at the proposed Waste Isolation Pilot Plant site, located in southeastern New Mexico, to evaluate the fluid-transmitting properties of several zones above the proposed repository zone. Apparatus used to conduct these tests included a pressure-transducer system connected to a recording device at the land surface. All three testing methods were used in various combinations to obtain values for the hydraulic properties of the test zones. Multiple testing on the same zone produced similar results. Transmissivities of the zones tested range from 9.29×10^{-7} m²/d to 0.929 m²/d.

Depth of supply well and efficiency of heat pumps

A. L. Hodges, Jr., completed a study of ground-water temperature with application to heat pumps in the Wyoming, Del., quadrangle. Analysis of data collected between March 1980 and May 1981 from 20 wells showed that ground water at 3 m below land surface had an

annual temperature fluctuation of 8.4° C, whereas that at 10 m fluctuated 1.6° C during the same period. Ground-water temperature at or near land surface closely followed air temperature, as expected. Changes in ground-water temperature with depth, however, exhibit a dampening of change and an increasing lag in maximum and minimum temperature as depth increases. Water temperature at 3 m reached a maximum in September (19.4° C) and a minimum (10.0° C) in February. At 10 m below land surface, temperature was at a maximum (15.5° C) in January and at a minimum (13.2° C) in August. Heat pumps supplied with water from wells screened 10 m below land surface will, therefore, operate more efficiently in both heating and cooling modes than those supplied from shallow buried heat exchangers or surface-water sources.

Time-of-water sampling in tidal-affected chloride monitor well in west-central Florida

During an areal study of coastal Citrus, Hernando, and Levy Counties, Fla., J. D. Fretwell observed a wide range in specific conductance values during bimonthly sampling of a well. The well, located 3.7 km from the coastline, is one of a network of wells used to monitor saltwater movement along the gulf coast. Variations appeared to be random but ranged from 612 to 9,500 μ mhos. A continuous recording monitor was placed on the well in November 1980 to define the nature of the variations in specific conductance. Specific conductance and temperature were recorded at 30-minute intervals for a 10-day period. Results of the study showed that sharp peaks in specific conductance occurred in the well shortly after high tide and returned to a base level soon thereafter. Time-of-sampling relative to the phase of the tide is critical to understanding the relation of chloride concentrations in the well to long-term movement of the saltwater-freshwater interface.

SURFACE-WATER HYDROLOGY

MODEL STUDIES

Potomac River Reservoir release routing

Tom Trombley has completed a computer flow-routing model of the Potomac River between Luke, Md., and Washington, D.C. The purpose of the model is to determine the downstream response to flow releases from Bloomington and Savage River Reservoirs located approximately 370 km upstream from Washington. A 24-hour sustained reservoir release at Luke, Md., will result in 35 percent of the flow passing Washington, D.C., during the fourth day after the release, 61 percent

passing on the fifth day, and the remaining 4 percent passing Washington on the sixth day.

Dynamic streamflow model and hysteretic stage-discharge relations

R. E. Faye and M. E. Blalock applied Faye's dynamic streamflow model (Faye and Cherry, 1980) to stage-hydrograph data from Levisa Fork in Kentucky. A series of discharge measurements made over the rising and falling stages of a flood at Levisa Fork indicated a hysteretic (looped) stage-discharge relation. The model showed excellent agreement with the data from Prestonsburg, Ky., but was less satisfactory with the data from Paintsville, Ky. Application of the model to other data sets is necessary to demonstrate the feasibility of using the model at sites with hysteretic stage-discharge problems.

Mathematical model of the Alabama River

Flow in a regulated reach of the Alabama River and its major tributaries in central Alabama was modeled by R. A. Gardner who used a one-dimensional open-channel flow simulator developed by J. P. Bennett. The calibrated model was used to simulate flows ranging from less than 5 m³/s to more than 1,500 m³/s. Within this range, discharge is characterized by very steep transients with flow changing from 3 m³/s to 750 m³/s or more in one time step (900 s). Steep transients in the flow system are frequently accompanied by negative flows extending several kilometers up the major tributaries. These negative flows may be 100 m³/s or more. The model, which consists of 20 interconnected reaches with 88 cross sections, was calibrated and verified with two continuous-discharge records and three continuous-stage records.

Flow model of Saginaw River

An unsteady, open channel flow model of the Saginaw River developed by D. J. Holschlag (1981) provides a method of determining instantaneous discharge through the normal range, -225 to +340 m³/s, from measurements of water stage and wind velocity. To compute flows greater than 340 m³/s, the model was modified by increasing flow-resistance coefficients about 17 percent on the basis of historic high-flow measurements.

Model simulation of runoff hydrographs in the Coon Creek watershed, Anoka County, Minnesota

A. D. Arntson has simulated hydrographs of runoff in Coon Creek and its tributaries for 17 storms by using the HEC-1 model. Linear equations developed by Arnt-

son were used to calculate parameter values relating rainfall characteristics to flow data from individual storm hydrographs. The equations significantly improved model simulation of 17 of the 19 recorded hydrographs. Use of average values of optimized parameters, which has been common practice in the past, produced satisfactory simulation of only one of the hydrographs.

Watershed-model-evaluation study

Twelve deterministic watershed models that have potential use in surface-mining hydrologic-impact assessments were evaluated by the USGS Gulf Coast Hydroscience Center. The principal investigators were P. B. Curwick, W. H. Doyle, Jr., and K. M. Flynn. Two types of models, discrete-event models and continuous daily simulation models, were evaluated on the basis of three tests: (1) accessibility test; (2) hypothetical catchment test; and (3) real catchment test. Both flow and sediment subcomponents were tested. The hypothetical tests demonstrated the magnitude of implicit differences between the models, while the real catchment data tests provided comparison information on model accuracy and performance. The accessibility test eliminated four models from the evaluation. Five discrete-event models and three continuous daily simulation models were tested in the hypothetical test. Two models of each category were further tested in the real catchment test; these were the discrete-event models, ANSWERS (Beasley and Huggins, 1980) and TENN II (Overton, 1980), and the continuous models, HYSIM (Betson and others, 1980) and PRMS (Leavesley and Striffler, 1979). ANSWERS requires many input data whereas the inputs to TENN II are few and simple. However, after calibration, the two models were essentially equal in performance. Of the models tested, HYSIM is one of the easier models to use. It is a highly regionalized model developed for areas in the Tennessee Valley, and, to be applicable elsewhere, data are needed to verify the model. PRMS, because of its modular design concept, is probably the easiest model to adapt to specific-site conditions. Optimization and sensitivity routines make PRMS very useful in watershed modeling. The main intent of this study was to evaluate a few of the available models and to provide some insight into the model-selection process.

STATISTICAL STUDIES

Ridge regression estimates of peak flow at ungaged sites

G. D. Tasker combined a regression-simulation model with a multisite streamflow generator to simulate a regional regression of 50-yr peak discharge against a

pair of basin characteristics. He compared the unbiased ordinary least-squares parameter estimator with the biased ridge estimator. The results indicate a substantial improvement in parameter estimation and prediction error by use of the ridge estimator when the correlation between basin characteristics is more than about 0.90.

Bias in standard deviation due to autocorrelation

G. D. Tasker and E. J. Gilroy used random-number simulation to generate factors to correct for bias in sample standard deviation, given a Gaussian lag-one Markov process with known serial correlation. Using Monte Carlo techniques, they compared the performance of several estimators of σ , given a sample with unknown serial correlation. They found two estimators of σ which were much less biased but had greater mean-square-errors than the usual estimator. The estimators may be briefly characterized as resulting from (1) a method using a maximum likelihood estimate of the unbiassing factor, and (2) a method using an empirical Bayes estimate of the unbiassing factor.

Errors due to time-sampling bias for streamflow statistic in Georgia

R. F. Carter and J. D. Lewis used methods described by Hardison (1969) to compute the average standard errors due to time-sampling bias of statistics of monthly minimum flows for streamflow stations in Georgia. The average standard errors were found to be similar over a wide area comprising approximately the northern two-thirds of the State. In this area, the average standard error of estimate for a low-flow statistic with a recurrence interval of 20 yr and estimated on the basis of 10 yr of record is about 14 percent. In the southern third of the State, the average standard errors were found to lie in a narrow range but were significantly greater than in the north. In the southern area, the average standard error of estimate for a low-flow statistic with a recurrence interval of 20 yr and estimated on the basis of 10 yr of record is about 34 percent.

Hydrologic regionalization by cluster analysis

G. D. Tasker compared methods of determining "homogeneous" hydrologic regions by data splitting. The compared methods use cluster analysis based on similarity of hydrologic characteristics or similarity of basin characteristics. Tasker used the complete-linkage algorithm for cluster analysis and computed weighted average estimates of hydrologic characteristics at ungaged sites. The weights used were proportional to

the probability of the ungaged site falling into a particular region. He used data for 221 stations in Arizona to show that these methods improve the fit of estimation data but do not necessarily improve the accuracy of predictions at ungaged sites.

DATA-NETWORK STUDIES

Evaluation of streamflow-data networks

One use of gaging-station data is to develop relations between various flow characteristics and basin characteristics for use in estimating flow characteristics at ungaged sites. The optimum length of record at gaged sites and the optimum number of gaged sites for this purpose can be estimated by a program called Network Analysis for Regional Information (Moss and Karlinger, 1974). The program has been applied to existing gaging-station networks in three States. According to R. R. Squires, the collection of additional data at existing sites, or the addition of data from new sites, probably would produce little improvement in flow estimations for Nevada. Improvement in estimates at ungaged sites can be achieved only after development of better models for relating flow characteristics to basin characteristics.

A related evaluation program, Cost-Effectiveness Procedure (Moss and Gilroy, 1980), was used to evaluate data-collection procedures in Pennsylvania and Idaho. H. N. Flippo showed that the cost of operating 203 continuous-record gages and 49 crest-stage gages in Pennsylvania could be reduced 18 percent without reducing reliability of results by visiting the sites at 10-week rather than at 6-week intervals. Possible cost reductions were also shown by the Idaho analysis.

Attempts by E. W. Quillian and W. A. Harenberg to apply the above models to networks that also included sites for collection of ground-water and water-quality data were not successful.

An evaluation of Idaho stream-gaging networks

NARI (Network Analysis for Regional Information) and the Cost-Effectiveness Procedure were tested by applying them to stream-gaging networks in Idaho. E. W. Quillian and W. A. Harenberg used NARI to determine network design strategies that would maximize the value of additional data. Value of data was measured as the decrease in the probable true standard error of regional regression equations. NARI indicated that no significant decrease in regression error can be achieved by the collection of additional data and that

better models should be sought. No major modifications to NARI are necessary to make it widely applicable. The Cost-Effectiveness Procedure was used to determine optimal network operation strategies. It showed network uncertainty can be reduced when one- or six-visit per year minimum constraints are in force. Attempts were unsuccessful to model networks that also included sites for collection of ground-water and water-quality data.

Streamflow data network for Nevada

The Nevada streamflow-gaging network has been evaluated to determine whether it produces information that can efficiently be transferred to ungaged sites. Streamflow characteristics evaluated by regional regression analyses were the annual mean discharge, the standard deviation of that discharge, and the 50-yr peak discharge. The modeling technique Network Analysis for Regional Information (NARI) (Moss and Karlinger, 1974) was used to evaluate the effect of changes in the network on the standard errors of estimate for the regression analyses. The results indicate that the collection of additional data at existing sites or the establishment of new sites would produce little improvement in the regression relations. Future studies using other modeling techniques and different independent variables, however, may improve the reliability of estimated streamflow characteristics at ungaged sites.

Cost-effectiveness in stream gaging in Pennsylvania

H. N. Flippo reports a pilot study was made in the Pennsylvania District, WRD, to test the applicability of recently-developed statistical techniques (Moss and Gilroy, 1980) for relating accuracies of discharge estimates to operational costs. Accuracies of daily-flow records would not deteriorate noticeably if field trips that are presently made at 6-week intervals were made at 8- or 10-week intervals.

A modest savings in expenditure of \$176,500, representing 17.7 percent of the present operational budget for the 203 continuous-record gages and 49 crest-stage gages considered in this study, could be achieved by adoption of a 10-week visitation plan. A more cost-effective distribution of gages among field trips for three of the four offices would be necessary to effect this savings. Losses of gage-height record, which are presently about 5 percent, would increase to approximately 6 percent if a 10-week visitation plan were adopted.

MISCELLANEOUS STUDIES

Hydraulic-model study of impact of Interstate route 10 crossing on backwater and flow distribution of lower Pearl River

In April 1979 and April 1980, major flooding on the lower Pearl River in Louisiana and Mississippi caused extensive damage to homes located in the flood plain of the Pearl River in the area of Slidell, La. Constrictions created by highway embankments, together with other physical features of the flood plain, caused significant lateral variations in water-surface elevation and flow distribution during the floods.

J. K. Lee, G. J. Wiche, J. J. Gilbert, and D. C. Froelich have used a two-dimensional finite-element surface-water modeling system based on the shallow-water equations to study backwater and flow distribution at the Interstate-10 crossing of the Pearl River basin near Slidell, La.

Model results showed that the highway embankment caused a redistribution of flow from the west to the east side of the flood plain during the April 1980 flood, that the maximum backwater was 0.46 m on the west side of the flood plain but only 0.34 m on the east side, and that backwater effects extended further upstream on the east side than on the west side. On the downstream side of the embankment, a maximum negative backwater of 0.09 m was computed on the west side of the flood plain and a maximum positive backwater of 0.18 m on the east side.

Effects of channel excavation in North Carolina

Hydrologic changes due to channel excavation on Black River near Dunn, N.C., were defined by C. E. Simmons. An 8-km reach was cleaned and deepened about 0.6 m. Streamflow records were obtained before and after excavation both upstream from and within the excavated reach.

The principal changes in the excavated reach were (1) over a 100 percent increase in flow velocities, (2) a one degree Celsius increase in water temperature due to removal of trees and the consequent reduction in shade, (3) increases of 20 to 25 percent in dissolved-oxygen concentrations at the lower discharges, and (4) increases in maximum concentration of suspended sediment from about 25 times soon after excavation to 5 to 10 times one year later.

Deepening of the channel caused a similar decline in ground-water levels within 30 m of the channel but no effect 150 m away. Little or no change was found in pH, total dissolved solids, nitrogen, phosphorus, or bacteria.

Streamflow changes in Platte River basin

J. E. Kircher and M. R. Karlinger (1981) analyzed changes in streamflow in the Platte River basin in Colorado, Wyoming, and Nebraska upstream from Duncan, Nebr., an area of 157,700 km².

Nine stream-gaging stations in the basin were selected for analysis of streamflow changes. Flow-duration curves, 1-, 3-, 7-, 14-, and 30-day mean low flows, and 1-, 3-, 7-, 15-, and 30-day mean high flows were determined for these stations. Beginning about 1950, flow-duration curves for all stations, except the South Platte River near Kersey, Colo., show a change with time of the low-flow segment of the distribution curve in a downstream direction. The analyses indicate that high flows have been relatively unaffected by water development in the Platte River basin. Low flows in the North Platte River increased following the closure of Kingsley Dam in 1941. Low flows in the South Platte River at Julesburg, Colo., increased around 1920, and at North Platte, Nebr., around 1932. Statistical analyses of data from six selected sites were performed to determine (1) the significance of major water developments capable of producing abrupt changes in the time series of streamflow statistics, and (2) the significance of water developments that caused a more gradual change or time trend in the streamflow statistics.

Effects of a flood-retarding dam

D. J. Graczyk, S. J. Field, and D. A. Wentz determined the primary effects of a floodwater-retarding structure (FRS) on streamflow, sedimentation, and channel morphology. The primary effects of the FRS on the streamflow of Trout Creek are the attenuation of flood peaks and extension of the time base of the flood hydrographs. The FRS also affects the sediment transport of Trout Creek. Most sediment stored in the flood pool during floodflows is released from the reservoir during subsequent reduced discharges. Sediment-trapping efficiency was about 7 percent for the 4-year period of the study. It was found that the structure reduced bankfull discharge by about one-half from upstream of the flood pool to downstream of the FRS. Mean bankfull depth below the FRS has adjusted to a value 45 percent less than the depth above the structure because of sedimentation of material transported from the FRS during reduced flows.

Preliminary analysis of historical streamflow and water-quality records for the San Juan River basin, New Mexico and Colorado

Long-term streamflow and water-quality records are available at the U.S. Geological Survey gaging stations located along the San Juan River and its tributaries in

New Mexico and Colorado. C. L. Goetz compared long-term records and records for 1963-79 in an attempt to detect significant changes in streamflow quantity and water quality. The t-test and Wilcoxon Rank Sum statistical procedures were used to detect changes.

Results show that streamflow characteristics have remained unchanged at San Juan River at Pagosa Springs, Colo., which is located in the headwaters of the river. However, at a downstream station, San Juan River at Shiprock, N. Mex., daily streamflow, specific conductance, and sediment load have decreased. The discharge-weighted specific conductance means for the two periods have increased at the same station. This implies that the decrease in daily specific conductance is not due to a decreased dissolved-solids load but to dilution effects caused by a difference in streamflow characteristics. The change in streamflow characteristics is partly a result of reservoirs that became operational after 1963 and are located on tributaries and the mainstem between the headwaters and the downstream station. Daily precipitation was tested and found to be unchanged for the pre-1963 and post-1963 periods. Other causes for the changes may be related to increasing population, changes in agricultural irrigation, mining, increased industrialization, or a combination of these factors.

Vertical velocity profiles in stratified open-channel flows

Experiments by S. C. McCutcheon involving mildly stratified turbulent flows (a gradient Richardson number ≤ 0.025) in a laboratory flume have shown that the logarithmic velocity profile is invalid unless it is modified by using arguments first developed by Monin and Obukhov for the atmospheric boundary layer (McCutcheon, 1981a). This modified profile makes it possible to compute the vertical velocity profile and velocity gradient in two-dimensional unidirectional continuously stratified shear flows from the density gradient, distance above the bottom boundary, average density, shear velocity, local acceleration of gravity, von Karman's constant ($\times 0.4$), and the Monin-Obukhov coefficient, α (determined to be 5.8 for stratified open channel flows). In addition, these results show that the width-to-depth ratio and degree of stratification are important factors in producing two-dimensional stratified flows in flumes.

Arkansas traveltime study

At various times during the past 10 years, T. E. Lamb has injected tracers into selected streams in Arkansas to measure traveltimes and dispersion characteristics. Flow about 20 percent of the average discharge generally yields predictable traveltimes in streams with

channel control. Streams with "pool and riffle" type channels are less predictable, especially during low flow; at discharges in the 7-day, 10-year frequency range, travel-times are very erratic and time-concentration curves often have multiple peaks. On two large navigable streams, the Arkansas and Ouachita Rivers, travel-time predictions are unreliable because of nonsteady flow created by several upstream power-generation dams.

Stage-discharge relations at dams on the Illinois and Des Plaines Rivers in Illinois

J. R. Gray and D. M. Maden report that measurements of discharge that ranged from 2.8 to 2,450 m³/s were used to determine stage-discharge relations for hydraulic control structures at four navigation dams on the Illinois and Des Plaines Rivers. Discharge coefficients in equations for steady flow under a taintor gate were determined for gates at the Dresden Island, Marseilles, and Straved Rock Dams. The coefficients ranged from 2.71 to 3.22 for free weir flow, 0.54 to 0.79 for free orifice flow, and 0.05 to 0.64 for submerged orifice flow. A free orifice discharge coefficient of 0.69 was determined for flow past headgates at the Brandon Road Dam.

Two estimates of leakage, 24.2 and 18.1 m³/s, were made for the Brandon Road Dam during different flow conditions. The estimates were based on discharge measurements and stage-discharge relations for the taintor gates and headgates at the dam. Leakage of 4.96 m³/s was measured at the downstream edge of the Marseilles Dam stilling basin on April 7, 1981, when all main channel taintor gates were closed.

Channel-geometry relations for Wyoming streams

The use of channel geometry has been found to be a worthwhile technique for estimating streamflow at ungaged sites, especially in arid and semiarid regions of the West. The procedure involves relating dimensions of channels to estimate streamflow at ungaged sites. H. W. Lowham (1976) previously developed such relations for Wyoming streams and he is presently updating the data and refining the relations.

Part of the residual error in these relations is due to variations in channel shape. On the basis of findings by Schumm (1960) that the percentage of silt and clay in the bed and banks has a significant influence on channel shape, Lowham collected samples of the bed and bank material for a test group of 23 gaged sites mainly on ephemeral streams in the plains areas of the State.

Median grain size, percent silt and clay, a sorting index that describes the variability of the particle sizes, and a plasticity index were determined for each of these

samples. Regressions of bankfull discharge on channel width and these bed and bank material indexes showed that none of the indexes were significantly related to bankfull discharge.

Hydraulic geometry of stream channels in the Piceance basin area

Hydraulic and geomorphic characteristics of relatively stable alluvial stream channels have been documented by J. G. Elliott and K. D. Cartier as a basis for assessing the impact of future energy development on channel stability. The study involved 21 stream channels in the semiarid shale region of northwest Colorado. Sediment size, basin characteristics, and channel form were measured. Bankfull discharge was available from streamflow records.

The sample was divided into two subgroups, perennial and ephemeral, and various channel characteristics were related to bankfull discharge, basin characteristics, and median grain size of bed and bank material. The relations for perennial streams are consistent with those for perennial streams in other semiarid regions of the United States. The relations for the ephemeral streams are markedly different.

Most of the variation in channel geometry is explained by bankfull discharge and valley slope. Drainage area and median grain size of bed material were found to be relatively unimportant.

Times of concentration and storage coefficients for Illinois streams

Values of time of concentration (*TC*) and storage coefficient (*R*) were computed for 98 drainage basins in Illinois that range from 1.17 to 938 km². According to J. B. Graf, the computed values of *TC* and *R* were compared with those computed by other investigators, and no significant differences were found. Therefore, *TC* and *R* values computed in this investigation and those computed by other investigators can be used in any application in Illinois for which they are needed.

A two-step technique for estimating *TC* and *R* for ungaged basins in Illinois was developed. The sum (*TC+R*) is related to stream length and main channel slope. This sum is used with regional values of the variable *R/(TC+R)*, which may account for regional physiographic differences in Illinois, to compute values of *TC* and *R*.

Low-flow characteristics of Massachusetts streams

S. W. Wandle, Jr., stated that annual minimum 7-day mean flows at the 2-yr and 10-yr recurrence intervals ranged from 0.11 to 4.04 and from 0 to 2.08 dm³/s/km², respectively. Station records for 39 sites based upon daily flows through 1979 were selected to represent

essentially natural conditions or consistent regulation patterns. The average length of record at these sites is 25 yr, and the daily flow exceeded 90 percent of the time varied from 0.44 to 4.26 dm³/s/km². An up-to-date data base of low-flow frequency values and duration of daily flows is being prepared for the evaluation and design of wastewater disposal and water-supply activities and for management of activities which affect streamflow in Massachusetts.

Applications of draft-storage diagrams for Georgia streams

R. F. Carter computed regional storage requirements to develop as much as 60 percent of the mean annual flow of streams in Georgia. These storage requirements were regionalized and expressed by draft-storage diagrams applying to four regions of the State. Draft-storage diagrams are useful for estimating in-channel storage required for low-flow augmentation, for estimating the volume of off-channel storage required to retain wastewater during low-flow periods for later release, and for estimating the volume of wastewater to be disposed of by spraying on land, provided that the water disposed of in this matter is only that for which stream-flow dilution water is not currently available.

Hydrologic evaluation of streamflow records at gaging stations in the Upper Columbia River basin and Bear River basin in Idaho

As part of a study to determine the adequacy of streamflow measured at gaging stations to represent water yield from basins, R. L. Moffatt reports that records from 14 of 22 stations in the Upper Columbia River basin in northern Idaho are affected by upstream regulation or diversions. However, the volume of water consumptively used or depleted from tributary areas as a result of man's activities and (or) that which bypassed the stations as underflow was generally less than 2 percent of the volume measured as surface flow at the stations. Thus, in most places, the gaged records were considered to adequately represent yield from drainage areas tributary to the Upper Columbia River. In comparison, 11 of the 18 gaging stations in the Bear River basin in southeastern Idaho are affected by upstream regulation or diversion. Unlike conditions in northern Idaho, the volume of water depleted from tributary areas as a result of man's activities and (or) that which bypassed the stations as underflow was, in most places, a significant part of basin yield. The most extreme condition was in Soda Creek subbasin, where about 75 percent of the water yield was estimated to bypass the gage as underflow. About 18 percent of the yield in this subbasin was attributed to interbasin movement of water from the Blackfoot River subbasin within the Up-

per Snake River basin, which is immediately north of the Bear River basin.

Flow losses along the Nueces River, Cotulla to Simmons, Texas

Analysis of the discharge hydrographs for gaging stations on the Nueces River at Cotulla, Tilden, and Simmons indicates that significant water losses occur along this reach during storm-runoff periods. According to B. C. Massey and W. E. Reeves, losses between Cotulla and Tilden ranged between 32 to 59 percent of the total runoff volume at Cotulla for 15 storm periods. The losses between Tilden and Simmons ranged from two to eight percent of the total runoff at Cotulla in an analysis limited to six storm periods.

Reach velocities in Illinois streams

Twelve measurements of time of travel and longitudinal dispersion were made on 7 uncontrolled Illinois streams ranging in drainage area from 326 to 3,926 km², according to Julia B. Graf. Measurements were made by tracing clouds of rhodamine WT dye through 26.9 to 67.3 km reaches at conditions corresponding to 20, 50 and 80 percent flow duration frequency. Preliminary analysis of all 26 measurements on 10 streams made to date indicates that best estimates of average reach velocity can be obtained from a relation based on flow duration frequency and discharge at the downstream end of the reach.

PALEONTOLOGY

Research by paleontologists of the USGS involves biostratigraphic, paleoecologic, taxonomic, and phylogenetic studies of a wide variety of plant and animal groups. The results of this research are applied to specific geologic problems related to the USGS program of geologic mapping, to resource investigations, and to the provision of stratigraphic framework for synthesis of the geologic history of North America and the surrounding oceans. Some of the significant results of paleontological research attained during the past year, many of them as yet unpublished, are summarized in this section by major geologic age and area. Many additional paleontologic studies were carried out by paleontologists of the USGS. In 1981, a total of 4,656 samples were analyzed from 36 States, the District of Columbia, and 22 foreign countries. Nearly 720 reports were issued to colleagues in the Geologic Division, Conservation Division, Water Resources Division, and the Office of International Geology of the USGS, among others. The results of some of these investigations are reported under other sections in this volume.

MESOZOIC AND CENOZOIC STUDIES

Atlantic offshore stratigraphy—Georges Bank Basin and Blake Escarpment

Continuing studies of the Atlantic margin rely on the integration of drill-hole data, samples collected from research submersibles, and the interpretation of seismic profiles. A stratigraphic analysis of a multichannel seismic profile across the Georges Bank Basin by C. W. Poag has shown that Triassic(?) and Jurassic evaporites and shallow marine carbonates are overlain by Cretaceous and Cenozoic units that are predominately siliclastic rocks indicative of nonmarine and marine depositional environments. The lithology, unconformities, and paleoenvironmental cycles of the sequence are similar to those of the Scotian Basin situated immediately to the north on the Canadian margin. A biostratigraphic study by P. C. Valentine of samples collected by the submersible Alvin on the Blake Escarpment off Florida, in conjunction with seismic stratigraphic interpretations of the region, has led W. P. Dillon and his coworkers to conclude that (1) the 3,500 m escarpment is an erosional feature; (2) it is constructed of predominately Lower Cretaceous shallow water limestone; and (3) it is a carbonate platform probably analogous to a feature that has been observed in seismic profiles to extend northward along the Atlantic margin beneath the Continental Slope.

Cretaceous-Tertiary boundary iridium anomaly

The Cretaceous-Tertiary boundary in marine rocks is recognized by an abrupt change in microfossil content. At several localities in the world an anomalously high iridium concentration has been found at this horizon. It is postulated that the iridium anomaly originated from debris generated by the impact of a large extraterrestrial object.

Search for a similar iridium anomaly was undertaken by R. H. Tschudy in the nonmarine rocks of the Raton Basin of New Mexico where deposition was apparently continuous across this boundary. In these rocks the boundary is identified by an easily recognizable change in the pollen content of the rocks. Several species that characterize the Upper Cretaceous of the Western Interior abruptly disappear. This palynological boundary was identified from core material; when these rocks were then tested for iridium content by C. J. Orth and others at the Los Alamos laboratory it was found that an anomalously high iridium concentration was present at this boundary. This coincident occurrence of iridium at the palynological boundary has been narrowed to a 2 cm interval. The iridium anomaly at the Cretaceous-Tertiary boundary in both marine and nonmarine rocks

invites speculation regarding a cause-effect relationship for the apparent widespread biotic extinctions at the end of Cretaceous time. Work is continuing at several additional localities in the Raton, San Juan, and Denver basins.

Tertiary Studies, Arctic Coastal Plain, Alaska

A series of offshore boreholes taken in the western Beaufort Sea have yielded a diverse assemblage of ostracodes and foraminifers that are currently being studied by K. A. McDougall and E. M. Brouwers. Several of the cores examined penetrated upper Pliocene and lower Pleistocene sediments. The climatostratigraphy established indicates a sequence of repeated eustatic sea-level changes, with well preserved Wisconsinan, Sangamon, ?Kotzebuan, and Beringian marine transgressions. The Sangamon/?Kotzebuan transgression was accompanied by a major invasion of deeper water Arctic species presently endemic to the North Atlantic. Amino-acid analyses (isoleucine/alloisoleucine racemization) of the benthic foraminifers by Julie Brigham (Univ. of Colorado) is providing the relative timing of the transgressions as well as serving as a tool to assist in correlation of the offshore boreholes to onshore sediments.

Studies of amino acid dates derived from mollusks and benthic foraminifers from the Pleistocene Gubik Formation exposed along Skull Cliff, southwest of Point Barrow, suggest the presence of three marine transgressions. The abundance of megafossils and microfossils at several Skull Cliff sections, combined with the amino acid dating techniques, is providing a tentative biostratigraphic framework for dating and correlating Gubik outcrops elsewhere on the North Slope.

Baseline studies of modern ostracode (E. M. Brouwers), foraminifer (K. A. McDougall), and mollusk (L. N. Marinovich) species of the western Beaufort, Chukchi, and Bering Seas are nearly complete and include the geographic distributions and the controlling physical-chemical parameters. The data document habitat preferences, depth assemblages, and salinity-temperature assemblages. This information forms a vital key in the accurate interpretation of Arctic Neogene paleoenvironments, paleoclimate and paleogeography, and the resultant chronostratigraphic framework.

L. N. Marinovich and E. M. Brouwers have identified a major early Tertiary assemblage of mollusks and ostracodes at Ocean Point, along the Colville River Arctic Coastal Plain. Preliminary studies suggest that this is an endemic fauna that evolved in a basin that was isolated from the rest of the world oceans. Fission-track analysis of an interfingering ash layer has an age of 50.9 ± 7.7 m.y.; in addition, plots of the known ranges

of the ostracode genera indicate an Eocene and Oligocene age. These are the first Paleogene marine beds recognized north of the Brooks Range.

Megafossil plant zonation, Raton Basin, New Mexico

New analyses of fossil leaf assemblages collected by J. A. Wolfe in the Raton Basin in New Mexico indicate that at least four floral zones can be recognized. The lowest zone is presumed to be latest Cretaceous in age, and the other three are presumed to be early Paleocene. The flora of the three lowest zones indicate very warm climates, but cooling is evidenced in the uppermost zone. No climatic difference is apparent between the latest Cretaceous and earliest Paleocene floras.

Eocene montane floras

Analysis of plant megafossils from montane Eocene floras in the northern Rocky Mountain region, particularly northeastern Washington, is providing much new information on the distribution in time and space of temperate plants. The analysis by J. A. Wolfe (USGS) and Wesley Wehr (University of Washington) indicates that the floras include an admixture of totally extinct and relict angiosperms and early occurrences of extant genera. Comparison to lowland floras in adjacent areas suggests that the depositional basins in these montane areas were at an altitude of 900 m during the middle Eocene.

California Eocene Kellogg Shale correlated to Atlantic cores

Study of 34 samples (J. A. Barron collection, 1977, 1981) from the 30-m section of Eocene Kellogg Shale of Clarks and Campbell (1942) exposed west of Byron, Calif., shows that the silicoflagellate assemblage contains many species in common with a middle Eocene flora described in marine cores from DSDP Site 356 on the Sao Paul Plateau in the South Atlantic Ocean (J. D. Bukry, 1977). Distinctive, short-ranging guide species, such as *Macrora najae* Bukry and *Mesocena venusta* Bukry, occur with more cosmopolitan guide species, such as *Distoyocha spinosa* (Deflandre), *Macrora barbadensis* Deflandre), *Mesocena oamareunsis* Schulz, and *Naviculopsis foliacea* Deflandre, at both locations. J. D. Bukry reports that Kellogg specimens of *M. Najae* and *M. venusta* are the first reported from anywhere in the Pacific basin. At DSDP Site 386 in the North Atlantic and at DSDP Site 356 in the South Atlantic, they are reported in the middle Eocene lower *Dictyocha hexacantha* Zone or upper *Naviculopsis foliacea* Zone. The first occurrence of *Dictyocha hexacantha* Schulz in California and the Atlantic sites is sporadic; only two samples

near the base of the Kellogg section contain it. Therefore, the Kellogg can be assigned to the lower *Dictyocha hexacantha* Zone of cosmopolitan usage, but auxiliary guide fossils *M. barbadensis*, *M. najae*, and *M. oamaruensis* are used for zonal assignment of most of the samples.

Tropical Miocene silicoflagellates near Barbados

Although only one silicoflagellate-rich level is available from the upper lower Miocene cores for study at DSDP 543 (15° 42.7' N., 58° 39.2' W.) north-northeast of Barbados, several stratigraphic and ecologic relations can be explored through this assemblage. Biostratigraphically, the lack of cosmopolitan *Actinocyclus ingens* Rattray and *Naviculopsis* indicates a brief interval just below the early to middle Miocene boundary. But the species array of the assemblage is unusual because of the combined paucity of *Corbisema triacantha* (Ehrenberg) and *Distephanus crux* (Ehrenberg) s. ampl. and the absence of *Mesocena apiculata curvata* Bukry, which can be rather common in late early Miocene assemblages. J. D. Bukry reports that the common *Mesocena elliptica* (Ehrenberg) helps to suggest a level of comparison to other assemblages. For example, DSDP 370 Core 3 contains *Corbisema triacantha* and *M. elliptica* but is predominated by *Distephanus crux*. *D. crux* is considered to be favored in waters of temperate coastal influence (Bukry and Foster, 1973). Although the genus *Corbisema* is considered to have favored warmer waters than *Distephanus*, the maximum abundances of the terminal species, *Corbisema triacantha*, in the *C. triacantha* Zone at DSDP sites, are also at temperate coastal sites such as DSDP 415 and 470. Lower-latitude (DSDP 158 and 495) and open-ocean (DSDP 66) sites have less abundant *C. triacantha*. Therefore, the high relative paleotemperature value of $T_s=91$ for DSDP 543 and paucity of these high-latitude taxa are appropriate to its more tropical and oceanic location.

Asiatic mollusks in Miocene faunas of the Alaska Peninsula

Intensive studies of Miocene molluscan faunas of the Alaska Peninsula by L. N. Marincovich have yielded unexpectedly high numbers of Asiatic taxa which provide the basis for correlating Alaskan strata with those in the northwestern Pacific (Japan, Kamchatka, Sakhalin, and Chukotka). The Tachilni Formation, which crops out near the tip of the Alaska Peninsula, contains 53 molluscan taxa (36 bivalves and 17 gastropods), and about one-third of these have their main occurrences in Asiatic formations and have not previously been recognized in Alaska or other parts of North America. The Tachilni is of early late Miocene age and its exotic

mollusks suggest correlation with the Etolon Formation of western Kamchatka, the Nutovo Formation of northern Sakhalin, and possibly with the Togeshita and Okkopezawa Formations of Hokkaido. A molluscan fauna larger than that of the Tachilni, but not yet well studied, occurs in the Bear Lake Formation which crops out in the middle portion of the Alaska Peninsula and is of middle and late Miocene age. Numerous Asiatic mollusks, including some known in the Tachilni fauna, are now recognized in the Bear Lake fauna. Ongoing studies will document the extent to which Asiatic taxa are present in the Bear Lake fauna and the possibilities for developing even better faunal ties between Alaska and Asia.

Also present in the Tachilni and Bear Lake faunas are a number of mollusks best known from occurrences in Miocene formations of Oregon and Washington. For example, the Tachilni fauna correlates with mollusk faunas of the Empire Formation in Oregon and the lower part of the Montesano Formation of Weaver (1912) in Washington. Similarly, Pacific Northwest taxa are known to occur in the Bear Lake Formation, but to a yet unknown extent. Thus, Alaska Peninsula Miocene molluscan faunas, with their mixture of Asiatic, Pacific Northwest, and endemic Alaskan species, comprise a paleontological Rosetta stone that has yielded correlations spanning the North Pacific from Hokkaido to Oregon.

Pacific climatostratigraphy by oceanic silicoflagellates

Relative paleotemperature values (T_s) calculated from abundances of warm- and temperate-water silicoflagellates can be used for correlation in the time interval 4.4 to 5.3 Ma at DSDP Sites 503A (4° N., 96° W.) and 504 (1° N., 84° W.). J.D. Bukry reports that for the identical time interval bracketing the Miocene/Pliocene boundary (5.0 Ma), the T_s cool and warm peaks show a similar sequence. Using diatom datums and the latest Miocene silicoflagellate acme of *Mesocena quadrangula* as time references, the following sequence occurs. At 5.3 Ma a cool peak of $T_s=42$ at DSDP 503A and $T_s=46$ at DSDP 503 is followed by a warming trend to $T_s=72$ and $T_s=63$, respectively, and the warm peak is within the latest Miocene acme of *M. quadrangula*. After a brief cooling, a warming trend proceeds across the Miocene/Pliocene boundary at 5.0 Ma. Values of $T_s=86$ for both sites occur adjacent to the boundary at Core 31 at DSDP 503A and Core 48 at DSDP 504. The maximum values of this trend are slightly higher at $T_s=92$ for Core 29 (4.8 Ma) at DSDP 503A and $T_s=91$ for Core 47 (4.8 Ma) at DSDP 504. Therefore, silicoflagellates provide an excellent local climatostratigraphic aid for the eastern Pacific marine correlations.

Hemphillian vertebrate fauna from Mobile County, Alabama

A vertebrate fauna of Hemphillian age, late Miocene to early Pliocene, about 10 to 3.5 m.y. ago (Berggren and Van Couvering, 1974, fig. 1), was collected by F. C. Whitmore on the right bank of Chickasaw Creek in northern Mobile County, 1.5 km northeast of the town of Mauvilla. The bones are found in a gray clay with thin intercalated sand beds, mapped by the Alabama Geological Survey as Miocene undifferentiated and underlying the Citronelle Formation. The bones, occupying a stratigraphic thickness of about 60 cm and lying about 2 m below the top of the clay, were associated with large logs, ranging from 0.5 cm to almost 1 m in diameter and oriented subparallel, between N. 30° E. and N. 50° E. The largest concentration of bones, all of which were disarticulated, lay close against the west sides of the logs in association with large amounts of woody trash. Soft-shelled turtles (*Trionyx*) were the most numerous components of the fauna. Land tortoises were also present and gar scales were very numerous. The lower jaw of a long-beaked porpoise (*Pomatodelphis inaequalis*) was collected by F. C. Whitmore and George Lamb (University of South Alabama) at the site in 1967, but further digging has produced no more porpoise bones.

Land mammals of the fauna included the rhinoceros *Teleoceras*, the horses *Hipparion* and *Nannippus*, the protoceratid (horned ruminant) *Synthetoceras*, a large camel, a peccary, and a large beaver similar to *Castoroides*. The bones are fresh and unabraded, so they do not appear to have been transported far; some of them show signs of having rotted, probably subaqueously. A jawbone of an infant protoceratid bears tooth marks on both sides that are from the canine teeth of a carnivore. No carnivore bones have yet been found in the collection, preparation of which has just begun.

The clay in which the bones are found shows cyclic sedimentation, having repeated alternation of clay beds (about 10 cm thick) and gray sand stringers (2 to 3 cm thick). Most of the bones are in sand stringers, embedded in the top of the clay bed. Judging from the freshness of the bones, the investigators think it is probable that they represent a fauna inhabiting a single small drainage basin. They were probably deposited during floods in a backwater where there was little current except during flood stage. The puzzling presence of a long-beaked porpoise may be explained by the hypothesis that *Pomatodelphis* was a freshwater porpoise.

Uplift of the San Bernadino Mountains, California

Deposits in the San Timoteo Badlands, south of the San Bernadino Mountains, record the first appearance in this area of debris derived from the rising Transverse

Ranges source area to the north along the San Andreas fault. The Mount Eden fauna occurs in this part of the section and has been known for 60 yr as being of late Hemphillian age (about 7-5 m.y. B.P.). A more precise date was needed, and the application of the developing neotomine rodent biochronology, by S. R. May, A. H. Walton, and C. A. Repenning indicated an age of between 5.0 and 5.4 m.y. B.P. for this change in source area. Earlier work by May and Repenning, based upon the microtine rodent biochronology, indicated that deposition derived from the Transverse Ranges continued in the San Timoteo structural block at least until about 1.2 m.y. ago before deformation halted.

To the north of the San Bernadino Mountains, near Lucerne Valley, the Old Woman Sandstone also records the first appearance of debris from the Transverse Ranges on the Mojave Block; the formation was subsequently overthrust from the south. Two poor faunas are known from the Old Woman Sandstone in that part of the section underlying the earliest clasts derived from the San Bernadino Mountains. Use of the neotomine rodent biochronology by May, Walton, and Repenning indicates that these faunas are between 2.5 and 3.0 m.y. old.

Farther west along the San Andreas Fault near Palmdale, the Harold Formation, previously considered younger than 400,000 yr, is now known to be between 800,000 and 1 million yr old on the basis of the rodent biochronology.

Elk Hills, California

The youngest sediments involved in the first upwarping of the Elk Hills anticline of Naval Petroleum Reserve No. 1 contain micromammals (both neotomine and sigmodontine rodents) which indicate an age of deposition of about 2.2 m.y., according to S.R. May and C. A. Repenning. These beds subsequently were upwarped, beveled, and overlain by fluvial gravels that are as yet undated and that were themselves subsequently upwarped to produce the present total structural relief.

Gubik Formation, Alaskan North Slope

At two localities southeast of Point Barrow, marine mammals from a basal unit of the Gubik Formation indicate great differences in age, according to C. A. Repenning. These indications are based upon the known biochronology of these marine mammals as calibrated around the Northern Hemisphere by micromammal biochronology. At one locality the basal marine unit of the Gubik is within 200,000 yr of being 2 m.y. old; at the second the basal (?) marine unit is most likely only about 120,000 yr old. Dating is through micromammal chronology as correlated to the oxygen isotope records of the

deep-sea cores. Formerly, all Gubik deposits were thought to be middle to late Pleistocene in age, and the depositional picture seems more complex since such extreme age variation within the formation has been recognized.

Cenozoic Studies, Gulf of Alaska Tertiary province

E. M. Brouwers has identified 150 Pleistocene and Holocene ostracode species in 268 offshore bottom grab samples examined from the Gulf of Alaska continental shelf, between Prince William Sound and Cross Sound. The Gulf of Alaska forms part of the Aleutian Zoogeographic province, having a cold temperate (boreal) marine climate. The modern ostracode species permit a definition and characterization of the Aleutian province. The southern provincial boundary, at Dixon Entrance (54° N. latitude), corresponds to the change from California Current water to the Alaska Current system. The northern provincial boundary, at the Aleutian Island Arc (about 62° N. latitude), corresponds to the change in water masses from the Alaska Current to the Bering Sea system.

Five distinct ostracode assemblages have been defined by means of Principal Coordinate Analysis (PCOORD). Four of these assemblages correspond to physical and chemical parameters that change with depth, primarily water temperature and salinity; to a lesser extent, oxygen content, turbidity, substrate, nutrient supply, and wave and storm activity are involved. The fifth assemblage is composed of ostracode species that correspond to environments no longer existing in the Gulf of Alaska.

Late Quaternary vegetation and climate history from western Alaska

See same title under the Climate section of this chapter.

PALEOZOIC STUDIES

Middle Cambrian fossils in central Brooks Range, Alaska

During the 1981 field season, Middle Cambrian fossils were discovered in sandy limestone that is intimately associated with marble and black fine-grained clastic rocks in the Doonerak anticlinorium of the central Brooks Range. Trilobites, identified by A. R. Palmer (Geological Society of America) include: *Kootenia* cf. *K. anabarensis* Lermontova, cf. "*Parehmania*" *lata* Chernysheva and *Pagetia* sp. Brachiopods are *Nisusia* sp. and acrotretids. The paraconodont *Westergaardina* sp. was identified by J. E. Repetski. The age of this

assemblage is most likely early Middle Cambrian, correlative with the Amganian stage of Siberia. The fossiliferous sequence is cut by two generations of mafic dikes, dated previously as 470 m.y. and 350 m.y. old. This autochthonous anticlinal structure may be part of the southern Brooks Range terrane that also contains Precambrian metamorphic and intrusive igneous rock farther west in the Survey Pass and Ambler River quadrangles.

Early Paleozoic Basin margin, Antelope Range, Nevada

Field and laboratory studies (1978–81) conducted by M. E. Taylor and J. E. Repetski in the Antelope Range, central Nevada, show that the Windfall Formation and overlying *Caryocaris* shale member of the Goodwin Limestone record a basin-slope facies in contrast to shoal-water facies of similar age in eastern Nevada. The upper part of the Whipple Cave Formation of the central Egan Range, east-central Nevada, consists of light- to medium-gray, medium- to thick-bedded limestones with high-relief domal stromatolites and thrombolites deposited in shoal waters of a carbonate shelf. The richly fossiliferous strata contain abundant and diverse conodont and trilobite faunas that have paleobiogeographic affinities with the North American Midcontinent Faunal Province. The Cambrian-Ordovician boundary occurs within the *Hirsutodontus hirsutus* Subzone of the *Cordylodus proavus* Zone, approximately 40 to 50 m below the top of the Whipple Cave Formation. Coeval strata in the Antelope Range, central Nevada, 130 km west from the Egan Range, are assigned to the Windfall Formation and *Caryocaris* shale member of the Goodwin Limestone. In the Antelope Range, the Windfall consists of isoclinally folded, thinly interbedded dark-gray limestone and dark-brown to black chert. The Windfall is overlain by dark-gray to dark-brown calcareous and phosphatic shales of the *Caryocaris* shale member.

The Windfall and *Caryocaris* shale member are interpreted to have formed on an ocean-facing slope in Late Cambrian and Early Ordovician time. The *Caryocaris* shale member may reflect ponded sediment deposited in an intraslope basin formed by penecontemporaneous slumping of the Windfall strata during the Early Ordovician.

Paleobiogeographic affinities of the conodont faunas from the Antelope Range section are cosmopolitan below the top of the *C. proavus* Zone and mixed North American and North Atlantic faunas in higher strata, whereas trilobites show affinities with Asia, South America, and with the Acado-Baltic Faunal Province. Conodont faunas from the basin slope environments of the Antelope Range are generally low both in numbers of individuals and in taxonomic diversity. The *Pro-*

conodontus Zone (Upper Cambrian) and the *C. proavus* Zone undivided are recognized in the upper part of the Windfall; Early Ordovician Faunas B and C are recognized in the uppermost part of the Windfall and in the *Caryocaris* shale member.

Pre-Carboniferous "basement" map of northern Alaska and northern Yukon

A Pre-Carboniferous paleogeologic map of northern Alaska and northern Yukon, compiled by W. P. Brosge and J. T. Dutro, Jr., depicts the geologic setting at the end of the Devonian, prior to major Carboniferous transgression in the Arctic regions. The map shows distribution of Precambrian and early Paleozoic rocks and the structures developed during Taconic and Acadian orogenic episodes. Possible source terranes for the Upper Devonian to Lower(?) Carboniferous Kanayut clastic wedge are suggested. The map serves as a "basement" map for the northern Alaska petroleum and gas province.

Fusulinids of the type Atokan Provincial Series, southern Oklahoma

Fusulinids, known previously from only limited horizons and localities in type area of Atokan Series are now known from at least six horizons and are widely distributed in outcrops of the Atoka Formation in Coal, Johnston, and Pontotoc Counties in the area west and northwest of Atoka, Okla. Studies by R. C. Douglass (USGS) and M. K. Nestell (University of Texas at Arlington) show that species of *Profusulinella* near the base of the Atoka Formation are succeeded stratigraphically by several species of *Fusulinella*. The overlying Deese Formation contains species of *Beedeina*, *Wedekindellina*, and *Pseudostaffella* of Des Moinesian age. No standard reference section for the Atokan Series has been proposed because of the lack of available diagnostic fossil evidence. Douglass and Nestell are working with P. K. Sutherland (University of Oklahoma) to establish a stratotype for the provincial series. The most appropriate locality may be on the Lewis Ranch in the Mill Creek syncline in Johnston County, Okla., where at least five of the Atokan fusulinid horizons are represented in the stratigraphic section.

Late Kinderhookian (Early Mississippian) ammonoids from the Western United States

Ammonoids of Early Mississippian age are rare in the western part of the United States. However, Mackenzie Gordon, Jr., has identified significant new ammonoid faunules from Nevada, Idaho, Montana, and New Mexico. The ammonoids occur in strata of late Kinderhookian age; they occur sparingly in the lower part of the

Siphonodella crenulata conodont zone and more commonly in the *Siphonodella isosticha* Zone through the upper part of the *S. crenulata* zones. Three collections from Nevada, occurring in an isolated fault block surrounded by Ordovician rocks, are associated with radiolarians. Preliminary analysis of the western Kinderhookian ammonoids indicates that 15 species referable to 6 genera are present. These western ammonoid faunules are decidedly different in composition from those of the same age in the Midcontinent region. The dominant group in the western faunules are members of the subfamily Pericyclinae. The genus *Pericyclus*, known east of the Cordillerian area only by three specimens, is represented in the western faunules by at least six species; the genus *Rotopericyclus* is represented by two. *Protocanites* is fairly common in both regions; however, in the Midcontinent, most of the *Protocanites* occur in rocks of early Osagean age. Two species of *Protocanites* are recognized in Nevada, and both are late Kinderhookian in age. The most common Kinderhookian genus in the Midcontinent is *Imitoceras*, which is rare in the West. Three species of *Gattendorfia* and one of *Kazakhstania* complete the western roster. No early Kinderhookian ammonoids have been found anywhere in the United States in beds equivalent to the *Gattendorfia* ammonoid zone of Europe.

Upper Mississippian invertebrate biostratigraphy, eastern Appalachians

Investigations in 1981 of the invertebrate megafauna from the Hinton Formation through the Bluestone Formation (upper and uppermost Chesterian) in the region of the proposed Pennsylvanian System stratotype in the eastern part of the central Appalachian basin have produced significant new information on the correlation of this sequence with the Midcontinent. The macrofaunas are being studied by Mackenzie Gordon, Jr., and T. W. Henry, and the conodonts by J. E. Repetski. The faunas, particularly the brachiopods, of the Hinton correlate with those of the middle and upper parts of the Fayetteville Shale and with the Pitkin Limestone of northwestern Arkansas, confirming Cooper's (1944) tentative correlation of the Hinton with the Menard through Clore Limestone sequence of the upper Mississippi Valley. *Goniatites* from the lower part of the Pride Shale Member, the basalmost member of the Bluestone Formation, are identified tentatively as *Stenoglyphyrites involutum?* (Gordon). This species occurs in northern Arkansas in the "upper Pitkin Shale" of Gordon (1965), which is referred to the basalmost part of the Cane Hill Formation by most authors (Saunders, 1974; Saunders and others, 1977) and which apparently correlates with the Grove Church Shale of Swann (1963) in Illinois. The macrofauna from the Bramwell Member of

the Bluestone, which is the member just below the proposed Mississippian-Pennsylvanian point-boundary stratotype (Englund, 1979), also is similar to that from the middle and upper parts of the Cane Hill Formation. The Bramwell conodont fauna suggest correlation with either the *Adetognathus unicornis* conodont zone or the lower part of the *Rhacistognathus muricatus* conodont zone. Thus, the Bramwell Member correlates with either the Grove Church Shale or with uppermost Chesterian (pre-Morrowan) strata apparently not represented in the Eastern Interior basin.

Mississippian coral zonation, western North America

A new system of coral zones has been devised by W. J. Sando and E. W. Bamber (Geological Survey of Canada) for the Mississippian System in the Western Interior province, which extends from the southwestern District of Mackenzie in western Canada to southern California in the Western United States. The zonation is based principally on the distribution of 45 coral genera and subgenera and comprises 6 Opperl-zones, 4 of which are divided into locally useful subzones. The coral zones are correlated with foraminifer and conodont zones, which provide the primary bases for establishing ranges of coral taxa. Recognition of deep-water and shallow-water coral biofacies is an integral part of the zonation and obviates errors in correlation that plagued previous zonation systems based on corals. The coral zones compliment zonation systems based on conodonts, cephalopods, and foraminifers because corals are more abundant and widespread in shallow-water carbonate facies than conodonts and cephalopods and they are more abundant and widespread in deep-water carbonate facies than foraminifers. The coral zones are particularly effective in solving structural and stratigraphic problems encountered during field work because many taxa useful for zonation can be identified with a hand lens, whereas microfossils can seldom be identified in the field.

Cambrian mollusk studies

Collections have been assembled to obtain an overview on the paleontology and biostratigraphy of American Cambrian mollusks by John Pojeta, Jr. Material is now available from the Great Basin, Oklahoma, and the Northeastern U.S. Collaborative projects are underway with James H. Stitt (University of Missouri, Columbia), Stephen Rowland (University of Nevada, Las Vegas), and Ed Landing (New York Geological Survey). Selected international correlations are under study with G. F. Webers (Macalester College, St. Paul), and E. L.

Yochelson (USGS), for Antarctica, and Roger Cooper (New Zealand Geological Survey).

PLANT ECOLOGY

Botanical evidence of historic floods on Passage Creek, Virginia

Over 200 flood-damaged trees and shrubs along Passage Creek were analyzed by C. R. Hupp to determine date of flood damage. Dendrochronological analysis indicated 17 dates of major floods on the stream. Thirteen dates of floods were prior to the period of record for Passage Creek. Adjacent Shenandoah River gage records were treated by regression analysis on the Passage Creek record to estimate stage for floods which occurred prior to the Passage Creek record (1932 to present). Shenandoah River had stage records back to 1870. Seven flood dates indicated by botanical evidence occurred between 1932 and 1870. Stages for these floods were estimated from the regression analysis and incorporated into a standard flood-frequency analysis as historic peaks. The flood-frequency curve was shifted by the addition of these peaks such that extreme flows have a higher recurrence interval than before the addition of the peaks. Six additional dates of flooding from botanical evidence, prior to 1870, were determined and extend the record of flood dates back to 1720.

Vegetation distribution relative to stream-channel morphology and sediment size characteristics

Three streams of different size in northern Virginia were investigated by C. R. Hupp and W. R. Osterkamp to determine botanical relations with various channel features and sediment sizes. The Potomac River, Passage Creek, and South Fork Quantico Creek were observed to determine the occurrence and characteristics of certain geomorphic levels and their associated sediment sizes. Depositional bar, active channel shelf, flood plain, and terrace were recognized as discrete widespread geomorphic levels. Woody-plant distribution analysis revealed particular species affinities for particular levels. Many species were found on the same geomorphic level on all streams but not on other levels. Natural breaks in plant community types coincided with the break in slope of geomorphic levels investigated. Results indicate a strong relation between geomorphic level and vegetation distribution. Only a few species were highly correlated with sediment size. Vegetation distribution supports the integrity of the geomorphic levels, especially the active channel shelf, heretofore seldom recognized in the literature.

Computer model of wetlands forest

A computer model of a wetlands forest, developed by R. L. Phipps and L. H. Applegate, has been applied to data from the Dismal Swamp on the coastal plain along the border of Virginia and North Carolina. Simulations indicate that the present abundance of *Acer* (maple) in the swamp has been enhanced by decreased inundation (allowing establishment of seedlings), severe disturbance (lumbering, allowing release of young trees), and reduction in fire occurrences (ensuring survival of young *Acer*). Without further disturbance, the importance of *Acer* in the swamp will likely increase. Data presently available for inclusion in simulations indicate that management procedures to control *Acer* include water level control, selective lumbering, and controlled burning. Simulation indicates that the most efficient combination of procedures to use varies strikingly from site to site within the swamp.

Patterns of vegetation in the Loxahatchee River estuary, Florida

The distribution of sea grass and wetland vegetation in the Loxahatchee River estuary has been studied by B. F. McPherson. Shoal grass, *Halodule wrightii*, by far the most abundant sea grass in the estuary, grows where suitable undisturbed bottom sediment occurs and where tides maintain adequate salinities. Biomass of shoal grass in the estuary is low compared with that of other sea grasses, *Syringodium filiformis* and *Thalassia testudinum*, in a nearby marine environment. Shoal grass has a relatively wide range of tolerance for temperature, salinity, and tidal exposure, all of which can vary in the estuary more than in the adjacent marine environment. This tolerance probably explains why it is dominant in the estuary.

Cypress forest is restricted to the upper reach of the river and is being replaced by mangrove forest along several kilometers near its downstream limit. Dead cypress snags stand over a dense mangrove forest at 9.5 km upstream of the estuary inlet. Shallow (1 to 3.5 m) ground water at this location is unstratified and saline. Farther upstream (10.5 km), some cypress trees survive tidal inundation by brackish water. At this location, shallow ground water is brackish near the land surface and fresh at depths below 2 m. The fresh ground water, attributed to adjacent high ground water levels that induce flow toward the river, serves as a buffer for the cypress community in the tidal environment. Attempts to manage or protect the cypress community should include consideration of both surface freshwater inflow and ground-water head.

CHEMICAL, PHYSICAL, AND BIOLOGICAL CHARACTERISTICS OF WATER

CHEMICAL AND BIOLOGICAL QUALITY OF SURFACE WATER

Temporal changes in chlorida, sulfate, and sodium concentration in four eastern Pennsylvania streams

Trend analyses of 20 years or more of chemical-quality and streamflow data reported in a 1981 study by J. B. Barker indicate that sulfate has decreased significantly in three of the four streams studied, while sodium and chloride generally have increased. The majority of chemical-quality changes occurred in the late 1950's and early 1960's coincident with significant changes in population.

Decreases in sulfate follow a regional trend resulting from the conversion of home and industrial heating units from high to low sulfur coal, gas, and oil. The most significant decreases were observed in those stream basins severely affected by mine-drainage where pumpage has decreased significantly in the past 25 years, the effect being a further reduction in the sulfate content of the streams. The observed increases in chloride and sodium are attributed to population growth and shifts from rural to suburban communities, both of which have resulted in increased demand for municipal waste treatment facilities and use of ice-melting salt on roadways.

Effects of nonpoint sources to concentrations and loads of water-quality constituents in Pequea Creek basin, Pennsylvania

J. R. Ward and P. L. Lietman measured concentrations and loads of suspended sediment, nutrients, and herbicides from the Pequea Creek basin and four predominant land use areas in the basin. They found that during the 1980 calendar year Pequea Creek discharged into the Susquehanna River 11,000 Mg of suspended sediment, 760 Mg of nitrate-nitrogen, 65 Mg of organic nitrogen, 19 Mg of phosphorus, 490 Mg of organic carbon, 42 kg of atrazine, 24 kg of simazine and 2.3 kg of prometone. These loads represent significant contributions to the total discharge of these constituents in the Susquehanna River.

The four land uses monitored were forest, corn, residential, and pasture. During baseflow, concentrations of organic nitrogen and phosphorus from the pasture, nitrate and atrazine from the cornfield, and prometone from the residential area were significantly higher than concentrations observed at any of the other sites. Nitrate concentrations during baseflow at the cornfield ranged from 18 to 24 mg/L, exceeding the Na-

tional Interim Primary Drinking Water Regulations standard of 10 mg/L in every sample collected. During storms, mean concentrations of suspended sediment, nitrate, phosphorus, and atrazine were highest at the cornfield, organic nitrogen highest at the pasture, and prometone highest at the residential area.

Agricultural practices have a significant effect on nonpoint discharges to receiving streams. The highest discharge of nutrients and herbicides usually occurred at the cornfield during storms that followed applications of manure, fertilizer, and herbicides. The residential area exhibited a washout effect, the highest suspended-sediment and nutrient concentrations occurring during the first part of runoff.

Chemical and biological characteristics of Indiana Dunes National Lakeshore streams

Indiana Dunes National Lakeshore streams (Grand Calumet River, Little Calumet River, Kintzele Ditch, Derby Ditch, and Dunes Creek) were studied by M. A. Hardy to provide information for resource management to the National Park Service. The most significant water-quality changes are: shifts from the normal calcium-bicarbonate water type because of sodium and chloride enrichment, and enrichment in concentrations of nutrients, general organic substances, lead, zinc, pesticides, and PCB's, and bacteria. In most cases these changes are associated with differences in land-use patterns.

Urban sewers and industrial-waste discharges generally caused enrichment of sodium, chloride, nitrogen, phosphorus, and zinc concentrations, particularly in the Little Calumet River. Ammonia concentrations in the lower reaches of the Little Calumet River occasionally exceed 0.02 mg/L, the maximum concentrations recommended for freshwater organisms. Urban sewers are also sources of decomposable organic substances, chlor-dane, PCB's, and fecal coliform bacteria. Runoff from road crossings or bordering streams contribute lead, zinc, and PCB's.

Industrial landfills near a headwater lagoon of the Grand Calumet River may cause ammonia nitrogen enrichment in the lagoon. Ammonia nitrogen concentrations are more than 100 times the maximum recommended concentration for aquatic life.

In agricultural areas, enrichment of dieldrin, DDT, and breakdown products of DDT are common, probably because of field applications near the streams. Feedlots in the upper reaches of Kintzele Ditch may be a primary source of fecal coliform bacteria during high-flow events. Wetlands are a major natural source of organic materials to streams at high-flow events.

Suitability of surface-water of the Red River basin, Oklahoma, for water supply

Surface water of the Red River basin upstream from Lake Texoma generally is unsuitable for potable-water supply or irrigation use because of high chloride concentrations, as determined in a recent investigation by J. D. Stoner, and the Washita River generally is unsuitable for potable-water supply because of high sulfate concentrations. However, numerous tributaries of the Washita River are suitable, and the suitability of the Washita River tends to improve downstream. Oklahoma tributaries to the Red River downstream from Lake Texoma are generally of very good quality and are suitable for both water supply and irrigation. The dilution effect of surface water from these tributaries tends to improve the surface-water quality of the Red River downstream from Lake Texoma.

Water quality of the Susquehanna, Potomac, and James Rivers

Water-quality constituent loads at the Fall Line stations of the Susquehanna, Potomac, and James Rivers, the three major tributaries to the Chesapeake Bay, can be estimated with reasonable accuracy by using regression techniques, especially for periods of 1 year or more of above average streamflow. D. J. Lang determined that the net transport of all nutrient species and other constituents (especially those associated with suspended sediment) is dominated by a relatively few spring and storm-related high-flow events. Atrazine and 2,4-D are the two pesticides most consistently detected at the Fall Line of the Susquehanna and Potomac Rivers. Concentrations of total residual chlorine and low-molecular-weight halogenated hydrocarbons at selected sites in major tributaries to the upper Bay are generally at or below detection limits. Compared to the two other major tributaries, the James River has the lowest discharge-weighted-sulfate concentrations, presumably because of the lack of coal mining activity in this basin. This river also has lower average concentrations of total nitrogen and nitrite plus nitrate. Ammonia concentrations and loads are decreasing at all three Fall Line stations, as is orthophosphate in the Susquehanna and Potomac Rivers. Slight increases in total nitrogen and nitrite plus nitrate in the Susquehanna River from 1969 to 1980 may cause increased algal growth if nitrogen is the limiting nutrient in the upper Chesapeake Bay.

Analyses of data confirm the suggestion by Gross and others (1978) that at a discharge below approximately 11,200 m³/s for the Susquehanna River at Conowingo, Md., suspended sediment (and associated sorbed nutrient and other water-quality constituents) is deposited upstream of the three hydroelectric dams be-

tween Harrisburg, Pa., and the river's mouth. Peak discharges above 11,200 m³/s resuspend and transport the sediments and their associated water-quality constituents to the Bay in loads that are in excess of those transported by the Susquehanna River at Harrisburg.

Effects of irrigation-return flows on water quality in Marsh Creek, Rock Creek, and Cedar Draw in south-central Idaho

In a 2-year study to monitor nonpoint sources of pollution in three streams in rural Idaho, T. K. Edwards reports that at all main-stream sampling sites, suspended-sediment loads ranged from 600 Mg/d to less than 0.01 Mg/d. Sediment loads related to availability of materials for transport more so than to stream discharge. Peak loads generally occurred in May and June, after cultivation and during initial irrigation of cropland, except at two sites in the Marsh Creek basin, where the peak load occurred in January during a flood period. Nitrate concentrations ranged from 0.0 mg/L to 4.5 mg/L, generally exhibiting a seasonal variation. Peak nitrate concentrations occurred in September and December except for one site on Rock Creek where the maximum concentration was measured in August. In contrast, dissolved-oxygen and fecal coliform concentrations were less predictable in occurrence, showing wide variations throughout the areas studied.

Water-quality studies of the Snake River Plain in southern Idaho and eastern Oregon

W. H. Low determined that water in 25 of the 26 major tributaries to the Snake River Plain is of the calcium-bicarbonate and calcium-magnesium-bicarbonate type. The exception is sodium-bicarbonate type water in Falls River, which drains silicic volcanic rocks in the Yellowstone National Park area. Dissolved-solids concentrations in surface water range from 50 mg/L in the Boise River drainage (composed chiefly of granitic rocks of the Idaho batholith) to 400 mg/L in the Owyhee and Raft River drainages (composed chiefly of older Banbury Basalt and older alluvium of the Salt Lake Formation, respectively). Dissolved-solids concentrations in approximately 80 percent of all ground-water samples are less than 400 mg/L and range from 60 to 5,900 mg/L. Much of the ground water is pumped from the Snake River Basalt aquifer. Increases in dissolved-solids concentrations can be attributed to agricultural land-use practices.

Surface-water quality in east-central Montana

An appraisal of the water resources of the Big Dry Resource area in east-central Montana by S. E. Slagle has shown that water quality in smaller perennial

streams is variable and dependent on flow conditions. Dissolved-solids concentrations are generally greatest during periods of low flow when streamflow is sustained by ground-water inflow and generally smallest during periods of high flow resulting from snowmelt or storm runoff. Dissolved-solids concentrations of 382 to 4,570 mg/L have been observed within the study area.

A reflection of the ground-water quality and geology in the area is that water in most streams is of the sodium-sulfate type during low-flow periods. Water in the downstream reaches of Prairie, Elk, and Sand Creeks is of the sodium-bicarbonate type, probably as a result of inflow from the Fox Hills Sandstone and the lower part of the overlying Hell Creek Formation both of Cretaceous age. During periods of high flow, the percentages of sodium and sulfate decrease and calcium, magnesium, and bicarbonate increase because of the replacement of ground-water inflow with water derived from overland flow.

Because of the large dissolved-solids and sodium concentrations, most streams are considered to have a high to very high salinity hazard and a medium to very high sodium hazard during low-flow periods. The water is generally suitable for livestock watering.

Water quality of the Cape Fear River, North Carolina

Dr. J. K. Crawford conducted a study of water quality of the Cape Fear River, N.C. The study was part of a larger project to examine water-quality variability, constituent loads, and long-term trends in several major rivers in North Carolina.

Preliminary results from the Cape Fear study indicate that from 50 to 75 percent of the load of major ions in the river come from human-related activities. These percentages were calculated by comparing water-quality data from baseline sites in undeveloped areas of the basin with water-quality data at a main-stream station.

Twenty-five years of water-quality data were examined to detect water-quality trends. Effects of discharge were accounted for in the analysis by a discharge-frequency-weighting technique. Statistically significant increasing trends were found for dissolved solids, specific conductance, dissolved sulfate, total nitrite plus nitrate nitrogen, dissolved sodium, dissolved magnesium, and dissolved potassium. Slight downward trends in pH, bicarbonate ion concentration, and total alkalinity are not statistically significant, but coupled with increasing concentrations of sulfate and nitrate suggest an influence of acid precipitation. Results from previous studies in the overall project indicate these trends are typical of the entire Piedmont portion of the State.

Water-quality assessment of the Merced River, California

A study of water quality of the Merced River, Calif. by S. K. Sorenson showed that the overall water quality was adequate for most beneficial uses, although water-quality standards for dissolved oxygen, pesticides, and pH were exceeded in some parts of the basin. The most likely cause of excessive dissolved oxygen and pesticide concentrations was the return of agricultural irrigation water to the lower 48 km of the river. Standards for pH were exceeded in the poorly buffered headwaters of the river.

CHEMICAL AND BIOLOGICAL QUALITY OF GROUND WATER

High sodium and sulfate in ground water in Brown County, Wisconsin

J. T. Krohelski has found that ground water in wells drilled in the Maquoketa Shale or units below the area between the Fox River and the Niagara Escarpment in Brown County have higher concentrations of sodium and sulfate than water from other areas of the county. The probable source of sodium and sulfate is the Maquoketa Shale of Ordovician age. Preliminary flow-model results indicate that ground water in these wells is recharged just east of the Niagara Escarpment and moves downward through the shale before flowing westward to the wells.

Anomalous radioactivity levels in central Louisiana water well

Gross alpha concentrations of 40 times the maximum limits recommended by the EPA for drinking water were found in a freshwater well located in the central Louisiana area. This well is 237 m deep and screened in sand of Miocene age.

Nineteen water samples were collected from the well for analyses during the period September 16, 1980, to May 26, 1981. These samples were analyzed by the Office of Health Services and Environmental Quality, Louisiana Department of Health and Human Resources. C. W. Smoot reported that gross alpha concentrations ranged from 104 pCi/L (September 26, 1980) to 607 pCi/L (May 8, 1981) and gross beta concentrations ranged from 13 pCi/L (September 26, 1980) to 32 pCi/L (May 12, 1981).

Duplicate splits of samples submitted to the State laboratory October 6, 1980, and January 13, 1981, were also sent to the USGS Denver Central Laboratory and the U.S. Department of Energy Radiological and Environmental Science Laboratory at Idaho Falls, Idaho, respectively, as a quality assurance and corroborations measure. The respective laboratories confirmed the

gross alpha and gross beta levels reported by the State laboratory, and the Idaho Falls laboratory further reported that the source of the radioactivity in the sample taken January 13, 1981, was polonium-210, but neither radium-226 nor radium-228 was detected.

Analyses of water samples collected periodically during continuous pumping from the 8th through the 22d of May revealed that the gross alpha and gross beta concentrations fluctuated throughout the pumping period. In the first 8 h of pumping, gross alpha concentrations increased from 341 pCi/L at 1 hour to 607 pCi/L at 8 h. Although the net concentration decreased to 290 pCi/L, during the next 328 h intermediate high-concentration peaks of 456 pCi/L and 432 pCi/L at 144 h and 264 h, respectively, and intermediate lows of 404 pCi/L and 359 pCi/L at 72 h and 168 h, respectively, were noted. The concentration of gross alpha remained the same from 336 to 432 h and then increased to 332 pCi/L after 500 h. The values determined for gross beta were an order of magnitude lower but followed a similar trend.

A water sample from a well located 670 m from the study well and completed at a depth 60 m lower stratigraphically did not show anomalous levels of radioactivity.

Elevated nitrate concentrations in the Widefield aquifer south of Colorado Springs, Colorado

An evaluation of sparse historical data from the Widefield aquifer indicates a large increase in nitrate concentrations has occurred in the last 20 yr. The Widefield aquifer is an approximately 8-km² band of high transmissivity alluvium along Fountain Creek. The aquifer is an important source of municipal water supply for several communities. On the basis of water-quality samples collected during summer 1981, D. L. Cain reported the mean concentration of nitrate nitrogen in water from 51 wells completed in this aquifer was 7 mg/L. Compared to mid-1960 when background nitrate in the aquifer was less than 2 mg/L, the nitrate concentration of samples during 1981 varied from 4 to 11 mg/L, with water from several wells containing nitrate in excess of the 10-mg/L (as N) limit for drinking water.

Five wells in the area were sampled on a monthly basis to determine the pattern and magnitude of seasonal variations in nitrate. Although a single consistent pattern of seasonal variation was not observed, some variation in nitrate concentration was present at all five wells. The magnitude of the variation was from 16 to 53 percent of the maximum nitrate concentration observed during the monthly sampling.

Possible sources of the elevated nitrate concentrations include infiltration from Fountain Creek, which

has relatively high concentrations of nitrogen due to discharge of sewage effluent, leakage from an irrigation canal which diverts water from Fountain Creek, artificial recharge using water diverted from Fountain Creek, fertilizer applied to crops and lawns, and direct seepage from sewage lagoons.

SURFACE-WATER QUALITY MODELS AND PROCESSES

Modified version of one-dimensional, steady-state, stream water-quality model in Arkansas

J. E. Terry and E. E. Morris have modified program G475 by Bauer, Jennings, and Miller (1979) to correct some problems in the code and to provide the capability of simulating a more varied set of conditions for any given receiving stream. The primary modifications include the following:

1. A new subroutine was added to compute reaeration coefficients for each subreach by any one of eight predictive equations;
2. A temperature-correction factor for net photosynthesis was added;
3. During projections, dissolved-oxygen concentrations are not allowed to exceed saturation due to photosynthesis;
4. A correction of dissolved-oxygen mass-balance computations at point-source inflow locations is now incorporated;
5. Dissolved-oxygen saturation is computed in accordance with WRD standard procedures.

Gas- and dye-tracer-estimation program in Arkansas

J. E. Terry and M. L. Farmer have developed a computer program, GDEST, that is used in a gas- and dye-injection study to determine reaeration coefficients for flowing waters. Injection rates for ethylene, propane, and (or) rhodamine WT dye and total quantities of each substance needed to inject for a given period of time are estimated.

Basic calculations are as presented by Rathbun (1979). Modifications have been made to the basic procedure to allow the user a choice of ten different predictive equations for reaeration coefficient (upon which the gas-desorption coefficients are dependent) and the three different predictive methods for estimating longitudinal dispersion.

Any number of reach lengths and sets of stream characteristics may be analysed for a given stream segment. Every set of stream characteristics will be analysed for

each reach length entered, and from one to eight different reaeration-estimation equations may be tried for each set of stream characteristics. GDEST has been made as flexible as possible so that as much information as possible can be obtained from a single run of the program.

Evaluation of selected one-dimensional stream water-quality models with field data

S. C. McCutcheon (1981b, 1982) compared and evaluated five one-dimensional stream water-quality models (digital computer programs applicable to streams and rivers that are laterally and vertically mixed). Data used in the models were collected during the river quality assessments of the Willamette River in Oregon, Chattahoochee River in Georgia, and Arkansas River in Colorado. The models included the USGS One-Dimensional Steady-State Stream Water-Quality Model (a modified Streeter-Phelps model), the QUAL II model (Southeast Michigan Council of Governments version), the Water-Quality for River-Reservoir Systems (WQRRS) model, the Velz rational technique, and the MIT Transient Water Quality Network Model.

Except for the MIT model, these models were of comparable accuracy and were equally valid for steady flows. Program or documentation errors in the MIT model made it impossible to apply the model to the data collected in this study. Except for the Velz model applied to the Willamette and Chattahoochee Rivers, which was not checked, the other models also had programming errors in their computer codes that have since been corrected. Although a number of differences exist between models in the way they were formulated, each model has the flexibility to make the differences relatively unimportant for typical stream water-quality studies.

In general the USGS and the QUAL II models are best adapted for steady flow and water quality. The added flexibility of the Velz technique makes it somewhat more tedious to apply. The WQRRS model should be limited to the simulation of dynamic (time varying) changes in flow and water quality except when special predictions of bicarbonate, pH, detritus, suspended sediment, and biota are needed. Application of WQRRS model for steady conditions is tedious and time consuming.

Transport mechanisms of solutes sorbing onto sediment in pool-and-riffle streams

K. E. Bencala demonstrated that mathematically simple formulations of reactive solute transport can simulate stable strontium concentrations in a pool-and-riffle stream. With the cooperation of V. C. Kennedy, G. W. Zellweger, R. A. Avanzino, A. P. Jackman, and

R. A. Walters, data from a multitracer injection experiment showed that strontium transport is influenced by both complex hydrology and interaction with bed sediment. The simulation exercises served to quantify the roles of surface-water hydrology and sediment interaction. The simulation coupled nonreactive, transient storage with a kinetic mass-transport model for sorption.

Microcomputer program for time-of-travel and dispersion characteristics of streams in Florida

An investigation by J. E. Coffin, in cooperation with the State of Florida, Department of Environmental Regulation, uses dyes and tracing techniques to measure the time-of-travel and dispersion characteristics in streams in Florida. In all dye studies, numerous mathematical formulas are needed to calculate variables such as volume of dye injected and time of travel. Reliance on and use of calculators is time consuming. These formulas have been incorporated into a microsoft Fortran computer program developed by L. J. H. Geiger for use on the microcomputer Superbrain QD, which is available in several WRD offices. The computer program calculates all necessary variables with minimal user input.

Dissolved-solids model of the Tongue River, Montana

A computer model has been developed by P. F. Woods for assessing potential increases in dissolved solids of streams as a result of leaching of overburden materials used to backfill pits in surface coal-mining operations in southeastern Montana. The model allows spatial and temporal simulation of streamflow and dissolved-solids loads and concentrations for user-defined plans of surface coal mining and agricultural development. The model specifically addresses the Tongue River from the Tongue River Dam to Miles City, Mont., and its three major tributaries, Hanging Woman, Otter, and Pumpkin Creeks. Provision is made to simulate releases from the present Tongue River Reservoir or the increased releases expected from a larger dam and reservoir proposed as a replacement for the present Tongue River Reservoir.

A hypothetical plan was formulated for the mining of all federally owned coal judged potentially available for mining. Under this plan, a simulation using mean streamflow from the present Tongue River Reservoir indicates that the mean annual dissolved-solids concentration of 646 mg/L with no mining is increased by mining to 677 mg/L. When the proposed Tongue River Reservoir is used in the simulation, the shift in dissolved-solids concentration is from 436 to 451 mg/L, which is illustrative of the dilutional effect of increased streamflow on concentration. Calculations were made with data representing the study area to determine the

relative impacts of irrigation and surface coal mining on a unit-area basis in a hypothetical stream. The dissolved-solids concentration of the hypothetical stream was determined to increase annually by 2.94 percent as a result of withdrawal and return flow of irrigation water and by 0.22 percent as a result of leachates from surface coal mines.

GROUND-WATER QUALITY MODELS AND PROCESSES

Projected effects of proposed salinity-control projects on fresh ground water in the upper Brazos and Wichita River basins, Texas

The U.S. Army Corps of Engineers recommended construction of total impoundment brine reservoirs as part of plans to control the natural salt pollution in the upper Brazos River basin and in the upper Wichita River watershed of the Red River basin. Sergio Garza found that the proposed reservoirs would have relatively minor effects on the existing fresh to slightly saline ground water in the area.

Two-dimensional digital-computer models were developed for aquifer simulation of steady and transient conditions in which the density effects of saltwater are considered. The models were used to project the effects on fresh ground water by the proposed 100-yr impoundments of brines on two reservoirs in North Corton Creek (upper Brazos River basin) and on one reservoir in Bluff Creek (tributary to North Wichita River). The projected rises in aquifer head in the area about each reservoir are not extensive; increases of less than 3 to about 15 m are projected only for areas near each dam and along each lake shoreline. Estimates of the maximum migration of saltwater downstream from each dam are projected to be about 1.6 km or less; these estimates are considered only as approximations due to exclusion of the effects of hydrodynamic dispersion.

Appraisal of coal-tar derivatives in ground water in St. Louis Park, Minnesota

M. F. Hult reports that coal-tar derivatives entered the Prairie du Chien-Jordan aquifer (in the Ordovician Prairie du Chien Group and Cambrian Jordan Sandstone) through multiaquifer wells near the former site of a coal-tar distillation and wood-preserving plant in St. Louis Park, Minn. The aquifer is the region's major ground-water resource and provides about 50 percent of consumptive use of water in the Minneapolis-St. Paul metropolitan area.

Preliminary solute-transport modeling showed that contaminants, if not degraded or removed by wells, could have moved many miles since the aquifer was first

reported to be contaminated in 1932. This was supported by measurement of the concentration of polynuclear aromatic hydrocarbons (PAH) in 80 wells in an area of about 100 km². Trace concentrations of PAH were found in all but one well downgradient from the former plant site but not in wells located upgradient. It is unlikely, however, that all the PBH's detected are from that site, because other sources are known in the area. Moreover, measurement of PAH below about 1 µg/L is difficult, and some analyses are doubtless in error.

It was found that even though high molecular weight PAH compounds (acenaphthene, fluorene, phenanthrene, pyrene, fluoranthene) are strongly sorbed and sparingly soluble in water, they are present in wells near the site in higher concentrations than aromatic compounds with lower molecular weight (ethylbenzene, naphthalene, 2-methylnaphthalene). However, because contaminated water entering the aquifer contains a high proportion of these soluble, low-molecular-weight compounds, it seems likely that they are being degraded by aerobic bacteria within the Prairie du Chien-Jordan aquifer.

AREAWIDE CHEMICAL LOADING

Water-quality loads of the Susquehanna River

D. K. Fishel determined that annual loads for 35 constituents indicate that about 2,090,000 Mg of suspended sediment and 2,710,000 Mg of dissolved solids were transported by the Susquehanna River to Harrisburg, Pa., from April 1, 1980, to March 31, 1981. Streamflow and sediment discharges were 77 and 72 percent, respectively, of the average annual discharges. About 79 percent of the nitrogen was dissolved. Nearly 84 percent of the phosphorus and 93 percent of the iron, aluminum, and manganese were associated with suspended sediment.

Water-quality loads of the Susquehanna River at Harrisburg, Pennsylvania

Loads of suspended sediment, nutrients, pesticides, trace metals, and major ions for the Susquehanna River at Harrisburg, Pa., were measured during base-flow periods and during five selected storms. According to D. K. Fishel, regression analysis showed that constituent loads and streamflow were directly related and had coefficients of determination greater than 0.80 for 35 of the 42 constituents analyzed.

There was less than 5 percent difference in annual constituent loads as computed by three separate

methods: hydrograph and subdivided day, flow duration and transport curve, and regression equation using mean daily streamflow. The annual suspended-sediment load for April 1, 1980, through March 31, 1981, was 2.09×10^6 Mg. Streamflow and sediment discharge during the study were 77 and 72 percent, respectively, of the long-term average annual discharges. About 79 percent of the 3.8×10^4 Mg annual total nitrogen load was dissolved; 60 percent was dissolved nitrate, and 20 percent was suspended organic nitrogen. The annual total phosphorus load was 2.7×10^3 Mg, of which 83 percent was suspended. The annual dissolved-solids load was 2.71×10^6 Mg; 32 percent sulfate, 17 percent calcium, and less than 1 percent chloride. Ninety-eight percent of the 1.03×10^4 Mg annual metal load was suspended iron, aluminum, and manganese. Atrazine and 2,4-D were the only pesticides detected in significant concentrations; however, annual loads were not calculated for these constituents.

Nutrient and detritus transport in the Apalachicola River, Florida

The Apalachicola River in northwest Florida flows 172 km from Jim Woodruff Dam to Apalachicola Bay on the Gulf of Mexico. The basin is approximately 3,100 km², of which 15 percent is bottom-land hardwood flood plain that is relatively undeveloped. The dense flood-plain forest produces approximately 800 Mg/km² of litter fall annually. According to J. F. Elder and H. C. Mattraw, spring floods of March and April 1980 carried 35,000 Mg of the decaying litter fall (detritus) into Apalachicola Bay. The estuary is predominantly a detrital-based food-web ecosystem which produces important commercial quantities of oyster, shrimp, blue crab, and various species of fish.

During the 1-yr study period, June 1979 to June 1980, 214,000 Mg of organic carbon were transported into the bay. Nitrogen transport during the same period was 21.5×10^3 Mg and phosphorus was 1.7×10^3 Mg. The Apalachicola River floodplain contribution to the annual transport of carbon, nitrogen, and phosphorus was 34,200 Mg, 668 Mg, and 197 Mg, respectively. Sixteen percent of the organic carbon is derived from less than 1 percent of the Apalachicola-Chattahoochee-Flint River basin.

Carbon transport from forested wetlands in a large Florida river basin

J. F. Elder and H. C. Mattraw, Jr., recently completed the Apalachicola River Quality Assessment.

The Apalachicola River in northwestern Florida receives runoff from a watershed more than 50,000 km² that extends over parts of Georgia, Alabama, and

Florida. Spring floods, which occur most years after rainstorms in the watershed, increase the discharge from the annual average of 825 m³/s to rates in excess of 3,000 m³/s and inundate some 450 km² in the Apalachicola basin, Florida. Bottomland hardwood trees in the flood plain annually produce 3.6×10^5 Mg of litter fall, approximately 60 percent of which consists of leaf material subject to rapid decomposition. Flooding provides the transport mechanism, and forest litter provides the source from which large amounts of allochthonous carbon can enter the main river channel and eventually reach the highly productive Apalachicola Estuary. Measurements of various components of the Apalachicola carbon budget suggest that the floodplain at times acts as a carbon sink. On an annual basis, however, it is an important source, releasing in excess of 80 g/m² of carbon per year. Seasonally dependent detrital carbon is particularly valuable to estuarine food webs in Apalachicola Bay.

RELATION BETWEEN SURFACE WATER AND GROUND WATER

Stream-aquifer interrelations in southeast Nebraska

A reconnaissance investigation was made by M. J. Ellis to determine the significance of stream-aquifer interrelations in the Big Blue and Little Blue River basins in Gage and Jefferson Counties, Nebr. Seepage measurements made at 21 sites in the Big Blue River basin and at 35 sites in the Little Blue River basin were used to determine stream gains or losses in 20 drainage areas in the Big Blue River basin and 31 drainage areas in the Little Blue River basin. Analyses of data from these seepage measurements and of available hydrogeologic data indicate that the most significant groundwater contributions to streamflow in the Big Blue and Little Blue River basins occur where a direct hydraulic connection exists between a stream and buried coarse-grained deposits of Quaternary age. These deposits occur in two buried bedrock valleys that trend east-northeasterly across the area.

The largest ground-water contributions to streamflow in the Big Blue River occur in the reaches of the river between the mouth of Mud Creek and the dam at Blue Springs (about 0.4 m³/s) and between the mouth of Turkey Creek and the Beatrice gaging station (about 0.6 m³/s). Ground-water contributions to streamflow also occur in two tributaries of the Big Blue River: Bear Creek (0.12 m³/s) and Big Indian Creek (0.18 m³/s). In the Little Blue River basin the largest contributions to streamflow occur between the mouths of Big Sandy and Little Sandy Creeks (about 0.18 m³/s) and in the vicinity

of Fairbury (about 0.5 m³/s). A ground-water contribution to streamflow of about 0.18 m³/s also occurs in Rose Creek, a tributary of the Little Blue River.

Hydrology of Wisconsin lakes potentially affected by acid deposition

D. A. Wentz and W. J. Rose are determining hydrologic and chemical budgets of four seepage lakes in sandy glacial deposits in northern Wisconsin. Lake surface area of 13 to 39 ha and drainage basins of 52 to 145 ha result in drainage/surface area ratios of 3.5 to 5.0. Daily measurements at two or more sites at each lake indicate that rainfall is homogeneous within each basin. Monthly water-level measurements allow categorization of three of the lakes as ground-water flow-through systems; ground water discharges to the lakes along part of the shoreline and is recharged from the lake along another part (generally the opposite shore). The fourth lake appears to be predominantly a ground-water recharge lake, although the lake may receive some contribution from a perched water table along one side. Preliminary data suggest that hydraulic conductivities of the aquifer at this recharge lake are less than at the other three; this lake also is the only one of the four where overland flow has been observed.

Data indicate that three of the lakes are susceptible to adverse effects from acid deposition (alkalinity less than 300 $\mu\text{eq/L}$, according to the classification scheme of Glass and others (1980). The fourth lake is potentially susceptible to adverse effects (alkalinity from 300 to 625 $\mu\text{eq/L}$).

Hydrology of Big Marine Lake, Washington County, Minnesota

Hydrologic instrumentation at Big Marine Lake in Washington County, Minn., was installed by G. E. Groschen to estimate the annual water budget and to establish the relation between water-level fluctuations in the lake and head in the ground-water system. Test-hole drilling showed that several types of glacial drift are present in the watershed but that there are no extensive confining layers in the drift. This finding suggests that the drift and the underlying Prairie du Chien-Jordan aquifer act as a single hydrologic unit. Water levels in drift and bedrock wells west of the lake are 1 to 8 m above lake level, which, with the presence of springs, indicates that ground water is discharging to the lake along its western shore. The water table in the drift-bedrock aquifer east of the lake slopes easterly toward the St. Croix River. Water seeps out of the lake along the eastern shore into the ground-water system.

Both the lake water and ground water are predominantly dilute calcium-magnesium-bicarbonate type. Concentrations of major ions average about 140 mg/L in ground-water samples from shallow wells along the east

and north shores of the lake. However, water from a water-table well 1.2 m deep on the northeast shore had a major-ion concentration of only 27 mg/L, which is significantly less than concentrations in lake water (about 120 mg/L). The low-concentration ground water probably is related to a ground-water mound northeast of the lake that prevents outseepage from the lake in that area. Concentrations of major ions from deeper wells (26 m) in the drift on both the east and west sides of the lake average about 240 mg/L, which is similar to major-ion concentrations in water from the Prairie du Chien-Jordan aquifer and twice the concentration in lake water. Results of tritium analyses of water samples from the lake and from a well in the Prairie du Chien show that water in the bedrock is much older than lake water and apparently is from a source other than the lake.

The hydraulic and geochemical data suggest that shallow localized ground-water systems have the greatest effect on the hydrologic regime of the lake. The data also show, however, that ground-water discharge to the lake from bedrock aquifers is significant.

Geohydrology of stream-aquifer system, Finney and Kearny Counties, Kansas

Unconsolidated deposits of Miocene and Pleistocene age are the major source of water in Kearny and Finney Counties. L. E. Dunlap, R. J. Lindgren, and C. G. Sauer classified these deposits into three aquifers—lower, upper, and alluvial valley aquifer. The use of ground water for irrigation caused the altitude of the water level to decline 6 to 24 m in the lower aquifer from 1974 to 1980. This decline induced downward leakage from the alluvial valley aquifer and now little or no ground water discharges to the Arkansas River. Consequently, the river is frequently dry. Seepage losses from the river can be as high as 75 percent when reservoir water is transported 35 km through the study area to irrigation canals.

When streamflow occurs, water levels in the alluvial aquifer rise. However, the rising water level usually does not reach the altitude of stream stage, and river seepage continues to occur. Additionally, a water-level rise in the valley aquifer corresponds to an increase in the downward leakage rate to the lower aquifer, which hinders the rise in water level.

The water budget for 1980 shows that 42 percent of the water pumped in Finney and Kearny Counties came from storage in the lower aquifer. The remaining water came from downward leakage from the overlying upper and alluvial valley aquifers.

Computer model projections from 1981 to 2005 indicate that under conditions of normal precipitation, 1980 irrigated acreage, and 1979 rates of recharge from

the river and canals, the additional water-level decline would be less than 15 to about 46 m by 2005. Saturated thickness will range from 15 to 76 m. Solely on the basis of the remaining saturated thickness, water will still be available in 2005 for irrigation in Finney and Kearny Counties.

LIMNOLOGY AND POTAMOLOGY

Although the term "limnology" originally applied only to the study of lakes, in its current usage it also refers to the study of streams and rivers. Limnology is the study of sources and nature of freshwater, its motion and changing condition, and, perhaps most significantly, the life it supports. The term "potamology" is more restrictive, applying only to river investigations.

Primary productivity at Lake Koocanusa, Montana

Limnological data collected at Lake Koocanusa were used by P. F. Woods to investigate the interrelation of nutrient loadings, primary productivity, and trophic condition of the reservoir from 1972 to 80. The 7.16-km² reservoir on the Kootenai River was impounded by Libby Dam on March 21, 1972. On the basis of loadings of nitrogen and phosphorus prior to and following impoundment, Lake Koocanusa was found to be potentially eutrophic. Beginning in 1976, total phosphorus loadings, but not total nitrogen loadings, were substantially lowered following improvements in wastewater treatment at a fertilizer plant located upstream from the reservoir. Daily areal primary productivity varied widely in each year at four sampled stations. During the 9 yr studied, daily areal primary productivity (mg carbon fixed/m²) ranged from 0.4 to 420.0; the mean of the 313 sampled days was 128.5. Annual areal primary productivity ranged from 23.2 to 38.5 g carbon fixed/m², which categorizes Lake Koocanusa as oligotrophic. The distribution of chlorophyll *a* within the water column indicated that, on the average, more than half of the phytoplankton in the reservoir was below the euphotic zone. These results support the hypothesis that the reservoir's weak thermal structure had allowed circulation of phytoplankton out of the euphotic zone. The trophic condition of Lake Koocanusa was categorized as eutrophic on the basis of the relationship of the nutrient loadings and the reservoir's ratio of mean depth to retention time. This result conflicts with the oligotrophic ranking the reservoir received on the basis of its areal primary productivity. The discrepancy in trophic condition was attributed mainly to the failure of nutrient-loading models to account adequately for physical processes within reservoirs.

Water-quality of small reservoirs in northeastern Montana

Limnological data were collected from several stock-watering reservoirs in northeastern Montana by R. F. Ferreira to provide information for their multiple-use management. Four of these reservoirs, considered suitable for fish propagation, were sampled intensively during the summer of 1981. Depths ranged from 1.1 to 4.3 m and surface areas ranged from 1.3 to 3.8 ha. Concentrations of dissolved constituents generally increased as summer progressed, probably as a result of water loss by evaporation. Specific conductances ranged from 200 to 4,600 μ mhos/cm and slightly increased with depth as the lakes thermally stratified in late summer. Temporal changes also occurred in the composition of phytoplankton communities during the summer. Large populations of phytoplankton, in conjunction with organic decomposition, resulted in decreased dissolved-oxygen concentrations in the bottom waters of all the reservoirs. At night, phytoplankton respiration near the surface resulted in dissolved-oxygen concentrations less than 5.0 mg/L. This finding suggests that these reservoirs do not provide a suitable habitat for fish.

Sensitivity to acidification of Flat Tops Wilderness Area lakes

A 2-yr study of lakes of the Flat Tops Wilderness Area of Colorado by J. T. Turk investigated the sensitivity of the lakes to impact by precipitation as acidic as that of the Northeastern United States. Alkalinity of the studied lakes ranges from about 70 to 1,400 μ eq/L. Most lakes at altitudes greater than about 2,700 m are predicted to have alkalinity values less than 200 μ eq/L, on the basis of highly significant ($r^2=0.76$) alkalinity/altitude regression. If the precipitation is assumed to be as acidic as that of the Northeastern United States, the 200 μ eq/L alkalinity is the minimum value necessary to prevent lake pH from decreasing to less than 5.5, the value at which fisheries often are adversely affected. Precipitation pH presently fluctuates from about 4.5 to about 6.0 in the area, having a median value of about 5.0. No degradation of the lakes has been observed, but the study indicates that many lakes could be severely impacted if precipitation pH is significantly lowered.

Field experiment on in-stream uptake and regeneration of nitrate

Nitrate uptake and regeneration was determined by downstream increase in nitrate concentration in a darkened flow-through channel. The study was conducted by F. J. Triska, V. C. Kennedy, and R. J. Avanzino at Little Lost Man Creek, Humboldt County, Calif. Nylon screen shading (92 percent) simulated near-surface intragravel conditions. The plexiglass channel

was augmented with nitrate (7.0 $\mu\text{g-atoms N/L}$) and phosphate (0.8 $\mu\text{g-atoms P/L}$) to mitigate nutrient limitation and minimize dark uptake by algal autotrophs. The stone-dwelling biotic community removed 0.51 g-atoms NO_3 per channel within 15 d, then generated 0.52 g-atoms NO_3 during the next 7 d. Nitrate regeneration was highest at night and lowest during daylight hours. At a flow rate of 9.5 L/min, maximum observed instantaneous nitrate formation was 0.6 $\mu\text{g-atoms N/L}$ and maximum average nitrate formation for a full day was 0.4 $\mu\text{g-atoms N/L}$. Daily net community primary production was always negative. Dissolved organic nitrogen and particulate detritus were potential sources of reduced nitrogen. Nitrate regeneration under darkened field conditions, despite low ammonium concentration, is consistent with previous observations of nitrate increases with increasing stream order in pristine, nitrogen-limited watersheds.

Trophic classification of Washington lakes

During the summer of 1981, S. S. Sumioka, N. P. Dion, S. S. Embrey, T. D. Olsen, and J. M. Jacoby collected physical, cultural, and biological data for 134 lakes in Washington State. Each lake then was classified trophically by using two methods:

1. A relative, multivariate technique (based on principal component analysis) using Secchi-disc visibility and concentrations of total phosphorus, total organic nitrogen, and chlorophyll *a* in the epilimnion.
2. An absolute univariate technique using any one of three water-quality parameters: Secchi-disc visibility, total phosphorus concentration in the epilimnion, or chlorophyll *a* concentration (Carlson, 1977).

The first method yielded characteristic values (CV's) that ranged from 45 to 1,047; the second method yielded trophic state indices (TSI's) that ranged from 0 to 106. In both approaches the higher numbers represent the more "eutrophic" conditions. On the basis of guidelines provided by Carlson (1979) and the range of observed TSI's, study lakes ranged from highly oligotrophic to highly eutrophic.

Nutrient Loads to Lahontan Reservoir, west-central Nevada

Lahontan Reservoir, located on the Carson River in west-central Nevada, is a major recreational site that stores water for irrigation in the nearby Fallon area. The reservoir is fed by the river and by the Truckee Canal, which diverts streamflow from the adjacent Truckee River basin. Nitrogen and phosphorus input to the

reservoir has resulted in increased eutrophication in recent years, as evidenced by a bloom of the blue-green alga, *Aphanizomenon*, in 1980. Estimated nutrient loads to Lahontan Reservoir from the Carson River have averaged approximately 300 Mg/yr for nitrogen and 100 Mg/yr for phosphorus during water years 1973-80, according to K. T. Garcia and R. L. Carman. Comparable long-term values of nitrogen and phosphorus for the Truckee Canal are approximately 300 and 70 Mg/yr, respectively. During water year 1980, nutrient loads from the Carson River were significantly greater than the estimated long-term average, due largely to above-normal streamflow. In contrast, nutrient data for the canal, which has a regulated flow, did not show greater than average loads in 1980.

Bacterial denitrification in small streams in California

Bacterial denitrification (measured by using acetylene inhibition) associated with algal mats was estimated in a small, nutrient-rich urban drainage basin (San Francisco Creek, San Mateo County, Calif). Three sizes of incubation chambers (0.05, 0.65, and 40 L) were placed in the dark and filled with nitrogen and acetylene gas having a concentration and temperature similar to the background nitrate concentration and temperature of the creek. Nitrate concentration ranged from 150 to 200 mg/L $\text{NO}_3\text{-N}$ and water temperature ranged from 16 to 25° C over the course of the experiments. F. J. Triska and J. H. Duff found denitrification (nitrous oxide production) to be 288 ± 257 , 481 ± 248 , and 304 ± 49 nmol $\text{N}_2\text{O/g/h}$ for the small, medium, and large chambers, respectively. Anomalously high rates in the 0.05-L chambers, which contained 15 to 25 mat-covered cobbles, provided the most reliable estimates and apparently minimized environmental variability by the large sample size. The 40-L chambers subsequently were used to examine the effect of photosynthetically produced oxygen from the mat as an inhibitor of denitrification. Three oxygen concentrations (0, 0-1, and 0-4 mg/L) were attained as a result of algal photosynthesis by regulated light. Production of N_2O in the gas phase was 3,580 nmol/g dry wt in the anaerobic chamber and 813 and 313 nmol/g dry wt, respectively, at 0 to 1 and 0 to 4 mg/L O_2 after 12 h. The above data were used to calculate a 24-hour field rate (2.9 $\mu\text{mol N}_2\text{O/g dry wt/d}$), assuming 6 h of uninhibited denitrification, 6 h of transitory inhibition, and 12 h of total photosynthetic oxygen inhibition. Areally, the rate was 134 $\mu\text{mol N}_2\text{O/m}^2$, which compares favorably with published rates from marine and lake sediments. Chambers of 40-L capacity also were used in a pristine environment (Little Lost Man Creek, Humboldt County, Calif.), where background nitrate concentration was approximately 40 $\mu\text{g/L NO}_3\text{-N}$. In the pristine environment, N_2O was not

produced by stream periphyton under aerobic or anaerobic conditions with or without NO_3 amendment.

Derivation of net photosynthetic production from community-metabolism analysis in Arkansas

J. E. Terry and E. E. Morris devised a method for determining net photosynthetic dissolved-oxygen production (production-respiration) from the community-metabolism program J330 of Stephens and Jennings (1976). This program is an Odum technique to analyse diel temperature and dissolved-oxygen data. Data needs for the derivation are output from programs J330 and chlorophyll *a* content of stream phytoplankton and periphyton. The resulting net-production data define a very important process in modeling dissolved-oxygen in a stream system.

NEW HYDROLOGIC INSTRUMENTS AND TECHNIQUES

New plastic pygmy-meter bucket wheels

Several prototype pygmy meter plastic bucket wheels have been successfully molded from lexan polycarbonate in one monolithic piece. According to J. C. Futrell, these lexan bucket wheels are a direct retrofit to the existing pygmy meters and require no modifications. These new bucket wheels weigh 40 percent less and are considerably more durable than previous versions. A cost reduction of 800 times is anticipated for the new lexan polycarbonate bucket wheels.

New lightweight fiber wading tagline

A new wading tagline has been developed for Kevlar, an Aramid-P fiber. According to J. C. Futrell, this braided line with jacket is made by a high speed machine process and is paint marked under tension. The new line has no beads and weighs one-sixth that of the previous steel version. It presently is being field tested.

Retrofitting the Survey's battery-powered water-quality monitor

According to J. H. Ficken, systems for measuring dissolved oxygen and pH have been designed for the Geological Survey's battery-powered water-quality monitor, which originally measured and recorded only river temperature and specific conductance. Information is recorded at specified timed intervals on punched paper tape from sensors placed directly in the river. The monitor can be connected directly to satellite data-collection platforms for real-time transmission.

Measurement of water stage with ultrasonic-ranging instrumentation

J. H. Ficken also reports that an ultrasonic ranging instrument has been designed for the measurement of the water stage of rivers. The instrument can be suspended above the river surface to a maximum height of about 10 m. Sound waves, generated by the instrument, reflect back to the device from the water surface. The time taken for the soundwaves to traverse the distance is a measure of the water stage. The ultrasonic ranging device is battery powered and can be used for the non-contact detection of high water and floods by interfacing it to satellite data-collection platforms. It has been field tested successfully at stream-monitoring stations in the vicinity of Mount St. Helens Volcano.

New point-integrating and depth-integrating bag-type samplers

J. J. Szalona devised a method for compensating for the effects that temperature has on the inflow rate to a bag-type suspended-sediment sampler. New point-integrating and depth-integrating bag-type samplers were designed for field use.

Evaluation of Helley-Smith bedload samplers

J. N. Skinner, J. P. Beverage, and J. J. Szalona, in cooperation with D. W. Hubbell and H. H. Stevens, Jr., completed studies of several different type of Helley-Smith types of bedload samplers. The instantaneous rate of bedload discharge is cyclical and varies over wide limits. The mean rate can be estimated from the probability distribution of a large number of samples; however, each sample must be corrected both for sampling errors characteristic of the sampler used and the instantaneous sampled rate.

Replacement for discontinued Pakron wading tagline reel

J. C. Futrell reports that a steel-tie-wire reel has been modified to replace the discontinued Packron wading tagline reel. The new reel has double the line capacity and a more simplistic design than the previous Packron reel. Fifty tagline and reel prototypes are currently being field tested.

New continuous-flow sediment-concentration samples

J. V. Skinner and J. P. Beverage completed laboratory tests of a new sediment-concentration meter. Tested fluvial-sediment concentrations ranged from zero to 97,000 ppm. The meter, which is a continuous-flow type, is slightly more sensitive to clay-size particles

than to sand-size-particles. After readings are compensated for variations in water temperature and dissolved solids, a random measurement error remains. For concentrations less than 500 ppm, the error is about ± 12 percent of the indicated concentration. For clay concentrations, the error is ± 3 percent.

Development of a new microprocessor controller for National Urban Runoff data collection

An AC line-powered microprocessor controller was developed for the National Urban Runoff Program and implemented in the spring of 1980. This system uses hydrologic measurements to make decisions on automated water-sample and data collections. Jack Hardee reports that a battery-powered microprocessor controller will soon be available and is scheduled for use in remote areas to support coal-hydrology investigations.

Contracted development of electronic current-meter pickup systems

J. C. Futrell reports that a contract has been advertised and bids received to develop several new electronic pickup systems to be tested with USGS current meters. The most successful electronic pickup will replace the existing catwhisker pickup in current meters. The nearly frictionless electronic pickup systems that will be examined are Hall effect, Weigand wire, and optic-sensing types.

Feasibility study for developing a depth-integrating pumping sampler

J. H. Ficken reports that a study by the Computer Sciences Corporation, a Geological Survey contractor, shows the feasibility of developing a depth-integrating pumping sampler for obtaining water-quality and water-sediment samples from rivers. Existing cable-suspended bottle-type samplers can be used by developing a small rate-controlled pump. The cable and pump lines will need to have streamlined fairing in order to reduce drag and setback.

Completion of Phase I of the Power System Study

K. V. Sharp reports that Phase I of a Power System Study is complete, and Phase II is midway to completion. Selection of an appropriate battery technology and a system design was completed in Phase I and resulted in definition of an alternative for providing power at Geological Survey hydrologic stations. This alternative is an improved system of hydrologic instrumentation and consists of the usual Fisher-Porter and Leopold Stevens recorder, stacom, and servo manometer modified to reduce current and conform to a single voltage of

12 V. Other essential components are sealed lead-acid batteries and charging systems.

Water-use monitoring equipment

E. H. Cordes reports that equipment to monitor the running time of water-pumping machinery is helping to collect water-use data around the country. By combining the operating time of pumps with their pumping rates, the quantities of water in use can be calculated. Two time-totalizer designs are in use, one that senses vibration of the system to which it is attached and one that relies on inductive pickup from electrical wiring. The vibration time totalizer (VTT) is triggered by a threshold vibration-level sensor and requires self-contained battery power. The inductive time totalizer (ITT) is completely passive and will only be activated when electric current is flowing through a conductor, as is the case with submersible pumping wells. Between the two totalizing units, the operating time of most water-pumping facilities can be monitored.

New stream-gaging equipment

Wayne Rodman and J. C. Jelinski are developing a portable hydraulic power unit to operate a B-56 sounding reel. The power unit and reel provide constant, repeatable sounding line speeds and fast sample retrieval with less operator fatigue. As development continues, the power unit will be used to operate E-53 reels, ice augers, cable car drives, and other hydrologic equipment.

Theoretical methods for interpreting shear and head waves in fluid-filled boreholes

F. L. Paillet conducted a theoretical analysis of the physical mechanisms associated with shear and head wave propagations along the fluid-rock interface in fluid-filled boreholes. The theory showed that although there is an important difference between head waves in cylindrical boreholes and the usual interpretation model involving waves along a plane interface, the radius of curvature of the borehole wall does not introduce severe complications to the interpretation of head waves. However, the coupling of shear waves in the borehole wall with internal resonances in the borehole fluid severely distorts the measured frequency response. The practical aspects of these results were summarized by Paillet (1981a) and simple numerical methods were developed for the prediction of resonant frequencies for a given borehole diameter and different seismic velocities. It was also determined that the pseudo-Rayleigh wave does not exist in the borehole. The slower traveling normal acoustic modes actually represent a hybridization

of the Rayleigh-like wall mode with the internally reflected fluid waves in the borehole. Since the complexity of the full mathematical theory made physical insight into the problem difficult, a much simplified plane-geometry analog to the borehole problem was developed (Paillet and White, 1982). The simplified model has proven especially useful in understanding how fluid responses in a borehole influence waveform character. The model is expected to remain an important research tool in future efforts to understand acoustic waveforms in boreholes.

Heat-pulse flowmeter

A low velocity heat-pulse flowmeter was modified by A. E. Hess to operate on standard four-conductor logging cable and to be used to study water-flow patterns with average velocities of as low as 2.5 m³/s. Velocity systems studied included forced convection in a sealed 15-m deep igneous-rock test pit and naturally occurring flow in a 60-m deep uncased well in sedimentary rocks. Initial results show that the system is very sensitive to debris clogging and other perturbations involving the flow sensors. Interpretation of the test results was also complicated by the fact that natural convection patterns in wells are poorly understood; perhaps different flow regimes for very similar external boundary conditions are involved.

Correlating surface geophysical surveys with borehole data

Ulrich Schimschal has investigated the use of downhole geophysical data derived from conventional well logs as a means of controlling the interpretation of surface resistivity measurements. The incorporation of resistivity and porosity data derived from logs may permit the association of interpreted resistivities from surface surveys with quantitative values for hydrogeologic constants. The method has been illustrated by two recently published papers (Schimschal, 1981a; Schimschal, 1981b).

Prototype compensated neutron porosity probe

W. S. Keys has undertaken the development of a compensated neutron porosity logging system for use in hydrogeology and engineering geology applications. The importance of an improved neutron logging system was indicated by the application of this tool in the direct characterization of water-filled pore space, coupled with the ambiguity between very small borehole wall effects and large formation porosities associated with existing neutron-logging systems. A theoretical analysis of the response of a multiple-detector, sidewall decentralized, and collimated neutron-logging sonde to expected

values of wall standoff and formation porosity was completed by using numerical models of neutron fluxes. The study identified the ranges of source-detector spacings required to maximize sensitivity to formation porosity while allowing correction for wall rugosity and providing reasonable count rates. The initial theoretical results were tested in the laboratory with simple detector and shield configurations. These results were then used to fabricate a prototype compensated neutron probe for field testing. The probe consisted of five helium-3 detectors with downhole digitization of measured count rates. Initial tests of the probe at the API test pits in Houston, Tex., and the DOE geothermal test pits at the Denver Federal Center, Denver, Colo., showed excellent sensitivity to formation porosities. Continuing field testing of the probe and compensated neutron-logging system has been directed toward the development of calibration techniques and system software that will allow corrections for the various borehole effects that normally impose severe limitations on the quantitative interpretation of single-detector neutron logs.

Improvements to borehole acoustic-televiever logging system

A. E. Hess has made several improvements in the basic borehole televiever system used to produce photographic images of the patterns of ultrasonic reflectivity on the borehole wall. These improvements include the replacement of noise-prone slip rings by a custom designed rotary transformer, use of a modified video-cassette recorder to record the unprocessed televiever signal prior to subsequent image-enhancement techniques, and development of a continuous televiever chart recording system to supplement the cumbersome Polaroid film system normally employed. The continuous recorder system automatically prints borehole depths on the continuous recording at preselected intervals. A numerical program also has been written to calculate the true orientation of fractures identified on the televiever log. This is done by making corrections for borehole deviation and for the deviation between the local magnetic vector and true north.

Hydraulic-conductivity logging

Ulrich Schimschal developed a computer program to calculate the hydraulic conductivity distributions along the borehole from volumetric flow changes produced by losses into formations around the borehole during fluid injection. The calculation of apparent hydraulic conductivity requires flowmeter and other supporting log data obtained during fluid injection. Continued refinement of this method was identified as a possible replacement for the time-consuming process of interval isolation and

pressure testing. The methodology has recently been tested in fractured dolomites (Schimschal, 1981c) and igneous and metamorphic rocks (Schimschal, 1981d).

Development of a hydrologic data-acquisition system

A program for the development of a modern, state of the art Adaptable Hydrologic Data Acquisition System (AHDAS) is being conducted by R. H. Billings. AHDAS is being custom designed to provide universal instrumentation support to the automatic field data collection programs of the WRD. AHDAS will be an intelligent, programmable, microprocessor-based system having solid-state data memory and facilities for interfacing a full spectrum of hydrologic sensors and peripherals. The system will operate with combinations of quantitative and qualitative parameters and provide active control to a variety of external samplers, pumps, and other devices. Data collection in either real-time or batch mode will be provided.

Characterizing hydraulic properties of fractured rock bodies with borehole geophysics

W. S. Keys and F. L. Paillet have analyzed the effectiveness of various geophysical techniques for identifying and characterizing natural fracture systems intersecting a fluid-filled borehole. Most of these techniques have been applied to igneous and metamorphic rocks, but at least one set of measurements has been obtained in low porosity limestones (Paillet, 1981b) and massive sandstones (Paillet and White, 1982). Analysis showed that conventional neutron and acoustic traveltime logs were most effective in identifying natural fractures in the borehole. The acoustic televiewer (an ultrasonic borehole-wall-imaging device) provided even more detail concerning the location and orientation of fractures. Initial attempts to develop a quantitative correlation between televiewer data and fracture permeability have not been successful because of the shallow viewing depth of the borehole wall provided by the televiewer and the complexity of the interaction between drill bit and natural fracture openings during drilling. Various crossplotting and correlation techniques involving more than one type of geophysical log were shown to be more effective in delineating fracture zones than any one kind of individual logs were. Acoustic waveform logs were also run in these boreholes, and the finite penetration depths of the acoustic waves were used to construct synthetic amplitude logs that correlated well with independent measurements of fracture permeability (Paillet, 1981c). Televiewer and waveform logs were also run over depth intervals containing hydraulically induced fractures. Even though these fractures were not

propped or subjected to repeated cycles of pressurization, all could be identified on acoustic televiewer logs, and all were associated with weak acoustic amplitude anomalies on the waveform logs.

Minimum standards for water-level sensing instruments

A detailed specification for water-level (stage) sensing instrumentation was prepared by D. H. Rapp and reviewed by the Branch of Surface Water, the staff at the Gulf Coast Hydrosience Center, and the Hydrologic Instrumentation Facility; legal aspects were evaluated by the Office of the Solicitor, Department of the Interior. This specification is part of a program to communicate the USGS requirements to instrument manufacturers. The specification covers systems for sensing the elevation of the water surface in open channels, rivers, lakes, reservoirs, storm-sewer pipes, and observation wells at Survey gaging sites. The signal output (mechanical or electrical) must meet the signal-input requirements of analog to digital and digital input recorders used by the Survey.

A classification of stage-sensing systems according to common characteristics is used to aid Survey personnel in making system selections. These characteristics are (1) contact or noncontact, (2) sensor type, (3) accuracy, (4) range, (5) power requirements, (6) system size and weight, and (7) data output signal. System requirements cover acceptable system configurations, signal outputs, materials, operation manuals, detailed environmental conditions, calibration procedures, system accuracy, power requirements, installation limitations, maintainability, safety, and workmanship. An outline of the qualification tests, procedures, and failure criteria is also given.

Sediment-oxygen-demand measurements by use of a laboratory respirometer in Arkansas

Water-quality modeling studies of various Arkansas streams by E. E. Morris and J. E. Terry have shown that one of the major demands on stream-dissolved oxygen is that imposed by the biological and chemical processes occurring on and in the bed of a stream. The studies used an in vivo approach to measuring this demand. An acrylic, airtight container is used to hold the sediment sample. Overlying water is circulated by use of a peristaltic pump. A continuous recorder is used in conjunction with an inline polarigraphic dissolved-oxygen probe to measure dissolved-oxygen depletion with time. Sediment-oxygen-demand results are expressed in $(g/m^2)/d$.

New dissolved-oxygen probe in Arkansas

E. E. Morris has observed increased precision of dissolved-oxygen measurements during the analysis of biochemical-oxygen demand. The Arkansas district has been using a nonoxygen-consuming Clark-type membrane dissolved-oxygen probe. The probe has shown drift of less than 0.05 (mg/L)/d. Membrane changes due to contamination are infrequent. Sample stirring is not needed during measurement.

ANALYTICAL METHODS**ANALYTICAL CHEMISTRY****Optimizing the selectivity of standard spectrofluorometers with computer control**

The potentially greater selectivity of fluorescence spectroscopy over absorption spectroscopy is shown by E. R. Weiner and M. C. Goldberg to be due to the larger number of variables that are related to the internal energy level structure of the sample molecules and that can be measured with fluorescence techniques. Until very recently, commercial spectrofluorometer design did not fully utilize the selectivity advantages of fluorescence spectroscopy. Many older instruments can be adapted to computer control for measuring the total excitation-emission matrix (EEM), and, thereby, enhance the selectivity of their fluorescence measurements. Details are given for converting a particular instrument for automatic recording of the EEM.

ENVIRONMENTAL GEOCHEMISTRY**Composition of saltbush grown on oil-shale reclamation test plots, Colorado**

Atriplex canescens (Pursh.) Nutt. (four-wing saltbush), a native browse species for livestock, is one of the most widespread and adaptable western shrubs. Because of its preference for saline soils, four-wing saltbush is being used more and more on spoil-pile reclamation sites throughout the arid and semiarid regions of the Western United States.

Samples of four-wing saltbush were collected from the Colorado State University Intensive Oil Shale Revegetation Study Site test plots in the Piceance Basin, Colo. The test plots were constructed to evaluate the effects on plant growth of soil cover thickness over processed shale and (or) over a gravel barrier between the shale and soil. Generally, the thicker the soil cover, the less

different the plant concentrations were from the control plot sample.

B. M. Anderson reports that concentrations of boron, copper, fluorine, iron, lithium, molybdenum, nickel, selenium, silicon, and zinc were larger in the samples grown over processed shale compared to those from the control plot, and concentrations for barium, calcium, lanthanum, niobium, phosphorus, and strontium were smaller. Twenty-one element concentrations in the ash of four-wing saltbush were larger on the plot with the gravel barrier between the soil and processed shale compared to the control plot sample. A greater water content in the soil on this plot has been reported, and the interaction between the increased percolating water and shale may have increased the availability of these elements for plant uptake.

Changes in trace-element composition of sagebrush close to Bridger Powerplant, Wyoming

To assess the possible effects of a coal-fired powerplant on the local geochemical environment, a sampling network around the Jim Bridger Powerplant, Wyo., was established in 1973 before the plant became fully operational. The sampling network consisted of four traverses (north, east, south and west) with stations located at geometrically increasing distances from the powerplant. Duplicate samples of big sagebrush (*Artemisia tridentata* Nutt.) and soils were collected at each station. After the powerplant had been in operation for 5 yr (1978), sampling on the east, west, and south traverses was repeated.

B. M. Anderson reports that from 1973 to 1978 16 element concentrations in the ash of big sagebrush have increased along the east and west traverses: B, Ba, Cr, Cu, Fe, Hg, Mg, Mn, Na, Ni, P, Sr, V, and Zr on the east traverse, and Cu, Hg, K, Mg, Mn, Ni, P, Sr, and Zn on the west traverse.

Regression analyses of the 1973 east traverse data indicated statistically significant trends for F and P at the 0.05 probability level and Pb, Zn, and Zr at the 0.10 level. These and nine additional element trends at the 0.05 level (Co, Fe, Mg, Mn, Na, Ni, Se, Si, and V) and three elements (Al, As, and K) at the 0.10 level were significant in the 1978 data.

The changes in the element composition of sagebrush from 1973 to 1978 indicate that the siting and operation of the Jim Bridger Powerplant has affected the local geochemical environment.

Geochemistry of vegetation, soils, and spoil materials, Jarvis Creek, Alaska

L. P. Gough and R. C. Severson studied the geochemistry of vegetation, soils, and spoil materials in the Jar-

vis Creek coal field to contribute to a feasibility and environmental assessment for potential development of this preference coal base. The vegetation of the area is classified as "birch and ericaceous shrub-sedge tundra." A broad plain of low relief at the extreme upper tree limit is bisected by the small channel formed by Ober Creek. North of Ober Creek, the native vegetation and soil is undisturbed. The coal excavation trench and spoil piles lie adjacent to, and west of, the undisturbed area that was studied.

The pH of the native soils and spoil material generally is less than 6.0, so that trace metals such as Al, Cd, Cu, Fe, Mn, Ni, and Zn should be available for plant uptake. Except for Cu and Zn, the concentrations of these elements are larger than concentrations in similar plants growing in near-neutral soils. Cadmium concentrations in willow stems are unusually large and are slightly larger in willows growing on spoil material than in those growing on undisturbed soils (3.5–6.2 ppm and 1.6–3.7 ppm, respectively). Willow may be a low-level accumulator of cadmium inasmuch as willow at the Isibelli Mine, where the pH is near neutral, contains similar amounts of cadmium (2.0–3.7 ppm). Willow plants at both Jarvis Creek and the Isibelli Mine also contain large amounts of zinc (240–330 ppm and 140–200 ppm, respectively). The amounts are truly unusual for plant material but are not so large as to suggest phytotoxic soil conditions.

Grasses growing on the spoil material at Jarvis Creek contain large amounts of aluminum (1,100–1,700 ppm). This may indicate that the spoil material has a potential for aluminum-toxic conditions.

Geochemical variability of soils and plants in the Piceance Basin, Colorado

Baseline values for 52, 15, and 13 properties in native soils, big sagebrush, and western wheatgrass, respectively, have been established for the Piceance Basin of western Colorado by Michele Tuttle, R. C. Severson, and Walter Dean (USGS), and Ronald Klusman (Colorado School of Mines). These baselines can be used to assess geochemical and biogeochemical effects of oil-shale development, to monitor changes in the geochemical and biogeochemical environment during development, and to assess the degree of success of rehabilitation of native materials after development. Map patterns for those geochemical properties that have statistically significant regional trends all show general north to south trends across the basin reflecting differences in lithology of soil parent material, elevation, and hydrology.

Soils in the Piceance Basin were classified into three geochemical groups by using Q-mode factor analysis. In

general, the three groups correspond to the three soil groups described by Dean and others (1979). The first group represents soils that contain high concentrations of vegetative debris. These soils occur in areas of high elevation where decomposition of organics is slow. Group one soils contain high concentrations of many DTPA-extractable elements, which means that these elements are chemically available to plants. The second group of soils is characterized by an enrichment of carbonates and carbonate-related elements such as strontium. Group two soils occur in areas where ground waters reach the surface. The third group of soils occurs in areas of low elevation. Group three soils are enriched in clay and have high pH values and have the highest trace-element concentrations of the three types of soils.

Chemical and mineralogical analyses of soil and chemical analyses of western wheatgrass samples from Colorado State University's experimental revegetation plot at Anvil Points provide data useful in assessing potential effects on soil and plant properties when large-scale revegetation operations begin. The concentrations of many major and trace elements in soils and in western wheatgrass are related to thickness of topsoil over spent oil shale. Concentrations of lead, zinc, organic and total carbon, and DTPA-extractable cadmium, iron, manganese, nickel, phosphorous, and zinc in soils in the revegetation plot samples are significantly higher than baseline values. Concentrations of all elements in western wheatgrass were within the baseline values established in the regional study.

Element content of rehabilitation plant species and their relation to mine-soil geochemistry

The surface mining of coal can either mobilize environmentally important elements found in the mine-soil material used for rehabilitation or make these elements less available. Regulatory agencies are expressing increased concern for an understanding of potential geochemical problems that may occur at individual mines. This concern means that both before- and after-mining inventories may be required in order to quantify changes.

In the fall of 1978, L. P. Gough and R. C. Severson collected samples of replaced cover soil, spoil, and seven plant species in rehabilitated areas that varied in age from 2 to 10 yr from 11 mines in the northern Great Plains, Powder River Basin, and Green River coal regions. Gough and Severson report that differences in the concentrations of 32 elements in crested, slender, and intermediate wheatgrass, alfalfa, and fourwing saltbush from rehabilitation sites reflect variability in cover-soil and spoil mineralogy, lithology, and bioavailability. Comparisons of element levels were made

among (1) species from mine-site and adjacent control-site areas, (2) species from different mine sites, and (3) species within mine sites.

The element content of intermediate wheatgrass at five mines in Colorado and North Dakota was significantly different among mines but usually by a factor of only two or three. Concentrations of elements in wheatgrasses from all mines were smaller than the amounts considered to be potentially toxic to plants or grazing animals; concentrations of phosphorus and magnesium in wheatgrasses, however, were consistently below critical dietary levels for cattle. Concentrations of elements from six mines in three States were fairly uniform; large variability among mines (factors of 5 to 10) was noted, however, for levels of Al, Cd, Li, and Na. Concentrations of boron in alfalfa at one North Dakota mine are indicative of available mine soil B levels that may be phytotoxic. Also, molybdenum levels of >4 ppm in alfalfa at a Montana and North Dakota mine have the potential of being toxic to grazing cattle. Variability in the levels of most elements in fourwing saltbush collected at two mines (Montana and Wyoming) was less than a factor of four. Extremely large B concentrations in saltbush from the Wyoming mine (110–610 ppm) are indicative of phytotoxic conditions, and only the most B-tolerant species should be expected to survive.

Chemical composition of overburden rocks and sampling needs for reclamation of surface coal mines

Data on major, minor, and trace element composition for rocks of discrete types from five mine sites in rocks of Cretaceous age from the western U.S. were assessed for uniformity, variation, and regional trends by T. K. Hinkley and K. S. Smith. The data were compared to other data from analogous suites of Tertiary rocks from

the northern Great Plains. At most sites, the knowledge of the available proportions of the distinct rock types, such as sandstone or carbonaceous shale, with their observed concentrations and variability of environmentally benign and troublesome chemical elements, allows researchers to make confident projections in advance for reclamation strategies. Much of the analytical chemical work on overburden rocks at new mine sites that has been recommended by regulatory agencies may be simplified by application of the results of this study.

Molybdenosis associated with uranium-bearing lignites in South Dakota

In the fall of 1975, cattle grazing to the north of an abandoned uranium mine on Flint Butte in Harding County, S. Dak., showed signs of molybdenosis, a molybdenum-induced copper deficiency. To identify the source of the problem, L. R. Stone, J. A. Erdman, and G. L. Feder collected plant, water, and soil samples on a grid design over a 16-km² area around Flint Butte. Uranium, molybdenum, and copper concentrations were determined in western wheatgrass (*Agropyron smithii*) and sweetclover (*Melilotus officinalis*), molybdenum and copper concentrations and pH were determined in pond waters, and pH determinations were made on the soils. Ratios of copper to molybdenum in the forage were found to be below the critical threshold of 2:1. Copper to molybdenum ratios below 2:1 are considered unhealthy to cattle. Molybdenum levels in some surface waters were extremely high. These conditions are related to outcrops of uranium- and molybdenum-bearing lignites at Flint Butte and at the Flint Hills nearby. A comparison of the regional geology with the local geology indicates that this nutritional problem in cattle may exist in similar geologic terranes over a broad region of the northern Great Plains.

GEOLOGY AND HYDROLOGY APPLIED TO NATURAL HAZARDS

EARTHQUAKE STUDIES

SEISMICITY

NETWORKS

Operations

The World Wide Standardized Seismograph Network (WWSSN), installed by the Albuquerque Seismological Laboratory (ASL) beginning in 1961, has been the principal source of geophysical data for the delineation of global plates and interior structure of the Earth. In FY 81 the ASL continued to provide supplies, replacement parts, and technical assistance to 106 stations of the WWSSN, according to O. J. Britton. Original seismograms were sent from 98 WWSSN stations to the USGS for quality checking and then were forwarded to NOAA/EDIS to be duplicated on film. R. P. McCarthy reported that the overall quality of the seismograms and the standards of performance of the WWSSN show no decline after twenty years in operation.

At the end of FY 81 the Global Digital Seismograph Network consisted of 16 Seismic Research Observatory (SRO/ASRO) stations and 11 Digital WWSSN stations operating in the United States and 19 foreign countries, according to R. D. Reynolds. The data acquisition systems for the GDSN were developed and installed by the ASL, which continues to supply and maintain the network. Magnetic tapes from each GDSN station are sent to the ASL, where the data are rigorously checked for quality and then assembled onto Network day tapes. J. P. Hoffman reports that the Network-Day tapes now provide most of the data for the rapidly expanding interest in the determination of earthquake source characteristics and phase attenuation properties.

Research and development

J. R. Peterson and C. R. Hutt (1981) completed a design study for a national digital seismograph network. They considered the types of seismic data that might be acquired by using broadband sensors with high

dynamic range, data system concepts, and data management concepts. Several methods were investigated for improving seismic stations at the South Pole and McMurdo-Dry Valleys region, Antarctica (L. G. Holcomb, 1982). Feasible alternatives ranged from a short-period vertical-component seismometer installed in a shallow borehole at the Pole to a three-component short- and long-period seismometer installed in a deep borehole in the Dry Valleys with data acquired by telemetry.

J. N. Murdock and C. R. Hutt (unpub. data, 1981) developed software for an improved event detector for digital signals that picks short-period events with no false alarms and also lists direction of first motion, exact arrival time, and quality of the pick. J. R. Peterson (1982) investigated the transients that occasionally appear in the SRO and ASRO data and found them to be caused in some cases by a nonlinear disturbance (sensor clipping) and in other cases by a predictable impulse response of the long-period filters. L. G. Holcomb (unpub. data, 1981) analyzed calibration data from all SRO and ASRO stations for the calendar year 1980 to test and evaluate the algorithm being used to compute the calibration constants for the network day-tape operation and to compile statistics on the performance of the overall calibration scheme. The study indicated that the station calibration amplitudes can be evaluated with a precision of better than ± 1 percent and that the phase angle can be determined to within ± 0.5 degree. L. G. Holcomb and J. R. Peterson (1981) reported on a method for compressing digital data in which only key characteristics of the digital waveform are retained and the dynamic range of the data word is tailored to the instantaneous requirement.

L. G. Holcomb (1981a) investigated simultaneous background Earth noise levels at stations distributed around the world. Power spectral estimates at periods from 0.1 to 600 s during the first two weeks of October, 1980, were calculated for 15 stations. L. G. Holcomb (1981b) reported that maximum entropy spectral analysis of the 26-s spectral line in long-period Earth background noise reveals that this line is much narrower than originally believed. The indication is that a very high Q source must be generating this energy.

DATA AND INFORMATION

National Earthquake Information Service

The National Earthquake Information Service (NEIS) continued its function as a focus for the collection of worldwide seismic data, the determination of earthquake locations, and the rapid issuance of bulletins containing accurate information on earthquakes worldwide with magnitude (M) ≥ 6.5 or in the United States with $M \geq 5.0$. According to W. J. Person, the NEIS in FY 81 determined the parameters (origin time, epicenter, focal depth and magnitude) of 6,670 earthquakes from data supplied by seismic observatories located in nearly every country in the world. These parameters were published in the weekly Preliminary Determination of Epicenters (PDE), usually within four weeks after the earthquakes occurred. The complete lists of these and other parameters were published in the PDE monthly listing about 5 months after the earthquake occurrences. The companion Earthquake Data Report, also published monthly, contained the earthquake parameters plus the observed station data for each earthquake.

Earthquake Early Alerting Service (EEAS)

According to W. J. Person, 52 of the earthquakes located by the NEIS during FY 81 were considered significant because they had $M \geq 6.5$, caused damage, or resulted in casualties. The worldwide total of earthquake-caused fatalities during FY 81 was reported at 14,600. The EEAS issued 89 bulletins on potentially damaging earthquakes worldwide and smaller United States earthquakes of significant interest. These bulletins provide disaster relief agencies, public safety organizations, the press, and the public with the first factual and accurate information on potentially damaging earthquakes. In addition, the EEAS reported 11 earthquakes with $M \geq 7.0$ to the Pacific Tsunami Warning Center within 20 minutes after the arrival of the triggering signal within the NEIS seismic network.

At the end of FY 81 the NEIS seismic network consisted of 9 cooperating stations in Alaska, 62 cooperating stations in the conterminous States, and 4 stations operated by the NEIS. Signals telemetered from these stations are recorded on a common time base in Golden, Colo. The wide distribution of the stations provides excellent coverage for the rapid investigation of earthquakes in the United States and good coverage for many of the areas of heavy seismicity elsewhere. Digital recording of the network signals was begun on an experimental basis in FY 81, according to M. A. Carlson.

United States earthquakes

C. W. Stover reported that 116 earthquakes in 26 States were canvassed during FY 81 by questionnaire and or field studies. The data has been interpreted and is published in the quarterly USGS Circulars, United States Earthquakes, which describe the effects on communities and show the geographical extent of the effects. The most damaging earthquakes to occur in the United States during FY 81 were both in California. One of these earthquakes, off the coast of northern California, collapsed a highway overpass near Fields Landing. The other earthquake caused extensive damage to buildings in Westmorland in the Imperial Valley. Both earthquakes had Mercalli Scale maximum intensity VII.

C. W. Stover, B. G. Reagor, and S. T. Algermissen published seismicity maps for 8 States in 1981. These maps and the accompanying tables show all historically felt earthquakes and all instrumentally located earthquakes with magnitudes ≥ 3.0 .

Observatories

During FY 81 the USGS operated five observatories that record both seismic and geomagnetic signals. Short-period vertical-component seismic signals were transmitted from three observatories to the NEIS in Golden, Colo. In addition, the observatories at Agana, Guam, and Cayay, P.R., communicated by telegraph and telephone with the NEIS when major earthquakes were recorded. The Guam observatory also participated in the Pacific Tsunami Warning Service. The magnetic data from the observatories was used to update regional and world magnetic charts and correction factors.

SPECIAL INVESTIGATIONS

Aftershock investigations

C. J. Langer reported that the aftershocks of the November 23, 1977, western Argentina earthquake ($M_s=7.4$) occupied a volume of considerable width and depth, rather than a planar or tabular zone. Extensive north-northwest and north-northeast fault systems, as well as a cross-cutting east-northeast fault system, may have been reactivated in the Sierra Pie de Palo and surrounding region by perturbation of the local stress regime as a result of the main shock displacement.

W. J. Spence and C. J. Langer (1982) completed an investigation of the aftershocks of the great ($M_s=7.8$, $M_w=8.1$) Peru earthquake of October 3, 1974. The aftershocks clustered spatially and temporally in zones that apparently had not been completely distressed

during the main shock. Much broader distressed regions surrounding the clusters were essentially free of detected aftershocks. A major ($M_s=7.1$) aftershock terminated the sequence by distressing the principal cluster zone.

Regional investigations

D. H. Warren found that microearthquakes in the vicinity of the San Pablo and Suisin Bays tended to be concentrated in isolated clusters, in contrast to the typical linear alignments of epicenters further to the southeast. These clusters were mostly along known faults. A seismic gap spanned the water-covered areas beneath both bays and extended inland on either side. The south boundary of the gap was well defined just south of the bays, but the north boundary was irregular and extended as far as 20 km northwest of the San Pablo Bay on the Rogers Creek fault. The gap is terminated to the east of Suisin Bay by the active Antioch fault. Most focal mechanisms from earthquakes ($M \geq 2.4$) close to the Bays show north-northwest, right lateral, strike-slip motion.

Oppenheimer and Herkenhoff (1981) performed a joint hypocenter-velocity inversion of earthquake traveltimes data that resulted in an improved velocity model for the Geysers region, California. Over 5,000 earthquakes were relocated with this model and the spatio-temporal seismicity pattern clearly documents induced activity about areas of concentrated geothermal production. An anomalously low velocity zone beneath Mount Hannah near the Geysers, California, is most readily attributed to a crustal magma body. Regional Pn traveltimes also indicate that the Moho dips 5 degrees to the northwest.

L. H. Jaksha and D. H. Evans (unpub. data, 1982) completed a crustal structure study in the San Juan basin, New Mexico, using seismic refraction-reflection techniques. In the vicinity of Farmington, N. Mex., they found the crust to be 48 km thick over a mantle Pn velocity of 7.99 ± 0.12 km/s. The crust is subdivided into (1) a 3-km-thick sedimentary layer with a P-wave velocity of 3.2 km/s, (2) a 29-km-thick granitic layer with $P_g=6.0$ km/s, and (3) a 16-km-thick gabbroic layer with $P^*=6.9$ km/s.

W. J. Spence and R. S. Gross completed an inversion of a large set of teleseismic P-wave data recorded at a seismograph network in the central Rio Grande Rift, New Mexico. The inversion showed that the upper mantle in the region of the Rift, to a depth of about 200 km, has a P-wave velocity about 4 to 6 percent lower than the adjacent mantle beneath the High Plains.

A. C. Tarr and B. S. Rhea (1981) completed an investigation of seismicity in the source area of the

Charleston, S.C., earthquake of August 31, 1886. They suggest that the current activity in the Middleton Place-Summerville seismic zone is in the fault zone of the 1886 main shock. The newly determined hypocenters define a three-segmented seismic zone composed of two en-echelon segments that strike northwest and dip nearly vertically southwest and a third segment that strikes east-northeast. A composite focal mechanism of 16 earthquakes suggests reverse dip-slip motion, on a northwesterly trending plane, in response to a generally northeasterly trending greatest principal compressive stress. Two other important clusters of epicenters near Bowman and Adams Run are spatially distinct from the Middleton Place-Summerville seismic zone.

According to A. M. Pitt, earthquakes (up to $M=3.8$) that occurred within the southwest Yellowstone caldera, Wyoming, in 1980 and 1981 defined a 15-km-long, north-trending zone which is aligned with the currently inactive Teton fault south of the caldera. This seismic activity suggests that the Teton fault may extend beneath the 75,000-150,000-yr-old rhyolite flows filling the caldera. Because the length of this seismic zone is comparable to the aftershock zone associated with the 1975 $M=6$ earthquake that occurred in the north-central part of the caldera, earthquakes up to $M=6$ should be possible in the southwest caldera.

Theoretical investigations

According to R. P. Buland, basic research has been completed on techniques for estimating various earthquake source parameters from digitally recorded teleseismic ground motion. In particular, S. A. Sipkin (unpub. data, 1982) has developed two different body phase waveform inversion techniques that are capable of estimating faulting geometry by using waveforms from four or more far field stations. Buland and Taggart (1981) have developed a method for estimating earthquake moment from long-period surface waves. In addition, software developed by M. D. Zirbes has greatly facilitated user access to Global Digital Seismograph Network day tapes and enabled R. E. Needham to estimate fault plane solutions for 33 large 1981 earthquakes (published in the PDE monthly listing).

B. R. Julian (1982) completed a theoretical analysis of the scattering of seismic waves in media with anisotropically distributed inhomogeneities. The analysis showed that at low frequencies (long wavelengths) scattering is independent of the distribution of the heterogeneities. For wavelengths comparable to the dimensions of the heterogeneities, resonance effects occur. At high frequencies only P-to-P and S-to-S scattering persist but are concentrated strongly into the forward direction, where they interfere with the direct wave and

produce fluctuations in its phase and amplitude. If the heterogeneities in elasticity and density are independently distributed, forward and backward scattering are equally strong. Pronounced back scattering, thought to be important in the generation of local earthquake coda waves, occurs only when the different types of inhomogeneities are correlated.

G. L. Choy reported two important advances in the development and application of digital waveform data for the investigation of both earthquake sources and the interior structure of the Earth. V. F. Cormer (Cooperative Institute for Research in the Environmental Sciences) and Choy applied full-wave theory to test different velocity models of the Earth's interior. They concluded that secondary arrivals such as interference head waves, not included in ray theory, can be important constraints on Earth structure (V. F. Cormer and G. L. Choy, 1981). Danny Harvey and G. L. Choy (1982) developed a technique for the simultaneous deconvolution of long- and short-period data from GDSN stations. They obtained broad-band records of body-wave ground displacement and velocity with spectral information from several hertz to tens of seconds. Frequency-dependent effects in body waves that may arise from source complexity or from propagation through the Earth are much more apparent and measurable in the broad-band records than in the original seismograms.

EARTHQUAKE MECHANICS AND PREDICTION STUDIES

Experimental studies of fault mechanics

Experimental deformation studies of simulated faults and samples of San Andreas fault gouge have been conducted by J. D. Byerlee. Strain hardening and velocity dependence of fault strength were consistently observed. The experiments were conducted under drained conditions, either nominally dry or with constant 2 MPa pore pressure. At both moderate (30 MPa) and elevated (300 MPa) confining pressures, increased strain rate elevated the frictional stress level and decreased strain rates lowered the frictional stress level. This finding suggests that in-situ frictional strength may be significantly less than that measured under relatively rapid strain rates in laboratory simulations. In addition, the experiments indicate that the strength of fault gouge increases during sliding with increased permanent strain.

D. A. Lockner, P. G. Okubo, Gerry Conrad, and J. H. Dieterich measured the heat generated during unstable slip on a simulated fault in granite. Frictional heating was measured to be 92–96 percent of the total energy

released during sliding. This result implies a maximum seismic efficiency of only 4–8 percent. Calculations of heat generated during slip agree with independent measurements of frictional sliding energy released and support a simple dynamic friction model for fault energetics.

Theoretical mechanics of earthquake precursors

Model simulations were made by G. M. Mavko to help clarify the relations among seismicity, fault creep, and fault trace geometry. In the model, fault strength obeys a pressure-dependent law, which is assumed to have the form of a constant coefficient of friction. Mavko developed a steady slip-rate model that predicts the spatial variation of slip rate in the region of interaction of the Calaveras, Paicenes, and San Andreas faults in close agreement with geodetically determined slip rates. The response of theoretical fault models incorporating detailed fault zone constitutive laws inferred from laboratory measurements of frictional sliding was also studied. These model simulations explored the effect of laboratory-inferred friction on the sliding behavior of in-situ scale faults. The fault zone "frictional" strength is characterized by two competing effects: an instantaneous dependence of fault strength on velocity (strength increases with velocity) and also an inverse dependence of strength on velocity that takes full effect only after a finite amount of slip has occurred. Two-dimensional simulations in a plate predict recurring rapid strike-slip events, similar in size to the 1906 San Francisco earthquake, separated by periods of strain accumulation. In addition, the model predicts an interval of precursory displacements shortly before the rapid slip and an extended interval of decaying afterslip.

Rupture processes of earthquakes

G. L. Choy, Jack Boatwright, and D. Harvey have analysed data from the Global Digital Seismic Network (GDSN) to infer rupture processes of earthquakes. Choy and Harvey developed a technique for the simultaneous deconvolution of long- and short-period data channels from GDSN stations to construct broad-band records of ground displacement and velocity. Choy and Boatwright have demonstrated that broad-band data could be used to infer detailed rupture histories for deep earthquakes and provide constraints on dynamic and static stress drops, earthquake rupture velocity, and source geometry. Choy and Boatwright also examined the temporal and spatial changes in static and dynamic source parameters of a sequence of four moderate-sized earthquakes that encircled the eventual rupture zone of the

large Miyagi-Oki earthquake of June 12, 1978. The third event of the sequence had a dynamic stress drop much higher than the previous two events. The main shock followed this event by four months.

California seismicity studies for earthquake prediction

Results for northern and central California support a three-stage model of seismicity: quiescence, following a great earthquake, renewed activity of moderate-sized events during the latter half of the time period between great earthquakes, and the next great earthquake. The historic record in southern California, although not as complete or extensive as that for the northern part of the State, tentatively supports the identification of the same stages of seismicity. Re-analysis of historical reports during the period from 1857 to 1920 by W. L. Ellsworth and B. L. Moths has failed to uncover any events as large as $M=6$ in the southern California region at latitudes parallel to the 1857 surface rupture and indicates that magnitude values of several previously reported $M=6$ events are overestimated. For southern California the pattern is one of relative quiescence at the $M=6$ level until about 1920 in the part of the San Andreas system that is parallel to the 1857 earthquake. Since 1920 there have been at least seven $M=6$ events. Seismicity in southernmost California, parallel to the segment of the San Andreas fault that has not ruptured during a large earthquake in historic time, has been at a high level since at least the 1890's, when the reliable record begins.

The 430-km-long segment of the San Andreas fault that ruptured in the great 1906 earthquake ($M=8$) has been seismically quiet at the $M=6$ level for the last 75 yr. Analysis of the historic record by A. G. Lindh and W. L. Ellsworth indicates that the southernmost 100 km of the fault break, extending from San Francisco to just north of San Juan Bautista, was the site of three or four $M=6$ or greater earthquakes in the 110 yr preceding 1906, with events occurring in 1800, 1838, 1865, 1890. These earthquakes are plausibly accounted for by repeated slip on the southernmost 50 km of fault, just to the northwest of San Juan Bautista. Geodetic data indicate that strain is currently accumulating across this zone at a rate (0.6 micro-strain/a) which can be explained if the right lateral displacement across the fault is 2 cm/a and the upper 10 km of the fault are locked. This rate of strain accumulation is consistent with short- and long-term geologic determinations of displacement rates in the region and is sufficient to account for a magnitude 6.5 earthquake every 30 yr, a close approximation to this segment's behavior in the nineteenth century. The long interval without a large event since 1906 can plausibly be accounted for by the 1.5 m of slip

that occurred on this portion of the fault in the 1906 earthquake. If this model is correct, it suggests that a large ($M=6+$) earthquake could occur in this region at any time. This idea is reinforced somewhat by the pattern of lower magnitude seismicity following 1906. Quiescence extending down to the $M=4.5$ level lasted for 40 yr; activity resumed in the mid-1940's. These variations are suggestive of a small scale, stress modulated "seismic cycle." Temporal variations in the rate of microearthquakes indicate that this region has been unusually active since mid-1979. The increase in activity apparently began with an intense swarm of activity that occurred on the San Andreas fault 4 d before the M_L 5.8 Coyote Lake earthquake that ruptured the Calaveras fault immediately to the east of the region.

The seismic moments for the Parkfield, Calif., main shocks of 1922 and 1934 have been determined by using seismograms recorded at Berkeley, Calif. The ratios of the 1922 and 1934 seismic moments (1:3) is nearly equal to the ratio of the time intervals to the subsequent Parkfield sequences (12 yr:32 yr), consistent with the "time-predictable" earthquake model. W. H. Bakun (USGS) and T. V. McEvelly (University of California, Berkeley) have employed the seismic moment of the 1966 Parkfield mainshock determined from Berkeley seismograms to estimate the time of the next Parkfield earthquake sequence. If it is assumed that the seismic moment-time interval proportionality holds, the sequence will occur between 1994 and 2003.

A detailed study of the seismicity of the San Andreas fault system north of San Francisco Bay has been initiated by R. S. Cockerham. The study uses earthquake data acquired by the USGS California network since January 1980. Two distinct seismic regions are evident: north of 40° N., and from latitude 38° N. to 40° N. In the northernmost region, the epicenters are widely scattered with a small clustering of events in an area approximately 25 km off Cape Mendocino. Most focal depths in this northern region range from 10 to 40 km; some deep events are between 50 and 60 km. These earthquakes outline a $20-25^\circ$ southeast-dipping Benioff zone, which represents subduction of the Gorda plate. Between 38° N. and 40° N., in the southern region, the pattern of seismicity consists of two N. 39° W. trending zones that parallel an essentially aseismic San Andreas fault. All focal depths within this region are shallower than 18 km. The western zone coincides with the Rodgers Creek-Maacama faults whereas the eastern zone of seismicity coincides with the Green Valley-Bartlett Springs faults. Geologic mapping of these faults in the northern San Andreas fault system has revealed abundant evidence for repeated displacement during the Holocene. Fault creep is locally occurring at a rate of several millimeters per year on the Maacama and Green Valley faults.

El Salvador seismic gap

D. H. Harlow, R. A. White, I. L. Cifuentes (USGS) and A. Aburto (Nicaragua Seismology Institute) studied the southeast end of the El Salvador seismic gap, an area apparently overdue for an earthquake of magnitude greater than 7.5. From teleseismic data they discovered a zone within this gap that has been almost totally quiet for magnitude 5 and greater earthquakes for the 30 yr preceding 1980. From local data recorded by the Nicaragua network it was discovered that this zone has also been almost totally quiet for magnitude 3 and greater earthquakes for at least 5 yr preceding 1980. The investigators conclude that this quiet zone is of sufficient dimensions to generate an earthquake of magnitude 7.5 or greater. On the basis of these observations they suggest that this area is an appropriate subject for continued monitoring and study.

Seismic velocity measurements in the San Andreas fault zone

H. P. Liu has developed equipment and conducted field tests to determine the feasibility of measuring changes in seismic wave traveltimes for monitoring changes in strain near active faults. Digitally recorded seismic wave forms were collected along a 600 m baseline located along a fractured granitic mass 2 km west of the San Andreas fault near Hollister, Calif. A 656 c³ air gun fired in the mud-filled pit provided a repeatable seismic source. The signals from two geophones 600 m apart were digitized by two cassette recorders synchronized to within 0.05 ms. The single-shot accuracy and repeatability of traveltime is ± 0.04 percent for the first surface wave arrival following the direct body waves. A 1-ms-variation (0.02 percent) of this traveltime is observed which correlates with the solid-earth tidal strain.

Correlated changes in gravity, elevation and strain

High-pressure measurements of crustal deformation are essential for earthquake prediction monitoring and for study of tectonically active areas. Uncertainties pertaining to the precision of measurement techniques has brought into question some potentially significant observations and has limited the analysis of some data. Gravity, elevation, and strain changes have been compared by R. C. Jachens and C. W. Roberts. Yearly or half-yearly repeated measurements show large correlated changes in gravity, elevation, and strain along the San Andreas fault in southern California during the 1977-1982 period. Precise gravity surveys indicate changes as large as 25 μ Gal between surveys 6 months apart. Repeated leveling surveys reported by W. Thatcher and R. S. Stein show that annual changes of as

much as 100 mm occurred over 40-100-km-long base lines. Area strain surveys by J. C. Savage reveal that coherent changes of 1-2 ppm occurred over much of southern California from 1978 to 1980. Based on plots of strain change and elevation change versus gravity change, the various quantities are related by approximately -0.01 ppm/mm and -0.1 μ Gal/mm. Although some doubts may exist concerning the precision of each of these measurement systems, the rather good agreement among them argues that the changes reflect true crustal deformation. The style of deformation revealed by the data is that of rapid aseismic fluctuations during which uplift is accompanied by gravity decrease and areal compression, whereas subsidence is associated with gravity increase and areal dilatation. That deformation of this style occurred during the past 5 yr has implications for many of the deformation monitor programs being conducted in southern California. The short-period nature of the deformation suggests that measurements of various parameters must be nearly coincident if the relations between them are to be accurately portrayed. For example, changes in relative elevation determined by repeated level surveys between widely separated points could reflect both intersurvey and intrasurvey movements.

M. J. S. Johnston has compared magnetic field data from southern California with the results by Jachens for gravity, elevation and strain. Johnston found that over a 5-yr period the four data sets generally tracked. This correlation increases confidence in each data set and allows critically important scaling factors to be determined.

Geodetic strain near Mammoth Lakes, California

Geodetic measurements were made near Mammoth Lakes, Calif., in support of studies of continuing high seismicity in that region. J. C. Savage and M. M. Clark report that the measurements demonstrate crustal deformation within the area of the Long Valley Caldera. On the basis of an analysis of the pattern of deformation, Savage and Clark suggested that the magma chamber beneath the resurgent dome within the Long Valley Caldera may have expanded because of the injection of new magma in late 1979 or early 1980. This result is important evidence for increased potential for volcanic activity. In addition, the inflation of the magma chamber may have induced stresses around the caldera and caused the 1980 sequence of earthquakes southwest of Mammoth Lakes.

Triggering of earthquakes by aseismic crustal movements

According to Wayne Thatcher and J. C. Savage, triggering of aseismic crustal movements has been convinc-

ingly demonstrated by observations and theoretical analysis for three large ($M=7$) tectonic earthquakes from central Japan. Other examples from both California and Japan support a similar conclusion. These results suggest that episodic aseismic movements can play a critically important role in the prediction of at least some earthquakes because the episodic movements can be detected by geodetic surveys.

EARTHQUAKE HAZARDS STUDIES

Studies of earthquake hazards include topical research on ground motion, earthquake-induced ground failure, the distribution, size, and frequency of damaging earthquakes, and the location and degree of activity of faults and regions of tectonic instability. These studies also include relatively detailed assessments of specific earthquake hazards in such areas of high risk as Los Angeles, San Francisco, Salt Lake City, and Seattle; localized assessments on hazards for such critical facilities as dams, nuclear reactors, and defense installations; and collaborative efforts with engineers, professional societies, and elected officials to improve earthquake safety through better building codes and construction practices.

The research described here constitutes the core of the USGS Earthquake Hazards Program and is supplemented by a diversified research effort supported by USGS contracts with universities, State geological surveys, and private research and engineering institutions; the results of the contract research program are summarized twice a year in open file reports issued by the USGS.

SEISMOLOGIC APPRAISAL OF EARTHQUAKE POTENTIAL

National earthquake data base

Accurately locating earthquakes, recording their effects and magnitude, and systematically incorporating them into a national data base is essential to realistic assessments of hazards. Carol Thomasson, Frank Baldwin, and James Taggart checked 33,000 earthquake listings against original published sources. Glen Reagor developed a versatile computer code with the capacity to edit, add, or delete any of the 45 parameters of the earthquakes listed in the files. Parametric uncertainties have been estimated by Taggart for many of the earthquakes in the Montana and New Mexico files.

W. H. K. Lee has made preliminary relocations of 200 pre-1960 earthquakes ($M>5$) by using computer program HYPO 79 and a standardized velocity model. The quality and distribution of the arrival times are not

uniform, and standard errors are unacceptably large for many of the relocations.

Southern Alaska seismicity during FY 81

During FY 81 J. C. Lahr, C. D. Stephens, R. A. Page, J. A. Rogers, and their co-workers collected and analyzed data from a network of 51 high-gain short-period seismograph stations that extend across southern Alaska. Their data show that the region west of Prince William Sound is dominated by Benioff zone activity, which dips northwestward beneath Cook Inlet and the Alaska Range. Events of about magnitude 2 and larger are routinely detected and processed in this region; more numerous and smaller events are detected and processed near Anchorage and the southern Kenai Peninsula, where special studies are underway. Below 70 km, the Benioff zone events are non-uniformly distributed along the strike of the subducted Pacific plate. Clusters of deeper events occurred beneath Iliamna Volcano west of Cook Inlet and in two areas to the southwest and northeast of Mount McKinley.

East of Prince William Sound earthquakes are shallower than 35 km, and those as small as magnitude 0.5 are routinely detected and processed. Clusters of events, the most noteworthy feature of this seismicity, include a northeast-trending zone 40 km northwest of Valdez, activity around the Copper River delta, a cluster 75 km northeast of Kayak Island in the Waxell Ridge area, aftershocks of the 1979 St. Elias earthquake north of Icy Bay, and a zone of seismicity that parallels the Duke River fault north of the network. Among a few shallow events aligned with the Denali fault was one of magnitude 4.4 in April, 1981. A line of epicenters also follows the northeastern boundary of the Yakutat foreland north and east of Yakutat Bay and coincides with an inferred northeast-dipping thrust fault that is the assumed focus of a series of great earthquakes in 1899-1900 (Thatcher and Plafker, 1977).

D. W. Gordon has relocated, by means of joint hypocenter determination, more than 250 instrumentally recorded earthquakes in the central U.S. (between 85° W. and 104° W.). The earthquakes occurred between 1930 and 1980 and all were of magnitude, based on the early arriving Love wave phase ($mdbLg$), 3.0 or greater. The completeness of this catalog can be tested by comparing it with catalogs of felt earthquakes, most of which were greater than magnitude 3.0. For 1930-1960, only about 5 percent of felt earthquakes listed by Nutthi (1979) could be located with instrumental data, for 1960-1969, about 50 percent of the felt earthquakes (Nutthi, 1979) could be located, and for 1970-1975 more than 75 percent of the felt earthquakes (Nutthi, 1979) could be located. For 1976-1980, nearly 95 percent of felt earthquakes reported to the NEIS of the USGS

could be located with instrumental data. For the entire period 1930-1980, the largest earthquakes that could not be located from instrumental records occurred in the 1930's and are estimated at magnitude (mbLg) 4.7, on the basis of the felt areas reported in Nuttli's catalog.

J. W. Dewey's study of the seismicity of Colorado, New Mexico, and southern Wyoming has demonstrated radical differences in properties of seismic wave attenuation across the Rocky Mountain front. To better estimate mbLg for Rocky Mountain earthquakes, he has determined regionally dependent and azimuthally dependent attenuation functions. If attenuation of Lg waves propagating to the east from the Rocky Mountain front is described by an anelastic attenuation coefficient of 0.07 deg^{-1} , a value typical of the central U.S., then attenuation coefficients for Lg to the west of the mountain front must have values of 0.3 deg^{-1} or 0.4 deg^{-1} if the mbLg values computed for westerly traveling waves are to agree with those computed for easterly traveling waves.

The Yakataga seismic gap is in the northeastern Gulf of Alaska and between Icy Bay and eastern Prince William Sound. During FY 81 most of the earthquakes in the gap were at or near its eastern and inferred northern perimeter. The central part of the gap, north of the Aleutian trench, was nearly aseismic.

Probable cause of earthquakes in southwestern Virginia

Giles County, in southwestern Virginia, often experiences small earthquakes; it suffered a moderately damaging shock in 1897. R. L. Wheeler, collaborating with G. A. Bollinger of Virginia Polytechnic Institute and State University, has concluded that those earthquakes are 5 to 25 km deep and are most likely on a fault that is buried beneath the Appalachian folds and faults that are visible at the surface. The fault may have formed when an ancient ocean opened about half a billion years ago, and now it has been reactivated in the same stress field that characterizes much of the Midwest.

Location and intensity of the 1872 Washington State earthquake

D. M. Perkins reanalyzed the location of the 1872 Washington State earthquake by using intensity data from 10 researchers. He concludes that the epicenter of the main shock was near Lake Chelan. The centers of the Intensity VI contours for all of the isoseismal maps lie within a radius of 60 km of lat 47.9° N . and long 120.3° W .; the circular area having this radius contains Lake Chelan, the town of Wenatchee, parts of the eastern Cascade Range, and parts of the Columbia Plateau. The reevaluation indicates that the maximum Modified

Mercalli Intensity is IX, and the depth, though uncertain, is probably shallow.

GEOLOGIC APPRAISAL OF EARTHQUAKE POTENTIAL AND FAULT ACTIVITY

Surface evidence of fault activity in California

A complex pattern of normal faults in and north of the Superstition Hills, as well as the Superstition Hills fault, which bounds the hills on the southwest, has been mapped by R. V. Sharp. He discovered structural evidence of movement along the Superstition Hills fault during deposition of the continental sediments now exposed at the surface. From regional stratigraphic relations, the age of these sediments is estimated as late Pleistocene. Scarps along some of the normal faults cut young alluvium, and although the latest fault movement is unknown, current seismic activity suggests that all of these structures are potentially active.

Surface expression of the San Andreas fault in the San Bernardino Mountains varies from well-defined to obscure. South of Thermal Canyon, where the fault is well-defined by geomorphology and vegetation, many of the scarps, bends, and other evidence for recent displacement coincide with intermittent ground rupture triggered by distant earthquakes in 1968 and 1979. The coincidence of triggered creep and evidence for Holocene offset, particularly below the high shoreline of prehistoric Lake Cahuilla suggests to R. V. Sharp that (1) triggered creep may locally contribute a significant fraction of total Holocene surface displacement; (2) neither large earthquakes nor faulting have displaced that part of the fault uncovered by the lowering of Lake Cahuilla 200-300 yr ago; and (3) those well-defined segments of the fault northwest of the zone of triggered creep in 1968 and 1979 may owe their character to triggered creep during other distant earthquakes.

M. J. Rymer's geologic studies of the central, creeping section of the San Andreas fault zone near Monarch Peak show the zone consists of six fault classes, three of which can be related to the late Quaternary tectonic history. The most obvious fault class, the main trace, consists of straight, discontinuous segments separated by steps and bends, which accommodate changes in the fault azimuth of as much as 20 degrees. Right steps with associated depressions are more numerous than left steps. Northeast of the main trace, and within 3 to 4 km of Monarch Peak, straight to slightly curved subsidiary faults trend approximately north and exhibit relative displacements that are down to the west; their true displacement, however, may be dextral oblique slip. The third class of late Quaternary faults consists of two boundary faults that contain the fault zone and enclose

a diapiric wedge that is nearly centered on the main trace. Within 100 m of the surface these faults dip toward each other at 20 to 80 degrees; they steepen at depth. Aseismic creep along the main trace and disperse deformation across the fault zone have long been known. Alinement arrays and other measurements of distance now show that the subsidiary faults slip as much as 12 mm/yr (Rymer, Lisowski, and Burford, 1982). The boundary faults may also be active, but data confirm only late Cenozoic, probably Pleistocene, movement.

Emergent Holocene marine terraces are common throughout the Pacific basin, especially where convergent tectonics accelerate uplift. K. L. Lajoie reports that most of coastal California deforms by strike-slip faulting and shearing and that regional uplift rates are relatively low. He finds greater uplift rates, however, in emergent Holocene terraces near Cape Mendocino in northern California and near Ventura in southern California; in both areas local convergence controls the rate of uplift. In Japan and Alaska, episodic crustal uplifts of 1-6 m, accompanying historic coastal earthquakes, have produced emergent marine terraces. If the multiple beach ridges and terraces on the main emergent terraces at Ocean House and Big Flat, near Cape Mendocino, and at Pitas Point, near Ventura, are coseismic in origin, they represent a rather complete history of major earthquakes in these areas over the past 6,000 yr.

Diffusion-equation model and degraded fault scarps, Colorado

Diffusion-type equations, sometimes used to simulate the evolution of hillslopes, are difficult to solve for general boundary conditions. S. M. Colman has developed an explicit solution of the diffusion equation by using simplifying fault-scarp boundary conditions. This solution has the form of an error function and directly relates the age of a fault scarp to the maximum scarp angle and to the scarp height.

The diffusion equation and measurements of scarp morphology suggest that the relations among height, slope angle, and age are valid for fault scarps formed by multiple-event or single-event surface ruptures. However, morphometric comparisons between these types of scarps are invalid because multiple-event scarps have lower slope angles for the same heights and ages of last rupture. Compared to the prior history of a fault, maximum slope angles of multiple-event scarps are primarily controlled by their cumulative scarp height and by the recency of faulting.

Within local areas of Colorado, the ages of most recent movement of late Quaternary fault scarps estimated by using the diffusion equation are generally consistent with ages estimated by using soil stratigraphy and radiocarbon dates. However, that apparent

rates of scarp degradation differ greatly between areas suggests that lithologic factors such as grain size, cementation, and soil development and past and present climates significantly affect rates of scarp degradation.

Surface faulting in the Sonora, Mexico, earthquake of 1887

On May 3, 1887, a large earthquake in the San Bernardino Valley of northern Sonora shook the Southwestern United States and northwestern Mexico. Contemporary investigations reported normal faulting for 56 km along the east side of the valley and an average throw of 2.1 m. Fieldwork in 1980 and 1981 by D. G. Herd and C. R. McMasters has traced the 1887 fault break for nearly 76 km. Beginning 8 km south of the U.S.-Mexico Border, the main fault trends along the southeast edge of the valley about S. 8 degrees W. and is expressed as a sinuous line of west-facing scarps. At the south end of the valley, the fault steps westward about 2.5 km and then continues 21 km southward in the Sierra Pilares de Teras, following a linear S. 12 degrees W. trend. This is now the longest historic normal fault; it exceeds the length of the fault (61 km) at Pleasant Valley, Nev., of 1915 by about 15 km. In the San Bernardino Valley a 30-km-long zone of secondary faults parallels the main break and lies 4 to 7 km west of it.

The throw on the main fault increases southward to at least 5.1 m about 30 km south of the border and then gradually diminishes to about 1 m in the Sierra Pilares de Teras. Almost all 1887 scarps are now gravity- and debris-controlled slopes; erosion of the scarps has increased the apparent scarp width to as much as 6.9 m in some places. In 1887 the scarp faces reportedly stood at 45-90 degrees; today they slope at angles of 50 degrees or less. From the measurements made in 1980 and 1981, the average dip-slip in 1887 (area under slip curve divided by fault length) is judged to have been at least 1.9 m (average throw) but less than 3.8 m (apparent dip slip). If faulting extended to a depth of 15 km along a fault surface dipping 70 degrees, the seismic-moment magnitude (M) was between 7.2 and 7.4.

Structural framework and earthquake hazards of the Mississippi embayment

D. P. Russ and A. J. Crone analyzed small boat and Vibroseis reflection profiles and subsurface data from well logs to interpret geologic structure and earthquake source zones near New Madrid, Mo. Russ, S. T. Harding, and D. W. O'Leary directed about 245 km of seismic reflection surveys along the Mississippi River between Osceola, Ark., and Wickliffe, Ky.; Kaye Shedlock has processed the data from the southern half of the survey. The processed profiles reveal several

previously undetected faults that offset Cenozoic sediments as much as 60 m. They also show that the Cottonwood Grove fault, which cuts the Mississippi River about 8 km southeast of Caruthersville, Mo., is at least 40 km long. Vibroseis reflection profiles from elsewhere in the Mississippi embayment define zones where the buried Paleozoic bedrock reflector is poorly developed or absent; these zones correspond to areas of repeated earthquakes and reactivated faults.

E. E. Glick and A. J. Crone reinterpreted subsurface well logs to construct a series of structure contour and isopach maps. The maps help in interpreting the late Mesozoic and Cenozoic depositional and tectonic history, and they document recurrent movement in excess of 75 m along a northeast-trending fault that coincides with the southeast edge of Reelfoot rift. Seismic intensity data for earthquakes near New Madrid from 1838 to 1982 suggest that the threshold for eruptive liquefaction (primarily sand blows) is $MM=8$ ($mb=6.2$). Since the great 1811-12 earthquake series, only the October 31, 1895, Charleston, Mo., shock is known to have caused sand blows in this region.

The first and last major shocks of the 1811-12 New Madrid earthquakes were on December 16, 1811, and February 7, 1812. S. F. Obermeier has located the epicenters of these earthquakes within a circle of 10 mi diameter by (1) mapping the distribution of sand blows, (2) calculating the peak (or sustained) horizontal ground surface acceleration required to cause sand blows along the outer margin of the sand-blow area, and (3) then using a relation between acceleration and distance from epicenter, striking arcs along the sand blow border. The epicenters are located where the arcs intersect. Obermeier also finds evidence of pre-1811, earthquake-induced liquefaction and deformation in sediments that overlie glacial outwash sands in alluvial lowlands near Truman, Ark. About a foot above the outwash sands, liquefied dikes of sand, sand blows, and warped beds are truncated by an erosional unconformity and capped by a thin, widespread layer of clay. This site is about 15 mi northwest of Marked Tree, Ark., in the area that was shaken severely by the 1811-1812 earthquakes.

Quaternary faulting along the La Jencia fault, central New Mexico

The La Jencia fault zone, a recently reactivated Cenozoic structure of major proportions, bounds the west side of the Rio Grande rift along the northern Magdalena and southern Bear Mountains in central New Mexico. M. M. Machette reports that the most recent movement on this fault zone produced a nearly continuous series of prominent scarps, less than 7 m in height, that extend northwesterly for 35 km. Because fault displacements are about the same in deposits that range in age from middle Pleistocene to middle

Holocene, Machette suggests that the scarp is young. Four exploratory trenches excavated across scarps of the La Jencia fault permit Machette to estimate the age of fault events. His estimates are based on the maturity of soils as shown by the content and rate of accumulation of secondary clay and calcium carbonate in these soils. In two trenches, the stratigraphic, structural, and pedogenic evidence indicates that at least two and probably three discrete episodes of surface rupturing occurred on three discrete segments of the fault during the Holocene (last 10,000 yr). In the other two trenches, geologic evidence suggests that two segments along the central part of the fault last ruptured about 15,000 and 33,000 B.P. The trenches also revealed evidence of still older, but minor faulting, which occurred about 150,000 yr B.P. along the northern one-third of the fault.

The relationships between maximum scarp-slope angle and scarp height indicate different ages for the most recent movement along segments of the La Jencia fault zone and support the fault history determined from the trenches. The youngest fault segments have scarp morphologies similar to those of the Drum Mountain fault of central Utah and the Cox Ranch fault of southern New Mexico. All of these scarps are thought to have formed in the last 4,000-6,000 yr. The next older segment of the La Jencia fault morphologically resembles the highest wave-cut shoreline of Lake Bonneville in Utah; both features are considered to be about 15,000 yr old. The older scarps along the La Jencia fault are about 33,000 yr old and are more degraded than the Bonneville shoreline.

Machette thus interprets four to seven separate surface ruptures along five areally discrete segments of the La Jencia fault. These movements occurred from about 33,000 yr B.P. to less than 3,000 yr(?) B.P., an interval of some 30,000 yr. During the past 33,000 yr the average recurrence interval for movement of the La Jencia fault is as much as 10,000 yr for four separate ruptures to as little as 5,000 yr for seven surface ruptures. Estimates of the maximum magnitudes of these late Quaternary paleoearthquakes range from $M=6.8$ to $M=7.1$, based on various combinations of surface rupture lengths, surface offsets, and source lengths and widths for the La Jencia fault. These earthquake magnitudes are commonly associated with moderate to extensive ground breakage, property damage, and potential loss of life.

Soils chronology and fault history

Rates and processes of soil development are becoming better known through use of a soil development index derived by Jennifer Harden (1982). Harden and her colleagues have collected about 1,200 samples from 175 soil profiles in 14 chronosequences of the Western

United States. These chronosequences were chosen to help evaluate the effect of parent material and climate on soil formations and to provide good age control from independently dated material. Jennifer Harden and the late Denny Marchand, along with Michael Singer, Alan Busacca, and Peter Janitzky of the University of California at Davis, have completed most of the chemical, physical, and mineralogical analyses of these samples. During 1981, Emily Taylor and Harden showed that the degree of development for many soils can be quantified and that some soil properties vary with age and are relatively independent of climate effects. This has challenged the prevailing view that climate is an influential factor in the rate of soil development. Other workers are now using the soil development index to quantify and compare soil development. The method has broad applications in Quaternary stratigraphy and in dating prehistoric earthquakes recorded by faulted soils.

Along the Wasatch front of north-central Utah, morphologic and textural properties of soil B-horizons are useful for estimating the ages of range front faults that have been active during the latest Pleistocene and Holocene. Soil studies by R. R. Shroba indicate that Holocene deposits can be distinguished by the amount and type of B-horizon development; deposits of late Holocene age lack B-horizons, those of middle Holocene age (4,000–6,000 yr old) commonly have cambic B-horizons, and those of early Holocene age typically have thin, weakly developed, argillic (textural) B-horizons. Argillic B-horizons formed in deposits of latest Pleistocene age (11,000–20,000 yr) are thicker, redder, and more clayey than those of early Holocene age and are much less developed than those of more than 100,000 yr in age.

Evaluation of faulting near Monticello Reservoir, South Carolina

D. T. Secor, Jr., of the University of South Carolina, and D. C. Prowell have located and investigated the Wateree Creek fault. The near vertical fault is of late Paleozoic age, exhibits evidence of brittle failure, and has about 600 m of vertical offset; it is cut by Mesozoic diabase dikes and is covered by late Tertiary(?) alluvial fans. The fault surface passes near seismic activity at the Monticello Reservoir; similar faults with less displacement have been mapped at the R. B. Russell Reservoir. Geologically evaluating these faults may aid our understanding of any seismic activity induced by reservoir filling.

Late Holocene geomorphic features near Cedar City, Utah

Geomorphic features along three aligned streams in the Hurricane Cliffs about 8 km northeast of Cedar City,

Iron County, southwestern Utah, suggest to E. G. Sable that late Holocene tectonic stresses may still be deforming the surface there. The inner gorges of the West Fork of Braffits Creek, the stream in Hells Canyon that is a tributary of Fiddlers Canyon, and an unnamed tributary of Coal Creek have been deeply incised and gulleyed into deformed Cretaceous and Tertiary sedimentary rocks and semiconsolidated colluvium and alluvium of probable Holocene age. Evidence for possible young tectonic activity includes: raw, vegetation-free slip faces, some of which may be fault scarps, in the colluvium and alluvium along valley walls; small local folds in Quaternary sediments that contain clasts of middle Tertiary volcanic rocks; small waterfalls in texturally homogeneous Quaternary sediments; and landslides that are estimated to be less than 50 yr old. These geomorphic features follow the three streams for at least 9 km, defining a N. 20 degrees E. trend, which is subparallel to the trend of the nearby Hurricane fault system. These observations of youthful geomorphic features confirm those reported earlier along the West Fork of Braffits Creek (Anderson, 1980, p. 528–530; Anderson and Buckman, 1979, p. 424).

Gravity evidence of crust and mantle structure and seismicity

M. F. Kane, T. G. Hildebrand, and R. W. Simpson have filtered, by wave length, a gravity data set for the conterminous United States and have produced a series of maps that offer new opportunities for deciphering the structure of the crust and upper mantle. The most significant of these maps is a complementary pair composed of wavelengths less than 250 km (residual) and those more than 250 km (regional). Few gravity anomalies have wavelengths near 250 km, so the fields shown by the two maps are well separated. Model studies suggest that the 250 km residual map records chiefly crustal sources, whereas the 250 km regional map records Moho topography and mantle sources. Crustal anomaly patterns are highly coherent and display, among other things, features which seem to be related to plate-margin tectonics. Kane and his colleagues interpret other patterns as evidence of rifting. The map of mantle anomalies shows a major northeast-trending gravity gradient in the Eastern United States that may be evidence of a suture. The fact that many gravity highs are associated with sedimentary basins suggests crustal thinning and supports the McKenzie stretching model for sedimentary basins. Seismicity can be related to the interpreted suture zone, to interpreted rift elements extending from the Gulf of St. Lawrence to the Mississippi embayment, and to a transverse feature that separates the central and southern Appalachians.

GEODETTIC APPRAISAL OF EARTHQUAKE POTENTIAL

Leveling surveys in southern California

Continued monitoring of vertical deformation across creeping traces in the Garlock fault zone in Fremont Valley has convinced T. L. Holzer, D. H. Pampeyan, and R. V. Sharp that the creep is related to ground-water pumping. The displacement rate is seasonal, with the greatest rates occurring during summer periods of maximum pumping and the lowest rates occurring during the winter when little water is pumped. Protruding well casings and tilting of the Koehn Lake playa surface toward the area of maximum pumping confirm the removal of ground water as the cause of subsidence and nearby faulting.

R. V. Sharp installed leveling arrays to monitor tilt and displacement on the Coyote Creek fault at Middle Willows and Coyote Mountain and on the Clark fault at Jackass Flat and southeastern Clark Valley. These arrays are within the southern part of the San Jacinto fault zone, which is currently viewed as a seismic gap. He also constructed a new array across the San Andreas fault at North Shore and connected two preexisting leveling arrays on Harris Road in Imperial Valley; one of them crosses the Imperial fault, the other crosses multiple strands of the Brawley fault zone.

Deformation of the southern California uplift and the Colorado River delta

Rapid and predominantly downward vertical displacements have nearly erased the southern California uplift since 1976. This phase of vertical deformation roughly corresponds with the pattern of horizontal deformation, which has changed from north-south contraction and areal contraction to east-west extension and areal expansion. The change in vertical deformation was disclosed by repeated levelings between Los Angeles and Palmdale, according to R. D. Burford and J. D. Gilmore. A relict of the original uplift probably remains along the Pinto Mountain fault between Twentynine Palms and Yucca Valley.

The geology and deformational history of the Salton Trough may provide Burford and Gilmore with several clues concerning the nature and origin of the oscillatory vertical movements in southern California. Records of vertical control in the Imperial Valley and Salton Trough suggest that the drainage divide between Salton Sea and the Gulf of California is not simply a result of deltaic sedimentation, but is at least partly the result of aseismic tectonic uplift. First-order level data indicate that the southern Imperial Valley, north of the crest of the Colorado River delta, rose more than 0.40 m during the period from 1926 to 1974 and partly col-

lapsed between 1973 and 1978; the net uplift, relative to the San Diego tide station, was 0.15 m. This evidence, as well as geologic and geophysical data, suggests to Burford and Gilmore that Holocene crustal swelling along the deltaic crest has diverted the Colorado River away from the Salton basin and toward the southeast flank of the delta.

ENGINEERING SEISMOLOGY AND GROUND MOTION RESEARCH

Regional and national seismic risk assessment

S. T. Algermissen revised probabilistic ground acceleration and velocity maps for the U.S. The maps are based on an extreme probability of 90 percent for exposure times of 10, 50, and 250 yr. The 50-yr acceleration map for Alaska has been published; other maps are in review.

Carl Stover completed and published seismicity maps for 12 States in 1981; 28 of these maps have been produced to date and approximately 10 more are in review. The maps summarize reviewed and revised data on historical seismicity for each State.

Attenuation of particle velocity in California

A. F. Espinosa has derived a magnitude scaling law from the strong-motion data base of the San Fernando earthquake of February 9, 1971, and has compared his results with strong motion records from 62 earthquakes in the Western U.S. His M_L values agree well with those evaluated by Hiroo Kanamori and Paul Jennings of California Institute of Technology. The empirical scaling law applies to significant earthquakes in the Western U.S. from 1933 through 1971; local magnitudes of these earthquakes, recorded at epicentral distances of about 5 to 300 km, range from about 4.0 to 7.2. The proposed method extends the procedure of using strong motion records to determine the local magnitude of moderate and large earthquakes at near- and intermediate-epicentral distances.

New computer codes for ground motion studies

Paul Spudich, Tom Heaton, and Steve Hartzell, together with Uri Ascher of the University of British Columbia, have written a computer code which uses a collocation method to solve the wave propagation equation $du/dz = A(z)u$, where u is a stress-displacement vector, z is depth, and $A(z)$ is a matrix of coefficients dependent on the velocity structure. The P and S velocity structures, and the attenuation structure, may be arbitrary functions of depth. Spudich and his colleagues

are currently comparing synthetic seismograms generated by this method to those generated by other methods.

Spudich, Heaton, and Hartzell have also written a computer code that will combine arbitrary kinematic fault rupture descriptions with Green's functions generated by the discrete-wavenumber finite-element method of A. H. Olson (University of California, San Diego). They have used this code to calculate near-source seismograms from extended earthquake sources in laterally homogeneous earth structures having arbitrary velocity-depth profiles. The method can now be used for strike-slip earthquakes on faults having any dip; with minor changes it should be adaptable to earthquakes of any mechanism.

HAZARDS AND RISKS IN URBAN REGIONS

Rates of slip on faults in the Los Angeles region, California

Geologic investigations of young faults in the Los Angeles region seek to measure rates of late Quaternary slip and thereby evaluate the relative hazard of these faults as sources of earthquakes or of surface faulting. Such studies are facilitated in this region by widespread marine and nonmarine sedimentary deposits formed within the past 500,000 yr and dated locally by carbon-14, amino-acid racemization, and soils-chronology methods. J. I. Ziony reports that although more than 100 faults exhibit evidence of late Quaternary activity, measured offsets are available for only half of these, and less than a quarter of the faults displace well-dated deposits that afford reliable estimates of slip or separation. Well-constrained estimates of slip yield 20–30 mm/yr for the San Andreas fault, 8–12 mm/yr for the Clark strand of the San Jacinto fault zone, and 2 mm/yr for the Cleghorn fault. Vertical separations on late Quaternary faults of the Transverse Ranges suggest typical rates of about 1 mm/yr or less; rates on the Sierra Madre and Cucamonga faults are about 1–3 mm/yr. The Newport-Inglewood Zone, a dominantly strike-slip system, yields vertical separation rates of as much as 0.6 mm/yr; these rates imply that rates of horizontal or oblique slip are considerably greater. Limited data suggest a much lower offset rate, 0.06 mm/yr of vertical separation, for the Chino-Elsinore fault zone. These results demonstrate the range of fault-slip rates to be expected and provide a base for estimating risk.

Ground motion and ground failure hazards in the Los Angeles region, California

J. C. Tinsley obtained new information on earthquake hazards from 14 exploratory holes drilled to depths of

about 20 m at 7 sites in the Canoga Park–Reseda area. He used standard and Dutch cone penetrometer tests and continuous-flight augering techniques to examine, sample, and test near-surface geologic materials. Most of the sediments outside modern stream channels are cohesive and not susceptible to liquefaction, but buried fluvial channels 3 to 12 m beneath the surface contain well-sorted medium- to fine-grained sand and silty sand that is locally gravelly; these buried channel deposits are cohesionless and, where exposed by excavations, they cascade from the cut face. Where water-saturated, the channel deposits commonly flow into boreholes and yield Standard Penetrometer Test blow counts ranging from 2 to 8 blows per foot. Tinsley found that many of these cohesionless, water-saturated channel deposits in the western San Fernando Valley are so low in density that they may liquefy and cause ground failure during earthquakes. Because surface landform rarely gives clues of these buried channels, subsurface investigations are necessary to evaluate liquefaction susceptibility at most sites. Current work indicates that sites on Holocene deposits have greater impedance contrasts, lower shear-wave velocities, higher void ratios, and greater amplification of ground motion than sites on Pleistocene deposits. Thickness of geologic units is also important in evaluating ground response. Thus, sites underlain by thick deposits of Holocene sediment are expected to have the most severe ground motion during future earthquakes.

A. M. Rogers found that short-period horizontal ground shaking (0.2–0.5 s) is controlled by the shear velocity of near-surface layers and by the thickness of Holocene materials. Sites underlain by 10–20 m of alluvium with nominal shear velocities of 200 m/s demonstrate a strong site period with short-period spectral ratios as high as 6 to 7, relative to crystalline rock.

Long-period horizontal ground shaking (3.3–10 s) is controlled by the thickness of Quaternary materials and the depth to basement. Mean response in this period band relative to crystalline rock increases from 1 to 6 as depth to basement increases from 0 to about 6 km (for an average Quaternary thickness of 200–300 m).

Theoretical damped site transfer functions (STF) do not match observed data in detail but do accurately predict the mean response, especially at periods less than 0.5 s. At longer periods these body-wave models underestimate the mean observed STF by 50 percent.

Quaternary geology and earthquake hazards in the Puget Sound region, Washington

Depth to bedrock, determined from drilling information and marine seismic-reflection profiles, has helped Jim Young, Fred Pessl, Jr., S. A. Safioles, and Mark Holmes clarify the relation between the thickness of

Quaternary sediment and the configuration of Tertiary basement in Puget Sound. The Quaternary section on the southwest side of the Marysville basin thins by nearly 400 m across a major northwest-trending gravity and aeromagnetic feature; the linear gravity and aeromagnetic feature has been interpreted by H. D. Gower and J. C. Young (unpub. data, 1981) as a fault bounding the upthrown southwest side of the basin. The Quaternary section also thins markedly north of Oak Harbor, across the east-trending northern Whidbey Island fault, which defines the north boundary of the Marysville basin. Further south, near Seattle, structural basins also contain thick deposits of Quaternary sediment that appear to thin over a prominent structural arch. This relationship between thickness of Quaternary sediment and Tertiary basin configuration suggests that basin margin structures have been active during the last 2 million yr.

Preliminary compilation of the thickness of post-glacial alluvium in the region east of Whidbey Island indicates that maximum thicknesses of 30 m, 70 m, and 90 m of alluvium exist at the mouths of the Snohomish, Stillaguamish, and Skagit Rivers. Within these alluvial deposits geotechnical wells have encountered some layers of fine-grained sand with anomalously low resistance to penetration. Some of these weakly resistant sediments may liquefy during ground shaking and may therefore constitute a significant hazard.

Plots of earthquake epicenters against depth in profiles transverse and longitudinal to the past position of the Puget lobe of the Cordilleran ice sheet show that shallow (less than 35 km deep) seismicity coincides closely with the margin of the ice sheet. Moreover, the pattern of seismicity, particularly in transverse profiles, mirrors ice thickness, having deeper earthquakes where ice was thickest and shallower earthquakes near the ice margin. This relation suggests, but does not prove, that residual stress from past ice loading may play a role in triggering shallow earthquakes beneath Puget Sound.

Mapping in the Puget Sound region has also identified a potentially useful stratigraphic marker, a till of probable early Wisconsin age, that correlates with the Possession drift of Easterbrook and others (1967). The till is well exposed at Possession Point and Indian Point on southern Whidbey Island and just south of Richmond Beach on the mainland (Minard, 1982); it is at least 25 m thick and lies between younger Vashon drift and older Double Bluff drift.

POST EARTHQUAKE INVESTIGATIONS

Earthquake, new reverse fault, and crustal unloading near Lompoc, California

At 01:21 PST on April 7, 1981, a local magnitude 2.5

earthquake was felt strongly at a 24-hr processing plant and quarry near Lompoc in the northwestern Transverse Ranges, a region noted for compressive deformation across east-west folds and seismically active reverse faults. After daybreak a 575-m-long zone of closely spaced reverse faults was observed on the flat floor of the quarry. According to R. F. Yerkes the zone trends about N. 84° E. and dips 39° to 59° S., parallel to bedding in diatomite, shale, and claystone of the Neogene Sisquoc Formation on the north limb of an open, symmetrical syncline. Displacement along thin clay interbeds showed the following maxima: of net slip, 25 cm; dip slip, 23 cm; and right-lateral strike slip, about 9 cm. Average net slip was about 12 cm. Slip vectors plunge 32° to 39° toward azimuth 142° to 150°. A tunnel 33 m below the quarry floor and at least 5 m stratigraphically below the down-dip projection of the surface ruptures showed only minor shaking damage. The fact that P-wave first arrivals recorded as near as 20 km were very emergent for this size earthquake indicates a shallow focus. Estimated radiated seismic moment from P waves is less than 2×10^{18} dyne/cm, compared to less than 10×10^{18} dyne/cm from field data; static stress drop was less than 3 bars. The removal of an average of 44 m of diatomite from an area of 5.4 km² during about 25 yr of quarrying accounts for an average pressure reduction at the quarry floor of about 5 bars and an increase of shear stress on the inclined fault plane of about 2 bars. Landsliding was not involved in the failure; the earthquake and fault are attributed to release of natural tectonic stresses triggered by unloading.

Mammoth Lake, California, earthquake studies

Of 1,500 Mammoth Lake earthquakes studied by Paul Spudich, 150 were locatable; their epicenters formed a diffuse pattern unrelated to mapped surface faults. One cluster of hypocenters defined a vertically dipping plane parallel to the south lip of the Long Valley caldera, and fault plane solutions indicated right-lateral strike-slip motion on this plane. The earthquake of May 27, 1980, at 14:50 GMT ($M_L=6.3$) recorded a peak horizontal acceleration of 0.4 g at a hypocentral range of 16 km.

Releveling of a first-order level line along U.S. 395 shows local vertical displacement of 120 mm, west side relatively up. The displacement, bracketed by leveling in 1975 and October, 1980, is in the epicentral region of the May, 1980, Mammoth Lakes earthquakes and at the Hilton Creek fault. Additional vertical displacement of about 100 mm is distributed westward from the Hilton Creek fault for about 10 km. The line, established in 1932, was also resurveyed in 1957 and 1975; it showed total vertical changes of less than 25 mm between 1932 and 1975. M. M. Clark interprets the recent fault dis-

placement of 120 mm along nearby parts of the Hilton Creek fault, and 60–80 mm of regional extension normal to the Hilton Creek fault between 1979 and September 1980, as evidence of normal tectonic slip on the Hilton Creek fault at the time of the earthquake. The level line crosses a Hilton Creek fault scarp that offsets glacial outwash from Convict Creek. Tioga glacial outwash, deposited about 15,000 yr ago, is offset about 25 m, and Tahoe glacial outwash, deposited about 50,000 to 130,000 yr ago, is offset 110 m. The 25-m scarp in Tioga outwash could have been built by about 200 1980-type events with an average recurrence interval of 75 yr. The historic record of earthquakes since 1870 is too short to test the validity of this estimated recurrence interval.

On November 16, 1980, a rockfall destroyed part of the Yosemite Falls trail killing 3 hikers and seriously injuring several others. M. M. Clark witnessed the rockfall from Sierra Point, 5 km away. Sierra Point was the site of the largest of several Yosemite Valley rockfalls triggered by the May 1980 earthquakes at Mammoth Lake, 65 km to the east. Gerald Wieczorek and Clark briefly inspected the rockfall on the Yosemite Falls trail 5 d later; they noted that the slab that failed had survived shaking during the earthquakes, and they concluded that although earthquakes trigger many rockfalls they also may reduce the stability of other rock masses and cause them to be susceptible to later failure. The many rockfalls triggered by the Mammoth Lakes earthquakes and the high seismicity along the eastern base of the Sierra Nevada suggest to Clark and Wieczorek that earthquakes may be the chief cause of Sierran rockfalls.

Westmorland, California, earthquake studies

Surface traces of the Imperial and Superstition Hills faults moved right-laterally during or shortly after the M_L 5.6 Westmorland earthquake of April 26, 1981, and before any significant aftershocks. The displacements are classed by R. V. Sharp as sympathetic. The main shock, about 20 km distant from either fault, was in an exceptionally seismogenic part of Imperial Valley, but no clear evidence of surface faulting has yet been found in the epicentral area. Sharp measured horizontal displacements of 8 mm on the Imperial fault southeast of the epicenter and 14 mm on the Superstition Hills fault southwest of the epicenter. He recorded discontinuous surface faulting for about 16 km along the northern segments of both faults. The maximum vertical component of slip, 6 mm, was observed on the Imperial fault 3.4 km north of the point of largest horizontal slip. No slip was detected along the Brawley fault zone, the San Andreas fault, or the part of the Coyote Creek fault that slipped during the 1968 Borrego Mountain earthquake.

VOLCANIC HAZARDS

VOLCANO MONITORING

Cascades Volcano Observatory

Continuing eruptions of Mount St. Helens through 1981 and the prospect, based on historical behavior of the volcano, that eruptions could continue another 2 or 3 decades resulted in establishment of a permanent facility for USGS monitoring operations and activities in Vancouver, Wash., about 75 km south of the volcano. This new facility, named the David A. Johnson Cascades Volcano Observatory, was officially dedicated on May 18, 1982, in memory of David A. Johnson, USGS geologist, who died while on duty during the May 18, 1980 eruption of Mount St. Helens. The Observatory includes office, laboratory, and storage facilities and is staffed by about 60 personnel, including volcanologists, geologists, hydrologists, geophysicists, geochemists, technicians, and other support personnel. Although primarily dedicated to monitoring the activity of Mount St. Helens, it also serves as a base of operations for monitoring all volcanoes in the Cascade Range, which extends through Washington, Oregon, and northern California. The Observatory has a direct communications link and closely collaborates with the joint University of Washington/USGS seismic monitoring center in Seattle, Wash., which maintains seismic monitoring networks on all potentially active Cascade volcanoes from Mount Hood, Ore., north to Mount Baker, Wash. (Volcanoes in central Oregon and California are monitored seismically from facilities at USGS Western Regional Headquarters in Menlo Park, Calif.).

Mount St. Helens activity

Mount St. Helens continued to erupt at about 2- to 3-mo intervals through 1980 and 1981. Most of the activity consisted of nonexplosive, dome-building eruptions typically lasting several days. All eruptions were preceded by significant increases in ground deformation, seismicity, and gas emissions within the crater. Careful monitoring of these precursory phenomena enabled the joint Cascades Volcano Observatory/University of Washington monitoring team to accurately predict all of the eruptions through 1981 as much as 3 weeks in advance, with no false alarms. According to Donald W. Peterson, Scientist-in-Charge at the Cascades Volcano Observatory, this remarkable record was made possible by early recognition of characteristic pattern changes within the crater prior to eruptions. Horizontal distance changes measured by Don A. Swanson, using electronic-distance-measurement (EDM) instruments, ground tile measurements by Daniel

Dzurizin, using dry-tile methods and inexpensive electronic tiltmeters developed by Jon Westphal (California Institute of Technology), level-line changes and mapping of fractures, fissures, and faults by R. T. Holcomb, and carbon dioxide and sulfur dioxide emission rates measured by T. J. Casadevall by means of an airborne correlation spectrometer (COSPEC) generally provided diagnostic information sufficient to issue "extended outlook" statements 2 to 3 weeks before eruptions. Changes in seismicity monitored by S. D. Malone, Christina Boyko, C. S. Weaver, and E. T. Endo of the University of Washington/USGS team in Seattle enabled the issuance of "eruption alerts" 1 or 2 days before the actual onset of eruptions.

Seismic monitoring, Oregon and California volcanoes

Seismic monitoring of potentially active Cascade volcanoes in Oregon and California was maintained throughout 1981 by means of a 32-station network in Oregon and two 8-station networks at Mt. Shasta and Lassen Volcanic National Park, Calif. All three networks were telemetered to Western Regional Headquarters in Menlo Park for analysis. H. M. Iyer, Alan Rite, Auriel Kollman, and David Knapp reported that in 1981 seismic activity in the Oregon Cascades was concentrated mainly in the central and northern part of the State and was at a low level, without swarms. In early 1981, a swarm of several hundred shallow earthquakes occurred about 30 km northeast of Mt. Shasta near Tennant, Calif. Lassen Volcanic National Park seismicity was relatively high, as in previous years, with most swarm activity occurring immediately south of Lassen Peak.

Hydrogen monitoring, Cascade volcanoes

By using bottled oxygen instead of air as the reference gas for their hydrogen sensor, Moto Sato, K. A. McGee, and A. J. Sutton monitored hydrogen concentration in the atmosphere near the crater rim of Mount St. Helens. Substantial diffusion of hydrogen from the crater plume to the surrounding atmosphere was indicated by previous experiments. Two sites, one on the south flank and the other on the northwest flank, both at about 2,100-m level, were chosen for the atmospheric hydrogen monitoring. Rapid increases (up to 700 ppm hydrogen) were observed at both sites, on June 16-17 and September 2, 1981, preceding dome-building eruptions that took place on June 18-19 and September 5-7, 1981, respectively. The hydrogen concentration in a rootless, crater fumarole showed somewhat antipathetic behavior to the atmospheric hydrogen. Coincident with the large increases in the atmospheric hydrogen, the fumarolic hydrogen decreased markedly. This observa-

tion may be interpreted to mean that when the central vent is closed, hydrogen is forced to permeate through the side of the magma chamber and mix with percolating ground water, but as soon as a substantial opening develops in the central vent, most hydrogen escapes vertically directly through the vent. The ratio between the atmospheric hydrogen (which is derived from the central plume) and the fumarolic hydrogen may thus indicate the openness of the central vent system.

Satellite-relayed hydrogen stations were established at Sherman Crater on Mount Baker, Wash. and at Bumpas Hell near Lassen Peak, Calif.

Gravity monitoring, Mount Shasta and Lassen Peak, California

Precision gravity networks for the purpose of monitoring deformation and magma movement associated with volcanic activity were established by R. C. Jachens at Lassen Peak (12 stations) and Mount Shasta (6 stations). Gravity changes of the order of 20 microGal (2 standard deviations), corresponding to elevation changes of approximately 10 cm, should be detectable. In addition to the precision gravity network at Lassen Peak, approximately 250 other measurement sites in a 400-km² area roughly centered on Lassen Peak could be reoccupied at future times. Although data from these sites are less precise than those from the precision network, elevation changes of the order of 35 cm (2 standard deviations) should be detectable.

Thermal-infrared surveys, Cascades volcanoes

Calibrated digital thermal-infrared measurements have been obtained for 14 potentially active volcanic areas in the Cascade Range by Hugh Kieffer, Jules Friedman, and David Frank, in cooperation with the Department of Energy. All observations (except at Crater Lake) were obtained shortly before dawn when sensitivity to geothermal heat is greatest. At Mount St. Helens, approximately 100 km² was covered and at Lassen Volcanic National Park, about 200 km² was measured. Ground resolution was typically 2 to 4 m. Quantitative assessment of excess radiant power can be derived from these data.

VOLCANIC HAZARDS ASSESSMENT STUDIES

Eruptive recurrence, Mauna Loa volcano, Hawaii

Over 50 radiocarbon dates have been obtained over the past 4 yr from charcoal collected by J. P. Lockwood beneath prehistoric lava flows of the northwest rift zone of Mauna Loa volcano. These 14 radiocarbon dates, determined by Meyer Rubin of the USGS Radiocarbon

Laboratory, have allowed preliminary determination of eruptive recurrence intervals for different parts of the eastern flank of Mauna Loa. Detailed geologic mapping shows that there are more short flows than long ones; areas near the active rift zone are consequently more frequently covered by lava than are areas further down the volcano flanks. Along the active rift zone, where lavas from only the last few thousand years are preserved, the eruptive recurrence interval is 35–60 yr. Further downslope, where lava flows have been less frequent during the past 10,000 yr, the recurrence interval is 900–1,200 yr. If past activity is typical of the future, these new data imply that Mauna Loa will continue to erupt rather frequently on the northeast rift zone, but most lava flows will not be of sufficient length to seriously threaten Hilo, the capital city of the “Big Island.”

Engineering studies, May 1980 eruption, Mount St. Helens

An assessment of engineering structures by R. L. Schuster has shown that the most serious results of the May 1980 eruptions of Mount St. Helens were flooding, burial, and erosion of highways and railways, destruction of bridges and buildings; partial mudflow-filling of a major reservoir; and disruption of water-supply, sewage-disposal, and flood-control systems. Major damage was caused by the lateral blast, the debris avalanche, and mudflows in the immediate vicinity of Mount St. Helens, in the Toutle River drainage, and along Lewis River tributaries that drain the volcano. An example was destruction by the debris avalanche and mudflows of 53 highway and railway bridges on the Toutle and Lewis Rivers. Significant damage by mudflows, floods, and sedimentation also occurred further downstream along the Cowlitz and Columbia Rivers.

Ash from the May 18 eruption disrupted civil works and operations in eastern Washington, northern Idaho, and western Montana. Removal and disposal of ash from roads, highways, and municipal sewage-disposal and storm-drain systems required costly efforts, particularly in eastern Washington. The May 25 and June 12 eruptions affected western Washington and the Portland, Oreg., areas to a lesser degree.

Pre-1980 eruptions of Mount St. Helens, Washington

Petrochemical data acquired by R. P. Hoblitt indicate that in the two youngest pre-1980 eruptive episodes at Mount St. Helens, the chemical composition of eruption products did not vary continuously from early dacite to late andesite. Apparently there was an abrupt change from dacite to andesite in each case. Furthermore, the early dacites and later andesites of the Kalama episode (approximately 450 to 350 yr ago) are not distinguish-

able by paleomagnetic secular variation results suggesting, but not proving, that eruption of the two lithologic types was closely spaced in time. Together, the chemical and paleomagnetic data show that abrupt chemical changes, typically accompanied also by changes in eruptive style, have occurred in the past and could occur in the future.

Late Holocene eruptions, South Sister Volcano, Oregon

During late Holocene time, domes, short, thick lava flows, tephra, and pyroclastic flows of rhyodacitic composition erupted during two episodes from vents on and just beyond the south and southeast flanks of South Sister volcano in the central Oregon Cascades. Stratigraphic investigations by W. E. Scott indicate that the older, more voluminous tephra erupted from the site of Rock Mesa lava flow, whereas the younger tephra erupted from a chain of seven vents along a rift to the south. The two groups of tephra are chemically and mineralogically similar but can be differentiated by stratigraphic position, relative amounts of pumice, obsidian, and lithic clasts, and presence of diagnostic accidental fragments. From radiocarbon dates of peat interbedded with the tephra, D. R. Mullineaux has determined that the episodes occurred about 2,500 and 2,000 yr B.P. Each episode began with the eruption of tephra, was accompanied at some vents by small pumiceous pyroclastic flows, and ended with emplacement of an obsidian dome or lava flow. Close to some vents, beds of angular obsidian fragments interlayered with beds containing pumice and obsidian suggest explosive clearing of vents or explosions from growing domes or flows. The tephra deposits are restricted to within 20 km of their vents. At their distal margins, the tephra are commonly thin beds of lapilli rather than fine ash.

Distal debris from Glacier Peak Volcano, Washington

S. A. Safioles and D. P. Dethier report that volcanoclastic sands containing lithic dacite fragments are associated with flowage deposits from Glacier Peak that occur 75 to 145 km from the volcano in the Skagit and Stillaguamish River valleys. The sands record deposition of volcanically derived sediments during intervals of volcanic activity about 1,800, 4,800 and 10,350 yr age.

Acoustics of the May 18, 1980, lateral blast, Mount St. Helens

S. W. Kieffer has attempted to determine why the approach of the lateral blast at Mount St. Helens was so amazingly silent when, within the expanding flow, a forest was being uprooted and destroyed, soils were

being ripped from the ground, and boulders, trees, and glacial blocks of ice were being mixed and transported kilometers from their source. There were two causes of this silence: (1) supersonic focusing of sounds in a downstream direction, and (2) strong attenuation of sound by the multiphase particulate cloud of the blast. Consideration of the difference in the behavior of sound in subsonic and supersonic flows is important. In subsonic flow, sound pulses generated within the flow travel faster than the fluid itself advances, and therefore, eventually reach all external observers. In such a flow, a falling tree would be heard eventually in all directions. However, in supersonic flow, sound pulses propagate downstream only within a cone, called a Mach cone, whose angle is related to the Mach number of the flow. Kieffer has proposed that the lateral blast was supersonic within about 10 km of the volcano with Mach numbers between one and three. For such a flow, the sound should be focused within ± 20 km of the local direction of flowage streamlines. Thus, observers not positioned on streamlines or their extensions (e.g., observers to the west or east of the generally northward-trending flow) would have been in a zone of silence. Probably a more important explanation is that sound is strongly attenuated in a dense particulate cloud. In clear air, sound is attenuated to about one-third of its original strength in a distance of about 10 km; for a cloud with the characteristics of the blast at a distance of 20 km from the volcano, the corresponding attenuation distance would have been on the order of 10 m, an attenuation more than 10,000 times that of clear air.

Postdepositional changes in Mount St. Helens ash

Stratigraphy, thickness, and grain size of the ash layer formed by the May 18, 1980, eruption of Mount St. Helens was studied by Susan Shipley to monitor changes that have taken place over the last 2 yr as a consequence of erosion and redeposition. At many downwind locations, the original three-fold and two-fold stratigraphy was little modified since initial deposition, except for compaction of as much as 45 percent over the May 18, 1980, thickness. At other localities, the ash-lobe axis had shifted as a consequence of reworking by wind. In several small basins, considerable thickening of the May 18 air-fall layer was observed, a consequence of local reworking. At such sites, the original air-fall stratigraphy is preserved beneath a massive, poorly stratified layer of reworked ash. These observations are being applied to studies of the stratigraphy of prehistoric tephra layers in the Pacific Northwest in order to estimate the original thickness of such layers and the magnitudes of the associated eruptions.

ENGINEERING GEOLOGY

ENGINEERING GEOLOGIC MAPPING

Swelling clays map of the United States

The first draft of a map showing the occurrence of swelling clays in the conterminous United States has been completed by a group directed by R. L. Schuster. The map is based on geologic units on the USGS "Geologic Map of the United States" (King and Beikman, 1974). These units are divided into five categories of swelling potential, ranging from "all (or more than half) highly expansive clay" to "little or no expansive clay." Swelling clay soils represent one of the most troublesome and costly problems confronting the construction industry. The map will be of assistance in alerting public officials and planners to the location and extent of such problem areas.

Physical properties evaluation of the Wasatch Formation near Sheridan, Wyoming

Near-surface coal-bearing sedimentary rocks in the Wasatch Formation of Eocene age were sampled in August and September of 1981 by A. F. Chleborad at a landslide-prone area about 10 km south of Sheridan, Wyo. Thin-wall (7.6 cm diameter) tube samplers were used at five locations to obtain core samples of weathered and stratigraphically equivalent unweathered Wasatch strata for geotechnical, mineralogical, and chemical analyses. Preliminary logging and index testing support previous findings (Chleborad, 1980) of an association between physicochemical changes and strength reduction in the weathered zone. Compositional analyses and strength testing are underway to provide correlations which will help identify the weathering processes that most affect strength characteristics.

Subsurface movements in abandoned coal mine

Unexpectedly large movements on a tiltmeter located along Interstate Highway 90 over abandoned workings of the New Monarch coal mine north of Sheridan, Wyo., led to the installation of three additional tiltmeters by F. W. Osterwald and J. B. Bennetti, Jr., in December 1980. During 1981, the apparent pattern of tilt indicated by the four meters suggested that an area immediately north and east of the northwest-trending highway was subsiding. A level line surveyed repeatedly by the Wyoming Highway Department, however, indicated only small elevation changes along the pavement. Drilling by the Highway Department in cooperation with the Geological Survey indicated that the

pillars along the north side of an east-west multientry set of mine openings were intact but that the pillars along the south side had yielded, the mine roof had partially caved, and the floor was covered with loose rubble and soft clay. The tiltmeter results, when interpreted with the results of the leveling and drilling, indicate irregular movements of the pavement as a result of coal pillars punching into an underclay beneath the abandoned workings.

Liquefaction studies in the Imperial Valley, California

A large earthquake ($M_L=6.6$) occurred in the Imperial Valley near El Centro, Calif., on October 15, 1979, generating sand boils, ground fissures, and other liquefaction effects at 36 localities. Damage resulting from liquefaction included disrupted highways, cracked canal linings, broken tile drains, slumped canal banks, and a variety of differential settlements in irrigated fields. At two sites where liquefaction effects were particularly pronounced, materials were sampled and tested by M. J. Bennett, T. L. Youd, E. L. Harp, and G. F. Wieczorek (1981). Because of the occurrence of sands that liquefied and adjacent sands that did not and the amount of basic information produced from the testing, these sites have generated a great deal of interest from researchers outside the Geological Survey. Continuing studies and some innovative testing techniques are producing a new understanding of the physical properties controlling the liquefaction process and engineering assessments for liquefaction susceptibility.

1906 earthquake fault offsets in northern San Mateo County, California

Historic data concerning the April 18, 1906, San Francisco earthquake were uncovered in the course of geologic studies in the Montana Mountain and San Mateo 7.5-minute quadrangles, northern San Mateo County, Calif., by E. H. Pampeyan. Confirmation of this information by field work and the aid of E. L. Fonseca and Gary Halkens of the San Francisco Water and Utilities Engineering Departments has established the locations and amounts of 1906 fault offsets at several sites whose whereabouts were previously uncertain or unknown to the geologic community. These sites are shown on a map (Pampeyan, 1982) covering 17 km of the San Andreas fault zone and including annotations describing the known offsets. Records of right-slip offsets in the literature for this area, some of which are based on questionable interpretations of the original information, show a range from 2.1 to 5.2 m. The recently uncovered data show right-slip offsets of 2.4 to 2.7 m at

three widely spaced sites in the map area and are in agreement with other nearby measurements. They also pinpoint the 1906 surface rupture in areas where previous locations were uncertain. In addition to right slip along the ruptures, there are three sites where dip slip is recorded, which in one place amounts to 30.5 cm.

Engineering geologic mapping in New York City

Geologic field mapping of the Bronx County area of New York City, under the direction of C. A. Baskerville, was 98 percent completed in 1981. Large quantities of archival subsurface data were obtained from local government agencies and some private contractors. Most of the field data and about 25 percent of the archival data have been plotted on the map. G. R. Roberts, J. A. Harris, Jr., and Fernando Martinez, field assistants, accomplished a good percentage of the west Bronx field mapping. Martinez and Harris also completed about 2.5 km² of field mapping on Manhattan Island. All of the field personnel, who are full-time college students majoring in geology, entered some of the archival subsurface data onto coding sheets for computer applications. To date, field mapping has indicated need for adjustments in formation contacts as compared to Merrill and others' 1902 map. In addition, some locations of units on the 1902 map no longer exist.

LANDSLIDE HAZARDS

Ground Failure Hazards Reduction Program

A USGS plan for the landslide part of a national program in ground failure hazards reduction has been published (USGS Circular 880). Mechanisms for coordination of efforts of the many agencies involved have been examined by a working group of the National Research Council (NRC). As a result of the recommendations of the working group, the NRC has proposed the formation of a multidisciplinary committee of the Nation's best earth scientists and engineers to provide the focus for a national program.

National landslide hazards assessment

Six new projects started in 1982 are cooperative efforts with State agencies to begin a landslide hazards assessment mapping effort having a nationwide scope. These cooperative projects have begun to map selected areas in California, Idaho, New York, Pennsylvania, Virginia, and Wyoming.

Landslide processes in the San Francisco Bay region

Detailed mapping (scale, 1:4,800) by G. F. Wieczorek (1982) in a 13 km² area near La Honda, Calif., has identified more than 230 dormant and recently active landslides. Continuous-recording rain gages and piezometers were installed in the area to monitor rainfall and ground-water levels which could trigger landslides. The instruments in California recorded the association of changing water levels and landslide movement during the December and January storms that hit the San Francisco Bay region and left disastrous results. Soil slip-debris flow events were a major cause of death and injury, and the instrumental data provide for significant modifications to the predictive model as developed for these kinds of landslides in southern California.

Landslide hazards mapping in the San Francisco Bay region

In the Marin County part of the San Francisco Bay region, experimental geomorphologic mapping by Stephen Ellen, D. M. Peterson, and G. O. Reid (in press) has identified areas where debris flows have occurred repeatedly in the past. A comparison of the map with inventory data on occurrences of debris flows associated with the storm of January 3-4, 1982, indicates that the mapping methodology provides a successful approach to predicting the most likely areas of future hazards from debris flows and other shallow landslides.

Landslide and flood disaster in the San Francisco Bay region

The rainstorm of January 3-4, 1982, in the San Francisco Bay region provided a rare opportunity for research on debris flows. Soil slip-debris flow events were a major cause of death and injury, and reconnaissance investigations by about 25 USGS personnel from Menlo Park, Calif., compiled inventory data on location, rainfall intensities, seasonal rainfall, damage, and costs. These data were reported in a multidisciplinary conference on landslides and flooding held at Stanford University, August 23-26, 1982. The conference was organized by the USGS, with joint sponsorship by the National Research Council, Stanford University, the Federal Emergency Management Agency, the State of California, the Association of Bay Area Governments, the Association of Engineering Geologists, and the American Society of Civil Engineers. The conference proceedings are being prepared for publication by the National Research Council.

Historic and prehistoric landslides in coastal southern California

A detailed map (scale, 1:4,800) of the Pacific Palisades area, Los Angeles County, Calif., compiled by J. T.

McGill has been published (McGill, 1982). It shows the complete distribution of prehistoric landslides for which there is evidence (evidence for shallow landslides is obliterated by natural processes more quickly than for more deeply seated landslides) and their relations to historic landslides. Of 74 prehistoric landslides, 18 (24 percent) are sites of shallow failures and 56 (76 percent) are moderately thick to deep seated. Of 201 discrete areas of historic landslides, 159 (79 percent) are sites of shallow failures and 42 (21 percent) are deeper seated. Prehistoric landslides clearly foreshadowed further extensive slope failures in several general parts of the Pacific Palisades area and in many specific localities as well. More than half of the number and about 40 percent of the total area of more deeply seated prehistoric landslides have been partly or wholly active in historic time. As much as two-thirds of the number and about half of the total area of these historic landslides have occurred in areas of prehistoric landslides. Some of these historic landslides were triggered by grading of prehistoric landslide deposits, especially along the coastal palisades. Most of the mapped prehistoric shallow landslides have become sites of historic shallow failures.

Landslides in the White Bluffs, north of Pasco, Washington

The White Bluffs of the Columbia River consist of Pliocene continental sedimentary strata, ranging from claystone to conglomerate, and a thin cover of Quaternary sand and silt. About 13 to 60 km north of Pasco, Wash., the bluffs are 70 to 160 m high and form the east side of the river valley. There are many inactive landslides in the bluffs, including some that are clearly older than latest Pleistocene flooding. Some of the oldest landslide deposits extend downslope to the present river level and indicate that the valley floor was incised to approximately its present level before Holocene time. Investigations by R. L. Schuster and W. H. Hays have identified about 50 currently active landslides in the bluffs. Most are small, but 14 have surface areas exceeding 10,000 m² each. The largest active landslide covers about 440,000 m². Other large landslides are encroaching on the river, periodically silting it and perhaps endangering a significant spawning bed for anadromous fish.

Landslides caused by intense storms in Pennsylvania

Continuing study by J. S. Pomeroy of slope failures from intense, short duration storms in western Pennsylvania indicates that these storms give rise to debris avalanches as much as 300 m long and 30 m wide. Most are on slopes of 31 to 37 degrees, which is close to the angle of repose for the material involved. No large slump-earth flow landslides occurred after a wet period

during which repetitive periods of several days of moderate rainfall extend for a month or more.

Large, old debris avalanches in the Appalachians

Investigation of five large debris avalanches on the east side of Dans Mountain, southwest of Cumberland, Md., indicates that these slides are probably Pliocene in age. W. E. Davies found the debris avalanches to be as long as 5 km, 800 m wide at the top, and spread out at the base in lobes as wide as 1,200 m. The difference in elevation from head to toe of the slides is as much as 300 m. The debris deposits contain large subangular boulders of sandstone from the Pottsville Formation of Pennsylvanian age and weathered shale and sandstone fragments from Upper Mississippian rocks. The deposits have been cut and reworked by the Potomac River to form high terraces of Pliocene to Pleistocene age. R. E. Thomas, working on landslides in Tennessee, has identified an area of similar large old debris avalanches on the east side of Wind Rock Mountain, which is about 10 km northwest of Oak Ridge.

Repetitive nature of Appalachian landslides

Observations by W. E. Davies and S. F. Obermeier in trenches and pipeline excavations show that the majority of slides in the Appalachian Plateau move along multiple shear planes roughly parallel to the slope. The material between shear planes is 0.5 to 3 m thick. Generally, the topmost shear is at the root line and is the plane along which most creep occurs. Landslides develop when movement occurs along the lower shear planes. Degraded illite is the dominant clay mineral present in the landslide material. Slope failure is progressive and continual. After failure along an upper plane, lower shear planes are brought into the zone where hydrologic changes are maximum and the processes leading to slope failure are continued. It is probable that landsliding at most of the sites in the Appalachians originated in middle or late Tertiary time and the present topography is a result of successive landsliding along the slopes since then.

Landslides in the greater Cincinnati area

Studies by R. W. Fleming of landslides in colluvium in the greater Cincinnati, Ohio, area concentrated on relations between ground-water levels, precipitation, and slope movement. Field measurements in two typical locations, thin colluvium (approximately 1 m) and thick colluvium (approximately 4 m), revealed that water pressures are significant but operate differently in each location. In thin colluvium, water accumulates during late winter and early spring in the area of contact

between bedrock and colluvium. During the brief period of March through early May, excess water pressures develop along the contact and facilitate landsliding. The water pressures increase in direct response to precipitation events with lag times of response of only a few hours. In thick colluvium, excess water pressures are developed in more permeable, fractured limestone in the bedrock. These water pressures do not change in response to individual storms but vary seasonally with the highest water pressures developed in early May and the lowest in early September. Movement of the thicker colluvium corresponds in time to the highest water pressure.

Dating landslides and other upper Pleistocene and Holocene features

Preliminary results of investigations by M. J. Pavich (USGS), Louis Brown and Fouad Tera (Carnegie Institute), and Roy Middleton and Jeffrey Klein (Univ. of Pennsylvania) in dating modern soils and paleosols by using ^{10}Be have been promising (Pavich and others, 1982). ^{10}Be is a cosmogenic isotope produced in the upper atmosphere and deposited on the lithosphere by rainfall, where it is quickly sorbed by clays. It has a half-life of 1.5×10^6 yr, and preliminary results indicate that soils have ^{10}Be concentrations that fit a simple model for accumulation and radioactive decay that is proportional to age over a range of about 10^5 to 10^7 yr. Soils of this age range are critical in determining recurrence intervals for prehistoric landslides.

Economics of landslide research

A methodology has been developed for estimating expected 10-yr losses from landslide events in the Cincinnati area. The development was done by an interdisciplinary USGS team consisting of R. L. Bernknopf, R. H. Campbell, R. W. Fleming, P. R. Beauchemin, C. D. Shapiro, S. F. Obermeier, S. W. Fleisig, and L. S. Gordon. The methodology can probably be applied to a wide area of the Appalachian Plateau province. It is being tested for its applicability, in modified form, to parts of the San Francisco Bay region, Calif., by utilizing data obtained as a result of the landslide and flood disaster of January 1982 in that region.

Establishment of slope-movement monitoring stations in West Java, Indonesia

J. R. Ege, in a cooperative engineering geology program between the USGS and the Directorate of Environment Geology (Indonesia), assisted in establishing four slope-movement monitoring stations in West Java. The region of investigation in southern Cianjur Regency experiences massive slope movements involving areas

as great as 100 km². Wet-land rice farming results in saturated ground conditions all year around. Movement is accelerated during the rainy season (November through March) when intense rainfall increases both surcharge and pore pressures. Extensive damage to villages, highways, irrigation works, and engineered structures occurs during this period. At selected sites, exploratory drilling revealed upper slip zones ranging between 3 and 15 m in depth and surficial materials comprising highly weathered volcanic products. Ground water is generally less than 1 m below the surface. The monitoring sites consist of survey lines as long as 100 m, open pipe piezometers, and rainfall gages which allow for periodic measurements of amounts and rates of surface movements, ground-water-level fluctuations, and rainfall.

REACTOR HAZARDS RESEARCH PROGRAM

The Reactor Hazards Research Program comprises over 30 projects in regional tectonics, engineering geology, geophysics, seismology, and geochronology. Most of the progress reports, particularly those summarizing regional tectonics, are included in the appropriate chapter.

Regional tectonics

Regional tectonic studies include six projects in the Atlantic Coastal Plain province, one in the Mississippi Embayment, three in the Appalachian Highlands, three in the Sierran foothills, and one in the northern Cascades. Results of the studies in the Mississippi Embayment and one of the projects in the Sierran Foothills are described in the following paragraphs; the results of other projects are reported in the third chapter of this volume, "Regional Geologic Investigations," in the "New England," "Appalachian Highlands and the Coastal Plains," and "Pacific Coast Region" sections.

Tectonic history of the Mississippi Embayment

E. E. Glick has prepared a structural map of the Mississippi Embayment, with contours drawn on the base of the Upper Cretaceous sequence, which illustrates the relationship of this broad embayment and its axis to the Mississippi Valley graben and associated plutons, as well as to areas in or near the graben where seismic activity is abnormally high. Apparently the northeast-trending graben formed during Precambrian time and probably was filled with detritus prior to the beginning of deposition of the thick Upper Cambrian to Middle Pennsylvanian marine sequence of the ancestral Mississippi Embayment. No younger Paleozoic beds are

known to have been preserved within the graben, but older Cambrian beds may be included in the graben fill.

During Cretaceous and early Tertiary time, plutons were emplaced along the ancient bordering faults of the graben, largely prior to but partly during the development of the modern Mississippi Embayment. The axis of the embayment, trending slightly east of north, crosses the Precambrian graben at an angle of about 20 degrees. Investigations by E. E. Glick and A. J. Crone show that some segments of the southeastern bordering fault of the graben were reactivated intermittently as high-angle reverse faults during and after the Late Cretaceous through early Tertiary development of the embayment. During historical time, seismic activity was concentrated both along the axis of the graben in northeastern Arkansas and along a trend normal to the axis in southeastern Missouri and western Tennessee, areas in which some, but not all, post-Cretaceous faults of the embayment areas are located.

Quaternary deformation of the Sacramento Valley and northern Sierra

Late Cenozoic deposits of the Sacramento Valley have been correlated by E. J. Helley and D. S. Harwood with those of the San Joaquin Valley. The Tehama and Tuscan Formations have been correlated with the Laguna Formation because all contain the Nomlaki tuff (3.2 m.y.) at or near their bases. The Red Bluff Formation pediment is correlated with the Turlock Lake Formation. The Red Bluff overlies the Deer Creek basalt (1.1 m.y.) and is overlain by the Maida ash (0.45 m.y.). The Turlock Lake Formation contains the Friant ash (0.6 m.y.). Terraces nested below the Red Bluff surfaces have been correlated with the Riverbank and Modesto Formations based on soil profile development, geomorphic position, and superposition. Post-Red Bluff folding and faulting is common throughout the valley. Late Quaternary deformation continues and appears to be similar to deformation which has occurred since the Late Cretaceous.

Applied geophysics

Applied geophysics research conducted under the Reactor Hazards Program included interpretation of marine seismic-reflection profiles of Lake Ontario. This project was done in cooperation with and was funded by the U.S. Nuclear Regulatory Commission. D. H. Hutchinson reports that the high-resolution seismic data obtained in Lake Ontario have been analyzed and large areas where the near-surface reflectors are discontinuous have been delineated. The epicenters of earthquakes in Lake Ontario are not confined to one part of the lake nor are they uniquely associated with these

zones of reflection disturbance, findings which suggest that the earthquakes are unrelated to the observed distribution of discontinuous reflectors. Studies of high-resolution seismic data obtained in Lake Erie also fail to show any significant geologic hazards.

Geochronology

Geochronologic research is directed towards developing new techniques and chronologies particularly for the past several million years so that fault histories and timing of relatively recent tectonic events can be established. One of the most promising areas of research is in the field of soils chronology. M. N. Machette reports that the morphology and amount of pedogenic CaCO_3 comprise a useful correlation tool and potential soil-dating technique for calcic soils and pedogenic calcretes formed on Quaternary surficial deposits in arid and semiarid portions of the Southwestern United States. Soils in chronosequences from this region have regional and temporal variations in the amount of pedogenically formed secondary CaCO_3 that have resulted from the combined effects of age, climate (amount and seasonal distribution of precipitation), and amount and distribution of airborne calcareous dust and Ca^{++} in rainfall. Potential applications of calcic soil development include correlation of soils, measurement of calcium carbonate accumulation rates, and a variety of landscape evolution studies including earthquake hazards assessment.

Two additional advanced stages of carbonate morphology are recognized in middle Pleistocene and older pedogenic calcretes. Stage V morphology is characterized by laminar and concentrically banded, pisolithic structures, whereas Stage VI is the terminal product of multiple cycles of brecciation, pisolith development, and relamination. Stage VI morphology has been found in calcretes developed on the constructional surface of the Miocene Ogallala Formation of eastern New Mexico and western Texas and on the constructional Pliocene(?) Mormon mesa surface of the Miocene Muddy Creek Formation east of Las Vegas, Nev.

A quantitative measure of the secondary CaCO_3 content (CS) of a soil is determined from horizon thickness, percent CaCO_3 , and bulk density; this measurement integrates the sum of these parameters over the total soil profile thickness. Our investigations have shown that the CaCO_3 contents, maximum stages of CaCO_3 morphology, and accumulation rates of calcic soils and pedogenic calcretes in the Southwestern U.S. are variable over large regions and through time. These variations are believed to be largely the result of changes in regional patterns of annual precipitation and airborne Ca^{++} and CaCO_3 .

Soils data from near Las Cruces and preliminary U-trend ages suggest that relict soils 100,000 to 500,000

yr in age have comparable average CaCO_3 accumulation rates. Soils that have formed in the past 50,000 yr have accumulated CaCO_3 about twice as fast; this change in rate probably is the result of decreased vegetative cover and thus increased supply of airborne Ca^{++} and CaCO_3 in the Holocene. In the Western U.S., identification and age determinations of volcanic ashes by Andre Sarna-Wojcicki are continuing to be useful in establishing the tectonic history of faults which displace alluvium. These results are discussed further in the chapter "Regional Geologic Investigations," in the "Pacific Coast Region" section.

Reactor site reviews

R. H. Morris, M. H. Hait, Jr., and S. T. Algermissen report that technical investigations and reviews of geologic and seismologic aspects of license applications to the Nuclear Regulatory Commission for power reactors were continued. The reviews evaluate geologic reports on the regional and local geologic structure, seismology, and geologic foundation conditions that become part of the public record of the licensing proceedings of the commission.

During the year, many Survey scientists prepared reviews and investigated geologic aspects of ten sites for nuclear power reactors or facilities in California, Illinois, Ohio, Pennsylvania, South Carolina, Tennessee, and Washington. The multidisciplinary nature of this work required consultation with other members of the USGS on specialized aspects of geology, geophysics, marine geology and geophysics, petrology, and geochronology. Geologic expertise was provided by C. A. Baskerville, E. E. Brabb, D. D. Dickey, G. S. Gohn, H. G. Greene, W. H. Hays, D. G. Herd, and R. C. McDowell. Seismologic expertise was provided by J. S. Andrews, E. P. Arnold, S. R. Brockman, J. F. Devine, W. L. Ellsworth, M. G. Hopper, D. M. Perkins, and P. C. Thenhaus.

The continuing experience indicates that regional and local geologic and seismologic knowledge, applied to evaluations of specific sites, provides a sound basis for closely adapting engineering-design criteria to the siting of nuclear reactors.

HYDROLOGIC ASPECTS OF COAL- AND MINERAL-RESOURCE DEVELOPMENT

Watershed model for Warrior coal basin, Alabama

A small watershed precipitation-runoff modeling system is being developed to provide hydrologists and land managers the capability of assessing water-resources impacts from coal development. Small-basin

watershed modeling in the Warrior coal basin of Alabama has been in progress since September 1979. R. E. Kidd and C. R. Bossong have expanded the effort to include five small basins in contrasting hydrologic settings and in mined and unmined basins within the coal field.

Daily mode-streamflow simulation performed on basins has resulted in predictions of annual runoff within 1 to 5 percent of observed runoff. Simulated seasonal-runoff distribution, hydrologic-response timing, peakflows, and recession rates appear to be very reasonable during the wet season (December–April). Peakflows and recessions during the dry season (May–November) were not as predictable.

Methodology for hydrologic evaluation of a potential surface mine, Tuscaloosa County, Alabama

L. M. Shown, D. G. Frickel, R. F. Miller, and F. A. Branson presented a method for evaluating premining hydrology and effects of mining and reclamation on the hydrology of a small basin (6.4 km²) containing a potential surface-coal-mine permit area. Estimation techniques were used to develop data for reconstructed topography, soil-water relations, vegetation cover, peak flows, flow volumes, soil losses, and sediment yields.

Streamflow response of the basin is described by the variable-source-area concept (Nutter and Hewlett, 1971); nearly all water moving from slopes flows through coarse-textured soils and unconsolidated sand and gravel deposits that are underlain by an impermeable clay zone. The resultant peak discharges per unit area are small to moderate and there is very little erosion of slopes or channels. Susceptibility of the soils to compaction by heavy machines and the effects of compaction on soil-water relations and peak flows are demonstrated.

Estimates of peak discharges made with three regression methods and one empirical method were divergent, particularly for recurrence intervals of 2, 5, and 10 yr; divergence is less for 25-, 50-, and 100-yr discharges.

The Universal Soil Loss Equation and sediment-delivery ratios were used to estimate sediment yields for various land and cover conditions from premining until 20 yr after reclamation began. A premining estimate of sediment yield made with the Universal Soil Loss Equation and a sediment-delivery ratio was about 2.5 times larger than an estimate made with the sediment-rating curve and flow-duration method.

Impact of ground-water pumpage for coal slurry, Navajo and Hopi Indian Reservations, Arizona

J. H. Eychaner (1981) estimated that water levels in the N aquifer have declined more than 30 m in an area of 500 km² near Black Mesa in northeastern Arizona. The

aquifer, which includes the Navajo Sandstone, is the main source of water in a 14,000-km² area. Since 1970, the aquifer has been used to supply water for a coal-slurry pipeline. Eychaner used a digital model to analyze data from 8 yr of monitoring. The largest declines occurred in the central part of the aquifer, where water is under confined conditions; during the years 1972–79, the water level in an observation well 50 km from the coal mine declined 5 m. Nearer the mine, no declines were measured in wells in areas of unconfined conditions or in two overlying aquifers. At least 220,000 hm³ of water is in storage in the aquifer, but recharge is only about 16 hm³/yr. Withdrawals averaged 5.6 hm³/yr during the years 1976–79. Eychaner estimated that about 95 percent of the withdrawals were derived from water in storage. On the basis of projected withdrawal rates, he estimated that in the year 2001 water-level declines would exceed 30 m in an area of 1,100 km². Substantial recovery of water levels would be possible if withdrawals were reduced. Municipal water systems, however, are increasing their withdrawals from the aquifer.

Toxicity of leachate from spent oil shale on a blue-green alga

Water-quality effects have been a major environmental concern associated with the anticipated development of Colorado's oil-shale resources. D. M. McKnight, W. E. Pereira, and C. E. Rostad studied the response of a blue-green alga, *Anabaena flos-aquae*, to a range of concentrations of leachate from spent shale produced by two different retorting processes, Tosco and Parahoe. Blue-green algae are important microflora in both streams and soils. One hundred g of spent oil shale was leached with 250 mL of distilled water for one week. At high concentrations of Parahoe spent-shale leachate (2:5 dilution with algal culture medium), calcium carbonate precipitated and the inoculum of *Anabaena* did not grow. Further experiments showed that growth inhibition was caused by calcium-carbonate precipitation. The Tosco spent-shale leachate is less alkaline and there was no calcium-carbonate precipitation observed on dilution of the leachate with algal culture medium. High concentrations of Tosco spent-shale leachate (2:5 and 1:10 dilutions) caused a decrease in the cellular content of C-phycoyanin, an important pigment of the photosynthetic system of blue-green algae. On the basis of additional experiments, this shift in the photosynthetic system was found to be caused by trace constituents in the Tosco spent-shale leachate. For both the Parahoe and Tosco spent-shale leachates, low concentrations (1:250 dilutions) have no effect on *Anabaena flos-aquae*. Results of the study indicate that blue-green algal communities may be affected by leachate in the vicinity of spent-shale piles.

Hydrology and water quality in coal areas of Illinois

E. E. Zuehls and others (1981a, b) report that the mean annual flows of ungaged streams in the coal areas of west-central and southern Illinois can be estimated from their drainage areas and regression equations developed for each coal area. Regression equations were also developed to estimate sulfate and dissolved-solids concentrations in streams from known values of specific conductance.

Zuehls also reports that annually, during the 36 days (10 percent of the year) of highest daily streamflow in west-central Illinois, 40 to 45 percent of the total annual streamflow and 71 to 97 percent of the annual sediment discharge will occur. Annually, suspended-sediment yields ranged from 20 to 166 (Mg/km²)/yr in west-central Illinois and from 29 to 44 (Mg/km²)/yr in southern Illinois.

Mine-reclamation hydrology in Fulton County, Illinois

C. A. Peters noted that three storms in June carried 52 percent of the total suspended sediment for the 1981 water year at the downstream Big Creek station near Bryant, Ill. In 1 day (June 22), the 104 km² drainage basin yielded 6,050 Mg of sediment out of a total of 20,200 Mg for the water year. Ammonia, sulfate, and fecal coliform values exceeded EPA drinking-water quality criteria for all of eight water samples taken for chemical analyses during the water year.

Aquifer studies at a proposed coal strip mine near Industry, Illinois

Two aquifers associated with the Colchester No. 2 coal seam near Industry, Ill., have been identified during a study of the premining hydrology by D. L. Gallo-way and J. V. Borghese. The upper, unconfined aquifer ranges in thickness from 0 to 25 m and is separated from the lower, confined sandstone aquifer by the 0.61-m-thick coal seam and a dense underclay 0.5 to 1 m in thickness. Hydraulic conductivities average 2.8×10^{-2} m/d for the unconfined aquifer and less than 1×10^{-3} m/d for the confined aquifer.

The unconfined aquifer is a calcium carbonate water with concentrations of dissolved iron ranging from 1 to 7 mg/L and total dissolved solids ranging from 229 to 381 mg/L. The confined aquifer is a calcium sulfate water with dissolved iron ranging from 3.8 to 39 mg/L and total dissolved solids ranging from 1,010 to 2,070 mg/L. Premining aquifer hydraulic conductivity and water quality will be beneficial in assessing the effects of strip mining on this hydrologic system.

Preliminary biological assessment of streams in the coal-mining regions of southwestern Indiana, October–November 1979

A study was done in the coal-mining region of south-west Indiana by D. J. Wangness to relate benthic-invertebrate and periphytic-algal communities in streams draining agricultural, forested, active/reclaimed-mined, reclaimed-mined, and unreclaimed-mined watersheds to the physical and chemical characteristics of the streams.

Alkalinity and pH were lower and the concentrations of dissolved solids, suspended solids, Ca, Mg, Na, K, SO₄, Fe, Mn, Al, and Zn were higher in streams draining unreclaimed-mined watersheds than in streams draining watersheds with other land use.

Numbers and community diversity of benthic invertebrates were less at sites affected by mining than at agricultural or forested sites, because of (1) synergistic effects of pH, metals, and unsuitable habitat, and (2) lack of colonizing drift organisms because of the small drainage area upstream from the mined area. Only a few organisms, such as the caddisflies *Cheumatopsyche* and *Hydropsyche* and the chironomids *Chironomus* and *Cricotopus* were found in streams draining mine areas.

Comparison of metal and other trace-element concentrations on streambed sediments from forested, agricultural, and coal-mining areas of southwestern Indiana

Streambed sediments were collected from 69 sampling sites in areas of predominantly forested, agricultural, reclaimed, and unreclaimed mined land in the glaciated and unglaciated parts of southwestern Indiana to determine concentrations of sorbed metals and other trace elements. According to W. G. Wilber and R. R. Boje, the objectives of this reconnaissance were to (1) provide baseline information for future comparison, and (2) determine whether the concentration of the elements was affected by land use and surficial geology.

Streambed sediments smaller than 2.0 mm and 0.062 mm were collected in May and October 1979, respectively, and analyzed for sorbed and acid-soluble Al, B, Cd, Cr, Cu, Co, Fe, Pb, Mn, Hg, Zn, and total As and Se. Nickel was determined only for samples collected in October 1979.

Analysis of variance indicates that differences in land use accounted for 10 percent or more of the total variation in Al, As, B, Co, Fe, Mn, Ni, Se, and Zn concentrations on streambed sediments for at least one of the two surveys. Differences in glacial province (surficial geology) did not significantly affect the concentrations of metals and other trace elements on streambed sediments. Concentrations of Al, Co, Fe, Ni, Se, and Zn on the less-than-0.062-mm fraction of streambed sediments from mined watersheds were significantly higher than

the concentrations of these elements on streambed sediments from agricultural and forested watersheds. The higher concentrations of these elements are due to (1) their presence in mine drainage and their subsequent adsorption and (or) coprecipitation with the oxides and hydroxides of aluminum and iron, and (2) their presence in coal and pyritic material found in streambed sediments.

Effects of abandoned lead and zinc mines on water quality in Kansas

Results from a study of T. B. Spruill on the effects of abandoned lead and zinc mines on water quality indicate that three streams that were studied are affected by mine drainage. Short Creek, a tributary to the Spring River, receives discharges from chat piles and Mississippian rocks that result in high concentrations of dissolved solids, sulfate, zinc, cadmium, manganese, and copper during low-flow periods. High total concentrations of iron, lead, and aluminum were observed in samples obtained during high-flow periods. Two other streams that are affected by mine drainage, Willow Creek and Tar Creek, drain Pennsylvanian shales overlying the mined Mississippian rocks. Drainage from chat piles currently exerts the greatest effect on water quality in these streams. High concentrations of sulfate, zinc, iron, manganese and, in Tar Creek, cadmium result from mine drainage.

Water samples, obtained from mine shafts, wells, and drill holes located in Mississippian rocks east of the Spring River indicate that ground water within and downgradient from the mined area near Galena, Kans., is characterized by pH values ranging from 3.5 to 6.8 and specific conductance values ranging from 250 to 690 μmhos . Concentrations of zinc ranged from 320 to 60,000 $\mu\text{g/L}$, cadmium from 1 to 340 $\mu\text{g/L}$, copper from 0 to 340 $\mu\text{g/L}$, and lead from 0 to 2,600 $\mu\text{g/L}$.

Water from mine shafts and drill holes located in Mississippian strata west of the Spring River that are overlain by Pennsylvanian shales that thicken toward the western edge of the study area is characterized by pH values ranging from 2.5 to 7.5 and specific conductance values ranging from 550 to 5,500 μmhos . Concentrations of zinc ranged from 1,100 to 43,000 $\mu\text{g/L}$, manganese from 100 to 6,400 $\mu\text{g/L}$ and iron from 20 to 560,000 $\mu\text{g/L}$.

Since mining ceased in 1970, water levels have been rising in Mississippian rocks west of the Spring River. A water-level measurement obtained west of Baxter Springs, Kansas, in October 1981 at the Lucky Jew Mine revealed that the water level in the mine had risen over 46 m since it was measured in April of 1976.

Geohydrologic appraisal of potential surface lignite mines in northwestern Louisiana

Energy companies are evaluating three areas west of the Red River in northwestern Louisiana for surface mining of lignite beds in the Tertiary Wilcox Group. At the first site in southeastern De Soto Parish the lignite bed is overlain by a massive sand. At the second site in western De Soto Parish the lignite is overlain by sands interbedded with clay. A saltwater-bearing sand below the lignite at the second site will be pumped to lower the potentiometric surface below the lignite. At the third site, which is mostly in eastern De Soto and western Red River Parishes, the lignite is overlain by sand and gravel of the Red River alluvial aquifer. According to J. L. Snider, quality of water in the aquifers at each site may cause different overburden-disposal problems.

Water from sands above the lignite has high concentrations of iron at all three sites and high concentrations of manganese at two sites. At sites one and two, water in sands above the lignite is soft, but water in the alluvial aquifer at site three is hard to very hard. The sand below the lignite at site two and the alluvial aquifer in part of site three contain water with a high concentration of chloride. High concentrations of iron and manganese might be lowered by treatment in settling ponds before the water is allowed to drain into the streams. Water with high chloride concentrations might be injected into deeper formations. Water in the Red River is hard to very hard at low stages. When stages are high and hardness is much lower, water from the alluvial aquifer would represent only a small part of the flow. Because of dilution, hardness probably would increase only slightly.

Hydrologic effects of underground coal mining, Garrett County, Maryland

M. T. Duigon (Maryland Geological Survey) and M. J. Smigaj completed fieldwork for the initial phase of a long-term study of the hydrological impact of a recently opened underground coal mine in southwestern Garrett County, Md. This phase was intended to determine baseline conditions; however, some effects were observed during this period.

As a lateral mine shaft approached a cluster of four observation wells (open to various depth intervals), water levels dropped about 23 to 113 m in a period less than three months. The greatest drop was in the interval directly above the coal seam; the interval below the coal seam dropped only slightly more than the shallowest interval (about 110 m above the coal seam). When progress along the mine shaft ceased, the water levels stabilized.

One stream reach measured as part of a seepage investigation was found to be losing water at a rate of about 0.013 (m³/s)/km. Mining had progressed to the area below this reach. A set of measurements made about nine months earlier, before the area was undermined, showed a gain of about 0.018 (m³/s)/km.

Water quality of coal deposits and abandoned mines in Saginaw County, Michigan

Analyses of water from 12 wells and 17 surface-water sites were used by A. H. Handy to study the effect of past mining practices on water resources in Saginaw County, Mich. Surface water and shallow ground water have not been affected. However, water from abandoned mines and undisturbed coal deposits is significantly high in B, phenol, Fe, L, Sn, V, Cr, Cu, Ga, Ge, Sr, SO₄, Cl, and Na.

Quality of streams in the Bull Mountains region, south-central Montana

As part of a program to assess surface-water quality in potential coal-mining areas, J. R. Knapton has been studying several small streams and the Musselshell River in the Bull Mountains region. In the small streams, bicarbonate and sulfate were the dominant anions and were found in early equal proportions. Magnesium was generally the dominant cation. Dissolved-solids concentrations for all small streams ranged from about 800 to 2,100 mg/L. Individually, the streams had much smaller ranges.

The Musselshell River had a larger annual variability than did the other streams for both dissolved solids and ion types. Dissolved solids ranged from about 450 mg/L during spring runoff to 1,800 mg/L for base flow. Sodium sulfate-type water, which was common during base-flow periods, was diluted during spring runoff with water principally containing calcium, magnesium, and bicarbonate. Calculations based on sediment-transport equations and flow-duration tables for the Musselshell River at Roundup showed an annual mean sediment load of 199,000 Mg/yr during the study.

Geochemistry and geohydrology of the Decker and Big Sky coal-mining areas, southeastern Montana

A study of the cause and magnitude of ground-water-quality changes in two coal strip-mining areas in southeastern Montana is being conducted by R. E. Davis. Water from coal aquifers in the Decker area is mainly a sodium bicarbonate type having an average dissolved-solids concentration of about 1,800 mg/L. Water from resaturated mine-spoils aquifers in the Decker area is

also a sodium bicarbonate type having an average dissolved-solids concentration of about 2,600 mg/L.

Water from coal aquifers in the Big Sky area is mainly a calcium-magnesium sulfate type having an average dissolved-solids concentration of about 1,800 mg/L. Water from resaturated mine-spoils aquifers is also a calcium-magnesium sulfate type having an average dissolved-solids concentration of about 3,000 mg/L.

The dissolved solids are principally derived from combinations of the dissolution of carbonate minerals and the dissolution of calcium sulfate, which is derived from the oxidation of iron sulfide. Sodium concentrations are the result of cation-exchange reactions. In some localized areas, sulfate-reducing bacteria have decreased the sulfate concentration and increased the bicarbonate concentration.

Hydrology and potential effects of mining in the Cook Creek and Snider Creek areas, Montana

M. R. Cannon completed studies of the hydrology and potential effects of surface mining in the Cook Creek area, 5 km northeast of Ashland, Mont., and the Snider Creek area, 30 km north of Ashland. Principal shallow aquifers in the Cook Creek area are alluvium, clinker, and coal beds; alluvium and sandstone lenses are the principal shallow aquifers in the Snider Creek area. The primary use of water in both areas is watering of livestock. Surface coal mining in the Cook Creek area would remove springs and wells used for livestock watering. Wells would also be lost as the result of mining operations in the Snider Creek area. In both areas, alternative water supplies are available to replace those lost through mining. After mining of the Cook Creek area, the alluvial aquifer downgradient from the mine area may show a long-term decrease in water quality as a result of leaching of soluble salts from overburden materials used to backfill mine pits.

Potential impacts of coal mining in selected areas of eastern Montana

Study on the Corral Creek area, a 68 km² basin between Decker and Otter in southeastern Montana, was completed by N. E. McClymonds in 1981. McClymonds, assisted by T. E. Reed and others, conducted aquifer tests and collected water samples for chemical analyses from 15 alluvial and 10 coal or sandstone observation wells in the basin. The main coal in the area is the 9-m-thick Anderson coal bed near the upper part of the Tongue River Member of the Fort Union Formation (Paleocene age). The transmissivity of the alluvial aquifer varied widely, from 2.5 to 700 m²/d; the average is about 20 m²/d. The alluvial water is mostly a sodium

sulfate type having an average dissolved-solids concentration of about 3,200 mg/L. The transmissivity of the Anderson coal bed varied from 0.1 to 2 m²/d; the average was about 0.5 m²/d. The coal water was tested mostly in the Horse Creek and Little Bear Creek areas, but it was also tested between Decker and Otter, Mont. Six new observation wells were drilled to coal beds within the Tongue River Member in the Horse Creek area; eleven new wells were drilled to the coal and sandstone aquifers in the Little Bear Creek area. Seven observation wells were completed in the West Glendive area of east-central Montana during 1981.

Ground water in the Oklahoma coal field

The ground-water resources of the eastern Oklahoma coal field are limited, according to M. V. Marcher and R. L. Coemaat. Rocks in this area consist of an alternating sequence of shale, siltstone, and sandstone. Ground-water movement and storage is largely limited to bedding planes, fractures, and joints. Locally, however, thick sandstones may be significant aquifers. Most wells yield only a few liters per minute. Water in the zone of weathered bedrock is generally under water-table conditions. Below this zone the water is under artesian conditions and generally stands less than 10 m below the surface; a few wells flow.

The chemical quality of the ground water is extremely variable. Total dissolved solids concentrations range from 200 to 3,000 mg/L. Sodium and calcium are the dominant cations and bicarbonate or sulfate is the dominant anion. Iron and manganese are the most troublesome constituents. No relation between water quality and well depth, geographic distribution, or geologic formation is apparent.

Because of the limited storage of ground water, and because most stream channels are above the saturated zone, streams with drainage areas of less than about 130 km² are ephemeral and have no flow about 30 percent of the time. Consequently, water for stock, the principal agricultural activity in the area, is provided by manmade ponds. Water for the rural population in large parts of the coal field is provided by rural water districts that obtain their supply from major reservoirs in the area.

Quality of water from coal-mine spoil, eastern Oklahoma

The quality of water from four wells drilled into abandoned coal-mine spoils is generally acceptable for drinking-water use with regard to toxic metal concentrations, according to L. J. Slack. Samples collected from the wells from October 1980 through September

1981 showed that As, Cd, Cr, Pb, Hg, Se, Cl, Cu, and Zn did not exceed the maximum contaminant levels established by primary or secondary drinking-water regulations. However, the maximum levels for Fe, Mn, SO₄, and total dissolved solids were generally exceeded. Water from the four wells is generally the same as that from nearby wells in alluvium and coal-mine ponds in the vicinity. The water from all wells and the mine ponds is predominantly a sodium sulfate type.

Suspended sediment in the southern Oklahoma coal field

Preliminary analysis of data from the southern Oklahoma coal field by S. P. Blumer shows that suspended-sediment concentrations ranged from nearly 0 at low flows to about 5,000 mg/L during major runoff events. Generally, 85 percent or more of the suspended material is finer than 0.062 mm. A large percentage of the annual suspended-sediment discharge commonly occurs during a single storm runoff. Suspended-sediment yield for 17 basins ranged from 0.75 to 4.0 Mg/km²/yr. Sediment yields in the extreme southern part of the coal field are higher than yields from basins farther north. Suspended-sediment yield from 12 unmined basins ranged from 0.75 to 2.2 Mg/km²/yr, whereas yields ranged from 2.2 to 3.2 Mg/km²/yr in 3 adjacent or nearby basins where there is current mining or recent mining has taken place.

Hydrology of the Eastern Coal Province, Pennsylvania

The USGS collected streamflow and water-quality data at about 380 locations in the bituminous-coal areas of Pennsylvania during the 1979-1981 water years to define the general area hydrology as required for mine-permit-application preparation and evaluation, according to W. J. Herb, L. C. Shaw, and D. E. Brown. Most sites in the data-collection network were sampled six times during the investigation, although selected stations were sampled more frequently. Water-quality data which were collected included specific conductance, dissolved solids, pH, total and dissolved iron, total and dissolved manganese, acidity, alkalinity, dissolved sulfate, bottom-material coal, bottom-material metals, and benthic-invertebrate-community composition.

Hydrologic information and sources of additional information were published for the Monongahela River basin (Herb, Shaw, and Brown, 1981a), the lower Allegheny and Kiskiminetas River basins (Herb, Shaw, and Brown, 1981b), and the Beaver and upper Ohio River basins (Roth, Engelke, and others, 1981).

Streamflow duration during low-flow periods in strip-mined areas of southwestern Virginia

J. D. Larson, P. W. Hufschmidt, and J. D. Powell report that the flow-duration curves of strip-mined basins in southwestern Virginia show extensions at low flow with respect to adjacent unmined basins. The flow-duration curves from the Russell Fork at Haysi, Va., show distinct differences at low flow when data prior to 1950 are compared with more recent data; active strip mining began in the study area about 1950. There is no difference in flow-duration curves for similar periods in the area of Clinch River at Cleveland, Va., a basin adjacent to the Russell Fork. Increased permeability of strip-mined areas, reduced evapotranspiration, and increased ground-water storage are probable mechanisms affecting the shape of the flow-duration curves. Synoptic, area-wide sampling during a low-flow period in the Russell Fork basin in August 1981 indicates that strip-mined basins discharge significantly more water per unit area than adjacent unmined basins.

Effects of chemical weathering on mine drainage in southwestern Virginia

J. D. Powell and P. W. Hufschmidt report that the primary source of buffering capacity in the southwestern Virginia coal-mining area is from chemical weathering of siderite and silicate minerals. Iron to sulfate ratios indicate an excess of iron over what would be expected from pyrite oxidation; large percentages of siderite in core samples probably are the source of the high iron concentrations. The system has typically low acidity and is well buffered. Weathering of the silicates plagioclase and chloride and the carbonate siderite are thought to be the main sources of the neutralization.

Joints and ground-water flow in oil shale in Wyoming

Joints, discernible on large-scale areal photographs, may have a pronounced effect on the ground-water-flow pattern at the Department of Energy's White Mountain in-situ oil-shale experimental retorts near Rock Springs, Wyo. E. A. Zimmerman reports that the joints form distinct patterns where soil has been removed by erosion or where vegetation growing in thin soil forms strips along the joints.

The joint pattern approximates the pattern of some of the experimental "burns" mapped out by surface thermometry and reported by Department of Energy personnel. The fracturing experiments, which were undertaken to increase permeability of the oil shale to permit propagation of the "burns", were mainly effective along the joint and bedding planes.

Although the dolomitic marlstone, called oil shale, has only slight primary permeability, the joints may produce a much greater secondary permeability that can conduct combustion byproducts away from the retorts toward Bitter Creek. The anisotropic permeability may account for the fact that byproducts have not been found in nearby wells although they are detectable in more distant wells in a slightly different direction from the retorts.

Solute transport of in-situ oil-shale retort water in Wyoming

Thiocyanate, a chemical associated with process water, has been observed in wells 0.8 km from an in-situ oil-shale retort near Rock Springs, Wyo., according to K. C. Glover. The retort experiment was conducted during a 180-day period in 1976 by the Department of Energy in a 12-m section of the Tipton Shale Member of the Green River Formation of Eocene age. Glover reported that thiocyanate concentrations of 3.7 to 49 mg/L have been detected in water from wells drilled during the past year. This compares with thiocyanate concentrations of 80 mg/L obtained from samples of water taken during the retort experiment and concentrations of less than 0.25 mg/L for water in wells not affected by retort water.

A drilling program was undertaken when chemical analyses of samples taken from Department of Energy observation wells showed that the retort water had migrated beyond the original monitoring area. Wells were installed in both the Tipton and the underlying Wasatch Formation. The Wasatch is a major water-bearing formation throughout the area. Results of geophysical logging and hydraulic head measurement indicate that flow within the Tipton may be three dimensional.

HYDROLOGIC EFFECTS OF VOLCANISM

Mount St. Helens posteruption flood hazards

M. E. Jennings, V. R. Schneider, and P. E. Smith performed an emergency assessment of Mount St. Helens posteruption flood hazards on the Toutle and Cowlitz Rivers, Washington (Jennings, Schneider, and Smith 1981). Flood hazards created by natural dams on the Toutle and Cowlitz River systems formed by rock and debris deposits derived from the May 18, 1980, eruption of Mount St. Helens were analysed by a finite-difference dam-break and flood-routing program. The posteruption structures investigated included the dam impounding Spirit Lake and the dam at Elk Rock on the North Fork Toutle River. Working under emergency conditions

with minimal data, the investigators made efforts to adapt computer models for a successful assessment. Three cases of dam failure were hypothesized for Spirit Lake, leading to peak discharge estimates ranging from 4,872 to 31,640 m³/s at the dam and from 3,556 to 13,272 m³/s at the mouth of the Toutle River 85.3 km downstream. These hypothetical discharges correspond to at least the 500-yr flood for the Cowlitz River, which receives flow from the Toutle River.

A small (3.08×10⁶m³) lake that formed at Elk Rock on the Toutle River also was analysed with the dam-break flood model when it became obvious that failure was imminent. Elk Rock dam failed the day following the theoretical failure analysis. This failure provided an opportunity to compare hypothetical and actual peak discharges. Simulated and observed discharges at the dam were 560 and 448 m³/s, respectively, and were 42 and 39 m³/s, respectively, at the mouth of the Toutle River 67 km downstream.

Debris-flow monitoring at Mount St. Helens

A 3-year project has been initiated at Mount St. Helens to monitor the behavior of active debris flows so that empirical equations for the flow of these non-Newtonian fluids can be developed. Since the catastrophic eruption of May 18, 1980, glacial outburst floods, rainstorms, and landslides on the debris-covered Shoestring Glacier regularly have been triggering small debris flows. T. C. Pierson has instrumented a reach of channel immediately downstream from the glacier terminus in order to collect data on flows of varying magnitude and composition that flow through the reach. Information on average flow velocities, flow regime, flow depth, and shape of the flow front is collected with still and movie photography and sonar distance meters mounted as "stream gages." Samples also are collected from each flow.

The data collected are being used to define relations between a dependent variable (flow velocity) and a number of independent variables, including flow depth, channel gradient, water and air content of the slurry, and particle-size distribution of the solid fraction.

Effects of volcanic ash on aquatic environments in northern Idaho

In a study to determine the effects of Mount St. Helens ash on substrate colonization and existing invertebrate communities in streams, S. A. Frenzel collected biologic and water-quality data from Big Creek near Calder, Id., inside of the ash-fallout area. In addition, Frenzel conducted controlled experiments on Gedney Creek near Selway Falls Guard Station, Id., outside of the ash-fallout area. Frenzel reports no detectable increase in concentrations of constituents

common to volcanic ash in Big Creek. Maximum concentration of suspended sediment was 5 mg/L at a discharge of 7.7 m³/s. Twenty-nine percent of the streambed material smaller than 63 microns was volcanic ash. Benthic invertebrates were abundant and diverse in Big Creek. For example, from May to December 1980, 80 taxa were collected by using 210-micron mesh nets. In Gedney Creek, by using artificial substrata (ceramic balls) covered with varying amounts of volcanic ash (0, 0.5, and 2 cm in thickness), greatest numbers of taxa (54) and fewest individuals (1,759/m²) collected on the substrata covered with 0.5 cm of ash; fewest taxa (49) and most individuals (4,186/m²) collected on the substrata covered with 2 cm of ash. Artificial substrata, which were allowed to colonize for 24 d before being covered with ash, showed little change in the number or mean density of taxa. Mean density of invertebrates on the untreated (control) substrata compared to that on treated substrata was 53 percent at 25 d after treatment, 63 percent at 38 d, and 94 percent at 54 d.

Effects of 1980 eruption of Mount St. Helens on selected lakes in Washington

The cataclysmic eruption of Mount St. Helens on May 18, 1980, altered the physical, chemical, and biological characteristics of several Washington lakes, according to N. P. Dion and S. S. Embrey. Lakes closest to the volcano were affected most by the eruption. Spirit Lake can now be considered a completely different lake because of its higher altitude, larger area, decreased depth, and altered hydrology, biology, and water chemistry (Dion and Embrey, 1981).

Extreme water-quality changes were observed only in lakes situated in the blast zone of the volcano. The changes included increases in concentrations of most chemical constituents and reductions in light transparency.

Concentrations of phytoplankton were similar among all western Washington study lakes in 1981 and ranged between 400 and 600 million organisms per cubic meter in July. The phytoplankton community of Spirit Lake was dominated by the Cyanophyta from October 1980 to September 1981. Zooplankton concentrations in Spirit, St. Helens, and Venus Lakes increased from 10 to 12 individuals per cubic meter in late summer 1980 to about 1,000 individuals per cubic meter in summer 1981 but remained lower than in Deadmans Lake, the control lake.

Chemical characteristics of the new lakes created by the blockage of the headwaters of the North Fork Toutle River are intermediate between those of Spirit Lake and St. Helens Lake, except for light transparency and dissolved iron. Light transparency is two to four times

greater in the new lakes than in Spirit and St. Helens Lakes. Dissolved-iron concentrations also exceed the concentrations in Spirit and St. Helens Lakes.

GEOLOGY RELATED TO NATIONAL SECURITY

Geology of Nuclear Test Sites, Nevada Test Site

The USGS, through interagency agreements with the U.S. Department of Energy (DOE) and the Department of Defense (DOD), investigates the geologic, geophysical, and hydrologic environment of each location within the Nevada Test Site (NTS) where underground nuclear explosions are conducted. Geologic and hydrologic data are needed to assess the safety, engineering feasibility, and environmental effects of nuclear explosions. In addition, the USGS compiles geologic and hydrologic information pertaining to underground nuclear explosions conducted within the Soviet Union. The USGS does research on specialized techniques needed to acquire geophysical and hydrologic data at nuclear explosion sites; some of the results of this research follow.

Containment of all underground nuclear tests (no release of radioactivity into the atmosphere) is a national commitment. Containment requires an expert appraisal of the geological, geophysical, and hydrologic environment for each test. In support of the containment program, W. S. Twenhofel as senior geology consultant and A. T. Fernald as alternate attended nine meetings of the Containment Evaluation Panel. E. C. Jenkins and others also acted as official observers as required to obtain, analyze, and present data relating to the stratigraphy, structure, media properties, and depth to the Paleozoic rocks for each event.

Geological and geophysical investigations at the NTS contribute to programs of the Los Alamos National Laboratory (LANL), the Lawrence Livermore National Laboratory (LLNL), and the Defense Nuclear Agency (DNA). A. T. Fernald updated the isopach map of the surficial deposits of Yucca Flat, and D. L. Healey updated the isopach map of the Cenozoic rocks of the same area, on the basis of new drill-hole data, 3-dimensional gravity analyses, and seismic surveys. Healey also continued updating and revising gravity data in Yucca Flat showing the configuration of the Paleozoic rock surface below Cenozoic rocks. G. E. Brethauer, D. C. Muller, and J. E. Kibler continued the synthesis of material properties into the GRASP system (Geologic Retrieval and Synopsis Program) for additional areas of Yucca Flat based on precise quality control of data. This program is designed for use in predicting material properties by extrapolation and interpolation from the data base in order to effect substantial savings by reducing

exploratory drilling, coring, and geophysical logging for new sites.

G. S. Corchary continued to manage the Geologic Data Center at the NTS, where drill cores and cuttings are collected for both nuclear weapons programs and the radioactive waste management programs.

Shear-wave velocity and changes in tuff due to shock loading

Shear- and compressional-wave-velocity data compiled in seven tunnels near chimneys resulting from the collapse of cavities produced by nuclear explosions indicate zonation of the tuff. These zones are most clearly defined on the basis of the lowering of the shear-wave velocity from preexplosion values. Core tests and velocity data suggest that, progressing outward from the explosion point, these zones consist of (1) the chimney, (2) a zone of pervasive microfailure of the tuff, (3) a zone of macrofailure, and (4) a zone of discrete failure which also includes the undisturbed tuff. The zone of microfailure may be defined by changes in the in-situ shear-wave velocity which are spatially coincidental with similar but less dramatic changes in core velocity. The tuff in this zone has dilated and microcracked as a result of explosion effects. The maximum extent of this zone appears to be about two chimney radii from the working point. The zone of macrofailure is seen only in in-situ shear-velocity measurements and is presumably associated with pervasive dislocations along bedding planes and joints. Available measurements indicate this zone is generally restricted to a range of less than four chimney radii from the working point. The zone of discrete failure is dependent on local geologic conditions, not generally measurable by other than direct observations, and can occur at ranges easily in excess of an order of magnitude beyond the zone of macrofailure.

The maximum range of explosion effects on the tuff may be obtained by noting the range at which the shear-wave velocity moves outside the experience histogram of preshot shear velocity. This is a useful approach when preshot velocity data are not available for comparison. These results help remove some of the speculation concerning close-in range effects of nuclear explosions in tuff.

U.S.S.R. underground nuclear explosions

The USGS continued to be responsible to the DOE for selection and training of a cadre of geologists for a Geology Verification Team as set forth in the Treaty of Underground Nuclear Explosions for Peaceful Purposes. In addition, a number of areas in the U.S.S.R. where underground nuclear explosions have taken place were studied. This was done in cooperation with the Department of Defense and other U.S. Government

agencies. The studies were based on the published scientific literature, geologic maps, stratigraphic sections and other relevant geologic and geophysical information from the areas of the Soviet tests. Using this basic data, together with information provided by the Soviets at international meetings and other materials, William J. Dempsey, Selma Bonham, and Jack Rachlin analyzed the explosion sites and their regional geologic setting in a series of classified reports. This work included computational analyses and comparison with U.S. experience.

Study continued on the Soviet deep seismic sounding program for information on the structure and physical properties of the crust and upper mantle in relation to the propagation of seismic waves, especially in areas of nuclear explosions and monitoring stations.

RELATION OF RADIOACTIVE WASTE TO THE GEOLOGIC ENVIRONMENT

Quaternary deformation in the Fisher Valley area, Utah

A study of the Quaternary history of the Fisher Valley area, Utah, is being done for the Department of Energy as a part of its program to evaluate potential nuclear waste repository sites in the Paradox basin; the Fisher Valley area contains the most complete record of the Quaternary in the basin.

Mapping of the surficial geology of the Fisher Valley area by S. M. Colman, assisted by F. F. Hawkins and A. F. Choquette, suggests a complex pattern of deformation of the Quaternary sediments. The sediments define a depositional basin that corresponds approximately to the present erosional basin which is coincident with the erosional amphitheatre at the head of Onion Creek. Most of Fisher Valley itself is underlain by relatively thin Quaternary sediments and shallow bedrock. The sediments contain several buried soils and two volcanic ashes and appear to record at least the last 1 million yr. The salt diapir apparently blocked Fisher Creek; this action in turn led to the deposition of the thick Quaternary section.

The lower part of the Quaternary section dips radially away from the nose of the salt diapir, and deformed remnants of these sediments occur on top of the diapir caprock. The diapir has thus clearly moved in Quaternary time, probably since the end of the deposition of the lower Quaternary sediments 600,000 to 700,000 yr ago. The upper part of the Quaternary section are not in contact with the caprock of the diapir, so younger movement of the diapir is difficult to identify. However, the Quaternary section dips inward around the edges of the depositional basin and contains several angular unconformities, especially between the major units. These units become nearly flatlying and conformable in the

center of the basin. This pattern of deformation suggests periodic subsidence of the depositional basin. The subsidence could be due either to solution of salt below the basin or to flowage of salt toward the diapir. Because solution of the salt would occur primarily near the diapir rather than beneath the adjacent depositional basin, salt has apparently flowed toward the diapir in Quaternary time.

Investigation of a potential nuclear waste repository site, Nevada Test Site

The USGS is assisting the DOE in evaluating the suitability of various geologic environments and rock masses for locating nuclear waste repositories. In 1981, work was focused on Yucca Mountain at the western edge of the Nevada Test Site.

Two additional core holes to depths of 1,219 and 1,829 m provided a framework for evaluating the subsurface lateral continuity of units underlying Yucca Mountain. In general, underlying units consist of a thick sequence of alternating welded and porous zeolitic tuffs to 1,829 m; however, the base of Tertiary volcanic rocks was not encountered. The existence and lateral continuity of several welded tuffs having substantial thermal resistance, coupled with interlayered zeolitic tuff having high sorptive capabilities, enhances the potential of Yucca Mountain for long-term storage of high-level nuclear waste.

Geomagnetic methods of geophysical prospecting have been adapted in the Climax stock and Yucca fault areas of the Nevada Test Site for application in nearby areas that are presently under study as possible sites for storage of radioactive waste. Geophysical models of the Climax stock intrusive were previously reported by Allingham and Zietz (1962) and Whitehill (1973). New interpretations by G. D. Bath, C. E. Jahren, J. G. Rosenbaum (USGS), and M. J. Baldwin (Phoenix & Scission Inc.) used new data that included additional aeromagnetic surveys, ground magnetic surveys, and magnetic properties of drill core. These interpretations gave a new model for the stock and for structures at the Boundary and Tippinip faults that border the stock. New models developed for the Yucca fault by G. D. Bath, G. L. Dixon, and J. G. Rosenbaum (1982) were consistent with the geology and magnetic properties found in numerous holes drilled in Yucca Flat on both the high- and low-standing sides of the fault.

Dc resistivity survey at Gibson Dome and Lockhart basin, San Juan County, Utah

A dc resistivity (Schlumberger) survey at Gibson Dome and Lockhart Basin was made by R. D. Watts (1982) as part of an evaluation for possible nuclear

waste repository sites by DOE. The investigation revealed the following: (1) A large, uniform, resistive area between Indian Creek and Davis and Lavender Canyons (locations under consideration for potential nuclear waste repository sites). The uniformity and high resistivity is consistent with a model of massive salt deposits with little or no ground water in contact with the salt. (2) A deep (300 m elevation) conductive anomaly near Horsehead rock. This anomaly may be due to unknown geologic structures beneath the salt formation or may be due to the presence of saline water there. (3) Major, high-contrast, conductive anomalies near the Lockhart fault system north of Lockhart basin. These anomalies are interpreted as being due to brine formed by water moving through the fault zone and coming into contact with the salt formation. One anomaly is adjacent to a recent oil discovery well, which penetrated an abnormally thick section of Moenkopi Formation rocks; this is interpreted as representing ancient dissolution of salt and collapse of the overlying formations.

Evaluation of the Basin and Range province for possible nuclear waste disposal

A cooperative project between the USGS and eight Western States is aimed at determining the suitability of areas in the Basin and Range province for deep storage of high-level radioactive waste. Meetings were held with State officials of Arizona, California, Idaho, Nevada, New Mexico, Oregon, Texas, and Utah by M. S. Bedinger, K. A. Sargent, Robert Schneider, and Department of Energy representatives to explain the project, propose work plans and budgets, and develop cooperative agreements for fiscal year 1982.

Preliminary data on potential host rocks, ground-water flow systems, gravity, heat flow, and seismicity were compiled for the Basin and Range province. Contract work was initiated to computerize bibliographic data and investigate the feasibility of digitizing map data.

Geomechanical characterization methods for potential radioactive-waste repository sites

In order to evaluate the performance of borehole geomechanical instruments under actual field conditions, a testing facility near Idaho Springs and an evaluation test site near Golden, Colo., were established. The test facility is being used to examine instrumental response to known boundary loads, whereas the evaluation test site is used to assess the effectiveness of these instruments in accurately characterizing a wide range of in-place rock-mechanical properties (state of stress, displacement, modulus, temperature, and hydraulic response).

These comparative studies are still in progress. However, initial modulus determinations by borehole jacking underestimated the true deformation modulus of rock by a factor of three or more for reasons that are not yet understood. Similarly, side-by-side evaluations of two different methods of stress measurement yield results that are contradictory in sign and magnitude. These difficulties are primarily due to shortcomings in instrumental design and construction and, to a lesser degree, due to over-simplified assumptions concerning the behavioral properties of rock. A major goal of this research is to resolve these ambiguities and establish a site-characterization methodology centered on efficient instrumental techniques.

Water analysis of salt deposits being considered for radioactive waste depositories

A neutron gamma-ray spectroscopy method was developed to measure the water concentration in a salt deposit being evaluated as a host rock for a radioactive waste depository. The ratio of the intensity of the gamma ray from a neutron inelastic scattering reaction to that of a capture gamma ray was used as an index of the water concentration. The method was shown to be feasible in wet and dry boreholes as long as the sonde is not constructed with hydrogenous materials.

Development of a borehole radar system

During FY 1981, a short-pulse prototype borehole radar system was completed and successfully tested in granite by D. L. Wright and R. D. Watts. Because data were recorded on analog tape, in-the-field examination of data was permitted. The system did respond to the geologic environment, though tests in more favorable sites are needed. Some of the analog records were successfully digitized as tests and two types of computer generator displays of the data have been made.

RELATION OF RADIOACTIVE WASTE TO THE HYDROLOGIC ENVIRONMENT

Liquid-waste disposal at the Idaho National Engineering Laboratory

Low concentrations of chemical and low-level radioactive wastes are discharged directly into the Snake River Plain aquifer through the Idaho Chemical Processing Plant disposal well. Tritium, a component of the waste effluent since 1953, has formed the largest waste plume (about 73 km² in area) in the regional aquifer; minute concentrations extend downgradient a horizontal distance of 12 km (Barraclough, Lewis, and Jensen, 1981).

Plumes of waste sodium, chloride, nitrate, and resultant increased specific conductance have similar configurations, flow southward, and are laterally dispersed in that portion of the aquifer underlying the Idaho National Engineering Laboratory. Other waste plumes containing strontium-90 and iodine-129 cover small areas near their points of discharge because strontium-90 is sorbed from solution as it moves through the aquifer and iodine-129 is discharged in very low quantities. Cesium-137 is also discharged through the well, but it is strongly sorbed from solution. Radionuclide-plume size and concentrations are controlled by aquifer flow conditions, the quantity discharged, radioactive decay, sorption, dilution by dispersion, and perhaps other chemical reactions.

Sealed monitoring wells for a radioactive environment

Dust from air and from measuring equipment (tapes, logging probes, bailer, pumps) enter monitoring wells near hazardous waste sites and therefore give researchers false indications of waste migration in ground water (Bagby and others, 1981). Opportunities for such contamination could be reduced by minimizing insertion of tools or equipment in the well and by keeping the well sealed against dust.

Four aquifer-monitoring wells located just outside the Radioactive Waste Management Complex at the Idaho National Engineering Laboratory, used for disposal of solid low-level radioactive wastes, have been equipped with submersible pumps and differential pressure transducers and then have been sealed at the surface. The pumps are used to collect water samples and the transducers provide water-level information. Sealing the wells at the surface after this equipment has been installed has allowed hydrologic data to be collected and has minimized the risks of contaminated water samples.

Estimating radioisotope concentrations with gamma-radiation well logs

Ulrich Schimschal has developed analytical techniques for the quantitative estimation of subsurface radioisotope concentrations on the basis of gamma spectral well logs. A computer program was written to perform the analysis numerically (Schimschal, 1981e), and the approach was tested with a borehole in granite located in central Wyoming. The study showed that radioisotope concentrations derived from moving and stationary spectral logs compared favorably with independent radioisotope analyses obtained from core samples. The computer program has been extended to permit stripping of natural background radiation from

the gamma spectral logs obtained at radioactive waste-disposal sites. The method has been designed to allow quantitative identification of unnatural or waste radioisotopes against a background of naturally occurring radioisotopes for use in monitoring radioactive waste-disposal sites.

Analysis of soil cores beneath radioactive-waste-disposal site, Sheffield, Illinois

Sample cores obtained by R. W. Healy from a 120-m-long tunnel which underlies four waste-filled trenches at the Sheffield, Ill., low-level radioactive-waste-disposal site were used to describe the stratigraphy of the glacial deposits within which the waste is buried, to determine hydraulic properties of these deposits, and to define the extent of migration of radionuclides from the trenches. The unsaturated zone consists of a layer of coarse pebbly sand confined between layers of fine clayey silt. Much less soil moisture is present in the pebbly sand than in the clayey silt. Volumetric moisture content ranged from 0.03 to 0.04 cm³/cm³ for the pebbly sand and from 0.19 to 0.31 cm³/cm³, averaging 0.24 cm³/cm³, for the clayey silt. Soil moisture was extracted from sample cores and radiometric analyses were performed on both the moisture and solids. No radionuclides above background concentrations were detected in the solids and tritium was the only radionuclide detected above background concentrations in the soil moisture. Tritium values from soil moisture ranged from 1,600 to 200,000 pCi/L in the coarse material and from background to 35,000 pCi/L in the fine material.

Ground-water flow to strip-mined lake from low-level radioactive-waste-disposal site near Sheffield, Illinois

The pebbly sand unit that underlies 67 percent of the Sheffield low-level radioactive-waste-disposal site has been found to extend into an area east and down-gradient from the site, according to J. B. Foster, R. W. Healy, and G. W. Mackey. Core samples from test wells and an earth resistivity survey indicate that the unit extends from the site to a strip-mined lake about 280 m east and northeast of the site. The pebbly-sand unit is the principal flowpath of ground water leaving the site. Water samples collected from two of the test wells contained above-background tritium. Water from well 563 located about 82 m east of the nearest waste trench contained 89 nCi/L. Well 575, 110 m from the nearest trench and downgradient from well 563, contained 56 nCi/L. The presence of tritium in water from these wells represents the greatest distance for migration of a radionuclide detected at the Sheffield site at this time.

Radionuclide transport in glacial outwash, Wood River Junction, Rhode Island

From 1964 to 1980, wastes from a scrap uranium-fuel recovery plant were discharged to polyethylene-lined lagoons underlain by a highly permeable glacial-outwash aquifer. Water-quality data from observation wells indicated leakage from the lagoons had occurred as early as 1973. According to B. J. Ryan and K. L. Kipp, the contaminant plume, which extends from the lagoons northwestward to the Pawcatuck River, is approximately 450 m long, 100 m wide, and appears to be confined to the upper 12 to 24 m of saturated thickness where sediment consists of medium to coarse sand and gravel. Specific conductance of plume water ranges from 150 to 5,000 μ inhos; contaminants include nitrate (5 to 500 mg/L) and gross beta calculated as cesium-137 (11 to 845 pCi/L).

Piezometric-head and water-quality data from wells screened at several depths on both sides of the river indicate that the plume discharges to the river and to an adjacent swampy area northwest of the river. An electromagnetic conductivity survey of the swamp indicates the presence of anomalous water-quality conditions in an area approximately 1,000 m², apparently caused by dissolved waste products in the water.

Radionuclide movement at a radioactive-waste burial site in Illinois

A plume of waste tritium has formed in a 40-m-thick glacial-drift deposit beneath the world's first radioactive waste burial site near the Argonne National Laboratory in Illinois. The plume moves slowly downward at a rate to 6.3×10^{-6} cm/s into underlying bedrock, according to J. C. Olimpio. Also, a small amount of horizontal, downgradient movement occurs. No other radionuclides have been detected in either soil or water below the site. Core samples from the site were analyzed in the laboratory to determine the distribution coefficient (K_d) of selected radionuclides, including tritium, strontium-85, cesium-137, and plutonium-238. Tritium results show a K_d value near zero; therefore, tritium movement will coincide with ground-water flow. Conversely, the K_d values of strontium, cesium, and plutonium are large and show that the glacial drift has a large capacity to absorb these radionuclides. Thus, the results of the laboratory analyses agree well with current field observations of the extent of radionuclide migration in the drift. With the aid of a computer model, tests are underway to evaluate the effectiveness of the drift in restricting the direction and rate of ground-water flow during changes in hydrologic stresses.

Hydrology of a low-level radioactive-waste burial site in South Carolina

The commercial low-level radioactive waste burial site located in the southwestern part of South Carolina is in a humid environment that receives about 1,200 mm of precipitation annually. Radioactive waste is buried in the upper 10 of 13 m of unsaturated Tertiary clayey sand. Aeolian sand, ranging in thickness from a few mm to about 3 m, covers the Tertiary sediments. J. M. Cahill is gathering geohydrologic data to study the migration of radionuclides in unsaturated and saturated coastal sediments.

Special soil-moisture monitoring techniques are being used to determine moisture movement in the unsaturated sediments. Air samples above trench covers are passed through cold traps and the condensed water is analyzed for radionuclide activity. Analyses of sediment core, soil moisture, ground water, and atmospheric samples indicate that tritium has migrated downward, outward, and upward from the buried waste. In 1981, tritium activity in water from a 21-m-deep well increased from background levels of 1,000 pCi/L to about 116,000 pCi/L, the increase indicating downward movement of radionuclides into the more permeable sands beneath the clayey sediments. Tritium activity was near background level in water from most other wells.

Tritium activity ranged from 2,400 to 16,700 pCi/L in water condensed from air samples collected 20 mm above land surface at a trench completed in 1975. Tritium activity of 17,500 pCi/L occurred in a sample collected 0.6 m above the land surface. Tritium activity at 1 m above land surface was lower than at 0.6 m but increased during daylight hours because of evapotranspiration.

FLOODS

Flood frequency of urban streams in Alabama

D. A. Olin and R. H. Bingham have developed equations for estimating future flood characteristics for 2-, 5-, 25-, 50-, and 100-yr recurrence intervals on ungaged urban streams in Alabama. Flood characteristics at 23 urban sites were based on flood records at those sites supplemented by floods synthesized from rainfall records by methods described by Lichty and Liscum (1978). These flood characteristics were related to drainage area and two percent of drainage area occupied by impervious materials. Flood characteristics at an ungaged site can be computed from these two basin characteristics.

Flood potential, Fortymile Wash and tributaries, southern Nevada

The floodplains of Fortymile Wash and three of its southwestern tributaries—Busted Butte, Drillhole, and Yucca Washes—were studied to determine areas of inundation by 100-yr, 500-yr, and maximum-potential floods, according to R. R. Squires and R. J. Young. By means of regression analysis of data from selected nearby crest-stage gages, equations were developed to determine discharge values for 100- and 500-yr floods; equation parameters include discharge drainage area, mean basin altitude, and basin latitude. Discharge values for the maximum potential flood were estimated from an envelope curve developed by Crippen and Bue (1977).

Flood estimation in Montana

Revised techniques for estimating flood magnitude in Montana were developed by Charles Parrett and R. J. Omang. Multiple-regression equations relating flood magnitude to drainage basin and climatic parameters were developed for eight different geographic areas in the State. In all areas, the drainage area was the most significant independent variable in the regression equations. Independent variables found to be important in at least two of the geographic areas were mean annual precipitation, mean basin elevation, percentage of basin above 1,829 m elevation, and a mapped geographical factor.

Appraisal of methods for delineating flood-hazard areas in the Great Basin

Five types of methods—detailed, historical, analytical, physiographic, and reconnaissance—have been evaluated with regard to their suitability for mapping flood-hazard areas in the 540,000-km² Great Basin of Nevada and adjacent States, according to D. E. Burkham. The five methods range in level of sophistication from comprehensive to approximate. A comprehensive method should be most suitable from a scientific standpoint for urban areas, whereas an approximate procedure seems adequate for undeveloped areas. The appropriate mapping method depends on the physiographic character of the area of interest—for example, a mountain stream, an alluvial fan, or a valley floor—because dominant flood hazards are somewhat different in each type of setting.

Effects of urbanization on flood peaks, Missoula, Montana

The potential effects on flood peaks of urbanization of a forested watershed near Missoula, Mont., are described in a report by Charles Parrett (1981). A com-

puterized hydrograph model was used to evaluate three potential scenarios of future urban development in the Rattlesnake Creek watershed. The modeling results indicated that none of the three potential development scenarios would significantly increase peak flows at the mouth of the stream. The study did indicate, however, that the peak runoff from just that part of the watershed subject to urban development could be increased by as much as 65 percent over expected peak flows under existing conditions.

Flood hydrology of foothill streams in Colorado

A study of floods by R. D. Jarrett and J. E. Costa shows that conventional hydrologic analyses fail to describe adequately the flood hydrology of foothill streams in Colorado. Annual flood peaks are derived from snowmelt, rainfall, or a combination of rain on snow. When snowmelt-runoff and rainfall-runoff peak flows are examined separately, flood-frequency analyses show different trends based upon elevation. Above about 2,300 m, snowmelt-runoff dominates; rainfall-runoff generally does not contribute to the flood potential for recurrence intervals in excess of the 100-yr flood. Where rainfall does significantly contribute to flooding above about 2,300 m, discharges per unit of drainage area are small when compared to lower elevation floods resulting from rainfall. Below about 2,300 m, rainfall-runoff peak flows predominate. Stratigraphic and geomorphic evidence supports these conclusions and indicates that catastrophic cloudburst-produced floods in foothill zones have recurrence intervals on the order of thousands of years at any given site. In small basins above 2,300 m, many large floods attributed to intense rainfall were, in fact, debris flows and not waterfloods. A paleohydrologic method using maximum boulder sizes was developed to reconstruct historic maximum flood peaks in small unaged basins.

EFFECTS OF POLLUTANTS ON WATER QUALITY**SURFACE-WATER POLLUTION****Effects of scrubber sludge disposal on hydrology of Beaver County, Pennsylvania**

Sludge consisting primarily of fly ash, calcium salts, lime, water, and a calcium-based stabilizing additive is produced by a coal-fired power plant in Beaver County, Pa., and deposited in Little Blue Run Lake, an impoundment constructed by the utility specifically for waste disposal. T. F. Buckwalter and D. R. Williams report that water levels and water quality in observation wells

adjacent to Little Blue Run Lake were not affected by sludge disposal from March 1978 through September 1980. The most probable reasons that Little Blue Run Lake has not yet affected water levels and water quality in the wells include: (1) total depths of some wells are above the lake surface elevation, (2) the hydraulic conductivity of bedrock is low, (3) the sludge blanket on the lake bottom retards lake water from seeping into the ground-water system, and (4) ground water moves too slowly to cover the horizontal distances of as much as several thousand feet between the wells and the lake. The sludge is believed responsible for high concentrations of fluoride, selenium, sulfate, dissolved solids, and high pH observed in water samples from Little Blue Run Lake and its outflow to the Ohio River. The observed concentrations exceed drinking water limits of the EPA.

Organochlorine pesticide and polychlorinated biphenyl residues at four trophic levels in the Schuylkill River, Pennsylvania

Various biological components within four trophic levels of the Schuylkill River in eastern Pennsylvania were found to contain high levels of organochlorine insecticides and polychlorinated biphenyls (PCB's). In the 1980 study, J. L. Barker of the USGS examined samples of periphyton, green algae, hydrophytes, snails, and whole body and fillets of nine common fish species from four locations.

Chlordane, DDT and its metabolites, dieldrin, and PCB's were detected at all trophic levels. Endrin and heptachlor epoxide were detected at all trophic levels except primary consumers (snails).

There is some evidence that these residues are being bioaccumulated in selected species at the higher trophic levels of the food web. The edible flesh of some fish such as American eel and sunfish contain concentrations of chlordane and PCB's that exceed Food and Drug Administration guidelines.

GROUND-WATER POLLUTION

Possible sources of degradation of water quality of the Vamoosa-Ada aquifer, east-central Oklahoma

A multiapproach study of the water resources in the Vamoosa-Ada aquifer by R. B. Morton suggests a petroleum-industry source for the 83 occurrences of degraded water identified. A total of 357 ground- and surface-water samples were collected and analyzed. Semilogarithmic plots were made of constituent ratios against different constituents for values of sodium, chloride, bromide, lithium, and residue at 180° C (ROE).

The plots indicated degradation of water where (1) chloride concentration is about 400 mg/L, or more, (2) bromide concentration is about 2 mg/L, or more, (3) the ratio of lithium to sodium is about 0.01, or less, and the chloride concentration is about 400 mg/L, or more, and (4) the ratio of sodium plus chloride to ROE is about 0.64, or more.

Data on concentrations of Br, Li, Sr, ROE, Ca, Mg, Na, Cl, and SO₄ were segregated according to these indices and an analysis of variance and Duncan's multiple-range test were used to test the significance of differences between segregated and nonsegregated data. Differences were significant at the 95 percent confidence level for all constituents but SO₄. Constituents whose concentrations are not within the limits of the indices represent fresh water, while those within the indices limits represent degraded water.

The total of 83 sites indicating evidence of water degradation were plotted on a map showing oil and gas-producing areas, active and abandoned. All 83 sites are closely related geographically with oil and gas-producing areas. None of the sites occur where petroleum activity is absent.

Contamination delineated at Wurtsmith Air Force Base, Michigan

A study of ground-water contamination at Wurtsmith Air Force Base, near Saginaw, Mich. by J. R. Stark, T. R. Cummings, and F. R. Twenter revealed that the principal aquifer underlying the base contained, at places, considerable concentrations of trichloroethylene, dichloroethylene, and benzene. The most highly contaminated area is in the east-central part of the base where a major plume—915 m long and 245 m wide—contained water having concentrations of trichloroethylene ranging from 1 to more than 1,000 µg/L. Water from a nearby observation well contained 266 µg/L dichloroethylene. Also, in the east-central area, water in a plume 300 m long and 90 m wide contained benzene concentrations as great as 1,450 µg/L. In the northern part of the base, trichloroethylene concentrations ranging from 1 to 1,150 µg/L were found in water in a plume that was 1,600 m long but only 120 to 150 m wide. Model simulations indicate that purge pumping can effectively contain the contaminants and eventually remove them from the ground-water system.

Treated-sewage plume in a sand and gravel aquifer, Cape Cod, Massachusetts

Infiltration of treated sewage to a sand and gravel aquifer through sand beds at Otis Air Force Base, Cape Cod, Mass., since 1936 has resulted in a plume of sewage-contaminated ground water that is more than 3,300 m long and 760 to 1,060 m wide, according to

Denis LeBlanc. At 900 m downgradient of the beds, the plume is 23 m thick and 15 m below the water table.

Specific conductance as high as 405 μmho , boron concentrations as high as 400 $\mu\text{g/L}$, ammonia-nitrogen concentrations as high as 20 mg/L , and detergent concentrations as high as 2.6 mg/L as methylene-blue-active substances (MBAS) were measured in the center of the plume. In uncontaminated ground water in the study area, the specific conductance is less than 80 μmho , the boron concentration is less than 50 $\mu\text{g/L}$, the ammonia-nitrogen concentration is less than 0.1 mg/L , and the detergent concentration is less than 0.1 mg/L as MBAS.

Chloride, sodium, and boron concentrations in the plume seem to be diluted only by hydrodynamic dispersion, but phosphorus concentrations are greatly attenuated by sorption. Detergent concentrations are highest between 900 and 3,000 m from the sand beds. The decrease in detergent concentration near the source reflects the change from nonbiodegradable to biodegradable detergents in 1964. The center of the plume as far as 1,500 m from the sand beds contains nitrogen as ammonia, no nitrate, and no dissolved oxygen. Ammonia in the center of the plume apparently is nitrified between 1,500 and 2,400 m from the sand beds as water in the plume mixes with uncontaminated ground water that contains up to 11 mg/L dissolved oxygen. Nitrification of ammonia is essentially complete at distances greater than 2,400 m downgradient of the sand beds.

No polychlorinated biphenyls in induced recharge from the Housatonic River, Massachusetts

Water samples from a network of wells between the Housatonic River and a large-capacity well field pumped continuously since 1956 contained no detectable amount of polychlorinated biphenyls (PCB), according to F. B. Gay. Fine-grained organic sediments in ponded areas along the Housatonic River in Massachusetts and Connecticut contain up to 110,000 $\mu\text{g/kg}$ of total PCB and were thought to be a potential source of PCB contamination of ground water induced to recharge through the streambed.

Ten wells were drilled in a glacial sand and gravel aquifer 1.5 m from the shore of Woods Pond on the Housatonic River and near a well field pumped continuously at about 82 dm^3/s . Water samples collected from these wells at about 1.6-m intervals down to 19 m below the pond level were analyzed for total PCB concentrations of aroclors 1016, 1221, 1232, 1242, 1248, 1254, and 1260 known to be in the river sediment. Concentrations of the aroclors were all below the analytical detection limit of 0.1 $\mu\text{g/L}$. In addition, total PCB concentrations in all samples of aquifer material collected at about 3.2-m intervals down to 19 m below pond level

were below the detection limit of 1.0 $\text{mg}/\mu\text{g}$. Analyses of hydraulic-head distribution in the aquifer and analyses of water from the wells for dissolved oxygen, total iron, manganese, ammonia, nitrite plus nitrate, and temperature indicate that about half the water produced from the well field is derived from the river. The implication of these results is that, although river water flows through the PCB-laden sediments, it does not cause the transport of PCB into and through the aquifer to adjacent wells and that the likelihood of PCB contamination of ground-water supplies from the river probably is very small.

Aldicarb pesticide contamination in ground-water in eastern Suffolk County, Long Island, New York

A preliminary investigation of contamination by the pesticide aldicarb of ground water in glacial aquifer in eastern Suffolk County is being conducted by Julian Soren and W. G. Stelz of the USGS, in cooperation with the Suffolk County Department of Health Services. Data from wells sampled in the Riverhead-Jamesport area showed widespread aldicarb contamination, with water from many wells exceeding the New York State health standard of 7 ppb; areas of lesser contamination have also been delineated. The contamination is believed to have resulted from the use of the pesticide on potato fields from 1975 to 1980.

The authors also have prepared water-table, depth-to-water, and well-location maps of the study area. Twelve shallow observation wells and 1 deep observation well screened at a depth of 137 m in the underlying Magothy aquifer have been installed. Preliminary hydrogeologic data from these wells indicate the presence of a significant uncontaminated freshwater supply in a deeper aquifer system that previously was believed to be salty. Freshwater was found to a depth of 152 m. The shallow aquifer system appears to be separated from the deeper aquifer by clay beds whose aggregate thickness is about 15 m. The areal extent of the clay beds is great but not exactly known.

Ground water near wastewater-treatment facilities in Glacier National Park, Montana

Ground water at wastewater-treatment facilities in Glacier National Park has not been significantly affected by percolating sewage effluents, according to J. A. Moreland and W. A. Wood. Analyses of water samples from 12 existing monitoring wells at the Headquarters, Many Glacier, and Saint Mary facilities indicate that the sewage effluents have only slightly altered ground-water quality. Analyses of samples from five shallow wells installed within the spray field used

to dispose of wastewater at the Headquarters facility indicate that dissolved-constituent concentrations are slightly higher in the shallow ground water than in the deeper part of the aquifer.

LAND SUBSIDENCE

Mining depth and geology affect coal mine subsidence hazards

Subsidence studies above selected underground coal mines in the Western United States by C. R. Dunrud indicate that overburden thickness, lithology, and structure affect the extent and severity of hazards caused by subsidence pits and depressions. Subsidence pits, which can be the greatest hazard to life and property, commonly are limited to areas where the mining depth (overburden thickness) is less than about 10 to 15 times the thickness of coal mined. The area affected by subsidence depressions increases, in relation to the mining area, as the overburden thickness increases. Slope change (tilt) and horizontal strain at the ground surface, which often do the most damage to structures in down-warped areas, commonly increase with increasing vertical displacement and decrease with increasing overburden thickness.

The incidence of subsidence pits commonly is reduced, for a given mining depth and area, where the overburden is composed of strong rocks, such as well-cemented sandstones and siltstones, compared to areas where the overburden consists of weak rocks, such as shales and mudstones. The area affected by a subsidence depression is less, for a given mining depth and area, where the overburden is composed of strong, massive, jointed rocks than it is where the overburden consists of weak rocks. Vertical displacement, relative to thickness of coal mined, commonly is less where the overburden consists of strong rocks than it is where the overburden consists of weak rocks. Vertical displacement also may be concentrated along faults that are located within subsidence areas.

Vertical displacements of a subsiding elastic layer

Subsidence above an underground cavity was modeled by assuming the subsiding region to be an infinitely long elastic layer that deforms under its own weight into an opening beneath its lower surface. An approximate analytic solution based on Fourier transform methods was found for vertical displacements of the ground surface and the roof of the opening when the layer thickness is much greater than the width of the opening. This model differs from previous analytic models in that both the ground surface and cavity roof

can be traction free. The shape of the surface subsidence trough was found to be controlled by the ratio of the layer thickness to the width of the opening; as the value of this ratio decreases the subsidence trough narrows and deepens, and a peripheral ridge forms.

Differential subsidence at Houston, Texas, oil fields

Evaluation by T. L. Holzer and R. L. Bluntzer (Texas Department of Water Resources) (1981) of releveling data from leveling-line crossings of 29 oil and gas fields in the Houston-Galveston, Tex., subsidence area suggests that the contribution of petroleum withdrawal to land subsidence and surface faulting there is minor. The regional subsidence, which is caused by aquifer compaction and is related to man-induced water-level decline, locally has reached a maximum of 2.7 m. Regional subsidence was inferred at each field by interpolation of subsidence data from the area surrounding the oil field. Of the 29 fields examined, subsidence at only the Chocolate Bayou, Goose Creek, South Houston, and possibly Hastings fields exceeded regional subsidence by more than 0.13 m. In all four of these fields, the component of subsidence possibly due to petroleum withdrawal was only a small fraction of the regional subsidence at the field as of 1978. In four fields—Barber's Hill, Cedar Bayou, Humble, and Pierce Junction—subsidence was substantially less than the regional subsidence. Excluding Cedar Bayou, these fields are associated with shallow-seated salt domes that partially pierce the aquifer system and cause it to thin. Subsidence at these fields was less than half the regional subsidence during the periods of record.

Inventory of active carbonate karst subsidence sites in Eastern U.S.

J. G. Newton and J. R. Ege are investigating mechanisms and extent of ground subsidence in karst areas of the Eastern United States. Newton, conducting on-site inspections in regions of active subsidence in carbonate terranes, has compiled a statistical and map inventory of subsidence locales in 17 States between Minnesota and Florida.

An arcuate band of active subsidence about 1,500 km long and 800 km wide extends from southern Pennsylvania through parts of West Virginia, Virginia, Kentucky, Indiana, Tennessee, Georgia, Alabama, Missouri, and Arkansas. A second band of active subsidence extends from southern Florida northward through South Carolina and North Carolina. Much of the current subsidence is attributed to the lowering of ground-water levels, either by pumping or drought conditions.

Sinkholes in west-central Florida

Studies of sinkhole development in Florida indicate that thickness and composition of surficial sediments overlying the limestone bedrock commonly control the size, type, and frequency of sinkhole development. Difference between the water level in the surficial sand and the underlying limestone aquifer often is the triggering mechanism that induces collapse of naturally developing sinkholes.

Areas with different types of sinkholes have been delineated by William C. Sinclair on the basis of existing sinkhole size, shape, and density, along with local topography, geology, hydrology, and other factors. In areas with a cover of cohesionless sand, sinkholes are sometimes shaped like an hour glass in cross section. More commonly, surficial sand has a clay fraction that, in conjunction with plant roots, gives the sand some cohesion and causes the sinkholes to develop as vertical pipes (natural wells) with diameter-to-length ratios on the order of 1 to 10. The diameter apparently is a function of the size of the cavity in the underlying limestone. Most of the west-central Florida area is underlain by a clay layer of variable thickness. Where present, the clay may have enough cohesive strength to bridge a cavity in the limestone surface for a considerable time, but eventually, the clay may collapse abruptly. The size of the sinkhole in these cases is a function of the thickness and bearing strength of the clay. Clay thickness in the range of 30 to 40 m generally precludes sinkhole development because it retards local solution of the limestone.

Land subsidence and earth-fissure hazards in central Arizona

H. H. Schumann reported that surface-geophysical surveys and test drilling, which were completed along the Salt-Gila aqueduct alignment of the Central Arizona Project east of Mesa, Ariz., were used to evaluate geohydrologic conditions that produce earth fissures related to land subsidence. Earth-fissure hazards were identified along two reaches of the aqueduct alignment. Long-term estimates of land subsidence indicate that approximately 2 m of subsidence may occur near Picacho Reservoir by the year 2035.

Active subsidence in carbonate terranes in the Eastern United States

J. G. Newton reports that about 750 sites of active subsidence have been inventoried in 19 States that are underlain by carbonate rocks. The number of collapses or areas of subsidence related to sinkhole development at individual sites generally ranged from 1 to 1,000

(estimated). Individual collapses ranged in diameter from 1 to 105 m and in depth from 1 to 45 m.

Subsidence at the inventoried sites was both natural and induced (man-related). The latter was significant and resulted primarily from lowering of the water table by ground-water withdrawals and by the impoundment or diversion of surface-water drainage. The largest amount of damage reported was associated with induced activity. Most significant damage costs or costs for safety measures resulting from sinkhole development involved large structures such as dams, highways, and buildings.

HAZARDS INFORMATION AND WARNINGS

The dissemination of earthquake hazard information was studied in Charleston, S.C., by P. L. Gori (USGS) and M. R. Greene (Battelle Human Affairs Research Centers) to determine how public officials and representatives of the private sector receive information regarding natural hazards and what type of information they find most useful. The Charleston metropolitan area was selected for study because it is the object of current USGS scientific investigations and because it suffered a major destructive earthquake in 1886.

Through personal interviews with public officials and private sector representatives, Gori and Greene documented a general awareness of the earthquake threat in Charleston. However, they found that this awareness was not translated into actions that would mitigate the earthquake hazard. The researchers affirmed past findings that information alone is not sufficient to mitigate hazards.

Some of the significant recommendations generated by the study are

- Local response agencies need to know what would happen to Charleston in the event of an earthquake in order to understand what their responsibilities and duties should be and to devise an effective preparedness plan that can be implemented at all levels of government.
- Maps need to be compiled showing locations of the 1886 earthquake damage distribution and current hazards potential. The preparers of these maps need to translate and interpret the maps for local officials.
- Because the Charleston area is prone to hurricanes and other natural hazards which occur more frequently than damaging earthquakes, efforts should be made to tie mitigation and response planning, education, and awareness efforts together for all natural hazards.

- Various jurisdictions in the Charleston area are in the very early stages of using the tools and information available to them to regulate land use. Planning commissions, zoning and subdivision ordinances, and building codes are being increasingly used to guide land development. Earth-science information is a necessary factor in this process. While Charleston expands its base of earth-science information to meet the land planning and regulating needs of the area, it should include those factors peculiar to earthquake-prone areas, such as maps showing areas prone to liquefaction. Since the majority of respondents in this study indicated substantial interest in attending a workshop that would explain the earthquake hazard, mitigation, and response, the USGS and others will consider coordinating such a local workshop.
- The news media play an important role in Charleston. They educate the entire public, including officials and professional people. They have been doing an excellent job of keeping people informed and tying what happens elsewhere to what could happen in Charleston. However, the media need more information about the earthquake hazard in Charleston to continue to perform their job. USGS and other geologists, engineers, and social scientists will provide briefings and maintain ongoing contact with media representatives.
- Professional and trade societies, newsletters, and journals are widely trusted and read by officials, professionals, and private industry. They should be used to educate and inform. The USGS and others can prepare short, nontechnical articles for journals and newsletters that explain, among other subjects, the earthquake hazard and potential mitigation actions.

ASTROGEOLOGY

PLANETARY STUDIES

SATURN INVESTIGATIONS

Voyager 2 Encounter

During FY1982, accomplishments from the U.S. Geological Survey's participation in the Voyager Imaging Science Experiment, under the direction of L.A. Soderblom, were centered on the Voyager 2 Saturn encounter. In addition to L.A. Soderblom, E.M. Shoemaker and Harold Masursky were deeply involved in the initial analysis and publication of the results derived from images of the Saturnian satellites. Published results of their analyses include the 30-day preliminary report that appeared in *Science* in January of 1982 (Smith and others, 1982) and other formal papers such as that by L.A. Soderblom and T.V. Johnson (1982). The activities of the investigators during the entire period involved final modifications of the Voyager 2 imaging encounter sequence, planning for the mission operation activities, and planning and implementation of the preliminary and second-order data reduction products at the Jet Propulsion Laboratory (Pasadena, Calif.).

JUPITER INVESTIGATIONS

Volcanism on Io

A.S. McEwen and L.A. Soderblom report that comparison of Voyager 1 and 2 images of Jupiter's moon, Io, shows the emergence of yet another active volcanic center near Io's south pole. Voyager scientists earlier reported discovery of an active volcanic plume near the north pole, at the same longitude. Analysis of these data by McEwen strongly suggest the existence of two classes of volcanic plumes, differing in chemistry and energy, which may be driven by separate volcanic processes. The plumes of the larger class show ringed deposits of dark brown and red materials as much as 1,500 km in diameter surrounding the vents. These plumes appear to be intermittently active and are restricted to the trailing hemisphere of the satellite. They could be driven by the interaction of molten silicate material with sulfur or sulfur dioxide. The second class shows rings of bright material only 100 to 200 km in diameter surrounding the vents. Most were seen to be continually active during both encounters. These plumes are restricted to the equatorial band

($\pm 30^\circ$) and may be driven by a lower temperature interaction, perhaps molten sulfur interacting with sulfur dioxide.

Europa

L.A. Soderblom (USGS) has collaborated with T.V. Johnson and J.A. Mosher of the Jet Propulsion Laboratory (Pasadena, Calif.) and T.B. McCord of the University of Hawaii (Oahu, Hawaii) to reduce the global multispectral images of the Galilean satellite Europa acquired by Voyager 1 and 2. They find that discrete material units, classifiable from spectral properties in the range 0.45 to 0.6 μm , correspond to geologic units mapped by L.A. Soderblom and B.K. Lucchitta. In the ultraviolet part of the spectrum, however, a broad global pattern uncorrelated to these surface units is present. This pattern is instead correlated to the distance from the apex of orbital motion. Evidently, a combination of charged particle bombardment and impact crater gardening is responsible.

Lucchitta and Soderblom (1982) report that the surface of Europa consists of two basic units, plains and mottled terrain. Both plains and mottled terrain units are transected by numerous varied bands, usually brown or dark gray, that appear to have formed as dark material infilling fractures, grabens, or gaps in the crust. The light central stripes found in some dark bands may result from dike-like filling of fractures by fluids that expanded on freezing. Numerous narrow ridges visible near the terminator in Voyager images may have similarly formed as dikes. A large brown spot appears to be an impact crater scar analogous to crater palimpsests or collapsed craters found on Gany-mede. A few small (10 to 30 km diameter) impact craters superposed on Europa's surface are confidently identified in the highest resolution Voyager images.

Plains units are the oldest geologic materials; other units, including mottled terrain and spots and stripes, formed by disruption or replacement of the plains. Ridges appear to be the youngest geologic features on Europa and locally postdate even young impact craters. The dark stripes and dark spots in mottled terrain units suggest that debris-laden materials were transported, perhaps as muddy slurries, through Europa's icy crust to the surface. Such movement could have occurred if the outer ice shell were not thicker than a few tens of kilometers. A thin ice shell suggests that most of Europa's water has remained in the interior, possibly tied up in hydrated

silicates. Alternatively, evidence of rafting and rotation of sections of the crust suggests that the ice shell is thick enough in places to have been decoupled from the subjacent silicate sphere.

Lineation patterns on Europa in the area covered by high-resolution Voyager 2 images were divided by Lucchitta and Soderblom into four classes and were analyzed for their systematic trends. Most major structures on Europa's surface were apparently influenced by tidal forces centered on the axis pointing towards Jupiter, but variations in the detail of structural patterns may have been caused by internal forces.

Ganymede

E.M. Shoemaker and B.K. Lucchitta (Lucchitta, 1982; Shoemaker and others, 1982) report that the icy crust of Ganymede comprises bright and dark areas. Investigations of Voyager 1 and 2 images have shown that bright terrain is grooved and separates dark polygons of cratered terrain. The grooved terrain contains alternating ridges and grooves in straight and curvilinear sets, which are locally interrupted by smooth patches and swaths. Cratered terrain, where it occurs in small wedges and slivers, has a pervasive grain of narrowly spaced furrows and thus is transitional to grooved terrain. An analysis of the morphology of terrain types, and of superposition and crosscutting relations, suggests that grooved terrain grew at the expense of cratered terrain, that tracts of cratered terrain were converted into grooved terrain in situ, and that vertical tectonism and shear movements dominated the resurfacing of Ganymede. Lucchitta and Shoemaker postulate that, during a period in the satellite's history when the lithosphere was thin, upwelling convection currents caused incipient rifting accompanied by intensive normal faulting; where rifting went to completion, crustal segments separated, locally spread apart, and sheared past one another. In places subduction and compression may have occurred, but the evidence is inconclusive. Thus, according to the USGS researchers, the grooved terrain on Ganymede (the largest satellite in the solar system) may record an early phase of ice-plate tectonics that caused rifting and drifting of the icy lithosphere but, unlike silicate plate tectonics on Earth, may have resulted in only minor vertical turnover.

Cratering rate of the Galilean satellites

An initial evaluation of the impact cratering rate on the Galilean satellites of Jupiter was completed in 1981 by E.M. Shoemaker and R.F. Wolfe (1982). Impact craters on the Galilean satellites have been

produced in the recent geologic past primarily by active and extinct comet nuclei (Passey and Shoemaker, 1982). Both short-period comets, sometimes called Jupiter-family comets, and long-period comets are represented in the flux of active comets in the vicinity of the Galilean satellites. Although the number of Jupiter-family comets is relatively small, their flux in the neighborhood of Jupiter is relatively high because of their short periods and because of their low velocities at Jupiter-crossing; these low velocities permit strong concentration of the flux by Jupiter's gravity field. The much more numerous long-period comets possibly account for about one-eighth to one-third of the present production of impact craters. According to Shoemaker, planet-crossing asteroids, consisting chiefly of recently extinct short-period comets, may be responsible for roughly one-half of the present production of impact craters. Because of the high orbital velocities of the Galilean satellites, the present cratering rate at the apex of motion is about twice the mean rate for each satellite, and the cratering rate at the apolapse is about 5 to 20 times less than the mean rate. Shoemaker and Wolfe suggest that the majority of craters on Callisto and on Ganymede probably date from a period of heavy bombardment early in the history of the solar system.

MARS INVESTIGATIONS

Martian geology

M.H. Carr has summarized the geology of Mars in several review articles and in a book published by Yale University Press (Carr, 1981). He notes that the evolution of Mars differs from that of the Earth for two basic reasons: Mars' lack of plate tectonics and, under martian climatic conditions, liquid water is unstable. The Earth's surface is a complicated system in which material is being recycled through the mantle, by subduction and ocean-floor spreading, and within the lithosphere and hydrosphere by weathering, metamorphism, erosion and deposition. The dynamics of the martian crust are totally different. Although the planet has been volcanically and tectonically active throughout much of its history, the lithosphere has not been recycled through the underlying asthenosphere. The huge volcanoes and vast fracture systems have not concentrated in linear zones, as on Earth, but rather have affected areas of broad regional extent. Furthermore, although water has flowed across the martian surface at times in the past, fluvial erosion has been trivial. On Earth uplift is followed by enhanced erosion, and downwarping by rapid sedimentation, so

that a rough equilibrium is maintained between the relief-forming processes and gradation by running water. On Mars, because of the limited fluvial erosion and deposition, no such equilibrium is achieved, and so despite its smaller size Mars has considerably more relief than the Earth. Volcanoes have grown to three times the height of Mt. Everest and canyons several kilometers deep have survived for billions of years. The lack of significant sediment transport implies in addition that weathering products are not recycled. Weathering probably does occur, since an extensive ground-water system is suspected, but without erosion and removal of weathered products the process must be extremely slow. In effect the subsurface rocks may be in a state of static equilibrium with the hydrosphere and atmosphere, in contrast to the dynamic interaction that occurs on Earth. Thus, the absence of plate tectonics on Mars prevents cycling of the lithosphere through the upper mantle; the absence of flowing water at the surface hinders cycling of surface materials and their interaction with the hydrosphere and atmosphere. The result is an active planet, having enormous surface relief, on which features with a wide range of ages are preserved in almost pristine condition.

Martian valleys and channels

M.H. Carr and G.D. Clow (1981) examined the distribution and characteristics of martian valleys and channels. The martian valleys resemble terrestrial valleys in that they increase in size downstream and have numerous tributaries. They are widely believed to have formed by slow erosion of running water. Most of the valleys are in the densely cratered terrain, which dates back to around four billion years ago. Individual drainage networks are generally open, the drainage basins are widely spaced with little evidence of competition between adjacent basins, and the networks rarely exceed 300 km in length from the most distal tributary to the mouth of the trunk channel. These characteristics suggest an immature drainage system in which single networks have not had time to dominate large areas. Restriction of the channel networks mainly to the oldest terrain suggests that the period of most active growth was early in the planet's history, possibly at a time when the atmosphere was thicker than at present. In contrast, the large channels appear to have formed by catastrophic floods rather than slow erosion. They are much larger than the valleys, many being several tens of kilometers across and thousands of kilometers long. They have few or no tributaries and do not necessarily become broader downstream. The channels have a wide range of ages,

in contrast to the predominantly old ages of the valleys. If they are the result of floods, these large channels could form under present conditions; no dramatic climatic changes are required to explain their presence. All these observations suggest that water is abundant close to the martian surface, possibly sealed below a thick permafrost, and that it bursts out occasionally to form the enormous flood features observed.

Martian topography—a new method for rapid extraction

Philip Davis and L.A. Soderblom report completion of development and testing of a computer-operated system to extract topographic information from radiometrically calibrated monoscopic Viking Orbiter images. The technique integrates topographic profiles from radiometric profiles by means of surface photometric functions, models of atmospheric scattering, and symmetry constraints with the topography.

The Basal Scarp of Olympus Mons

E.C. Morris reports that the origin of the escarpment that surrounds the perimeter of the large shield volcano Olympus Mons has been the subject of much speculation since the escarpment was first observed in the Mariner 9 pictures (Morris, 1981). Erosional, depositional, and tectonic processes have all been proposed for its origin. The scarp is complex in its structure; though roughly concentric, it is composed of linear, concave, and convex segments. Radial fractures, some extending partway up the flank of the volcano, divide the scarp into segments. One radial fracture shows compressional features—several imbricate, steeply dipping blocks along its trace. The north and northwest segments of the scarp have the greatest elevation, rising 8 to 10 km above the basal plain. The southeast segment is 4 to 5 km high. Morris reports that the southwest, east, and northeast parts of the scarp are nearly buried by young lava flows. The height of the scarps in these areas is about 2 to 4 km. Layered material is exposed in the north, northwest, and southeast segments of the scarp. This material is probably, according to Morris, the basal unit upon which Olympus Mons was built. Blocks of this material are found along the rim of the scarp dipping towards the center of the volcano. The scarp appears to truncate some old flows that stream down the flanks of Olympus Mons; in other areas the flows are ponded behind a raised rim of the scarp. These relations seem to indicate that the scarp formed late in the history of Olympus Mons during a relatively short time. Except where buried by young flows or modified by a few

debris flows and landslides along the west segments, the scarp has changed little since its formation. The complex nature of the basal scarp of Olympus Mons implies a tectonic origin. The scarp is interpreted by Morris to have formed by thrust faulting as a consequence of compressional forces developed in the crust during subsidence of Olympus Mons.

Geologic mapping of Mars

Geologic mapping of the western hemisphere of Mars has been completed in six quadrangles and in parts of eight other quadrangles. D.H. Scott reports that major subdivisions of rock units have been made in the highlands and northern plains and around the volcanic complexes in Tharsis Montes, Tempe Terra, and southern highlands of Mars. Lava flows from the Tharsis volcanoes have been subdivided into 15 major units, and materials provisionally mapped as ignimbrites (Scott and Tanaka, 1982) in Amazonis Planitia have been divided into 7 map units. Materials forming the lowland plains are more difficult to distinguish as separate units and subdivision there is presently being made on the basis of variations in impact-crater density.

Lava-flow maps of Tharsis Montes

D.H. Scott reports that sixteen 1:2,000,000-scale lava-flow maps of the Tharsis Montes volcanic province were completed during 1981 and were published in 1982 as U.S. Geological Survey Miscellaneous Investigations Maps (I-1266 to I-1281). The lava flows are among the youngest on Mars; they consist of about 15 major units covering some 18 million km². They have been erupted from five large volcanoes as well as from fissure vents in the martian plains. The flows have been relatively dated by superposition relations and by crater counts. They record the waning stages of major volcanism on Mars.

Mars highland volcanic province

D.H. Scott and K.L. Tanaka (1981) report that regional geologic mapping from Viking images indicates that many of the mountains in the highland region southwest of Tharsis Montes have morphologies characteristic of volcanoes. Some of the postulated volcanoes may be composite structures formed by lava flows and interbedded pyroclastic deposits. Generally, they do not resemble other highland volcanoes, which are more subdued. The mountains are partly buried or embayed in places by lava flows from Arsia Mons; this observation indicates that Tharsis volcanism occurred after an earlier period of volcanic mountain building and major tectonic activity.

Composite origin for martian outflow channels

The origin of martian outflow channels has been ascribed variously to wind, flood, mud, or ice. All these hypotheses rely primarily on the morphologic resemblance between martian outflow-channel features and features of channels formed on Earth by these agents. In order to satisfy the observations, B.K. Lucchitta and H.M. Ferguson (1982) proposed the following composite origin for the martian outflow channels: The channel-forming fluid emerged from the chaotic terrain as liquefaction mudflows that became more viscous and moved more slowly downstream, where the liquid was frozen and the channels choked in the manner of ice drives. Such slugs of debris may have moved through the channels as hybrids between very viscous mudflows and very debris-rich and wet glaciers; confined brines at their base may have buoyed the flow locally. Increased friction on steeper gradients may have partly liquefied the material so that it reverted, in some places, to true mudflows or floods. The debris was carried into the northern plains, where it may have created some of the irregular topography seen in that region. After the channels were formed, wind erosion modified many of the previously developed landforms.

Geology of Valles Marineris

Excellent stereographic pictures at resolutions near 100 m/line-pair cover parts of the Valles Marineris on Mars. The Viking Orbiter images were studied in detail by B.K. Lucchitta; these images provided new insights into the interplay between faulting, possible volcanism, basin-bed deposition, and channel erosion in the chasmata. The oldest geologic rocks in Valles Marineris were found to be buried under talus in the lower trough walls; the composition of these rocks is unknown, but they apparently form unstable walls and liquefy easily, actions that suggest high water content. The cap rock on the walls is layered and is commonly interpreted as lava of the Lunae Planum Plateau. After eruption of plateau lava ceased, east-west-trending grabens several thousand meters deep formed most of the chasmata. The graben walls were vigorously eroded into gullies, spurs, and tributary canyons.

Erosional debris from the walls apparently accumulated in the center of the troughs and formed layered basin beds. Even though some lower layers appear to be in fault contact with the trough walls, most layers were deposited against the walls and overtopped median ridges. The basin beds are stacks of layered rocks. Some layers are soft, thick, extremely bright, and erode easily into steep subparallel gullies,

transformed by wind erosion into yardangs. Other layers are coarse and rubbly; others again are smooth, or finely gullied at various spacings. Conspicuous are interbedded resistant, dark layers that form steep-sided caprocks, supporting ledges, or small mesas. These interbedded dark and light layers resemble basin beds in Arizona and Nevada that are composed of basalts and tuffaceous sediments. The similarity suggests that martian basin beds contain volcanic materials of varying compositions. The volume of the interior deposits appears to be larger than the volume eroded from trough walls, most of which are steep fault-line scarps, so that a contribution from elsewhere is required. As the surrounding plateau surface is little dissected, the contribution probably comes from the trough interior by volcanism or from the outside by wind; photogeologic considerations favor volcanism. Thus, the basin beds may be composed of interfingering fluvial deposits from the walls, volcanic flows, tuffs, and tuffaceous sediments. The level top surface suggests processes of deposition similar to those in terrestrial playas. At some time after basin-bed deposition ended, the fluvial processes that formed the spurs and gullies also stopped. Late faults truncated spurs, left gullies as hanging valleys, and formed straight fault scarps blanketed by smooth talus.

Huge landslides and small debris lobes continued to fall or flow from the walls into troughs deepened by renewed faulting or erosion. Some of these deposits are in turn faulted. Large new landslides have smooth headwalls, probably because they post-date the episode of spur and gully formation. The landslide deposits lapped upon or spilled around basin-bed remnants. Fluids emerged from their lobes and flowed into low areas in Candor Chasma, which they filled with level deposits traversed by polygonal cracks. Wind erosion continued to the present. Basin beds show intense deflation. Most landslide deposits, like the wall and cap rock of the troughs, are little eroded by the wind. Most diffuse dark wind streaks are found near dark rock outcrops or possible volcanic vents; that other dark wind deposits tend to be concentrated near small, rugged features suggests preferential dropping of dark suspended materials in the turbulent air. Some interior mesas are covered by smooth deposits with vague, dunelike forms, and large areas of the chasma floors are buried by apparent wind deposits, which form a gently rolling topography.

Probable fluvial sources for dune sand on Mars

J.F. McCauley, C.S. Breed, and M.J. Grolier report that field studies and satellite-image analysis of terrestrial sand sheets and dunes, particularly in relation to the newly recognized relict fluvial patterns and

distribution of inselbergs in the Western Desert of Egypt, provide a model for interpretation of eolian features on Mars. A fluvial origin is proposed for much of the sand in martian dune fields, as on Earth. On Mars, fluvial sources are now defunct and most of the sand particles have been winnowed and transported by surface winds to depositional sites throughout the planet. These sites consist of various kinds of topographic traps and include the north circumpolar erg, numerous crater and valley floors, and low or sheltered plains areas. Their model implies former martian climatic conditions that permitted rivers to flow and an absence of the polar ice caps that presently control global wind-circulation patterns.

Physical properties at the Viking landing sites

H.J. Moore (Moore and others, 1982) reports analyses of sample trenches excavated by the Viking landers on Mars and, using a theory for plowing with narrow blades, has provided estimates of the angles of internal friction and the cohesions of the martian soil-like surface materials. Angles of internal friction appear to be the same as those of many terrestrial soils because they are generally between 27° and 39°. Drift material, at the Lander 1 site, has a low angle of internal friction—near 18°. All the materials excavated have low cohesions, generally between 0.2 and 10 kPa. The occurrence of crossbedding, layers of crusts, and blocky slabs shows that these materials are heterogeneous and that they contain planes of weakness.

The results reported by Moore have significant implications for future lander missions, martian eolian processes, and interpretation of thermal inertia. Foot pads of future Mars landers must be designed to be able to land on a surface entirely underlain by drift material; the Viking landers would probably have penetrated too deeply into a surface entirely underlain by drift material. The magnitudes of the cohesions of the materials (and their grain size) indicate that they are not easily entrained and transported by martian winds. Finally, Moore suggests that cohesions of the materials require that models that employ cohesionless grains should not be used to explain infrared thermal inertias.

VENUS INVESTIGATIONS

Venus tectonics

G.G. Schaber reports that three global-scale zones of possible tectonic origin have been described as occurring along broad, low rises within the Equatorial Highlands on Venus (Schaber, 1982). The two longest

of these tectonic zones, the Aphrodite-Beta and Themis-Atla zones, extend for 21,000 and 14,000 km, respectively. Several lines of evidence indicate that the Beta and Atla Regiones, located at the only two intersections of the three major tectonic zones, are dynamically supported volcanic terrains associated with currently active volcanism. Rift valleys south of Aphrodite Terra and between Beta and Phoebe Regiones are characterized by 75- to 100-km widths, raised rims, and extensions of only a few tens of kilometers, about the same magnitude as in continental rifts on Earth. Horizontal extension on Venus was probably restricted by an early choking-off of plate motion by high crustal and upper mantle temperatures and the subsequent loss of water and an asthenosphere.

THE SOLAR SYSTEM

Measurement of cratering

As part of a broadly based study of the morphologic transition from large complex craters to small multiring basins, R.J. Pike (1981a) has developed a method for ascertaining and expressing mathematical regularity in the radial separation of basin rings. The simple procedure, which thus far has been applied to measurements of 92 ring sizes for 24 basins on seven planets and satellites, establishes a numerical relation between ring size and ring rank within each basin. Rank is the relative radial position of a ring in a given basin, with the innermost possible ring ranked as I. Ranks as high as VII have been tentatively identified. The new system adapts well to existing ring nomenclature: the main, or topographic, ring is ranked as IV; the central-peak ring is II; the intermediate ring is III; and outer arcs rank as V or higher. The resulting statistical scheme for size:rank of multiring basins suggests that radial separation of adjacent rings is essentially $\sqrt{2}$ as previously hypothesized. Differences in ring prevalence and topographic prominence revealed by size:rank analysis may have generic significance. The systematic decrease of both attributes, inward and outward, from Ring IV and Ring V suggests the radial decay of a damped-wave phenomenon.

Morphometry of the volcanoes

R.J. Pike and G.D. Clow have largely completed their work on the topographic geometry of volcanic edifices (Pike and Clow, 1981). The taxonomy of central volcanoes has been expanded to 25 terrestrial classes and 6 extraterrestrial classes. Categories for breached stratocones (the Mount St. Helens type) and

for submarine caldera-bearing shields have been added, and other classes have been subdivided. Multivariate analysis of edifice dimensions yields eight fundamental, process-related groups of central volcanoes. The three classes of volcanoes on both Mars and the Moon are distinctively different from one another. Current applications of cluster and principal-component analysis, however, have not been able to uniquely infer the mode of origin of martian volcanoes from the gross topography of terrestrial volcanoes; too much overlap is present in the data. The depth of burial of large caldera-bearing shields on Mars is calculated as typically 1 to 4 km, on the basis of revised photogrammetric data and a method applied initially by M.H. Carr. The data file on topographic dimensions has been extended to 697 volcanoes. Mean volumes for different classes of volcanic edifices vary by some ten orders of magnitude, from 10^5 m^3 (terrestrial pseudo-craters) to 10^{15} m^3 (martian shield volcanoes).

Planimetric mapping of the planets

The surfaces of 14 planets and satellites, including Mars, Venus, Mercury, the Earth's Moon, four Jovian satellites (Io, Europa, Ganymede, and Callisto), and six Saturnian satellites (Mimas, Tethys, Dione, Rhea, Iapetus, and Enceladus), have been mapped from spacecraft data. Of these bodies, 11 were mapped from digital television pictures that have almost negligible potential for measuring topographic elevations; only the data sets for the Moon, Mars, and Venus will support extensive contour mapping.

Three general categories of map products are compiled during two phases. In the first phase, preliminary maps required to support preliminary mission science reports are compiled immediately after receipt of data; these products include uncontrolled photomosaics, semicontrolled "pictorial" maps drawn by airbrush, and special-purpose uncontrolled mosaics and airbrush maps. In the second phase, controlled maps are prepared for formal publication, including controlled photomosaics, airbrush shaded-relief and albedo maps, and special maps required to support topical studies or future mission planning. Scales of map products are based on the resolution of available map data. The primary scale for maps of all extra-terrestrial objects is 1:5,000,000; reconnaissance or planetwide maps of the larger bodies are drawn at 1:25,000,000 or 1:50,000,000; scales of 1:2,000,000, 1:1,000,000 and 1:500,000 are used when data resolution supports these larger scales. Projections are usually conformal, to preserve landform shapes for geologic investigation. Some maps that were originally compiled on conformal projections have been digitally

transformed to equal-area projections to facilitate scientific investigations involving the size-frequency distributions of certain geologic structures.

Compilation processes include level 1 digital processing for image cleanup, artifact removal, and radiometric correction. Level 2 digital processing includes photometric correction, correction for imaging-system distortions, and transformation to appropriate map projections. Spatial filtration and contrast enhancement are applied as appropriate. The resulting images are used in mosaics, assembled manually or digitally, that are either published as photo-maps or used to support airbrush compilation.

LUNAR INVESTIGATIONS

Lunar geology

D.E. Wilhelms has found that the Moon's largest ringed impact basin, the 3,200-km Procellarum basin identified by Cadogan (1974) and Whitaker (1981), is responsible for a remarkably long list of lunar phenomena:

1. Terra elevations are lower inside the basin than on the rest of the near side and on the far side, except in a few other large basins.
2. Ridges and troughs of the near-side terra not previously accounted for by ringed basins are parts of the three rings of Procellarum.
3. The feldspathic, low-density terra crust is thinner inside Procellarum than on the rest of the near side, as a result of the original impact excavation.
4. Most mare volcanism and all Eratosthenian and Copernian mare volcanism took place inside Procellarum, probably as a result of the thin crust and

correspondingly elevated mantle sources of the basalts.

5. Isostatic adjustment of basins and the contained mare basalts was more complete inside Procellarum than outside, because of the differences in crustal thickness. The crust and the elastic lithosphere were equivalent at the time of mare volcanism.
6. Arcuate grabens, which are caused by mare subsidence, formed inside but rarely outside Procellarum.
7. More crater floors rebounded in and near Procellarum than elsewhere on the Moon.
8. The Al:Mg of terra material is higher outside than inside Procellarum, probably because feldspathic materials of the upper crust were ejected by the impact.
9. The concentration of KREEP that has been noted in Procellarum is a result either of KREEP volcanism or of unroofing a deep-seated KREEP layer by the basin (Cadogan, 1974).
10. Thin, aluminous mare basalts, which are formed by refractory, dense magmas, were extruded in much greater volumes and at later times inside Procellarum than outside the basin.

Lunar crater studies

In related work on lunar impact craters, R.J. Pike (1981b) has documented the target-dependence of crater geometry by using depth/diameter ratios calculated from Apollo photogrammetry. The high-quality depth data reveal a substantial mare/terra contrast. Although depth/diameter ratios are similar for simple (small, bowl-shaped) craters on mare and terra surfaces, fresh terra craters that are complex (large, with central peaks, flat floors, and wall terraces) are systematically deeper than those on the maria. The morphometric contrast could reflect contrasts in lunar target materials: the terra breccias may be weaker and (or) more poorly layered than the mare basalt flows, thus accommodating deeper excavation by the initial impact or deeper structural adjustment in the modification stage.

REMOTE SENSING AND ADVANCED TECHNIQUES

EARTH RESOURCES OBSERVATION SYSTEMS OFFICE

The Earth Resources Observation Systems (EROS) Office supports and coordinates research and demonstrates applications of remote sensing technology within bureaus and offices of the DOI and in cooperation with other Federal and State agencies. The cost effectiveness and utility of techniques are assessed and documented, and the user agencies gain experience in carrying out procedures. Training and assistance in the use of remotely sensed data are also provided to the public, private, and international sectors.

EROS staff are located at the EROS Office headquarters in Reston, Va., the EROS Data Center (EDC) in Sioux Falls, S. Dak., and the field offices in Anchorage, Alaska, and Flagstaff, Ariz. In addition to its applications, demonstrations, training, and assistance functions, EDC is the principal archive for and distributor of the National Aeronautics and Space Administration's (NASA's) Landsat data, photographs acquired by NASA from research aircraft and manned spacecraft, and aerial photographs acquired by bureaus and agencies of the DOI. A central computer complex provides access to a data base that contains approximately 7 million images and photographs of the Earth's surface; searches for and identifies images of specified geographic areas of interest; and serves as a management tool for the entire data archival, reproduction, and dissemination process.

SPATIAL DATA HANDLING RESEARCH AND DEVELOPMENT

Spatial data handling capability assessment

D.L. Murphy (Technicolor Graphic Services, Inc.) assessed the need for digital spatial data handling and analysis capabilities at EDC. He recommended acquisition of a proprietary spatial data management system based on hexagonal structures. The recommended software would satisfy some short-term data base needs but would be implemented with the long-term needs in mind.

Computer system networking

Preliminary developmental steps have been taken to implement a high-speed local computer network at EDC. The network uses HYPERchannel, a product developed by Network Systems Corporation

(NSC). Five HYPERchannel processor adapters and two minicomputer interface devices were procured. The first two adapters were installed on the SEL 32/77 and Burroughs 6700 computer systems. Preliminary software was designed and developed for both computer systems to ensure that the network was functional and compatible with the HYPERchannel processor adapters. Operating system input/output handlers, diagnostics, and a simple file transfer program were developed.

Additional research was then conducted on higher level communications protocols that would be consistent with the International Standards Organization's Open Systems Interconnections Reference Model.

Remote image processing station (RIPS) research, development, and technology transfer

H.L. Wagner (Technicolor Graphic Services, Inc.) has designed and built three prototype models of a remote image processing station. The station is designed to facilitate the use of Landsat and other remotely sensed data in USGS and other DOI field offices. RIPS is not intended to compete with large-scale or minicomputer-based systems, but to complement them through local processing and remote access to network host computers. This phased-development project included prototype hardware design, definition of user requirements, development of data-compression techniques and data-transmission protocols, remote-unit software design, host-unit software design, system testing, field evaluation, and solicitation of industry involvement.

Image processing software has been written to handle routine analysis functions such as haze removal, histogramming, contrast stretch, edge enhancement, ratioing, and image classification. These and numerous other processing functions and the ability to interface with many host computers enable RIPS to input and analyze several types of geographically referenced image data such as meteorological, Landsat, and topographic data, as well as polygonal cartographic data structures. A procurement specification for quasi-operational RIPS stations was developed on the basis of experience gained from operational tests of the three prototypes and user input from a national RIPS workshop held at EDC.

Representatives from government, academia, and industry were invited to participate in the workshop, which was planned and coordinated by F.A. Waltz and H.L. Wagner. The RIPS workshop provided a forum for discussing concepts and sharing

innovative ideas about microprocessors, other hardware devices, accompanying software, and system specifications. Data availability, software exchange, cost recovery, cost effectiveness, and private industry versus government responsibilities were among the topics discussed. Several hardware demonstrations were conducted at the workshop.

Although the RIPS concept had not been fully formulated, workshop participants were interested in low-cost image processing systems, and several participants had low-cost systems in various stages of development. The workshop brought together potential users of RIPS technology with industrial representatives who might eventually be the providers of equipment and demonstrated that the technology now exists to fulfill the RIPS concept of low-cost image processing capabilities. A consensus was reached by all workshop participants that user acceptance must be built via active development and demonstration of the RIPS concept.

Data availability and the mechanism by which data are input to RIPS were identified as potential problem areas unless floppy disks, tape cartridges, television scanners, and communications links become readily available. Also, the production of quality output products on low-cost equipment remains a problem; however, a possible solution would be the development of a service bureau within private industry for providing quality output for RIPS users. The building of data bases with inputs of 30 to 40 variables and the use of spatial data handling and analysis techniques on these systems were considered by all participants to be important areas of future research and development.

Geometric registration

Software and procedures are being developed to produce and integrate geometrically registered Landsat data products and integrate them with other spatial data. This project was a phased development task to define, contract, purchase, and install hardware; design software; implement image-to-map registration; implement image-to-image registration; and incorporate the Landsat ground control point library from the NASA Goddard Space Flight Center.

Currently, hardware support for the project is provided by the Image 100 display system driven by a DEC PDP 11/35 processing system. The software has been defined and is being implemented. The image-to-map registration is nearly complete. Final enhancements are currently being made along with the documentation. The image-to-image automatic correlation software is under development and will be tested early in 1982. The incorporation of the Goddard ground control point library is still in the analysis stage.

Digital topographic data

EROS has incorporated digital topographic data into the data bases of various projects. At first, the Digital Terrain Tapes (DTT) were the sole source of digital topographic data. They were produced from 1:250,000-scale map sources by the Defense Mapping Agency and distributed by the National Cartographic Information Center (NCIC). Due to a lack of continuity of data at the 1° by 1° data block edges, problems were encountered in registering DTT data to map bases. The DTT's were edited and reformatted to the USGS Digital Elevation Model (DEM) format. All existing 1:250,000-scale DEM data files for Alaska and the United States are in the EDC tape library to facilitate usage in cooperative projects. Software was developed to streamline mosaicking and registering of DEM data to bases at any scale and in twenty map projections.

Spatial data analysis technique development

D.D. Greenlee (USGS) and D.A. Nichols (Jet Propulsion Laboratory) reported that three software functions that allow classifications to be converted to polygonal formats have been implemented on the Interactive Digital Image Manipulation System (IDIMS). By use of this technique, landcover type classes can be "area filtered" with a minimum-size threshold, choropleth plots can be generated on a pen plotter, and cartographic generalization can be effected. The technique utilizes virtual arrays to avoid size limitations and utilizes a component labelling procedure described by Rosenfeld (1978) and a polygon generalization method by Douglas and Peucker (1973). This technique provides an important bridge from image processing of raster data to spatial analysis techniques employing vector representations (Greenlee, 1981).

Jay Feuquay (Technicolor Graphic Services, Inc.) has designed applications software for the raster-to-vector conversion technique and has enhanced existing vector-to-raster spatial data format conversion capabilities. These techniques allow analysis of grid cell and vector data to occur within the same image processing system (for example, tabular summaries of grid cell data within polygons and overlay analysis with vector data as input).

Techniques for the storage of very large spatial data sets

Technological advances in scan digitizing have made the production of very large spatial data sets possible. Vector-based structures have been used for such files, and raster-based structures are being investigated. Both have deficiencies. Some vector

mode functions require lengthy processing, and some are impractical in raster mode. Donna Peuquet (USGS) has proposed a totally new, hybrid structure for large geo-based files which may permit the economic and efficient use of both vector- and raster-based algorithms. Software implementation of the new data structure has begun for proof-of-concept test and evaluation.

Inventory of computer software for spatial data handling

The three volume "Inventory of Computer Software for Spatial Data Handling" was compiled for the USGS by the International Geographical Union (IGU), Commission of Geographical Data Sensing and Processing. Copies of the inventory were distributed to 1,500 persons or organizations, worldwide, known to be involved in research or development in digital cartography or quantitative geography. On April 30-May 1, 1981, a follow-up workshop on "Spatial Data Handling R&D Needs for the 1980's," co-sponsored by the IGU and USGS, was held in Reston, Virginia.

TECHNIQUES IN PROCESSING DIGITAL DATA

Analysis of return beam vidicon (RBV) radiometric response and development of correction techniques

Studies of Landsat RBV response properties in 1981 were divided into two phases: (1) the characterization of the response of each camera as a function of both object plane position and time, and (2) the development of techniques to compensate for vidicon shading.

The RBV response was analyzed for selected scenes acquired between February and May. Approximately 100 relatively featureless scenes (oceans, deserts, ice) were identified as candidates for control in recalibration techniques. The scenes were organized into three broad categories of assumed overall scene brightness (on the basis of ground cover and Sun angle) from which vidicon biases and gains were derived. Finally, recurrent higher frequency artifacts (faceplate blemishes, stairsteps, shade stripe, and periodic noise) were noted and cataloged.

Techniques for radiometrically correcting RBV images were developed that centered the low spatial frequencies of the images. Similarities in the continuous tone information among the images were identified by using spatial filtering and signal averaging techniques for the scenes in each of the three brightness categories. The resulting three calibration points for each object plane position were used to calculate

bias and gain distributions. The effects of bias correcting alone on an RBV image were described and illustrated in the October 1981 issue of the "Landsat Data User's Notes."

Multispectral classification procedures

A new procedure to cluster and classify Landsat MSS data has been developed by S.K. Jenson (Technicolor Graphic Services, Inc.) and Jack Bryant (Texas A&M University). The new procedure, called Amoeba, locates spatially and spectrally homogeneous areas in an image and calculates cluster centers within these areas. Arbitrary parameters such as location and size of training sets or number of land cover clusters need not be specified by the analyst. The result of the Amoeba algorithm is a classification of land cover based on both spectral reflectance and image texture (the spatial variability of reflectance).

Tests of the Amoeba algorithm have shown that the resulting land cover classification can be obtained faster with it than with most other algorithms and with an accuracy that is comparable to other methods.

Image generation using film recorder

A project begun in 1980 was expanded in scope to study the causal relationship between film response curve manipulation and subjective image quality. The necessity for using a lookup table to linearize a digitally exposed film-response curve was well known. Not so well understood was how to modify the linear or exponential response curve to enhance image contrast and feature discrimination. The current study used three slightly different, high-gamma exponential curves to generate black-and-white film separates that are the component image sources for false-color composites. Film response curves were specifically tailored to individual scenes of the London, England, Damascus, Syria, and Volgograd, USSR, regions. The resulting images had improved image clarity and feature discrimination when compared to the standard, single-lookup-table product (Boyd, 1981).

Innovative techniques for display of thematic maps

Newly emerging automated, geobased decision-support systems allow scientists, engineers, and managers to generate maps and display data on geographic bases, but sometimes such computer-generated displays are inaccurate or unintentionally misleading. The USGS, in cooperation with the George Washington University, Institute for Information Science and Technology, began examining means of building cartographic intelligence into such systems. To eliminate

many of the statistical problems associated with classed choroplethic displays, USGS, in conjunction with Michigan State University (continuous-tone mapping) and George Washington University (continuous-color mapping) has developed choropleth mapping software.

HYDROLOGIC APPLICATIONS

Determination of irrigation potential, Lower Brule and Crow Creek Indian Reservations

P.M. Seevers, D.O. Ohlen, and J.C. Eidenshink (all of Technicolor Graphic Services, Inc.), in a cooperative project with the Bureau of Indian Affairs (BIA), Aberdeen, S. Dak., office, developed a digital data base for the Lower Brule and Crow Creek Indian Reservations. The data base was used to determine irrigation potential of the reservation lands and to assist in meeting other resource management needs of the BIA.

Visual interpretation of Level I agricultural activity on late-summer, 1:250,000-scale Landsat images from 1974, 1976, 1978, and 1980 showed the study area to be about 65 percent rangeland, 20 percent agricultural crops, and 15 percent surface water. These data also showed a marked increase in the amount of land under irrigation for the 6-year period.

The multiple data base consisted of digital terrain data, digital line graph data, and digitized soil, ground water, road network, and ownership boundary maps. Crop water use, energy needs, and energy costs were calculated and entered into the data base. An irrigation model was developed that allowed manipulation of the data with a variety of parameter restrictions to determine irrigability under several sets of conditions.

Color-infrared aerial photographs at 1:24,000 were obtained on September 1, 1981, and used with ground data collected in May and August 1981 to identify the crops growing on randomly picked sample plots. Landsat digital data from August 1981 were then spectrally classified to identify irrigated crops and crop types. The sample plots will be used for an accuracy assessment of the classification results.

Hydrologic information systems in Black Hills and Cheyenne River Basin

Multiple spatial data sets have been compiled into a hydrologic information system for the Black Hills, S. Dak. This work is being done in cooperation with the South Dakota District Office, Water Resources Division. The objective is to derive stream basin characteristics for use in calculating of runoff curve numbers, ground-water recharge, and a water budget. The information system includes Landsat data, digital

terrain data, land cover, geology, drainage lines and divides, and precipitation and streamflow indices. Data set formatting and parameter evaluation was done by L.G. Batten (Technicolor Graphic Services, Inc.). Research by S.K. Jenson (Technicolor Graphic Services, Inc.) began on the calculation of surface drainage areas and the automated delineation of drainage lines from digital topographic data.

Satellite glaciology

The preparation of the "Satellite Image Atlas of Glaciers" (Williams and Ferrigno, 1981), has produced a 1:5,000,000 "Landsat Index Map of Antarctica," in which each of the 2,470 Landsat nominal scene centers is represented by a symbol showing the suitability of available Landsat images for the preparation of planimetric image maps and for glaciological studies. Landsat has the potential for imaging about 79 percent of the area of Antarctica; 70 percent of the Landsat imaging area, or about 55 percent of the continent, was found to have excellent or good (less than 10 percent cloud cover) coverage.

Australia, Japan, New Zealand, the United Kingdom, and the United States have published Landsat image maps, either as single Landsat scenes or as mosaics of two or more images. The Federal Republic of Germany and South Africa also plan to publish Landsat image maps in the near future (Williams and others, 1981).

Available Landsat images could be used, in combination with doppler satellite technology for geodetic control, to triple the area of Antarctica currently mapped at scales of 1:250,000 or larger. Landsat 3 RBV images can also be used to prepare 1:100,000 image maps. In addition to eventually using Landsat images to compile an accurate map of the coastline of Antarctica, Landsat images have been successfully used for glaciological studies. Recent measurements of successive images of the Pine Island Glacier, Walgreen Coast, West Antarctica, showed an average speed of flow of the terminus of 6 m/d over 750 d.

GEOLOGIC APPLICATIONS

Global Magsat anomaly signatures emphasizing west Africa and eastern South America

The preliminary Magsat scalar (total field) 2° by 2° anomaly map was refined during 1981 by NASA's Goddard Space Flight Center. The first preliminary versions of vector (component field) anomaly maps were also produced by Goddard for Magsat investigators.

D.A. Hastings (Technicolor Graphic Services, Inc.) applied Magsat anomaly signatures to a study of regional crustal structure. Ancillary data were compiled and interpreted, and Hastings' (1980) model of the geologic framework of west Africa's mineral deposits was further refined. In addition, Hastings, D.E. Laux, and Gary Walvatne (all of Technicolor Graphic Services, Inc.) prepared a geological map of the world on one sheet to use as a base map for the geological correlation of Magsat anomalies with ancillary data such as seismicity and mineral deposits.

When corrected for the effects of magnetic latitude, the anomaly map shows patterns that correlate spatially with specific tectonic features (Hastings, 1981a, b). Uplifted tectonic provinces (such as shields and oceanic plateaus) tend to produce negative scalar Magsat anomalies for magnetic latitudes (inclinations) less than 45° (north or south), with the strongest anomalies tending to be associated with the oldest (Archean) provinces. Depressed tectonic provinces (such as basins) tend to produce positive scalar Magsat anomalies at the same latitudes, with the strongest anomaly values appearing to correlate with the postulated greatest amounts of depression of the provinces. These anomalies tend to have opposite signs at magnetic latitudes greater than 45° (north or south). These correlations were noticed for Africa but are also found generally over the whole Earth.

Preliminary interpretation and modeling of these Magsat data as well as comparison with ancillary data appear to be consistent with a greater magnetic susceptibility (probably caused by a combination of greater regional metamorphism and greater uplift of more highly susceptible deeper crustal materials) above the Curie point isotherm for the older shields, and lower susceptibility (probably caused by a combination of a veneer of relatively nonmagnetic sediments near the surface and a depressed crustal column containing relatively less magnetic upper crustal materials) above the Curie isotherm in the basins.

Geologic applications of Landsat 3 RBV images

Scott Southworth (USGS) investigated the use of Landsat 3 RBV images for geologic applications. Landsat 3 contains two modified RBV cameras that operate in a broad 0.505- to 0.750- μm wavelength region and acquire data with a spatial resolution of 30 m. The improved geometric accuracy and high spatial resolution of the RBV images provide a superior planimetric base for regional geologic mapping.

RBV data were used to map structural lineaments in the Wind River Range, west-central Wyoming. Three images acquired August 11, 1978, Sep-

tember 5, 1978, and September 29, 1978, were analyzed for the effects of variations of Sun elevation and azimuth direction on topographic expression. Observable lineaments increased as the Sun azimuth changed from N. 52° W. to N. 35° W. and the Sun elevation dropped from 52° to 38° off the horizon. The number of lineaments mapped increased because the additional lineaments observed had topographic relief that required a lower Sun angle for enhancement and had trends that were near perpendicular (N. 55° E.) to the Sun azimuth (N. 46° W. to N. 35° W.).

Landsat 3 RBV images acquired October 9, 1980, over the Red Sea off the coast of Saudi Arabia, and October 22, 1980, over the Persian Gulf near Bahrain, were analyzed for shallow seas mapping. Defense Mapping Agency 1:500,000 nautical charts (revised in 1981) were photographed to produce a transparent overlay for the RBV images. Although the RBV data have poor radiometric fidelity compared with multispectral scanner (MSS) image data, the improved spatial resolution and geometric fidelity provide an image base on which subsurface reef structures can be identified and delineated. The availability of RBV data over shallow seas regions provides a means of revising nautical charts, but the compilation of MSS and bathymetric data is essential for optimal results.

Landsat 3 RBV images acquired August 26, 1978, and September 8, 1978, over the Columbia Glacier, Alaska, were analyzed for monitoring dynamic geologic phenomena. In 1979, the lower glacier was reduced in mass, both by retreat and thinning, the greatest amount yet recorded. RBV positive film transparencies at a scale of 1:500,000 were cropped to a 70-mm format and processed on a color additive viewer. Variations in the glacier terrain were enhanced by combining the 1979 image (projected through a red filter) with the 1978 image (projected through a green filter). Areas that remained constant appeared as yellow, and other colors identified other features that changed during the 1-yr period.

A Landsat 3 RBV image acquired on October 15, 1978, over Hobbs, N. Mex., was compared by Scott Southworth and W.D. Carter (USGS) to the 1976 Geologic Atlas of Texas, Hobbs Sheet, and to the USGS topographic quadrangle map to monitor the growth of oil and gas fields in the region over a 2-yr period. Existing maps of the Hobbs, N. Mex., area show that 1,339 oil and gas wells were mapped at a scale of 1:250,000 on the USGS 1° by 2° topographic map of Hobbs (revised in 1973) for an area covering 85 km by 67 km. An additional 3,365 oil and gas wells, mostly offset development drill holes, were identified over the same area on the October 15, 1978, RBV image, a 250-percent increase in oil and gas wells. The increased

availability of Landsat 3 RBV images provides scientists and energy resource managers with an important data base for accurate assessment and monitoring of exploration and development of hydrocarbon resources. Regional maps of active oil and gas fields can be adequately inspected and revised by using the RBV image as a planimetric base, thus reducing the need for expensive aircraft programs to only those areas where map revision is warranted.

Evaluation of data from new satellite imaging systems for geologic applications

Scott Southworth and W.D. Carter continued evaluating the usefulness of Heat Capacity Mapping Mission (HCMM) and Seasat Synthetic Aperture Radar (SAR) data for geologic applications. HCMM day-visible (0.55–1.1 μm) and day-thermal infrared (10.5–12.5 μm) data having respective spatial resolutions of 500 and 600 m were analyzed for the Southwestern United States. Differences in the physical properties of vegetation cover, soil moisture, rock types, and structural features were observed in both the visible and infrared response regions. Pat Chavez (USGS) Flagstaff, Ariz., digitally processed computer compatible tapes of the same region for geologic interpretation of the enhanced images. High-pass filters and diagonal-derivative images accentuated the linear components of the data. Lineaments accentuated on the thermal-infrared data appear to be related to differences in ground materials and moisture concentration.

Seasat SAR images (revolution 378) acquired July 23, 1978, from Lake Erie to Cape Hatteras, N.C., were analyzed for geologic application. The SAR is an L-band (23.5- μm wavelength) system with 25-m resolution. The 100-km wide image swath was produced on a southeast-to-northwest ascending satellite node with a look direction of N. 67.5° E. The look direction and look angle (20.5° off vertical) enhanced the cross strike structures of the northeast-trending Appalachian Mountains. The SAR image covers major physiographic provinces of the Eastern United States, specifically, the Cumberland Plateau, Valley and Ridge (Appalachians), Blue Ridge Mountains, Culpeper Basin, Piedmont, and the Coastal Plain. Ordovician age shale was differentiated from dolomite of the same age on the basis of drainage variation in the Shenandoah Valley. Resistant chert formations that form prominent topographic remnants were identified on SAR although they could not be detected on Landsat images. Topography, structure, drainage patterns, and vegetation differences were accentuated and provide a complementary data base for geologic investigations.

The optical-thermometric structure of volcanic eruption clouds was studied by A.S. McDade (USGS) and Michael Matson of the National Earth Satellite Service Branch of the National Oceanic and Atmospheric Administration (NOAA/NESS). Advanced high resolution radiometer (AVHRR) data, recorded from the NOAA-6 satellite during the April 1981 eruption of Alaid Volcano, USSR (50.86° N., 155.56° E.), were used to analyze changes in the shape and temperature of the eruption clouds during a contiguous data collection period from April 27, 1981, through April 29, 1981. Correlation and regression analyses were applied to multispectral combinations and single channel data sets to determine plume dispersal properties and temperature-height relationships of volcanic clouds. Microbarographic and radiosonde data from the area surrounding Alaid were used to study the nature of temperature extremes observed in the plumes from the AVHRR data.

Landsat evaluation of mineral production areas of the United States

Mineral deposits were plotted by commodity on a separate 1:5,000,000 lineament map of the United States by Scott Southworth and W.D. Carter, and the locations were compared to local lineament trends to define possible exploration targets. Landsat index maps were compiled by commodity and by State to facilitate the data search by mining geologists. The following nine U.S. mining districts were selected for analysis: Franklin Furnace, N.J. (Pb, Zn); Adirondacks, N.Y., (Fe); Mesabi Range, Minn., (Fe); Homestake, S. Dak. (Au); Butte, Anaconda, Mont., (Cu); Ajo, Ariz., (Cu); Bingham Canyon, Utah, (Cu); Climax, Colo., (Mo); and the Missouri lead belt. Topographic and geologic maps and Landsat RBV and MSS images of the mining areas were compiled in a booklet. Overlays were produced to define known structure as well as observed lineaments. Computer processing (linear stretches, low and high pass filters, lineament enhancements and extractions) of Mesabi and Bingham scenes enhanced interpretation.

Mineral resource assessment with digital geologic data bases

D.D. Greenlee (USGS) and C.M. Trautwein (Technicolor Graphic Services, Inc.) expanded development of a geologic data base for the southern half of the Nabesna quadrangle, Alaska, to investigate the utility of digital processing techniques applied to mineral resource assessment. A spatial analysis model for evaluating porphyry-type copper potential was developed to analyze the digital geologic data base consisting of 16 original data types and 18 derived data sets. Landsat MSS data, digital terrain data, and regional

geochemical, geophysical, and geologic data from the Alaskan Mineral Resources Assessment Program were the primary data types in the data base. All data were geometrically rectified and transformed to a 50-m Universal Transverse Mercator (UTM) coordinate grid reference.

Model parameters were quantified with arithmetic and statistical integration of multivariate data sets. The resultant model has 10 parameters that identify 3 areas of significant porphyry copper potential, 2 of which are known occurrences. Bouguer gravity anomaly data, residual aeromagnetic data, the ratio of stream-sediment copper to chromium, and geochemical copper data were used to establish regional geologic environments favorable for porphyry copper occurrence. Topographic slope, solar incidence angle, and the ratio of Landsat MSS band 5 (0.6–0.7 μm) to MSS band 4 (0.5–0.6 μm) were used to isolate areas of spectrally defined gossan. Known igneous intrusive bodies, distance to these intrusives, and distance to known mineral occurrences were used to define mineralized centers and to partially reinforce other model parameters.

C.M. Trautwein, J.E. York (Technicolor Graphic Services, Inc.), and D.G. Orr (USGS) conducted field studies in areas in the Nabesna quadrangle that were indicated by the model as having high mineral potential. Rock samples from Orange Hill, Bond Creek, Cross Creek, Horsfeld Creek, and Baultoff Creek were collected for geochemical analysis to test the results of digital data base analyses. All areas indicated by the model as having high potential for copper mineralization were intensely altered.

Improved lithologic separation and data base application

Studies using remotely sensed data to improve discrimination of sedimentary rock lithologies and detection of surficial effects related to subsurface hydrocarbon occurrences are being conducted by G.B. Bailey (USGS), J.R. Francica, J.L. Dwyer, K.M. Walker, D.A. Hastings, and S.K. Jenson (all Technicolor Graphic Services, Inc.), and M.S. Feng (Visiting Scholar, People's Republic of China) in the Uinta and Piceance sedimentary basins of northeastern Utah and northwestern Colorado. Initial results show that Landsat and Thematic Mapper Simulator (TMS) data (acquired by NASA/NSTL over selected areas in the region) can be digitally processed to produce images which permit significantly greater separation of lithologic variation than can be accomplished with unenhanced, false-color Landsat images. Ground-field spectral data (760 wavelength bands between 0.40 and 2.50 μm), collected from more than 200 localities within the

TMS coverage areas, and 760-band airborne spectral data are being used to help design optimal digital processing approaches as well as to calibrate TMS data.

Photointerpretation manual for surface mining inspectors

In cooperation with the Office of Surface Mining Reclamation and Enforcement, D.G. Moore (USGS) and D.O. Ohlen (Technicolor Graphic Services, Inc.) are preparing a self-instructional manual for interpretation of low-altitude photographs of coal surface mines. The manual was designed to be used by Federal and State mine inspectors to identify specific familiar features, problems, and activities associated with a mining operation. Mine features and conditions were identified and described, and aerial photographs illustrating mining problems unique to each coal-producing region within the United States are included in the manual. A contract was awarded to Resource Technologies Corporation of State College, Pennsylvania, to assist in preparing the illustrations and layout of the manual.

Side-looking airborne radar program

The Survey's side-looking airborne radar (SLAR) program, which was initiated in fiscal year 1980, involves evaluating the technology for geologic (including hydrologic) and cartographic applications. During 1980 and 1981, SLAR data, including multilook and stereographic coverage, were acquired for approximately 155,400 km^2 in the Alaska Peninsula and in northern Alaska. During 1981, the Survey completed 20 research projects and published a summary report of these investigations (Moore and Sheehan, 1981). The studies showed that radar images are useful for geologic mapping and resource surveys, particularly for mineral and petroleum exploration, and are also useful for geologic site studies and hazard mapping. The studies concluded that radar images, although best suited as a supplemental information source, may be used as a primary data source in areas of persistent cloud cover.

LAND RESOURCE APPLICATIONS

Landsat applications for soil-vegetation inventory

The Bureau of Land Management (BLM) is responsible for the management of approximately 100 million hectares of arid and semiarid lands in the Western United States. The Federal Land Policy and Management Act of 1976 requires current resource

inventories to be maintained on public lands. Costs of inventorying soil and vegetation resources have escalated rapidly and have become a major constraint on the amount of land that can be inventoried each year.

W.J. Bonner (BLM) and R.H. Haas, W.A. Miller, E.H. Horvath, and J.A. Newcomer (all of Technicolor Graphic Services, Inc.) initiated a cooperative project to investigate the potential of using Landsat MSS data and other digital data to map ecologically significant soil-vegetation landscapes called site write-up areas. A digital data base was assembled for the Grass Creek Resource Area (594,000 hectares), Worland District, in north-central Wyoming. Landsat MSS data from June 1978 soil boundaries, digital terrain data, and digitized administrative boundaries were registered to a common 50-m UTM grid base.

The Landsat data were stratified into four spectral classes and training statistics were developed for each strata using unsupervised clustering techniques. The resulting 94 spectral classes were aggregated to represent 21 plant community types based on a physiognomic vegetation classification framework. Digital terrain data were used in postclassification procedures to eliminate confusion among spectral classes.

The 21-class-present vegetation digital map and digitized soil and allotment boundaries were used to delineate and map ecologically significant soil-vegetation landscapes. Eight sets of decision rules were developed for aggregating vegetation classes within 32 dominant range sites (derived from soils data). The resulting 42 vegetation group classes were subsequently mapped within soils boundaries and output as 1:24,000-scale transparent overlays for 7.5-minute quadrangles. Two methods were evaluated for producing the final site write-up area maps. The final mapping of vegetation groups within soil boundaries was performed manually in one method and by software developed by D.D. Greenlee (USGS) and J.W. Feuquay (Technicolor Graphic Services, Inc.) in the second method.

Although a final evaluation remains to be completed by BLM, a preliminary field evaluation of the products supports the following conclusions:

1. Digital soils data and vegetation information derived from Landsat MSS data can be used for mapping ecologically significant soil-vegetation landscapes.
2. Misclassification of present vegetation, caused primarily by variations in the amount of ground cover within plant community types, did not adversely affect site write-up area delineation.
3. Maps of ecologically important soil-vegetation landscapes can be produced for less than 20 cents per

hectare. The resulting digital data base also forms an important information source for post-inventory land management activities.

Estimating rangeland plant cover proportions with large-scale color-infrared aerial photographs

C.J. Van Zee (Technicolor Graphic Services, Inc.), in cooperation with K.G. Bonner (U.S. Forest Service), studied rangeland plant cover using a double sample of photograph and ground plots. The study was conducted in an open shrub/grassland area in northeastern California. Field data were collected 2 weeks before photograph acquisition. Color-infrared aerial photographs were acquired at scales of 1:1,200 and 1:1,500 on August 3, 1980. Fifty plots were interpreted for 12 rangeland plant cover classes and 25 of these plots were used for collecting ground data. Field and photointerpretation data were summarized by calculating percent occurrence per plot for each of the 12 cover classes. A regression model was constructed by using one cover class as the base model with a corresponding indicator variable and a cross-product variable for each of the remaining 11 classes.

Resolution of the photographs at these very large scales was adequate for accurate identification of major shrub species. Nine-inch format photographs proved excellent for locating previously marked ground plots. A 92 percent correlation was found between photograph and ground measurements of cover when all 12 cover classes were considered simultaneously in multiple regression analysis (Van Zee and Bonner, 1981).

Using aircraft and satellite acquired data to estimate food available to refuge waterfowl

The Iowa Cooperative Wildlife Research Unit of the U.S. Fish and Wildlife Service (USFWS) has been conducting a long-term research project to study the behavior and energetics of migrating snow geese in relation to various environmental factors, particularly the amount of food available in agricultural fields. Part of this study, completed by W.H. Anderson (Technicolor Graphic Services, Inc.), evaluated the use of remotely sensed data to monitor the changing quantity of food within the feeding territory of snow geese utilizing the DeSoto National Wildlife Refuge near Omaha, Nebr. Estimates of agricultural cover type (unharvested and harvested crop, plowed fields, etc.) were derived from Landsat data and aerial photographs and were combined with ground estimates of waste grain per unit area to estimate total available food within the 379 hectare study area. The regression

estimation procedure resulted in less than a 0.05 percent sampling error, well within desired limits. The techniques developed for this project are directly applicable in other refuges where timely and reliable information is desired about the food supply for waterfowl.

Utility of a digital data base for improving Landsat classification results and managing a forested wetland

The USGS Water Resources Division, Northeast Region, previously used Landsat multitemporal data to map vegetation in the Great Dismal Swamp, Virginia/North Carolina. The resulting map was less accurate than desired. Recent research has demonstrated that Landsat classification can be improved by incorporating ancillary data (Miller and others, 1981). Multiple data sets, when registered to a common map base, can be manipulated by using geographic information system techniques to provide resource managers with an improved resource map.

In a cooperative EROS Office/Water Resources Division project, S.P. Prisley (USGS) and W.A. Miller (Technicolor Graphic Services, Inc.) developed a digital data base for the Great Dismal Swamp. January 1978 Landsat data, photointerpreted vegetation classes, ground surface elevations, organic soil (peat) depths, and road, ditch, and refuge boundary locations were registered to a common map projection (50-m UTM grid). Landsat data were classified by using unsupervised classification techniques (1) without spectral stratification or discriminant analysis reclassification, (2) with spectral stratification only, and (3) with spectral stratification and discriminant analysis reclassification. Photointerpreted vegetation data compiled by Carter and Gammon (1976) were used to aggregate the results of the three classification approaches into vegetation categories specified by Water Resources Division and to determine classification accuracy for each of the three approaches.

Classification accuracy was improved by incorporating spectral stratification and discriminant analysis reclassification techniques into the classification process, but the resulting classification accuracy and level of detail required by refuge managers was still limited. However, when the photointerpreted vegetation data (rather than the Landsat data) were used with other elements of the digital data base, invaluable information was supplied to the refuge managers to support specific management activities. Thematic maps are being used in the improvement of wood-duck habitat and in the control of the eastern forest tent caterpillar. As additional information was added to the data base, the refuge managers began to realize

fully its potential for providing decisionmaking information quickly and economically.

Accuracy assessment of Landsat-derived Arizona wildland vegetation map

D.S. Linden and John Szajgin (Technicolor Graphic Services, Inc.) developed a cost-effective sampling design (Linden and Szajgin, 1981) to evaluate the Landsat-derived wildland vegetation map for Mojave County, Ariz., produced by W.G. Rohde (USGS), W.A. Miller (Technicolor Graphic Services, Inc.) and BLM personnel in 1980. The sample design consisted of a stratified two-phase cluster sample with equal probabilities of selection within strata (Cochran, 1977). The strata were defined by the eight hierarchical level II vegetation classes represented in the map. Phase I consisted of interpretation of large-scale (1:2,000) natural-color aerial photographs of 160 three-by-five-pixel sample clusters. Classification accuracy was estimated by comparison of photointerpretation classification with the corresponding Landsat digital classification. In Phase II, ground data for a subsample of 80 clusters were used to refine the accuracy estimate. A least-squares method was used to develop a regression relationship between photointerpretation accuracy estimates and ground data accuracy estimates. Overall accuracy of the vegetation map was estimated at 64 percent with a standard error of 2 percent.

Mapping forest fuels and predicting wildland fire behavior

M.B. Shasby (Technicolor Graphic Services, Inc.) and R.R. Burgan (U.S. Forest Service) investigated the impact of using digital terrain tape (DTT) data produced by the Defense Mapping Agency to map forest fuels and predict fire behavior. A previous study (Shasby and others, 1981) proved that a spatially registered digital data base containing DEM data and Landsat MSS data could be used to map forest fuels and provide forest managers with real-time predictions of fire behavior for a test site in the Lolo National Forest. DEM data are available for relatively few specific areas; therefore, to apply these methodologies to large areas, DTT data, available nationally, were tested.

The forest fuels cover map produced when DTT data were incorporated into the Landsat classification process was less accurate than the one produced when DEM data were used (60 versus 73 percent accurate, respectively). Also, the slope estimates derived using the DTT data were unacceptable for use in the mathematical fire behavior model.

Land cover and terrain mapping for the Kenai National Wildlife Refuge using Landsat MSS data

Landsat MSS data acquired in August 1980 were used by Mark Shasby (Technicolor Graphic Services, Inc.) of the EROS Field Office to classify over 1 million hectares of land cover within the Kenai National Wildlife Refuge. Digital terrain data for the project area were registered to the Landsat data and used to calculate the elevation, slope, and aspect corresponding to each Landsat picture element. The land cover, terrain, and surficial geology data were combined within a multiple data base to produce resource maps from each data type and from combinations of each data type. This digital data base was produced for the USFWS as a cooperative project by the EROS Office and the National Mapping Division. The resource maps are being used by the USFWS for comprehensive planning for the refuge as mandated by the Alaska National Interest Lands Conservation Act, 1980. Of particular importance to the USFWS are the water cover and habitat maps produced from combinations of vegetation cover types and terrain variables. In addition, the Alaska Department of Natural Resources (ADNR) is using the land cover data to produce vegetation maps for their resource assessment program.

Land cover and terrain mapping for the Bristol Bay Subregion using Landsat MSS data and digital terrain data

Personnel from the ADNR and the USFWS have used the computer analysis equipment of the EROS Field Office in Anchorage to produce land cover and terrain maps of the Bristol Bay Subregion, an area of approximately 12 million hectares, including all or portions of the Togiak, Izembek, Alaska Peninsula, and Bechar of National Wildlife Refuges. The land cover maps were produced from geometrically corrected Landsat data that have been reformatted for the 1:250,000-scale USGS quadrangles covering the area. Digital terrain data from the quadrangles were registered to the Landsat data to produce elevation, slope, and aspect maps. The elevation and slope data, together with winter Landsat scenes, were used to improve classification accuracy of the land cover maps. The winter Landsat scenes were extremely valuable for clearly separating wetland from conifer cover types. The land cover maps were produced at a scale of 1:250,000 and used by ADNR and USFWS in preparing a comprehensive plan for the subregion as mandated by the Alaska National Interest Lands Conservation Act, 1980. The digital data base, comprised of the land cover and terrain data, was transferred to

the ADNR for further manipulation and production of habitat maps.

Land cover mapping with merged Landsat RBV and MSS stereoscopic images

D.T. Lauer (USGS) and W.J. Todd (Lockheed Missiles and Space Co.) used computer processing techniques to merge Landsat RBV and MSS digital data to form a 40-m resolution, three-channel, color-composite image (Sheehan and Gehring, 1980). Further processing used digital terrain data to introduce parallax into a "left conjugate" image and thus create a stereoscopic image (Batson, Edwards, and Eliason, 1976). These RBV/MSS stereo images were analyzed for information about a wildland area in the Coast Range of California. Interpretations of vegetation types, densities, canopy characteristics, and boundaries were improved when using the RBV/MSS stereo image compared to the MSS or RBV image alone. However, images with a resolution greater than 40 m are needed to consistently detect and identify canopy characteristics related to forest stand structure. The location of, and association between, vegetative features and topography were readily seen on the RBV/MSS stereoscopic pair. Analysis of the RBV image alone produced results on vegetation type and boundary placement nearly as good, but not as quickly, as those derived from analysis of the merged RBV/MSS image.

The results of the work reported by Lauer and Todd (1981) suggest that data acquired from the proposed Mapsat sensors, the planned Thematic Mapper on Landsat D, high-resolution visible imaging instrument on the French SPOT (Système Probatoire d'Observation de la Terre) Satellite, and Large Format Camera on the space shuttle will allow improved classifications of forestlands using visual interpretation techniques, as compared to classifications performed using data currently available from Landsats 1, 2, and 3.

Sioux Falls area geographic analysis

J.A. Sturdevant (Technicolor Graphic Services, Inc.) conducted a cooperative project with three Sioux Falls, S. Dak., area planning agencies to demonstrate the application of remote sensing and geographic data base techniques to land management problems in the Sioux Falls area. The specific objectives were to develop (1) a rural land use inventory using interpretation of aerial photographs, (2) a geographic digital data base consisting of land use, soils, and slope data, and (3) maps and statistics describing physical limitations of rural land to development.

Sioux Falls area planners interpreted USGS Level II and Level III land use categories on color-infrared, 1:24,000-scale aerial photographs. The interpretations were digitized, registered to the UTM coordinate system, and converted to digital images consisting of 50- by 50-m grid cells. Similarly, digitized soil and slope data were input to the data base.

The digital land use, soils, and slope data were composited to produce images and statistics describing limitations of rural land to septic tank operation, dwelling unit construction, road and street construction, and agriculture (Sturdevant, 1981a and 1981b). The products are currently being used by Sioux Falls area planners to formulate long-term plans and to aid in public hearings and planning commission meetings.

Using principal components analysis to monitor arid land change

A.S. Walker applied principal component analysis to Landsat data to monitor arid lands in the Turpan Depression, a 50,000-km² fault-formed interior drainage basin in Xinjiang Autonomous Region, People's Republic of China. The depression is named after Turpan County (43° N., 89° E.), in the north-central part of the basin and is bounded on the north, east, and west by the Tian Shan.

Principal component analysis is a technique developed to reduce redundancy in digital Landsat data by rotating the axes into principal component axes which maximize variance in the data. The transformation is determined such that the largest possible amount of the total variance is contained in the first principal component; the second component contains the largest possible amount of the remaining variance, and so on (Jenson and Waltz, 1979). For this study, principal components were calculated for 1976 and 1972 Landsat images of a subscene of the Turpan Depression. The second principal component contained information most readily associated with vegetation.

By using the additive properties of filtered light, changes in arid land characteristics were readily observed by displaying the second principal component of 1976 data in green light and the second principal component of 1972 data in red light. With this color combination, black and yellow (a result of green light added to red light) indicate areas which have not substantially changed. The red rim around the black area, however, indicated where the farmland had increased during the 4 yr. The observed increase in cultivated land has been verified by field work. The occasional areas of green in the oasis represent areas where vegetated land has decreased. This technique thus shows changes in vegetated area.

APPLICATIONS TO GEOLOGIC STUDIES

Paleoshorelines in the Point Lookout Sandstone, San Juan Basin, New Mexico

Landsat images reveal several parallel linear features as much as 17 km in length and 0.7 km in width on the Upper Cretaceous Point Lookout Sandstone capped mesas 32 km northeast of Gallup, N. Mex. Detailed studies by R.S. Zech of sections normal to the linear feature show it to be an exhumed paleoshoreline containing a range of depositional environments and abrupt linear pinchouts of well-sorted coastal barrier sandstones into carbonaceous shales and fluvial sandstones of the overlying Menefee Formation. All of these linear elements have contrasting resistance to erosion and control modern drainage normal to the regional drainage. The resulting trellislike pattern makes these linear features easily discernible on aerial photography and Landsat images. The rapid lithologic and thickness changes of the upper Point Lookout Sandstone in these features provide an excellent example of a stratigraphic trap for hydrocarbon accumulation which may occur in similar features deeper in the basin.

Analysis of Landsat linear feature data of southern Colorado Plateau

Statistical analysis of 6,050 linear features mapped from Landsat images of the Colorado Plateau south of 38° N. by D.H. Knepper, Jr., revealed three important trend intervals: N33-59 W, N10-16E, and N35-72E. These intervals could be further subdivided on the basis of the shape of the strike/frequency curve. Contour maps of the concentrations of linear features in the major intervals and subdivisions helped define 20 lineaments in the region. One northwest-trending lineament is a prominent boundary between high and low concentrations in the southwestern part of the area. The remaining lineaments are defined by clusters of parallel linear features. Preliminary evaluation indicates that some of the lineaments are spatially related to the distribution of uranium deposits in the region. The nature of this relationship has not been determined.

Identification of altered minerals by using airborne spectral reflectance

L.C. Rowan made high spectral-resolution reflectance measurements in Nevada by using an airborne spectrometer designed and operated by William Collins of Columbia University. Results indicate that some common alteration minerals can be identified on

the basis of spectral absorption bands in the 1.5 to 2.5 micrometer region. The system records reflected solar radiance in 64 channels in the wavelength region, and base-sighted color photographs are acquired simultaneously for location purposes. The minerals which have been identified thus far include alunite, jarosite, kaolinite, montmorillonite, and calcite. These results suggest that alteration zones can be mapped by using this nonimaging system and that very detailed mapping of mineralogical variations could be achieved by using high spectral-resolution images.

Landsat studies of uranium settings, Australia and France

Computer-enhanced Landsat images were used by G.L. Raines for mapping linear features in an area of huge unconformity-vein uranium deposits in northern Australia and in a granite area containing uranium vein deposits in France. Synthesis of this data, together with results of similar studies by other investigators in Canada, Sweden, and England, resulted in an hypothesis of structural control in each area. Analysis of linear-feature distributions, with respect to local sequences of tectonic and mineralization events, suggests that a single dominant structural direction at time of mineralization was the major influence on distribution of uranium deposits in each area. Field work in Australia and France provided more detailed information that supports the hypothesis.

Thematic mapper detection of hydrothermal alteration in Marysvale, Utah

Detailed field sampling of rocks was done by M.H. Podwysocki and D. Segal in the Marysvale, Utah, mining area. These samples are being analyzed in the lab for (1) their spectra between 0.4 and 2.5 micrometers, (2) the hydroxyl-bearing portion of their mineral content, and (3) their total iron content. Selected samples are also being analyzed for their ferric iron content. These data will be used in an attempt to relate the intensity of absorption bands caused by the presence of ferric iron and hydroxyl-bearing minerals to band ratios created from airborne multispectral scanner data collected for the area.

Preliminary analysis of airborne Thematic Mapper Simulator multispectral scanner images for Marysvale, Utah, shows that many areas of zeolites and argillic sediments are initially confused with areas of hydrothermally altered rocks. Work will continue to numerically define the values of the 1.6 micrometer to 2.2 micrometer ratio that are related to each type of argillic rock.

Remote sensing in vegetated areas

Dennis Krohn, Nancy Milton, and Don Segal are conducting research in microwave remote sensing to learn how to develop techniques for applying radar images to geologic problems, particularly in vegetated areas. Radar data in digital form greatly extend the ability to enhance the images and to understand the complex microwave backscatter from vegetation. The USGS contracted and flew, in conjunction with A.W. England from NASA, a digital radar mission over eastern Virginia on June 24-June 28, 1981. The WB-57 aircraft flew an X-band synthetic aperture radar with two look angles and two polarizations supplemented by selected areas of color infrared photography. Digital correlation for selected areas is presently being completed at Johnson Space Center. Preliminary optically-correlated X-band (3 cm) radar show some interesting comparisons to digitally-correlated L-band (25 cm) radar from Seasat. Over lowland areas, the X-band data have a lower dynamic range than L-band, which supports the hypothesis that the large increase in signal strength, up to 5 db, may result from interaction of vegetation canopy and standing water surface. In upland areas, loblolly pine forests appear darker than neighboring deciduous and coniferous forests, which appear as diffuse scatterers. These observations contrast with results from Seasat where Virginia pine forests appear brighter than neighboring deciduous and coniferous forests. The specificity of different wavelength radars to individual tree species suggests that some consistent interaction mechanism, which might be applied in other areas, is occurring between radar signal and tree canopy.

Method to improve reproducibility of Landsat color images

J.S. Duval has developed a method to improve the reproducibility of Landsat color images. This method uses film transfer functions to ensure that a given set of data values for the primary colors (red, green, and blue) will always produce the same resultant color. The transfer functions are calculated by using analytical equations that represent the relation between data values and film density measurements. By using film transfer functions defined in the same way, different film writing machines can be made to produce visually identical film products. The film transfer functions also make it possible to control image contrast and exposure in an objective manner. The development of the transfer functions also led to the development of procedures for overall quality control for the image-making process.

Geologic mapping with HCMM data in the Powder River Basin, Wyoming and Cabeza Prieta, Arizona

Kenneth Watson, Susanne Hummer-Miller, and T.W. Offield (1981) have shown that the experimental thermal satellite, HCMM (heat capacity mapping mission), has provided unique thermal data for mapping geologic features and exploring for energy resources and mineralized areas. Using a new thermal-inertia mapping algorithm which provides greater discrimination capability than those in current use, they have examined data of two areas: Powder River Basin, Wyoming, and Cabeza Prieta, Arizona. Results include discrimination of igneous rocks, delineation and subdivision of geologic units, detection of tectonic framework elements, and demarcation of anomalies coincident with areas of helium leakage. The most important results have been the discovery of two linear features associated with thermal-inertia contrasts. In the Powder River Basin, a feature not on existing geologic maps and not detected on Landsat images appears to reveal a basement discontinuity which involves the famous Homestake Mine in the Black Hills, a zone of Tertiary igneous activity, and facies control in oil-producing horizons. A feature in Cabeza Prieta, initially seen on an image formed as a difference of two thermal-inertia images, was found to be the extension of a bilaterally symmetrical aeromagnetic feature which trends northeast for a distance of at least 1,200 km.

Aerial infrared surveys at Mount St. Helens, Washington

Thermal infrared observations by H.H. Kieffer, David Frank, and J.D. Friedman (1982), and J.D. Friedman, David Frank, H.H. Kieffer, and D.L. Sawatzky (1982) were begun on March 30, 3 days after the first 1980 Mount St. Helens eruption. The objectives of these observations were hazards prediction, identification of enhanced heat flow that might precede a flank eruption, and quantitative measurements of the thermal changes associated with the sequence of eruptive events.

Aircraft-based instruments used included: film-recording uncalibrated scanners, moderate- and very high-resolution video-recording systems, handheld imaging systems and radiometers, and calibrated digitally recording scanners. March 30 observations showed anomalous heat in the summit crater, locally along the southern bounding fault of the newly developed summit graben, in two large fractures in a region of historic thermal emission on the upper north slope that later became the bulge, and at the other historic thermal area high on the southwest slope. In the area

of the bulge, infrared anomalies increased in abundance from early April until just prior to the May 18 eruption, when the upper part of the bulge appeared to be perforated by heat leaks of a few to 100 m lateral extent. All these areas of excess thermal emission were removed by the May 18 eruption. During periods between eruptions, excess thermal radiation from the summit of Mount St. Helens on May 16 was approximately 3 MW. The traces of the first two May 18 landslide failure surfaces were through clusters of thermal anomalies.

Qualitative infrared images in the 8- to 11.5- and 8- to 14-micrometer spectral region were obtained over Mount St. Helens by forward-looking and vertical-mount aerial scanning systems on May 31, June 3, 6-8, 19, and July 15, 1980. Quantitative or calibrated images were obtained August 11-13, 19, and 20. Night and predawn images, obtained during times of diurnal surface-temperature minima, depict the spatial pattern of high thermal emission associated with the crater and vent area on June 7 and 8. Following the eruption of June 12, the emergence of a dacite dome was confirmed by radar images on June 13, and subsequently on June 15 by visual observation. The infrared images of June 19 show a concentric and annular distribution of thermal emission associated with the emergent dome. On June 19 the emergent dome, the rampart, and a southeast-striking fracture controlling alignment of fumaroles within the crater floor area were studied in detail by three different scanning systems. A large circular area also appeared in the images of June 19 southeast of the dacite dome; the area was about equal in size to the dome and was outlined by a ring of fumaroles. Infrared images of July 15 show the annular and radial fracture pattern of the dome prior to its destruction on July 22. An en-echelon set of northwest-striking fractures in the crater and amphitheater region was also clear on the July 15 image. These fractures were related to the location of the first and subsequent lava domes and at least two of three smaller hot spots. The calibrated surveys of August 13-17 gave the temperature of the partly cooled rind of the August dome and the day-night temperature differences of an array of pyroclastic-flow deposits, as well as the temperature of Spirit Lake, several secondary phreatic fumaroles, and surrounding terrain.

Tectonic implication of lineaments in the northern Paradox Basin, Utah and Colorado

J.D. Friedman, S.L. Simpson, and J.E. Case report that computerized rose diagrams were prepared uniformly from azimuthal histogram plots of

several thousand lineaments of the Moab 2 degree quadrangle, permitting detailed statistical comparison of Landsat MSS lineaments trends and those of magnetic-field and gravity-field lineaments and fault fold-axis strike trends.

A good correlation, statistically more than coincidence will allow, was found to exist between major Landsat lineaments, magnetic- and gravity-field lineaments, fold northwest axes, and northwest fault trends. A similarly good correlation exists between the first-order surface azimuthal trends of all lineaments mapped from Landsat and a Precambrian structural discontinuity trending northeast and mapped in the magnetic and gravity fields. This Precambrian structural discontinuity may be on a strike projection of the pre-Sinyala fault system of northern Arizona.

The good correspondence of azimuthal trends of magnetic and gravity lineaments, presumably of Precambrian basement origin, and surface lineaments and mapped faults suggests that equivalent structural patterns are likely to be present in the intervening Phanerozoic sequence. The post-Sonoman, Laramide, and possible Pleistocene age of the above-mentioned faults (dating based on stratigraphic cutting relations) supports this conclusion. The surface lineaments and faulting are thus interpreted to represent Precambrian basement-controlled structures in the younger Phanerozoic cover. The major lineaments mapped (those longer than 20 km) show the best azimuthal correlation with lineaments of the magnetic field and mapped northwest-striking faults and fold axes and probably represent deep and long-lived faults in the Earth's crust.

The laccolith cluster of the La Sal Mountains and several circular features occur at intersections of some of the major northwest and northeast lineaments of the Paradox Basin and are thus of special tectonic significance. Circular features such as Lockhart Basin, below which salt solution and subsidence of the overlying sequence of elastic rocks has occurred, may represent the negative analog of salt diapirism and laccolithic intrusive activity in the Paradox Basin. Surface faulting, such as fault clusters of en-echelon character, that lie astride the northeast-trending Precambrian structural discontinuity, may thus have played a significant role in halokinetic processes of salt flowage dissolution.

Landsat hydrothermal alteration mapping of Richfield—CUSMAP

The remainder of the Richfield 1 by 2 degree quadrangle has been field checked by M. Podwysocki and D. Segal for hydrothermally altered rocks by

using a map of limonitic materials as a guide for locating prospective areas. The map was derived from a digital classification of Landsat band ratios. Numerous small areas of mineral shows were not detected because of (1) the relatively coarse resolution (approx. 80 m) of the satellite scanner; (2) the lack of telltale limonite staining at the locality, or (3) the presence of vegetation masking the alteration. However, some localities which contained highly limonitic rocks did show through as much as 40 percent vegetation cover.

To make the map of alteration more comprehensive, all occurrences of lithophile, base, and precious metal mineralization, derived from the USGS CRIB data base, also were examined. Those occurrences which did not correspond to any detectable alteration as determined from the Landsat classification or prior geologic mapping were added to the map. A number of these localities were field checked.

Nearly all the altered volcanic rocks examined were in the argillic or advanced argillic category of alteration, with minor amounts of silicified and sericitized altered rocks. Propylitically altered rocks were not included in the map because of the pervasiveness of this alteration type. Sericitic alteration occurs primarily at the boundary or within several igneous intrusive stocks. Several occurrences of skarns and contact metamorphic marbles along the boundaries of intrusives also were noted. The argillic or advanced argillic phases of alteration appear in a number of cases to be related to the uppermost levels of volcanic extrusive complexes with known or inferred intrusive bodies at depth.

Structural analysis—Valley and Appalachian Plateau, Pennsylvania

Field studies of structural geology in the Appalachian Plateau and Valley and Ridge provinces in Pennsylvania by H.A. Pohn and T.L. Purdy have substantiated several existing concepts and generated new ideas concerning Appalachian tectonics. Field observations suggest that almost all structures are scale independent. Virtually every structure seen in seismic section or in megascopic map scale can also be seen in mesoscopic, or even microscopic scale; the reverse is usually, but not always, true. Only two kinds of thrust faults are present in the study areas—uplift thrusts, which are a specific type of ramp fault, and overcore faults, a specific type of detachment fault. Both types of structures are related to the formation of anticlines.

Observations further indicate that contrary to current concepts, most of the thrust faults in the Valley and Ridge and the Appalachian Plateau provinces precede or are contemporaneous with the associated

folds. Two lines of evidence support this idea. First, the anticlines which form through buttressing in the hanging walls of ramp faults do not have associated synclines in the foot walls. Synclines should occur if the folding preceded the faulting (structures related to prior faulting may be present in the foot walls). Second, in a regional sequence of multiple folds and faults, if folding preceded faulting the folds in both the hanging walls and foot walls should have similar amplitudes and wavelengths. Field observations, however, indicate that folds in the hanging walls are generally of considerably different amplitude and wavelengths than folds in the foot walls.

A majority (perhaps up to 80 percent) of thrust faults in the region studied are paired or multiple faults. In each case where a time sequence has been deciphered, the younger faults progress into the hanging walls. In the process in which paired faults or multiple faults are formed, the strata between the faults usually become highly deformed and folded. These disturbed zones have been called drag folds, disturbed rocks, or highly faulted and folded rocks, but they have not been mapped as zones of faulting. Two lines of evidence indicate that these disturbed zones are bounded by pairs of faults. First, the zones are linear, usually a few tens to hundreds of meters wide and kilometers to tens of kilometers long, and they occur in otherwise undisturbed sequences of rocks. These long and narrow zones could not be formed by a mechanism other than buttressing against faults. Second, seismic sections in southern Pennsylvania show subsurface faults that, when extended, are coincident with the disturbed zones mapped at the surface.

Disturbed zones are common within the section from the lower paleozoic carbonate sequence to the thick Devonian sandstones of the upper part of the Lock Haven Formation, equivalent to the Foreknobs Formation in southwestern Pennsylvania. Lithotectonic units (brittle versus ductile units as controls to ramp and detachment faults) do not necessarily control disturbed zones. Disturbed zones are more common in ductile units, but they have been noted in thick brittle sequences where these are the only rocks available.

Disturbed zones, due to the nature of the intense folding and faulting, produce areas of high fracture porosity which should be excellent gas traps where the zones are present in the subsurface.

Thermal energy yield of Mt. St. Helens

The heat content of the dacite dome of June 1980 was estimated by J.D. Friedman, G.R. Olhoeft, G.R.

Johnson, and D. Frank (1982) from laboratory measurements of thermophysical properties, supplemented by published data on latent heat of fusion. A crystallization temperature of 970°–990°C was inferred from melting experiments and Fe-Ti-oxide geothermometry (Melson and Hopson). The volume of the visible dome was estimated to be 4.6×10^6 m³ from vertical aerial photographs. The thermal energy of the visible dacite dome was 1.5×10^{16} J, calculated from data on volume, crystallization temperature, bulk density (2.2 g/cm³), specific heat (1.059 J/g/K), latent heat of fusion (350 J/g), and heat content (1.385 J/g for solid dacite and 140 J/g for associated volatiles). Including inferred subsurface dome material above the conduit, the total energy would be approximately 3.4×10^{16} J. Eruption of the dome was comparable to an eruption of intermediate magnitude, intensity III+ on the Tsuya scale, or intensity IV+ on the Hedervari scale. The total thermal energy released at Mt. St. Helens between May and October 1980 was estimated conservatively at 1.2×10^{16} J, about 93 percent of the total released during this period.

Additions via domal growth to the earlier 1980 volcanic eruption energy bring the cumulative energy yield from May 18, 1980, through April 1981 to about 1.4×10^{25} ergs. Volcanic power was expended from June 12, 1980, through April 1981 at a rate of 2.3×10^3 megawatts, on the basis of steady-state eruption conditions. This represents May 18, 1980, through August 13, 1980 (which was 4 to 10×10^3 megawatts). The gradual change in eruption style from explosive eruptions to generally nonexplosive dome growth may thus correspond to the reduction in volcanic power.

APPLICATIONS TO HYDROLOGIC STUDIES

Real-time data processing

The Water Resources Division is improving its capabilities to process hydrological data received from WRD data collection stations by means of NOAA's Geostationary Operational Environmental Satellites. During fiscal year 1981, WRD operated the Hydrological Data Real-Time Computer Processing System (Hydrecs) which resides on the USGS's Honeywell 68/80 computer. This system allows WRD district personnel and their cooperators to access hydrological data from sites equipped with GOES transmitters within one hour after the data are transmitted. Hydrecs also automatically forwards the hydrological data into Watstore, the Water Resources Division's National water data base. Hydrecs has two main problems: (1) it requires too many data communication links to obtain

data after the data have been relayed by the satellites, and (2) it is a highly centralized system. A failure of one of the communication links or the Honeywell 68/80 computer makes the data transmitted by satellites inaccessible to all districts. To eliminate these problems, WRD began developing a real-time data processing system that will perform the same functions as Hydrees but will operate on minicomputers and microprocessors operated by WRD districts. A prototype minicomputer real-time processing system will be tested by the Arizona district in June of 1982. This system will connect directly with a satellite receive station that has been purchased by the Arizona district and will permit the district and their cooperators to receive data from sites equipped with GOES transmitters directly from the satellite. These data will be immediately available for processing by the district's own computer, thus enabling them to monitor data collection networks in real time.

Contracted satellite data relay study

The first phase of the contracted effort between the USGS and COMSAT General for the collection of hydrologic data via the GOES was completed January 31, 1982. The 104-site pilot test resulted in several improvements to the data collection platforms, as well as the introduction of the new technology to many water data users in Texas, New England, Pennsylvania, Colorado, and Arizona. The system performed

well with 95 percent of expected data transmissions received and processed. Problem areas included data quality and the high costs (approximately \$1,000.00 per site, per month) for contracted data collection. The second phase of contracted effort with COMSAT General involves approximately 70 hydrologic data collection and water management sites in the Arkansas River basin in central Colorado.

District satellite receive sites

The Water Resources Division of the USGS is deploying local receive sites in Washington, Arizona, and Hawaii to improve satellite data relay operations. The receive sites provide for reduced communications costs, improved reliability, increased control, and faster access to hydrologic data transmitted via the GOES satellites. The Washington (Tacoma) receive site began operations in February 1981, and the Arizona site (Phoenix) started receiving data in January 1982. The Hawaii site is a joint NASA, NOAA, and USGS effort that includes development of a state-of-the-art reception and processing facility that is scheduled to begin operations in March 1982. The first year of operation of the Washington site has been successful in providing real-time data from the streams and rivers surrounding Mount St. Helens. The Phoenix receive site supports the 43-site flood warning network operated by the USGS in central Arizona.

LAND USE AND ENVIRONMENTAL IMPACT

Planning for use of land and its resources should consider the long-term consequences of each type of use to prolong the well being of the society in the future and to protect the integrity of the land and its biota. Three kinds of land use can be distinguished for planning purposes. Reversible land use leaves the land, after use, essentially as it was before; little or no man-induced modification remains. An example of reversible use in the United States is the designation of certain public lands as wilderness. Terminal land use commits the land to a particular use in such a way that an attempt at reversal requires either usage on a time scale that is long compared with the expected life span of the social and political institution or a commitment of resources that is too high for the society to consider worth bearing. Examples of terminal land use are location of metropolises and sites of toxic and (or) radioactive waste disposals. A current source of some social tension arises from the fact that wilderness designation appears to assign a terminal-use status by legislative fiat, whereas in fact the land is being used reversibly. Between these two extremes, the bulk of the land use is sequential; each use of land changes its potentials and configurations and these changes are mainly irreversible. One goal of geologic input to land-use planning is to identify the various pathways along which a given land may be used in order to extract the greatest benefit to society with least harm to the land and its life. However, all planning formats must be considered in deciding how the land should be used, and both internal and environmental costs need to be included in the planning. Predictive methodology for land-use planning and for estimations of uncertainties must be developed to allow for the needs and consequences of both land use and land recovery.

Land-use decisions involve value judgment and are problems without technical solutions, but they require technical input, and earth scientists have a major role to play in both providing the input and in pointing out the implications of alternative decisions.

LONG RANGE PLANNING

Work was initiated on this subject in the form of a cooperative agreement with Virginia Polytechnic Institute and State University. A series of activities were carried out that produced 20 background papers and working papers, which were prepared in conjunction with meetings and discussions with persons involved in the long-range planning process. A 3-day workshop for USGS Water Resources Division personnel was

held, at which the group dynamics technique of meeting facilitation was introduced as an aid to achieving consensus on goals and issues to be investigated.

The monograph series instituted by Virginia Polytechnic Institute produced six reports. C.W. Steger (1981a, b) completed two reports on an introduction and summary of long range planning. R.C. Stuart (1981) completed a survey of strategic planning in Federal agencies. J.W. Dickey (1981) completed a computer model to analyze and integrate trends mathematically. T.D. Fuller (1981) completed the trends report on population, and John Randolph (1981) completed the one on energy trends.

An explanatory planning study was also undertaken in cooperation with the USGS Conservation Division. A report was produced by Dames & Moore (1981) that includes global and national long range trends in population and natural resource consumption, alternative hypothetical scenarios of future events, and priority planning concerns involving oil and gas production, coal, oil shale, uranium, geothermal, and non-fuel minerals development.

E.T. Smith and D.W. Moody (1980) prepared a paper on alternative futures studies that was presented at the American Water Resources Association conference. This study described four components of long range planning: futures studies, goal development, alternative scenario planning, and model formulation. The methods of scenario building were covered, including the use of factors that act to cause change in conjunction with impact areas that show the effects of change. The use of mathematical models was discussed as a technique to provide quantitative estimates of the variables that form the trends and forecasts in future scenarios.

ENVIRONMENTAL IMPACT STUDIES

Simulations of seabird damage and recovery from oilspills in the northern Gulf of Alaska

An oilspill trajectory analysis was performed for Proposed Outer Continental Shelf Lease Sale 55 (Northern Gulf of Alaska) to analyze the probability of spill occurrence, likely movement of the spills, and the locations of biological resources vulnerable to oilspills. Ecological damage assessment and recovery of glaucous-winged gulls and common murrelets in the northern Gulf of Alaska was approached in two ways:

1. Oilspill contacts were simulated in Monte Carlo fashion for a large number of simulated lease life-

times (a lease lifetime is defined as the number of years oil production will occur). Oilspill contacts to seabird colonies, during the lease lives, were randomly sampled according to their probability distribution. Population effects were modeled according to a specified growth curve.

2. Damage and recovery for a specific number of oilspill contacts were calculated to examine the sensitivity of the population model to growth and mortality parameters.

If an oilspill contacts a colony of gulls, reducing the population by 50 percent, the population is expected to recover to its prespill level in about 20 years. For common murrelets this same situation yields a recovery time of approximately 70 years. If oil is found and if each oilspill contact causes a fractional population loss of 0.95, on the basis of the expected number of oilspills to occur and contact these colonies during the lease lifetime the probability of reducing the population to some fraction of its initial level was calculated. For gulls, only a 10 percent chance of population reduction to less than one-half the prespill level was calculated for the lease lifetime. For murrelets, only a 4-percent chance of similar reduction was calculated.

A comparative study of change and disorganization in energy development communities of the Great Plains

R.R. Reynolds, Jr. (USGS), J.G. Thompson (Western Research Corporation), K.P. Wilkinson (Pennsylvania State University), and L.M. Ostresh, Jr., (University of Wyoming) participated in a four phase cooperative project designed to develop and validate, to the extent possible, a systematic framework for determining the nature and extent of the social effects of energy development on communities in the western Great Plains. The first phase is completed, as are major aspects of the second phase. The first phase has

involved critical explication of the western "boomtown" social science literature in order to identify key theoretical assumptions, propositions, and prevailing assertions. This assessment revealed that the literature offers a number of suggestive propositions, but apparent biases of the researchers have limited the range of fruitful theoretical development, the result being premature conclusions without adequate empirical evidence (Wilkinson and others, 1980). The prevailing hypothesis/assertion is that energy development-induced increases in scale of place and (or) rate of growth are disruptive to community social organization and this in turn results in a wide range of personal and interpersonal maladjustments reflected in accelerated divorce rates, crime rates, child abuse, welfare dependency, substance abuse, suicide, etc. Much of the literature also dwells heavily on negative effects, i.e., disruption, and has little to say about the potential positive effects of development.

The second phase of the project has been designed to test hypotheses in the literature regarding energy development-related social change. Results in several project analyses conducted to date suggest that community level social organization change is probably more limited in scope and transitory in effect than most of the literature developed in the region has suggested (Ostresh and others, 1981). Moreover, changes in the rates of disruptive behavior and instability in relationships, to the extent it actually occurs, may not be directly attributable to population growth rate and (or) change in scale of community associated with energy development (Wilkinson and others, 1980).

Further empirical analysis together with specification and testing of alternative theoretical frameworks for conducting and organizing balanced social impact input to environmental impact assessments is anticipated in the third phase of the project. The final phase will consist of a statement of research and policy action recommendations.

INTERNATIONAL ACTIVITIES IN THE EARTH SCIENCES

The USGS carries on an international program which in part is an extension of its mandated domestic program and in part is undertaken in support of United States foreign policy goals. The international activities include a variety of studies or investigations that can be categorized as follows: scientific and technical assistance to developing countries, accomplished under the sponsorship of other agencies or host governments; training of participating foreign nationals; topical resource studies of various areas around the world; scientific cooperation and exchange in support of domestic programs; and representational duties in international congress, conferences, and unions.

The number of personnel assigned overseas and their fields of expertise are given in table 3. Results of the overseas studies are made available to the sponsoring countries and (or) agencies and most such data are released to the public through formal publication and (or) open files. The country involved, type of publication, and number of reports prepared in FY 1981 are given in table 4. Since 1940, more than 3,160 technical and administrative documents describing USGS international work have been authored or their preparation closely supervised by Survey personnel. During FY 1981, 100 administrative reports were issued and a total of 63 reports and maps were published.

TABLE 3.—*Technical assistance provided by the USGS to other countries during FY 1981*

Country	USGS personnel assigned to other countries			Scientists from other countries trained in U.S.	
	Number	Title	Type of Program ¹	Number	Field of Training
Latin America					
Argentina	3	Geologist	A, B	1	Geological interpretation
	1	Geophysicist	B	2	Remote sensing
	1	Physical scientist	A		
Brazil	2	Geologist	A	1	Geology
	2	Geophysicist	A	1 ²	Geology
Chile				1 ²	Geophysics
				1	Hydrology
				1	Aerial radiometric prospecting
				2	Explor. data processing
				1	Geologic interpretation
Costa Rica				2	Remote sensing
				1	Remote sensing
Guatemala	1	Geophysicist	A	1	Remote sensing
Guyana				1 ²	Mineralogy
Honduras				1	Remote sensing
Mexico	3	Hydrologist	A, B	1	Data processing
	5	Geologist	A, B	4	Remote sensing
	2	Geophysicist	A		
	2	Res. chemists	A		
Panama	1	Geophysicist	A		
Peru	2	Geologist	A		
Venezuela	1	Geologist	A		
Africa					
Algeria	1	Geologist	A		
Benin	1	Physical scientist	C		
Botswana				1	Surface and ground-water hydrology
Egypt	2	Geophysicist	A	1	Paleomagnetism
	3	Geologist	C	3	Remote sensing
	1	Cartographer	C	1	Ground-water studies and mgmt.
				1	Geophysical elect. meth.
			1	Spectrographic analysis	
Ethiopia				1	Hydrologic techniques
Gambia				1	Hydrologic techniques
				1	Remote sensing

See footnotes at end of table.

TABLE 3.—*Technical assistance provided by the USGS to other countries during FY 1981—Continued*

Country	USGS personnel assigned to other countries			Scientists from other countries trained in U.S.	
	Number	Title	Type of Program ¹	Number	Field of Training
Africa—Continued					
Ghana	--	1	Hydrologic techniques
Kenya	1	Photographer	C	1	Hydrologic techniques
Lesotho	--	1	Digital image processing
Libya	--	1	Remote sensing
Morocco	--	2	Remote sensing
Nigeria	--	9	Remote sensing
				1	Hydrology/hydrogeology
				2	Geological interpretation
				1	Hydrology
				6	Hydrologic techniques
				2	Preparation of thematic maps
				1 ²	Petroleum geology
Sierra Leone	--	1	Remote sensing
Swaziland	--	1	Hydrologic techniques
Tunisia	1	Cartographer	C	1	Remote sensing
	1	Photo. technician	C		
Near East and South Asia					
Bangladesh	2	Geologist	A	1	Techniques of data processing
	1	Geophysicist	A	1	Hydrologic data processing
				1	Hydrogeologic equipment
				1	Quantitative evaluation of ground-water resources
				1	Water balance
				1	Organization & maintenance of hydrological instr. works
India	1	Geologist	A	1	Geochemistry
	1	Geophysicist	A	2	Uranium exploration
	1	Chemist	A	1	Remote sensing
				1	Computerized information systems
				1	Uranium geology
				1 ²	Geochemical methods
Israel	--	2	Analytical techniques
Jordan	2	Geophysicist	A	2	Remote sensing
	1	Hydrologist	B	1	Geologic & electromagnetism
Nepal	--	1	Ground-water invest.
Oman	--	1	Hydrologic techniques
Pakistan	1	Graphic arts spec.	C	1	Hydrologic techniques
				1	Uranium exploration
				1 ²	Uranium exploration
Saudi Arabia	19	Geologist	A	1 ²	Coal resource mapping
	3	Geophysicist	A, C	1	Distribution, geologic publications
	1	Mathematician	A		
	1	Chemist	A	2	Cartography
	7	Technical advisor	A, B, C	4	Remote sensing
	3	Computer specialist	C	1	Academic
	4	Cartographer	A	4	Administration
	1	Hydrologist	B	10	English
				1	Photo lab techniques
				2	Analytical lab techniques
				1	Computer programming
				3	Geology
				1	Geologic interpretation
				4	Photo lab technology
				1	English, type composing
				1	X-ray analysis
				4	Spectroscopy

TABLE 3.—*Technical assistance provided by the USGS to other countries during FY 1981—continued*

Country	USGS personnel assigned to other countries			Scientists from other countries trained in U.S.	
	Number	Title	Type of Program ¹	Number	Field of Training
Near East and South Asia—Continued					
Saudi Arabia— continued				1	Business administrative
				1	Health physics
				2	Design of hazardous waste landfill
				2	Ground-water hydrology
				1	English, property management
				2	Induced polarization
				1	Property management
				1	English/Photo lab tech.
				1	Geologic administration
				1	Computer science
				1	Fission track studies
				1	Distribution of printed mat.
				2	Well drilling
				1	Editorial/type composition
				2	English/computer graph
			1	Seismological equipment	
Turkey	1	Geologist	A	1 ²	Stratiform chromites
				1	Iron-ore geology
Yemen	1	Hydrologist	B	1	Remote sensing
				1	Irrigation
				2	Surface-water hydrology
Far East and Pacific					
Australia	2	Geologist	A		
Burma	--			1	Data banks
				1	Hydrologic techniques
China					
Mainland	3	Geologist	A, B	1 ²	Petroleum geochemistry
	5	Geophysicist	A	2	Remote sensing
	2	Hydrologist	B	2 ²	Coal petrology
	1	Computer scientist	A	2 ²	Light stable isotope
				2 ²	Crustal/mantle studies
				1 ²	Uranium geology
				3 ²	Geophysics/seismology
				1 ²	Geothermal studies
				1 ²	Analytical chemistry
				1 ²	Geothermal research
				1 ²	Earthquake prediction
				1 ²	Fluid inclusions/ore deposits
				1 ²	Organic geochemistry
				1 ²	Impact metamorphism
				1 ²	Tectonics
Taiwan	--			2	Remote sensing
				1	Water resources development
Indonesia	3	Geophysicist	C		
	2	Geologist	A		
	1	Physical science tech.	A		
	1	Hydrologist	B		
	1	Soils scientist	A		
Japan	1	Geophysicist	A	2	Remote sensing
	1	Engineer	C	1	Environmental geology
				1 ²	Environmental geology
				1 ²	Electromagnetism/geology
				1 ²	Marine geology
				1 ²	Paleontology and stratigraphy
Korea, South	2	Geologist	A	1	Data bank system
Malaysia	6	Geologist	A, C	1	Remote sensing
	1	Engineer	C		

TABLE 3.—*Technical assistance provided by the USGS to other countries during FY 1981—continued*

Country	USGS personnel assigned to other countries			Scientists from other countries trained in U.S.	
	Number	Title	Type of Program ¹	Number	Field of Training
Far East and Pacific—Continued					
	1	Petroleum engr. tech.	C		
New Guinea	1	Cartographer	C		
New Zealand	1	Chemist	A		
Philippines	--			2	Remote sensing
				1	Ground-water supply
				1	Cartography and map production
				2	Hydrologic techniques
Singapore	--			1	Hydrologic techniques
Thailand	2	Geologist	A		
	1	Geophysicist	A		
Europe					
Austria	1	Geologist	C		
Belgium	--			1	Data processing
Finland	--			1	Geologic interpretation
				1	Data processing
France	1	Chemist	B	1 ²	Seismology
				1 ²	Tectonophysics
				1 ²	Sulfides
				1 ²	Petrophysics and R.S.
				1 ²	Geoelectrical methods
				1	Geochronology labs
				1	Metallurgy
Germany	1	Physicist	A		
	1	Geologist	A		
Greece	1	Civil engineer	A	2	Pollution of ground-water aquifers
				1	Uranium exploration tech.
				1	Ground-water pollution
Hungary	1	Mathematician	A	1	Sedimentation models
	1	Chemist	A	1	Seismic risk
	2	Geophysicist	A	1	Electromagnetic methods
				1	Seismic modeling
				1	Geophysical instrumentation and tech.
				3 ²	Geophysical instrumentation and tech.
Italy	1	Physical scientist	A	1	Geological interpretation
				5	Remote sensing
				2 ²	Isotope geology
				1 ²	Seismology
				1	Geologic interpretation
Netherlands	--			2	Ground-water modeling
				1	Eolian sand deposits
				1	Radiometric dating
Norway	--			1	Remote sensing
				1 ²	X-ray spectroscopy
				1	Radio chemistry
				1	Regional geophysics
Poland	3	Geologist	A		
Portugal	3	Geologist	A	1	Remote sensing
	2	Chemist	A		
	1	Physical scientist	B		
Spain	1	Physical sci. tech.	A		
Sweden	1	Hydrologist	A	1	Isotope geology
	1	Chemist	A		

TABLE 3.—*Technical assistance provided by the USGS to other countries during FY 1981—Continued*

Country	USGS personnel assigned to other countries			Scientists from other countries trained in U.S.	
	Number	Title	Type of Program ¹	Number	Field of Training
Europe—Continued					
Switzerland	--			1 ²	Isotope geology
				1	Geothermal resources
United Kingdom	--			1	Geologic interpretation
				1 ²	Geology
				2	Petrochemistry
USSR	1	Geophysicist	A	1 ²	Petrochemistry
				2 ²	Seismology
Other					
Antarctica	2	Cartographic tech.	C		
	3	Physical scientist	A		
Canada	4	Geologist	A	1	Remote sensing
Deep-sea drilling program	1	Geologist	A		
Iceland	--			1	Geothermal resource asst.

¹A. Geologic mapping and resource appraisal; B. Studies of hydrologic phenomena; C. Other assistance in developing or strengthening earth-science institutions.

²Visiting scientist.

TABLE 4.—*Technical and administrative documents issued during FY 1981 as a result of USGS technical and scientific cooperation programs*

Country or region	Reports or maps prepared			
	Project and administrative reports	Approved for publication by counterpart agencies or USGS	Published	
			In technical journals	By USGS
Arctic	--	--	2	--
Argentina	7	6	--	--
Bahamas	--	--	1	--
Bangladesh	1	--	--	--
Botswana	1	--	--	--
British Indian Ocean Terr.	1	--	--	--
Caribbean	--	--	--	1
Chile	--	--	--	1
Circum Pacific	--	6	--	1
Costa Rica	1	--	--	--
Egypt	3	1	--	2
Greece	--	--	--	1
Indonesia	4	--	--	--
Jordan	3	--	--	--
Korea	7	8	--	--
Liberia	1	--	--	--
Mauritania	1	--	--	--
Mexico	--	--	1	--
Oman	--	2	--	1
Portugal	10	5	--	3
Saudi Arabia	51	40	8	33

TABLE 4.—*Technical and administrative documents issued during FY 1981 as a result of USGS technical and scientific cooperation programs—Continued*

Country or region	Reports or maps prepared			
	Project and administrative reports	Approved for publication by counterpart agencies or USGS	Published	
			In technical journals	By USGS
Spain	--	--	--	1
Taiwan	--	--	--	1
Thailand	3	--	--	--
Tunisia	1	--	--	--
Venezuela	1	--	--	--
Yemen	1	--	1	1
Zambia	1	--	--	--
General	2	1	2	2
Total	100	69	15	48

TECHNICAL ASSISTANCE

In FY 1981 the USGS provided some type of assistance to 10 countries and 2 regional organizations through projects authorized under the Foreign Assistance Act of 1961 as amended. Most of the assistance projects are sponsored by the Agency for International Development, the Department of Energy, by UNESCO or other international organization, or by the recipient country.

Examples of such activities are the long-continued Saudi Arabian program, encompassing regional and areal geologic mapping, geophysical surveys, geochronologic studies, genesis of ore deposits, geochemistry, plutonic rock study, and computer science; the Indonesian program of land use and hazard mitigation now in the fifth year; and short-term studies of geothermal resources and potash resources in Thailand. additional information is given in the section of this chapter entitled "Summary of Selected Activities by Country or Region."

PARTICIPANT TRAINING

Training of foreign nationals is an important part of the technical assistance projects, and in FY 1981, 323 earth scientists from 54 countries were engaged in academic, observation, or intern training in the U.S. Since the assistance programs began in the late 1940's, more than 2,300 earth scientists and engineers from 130 countries have completed study assignments in the United States either provided by, or coordinated by, the USGS. The training projects ranged from short term to long term and covered a wide variety of subjects, including, but not limited to, cartography and geologic map compilation, seismic studies, geothermal research assessment, volcanic hazard investigation, data processing, hydrology, mineral resources exploration techniques, and remote sensing.

James Lucas participated in a United Nations/Food and Agricultural Organization (UN/FAO) regional training seminar on remote sensing applications for land resources, held in Athens, Greece, October 7 to 17. The seminar was organized in cooperation with the Government of Greece. Twenty-seven persons attended the seminar, which provided an overview of remote sensing techniques and emphasized application in Mediterranean areas. Landsat data were used during a field trip to the Atalanti area to assess the geology and the nature of land cover.

C.M. Trautwein was part of an instructional team for a 3-week training course titled "Applications of Remote Sensing to Geological/Mining Surveys" held in Buenos Aires, Argentina, October 6 to 24, 1980. The course was co-sponsored by the Organization of American States and the Argentina National Commission on Space Investigations. Twenty-one South and Central American geoscientists participated in the training course. A field trip to Catamarca Province in northwestern Argentina was also conducted.

Robert Christiansen, Wendell Duffield, Robert Smith, Alfred Truesdell, and Donald White spent October 20 to November 3, 1980, in Mexico conducting

a 2-week training course in volcanology and volcano-related geothermal systems. Approximately 65 students, geologists, and geochemists of Mexico's Comision Federal de Electricidad (CFE), plus a few counterparts from the University of Mexico, met at Guadalajara, where the first week was devoted to alternating days of lectures and field trips to nearby La Primavera caldera and the associated volcanic field. Upper Pleistocene lava flows and domes, air-fall and ash-flow pyroclastic deposits and caldera-related structures, and active hot springs and fumaroles were visited. The area is a promising geothermal prospect, where exploratory drilling has encountered temperatures in excess of 250° C at a depth of about 1 km. Both the USGS and the Mexican participants judged the training course to be a worthwhile and rewarding experience. CFE officials invited the USGS team to return with a similar program next year. Such collaboration is in the spirit of U.S.-Mexico relations espoused at executive levels by the two governments and helps address current worldwide energy problems.

TOPICAL RESOURCE STUDIES

In FY 81 the Geological Survey initiated a World Energy Program for which the goals include: (1) development of an independent, publicly available, and updateable assessment of energy resource potential worldwide; (2) the ability to analyze production and exploration potential, including media analysis, in key international areas of concern; and (3) the development of exploration analogs to apply to domestic assessment/exploration activities. These goals are compatible with various user agency needs such as Department of State, Treasury Department, and Department of Energy. The studies are based largely on analysis of available literature and data bases. The Survey's World Energy Program focuses primarily on oil and gas but also includes some investigations of coal and uranium, and, although it concentrates on maximum short-term benefits, it is designed to provide a solid base for continued work. Results will be computerized for easy updating as new information becomes available.

Regional areas of investigation in FY '81 include the major free-world export areas: Nigeria, Trinidad, Venezuela, the Middle East, Indonesia, North Africa, Mexico, and the North Sea; in addition, preliminary compilations were made for some fields in the USSR. Most of the areas of important free-world export potential are included in the Foreign Energy Supply Assessment Program (FESAP) conducted in coordination with the Department of Energy. The

specific goals of FESAP are to develop a technical understanding of the production potential of a given country and, based on its past history of discovery and assessed resource potential, render a technical judgment on the ability of the given country to sustain or increase that production. Studies of potential in the USSR, the world's leading producer of petroleum and the source of oil for most of the communist-block nations, will continue; longer term studies will address the extraordinary potential of the Soviet Arctic, including the Barents Sea, which is in general a continuation of North Sea geology. Still another regional study will address the occurrence of petroleum off shore, in an attempt to analyze the distribution of giant fields, the field-size distribution, and the discovery rates.

The topical areas of study will concentrate on worldwide paleo-zones of oxygen minima that have contributed to the major source rocks of petroleum. A companion study to that effort involves the projection through time of geologic-plate locations relative to the equator and major oceans, the understanding of which provides important components of predictive petroleum occurrence models. The topical program also will serve in basic data development in such vast but little understood or reported areas as China and Antarctica.

Under an agreement with AID (Agency for International Development) the USGS prepared preliminary administrative reports that assess the conventional sources of energy (oil, gas, coal, and geothermal) and their potential for development for approximately 40 countries supported by AID mission activities. M.J. Bergin, R.L. Miller, Keith Yenne, E.R. Landis, V.E. Swanson, Eleanor Crosby, P.T. Hayes, Mahlon Ball, and P.R. Woodside were among those compiling the reports on the basis of literature surveys. More detailed follow-on investigations, including in-country visits, were made for Bangladesh, Costa Rica, and Ecuador; more specific information is reported in the section summarizing selected activities by country or region.

SCIENTIFIC COOPERATION AND RESEARCH

Two new agreements to cooperate in remote sensing and in geological science were signed on April 2, 1981, by representatives of the USGS and the Canadian Department of Energy, Mines and Resources. One agreement is with the Canadian Centre for Remote Sensing and the other is with the Geological Survey of Canada. The agreements provide for consultations, exchanges of scientific and technical data, and joint research on geoscience problems, techniques,

and methods of mutual interest in those subjects. Under each agreement specific exchanges and joint projects will be defined, including cooperation in such areas as marine geophysical studies, compilation of an aeromagnetic map of Canada and the United States, and preparation of a Landsat satellite image map of North America.

In another program, the USGS began to participate in a cooperative project between the United States, West Germany, Canada, and South Africa to develop an international mineral resources inventory of major mineral deposits. The initial program will be a pilot study, limited to the commodities nickel, chromium, manganese, and phosphate. The inventory will compile information on major mines and deposits of each of those minerals as a basis for each country to make its own policy decisions. The pilot study is to be completed by December 1982, and a report is to be prepared and published.

SPECIAL FOREIGN CURRENCY PROGRAM (SFCP)

Poland

During 1981, research on two cooperative projects in coal geology ("Cooperative Research on the Characteristics of Coal Basins" and "Geochemistry of Coal and the Computerization of Core Data") was completed and final reports were prepared. USGS coinvestigators K.J. England, M.D. Carter, and T.W. Henry spent Feb. 14-March 4, 1981, in Poland working with Polish coinvestigators in editing for publication English translations of 11 final reports that have resulted from the two projects. Unfortunately, since the declaration of martial law in Poland in December 1981, no communication has been received on the status of the reports.

Three other research projects in Poland ("The Comparative Study of Native Sulfur Deposits," "Copper Mineralization in Black Shales," and "The Thermal History of Intrusive Bodies by Fission Track Dating") were active in 1981. Three Polish geologists, coinvestigators on the sulfur project, visited sulfur deposits in the United States, under the guidance of USGS project officer Alfred Bodenlos, in October 1981. Plans were well under way for exchange visits of scientists in the other two projects ("Copper" and "Fission Track Dating") but were halted when martial law was declared in December 1981. Since then, there has been no communication on project activities, but personal communication between several USGS project officers and Polish counterparts has continued.

A.H. Chidester visited Poland Sept. 19-Oct. 1, 1981, to review ongoing projects and discuss proposals

for new projects under the SFCP program and to attend the meeting in Warsaw of the U.S.-Poland Joint Board on Science and Technology (S&T) Agreements. In the discussion, agreement was reached with the Polish Geological Institute on proposals for two new coal projects ("Research on Methods of Exploration for and Evaluation of Coal Deposits" and "Analysis of Characteristics of Lignite Deposits in the Pozan Graben") to be funded from the allocation to the Polish Ministry of Mining and Energetics but to be carried out by the Geological Institute. It was also agreed that the USGS would consider proposals for an extension of the project "Copper in Black Shales" and for a new project on Precambrian ore deposits in the crystalline basement of northeastern Poland. At the Joint Board meeting, an understanding was reached on the allocation of funds to finance the proposed projects between the Geological Institute and the USGS. These proposals were, of course, brought to nought by the events of December 1981.

Yugoslavia

Martin F. Kane represented the USGS at the Meeting of the U.S.-Yugoslavia Joint Board on Science and Technology Agreements, held in Sarajevo, Yugoslavia October 5-9, 1981. At the meeting a new project on "Terrain Subsidence Due to Salt Solution and Coal Mining" with the Institute for Mining Research in Tuzla was approved; a proposal for a project on "Geochemical Surveys Based on Statistical Sampling Design" with the Geological Institute of the University Edvard Kardelj in Ljubljana was submitted. The projects "Investigation of Ground Motion During Earthquakes and the Behavior of Surface Layers and Structures" with the Institute for Earthquake Engineering at Skopje and "Crustal Structure in Relation to Earthquakes" with the Geophysics Institute in Belgrade continue on planned schedules.

CIRCUM-PACIFIC MAP PROJECT

The Circum-Pacific Map Project will show, at a common scale (1:10,000,000) and projection (equal-area), coordinated geologic and resource data for the Pacific basin and the peripheral continental areas that were affected by geologic phenomena in the development of the basin during the Mesozoic and Cenozoic. Five panels, one for each quadrant of the Pacific region and one for Antarctica, are compiling the thematic maps of their respective quadrants (1:10,000,000); they also contribute data for composite Pacific basin maps at a scale of 1:20,000,000. The chairmen of the

panels are Chikao Nishiwaki of Japan (Northwest), Fred Douch of Australia (Southwest), Campbell Craddock of the United States (Antarctica), Jose Corvalan of Chile (Southeast), and Kenneth Drummond of Canada (Northeast). The USGS participation involves the overall coordination of the project, as well as expert consultation and final cartographic work; the USGS also hosts an annual Panel Chairmen's Meeting. The set of maps will comprise the following thematic series: plate tectonic, geologic, tectonic, geodynamic, mineral resources, and energy resources. Of the projected total of 44 map sheets, 15 were published by the end of 1981.

During the year, the Northeast, Northwest and Southeast Quadrants of the Plate Tectonic Map at 1:10,000,000-scale were published. The plate tectonic series, which will be the first thematic series to be published, depicts active plate boundaries, major intraplate faults, plate-motion vectors, seismicity, Holocene volcanic activity, and magnetic lineation on the sea floor. The Geological Map Series will be the next main target.

The Circum-Pacific Maps are being published and distributed by the American Association of Petroleum Geologists. Each series consists of five overlapping maps, each measuring 54 by 40 inches. The geographic maps sell for \$12 each or 6 for \$30; the base maps sell for \$6 each or 6 for \$20, and the plate-tectonic maps sell for \$8 each; they are available from the American Association of Petroleum Geologists Bookstore, P.O. Box 979, Tulsa, Oklahoma, 74101, or Brown's Geological Information Services, Ltd., 160 North Gower St., London England, NW1, 2ND.

G.W. Moore visited the U.S.S.R. September 18 to October 10, 1980, at the official invitation of Viktor B. Kurnosov, Far East Geological Institute, Vladivostok. One of his primary objectives was to familiarize Soviet geologists with the Circum-Pacific Map Project and to stimulate their participation in the project.

Moore briefed many U.S.S.R. geologists on his recent work on the Circum-Pacific Map Project's plate-motion maps of the Pacific basin. Leonid Parfenov of the Institute of Tectonics and Geophysics, Khabarovsk, drew a boundary marking the edge of the continent at the beginning of the Jurassic for the Plate-Tectonic Map of the Northwest Quadrant. Lev. P. Sonenshayn and Leo Savostin of the Moscow Institute of Oceanology were helpful in delineating the plate boundaries within eastern Asia for the map. Soviet geologists will supply percent-of-manganese coverage for all Soviet bottom photographs to be used in the Circum-Pacific Mineral Resource Map series, as well as the marine data for the geologic maps.

INTERNATIONAL GEOLOGIC CORRELATION PROGRAM

The United States has been a member of the International Geologic Correlation Program (IGCP) since its beginning in 1973. Several U.S. geologists helped formulate the program and others have served on the Board and Scientific Committee. A U.S. National Committee for IGCP (USNC/IGCP) was organized in 1974 as a subcommittee of the U.S. National Committee on Geology, under the joint sponsorship of the National Academy of Sciences and the U.S. Department of the Interior (Geological Survey). The USNC/IGCP performs the planning and organizing functions typical of national committees, issues periodic newsletters, and solicits and disburses funds to support in part the United States contribution to the program.

Project 115, "Siliceous Deposits in the Pacific Region," was led by J.R. Hein. It held its second international conference in Japan in 1981 to mark the close of the project, which had been active for 5 yrs. A paper presented by Hein and S.M. Karl compared deep-sea ocean cherts with those found in circum-Pacific orogenic belts. The latter probably formed in young ocean basins, in block-faulted continent margins, in back-arc basins, or adjacent to island arcs. Other papers discussed siliceous deposits as sources of metals, silica, and petroleum, and the origin, age, and distribution of siliceous deposits.

P.C. Bateman leads Project 30, "Circum-Pacific Plutonism." The project has worked to determine the origin and relation to tectonism, volcanism, and ore deposits of the batholiths that make up a large part of the Pacific margins. Final products, a symposium volume, and a map of plutonism marginal to the Pacific basin, are near completion.

W.D. Carter, co-leader of IGCP Project 143, "Remote Sensing and Mineral Exploration," attended the project's Spanish Working Group meeting at the Escuela de Ingenieros de Minas in Madrid, Spain, October 28, 1980. Although the Working Group began their activities only in 1980, they have completed a Landsat mosaic of the Iberian Peninsula and are about ready to publish a national lineament map, both of which are at scales of 1:1,000,000. With co-leader L.C. Rowan, Carter led a 2-week workshop at the Regional Remote Sensing Center, Nairobi, Kenya, for participants from seven African countries.

OTHER

A.H. Chidester, J.A. Briskey, M.F. Kane, and Helmuth Wedow participated with Wolfgang Klau (BGR), Don Sanopter (Geological Survey of Canada),

and Helfried Mostler (Univ. of Innsbruck) in a meeting of the Joint Committee on Base-Metal Deposits in Carbonate Rocks, held in Innsbruck Oct. 10-11, 1981. Following the meeting, the committee went on a field trip to zinc-lead mines and deposits in Austria, northern Yugoslavia, and northern Italy, led by Klau and Mostler, and by local experts at each mine.

October 19th through the 21st, 1981, Martin F. Kane met with staff of the Bureau de Recherches Géologiques et Minières (BRGM) at Orleans, France, to negotiate renewal of the agreement between USGS and BRGM. While there, he presented a report on recent developments in the USGS in the use of regional gravity and magnetic data.

From October 15 to 21, 1981, the second meeting of the United States/People's Republic of China Working Group was held in Reston, Va., to complete negotiations on the Annexes to the Earth Science Protocol. Three major US/PRC geoscience protocols were formulated on the basis of mutually beneficial disciplinary interests—an Earthquake Studies Protocol signed by USGS and NSF, an Earth Sciences Protocol signed by USGS and involving NSF, and a Surface-Water Hydrology Protocol signed by USGS and involving NOAA. As now envisioned, the three protocols will involve about 31 different projects and more than 100 scientists over the next several years. On the Chinese side, eight major agencies and some two dozen subsidiary institutes or bureaus are participating. It is apparent that the evolving USGS-China connection will become one of the largest and most diversified cooperative geoscience programs ever initiated with another country.

The U.S.-Japan Natural Resource Program (UJNR) cooperative explores a variety of subject areas via scientist exchange and other means. The USGS has been most active in its joint Marine Geology Panel Meetings.

Joint United States-Canada study of flow of Milk River at the Montana-Alberta border

The United States and Canada have initiated a study to define the natural flow of the Milk River at its eastern crossing of the international boundary between Montana and Alberta. The principal investigator in the study is R.E. Thompson. A treaty between Canada and the United States apportions water from the Milk River to the two countries on the basis of natural flow. In the past, the determination of natural flow has been complicated by the fact that during the irrigation season, the United States uses the Milk River as a conduit to transport water from the upper reaches of the St. Mary River through Canada to the downstream (U.S.)

end of the Milk River. The Canadians are now planning the construction of a dam(s) on the Milk River, which will further complicate the computation of natural flow.

During the year, the United States and Canada made numerous measurement runs throughout the entire 200-mile reach of channel through Canada to determine sites of loss or gain in the river system. Analysis of the data gathered from the field work resulted in the installation of one continuous-stage recording station and three different sets of ground-water wells to monitor the effects of evapotranspiration and ground-water movement on the surface flow. All existing data were compiled, and testing and evaluation of different mathematical models was begun.

INTERNATIONAL COMMISSIONS AND REPRESENTATION

Participation in international congresses, conferences, and meetings serves the objectives of the USGS as well as the foreign policy goals of the United States, inasmuch as accredited official delegates represent the United States rather than their own bureau or agency. U.S. delegations to multilateral, intergovernmental conferences are accredited since 1948 under authority delegated from the President to the Secretary of State and exercised on behalf of the Secretary by the Assistant Secretary for International Organization Affairs.

D.F. Davidson, accompanied by J.S. Rosenshein, led the U.S. delegation to the 7th session of the ESCAP Committee on Natural Resources in Bangkok from September 30 through October 6. The session was devoted principally to water resources appraisal, development, and management. Interest was shown by ESCAP member countries in the use of remote-sensing techniques to address various water resources issues and in the development of water-use data systems, models, and hydrological skills.

The 17th session of Committee for Coordination of Joint Prospecting for Mineral resources in Asian Offshore Areas (CCOP) and the concurrent session of its Technical Advisory Group (TAC) was held in Bangkok, Thailand, in November 1980. The U.S. was represented by J.A. Reinemund, J.M. DeNoyer, D.E. Kash, M.J. Terman, F.H. Wang, and H.G. Green from the USGS. Reinemund and M.J. Terman were also U.S. delegates at the November 1981 18th Session in Seoul, Korea. M.J. Terman and H.G. Greene were technical advisors to the October 1980 9th Session of the Committee for Coordination of Joint Prospecting

for Mineral Resources in South Pacific Offshore Areas (CCOP/SOPAC).

P.G. Teleki was a member of the U.S. delegation at the meeting of the United States-France Cooperative Program in Oceanography in Paris, October 28-30, 1980.

A.H. Chidester, J.A. Briskey, and Helmuth Wedow attended the Fourth International Symposium on Mineral Deposits of the Alps, held in Berchtesgaden, West Germany, October 4-10, 1981.

R.M. Hamilton attended the Conference on Large Earthquakes in Napier, New Zealand, January 31 through February 4, 1981, where he presented an invited paper, "Science and Politics of Earthquake Prediction." The conference was sponsored by the Government of New Zealand to plan for research and mitigation of hazards of large earthquakes. During the trip Hamilton also presented a seminar on "Seismic Reflection Studies in the Earthquake Regions of the Eastern United States."

J.A. Reinemund and G.E. Tolbert attended the Regional Conference on the Development and Utilization of Mineral Resources, February 2 to 6, 1981, in Arusha, Tanzania. Reinemund represented the International Union of Geological Sciences (IUGS) of which he is Treasurer and member of the IUGS Executive Committee. Tolbert represented the USGS, which had also been requested to send a representative.

D.F. Davidson represented the USGS at the International Energy Technical Cooperation and Foreign Policy Workshop in April 1981, at the Los Alamos National Laboratory (LANL), sponsored by the Office of International Affairs of the Department of Energy and the Bureau of Oceans and International Environmental and Scientific Affairs of the Department of State. The objective was to promote better coordination among U.S. organizations involved in international energy activities and to make better use of technical cooperation as a cost-effective tool of foreign policy.

J.A. Reinemund represented the United States at the Fourth Arab Conference on Mineral Resources held in Amman, Jordan, April 29 to May 1, 1981. The conference was attended by representatives of Saudi Arabia, United Arab Republic, Iraq, Jordan, Kuwait, Libya, Morocco, Mauritania, Qatar, Somalia, Sudan, Syria, and Tunisia. Also, as Treasurer of the International Union of Geological Sciences (IUGS), he met in Paris in January 1981 with Christian Weber, Secretary-General of IUGS, concerning the operating program and budget for IUGS spring 1981.

At the request of the Chairman, Research Development Program, International Union of Geological

Sciences (IUGS), J.E. Case participated in a field-oriented planning meeting in Guatemala, October 1 to 9, 1981. The purpose of the meeting was to develop a program on "Metallogenesis of Mafic and Ultramafic Belts in Latin America." The objective of the field trip, to see the regional setting of various mafic and ultramafic (MUM) belts in Guatemala and their associated mineral deposits, was accomplished, as was the development of an IUGS program plan.

L.F. Konikow, hydrologist, attended a seminar and workshop on land and stream salinity in Perth, Australia, sponsored by the State Government of Western Australia, November 10 to 20, 1980. J.O. Morgan attended the 15th International Remote Sensing Symposium at the University of Michigan May 11 to 15, 1981.

D.F. Davidson and J.A. Reinemund acted as co-leaders of the United States delegation to the biannual meeting of the Committee on Natural Resources of the Economic and Social Council of the United Nations. The meeting was held at the U.N. headquarters in New York, May 18 to 28, 1981, and dealt with a wide-ranging series of international earth-science subjects.

M.J. Terman represented the United States at the Expert Working Group Meeting on the third edition of the Oil and Natural Gas Map of Asia, May 12 to 14, 1981, at Bangkok, Thailand. Representatives from India, Indonesia, Iran, Malaysia, Pakistan, Philippines, Thailand, and the USSR attended the meeting, as well as the Senior Petroleum Geologist of CCOP. The participants generally agreed that the basic objectives of the map should be to show boundaries and 1,000 m isopachs, geometry, facies, structures, petroleum deposits, and main petroleum industry installations.

J.A. Reinemund and Roger Stewart participated in the initial meeting of the Working Group on Science and Technology in Athens, Greece, September 30 to October 3, 1980. The Working Group was established under the cooperative agreement between Greece and the United States signed earlier in the year. The meeting was co-chaired by Dr. George Argyropoulos, Director General of the Scientific Research and Technology Agency, and Assistant Secretary of State, Thomas Pickering, for the U.S. side. The group discussed cooperation in the fields of energy assessment, geothermal investigations, remote sensing (training and applications), and seismic studies and risk analysis. J.R. McCord followed up in November to assist in planning a new space research center for Greece.

A.H. Watkins represented the U.S. Department of the Interior at the User Services/Data Management Working Group meeting, May 18-19, 1981, and the

Landsat Ground Station Operations Working Group meeting, May 20-22, 1981, both in Canberra, Australia.

F.E. Senftle represented the U.S. at the International Atomic Energy Agency (IAEA) Advisory Group meeting in Vienna, Austria, November 24 to 28, 1980, which met to discuss organization and objectives of training courses in nuclear sciences for the developing countries. The necessity to train personnel in the developing countries in nuclear electronics was discussed in detail.

L.J.P. Muffler attended the Standing Advisory Committee on Geothermal Training of the United Nations University in Pisa and Rome, Italy. This committee serves to coordinate the four international geothermal training courses (New Zealand, Iceland, Italy, and Japan) and to make recommendations to the sponsoring agencies on geothermal training needs. Three ad hoc working groups were established at the session, one of which was chaired by Muffler.

J.R. Wray, senior geographer-cartographer, has been appointed as a member of the U.S. National Committee (USNC) for the International Geographical Union (IUGS), by Dr. Philip Handler, Chairman of the National Research Council. Wray will serve through 1984. R.P. Southard is the U.S. Member, Commission on Cartography, and K.I. Daugherty is Alternate Member.

J.A. Reinemund also participated in a seminar at Accra, Ghana, on Geology and Mineral Resources of Precambrian Rocks in Africa, jointly sponsored by IUGS and UNESCO, to develop plans for a new research program on the Precambrian in Africa and to attend the annual meeting of the IUGS Executive Committee.

In July 1981, D.F. Davidson represented the IUGS in a meeting with the Trade and Development Program (TDP) of the International Development Cooperation Agency (IDCA). The purpose of the meeting was to explore possible directions in which a TDP-supported program for mineral resources might go. The Bureau of Mines and the Economic Bureau of the Department of State were also represented. As a result of the meeting, TDP may play a role in developing mineral deposits that are presently not economically attractive because of technologic problems, especially metallurgical problems. USGS and USBM listed potash, refractory bauxite, cobalt, chromite, the platinum group, vanadium, rutile, columbium/tantalum, and fluorspar as mineral commodities for which stock piles are in short supply. An attempt will be made to identify and list problem deposits of these minerals in a few countries of the world.

At a session of the Committee for Coordination of

Joint Prospecting for Mineral Resources in Asian Offshore Areas (CCOP), F.H. Wang presented isotopic ages, lithology, and the data compiled from bases of basement rocks in offshore wells and Deep Seismic Drilling Program holes on a preliminary map showing crustal and basement rocks in Asia marine areas.

INTERNATIONAL HYDROLOGICAL PROGRAM AND RELATED ACTIVITIES

The International Hydrological Program (IHP) sponsored by the United Nations Educational, Scientific and Cultural Organization (UNESCO), is an outgrowth of the International Hydrological Decade and began in 1975. The major functions of the IHP are (1) the promotion of a scientific program, including studies of the hydrological cycle, assessment of water resources, and evaluation of the influence of man's activities on water regimes; (2) the promotion of education and training in hydrology; (3) the enhancement of exchange of information; (4) support of technical assistance programs; and (5) the promotion of regional cooperation.

International guidance and supervision of the program is carried out by an Intergovernmental Council consisting of 30 member countries, half of which are elected every 4 years from the 130-nation IHP membership by the General Conference of UNESCO. The United States was not a member of the IHP Intergovernmental Council during the Phase I period 1975-79, but was elected to membership for the shortened Phase II, 1979-81 term. The IHP Bureau is composed of one representative from each of the five IHP regions and is elected for each phase of the IHP by the Intergovernmental Council members. Philip Cohen, Chief Hydrologist, USGS, was elected to represent Region One, which includes Western Europe, Canada, Australia, New Zealand, Israel, Turkey, and the United States, for the period 1979-81. The Bureau prepares for sessions of the Council, supervises the implementation of resolutions, monitors the status of the IHP activities, and during 1979-81 prepared the work plan for Phase II, 1985-89, of the IHP.

United States participation in the IHP is guided by the U.S. National Committee on Scientific Hydrology (USNC/SH) chaired by Chief Hydrologist Cohen. The membership includes representatives of eight other Federal agencies and six nongovernmental organizations. Associate Chief Hydrologist, R.H. Langford (USGS), is the Alternate Chairman; Della Laura (USGS), Chief, the Office of International Hydrology, is Executive Secretary of the USNC/SH. The USGS

Office of International Hydrology (OIH) serves as secretariat of the USNC/SH.

The major functions of the USNC/SH are (1) to formulate the United States program of participation in the IHP; (2) to serve as a channel of communication for United States international hydrological activities; (3) to promote international hydrological activities; (4) to aid the Department of State in preparing U.S. positions on hydrology; and (5) to coordinate United States activities related to requests concerning hydrology from other countries and international organizations.

Much of the work of the IHP is done through individual Rapporteurs and Working Groups. The Rapporteurs generally work alone to prepare short reports summarizing the state of knowledge on specific topics. Working Groups are composed of two to eight members representing different countries and generally are concerned with broader topics than Rapporteurs. Phase II of the IHP has projects requiring 14 Rapporteurs and 7 Working Groups. Seven Rapporteurs and five Working Group members are from the United States; of these, one Rapporteur and one Working Group member are from the USGS.

USGS staff engaged in several IHP-related activities during the year. H.H. Barnes attended the first joint meeting of the U.S. and Canadian Committees for the Hydrological Operational Multipurpose Subprograms (HOMS) of the World Meteorological Organization (WMO) in Ottawa, October 13-17, 1980. Mr. Barnes attended a meeting of the WMO Working Group for the Guide, Standardization, and Technology Transfer of which he is the Rapporteur for the Technical Regulations on November 8-15, 1980.

L.F. Konkow and J. Vecchioli attended the International Symposium on quality of Ground Water co-sponsored by the UNESCO and WMO, during March 20-30, 1981.

The Ninth Session of the Bureau of the Intergovernmental Council of the IHP was held in Paris, March 6-15, 1981. Philip Cohen represented the hydrologic communities of the United States, Canada, Western Europe, and Australia, and Della Laura, Executive Secretary of the U.S. National Committee on Scientific Hydrology, participated in the session.

G.D. Bennett attended a session of the UNESCO International Scientific Council to plan and coordinate a project entitled "Protection of the Lithosphere as a Component of the Environment," during September 4-13, 1981.

An International Conference on Hydrology and the Scientific Bases for the Rational Management of Water Resources, attended by over 100 nations, was convened jointly by UNESCO and WMO in Paris,

France, August 17-27, 1981. This conference reviewed progress on UNESCO's International Hydrological Program and WMO's Operational Hydrology Program, and planned activities for these programs for the 5-yr period beginning in 1983. The fourth meeting of the UNESCO Intergovernmental Council of the IHP was held in Paris August 28-29, following the joint conference. The U.S. Delegation, headed by R.H. Langford, included D. Laura and D.M. Thomas of the USGS and R.A. Clark and A.F. Flanders of NOAA. M.F. Meier, President of the International Association of Hydrological Sciences (IAHS), represented that organization at the joint conference. N.C. Matalas assisted Mr. Meier at the joint conference and both attended the concurrent session of the Committee of Reorganization of the IAHS.

Two out of six keynote addresses made at the joint conference were given by Survey employees. Meier presented a paper entitled "Snow and Ice, Climate, and Water Supply: Activities of the IHP," and Laura presented a paper entitled "Assessment of Water Resources: The U.S. Experience." The U.S. Delegation presented 10 technical films and 33 technical publications for review by the delegates. Thomas made a presentation on the hydrological effects of the Mount St. Helens eruption.

ACTIVITIES RELATED TO OTHER INTERNATIONAL ORGANIZATIONS

The International Standardization Organization (ISO), an agency with which the USGS cooperates regularly, has among its aims the standardization of hydrologic equipment and data collection methods to assure that data obtained in diverse countries are mutually acceptable and compatible. During the first half of October 1980 in Paris, A.F. Pendleton, H.H. Barnes, and E.D. Cobb participated in sessions of the Technical Committee 113 (Measurement of Liquid Flow in Open Channels) of the ISO as follows: Pendleton on subcommittee 1, velocity-area methods, Barnes on subcommittee 7, methods for measurement under difficult conditions, Cobb on subcommittee 4, dilution methods.

INTERNATIONAL COMMISSIONS

In a collaborative effort on behalf of the Department of State, the USGS continued its participation in the work of the U.S.-Canadian International Joint Commission (IJC). The principal activity is continua-

tion of stream-flow data collection at stations along the international boundary.

R.H. Langford attended the International Souris-Red Rivers Engineering Board meeting in Ottawa, Canada, and presented the Board's annual report to the International Joint Commission, October 6-10, 1980.

A.J. Horowitz attended a meeting of the International Joint Commission in Windsor, Ontario, during May 13-15, 1981, representing the Survey's National Water Quality Laboratory in discussions of analytical procedures.

OTHER INTERNATIONAL MEETINGS AND CONFERENCES

From October 24 to November 2, 1980, M.E. Moss participated in the founding session of the working group on "Scale Problems in Hydrology" of the IAHS, and on the concurrent workshop of the IIASA on "Criteria, Conflicts, Uncertainty, and Institutions in Regional Water Management," in Laxenburg, Austria.

M.F. Meier attended the 1980 officers' meeting of the International Commission on Snow and Ice in Sapporo, Japan, at the end of October.

In late November 1980, L.F. Konikow attended the Land and Stream Salinity Seminar and Workshop sponsored by the State Government of Western Australia in Perth, Australia.

R.J. Janda presented a paper on sedimentation of Mount St. Helens at the January 1981 meeting of the American Association for the Advancement of Science in Toronto, Canada. Also in January and in Toronto, R.J. Pickering attended a meeting of the Policy and Coordination Work Group, established to guide implementation of the U.S.-Canada Transboundary Air Pollution Agreement.

R.J. Janda, R.M. Meade, and K.M. Noland attended the International Symposium on Erosion and Sediment Transport in Pacific Rim Steeplands in Christchurch, New Zealand, from January 15 to February 5, 1981.

J.H. Eychaner and K.J. Hollett went to Hermosillo, Sonora, Mexico, to present a paper at the annual meeting of the Cordilleran Section of the Geological Society of America in late March 1981.

M.F. Meier attended the first meeting of the Climate Coordinating Forum established by ICSU in Paris and visited the Secretariat of IAHS in London during the period April 26-May 2, 1981.

M.S. Bedinger participated in a Workshop on Siting of Radioactive Waste Repositories in Geological

- Formations sponsored by the Nuclear Energy Agency of the Organization for Economic Cooperation and Development in Paris during May 19-22, 1981.
- M.F. Meier attended the July 1981 meeting of the International Union of Geodesy and Geophysics Executive Committee as President of the International Association of Hydrological Sciences, in London, Ontario.
- R.T. Cheng delivered a series of lectures on the hydrodynamics of tidal estuaries at the IAC, an institute of applied mathematical research in Rome, Italy, in late June 1981.
- C.F. Nordin and W.W. Emmett attended the IAHS sponsored International Symposium on Erosion and Sediment Transport Measurements in Florence, Italy, in late June 1981.
- In Leningrad, USSR, in June 1981, E.T. Sundquist participated at a workshop on the Potential Effect on Global Climate of Carbon Dioxide Produced by Burning Fuels.
- F.L. Paillet attended the annual symposium of the Society for Professional Well Log Analysts in Mexico City, Mexico, in June 1981.
- L.F. Konikow and William Back (principal lecturer) participated in the International Course on New Methods for the Study of Geochemistry and Contamination of Ground Water given by the University of Madrid, Spain, in early June 1981.
- S.N. Luoma attended a Marine Chemistry Symposium held in Halifax, Nova Scotia, in June and was the lead speaker at a session on chemical processes in estuaries.
- Edward Collender attended the Second International Symposium on the Interactions Between Sediments and Freshwater and presented the invited paper "Interactions between Benthic Sediments and Water in the Potomac River Estuary," in Kingston, Ontario, in June 1981.
- M.F. Meier attended the Review Meeting on World Glacier Inventory held in Zurich, Switzerland, from August 21 to September 3, 1981.
- C.R. Wagner and J.C. Futrell, III, conferred with personnel of the Water Survey of Canada on hydrologic instrumentation in Ottawa in September 1981, continuing the information exchange initiated by a Canadian visit to the Survey's Hydrologic Instrumentation Facility in Mississippi.
- I.K. Barnes attended the Second International Symposium on Methods of Applied Geochemistry held in Irkutsk, Siberia, USSR, while en route to visit the People's Republic of China at the invitation of the State Seismological Bureau in Beijing during the period September 16 to October 5, 1981.
- E.D. Andrews attended the Second International Symposium on Modern and Ancient Fluvial Sediments held at the University of Kelle, England, in September.
- H.E. Taylor was a plenary lecturer at the Sixth Australian Symposium on Analytical Chemistry in Canberra City, Australia, and a participant at the Ninth Conference on Atomic Spectroscopy/Colloquium Spectroscopicum International in Tokyo, Japan, in August and September 1981.
- B.B. Hanshaw presented a keynote paper at the GSA Conference "Controls of Carbonate Platform Evolution" in Naples and visited the IAEA in Vienna to discuss isotopic work in geothermal areas in early September 1981.
- D.D. Eberl attended the 7th International Clay Conference in Bologna and Pavia, Italy, during the period September 6-12. He also visited clay mineral laboratories in Krakow, Poland, and Leuven (Louvain), Belgium, during the period September 13-26.

SUMMARY OF SELECTED ACTIVITIES BY COUNTRY OR REGION

ANTARCTICA

Antarctic studies under the World Energy Program are being negotiated with the German Geological Survey as a coordinated seismic processing and interpretation of data gathered by the German Survey in the Ross Sea in 1980. Such a study and its publication would constitute the first public seismic data from that vast, unexplored land. Plate tectonic reconstructions indicate that the oil-bearing Bass Straits of South Australia were once joined to the Ross Sea; such an earlier connection would suggest the strong possibility of oil occurrence in Antarctica. The geophysical analysis program with the German Survey will assess that possibility.

AUSTRALIA

G.I. Smith, as a Fulbright Scholar, examined Quaternary lake records from April to September to provide Southern Hemisphere correlatives to the USGS Climate Change Program. G.L. Raines examined large unconformity-type uranium deposits in June as part of his research to determine regional relations of such deposits for their potential exploration by Landsat imagery analysis.

BANGLADESH

P.W. Richards, J.M. DeNoyer, M.J. Terman, and L.L. Benton examined the organizational structure, facilities, and training level of the Geological Survey of Bangladesh (GSB) and proposed a staged program for GSB modernization with USGS assistance that is to begin in 1982 and probably include some 18 visiting experts over the next 3 to 5 years. This program is fully reimbursable through a loan to GSB from the Asian Development Bank.

During 1981 the energy resource potential of Bangladesh was assessed by the USGS under auspices of AID. Mahlin Ball spent 2 weeks in Dacca conferring with Bangladesh energy resource officials and ascertaining availability and value of data on oil and gas resources and seismic investigations.

BRITISH INDIAN OCEAN TERRITORY

In January 1981, D.A. Davis and C. Hunt departed from Honolulu on a 45-day mission to the strategically important island of Diego Garcia, where they investigated the feasibility of developing freshwater supplies for the U.S. Naval Support Facility.

CANADA

In October, A.M. LaSala, Jr., and G.D. DeBuchanne conferred with Canadian officials in White Shell, Ontario, on the establishment of a subsurface test facility in the crystalline rocks of the Canadian Shield to study response to the storage of high-level radioactive waste. In April, W. Scott Keys attended a symposium workshop on hydrogeologic research on Canadian high-level nuclear waste disposal at the White Shell Nuclear Research Establishment in Pinawa, Manitoba.

CCOP

F.H. Wang continued to serve as technical adviser in marine geology to the United Nations Committee for Coordination of Joint Prospecting for Mineral Resources in Asian Offshore Areas (CCOP), which is an intergovernmental body composed of 13 countries in east and Southeast Asia.

Working at the request of the Commission for the Geological Map of the World (CGMW) and in cooperation with the Circum-Pacific Map Project, geological

maps of the seafloor and continental margin of eastern Asia at the scale of 1:5,000,000 are being compiled. These maps will constitute parts of the third edition of the Geological Map of South and East Asia to be published by CGMW.

During 1981 Wang's preliminary map of the seafloor bedrock and surficial sediments off eastern Asia was revised to standardize legends used with those of comparable maps in other parts of the world and to make use of new data from the oil industry. The general lack of seafloor outcrop data, except around Japan, has been a severe constraint. Cooperation with China is being sought.

Planning began for a CCOP 1982 workshop in Indonesia on offshore geological and natural environmental hazards in petroleum exploration and exploitation in Asian offshore areas. The USGS and the East-West Central Environmental and Policy Institute (EAPI) have been requested by CCOP to contribute leadership roles.

CCOP/SOPAC

In 1981 the USGS began planning offshore and onshore phases of energy resources work for the U.N. Committee for Coordination of Joint Prospecting for Minerals Resources in South Pacific Offshore Areas (CCOP/SOPAC). The USAID-supported research should contribute to the understanding of the structural framework of the region, to a basin-by-basin analysis, and to an evaluation of the total petroleum potential. The USGS offshore work would include 60 days of basic geophysical work using the USGS Research Vessel *S.P. Lee*. Onshore work would include as much as 90 days in Tonga, Vanuatu, and the Solomon Islands.

CHINA

Under the joint sponsorship of UNESCO and the USGS, A.L. Clark, R.B. McCammon, J.L. Cook, and J.M. Botbol organized and conducted a 2½-week training workshop in resource data handling and resource assessment in Beijing, People's Republic of China, June 8 to 20, 1981. The workshop was a continuation of assistance provided by the USGS in Southeast Asia to help standardize international resource data collection and analysis procedures and to promote compatibility with U.S. procedures. Forty-five participants from the Ministries of Geology, Petroleum, Coal, Metallurgy, the Second Machine-Building Industry,

and the Chinese Academy of Sciences attended the workshop.

Chinese petroleum geology is dominated by the petroleum-generating process peculiar to environments of high-heat flow and lacustrine (lake) sedimentary environments. These types of situations are rare in the United States but prominent in some other areas of the world, notably Africa and Brazil, so the project activities will have broad application in the overall program. Another unique aspect of the China program involves investigation of the largest Triassic marine carbonate basin in the world; this study will have application to petroleum occurrence in carbonate basins of all ages.

The Chinese delegation from the Bureau of Hydrology of the Ministry of Water Conservancy in Beijing, China, arrived in Washington on April 23, 1981, and began a 1-month program of information exchange with a meeting at the Survey's National Center on April 24. This activity initiated the cooperative effort in surface-water hydrology between the United States and China under the Science and Technology Agreement signed by the President. A protocol for joint cooperation in surface-water hydrology between the USGS and the Chinese was drafted. The delegation met with several USGS scientists as it toured the National Center.

In October 1980, M.F. Meier visited hydrology and glaciology institutes in the People's Republic of China in his capacity as Project Chief for Glaciology, USGS, and President of IAHS. In July 1981, Robert M. Meade participated in a sediment-sampling cruise on the Yangtze River estuary and lectured at Chinese universities and research institutes on sediment problems in rivers. In September, William Back discussed ground-water pollution with scientists of the Chinese Association of Science and Technology. He also conducted a field study of the karst of China.

COSTA RICA

During 1981, E.R. Landis and R.L. Miller completed a preliminary investigation of the coal resources of Costa Rica. In common with deposits in other Central American and Caribbean nations, the coal of Costa Rica has received little study, though its presence has been known for many years.

As yet, available information is not sufficient to properly categorize and prepare internationally comparable estimates of the coal resources of Costa Rica or of any of the nine areas within the country that are known to contain coal. However, enough data are available to indicate that known coal beds are equal in

thickness and persistence to beds that are minable in other parts of the world and that the coal is high enough in quality to be used for the generation of electricity and for other conversions such as gasification and manufacture of fertilizers. With widespread interest in diversifying energy sources, the solid fossil fuel resources found in many areas that traditionally have been dependent on other forms of energy should be investigated in the future.

EGYPT

A participating Agency Services Agreement with AID, extending the geological mapping and mineral resources assessment program with the Egyptian Geological Survey and Mining Authority (GSE) for an additional year, was approved by AID and by USGS.

The first full-color Geologic Map of Egypt at 1:2,000,000-scale was printed at USGS Reston during July 1981, and 10,000 copies were shipped to the Chairman of the Egyptian Geological Survey and Mining Authority. The map was printed at USGS in order to speed its publication and also to involve GSE trainees in the printing process. D.L. Rossman advised the GSE on compilation of a metallogenic map of the Aswan quadrangle.

Interpretation of aeromagnetic and radiation surveys, reinforcing results inferred from investigations by means of other criteria, provided new magnetic evidence for 107 km of left-lateral movement along the Dead Sea transform fault.

INDIA

H.L. Berryhill, marine geologist, was in India during January and March responding to a request from the Centre for Earth Science Studies to assist in their organization of a Marine Division and to plan for joint studies and staff training. A program for USGS cooperative assistance in nearshore bathymetric data acquisition, the determination of seafloor depth and various stratigraphic horizons, including potential monazite-bearing beds, is under review.

INDONESIA

The USGS continued its 4½-year program of technical assistance to increase Indonesia's ability to collect and interpret earth science data related to land-use and hazard mitigation; this program is fully reimbursable through a loan to Indonesia from USAID.

P.F. Narten continued work on the prototype environmental geology and land-use studies for transmigration problems into East Kalimantan and broadened the project's goal into three scales of mapping—1:10,000, 1:50,000 and 1:250,000. A short examination for geologically controlled land-use problems related to the overpopulated Pacitan area in Central Java was made prior to December 1980.

In March 1981, Allen Sinnott, hydrologist, and G.J. Post, soil scientist from USDA's Soil Conservation Service, provided guidance and training in their respective fields to the East Kalimantan project. Test wells indicated that adequate supplies of ground water can be provided from properly developed drilled wells. Moderately mineralized ground waters contain as much as 700 mg/L of total dissolved solids. Electrical conductivities of less than 50 microhms in most surface waters indicate total dissolved solids of as much as 40 milligrams per liter. The surface soils in the area range from acid to very acid and are generally of low agricultural productivity. Slumping and settling along the Balikpapan-Samarinda Highway have resulted from insufficient compaction of fill reaches during construction. Erosion along roadcuts and elsewhere can be controlled by proper grading and the use of suitable vegetative cover.

Between October and January, engineering geologist J.E. Ege followed up the USGS's landslide assistance work begun in July 1980 in the southern Cianjur Regency, Java, by identifying relevant field-measurement methods and by training his counterparts in the means of instrumentation. Ege established monitoring sites that will permit detection of landslide movements in southern Cianjur Regency; the data thus derived will provide information on causes of land movement, means of impeding movements and mitigating disastrous effects, and a basis for alerting the populace in areas threatened by future slides.

In October 1980 Simon Cargill, computer applications specialist, assessed the existing computer system uses and personnel in the geoscience directorates and related organizations, recommended programs for training and data manipulation and management, and suggested an organizational means of coordinating all computer activities in the earth science fields.

D.B. Krinsley made a brief visit in early 1981 to discuss and review disaster emergency response plans with the Director of the Volcanological Survey of Indonesia (VSI) and the Secretary of the National Coordination Board for Dealing with National Disasters. He received a request that a U.S.-Indonesian memorandum of understanding be prepared so that U.S. experts could be dispatched to assist Indonesia during natural disasters.

In October 1980 J.P. Lockwood began a 1-month case history of the Gunung Gamalama Volcano on Ternate Island of the Halmahera Islands. He returned in September 1981 to complete the revision of the joint Indonesian and USGS Geologic Map of the Gamalama Volcano, Ternate Island, Indonesia, and to consult with the Director of VSI on disaster response plans.

In early 1981 A.T. Okamura, volcanologist, assisted in the installation and instruction in the use of tiltmeters on the Hangkuban Prah Volcano.

From September into January, C.G. Newhall initiated and developed the planned 2-yr-long USGS assistance for studies and monitoring at the Merapi Volcano Observatory. C.D. Miller made a 2-mo study of volcanic hazards prediction means and methods for VSI.

Allen Sinnott completed a 4-mo mission in July 1981, supporting the US AID/USGS Science and Technology Project, Jakarta, by participation in hydrogeologic investigations of the East Kalimantan Environmental Geology Project area. Activities included examination of the quality and quantity of potential sources of water, existing and possible pollution problems, and potential flooding and erosion, particularly in relation to land development.

ITALY

On the basis of a study at Le Castella, Italy, of planktonic Foraminifera and calcareous nannoplankton whose first and last appearance datums (FAD's and LAD's) could be tied to the biostratigraphy of paleomagnetically dated deep sea cores, Haq, Berggren, and Van Couvering (1977) estimated the age of the Pliocene-Pleistocene boundary to be about 1.65 m.y. Because of numerous problems surrounding the Le Castella section (hiatuses, reworking of fossils, faulting, slumping, plus a very abbreviated section), a new stratotype section at Vrica (approximately 18 km northeast of Le Castella) was proposed. However, K-Ar and fission-track dating of volcanic ash (m marker bed) and pumice found in the interval that should encompass the Pliocene-Pleistocene boundary at Vrica yielded ages of 2.0 to 2.5 m.y. (Selli and others, 1977). These results contrast sharply with that of Haq, Berggren, and Van Couvering (1977) for what is thought to be essentially the same biostratigraphic level. J.D. Obradovich, C.W. Naeser, and G.A. Izett, working in cooperation with Italian scientists Giancarlo Pasini (Istituto de Geologia Marina del Consiglio Nazionale delle Ricerche, Bologna, Italy) and Giulio Bigazzi (Istituto di Geochronologia e Geochimica Isotopica del Consiglio Nazionale delle Ricerche, Pisa,

Italy) have now established a chronology for the Vrica section that invalidates all earlier dating efforts. An ash, 280 meters below the m marker bed ash, has been dated at 2.22 ± 0.03 m.y. (K-Ar, hornblende), 2.0 ± 0.16 m.y. (F-T, zircon), and 2.2 ± 0.2 m.y. (F-T, glass shards, plateau annealing method). Selli (1970) had previously reported K-Ar ages of 3.4 and 3.6 m.y. for glass shards from this same ash. Clearly the glass shards contain excess radiogenic argon. Some of the results reported by Selli and others (1977) are, in fact, for this same Pliocene ash because of an inadvertent mislabeling of one of the samples collected at Vrica. Efforts to date on the m marker bed ash were only partly successful. This thin (2-3 cm), lenticular ash is contaminated (determined by electron-microprobe analysis, indicating three populations of biotite), and the youngest age we obtained (1.99 ± 0.08 m.y.) simply provides a maximum that the age of the boundary cannot exceed. The ultimate question, though, is just how much younger can this ash, and, of course, the Pliocene-Pleistocene boundary, be? Using rates of sedimentation of 45 cm/1,000 yr derived from the underlying sedimentary column would indicate that the m marker bed level could be as young as 1.6 m.y. Use of the FAD's and LAD's of certain calcareous nannoplankton and planktonic Foraminifera found in the Vrica section would suggest an age for the boundary near 1.7 m.y. At present, paleomagnetic criteria cannot be used because of conflicting data and interpretations. What is clear is that estimates of a Pliocene-Pleistocene boundary older than 2 million yrs are inappropriate.

JAPAN

Earl Brabb and D.R. Nichols, engineering geologists, were the USGS representatives in a 24-person U.S. delegation invited by the Japanese Landslide Society to examine landslide problems in Japan in October 1980. This exchange of scientific data on landslides and mitigation of associated hazards resulted in arrangements for a similar U.S. meeting to be organized by the USGS in 1982.

JORDAN

C.L.R. Holt, Jr., conferred with the government of Jordan intermittently throughout the year in developing and coordinating implementation of an expanded program of ground-water investigations.

MALAYSIA

A.L. Clarke and J.L. Cook completed work on petroleum-data-handling studies and prepared a handbook on geologic and geophysical data handling, storage, and retrieval for PETRONAS, the national petroleum corporation for Indonesia.

MEXICO

The cooperative program was continued between the U.S. Department of Energy and the Mexican Comision Federal de Electricidad for research, development, and demonstration of applications of geothermal energy in the Cerro Prieto geothermal field in the Mexicali Valley, the southern extension of the Imperial Valley of California. R.L. Ireland, R.M. Jensen and W.D. Zimmerman resurveyed the horizontal control network of the Cerro Prieto geothermal well field in January 1981.

Detailed geologic, geochemical, geophysical, and remote-sensing studies within the El Correo hydrothermal system in northern Sonora, Mexico, augmented by trenching and drilling on the part of the Consejo de Recursos Minerales, have allowed a definition of several components of the system. Stockwork and vein-type copper and molybdenum mineralization in the center of the system is associated with an intrusive center at a fairly high level in a volcanic system. Peripheral lead-zinc-silver mineralization is in brecciated rocks of the volcanic pile in a ringlike fracture system that, determined from audiomagnetotelluric studies, persists to several kilometers of depth. Drilling in the lead zone has not penetrated the zone of hypogene alteration but has provided a clear sequence of supergene mineralogic changes. The pyritic zone, outside of the lead zone, is an intense stockworklike set of fractures localized at least in part around breccia pipes. Pyritization, along with some enrichment in copper and molybdenum, persists to a depth of at least 400 m.

In the Cerro Chile area, west of the El Correo system, an initial reconnaissance in the rare-element-rich zone on the west side of the range found numerous localities containing a series of thorium and rare-earth minerals, but this phase of the study was abandoned before a bedrock source was found. An aeromagnetic survey of the entire area has been completed. In the southern part of the Cerro Chile block, wildly anomalous waters in the Los Tomales area feed an equally

anomalous biogeochemical system. The apparent source for these anomalies is in chalcopyrite- and molybdenite-rich veins forming a long, linear stockwork in old granodioritic rocks that are intruded and segmented by a sequence of younger porphyritic rocks.

There is exceptional access to a wide range of hydrothermal gases from the Cerro Prieto geothermal field which has been extensively drilled and has produced from depths of 1 to 2.5 km with temperatures ranging from 240° to greater than 340° C. Fluids have also been collected from cool to boiling surface discharges adjacent to the field. The gases consist of H₂O, CO₂, H₂S, CH₄, H₂, N₂, higher hydrocarbons, and noble gases.

Carbon dioxide in well samples could be juvenile from its isotopic composition ($\delta^{13}\text{C} \sim -5$ to -8) but is in thermodynamic equilibrium with C, H₂, and H₂O. It probably originates from thermal alteration of deltaic sediments containing carbonate ($\delta^{13}\text{C} \sim 0$) and organic matter ($\delta^{13}\text{C} \sim -15$ to -25). H₂S ($\delta^{34}\text{S} \sim -1$) is in equilibrium with H₂, H₂O, pyrite and pyrrhotite (which control sulfur fugacity) and could have either a volcanic or sedimentary origin. CH₄ ($\delta^{13}\text{C} \sim -30$) is in equilibrium with H₂, CO₂, and H₂O and could have originated by reaction of these gases, but appears isotopically cogenetic with C₂-C₇ hydrocarbons. C₆ hydrocarbon gases are isotopically similar to coal ($\delta^{13}\text{C} \sim -24$), while C₅ to C₇ gases are progressively lighter. Relative concentrations of C₄-C₇ gases are greater at lower temperatures, behavior consistent with thermal breakdown of large organic molecules to smaller ones at rates proportional to temperature. H₂ is in equilibrium with CO₂, H₂O, and C (coal), which appear to control the O₂ fugacity in the reservoir. N₂, H₂, and NH₃ are in equilibrium, but atmospheric N₂/Ar ratios are observed. Hence, the nitrogen for the NH₃ formation must come from organic breakdown.

Recharge by meteoric water at about 10° C is indicated because He, Ar (36 and 38), and Kr are of atmospheric isotopic compositions and elemental abundances. Additions of radiogenic ⁴He (up to 5.5×10^{-5} c³ STP/g fluid) and ⁴⁰Ar (up to 1.7×10^{-5} c³ STP/g fluid) are observed. Positive correlations between the atmospheric and radiogenic noble gases indicate deep recharge and subsequent steam losses. Varying degrees of depletion of noble gas indicate steam formation in the range of 0-3 percent of the fluid. The ³He/⁴He ratio is 6× atmospheric.

All Cerro Prieto gases appear to have a local origin from recharge waters or heating of water-saturated organic- and carbonate-rich deltaic sediments. Even ³He may have been leached from intrusive igneous rocks rather than having come directly from mantle fluids.

NICARAGUA

A.F. Espinosa, under the sponsorship of the Foreign Disaster Assistance office of AID, visited Managua to advise on problems related to seismic risk, strong ground motion, and attenuation. These studies have a direct impact on the new building code for reconstruction proposed in Nicaragua.

PHILIPPINES

A.L. Clark and J.L. Cook conducted a workshop on standardization of terminology and formats for energy data sponsored by CCOP and the Philippine Bureau of Energy Development. Member countries of CCOP participated and produced a regional thesaurus of geographic/geologic terms for each country, as well as detailed formats and pool files for use in each country.

PORTUGAL

J.D. Bredehoeft, N.E. Hutchison, and Morris Deutsch worked in Portugal during September 1980 providing technical assistance to governmental officials on water-resources management programs, development of a water data storage and retrieval system (Hutchison, 1981), and use of remote-sensing data in hydrologic evaluations. The emphasis of the three assignments was on the Algarve region.

From March to June 1981, W.W. Doyel was detailed to the U.S. Agency for International Development to develop programs for systematic investigation of the ground-water resources of the islands of the Azores and Madeira. For Madeira, a conventional program of fundamental and special studies by a full-time technical staff was proposed. Comprehensive study of the several islands of the Azores Archipelago however, requires establishment of a regional management structure under which the necessary technical activities, coordination, and cooperation might be effected. Administrative and technical requirements for the studies of both areas were given to U.S. AID.

SAUDI ARABIA

Reconnaissance geology of the Al'Awshaziyah quadrangle

G.W. Leo reports that the Al 'Awshaziyah 30-minute quadrangle in the northeast part of the Arabian Shield (northeast corner: 27° N., 42° E.) is under-

lain by a variety of layered volcanogenic rocks and plutonic rocks of probable Late Proterozoic age. The layered rocks constitute two generally distinct sequences. The older of these (Jabal Aqab sequence) consists of volcanic rocks ranging from basalt to quartz keratophyre and rhyolite(?), in addition to tuffaceous siltstone, sandstone, and coarser, poorly sorted sedimentary breccia. The younger sequence (Al 'Awshaziyah sequence) discordantly overlies the Jabal Aqab sequence. It consists dominantly of felsic ignimbrite and fragmental tuffs but includes some volcanoclastic sandstone and siltstone. The Al 'Awshaziyah assemblage is an eruptive sequence related to a large caldera (20–25 km diameter) centered in the western part of the quadrangle. The mineralogy of the caldera sequence suggests compositions ranging from dacite to quartz latite or rhyolite.

Plutonic rocks include granites of several distinct ages, as well as subordinate granodiorite, tonalite, diorite, gabbro, and at least one small layered mafic-ultramafic intrusion. The granitic rocks seem to be calc-alkaline, with the exception of a relatively young, subcircular peralkaline pluton (Jabal ar Ruman Batholith) that cuts into the western part of the quadrangle. One of the older granites is intimately associated with the Al 'Awshaziyah volcanics and may be comagmatic. Most of these rocks are pervasively hydrothermally altered and metamorphosed at lower to middle greenschist facies.

Tectonism in the region is confined to relatively small-scale faulting, locally intense fracturing, and moderate folding and tilting. The Jabal Aqab rocks commonly are steeply tilted and locally overturned; the Al 'Awshaziyah sequence shows gentle to moderate tilts radial to the caldera center and is demonstrably right-side-up. There is little indication of potentially economic mineral deposits.

Age and strontium initial ratio of plutonic rocks

Geochronic studies by R.J. Fleck and D.G. Hadley by means of Rb-Sr, K-Ar, and $^{40}\text{Ar}/^{39}\text{Ar}$ techniques document a southwest to northeast decrease in age of orogenic events in the Arabian Shield. These events include the emplacement of the oldest (dioritic) plutonic units, the deformation of these dioritic units and stratified units intruded by them, and the intrusion of late-orogenic and postorogenic plutons.

Initial $^{87}\text{Sr}/^{86}\text{Sr}$ ratios in the northern and eastern parts of the shield are generally below 0.704. The few exceptions are restricted to low-strontium, postorogenic plutons that may have incorporated marine sedimentary materials. No evidence of lower Proterozoic units was found, and the low initial ratios

support the contention that no sialic crust of that age is present in the areas studied. Elevated lead isotopic ratios reported for galenas from the eastern part of the shield (Stacey and others, 1980) may have resulted from mobilization or incorporation of lead from middle or upper Proterozoic sedimentary units derived from older rocks. Alternatively, these ratios may have resulted from partial melting of a lower Proterozoic continent. Rb/Sr results are consistent with an origin by accretion of intraoceanic island arcs, the more easterly of which may have included substantial sedimentary materials from an older continental source.

Age of diorite-granodiorite gneisses

Total-rock rubidium-strontium isochron ages were obtained by R.J. Fleck from dioritic to granitic plutons in the Jiddah-Makkah region, most of which are between 760 and 780 m.y. These results and the low initial $^{87}\text{Sr}/^{86}\text{Sr}$ ratios (about 0.70267) suggest that granites older than 1,000 m.y. are not present in this area. The low ratios also indicate that orogenesis during and shortly after formation of the plutons occurred within a crust having a low Rb/Sr ratio, probably at an intraoceanic convergent plate margin. The results are consistent with previous suggestions that this part of the Arabian Shield formed in an island-arc environment.

Implications of common lead measurements

John Stacey reports that the oldest igneous rocks found in the Al Amar region of the eastern Arabian Shield are in a gabbroic gneiss from the Urd ophiolite sequence just west of the village of Halaban. Zircons from this sample yielded an almost concordant U-Pb age of 700 m.y. U-Pb zircon ages of the more evolved continental rocks west of the Al Amar fault range from 680 m.y. for a granodiorite to approximately 580 m.y. for posttectonic granites that intrude the Abt schist. East of the Al Amar fault, a tonalite has a U-Pb zircon age of 660 m.y., and later dioritic rocks are 640 m.y. old.

Lead in feldspar from these rocks in the Al Amar region seems to contain a continental component, perhaps as old as 2,000 m.y. Zircons yielding a rather discordant U-Pb age of 2,000 m.y. have been found by Calvez (written commun.) in a leucogranite near the Al Amar fault. To the south of Al Amar at Jabal Sitarah, and 200 miles west at Afif, feldspar leads in upper Precambrian rocks have very much higher $^{207}\text{Pb}/^{206}\text{Pb}$ and $^{208}\text{Pb}/^{206}\text{Pb}$ ratios than those at Al Amar and therefore exhibit a more pronounced old crustal component. This is in contrast to the situation

in the southern part of the shield (southeast Asir) where lead-isotope ratios from feldspars in igneous rocks are consistent with evolution from a single oceanic crustal source approximately 750 m.y. old.

As strontium-isotope ratios are only slightly elevated in the rocks that contain continental-type lead, a lower crustal source seems probable. However, the search for the source of the older lead continues because this may lead to a better understanding of the structure and evolution of the whole Saudi Arabian Shield.

Granitoid plutonic rocks of the Arabian Shield

D.B. Stoesser, in collaboration with J.S. Stacey, completed a study on the U/Pb zircon geochronology of granitoid plutonic rocks in the southern part of the Arabian Shield. The results indicate that the Wadi Tarib composite batholith was emplaced during the approximate period 700–735 m.y. (Halaban/Hulayfah age) and is significantly younger than the An Nimas batholith (older than 815 m.y.) to the west. The batholith is interpreted to be the result of continental or island-arc to island-arc collision somewhere east of the exposed shield. The results also indicate that the southernmost shield experienced major tectonism in the period 650–670 m.y., at which time the Khamis Mushayt gneissic complex, the Malahah dome, and other major gneissic complexes were emplaced. Postorogenic granites in the region were emplaced during the period 625–650 m.y.

Zircon dating of plutonic and volcanic rocks of the Wadi Wassat region indicate that the oldest sampled plutonic rocks there generally fall in the range 640–660 m.y. This result was derived from the dating of quartz diorite bodies from the northeastern Malahah quadrangle (lat. 18°30' N., long 44° E.), which gave an age of 660 m.y., and those from the Najran Airport area (lat 16°30' N., long 44°30' E.), which yielded a date of 640 m.y. These results support the interpretation that the layered rocks intruded by the quartz diorite plutons in the Wadi Wassat region are of Halaban age.

Cenozoic volcanic rocks

R.C. Coleman and R. Gregory completed fieldwork over an area of about 90,000 km² in a study of volcanic fields (harrats) in the Arabian Shield. The studies suggest that Harrat Hadan is the oldest field (probably similar in age to the As Sirat) followed by Harrats Kura, southern Rahat, southern Uwayrid, and parts of Al Hamad. Harrats Kishb, Ithnayn, northern Rahat, northern Uwayrid, Khaybar, Lunayir, and Nawasif are all young fields exhibiting Holo-

cene activity. The historic flow at Madinah was examined to compare its features with those of the younger flows in other harrats. The presence of buried "Neolithic" rock monuments in several of the Holocene harrats suggests significant activity within the last 10,000 yr.

Fissure eruptions of olivine basalt delivered the youngest lavas to the harrat, and during the later stages of the eruptive events, extrusion of material was centered at cones that formed along the north-trending fissures. Peridotite-nodule-bearing tuff rings are common within the harrat. Harrats Rahat, Kishb, Khaybar, and Uwayrid are bio-modal, containing both basaltic and silicic rock types. Intermediate magmas are conspicuously absent in the Cenozoic volcanic suites.

Regional assessment of the Wadi Bidah district

C.W. Smith, A.M. Helaby, Mohammed Naqvi, and Mir Amjed Hussein completed the final phase of fieldwork and compilation to assess the Wadi Bidah mineral district. The fieldwork consisted of geologic mapping and rock sampling for trace-metal analysis in an area about 10 km southwest of the USGS Baha camp (lat 20° N., long 41°15' E.). This area includes two adjoining aeroelectromagnetic anomalous zones that cover about 10 km².

The rocks are predominantly metasedimentary, dip steeply, and strike north. Much of the section consists of chemical precipitates, including massive chert beds locally containing pyrite and minor copper staining. Cherty iron-manganese formations are a major feature of the stratigraphic section. These formations closely resemble the rocks found in Wadi Bidah proper, and in a few places they grade into goethitic-hematitic gossans stained by secondary copper. The gossans, where exposed, are small; some are almost covered by alluvium.

The area appears to be part of an eroded anticlinorium that has a north-trending fold axis. A small gold deposit in chert is associated with east-trending shears.

Baid al Jimalah tungsten deposit

Significant tungsten mineralization is within and marginal to a small irregular cupola and dike network of upper Proterozoic porphyritic, biotite-bearing microcline-albite granite at Baid al Jimalah (lat 25°09' N., long 42°41' E.). The granite is highly enriched in lithium, fluorine, beryllium, tungsten, and tin, and has been heavily veined and greisenized, probably during an intense hydrothermal event related to the emplacement of the granite. Mineralization consists principally of very coarse crystals of wolframite,

lesser cassiterite, and minor scheelite in stockworks and in dense, subvertical veins of vuggy quartz. Greisenized granite and country-rock hornfels contain some disseminated cassiterite, wolframite, and lesser pyrite. Composite samples collected by J.C. Cole and J.E. Elliott from excavated trenches contain significant amounts of tungsten and minor amounts of tin. The outcrop of the mineralized area exceeds 700 m by 800 m and consists chiefly of subparallel zones of closely spaced quartz veins. In the northern zone, sample material from 120 m of the 320 m of trenching contains more than 2,000 ppm tungsten, the highest value being 12,500 ppm. The southern zone is somewhat distinct, containing higher median concentrations of lithium, fluorine, tin, beryllium, and sulfides, and may have been formed at slightly lower temperatures. In the southern zone, sample material from 25 m of the 275 m of trenching contains greater than 2,000 ppm tungsten, the highest value being 5,000 ppm. A total of 210 m of trenching was done in outlying zones. In these, samples taken over a distance of 20 m contain more than 2,000 ppm tungsten, the highest value reaching 12,950.

The granite and veins were emplaced in fine-grained clastic rocks of the Murdama group, just below the subhorizontal unconformity that marks the base of the younger Al Jurdhawiyah group of continental andesitic volcanic and volcanoclastic rocks. Tungsten mineralization is most likely younger than the Al Jurdhawiyah group and may be cogenetic with a vein- and fracture-controlled lead-zinc-silver deposit 2 km to the east.

The Baid al Jimalah tungsten deposit is similar in terms of its structural setting, chemistry, mineralogy, and paragenesis to other tungsten and tin deposits around the world that are associated with granitoid plutonic rocks. The size of the mineralized area is comparable to that of producing economic deposits elsewhere, but the depth and grade of the ore at Baid al Jimalah are as yet undetermined, though under study. The USGS and the Riofinex Geological Mission are jointly examining the prospect and adjoining areas. The work includes but is not limited to large-scale mapping, core drilling, trenching and sampling, bulk sampling, detailed colorimetric and instrumentation analysis, petrological studies, geochemical surveys, and geophysics (spectrometry, magnetometry, induced polarization, gravimetry, electromagnetometry, and downhole logging).

Mineralization at the Mahd adh Dhahab gold mine

A special study of mineralization at the Mahd adh Dhahab gold mine was made by a team of USGS

geologists: R.G. Worl and R.J. Ebens (geochemistry); R.O. Rye (stable isotopes); C.G. Cunningham (fluid inclusions); J.S. Stacey (U/Pb geochronology, common Pb isotopes); W.E. Hall (ore petrography); and J. Doebrich and J. Leanderson (host-rock alteration).

Field investigations by the team indicated that the mineralization is associated with a hypabyssal rhyolite stock that intruded its own volcanic ejecta. The later stages of intrusion were dominated by forceful emplacement, which domed the overlying country rocks. A metamorphic aureole or hornfels was formed and xenoliths were incorporated in the stock. Pervasive silicification and sericitization grade locally into chlorite and potassium-feldspar alteration as the dominant assemblage.

Pressure gradients at the margin of the stock resulted in the formation of a crackle breccia by hydrofracturing. The breccia is pervasive and extends into the country rock. At the highest levels of the dome, the spalling of slabs of country rock and solidified rhyolite produced cracks which filled with clastic debris.

Ore deposition was largely controlled by the pressure gradients and attendant thermal, physical, and chemical changes at the margins of the stock. In the course of passing from a lithostatically dominated rhyolite magma system to a hydrostatically dominated system in the adjacent country rocks, the fluids would be expected to boil and cool, losing H₂S and CO₂, and undergo resulting pH changes.

Continued extensional tectonism produced regional north-striking fractures, which cut the rhyolite. Some of these vein systems at the surface are mineralized and others are barren. Some of these veins may result from continued activity during waning stages of the hydrothermal system or may be related to an undiscovered, younger system at depth.

The results of biogeochemical sampling indicate that samples of ash of *Acacia* branches contain amounts of trace elements (particularly lead and zinc) that show a high positive correlation with bedrock geology, and that they reflect mineralized versus nonmineralized ground, even where covered by alluvium.

Bouguer gravity of a part of the southern Arabian Shield

Reductions and analysis of gravimetric ties to the International Gravity Standardization network were completed by M.E. Gettings. This work resulted in a first-order tie to IGSN71 network at Port Sudan, Khartoum, and Nairobi for the Jiddah base, thus improving its reliability to the level of about ± 0.03 mgal. The results for the gravity meter calibration line from Jiddah to At Taif are of high quality, having

been established at 20 occupations of the loop stations using 4 different instruments in 5 runs. The calibration range covers about 500 mgal in the central part of the range of observed gravities in Saudi Arabia.

Reduction of existing regional data for the southern shield (approximately 1,800 stations) was completed, and a simple Bouguer anomaly map has been prepared at contour intervals of 5 mgal. The map clearly delineates the principal greenstone belt as a north-trending high, and also shows important regional discontinuities trending east and northwest.

Interpretation of seismic deep-refraction line

W.D. Mooney and M.E. Gettings completed work on the seismic deep-refraction line. Many USGS staff contributed time, effort, and support for the refraction work.

The data have been interpreted on the basis of horizontally layered models and standard two-dimensional ray-tracing techniques. To a first-order approximation, the shield is composed of two layers, each about 20 km thick, one having 6.3 km/s and the other 7.0 km/s average velocity. At the western margin of the shield the crust thins to less than 20 km in thickness; the Red Sea coastal plain and shelf are interpreted to be underlain by oceanic crust.

A major lateral inhomogeneity in crustal velocities northeast of Sabhah is interpreted as two crustal blocks of different compositions. Several high-velocity anomalies in the upper crust correlate with gneiss dome structures. Two intracrustal reflectors at 13 km depth have been identified and are interpreted as the tops of mafic intrusives.

The Mohorovicic discontinuity beneath the shield ranges from 43 km in depth and 8.2 km/s in mantle velocity in the northeast to 38 km in depth and 8.0 km/s in velocity in the southwest. Two velocity discontinuities in the upper mantle at 59 and 70 km depth are identified.

The basement beneath the sediments of the Arabian platform near shot point 1 at the extreme northeast end of the seismic line appears to vary in depth in agreement with mapped fault zones. The total vertical relief is about 1,000 m and is interpreted to reflect horst-graben structure.

The Geophysical Observatory

H.M. Butler and H. Merghelani (DMMR), assisted by M. Bassari, identified a new site for the planned Geophysical Observatory. The new site is at approximately lat 21°14' N., long 40°33' E., 17.5 km southeast of the city at At Taif and about 2 km north of the At Taif-Abha Highway. It is about 2 km east of Wadi

Liyah, in a small basin enclosed by outcrops of fresh, structureless granite, well isolated from any cultural disturbances and easily accessible from the main paved highway. An on-site noise survey was made to compare the background noise levels of the Wadi Urudah (former proposed site, which could not be made available for the observatory) and Wadi Liyah locations. The normal microseism intensity does not differ significantly between the two sites (both could operate at a magnification of 200,000). It was found, however, that an increase in the level of noise generated by cultural activity in the area has occurred at the Wadi Urudah site since its previous noise-level survey, making that site less desirable than originally considered.

The process of land acquisition is being handled by officials of the Kingdom and the city of At Taif. The title held by the present land owner was determined to be free and clear, and it is expected that the government will conclude the purchase of the property. Architectural and engineering work will commence immediately afterwards.

The development, fabrication, assembly, and testing of seismic systems that will be installed at the Observatory are being carried out at USGS, Albuquerque, N. Mex., by B.W. Thompson, under the direction of H.M. Butler. The geomagnetic system is being developed by J.D. Wood, USGS, Denver, Colo.

Water resources advisory service

The U.S. Departments of the Interior and Agriculture provide a variety of technical and advisory services to the Saudi Arabian Ministry of Agriculture on water resources and related programs. These services are made available to support the Agriculture and Water Project (AGWAT) of the U.S.-Saudi Arabian Joint Commission on Economic Cooperation (JECOR). Under the agreement, technical specialists of the USGS work directly with the Saudi Water Resources Development Department (WRDD) in the collection, processing, and analysis of data on surface water, ground water, and water quality for the Kingdom.

During 1981, Ministry officials were advised on a number of water development projects and significant progress was made in computerizing the water resources data base for the Kingdom. A ground-water model of the Minjur aquifer system was completed and used to provide development, planning, and management information. A joint project to install 250 crest-stage gages for documentation of peak runoff events was underway. The Ministry of Agriculture and Water initiated several new programs for 1981,

including Water Atlas, Water Reuse, and Agricultural Meteorology projects. The Water Atlas project is to provide a series of maps portraying topographic geologic, hydrologic and climatologic conditions throughout the Kingdom. These new programs increased the USGS representation in AGWAT from 5 to 13 specialists.

SWEDEN

Age and genetic constraints for the uranium deposit at Lilljuthatten

Geologic, petrographic, geochemical, and isotopic studies have been made to examine the genesis of the uranium deposit at Lilljuthatten, Sweden, and its relationship to the Olden Granite (Stuckless and others, 1982b). The complex geologic history of the area precludes unique interpretations of the data, but internally consistent and geologically reasonable models can be developed.

Analyses of whole-rock drill-core samples from the ore deposit, six of which are mineralized, yield a Pb-Pb age of 420 ± 3 m.y. This age corresponds to the last stage of the Caledonian orogeny, and therefore, the investigators conclude that the uranium deposit formed as a result of that event.

None of the isotopic systems examined have completely retained the intrusive age of the granite, but data for Rb-Sr whole-rock, Pb-Pb whole-rock, and Pb-Pb galena all suggest an age of approximately 1,650 m.y. Zircon U-Pb data yield a three-stage history for which a minimum age of 1,570 m.y. can be calculated. There is a general correspondence between samples that exhibit open-system behavior isotopically and samples that are displaced from the polybaric minimum in the system Q-Ab-Or. This suggests that most of the Olden Granite was affected by hydrothermal activity during the Caledonian orogeny. An effect of the hydrothermal activity was to deplete most of the granite in uranium so that most samples contain excess radiogenic lead relative to uranium. Only oxygen isotope values, rare-earth-element contents, and possibly thorium contents seem to have been unaffected by hydrothermal activity. If thorium was immobile, then most samples also lost some radiogenic lead.

A model for the genesis of the uranium deposit at Lilljuthatten is proposed as follows: (1) derivation of a highly evolved granite, probably by partial melting of crustal materials, at approximately 1,650 m.y. ago; (2) pervasive hydrothermal alteration and fracturing of the granite in response to the Caledonian orogeny at approximately 420 m.y. ago with mobilization of uranium and lead and precipitation of these elements in

open fractures; and (3) recent modification of uranium distribution in response to near-surface hydrologic conditions.

THAILAND

R.O. Fournier, under AID sponsorship and in cooperation with the Electric Generating Authority of Thailand, the Department of Mineral Resources (DMR), and Chiang Mai University, examined nine geothermal localities in October 1980. On the basis of his work five localities in northwest Thailand appear promising as prospects for geothermal resources.

R.J. Hite returned to Thailand in October 1980 to assist DMR in evaluating corehole data of the potash deposits drilled since 1974. He examined the proposed rock-salt carnallite mining area of Banmet Narong District in the Central Khorat Plateau, suggested the controlling structural and age relations between carnallite and sylvite, and predicted that they would be effective guides for potash exploration. In brief, the cutting of deep stream channels in the overburden rocks during the Pleistocene caused differential unloading in the underlying carnallite-capped salt beds. These beds responded by rising anticlinally below the channels. The carnallite on the crests of the anticlines has been altered by solution to sylvite, the potash ore, and redeposited on the flanks of the anticlines. In Hite's model the location of the now buried and concealed stream channels would be a primary guide for potash prospecting on the Khorat Plateau. These old elastic-filled channels, which are probably of major significance to ground-water distribution and supply, can be located by gravity and electrical geophysical techniques.

In parallel geophysical studies, J.C. Wynn returned to Thailand in August 1981 to provide guidance and training in the analysis of geophysical data and to give 2 weeks' training in electrical exploration geophysical methods. He designed a program to verify the Hite model and made detailed interpretations of the resistivity profiles in the Bamnet Narong District, which confirmed veracity of the model there. Wynn also provided the DMR with petrophysical analyses of 25 samples from the Khorat Plateau and computer-generated color maps of gravity data and models of the buried channel at Mahasarakam. The very low frequency electromagnetic data acquired by Wynn at Mahasarakam in 1980 had one anomalous area interpreted to be a breached anticline. This was confirmed by Thai drilling in the spring of 1981.

V.E. Swanson also returned to Thailand as a follow up to his 1980 drilling recommendations for the development of lignite resources. Swanson, as monitor

of the TDP-sponsored exploratory drilling program being done by a U.S. private company, reviewed the program results in June. He examined outcrops and drill cores, evaluated ongoing drilling in four coal basins, and concluded that the Mae Ramat basin has no economically minable lignite but the Chao Hom basin does have potential.

In a November 1980 visit J.R. McCord, photographic specialist, explored the means to establish photographic reproduction facilities in remote-sensing laboratories at the national level.

TUNISIA

M.J. Grolier, P.A. Davis, and P.A. Schultejan completed a study of Landsat image analysis as a tool in exploration for phosphate in Tunisia. Their study covered digitizing techniques that can be useful in detecting phosphate-, halide-, and gypsum-bearing areas on Landsat images. The work is part of an AID-sponsored remote sensing project with Tunisia.

UNITED KINGDOM

Geophysical study of shallow coals

During FY '81, the U.S. Geological Survey and the National Coal Board of Great Britain conducted a joint study on the use of shear-wave seismics for evalu-

ating strippable-depth coals. First findings of this effort indicate that in two test areas shear-wave reflection from depths of 5 to 50 m could be seen, shear-wave refractions could be used to find subcrops, and shear-wave methods could be used to delimit the extent of an abandoned, shallow coal mine.

YEMEN ARAB REPUBLIC

The ground-water potential and hydrogeology of the Amran Valley north of the capital city of Sana have been described in a report by G.C. Tibbitts, Jr., and James Aibel (1980). The work was an element of the Water Survey of North Yemen Project carried out under the auspices of the U.S. Agency for International Development. It was the first such investigation undertaken in North Yemen in which an appreciable number of Yemeni technical personnel participated. In another element of the project, a qualitative appraisal of the hydrology of the Republic has been made from a series of Landsat images (Grolier, Tibbitts, and Ibrahim, 1981) describing the flow regimens of streams and the regional distribution of vegetation as an indication of the occurrence of ground water at shallow depth.

R.M. Beall was detailed to U.S. AID in June to assist in an evaluation of progress being made on the establishment of a Department of Hydrology within the Yemen government.

CARTOGRAPHIC AND GEOGRAPHIC RESEARCH

AUTOMATED SPATIAL DATA HANDLING

Data base development

One of the major activities of the NMD is the development of the Digital Cartographic Data Base (DCDB). Plans call for the data base to consist initially of the boundaries, public land net, streams and water bodies, and transportation features shown on 1:24,000-scale maps; of elevation data largely obtained concurrently with the orthophotoquad program; of planimetric features from the 1:2,000,000-scale sectional maps of the "National Atlas of the United States of America"; of elevation data obtained from the 1:250,000-scale map series; of land use and land cover data; and of geographic names. The potential size of the data base is extremely large; with complete coverage of the conterminous United States at 1:24,000-scale requiring nearly 54,000 maps, the data base would eventually contain several trillion bits of spatial data. For comparison, a typical typewritten page contains about 25,000 bits.

In its configuration, the DCDB is a unified set of smaller generic data sets that are managed by the SYSTEM 2000 data base management system (DBMS). It is important to note that only the files are managed and not the coordinate and attribute data within the files.

There is, however, a standard file format for the map information managed by the DBMS. This format describes the parameters and characteristics of the individual map data files. General information such as map name, scale, projection, and data resolution is stored. In addition, data on the numbers of points, lines, and areas, as well as the attributes of these features, are specified for each map.

The purpose of the DBMS is to accept, catalog, and archive digital cartographic data files in a standard way and to access the files or report information about the files upon request. Certain file data, such as name, date, geographic coverage, data categories, and accuracy, are extracted and stored in the DCDB SYSTEM 2000 index. The DCDB system, providing at least two backup copies of each file on high-density tape, is also used to produce archival magnetic tapes.

Research is being conducted to expand the DBMS from a file management system to a spatial data base management system that would enable the user to query the actual spatial data currently contained in individual files. To do so will require not only a greater understanding and formalization of the types of queries

that are going to be placed upon the data base but also a rigorous definition of the spatial operations that must be performed in order to answer a question. In such a configuration, the formal query will invoke a sequence of spatial operators to manipulate the required data sets and produce the desired output product.

The 1:2,000,000-scale data base

Most Federal programs are established on a nationwide basis, and many of these require definitive information about the spatial relations of features routinely shown on base maps. Such feature data can be practically combined, manipulated, and analyzed only by digital means. To satisfy the expressed needs of both the USGS and other user agencies for a small-scale national data base, the data base had to contain cartographic information that was current, topologically structured, no smaller in scale than 1:2,000,000, and sufficiently flexible to permit the generation of smaller-scale derivative maps, thematic overlays, and other graphic products. Existing cartographic data bases, related applications software, and data collection hardware systems were investigated, but all had limitations. After considerable study and planning, NMD defined a series of tasks directed toward the generation of a comprehensive nationwide data base.

The 1:2,000,000-scale general reference maps of the "National Atlas of the United States of America" were selected as the available source materials best able to meet the requirements. The resulting data are current to 1980, comprehensive, and available in two file organizations, one topologically structured and the other compatible with the Cartographic Automatic Mapping (CAM) Program. The data include political and Federal administrative boundaries, roads, railroads, streams, water bodies, and airports. The coding scheme allows maps to be generated with appropriate detail for a particular map scale and theme.

DEM editing using a polygon scan-conversion process

One device the NMD uses to produce DEM's is the GPM-2. The GPM-2 electronic image correlator derives a gridded array of elevations from stereophotographs. However, because of problems in automatic correlation on certain topographic features, such as large water bodies, elevation data derived for these features must be further edited. A polygon scan-conversion routine was developed on an interactive computer graphics system to edit GPM-2 elevation data for uncorrelated water bodies. DEM's in both the

GPM-2 patch format and DCDB profile format can be edited with this routine. Complex polygon structures, such as multiple islands within a lake boundary, can be processed efficiently.

The DEM for the Shadow Mountain, Colo., quadrangle was selected for testing the editing software. A total of 22 edit polygons were digitized (2 large reservoirs, 6 ponds, and 14 islands). The digitizing and attribute tagging of the polygons took 1.5 h and the polygon scan-conversion routine took 15 min. The output from the editing process is an edited DEM, captured on a magnetic tape, having the same logical and physical file layout as the input DEM. Relative accuracy tests on the unedited and edited DEM showed RMSE's of 17.75 m and 11.95 m, respectively.

Automated cartography

The use of the computer has been incorporated into nearly all computation phases of map production, and cartographers have taken advantage of this technology to enhance many of their production procedures. With the modern digital cartographic equipment now available, it is possible to utilize computer-assisted techniques in many phases of map production to allow greater flexibility in mapping techniques and products.

In conventional map compilation operations, the map features are traced out on the stereoplotter tracing table, which is linked either mechanically or electronically to a pantograph or slave plotter, which produces a drawing of the features on a Mylar manuscript. The manuscript is then usually scribed with proper symbology to produce the color separate guides.

In late 1977, research was initiated to test the feasibility and cost-effectiveness of capturing digital cartographic data directly from the stereoplotter. New equipment and techniques now permit the use of stereomodel digital-data capture, interactive editing, and cartographic machine-plotting techniques for the automated production of conventional map color-separate guides. The corresponding digital data stored on magnetic tape or disk can be processed further to generate other products, such as USGS standard DEM and DLG files, and to establish digital topographic data bases for revision.

Currently, four Kern PG-2 stereoplotters are dedicated to collecting digital data on a production basis. The stereoplotters are equipped with shaft-angle encoders, which output to an Altek AC/189 three-axis digitizer and tape unit. The digitizer captures X-Y movement of the plotter tracing table either by an incremental vector criterion (usually about 4-6 ft at

ground scale) or through an angle-based hardware filter, which eliminates unnecessary vertices. Attribute codes are entered through an Interstate Voice Data Entry System (VDES) interfaced to the digitizer. The VDES, supported by a Data General Nova 2 minicomputer, allows the operator to enter attributes without breaking concentration or moving away from the stereoplotter. The VDES also reduces coding errors by prompting the operator to enter additional attributes as required for special features.

Processing of digital data is accomplished on a Pekin-Elmer (PE) 3220 System. Interactive editing capability is available on the DDES supported by a DEC PDP 11/70 computer. Verification plots are generated on a Versatec 8242A raster plotter, while color separation guides are photoplotted on a Gerber 4477 flatbed plotter.

As a result of research in stereomodel digitization, the Digital Cartographic Software System (DCASS) was developed. DCASS is a system of programs used to collect, process, manipulate, and derive useful products from digital data obtained directly from the stereoplotter or digitizing table. All DCASS software utilizes a feature-indexed file structure for representation and storage of digital cartographic data. This commonality allows maximum flexibility as well as reduced software development costs, as many programs share the same routines for feature storage and manipulation.

The DCASS structure is vector based and was designed to maximize the ease of performing cartographic manipulations, such as joining of features across photogrammetric models and resampling of contours for DEM production. Although the usual processing unit is one 7.5 minute quadrangle, DCASS can process maps of any scale within resolution limits. The DCASS structure consists of two files: an attribute file and a coordinate file.

DCASS consists of six major subsystems. Each subsystem, comprised of one or more programs, exists for one of three primary functions. The subsystems can be categorized as: (1) manipulation (having the power to alter the contents, but not the structure); (2) application (using a read-only mode to generate some other product); and, (3) utility (reformatting and support functions).

DCASS is being used in a production mode. Test results show that the accuracy of DEM's produced by DCASS range between one-fourth and one-half the contour interval of the compiled quadrangles. DCASS is also being used to produce Provisional Edition 1:24,000-scale topographic maps. Approximately fifty of these maps have been completed and are now in the

map-finishing stage. Initial results indicate a savings of about 20 h per quadrangle for digitally produced maps.

Geographic Information System Development

Two primary goals of the digital mapping program are to (1) create, maintain, manage, and distribute the national cartographic and geographic digital data base for multipurpose needs; and (2) implement digital techniques in cartographic and geographic operations. To accomplish both of these goals, capabilities in the areas of spatial data manipulation, retrieval, and analysis must be developed. Research to address these goals is being conducted to develop prototype geographic information systems components designed to utilize the digital products of the land use and land cover mapping program that are incorporated in the DCDB. The intended applications of the results of this project are twofold: (1) to assist users, especially USGS personnel, in applying the land use and land cover and DCDB data to research and production tasks; and (2) to provide feedback mechanisms to the ongoing task of designing and developing the DCDB and the system to build and manage it.

One study is addressing the impact of spatial operators on data base management system design criteria. Spatial operators provide a common foundation for many different applications routines and perform the fundamental computations of locational, geometric, or topological attributes needed in spatial analysis. A survey of existing geographic information systems illustrates a high degree of commonality in capabilities. This would seem to suggest that a relatively small set of spatial operators could support a widely varying set of applications.

The set of spatial operators would provide data base design criteria in terms of required data elements and structural elements that will need to be explicitly encoded or derived. The objectives of this research are to identify a set of spatial operators, delineate the data requirements of the spatial operators, group like data requirements to define subschemas of archival data structures, and inspect the set of subschemas to provide data base management system design criteria.

Geographic Names Information System

Uniformity in the spelling and application of geographic names is essential at all levels of government and industry, and for those sciences that deal with the Earth and geographic location. Large amounts of interrelated data involving names and their appli-

cation to specific features, places, and areas must be collected, processed, stored, retrieved, manipulated, and disseminated to a wide variety of users.

After several years of researching user needs and information systems, the USGS developed an automated Geographic Names Information System (GNIS) and is building a national geographic names data base. Although the system is operational, further research and analysis is being conducted in regard to methodology and the necessary expansion and development of the system. GNIS is presently capable of providing basic information for about 2 million names used in the United States and its territories and is designed for governmental, industrial, educational, and public use. Data from the system can be retrieved, manipulated, and arranged to meet the special needs problems of users. Data collection is based mainly on the standard topographic map series published by the USGS but also includes names information derived from records of the Board on Geographic Names, U.S. National Ocean Survey charts, U.S. Forest Service maps, and reliable historical records, as well as other reputable sources of name information.

GNIS was developed to meet national needs in the following six ways: (1) to assist in establishing uniform name usage throughout the Federal Government in cooperation with the U.S. Board on Geographic Names, which works with State and local governments and the public; (2) to provide an index of names found on Federal, State, and private maps; (3) to eliminate duplication and excess time and expense by government agencies, industry, and others in organizing similar basic data files for their specific needs; (4) to provide an interface to integrate data from other systems for multidisciplinary use; (5) to provide for standardization of data elements and their coded representation for information exchange use within the information processing community; and (6) to meet public information requirements prescribed by Federal law.

GNIS furnishes information to two types of users: those who use the data for reference purposes and those who reformat the information for individual or specialized use. GNIS lists primary data for various kinds of features identified by a name. The information includes all named natural features (about 80 percent of the data base) and most major and minor civil divisions, dams and reservoirs, airports, and national and State parks. However, named streets, roads, and highways are not included at this time.

GNIS is capable of providing information on a number of data elements: official name, feature class, location of named feature (State, county, and geogra-

phical coordinates), variant names, USGS map sheet, and elevation. Information from the GNIS State name files is presently available in several ways: direct on-line access by an outside computer terminal; USGS computer products such as magnetic tapes, computer printouts, and microfiche; and printed and bound products such as alphabetical and topical lists.

Applications software development for land use and land cover data

As a result of a 2-yr demonstration project, software has been developed to support applications of digital land use and land cover data. The resultant software and procedures are rudiments of a spatial data base management subsystem which can be linked to existing software systems within the NMD.

To date, applications largely have utilized area data sets developed by the Geographic Information Retrieval and Analysis System (GIRAS) software. These data sets are efficiently handled through the use of a compact raster data format which reduces the volume of data for storage and processing. Spatial operations, such as compositing data sets, windowing an area, and merging data from adjacent map sheets, can be performed on the data in the compact raster format (Miller, 1980).

In addition, prototype methods for spatial retrieval have been developed for relating point and linear features in vector format to the areal data sets in the compact raster format. This allows radial and corridor searches of extensive data sets (Miller, 1980). To date, these radial and corridor search procedures have been utilized in several applications involving land use and land cover data sets. They could, however, be adopted to interrelate other raster and vector data developed from the national topographic map series. This would include DEM's in raster format and terrain data (such as water bodies) which could be converted from vector to raster format. These data sets can be interrelated with various line and point features from the maps, which are retained in vector format.

Algorithms for generalization of land use and land cover map content

Computer algorithms for content generalization in scale reduction of digital land use and land cover data, with particular emphasis on reduction from 1:250,000 to 1:2,000,000, are being developed and tested. A frequency analysis of land use polygons, based upon seven representative 1° by 2° 1:250,000 quadrangles, explores the extent to which land use and land cover polygons and islands might be eliminated in a scale reduction because of small area or

noncompact shape. Two conceptually independent shape indexes are warranted: one to measure boundary inefficiency (a ratio of the polygon's perimeter length to the square root of its area) and the other to indicate elongation of gross shape. Shape is related to area, but only moderately so. Through area, shape also affects land use and land cover, for example, transportation corridors are quite linear. Absorbing small enclaves with a different aggregate attribute will not seriously dilute the "class purity" of most surrounding polygons. Marked patterns of topological nesting of landscape types are related to regional physiography.

CARTOGRAPHIC AND GEOGRAPHIC STUDIES

Map projections

Map projection, the science of showing a spherical body, especially the Earth, on a flat surface with defined characteristics, has been researched with increased concentration by the USGS. The advent of space technology has led to a need for map projections which have not existed before. The generation of maps by computer has led to an increased need for mathematical formulas for projections and for more efficient computation of coordinates for high-volume production. On the other hand, the computer permits easy handling and analysis of projections which previously were too complicated for routine manual use.

A new series of projections, called satellite-tracking projections, has been developed (Snyder, 1981). These projections permit groundtracks to be shown as straight lines on conic and cylindrical projections with restricted distortion of land masses.

An expanded computer program to transform coordinates from one map projection to another was developed and tested under the name General Cartographic Transformation Package. It supersedes other projection packages used by the USGS and includes additional projections and both forward and inverse computations for all the projections contained. Another project generating considerable interest is the first detailed working manual describing all map projections used by the USGS (Snyder, 1982).

A computer program currently nearing completion is intended to permit determination of the projection parameters such that data can be accurately transferred from one map to another. Over twenty paper maps have been tested through this program, and data transfer is generally accurate to within 1 mm.

Mount St. Helens mapping

The volcanic eruption of Mount St. Helens in 1980 resulted in a series of special cartographic products which required special procedures because of time, cartographic, and logistical constraints. The five major efforts involved 1:100,000-scale base maps, orthophotoquads, contouring sequential topographic changes, surveying and mapping along drainage basins, and generation of digital cartographic data.

The 1:100,000-scale base maps were the first products prepared in response to local planning requirements after the May 1980 eruption. Both pre- and post-eruption versions were made. This was a cooperative effort with the U.S. Forest Service and the State of Washington's Department of Natural Resources. Special symbols were used and the hazardous area received special editing treatment.

Post-eruption 1:24,000-scale orthophotoquads were also produced. These orthophotoquads were made from NASA 1:130,000-scale photos taken from a U2 aircraft in June 1980. Because bad weather lingered, this was one of the earliest sets of mapping photos taken after the eruption. Higher-resolution orthophotoquads were produced later from 1:40,000-scale photographs taken in September 1980.

A new series of 1:24,000-scale topographic maps was started with the discovery of the "bulge" in March 1980, prior to the major eruption in May 1980. The mapping was used to monitor the changes on the mountain. The earlier 15-minute map was compiled in 1952 at 1:48,000 scale. The first topographic map in the series was compiled from the 1952 photographs at 1:24,000 scale. As a basis for monitoring the bulge, a 1:24,000-scale map was compiled from July 1979 photographs. Pre-eruption mapping was produced from photographs taken in April and May 1980, and post-eruption mapping was completed from photographs taken from June through October 1980. The photographs taken in September 1980 were used to compile the 1:24,000-scale map which was published. These maps were compiled in most cases within a few days of the flight day to assist others in their monitoring of the mountain and its surroundings.

The USGS Water Resources Division had an immediate requirement in the Mount St. Helens area for large-scale (1:4,800) maps of drainage basins for erosion monitoring and watershed analysis. Most of this mapping was done under contract. However, due to short-term needs in critical areas, the NMD produced some maps prior to the contract mapping. This effort required ground surveys and photogrammetric mapping with large-scale accuracy on extremely short

notice. Ground crews performing field surveys required for the photogrammetric work found access difficult and conditions hazardous. Analytical aerotriangulation was used to extend field control through the use of accurate procedures which minimized the field requirements. The final products were compiled photogrammetrically at 1:4,800 scale with 4-ft contour intervals.

Perhaps the most widely seen products of the mapping activities in the Mount St. Helens vicinity have been the pre- and post-eruption isometric views generated from DEM data of July 15, 1979, and September 6, 1980, respectively.

The pre- and post-eruption DEM's also were used to project local ejecta deposition volume by algebraic subtraction of the two data sets. The resultant data set was used to produce a volumetric data isometric plot. Additional products generated from the DEM data include a post-eruption contour plot and a contour plot indicating ejecta contours used for volumetric analysis. Plots made from DEM data are not standard USGS products. They are examples, however, of applications of DEM data which, in this case, met immediate needs of geologists and land management agencies.

Provisional map standards development

A primary goal of the NMD is to complete nationwide large-scale map coverage by the late 1980's. To provide a realistic means to meet this goal, the NMD has developed technical standards and has initiated an accelerated program for the production of Provisional Edition topographic maps. The provisional map standards modify certain conventional mapping procedures whereby significant reductions in map finishing operations and moderate modifications to standard field and photogrammetric operations are applied. These modifications permit provisional maps to be produced at approximately 20 to 25 percent less cost and on a more timely basis than production of standard topographic maps. Provisional maps are prepared to NMAPS, printed in four or five colors, and made available through normal distribution procedures. They generally contain the same level of information as shown on standard topographic maps but have a provisional rather than a finished map appearance.

Provisional maps will be produced in three categories, depending on the status of the individual maps or projects in the mapping cycle at the time the provisional mapping program was implemented: (1) category 1 maps for which map preparation materials

have not been through field phases; (2) category 2 maps which have not been compiled, but for which map preparation materials have received advanced field interpretation; and (3) maps that have been through the field and compilation phases but not through the map-finishing (color separation) phases. Content, symbolization, and map-finishing procedures will differ somewhat for each category.

Copies of the compiled map manuscripts are used as the final drawings for lithographic printing of provisional maps. In general, standard compilation procedures apply, with the addition of separate manuscripts for water features, which are printed in blue, and public-land survey information, which is printed in red.

Map collars are generated either from master collars or directly on the DDES (except for grid and graticule values). The appearance of provisional maps is readily distinguishable from standard maps because of the modified treatment and the printing of all map collar information in brown. With minor exceptions, provisional maps will be prepared for all remaining unmapped 7.5-minute quadrangles (approximately 12,000), including those currently covered by 15-minute maps, and all unmapped Alaska 15-minute areas.

Application of linear algebra to computation of gridded data

In several mathematical studies, the application of linear algebra to the computation of gridded data has been considered. The motivation behind these preliminary studies is the desire to develop efficient algorithms for handling DEM's in which elevation values are assigned on a regular, horizontal rectangular-coordinate grid.

One line of investigation has been into filtering and interpolation on perfectly spaced rectangular grids, on imperfectly spaced rectangular grids (where spacings vary slightly about a perfect spacing), and on grids for which some of the grid intersections may be absent. The analytical form of the solution is couched in terms of the direct or Kronecker product, a specific form of matrix multiplication. Normal equations are formed, and through identities a convenient solution algorithm is outlined.

A second line of investigation involves the sparse factorization of matrices with application to interpolation, filtering, and the fast Fourier transforms. The derivation of the sparse factorization is obtained in two steps: simplifying the structure of the algebraic equations and defining matrix elements with the Kronecker delta symbol. For strictly computational pur-

poses, the second step is unnecessary. The value of defining sparse matrices is that often the inverse or pseudo-inverse of a sparse matrix is itself sparse. If so, it may be possible to factor these sparse matrices even further, although this possibility may not be evident from the straightforward algebraic equations.

The third line of investigation compares several techniques of solving the interpolation problem. The first technique is the direct method which requires n^6 multiplication where n is the dimension of a square matrix; a second is the so called array algebra method which requires $2n^3$ multiplications; and a third is the tensor-product method, which also requires $2n^3$ multiplications. Two other methods investigated also require $2n^3$ multiplications. It is found that the array algebra technique is simply a notational device by which a user can express tensor products by multiple indices in a way which is consistent with the FORTRAN compiler.

Generalized adjustment by least squares

The least-squares principle is the universally accepted basis for adjustment procedures in the allied fields of geodesy, photogrammetry, and surveying. A prototype software package for Generalized Adjustment by Least Squares (GALS) was recently developed. The package is designed to perform all least-squares related functions in a typical adjustment program. GALS is capable of supporting development of adjustment programs of any size or degree of complexity.

GALS is a software system aimed at removing from the process of building adjustment programs all those mathematical and algorithmic aspects associated with application of the least-squares principle to the adjustment of linear mathematical models. It is intended to be the general tool that might lead to a standardization of least-squares operations in adjustment software.

GALS is a software subsystem which must be executed from a higher level program. It can be viewed as a subroutine package with somewhat involved interface requirements. Knowledge of the detailed internal operations of GALS is not essential for its use. It is possible to deal with GALS as a "black box" and still create very involved adjustment systems.

A prototype of GALS was built to operate on the USGS Amdahl computer. The prototype was written exclusively in FORTRAN, except for two small subroutines for bit manipulation which are written in Assembly language. GALS requires the services of a sort-merge software facility which is assumed to exist within the operating environment. The development

of GALS is largely a software engineering project. As such, a prototype was needed to satisfy the important functions of system design verification for correctness and completeness; experimentation with the many possible design tradeoffs, under closely realistic conditions; and actual simulation of GALS in connection with various types of adjustment problems.

Because of the inability to access computer resources from within a FORTRAN environment, the prototype is configured as a sequence of six independent program tasks. This configuration will be changed in the second phase of GALS development by using PL/1 programming language. This will make possible a single step, "black box" type of service. It will also provide for the automatic allocation of all necessary computing resources by GALS, depending on an assessment of actual needs.

Experimental 1:63,360-scale orthophotoquad of Kodiak A-6 quadrangle, Alaska

The NMD has been requested to prepare 1:63,360-scale orthophotoquads for the State of Alaska. The primary image sources for the project are the 1:120,000-scale photographs taken by NASA. By specification, up to 10 percent cloud cover is acceptable. New snow cover, film scratches, smoke, and density variations on the source photographs of Alaska will not be controlled to the same degree as photographs used for the standard USGS orthophotoquad program. A research project was undertaken to prepare a sample 1:63,360-scale orthophotoquad to present to the State of Alaska and interested government agencies for comment before NMD embarked on the full-scale program. The Kodiak A-6 quadrangle was selected as a typical example of a quadrangle having both clouds and new snow.

Two versions of the Kodiak A-6 orthophotoquad were prepared for evaluation by different procedures. The first version was prepared from stereomodels scanned on the GPM-2. Five stereomodel scans were mosaicked into a single negative at 1:63,360 scale. A collar was prepared and black-and-white prints were made, including one with a contour overprint. The main problem encountered by the GPM-2 was the loss of correlation in cloud and water areas. The second version was prepared on the Wild OR-1 using a profile drive tape generated from Defense Mapping Agency DEM data derived from 1:250,000-scale maps. These are the only DEM data available in Alaska. Three OR-1 scans were mosaicked into a single negative at 1:63,360-scale, and composite prints were made. Extra effort was required to generate the profile tapes because formats and units of the DMA DEM tapes

were not compatible with available software. The profile tapes provided uninterrupted scanning across snow, water, and cloud areas. Horizontal and vertical accuracy tests based on aerotriangulated test points were applied to the resulting OR-1 stereomodel and orthophoto. Preliminary test results indicate a good probability that DEM tapes can be used to produce 1:63,360-scale orthophotos that meet NMAS in areas of moderate relief.

Identifying changes in land use and land cover

Because effective management of land resources requires current information on land use and land cover, maps that portray these data need to be updated periodically. In addition, data on land use and land cover change are of value to planners, land managers, and other decisionmakers in understanding and dealing with the varied and complex issues associated with the use of the Nation's lands. At the present time, the NMD is studying ways to maintain the currency of USGS land use and land cover maps and associated digital data. Some of this research has focused on ways to both produce and use data on land use change in the updating process. Particular emphasis is on identifying likely products that would provide information on land use changes for use in data analysis, modeling, and other land resources applications.

In one updating approach, spatial data on land use change are used to directly update existing land use maps and statistics. To accomplish this, researchers compare the old land use map with new remotely sensed source materials and map only the areas of change between them. By then incorporating only the new polygon information, maps and digital data are updated in an efficient manner without the need for complete and costly remapping and redigitization of all polygon data.

A variety of graphic products and formats could be used to portray the land use change data derived from this map-revision process. Such products could be produced quickly and inexpensively either by conventional cartography or as specialized products of a computerized geographic information system.

A single overlay can show both "from" and "to" land use change categories. Each change is coded to identify the original Level II land use and land cover category (from the old map) and the new category (from the new photographic source). A separate polygon is delineated for every change in category and boundary that occurs.

In addition to graphic products, detailed statistics on land use change can serve as useful aids for analyzing and interpreting land use, land cover, and

land changes. Statistical products can be generated from the computerized data in the form of standard area summary tabulations, charts and graphs, or as change category or land conversion matrices.

Land use and land cover statistics

The nationwide land use and land cover mapping program of the USGS began in 1975; since that time approximately 53 percent of the United States (excluding Alaska) has been mapped. An important aspect of this mapping effort has been the development of digital data files which can be used to generate areal statistics of land use and land cover. Approximately 21 percent of the United States (excluding Alaska) has been digitized to date.

An assessment of the accuracy of land use and land cover maps

An advanced statistical technique for testing the accuracy of land use and land cover and other National Mapping Program thematic maps was completed and tested during the past year. The minimum sample size needed to validate the accuracy for each land use and land cover category with specified confidence is developed from the cumulative binomial distribution. The critical level, also developed from the cumulative binomial distribution, is used as the criterion to determine if the identification from remotely sensed data of a thematic category meets a specified accuracy. The algorithm for selecting a sample for thematic map accuracy testing is based on sampling from two statistical frames and uses: a stratified systematic unaligned sampling technique based on the map as a whole, and an additional random sample of points for under-represented categories from all points in that category.

A computer program compares the category classifications interpreted from remotely sensed data to the field-identified classifications and lists the statistical and tabular results of this comparison. The estimated overall accuracy of the map and the estimated accuracy for each category on the map are considered with associated confidence limits.

Further research determined a methodology for analysis of accuracy of area data acquired in land use and land cover mapping experiments. Some techniques of nonparametric statistics are applicable to the analysis of area data in thematic mapping experiments: (1) for the analysis of multiple related samples—Kendall's coefficient of concordance test and Freedman's method of ranks test; and (2) for the analysis of paired samples—the Kendall tau statistic test and the

Wilcoxon signed rank test. In each analysis, the two-test procedure is analogous to testing the shape of two curves and the distance between them in order to determine if they are statistically identical.

In a multiple sample experiment of Level II land use and land cover classification at three scales (1:24,000, 1:100,000 and 1:250,000), the area of individual categories delineated at 1:250,000 scale was determined to be significantly different from that of the other two scales. Thus, the classification at 1:250,000 scale results in significantly smaller areas for more of the categories than the other two scales, as determined by area measurement.

Evaluation of the variables of thematic mapping experiments, such as scales, images, and algorithms, that affect classification by thematic categories was also undertaken to aid in developing specifications and techniques for producing thematic maps.

The data acquired for analyzing the accuracy of thematic mapping methods usually consisted of the population of agreements and disagreements between the classifications based on field observations and the classifications interpreted from remotely sensed data, such as aerial photographs. These data were assumed to be binomially distributed. A weighted analysis of variance adjustment rigorously accommodated the different numbers of sample points that fell within each of the various thematic categories. A posteriori multiple range tests are tests applied to population means found to be significantly different in the analysis of variance table. An experiment showed evidence of a significant difference in accuracy among three scales of land use and land cover mapping (1:24,000, 1:100,000, and 1:250,000) when using the data transformed by a weighted analysis of variance adjustment. Multiple range tests showed that all three scales are different for the arcsine transformed data.

Computer graphics experiments and techniques

Cartographic information can be collected, organized, and sorted in such a way that a single digital data base may serve a wide range of applications. One use of the data is graphic production. Computer graphics techniques applied to digital spatial data can produce cartographic products that would be difficult, time consuming, and, in some cases, impossible to produce by traditional methods. One example of this application is the preparation of thematic maps for color lithographic reproduction from digital spatial data. The thematic map depicts the land use and land cover information of the type being collected by the USGS. After compilation, the maps are digitized and

the data edited and incorporated into a data base.

The land use and land cover digital data are maintained in a topologically structured polygon/arc-segment format. In this format the arc segments are defined by a series of x,y coordinate pairs. The requirements of the device used to display these digital data as a color thematic map made it necessary to convert the data from their vector format to grid cells in a run-encoded raster format. The polygon-to-grid computer program was used to perform this conversion.

A grid cell size of 200 μm on a side, at a publication scale of 1:250,000 was chosen for this example. Each cell represents 0.25 ha in ground area.

To prepare the data for display (and ultimately printing) on this map, each Level II data category is assigned a color value. The Level II color values are chosen within Level I tint groupings. The colors are preselected from color printing charts prepared by the Geological Survey. Using these charts, the map designer can choose colors with the assurance that the desired colors will appear identical in published form. The color chosen for each Level II data category is composed of a unique combination of transparent lithographic process ink colors (yellow, magenta, cyan, and black). Colors are developed by using various densities of dot screens for each ink. To minimize moire patterns these screens (120 lines per inch) are also angled separately from horizontal for each color, 60°, 75°, 105°, and 45°, respectively, for yellow, magenta, cyan, and black inks.

The Scitex Response 250 Cartographic System creates from the digital data the required color separate materials. The Scitex generates the desired dot screen (in terms of density, lines per inch, and angle) and assigns this screen pattern to the chosen input raster data elements, in this case land use data categories that create the image of the land use map. The laser plotter component of the system then permits the plotting, at publication size and scale, of the color separation films that are used directly to make printing plates.

For example, the red used to depict land use category 11 (residential land) is comprised of 39 percent yellow ink, 50 percent magenta, 0 percent cyan, and 0 percent black. In plotting the yellow separate, wherever the raster image contains data elements with category 11, the plotter would draw on film, within the 200- μm ×200- μm area covered by that raster element, a 120-line screen, angled at 60°, with a density of 39 percent. This procedure is repeated for the other separates. When the separates are used for printing the color inks, the result is a color map.

This entire process is very cost efficient. The conversion of the land use data from polygon/arc-segment

format into raster format suitable for plotting requires less than 3 min of computer time. The four-color separation films can be generated in less than 2 h. Other computer-aided methods are at least an order of magnitude slower. Thus, the combination of digital spatial data bases with state-of-the-art computer software and hardware allows the rapid preparation of the materials necessary for the lithographic production of a color thematic map.

Level III land use and land cover mapping in Connecticut

The State of Connecticut requested Level III land use and land cover maps for the entire State that could be correlated effectively with water use and evapotranspiration coefficients to produce data for the Connecticut Water Use Information System and to water balance models for drainage basins in Connecticut. A preliminary Level III land use and land cover classification system has been developed with category definitions and mapping specifications established. A pilot study to compile a land use and land cover map of the area covering the Norwich 7.5-minute quadrangle is currently underway to test the proposed classifications and specifications.

Land use and land cover and environmental photographic interpretation keys: a guide for Missouri

In 1975, the USGS initiated production of land use and land cover and associated maps for the United States. Documenting the land use categories shown on the maps and providing insight into the environmental effect of land use have been longstanding user requirements. These two requirements have been addressed in this joint project by the USGS and the Environmental Protection Agency, production of a photointerpretation guide. This prototype guide is designed to demonstrate the applicability of land use an environmental keys, to develop data acquisition techniques for compilation of the keys, and to indicate the potential effects of land use on the environment.

The guide is divided into seven sections dealing with (1) the source materials; (2) selected types of remote sensors and their characteristics; (3) the background for the development of the land use and land cover classification system; (4) the techniques for compiling land use and land cover maps; (5) a general description of the potential adverse impact of some land uses on the environment; (6) photointerpretation keys for Missouri; and (7) Missouri land use statistical tabulations.

REMOTE SENSING AND SPACE TECHNOLOGY RESEARCH

Landsat cartographic research

The application of Landsat data to mapping has been a continuing research effort over the last decade. During FY 1981 insight from investigations refined specific processing techniques and applications. These investigations include the exchange of technical information with foreign mapping agencies.

Analysis of the geometry, resolution, and radiometric qualities of Landsat-3 Return Beam Vidicon (RBV) imagery confirmed that the RBV on Landsat-3 is suitable for image map presentation at scales as large as 1:100,000. Tests indicate that one of the most common radiometric anomalies found in the standard RBV images, shading, can for the most part be removed by relatively simple analog processing.

As the result of experimental image map compilation, new methods were developed for processing Landsat data to cartographic form. Experimental image maps of Cape Cod, Mass., and Ikpikpuk River, Alaska, were prepared at 1:100,000 and 1:250,000 scale. In response to requests for technical assistance, areas in Saudi Arabia, Pakistan, Antarctica, and Africa were mapped to demonstrate these new techniques. Both digital and analog enhancement are involved, as well as the use of various new reproduction techniques such as screenless printing.

Characteristics of Landsat data such as currency of images, repeating cycle of 18 d, simple enlargement without rectification, and the broad coverage of a single image render them advantageous for map revision. Experiments with RBV data have verified these advantages and demonstrated that RBV imagery can be used to update specific features such as woodland, new highways, and streams on maps at scales of 1:100,000 and smaller where conventional sources of revision data are absent.

Through contacts with other national mapping agencies, it was also verified that Landsat multispectral scanner (MSS) and RBV data have been successfully applied to the revision of 1:250,000 and smaller scale line maps on an operational basis. Canada has also utilized Landsat as an inspection tool for its 1:50,000-scale mapping program to determine which quadrangles require revision and thus will require the acquisition of new aerial photography. The implementation of this procedure has resulted in substantial savings and is considered applicable to many other areas of the world.

As a result of the distribution of the Landsat

image map of Berry Islands, the Bahamas, produced in cooperation with the Defense Mapping Agency from combined Landsat and hydrographic data, the value of MSS data for delineating shorelines and mapping shallow seas has become more widely known. Inquiries and requests for assistance from those concerned with island and shallow seas mapping programs have been received. During FY 1981 assistance was rendered to officials of Papua, New Guinea, which contributed to a new mapping program aimed at covering the extensive shallow seas north and east of the island country.

Mapsat

After 15 yr of study and experimentation with cartographic applications of space technology, the NMD developed a concept for a cost-effective Earth resources mapping satellite called Mapsat. In 1980 a contract was arranged to perform a feasibility study relative to the conceptual design of this new form of mapping satellite. The final report, received during FY 1981, verified the validity of the concept and its cost-effective qualities. The several unique facets of the Mapsat system are the result of a USGS effort to define an operational Earth-sensing system based on Landsat technology which includes the following objectives: global coverage on a continuous basis; data dissemination in a reasonable time and at reasonable cost; variable resolution (down to 10-m elements) and swath width, with stereoscopic and multispectral capabilities; capability of image mapping at scales as large as 1:50,000 with contour intervals as small as 20 m; continuity with respect to Landsat-1, -2, and -3, including the same orbit and basic data transmission and reception system; and cost effectiveness.

Mapsats, as opposed to aerial photography, is a completely different concept for imaging the Earth's topography. It uses three sets of optics, two of which look fore and aft of the satellite and the third which looks vertically. Any two of the three optics view the Earth from two different positions as the satellite proceeds in its orbit. The data are detected by thousands of solid-state elements with one detector of one array (one optic) imaging the same line segment of the Earth as a corresponding detector on the other array (other optic). When such a line segment is imaged from two separate points in space, an epipolar condition exists. This results in the generation of one-dimensional data from each pair of imaging detectors. One-dimensional data processing is relatively simple and cost effective. Mapsat is multispectral as well as stereoscopic and thus has thematic as well as topographic mapping capabilities.

High geometric fidelity is achieved by defining a spacecraft and sensor system having virtually no moving parts and very precise position and attitude determination. The sensor system is solid-state, the antenna is fixed, and solar panels are not actuated during periods of data acquisition.

Mapsat is designed for operations using three spectral bands at various resolutions and swath widths. The three bands selected for Mapsat are a blue-green (0.47 to 0.57 μm), a green-red (0.57 to 0.70 μm), and a near-infrared (0.76 to 1.05 μm). These selections are based on demonstrated practical uses of Landsat spectral bands and the need to limit data rates and achieve a high signal to noise ratio. The effective resolution element may be as small as 10 m, and various spectral bands, stereo combinations, and swath widths can be employed, depending on the areas of interest. However, the data transmission rate is limited to 48 megabits per second for reasons of economy. This data rate is achieved by relatively minor modifications to the existing Landsat receiving stations. The existing S-band Landsat transmission system or X-band defined for the Landsat D Thematic Mapper may be utilized.

The delineation of the Earth's surface in three dimensions is essential for many applications. Mapsat will provide two base-height ratios for the stereo mode. This mode, providing for the automated production of contour maps and digital elevation data, is a relatively new and powerful tool for defining and analyzing the Earth's terrain.

A patent for Mapsat has been issued by the U.S. Patent Office.

Combination of unlike data sets

Since 1979, the USGS has been graphically combining two unlike data sets of which one or both were Landsat records. The first product was the stereocombination of Landsat MSS and aeromagnetic data. A Landsat stereomodel was created in which the apparent elevation differences or parallaxes were actually the differences in the strength of the magnetic field.

During 1980 and 1981, data from the Heat Capacity Mapping Mission (HCMM) were compared and correlated with Landsat MSS band 7 (near-infrared) data. Although the HCMM data were of 600 m resolution and the MSS of 8 m resolution, the two data sets were well correlated and permitted the extrapolation of the low-resolution HCMM data set to the higher resolution MSS data set.

Multispatial data acquisition and processing

The term "multispatial" describes multispectral data taken simultaneously from the same platform but

at different spatial resolutions in the different spectral bands. Concern about excessive data acquisition and transmission rates, especially with the latest generation of high spatial and radiometric resolution sensors, such as multispectral linear arrays, the Thematic Mapper, and the Multispectral Resource Sampler, has triggered experiments in data compaction techniques.

When more than one spectral band is involved, considerable redundancy exists in the acquired data. Because the same boundaries (continuous spectral signature differences) are often recorded in more than one spectral band, it should be possible to record one dominant band at high resolution for a reduction in data transmission without a corresponding loss of information. The USGS sponsored research at the University of Arizona to demonstrate that the multispatial principle applies to digital image data as well as to analog data.

Reconstruction of two lower resolution bands based on boundaries resolved in the higher resolution band yields significant improvement in radiometric quality and, by inference, in information content. The extent of this improvement will depend on the number of bands, their difference in resolution, the reconstruction method applied, and on the scene itself. For any multispectral sensor similar to the Thematic Mapper, or the linear arrays on the proposed Mapsat, the proper application of the multispatial concept will result in an increase in information content per bit of data transmitted of at least 100 percent, as compared to the acquisition of all data at the same resolution. This project indicates that for any general-purpose multispectral system on which a data rate limit is imposed or from which data costs are based on the number of bits, the multispatial concept has considerable advantage to make the system cost-effective.

Image map research

Image maps derived from Landsat, aerial photographs, radar, and computer-generated image data require new and different techniques and equipment from those used to produce standard line maps. The primary goal in image map research is to develop an ideal map tone curve (D log E curve) compatible with equipment, techniques, cost, and production considerations.

The selection of the midpoint in the tone curve is the most important factor in final image quality. The midpoint should be a transmission density of 0.86 ± 0.05 for lithography with a density minimum above the base fog of the film. A "gray-scale" representative of the imagery is computer generated along with the imagery for subsequent photographic/lithographic

processing control and quality assurance.

Experimental image maps have been printed for Saudi Arabia, Pakistan, Bangladesh, Nepal, Yemen, Ethiopia, Nigeria, Liberia, and Brazil, in addition to the NMD orthophotoquads, State Landsat maps, the Grand Canyon National Park Landsat map, and the map series of the Canadian/Mexican borders. Image map projects in progress include (1) a duotone 1:2,000,000-scale halftone Landsat map of Saudi Arabia; (2) a series of 1:250,000-scale screenless duotone Landsat maps of Saudi Arabia; (3) a new series of 1:500,000-scale Saudi Arabia maps computer tone controlled and mosaicked by the Environmental Research Institute of Michigan; (4) various scale process-color Landsat maps for Mexico; and (5) duotone Alaskan radar maps.

Both screenless and halftone lithographic printing are used on these experimental and semiproduction products. The latest pre-press development is to proof the screenless process color maps by using relatively inexpensive photographic color paper. This new color proofing method is expected to significantly reduce costs and improve the quality of future image maps.

Mapping of irrigated cropland with Landsat digital data

The primary purpose of this research was to demonstrate the use of Landsat digital data to indirectly estimate water withdrawal from irrigated cropland acreage. The High Plains aquifer, covering parts of eight States, supplies water for one-quarter of the Nation's irrigated agriculture. That supply of water is being depleted rapidly, and there is little natural recharge. A computerized hydrologic model to assist in evaluating effects of future ground-water pumpage was constructed by staff members of the USGS High Plains Regional Aquifer Systems Analysis project.

The key model parameter is water pumpage, which is estimated from knowledge of the amount of land that is irrigated and the amount of water used to irrigate an average acre. Landsat digital data were used to map irrigated cropland by analyzing 26 Landsat scenes from the 1978 crop season. After computer processing to establish spectral classes (classes where spectral reflectances in the four wavelength bands are similar) and after using a process known as clustering, each scene was classified into spectral types that were based on the clustering results. An analyst then interpreted each spectral class to identify irrigated cropland and general land cover types. A 1' by 1' latitude/longitude grid was used to establish the percentage of irrigated cropland for each area of the classified scenes. These data, in turn, were aggregated into a

mosaic showing intensity of irrigated agriculture on the High Plains and were used to produce a computer tape as input to the hydrologic model.

Although most of the irrigated cropland can be identified by using just one midsummer Landsat scene when crops are green, in some areas of the region a significant portion (more than 10 percent) of crop acreage was not mapped as irrigated land because some crops (mostly wheat) were not green during that time. For this reason, the central and southern portions of the High Plains aquifer required the interpretation of two, or sometimes three, seasonally related Landsat scenes. In areas where spring crops such as wheat are important, it is necessary to use spring as well as summer data. In the southern portion of the region, a late summer scene is needed to indicate the cotton crop which matures late in the season. In areas where both wheat and cotton are raised, scenes from spring, midsummer, and late summer are necessary.

By using 1980 Landsat data, a second analysis has been prepared to refine the estimate. In 1980, rather than clustering and classifying the data, the irrigated cropland acreage was identified by ratioing the red and infra-red bands and establishing one ratio value per scene as a cutoff separating irrigated from nonirrigated land. Where two or three scenes were required, they were registered to one reference scene through a remapping procedure. Each scene was then analyzed separately and combined with the others to produce a composite analysis of irrigated cropland. Aggregation of data to grid cells and generation of a tape for the hydrologic model completed the process.

MAPPING VEGETATION AND LAND COVER IN ALASKA WITH LANDSAT DIGITAL DATA

National Petroleum Reserve in Alaska

In 1981, work continued on the completion of a land cover classification of the National Petroleum Reserve in Alaska (NPRA) (Morrissey and Ennis, 1981). The Landsat digital data were formatted into quadrangles, the data sets mosaicked, and photo prints of the result were scaled to topographic base maps. A map of vegetation and land cover at the scale of 1:500,000 has been compiled from 1975 data. Digital tapes containing land cover classifications for areas mapped on the Barrow, Wainwright, Meade River, Teshekpuk, Harrison Bay, Utukok River, Lookout Ridge, Ikpikpuk River, Umiat, Misheguk Mountain, and Howard Pass 1:250,000-scale quadrangles will be released through the National Cartographic

Information Center. The land cover digital data were combined with DEM data to help assess impacts in NPRA lease areas.

Prudhoe Bay region

Additional land cover mapping was done in the Prudhoe Bay region and to the south along the pipeline haul road into the Sagavanirktok quadrangle area. With the help of the U.S. Army Corps of Engineers Cold Regions Research and Engineering Lab, and their contractor, the Institute of Arctic and Alpine Research at the University of Colorado, an existing land cover classification prepared from Landsat data was evaluated, refined, and field checked during the summer. Land cover in the Beechey Point and Sagavanirktok 1:250,000-scale quadrangles will be reclassified by using information obtained during field investigations. Field sites for areas in the Dietrich and Bettles quadrangles also were selected and visited during the summer of 1981.

Land cover of the Arctic National Wildlife Refuge coastal area

Late in 1981, efforts were focused on preparing a land cover map of the Arctic National Wildlife Refuge coastal plain for an environmental impact statement being prepared by the U.S. Fish and Wildlife Service, supported by the USGS. Three Landsat scenes were selected for analysis. Knowledge of field-mapped sites was used along with clustering techniques to establish spectral classes for the land classification. Results were then viewed on an interactive color display for verification with field reconnaissance notes, and a description of vegetation associated with each category was compiled. The data were then geometrically corrected and mosaicked.

A laser plotter was then used to plot the land cover and vegetation data on plates for a four-color printing process of the map at a scale of 1:250,000. This unique thematic map depicts twelve land cover classes on a topographic base mosaic of the Barter Island, Flaxman Island, Demarcation Point, and Mt. Michelson quadrangles. Information printed on the map margin includes corresponding surface area measurements.

Land use and land cover mapping in south-central Alaska

In preparation for the 1:250,000-scale land use and land cover mapping of several quadrangles in south-central Alaska, a land use and land cover map of the Valdez B-6 1:63,360-scale quadrangle was prepared by using August 1978 1:60,000-scale color

infrared photographs. Land cover types in the region were correlated to the USGS land use and land cover classification system. Interpretation and classification problems were identified, and category specifications and guidelines for compilation were developed. In October 1981 operational land use and land cover mapping of the Valdez 1:250,000-scale quadrangle was begun. Researchers found it difficult to make consistent interpretations of certain land cover categories when viewing the 1:20,000-scale black-and-white photographs in stereo or the 1:60,000-scale color infrared photographs without stereo. However, most of these problems were resolved by stereoscopic interpretation of the color infrared photographs.

Studies were also begun to compare the USGS classification system with selected land cover or vegetation classification systems being used in Alaska by other Federal or State agencies. This review may prompt possible modifications to the tundra categories in the USGS mapping classification system in all regions of Alaska.

RADAR STUDIES

The USGS is participating in a project to acquire and evaluate side-looking airborne radar (SLAR) imagery. As a result of legislative directives, the USGS initiated the SLAR program in January 1980. The SLAR program required three major tasks: (1) the purchase of existing SLAR imagery of the conterminous United States acquired by two distinctly different radar systems—synthetic-aperture and real-aperture; (2) acquisition of new imagery by the two radar systems in Alaska; and (3) the initiation of research projects in the National Mapping and Geologic Divisions. Most of the research has involved the evaluation of real-aperture imagery acquired by the Motorola Aerial Remote Sensing System (MARS) and synthetic-aperture imagery acquired by the Goodyear Electronic Mapping System (GEMS).

Comparison of SLAR and DEM shaded relief imagery

Shaded-relief imagery is useful for the interpretation of geologic information. Radar images, which simulate shaded-relief images in appearance, are used for this purpose. Because shaded-relief images can also be generated by computer from DEM data, a comparison was made between GEMS synthetic-aperture SLAR imagery and shaded-relief imagery produced from DEM data. A portion of the Butte, Mont., quadrangle, for which DEM data and a 1:250,000-scale radar mosaic were available, was chosen for the

test. Shaded relief imagery was generated by digitally mosaicking the twelve 1:24,000-scale DEM's that comprise the test area. A sun elevation angle of 30° and a sun azimuth of 90° were selected to simulate the look and depression angles of the radar beam. The portion of the Butte radar mosaic corresponding to the test area was printed for comparison with the DEM shaded relief image. The two images were compared for utility, information content, accuracy and cost.

The DEM shaded-relief imagery minimizes surface features such as streams, roads, and towns which appear on the radar imagery and which may be a distraction to the analysis of structural detail such as lineaments. It has been advocated that at least two orthogonal radar looks are needed in order to detect all ground structure. However, this entails re-flying each area at a considerable increase in cost. It is quite simple and economical to generate shaded-relief images with multiple look and depression angles by using DEM data. DEM shaded-relief images have the added advantage of not being subjected to radar shadowing, which can be detrimental to interpretation. Geometrically, a more accurate product results from the DEM shaded-relief image. Radar imagery is less accurate because of characteristics such as radar layover, and DEM collection procedures are more precise than those for radar imaging.

Control extension using stereo radar strip imagery

One of the uses of radar imagery is to make radar mosaics in 1:250,000-scale quadrangle format. The production of controlled mosaics requires geodetic control points. If the number of field-determined control points can be decreased, mosaic cost is also decreased. One of the potential uses of SLAR data that has been investigated is the extension of ground control based on stereo radar strips. Radar imagery from both real- and synthetic-aperture systems was evaluated. Due to the radical geometric differences between radar imagery and photographic imagery, the computational procedures are quite different from those used in phototriangulation. The geographic area used as the test area is a portion of the Ugashik 1:250,000-scale quadrangle on the Alaska Peninsula.

The control-extension process was divided into three general phases: interior orientation, exterior orientation, and pass-point intersection. The techniques that were used involved performing a space resection of each image strip individually and then intersecting common image rays of pass points. Constant aircraft altitude and straight flight lines were assumed. Computation of planimetric positions did not present any

computational difficulty. However, due to poor image geometry, elevations proved impossible to compute accurately. The GEMS synthetic aperture system achieved a slightly lower RMSE for planimetric point position than the MARS real-aperture system (GEMS RMSE = 90.4 m; MARS RMSE = 102.2 m).

The relatively high planimetric RMSE's and the inability of either system to provide data that would permit reasonable elevation computations can be attributed to several sources of error. Ground control was obtained from existing 1:63,360-scale maps. Because there are only a few cultural features, identifiable image points were limited primarily to water features. Such features are likely to change shape with time. No data such as output from the inertial navigation system and gyro compasses were available to determine sensor position and attitude. Because registration marks were lacking, corrections for film deformation were limited to an overall correction for a variety of errors. For example, a non-orthogonality correction accounted for non-orthogonality due to image deformation as well as azimuthal errors in the radar. In addition, the imagery was acquired at low depression angles.

The low depression angles, imprecise knowledge of sensor position and attitude, and the use of same-side imagery result in very poor intersections, especially for elevation determinations. It is unlikely that SLAR imagery can be used for control extension until sensor position and attitude data are made available for radar images acquired at steeper depression angles in areas containing more identifiable image control points.

Detection of forested wetlands and perennial snow or ice using SLAR imagery

Investigations were conducted concerning the value of X-band airborne radar imagery in detecting either forested wetland areas or areas of perennial snow or ice. These are categories shown on USGS maps of land cover and commonly on topographic maps; however, they are often difficult to detect on aerial photographs because of concealing tree canopies in the case of wetlands and prevailing summer cloud cover in the case of perennial snow. Radar may be able to penetrate such concealment and to permit interpretation of hydrologic conditions. Tests showed the necessity of tailoring the radar collection to a specific type of investigation and for having ground investigators to collect hydrologic data at time of overflight of the radar aircraft. Nevertheless, it was found that an airborne synthetic-aperture radar image obtained

in wintertime could assist in the discrimination of frozen wetland from surrounding areas of dry forest and snow-covered rangeland in western Montana. Efforts were also made to delineate snow or ice fields in the Olympic Mountains of Washington as seen in a real-aperture radar image; however, strong radar reflection from mountainous terrain saturated the image and obscured the snowfield boundaries.

Screenless lithographic printing of 1:250,000-scale SLAR imagery

Experimental maps of real- and synthetic-aperture SLAR imagery have been printed in different hues and colors by the screenless printing process, which is currently the best cost-effective method of reproducing SLAR imagery. A 1:250,000-scale mosaicked radar quadrangle of Seattle, Wash., furnished by MARS, was printed by the screenless process in a single mixed black-brown ink. The screenless process results in an effect of two-color printing without the cost and time of making two impressions with two ink colors on the press. A collar was designed to specify the pertinent data concerning the radar images and to diagram the flight strips that comprise the mosaic. A fitted UTM grid was generated by measuring control points on the mosaic and on the corresponding line maps. A fitted grid was similarly made for the 1:250,000-scale radar mosaic of Butte, Mont., furnished by GEMS. Control points were chosen to lie at approximately the same elevation. The fitted grids for both radar mosaics produced planimetric RMSE's of approximately 250 m. However, radar layover produced discrepancies up to a kilometer in mountainous terrain. A 1:250,000-scale radar mosaic of Hoquiam, Wash. (which includes Mount St. Helens), supplied by MARS, was printed in a black-green ink as a comparison to the black-brown ink used for the Seattle quadrangle.

Analysis of SLAR imagery for identification of base map categories

Four types of radar imagery were evaluated in three separate studies for the detection of base map category data: (1) ERIM L- and X-band synthetic-aperture radar; (2) Seasat L-band synthetic-aperture radar; (3) GEMS X-band synthetic-aperture radar; and (4) MARS X-band real-aperture radar. The five base categories studied were hydrography, landforms, transportation networks, boundaries, and culture. The results of each study were essentially the same for all base map categories regardless of the type of radar imagery evaluated. Hydrography and landforms were easiest to detect and closely followed the configuration found on corresponding line maps. Cultural features tend to lose form on radar imagery and appear only as

bright areas. Transportation networks are intermittent and difficult to follow unless orthogonal to the radar beam. Overall results indicate that SLAR imagery is not useful for the detection of base map category data and therefore has little application for topographic mapping except as a substitute data source in persistently cloud-covered areas where high-quality aerial photographs and satellite images are difficult to obtain.

Seasat altimeter

Recent studies indicate that Seasat altimeter measurements over land are a useful data base for mapping smooth terrain. The Seasat altimeter was "on" nearly continuously from June 1978 until the spacecraft's electrical failure in October 1978; Seasat provided about 400 h of overland altimeter measurements. Although the altimeter was designed for relatively small dynamic height changes over the ocean surface, profiles derived from some Seasat altimeter overland data agree with the true terrain profiles within a few meters. Adjusting the sampled waveforms from the satellite's onboard tracking device, or retracking the waveforms, may result in terrain profiles within 10 cm of the true profiles over nonmountainous areas.

A study of retracking of Seasat radar altimeter waveforms has been initiated under contract. The objectives of this study are to: (1) use the Seasat altimeter data collected over the Meade River, Alaska, 1:250,000-scale quadrangle to determine spot elevations and, from these, derive a topographic overlay of the quadrangle with a 2-m contour interval; (2) make the computer software for altimeter retracking operational on the USGS Amdahl computer and train USGS personnel in the use of the software; and (3) perform a study of considerations required for the design of a satellite altimeter capable of determining elevations over mountainous terrain to within 1 m. The Seasat altimeter was designed for use only over the relatively flat ocean surface and, hence, its overland use is limited to terrain with very little slope change.

The Seasat altimeter overland data base contains potential overland profiling lengths of approximately 1×10^7 km. Even if only 10 percent of the data can be made geodetically useful, this amount represents a significant data base for providing terrain profiles over nonmountainous areas at relatively low cost.

Satellite surveying system

In order to take advantage of rapid development in Earth satellite technology, the USGS teamed with

the Defense Mapping Agency and the National Geodetic Survey in 1980 for development of geodetic application of the NAVSTAR Global Positioning System (GPS). GPS is a worldwide satellite navigation and positioning system under development by the Department of Defense. The GPS is scheduled to replace the TRANSIT satellite navigation system, now maintained by the U.S. Navy, in the 1986-1988 time frame. Use of the GPS promises to provide the capability of attaining geodetic positional data with much less effort and in less time than is required for current field-data-collection techniques.

The results of this team effort have led to a contract awarded to the University of Texas, Applied Research Laboratory (ARL), to develop an Advanced Geodetic Receiver (AGR) to exploit the GPS signals. The AGR is a single-channel multiplex receiver which will track four satellites simultaneously and will be capable of achieving accuracies in the sub-meter range. ARL has subcontracted AGR hardware development to Texas Instruments. The Naval Surface Weapons Center is developing hardware and software for the navigation processor which will be used with the AGR. The first delivery of AGR's is planned for late 1982.

SYSTEMS AND TECHNIQUES RESEARCH AND DEVELOPMENT

Automated cartographic lettering

Since 1975 the NMD has used a second-generation Mergenthaler VIP phototypesetter located in the printing plant in Reston, Va., for preparing film copy of nearly all map product lettering. Map lettering is a major labor-intensive activity in map production. The activity involves: (1) design—selection, size, style, and placement; (2) ordering—listing, keyboarding, and proofing; (3) production—typesetting, proofing, photolab processing, production of film positive copies, and waxing; (4) stick-up—locating lettering on order, cutting, and applying to film overlay; and (5) editing—additions, corrections, and changes. Several research projects are in progress to modernize the map lettering process, which has remained essentially unchanged for the past 40 yr.

A research project was conducted to determine the cost-effectiveness of developing quality type fonts in digital form for the DDES by using interactive graphic editing terminals to enter and manipulate data and a Gerber 4477 plotter to produce photographic film images for map lettering plates. Initial research

was directed toward determining the usefulness, for map lettering, of those fonts currently existing; then a search began for other sources of digital fonts. Other agencies, both Federal and State, were contacted to learn what advances have been made in automated type placement. A limited number of digital fonts were located, but few were suitable for mapping purposes.

Most of the research effort has been devoted to user command development on the DDES; limited time has been spent on actual digitization of type. Refinement of user commands is continuing and cost analyses cannot be finalized until all tasks are completed. However, preliminary results indicate that interactive type placement is a cost-effective approach, particularly in light of the new Provisional Edition topographic maps. The primary advantages of this approach are speed, accuracy of text placement, and reduction in visual checking, all of which lead to a significant reduction in the cycle time for the editing phases of map production.

A separate project was conducted by NMD staff in Reston to decentralize typesetting and increase efficiency through automated type placement of map lettering on a film overlay. Simultaneously, the Geologic Division (GD) was investigating methods to reduce their type cost for book publications and had obtained authorization from the Congressional Joint Committee on Printing for purchase of typesetters in Menlo Park, Calif., and Denver, Colo. A cooperative agreement was made between GD and NMD to procure the fourth-generation Mergenthaler Omnitech 2100—a digital font, laser printer which met GD's requirements for a word-processing interface and NMD's requirement for automating horizontal letter placement on maps. Omnitech 2100 typesetters are now operational in all four mapping centers.

The Omnitech 2100 has 30 graphic-arts quality digital fonts online, a point size selection from 4.5 to 127.5, a 12-inch film cassette, full editing capability, and imaging capability at a speed of 68 in²/min at a resolution of 362 scanlines per inch. Software features permit modifying those fonts online to double resolution and modifying fonts to expanded, condensed, or slanted versions, which effectively increase the resolution and available selection of online fonts. Horizontal type can be placed to an accuracy of 0.014 inch in any position 11-inches wide by the length of the map with a "go-to" keystroke command. Two or more overlay strips from the Omnitech 2100 will cover a map product. Nonhorizontal and curved lettering continue to require hand placement.

Savings with the new Omnitech 2100 will be

realized in the discontinued use of the teletype punch paper tape transmission, near elimination of correction cut-in due to editing capabilities, and rapid type delivery by on-site equipment. The printing of film negatives or positives directly from the typesetter will save photolaboratory labor and materials. The major saving, however, is in automated type placement of horizontal lettering. With the computer interface, future applications may include direct name input from the Geographic Names Information System.

Screenless lithography

For over 25 yr, the NMD has explored a variety of lithographic printing techniques that do not use halftone screens for reproducing continuous tone images. In lithography, a halftone screen is used to break a continuous-tone or screenless image into dots of ink. The halftone dots tend to obscure fine detail such as houses, streets, and railroads at the scale of orthophotomapping used in NMD. In order to preserve the fine detail, "Image-Tone" and "Photolytic" systems of screenless printing were developed. Recently, new photo polymers and new processes of anodizing and graining of aluminum printing plates became available to produce similar fine-grain random dots through improved photographic and lithographic printing controls. In comparison, a random dot, lithographic screenless print is equal to 600 to 700 lines per inch while the finest halftone print possible is 300 lines per inch. Many experimental image maps using the screenless plate process have been printed by the USGS.

The screenless plate process requires exposure and chemical processing that is as critical as that of a photographic film system. To facilitate processing and meet the exacting chemical requirements, the National Mapping Division has designed and built a rocking development tray with temperature and time control to accommodate 60-inch plates. Previously, plates were limited to 40 inches and processed in a vertical dip tank. The new large-tray processor will permit the production of maps as large as 42 by 60 inches by the screenless process.

Analysis of the image chain in the orthophoto production system

A study is in progress to determine the loss in resolution at each stage of the multiple processes that transform an aerial photo image into a lithographed orthophotoquad or orthophotomap. From the original aerial image to the final lithographic printing, the image is processed through six to nine steps, depending on the instrument used for simple or differential

rectification. As an aid to the study, an image control target chart was designed and produced on film to evaluate resolution, tone reproduction, and flare characteristics. This control target evaluated, along with the image, in an effort to determine the loss of resolution occurring with each step in the process. The study also includes an analysis of resolution loss by photolab processing, pressplate processing, and the printing system. Upon completion of the study, calibration of and modifications to equipment and changes in processing of materials will be recommended to minimize losses.

Aerial Profiling of Terrain System

The Aerial Profiling of Terrain System (APTS) has been under development since 1974. It will be a precision airborne surveying system capable of measuring elevation profiles across various types of terrain from a relatively light aircraft at flight heights up to 1,000 m above the ground. A laser profiler measures the distance from the aircraft to the terrain, and an inertial measuring unit (IMU) and a laser tracker provide the aircraft position datum. The tracker measures the distance to previously placed retroreflectors to provide a high-precision positional update to the IMU.

This research work is being done at the Charles Stark Draper Laboratory, where the fabrication of components (navigation, tracker, profiler, and video subsystems) was recently completed. Integration of the components has begun and will be followed by extensive laboratory testing. In a parallel effort, a Twin-Otter aircraft is being modified for the APTS installation which will begin in mid-summer of 1982. The APTS is expected to meet system accuracy goals of ± 0.5 feet vertically and ± 2.0 feet horizontally.

Applications and techniques development for raster-formatted data

The NMD is conducting applications research and software and techniques development with respect to raster-formatted data for digital cartographic applications. These efforts center on the capabilities of the NMD's Scitex RESPONSE 250 map scanning and digitizing system. This system is composed of four major subcomponents: (1) two large-format (36 by 36 inch) color raster scanners capable of encoding up to 12 colors or gray levels; (2) two interactive digital graphic editing and design consoles; (3) a large-format (40 by 60 inch) laser printer capable of producing raster-format positive and negative film transparencies; and (4) a DEC PDP 11/60 minicomputer for raster-to-vector data conversion and batch-oriented processing.

NMD personnel are currently in the process of developing special applications software for this system; however several digital cartographic applications have already been investigated:

Map replication. Reproduction of a 1931 edition of a USGS map demonstrated the application of the Scitex for map manuscript production. The only available copy of the map was a paper copy that showed its age through fold marks, age stains, and other signs of use. The original color separates were hand-engraved on copper plates that are no longer usable for reprint purposes. The paper copy was scanned and, through the use of the editing functions of the Scitex electronic design console, the age stains, fold lines and other blemishes were erased from the digital copy. Lines and symbols were retouched and repaired and the map was rescaled to more modern dimensions. The laser printer was then used to generate reproduction-quality color separates for printing.

Processed-image graphic generation. Through contractual arrangements, digital images of Landsat MSS scenes are computer processed to obtain land use classifications and other thematic data sets. These data sets are input, via magnetic tape, to the Scitex interactive design console to view multicolor display and to perform several editing functions, such as the resolving of indeterminate feature boundary situations and the performance of edge enhancements.

Shaded-relief map separates. DEM data can be used to computer-generate topographic shading representations based on slope aspect, sun angle, and sun azimuth. These representations, coded with numeric color or gray levels, are input to the design console via magnetic tape for editing. Electronic artifacts are removed or corrected as needed, and line screens are added to the digital data to produce desired patterns and densities of shading. The laser printer is used to generate a film transparency that can be composited with other map separates to produce a shaded-relief representation.

Slope map thematic graphics. The DEM's can also be used for generating digital and slope-zone thematic graphics. Each DEM grid cell or pixel is assigned a numeric color or density code as with the shaded relief separate; but in this case the code is based only on percent of slope. The data set, once generated, is formatted for the Scitex hardware and then input to the design console via magnetic tape and edited. The various slope zones are assigned colors or color intensities (line-screening densities) as needed to graphically portray the data for the intended application. The slope zone graphics produced by the laser printer can then be composited with such map separates as may be required to print a particular thematic graphic.

Open-window thematic graphics. NMD land use and land cover map graphics often contain thousands of polygons, each carrying one of 37 different classification numbers. Manually etching and peeling an open-window color separate for just one classification is a labor-intensive task. A large quantity of polygon data exists in a digital data base in vector form. These data can be retrieved from the data base and converted to color-coded raster form that can be input to the Scitex via magnetic tape. The console controls are then used to perform color design operations to produce the desired pictorial rendition. Variable-density line screening or other symbolic pattern fill are added to selected polygons, or sets of polygons, for either feature enhancement or general readability. The open-window graphics output by the laser printer can be composited or overprinted in any combination to produce a particular thematic graphic.

Production of DLG data. Another important application of raster scanning technology is the production of DLG data. Hypsographic (contour) color separates are raster scanned at a density of 40 cell points per millimeter. The data are then reduced (centerlined) so that the line data are represented in one-cell-wide centerline form. These data are then displayed and edited to erase name information, contour numbers, depression ticks, spot elevations, and other extraneous information. Line spurs, overruns, and other spurious artifacts of the scanning and data reduction processes are deleted. Unwanted line gaps are closed and congested areas are erased. The edited raster data are then converted to vector data, compacted (filtered) to remove any nonessential line vertices, and reformatted for input into the vector-oriented DDES equipment. Once in the DDES, residual line gaps are closed and any residual line continuity and directional problems are corrected. The feature code and name (height) of each contour line are appended to its x,y spatial data string, and the data are formatted into standard form for use by the USGS and its customers. From this general form, the data can be further computer-processed into digital elevation matrices, perspective views, contour line graphs, contour plot tapes, or other forms required by the user.

The NMD digital raster hardware is still in the developmental stage, with most of the current efforts centered on the development of operating procedures for the previously described applications. Development of optimal raster-to-vector software for hypsography is well underway, and NMD will soon begin developing raster-to-vector conversion software and techniques for hydrography, transportation networks, and polygonal data.

Pass point marking system

The NMD has designed a computer-controlled pass point marking system that will be used to mark pass points on new copies of original photographs for customers outside the USGS, perform point transfer, and gather pass point data without marking the points for input to analytical plotters.

The hardware consists of a Kern CPM-1 mono-comparator/stereoscopic point marker interfaced with an Altek AC-74 digitizer. The left stage of the CPM-1 is equipped with linear encoders and serves as a mono-comparator. The digitizer is interfaced to a Hewlett-Packard desktop computer (HP-85) which is supported by a flexible-disk drive.

The original pass point coordinates are obtained from a magnetic tape and transferred to a flexible disk. These pass points are transformed into the stage coordinate system of the CPM-1 by using a six-parameter affine transformation and measurements of the fiducial marks. The operator manually moves the stages to the displayed coordinates and marks the left photographic plate by drilling holes in the emulsion.

Map revision module for Kern PG2-AT stereoplotter

The NMD is engaged in the continuing task of updating topographic maps of the United States and its territories. The map revision phase now makes up about one-eighth of the NMD workload. To meet the increasing production requirements for map revision, the NMD has purchased a prototype map revision module for the Kern PG2-AT stereoplotter. The basic function of the revision module is to superimpose the map manuscript image into the optical train of the stereoplotter and allow the instrument operator to simultaneously view the stereomodel and the map manuscript being revised. Because the PG-2 operator is no longer required to shift attention between the stereo instrument and the map manuscript, an increase in productivity should result. This simultaneous viewing capability is accomplished by integrating a TV camera and a special high-contrast TV monitor, a beam splitter, and auxiliary optics into a unit capable of being retrofitted to the PG2-AT stereoplotter. The prototype module has met the basic functional requirements. However, the NMD is currently modifying some of the components and the location of operator controls to further increase ease of operation, hence efficiency.

Automatic Map Symbol Placement System

The NMD is developing an Automatic Map Symbol Placement System based on the capabilities of the Kongsberg automatic plotter. In this application

the Kongsberg is used to position and imprint topographic and geologic symbols during the map-plotting process. The map symbols are placed at precise x,y coordinates and rotated to specific angles by using commands stored on digital tapes which direct the plotter's movements.

Tests were made of geologic formation and letter symbols through the use of digital data tapes collected on the Altek angle-measuring data acquisition system. The Altek generates a drive plot tape that provides the proper symbol identification, location, and angle of orientation. Software was also developed to produce plot tapes of design files stored on the DDES. These magnetic data tapes contain all of the commands and coordinate data needed to drive the photohead on the Kongsberg plotter.

This system can be used to produce high-quality ink, scribe, or photo plots. At this time, the primary advantage appears to be the quick, efficient generation of symbol overlays for geologic maps.

Voice data entry system

The NMD has purchased, tested, and accepted five new voice data entry systems for use in map digitizing work. The major advantage of these systems is the capability of their users to make voiced data entries with no interruption to their manual cartographic tasks. The operator of a digitizer, for example, is not required to enter attribute code changes by hand. When the operator simply speaks the appropriate word, the voice-recognition module recognizes the speech by comparing it to a previously stored vocabulary reference pattern for that user, and the proper code is entered. To verify that the word was properly interpreted, the voice synthesizer is used to "speak" the word for the entered code.

Each stand-alone system is composed of a micro-computer with an interactive terminal having an alphanumeric display, line printer, voice recognition module, voice synthesizer module, and magnetic floppy-disk storage. The floppy-disk storage is used to store system control software and users' vocabularies, applications, and programs.

A voice response capability has also been developed for the existing Threshold Technology Inc. T-600 voice recognition input terminals. The T-600's and digitizer/recorders are used to add spoken input feature codes to cartographic data being recorded from stereoplotters. The newly added voice output capability eliminates the need for an operator to look away from the stereoplotter in order to confirm voice data input; instead, a synthesized voice repeats each feature as it is entered and allows multiword feature

designations to be entered. Interactive editing is provided. A DEC LSI-11/03 microcomputer is used for control, input/output buffering, and vocabulary storage.

Online Aerotriangulation Data Collection and Edit System

The NMD presently collects aerotriangulation data by using manual comparators and plotters interfaced to Altek digitizers which then output to punch cards. There is presently no chance to verify the data while it is being collected. The Online Aerotriangulation Data Collection and Edit System (OADCES) is being developed to automate the collection and editing of coordinate data while aerial photographic plate measurements are being made. The system will detect mensuration blunders by performing interior orientation on a single photograph and relative orientation between successive photographs. Photo coordinates will be corrected for lens distortion and film deformation. Microcomputers will be interfaced to manual comparators and stereoplotters, and to peripherals such as flexible disk drives. The communication between each computer and its comparator/plotter will be through an Altek digitizer. The computer programs will be written in BASIC. Data from each system will be output to disk and then transferred to magnetic tape on the stand-alone system for input to an aerotriangulation program on a larger computer. Each mapping center will have one stand-alone system consisting of a microcomputer, flexible disk drive, magnetic tape drive, and printer.

The OADCES will increase the throughput of the aerotriangulation mensuration phase by (1) relieving the comparator operator of some of the present

bookkeeping tasks, (2) performing online data verification, (3) allowing online data editing/remensuration, and (4) making the aerotriangulation mensuration process operator-friendly.

ASSOCIATED ACTIVITIES

Testing and calibration of aerial cameras

During the past year the USGS NMD Optical Calibration Laboratory has continued work in aerial mapping camera calibrations, lens camera performance, and investigations in areas of calibration accuracy. A total of 96 cameras were calibrated during the year, submitted from private mapping contractors, State highway departments, the NASA Johnson Space Flight Center, and NOAA National Ocean Survey. Several special cameras used on contract work for the Nuclear Regulatory Commission in the investigation of nuclear generation station accidents and safety violations were also calibrated.

An investigation was completed into the spectral characteristics of calibration light sources to be used in the 53 collimators of the camera calibrator in order to change the output color temperature to that of average noon sunlight, which is considered to be from 5,000 to 5,500 K. A new illumination system was developed that has full-spectrum light with a color composition of approximately 5,200 K. Samples of these lamps were measured by the National Bureau of Standards along with calibration of NMD's color temperature-measuring equipment. The new system will allow a closer approximation of optimum theoretical results between film and camera lens performance in the photographic testing process.

COMPUTER RESOURCES AND TECHNOLOGY

During fiscal year 1981, the scientists of the U.S. Geological Survey gained an increasing awareness of the opportunities and challenges afforded by effectively using the technologies of ADP and information science. The Computer Center Division (CCD), working with the scientists, achieved significant accomplishments in many areas: small computer technology, teleconferencing and office automation, information management technology, and array processing.

MICROCOMPUTERS

During 1981, the use of microcomputers in the U.S. Geological Survey dramatically increased. Three major factors contributed to this increase: the extensive investigation, selection, and standardization of both synchronous and asynchronous data communications software packages by the CCD; a similar effort in the area of assisting management in making intelligent, informed decisions; and the research and development efforts involving the microcomputer user community in various state-of-the-art technological approaches to efficient, cost-effective microcomputer usage.

Because of the microcomputer explosion during the fiscal year 1981 period, the CCD initiated a competitive procurement for additional compatible microcomputers, based on the requirements of users within the Survey.

TELECONFERENCING AND OFFICE AUTOMATION

The Division completed developmental work in teleconferencing and office automation systems during fiscal year 1981. It implemented a system to allow Multics computer users from Menlo Park, Denver, and Reston to attend meetings held through the computer. The system encourages the use of computers for conferencing by providing an easy method for field offices to access a central computer. An office automation system was developed for use on the Multics computers. The system was designed to help personnel become more efficient and effective in carrying out day-to-day office functions. Some of the tools available on the office automation system are electronic mail, word processing, teleconferencing, on-line calendars, information storage, and retrieval capabilities.

INFORMATION MANAGEMENT TECHNOLOGY

During fiscal year 1981 the CCD investigated several tools that can be used to improve information management technology at the USGS and the Department. One of these tools that serves as an aid to systems planning was the software package SLIM, Software Life Cycle Management, a system life cycle management estimating and control model. The model's programs are used to forecast future events and their probabilities and impact on medium and large size programming projects. Historical data is reviewed by the model to produce forecasts, ranges of uncertainty and a schedule of significant events with a probability of their occurrences on software projects. SLIM provides: (1) life cycle costing; (2) simulation modeling; (3) risk profiles; (4) probability of success factors; (5) a linear programming subroutine to give best possible solutions to management constraints (maximum project cost, maximum development time and minimum and maximum manpower expenditures); and (6) the ability to size systems using PERT techniques which are internal to the SLIM system.

The CCD evaluated and purchased another management tool during fiscal year 1981, PSL/PSA (Problem Statement Language/Problem Statement Analyzer.) PSL is a computer-processible, English-like language designed primarily to describe a system during its formative stage, that is, during the description of the proposed system and logical system design phases in the system life cycle. PSA is a software package used to evaluate and enter system specifications into a database, integrate them with other specifications as they are generated, modify all specifications, and derive reports documenting the information in various stages of development.

ARRAY PROCESSING

The Flagstaff Field Computation Center installed a Floating Point System AP-120B array processor during fiscal year 1981. The array processor is connected to a PDP-11/45 computer system that users can access by using a terminal and a telephone. The internal organization of the AP-120B is particularly well suited for performing large numbers of reiterative multiplications and additions required in digital signal processing, matrix arithmetic, statistical analysis, geophysical data processing, simulation, modeling, and image processing. The structure allows for other

functions to be performed on the data simultaneously with arithmetic operations. The enhanced capabilities permit much faster execution than on a typical general purpose computer, where operations occur sequentially. The AP-120B is well-supplied with soft-

ware. Over 235 math subroutines cover a wide variety of arithmetic operations including data transfer and control, vector and matrix operations, and signal processing.

U.S. GEOLOGICAL SURVEY PUBLICATIONS

PUBLICATIONS PROGRAM

Books and maps

Results of research and investigations conducted by the USGS are made available to the public through professional papers, bulletins, water-supply papers, circulars, miscellaneous reports, and several map and atlas series, most of which are published by the USGS. Books are printed by the Government Printing Office, and maps are printed by the USGS. Both books and maps are sold by the USGS.

All books, maps other than topographic quadrangle maps, and related USGS publications are listed in the catalogs "Publications of the Geological Survey, 1879-1961" and "Publications of the Geological Survey, 1962-1970," available at nominal cost, and in yearly supplements, available free on request, that keep the catalogs up to date.

New publications, including topographic quadrangle maps, are announced monthly in "New Publications of the Geological Survey." A free subscription to this list can be obtained on application to the *U.S. Geological Survey, 582 National Center, Reston, VA 22092*.

State list of publications on hydrology and geology

"Geologic and Water-Supply Reports and Maps, [State]," a series of booklets, provides a ready reference to these publications on a State basis. The booklets also list libraries in the subject State where USGS reports and maps can be consulted; these booklets are available free on request to the USGS.

Surface-water, quality-of-water, and ground-water-level records

Surface-water records through water year 1970 were published in a series of water-supply papers titled "Surface Water Supply of the United States;" through water year 1960, each volume covered a single year, but the period from 1961 to 1970 was covered by two 5-yr volumes (1961-65 and 1966-70).

Quality-of-water records through water year 1970 were published in an annual series of water-supply papers titled "Quality of Surface Waters of the United States."

Both surface-water and quality-of-water records for water years 1971 to 1974 were published in a series of annual reports titled "Water Resources Data for [State]." Some of these reports contained both types of

data in the same volume, but others were separated into two parts, "Part 1: Surface-Water Records" and "Part 2: Water-Quality Records." Limited numbers of these reports were printed, as they were intended for local distribution only. Because the data in these reports will not be republished in the water-supply paper series, reports are sold by the National Technical Information Service.

Records of ground-water levels in selected observation wells through calendar year 1974 were published in the series of water-supply papers titled "Ground-Water Levels in the United States." Through 1955, each volume covered a single year, but, during the period from 1956 to 1974, most volumes covered 5 yr.

Starting with water year 1975, records for surface water, quality of water, and levels of ground-water observation wells are all published under one cover in a series of annual reports issued on a State-boundary basis. Reports for water year 1975 and subsequent water years appear in a series of reports titled "Water-Resources Data for [State]"; these reports are sold by the *National Technical Information Service, U.S. Department of Commerce, Springfield, VA 22161*.

State hydrologic unit maps

State hydrologic unit maps, which are overprints of the 1:500,000-scale State base maps, show culture in black, hydrography in blue, hydrologic subdivision boundaries and codes in red, and political (FIPS county) codes in green. The Alaska State map is at 1:2,500,000 scale, and the Puerto Rico map is at 1:240,000 scale. All river basins having drainage areas greater than 700 mi² (except for Alaska) are delineated on the maps. The hydrologic boundaries depict (1) water-resources regions, (2) water-resources subregions, (3) National Water-Data Network accounting units, and (4) cataloging units of the USGS "Catalog of Information on Water Data." These maps are available for every State and Puerto Rico. Also available is a Hydrologic Unit Map of the U.S.

State water-resources investigations folders

A series of folders titled "Water-Resources Investigations in [State]" is a project of the Water Resources Division to inform the public about its current programs in the 50 States and Puerto Rico, the U.S. Virgin Islands, Guam, and American Samoa. As the programs change, the folders are revised. The

folders are free on request as follows: for areas east of the Mississippi River, including Minnesota, Puerto Rico, and the Virgin Islands—*Eastern Distribution Branch, U.S. Geological Survey, 1200 South Eads Street, Arlington, VA 22202*; for areas west of the Mississippi, including Alaska, Hawaii, Louisiana, Guam, and American Samoa—*Western Distribution Branch, U.S. Geological Survey, Box 25286, Federal Center, Denver, CO 80225*.

Open-file reports

Open-file reports, which consist of manuscript reports, maps, and other preliminary material, are made available for public consultation and use. Reports and maps released only in the open files are listed monthly in "New Publications of the Geological Survey," which also lists places of availability for consultation. Most open-file reports are placed in one or more of the three USGS libraries: Room 4A100, National Center, 12201 Sunrise Valley Drive, Reston, VA 22092; 1526 Cole Boulevard at West Colfax Avenue, Golden, Colo. (mailing address: Stop 914, Box 25046, Federal Center, Denver, CO 80225); and 345 Middlefield Road, Menlo Park, CA 94025. Some open-file reports are superseded later by formally printed publications. Effective October 1, 1981, the Government Printing Office began distributing open-file reports to requesting depository libraries.

Microfiche and (or) paper copies of most open-file reports can be purchased from the *Open-File Services Section, Western Distribution Branch, U.S. Geological Survey, Box 25425, Federal Center, Denver, CO 80225*.

Earthquake publications

The "Earthquake Information Bulletin" is published bimonthly by the USGS to provide information on earthquakes and seismological activities of interest to both general and specialized readers. Each issue also lists a worldwide summary of felt earthquakes.

The USGS National Earthquake Information Service locates most earthquakes above magnitude 5.0 on a worldwide basis. A chronological summary of location and magnitude data for each located earthquake is published in the monthly listing "Preliminary Determination of Epicenters." The "Earthquake Data Report," a bimonthly publication, provides a chronological summary of location and magnitude data for each located earthquake and contains station arrival times, individual distances, azimuths, and traveltime residuals. "Earthquakes in the United States" is published quarterly as a USGS circular. The circulars supplement the information given in the monthly listing "Preliminary Determination of Epicenters" to the extent of providing detailed felt and intensity data as well as isoseismal maps for U.S. earthquakes.

"United States Earthquakes [year]" is published jointly by the USGS and the NOAA. This annual sourcebook on earthquakes occurring in the United States gives location, magnitude, and intensity data. Other information such as strong-motion data fluctuations in well-water levels, tsunami data, and a list of principal earthquakes of the world also is given.

PUBLICATIONS ISSUED

During fiscal year 1981, the USGS published 6,838 maps.

<i>Kind of map printed</i>	<i>Number</i>
Topographic	5,628
Geologic and hydrologic	731
Maps for inclusions in book report	47
Miscellaneous (including maps for other agencies)	432
Total	6,838

In addition, six issues of the "Earthquake Information Bulletin," 176 technical book reports, and 338 leaflets and maps of flood-prone areas were published.

At the beginning of fiscal year 1981, more than 104.6 million copies of maps and 2.1 million copies of book reports were on hand in the USGS distribution centers. During the year 9,388,682 copies of maps, including 493,118 index maps, were distributed. Approximately 6.1 million maps were sold, and \$5,079,879 was deposited to Miscellaneous Receipts in the U.S. Treasury.

The USGS also distributed 175,159 copies of technical book reports, without charge and for official use, and 1,581,663 copies of booklets, free of charge, chiefly to the general public; 384,000 copies of the monthly publications announcements and 600,000 copies of a sheet showing topographic map symbols were sent out.

The following table compares USGS map and book distribution (including map indexes and booklets, but excluding map-symbol sheets and monthly announcements) during fiscal years 1980 and 1981 :

Number of maps and books distributed

<i>Publication</i>	<i>Fiscal year</i>		<i>Change (percent)</i>
	<i>1980</i>	<i>1981</i>	
Maps	9,806,694	9,388,682	.04-
Books	436,817	208,307	.52-
Popular publications	1,319,115	1,581,663	.17+
Total	11,562,626	11,178,652	.03-

HOW TO OBTAIN PUBLICATIONS

OVER THE COUNTER

Book reports

Book reports (professional papers, bulletins, water-supply papers, "Techniques of Water-Resources Investigations," and some miscellaneous reports) can be purchased from the *Eastern Distribution Branch, U.S. Geological Survey, 604 South Pickett Street, Alexandria, VA 22304*, and from the USGS Public Inquiries Offices listed below under "Maps and Charts" (authorized agents of the Superintendent of Documents).

Some book publications that can no longer be obtained from the Superintendent of Documents are available for purchase from authorized agents of the Superintendent of Documents.

Maps and charts

Maps and charts can be purchased at the following USGS offices:

Distribution Branches:

Eastern Distribution Branch
1200 South Eads St.,
Arlington, Va.

Western Distribution Branch
Building 41, Federal Center,
Denver, Colo.

Alaska Distribution Section:

New Federal Bldg.,
101 Twelfth Ave.,
Fairbanks, Alaska

National Cartographic Information Center:

1400 Independence Rd.,
Rolla, Mo.

Public Inquiries Offices:

Rm. 108, Skyline Bldg.,
508 2d Ave.,
Anchorage, Alaska

Rm. 7638, Federal Bldg.,
300 North Los Angeles St.,
Los Angeles, Calif.

Rm. 122, Bldg. 3,
345 Middlefield Rd.,
Menlo Park, Calif.

Rm. 504, Customhouse,
555 Battery St.,
San Francisco, Calif.

Rm. 169, Federal Bldg.,
1961 Stout St.,
Denver, Colo.

Rm. 1028, General Services Bldg.,
19th and F Sts., NW.,
Washington, D.C.

Rm. 1C45, Federal Bldg.,
1100 Commerce St.,
Dallas, Tex.

Rm. 8105, Federal Bldg.,
125 South State St.,
Salt Lake City, Utah

Rm. 1C402, National Center
12201 Sunrise Valley Dr.,
Reston, Va.

Rm. 678, U.S. Courthouse,
West 920 Riverside Ave.,
Spokane, Wash.

USGS maps are also sold by some 1,950 commercial dealers throughout the United States. Prices charged are generally higher than those charged by USGS offices.

Indexes showing topographic maps published for each State, Puerto Rico, the U.S. Virgin Islands, Guam, American Samoa, and Antarctica are available free on request. Publication of revised indexes to topographic mapping is announced in the monthly "New Publications of the Geological Survey." Each index also lists special and U.S. maps, as well as USGS offices and commercial dealers from which maps can be purchased.

Maps, charts, folios, and atlases that are out of print can no longer be obtained from any official source. They may be consulted at many libraries, and some can be purchased from second-hand book dealers.

BY MAIL

Book Reports

Technical book reports and some miscellaneous reports can be ordered from the *Eastern Distribution Branch, U.S. Geological Survey, 604 South Pickett*

Street, Alexandria, VA 22304. Prepayment is required and should be made by check or money order in U.S. funds payable to the U.S. Geological Survey. Postage stamps are not accepted; please do not send cash. On orders of 100 copies or more of the same report sent to the same address, a 25-percent discount is allowed. Circulars, publications of general interest (such as leaflets, pamphlets, and booklets), and some miscellaneous reports can be obtained free from the Distribution Branch.

Maps and charts

Maps and charts, including folios and hydrologic atlases, are sold by the USGS. Address orders for maps of areas east of the Mississippi River, including Minnesota, Puerto Rico, and the U.S. Virgin Islands, to *Eastern Distribution Branch, U.S. Geological Survey, 1200 South Eads Street, Arlington, VA 22202*, and for maps of areas west of the Mississippi River, including Alaska, Hawaii, Louisiana, Guam, and American Samoa, to *Western Distribution Branch, U.S. Geological Survey, Box 25286, Federal Center, Denver, CO 80225*. Residents of Alaska also may order maps of their State from the *Alaska Distribution Section, U.S. Geological Survey, New Federal Building—Box 12, 101 Twelfth Avenue, Fairbanks, AK 99701*.

Prepayment is required. Remittances should be by check or money order in U.S. funds payable to the U.S. Geological Survey. On an order amounting to \$500 or more at the list price, a 50-percent discount is

allowed. Prices are quoted in lists of publications and in indexes to topographic mapping for individual States. Prices include the cost of surface transportation.

Earthquake Information Bulletin

Subscriptions to the "Earthquake Information Bulletin" and the "Preliminary Determination of Epicenters" are by application to the *Superintendent of Documents, Government Printing Office, Washington, DC 20402*. Payment is by check payable to the Superintendent of Documents or by charge to your deposit account number. Single issues can be purchased from the *Eastern Distribution Branch, U.S. Geological Survey, 604 South Picket Street, Alexandria, VA 22304*.

National Technical Information Service

Some USGS reports, including computer programs, data and information supplemental to map or book publications, and data files, are released through the National Technical Information Service (NTIS). These reports, available either in paper copies or on microfiche or sometimes magnetic tapes, can be purchased only from the *National Technical Information Service, U.S. Department of Commerce, Springfield, VA 22161*. USGS reports that are released through NTIS, together with their NTIS order numbers and prices, are announced in the monthly "New Publications of the Geological Survey."

REFERENCES CITED

- Adam, D. P., Sims, J. D., and Throckmorton, C. K., 1981, 130,000-yr continuous pollen record from Clear Lake, Lake County, California: *Geology*, v. 9, p. 373-377.
- Allingham, J. M., and Zietz, I., 1962, Geophysical data on the Climax stock, Nevada Test Site, Nye County, Nevada: *Geophysics*, v. 27, p. 599-610.
- Altschuler, Z. S., Silber, C. C., and Schnepfe, M. M., 1980, Distribution and genesis of primary pyrite in coal: U.S. Geol. Survey Prof. Paper 1175, p. 29.
- Anderson, C. A., 1941, Volcanoes of the Medicine Lake Highland, California: Univ. of California Publications, Bulletin of the Department of Geological Sciences, v. 25, p. 347-422.
- Anderson, L. A., 1981a, Rock property analysis of core samples from the Calico Hills UE25a-1 borehole, Nevada Test Site, Nevada. U.S. Geol. Survey Open-File Report 81-1337, 34 p.
- 1981b, Rock property analysis of core samples from the Yucca Mt. UE25a-1 borehole, Nevada Test Site, Nevada. U.S. Geol. Survey Open-File Report 81-1338, 36 p.
- Anderson, R. E., 1980, The status of seismotectonic studies of southwestern Utah, in Anderson, R. E., Ryall, Alan, and Smith, K. A., organizers, Earthquake hazards along the Wasatch and Sierra Nevada frontal fault zones, 10th, Proceedings: U.S. Geological Survey Open-File Report 80-801, p. 519-547.
- Anderson, R. E., and Buckman, R. C., 1979, Two areas of probable Holocene deformation in southwestern Utah, in Whitten, C. A., Green, R., and Meade, B. K., eds., Recent crustal movements: Amsterdam, Elsevier Scientific Publishing Company, no. 52, p. 417-430.
- Anderson, W. L., 1981, Calculation of transient soundings for a central induction loop system (Program TCLOOP): U.S. Geol. Survey Open-File Report 81-1309, 80 p.
- 1982a, Adaptive nonlinear least-squares solution for constrained or unconstrained minimization problems (Subprogram NLSOL): U.S. Geol. Survey Open-File Report 82-68, 65 p.
- 1982b, Calculation of transient soundings for a coincident loop system (Program TCOLOOP): U.S. Geol. Survey Open-File Report 82-378, 77 p.
- Anthony, T. R., and Cline, H. E., 1971, Thermal migration of liquid droplets through solids: *Journal of Applied Physics*, v. 42, no. 9, p. 3380-3387.
- Armstrong, R. L., Harakal, J. E., and Neill, W. M., 1980, K-Ar dating of Snake River Plain (Idaho) volcanic rocks—new results: *Isochron/West*, no. 27, p. 5-10.
- Armstrong, R. L., Leeman, W. P., and Malde, H. E., 1975, K-Ar dating, Quaternary and Neogene volcanic rocks of the Snake River Plain, Idaho: *American Journal of Science*, v. 275, p. 225-251.
- Arthur, M. A., 1982, Thermal history of Georges Bank basin, in Scholle, P. A., and Wenkam, C. R., eds., Geological studies of the COST Nos. G-1 and G-2 wells, United States North Atlantic Outer Continental Shelf Area: U.S. Geol. Survey Circular 861, p. 143-152.
- Ashwal, L. D., Mogk, D. W., Bergman, S. C., Gibson, E. K., Jr., Henry, D. J., Warner, J. L., and Lee-Berman, Richard, 1981, Liquid-vapor inclusions in achondrite meteorites (abstract): *Meteoritics*, v. 16, p. 290-291.
- Axelrod, D. I., 1964, The Miocene Trapper Creek flora of southern Idaho: California University Publication in Geol. Sci., v. 51, 180 p.
- Bagby, J. C., Ghering, G. E., Jensen, R. G., and Barraclough, J. T., 1981, A wind-powered, ground water monitoring installation at a radioactive waste management site in Idaho, U.S. Geol. Survey Open-File Report 81-493, 28 p.
- Barr, A. J., Goodnight, J. H., Sall, J. P., and Helwig, J. T., 1979, SAS user's guide, 1979 edition: SAS Institute, Inc., P.O. Box 10066, Raleigh, N.C., 494 p.
- Barraclough, J. T., Lewis, B. D., and Jensen, R. G., 1981, Hydrologic conditions at the Idaho National Engineering Laboratory, Idaho Emphasis: 1974-1978: U.S. Geol. Survey Open-File Report 81-526, 77 p.
- Bath, G. D., Dixon, G. L., and Rosenbaum, J. G., 1982, Relation of aeromagnetic anomalies to faulted volcanic terrains at the Nevada Test Site (abs.): Geological Society of America Abstracts with Programs, v. 14, no. 6, p. 302.
- Batson, R. M., Edwards, Kathleen, and Eliason, E. M., 1976, Synthetic stereo and Landsat pictures: Photogrammetric engineering and remote sensing, v. 42, no. 10, p. 1279-1284.
- Bauer, D. P., Jennings, M. E., and Miller, J. E., 1979, One-dimensional steady-state stream water-quality model: U.S. Geol. Survey Open-File Report 79-45, 215 p.
- Beasley, D. B., and Huggins, L. F., 1980, ANSWERS (Areal, Non-point Source Watershed Environment Response Simulation) User's Manual: Agricultural Engineering Department, Purdue University, West Lafayette, Indiana, 55 p.
- Bennett, M. J., Youd, T. L., Harp, E. L., and Wiczorek, G. F., 1981, Subsurface investigation of liquefaction, Imperial Valley earthquake, California, October 15, 1979: U.S. Geol. Survey Open-File Report 81-502, 83 p.
- Benson, L. V., 1978, Fluctuation in the level of pluvial Lake Lahontan during the last 40,000 yr: *Quaternary Research*, v. 9, p. 300-318.
- Berg, H. C., 1979, Significance of geotectonics in the metallogenesis and resource appraisal of southeastern Alaska—A progress report, in Johnson, K. M., and Williams, J. R., eds., The United States Geological Survey in Alaska—Accomplishments during 1978: U.S. Geol. Survey Circular 804-B, p. 115-118.
- Berg, H. C., Jones, D. L., and Coney, P. J., 1978, Map showing pre-Cenozoic tectonostratigraphic terranes of southeastern Alaska and adjacent areas: U.S. Geol. Survey Open-File Report 78-1085, scale 1:1,000,000, 2 sheets.
- Berggren, W. A., and Van Couvering, J. A., 1974, The late Neogene, biostratigraphy, geochronology and paleoclimatology of the last 15 million years in marine and continental sequences: *Palaeogeography, Palaeoclimatology, Palaeoecology*, 16:1-216.
- Betson, R. P., Bales, J., and Pratt, H. E., 1980, User's guide to TVA-HYSIM, A hydrologic program for quantifying land-use change effects: Tennessee Valley Authority for the U.S. Environmental Protection Agency, EPA-600/70-80-048, 107 p.
- Blake, M. C., Jr., and Jones, D. L., 1974, Origin of Franciscan melanges of northern California: *SEPM Special Paper* 19, p. 345-357.
- 1977, Tectonics of the Yolla Bolly junction and its significance to the plate tectonic history of northern California: *Field Trip Guidebook*, Geological Society of America, Cordilleran Section, 73rd Annual Meeting, Sacramento, California, p. 1-14.
- Bohor, D. F., and Triplehorn, D. M., 1981, Volcanic origin of the flint clay parting in the Hazard #4 (Fire Clay) coal bed of the Breathitt

- Formation in eastern Kentucky, in *Coal and coal-bearing rocks of eastern Kentucky: Guidebook*, Ann. Geol. Soc. America Div. Field Trip, November 5-8, 1981, Kentucky Geol. Survey, p. 49-54.
- Boudette, E. L., 1982, Ophiolite assemblage of Early Paleozoic age in central western Maine, in St. Julien, P., and Beland, J., eds., Major structural zones and faults of the northern Appalachians: Geological Association of Canada Special Paper 24 (in press).
- Boudette, E. L., and Boone, G. M., 1976, Pre-Silurian stratigraphic succession in central western Maine: Geological Society of America Memoir 148, p. 79-96.
- Boyd, J. E., 1981, Image enhancement through film recorder response contouring: Society of Photo-Optical Instrumentation Engineers, Bellingham, Wash., April 21-22, 1981, Proceedings, p. 157-166.
- Brew, D. A., and Ford, A. B., 1977, Preliminary geologic and metamorphic isograd map of the Juneau B-1 quadrangle, Alaska: U.S. Geol. Survey Miscellaneous Field Studies Map MF-846, scale 1:31,680.
- 1981, The Coast plutonic complex sill, in Albert, N. R. D., and Hudson, T. L., eds., The United States Geological Survey in Alaska: Accomplishments during 1979: U.S. Geol. Survey Circular 823-B, p. B96-B99.
- Brew, D. A., and Morrell, R. P., 1980, Intrusive rocks and plutonic belts of southeastern Alaska: U.S. Geol. Survey Open-File Report 80-78, 35 p.
- Brockway, R., Alexander, B., Day, P., Lyle, W., Hiles, R., Decker, W., Polski, W., and Reed, B., 1975, Bristol Bay region, stratigraphic correlation section, southwest Alaska: The Alaska Geological Society, 1 sheet.
- Brown, Andrew, Berryhill, H. L., Taylor, D. A., and Trumbull, J. V. A., 1952, Coal resources of Virginia: U.S. Geol. Survey Circular 171, 57 p.
- Brown, C. E., and Ayuso, R. A., 1982, Magnesian-tourmaline-rich metasedimentary rocks in the Grenville lowlands of New York: Potential for occurrence of massive sulfide deposits: Abstracts with Programs, Geological Society of America, North-eastern Section, v. 14, nos. 1 and 2, p. 101.
- Bucknam, R. C., and Anderson, R. E., 1979, Estimation of fault-scarp ages from a scarp-height slope-angle relationship: *Geology*, v. 7, p. 11-14.
- Bukry, J. D., 1977, Coccolith and silicoflagellate stratigraphy, South Atlantic Ocean, Deep Sea Drilling Project Leg 39: Deep Sea Drilling Project Initial Reports, v. 39, p. 825-839.
- Bukry, J. D., and Foster, J. H., 1973, Silicoflagellate and diatom stratigraphy, Leg 61, Deep Sea Drilling Project: Deep Sea Drilling Project Initial Reports, v. 16, p. 815-871.
- Buland, R. P., and Taggart, J. N., 1981, A mantle wave magnitude for the St. Elias, Alaska, earthquake of 28 February 1979: *Bulletin of the Seismological Society of America*, v. 71, no. 4, p. 1143-1159.
- Cadogan, P. H., 1974, Oldest and largest lunar basin?: *Nature*, v. 250, p. 315-316.
- Carlson, R. E., 1977, A trophic state index for lakes: *Limnology and Oceanography*, v. 22, no. 2, p. 361-369.
- 1979, A review of the philosophy and construction of trophic state indices, in Maloney, T. E., ed., *Lakes and reservoir classification systems*: U.S. Environmental Protection Agency, Report No. EPA-600/3-79-074, p. 1-52.
- Carr, M. H., 1981, *The surface of Mars*: Yale University Press, New Haven, Conn., 232 p.
- Carr, M. H., and Clow, G. D., 1981, Martian channels and valleys: Their characteristics, distribution and age: *Icarus*, v. 48, p. 91-117.
- Carr, W. J., 1981, Tectonic history of the Vidal-Parker region, California and Arizona, in Howard, K. A., Carr, M. D., and Miller, D. M., eds., *Tectonic framework of the Mojave and Sonoran Deserts, California and Arizona*: U.S. Geol. Survey Open-File Report 81-503, p. 18-20.
- Carter, L. D., 1981, A Pleistocene sand sea on the Alaska Arctic Coastal Plain: *Science*, v. 211, no. 4480, p. 381-383.
- Carter, Virginia, and Gammon, Patricia, 1976, Great Dismal Swamp vegetative cover map: U.S. Geological Survey Open-File Report 76-615.
- Cathcart, J. B., Sheldon, R. P., and Gulbrandsen, R. A., 1981, A summary of phosphate-rock resources of the United States—an analysis of past estimates: U.S. Geol. Survey Open-File Report 81-789, 9 p.
- Champan, R. M., and Patton, W. W., Jr., 1978, Preliminary summary of the geology in the northwest part of the Ruby quadrangle, in Johnson, K. M., ed., U.S. Geological Survey in Alaska: Accomplishments during 1977: U.S. Geol. Survey Circular 772-B, p. B39-B41.
- Chleborad, A. F., 1980, Investigation of a natural slope failure in weathered Tertiary deposits, western Powder River Basin, Wyoming: U.S. Geol. Survey Open-File Report 80-673, 66 p., 27 figs., 2 tables.
- Clark, B. L., and Campbell, A. S., 1942, Eocene Radiolarian faunas from the Mount Diablo area, California: Geological Society of America, Special Paper Number 39.
- Cochran, W. G., 1977, *Sampling techniques* (3d ed.): New York, John Wiley and Sons, 428 p.
- Colby, B. R., 1957, Relationship of unmeasured sediment discharge to mean velocity: *Transactions of American Geophysical Union*, v. 38, no. 5, 9 p.
- Colby, B. R., and Hembree, C. H., 1955, Computations of total sediment discharge, Niobrara River near Cody, Nebraska: U.S. Geol. Survey Water-Supply Paper 1357, 187 p.
- Collins, B. A., 1976, Coal deposits of the Carbondale, Grand Hogback, and southern Danforth Hills coal fields, eastern Piceance Creek Basin, Colorado: *Quarterly of the Colorado School of Mines*, v. 71, no. 1, 138 p.
- Connor, C. W., 1982, First recognition of crystal tuff in Montana coal bed: *Geotimes*, v. 27, no. 3, p. 1 and 3.
- Cook, H. E., and Egbert, R. M., 1981a, Carbonate submarine fan facies along a Paleozoic prograding continental margin, western United States (abs.): *American Association of Petroleum Geologists Bulletin*, v. 65, p. 913.
- 1981b, Late Cambrian-Early Ordovician continental margin sedimentation, in Taylor, M. E., ed., *Short papers for 2d International Symposium on Cambrian System*: U.S. Geol. Survey Open-File Report 81-743, p. 50-56.
- Cooley, R. L., 1977, A method of estimating parameters and assessing reliability for models of steady-state ground-water flow, 1, Theory and numerical properties: *Water Resources Research* 13 (21), p. 318-324.
- 1979, A method of estimating parameters and assessing reliability for models of steady-state ground-water flow, 2, Application of statistical analysis: *Water Resources Research* 15 (3), p. 603-617.
- Cooper, B. N., 1944, *Geology and mineral resources of Burkes Garden quadrangle, Virginia*: Virginia Geol. Survey Bulletin 60, 299 p.
- Cormier, V. F., and Choy, G. L., 1981, Theoretical body wave interactions with upper mantle structure: *Journal of Geophysical Research*, v. 86, p. 1673-1678.
- Counts, H. B., and Krause, R. E., 1976, Digital model analysis of the principal artesian aquifer, Savannah, Georgia, area: U.S. Geol. Survey Water-Resources Investigations 76-133, 4 sheets.
- Cox, D. P., Czamanske, G. K., and Bain, J. H. C., 1981, Mineral-rich fluid inclusions in the root zone of a porphyry copper system,

- Ajo, Arizona: Geological Society of America Abstracts with Programs, v. 13, no. 7, p. 433.
- Crippen, J. R., and Bue, C. D., 1977, Maximum floodflows in the conterminous United States: U.S. Geol. Survey Water-Supply Paper 1887, 52 p.
- Cronin, T. M., Szabo, B. J., Ager, T. A., Hazel, J. E., and Owens, J. P., 1981, Quaternary climates and sea levels of the U.S. Atlantic Coastal Plain: *Science*, v. 211, p. 233-240.
- Crowley, K. D., 1981, Large-scale bedforms in the Platte River downstream from Grand Island, Nebraska: Structure, process and relationship to channel narrowing: U.S. Geol. Survey Open-File Report 81-1059, 33 p.
- Dalrymple, G. B., 1980, K-Ar ages of the Friant Pumice Member of Turlock Lake Formation, the Bishop Tuff, and the tuff of Reds Meadow, central California: *Isotopes*, no. 28, p. 3-5.
- Dames & Moore, 1981, Exploratory planning study, 1980-1985: prepared under contract to Virginia Polytechnic Inst. and State University, 135 p.
- Daniels, J. J., 1982, Hole-to-surface resistivity measurements at Gibson Dome (drill hole GD-1), Paradox Basin, Utah: U.S. Geol. Survey Open-File Report 82-320, 23 p.
- Daniels, J. J., and Scott, J. H., 1981a, Interpretation of hole-to-surface resistivity measurements at Yucca Mountain, Nevada Test Site: U.S. Geol. Survey Open-File Report 81-1336, 23 p.
- 1981b, Interpretation of geophysical well logs from drill hole UE25a-4, -5, -6, and -7: U.S. Geol. Survey Open-File Report 81-289, 29 p.
- Daniels, J. J., Scott, J. H., and Olhoeft, G. R., 1981, Geophysical well logs for granite drill hole UPH-3, Stephenson County Illinois: U.S. Geol. Survey Open-File Report 81-237, 6 p., 4 plates.
- Davis, J. O., 1978, Quaternary tephrochronology of the Lake Lahontan area, Nevada and California: *Nevada Archeological Survey Research Paper 7*, 137 p.
- Davis, G. A., Anderson, J. L., Frost, E. G., and Shackelford, T. J., 1980, Mylonitization and detachment faulting in the Whipple-Rawhide-Buckskin Mountains terrane, southeastern California and western Arizona, in Crittenden, M. D., Jr., Coney, P. J., and Davis, G. A., eds., *Cordilleran metamorphic core complexes: Geological Society of America Memoir 153*, p. 79-130.
- Dean, W. E., Ringrose, C. D., and Klusman, R. W., 1979, Geochemical variation in soils in the Piceance Creek basin, Western Colorado: U.S. Geol. Survey Bulletin 1479, 46 p.
- DeGraw, H. M., 1969, Subsurface relations of the Cretaceous and Tertiary in western Nebraska: Open-File Report, Nebraska Geol. Survey, University of Nebraska, Conservation and Survey Division, Lincoln, 137 p.
- Dickey, J. W., 1981, TIP: trends integrator procedure: Virginia Polytechnic Inst., 67 p.
- Diment, W. H., Urban, T. C., Nathenson, M., Nehring, N. L., Shaeffer, M. H., 1981, Thermal convection in cased water-filled drill holes: Effect of small quantities of gas: EOS, *American Geophysical Union Transactions*, v. 62, p. 392.
- Dion, N. P., and Embrey, S. S., 1981, Effects of Mount St. Helens eruption on selected lakes in Washington: U.S. Geol. Survey Circular 850-G, 25 p.
- Dodge, K. A., and Levings, G. W., 1980, Measurement of discharge, gain or loss in flow, and chemical quality of the Poplar and Red-water Rivers, northeastern Montana, October 24-25, 1979: U.S. Geol. Survey Open-File Report 80-1210, 16 p.
- Douglas, D., and Peucker, T., 1973, Algorithms for the reduction of the number of points required to represent a digitized line or its caricature: *Canadian Cartographer*, 1973, v. 10, no. 2, p. 112-122.
- Doyle, W. H., Jr., and Lorens, J. A., 1981, Urban stormwater data management system, in *Proceedings of International Symposium on Rainfall-Runoff Modeling*, Mississippi State University, May 18-22, 1981, 22 p.
- Druse, S. A., Dodge, K. A., and Hotchkiss, W. R., 1981, Base flow and chemical quality of streams in the Northern Great Plains area, Montana and Wyoming, 1977-78: U.S. Geol. Survey Open-File Report 81-692, 60 p.
- DuBar, J. R., 1971, Neogene stratigraphy of the lower Coastal Plain of the Carolinas, in *Atlantic Coastal Plain Geological Association 12th annual field conferences guidebook: Myrtle Beach, South Carolina*, 128 p.
- Easterbrook, D. J., Crandall, D. R., and Leopold, E. B., 1967, Pre-Olympia Pleistocene stratigraphy and chronology in the central Puget Lowland, Washington: *Geological Society of America Bulletin*, v. 78, p. 13-20.
- Eaton, G. P., Wahl, R. R., Prostka, H. J., Mabey, D. R., and Kleinkopf, M. D., 1978, Regional gravity and tectonic patterns; their relation to late Cenozoic epeirogeny and lateral spreading in the Western Cordillera, in Smith, R. B., and Eaton, G. P., eds., *Cenozoic tectonics and regional geophysics of the Western Cordillera: Geological Society of America Memoir 152*, Chapter 3, p. 51-92.
- Edds, Joe, 1981, Ground-water levels in Arkansas, spring 1981: U.S. Geol. Survey Open-File Report 81-1114, 52 p.
- Ekren, E. B., Bucknam, R. C., Carr, W. J., Dixon, G. L., and Quinlivan, W. D., 1976, East-trending structural lineaments in central Nevada: U.S. Geol. Survey Professional Paper 986, 16 p.
- Ellen, Stephen, Peterson, D. M., and Reid, G. O., 1982, Map showing areas susceptible to different hazards from shallow landsliding, Marin County and adjacent parts of Sonoma County, California: U.S. Geological Survey Miscellaneous Field Studies Map MF-1406, scale 1:62,500 (in press).
- Englund, K. H., 1979, Mississippian System and Lower Series of the Pennsylvania System in the Proposed Pennsylvania System stratotype area, in Englund, K. J., Arndt, H. H., and Henry, T. W., (eds.), *Proposed Pennsylvanian System stratotype, Virginia and West Virginia: American Geological Institute Selected Guidebook Series no. 1*, p. 69-72.
- Eschner, T. R., Hadley, R. F., and Crowley, K. D., 1981, Hydrologic and morphologic changes in channels of the Platte River basin: A historical perspective: U.S. Geol. Survey Open-File Report 81-1125, 57 p.
- Evans, B. J., Johnson, R. G., Senftle, F. E., Cecil, C. B., and DuLong, F. T., 1982, The ⁵⁷Fe Mossbauer parameters of pyrite and marcasite with different provenances: *Geochimica et Cosmochimica Acta*, v. 46, p. 761-775.
- Evernden, J. F., and Kistler, R. W., 1970, Chronology of emplacement of Mesozoic batholithic complexes in California and western Nevada: U.S. Geol. Survey Professional Paper 623, 42 p.
- Evernden, J. F., Savage, D. E., Curtis, G. H., and James, G. T., 1964, Potassium-argon dates and the Cenozoic mammalian chronology of North America: *American Journal of Science*, v. 262, p. 145-198.
- Eychaner, J. H., 1981, Geohydrology and effects of water use in the Black Mesa area, Navajo and Hopi Indian Reservations, Arizona: U.S. Geol. Survey Open-File Report 81-911, 46 p.
- Fabiano, E. B., and Peddie, N. W., 1981, Total magnetic intensity in the United States—epoch 1980: U.S. Geol. Survey Miscellaneous Investigations Series Map I-1370.
- Faye, R. E., and Cherry, R. N., 1980, Channel and dynamic flow characteristics of the Chattahoochee River, Buford Dam to Georgia Highway 141: U.S. Geol. Survey Water-Supply Paper 2063, 66 p.
- Feltis, R. D., Lewis, B. D., Frasure, R. L., Rioux, R. P., Jauhola, C. A., and Hotchkiss, W. R., 1981, Selected geologic data from the Northern Great Plains area of Montana: U.S. Geol. Survey Open-

- File Report 81-415, 63 p.
- Fender, H. B., and Murray, D. K., 1978, Data accumulation on the methane potential of the coal beds of Colorado, Colorado Geological Survey Open-File Report 78-2.
- Ferry, J. M., and Spear, F. S., 1978, Experimental calibration of the partitioning of Fe and Mg between biotite and garnet: Contributions to Mineralogy and Petrology, v. 66, p. 113-117.
- Fieni, C. M., Bourte-Denise, M., Pallas, P., and Touret, J., 1978, Aqueous fluid inclusions in feldspars and phosphates from Peetz chondrite (abstract): Meteoritics, v. 13, p. 460-461.
- Fiske, R. S., Hopson, C. A., and Waters, A. C., 1963, Geology of Mount Rainier National Park, Washington: U.S. Geol. Survey Professional Paper 444, 93 p.
- Forbes, R. B., 1959, The geology and petrology of the Juneau Ice Field area, southeastern Alaska: Seattle, University of Washington, PhD thesis, 261 p.
- Ford, A. B., and Brew, D. A., 1973, Preliminary geologic and metamorphic isograd map of the Juneau B-2 quadrangle, Alaska: U.S. Geol. Survey Miscellaneous Field Studies Map MF-527, scale 1:31,680.
- Fournier, R. O., and Potter, R. W., II, 1979, Magnesium correction to the Na-K-Ca chemical geothermometer: Geochimica et Cosmochimica Acta, v. 43, p. 1543-1550.
- Friedman, J. D., Frank, David, Keiffer, H. H., and Sawatzky, D. L., 1982, Thermal infrared surveys of the May 18 crater, subsequent lava domes, and associated volcanic deposits, in The 1980 eruptions of Mount St. Helens: U.S. Geol. Survey Professional Paper 1250, p. 279-294.
- Friedman, J. D., Olhoeft, G. R., Johnson, G. R., and Frank, David, 1982, Heat content and thermal energy of the June dome in relation to total energy yield of Mt. St. Helens, May-October, 1980, in The 1980 eruptions of Mount St. Helens, U.S. Geol. Survey Professional Paper 1250, p. 557-568.
- Fuller, T. D., 1981, Population: Virginia Polytechnic Inst., 155 p.
- Gautier, D. L., 1982, Siderite concretions; Indicators of early diagenesis in the Gammon Shale (Cretaceous): Journal of Sedimentary Petrology (in press).
- Gilbert, W. G., Ferrell, V. M., and Turner, D. L., 1976, The Teklanika Formation—A new Paleocene volcanic formation in the central Alaska Range: Alaska Division of Geological and Geophysical Surveys, Geologic Report 47, 16 p.
- Gilluly, James, 1946, The Ajo mining district, Arizona: U.S. Geol. Survey Professional Paper 209, 112 p.
- Glass, N. R., Glass, G. E., and Rennie, P. J., 1980, Effects of acid precipitation in North America: Environmental International, v. 4, p. 443-452.
- Goolsby, J. E., and Miller, D. D., 1982, Energy exploration along the basin margin—mountain front in the Rocky Mountain area: Geological Society of America, Abstracts with Programs, v. 14, no. 6, p. 313.
- Gordon, Mackenzie, Jr., 1965, Carboniferous cephalopods of Arkansas: U.S. Geol. Survey Professional Paper 460, 322 p.
- Greenlee, D. D., 1981, Application of spatial analysis techniques to remotely sensed images and ancillary geocoded data, in Harvard Computer Graphics Week 1980: Harvard Library of Computer Graphics, Cambridge, Mass., 1980, v. 15, p. 111-120.
- Grolier, M. J., Tibbitts, G. C., Jr., and Ibrahim, M. M., 1981, A qualitative appraisal of the hydrology of the Yemen Arab Republic from Landsat images: U.S. Geol. Survey Open-File Report 80-565, Reston, Virginia, 103 p., 6 figs., 1 pl., 2 tables.
- Gross, M. G., Kariverit, M., Cronin, W. B., and Schubel, J. R., 1978, Suspended-sediment discharge of the Susquehanna River to northern Chesapeake Bay, 1966 to 1976: Estuaries, v. 1, no. 2, p. 106-110.
- Guffanti, Marianne, and Nathenson, Manuel, 1980, Preliminary temperature-gradient map of the conterminous United States: Geothermal Resources Council Transactions, v. 4, p. 53-56.
- 1981, Temperature-depth data for selected deep drill holes in the United States obtained using maximum thermometers: U.S. Geol. Survey Open-File Report 81-555, 100 p.
- Hale, L. A., 1960, Frontier Formation—Coalville, Utah, and nearby areas of Wyoming and Colorado: Wyoming Geol. Association Guidebook, 1960, p. 137-146.
- Ham, W. E., and others, 1964, Basement rocks and structural evolution, southern Oklahoma: Oklahoma Geol. Survey Bulletin 95.
- Haq, B. V., Berggren, W. A., and Van Couvering, J. A., 1977, Corrected age of Pliocene/Pleistocene boundary: Nature, v. 269, p. 483-488.
- Harden, J. W., 1982, A quantitative index of soil development from field descriptions: Geoderma, v. 28, no. 1, p. 1-28.
- Hardison, C. H., 1969, Accuracy of streamflow characteristics, in Geological Survey research 1969: U.S. Geol. Survey Professional Paper 650-D, p. D210-D214.
- Harris, L. D., Harris, A. G., de Witt, Wallace, Jr., and Bayer, K. C., 1981, Evaluation of the southern Eastern Overthrust belt beneath the Blue Ridge—Piedmont thrust: American Association of Petroleum Geologists Bulletin, v. 65, no. 12, p. 2497-2505.
- Harvey, Danny, and Choy, G. L., 1982, Broadband deconvolution of GDSN data: Geophysical Journal Royal Astronomical Soc., v. 69, p. 659-668.
- Hastings, D. A., 1980, On the tectonics and metallogenesis of West Africa: a model influenced by new geophysical data (abs.): International Geological Congress, 26th, Paris, Proceedings, p. 726.
- 1981a, A first look at the Magsat anomaly map, emphasizing Africa (abs.): American Geophysical Union Spring Meeting Program, p. 72.
- 1981b, An interpretation of the preliminary total-field Magsat anomaly map: Geological Society of America Abstracts with Programs, v. 13, p. 469.
- Havens, John, 1982a, Generalized altitude and configuration of the base of the High Plains regional aquifer, northwestern Oklahoma: U.S. Geol. Survey Open-File Report 81-1117, scale 1:250,000, 2 sheets.
- 1982b, Altitude and configuration of the 1980 water table in the High Plains regional aquifer, northwestern Oklahoma: U.S. Geol. Survey Open-File Report 82-100, scale 1:250,000, 2 sheets.
- 1982c, Altitude and configuration of the predevelopment water table in the High Plains regional aquifer, northwestern Oklahoma: U.S. Geol. Survey Open-File Report 82-275, scale 1:250,000, 2 sheets.
- Herb, W. J., Shaw, L. C., and Brown, D. E., 1981a, Hydrology of area 5, Eastern Coal Province, Pennsylvania, Maryland, and West Virginia: U.S. Geol. Survey Open-File Report 81-538, 92 p.
- 1981b, Hydrology of area 3, Eastern Coal Province, Pennsylvania: U.S. Geol. Survey, Open-File Report 81-537, 88 p.
- Holcomb, L. G., 1981a, The lower limits of seismic background noise levels: American Institute of Aeronautics and Astronautics, Proceedings of the Guidance and Control Conference, August 19-21, p. 249-252.
- 1981b, High resolution spectral analysis of long-period microseisms: International Association of Seismology and Physics of the Earth's Interior, Twenty-First General Assembly, London, Ontario, abs., p. C2.3.
- 1982, Preliminary study of methods for upgrading USGS Antarctic seismological capability: U.S. Geol. Survey Open-File Report 82-292, 40 p.
- Holcomb, L. G., and Peterson, J. R., 1981, A technique for compressing seismic digital data: International Association of Seismology

- and Physics of the Earth's Interior, Twenty-First General Assembly, London, Ontario, abs., p. A1.17.
- Holtschlag, D. J., 1981, Flow Model of Saginaw River near Saginaw, Michigan: U.S. Geol. Survey Open-File Report 81-1061, 20 p.
- Holzer, T. L., and Bluntzer, R. L., 1981, Significance of petroleum withdrawal to subsidence and surface faulting in the Houston-Galveston, Texas, area: Geol. Society of America Abstracts with Programs, v. 13, no. 7, p. 475-476.
- Hopson, C. A., 1964, The crystalline rocks of Howard and Montgomery Counties: Maryland Geol. Survey, The Geology of Howard and Montgomery Counties, p. 27-215.
- Hubbert, M. K., and Rubey, W. W., 1959, Mechanics of fluid-filled porous solids and its application to overthrust faulting: Geol. Society of America Bulletin, v. 70, no. 2, p. 115-166.
- Hudson, Travis, 1977, Map showing preliminary framework data for evaluation of the metallic mineral resource potential of northern Seward Peninsula, Alaska: U.S. Geol. Survey Open-File Report 77-167-B.
- Hutchison, N. E., 1981, Outline for a hydrologic data base for Portugal: U.S. Geol. Survey Open-File Report 81-424, Reston, Virginia, 142 p.
- Iivari, T. A., 1979, Cenozoic geologic evolution of the east-central Markagunt Plateau, Utah: Kent State University MS thesis, 154 p.
- Jennings, M. E., Schneider, V. R., and Smith, P. E., 1981, Emergency assessment of Mount St. Helens post-eruption flood hazards, Toutle and Cowlitz Rivers, Washington, U.S. Geol. Survey Circular 850-I, 7 p.
- Jenson, S. K., and Waltz, F. A., 1979, Principal components analysis and canonical analysis in remote sensing, in American Society of Photogrammetry Annual Meeting, 45th, Washington, D.C., Proceedings: Falls Church, Va., American Society of Photogrammetry, v. 1, p. 337-347.
- Johnson, W. H., 1976, Quaternary stratigraphy in Illinois: Status and current problems, in Mahaney, W. C., ed., Quaternary stratigraphy of North America: Stroudsburg, Pa., Dowden, Hutchinson, and Ross, p. 161-196.
- Jones, D. L., Silberling, N. J., Berg, H. C., and Plafker, George, 1981, Map showing tectonostratigraphic terranes of Alaska, columnar sections, and summary description of terrane: U.S. Geol. Survey Open-File Report 81-792, 2 sheets, scale 1:250,000, 20-page pamphlet text.
- Jones, D. L., Silberling, N. J., Csejtey, Bela, Jr., Nelson, W. H., and Blome, C. D., 1980, Age and structural significance of ophiolite and adjoining rocks in the Upper Chultina District, south-central Alaska: U.S. Geol. Survey Professional Paper 1121-A, p. A1-A21, 2 plates.
- Jones, D. L., Silberling, N. J., Gilbert, Wyatt, and Coney, P. J., 1982, Character, distribution, and tectonic significance of accreted terranes in the central Alaska Range: American Geophysical Union Bulletin, v. 87, no. B5, p. 3709-3717.
- Judy, J. R., 1974, Cenozoic stratigraphic and structural evolution of the west-central Markagunt Plateau, Utah: Kent State University MS thesis, 107 p.
- Julian, B. R., 1982, Seismic-wave scattering in a quasi-stratified earthquake: Seismological Society of America, Eastern Section, Earthquake Notes, abs., p. 78.
- Karlinger, M. R., Mengis, R. C., Kircher, J. E., and Eschner, T. R., 1981, Application of theoretical equations to estimate the discharge needed to maintain channel width in a reach of the Platte River near Lexington, Nebraska: U.S. Geol. Survey Open-File Report 81-697, 16 p.
- Keiffer, H. H., Frank, David, and Friedman, J. D., 1982, Thermal infrared surveys: Observations prior to the eruption of May 18, in The 1980 eruptions of Mount St. Helens, U.S. Geol. Survey Professional Paper 1250, p. 257-278.
- Kiilsgaard, T. H., Freeman, V. L., and Coffman, J. S., 1970, Mineral resources of the Sawtooth Primitive Area, Idaho, U.S. Geol. Survey Bulletin 1319-D, 174 p.
- King, P. B., and Beikman, H. M., 1974, Geologic Map of the United States (exclusive of Alaska and Hawaii): U.S. Geol. Survey, scale 1:2,500,000, 3 sheets [1975].
- Kirby, S. H., 1981, Hydrogen-bonded hydroxyl in synthetic quartz: analysis, mode of incorporation, and role in hydrolytic weakening (abs.): EOS, American Geophys. Union Transactions, v. 62, p. 396.
- Kircher, J. E., 1981, Sediment transport and effective discharge of the North Platte, South Platte, and Platte Rivers in Nebraska: U.S. Geol. Survey Open-File Report 81-53.
- Kircher, J. E., and Karlinger, M. R., 1981, Changes in surface water hydrology, Platte River basin in Colorado, Wyoming, and Nebraska upstream from Duncan, Nebraska: U.S. Geol. Survey Open-File Report 81-818, 77 p.
- Klein, F. W., 1982, Earthquakes at Loihi submarine volcano, Hawaii: Journal of Geophysical Research, v. 87, p. 7719-7726.
- Klitgord, K. D., Schlee, J. S., and Hine, Karl, 1982, Basement structure, sedimentation and tectonic history of the Georges Bank Basin, in Scholle, P. A., and Wenkam, C. K., eds., Geological Studies of the COST Nos. G-1 and G-2 wells, United States North Atlantic Outer Continental Shelf: U.S. Geol. Survey Circular 861, p. 160-186.
- Lajoie, K. R., Sarna-Wojcicki, A. M., and Yerkes, R. F., 1982, Quaternary chronology and rates of crustal deformation in the Ventura area, California, in Neotectonics in southern California: Field Trip Guidebook, Geological Society of America, Cordilleran Section p. 43-51.
- Langel, R. A., Estes, R. H., Mead, G. D., Fabiano, E. B., and Lancaster, E. R., 1980, Initial geomagnetic field model from Magsat vector data: Geophysical Research Letter, v. 7, no. 10, p. 733-796.
- Lauer, D. T., and Todd, W. J., 1981, Land cover mapping with merged Landsat return beam vidicon (RBV) and multispectral scanner (MSS) stereoscopic images, in American Society of Photogrammetry Fall Technical Meeting, San Francisco, Calif., 1981, Proceedings: Falls Church, Va., American Society of Photogrammetry, p. 68-89.
- Leavesley, G. H., and Striffler, W. D., 1979, A mountain watershed simulation model, in Colbeck, S. C., and Roy, M., eds., Proceedings model of snow cover runoff: Hanover, New Hampshire, U.S. Army Corp of Engineers, Cold Regions Research and Engineering Laboratory, p. 379-386.
- Lee, D. E., Kistler, R. W., Friedman, Irving, and Van Loenen, R. E., 1981, Two-mica granites of northeastern Nevada: Journal of Geophysical Research, v. 86, no. B11, p. 10607-10616.
- Lee, D. E., Marvin, R. F., and Mehnert, H. H., 1980, A radiometric age study of Mesozoic-Cenozoic metamorphism in eastern White Pine County, Nevada, and nearby Utah: U.S. Geol. Survey Professional Paper 1158-C, p. 17-28.
- Levings, G. W., 1981a, Selected hydrogeologic data from the Northern Great Plains area of Montana: U.S. Geol. Survey Open-File Report 81-534, 241 p.
- 1981b, Selected drill-stem test data from the Northern Great Plains area of Montana: U.S. Geol. Survey Open-File Report 81-326, 20 p.
- Levings, J. F., and Dodge, K. A., 1981, Selected hydrogeologic data from the Judith Basin, central Montana: U.S. Geol. Survey Open-File Report 81-1015, 98 p.
- Levings, J. F., Levings, G. W., Feltis, R. D., Hotchkiss, W. R., and Lee, R. W., 1981, Selective annotated bibliography of geology and ground-water resources for the Montana part of the Northern

- Great Plains regional aquifer-system analysis: U.S. Geol. Survey Open-File Report 81-401, 91 p.
- Lichty, R. W., and Liscum, R., 1978, A rainfall-runoff modeling procedure for improving estimates of T-year (annual) floods for small drainage basins: U.S. Geol. Survey Open-File Report 78-7, 44 p.
- Lind, C. J., 1982, Characterization of mineral precipitates by electron microscope photographs and electron diffraction patterns: U.S. Geol. Survey Water-Supply Paper 2204 (in press).
- Linden, D. S., and Szajin, John, 1981, Verification of land cover maps from Landsat data, in *Western Regional Remote Sensing Conference, Monterey, Calif., 1981, Proceedings: Moffett Field, Calif., National Aeronautics and Space Administration, Ames Research Center*, p. 1-119 to 1-125.
- Lowhan, H. W., 1976, Techniques for estimating flow characteristics of Wyoming streams: U.S. Geol. Survey Open-File Report 76-112, 83 p.
- Lucchitta, B. K., 1982, Ice sculpture in the martian outflow channels, *Journal of Geophysical Research*, v. 87, no. B.12, p. 9951-9973.
- Lucchitta, B. K., and Ferguson, H. M., 1982, Chryse basin channels: low gradients and ponded flow: *Proceedings, Thirteenth Lunar and Planetary Science Conference, Journal of Geophysical Research*, v. 82, pt. 2, Supplement, p. A553-A568.
- Lucchitta, B. K., and Soderblom, L. A., 1982, The geology of Europa, in *Morrison, David, ed., The Satellites of Jupiter: University of Arizona Press, Chapter 14*, p. 521-553.
- McCallister, R. H., and Nord, G. L., Jr., 1981, Subcalcic diopsides from kimberlites: chemistry, exsolution microstructures, and their thermal history: *Contributions to Mineralogy and Petrology*, v. 78, p. 118-125.
- McCutcheon, S. C., 1981a, Comparison of one-dimensional water-quality models, *EOS*, v. 62, no. 45, p. 868.
- 1981b, Vertical velocity profiles in stratified flows, *ASCE Journal of Hydraulics Division*, v. 107, no. HY8, p. 973-988.
- 1982, Evaluation of selected one-dimensional stream water-quality models with field data, *Technical Report E-82: Prepared by the Gulf Coast Hydroscience Center, Geological Survey, for the U.S. Army Engineers Waterways Experiment Station, CE, Vicksburg, Miss.*
- McGill, J. T., 1982, Map showing relationship of historic to prehistoric landslides, Pacific Palisades area, City of Los Angeles, California: U.S. Geol. Survey Miscellaneous Field Studies Map MF-1455, scale 1:4,800.
- Mack, F. K., and Thomas, W. O., Jr., 1972, Hydrology of channel fill deposits near Salisbury, Maryland, as determined by a 30-day pumping test: *Maryland Geol. Survey, Bulletin 31, part 1*, p. 1-60.
- Mack, F. K., Webb, W. E., and Gardner, R. A., 1971, Water Resources of Talbot and Dorchester Counties, Maryland: *Maryland Geol. Survey, Report of Investigations No. 17*, 107 p.
- Macke, D. L., and Denson, N. M., 1981, Contours on the pre-Oligocene surface and pre-Oligocene geologic map, in *Seeland, D. A., principal investigator, Uranium resource evaluation Torrington NTMS 1 degree and 2 degree quadrangle, Wyoming-Nebraska: U.S. Dept. Energy NURE Folio PGJ-067(81)*, 97 p., 800 p. appendices, 10 pl.
- MacLeod, N. S., Sherrod, D. R., Chitwood, L. A., and McKee, E. H., 1981, Newberry Volcano, Oregon, in *Johnston, D. A., and Donnelly-Nolan, Julie, eds., Guides to some volcanic terranes in Washington, Idaho, Oregon, and northern California: U.S. Geol. Survey Circular 838*, p. 85-103.
- Merriam, J. C., 1907, The occurrence of middle Tertiary mammal bearing beds in NW Nevada: *Science ns.*, v. 26, p. 380-382.
- Merrill, F. J. H., Darton, N. H., Hollic, Arthur, Salisbury, R. D., Dodge, R. B., Willis, Bailey, and Pressey, N. H., 1902, Description of the New York City district: U.S. Geol. Survey Geologic Atlas, Folio 83, 19 p., 13 sheets.
- Mertie, J. B., Jr., 1937, The Yukon-Tanana region, Alaska: U.S. Geol. Survey Bulletin 872, 176 p.
- 1938, Gold placers of the Fortymile, Eagle, and Circle Districts, Alaska: U.S. Geol. Survey Bulletin 897-C, p. 133-261.
- Miller, F. K., and Yates, R. G., 1976, Geologic map of the west half of the Sandpoint 2 degree quadrangle (Washington-Idaho): U.S. Geol. Survey Open-File Report 76-327.
- Miller, S. W., 1980, A compact raster format for handling spatial data: *American Society of Photogrammetry and American Congress on Surveying and Mapping Fall Technical Meeting, Niagara Falls, N.Y., October 7-10, 1980, Proceedings, ACSM Technical Papers*, p. CD-4-A-1-CD-4-A-18.
- Miller, W. A., Shasby, M. B., Rohde, W. G., and Johnson, G. R., 1981, Developing in-place data bases by incorporating digital terrain data into the Landsat classification process, in *In-Place Resource Inventories National Workshop, Orono, Maine, August 9-14, 1981, Proceedings: 8 p. (in press)*.
- Miller, W. J., 1934, Geology of the western San Gabriel Mountains of California: *Univ. California at Los Angeles Pub. in Math. and Phys. Sci.*, v. 1, no. 1, p. 3-12, 63-65.
- Miller, W. L., 1966, Petrology of the Putah Member of the Tehama Formation, Yolo and Solano Counties, California: *University of California, Davis, MS thesis*, 80 p.
- Minard, J. P., 1982, Distribution and description of the geologic units in the Edmonds East and adjoining eastern part of the Edmonds West quadrangles, Snohomish and King Counties, Washington: U.S. Geol. Survey, Open-File Report 82-829, scale 1:24,000.
- Modreski, P. J., and Chou, I-Ming, 1981, Silica content of magnetite from fayalite-magnetite-quartz assemblage and from hydrothermal ore deposits (abs.): *Geological Society of America, Abstracts with Programs*, v. 13, no. 7, p. 513.
- Molenaar, C. M., 1973, Sedimentary facies and correlation of the Gallup Sandstone and associated formations, northwestern New Mexico: *Four Corners Geol. Society Memoir no. 1*, p. 85-110.
- Moore, G. K., and Sheehan, C. A., 1981, Evaluation of radar imagery for geologic and cartographic applications: summary report of investigations: U.S. Geol. Survey Open-File Report 81-1358, 37 p.
- Moore, H. J., Clow, G. D., and Hutton, R. E., 1982, A summary of Viking sample trench analyses for angles of internal friction and cohesion: *Journal of Geophysical Research*, v. 89, p. 1043-1050.
- Morris, E. C., 1981, The aureole deposits of the martian volcano Olympus Mons: *Journal of Geophysical Research*, v. 87, no. 82, p. 1164-1178.
- Morrissey, L. A., and Ennis, R. A., 1981, Vegetation mapping of the National Petroleum Reserve in Alaska using Landsat digital data: U.S. Geol. Survey Open-File Report 81-315, 25 p.
- Moss, M. E., and Gilroy, E. J., 1980, Cost effective stream-gaging strategies for the Lower Colorado River basin—the Blythe field office operations: U.S. Geol. Survey Open-File Report 80-1048, 111 p.
- Moss, M. E., and Karlinger, M. R., 1974, Surface water network design by regression analysis simulation: *Water Resources Research*, v. 10, no. 3, p. 427-433.
- Mudge, M. R., and Earhart, R.L., 1980, The Lewis thrust fault and related structures in the Disturbed Belt, northwestern Montana: U.S. Geol. Survey Professional Paper 1174, 18 p.
- Muffler, L. J. P., 1967, Stratigraphy of the Keku Islets and neighboring parts of Kuiu and Kupreanof Islands, southeastern Alaska: U.S. Geol. Survey Bulletin 1241-C, 52 p.
- Mundorff, M. J., Crosthwaite, E. G., and Kilburn, Chabot, 1964, Ground water for irrigation in the Snake River basin in Idaho: U.S. Geol. Survey Water-Supply Paper 1654, 224 p.

- Myers, R. C., 1977, Stratigraphy of the Frontier Formation (Upper Cretaceous), Kemmerer area, Lincoln County, Wyoming, in *Rocky Mountain Thrust Belt Geology and Resources: Wyoming Geological Association, 29th Annual Field Conference Guidebook*, p. 271-311.
- Naeser, C. W., Izett, G. A., and Wilcox, R. E., 1973, Zircon fission-track ages of Pearlette family ash beds in Meade County, Kansas: *Geology*, v. 1, p. 93-95.
- Nathenson, Manuel, 1981, The relation between geothermometer, reservoir, and spring temperatures for low- and intermediate-temperature (less than 150 degrees C) hydrothermal systems in southwestern Montana: *Geothermal Resources Council Bulletin*, v. 10, no. 7, p. 3-7.
- Nichols, K. M., and Silberling, N. J., 1979, Early Triassic (Smithian) ammonites of paleoequatorial affinity from the Chultina Terrane, south-central Alaska: *U.S. Geol. Survey Professional Paper 1121-B*, p. B1-B5, 3 pl.
- Norvitch, R. F., Thomas, C. A., and Madison, R. J., 1969, Artificial recharge to the Snake Plain aquifer in Idaho; an evaluation of potential and effect: *Idaho Department of Reclamation, Water Information Bulletin No. 12*, 59 p.
- Nutter, W. L., and Hewlett, J. D., 1971, Streamflow production from permeable upland basins, in Monke, E. J., ed., *Biological effects in the hydrological cycle: Proceedings, Third International Seminar for Hydrology Professors, Purdue University, West Lafayette, Indiana, July 18-30, 1971*, p. 248-257.
- Nuttli, O. W., 1979, Seismicity of the central United States, in Hathaway, A. W., and McClure, C. R., Jr., *Geology in the citing of nuclear power plants: Geological Society of America Reviews in Engineering Geology*, v. IV, p. 67-93.
- Oaksford, E. T., 1978, Water-manometer tensiometers installed and read from land surface: *Geotechnical Testing Journal*, v. 1, no. 4, p. 199-202.
- Obradovich, J. D., and Cobban, W. A., 1975, A time-scale for the Late Cretaceous system in the Western Interior of North America, in Caldwell, W. G. E., ed., *Geological Association of Canada: Special Paper No. 13*, p. 31-54.
- Oliver, J., Johnson, T., and Dorman, J., 1970, Postglacial faulting and seismicity in New York and Quebec: *Canadian Journal of Earth Science*, v. 7, no. 2, p. 579-590.
- Ogle, B. A., 1953, *Geology of Eel River valley area, Humboldt County, California: California Div. Mines Bulletin 164*, 128 p.
- Olsen, H. W., McGregor, B. A., Booth, J. S., Cardinell, A. P., and Rice, T. L., 1982, Stability of near-surface sediment on the mid-Atlantic upper continental slope: 1982 Offshore Technology Conference, Houston, Texas, *Proceedings*, v. 3, p. 21-35.
- Olsen, P. E., Remington, C. L., Cornet, B., and Thomson, K. S., 1978, Cyclic change in Late Triassic lacustrine communities: *Science*, v. 201, p. 729-733.
- Oman, C. L., Meissner, C. R., and Kane, Jean, 1982, Chemical composition of Gulf Coast lignites: Data as of 1981: Abstract with Programs, Geological Society of America, Northeast-Southeast Meeting, Washington, D.C., Febr. 1982, v. 14, nos. 1 and 2, p. 70.
- Oppenheimer, D. H., and Herkenhoff, K. E., 1981, Velocity-density properties of the lithosphere from three-dimensional modeling at The Geysers-Clear Lake, California: *Journal of Geophysical Research*, v. 86, p. 6057-6065.
- Ostresh, L. M., Jr., Thompson, J. G., Banwart, A. L., Reynolds, R. R., Jr., and Wilkinson, K. P., 1981, Change in industrial composition in Western energy development communities: *Rural Sociological Society meetings, Guelph, Ontario, Canada, August*.
- Overton, D. E., 1980, Computer program TENN II, A nonlinear model for simulating stormwater runoff volumes, hydrographs, and pollutant yields for small watersheds: *User's manual*, D. E. Overton and Associates, Consulting Engineers, Knoxville, Tennessee, 21 p.
- Paillet, F. L., 1981a, Predicting the frequency content of acoustic waveforms obtained in boreholes: *Society of Professional Well Log Analysts, 22d Annual Logging Symposium, Mexico City, Mexico, Transactions*.
- 1981b, A comparison of fracture characterization techniques applied to near-vertical fractures in a limestone reservoir: *Society of Professional Well Log Analysts, 22d Annual Logging Symposium, Mexico City, Mexico, Transactions*.
- 1981c, The in-situ measurement of fracture permeability using acoustic normal mode attenuation in boreholes, Chalk River, Ontario, Canada: *Geological Society of America, Annual Meeting, Cincinnati, Ohio, abstract*.
- Paillet, F. L., and White J. E., 1982, Acoustic normal modes in the borehole and their relationship to rock properties: *Geophysics*, v. 47, no. 8.
- Palacas, J. G., Daws, T. A., and Applegate, A. W., 1981, Preliminary petroleum source-rock assessment of pre-Punta Gorda rocks (lowermost Cretaceous-Jurassic?) in south Florida: *Gulf Coast Association of Geological Societies Transactions*, v. 31, p. 369-376.
- Pampeyan, E. H., 1982, The 1906 San Andreas fault trace in the Montara Mountain and San Mateo 7 1/2-minute quadrangles, San Mateo County, California: *U.S. Geol. Survey Miscellaneous Field Studies Map MF-1488, scale 1:24,000 (in press)*.
- Parker, Gary, 1978, Self-formed straight rivers with equilibrium banks and mobile bed, Part I, The sand-silt river: *Journal of Fluid Mechanics*, v. 89, pt. 1, p. 109-125.
- Parrett, Charles, 1981, Potential effects of urbanization on peak flows in Rattlesnake Creek, Missoula County, Montana: *U.S. Geol. Survey Water-Resources Investigations 81-34*, 18 p.
- Passey, Q. R., and Shoemaker, E. M., 1982, Craters and basins on Ganymede and Callisto: morphological implications of crustal evolution, in Morris, David, ed., *The satellites of Jupiter: University of Arizona Press, chapter 12*, p. 379-434.
- Patton, W. W., Jr., and Hoare, J. M., 1968, The Kaltag fault, west-central Alaska, in *Geological Survey research 1968: U.S. Geological Survey research 1968: U.S. Geological Survey Professional Paper 600-D*, p. D147-D153.
- Pavich, M. J., Brown, Louis, Tera, Fouad, Middleton, Roy, and Klein, Jeffrey, 1982, Evaluation of 10-beryllium as a method for dating late Cenozoic soils (abs.): *Geological Society of America Abstracts with Programs*, 1982, v. 14, nos. 1 and 2, p. 72.
- Pavrides, Louis, 1981, The central Virginia volcanic-plutonic belt: an island arc of Cambrian(?) age: *U.S. Geol. Survey Professional Paper 1231-A*, p. A1-A34.
- Peirce, H. W., Damon, P. E. and Shafiqullah, M., 1979, An Oligocene(?) Colorado Plateau edge in Arizona: *Tectonophysics*, v. 61, p. 1-24.
- Peterson, Fred, 1980, Sedimentology of the uranium-bearing Salt Wash Member and Tidwell unit of the Morrison Formation in the Henry and Kaiparowits basins, Utah, in Picard, M. D., ed., *Henry Mountains Symposium: Utah Geological Association Publication 8*, p. 305-322.
- 1982, Fluvial sedimentation on a quivering craton; Salt Wash Member of the Morrison Formation (Upper Jurassic) in south-central Utah [abs.]: *Geological Society of America Abstracts with Programs*, v. 14, no. 4, p. 224.
- Perry, W. J., Jr., Ryder, R. T., and Maughan, E. K., 1981, The southern part of the southwest Montana thrust belt: A preliminary reevaluation of structure, thermal maturation, and petroleum potential, in Tucker, T. E., ed., *Field Conference and Symposium Guidebook to Southwest Montana: Montana Geological Society*, p. 261-273.
- Peterson, J. A., 1981, General stratigraphy and regional paleostructure of the western Montana Overthrust belt, in Tucker, T. E.,

- ed., Field Conference and Symposium Guidebook to Southwest Montana: Montana Geological Society, p. 5-35.
- 1982, A note on transients in the SRO and ASRO long-period data: U.S. Geol. Survey Open-File Report 82-702, 19 p.
- Peterson, J. R., and Hutt, C. R., 1981, Preliminary design study for a national digital seismograph network: U.S. Geol. Survey Open-File Report 81-1046, 55 p.
- Pike, R. J., 1981a, A size: rank model for basin rings [abs.]: Reports of Planetary Geology Program, National Aeronautics and Space Administration Technical Memorandum 84211, p. 123-125.
- 1981b, Target-dependence of crater depth on the Moon [abs.]: Lunar and Planetary Science XII, p. 845-847.
- Pike, R. J., and Clow, G. D., 1981, Revised classification of terrestrial volcanoes and catalog of topographic dimensions, with new results on edifice volume: U.S. Geol. Survey Open-File Report 81-1038, 40 p.
- Plummer, F. B., 1933, The geology of Texas, part 3, Cenozoic systems in Texas: Texas University Bulletin 3232, p. 519-818.
- Posner, Alex, and Zenone, Chester, 1982, Chemical quality of ground water in the Culpeper basin, Virginia and Maryland: U.S. Geol. Survey Miscellaneous Investigation Series Map I-1313-D, scale 1:125,000.
- Powell, R. E., 1981, Geology of the crystalline basement complex, eastern Transverse Ranges, southern California—constraints on regional tectonic interpretation: California Institute of Technology PhD thesis, 441 p.
- Prill, R. C., Oaksford, E. T., and Potorti, J. E., 1979, A facility designed to monitor the unsaturated zone during infiltration of tertiary-treated sewage, Long Island, New York: U.S. Geol. Survey Water-Resources Investigations Open-File Report 79-48, 14 p.
- Randolph, John, 1981, Energy: Virginia Polytechnic Inst., 325 p.
- Rathbun, R. E., 1979, Estimating the gas and dye quantities for modified tracer technique measurements of stream reaeration coefficients: U.S. Geol. Survey Water-Resources Investigations Open-File Report 79-27, 42 p.
- Reed, B. L., and Lanphere, M. A., 1973, The Alaska Aleutian Range batholith—Geochronology, chemistry, and relation to circum-Pacific plutonism: Geological Society of America Bulletin, v. 84, no. 8, p. 2583-2610.
- Reed, J. C., Jr., Bryant, Bruce, and Myers, W. B., 1970, The Brevard zone: a reinterpretation, in G. W. Fisher, F. J. Pettijohn, J. C. Reed, Jr., and K. N. Weaver, eds., Studies of Appalachian Geology: central and southern: New York, Wiley-Interscience, p. 261-269.
- Rehrig, W. A., 1981, Principal tectonic effects of the Mid-Tertiary orogeny in the Sonoran Desert province, in Howard, K. A., Carr, M. D., and Miller, D. M., eds., Tectonic framework of the Mojave and Sonoran Deserts, California and Arizona: U.S. Geol. Survey Open-File Report 81-503, p. 90-92.
- Robb, J. M., Hampson, J. C., Jr., and Kirby, J. R., 1982, Surficial geologic studies of the continental slope in the northern Baltimore Canyon Trough area—techniques and findings: 1982 Off-shore Technology Conference, Houston, Texas, Proceedings, v. 1, p. 39-59.
- Robbins, E. I., 1981, A preliminary account of the Newark rift system [abs.], in Papers Presented to the Lunar and Planetary Institute Conference on Processes of Planetary Rifting: St. Helena, Calif., Dec. 2-6, p. 180-182.
- Robertson, E. C., Fournier, R. O., Strong, C. P., 1976, Hydrothermal activity in southwestern Montana: Proceedings, Second United Nations Symposium on the Development and Use of Geothermal Resources, San Francisco, Calif., 1975, v. 1, p. 553-561.
- Rodder, Edwin, 1965, Liquid carbon dioxide inclusions in olivine-bearing nodules and phenocrysts from basalts: American Mineralogist, v. 50, p. 1756-1782.
- 1981, Carbon dioxide-, sulfide melt-, and silicate melt-inclusions in olivine nodules from Loihi Seamount, Hawaii [abs.]: EOS, Transactions of American Geophysical Union, v. 62, p. 1083.
- 1982, Possible Permian diurnal periodicity in NaCl precipitation, Palo Duro basin, Texas: The Univ. of Texas at Austin, Bureau of Economic Geology Circular 82-7, p. 101-104.
- Rosenfeld, Azriel, 1978, Extraction of topological information from digital images: Harvard Conference on Geographic Information Systems, 1978, v. 6, p. Rosenfeld/1 to Rosenfeld/14.
- Rosholt, J. N., 1980, Uranium-trend dating sediments: U.S. Geol. Survey Open-File Report 80-1087, 65 p.
- Roth, D. K., and Engelke, M. J., Jr., 1981, Hydrology of area 4, Eastern Coal Province, Pennsylvania, Ohio, and West Virginia: U.S. Geol. Survey Water-Resources Investigations Open-File Report 81-343, 62 p.
- Ryer, T. A., 1976, Cretaceous stratigraphy of the Coalville and Rockport areas, Utah: Utah Geology, v. 3, no. 2, p. 71-83.
- Ryer, T. A., Phillips, R. E., Bohor, B. F., and Pollastro, R. M., 1980, Use of altered volcanic ash falls in stratigraphic studies of coal-bearing sequences: an example from the Upper Cretaceous Ferron Sandstone Member of the Mancos Shale in central Utah: Geol. Society of America Bulletin, pt. 1, v. 91, p. 579-586.
- Rymer, M. J., Lisowski, M., and Burford, R. O., 1982, The case of the missing 12 mm/yr offset near Monarch Peak, central section of the San Andreas fault zone, and its tectonic implications [abs.]: Earthquake Notes, v. 54, p. 11.
- Sammel, E. A., 1981, Results of test drilling at Newberry Volcano, Oregon, and some implications for geothermal prospects in the Cascades: Geothermal Resources Council Bulletin, v. 10, no. 11, p. 3-8.
- Sandberg, C. A., 1980, Utility of conodonts in determining rates of synorogenic sedimentation and in timing Antler orogenic events, western United States [abs.], in 2d European Conodont Symposium; Guidebook, Abstracts: [Austria] Geol. Bundesanstalt Abhandlungen, v. 35, p. 209.
- Sandberg, C. A., and Dreesen, Roland, 1982, Phylogeny and ranges of late Devonian taxa of the conodont Family Icriodontidae: Geological Society of America Abstracts with Programs, v. 14, no. 5, p. 286.
- Saucier, A. E., 1974, Stratigraphy and uranium potential of the Burro Canyon Formation in the southern Chama Basin, New Mexico: New Mexico Geological Society Guidebook, 25th Field Conference, Ghost Ranch, p. 211-217.
- Saunders, W. B., 1973, Upper Mississippian ammonoids from Arkansas and Oklahoma: Geol. Society of America Special Paper 145, 110 p.
- Saunders, W. B., Mangere, W. L., and Gordon, Mackenzie, Jr., 1977, Upper Mississippian and Lower and Middle Pennsylvanian ammonoid biostratigraphy of northern Arkansas, in Sutherland, P. K., and Manger, W. L., eds., Upper Chesterian-Morrowan stratigraphy and the Mississippian-Pennsylvanian boundary in northeastern Oklahoma and northeastern Arkansas: Oklahoma Geol. Survey Guidebook No. 18, p. 117-137.
- Schaber, G. G., 1982, Venus: limited extension and volcanism along zones of lithospheric weakness: Geophysical Research Letters, v. 9, no. 5, p. 499-502.
- Schimschal, Ulrich, 1981a, The relationship of geophysical measurements to hydraulic conductivity at the Brantley damsite, New Mexico: Geoexploration, v. 19, p. 115-125.
- 1981b, Resistivity data analysis of a multi-layered medium by computer curve matching techniques: U.S. Bureau of Reclamation, Engineering and Research Center.
- 1981c, Flowmeter analysis at Raft River, Idaho: Ground Water, v. 19, no. 1, p. 93-97.

- 1981d, Logging hydraulic conductivity during injection testing in fractured dolomites: *The Log Analyst*, v. 22, no. 6, p. 7-12.
- 1981e, Mathematical model of gamma-ray spectrometry borehole logging for quantitative analysis: U.S. Geol. Survey Open-File Report 81-402, 23 p.
- Scott, D. H., and Tanaka, K. L., 1981, Mars: a large highland volcanic province revealed by Viking images: *Proceedings, Twelfth Lunar and Planetary Science Conference, Geochemica et Cosmochimica Acta*, v. 12, p. 1449-1458.
- Schumm, S. A., 1960, The shape of alluvial channels in relation to sediment type: U.S. Geol. Survey Professional Paper 352-B, p. 17-30.
- Scott, D. H., and Tanaka, K. L., 1982, Ignimbrites of Amazonis Planitia region of Mars: *Journal of Geophysical Research*, v. 87, p. 1179-1190.
- Scott, J. H., Seeley, R. L., and Barth, J. J., 1981, A magnetic susceptibility well-logging system for mineral exploration: *Transactions, SPWLA 22d Annual Logging Symposium*, June 23-26, Mexico City, Mexico p. CC1-CC21.
- Seiders, V. M., 1965, Volcanic origin of flint clay in the Fire Clay coal bed, Breathitt Formation, eastern Kentucky, in *Geological Survey Research 1965*: U.S. Geol. Survey Professional Paper 525-D, p. D52-D54.
- Selli, R., 1970, Report on the absolute age, Committee Mediterranean Neogene Stratigraphy, *Proceedings, IV Session, Bologna, 1967: Giornale di Geologia (2)*, XXXV, p. 51-59.
- Selli, R., Accorsi, C. A., Bandini, M. M., Bertolini, M. D., Bigazzi, G., Bonadonna, F. P., Borsetti, A. M., Cati, F., Cololongo, M. L., D'Onofrio, S., Landini, W., Menesini, E., Mezzetti, R., Pasini, G., Savelli, C., and Tampieri, R., 1977, The Vrica Section (Calabria, Italy), A potential Neogene/Quaternary boundary stratotype: *Giornale di Geologia (2)*, XLII, p. 181-204.
- Shasby, M. B., Burgan, R. R., and Johnson, G. R., 1981, Broad area forest fuels and topography mapping using digital Landsat and terrain data: 7th International Symposium on Machine Processing of Remotely Sensed Data, Purdue University, West Lafayette, Ind., June 23-26, 1981, p. 529-538.
- Sheehan, C. A., and Gehring, D. G., 1980, Generation of stereo high-resolution false-color composites using Landsat, topographic, and aeromagnetic data, in *Abstracts with Programs: Pecora Symposium, 6th*, Sioux Falls, S. Dak., 1980: Society of Exploration Geophysicists, p. 83-85.
- Shoemaker, E. M., Lucchitta, B. K., Plescia, J. B., Squyres, S. W., and Wilhelms, D. E., 1982, The geology of Ganymede, in Morrison, David, ed., *The satellites of Jupiter*: University of Arizona Press, chapter 13, p. 435-520.
- Shoemaker, E. M., and Wolfe, R. F., 1982, Cratering time scales for the Galilean satellites, in Morrison, David, ed., *The satellites of Jupiter*: University of Arizona Press, chapter 10, p. 277-339.
- Shackelton, N. J., and Opdyke, N. D., 1973, Oxygen-isotope temperatures and paleomagnetic stratigraphy of equatorial Pacific core V28-238—Ice volumes on a 100,000- and 1,000,000-year scale: *Quaternary Research*, v. 3, p. 39-55.
- Silberling, J. J., Wardlaw, B. R., and Berg, H. C., New paleontologic age determinations from the Taku terrane, Ketchikan area, southeastern Alaska, in *Alaska—Accomplishments during 1980*: U.S. Geol. Survey Circular 844, p. 117-119.
- Smith, B. A., Soderblom, L. A., Batson, R. M., Bridges, Patricia, Inge, Jay, Masursky, Harold, Shoemaker, E. M., Beebe, Reta, Boyce, J. M., Briggs, Geoffrey, Bunder, Anne, Collins, S. A., Hansen, C. J., Johnson, T. V., Mitchell, J. L., Terrile, R. J., Cooke, A. F., II, Cuzzi, Jeffrey, Pollack, J. B., Danielson, G. E., Ingersoll, A. P., Davies, M. E., Hunt, G. E., Morrison, David, Owen, Tobias, Sagan, Carl, Veverka, Joseph, Strom, Robert, and Suomi, V. E., 1982, A new look at the Saturn system: *The Voyager 2 images: Science*, v. 215, p. 504-537.
- Smith, E. T., and Moody D. W., 1980, Alternative future studies: presented at the American Water Resources Association annual conference, Minneapolis, Minnesota, Oct. 12-14, 1980.
- Smith, R. L., 1979, Ash-flow magmatism: Geological Society of America Special Paper 180, p. 5-27.
- Snook, J. R., Lucas, H. E., and Abrams, M. J., 1981, A cross section of Nevada-style thrust in northeast Washington: *Reports of Investigation—Washington, Division of Geology and Earth Resources*, no. 25, 8 p.
- Snyder, J. P., 1981, Map projections for satellite tracking: *Photogrammetric Engineering and Remote Sensing*, v. 47, no. 2, p. 205-213.
- 1982, Map projections used by the U.S. Geol. Survey: U.S. Geological Survey Bulletin 1532, 313 p.
- Soderblom, L. A., and Johnson, T. V., 1982, The moons of Saturn: *Scientific American*, v. 246, no. 1, p. 101-116.
- Speed, R. C., 1977a, Island-arc and other paleogeographic terranes of late Paleozoic age in the western Great Basin, in Stewart, J. H., Stevens, C. H., and Fritsche, A. E., eds., *Paleozoic paleogeography of the Western United States: Society of Economic Paleontologists and Mineralogists, Pacific Section, Pacific Coast Paleogeography Symposium 1*, p. 349-362.
- 1977b, Excelsior Formation, western-central Nevada stratigraphic appraisal, new divisions, and paleogeographic interpretations: *Society of Economic Paleontologists and Mineralogists, Pacific Coast Paleogeographic Symposium 1*, p. 328-332.
- Spence, W. J., and Langer, C. J., 1982, Was a barrier involved with the twin 1974 Peru earthquake?: *Seismological Society of America, Eastern Section, Earthquake Notes, Abs.*, v. 53, no. 1, p. 42.
- Spencer, J. E., 1982, Origin of folds of Tertiary low-angle fault surfaces, southeastern California and western Arizona, in Frost, E. G., and Martin, D. L., eds., *Mesozoic-Cenozoic tectonic evolution of the Colorado River region, California, Arizona, and Nevada*: San Diego, Cordilleran Publishers, p. 123-134.
- Spicer, H. C., 1954, A compilation of deep Earth temperature data: USA 1910-1945: U.S. Geol. Survey Open-File Report 64-147. Unpagged.
- Stacey, J. S., Doe, B. R., Roberts, R. J., Delevaux, M. H., and Gramlich, J. W., 1980, A lead isotope study of mineralization in the Saudi Arabian Shield: *Contributions to Mineralogy and Petrology*, v. 74, p. 175-188.
- Steger, C. W., 1981a, Introduction to long-range planning: Virginia Polytechnic Inst., 9 p.
- 1981b, Summary report on long-range planning: Virginia Polytechnic Inst., 27 p.
- Stephens, D. W., and Jennings, M. E., 1976, Determination of primary productivity and community metabolism in streams and lakes using diel oxygen measurements: *Water Resources Division computer contribution*, U.S. Geol. Survey, 100 p.
- Stern, T. W., Bateman, P. C., Morgan, B. A., Newell, M. F., and Peck, D. L., 1981, Isotopic U-Pb ages of zircon from the granitoids of the central Sierra Nevada: U.S. Geol. Survey Professional Paper 1185, 17 p.
- Steven, T. A., Lipman, P. W., Fisher, F. S., Bieniewski, C. L., and Meeves, H. C., 1977, Mineral resources of study areas contiguous to the Uncompahgre Primitive Area, San Juan Mountains, southwestern Colorado: U.S. Geol. Survey Bulletin 1391-E, p. E1-E126.
- Stone, B. D., and Force, E. R., 1980, The Port Leyden, New York, heavy mineral deposit: *New York State Museum Bulletin 436*, p. 57-64.
- Straut, R. C., 1981, Strategic planning in federal agencies: Virginia Polytechnic Inst., 59 p.

- Stuckless, J. S., and Nkomo, I. T., 1978, Uranium-lead isotope systematics in uraniumiferous alkali-rich granites from the Granite Mountains, Wyoming: implications for uranium source rocks: *Economic Geology*, v. 73, p. 427-441.
- Stuckless, J. S., Troeng, B., Hedge, C. E., Nkomo, I. T., and Simmons, K. R., 1981, Age of uranium mineralization at Lilljuthatten, Sweden, and constraints on ore genesis: *Geological Survey of Sweden bulletin*, C. 789, 45 p.
- Stuckless, J. S., and Vantrump, G., Jr., 1982a, An evaluation of the uranium content of zircons from igneous rocks of the contiguous United States as an aid to exploration and resource assessment: IAEA/NEA conference on uranium R and D, 22 p.
- 1982b, A compilation of radioelement concentrations in granitic rocks of the contiguous United States: IAEA/NEA conference on uranium R and D, 27 p.
- Sturdevant, J. A., 1981a, Assessing accuracy of digital land use and terrain data, in *American Society of Photogrammetry Technical Meeting*, San Francisco, Calif., 1981, Proceedings: Falls Church, Va., American Society of Photogrammetry, p. 101-112.
- 1981b, The development and application of a county-level geographic data base, in *Pecora Symposium, 7th*, Sioux Falls, S. Dak., 1981, Proceedings: Falls Church, Va., American Society of Photogrammetry, p. 383-392.
- Swann, D. H., 1963, Classification of Genevievian and Chesterian (Late Mississippian) rocks of Illinois: *Illinois Geol. Survey Report of Inv.* 216.
- Tarr, A. C., and Rhea, B. S., 1981, Seismicity near Charleston, South Carolina, in *Studies related to Charleston, South Carolina, Earthquake of 1886—Tectonics and seismicity* (collected abstracts): U.S. Geol. Survey Open-File Report 82-134, p. 32-33.
- Thatcher, Wayne, and Pfalker, George, 1977, The 1899 Yakutat Bay, Alaska, earthquakes: IASEPI/IAVECI Assembly, Durham, Abstract with Programmes, p. 54.
- Thayer, P. A., 1970, Stratigraphy and geology of Dan River Triassic Basin, North Carolina: *Southeastern Geology*, v. 12, p. 1-31.
- Thompson, A. B., 1976, Mineral reactions in pelitic rocks: I. Prediction of P-T-X (Fe-Mg) phase relations: *American Journal of Science* 276, p. 401-424.
- Tibbitts, G. C., Jr., and Aubel, James, 1980, Ground-water resources investigation in the Amran Valley, Yemen Arab Republic: U.S. Geol. Survey Open-File Report 80-774, Reston, Virginia, 138 p., 17 figs., 1 pl., 7 tables.
- Treuil, M., and Varet, J., 1973, Criteres volcanologiques petrologiques et geochemiques de la genese et de la differenciation des magmas basaltiques; exemple de l'Afar: *Bulletin de la Societe Geologique de France*, v. 15, no. 5-6, p. 506-540.
- Trexler, D. W., 1966, Stratigraphy and structure of the Coalville area, Utah: *Colorado School of Mines, Professional Contribution*, no. 2, 69 p.
- Triplehorn, D. M., and Bohor, B. F., 1981, Altered volcanic ash partings in the coal bed, Ferron Sandstone Member of the Mancos Shale, Emery County, Utah: U.S. Geol. Survey Open-File Report 81-775, 43 p.
- Tripp, R. B., Detra, D. E., and Nishi, J. M., 1982, Mineralized zones in bedrock near Miller Creek, Circle quadrangle, in *The United States Geological Survey in Alaska: Accomplishments during 1980*: U.S. Geol. Survey Circular 844, p. 62.
- Tweto, Ogden, 1982, Las Animas Formation (upper Precambrian) in the subsurface of southeastern Colorado: *U.S. Geol. Survey Bulletin* 1529-G.
- Urban, T. C., and Diment, W. H., 1980, Thermal convection in cased, water-filled drill holes: observations over a wide range in conditions: *EOS, American Geophysical Union Transactions*, v. 61, p. 1130.
- U.S. Geological Survey, 1980, U.S. Geological Survey research, 1980: U.S. Geological Survey Professional Paper 1175, p. 156.
- 1981, U.S. Geological Survey research, 1981: U.S. Geological Survey Professional Paper 1275, p. 126.
- Vail, P. R., Mitchum, R. M., Jr., and Thompson, S., III, 1977, Seismic stratigraphy and global changes of sea level: *American Association of Petroleum Geologists Memoir* 26, p. 83-97.
- Vance, J. A., 1982, Cenozoic stratigraphy and tectonics of the Washington Cascades: *Geological Society of America Abstracts with Programs*, v. 14, no. 4, p. 241.
- Van Zee, C. J., and Bonner, K. G., 1981, Estimating rangeland cover proportions with large-scale color-infrared aerial photographs, in *Eighth Biennial Workshop on Color Aerial Photography in the Plant Sciences*, Luray, Va., 1981, Proceedings: Falls Church, Va., American Society of Photogrammetry, p. 73-82.
- Villemont, Benoit, Jaffrezic, Henri, Joron, Jean-Louis, and Treuil, Michels, 1982, Distribution coefficients of major and trace elements: fractional crystallization in the alkali basalt series of Chaine des Prys (Massif Central France): *Geochimica et Cosmochimica Acta*, v. 45, p. 1997-2016.
- Vitrac, A. M., Albarede, F., and Allegre, C. J., 1981, Lead isotopic composition of Hercynian granitic K-feldspars constrains continental genesis: *Nature*, v. 291, p. 460-464.
- Wadsworth, W. B., 1968, The Cornelia pluton, Ajo, Arizona: *Economic Geology*, v. 63, no. 2, p. 101-115.
- Warner, J. L., Ashwal, L. D., Bergman, S. C., Gibson, E. K., Jr., Henry, D. J., Lee-Berman, Richard, Roedder, Edwin, and Belkin, H. E., 1982, Fluid inclusions in stony meteorites: Lunar and Planetary Science Conference, Proceedings 13th Journal of Geophysical Research, v. 88, Supplement, p. A731-A735.
- Watson, Kenneth, Hummer-Miller, Susanne, and Offield, T. W., 1981, Geologic applications of thermal-inertia mapping from satellite, USGS Open-File Report 81-1352, 72 p.
- Watts, R. D., 1982, Interpretation of Schlumberger dc resistivity data from Gibson Dome-Lockhart Basin Study Area, San Juan County, Utah: U.S. Geol. Survey Open-File Report 82-704.
- Weaver, C. E., 1912, A preliminary report on the Tertiary paleontology of western Washington: *Washington Geological Survey, Bulletin* no. 15.
- Weber, F. R., 1982, Two new tephra localities in the Yukon-Tanana Upland, in *Coonrad, W. L., ed., The U.S. Geological Survey in Alaska—Accomplishments during 1980*: U.S. Geol. Survey Circular 844, p. 61-62.
- Weigle, J. M., 1972, Exploration and mapping of Salisbury Paleochannel, Wicomico County, Maryland: *Maryland Geol. Survey, Bulletin* 31, part 2, p. 61-123.
- Whitaker, E. A., 1981, The lunar Procellarum basin: Multi-ring basins, *Geochimica et Cosmochimica Acta, Supplement* 15, p. 105-111.
- Whitehall, D. E., 1973, Automated interpretation of magnetic anomalies using the vertical prism model: *Geophysics*, v. 38, p. 1070-1087.
- Wieczorek, G. F., 1982, Map showing recently active and dormant landslides near La Honda, central Santa Cruz Mountains, California: U.S. Geol. Survey Miscellaneous Field Studies Map MF-1422, scale 1:4,800.
- Wijmstra, T. A., 1978, Palaeobotany and climatic change, in *Gribbin, John, ed., climatic change*: Cambridge, Cambridge University Press, p. 25-45.
- Wilkinson, K. P., Thompson, J. G., Reynolds, R. R., Jr., and Ostresh, L. M., Jr., 1980, Social disruption and rapid community growth: An examination of the "boomtown" hypothesis: *Rural Sociological Society meetings*, Ithaca, New York, August.
- Williams, H., 1942, *Geology of Crater Lake National Park, Oregon*: Carnegie Institute of Washington Publication No. 540, 162 p.
- Williams, Harold, 1978, Tectonic and lithofacies map of the Appala-

- chian orogen: Memorial University of Newfoundland, map no. 1.
- Williams, R. S., Jr., and Ferrigno, J. G., 1981, Satellite image atlas of the Earth's glaciers, in Deutsch, Morris, and others, eds., *Satellite Hydrology: Annual William T. Pecora Memorial Symposium on Remote Sensing*, 5th, Sioux Falls, S. Dak., 1979, Proceedings: Minneapolis, Minn., American Water Resources Association, p. 173-182.
- Williams, R. S., Jr., Ferrigno, J. G., Kent, T. M., and Schoonmaker, J. W., Jr., 1981, Landsat images, maps, and mosaics of Antarctica for glaciological studies, in *Abstracts of Papers: Third International Symposium on Antarctic Glaciology*, Ohio State University, Columbus, September 7-12, 1981, 4 p.
- Woillard, Genevieve, 1978, Grande Pile peat bog: A continuous pollen record for the last 140,000 years: *Quaternary Research*, v. 9, p. 1-21.
- Woods, P. F., 1981, Physical limnological factors suppressing primary productivity in Lake Koochanusa, Montana, in Stefan, H. G., ed., *Proceedings of the Symposium on Surface Water Impoundments: American Society of Civil Engineers*, v. II, p. 1368-1377.
- Yeend, Warren, 1981, Placer gold deposits, Mount Hayes quadrangle, Alaska, in Albert, N. R. D., and Hudson, Travis, eds., *The United States Geological Survey in Alaska—Accomplishments during 1979: U.S. Geol. Survey Circular 823-B*, p. B68.
- Young, R. A., and Brennan, W. J., 1974, Peach Springs Tuff; its bearing on structural evolution of the Colorado Plateau and development of Cenozoic drainage in Mohave County, Arizona: *Geological Society of America Bulletin*, v. 85, p. 83-90.
- Zapp, A. D., and Cobban, W. A., 1960, Some late Cretaceous strand lines in northwestern Colorado, and northeastern Utah, in *Short papers in the geologic sciences, U.S. Geol. Survey Professional Paper 400-B*, p. B245-B249.
- Zuehls, E. E., Ryan, G. L., Peart, D. B., and Fitzgerald, K. K., 1981a, Hydrology of area 35, eastern region, Interior Coal Province, Illinois and Kentucky: U.S. Geol. Survey Water-Resources Investigations Open-File Report 81-403, 68 p.
- 1981b, Hydrology of area 25, eastern region, Interior Coal Province, Illinois: U.S. Geol. Survey Water-Resources Investigations Open-file Report 81-636, 66 p.

INVESTIGATIONS IN PROGRESS IN THE GEOLOGICAL SURVEY

Investigations in progress during fiscal year 1981 are listed below together with the names and headquarters of the individuals in charge of each. Headquarters at main centers are indicated by NC for the National Center in Reston, Va., D for Denver, Colo., and M for Menlo Park, Calif. The lowercase letter after the name of the project leader shows the Division technical responsibility: c, Conservation Division; o, Office of Earth Sciences Applications; w, Water Resources Division; cc, Computer Center; n, National Mapping Division; no letter, Geologic Division.

The projects are classified by principal topic. Most geologic-mapping projects involve special studies of stratigraphy, petrology, geologic structure, or mineral deposits but are listed only under "Geologic mapping" unless a special topic or commodity is the primary justification for the project. A reader interested in investigations of volcanology, for example, should look under the heading "Geologic Mapping" for projects in areas of volcanic rocks, as well as under the heading "Volcanology." Likewise, most water-resource investigations involve special studies of several aspects of hydrology and geology but are listed only under "Water Resources" unless a special topic—such as floods or sedimentation—is the primary justification for the project.

Areal geologic mapping is subdivided into mapping at scales smaller than 1:62,500 (for example, 1:250,000) and mapping at scales of 1:62,500 or larger (for example, 1:24,000).

ADP systems:

Distributed information systems (S. M. Longwill, w, NC)

Minicomputers (S. M. Longwill, w, NC)

Northwest Water Resources Data Center (C. W. Alexander, w, Portland, Oreg.)

States:

Kansas (w, Lawrence):

Automatic data recorder applications development (J. M. McNellis)

Louisiana (w, Baton Rouge):

Special reports (M. J. Forbes)

New Jersey (w, Trenton):

Peaks above base, Delaware River basin (A. A. Vickers)

New Mexico (w, Albuquerque):

New Mexico data bank (E. V. Thomas)

New York (w, Albany):

Analysis of hydrologic data, Long Island (G. W. Hawkins, Syosset)

Vermont (w, Montpelier):

Automatic processing of hydrologic data (R. E. Hammond, Concord, N.H.)

Aluminum:

Resources of the United States (S. H. Patterson, NC)

Analytical chemistry:

Plant laboratory (T. F. Harms, D)

Radioactivation and radiochemistry (H. J. Rose; NC, D. M. McKown, D)

Rock chemical analysis (F. W. Brown, NC; L. L. Jackson, D; W. S. Updegrave, M)

Spectroscopy:

Emission (R. E. Mays, M)

Optical (D. W. Golightly, NC; F. E. Liche, D)

X-ray (H. J. Rose, NC; J. E. Taggart, D)

Aquifer characteristics:

Alabama (w, Tuscaloosa):

Hydrology of aquifers, Ft. Rucker (J. C. Scott, Montgomery)

Alaska (w, Anchorage):

Eagle River valley ground water (L. L. Dearborn)

Mendenhall hydrology (G. O. Balding, Juneau)

Aquifer characteristics—Continued

Arizona (w, Tucson):

Ground water, southern Apache County (L. J. Mann)

California (w, Menlo Park):

Ground water, U.S. Marine Corps, Twentynine Palms (J. H. Koehler, Laguna Niguel)

Colorado (w, Lakewood):

Aquifer testing (F. A. Welder, D)

Ground-water studies in coal areas (R. S. Williams, D)

Intensive monitoring in northwest Colorado (R. S. Parker, D)

USBM prototype mine (J. B. Weeks, D)

Connecticut (w, Hartford):

Water resources of Farmington Basin (E. H. Handnan)

Florida (w, Tallahassee):

Appraisal of shallow aquifers (John Fish, Miami)

Aquifer characteristics in southwestern Florida (R. M. Wolansky, Tampa)

Floridan aquifer: Withlacoochee (Warren Anderson, Orlando)

Shallow aquifer, Brevard County (J. M. Frazee, Winter Park)

Technical support Southwest Florida Water Management District (T. H. Thompson, Tampa)

Well fields, west-central Florida (D. M. Johnson, Tampa)

Kansas (w, Lawrence):

Aquifer test evaluation (T. B. Reed)

Chemical quality, deep aquifers (Jack Kume, Garden City)

Geohydrology of Wellington, Salina area (Joe Gillespie)

Wellington aquifer parameters (J. B. Gillespie)

Maryland (w, Towson):

Maryland aquifer studies III (F. K. Mack)

Missouri (w, Rolla):

Specific capacity, Missouri (W. S. Oakes)

New Mexico (w, Albuquerque):

Radioactive by-products in salt (J. W. Mercer)

New York (w, Albany):

Selected aquifers, western New York (R. B. Moore, Ithaca)

Ohio (w, Columbus):

Piketon investigation (S. E. Norris)

Subsurface mines as source of water (J. O. Helgesen)

Aquifer characteristics—Continued

- Oregon (w, Portland):
Underground injection, east Oregon (J. B. Gonthier)
- Puerto Rico (w, San Juan):
Water resources, Rio Cibuco area (A. E. Torres-Gonzalez, Ft. Buchanan)
- Utah (w, Salt Lake City):
Ground water in Jordan Valley (K. M. Waddell)
Northern Utah valley ground water (David Clark)
- Washington (w, Tacoma):
Muckleshoot ground water (W. E. Lum)
- West Virginia (w, Charleston):
Hydrology of stress-relief fracturing (J. W. Borchers)

Arctic geology:

- Engineering studies (Reuben Kachadoorian, M)
Environmental studies (O. J. Ferrians, Jr., Anchorage)

Artificial recharge:

- Borehole geophysics (W. S. Keys, w, D)
East Triassic waste-disposal study (G. L. Bain, w, Raleigh, N.C.)
- States:*
- Arizona (w, Tucson):
Salt-Gila recharge (L. J. Mann, Phoenix)
- California (w, Menlo Park):
Artificial recharge, San Joaquin County (H. T. Mitten, Sacramento)
Artificial recharge, southern California (J. H. Koehler, Laguna Niguel)
Confined aquifer, San Bernardino (W. F. Hardt, Laguna Niguel)
Palo Alto wastewater recharge (S. N. Hamlin)
- Colorado (w, Lakewood):
Artificial recharge (G. J. Leonard, Pueblo)
- Florida (w, Tallahassee):
Freshwater storage, saline aquifers (M. L. Merritt, Miami)
Lee County freshwater injection (D. J. Fitzpatrick, Fort Myers)
Subsurface waste injection, Florida (John Vecchioli)
Waste injection, St. Petersburg (J. J. Hickey, Tampa)
- Minnesota (w, St. Paul):
Aquifer thermal-energy storage (R. T. Miller)
- New York (w, Albany):
Nassau County recharge (E. J. Koszalka, Syosset)
Recharge of tertiary-treated sewage (T. M. Robison, w, Syosset)
Recharge of treated sewage (John Vecchioli, Mineola)
Saline hydrology (R. M. Waller, Ithaca)
Supplemental recharge by storm basins (D. A. Aronson, Syosset)
- Puerto Rico (w, San Juan):
Fort Allen recharge (J. R. Diaz, Ft. Buchanan)
- Washington (w, Tacoma):
Columbia River basalt recharge (M. R. Karlinger)

Atmospheric:

- Connecticut (w, Hartford):
Atmospheric deposition chemistry (K. P. Kulp)
- New York (w, Albany):
Snow survey (R. V. Allen)
- North Carolina (w, Raleigh):
Atmospheric deposition (H. B. Wilder)
- Oregon (w, Portland):
Mount St. Helens (S. W. McKenzie)
- Pennsylvania (w, Harrisburg):
Chemistry of precipitation (T. G. Ross, Malvern)

Atmospheric—Continued

- Utah (w, Salt Lake City):
Atmospheric fallout (D. W. Stephens)
- Washington (w, Tacoma):
Real-time data dissemination (R. R. Adsit)

Base metals. See base-metal names.**Basin characteristics:**

- Rehabilitation potential, energy lands (Lynn M Shown, w, D)
- States:*
- Idaho (w, Boise):
Special studies (H. W. Young)
- Illinois (w, Urbana):
T and K Studies on Illinois streams (J. B. Graf)
- Kansas (w, Lawrence):
Flood hydrology and hydraulics (R. W. Clement)
- Mississippi (w, Jackson):
Drainage areas, Mississippi streams (J. W. Hudson)
- New Jersey (w, Trenton):
Drainage areas of streams (A. J. Velnich)
Low-flow regionalization (B. D. Gillespie)
- New York (w, Albany):
Low-flow study (A. D. Randall)
Stream gazetteer (L. A. Wagner)
- North Carolina (w, Raleigh):
Data site information for 208 study (C. E. Simmons)
- Washington (w, Tacoma):
Newaukum Basin study (E. A. Prych)
- Wisconsin (w, Madison):
Drainage areas (E. W. Henrich)

Biologic, macroscopic:

- Limnology: stream ecosystems (K. V. Slack, w, M)
Toxic substances: aquatic ecosystems (H. V. Leland, w, M)
- States:*
- Colorado (w, Lakewood):
Aquatic biology of Piceance Creek (K. J. Covay, Meeker)
- Idaho (w, Boise):
Effects of ash (S. A. Frenzel)
- Indiana (w, Indianapolis):
Surface-water-quality study (M. A. Hardy)
- Pennsylvania (w, Harrisburg):
Biological monitoring, Chester County (C. R. Moore, Malvern)
- Wisconsin (w, Madison):
Nederlo Creek biota (P. A. Kammerer)
- Wyoming (w, Cheyenne):
Stream habitats, Wyoming (D. A. Peterson)

Biologic, microscopic:

- Atlanta Central Lab—biological analyses (R. G. Lipscomb, w)
Denver Central Lab—biological analyses (R. R. Grabbe, w, D)
Microbial biogeochemistry (R. S. Oremland, w, M)
Organic chemicals in subsurface (G. G. Ehrlich, w, M)

States:

- Alaska (w, Anchorage):
Arctic lakes (G. A. McCoy)
- Florida (w, Tallahassee):
Aquifer pollution, Lake County (G. F. Taylor, Orlando)
- Montana (w, Helena):
Lake Kocanusa productivity (P. F. Woods)
- Washington (w, Tacoma):
Rainier quality of water (G. L. Turney)

Channel morphology:

- Arctic fluvial processes, landforms (K. M. Scott, w, Laguna Niguel, Calif.)
Channel morphology (G. P. Williams, w, D)
Platte River hydrology (R. F. Hadley, w, D)

Channel morphology—Continued*States:***Alaska (w, Anchorage):**

- Arctic resources, Alaska (J. M. Childers)
- Kenai morphology (K. M. Scott)

California (w, Menlo Park):

- Channel changes, Sacramento River (J. C. Blodgett, Sacramento)

Colorado (w, Lakewood):

- Mannings "n" value study (R. D. Jarrett, D)

Kansas (w, Lawrence):

- Channel geometry, Kansas River (W. R. Osterkamp)
- Channel geometry, regulated streams (W. R. Osterkamp)
- Sediment-active channel geometry (W. R. Osterkamp)

Montana (w, Helena):

- Channel geometry studies (R. J. Omang)

Nevada (w, Carson City):

- Lake Mead recreational area flood hazards (Otto Moosburner)

Tennessee (w, Nashville):

- Tennessee bridge scour (W. J. Randolph)

Wisconsin (w, Madison):

- Flood control effects on Trout Creek (D. A. Wentz)
- Pheasant branch study (W. R. Krug)

Wyoming (w, Cheyenne):

- Green River basin water supply (H. W. Lowham)

Chromite. See Ferro-alloy metals.**Clays (NC):**

- Bentonite studies (J. W. Hosterman)
- Kaolin investigations (S. H. Patterson)

Climatic changes:

- California, Quaternary (D. P. Adam, M)
- Lakes, Holocene (W. E. Dean, D)
- Marine/nonmarine climates, Atlantic coast (T. M. Cronin, NC)
- Pluvial history, southwestern Great Basin (G. I. Smith, M)
- Rocky Mountain area, Quaternary deposits (K. L. Pierce, D)

Coal:

- Appalachia, Safe mine waste disposal (W. E. Davies, NC)
- Application of engineering principles to coal resource assessments (T. O. Friz, NC)
- Coal bed correlation and dating (B. F. Bohor, D)
- Coal contaminants, geology of (C. B. Cecil, NC)
- Coal petrochemistry and related investigations (E. C. T. Chao, NC)
- Coal resource assessment (G. H. Woods, Jr., NC)
- Experimental diagenesis of organic matter (C. B. Cecil, NC)
- Genesis of low-sulfur coal (Z. S. Altschuler, NC)
- Geophysical applications (W. P. Hasbrouck, D)
- Natural combustion and metamorphism of overlying rocks (J. R. Herring, D)
- Nuclear and electrical methods for coal evaluation (J. J. Daniels, D)
- Petrologic studies of coal-bearing clastic rocks (N. L. Hickling, NC)
- Petrology of North American coals (R. W. Stanton, NC)
- Stratigraphic analysis and modeling of Cretaceous coal-bearing formations (V. L. Freeman, D)
- Sulfur in coal and lignite (A. J. Bodenlos, NC)
- United States, National Coal Resources Data System (M. D. Carter, NC)

*States:***Alabama, Coal geology, Haleyville area (S. P. Schweinfurth, NC)****Alaska:**

- Coal resources (G. D. Stricker, D)

Coal—Continued**Nenana (Clyde Wahrhaftig, M)**

- Regional engineering geology of Cook Inlet coal lands (H. R. Schmoll and L. A. Yehle, D)

Colorado (D):

- Central Colorado coal fields (V. L. Freeman)
- Coal geology of the Walden area (R. F. Modale)
- Douglas Creek Arch area (B. E. Barnum)
- Rawlins coal field, Wyoming-COLORADO (C. S. V. Barclay)
- SE Uinta coal region (D. L. Gaskill)
- Smizer Gulch and Rough Gulch quadrangles (W. J. Hail)
- Trinidad coal field (D. A. Jobin)
- Yampa coal field (E. A. Johnson)

Kentucky (NC):

- Hazard quadrangle (C. L. Rice)
- Western Kentucky coal field (T. M. Keln)

Montana (D, except as otherwise noted):

- Birney quadrangle (W. C. Culbertson)
- Blackfeet Indian Reservation (W. J. Mapel)
- Broadus quadrangle (Marguerite McLellan)
- Bull Mountain coal field (C. W. Connor)
- Canoncito Indian Reservation (A. B. Olson, NC)
- Coal geology of the Forsyth area (Kim Manley)
- Coal resources, Fort Peck Indian Reservation (H. H. Arndt)
- Coal resources, Northern Powder River basin (W. W. Olive, NC)

Crow Indian Reservation (L. N. Robinson)

- Culbertson quadrangle (H. H. Arndt)
- Hardin quadrangle (L. N. Robinson)
- Tertiary basins (G. B. Schneider)

New Mexico (D, except as otherwise noted):

- Coal geology, Grants 1-degree quadrangle (D. A. Jobin)
- Coal geology, southern San Juan River coal region (J. W. Mytton)
- Coal resources, Alamo Indian Reservation (E. R. Landis); Jicarillo Indian Reservation (A. B. Olson, NC); Ramah and Navajo Indian Reservations (W. J. Mapel); Zuni Indian Reservation (G. D. Stricker)
- Western Raton field (C. L. Pillmore)

North Dakota (D):

- Coal geology, Bowman area (A. B. Gibbons)

Ohio, Coal geology, Ripley 1-degree quadrangle (P. C. Lyons, NC)**Regional studies:**

- Chemical analysis and geologic evaluation of coal in the Eastern United States (J. H. Medlin, NC); Western United States (F. O. Simon, NC)
- Coal geology, Central Fort Union region (J. S. Hinds)
- Coal geology and paleoenvironment of Mississippian and Upper Pennsylvanian Series, Central Appalachians (W. R. Sigelo, NC)
- Environments of coal deposition in Western Interior coal basins (R. M. Flores, D)
- Geology and coal resources, southern Appalachian Basin (K. J. Englund, NC)
- Geotechnical research in western energy lands (F. W. Osterwald, D)
- Gulf Coast lignites (C. R. Meissner, NC)
- Pennsylvanian System stratotype section (K. J. Englund, NC)
- Regional geotechnical studies, Powder River Basin (S. P. Kanizay, D)

Utah (D):

- Book Cliffs coal field (J. L. Gualtieri)
- Coal geology, Hams Fork region (J. W. M'Gonigle)

Coal—Continued

Coal geology, Kaiparowitz Plateau, Utah (H. D. Zeller)
 Coal geology, Salina area (F. R. Shawe)
 Engineering geologic studies, east-central Utah (E. E. McGregor)

Virginia and West Virginia, Central Appalachian Basin (K. J. Englund, NC)

West Virginia (NC):

Coal geology, central West Virginia (J. M. Back)
 Coal geology, Ripley 1-degree quadrangle (R. C. Lyons)
 Regional coal resources of northern West Virginia (J. O. Maberry)

Wyoming (D) except as otherwise noted:

Alluvial valley floor features and reclamation (H. E. Malde)
 Coal geology, Burgess Junction (J. L. Brown)
 Coal geology, Firehole Canyon (M. A. Kirshbaum)
 Coal geology, Hams Fork region (J. W. M'Gonigle)
 Coal geology, Hanna and Rock Creek coal fields (D. E. Hansen)

Coal geology, Red Desert basin (R. H. Affalter)
 Coal geology, Rock Springs uplift (H. W. Roehler)
 Coal geology, Wind River Indian Reservation (J. F. Windolph, Jr., NC)

Coal mine deformation studies, Powder River Basin (C. R. Dunrud)

Engineering geologic mapping, Sheridan-Buffalo area (E. N. Hinrichs)

Engineering geologic studies, Kemmerer 1:100,000 sheet (D. D. Dickey)

Rawlins-Little Snake River coal fields, Wyoming-Colorado (C. V. S. Barclay)

Sheridan 1-degree quadrangle (C. L. Molnia)

Stratigraphic framework of coal beds of the Powder River Basin (B. H. Kent)

Weston SW quadrangle (R. A. Katock, c. Casper)

Construction and terrain problems:

Electronics instrumentation research for engineering geology (J. B. Bennetti, D)

Fissuring-subsidence research (T. L. Holzer, M)

Geophysical studies for engineering geology (C. H. Miller, D)

Geotechnical measurements and services (R. W. Nichols, D)

Geotechnical research in western energy lands (F. W. Osterwald, D)

Ground failure hazards (W. H. Hays, D)

Reactor site investigations (M. H. Hait, Jr., D)

Regional geotechnical studies, Powder River Basin (S. P. Kanizay, D)

Rock deformation in New England (F. T. Lee, D)

Safe mine waste disposal, Appalachia (W. E. Davies, NC)

Solution subsidence and collapse (J. R. Ege, D)

Tephra hazards from Cascade Range volcanoes (D. R. Mullineaux, D)

Volcanic hazards (D. R. Crandell, D)

States:

Alaska:

Northern engineering geology (O. J. Ferrians, Jr., M)

Regional engineering geology of Cook Inlet coal lands (H. R. Schmoll and L. A. Yehle, D)

California:

Geology and slope stability, western Santa Monica Mountains (R. H. Campbell, NC)

Pacific Palisades landslide area, Los Angeles (J. T. McGill, D)

Palo Alto, San Mateo, and Montara Mountain quadrangles (E. H. Pampeyan, M)

Construction and terrain problems—Continued

Potential volcanic hazards to nuclear facilities, Washington, Oregon, and northern California (M. H. Hait, Jr., D)

Hawaii, Seismic hazards of the island of Hawaii with special emphasis on the Hilo 7½ min. quad. (J. Buchanan-Banks, Hawaii)

Oregon, Potential volcanic hazards to nuclear facilities, (M. H. Hait, Jr., D)

Utah, Engineering geologic studies, east-central Utah (E. E. McGregor, D)

Washington, Potential volcanic hazards to nuclear facilities, (M. H. Hait, Jr., D)

Wyoming (D):

Coal mine deformation studies, Powder River Basin (C. R. Dunrud)

Engineering geologic mapping, Sheridan-Buffalo area (E. N. Hinrichs)

Engineering geologic studies, Kemmerer 1:100,000 sheet (D. D. Dickey)

Weathering effects on geotechnical properties, Sheridan and Buffalo 1-degree quadrangles (A. F. Chleborad)

See also Land use; Urban geology; Urban hydrology.

Contaminants/pollutants:

Ground-water dispersion (W. W. Wood, w, NC)

Hydrology, nuclear-weapons testing (W. E. Wilson, w, D)

Hydrology of Amchitka Island (D. D. Gonzalez, w, D)

Hydrology of subsurface waste disposal-INEL, Idaho (J. T. Barraclough, w, Idaho Falls, Idaho)

NTS waste sites (F. F. Rush, w, Mercury, Nev.)

Radionuclide migration, NTS (W. E. Wilson, w, D)

Radioactive waste burial (G. D. DeBuchanne, w, NC)

Solute partitioning (J. A. Davis, w, M)

Transport modeling—saturated zone (L. F. Konikow, w, NC)

States:

California (w, Menlo Park):

Ground-water quality, Livermore-Amador Valley (M. A. Sylvester)

Stovepipe wells contamination (Anthony Buono, Laguna Niguel)

Colorado (w, Lakewood):

Colorado landfills (J. T. Turk)

Effects of sludge basins on ground water (S. G. Robson, D)

Hayden power plant study (R. L. Tobin, Meeker)

Inflows to lakes (M. H. Mustard, D)

Oil shale methods development (D. J. Ackerman, Grand Junction)

Florida (w, Tallahassee):

Bore hole phosphate mining (Paul Hampson, Jacksonville)

Geohydrology of drainage wells (J. O. Kimrey, Orlando)

Ground-water quality, Dade County (D. J. McKenzie, Miami)

Hydrogeochemistry, Florida phosphate (P. R. Seaber)

Movement and fate of wastes (E. R. German, Orlando)

Recharge Floridan aquifer, Alachua County (A. S. Navoy, Orlando)

Sewage effluent disposal irrigation (M. C. Yurewicz)

Solid waste, Hillsborough County (Mario Fernandez, Tampa)

Southeast spray field, Tallahassee (J. F. Elder)

Surface impoundment study (D. E. Troutman)

Traffic related contaminants (D. J. McKenzie, Miami)

Idaho (w, Boise):

Ground water, Michaud Flats (N. D. Jacobson, Idaho Falls)

Illinois (w, Urbana):

Contaminants/pollutants—Continued

- Palos waste-burial site (J. C. Olimpio)
 Sludge storage in strip-mine land (G. L. Patterson)
 Tritium migration, Illinois (J. R. Nicholas)
- Kansas (w, Lawrence):
 Quality of water, lead-zinc mined areas (T. B. Spruill)
 Solute transport in Equus beds, Kansas (J. B. Gillespie)
- Maryland (w, Towson):
 Nitrate in ground water, Delmarva (L. L. Bachman)
- Massachusetts (w, Boston):
 Impact of Otis AFB waste disposal (D. R. LeBlanc)
 Water-quality management (M. H. Frimpter)
- Minnesota (w, St. Paul):
 Derivatives in ground water (M. F. Hult)
 Karst well hydraulics (M. F. Hult)
 St. Louis Park transport model (M. F. Hult)
 Sand-plain in aquifer water quality (C. F. Myette)
- Montana (w, Helena):
 Geochemistry of spoils, Montana (G. M. Pike)
- New Jersey (w, Trenton):
 KMR water-quality (T. V. Fusillo)
- New Mexico (w, Albuquerque):
 In situ uranium hydrology, San Juan Basin (K. E. Stevens)
 San Jose water-table map, Albuquerque (J. D. Hudson)
- New York (w, Albany):
 Aldicarb pesticide in ground water, Suffolk County (Julian Soren, Syosset)
 Appraisal of selected aquifers (quality of water) (R. M. Waller)
 Brine disposal (R. M. Waller)
 Ground-water contamination on Long Island (G. E. Mallard, Syosset)
 Ground-water quality, Suffolk County (Julian Soren, Mineola)
 Hydrology of selected major aquifers (R. M. Waller)
 Landfill leachate model (E. J. Wexler, Syosset)
 Landfills in Oswego County (H. R. Anderson)
 Organic chemicals in ground water, Long Island (G. E. Mallard, Syosset)
 Symposium on impact of waste on ground water (R. P. Novitzki, Ithaca)
- North Carolina (w, Raleigh):
 Urban water quality, Charlotte (W. H. Eddins)
- North Dakota (w, Bismarck):
 Mining effects, Gascoyne area (M. G. Croft)
- Ohio (w, Columbus):
 Landfill impacts on ground-water system (A. C. Razem)
- Pennsylvania (w, Harrisburg):
 Nonpoint sources, Conestoga River (J. R. Ward)
 Water resources, anthracite region (A. E. Becher)
- South Carolina (w, Columbia):
 Disposal of wastewater by spray irrigation (G. K. Speiran)
 Radioactive waste burial study (J. M. Cahill)
- Tennessee (w, Nashville):
 Burial-ground studies at ORNL (D. A. Webster, Knoxville)
 Chemical character of shallow ground water (W. S. Parks, Memphis)
 Solute transport—Memphis Sand (J. V. Brahana)
 Waste disposal impact on ground-water quality (D. D. Graham, Memphis)
- Vermont (w, Montpelier):
 Ground-water quality, Vermont (R. E. Willey)
- Virginia (w, Richmond):
 Storm-water disposal (T. W. Danielson, Marion)
- Washington (w, Tacoma):

Contaminants/pollutants—Continued

- Clover-Chambers ground-water quality (B. W. Drost)
 Walla Walla ground water nitrate study (N. P. Dion)
- Wisconsin (w, Madison):
 Ground-water quality, Waukesha County (J. J. Schiller)
- Wyoming (w, Cheyenne):
 Effluent monitor, Yellowstone Wyoming (E. R. Cox)
- Copper:**
 New England massive sulfides (J. F. Slack, NC)
 Porphyry copper alteration zones (R. G. Schmidt, NC)
States:
 Colorado, Precambrian sulfide deposits (D. M. Sheridan, D)
 Maine-New Hampshire, Porphyry with molybdenum (R. G. Schmidt, NC)
 Virginia, Massive sulfides (J. E. Gair, NC)
- Crustal studies.** *See* Earthquake studies; Geophysics, regional.
- Current velocity/patterns:**
 Circulation, San Francisco Bay, California (T. T. Conomos, w, M)
 Numerical simulation (R. A. Baltzer, w, NC)
States:
 Alabama (w, Tuscaloosa):
 Travel-time studies (H. H. Jeffcoat)
 California (w, Menlo Park):
 Tidal river-discharge computation (R. N. Oltman, Sacramento)
 Colorado (w, Lakewood):
 Instream flow evaluation—Colorado (D. P. Bauer, D)
 Florida (w, Tallahassee):
 Impact of altered freshwater inflow (M. R. Fernandez, Tampa)
 Nassau estuary study, Florida (J. B. Largen, Jacksonville)
 Idaho (w, Boise):
 Water quality, Spokane River (H. R. Seitz)
 Illinois (w, Urbana):
 Stream dispersion (J. B. Graf)
 Louisiana (w, Baton Rouge):
 Velocity, Louisiana streams (G. J. Arcement)
 Nebraska (w, Lincoln):
 Travel data for Nebraska (L. R. Petri)
- Dam construction/design:**
 Illinois (w, Urbana):
 Dam ratings (J. R. Gray, DeKalb)
- Detergents:**
 New York (w, Albany):
 Long Island water quality (W. J. Flipse, Syosset)
- Droughts:**
 Colorado (w, Lakewood):
 Drought in Colorado (T. R. Dosch, D)
 Iowa (w, Iowa City):
 Northwest Iowa (M. R. Burkart)
 South Carolina (w, Columbia):
 Low-flow characteristics of South Carolina streams (W. M. Bloxham)
- Earthquake studies:**
 Active fault analysis (R. E. Wallace, M)
 Air-gun seismic measurements (H. P. Liu, M)
 Attenuation and seismic risk assessment (S. T. Harding, D)
 Borehole studies related to earth strain and other phenomena (T. C. Urban, M)
 Bounds on lower crust rheology (Marcia McNutt, M)
 Brittle tectonics and reservoir induced seismicity (D. C. Prowell, Atlanta)
 Comparative elevation studies (R. O. Castle, M)

Earthquake studies—Continued

Crustal evolution studies and isotopic measurements (J. S. Stacey, D)
 Crustal inhomogeneity in seismically active areas (S. W. Stewart, M)
 Crustal strain (J. C. Savage, M)
 Digital network data processing (J. P. Hoffman, Albuquerque)
 Digital network operations (N. A. Orsini, Albuquerque)
 Digital signal processing of seismic data (W. H. Bakun, M)
 Dynamic soil behavior (A. T. F. Chen, M)
 Earthquake control experiment (J. H. Dieterich, M)
 Earthquake field studies (W. J. Spence, C. J. Langer, and J. N. Jordan, M)
 Earthquake forecast models (W. D. Stuart, M)
 Earthquake-induced landslides (E. C. Harp, M)
 Earthquake-induced sedimentary structures (J. D. Sims, M)
 Earthquake observation system development (J. R. Van Schaack, M)
 Earthquake occurrence and statistics of crustal heterogeneity (B. R. Julian, M)
 Earthquake recurrence and history (R. D. Nason, M)
 Experimental liquefaction potential mapping (T. L. Youd, M)
 Experimental tilt and strain instrumentation (C. E. Mortenson, M)
 Fault creep (G. M. Marko, M)
 Fault-slip measurements (R. O. Burford, M)
 Fault zone water- and gas-well monitoring (C. Y. King, M)
 Field experiment operations (J. R. Van Schaack, M)
 Fluid injection, laboratory investigations (J. D. Byerlee, Louis Peselnick, M)
 Geologic parameters of seismic source areas (J. I. Ziony, M)
 Geothermal induced seismicity (D. H. Oppenheimer, M)
 Geothermal-tectonic seismic studies (C. S. Weaver, Seattle)
 Global ground-motion accelerometer instrumentation (N. A. Orsini, Albuquerque)
 Global telemetered seismograph network (N. A. Orsini, Albuquerque)
 Ground failures caused by historic earthquakes (D. K. Keefer, M)
 Ground-motion modeling and prediction (D. M. Boore, M)
 Ground-motion studies (R. D. Borchardt, L. M. Baker, M)
 In-situ stress measurement (J. H. Healy, M)
 Instrument development and geotechnical studies (R. E. Warrick, M)
 Interaction of earthquakes (T. C. Hanks, M)
 Interaction of ground motion and ground failure (R. C. Wilson, M)
 Large-scale fracture experiment (D. A. Lockner, M)
 Low-frequency data network (J. W. Herriot, M)
 Mechanics of geologic structures associated with faulting (D. D. Pollard, M)
 Microearthquake data analysis (W. H. K. Lee, M)
 National Earthquake Catalogue (J. N. Taggart, D)
 National Earthquake Information Service (E. P. Arnold, D)
 National Strong-Motion Instrumentation Network (R. B. Matthesen, M)
 New seismic instrumentation for geothermal surveys (P. A. Reasenber, M)
 Numerical studies of short-period ground motion near faults (D. J. Andrews, M)
 On-line seismic processing (R. V. Allen, M)
 Permeability of fault zones (J. D. Byerlee, M)
 Post-earthquake shaking effects and fault creep (Christopher Rojahn and R. D. Nason, M)
 Precursory phenomena (E. T. Endo, M)

Earthquake studies—Continued

Prediction, animal behavior studies (P. A. Reasenber, M)
 Prediction monitoring and evaluation (R. N. Hunter, D)
 Pressurized fractures in hot rock (D. D. Pollard, M)
 Quaternary dating and neotectonics (K. L. Pierce, D)
 Re-analysis of instrumentally recorded earthquakes (J. W. Dewey, D)
 Recurrence intervals along Quaternary faults (K. L. Pierce, D)
 Remote monitoring of source parameters for seismic precursors (G. L. Choy, D)
 Reservoir-induced seismicity, statistical approach (D. E. Stuart-Alexander, M)
 Seismic data library (W. K. Lee, M)
 Seismic-risk studies (S. T. Algermissen, D)
 Seismic slope stability (D. K. Keefer, M)
 Seismic-source studies (W. R. Thatcher, M)
 Seismic studies of fault mechanics (W. L. Ellsworth, M)
 Seismicity and tectonics, Southeastern United States (N. M. Ratcliffe, NC)
 Seismological data processing (B. R. Julian, M)
 Seismological observatories (H. S. Whitcomb, D)
 Seismological research observatories (J. R. Peterson, Albuquerque)
 Self-potential measurements near dams (D. V. Fitterman, D)
 Southern hemisphere seismic data collection (W. N. Green, NC)
 State seismicity maps and quarterly U.S. earthquake reports (C. W. Stover, D)
 Strong ground motion and dam site engineering (R. D. Borchardt, M)
 Strong ground-motion data analysis (J. B. Fletcher, M)
 Surface faulting studies (M. G. Bonilla, M)
 Synthetic strong-motion seismograms (W. B. Joyner, M)
 Systems development and testing for nuclear test monitoring (J. R. Peterson, Albuquerque)
 Tectonic studies (W. B. Hamilton, D)
 Tectonic tilt measurements using lake levels (S. H. Wood, M)
 Teleseismic determination of earthquake source parameters (John Boatwright, M)
 Teleseismic search for earthquake precursors (J. W. Dewey, D)
 Theoretical mechanics of earthquake precursors (G. M. Mavko, M)
 Theoretical seismology (A. F. Espinosa, D)
 Three-dimensional near-field modeling and strong-motion prediction in a layered medium (R. J. Archuleta, M)
 Tilt, strain, and field observations (M. J. Johnston, M)
 Tsunami network (H. E. Clark, Jr., Albuquerque)
 United States Seismic Network (M. A. Carlson, D)
 Worldwide Seismic Network (N. A. Orsini and J. R. Peterson, Albuquerque)
States and territories:
 Alaska:
 Eastern Gulf of Alaska seismic studies (J. C. Lahr, M)
 Earthquake hazards, southern Alaska (George Plafker, M; H. R. Schmoll, D)
 Microearthquake studies (R. A. Page, M)
 Seismic studies (J. C. Lahr, M)
 Arizona, Glen Canyon Dam seismicity (M. A. Carlson, D)
 California (M, except as otherwise noted):
 Basement rock studies along San Andreas fault (D. C. Ross)
 Central California network operations (W. D. Hall)
 Crustal changes north of San Francisco (P. L. Ward)
 Earthquake hazards, San Francisco Bay region (E. E. Brabb)
 Foothills fault system (D. E. Stuart-Alexander)
 Geodetic strain (A. F. McGair)

Earthquake studies—Continued

- Geophysical studies, San Andreas fault (J. H. Healy)
 Los Angeles Metropolitan area (R. F. Yerkes)
 Measurement of seismic velocities for seismic zonation
 (J. F. Gibbs, R. D. Borchardt, T. E. Fumal)
 Microearthquake studies:
 Central part (J. H. Pfluke)
 Southern part (D. P. Hill)
 Nonlinear soil response at Imperial Valley recording sites
 (A. T. F. Chen)
 Parkfield prediction experiment (A. G. Lindh)
 Quaternary reference core, Clear Lake (J. D. Sims)
 Recency of faulting, eastern Mojave Desert (W. J. Carr)
 Relative hazards of southern California faults (J. I. Ziony)
 Rupture processes and wave propagation effects from the
 Coyote Lake earthquake (P. A. Spudich)
 San Pablo—Suisun Bay seismic gap (D. H. Warren)
 Seismic zonation, Los Angeles basin (A. M. Rogers, D)
 Southern California cooperative seismic network (C. E.
 Johnson)
 Strong ground-motion studies, Imperial Valley 1979 earth-
 quake (T. C. Hanks)
 Tectonics:
 Central and northern part (W. P. Irwin)
 Central San Andreas fault (D. B. Burke, T. W. Dibblee,
 Jr.)
 Salton Trough (R. V. Sharp)
 Theory of wave propagation in an elastic media (R. D.
 Borchardt)
 Colorado, Desalinization of the Delores River and induced seis-
 micity (W. J. Spence, D)
 Hawaii:
 Earthquake studies (R. W. Decker, Hawaii)
 Seismic hazards of the island of Hawaii with special
 emphasis on the Hilo 7 1/2-min. quad. (J. Buchanan-
 Banks, Hawaii)
 Idaho, Active faults, Snake River Plain (P. L. Williams, D)
 Massachusetts, Fault definition, northeastern Massachusetts
 (A. F. Shride, D)
 Montana, Yellowstone National Park, Microearthquake studies
 (A. M. Pitt, M)
 New Mexico:
 Albuquerque observatory; Socorro magma bodies (L. H.
 Jaksha, Socorro)
 Seismotectonic analysis, Rio Grande rift (E. H. Baltz, Jr.,
 D)
 Puerto Rico, Preliminary assessment of liquefaction potential in
 and near San Juan (T. L. Youd, M)
 Regional (D):
 Hazard mapping, eastern Great Basin (R. E. Anderson)
 Mississippi Valley seismotectonics (D. P. Russ)
 Southern Great Basin seismicity studies (A. M. Rogers)
 Structural framework of seismic zones, Eastern United
 States (R. L. Wheeler)
 South Carolina, Seismic studies (C. J. Langer, D)
 Utah, Ground response, Salt Lake Valley (W. W. Hays, NC)
 Washington:
 Hanford microearthquake studies (J. H. Pfluke, M)
 Seismotectonic analysis, Puget Sound (J. C. Yount, M)

Ecology:

- Estuarine plankton dynamics (J. E. Cloern, w, M)
 Wetland studies (V. P. Carter, w, NC)
 States:
 Florida (w, Tallahassee):
 Water resources of the Everglades (K. W. Ratzlaff, Miami)

Ecology—Continued

- Hawaii (w, Honolulu):
 Biology-morphology, Wailuku River (J. J. Yee)
 Mississippi (w, Jackson):
 Hydrology-Tennessee-Tombigbee (D. J. Tomaszewski)
 Engineering geologic studies. See Construction and terrain prob-
 lems; Urban geology.
 Environmental assessment:
 Case study socioeconomic assessments of three energy develop-
 ment communities: Rangely, Colorado; Price, Utah; and
 Douglas, Wyoming (R. R. Reynolds, o, NC)
 Guidance to task force leaders for EIS preparation (P. Cheney;
 D. Schleicher, o, D)
 Validation and improvement of socioeconomic impact state-
 ment methodologies (R. R. Reynolds, o, NC)
 Environmental geology:
 Utah (D):
 Cedar City 2-degree quadrangle (K. A. Sargent)
 Central Utah energy lands (I. J. Witkind)
 Kaiparowits Plateau coal basin (K. A. Sargent)
 Wyoming:
 Bighorn Basin (R. M. Barker, NC)
 Hams Fork coal basin (A. B. Gibbons, D)
 See also Construction and terrain problems; Land use; Urban
 geology.
 Erosion/sedimentation:
 Cal Tech sediment management (J. K. Culbertson, w, NC)
 Coon Creek morphology (S. W. Trimble, w, Los Angeles)
 Forest geomorphology, Pacific coast (R. J. Janda, w, M)
 Hydrological-biological interactions (E. D. Andrews, w, D)
 Sediment in rivers (R. H. Meade, w, D)
 Stochastic transport processes (C. F. Nordin, w, D)
 States:
 Alaska (w, Anchorage):
 Sediment transport—Devils Canyon (L. S. Leveen)
 Tanana River sediment study (R. L. Burrows, Fairbanks)
 California (w, Menlo Park):
 Water—Redwood National Park (S. H. Hoffard)
 Idaho (w, Boise):
 Channel change, Big Lost River (R. P. Williams)
 Illinois (w, Urbana):
 Erosion at Sheffield site (J. R. Gray, De Kalb)
 Illinois bedload data (J. B. Graf)
 Urban construction stream quality (H. E. Allen, De Kalb)
 Missouri (w, Rolla):
 Sediment characteristics, Salt River (W. R. Berkas)
 Surface-water resources, Little Black River (W. R. Berkas)
 Nevada (w, Carson City):
 Edgewood Creek sedimentation (L. A. Bohner)
 Ohio (w, Columbus):
 Sediment yields, Ohio (P. W. Anttila)
 Pennsylvania (w, Harrisburg):
 Predicting sediment flow (L. A. Reed)
 Sediment discharge, logging mining (D. E. Stump, Pitts-
 burgh)
 Washington (w, Tacoma):
 Toutle rainfall-runoff model (J. J. Vaccaro)
 Wyoming (w, Cheyenne):
 Sediment yield from small basins, Wyoming (C. L. Joy)
 Estuarine studies:
 Dissolved oxygen and nutrient dynamics (W. E. Webb, w, NC)
 Geochemistry of rivers and estuaries (D. H. Peterson, w, M)
 Potomac Estuary benthic ecology (R. L. Cory, w, Edgewater,
 Md.)
 Potomac Estuary phytoplankton (R. R. Cohen, w, NC)

Estuarine studies—Continued

Submersed aquatic vegetation (Virginia Carter, w, NC)
Water quality and estuarine biology (R. L. Cory, w, Edgewater, Md.)

Water quality model development and implementation (R. A. Baltzer, w, NC)

States:

South Carolina (w, Columbia):

Effectiveness of Cooper River diversion (G. G. Patterson)
Reconnaissance, South Carolina estuaries (F. A. Johnson)

Wisconsin (w, Madison):

Milwaukee Harbor study (L. B. House)

Evapotranspiration:

Evapotranspiration data analysis (T. E. Van Hylckama, w, Lubbock, Tex.)

Evapotranspiration studies (E. P. Weeks, w, D)

Vegetation ecohydrology (R. M. Turner, w, Tuscon)

States:

Arizona (w, Tucson):

Lower Colorado River consumptive use study (L. H. Applegate, Phoenix)

Colorado (w, Lakewood):

Evaporation, Colorado lakes (N. E. Spahr, D)

Extraterrestrial studies (Flagstaff, Ariz., unless otherwise noted):

Cartography (R. M. Batson, D. W. G. Arthur)

Eolian processes (J. F. McCauley, M. J. Grolier, C. S. Breed)

Explosion craters (D. J. Roddy, J. F. McCauley, L. A. Soderblom, R. L. Pike, Jr.)

Galilean satellites (Harold Masursky, L. A. Soderblom, M. H. Carr, E. M. Shoemaker, B. K. Lucchitta)

Glacial processes (B. K. Lucchitta, Harold Masursky)

Jupiter-Saturn mapping (Harold Masursky)

Lunar geology (D. E. Wilhelm, M; G. A. Swann, P. D. Spudis)

Lunar sample investigations (NC):

Geologic thermometry (J. S. Huebner)

Highlands breccias (O. B. James)

Microstructure analysis (G. L. Nord)

Mars:

Boundary problems between heavily cratered/lightly cratered terrain (C. A. Baskerville, NC)

Geologic mapping (D. H. Scott)

Geologic studies (E. C. Morris, Harold Masursky, H. J. Moore, D. H. Scott, M. H. Carr, M)

Phanerozoic impact history of the Earth (E. M. Shoemaker)

Planetary nomenclature (Harold Masursky)

Planetary uplands evolution (D. E. Wilhelm, M)

Radar image processing, techniques and interpretation (H. H. Kieffer, Harold Masursky, G. G. Schaber, L. A. Soderblom, M. H. Carr, M)

Terrestrial planets book (M. H. Carr, M)

Thermal analysis (H. H. Kieffer)

Topographic synthesis (S. S. C. Wu)

Volcanic features and processes (R. J. Pike, Jr., C. A. Hodges, H. J. Moore, M)

Voyager mission (L. A. Soderblom)

Ferro-alloy metals:

Chromium:

Geochemistry (B. A. Morgan III, NC)

Resource studies (B. R. Lipin, NC)

Flood mapping/routing:

Flood-hazard mapping (G. W. Edelen, w, Washington, D.C.)

HUD flood insurance studies (E. J. Kennedy, w, NC)

Techniques of flood-plain mapping (R. H. Brown, w, Bay St. Louis, Miss.)

Flood mapping/routing—Continued*States:*

Alabama (w, Tuscaloosa):

Flood-hazard mapping (C. O. Ming, Montgomery)

Alaska (w, Anchorage):

Mt. Spurr study (R. P. Emanuel)

Arkansas (w, Little Rock):

Flood-hazard mapping (R. C. Gilstrap)

California (w, Menlo Park):

Flood-hazard mapping (J. R. Crippen)

Flood hydrology, Butte Basin (J. C. Blodgett, Sacramento)

Lassen Peak hydrologic hazards (J. C. Blodgett, Sacramento)

Mount Shasta hydrologic hazards (J. C. Blodgett, Sacramento)

Park and Monument flood risk (J. R. Crippen)

Colorado (w, Lakewood):

Flood-hazard mapping (T. R. Dosch, D)

Connecticut (w, Hartford):

Flood-hazard mapping (M. A. Cervione)

Florida (w, Tallahassee):

Flood-hazard mapping (S. D. Leach)

Georgia (w, Doraville):

Flood-hazard mapping (Mc Glone Price, Atlanta)

Idaho (w, Boise):

Flood-hazard mapping (W. A. Harenberg)

Iowa (w, Iowa City):

Flood-hazard mapping (O. G. Lara)

Kansas (w, Lawrence):

Flood-hazard mapping (C. A. Perry)

Kentucky (w, Louisville):

Flood-hazard mapping (J. N. Sullivan)

Louisiana (w, Baton Rouge):

Flood-hazard mapping (A. S. Lowe)

Maine (w, Augusta):

Flood-hazard mapping (R. A. Morrill)

Minnesota (w, St. Paul):

Flood-hazard mapping (G. H. Carlson)

Flood-plain coordination (George H. Carlson)

Montana (w, Helena):

HUD flood-insurance studies (R. J. Omang)

Willow Creek modeling (Charles Parrett)

New Jersey (w, Trenton):

HUD flood-insurance studies (R. D. Schopp)

New York (w, Albany):

HUD flood-insurance studies (R. T. Mycyk)

Schoharie Creek runoff-rainfall model (S. W. Wolcott)

Nevada (w, Carson City):

HUD flood-insurance study (R. R. Squires)

Ohio (w, Columbus):

Flood-hazard mapping (D. K. Roth)

Hydraulics of bridge sites (R. I. Mayo)

Oklahoma (w, Oklahoma City):

Urban flood analysis in Oklahoma City (T. L. Huntzinger)

Oregon (w, Portland):

Flood-hazard mapping (D. D. Harris)

Mt. Hood volcanic hazards (L. L. Hubbard)

Three Sisters volcanic hazards (D. D. Harris)

Pennsylvania (w, Harrisburg):

Flood-hazard mapping (Andrew Voytik)

Puerto Rico (w, San Juan):

Eloise floods, Puerto Rico, September 1975 (K. G. Johnson, Ft. Buchanan)

HUD flood-insurance studies (Eloy Colon-Dieppa, Ft. Buchanan)

Flood mapping/routing—Continued

- St. Croix flood of October 7-8, 1977 (K. G. Johnson, Ft. Buchanan)
- South Carolina (w, Columbia):
Flood-hazard mapping (W. T. Utter)
Savannah River streamflow simulation (B. B. McDonald)
- South Dakota (w, Huron):
Flood-hazard mapping (L. D. Becker)
- Texas (w, Austin):
Flood-hazard mapping (E. E. Schroeder)
- Utah (w, Salt Lake City):
Flood-plain mapping in Utah (K. L. Lindskov)
- Washington (w, Tacoma):
Cowlitz sediment (R. E. Lombard)
Flood-hazard mapping (C. H. Swift)
HUD flood-insurance studies (C. H. Swift)
Mount Rainier flood hazards (D. L. Kresch)
St. Helens photogrammetry (D. L. Kresch)
- Wisconsin (w, Madison):
Digital model-flood flow, Rock River (W. R. Krug)
St. Croix scenic river waste study (C. L. Lawrence)
- Wyoming (w, Cheyenne):
Flood-hazard mapping (B. H. Ringen)
- Flood reporting/analysis:**
Documentation extreme floods (H. H. Barnes, w, NC)
Floods, Big Sandy-Tug Fork (A. G. Scott, w, NC)
Flow frequency analysis (W. O. Thomas, w, NC)
States:
Alabama (w, Tuscaloosa):
Flood frequency in Alabama (D. A. Olin)
Arizona (w, Tucson):
Flood report (B. N. Aldridge)
1980 flood report (B. N. Aldridge)
California (w, Menlo Park):
Floods—small drainage areas (A. O. Waananen)
1980 flood report (R. J. Longfield, Laguna Niguel)
Colorado (w, Lakewood):
Foothill floods (R. D. Jarrett, D)
Florida (w, Tallahassee):
Regional lake stage evaluation (M. A. Lopez, Tampa)
Georgia (w, Doraville):
Atlanta flood characteristics (E. J. Inman)
Urban flood-frequency, Georgia (E. J. Inman)
Idaho (w, Boise):
HUD flood-insurance studies (W. A. Harenberg)
Indiana (w, Indianapolis):
Flood frequency, Indiana (D. R. Glatfelter)
Kentucky (w, Louisville):
Floods, Big Sandy-Tug Fork (C. E. Schoppenhorst)
Small area flood hydrology (C. E. Schoppenhorst)
Nevada (w, Carson City):
Environmental study, Nevada (T. L. Katzer)
New Mexico (w, Albuquerque):
Flood analysis (R. P. Thomas, Santa Fe)
New York (w, Albany):
Flood investigations—New York (T. J. Zembrzusi)
North Dakota (w, Bismarck):
Red River hydrologic response (J. E. Miller)
Oregon (w, Portland):
Pollalie flood (G. L. Gallino)
Virginia (w, Richmond):
Flood investigation in Virginia (B. J. Prugh)
Floods in Tug Fork, Virginia (T. W. Danielson)
West Virginia (w, Charleston):
Floods in Tug Fork, West Virginia (R. L. Bragg)

Flood reporting/analysis—Continued

- Wisconsin (w, Madison):
Flood documentation in Wisconsin (P. E. Hughes)
Flood-frequency—urban and rural (D. H. Conger)
- Wyoming (w, Cheyenne):
Flood investigations (G. S. Craig)
- Flood warning/forecasting:**
Nationwide flood-frequency (A. G. Scott, w, NC)
States:
Arizona (w, Tucson):
Flood-warning network (F. C. Boner)
New Jersey (w, Trenton):
Somerset County (J. B. Campbell)
Washington (w, Tacoma):
North Fork Toutle Lakes (P. J. Carpenter)
St. Helens monitoring (Dallas Childers)
- Fluorspar:**
Cenozoic lacustrine deposits of the United States (R. A. Sheppard, D)
Illinois-Kentucky district, regional structure and ore controls (D. M. Pinckney, D)
- Foreign nations, geologic investigations:**
Africa:
Advisory services relative to facilities for reception and processing of satellite data for earth resource information, West Africa remote sensing center, Ouagadougou (S. R. Address)
Remote sensing training, cartography (A. Warren, n)
Geological data management systems (R. W. Bowen, NC)
Antarctica, geology of the Lassiter/Orville Coasts (P. D. Rowley, D)
Asia:
Offshore geologic map of Southeast Asia (F. H. Wang, M)
Technical assistance for Southeast Asian environmental problems (F. H. Wang, M)
Technical assistance in East Asian sedimentary basin analysis (C. D. Masters, NC, petroleum; Keith Robinson, D, Malaysian petroleum)
Bangladesh, Technical assistance to modernize the Geological Survey (P. W. Richards, NC)
Brazil, Consultation on exploration program for oil and gas in the Parana Basin, with the Instituto de Pesquisas Tecnológicas, Sao Paulo State (C. W. Spencer, D; W. D. Stanley, D)
Canada:
Polymetallic sulfide investigations (W. R. Normark, M)
International Minerals Inventory (J. H. deYoung, Jr., NC)
China, People's Republic of:
Earthquake Studies:
Deep crustal structure (D. P. Russ, NC)
Investigations of premonitory phenomena and techniques for earthquake prediction (D. P. Russ, NC)
Investigations of intraplate active faults and earthquakes (D. P. Russ, NC)
Laboratory studies in rock mechanics (D. P. Russ, NC)
Earth Sciences:
Application of remote-sensing techniques to petroleum exploration (G. B. Bailey and T. D. Fouch, D)
Coal basin exploration and analysis (E. R. Landis, D)
Petroleum geology of carbonate rocks (P. A. Scholle, D)
Uranium deposits exploration and analysis (R. I. Grauch, D)
- Egypt:**
Eolian carbonates and calcareous eolianites, literature review of distribution and genesis (E. D. McKee, D)

Foreign nations, geologic investigations—Continued

- Mineral resources exploration methods and map production techniques; technology transfer (R. W. Schaff, Cairo)
- England, Sonar mapping of the seafloor (L. E. Garrison, c, Corpus Christi, Tex.; P. S. Chavez, Jr., Flagstaff)
- Federal Republic of Germany:
International Minerals Inventory (J. H. deYoung, Jr., NC)
Marine resource geology and geophysics (J. S. Schlee, Woods Hole, Mass.)
Modeling Mississippi-type ore deposits (J. A. Briskey, Jr., M)
- France:
Remote sensing data software development (E. M. Eliason, cc, Flagstaff)
Seafloor engineering (P. G. Teleki, NC)
- Hungary:
Coal geochemistry (Peter Zubovic, NC)
Computer-assisted geologic data management (R. W. Bowen, M. D. Carter, NC)
Electromagnetics (F. C. Frischknecht, D)
Induced polarization (B. D. Smith, D)
Magnetostratigraphy and paleomagnetism (D. P. Elston, Flagstaff)
Oil and gas resources (R. E. Mattick, NC)
Organic geochemistry (R. E. Miller, c, NC)
Paleoenvironments of Mesozoic sediments (H. E. Clifton, M)
Sedimentology (R. L. Phillips, M)
Vertical seismic profiling (F. K. Miller, Spokane)
- Iceland, Remote sensing, geology (R. S. Williams, Jr., n, NC)
- Indonesia:
Technical assistance in geologic hazards mitigation and environmental geologic mapping (G. W. Weir, Bandung)
Technical assistance in petroleum data systems (R. W. Bowen, NC)
- Jordan, Technical assistance in establishment of a seismic monitoring system for the National Resource Authority (G. E. Andreasen, NC)
- Latin American Region:
Andes, technical assistance toward earthquake disaster mitigation in the Andean region (R. W. Fary, Jr., NC)
Bolivia, Investigation of geology of tin deposits associated with calderas (G. E. Ericksen, R. L. Smith, R. G. Luedke, NC)
- Brazil:
Consultation on exploration program for oil and gas in the Parana Basin (C. W. Spencer, W. D. Stanley, D; I. G. Sohn, Wash., D. C.)
Consultation on program for geological evaluation of coal resources of Sao Paulo State (R. M. Flores, D)
- Colombia, Assessment of minerals resource base of Colombia (W. R. Greenwood, NC)
- Mexico:
Analysis of geologic conditions and monitoring of activity of El Chichon Volcano (R. I. Tilling, Daneil Dzurisin)
Baja and Durango reflectance measurements and interpretation of shuttle imagery (L. C. Rowan, NC)
Geochemical, geophysical, aerial, and satellite remote sensing exploration for copper in the Sonoran environment (P. K. Theobald Jr., H. N. Barton, J. G. Frisken, R. L. Turner, M. D. Kleinkopf, G. L. Raines, B. D. Smith, J. W. Rozelle, D)
Structural and stratigraphic relations to metallogenic

Foreign nations, geologic investigations—Continued

- provinces (D. G. Howell, J. H. Stewart, J. P. Albers, M)
- Peru, mineral resources assessment in southern Peru (C. R. Glenn, NC)
- Malawi:
Coal resources assessment (F. D. Simon, NC)
Oil and gas resources assessment (R. E. Mattick, NC)
- Morocco:
Cobalt resources (M. P. Foose, NC)
Mesozoic basins, ore deposits (A. J. Froelich, NC)
- Pacific:
Circum-Pacific map project (W. O. Addicott, M)
Technical assistance in offshore resources assessment, Southwest Pacific (H. G. Greene, M)
Technical assistance in onshore source-rock studies, Southwest Pacific (P. A. Scholle, D)
- Portugal, Geothermal resources, Azores (W. A. Duffield, Flagstaff)
- Roumania, Procurement of equipment for earthquake mitigation (S. T. Algermissen, D)
- Saudi Arabia:
Center for Science and Technology, Concepts for an Institute for Natural Resources and Environmental Research (R. W. Fary, Jr., NC)
Production of mosaics and Landsat image map bases (J. O. Morgan, Jidda)
Technical assistance in earth sciences and mineral resource studies from the Deputy Directorate for Mineral Resources, Kingdom of Saudi Arabia (R. O. Jackson, Jidda)
- South Africa, International Minerals Inventory (J. H. deYoung, Jr., NC)
- South America, mineral deposits of (G. E. Erickson, NC)
- South Korea:
Technical assistance in petroleum resources (Keith Robinson, D)
Technical assistance in geothermal resources (W. A. Duffield, Flagstaff)
- Spain, marine mineral resources (P. D. Snavelly, Jr., M)
- Syria:
Preliminary investigation of knowledge, data, and field conditions relative to chromite occurrences (B. R. Lipin, NC)
Technical assistance in establishment of a remote sensing user facility with the Syrian National Remote Sensing Center, J. R. McCord, n, Sioux Falls)
- Thailand:
Potash resources assessment (R. J. Hite, D)
Remote-sensing program (J. R. McCord, n, Sioux Falls)
Technical assistance in land-use studies (D. B. Krinsley, NC)
- Tunisia, training in remote sensing (M. J. Grolier, Flagstaff)
- U.S.S.R.:
Volga Urals oil and gas resource analysis (J. A. Peterson, D)
West Siberia oil and gas resource analysis (J. C. Clarke, NC)
- Yugoslavia:
Deep seismic soundings for crustal studies in active seismic areas (M. F. Kane, D)
Earthquake risk (R. C. Bucknam, D)
Engineering seismology (R. D. Borchardt, M)
Geochemical exploration (W. R. Miller, D)
Subsurface subsidence in mining areas (D. R. Nichols, D)
- Fuels, organic.** See Coal; Oil shale; Petroleum and natural gas.
Gas, natural. See Petroleum and natural gas.

General inorganic:

- Acid rain (R. J. Pickering, w, NC)
- Acid rain effects, monitoring (W. L. Bradford, w, NC)
- Air Force quality of water analysis (A. W. Beetem, w, NC)
- Atlanta Central Lab—atomic absorption (F. E. King, w)
- Atlanta Central Lab—automated methods (A. J. Horowitz, w)
- Atlanta Central Lab—manual methods (E. R. Anthony, w)
- Atlanta Central Lab—special methods (D. K. Leifeste, w)
- Atlanta Central Laboratory (D. K. Leifeste, w)
- Benchmark network (R. R. Pickering, w, NC)
- Chemical constituents of water (William Back, w, NC)
- Collection of basic data—chemical quality analyses (Alberto Condes, NC)
- Compact chemical quality analyses (Alberto Condes, w, NC)
- Denver Central Lab—ADP (R. E. Gust, w, D)
- Denver Central Lab—atomic absorption (H. J. Miller, w, D)
- Denver Central Lab—automated method (J. M. Schoen, w, D)
- Denver Central Lab—manual methods (S. A. Duncan, w, D)
- Denver Central Lab—physical properties (Tung-Ming Lai, w, D)
- Denver Central Lab—radiochem analyses (I. C. Yang, w, D)
- Denver Central Lab—special methods (M. L. Yates, w, D)
- Denver Central Laboratory (D. B. Manigold, w, D)
- Methods development support (D. E. Erdmann, w)
- Mineralogic control ground water (B. B. Hanshaw, w, NC)
- Mineral-water interaction in saline environment (B. F. Jones, w, NC)
- Modeling mineral-water reactions (L. N. Plummer, w, NC)
- National river quality (J. F. Ficke, w, NC)
- National trends network (W. L. Bradford, w, NC)
- NASQAN (R. J. Pickering, w, NC)
- NASQAN support activities (R. J. Pickering, w, NC)
- States:*
- Arkansas (w, Little Rock):
 - Soil Conservation Service watershed studies (J. C. Petersen)
- California (w, Menlo Park):
 - Quality of water, California streams (P. W. Anttila)
 - Water quality studies design—NPS (M. V. Shulters)
 - Water resources, Upper Coachella (Anthony Buono, Laguna Niguel)
- Colorado (w, Lakewood):
 - Acid rain study (J. T. Turk, D)
 - Quality of water characteristics of Colorado streams (M. W. Gaydos, D)
 - Roan/Parachute Creek spring study (D. L. Butler, Grand Junction)
- Connecticut (w, Hartford):
 - Water quality in Little River watershed (K. P. Kulp, Hartford)
 - Water resources lower Connecticut River basin (L. A. Weiss)
- Florida (w, Tallahassee):
 - Lakes Faith, Hope and Charity (E. R. German, Orlando)
- Idaho (w, Boise):
 - Ground-water quality assessments (D. J. Parlman)
- Kansas (w, Lawrence):
 - Ground-water quality network evaluations (A. M. Diaz)
- Maine (w, Augusta):
 - Chemical quality of precipitation (J. A. Smath)
- Massachusetts (w, Boston):
 - Highway deicing chemicals in ground water (S. J. Pollock)
- Michigan (w, Lansing):
 - Water resources, Van Buren County (F. R. Twenter)
- Mississippi (w, Jackson):
 - Ground-water hydrology and quality of water, Barnett area (W. T. Oakley)

General inorganic—Continued

- Missouri (w, Rolla):
 - Coal hydrology, Missouri (J. H. Barks)
- Nebraska (w, Lincoln):
 - Ground-water quality evaluation, Nebraska (R. A. Engberg)
- Nevada (w, Carson City):
 - Ground-water quality monitoring network (J. O. Nowlin)
- New Jersey (w, Trenton):
 - Problem river studies—New Jersey (J. C. Schornick)
- New Mexico (w, Albuquerque):
 - Southeast areas, northwest New Mexico (J. R. Hejl)
 - San Juan River valley (F. P. Lyford)
- North Carolina (w, Raleigh):
 - Effects of channelizing Black River (C. E. Simmons)
 - I-85 runoff (R. G. Garrett)
 - Water-quality of major North Carolina rivers (J. J. Crawford)
- North Dakota (w, Bismarck):
 - Ground-water sampling techniques (R. L. Houghton)
- Ohio (w, Columbus):
 - Limnology of selected Ohio lakes (C. G. Angelo)
 - Rattlesnake Creek water quality (K. F. Evans)
- Oklahoma (w, Oklahoma City):
 - Blue Creek quality (J. K. Kurklin)
 - Coal hydrology, eastern Oklahoma (M. V. Marcher)
 - Gaines Creek quality (J. K. Kurklin)
 - Zinc mine water quality (Jerry D. Stoner)
- Oregon (w, Portland):
 - Water in western Douglas County (D. A. Curtiss)
- Pennsylvania (w, Harrisburg):
 - Ground-water quality in Pennsylvania (H. E. Koester)
 - Quality of water, Francis E. Walter Reservoir (J. L. Barker)
 - Water resources, Washington County (D. B. Richards, Pittsburgh)
 - Water quality in Tioga River basin (J. R. Ward)
- Rhode Island (w, Providence):
 - Quality of Rhode Island streams (H. E. Johnston)
- South Dakota (w, Huron):
 - Water quality in Black Hills area (K. D. Peter, Rapid City)
- Texas (w, Austin):
 - Water quality of Lake Arlington (F. L. Andrews)
 - Water quality, bays and estuaries (J. C. Fisher, Houston)
- Utah (w, Salt Lake City):
 - Reconnaissance of Utah coal fields (K. M. Waddell)
 - Surface-water quality, Dirty Devil (J. C. Mundorff)
 - Virgin River basin water quality (K. R. Thompson)
 - Water quality, San Rafael River basin (J. C. Mundorff)
 - Weber River basin water quality (K. R. Thompson)
- Washington (w, Tacoma):
 - Ground-water quality network—Washington (J. C. Ebbert)
- Wisconsin (w, Madison):
 - Bench-mark water quality (D. A. Wentz)
 - Ground-water quality evaluation (P. A. Kammerer)
- Geochemical distribution of the elements (D, except as otherwise noted):**
- Basin and Range granites (D. E. Lee)
- Beryllium, distribution and application to geochemical exploration (W. R. Griffiths)
- Data of geochemistry (Michael Fleischer, NC)
- Data systems (R. V. Mendes)
- Element availability:
 - Soils (R. C. Severson)
 - Vegetation (L. P. Gough)
- Geochemical baselines for Atriplex sp. (B. M. Anderson)
- Geochemistry of belt rocks (J. J. Connor)
- Light stable isotopes (J. R. O'Neil, M)

Geochemical distribution of the elements—Continued

- Phosphoria Formation, organic carbon and trace element distribution (E. K. Maughan)
- Selenium and tellurium in geochemical exploration (J. R. Watterson)
- Statistical geochemistry and petrology (A. T. Miesch)
- Surficial geochemistry:
 - Craig-Meeker, 1:100,000 quad. (Colo.) (R. R. Tidball)
 - Green River Basin (Wyo.) (R. R. Tidball)
 - Recluse (Wyo.) (R. R. Tidball)
- Tippecanoe sequence, Western Craton (L. G. Schultz)
- Trace elements in oil shale (W. E. Dean, Jr.)
- Urban geochemistry (H. A. Tourtelot)
- Western coal regions:
 - Geochemical survey of rocks (T. K. Hinkley)
 - Geochemical survey of vegetation (J. A. Erdman)
 - Geochemical survey of waters (G. L. Feder, w)
 - Geochemistry of clinker (J. R. Herring)

States:

- Alaska, Geochemical census (L. P. Gough)
- California:
 - Geochemical mapping (W. R. Miller)
 - Sierra Nevada batholith, geochemical study (F. C. W. Dodge, M)
- Colorado, Mt. Princeton igneous complex (Priestley Toulmin III, NC)

Geochemical prospecting methods (D):

- Biological methods research (J. R. Watterson)
- Chemical patterns in zoned deposits (M. A. Chaffee)
- Epithermal gold-silver deposits (B. R. Berger)
- Gamma-ray spectrometry (J. A. Pitkin)
- Geochemical exploration:
 - Bureau of Land Management lands, Central and Western Regions (S. P. Marsh)
 - Development of analytical techniques for hydrochemical exploration (W. H. Ficklin)
 - Deep soil and saprolite (W. R. Griffiths)
 - Glaciated areas (H. V. Alminas)
 - Massive sulfide deposits (P. K. Theobald, D)
 - Research in methods of spectrographic analysis (E. L. Mosier)
 - Surface and ground water (W. R. Miller)
 - Volatile elements and compounds (M. E. Hinkle)
- Instrumentation development (R. C. Bigelow)
- Lamprohyre-ore association (G. J. Neuerburg)
- Lateritic areas, southern Appalachian Mountains (W. R. Griffiths)
- Nitrogen, sulfur, and oxygen as transports of heavy metal (J. G. Viets)
- Ore-deposit controls (A. V. Heyl, Jr.)
- Research in chemical methods for geochemical exploration (T. T. Chao)
- Sulfides, accessory in igneous rocks (G. J. Neuerberg)
- Techniques of geochemical, geophysical, and geological exploration in the Sonoran environment (P. K. Theobald)
- Volatile elements released by natural coal burning and baking of overlying rocks (J. R. Herring)

States:

- Puerto Rico, geochemical exploration (R. E. Learned)
- Wisconsin, geochemistry of volcanic rocks (K. J. Schulz, NC)

Geochemistry, experimental:

- Chemical and isotope studies of hydrothermal systems (G. P. Landis, D)
- Chemical methodology in geoanalysis (T. T. Chao, D)
- Coal combustion and rock metamorphism (J. R. Herring, D)

Geochemistry, experimental—Continued

- Combustion metamorphism (J. R. Herring, D)
- Experimental mineralogy (R. O. Fournier, M)
- Fluid inclusions in minerals (Edwin Roedder, NC)
- Fluid zonation in metal deposits (J. T. Nash, M)
- Fossil fuel geochemistry (P. G. Hatcher, NC)
- Geochemical characteristics, granitic plutons and porphyry type Cu-Mo deposits, northern Maine (R. A. Ayuso, NC)
- Geochemical composition, sources, and transport of atmospheric dusts (T. K. Hinkley, D)
- Geologic thermometry (J. S. Huebner, NC)
- Hydrothermal alteration (J. J. Hemley, NC)
- Kinetics of igneous processes (H. R. Shaw, NC)
- Mineral equilibria, low temperature (E-an Zen, NC)
- Neutron activation (F. E. Senville, NC)
- Oil shale:

- Colorado, Utah, and Wyoming (W. E. Dean, Jr., D)
- Organic geochemistry (R. E. Miller, D)

- Organic geochemistry (J. G. Palacas, G. E. Claypool, D)
- Organometallic complexes, geochemistry (Peter Zubovic, NC)
- Stable isotopes and ore genesis (R. O. Rye, D)
- Statistical geochemistry (A. T. Miesch, D)
- Thermodynamic data of minerals (J. L. Haas, Jr., NC)

Geochemistry and mineralogy, water:

- Gases in water (D. W. Fisher, w, NC)
- Geologic perspectives—global CO₂ (E. T. Sundquist, w, NC)
- Paleoclimatology and aquifer geochemistry (I. J. Winograd, w, NC)
- Redox reactions (D. C. Thorstenson, w, NC)
- Volcanic volatiles (Ivan Barnes, w, M)

States:

- Delaware (w, Dover):
 - Ground-water quality, southwestern Delaware (J. M. Denver)
- Florida (w, Tallahassee):
 - Mineralized ground waters, southwest Florida (W. C. Steinkampf, Tampa)
- Missouri (w, Rolla):
 - Geochemistry of coal spoil piles (D. C. Hall)
- North Dakota (w, Bismarck):
 - Fort Union coal region geochemistry (R. L. Houghton)
- Oregon (w, Portland):
 - Iron geochemistry at Coos Bay (J. E. Luzier)

Geochemistry and petrology, field studies:

- Anhydrite (W. E. Dean, D)
- Basalt, genesis (T. L. Wright, NC)
- Basin and Range granites (D. E. Lee, D)
- Clinker (J. R. Herring, D)
- Continental evaporite deposition processes (G. I. Smith, M; I. Friedman, D)
- Experimental petrology of basalt (R. L. Helz, M)
- Fluid-inclusion and light-stable isotope studies, sulfide minerals (W. E. Hall, M)
- Geochemistry and ore deposits of late magmatic environment (P. J. Modreski, D)
- Geochemistry of Tippecanoe Sequence, Western Craton (L. G. Schultz, D)
- Hydrothermal alteration in the Cascades (M. H. Beeson, M)
- Lake sediments (W. E. Dean, Jr., D)
- Late Cenozoic magmatic systems (R. L. Christianson, M)
- Layered Dufek intrusion, Antarctica (A. B. Ford, M)
- Layered intrusives (N. J. Page, M)
- Marine sediments (W. E. Dean, Jr., D)
- Metavolcanic terranes (Henry Bell III, NC)
- Organic petrology of sedimentary rocks (N. H. Bostick, D)

Geochemistry and petrology, field studies—Continued

- Petrogenesis and metallogeny—Western U.S. volcanic belts and ore deposits (C. M. Conway, M)
- Platinum-group elements from unconventional sources (R. R. Carlson, D)
- Platinum-group metals resources (N. J. Page, M)
- Recent volcanic processes (J. G. Moore, M)
- Regional geochemistry (W. E. Dean, Jr., D)
- Regional volcanology (R. L. Smith, NC)
- Residual minor elements in igneous rocks and veins (George Phair, NC)
- Solution transport of heavy metals (G. K. Czamanske, M)
- Sphagnum bogs (W. E. Dean, Jr., D)
- Thermal waters, origin and characteristics (D. E. White, M)
- Trace elements in oil shale (W. E. Dean, Jr., D)
- Ultramafic xenoliths in basalts (H. G. Wilshire, M)
- Uranium, radon, and helium—gaseous emanation detection (G. M. Reimer, D)
- Volcanic evolution of the Crater Lake region (C. R. Bacon, M)
- Western coal regions:
- Geochemical survey of vegetation (J. A. Erdman, D)
- Geochemistry of clinker (J. R. Herring, D)
- Western energy regions:
- Element availability—plants (L. P. Gough, D)
- Element availability—rocks (J. M. McNeal, D)
- Element availability—soils (R. C. Severson, D)
- States:
- Alaska (M, except as otherwise noted):
- Island arcs (Fred Barker, D)
- La Perouse layered intrusion (R. A. Loney)
- Petersburg quadrangle (D. A. Brew)
- Petrographic studies, Yukon-Tanana Upland (C. Dusel-Bacon)
- California:
- Clear Lake volcanics (B. C. Hearn, Jr., NC)
- Geochemistry of sediments, San Francisco Bay (D. S. McCulloch, M)
- Granitic rocks of Yosemite National Park (D. L. Peck, NC)
- Kings Canyon National Park (J. G. Moore, M)
- Long Valley Caldera-Mono Basin geothermal area (R. A. Bailey, NC)
- Colorado, Petrology of Mt. Princeton igneous complex (Priestley Toulmin III, NC)
- Hawaii (Hawaii National Park, except as otherwise noted):
- Earthquake studies (R. W. Decker)
- Eruptive history of Mauna Loa (J. P. Lockwood)
- Eruptive processes (R. I. Tilling, NC)
- Geothermal energy (R. W. Decker)
- Petrology of Hualalai Volcano (R. B. Moore)
- Idaho, Wood River district (W. E. Hall, M)
- Montana:
- Diatremes, Missouri River Breaks (B. C. Hearn, Jr., NC)
- Pioneer batholith (E-an Zen, J. M. Hammarstrom, NC)
- Wolf Creek area, petrology (R. G. Schmidt, NC)
- Pennsylvania, Geochemistry of Pittsburgh urban area (H. A. Tourtelot, D)
- South Dakota, Keystone pegmatite area (J. J. Norton, Rapid City)

Geochronological investigations:

- Carbon-14 method (Meyer Rubin, NC)
- Geothermal (M. A. Lanphere, M)
- Igneous rocks and deformational periods (R. W. Kistler, M)
- Lead-uranium, lead-thorium, and lead-alpha methods (T. W. Stern, NC)

Geochronological investigations—Continued

- Quaternary dating techniques, numerical and relative-age (K. L. Pierce, D)
- Radioactive-disequilibrium studies (J. N. Rosholt, D)
- Williston Basin geochronology (Z. E. Peterman, D)
- States:
- Alaska:
- Central and western (F. H. Wilson, M)
- Southeastern (J. G. Smith, M)
- Colorado, Geochronology of Denver area (C. E. Hedge, D)
- Montana, Geochronology, north-central Montana (B. C. Hearn, Jr., NC; R. F. Marvin, R. E. Zartman, D)
- See also Isotope and nuclear studies.

Geologic mapping:

- Map scale smaller than 1:62,500:
- Antarctica, Dufek Massif and Forrestal Range, Pensacola Mountains (A. B. Ford, M)
- Belt basin study (J. E. Harrison, D)
- Columbia River Basalt (D. A. Swanson, M)
- Ouachita Mountains, Arkansas-Oklahoma (B. R. Haley, Little Rock)
- States:
- Alaska (M):
- Hughes-Shungnak area (W. W. Patton, Jr.)
- Juneau and Taku River quadrangles (D. A. Brew)
- Metamorphic facies map (Cynthia Dusel-Bacon)
- Petersburg quadrangle (D. A. Brew)
- St. Lawrence Island (W. W. Patton, Jr.)
- Yukon-Tanana Upland (H. L. Foster, F. R. Weber, Cynthia Dusel-Bacon)
- California (M):
- Cascade Range (J. G. Smith)
- Tectonic studies, Great Valley area (J. A. Bartow, D. E. Marchand)
- Terrane boundary relations, northwest (R. J. McLaughlin)
- Yosemite National Park (N. K. Huber)
- Colorado (D):
- Denver 2-degree quadrangle (B. H. Bryant)
- Geologic map (O. L. Tweto)
- Leadville 2-degree quadrangle (O. L. Tweto)
- Neotectonic map of Colorado (S. M. Colman)
- Pueblo 2-degree quadrangle (G. R. Scott)
- Sterling 2-degree quadrangle (G. R. Scott)
- Connecticut, Cooperative mapping program (J. R. Stone, NC)
- Georgia (Atlanta)
- Atlanta 2-degree quadrangle (M. W. Higgins)
- Barnwell 1-degree quadrangle (D. C. Prowell)
- Idaho (D):
- Challis Volcanics (D. H. McIntyre)
- Idaho Falls 2-degree quadrangle (M. A. Kuntz)
- Preston 2-degree quadrangle (S. S. Oriol)
- Snake River Plain region, eastern part (S. S. Oriol)
- Maine:
- Bangor 2-degree quadrangle (P. H. Osberg)
- Lewiston 2-degree quadrangle (N. L. Hatch, Jr., NC)
- Montana (D):
- Butte, 2-degree quadrangle (C. A. Wallace)
- Dillon 2-degree quadrangle (E. T. Ruppel)
- Wallace 2-degree quadrangle (J. E. Harrison)
- Williston basin (R. B. Colton)
- Nebraska, central basin (George Prichard, D)
- New Hampshire:

Geologic mapping—Continued

- Glens Falls 2-degree quadrangle (J. B. Thompson, Jr., Cambridge, Mass.)
- Lewiston 2-degree quadrangle (N. L. Hatch, Jr., NC)
- New Jersey, Pennsylvania, New York, Newark 2-degree quadrangle (P. T. Lyttle, NC)
- New Mexico (D):
- North Church Rock area (A. R. Kirk)
- Sanostee (A. C. Huffman, Jr.)
- Santa Fe 2-degree quadrangle, western half (E. H. Baltz, Jr.)
- Tusas Mountains (Kim Manley)
- North Carolina, Charlotte 2-degree sheet (Richard Goldsmith, NC)
- North Dakota, Williston basin (R. B. Colton, D)
- Oregon (M)
- Cascade Range (J. G. Smith)
- State geologic map (G. W. Walker)
- South Carolina, Charlotte 2-degree sheet (Richard Goldsmith, NC)
- Utah (M), except as otherwise noted:
- Price 2-degree quadrangle (I. J. Witkind)
- Richfield 2-degree quadrangle (H. T. Morris)
- Tooele 2-degree quadrangle (W. J. Moore)
- Wasatch Front surficial geology (R. D. Miller, D)
- Wasatch-Uinta Tectonics, Salt Lake City and Ogden 2-degree quadrangles (B. H. Bryant, D)
- Vermont, Glens Falls 2-degree quadrangle (J. B. Thompson, Jr., Cambridge, Mass.)
- Washington (M):
- Cascade Range (J. G. Smith)
- Okanogan 2-degree quadrangle (K. F. Fox, Jr.)
- West Wenatchee 1-degree sheet (R. W. Tabor)
- Washington, Idaho, and Montana, Sandpoint 2-degree sheet (F. K. Miller, Spokane)
- Washington-Oregon, NW Olympic land-sea transect (P. D. Snively, Jr., M)
- West Virginia, Marlinton 1-degree quadrangle (W. L. Peterson, NC)
- Wyoming:
- Geologic map (J. D. Love, Laramie)
- Preston 2-degree quadrangle (S. S. Oriol, D)
- Teton Wilderness (J. D. Love, Laramie)
- Wasatch-Uinta Tectonics, Ogden 2-degree quadrangle (B. H. Bryant, D)
- Map scale 1:62,500 and larger:
- States and territories:*
- Alaska:
- Anatuvuk Pass (G. B. Shearer, c, Anchorage)
- Bering River coal field (R. B. Sanders, c, Anchorage)
- Geology and mineral resources of the Ketchikan quadrangle (H. C. Berg, M)
- Nelchina area, Mesozoic investigations (Arthur Grantz, M)
- Nenana coal investigations (Clyde Wahrhaftig, M)
- Regional engineering geology of Cook Inlet coal lands (H. R. Schmoll and L. A. Yehle, D)
- West Chichagof-Yakobi Islands (B. R. Johnson, M)
- Yukon-Tanana Upland (F. R. Weber)
- Arizona:
- Bagdad, vicinity of Old Dick and Bruce mines (C. M. Conway, M)
- Cummings Mesas quadrangle (Fred Peterson, D)
- Hackberry Mountain area (D. P. Elston, Flagstaff)
- Mt. Wrightson quadrangle (H. D. Drewes, D)

Geologic mapping—Continued

- California (M, except as otherwise noted):
- Elk Creek-Black Butte areas (R. J. McLaughlin)
- El Paso Mountains and Pilot Knob Valley areas (M. D. Carr)
- Lassen Volcanic National Park (L. J. P. Muffler)
- Long Valley caldera (R. A. Bailey, NC)
- Merced Peak quadrangle (D. L. Peck, NC)
- Metamorphic framework, Klamath Mountains (R. G. Coleman)
- Northern Sierra accreted terrane (D. S. Harwood)
- Pacific Palisades landslide area, Los Angeles (J. T. McGill, D)
- Palo Alto, San Mateo, and Montara Mountain quadrangles (E. H. Pampeyan)
- Peninsular Ranges (V. R. Todd, La Jolla)
- Regional fault studies (E. J. Helley, D. G. Herd, B. F. Atwater)
- Sierra Nevada batholith (P. C. Bateman)
- Western Santa Monica Mountains (R. H. Campbell, NC)
- Colorado (D, except as otherwise noted):
- Central City area (R. B. Taylor)
- Central Roan Plateau (W. J. Hail)
- Citadel Plateau (G. A. Izett, NC)
- Middle Dry Fork quadrangle (R. C. Johnson)
- Northern Park Range (G. L. Snyder)
- Rocky Mountain National Park (W. A. Braddock)
- Connecticut, Cooperative mapping program (J. R. Stone, NC)
- Georgia (NC):
- Coastal plain stratigraphy and structure (Juergen Reinhardt)
- Greenville 2-degree quadrangle (A. E. Nelson)
- Idaho (D, except as otherwise noted):
- Bayhorse area (S. W. Hobbs)
- Boulder Mountains (C. M. Tschanz)
- Goat Mountain quadrangle (M. H. Staatz)
- Malad SE quadrangle (S. S. Oriol)
- Wood River district (W. E. Hall, M)
- Maine:
- Rumford quadrangle (R. H. Moench, D)
- The Forks quadrangle (F. C. Canney, D)
- Massachusetts:
- Boston and vicinity (C. A. Kaye, Boston)
- Cooperative mapping program (B. D. Stone, NC)
- Michigan, Gogebic Range, western part (R. G. Schmidt, NC)
- Minnesota, Vermilion greenstone belt (P. K. Sims, D)
- Montana:
- Cooke City quadrangle (J. E. Elliott, D)
- Craig quadrangle (R. G. Schmidt, NC)
- Lemhi Pass quadrangle (M. H. Staatz, D)
- Northern Pioneer Range, geologic environment (E-an Zen, NC)
- Wolf Creek area, petrology (R. G. Schmidt, NC)
- Nevada:
- Austin quadrangle (E. H. McKee, M)
- Midas-Jarbridge area (R. R. Coats, M)
- Round Mountain and Manhattan quadrangles (D. R. Shawe, D)
- New Mexico (D, except as otherwise noted):
- Cretaceous stratigraphy, San Juan Basin (E. R. Landis)
- Hillsboro quadrangle (D. C. Hedlund)
- Iron Mountain (A. V. Heyl, Jr.)
- Lower San Francisco area (J. C. Ratté)

Geologic mapping—Continued

- Manzano Mountains (D. A. Myers)
- Mongollon quadrangle (J. C. Ratté)
- Raton coal basin, western part (C. L. Pillmore)
- Tusas Mountains (Kim Manley)
- Valles Mountains, petrology (R. L. Smith, NC)
- New York, Geologic correlations and mineral resources in Precambrian rocks of St. Lawrence lowlands (C. E. Brown, NC)
- North Carolina, Central Piedmont (A. A. Stromquist, D)
- Puerto Rico (R. D. Krushensky, NC)
- South Carolina:
 - Charleston region (G. S. Gohn, NC)
 - Greenville 2-degree quadrangle (A. E. Nelson, NC)
- South Dakota:
 - Keystone pegmatite area (J. J. Norton, Rapid City)
- Texas:
 - Tilden-Loma Alta area (K. A. Dickinson, D)
- Utah (D, except as otherwise noted):
 - Basin Canyon quadrangle (Fred Peterson)
 - Blackburn Canyon quadrangle (Fred Peterson)
 - Redmond quadrangle (I. J. Witkind)
 - Salt Lake City and vicinity (Richard VanHorn)
 - Sheeprock Mountains, West Tintic district (H. T. Morris, M)
 - Sunset Flat quadrangle (Fred Peterson)
 - Wasatch Front surficial geology (W. E. Scott)
 - Willard Peak area (M. D. Crittenden, Jr., M)
- Virginia (NC):
 - Culpeper Basin (A. J. Froelich)
 - Rapidan-Rappahannock (Louis Pavlides)
 - Rose Land district (E. R. Force)
- Washington (M):
 - Colville Indian Reservation (C. D. Rinehart)
 - Doe Mountain quadrangle (V. R. Todd)
 - Northern Okanogan Highlands (C. D. Rinehart)
 - Olympic Peninsula, offshore-onshore geologic transect (P. D. Snavely, Jr.)
- Wyoming (D, except as otherwise noted):
 - Banner quadrangle (E. N. Hinrichs)
 - Fortin Draw quadrangle (B. E. Law)
 - Gillette East quadrangle (B. E. Law)
 - Grand Teton National Park (J. D. Love, Laramie)
 - Moyer Springs quadrangle (B. E. Law)
 - Oriva quadrangle (B. E. Law)
 - Story quadrangle (E. N. Hinrichs)

Geologic mapping, water:

- Geochemical controls—quality of water (Ivan Barnes, w, M)
- Oregon coastal sedimentation (R. J. Janda, w, M)
- States:
 - Florida (w, Tallahassee):
 - Susceptibility of surficial aquifers (W. C. Sinclair, Tampa)
 - Michigan (w, Lansing):
 - Geohydrology—environmental planning (F. R. Twenter)
 - North Dakota (w, Bismarck):
 - Geohydrology of Jurassic-Tertiary (O. A. Crosby)
 - New York (w, Albany):
 - Hydrogeology of Nassau County (Chabot Kilburn, Syosset)

Geomagnetism:

- Geomagnetic applications (W. H. Campbell, D)
- Geomagnetic instrumentation (R. W. Kuberry, D)
- Geomagnetic observatories (J. D. Wood, D); data processing and analysis (R. G. Green, D)
- Geomagnetic polarity time scale and paleosecular variations

Geomagnetism—Continued

- and magnetization of sedimentary rocks (E. A. Mankinen, M)
- Geomagnetic secular variation (L. R. Alldredge; N. W. Peddie, D)
- Geomagnetic-telluric array investigations, geoelectrical structure, crust and upper mantle (J. N. Towle, D)
- Global geomagnetism (J. C. Cain, D)
- Magnetic-field analysis and U.S. charts (E. B. Fabiano, D)
- Paleomagnetism of mineralized terranes (D. P. Elston, Flagstaff)
- Paleomagnetism of accreted terranes, Alaska (J. W. Hillhouse, M)
- Paleomagnetism of hydrothermal ore deposits (D. L. Champion, M)
- Paleosecular variation (D. P. Elston, Flagstaff)
- World magnetic charts and analysis (E. B. Fabiano, D)
- Geomorphology:**
 - Fermentation and characteristics of clinker, Central United States (D. A. Coates, D)
 - Recovery rates, prehistoric roads (E. B. Newman, M)
 - Sedimentary structures (E. D. McKee, D)
 - States:
 - Utah, Quaternary geology (W. E. Scott, D)
 - Wyoming, Quaternary geology (G. M. Richmond, D)
 - See also Sediment; Geochronological investigations.
 - Surface processes in arid lands (H. G. Wilshire, M)
- Geomorphology, water:**
 - Field coordination (J. F. McCain, w, NC)
 - States:
 - Colorado (w, Lakewood):
 - Hydraulics of stream channels (J. G. Elliott, D)
 - Yampa River sediment (J. G. Elliott, D)
 - Florida (w, Tallahassee):
 - Geohydrology of sinkholes (W. C. Sinclair, Tampa)
 - Washington (w, Tacoma):
 - Pine and Muddy geomorphology (H. A. Martinson)
- Geophysics, regional:**
 - Airborne and satellite research:
 - Aeromagnetic studies (M. F. Kane, D)
 - Applications of airborne and satellite magnetic data (J. D. Phillips, NC)
 - Electromagnetic research (F. C. Frischknecht, D)
 - Gamma-ray research (J. S. Duval, D)
 - Cascade Range (D. L. Williams, D)
 - Crust and upper mantle:
 - Mafic/ultramafic belts (J. E. Case, M)
 - Seismicity and Earth structure (G. L. Chay, D)
 - Seismologic studies (J. P. Eaton, M)
 - Deep electromagnetic soundings, Western United States (J. N. Towle, D)
 - Engineering geophysics (H. D. Ackermann, D)
 - Gravity and magnetics, Eastern overthrust belt (J. D. Phillips, NC)
 - Gravity studies, San Andreas fault (R. C. Jachens, M)
 - Great Lakes (R. J. Wold, D)
 - Indian lands, Eastern United States (B. D. Smith, D)
 - Magnetic chronology, Colorado Plateau and environs (D. P. Elston, E. M. Shoemaker, Flagstaff, Ariz.)
 - Midcontinent rift system (R. J. Wold, D)
 - Mobile magnetometer profiles, Eastern United States (M. F. Kane, D)
 - Northern Rocky Mountain overthrust belt (M. D. Kleinkopf, D)
 - Rainier Mesa (J. R. Ege)
 - Reduction of aeromagnetic data to basement (L. E. Cordell, D)
 - Repeat magnetic surveys (J. D. Woods, D)

Geophysics, regional—Continued

Thermal modeling investigations (Kenneth Watson, D)
United States and North America magnetic map (D. R. Mabey, D)

*States and territories:***Alaska (D):**

Gravity and magnetic interpretations (J. W. Cady)
Mining geophysics (D. L. Campbell)
Northern geophysics (J. W. Cady)
Uranium geophysics (J. W. Cady)

Arizona, Aeromagnetic survey, San Francisco volcanic field (R. J. Blakely, M)

Arizona-California desert land, geophysical studies (R. W. Simpson, Jr., M)

California, Sierra Nevada, geophysical studies (H. W. Oliver, M)
Montana, Glacier National Park gravity studies (D. M. Wilson, D)

Nevada:

Cooperative aeromagnetic and gravity surveys (H. W. Oliver, M)
Engineering geophysics, Nevada Test Site (R. D. Carroll, D)
Petrophysics, Nevada Test Site (L. A. Anderson, D)

North Dakota-South Dakota, Precambrian basement magnetics (E. R. King, NC)

Washington, Colville Indian Reservation (V. J. Flanigan, D)

Geophysics, theoretical and experimental:

Borehole geophysical research in uranium exploration (J. H. Scott, D)

Deep geoelectrical soundings (F. C. Frischknecht, D)

Earthquakes, local seismic studies (J. P. Eaton, M)

Elastic and inelastic properties of Earth materials (Louis Peselnick, M)

Electrical properties of rocks (R. D. Carroll, D)

Electrical resistivity studies (A. A. R. Zohdy, D)

Electromagnetic induction applications to the Earth's conductivity structure (D. P. Klein, D)

Electromagnetic modeling and inversion of controlled source measurements (W. L. Anderson, D)

Gamma-ray spectrometry for uranium exploration in crystalline terranes (J. A. Pitkin, D)

Gamma-ray spectrometry in uranium (J. S. Duval, D)

Geophysical studies applied to mineral resource recognition (D. P. Klein, D)

Geophysical studies for engineering geology (C. H. Miller, D)

Geophysical studies relating to mineral deposits (W. F. Hanna, D)

Geophysical studies relating to uranium deposits in crystalline terranes (D. L. Campbell, D)

Magnetic and luminescent properties (F. E. Senftle, NC)

Mathematical geophysics (R. H. Godson, D)

Mineral research petrophysics (G. R. Olhoeft, D)

NASA, electrical properties for the detection and mapping of waters on Mars (G. R. Olhoeft, D)

NASA, laboratory microwave, radar, and thermal-emission studies of basalt soil in vacuum (G. R. Olhoeft, D)

Paleomagnetic dating (J. W. Hillhouse, M)

Paleomagnetism, Precambrian and Tertiary chronology (D. P. Elston, Flagstaff)

Petrophysics-geothermal (G. R. Olhoeft, D)

Remanent magnetization of rocks (C. S. Grommé, M)

Resistivity interpretation (A. A. R. Zohdy, D)

Rock behavior at high temperature and pressure (E. C. Robertson, NC)

Theoretical studies of potential field data (R. J. Blakely, M)

Geophysics, theoretical and experimental—Continued

Theory of gamma rays for geological applications (J. S. Duval, D)

Thermal modeling investigations (Kenneth Watson, D)

Thermodynamic properties of rocks (R. A. Robie, NC)

Uranium geophysics in frontier areas (J. W. Cady, D)

Uranium petrophysics (G. R. Olhoeft, D)

Volcano geophysics (E. T. Endo, M)

*States:***Nevada (D):****Nevada Test Site:**

Interpretation of geophysical logs (R. D. Carroll)

Seismic velocity measuring techniques (R. D. Carroll)

Geophysics, water:

Ground water geophysics research (A. A. R. Zohdy, D)

*States:***Arizona (w, Tucson):**

Borehole geophysics (Chester Zenone, Phoenix)

Connecticut (w, Hartford):

Surface geophysics in ground-water investigations (F. P. Haeni)

Hawaii (w, Honolulu):

Schofield geophysics (C. D. Hunt)

New Jersey (w, Trenton):

Geophysical characteristics (R. L. Walker)

Geotechnical investigations:

Computer modeling research for engineering geology (W. Z. Savage, D)

Dynamic soil behavior (A. T. F. Chen, M)

Earthquake-induced landslides (E. L. Harp, M)

Electronics instrumentation research for engineering geology (J. B. Bennetti, Jr., D)

Experimental liquefaction potential mapping (T. L. Youd, M)

Fissuring-subsidence research (T. L. Holzer, M)

Geomechanics of radioactive waste storage (H. S. Swolfs, D)

Geotechnical measurements (R. W. Nichols, D)

Interaction of ground motion and ground failure (R. C. Wilson, M)

Landslide investigations (R. W. Fleming, D)

Marine geotechnique (H. W. Olsen, D)

Research in rock mechanics (F. T. Lee, D)

Solution subsidence and collapse (J. R. Ege, D)

States:

Alaska, Regional engineering geology of Cook Inlet coal lands, Alaska (H. R. Schmoll and L. A. Yehle, D)

Montana-Wyoming, Regional geotechnical studies, Powder River Basin (S. P. Kanizay, D)

Wyoming, Coal mine deformation studies, Powder River Basin (C. R. Dunrud, D)

Geothermal investigations:

Broad-band electrical surveys (Mark Landisman, University of Texas)

Colorado Plateau, potential field methods (R. R. Wahl, D)

Convection and thermoelastic effects in narrow vertical fracture spaces:

Analytical techniques (Gunnar Bodvarsson, Oregon State University)

Numerical techniques (R. P. Lowell, Georgia Institute of Technology)

Development of first-motion holography for exploration (Keiiti Aki, Massachusetts Institute of Technology)

Electrical and electromagnetic methods in geothermal areas (D. B. Jackson, D)

Electrical techniques for shallow to medium depth exploration of geothermal systems (D. B. Hoover, D)

Fossil systems and roots of calderas (R. W. Lipman, D)

Geothermal investigations—Continued

- Geochemical exploration (M. E. Hinkle, D)
 Geochemical indicators (A. H. Truesdell, M)
 Geophysical characterization of young silicic volcanic centers, eastern Sierran Front (W. F. Isherwood, D)
 Geothermal geophysics (D. R. Mabey, D)
 Geothermal helium sniffing (Irving Friedman, D)
 Geothermal petrophysics (G. R. Olhoeft, D)
 Geothermal reservoirs (Manuel Nathenson, M)
 Geothermal resource assessment (L. J. P. Muffler, M)
 Geothermal resources data file (J. R. Swanson, M)
 Geothermal studies (A. H. Lachenbruch, M)
 Gravity variations as a monitor of water levels (J. M. Goodkind, University of California, San Diego)
 Heat flow (J. H. Sass, A. H. Lachenbruch, M)
 Low-frequency electromagnetic prospecting system (J. Clarke and H. F. Morrison, University of California, Berkeley)
 Magnetotelluric sounding, geothermal resource assessment (W. D. Stanley, D)
 Mapping of volcanic and conducted heat flow sources for thermal springs in the Western United States (William J. Jenkins, Woods Hole Oceanographic Institution)
 Mercury geochemistry as a tool for geothermal exploration (P. R. Buseck, Arizona State University)
 Multiphase fluid flow in geothermal systems (S. W. Kieffer, Flagstaff)
 Oxygen isotopes (J. R. O'Neil, M)
 Physics of geothermal systems (W. H. Diment, M)
 Regional volcanology (R. L. Smith, NC)
 Remote sensing (Kenneth Watson, D)
 Rock-water interactions (R. O. Fournier, M)
 Seismic exploration (P. L. Ward, M)
 Self-potential geothermal studies (D. V. Fitterman, D)
 Thermal waters (D. E. White, M)
States:
 Alaska, Geothermal reconnaissance (T. P. Miller, M)
 Arizona:
 Hackberry Mountain volcanic center (R. E. Lewis, Flagstaff)
 San Francisco volcanic field (E. W. Wolfe, Flagstaff)
 Springerville-White Mountains volcanic field (E. W. Wolfe, Flagstaff)
 California:
 Aeromagnetic measurements in the Cascade Range and Modoc Plateau (Richard Couch, Oregon State University)
 Coso area, passive seismology (P. A. Reasenber, M)
 Geology of Long Valley-Mono basin (R. A. Bailey, NC)
 Long Valley, active seismology (W. D. Mooney, M)
 Medicine Lake Volcano (J. R. Donnelly-Nolan, M)
 Microearthquake monitoring:
 Imperial Valley (D. P. Hill, M)
 The Geysers-Clear Lake (C. G. Bufe, M)
 Mt. Lassen thermal areas (L. J. P. Muffler, M)
 The Geysers area, seismic noise (H. M. Iyer, M)
 The Geysers-Clear Lake (B. C. Hern, Jr., NC)
 Volcanotectonics and thermogeology, southeastern part of the Cascade Range (L. T. Grose, Colorado School of Mines)
 Hawaii, Kilauea Volcano, potential field methods for subsurface magma mapping (C. J. Zablocki, NC)
 Idaho:
 Evaluation of detailed seismic refraction profiling for regional geothermal exploration in the Yellowstone and Snake River Plain regions and adjacent areas

Geothermal investigations—Continued

- (Lawrence Braile, Purdue University)
 Snake River Plain surface and subsurface geology (M. A. Kuntz, D)
 Montana, evaluation of detailed seismic refraction profiling for regional geothermal exploration in the Yellowstone and Snake River Plain regions and adjacent areas (Lawrence Braile, Purdue University)
 Nevada, Geothermal reconnaissance (R. K. Hose, M)
 North Carolina, Basement trends in metamorphism, plutonism, and heat flow under the Atlantic coastal plain for potential geothermal resources (Lynn Glover and John Costain, Virginia Polytechnic Institute and State University)
Oregon:
 Aeromagnetic measurements in Cascade Range (Richard Couch, Oregon State University)
 Gravity measurements in the Cascade Range near Breitenbush Hot Springs (Richard Couch, Oregon State University)
 Hydrothermal alteration, Cascade (M. H. Beeson, M)
 Interpretation of aeromagnetic measurements for geothermal assessment (Richard Couch, Oregon State University)
Wyoming:
 Evaluation of detailed seismic refraction profiling for regional geothermal exploration in the Yellowstone and Snake River Plain regions and adjacent areas (Lawrence Braile, Purdue University)
 Yellowstone thermal areas, geology (M. H. Beeson, M)
Geothermal investigations, water:
 Geochemistry of geopressured systems (Y. K. Kharaka, w, M)
 Geothermal, Coachella Valley (J. H. Robison, w, M)
 Geothermal coordination (F. H. Olmsted, w, M)
 Geothermal reconnaissance, Oregon (E. A. Sammel, w, M)
 Geothermal subsidence research (F. S. Riley, w, D)
 Nevada geothermal (F. H. Olmsted, w, M)
 Western U.S. geochemistry (R. H. Mariner, w, M)
States:
 Arizona (w, Tucson):
 Geothermal water, Salt River valley (P. P. Ross, Flagstaff)
 Colorado (w, Lakewood):
 Colorado geothermal (R. E. Moran, D)
 Hawaii (w, Honolulu):
 Geothermal hydrology (K. J. Takasaki)
 Idaho (w, Boise):
 Idaho geothermal (H. W. Young)
 Maryland (w, Towson):
 Maryland springs and thermal energy (E. G. Otton)
 Montana (w, Helena):
 Geothermal investigations in Montana (R. B. Leonard)
 Nevada (w, Carson City):
 Black Rock Desert geothermal (A. H. Welch)
 Humboldt House geothermal (D. H. Schaefer)
 Utah (w, Salt Lake City):
 Geothermal reconnaissance, Utah (F. F. Rush)
Glaciology and ice:
 Alaska glaciology (L. R. Mayo, w, Fairbanks)
 Changes in glacier volumes (M. F. Meier, w, Tacoma, Wash.)
 Glacier mass balances (L. R. Mayo, w, Fairbanks)
 Glacier response to climate (S. M. Hodge, w, Tacoma, Wash.)
 Knik Glacier (L. R. Mayo, Fairbanks)
 Reconstruction of streamflow (S. M. Hodge, w, Tacoma, Wash.)
Gold:
 Composition related to exploration (J. C. Antweiler, D)
 Disseminated gold (E. W. Tooker, M)

Gold—Continued*States:***Alaska:**

Placers, Mt. Hayes quadrangle, central district, Valdez Creek district, Ophir quadrangle (W. E. Yeend, M)

California, Klamath Mountains (P. E. Hotz, M)

Montana, Butte quadrangle (J. E. Elliott, D)

Nevada (M, except as otherwise noted):

Carlin mine (A. S. Radtke)

Comstock district (D. H. Whitehead)

Goldfield district (R. P. Ashley)

Round Mountain and Manhattan districts (D. R. Shawe, D)

Oregon-Washington, Nearshore area (P.D. Snavelly, Jr., M)

Wyoming, northwestern part, conglomerates (J. C. Antweiler)

See also Heavy metals.

Ground water, general:

Gulf coast hydrodynamics (P. C. Trescott, w, NC)

States:

Arizona (w, Tucson):

Ground water to Colorado River (S. A. Leake)

California (w, Menlo Park):

Technology transfer—CVAP (L. A. Swain, Sacramento)

Indiana (w, Indianapolis):

Assessment of reclaimed areas (S. E. Eikenberry)

Louisiana (w, Baton Rouge):

Lignite hydrology (J. L. Snider, Alexandria)

Maryland (w, Towson):

Coastal plain aquifers, Maryland-Delaware (W. B. Fleck)

Ground water from Maryland coastal plain (W. B. Fleck)

North Carolina (w, Raleigh):

North Carolina ground water ADP program (C. C. Daniel)

Washington (w, Tacoma):

Washington nonpotable aquifers (W. E. Lum)

Ground-water principles and relations:

Climax heater experiment (R. K. Waddell, w, D)

Consultation and research (C. V. Theis, w)

Energy transport in ground water (A. F. Moench, w, M)

Impact of mining on aquifers (N. J. King, w, D)

Information transfer (D. A. Rickert, w, NC)

Limestone hydraulic permeability (V. T. Stringfield, w, Washington, D.C.)

Modeling geothermal systems (M. L. Sorey, w, M)

Subsurface transport phenomena (C. I. Voss, w, NC)

Wilcox waste storage appraisal (R. H. Wallace, w, NSTL Station, Miss.)

States:

Arizona (w, Tucson):

Ground water, Vekol Valley, Arizona (J. R. Marie)

Florida (w, Tallahassee):

Quality of water study—ground water, eastern Indian River County (J. L. Smoot, Orlando)

Withlacoochee Basin, phase II (G. R. Schiner, Orlando)

Hawaii (w, Honolulu):

Oahu RASA (C. J. Ewart)

Idaho (w, Boise):

Hydrology of specified basins (R. P. Williams)

Indiana (w, Indianapolis):

Southeastern Indiana lineaments (T. K. Greeman)

Iowa (w, Iowa City):

Carbonate terrane hydrology, phase 1 (K. D. Wahl)

Kansas (w, Lawrence):

Water resources of Ford County, Kansas (Joseph Spinazola, Garden City)

Maine (w, Augusta):

Maine transition zone studies (W. J. Nichols)

Ground-water principles and relations—Continued

Michigan (w, Lansing):

Ground-water models—Muskegon County, Michigan (M. G. McDonald)

Minnesota (w, St. Paul):

Lake Williams—water balance (G. E. Groschen)

Montana (w, Helena):

Mining effects, shallow water (S. E. Slagle, Billings)

New Mexico (w, Albuquerque):

Hydrologic plan for Albuquerque Basin (G. E. Kues)

North Dakota (w, Bismarck):

Hydrology of James River, North Dakota (J. E. Miller)

Mining and reclamation, Mercer County (O. A. Crosby)

South Carolina (w, Columbia):

Framework Congaree National Monument (B. H. Whetstone)

Washington (w, Tacoma):

Hydrologic basin analysis (K. L. Walters)

Island County ground water (D. B. Sapik)

Lower Yakima summary (Dee Molenaar)

West Virginia (w, Charleston):

Ground water, Romney—Lost River (W. A. Hobba, Morgantown)

Wisconsin (w, Madison):

Ground water atlas—Wisconsin (G. G. Allord)

Wyoming (w, Cheyenne):

White Mountain oil shale (K. C. Glover)

Ground-water supplies and availability:

Ground water in northern Jordan (Della Laura, w, NC)

Ground water, Southeastern States (D. D. Cederstrom, w, NC)

Hydrologic remote sensing (G. K. Moore, w, Sioux Falls, S. Dak.)

Mississippi embayment—West Gulf Coast—RASA (H. F. Grubb, w, Austin, Tex.)

North Atlantic coast RASA (Harold Meisler, w)

Northeastern glacial valleys aquifers (F. P. Lyford, w, Albany, N.Y.)

Northern Great Plains aquifer study (G. A. Dinwiddle, w, D)

States:

Alaska (w, Anchorage):

Capps Creek coal study (G. L. Nelson)

Kenai Borough project (G. L. Nelson)

Point McKenzie hydrology (L. D. Patrick)

Arizona (w, Tucson):

Special site studies (R. D. MacNish)

Tucson-Phoenix urban study (E. S. Davidson)

Water resources of Coconino County (E. H. McGavock, Flagstaff)

Water supply, Lake Mead area (R. L. Laney, Phoenix)

Water use (S. G. Brown)

Arkansas (w, Little Rock):

Central Midwest RASA, Arkansas (A. H. Ludwig)

Hydrology of Claiborne and Wilcox (M. E. Broom)

California (w, Menlo Park):

Central Valley aquifers (G. L. Bertoldi, Sacramento)

Data, Antelope Valley-East Kern (D. J. Downing, Laguna Niguel)

Ground water, Indian Wells Valley (P. A. Lipinski, Laguna Niguel)

Ground-water model—Modesto (C. J. Londquist, Sacramento)

Ground water, northern Monterey County (M. J. Johnson)

Ground water, Seaside area (K. S. Muir)

Madera area ground-water model (C. J. Londquist, Sacramento)

Ground-water supplies and availability—Continued

- Mendocino County ground water (C. D. Farrar)
 Nevada County ground-water study (H. T. Mitten, Sacramento)
 Northeast counties ground-water investigation (M. J. Pierce, Sacramento)
 Pajaro Valley ground-water model (G. W. Kapple)
 Tassajara ground-water study (R. L. Glass)
 Water resources, Vandenberg AFB (J. A. Singer, Laguna Niguel)
 Water resources of Lanfair—Fenner Valleys (D. A. Freiwald, Laguna Niguel)
 Yosemite appraisal (W. R. Hotchkiss, Sacramento)
- Colorado (w, Lakewood):
 Colorado central Midwest RASA (S. G. Robson, D)
 Ground water, southwestern Colorado (Robert E Brogden, D)
 Roan-Parachute ground-water model (O. O. Taylor, D)
 Upper Colorado RASA (O. O. Taylor, D)
- Connecticut (w, Hartford):
 Evaluation of stratified drift deposits (S. J. Grady)
 Ground-water development in Simsbury, Conn. (J. W. Bingham)
 Recharge areas for stratified drift (E. H. Handman)
 Short-term studies (C. E. Thomas)
- Delaware (w, Dover):
 Digital model of southwestern Delaware (J. M. Denver)
- Florida (w, Tallahassee):
 Englewood Water District (H. R. Sutcliffe, Sarasota)
 Geohydrology of central Sarasota (H. R. Sutcliffe, Sarasota)
 Ground water, northeastern Seminole County (G. G. Phelps, Orlando)
 Ground-water reappraisal, Orange County (A. S. Navoy, Orlando)
 Ground-water sources of drinking water, Florida (B. J. Franks)
 Hydrogeology, Pinellas County (K. W. Causseaux, Tampa)
 Hydrology of Hernando County (J. D. Fretwell, Tampa)
 Investigation of hydrology of St. Johns County (P. S. Hampson, Jacksonville)
 Potentiometric maps in Southwest Florida Water Management District (D. K. Yobbi, Tampa)
 Quantitative study, Biscayne aquifer (Howard Klein, Miami)
 Water for Florida cities (G. W. Leve, Jacksonville)
 Water resources, Duval-Nassau (E. C. Hayes, Jacksonville)
 Water resources, Flagler County (A. S. Navoy, Orlando)
 Water resources, Hendry County (J. E. Fish, Miami)
 Water resources, Lee County (F. A. Watkins, Fort Myers)
 Water resources, Tequesta (A. L. Knight, Miami)
 Water supply, southwest Brevard County (Michael Planert, Orlando)
- Georgia (w, Doraville):
 Ground water, Atlanta region (C. W. Cressler)
 Ground water, post-Oligocene (E. A. Zimmerman, Brunswick)
 Ocala aquifer—Albany area (D. W. Hicks, Albany)
- Hawaii (w, Honolulu):
 Data management, Guam (C. J. Huxel, Agana, Guam)
 Kalaupapa water resources (W. R. Souza)
 Kauai water-resources survey (R. R. Burt)
 Kipahula water resources (W. R. Souza)
 Water resources, Kawailoa, Oahu (C. D. Hunt)
 Water resources of southeastern Oahu (K. J. Takasaki)

Ground-water supplies and availability—Continued

- Water-resources information, northern Marianas (D. A. Davis)
- Idaho (w, Boise):
 Banbury Hot Springs (R. E. Lewis)
 Ground water for irrigation on Bruneau Plateau (R. L. Moffatt)
- Indiana (w, Indianapolis)
 Decatur County (T. K. Greeman)
 Ground water, upper West Fork White River basin (W. W. Lapham)
 Indiana Dunes ground-water study (R. J. Shedlock)
 Jennings County fracture trace (T. K. Greeman)
 Johnson-Morgan ground-water study (Zelda Bailey)
 Southeastern Indiana lineament study (T. K. Greeman)
- Iowa (w, Iowa City):
 Water resources of north-central Iowa (R. C. Buchmiller)
- Kentucky (w, Louisville):
 Mississippian Plateau region (R. J. Faust)
- Louisiana (w, Baton Rouge):
 Ground-water conditions, New Orleans area (D. C. Dial)
 Site studies (J. E. Rogers, Alexandria)
 Southwestern Louisiana (D. J. Nyman)
- Maine (w, Augusta):
 Significant Maine aquifers (G. C. Prescott)
- Maryland (w, Towson):
 Ground-water quality, Baltimore industrial area (F. H. Chapelle)
- Massachusetts (w, Boston):
 Northeastern Massachusetts river basins (R. A. Brackley)
 Blackstone River basin (B. E. Krejmas)
- Michigan (w, Lansing):
 Ground water, west upper peninsula (C. J. Doonan)
- Minnesota (w, St. Paul):
 Carlton, Pine, and Kanebec Counties (C. F. Myette)
 Ground-water appraisal, Pelican River sand plain (R. T. Miller)
 Ground water in southwestern Minnesota (D. G. Adolphson)
 Ground water, Todd, Cass, Morrison Counties (C. F. Myette)
 Pomme de Terre—Chippewa ground water (R. J. Wolf)
 Reconnaissance of sand-plain aquifers (H. W. Anderson)
 Underground injective control (D. G. Adolphson)
- Mississippi (w, Jackson):
 Eutaw-McShan aquifer model (J. M. Kernodle)
 Ground water near Natchez (E. H. Boswell)
 Tupelo model (J. M. Kernodle)
- Missouri (w, Rolla):
 Barton, Bates, and Vernon Counties (L. F. Emmett)
- Montana (w, Helena):
 Geohydrology, Cascade County (K. R. Wilke)
 Ground water Fort Belknap (R. D. Feltis, Billings)
 Ground-water resources, Lake Creek (K. R. Wilke)
 Hydrology of lower Flathead (A. J. Boettcher)
 Northern Great Plains aquifer study (W. R. Hotchkiss)
 Shallow aquifers, Big Dry area, Montana (S. E. Slagle)
 Special investigations (J. A. Moreland)
 Stillwater Complex (R. D. Feltis, Billings)
 Tongue River inflow (R. D. Hutchinson)
 Water resources in National Parks (J. A. Moreland)
- Nevada (w, Carson City):
 Fernley area water resources (F. E. Arteaga)
 Great Basin aquifer systems (J. R. Harrill)
- New Hampshire (w, Concord):

Ground-water supplies and availability—Continued

- Ground water, Lamprey River basin (J. E. Cotton)
- New Jersey (w, Trenton):
 - Conjunctive-use modeling (A. W. Harbaugh)
- New Mexico (w, Albuquerque):
 - Delaware Basin freshwater aquifers (J. G. Wells)
 - Harding County ground water (F. C. Trauger)
 - Lower Rio Grande valley (C. A. Wilson, Las Cruces)
 - Northern High Plains, New Mexico (E. G. Lappala)
 - San Agustin Plains ground water (C. A. Wilson, Las Cruces)
 - Sandia-Manzano Mountains (D. W. Wilkins)
 - State Engineer—miscellaneous (D. P. McAda)
 - Tularosa Basin water resources (C. A. Wilson, Las Cruces)
 - Ute Creek buried channel (W. A. Mourant)
 - Water resources, Acoma Pueblo (F. P. Lyford)
 - Water resources, Laguna Pueblo (D. W. Risser)
 - Water resources, Santa Fe (W. A. Mourant)
 - Zuni water resources (B. R. Orr)
- New York (w, Albany):
 - Pine Bush hydrology (D. S. Snively)
- North Carolina (w, Raleigh):
 - Ground water in North Carolina piedmont and mountains (C. C. Daniel)
 - Ground water, Cochecho River basin (J. E. Cotton)
- North Dakota (w, Bismarck):
 - Ground-water availability, Fort Union coal (M. G. Croft)
 - Ground water, Bottineau-Rolette, North Dakota (P. G. Randich)
 - Ground water, Logan County (R. L. Klausning)
 - Ground water, McIntosh County (R. L. Klausning)
 - Ground water, McKenzie County (M. G. Croft)
 - Ground water, National Grasslands, McKenzie County (M. G. Croft)
 - Ground water, North Dakota (Q. F. Paulson)
 - Ground water, Ransom-Sargent (C. A. Armstrong)
 - Ground-water, Towner County (P. G. Randich)
 - Hydrologic changes due to mining (W. F. Horak)
 - Hydrology of M & M deposit, North Dakota (R. L. Klausning)
 - New Leipzig coal hydrology, North Dakota (C. A. Armstrong)
 - North Great Plains aquifer study (R. D. Butler)
 - Special investigations (C. A. Armstrong)
 - West Fargo aquifer evaluation (C. A. Armstrong)
- Ohio (w, Columbus):
 - Dayton digital model (S. E. Norris)
 - Southeast Ohio aquifer study (A. C. Sedam)
- Oklahoma (w, Oklahoma City):
 - Arbuckle aquifer, Oklahoma (R. W. Fairchild)
 - Ground water, Upper Red basin (M. V. Marcher)
 - Hydrogeology, Antlers Sand (D. L. Hart)
 - Roubidoux aquifer, Oklahoma (R. W. Fairchild)
 - Special computer services (J. H. Irwin)
- Oregon (w, Portland):
 - Bend-Redmond ground water (J. B. Gonthier)
 - Ground water, Clackamas County (A. R. Leonard)
 - Ground water, Rouge River basin (J. G. Gonthier)
- Pennsylvania (w, Harrisburg):
 - Aquifer model, Berwick-Bloomsburg (J. H. Williams)
 - Coal hydrology, Greene County (D. R. Williams, Pittsburgh)
 - Ground water of Cumberland Valley, Pennsylvania (A. E. Becher)
 - Ground water of Philadelphia area (C. R. Wood, Malvern)
 - Ground-water resources of Pike County (D. K. Davis, Malvern)

Ground-water supplies and availability—Continued

- Hydrogeology of Great Valley (A. E. Becher)
- Lower Susquehanna ground water (J. M. Gerhart)
- Major fracture systems, western Pennsylvania (J. D. Stoner, Pittsburgh)
- Philadelphia ground water (C. R. Wood, Malvern)
- Water resources, western Pennsylvania (G. R. Schiner)
- Puerto Rico (w, San Juan):
 - Ground water, Canovanas-Rio Grande area (A. E. Torres-Gonzalez, Ft. Buchanan)
 - Ground-water potential, College of Virgin Island area (Fernando Gomez-Gomez, San Juan)
 - Manati water resources (Fernando Gomez-Gomez, Ft. Buchanan)
 - Water resources, lower Rio Grande de Arecibo Valley (A. L. Zack, San Juan)
- Rhode Island (w, Providence):
 - Ground water, Pawcatuck River basin (H. E. Johnston)
- South Carolina (w, Columbia):
 - Assessment of ground-water resources (A. D. Park)
- South Dakota (w, Huron):
 - High Plains aquifer study (C. L. Loskot, Rapid City)
 - Hydrogeology Cheyenne-Standing Rock (L. W. Howells)
 - Northern Great Plains aquifer study (H. L. Case, Rapid City)
 - Water resources, Walworth County (E. F. LeRoux)
 - Water resources-Deuel Hamlin (Jack Kume, Vermillion)
- Tennessee (w, Nashville):
 - Tennessee aquifer delineation (M. W. Bradley)
- Texas (w, Austin):
 - Limestone County ground water (P. L. Rettinan, San Antonio)
 - Model study, Chicot and Evangeline aquifer (L. F. Land)
 - Orange County ground water (C. W. Bonnet, Houston)
 - Rusk County ground water (W. M. Sandeen, Houston)
 - Water resources, Big Bend (E. T. Baker)
- Utah (w, Salt Lake City):
 - Great Basin aquifer systems (J. S. Gates)
 - Ground water in Sevier Desert, Utah (W. F. Holmes)
 - Ground water, Wasatch Front (Don Price)
 - Hydrology of Tooele Valley area (A. C. Razem)
 - Morgan Valley, Utah (J. S. Gates)
 - Reconnaissance, Fish Springs Flat (E. L. Bolke)
 - Upper Colorado RASA-Navajo Sandstone (J. W. Hood)
- Vermont (w, Montpelier):
 - Ground water, Rutland area, Vermont (R. E. Willey)
- Virginia (w, Richmond):
 - Culpeper basin study (Chester Zenone, Fairfax)
 - Fairfax County urban area study (Chester Zenone, Fairfax)
 - Ground-water resources, Blue Ridge Parkway (H. T. Hopkins)
- Washington (w, Tacoma):
 - Horse Heaven Hills ground water (F. A. Packard)
 - Nisqually ground water (W. E. Lum)
 - San Juan water resources (K. J. Whiteman)
 - Shoalwater water resources (W. E. Lum)
 - Test drilling (D. R. Cline)
 - Tulalip ground water (W. E. Lum)
 - Water data for coal mining (F. A. Packard)
 - Water, north Cascades (D. R. Cline)
 - Water, Yakima Reservation (E. A. Prych)
- West Virginia (w, Charleston):
 - Elk River basin study (G. T. Tarver)
 - Ground-water atlases (Celso Puente)
 - Guyandotte River study (J. S. Bader)

Ground-water supplies and availability—Continued

- Remotely-sensed ground water (W. A. Hobba, Morgan-town)
- Water resources of Gauley River basin (G. G. Wyrick)
- Water resources of Tug Fork Basin, West Virginia (J. S. Bader)
- Wisconsin (w, Madison):
 - Digital model, lower Fox River area (R. S. Grant)
 - Ground water, Dodge County (R. W. Devaul)
 - Hydrogeology, Langlade County (W. G. Batten)
 - Hydrogeology, Vilas County (E. H. Reinen)
 - Hydrology, Mole Lake Reservation (R. A. Lidwin)
- Wyoming (w, Cheyenne):
 - Green River ground water, Wyoming (E. A. Zimmerman)
 - Hanna Basin water resources (P. B. Daddow)
 - Model of Bates Hole, Wyoming (K. C. Glover)
 - Northern Great Plains aquifer study (D. T. Hoxie)
 - Saratoga Valley, Wyoming (L. W. Lenfest)
 - Weston County, Wyoming (M. E. Lowry)
- Ground-water techniques and instrumentation:**
 - California (w, Menlo Park):
 - Palmdale Bulge earthquake prediction (W. R. Moyle, Laguna Niguel)
 - Drilling techniques (Eugene Shuter, D)
- Ground-water trends:**
 - California (w, Menlo Park):
 - Water resources, Indian Reservations (J. R. Freckleton)
 - Florida (w, Tallahassee):
 - Water atlas; potentiometric surface change, St. Johns River Water Management District (H. G. Rodis, Orlando)
 - Idaho (w, Boise):
 - Ground-water trends in Idaho (A. W. Grover)
 - Illinois (w, Urbana):
 - Shallow ground water—McHenry County (J. T. Krohelski, De Kalb)
 - Kansas (w, Lawrence):
 - Hydrologic data base, western Kansas Ground Water Management District No. 1 (J. M. Spinazola, Garden City)
 - Louisiana (w, Baton Rouge):
 - Red River waterway study (J. E. Rogers, Alexandria)
 - Massachusetts (w, Boston):
 - Water level users guide (M. H. Frimpter)
 - Mississippi (w, Jackson):
 - Hydrologic impact, lignite mining in alluvium (J. P. Crout)
 - Potentiometric mapping (B. E. Wasson)
 - Nebraska (w, Lincoln):
 - Hydrology, Platte-Loup area, Nebraska (J. M. Peckenaugh)
 - Nevada (w, Carson City):
 - Ground-water levels, Topaz Lake (J. O. Nowlin)
 - New Mexico (w, Albuquerque):
 - Malaga bend evaluation (J. J. Kunkler)
 - Mimbres Basin model (R. T. Hanson)
 - WSMR water levels (J. D. Hudson)
 - New York (w, Albany):
 - Technology for Ground Water Management Plan, Long Island (T. M. Robison, Syosset)
 - Ohio (w, Columbus):
 - Ground water in Geauga County (V. E. Nichols)
 - Tennessee (w, Nashville):
 - Memphis aquifer studies (D. D. Graham, Memphis)
 - Texas (w, Austin):
 - Ground water, Houston (R. K. Gabrysch, Houston)

Ground-water trends—Continued

- Ground-water studies—San Antonio area (R. D. Reeves, San Antonio)
- Water resources, El Paso (D. E. White, El Paso)
- Utah (w, Salt Lake City):
 - Ground-water conditions, Utah (J. S. Gates)
- Wisconsin (w, Madison):
 - Ground-water level fluctuations (G. L. Patterson)
- Wyoming (w, Cheyenne):
 - Saratoga model, Wyoming (M. A. Crist)
 - Wheatland Flats model, Wyoming (M. A. Crist)
- Heavy metals:**
 - Hydrogeochemistry and biogeochemistry (T. T. Chao, D)
 - Mineral paragenesis (J. T. Nash, M)
 - New England massive sulfides (J. F. Slack, NC)
 - Regional variation in heavy-metals content of Colorado Plateau stratified rocks (R. A. Cadigan, D)
 - Rocky Mountain region, fossil beach placers (R. S. Houston, Laramie, Wyo.)
 - Solution transport (G. K. Czamanske, M)
 - Southeastern States, geochemical studies (Henry Bell III, NC)
- States:**
 - Alaska (M):
 - Gulf of Alaska, resources (Gorge Plafker)
 - Hogatza trend (T. P. Miller)
 - Southeastern part (D. A. Brew)
 - Southern Alaska Range (B. L. Reed)
 - Southwestern part (J. M. Hoare)
 - Yukon-Tanana Upland (H. L. Foster)
 - Nevada, Basin and Range (D. R. Shawe, D)
- Highways and bridges:**
 - Hydraulics laboratory studies (V. R. Schneider, w, NSTL Station, Miss.)
 - Stream-channel behavior (J. C. Brice, w, M)
- States:**
 - Alabama (w, Tuscaloosa):
 - Flood studies, Alabama (C. O. Ming, Montgomery)
 - Florida (w, Tallahassee):
 - Flood assessment (W. C. Bridges)
 - Georgia (w, Doraville):
 - Flood studies, Georgia (McGlone Price)
 - Hawaii (w, Honolulu):
 - Hydrology, sediment, Moanalua (C. J. Ewart)
 - Iowa (w, Iowa City):
 - Flood profiles of Iowa streams (A. J. Heinitz)
 - Kentucky (w, Louisville):
 - Flood studies, statewide (C. E. Schoppenhorst)
 - Louisiana (w, Baton Rouge):
 - Flood hydraulics and hydrology (F. N. Lee)
 - Roughness coefficients (G. J. Arcement)
 - Mississippi (w, Jackson):
 - Multiple-bridge hydraulics (B. E. Colson)
 - Montana (w, Helena):
 - Bridge-site investigations (R. J. Omang)
 - Nevada (w, Carson City):
 - Flood investigations, Nevada (R. R. Squires)
 - Ohio (w, Columbus):
 - Flood volume (W. P. Bartlett)
 - Pennsylvania (w, Harrisburg):
 - Bridge waterways analysis (J. O. Shearman)
 - South Carolina (w, Columbia):
 - Flood studies and assessment (B. H. Whetstone)
 - Tennessee (w, Nashville):
 - Flood investigations (C. R. Gamble)
 - Virginia (w, Richmond):

Highways and bridges—Continued

Hydrology, Wytheville Fish Hatchery (J. R. Hendrick, Marion)

Hydrogeology:

Appalachian Basin—waste storage (P. M. Brown, w, Raleigh, N.C.)

Cretaceous shale hydrology (R. G. Wolff, w, NC)

Geopressed-geothermal resources (R. H. Wallace, w, NSTL Station, Miss.)

Hydrologic analysis of petrofabrics (R. T. Getzen, w, M)

Hydrologic laboratory (F. S. Riley, w, D)

Hydrology of NTS (W. W. Dudley, w, D)

Nuclear engineering (J. E. Weir, w, D)

Planning, Northern Coastal Plain (Harold Meisler, w)

Range water resources, Kenya (N. E. McClymonds, w, Helena, Mont.)

Tropical carbonate aquifers (William Back, w, NC)

Wells—strain meters (J. D. Bredehoeft, w, NC)

Yucca Flat hydrology (G. C. Doty, w, Mercury, Nev.)

States:

Alabama (w, Tuscaloosa):

Environmental hydrogeology, highways (J. C. Scott, Montgomery)

Hydrogeologic study (J. G. Newton)

Alaska (w, Anchorage):

Anchorage geohydrology (T. P. Brabets)

Arizona (w, Tucson):

Agua Fria water resources (R. P. Wilson)

Ground water-surface water, Verde Valley (S. J. Owen-Joyce)

Florida (w, Tallahassee):

Hydrogeologic maps, Seminole County (W. D. Wood, Orlando)

Hydrogeology—Middle Peace Basin (W. E. Wilson, Tampa)

Hydrogeology of northern Collier County, Florida (F. A. Watkins, Fort Myers)

Hydrogeology of shallow aquifers, southwest Florida (R. M. Wolansky, Tampa)

Hydrology of Floridan aquifer lower confining bed (W. C. Steinkampf, Tampa)

Santa Fe River Basin (J. D. Hunn)

Sulphur Springs quadrangle (J. W. Stewart, Tampa)

Georgia (w, Doraville):

Ground-water resources, coastal Georgia (H. E. Gill)

Hawaii (w, Honolulu):

Aquifer identification, Hawaii (C. J. Ewart)

Northern Guam aquifer study (C. J. Huxel)

Illinois (w, Urbana):

Regional aquifer study in Illinois (M. G. Sherrill)

Iowa (w, Iowa City):

Water resources, west-central Iowa (D. L. Runkle)

Kentucky (w, Louisville):

Hydrogeology of eastern Kentucky coal field (A. L. Knight)

Hydrogeology of landfills (H. H. Zehner)

Maryland (w, Towson):

Hydrologic impacts of power plants (F. K. Mack, Annapolis)

Michigan (w, Lansing):

Ground water of coal deposits, Bay County (J. R. Stark)

Minnesota (w, St. Paul):

Regional aquifer study in Minnesota (D. G. Woodward)

Montana (w, Helena):

EMRIA site studies (N. E. McClymonds)

Water-Tongue River area, Montana-Wyoming (R. R. McMurtrey)

Nebraska (w, Lincoln):

Hydrogeology—Continued

Butler County, Nebraska (M. H. Ginsberg)

Central Midwest RASA-Nebraska (M. J. Ellis)

Hydrology, southern Sand Hills, Nebraska (J. W. Goeke)

Nevada (w, Carson City):

Carson Valley ground-water model (D. K. Maurer)

New Mexico (w, Albuquerque):

Ground-water resources, Catron County (R. G. Roybal)

Ground water, Socorro County (J. A. Baldwin)

Jemez geothermal, New Mexico (A. M. Umari)

Northwestern New Mexico ground water (P. F. Frenzel)

Western Valencia County (Baldwin Joseph)

New York (w, Albany):

Geohydrology of North Brookhaven (E. J. Koszalka, Syosset)

Ground water, Oswego County (T. S. Miller, Ithaca)

Hydrogeology of southeastern Nassau County (H. F. Ku, Syosset)

Hydrogeology of Suffolk County (R. K. Krulikak, Syosset)

Ohio (w, Columbus):

Mine-site investigations (S. E. Norris)

Pennsylvania (w, Harrisburg):

Ground water, Columbia and Montour Counties (J. H. Williams)

Ground water, Williamsport (O. B. Lloyd)

Hydrogeology of Erie County (J. T. Gallaher, Meadville)

South Carolina (w, Columbia):

Ground-water quality, South Carolina piedmont (G. G. Patterson)

Water-resources evaluation: Horry, Georgetown (A. L. Zack, Conway)

Texas (w, Austin):

Ground-water resources, Ogallala Formation (C. A. Wilson, Lubbock)

Limestone hydrology study (R. W. MacLay, San Antonio)

Utah (w, Salt Lake City):

Ground water, Trail Mountain area (G. C. Lines)

Vermont (w, Montpelier):

Ground water—Mad River area (A. L. Hodges)

Wisconsin (w, Madison):

Ground-water quality (P. A. Kammerer)

Regional aquifer study in Wisconsin (P. J. Emmons)

Wyoming (w, Cheyenne):

Southern Powder Uranium, Wyoming (M. E. Lowry)

Hydrologic principles:

Glaciology (M. F. Meier, w, Tacoma, Wash.)

Hydrologic probability models (W. H. Kirby, w, NC)

Hydrologic techniques course (Della Laura, w, NC)

Infiltration and drainage (Jacob Rubin, w, M)

Modeling principles (J. P. Bennett, w, NC)

Solute transport at low flow (V. C. Kennedy, w, M)

Stratigraphy, Florida and Alabama (C. E. Simmons, w)

Unsaturated zone solutes (R. V. James, w, M)

States:

California (w, Menlo Park):

Great Basin flood hazards (D. E. Burkham, Sacramento)

Colorado (w, Lakewood):

Arkansas River basin (J. L. Hughes, Pueblo)

Evaluation, deep-well sites, Northwestern Colorado (F. A. Welder, Meeker)

Front Range urban corridor (D. E. Hillier, D)

Popularized Piceance Basin report (O. O. Taylor, D)

Connecticut (w, Hartford):

Estimating flow in aquifers (D. L. Mazzafarro)

Florida (w, Tallahassee):

Hydrologic principles—Continued

- Effects of urbanization on hydrology (M. A. Lopez, Tampa)
- Landfill and sewage effluent, Florida (M. R. Fernandez, Tampa)
- Seismic surveys, west-central Florida (R. M. Wolansky, Tampa)
- Indiana (w, Indianapolis):
 - Wabash River reaeration study (C. G. Crawford)
- Kansas (w, Lawrence):
 - Ground water-surface water (W. M. Kastner)
- Kentucky (w, Louisville):
 - Big Sandy River basin: Levisa Fork (R. W. Davis)
 - Ground-water levels, Louisville, Kentucky (D. V. Whitesides)
 - Hydrology of oil shale areas, Kentucky (R. W. Davis)
 - Hydrology of oil shales (D. W. Leist)
- Mississippi (w, Jackson):
 - Flood studies, statewide (K. V. Wilson)
- Missouri (w, Rolla):
 - Hydrology of Ozark's basins (John Skelton)
- New Jersey (w, Trenton):
 - Cohansey model (A. W. Harbaugh)
- New Mexico (w, Albuquerque):
 - Hydrologic contamination, New Mexico (J. F. Daniel)
 - Liaison, USGS-BLM (Kim Ong)
 - Water resources, San Juan Basin (S. D. Craig)
- New York (w, Albany):
 - Acid lakes (N. E. Peters)
- North Dakota (w, Bismarck):
 - Rattlesnake Butte area hydrology, North Dakota (W. F. Horak)
 - Wibaux-Beach deposit hydrology (W. F. Horak)
- Washington (w, Tacoma):
 - Bonaparte Creek ground-water study (F. A. Packard)
- Hydrology, general:**
 - Coal hydrology services (D. A. Goolsby, w, D)
 - Coal hydrology services (L. E. Young, w, M)
 - Commission support (T. J. Buchanan, w, NC)
 - Computational hydraulics (V. C. Lai, w, NC)
 - COOP-programs, training (Della Laura, w, NC)
 - Field coordination (C. L. Holt, w, Atlanta, Ga.)
 - Field coordination (D. L. Coffin, w, D)
 - International specialist training (Della Laura, w, NC)
 - NAWDEX project (M. D. Edwards, w, NC)
 - Other Federal Agencies training (Della Laura, w, NC)
 - OWDC activities, WR (L. E. Young, w, M)
 - Participant training—PL 80-402 (Della Laura, w, NC)
 - Section 607 (Della Laura, w, NC)
 - Unrestricted fund, Northeastern Region (J. E. Biesecker, w, NC)
 - Water data coordination (R. H. Langford, w, Washington, D.C.)
 - World Bank Projects Foreign (Della Laura, w, NC)
 - WRD training center (J. P. Monis, w, D)
- States:**
 - Colorado (w, Lakewood):
 - Program enhancement (E. A. Moulder, D)
 - Study plan for oil-shale hydrology (O. O. Taylor, D)
 - Idaho (w, Boise):
 - Kootenai Board—WWT (E. F. Hubbard)
 - Kansas (w, Lawrence):
 - ADP-GWSI consulting services (C. H. Baker)
 - Distributed systems, Kansas (J. M. McNellis)
 - Maine (w, Augusta):
 - Hydrology of peat bogs in Maine (W. J. Nichols)
 - Maryland (w, Towson):

Hydrology, general—Continued

- Small basin modeling (R. E. Willey)
- Massachusetts (w, Boston):
 - Otis plume model (D. R. LeBlanc)
- North Dakota (w, Bismarck):
 - Airborne snow surveys (D. G. Emerson)
- Utah (w, Salt Lake City):
 - Program enhancement (Ted Arnow)
- See also* Evapotranspiration; Marine hydrology; Plant ecology; Urban hydrology.
- Industrial minerals. See specific minerals.**
- Industrial wastes, inorganic:**
 - Iowa (w, Iowa City):
 - Water quality, Iowa coal region (M. G. Detrov)
 - Illinois (w, Urbana):
 - Coal hydrology—Illinois EPA coop agreement (G. G. Glysson)
 - Kansas (w, Lawrence):
 - Quality of water, mined areas in southeastern Kansas (A. M. Diaz)
 - Minnesota (w, St. Paul):
 - Mercury in lakes, Voyageurs Park (D. I. Siegel)
 - Nevada (w, Carson City):
 - Water contamination by explosive wastes (A. S. Van Denburgh)
 - New York (w, Albany):
 - Contaminants in the Saw Mill River (R. J. Rogers)
 - North Dakota (w, Bismarck):
 - Precipitation chemistry, North Dakota (R. L. Houghton)
 - Ohio (w, Columbus):
 - Quality of water monitoring network (M. S. Katzenbach)
 - Oklahoma (w, Oklahoma City):
 - Saltwater infiltration (R. B. Morton)
 - Pennsylvania (w, Harrisburg):
 - Little Blue Run Lake—fly ash (D. R. Williams, Pittsburgh)
 - Wyoming (w, Cheyenne):
 - In-situ coal, Wyoming (J. F. Busby)
- Industrial wastes, organic:**
 - Identification of organics in water (M. C. Goldberg, w, D)
 - Oil-shale wastewater and water quality (J. A. Leenheer, w, Arvada, Colo.)
 - Organic deep-waste storage (R. L. Malcolm, w, Arvada, Colo.)
- States:**
 - California (w, Menlo Park):
 - San Francisco Bay urban study (R. D. Brown, M)
 - Connecticut (w, Hartford):
 - PCB in the Housatonic River (K. P. Kulp)
 - Kentucky (w, Louisville):
 - Louisville alluvial aquifer test (K. E. Stevens)
 - New York (w, Albany):
 - Recharge and nitrates, Cornell Farm (A. D. Randall)
 - Pennsylvania (w, Harrisburg):
 - Schuylkill River quality (G. L. Pederson)
 - Puerto Rico (w, San Juan):
 - San Juan lagoons (S. R. Ellis)
- Inventory wells:**
 - Kansas (w, Lawrence):
 - Hydrologic data base, Ground Water Management District 3, Kansas (J. M. Spinazola, Garden City)
 - Nevada (w, Carson City):
 - Statewide ground-water-level network (P. A. Glancy)
 - Virginia (w, Richmond):
 - Geohydrologic data (H. T. Hopkins)
- Iron:**
 - Resource studies, United States (W. F. Cannon, NC)

Irrigation return-flow:

Unsaturated zone field studies (E. P. Weeks, w, D)

States:

Colorado (w, Lakewood):

Nitrogen levels, San Luis Valley (P. F. Edelmann, Pueblo)

Idaho (w, Boise):

Water quality of irrigation flows (H. R. Seitz)

Kansas (w, Lawrence):

Quality of irrigation return flow (S. A. Druse)

Washington (w, Tacoma):

Sediment data for irrigated agriculture (P. R. Boucher)

Isotope and nuclear studies:

Atmospheric carbon dioxide (Irving Friedman, D)

Carbon isotopes and the global carbon cycle (M. A. Arthur, D)

CUSMAP (C. E. Hedge, D)

CUSMAP (T. W. Stern, NC)

CUSMAP (R. W. Kistler, M)

Data bank (R. F. Marvin, D)

Geochronology (B. R. Doe, NC)

Geochronology (M. A. Lanphere, M)

Geochronology (C. W. Naeser, D)

Geochronology (T. W. Stern, NC)

Instrument development (J. D. Obradovich, E. E. Wilson, D)

Isotope ratios in rocks and minerals (Irving Friedman, D)

Lead isotopes and ore deposits (B. R. Doe, NC; R. E. Zartman, D)

Light stable isotopes (Irving Friedman, D)

Magnetic properties of coal (F. E. Senftle, NC)

Mass spectrometry and isotopic measurements (J. S. Stacey, D)

Mineral separation (G. T. Cebula, D)

Neutron activation (F. E. Senftle, NC)

Nevada Test Site isotopic evaluation for waste disposal (J. N. Rosholt, D)

Nuclear irradiation (C. M. Bunker, D)

Nuclear waste disposal (WIPP) (J. D. Obradovich, D)

Obsidian hydration dating (Irving Friedman, D)

Oxygen isotopes, geothermal (J. R. O'Neil, M)

Radiocarbon, geothermal (S. W. Robinson, M)

Radionuclide systems in Illinois deep drill holes (Z. E. Peterman and S. S. Goldich, D)

Stable isotopes and ore genesis (R. O. Rye, D)

Upper mantle studies (Mitsunobu Tatsumoto, D)

See also Geochronological investigations; Radioactive-waste disposal.

Lake and reservoir siltation:

Iowa (w, Iowa City):

Sedimentation study—Lake Panorama (A. J. Heinitz)

Missouri (w, Rolla):

Water quality of Creve Coeur Lake (D. W. Spencer, Maryland Heights)

Pennsylvania (w, Harrisburg):

Swatara preimpoundment (D. K. Fishel)

Lakes and reservoirs:

Relation of ground water to lakes (T. C. Winter, w, D)

States:

California (w, Menlo Park):

California lakes and reservoirs (W. L. Bradford)

Lake model test (W. L. Bradford)

Connecticut (w, Hartford):

Water quality of Lake Waramaug (K. P. Kulp)

Florida (w, Tallahassee):

Hydrology of Lake Butler (James Smoot, Orlando)

Hydrology of lakes (G. A. Irwin)

Indiana (w, Indianapolis):

Mapping of Big Long Lake, Indiana (R. R. Contreras)

Lakes and reservoirs—Continued

Minnesota (w, St. Paul):

Big Marine Lake (G. E. Groschen)

Montana (w, Helena):

Limnology of Valley County lakes (R. F. Ferreira)

New Mexico (w, Albuquerque):

Santa Rosa Reservoir leakage, New Mexico (D. W. Risser)

New York (w, Albany):

Discharges, Oswego River basin sites (Richard Lumia)

Otisco Lake water quality (T. S. Miller, Ithaca)

Ohio (w, Columbus):

Rush Creek water quality (Janet Hren)

Oregon (w, Portland):

Oregon lakes and reservoirs (D. D. Harris)

Puerto Rico (w, San Juan):

Islandwide 208 assistance study (Fernando Gomez-Gomez, Ft. Buchanan)

Water quality in Lago Carraizo (Ferdina Quinones-Marquez)

Washington (w, Tacoma):

Lakes classification (N. P. Dion)

Wisconsin (w, Madison):

Bridge Creek hydrology (L. B. House)

Hydrology of lakes in Wisconsin (D. A. Wentz)

Urban lakes (L. B. House)

Water resources of Apostle Islands (W. J. Rose)

Land and vegetation:

Powell arid lands centennial (R. F. Hadley, w, D)

State:

Washington (w, Tacoma):

Mt. Rainier aerial photography (L. M. Nelson)

Land drainage:

Florida (w, Tallahassee):

Golden Gate study (M. L. Merritt, Miami)

Maine (w, Augusta):

Drainage areas in Maine (R. A. Fontaine)

Land resources analysis:

Idaho, eastern Snake River Plain region (S. S. Oriol, D)

Landslide studies:

Chemical-thermal geotechnical effects on argillaceous sediments (H. W. Olsen, D)

Computer-based statistical modeling (R. K. Mark, M)

Earthquake-induced landslides (E. L. Harp, M)

Experimental landslide mapping (G. F. Wieczarek, M)

Gravitational spreading of ridges (D. J. Varnes, D)

Ground failures caused by historic earthquakes (D. K. Keefer, M)

Hazards information center (R. W. Fleming, D)

Interaction of ground motion and ground failure (R. C. Wilson, M)

Landslide investigations (R. W. Fleming, D)

Landslide mapping analysis, United States (E. E. Brabb, M)

Mechanics of debris-flow failure (E. L. Harp, M)

Miscellaneous landslide investigations (R. W. Fleming, D)

Rock deformation induced by subsurface excavation (T. C. Nichols, Jr., D)

Safe mine waste disposal, Appalachia (W. E. Davies, NC)

Seismic slope stability (D. K. Keefer, M)

Solution subsidence and collapse (J. R. Ege, D)

Swelling clays, United States (R. L. Schuster, D)

States:

California:

Areal slope stability, San Francisco Bay (S. D. Ellen, M)

Landslide hazard zonation (J. T. McGill, D)

Landslide studies—Continued

Pacific Palisades landslide area, Los Angeles (J. T. McGill, D)

Montana:

Birney area (R. M. Lindvall, D)

Hardin and Grass Lodge quadrangles (S. S. Agard, D)

Utah, Lynndyl 1-degree quadrangle (E. H. Pampeyan, M)

Washington, Engineering implications of Mt. St. Helens eruptions (R. L. Schuster, D)

Land subsidence:

Fissuring-subsidence research (T. L. Holzer, M)

State:

New Mexico, Land subsidence in the Known Potash Leasing Area (M. L. Millgate, c, Roswell)

Land use (NC, except as otherwise noted):

Accuracy assessment of land use and land cover maps produced from Landsat digital data (G. H. Rosenfield, o)

Development of automated techniques for land use mapping (J. R. Wray, o)

Geographic Information Systems operation and development (W. B. Mitchell, o)

Geographic Information Systems software development (W. B. Mitchell, o)

Hazard prediction and warning, socioeconomic and land use planning implications (R. H. Alexander, o, Boulder, Colo.)

Land use and land cover:

Land use pattern analysis (C. W. Spurlock, o, Gainesville, Fla.)

Mapping and data compilation (G. L. Loelkes, o)

Mapping in Alaska based on Landsat digital data (Leonard Gaydos, o, Moffett, Calif.)

Maps and data and other geographic studies (J. R. Anderson, o)

Land use and land cover map update (V. A. Milazzo)

Land use impact on solar-terrestrial energy systems (R. W. Pease, o)

Multidisciplinary studies:

Drainage basins as environmental planning units (T. A. Lewis)

Environmental mapping for the Ashburton-Arcola study area, Virginia (D. B. Harper)

Use of earth-science information by planners and decision-makers (W. J. Kockelman, M)

States:

California:

San Francisco Bay, use and protection (W. J. Kockelman; J. T. Conomos; A. E. Leviton, M)

Use of USGS information in the San Francisco Bay region by city, county, regional, State, Federal, conservation, and corporate planners and decisionmakers (W. J. Kockelman, M)

Virginia, Culpeper Basin earth-sciences applications study (A. J. Froelich)

See also Construction and terrain problems; Urban geology; Urban hydrology.

Lead, zinc, and silver:

Lead and zinc resources of Eastern United States (S. H. B. Clark, NC)

Lead resources of United States (C. S. Bromfield, D)

New England massive sulfides (J. F. Slack, NC)

Silver commodity research (R. B. Hall, D)

Zinc resources of the Western United States (H. T. Morris, J. A. Briskey, M)

States:

Colorado, Precambrian sulfide deposits (D. M. Sheridan, D)

Lead, zinc, and silver—Continued

Illinois-Kentucky district, Regional structure and ore controls (D. M. Pinckney, D)

Nevada (M):

Comstock district (D. H. Whitebread)

Silver Peak Range (R. P. Ashley)

See also Water quality, general.

Lunar geology. *See* Extraterrestrial studies.

Marine geology:

Atlantic Continental Shelf (Woods Hole, Mass., unless otherwise noted):

Coastal, estuarine, and lacustrine studies (H. J. Knebel)

Environmental assessment (D. W. Folger); Mid-Atlantic, Baltimore Canyon (J. M. Robb); North Atlantic (D. M. O'Leary)

Geochemistry and hydrochemistry (F. T. Manheim)

Geophysical studies (J. A. Grow)

Georgia embayment, environmental assessment (Peter Popenoe)

Magnetic studies (K. D. Klitgord)

Mass wasting processes on East Coast Continental Slope (J. S. Booth)

New England coastal zone (R. N. Oldale)

Organic geochemistry of Atlantic Continental Shelf and nearshore environments (R. E. Miller, NC)

Petroleum geology (M. M. Ball)

Petroleum potential of U.S. Atlantic Margin (R. E. Mattick, NC)

Site Surveys (W. P. Dillon)

Stratigraphy (J. C. Hathaway)

Stratigraphy and structure (J. S. Schlee)

Submarine Canyon dynamics (B. A. McGregor)

Caribbean and Gulf of Mexico (Corpus Christi, Tex.):

Coastal Plain estuaries (E. A. Martin)

Continental Slope (C. W. Holmes)

Geologic-tectonic map (R. G. Martin, Jr.)

Mississippi delta studies (L. E. Garrison)

Puerto Rico cooperative (J. V. A. Trumbull, San Juan, P.R.)

Quaternary history and sea floor stability (H. Berryhill)

Texas Barrier Island stratigraphy (G. L. Shideler)

West Florida Continental Shelf (C. W. Holmes)

Cartography and physiography (T. R. Alpha, M)

Current dynamics and sediment transport, continental shelves (Bradford Butman, Woods Hole, Mass.)

Geotechnical investigations (H. W. Olsen, D)

Marine geotechnique (H. W. Olsen, D)

Marine mineral resources, worldwide (F. H. Wang, M)

Pacific-Arctic Oceans (M, except as otherwise noted):

Acoustic measurement of in situ physical properties of shelf sediments (Gary Boucher)

Advanced geopotential data (collection, processing, modeling) (A. K. Cooper)

Advanced seismic systems (D. H. Tompkins)

Alaskan marine micropaleontology (P. J. Quinterno)

Benthic processes in San Francisco Bay (F. H. Nichols)

Biogenic sedimentary processes (G. W. Hill)

Comparative sedimentology of continental margin environments for exploration and recovery of energy resources (C. H. Nelson)

Computer systems analyses and applications programming (G. A. McHendrie)

Continental margin petroleum resources framework (T. H. McCulloh)

Continental margin processes (J. V. Gardner)

Continental margin sediment dynamics (D. A. Cacchione)

Marine geology—Continued

- Deep-sea fan studies (W. R. Normark)
 Depositional processes and facies coastal embayments (R. L. Phillips)
 Dynamics of sediment bedforms (D. M. Rubin)
 Eastern Gulf of Alaska resource assessment (George Plafker)
 Environmental geologic studies, Beaufort and Chukchi Seas (P. W. Barnes; Erk Reimnitz)
 Environmental geologic studies, eastern Gulf of Alaska (B. F. Molnia)
 Environmental geologic studies, northern and central California continental shelf and margin (D. S. McCulloch)
 Environmental geologic studies, southern California borderland (H. G. Greene); Northern California continental margin (M. E. Field, M)
 Geochemistry of sediments (W. E. Dean, D)
 Geologic and resource assessment, northern Bering Sea (M. A. Fisher)
 Geologic framework and resource assessment, Aleutian-Bering Sea area (M. S. Marlow)
 Geologic framework and resource assessment, Gulf of Alaska (R. E. von Huene)
 Geologic framework and resource assessment, northern and central California continental shelf and margin (D. S. McCulloch)
 Geologic framework and resource assessment, Oregon-Washington continental margin (P. D. Snavely, Jr.)
 Geologic framework and resource assessment, southern California borderland (J. G. Vedder)
 Geologic framework and resource assessment, Beaufort and Chukchi Seas (A. Grantz)
 Geologic hazards in Navarin Basin province (P. R. Carlson)
 Juan de Fuca Ridge, structure and metallogenic processes (W. R. Normark)
 Linear island chains, tectonic movements of the Pacific crust (D. A. Clague)
 Lithogenesis of deep margin sediments (W. R. Normark)
 Marine gas hydrates (K. A. Kvenvolden)
 Marine geochemical studies (J. L. Bischoff)
 Marine geotechnical studies (M. A. Hampton)
 Marine organic geochemistry (K. A. Kvenvolden)
 Metallic deposits in the oceanic crust (R. A. Koski)
 Nearshore sediment dynamics (A. H. Sallenger, Jr.)
 Ocean floor mineralization studies (J. L. Bischoff)
 Ocean floor mineral resources (D. Z. Piper)
 Oceanic micropaleontology (J. D. Bukry)
 Oceanic volcanology (D. A. Clague)
 Open-coast sedimentary lithogenesis (R. E. Hunter)
 Pacific Ocean, biostratigraphy, oceanic (J. D. Bukr, La Jolla, Calif.)
 Pacific reef studies (J. I. Tracey, Jr., NC)
 Petroleum geology of Cook Inlet-Shelikof Strait (L. B. Magoon)
 Properties of submarine volcanic rocks (J. G. Moore)
 Resource and geo-environmental assessment, Aleutian ridge and shelf (D. W. Scholl)
 Sediment processes and facies in the shelf-slope transition zone (M. E. Field)
 Sedimentary processes of submarine canyon heads (J. R. Dingler)
 Sediment transport and diffusion in abyssal benthic boundary layer (S. L. Eittrheim)
 Silica and clay mineral distributions and diagenesis in deep sea (J. R. Hein)

Marine geology—Continued

- Submarine Canyon transport processes (S. L. Eittrheim)
 Small Boat Surveys (H. J. Knebel, Woods Hole, Mass.)
 Spanish continental margin (Almeria Province) (P. D. Snavely, Jr., H. G. Greene, H. F. Clifton, W. P. Dillon, J. M. Robb, M)
 Trace-metal geochemistry, offshore sediments (M. H. Bothner, Woods Hole, Mass.)
 Volcanic geology, Mariana and Caroline Islands (Gilbert Corwin, NC)
 Volcanogenic manganese deposits (R. A. Koski, M)
States and territories:
 California, La Jolla marine geology laboratory (J. D. Bukry, San Diego)
 Oregon-Washington, Geologic framework (P. D. Snavely, Jr., M)
 Puerto Rico, Cooperative program (J. V. A. Trumbull, Santurce)
Marine geotechnique:
 Marine geotechnical investigations (H. W. Olsen, D)
Marine hydrology. *See* Water quality, general; Geochemistry and mineralogy, water; Marine geology.
Mercury:
 Deposits and resources (E. H. Bailey, J. J. Rytuba, M)
Meteorites. *See* Extraterrestrial studies.
Mine drainage:
 Chemical models—coal hydrology (D. C. Thorstenson, w, Dallas, Tex.)
 Hydrologic impacts of coal mining (A. M. Lumb, w, NC)
 Water monitoring, coal mining, northeast region (J. F. Bailey, w, NC)
 Water monitoring, coal mining, southeast region (C. A. Pascale, w, Atlanta, Ga.)
States:
 Alabama (w, Tuscaloosa):
 Hydrologic assessment of coal areas, Alabama (J. R. Harkins, University)
 Arizona (w, Tucson):
 Black Mesa hydrologic study (G. W. Hill)
 Colorado (w, Lakewood):
 Coal hydrogeology—Denver Basin (R. S. Williams, D)
 Hydrology of coal spoils piles (R. S. Williams, D)
 Illinois (w, Urbana):
 Research modeling in coal areas (A. R. Klinger)
 Strip mine modeling (D. L. Galloway)
 Water monitoring—coal mining, Illinois (E. E. Zuehls)
 Indiana (w, Indianapolis):
 Effect of strip mining on ground water and surface water (C. G. Crawford)
 Water monitoring—coal mining, Indiana (W. G. Wilber)
 Kansas (w, Lawrence):
 Coal hydrology of east-central Kansas (H. E. Bevans)
 Kentucky (w, Louisville):
 Downstream effects of coal mining (J. E. Dysart)
 Hydrologic data, coal areas of Kentucky (J. M. Bettendorf)
 Maine (w, Augusta):
 Hydrologic effects, northern Maine mining (R. A. Fontaine)
 Maryland (w, Towson):
 Hydrologic effects of coal mining (M. T. Duigon)
 Water monitoring of coal mining, Maryland (W. W. Staubitz)
 Montana (w, Helena):
 Surface water-quality of water analysis, eastern Montana (J. J. Knapton)
 Nevada (w, Carson City):
 Water-supply history, mining camps (H. A. Shamberger)
 New Mexico (w, Albuquerque):

Mine drainage—Continued

- Chaco Canyon, New Mexico, hydrology (H. R. Hejl)
- Individual coal mine effects (C. L. Goetz)
- San Juan coal monitoring (H. R. Hejl)
- Ohio (w, Columbus):
 - Acid mine-drainage characterization (C. G. Angelo)
 - Analysis of sediment data, coal states (G. F. Koltun)
 - Mine reclamation Lake Hope basin (V. E. Nichols)
 - Quality of water impact of reclamation (C. L. Pfaff)
 - Quality of water in Ohio coal areas (S. L. Westover)
 - Water monitoring, coal mining, Ohio (D. K. Roth)
- Oklahoma (w, Oklahoma City):
 - Abandoned zinc mines (C. J. Hill)
 - Hydrogeology of orphan lands, eastern Oklahoma (L. J. Slack)
- Pennsylvania (w, Harrisburg):
 - Coal hydrology, Stony Fork watershed (D. E. Stump, Pittsburgh)
 - Coal hydrology, Big Sandy Creek (D. E. Stump, Pittsburgh)
 - Daylighting—hydrology of Babb Creek (L. A. Reed)
 - Mine-site application for the Office of Surface Mining (W. J. Herb)
 - Water monitoring, coal mining, Pennsylvania (W. J. Herb)
 - Western middle anthracite hydrology (D. J. Growitz)
- Puerto Rico (w, San Juan):
 - Copper mining area, Puerto Rico (P. W. McKinley)
- Tennessee (w, Nashville):
 - Landsat basin characteristics (E. F. Hollyday)
 - Water monitoring, coal mining, Tennessee (V. J. May)
- Utah (w, Salt Lake City):
 - Ferron Sandstone, Castle Valley (G. C. Lines)
 - Huntington coal hydrology (T. W. Danielson)
 - Price River basin (K. M. Waddell)
 - Water monitoring, coal mining, Utah (G. G. Plantz)
- Virginia (w, Richmond):
 - Coal hydrology information transfer (P. W. Hufschmidt)
 - Geochemistry of mine drainage (P. W. Hufschmidt)
 - Ground-water coal mining, Virginia (J. D. Larson)
- Washington (w, Tacoma):
 - Centralia strip mining and monitoring (F. A. Packard)
 - Western Washington coal network (L. A. Fuste)
- West Virginia (w, Charleston):
 - Deep mine collapse hydrology (W. R. Hobba, Morgantown)
 - Effects of deep mining in West Virginia (J. W. Borchers)
 - Quantitative mine-water studies (G. G. Wyrick)
 - Water monitoring, coal mining, West Virginia (T. A. Ehlke)
- Mineral and fuel resources, compilations, and topical studies:**
 - Acid-altered volcanogenic mineral deposits, Eastern United States (R. W. Luce, NC)
 - Arctic mineral-resource investigations (R. M. Chapman, M)
 - Basin and Range, stratiform metals (F. G. Poole, D)
 - Chromium geophysical studies (J. C. Wynn, NC)
 - Computer characterization of selected sedimentary materials (M. W. Bodine, Jr., D)
 - Disseminated gold (E. W. Tooker, M)
 - Environment of ore deposition (P. H. Wetlaufer, NC)
 - Geochemistry of Alaskan Wilderness Areas (S. E. Church, D)
 - Geochemistry of Central Region Wilderness Study Areas (J. C. Antweiler, D)
 - Geochemistry of Eastern Region Wilderness Areas (W. R. Griffitts, D)
 - Geochemistry of Western Region Wilderness Areas (R. E. Learned, D)
 - Geology and resources of beryllium (W. R. Griffitts, D)
 - Geology and resources of marine manganese nodules and world manganese resources (W. F. Cannon, NC)

Mineral and fuel resources, compilations, and topical studies—Continued

- Geology and resources of niobium and tantalum (G. P. Landis, D)
- Geology and resources of selenium-tellurium (J. R. Watterson, D)
- Geology and resources of zirconium and hafnium (M. E. Paidakovich, NC)
- Geology, geochemistry, and resources of peat (C. C. Cameron, NC)
- Geophysical studies (C. K. Moss, D)
- Information bank, computerized (J. A. Calkins, NC)
- Kimberlites (B. C. Hearn, Jr., NC)
- Lithium resources, sedimentary environments of (Sigrid Asher-Bolinder, D)
- Metalliferous black shale (F. G. Poole, D)
- Methodology of minerals geophysics (F. C. Frischknecht, D)
- Mineral resource estimation (W. D. Menzie, M)
- Mineral-resource surveys:
 - Indian lands:
 - Mescalero Apache Reservation, New Mexico. (S. L. Moore, D)
 - Papago reservation (P. G. Schruben, NC)
 - Subsurface geology, Wisconsin and Michigan (W. F. Cannon, NC)
 - Nonmetallic deposits, mineralogy (B. M. Madsen, M)
- Oil and gas resources:
 - Offshore (R. B. Powers, E. W. Scott, D)
 - Onshore (G. L. Dolton, S. E. Frezon, Keith Robinson, A. B. Coury, K. L. Varnes, D)
- Ore deposits and processes in early magmatic environment (N. J. Page, M)
- Phosphate petrology and world resources (R. P. Sheldon, NC)
- Primitive, Wilderness, and RARE II Areas:
 - Anaconda-Pintlar, Montana (D. A. Wallace; J. E. Elliott, D)
 - Andrews Mountain, Mazourka, Paiute, Coyote, Table Mountain, and Buttermilk, California (E. H. McKee, M)
 - Arnold Mesa, Arizona (E. W. Wolfe, Flagstaff)
 - Arroyo Seco, California (J. C. Matti, M)
 - Big Butte-Shinbone, California (M. C. Blake, Jr., M)
 - Big Horn Desert lands, California (J. C. Matti, M)
 - Big Horn-White Water, California (Andrew Griscom, M)
 - Big Sandy-W. Elliotts Creek, Alabama (S. H. Patterson, NC)
 - Blanco Mountain Wilderness, California; Birch Creek, Black Canyon, Benton Range, and Sugarloaf Wilderness Areas, Nevada (E. H. McKee, M)
 - Bridger, Wyoming (R. G. Worl, D)
 - Buffalo Hump, Idaho (K. I. Lund, State College, Penn.)
 - Buffalo Peaks, Colorado (D. C. Hedlund, D)
 - Cactus Springs—Sugarloaf South, California (J. C. Matti, M)
 - Carson-Iceberg Wilderness, California (W. J. Keith, M)
 - Castle Crags, Mount Eddy, and Shasta, California (J. A. Peterson, M)
 - Cheat Mountain, West Virginia (K. J. Englund, NC)
 - Chips Creek, Middle Fork Feather, Bucks Lake, and Bald Rock, California; Stansbury Range, Utah (M. L. Sorenson, M)
 - Chugach National Forest, Alaska (S. W. Nelson, Anchorage)
 - Cohutta, Georgia-Tennessee (J. E. Gair, NC)
 - Columbine-Hondo, New Mexico (J. C. Reed, D)
 - Complanter, Pennsylvania (F. G. Lesure, NC)
 - Dennison Peak/Moses Mountain, California (J. F. Seitz, M)

Mineral and fuel resources, compilations, and topical studies—Continued

Devils Fork, Virginia (K. J. Englund, NC)
 Dinkey Lakes, California (F. C. Dodge, M)
 Dome Land Wilderness, California (J. R. Berquist, M)
 Dragoon Mountains, Arizona (H. D. Drewes, D)
 Eagle Rock Study Area, Washington (R. W. Tabor; V. A. Frizzell, Jr., M)
 East Yuba-West Yuba Wilderness Areas, California (J. R. Berquist, M)
 Electrical studies (D. B. Hoover, D)
 Elk Creek-Black Butte, California (R. J. McLaughlin, M)
 Florida RARE II (J. B. Cathcart, NC)
 Forest Service Further Planning Areas, Arkansas (M. H. Miller, D)
 Forest Service Further Planning Areas, Texas (B. B. Houser, D)
 Fossil Ridge, Colorado (E. H. DeWitt, D)
 Freel, Dardenelles, Tragedy-Elephants Back, and Raymond Peak Wilderness areas, California and Nevada (R. A. Armin, M)
 Gates of the Mountains Wilderness Area, Montana (M. W. Reynolds, D)
 Gearheart Mountain and Deschutes Canyon, Oregon (G. W. Walker, M)
 Glacier Peak Wilderness, Washington (A. B. Ford, M)
 Glacier View/Tatoosh, Washington (R. C. Evarts, M)
 Goat Rocks, Washington (D. A. Swanson, Vancouver)
 Grand Wash Cliffs, Arizona (R. G. Bohannon, D)
 Granite Chief, California (D. S. Harwood, M)
 Greenhorn Mountain, Colorado (M. I. Toth, D)
 Guadalupe Escarpment, New Mexico (P. T. Hayes, D)
 Hall Natural, Log Cabin-Saddlebag, Tioga Lake, and Horse Meadows Wilderness Areas, California (J. F. Seitz, M)
 Highland Ridge and Wheeler Peak Wilderness Areas, Nevada (D. H. Whitebread, M)
 Illinois (J. S. Klasner, Macomb, Ill.)
 John Muir Wilderness, California (N. K. Huber, M)
 Lincoln Creek, Nevada (J. R. Berquist, M)
 Little Frog, Tennessee (E. R. Force, NC)
 Los Padres Study Areas, California (V. A. Frizzell, Jr., M)
 Lost Creek, Colorado (B. R. Johnson, D)
 Madison—Gallatin Study Area, Montana (F. S. Simons, D)
 Marble Mountain, California (M. M. Donato, M)
 Mazatzal Wilderness, Arizona (C. T. Wrucke and C. M. Conway, M)
 Monte Cristo Study Area, Washington (R. W. Tabor; V. A. Frizzell, Jr., M)
 Mount Adams, Washington (E. W. Hildreth, M)
 Mount Henry, Montana (R. E. Van Loenen, D)
 Mount Raymond Wilderness Study Area, California (N. K. Huber, M)
 Mount Washington, Oregon (N. S. McLeod, M)
 Nephi, Birdseye, and Santaquin, Utah (M. L. Sorenson, M)
 Nopah and Resting Spring Ranges, California (A. K. Armstrong, M)
 North Fork John Day River, Oregon (J. G. Evans, Spokane)
 North Fork Smith and South Kalmiopsis Wilderness Areas, California and Nevada (J. P. Albers, M)
 North Georgia (A. E. Nelson, NC)
 Oh-Be-Joyful, Colorado (S. D. Ludington, NC)
 Oil and gas potential (Wallace de Witt, Jr., NC)
 Orleans Mountain, California (M. C. Blake, Jr., M)
 Orleans Mountain and Condrey Mountains, California (M. M. Donato, M)

Mineral and fuel resources, compilations, and topical studies—Continued

Otter Creek Wilderness, West Virginia (K. J. Englund, NC)
 Overflow, Georgia and North Carolina (A. E. Nelson, NC)
 Owens Peak, Little Lake Canyon, and El Paso Mountains, California (J. R. Berquist, M)
 Owlshead Mountain and Slate Range, California (E. H. McKee, M)
 Picacho Peak, California (G. B. Haxel, M)
 Piedra, Colorado (A. L. Bush, D)
 Polvadera and Caballo, New Mexico (Kim Manley, D)
 Rawah Wilderness Area and nearby study areas, Colorado (R. C. Pearson, D)
 Redding 2-degree quadrangle, California Wilderness areas (J. P. Albers, M)
 Saline Valley, California (C. T. Wrucke; R. J. Blakely, M)
 Sandia, New Mexico (D. C. Hedlund, D)
 Sangre de Cristo, Colorado (B. R. Johnson, D)
 Savage Run, Wyoming (Kenneth Segerstrom, D)
 Scodie and Tuolumne River Wilderness Areas, California (J. F. Seitz, M)
 Selkirk and Upper Priest, Washington and Idaho (F. K. Miller, Spokane)
 Selway-Bitterroot Wilderness, Idaho and Montana (M. I. Toth, D)
 Sill Hill, Houser, and Caliente, California (V. R. Todd, M)
 South Carolina (C. C. Cameron, NC)
 Spanish Peaks, Colorado (K. E. Budding, D)
 Superstition, Arizona (D. W. Peterson, D)
 Sweetwater, California and Nevada (G. F. Brem, M)
 Ten Lakes, Montana (J. W. Whipple, Spokane, Wash.)
 Ventana, Black Butte, and Bear Canyon, California (V. M. Seiders, M)
 Vermont Wilderness and RARE II areas (J. F. Slack, NC)
 Welcome Creek, Montana (C. A. Wallace, D)
 West Chichagof-Yakobi Wilderness Study Area, Alaska (B. R. Johnson, M)
 West Needles, Colorado (R. E. VanLoenen, D)
 Wheeler Peak, Colorado (W. H. Raymond, D)
 Whetstone, Arizona (C. T. Wrucke, Jr., M)
 White Mountains, New Hampshire (R. H. Moench, D)
 Wild Cattle, Heart Lake, Butt Mountain, Ishi, Polk Springs, and Mill Creek, Oregon (E. H. McKee, M)
 Wild Rogue, Oregon (Floyd Gray, M)
 Williams Fork, Colorado (P. K. Theobald, D)
 Winchester Mountains, Arizona (W. J. Keith, M)
 Windago Thielsen and Diamond Peak, Oregon (N. S. McLeod, M)
 Wonder Mountain Study Area, Washington (R. W. Tabor, M)
 Resources and geology of nickel and cobalt (M. P. Foose, NC)
 States:
 Alaska (M, except as otherwise noted):
 AMRAP Geochemical Exploration (S. E. Church, D)
 AMRAP Geophysical Studies (J. E. Case, D. F. Barnes, C. K. Moss, D)
 AMRAP Program (H. C. Berg)
 Cenozoic geology (D. M. Hopkins, D)
 Coastal environments (A. T. Ovenshine, NC)
 Mineral resources (D. F. Barnes)
 Ore-forming environments, Ambler District (D. P. Cox)
 Petersburg quadrangle (D. A. Brew, J. B. Cathrall, D)
 Southeastern Brooks Range (W. P. Brosgé)
 Arizona:
 Ajo 2-degree quadrangle, geochemistry (P. K. Theobald, D); mineral resources, (G. B. Haxel, M); remote sensing

Mineral and fuel resources, compilations, and topical studies—Continued

- (G. L. Raines, D); geophysics (D. P. Klein, D)
- Base and precious metal resources (J. A. Peterson, M)
- Metals in red-bed sequences (D. H. Lindsey, D)
- Needles 2-degree quadrangle (K. A. Howard, M)
- Ores related to rhyolites, southeastern Arizona (D. H. Richter, Santa Fe)
- Silver City 2-degree quadrangle, mineral resources (D. H. Richter, Santa Fe)
- California:
 - Mineral resources (J. P. Albers, M)
 - Needles 2-degree quadrangle (K. A. Howard, M)
 - Resource processes, West Shasta massive sulfides (J. P. Albers, M)
- Colorado (D):
 - Metals in red-bed sequences (D. H. Lindsey)
 - Precambrian sulfide deposits (D. M. Sheridan)
 - Summitville district, alteration study (R. E. Van Loenen)
- Idaho:
 - Challis 2-degree quadrangle, biogeochemical exploration (J. A. Erdman, M); geochemistry (G. J. Neuerberg, D); geology (W. E. Hall, M); mineral resources (F. S. Fisher, D)
 - Ore controls, Coeur d'Alene district (R. R. Reid, Moscow)
 - Ore genesis, Coeur d'Alene district (G. P. Landis, D)
- Maine, Sherbrooke-Lewiston 2-degree quadrangle, geochemistry (F. C. Carney, D); geology (N. L. Hatch, Jr., NC); geophysical studies (D. P. Klein, D); remote sensing (H. A. Pohn, NC)
- Missouri, Springfield 2-degree quadrangle, geochemistry (R. L. Erickson, D); geophysics (L. E. Cordell, D); mineral resource appraisal (W. P. Pratt, D)
- Montana:
 - Butte 2-degree quadrangle, geochemistry (J. C. Antweiler, D); mineral resources (J. E. Elliott, D); geophysics (W. F. Hanna, D); remote sensing (L. C. Rowan, NC)
 - Southwestern bedded Precambrian iron deposits (H. L. James, Port Townsend, Wash.)
- Montana-Idaho, Dillion 2-degree quadrangle, geochemistry (B. R. Berger, D); geophysics (W. F. Hanna, D); remote sensing (L. C. Rowan, NC)
- Nevada:
 - Jefferson-Belmont areas (D. R. Shawe, D)
 - Mineral resources (E. W. Tooker, M)
 - Ore genesis, Uinta trend (R. P. Ashley, M)
 - Southern Snake Mountains (K. B. Ketner, D)
 - Tonopah 2-degree quadrangle, mineral resources (D. H. Whitebread, M); geochemistry (J. T. Nash, D); geophysics (Donald Plouff, M); remote sensing (T. L. Purdy, NC)
 - Tungsten resources (H. K. Stager, M)
- New Hampshire-New York-Vermont:
 - Glens Falls 2-degree quadrangle, geochemistry (K. C. Watts, Jr., D); geophysics (D. L. Daniels, NC); mineral resources (C. E. Brown, NC); remote sensing (N. M. Milton, NC)
- New Mexico:
 - Mineral resources, Apache district (C. H. Maxwell, D)
 - Ores related to rhyolites, southwestern New Mexico (D. H. Richter, Santa Fe)
- New York, Mineral resources of Precambrian rocks, St. Lawrence County (C. E. Brown, NC)
- North Carolina:
 - Charlotte 2-degree quadrangle, geophysics (D. L. Daniels, NC); mineral resources, (G. E. Ericksen, NC)

Mineral and fuel resources, compilations, and topical studies—Continued

- North Dakota:
 - Geology, geophysics, and mineral potential of buried Precambrian rocks (J. S. Klasner, Macomb, Ill.)
- Oregon, McDermitt caldera complex (J. J. Rytuba, M)
- South Carolina:
 - Mineral resources, Charlotte 2-degree quadrangle (G. E. Ericksen, NC)
- South Dakota:
 - Geology, geophysics, and mineral potential of buried Precambrian rocks (J. S. Klasner, Macomb, Ill.)
 - Keystone area, Black Hills (J. J. Norton, D)
- United States:
 - Appalachian massive sulfides, Southeastern U.S. (J. E. Gair, NC)
 - Atlantic Coastal Plain, heavy minerals (A. E. Grosz, NC)
 - Bentonite resources, Rocky Mountains (C. G. Whitney, D)
 - Central States, mineral-deposit controls (A. V. Heyl, Jr., D)
 - Great Lakes Region, Precambrian tectonics, Lake Superior (P. K. Sims, D)
 - Metallogenic maps (P. W. Guild, NC)
 - Northeastern States, peat resources (C. C. Cameron, NC)
 - Phosphate, Southeastern States (J. B. Cathcart, D); Great Basin (K. B. Ketner, D)
 - Silica resources (K. B. Ketner, D)
- Utah:
 - Ore genesis, Uinta trend (R. P. Ashley, M)
 - Richfield 2-degree quadrangle, geochemistry (W. R. Miller, D); geophysics (D. R. Mabey, D)
- Washington:
 - Mineral resources (J. A. Peterson, M)
 - Mount St. Helens basement rocks (R. P. Ashley, M)
- See also specific minerals or fuels.*
- Mineralogy and crystallography, experimental:**
 - Crystal chemistry (Malcolm Ross, NC)
 - Crystal structure, sulfides (H. T. Evans, Jr., NC)
 - Electrochemistry of minerals (Motoaki Sato, NC)
 - Fluid-inclusion and light stable isotope studies of sulfide mineral deposits (T. G. Theodore, M)
 - Geochemistry (George Phair, NC)
 - Mineral identification (M. E. Mrose, NC)
 - Mineralogy of metalliferous shales (G. A. Desborough, D)
 - Mineralogy of sedimentary rocks (P. D. Blackmon, D)
 - Phosphoria Formation, stratigraphy and resources (R. A. Gulbrandsen, M)
 - Rapid mineralogical analyses (L. G. Schultz, D)
 - Research on ore minerals (B. F. Leonard, D)
 - See also Geochemistry, experimental.*
- Mineral resource investigations, resource information systems and analysis:**
 - Computer applications in mineral resource studies (R. B. McCammon, NC)
 - Computer-assisted mapping of critical minerals (P. G. Schruben, NC)
 - Computer-based mineral and energy resource system for the Navajo Tribe (J. D. Bliss, M)
 - Computer graphics, geologic and commodity maps (P. A. Fulton, NC)
 - Computerized coal resource assessments (A. L. Medlin, NC)
 - Computerized resource estimation and contouring techniques (W. D. Grundy, D)
 - CUSMAP Program (J. H. DeYoung, Jr., T. M. Cookro, NC)
 - Economics of mineral resources (J. H. DeYoung, Jr., NC)
 - Energy resource studies (R. F. Meyer, NC)
 - Geologic database management (R. W. Bowen, NC)

Mineral resource investigations, resource information systems and analysis—Continued

- Geostatistical analysis of resource potential of Maine, New Hampshire, and Vermont (W. J. Bawiec, NC)
- Geostatistical analysis of structure and distribution of ore in early magmatic environments (L. J. Drew, NC)
- Interactive data analysis of geologic data (J. O. Kork, D)
- Metallogenic studies (P. W. Guild, NC)
- Mineral assessment techniques in glaciated terrain (L. H. Filipek, D)
- Mineral Data System (MDS) (J. A. Calkins, NC)
- Petroleum resource appraisal and discovery process modeling (D. H. Root, NC)
- Processes controlling metal deposition in a fresh-seawater interface (L. H. Filipek, D)
- Research, development, and application of techniques for mineral assessment studies (R. W. Leinz, D)
- Resource analysis evaluation (E. D. Attanasi, NC)
- Resource assessment (D. W. Menzie, M)
- Resource assessment methods (D. A. Singer, M)
- Resources in sedimentary host rocks (W. D. Grundy, D)
- Statistical analysis of mineral assessment data (J. T. Hanley, NC)
- Uranium resource analysis (R. B. McCammon, NC)
- Model studies, geologic, geophysical, and mineral:**
- Characteristics of mineral occurrence (R. L. Erickson, D)
- Computer modeling:
- Research for engineering geology (W. Z. Savage, D)
- Rock-water interactions (J. L. Haas, Jr., NC)
- Exploration model for rutile in metasedimentary rocks (S. P. Marsh, D)
- Geochemical exploration model, Coeur d'Alene district, Idaho (D. L. Leach, D)
- Geochemical models, epithermal gold-silver deposits (B. R. Berger, D)
- Ice ages (D. P. Adam, M)
- Mineral scarcity model development (S. M. Cargill, NC)
- Occurrence models of mineral deposits (R. B. Taylor, D)
- Model studies, hydrologic:**
- Alluvial fan deposition (W. E. Price, w, NC)
- Atchafalaya River basin model (M. E. Jennings, w, Bay St. Louis, Miss.)
- Chattahoochee intensive river quality (R. N. Cherry, w, Atlanta, Ga.)
- Deterministic surface water models (M. E. Jennings, w, NSTL Station, Miss.)
- Estuaries-rivers dispersion (H. B. Fischer, w, M)
- Estuary hydrodynamics (R. T. Cheng, w, M)
- Ground-water quality modeling (D. B. Grove, w, D)
- High Plains aquifer study (J. B. Weeks, w, D)
- Modeling of hydrodynamic systems (R. W. Schaffranek, w, NC)
- Numerical simulation (V. C. Lai, w, NC)
- Physical modeling (V. R. Schneider, w, Bay St. Louis, Miss.)
- Potomac Estuary hydrodynamics (R. W. Schaffranek, w, NC)
- Radionuclide transport modeling (R. K. Waddell, w, D)
- Rainfall-runoff modeling (G. H. Leavesley, w, D)
- Regional studies coordination (G. D. Bennett, w, NC)
- Simulation of subsurface water flow (R. L. Cooley, w, D)
- Systems analysis lab (I. C. James, w, NC)
- Transient flow (C. E. Mongan, w, Cambridge, Mass.)
- Transport in fluid flow (Akio Ogata, w, M)
- States:**
- Alabama (w, Tuscaloosa):
- Southeast regional aquifer study, Alabama (M. E. Davis)
- Arizona (w, Tucson):

Model studies, hydrologic—Continued

- Coconino aquifer—Apache County, Arizona (P. P. Ross, Flagstaff)
- Southwest alluvial basins—RASA (T. W. Anderson)
- Arkansas (w, Little Rock):
- Illinois River model (E. E. Morris)
- California (w, Menlo Park):
- Digital model of Carmel Valley (M. J. Johnson)
- Ground-water model, Fresno County (H. T. Mitten, Sacramento)
- Impact of Marble Cone fire (K. W. Lee)
- Sacramento valley ground water (S. K. Sorenson, Sacramento)
- Salinas ground-water model (M. J. Johnson)
- Water supply forecast evaluation (K. L. Wahl)
- Colorado (w, Lakewood):
- Arkansas River basin model (J. L. Hughes, Pueblo)
- Closed Basin (G. J. Leonard, Pueblo)
- Geochemical investigation (R. L. Tobin, Meeker)
- In-situ uranium mining (J. W. Warner, D)
- Narrows Reservoir model (D. R. Minges, D)
- Rocky Mountain Arsenal DIMP (diisopropylmethylphosphonate) contamination (S. G. Robson, D)
- San Luis Valley modeling (E. L. Nickerson, Pueblo)
- Streamflow simulation (R. S. Parker, D)
- Water management—High Plains, Colorado (R. G. Borman, D)
- Delaware (w, Dover):
- Coastal aquifers study (A. L. Hodges)
- Florida (w, Tallahassee):
- Estuarine hydrology, Tampa Bay model (C. R. Goodwin, Tampa)
- Floridan aquifer ground-water flow model southwest Florida (E. C. Hayes, Jacksonville)
- Ground-water computer models (D. M. Johnson, Tampa)
- Hydrology of mining areas southwest Florida (W. R. Murphy, Tampa)
- Low flow in southwest Florida (K. M. Hammett, Tampa)
- North Tampa regional model (C. B. Hutchinson, Tampa)
- Southeast limestone, east-central Florida (C. H. Tibbals, Orlando)
- Southeast limestone, west-central Florida (P. D. Ryder, Tampa)
- Unconfined aquifer, Charlotte County (J. J. Hickey, Tampa)
- Water resources, Ft. Walton Beach area (P. R. Seaber)
- Watershed modeling (K. M. Hammett, Tampa)
- Georgia (w, Doraville):
- Coastal plain sand-aquifer study (R. E. Faye)
- Cretaceous-tertiary aquifer, Georgia (J. S. Clarke)
- Principal artesian aquifer (L. R. Hayes)
- Idaho (w, Boise):
- Rathdrum Prairie aquifer (H. R. Seitz)
- Illinois (w, Urbana):
- Loss rate effects on T & K (George Garklavs)
- Kansas (w, Lawrence):
- Central Midwest aquifer study (C. H. Baker)
- Ground water, north-central Kansas (L. E. Stullken, Garden City)
- Ground-water pumping effect on Arkansas River (L. E. Dunlap, Garden City)
- High Plains aquifer study (L. E. Stullken, Garden City)
- Streamflow models (P. R. Jordan)
- Water-supply planning, west-central Kansas (J. M. Spinzola)
- Kentucky (w, Louisville):

Model studies, hydrologic—Continued

- Assessment of models (D. E. Bower)
- Louisiana (w, Baton Rouge):
 - Hydrology of Pearl River basin (G. J. Wiche)
 - Modeling of Sparta Sand (G. N. Ryals, Alexandria)
- Maine (w, Augusta):
 - Maine surface-water network (R. A. Morrill)
- Maryland (w, Towson):
 - Aquia-Piney Point-Nanjemoy aquifers (F. H. Chapelle)
- Massachusetts (w, Boston):
 - Charles River basin model (D. J. Lang)
 - Mattapoissett aquifer study (Julio Olimpico)
- Minnesota (w, St. Paul):
 - Analog model of the Twin Cities Basin (R. F. Norvitch)
- Mississippi (w, Jackson):
 - Ground-water model—Yazoo River navigation (J. M. Kernodle)
 - Southeast regional aquifer study, Mississippi-Alabama (M. J. Mallory)
- Montana (w, Helena):
 - Rosebud, Armells Creek salinity models (P. F. Woods)
- Nebraska (w, Lincoln):
 - High Plains aquifer study (R. A. Pettijohn)
- Nevada (w, Carson City):
 - Jones-Galena Creek water resources (T. L. Katzer)
 - Las Vegas Valley ground-water models (David Morgan)
- New Jersey (w, Trenton):
 - Regional aquifer study, New Jersey (O. S. Zapecza)
 - Water resources, Wharton tract (A. W. Harbaugh)
- New Mexico (w, Albuquerque):
 - Cimarron Basin analysis (E. D. Cobb)
 - High Plains aquifer study (D. R. Hart)
 - High Plains study, Lea County (D. P. McAda)
 - Model study of Santa Fe area, New Mexico (K. F. Dennehy)
- New York (w, Albany):
 - Flow routing—upper Susquehanna (T. J. Zembrzuski)
 - Ground water in western Long Island (H. T. Buxton, Syosset)
 - Ground-water models, Long Island (T. E. Reilly, Syosset)
 - Impact and mitigation of sewerage (T. E. Reilly, Syosset)
 - Regional aquifer study, Long Island (M. S. Garber, Syosset)
 - Simulating ground water-surface water interaction (M. P. Bergeron, Ithaca)
 - Tioughnioga River ground water (O. J. Cosner, Ithaca)
- North Carolina (w, Raleigh):
 - North Carolina Coastal Plain aquifer study (R. W. Coble)
- North Dakota (w, Bismarck):
 - Surface-water modeling, Fort Union coal region (D. G. Emerson)
- Ohio (w, Columbus):
 - Franklin County aquifer study (A. C. Razem)
 - Ground-water evaluation of Geauga County (A. C. Razem)
 - Ground-water hydrology, strip-mining areas (A. C. Razem)
- Oklahoma (w, Oklahoma City):
 - Antlers aquifer model (R. B. Morton)
 - Coal Creek basin, Oklahoma (S. P. Blumer)
 - High Plains aquifer study (J. S. Havens)
 - North Canadian hydrology, phase II (S. C. Christenson)
- Oregon (w, Portland):
 - Umatilla structural basin model (Ann Zurawski)
- Pennsylvania (w, Harrisburg):
 - Anthracite region hydrologic model (D. J. Growitz)
 - Delaware River streamflow model (J. O. Shearman)
 - Laurel Run Dam failure (J. T. Armbruster)
 - Research modeling in coal areas (W. J. Herb)

Model studies, hydrologic—Continued

- West Branch Brandywine Creek stormwater model (R. A. Sloto, Malvern)
- West Branch flow-routing (S. A. Brua)
- Puerto Rico (w, San Juan):
 - North coast model (J. E. Heisel, Ft. Buchanan)
 - Water in the Lower Rio Loco Valley (Arturo E. Torres-Gonzalez)
- Rhode Island (w, Providence):
 - Hydrology, Providence-Warwick (H. E. Johnston)
 - Radionuclide transport (B. J. Ryan)
- South Carolina (w, Columbia):
 - Coastal Plain sand aquifer study (W. R. Aucott)
 - Flow and quality of water model (S. J. Playton)
- South Dakota (w, Huron):
 - Digital model, James River basin (L. K. Kuiper)
 - Digital model, Minnehaha County (N. C. Koch)
 - Water resources, Big Sioux valley (N. C. Koch)
- Tennessee (w, Nashville):
 - Hydrologic process model, coal basins (W. P. Carey)
 - Memphis ground-water model (J. V. Brahana)
- Texas (w, Austin):
 - High Plains aquifer study (L. F. Land)
 - Miocene aquifer study (E. T. Baker)
- Utah (w, Salt Lake City):
 - Hydrology of Beryl-Enterprise area (R. W. Mower)
- Virginia (w, Richmond):
 - Coastal Plain aquifers, Virginia (J. F. Harsh)
 - Research modeling in coal areas (T. W. Danielson)
- Washington (w, Tacoma):
 - Model simulation for water management (William Meyer)
 - Mt. Rainier flood discharge models (W. G. Sikonia)
- West Virginia (w, Charleston):
 - Hydrologic modeling (Celso Puente)
 - Research modeling in coal areas (S. M. Ward, Morgantown)
- Wisconsin (w, Madison):
 - Land-use changes, southwest Wisconsin (W. R. Krug)
 - Nonpoint pollution in Fox Basin (P. E. Hughes)
- Wyoming (w, Cheyenne):
 - Digital model, La Grange area, Wyoming (W. B. Borchert)
- Moon studies.** See Extraterrestrial studies.
- Municipal and domestic wastes, inorganic:**
 - Colorado (w, Lakewood):
 - El Paso County water quality (D. L. Cain, Pueblo)
 - Kansas (w, Lawrence):
 - Chemical quality of atmospheric fallout (K. D. Medina)
 - Urban storm-water quality (A. M. Diaz)
 - Montana (w, Helena):
 - Geohydrology of Helena Valley, Montana (A. J. Boettcher)
 - Nevada (w, Carson City):
 - Truckee-Carson assessment (J. O. Nowlin)
 - New York (w, Albany):
 - Irondequoit wetland hydrology (William Kappel, Ithaca)
 - Westchester County waste management (R. J. Archer)
 - Wisconsin (w, Madison):
 - Stream re-aeration (L. B. House)
- Municipal and domestic wastes, organic:**
 - Organic substances in streams (R. E. Rathbun, w, Bay St. Louis, Miss.)
- States:**
 - California (w, Menlo Park):
 - Waste water re-use (J. A. Izbicki, Laguna Niguel)
 - Colorado (w, Lakewood):
 - Northwestern Colorado water quality (T. R. Ford, Meeker)
 - Florida (w, Tallahassee):

Municipal and domestic wastes, organic—Continued

Intensive quality of water surveys of streams (J. E. Coffin)
Reaeration capacity, Florida (J. E. Coffin)

Georgia (w, Doraville):

Quality of water of West Point Reservoir (D. B. Radtke)

Illinois (w, Urbana):

Sludge irrigation hydrology (R. F. Fuentes)

Indiana (w, Indianapolis):

Water-quality assessment, White River (D. J. Wangness)

Kentucky (w, Louisville):

Chemical quality of ground water in Kentucky (D. S. Mull)

Missouri (w, Rolla):

Urban runoff in Springfield, Missouri (John Skelton)

New York (w, Albany):

Reaeration studies (D. A. Stedfast)

North Dakota (w, Bismarck):

Quality of water assessment, Souris River, North Dakota
(E. A. Wesolowski)

Oregon (w, Portland):

Portland Harbor study (S. W. McKenzie)

Network design:

National quality of water network design (R. A. Smith, w, NC)

Urban studies coordination (E. D. Cobb, w, NC)

States:

California (w, Menlo Park):

Monterey County network evaluation (D. A. Van Schoten)
Santa Barbara ground water (Peter Martin, Laguna Niquel)
Surface-water network study (J. R. Crippen)

Colorado (w, Lakewood):

Manual for hydrologic monitoring (J. T. Turk, D)

Connecticut (w, Hartford):

Connecticut stream quality (K. P. Kulp)
Integrated hydrologic network—Connecticut (R. L. Melvin)

Florida (w, Tallahassee):

Charlotte Harbor estuarine study (J. F. Turner, Tampa)
Florida ground-water quality network (P. R. Seaber)

Georgia (w, Doraville):

Georgia streamflow network evaluation (R. F. Carter)

Hawaii (w, Honolulu):

Network evaluation (Iwao Matsuoka)

Idaho (w, Boise):

Evaluation of stream-gaging (W. A. Harenberg)

Illinois (w, Urbana):

Ground-water network design (L. R. Frost)

Iowa (w, Iowa City):

Ground-water quality monitoring network (M. G. Detroy)

Massachusetts (w, Boston):

Ground-water quality network (R. V. Fowler)
Massachusetts surface-water network (R. A. Brackley)

Michigan (w, Lansing):

Design of ground-water network, Michigan (F. R. Twenter)

Nevada (w, Carson City):

Surface-water network evaluation (R. R. Squires)

New Jersey (w, Trenton):

Ground-water quality assessment (D. A. Harriman)

New York (w, Albany):

Surface-water network evaluation (T. J. Zembrzuski)

Pennsylvania (w, Harrisburg):

Gaging network, Pennsylvania (H. N. Flippo)

Nuclear explosions, geology:

Engineering geophysics, Nevada Test Site (R. D. Carroll, D)

Nuclear site studies:

Waste-disposal sites (L. A. Wood, w, NC)

States:

Illinois (w, Urbana):

Nuclear site studies—Continued

Ground-water flow, Sheffield site (J. B. Foster)

Sheffield unsaturated flow (R. W. Healy)

New York (w, Albany):

Hydrology of nuclear landfill (M. P. Bergeron)

West Valley nuclear storage study (W. M. Kappel, Ithaca)

Nutrients:

Polaris operations (T. T. Conomos, w, M)

Potomac River Estuary geochemistry (Edward Callender, w, NC)

States:

Florida (w, Tallahassee):

Apalachicola River quality (H. C. Mattraw)

River quality-Kissimmee Basin (A. G. Lamonds, Winter Park)

Maine (w, Augusta):

Maine lakes (W. J. Nichols)

Maryland (w, Towson):

Patuxent Estuary nutrient flux (W. W. Staubitz)

Massachusetts (w, Boston):

Hager Pond nutrient study (J. C. Briggs)

Lake Cochituate nutrients (F. B. Gay)

Minnesota (w, St. Paul):

Quality of water, Voyageurs National Park (G. A. Payne)

New York (w, Albany):

Switzer Creek nonpoint pollution (D. A. Sherwood, Ithaca)

Pennsylvania (w, Harrisburg):

Nonpoint sources, Pequea Creek basin (J. R. Ward)

Susquehanna River quality of water loads (D. K. Fishel)

Vermont (w, Montpelier):

Hydrologic system, Lake Morey (J. E. Cotton, Bow, N.H.)

Washington (w, Tacoma):

Hydrology of Pine Lake, Washington (N. P. Dion)

Oil shale:

Organic geochemistry (R. E. Miller, D)

Petrology (J. R. Dyni, D)

Regional geochemistry (W. E. Dean, Jr., D)

Stratigraphic studies, eastern Uinta Basin (W. B. Cashion, Jr., D)

Trace elements (W. E. Dean, Jr., D)

States:

Colorado (D)

Piceance Creek Basin:

Douglas Pass 1-degree quadrangle (R. C. Johnson)

East-central (R. B. O'Sullivan)

Geology (J. R. Donnell)

Mechanics of jointing (E. R. Verbeek)

Rangely 1-degree quadrangle (W. J. Hail, Jr.)

Sedimentary diagenesis of Tertiary/Cretaceous marine/nonmarine rocks (J. K. Pitman)

Stratigraphy of the Green River Formation (R. C. Johnson)

Tectonic controls (D. L. Sawatzky)

Colorado-Utah-Wyoming, geochemistry (W. E. Dean, Jr., D)

Colorado-Wyoming, Eocene rocks (H. W. Roehler, D)

Nevada, Investigations of oil shale of Tertiary age (B. Solomon, c, M)

United States (D):

Computer applications to resource appraisal and stratigraphy, Western United States (J. K. Pitman)

Geologic factors related to development (W. R. Hansen)

Utah (D):

Sedimentary diagenesis of Tertiary/Cretaceous marine/non-marine rocks, Uinta Basin (J. K. Pitman)

Oil shale—Continued

Seep Ridge and Vernal 1-degree quadrangles (W. B. Cashion, Jr.)

South 1/2 Nutters Hole quadrangle (W. B. Cashion, Jr.)

Overdevelopment of supplies:

New Mexico (w, Albuquerque):

Coal mining effects-San Juan Basin (P. F. Frenzel)

San Juan Crownpoint ground-water surveillance (P. F. Frenzel)

Washington (w, Tacoma):

Clallam County water resources (B. W. Drost)

Paleobotany, systematic:

Diatom studies (G. W. Andrews, NC)

Floras:

Cenozoic:

Pacific Northwest (J. A. Wolfe, M)

Western United States and Alaska (J. A. Wolfe, M)

Devonian (J. M. Schopf, Columbus, Ohio)

Paleozoic (S. H. Mamay, NC)

Fossil wood and general paleobotany (R. A. Scott, D)

Plant microfossils:

Mesozoic (R. H. Tschudy, D)

Paleozoic (R. M. Kosanke, D)

Paleoclimatology:

California, Southwestern Great Basin (G. I. Smith, M)

Paleoecology:

Insects and pollen, Quaternary Alaska (R. E. Nelson, Seattle)

Ostracodes, Recent, North Atlantic (J. E. Hazel, NC)

Pollen, Quaternary, California (D. P. Adam, M)

Vertebrate faunas, Ryukyu Islands, biogeography (F. C. Whitmore, Jr., NC)

Paleontology, invertebrate, systematic:

Brachiopods:

Carboniferous (Mackenzie Gordon, Jr., NC)

Upper Paleozoic (J. T. Dutro, Jr., NC)

Cephalopods:

Cretaceous (D. L. Jones, M)

Upper Cretaceous (W. A. Cobban, D)

Upper Paleozoic (Mackenzie Gordon, Jr., NC)

Conodonts:

Devonian and Mississippian (C. A. Sandberg, D)

Succession across the Lower/Mid-Ordovician boundary, Central Appalachians (A. G. Harris, NC)

Corals, rugose:

Mississippian (W. J. Sando, NC)

Silurian-Devonian (W. A. Oliver, Jr., NC)

Foraminifera, Mississippian (B. A. Skipp, D)

Gastropods, Mesozoic (N. F. Sohl, NC)

Graptolites, Ordovician-Silurian (R. J. Ross, Jr., D)

Mollusks:

Cambrian, biostratigraphy and correlation of shallow marine shelf sediments (John Pojeta, Jr., NC)

Planktonic biochronology (R. Z. Poore, NC)

Ostracodes:

Alaskan Paleogene floras (J. A. Wolfe, M)

Northern Alaska Carboniferous and Triassic (I. G. Sohn, Wash., D.C.)

Upper Cretaceous and Tertiary (J. E. Hazel, NC)

Upper Paleozoic (I. G. Sohn, NC)

Pelecypods:

Inoceramids (D. L. Jones, M)

Triassic (N. J. Silberling, M)

Trilobites, Ordovician (R. J. Ross, Jr., D)

Paleontology, stratigraphic:

Biostratigraphic and depositional framework, Atlantic Con-

Paleontology, stratigraphic—Continued

tinental Margin (P. C. Valentine, Jr., Woods Hole)

Conodont-based age determinations, low- to medium-grade metamorphic rocks, Appalachian orogen (A. G. Harris, NC)

Cenozoic:

Cryosphere and sea-level history (R. Z. Poore, NC)

Pollen and spores, Kentucky (R. H. Tschudy, D)

Tectonic history, northeastern North Carolina (L. W. Ward, NC)

Vertebrates:

Atlantic coast (F. C. Whitmore, Jr., NC)

Pacific coast (C. A. Repenning, M)

Panama Canal Zone (F. C. Whitmore, Jr., NC)

Mesozoic:

Pacific coast and Alaska (D. L. Jones, M)

Cretaceous:

Alaska (D. L. Jones, M)

Biostratigraphy of the Wasatch hinterland and thrust belt, Utah-Wyoming (D. J. Nichols, D)

Coastal Plain (N. F. Sohl, NC)

Depositional environment and biostratigraphy, Fort Union and Wasatch Formations (J. H. Hanley, D)

Gulf coast and Caribbean (N. F. Sohl, NC)

Molluscan faunas, Caribbean (N. F. Sohl, NC)

Western Interior United States (W. A. Cobban, D)

Triassic:

Biostratigraphy, organic metamorphism, overthrust belt, Western United States (B. R. Wardlaw, NC)

Marine faunas and stratigraphy (N. J. Silberling, M)

Paleozoic:

Biostratigraphy, Alaska (A. K. Armstrong, M)

Biostratigraphy, organic metamorphism, overthrust belt, Western United States (B. R. Wardlaw, NC)

Cambrian chronostratigraphic and depositional framework, Western United States (M. E. Taylor, D)

Conodont succession across the Lower/Mid-Ordovician boundary, central Appalachians (A. G. Harris, NC)

Devonian and Mississippian conodonts, Western United States (C. A. Sandberg, D)

Mississippian:

Stratigraphy and brachiopods, northern Rocky Mountains and Alaska (J. T. Dutro, Jr., NC)

Stratigraphy and corals, northern Rocky Mountains (W. J. Sando, NC)

Onesquethaw Stage (Devonian), stratigraphy and rugose corals (W. A. Oliver, NC)

Palynology of cores from Naval Petroleum Reserve No. 4 (R. A. Scott, D)

Silurian-Devonian Corals, Northeastern United States (W. A. Oliver, Jr., NC)

Upper Paleozoic, Western States (Mackenzie Gordon, Jr., NC)

Quaternary:

Chronostratigraphic framework, southwestern Alaska (T. A. Ager, NC)

Climate history and tephrochronology, south-central Alaska (T. A. Ager, NC)

Paleontology, vertebrate, systematic:

Artiodactyls, primitive (F. C. Whitmore, Jr., NC)

Cambrian chronostratigraphic and depositional framework, Western United States (M. E. Taylor, D)

Cenozoic biostratigraphy, southern Alaska (L. N. Marinovich, M)

Cretaceous Coastal Plain (N. F. Sohl, NC)

Paleontology, vertebrate, systematic—Continued

- Cretaceous-Tertiary palynology, Los Padres National Forest, California (N. O. Frederiksen, NC)
- Mid-Cretaceous events, Colorado (D. J. Nichols, D)
- Pinnipedia (C. A. Repenning, M)
- Pleistocene fauna, Big Bone Lick, Kentucky (F. C. Whitmore, Jr., NC)
- Quaternary, Clear Lake, California (J. P. Bradbury, D)
- Tertiary coal-bearing strata, Wind River, Wyoming, biostratigraphy and paleoenvironments (T. M. Bown, D)
- Tertiary marine basins, California, synoptic correlation (E. J. Moore, M)

Pesticides, organic:

- Atlanta Central Lab—organic analyses (L. E. Lowe, w)
- Denver Central Lab—organic analyses (R. R. Grabbe, w, D)
- Pesticide monitoring network (R. J. Pickering, w, NC)

States:

- Louisiana (w, Baton Rouge):
 - Limnological study, Lake Bruin, Louisiana (H. L. Leone)
- New Jersey (w, Trenton):
 - Quantification nonpoint pollution (J. C. Schornick)
- New York (w, Albany):
 - Organic compounds in ground water (J. T. Turk)
 - PCB transport in the upper Hudson (R. A. Schroeder)
- Wyoming (w, Cheyenne):
 - Herbicides, Wyoming streams (S. J. Rucker)

Petroleum and natural gas:

- Aeromagnetic detection of diagenetic magnetite over oil fields (T. J. Donovan, Flagstaff)
- Aromatic hydrocarbons, analyses of (T. G. Ging, Jr., D)
- Biogeochemical prospecting for petroleum (T. J. Donovan, Flagstaff)
- Borehole gravimetry, application to oil exploration (J. W. Schmoker, D)
- Borehole gravity studies and operations (S. L. Robbins, D)
- Carbonate submarine fans, depositional environments, processes, facies, and modeling (H. E. Cook, M)
- Catagenesis of organic matter and generation of petroleum (N. H. Bostick, D)
- Characteristics of carbonate reservoir rocks (R. B. Halley, D)
- Chemical and isotopic evidence, origin of natural gas (D. D. Rice, D)
- Computer applications to reservoir rock problems (T. S. Dyman, Pullman, Wash.)
- Computer well-log analysis and applications (S. E. Prenskey, D)
- Data storage and retrieval system (L. B. Alley, D)
- Deep-water reservoir rocks (Hugh McLean, M)
- Geochemical study (G. E. Claypool, D)
- Geology of the Volga-Ural petroleum province (J. A. Peterson, Missoula, Mont.; J. W. Clarke, NC)
- Geophysical data interpretation (D. J. Taylor, D)
- Hydrocarbon micro-seepage (J. D. Hendricks, Flagstaff)
- Hydrocarbon source rocks and paleoceanography (M. A. Arthur, D)
- Minor and trace element distribution in crude oil source rocks (J. R. Hatch, D)
- Oil and gas resource appraisal methodology and procedures (R. A. Crovelli, D)
- Organic and inorganic measures of thermal maturity, comparison of (C. E. Barker, D)
- Origin, migration, and accumulation of petroleum (L. C. Price, D)
- Origin of oil in continental basins (D. E. Anders, D)
- Permian reef (R. B. Halley, D)
- Petroleum geology and resource appraisal, Southern Mexico

Petroleum and natural gas—Continued

- and Guatemala (J. A. Peterson, Missoula, Mont.)
- Petroleum geology of Permian Phosphoria and Park City Formations (J. A. Peterson, Missoula, Mont.)
- Petroleum geology of siliceous shale and related rocks (L. A. Beyer, M)
- Petroleum prospecting utilizing gaseous emanations (A. A. Roberts, D)
- Petroleum resources of selected South Pacific offshore areas (P. A. Scholle, D)
- Petrology and reservoir characteristics, deeply buried rocks (C. W. Keighin, D)
- Petrology of organic matter in sedimentary rocks (N. H. Bostick, D)
- Reservoir rock properties (J. W. Schmoker, D)
- Seismic petroleum exploration research (A. H. Balch, D)
- Source bed evaluation, Appalachian basin black shale (J. B. Roen, NC)
- Stratigraphy and sedimentation of geopressed zones (R. Q. Foote, Corpus Christi)
- Thrust plate models of the Appalachian Orogen (K. C. Bayer and Wallace DeWitt, Jr., NC)
- Western United States:
 - Characterization of natural gas resources, low-permeability rocks, Piceance and Uinta Basins (T. D. Fouch, D); Green River Basin (B. E. Law, D); Northern Great Plains (D. D. Rice, D)
 - Characterization of natural gas resources, low-permeability sandstones, Wind River Basin (J. E. Fox, Rapid City, S. Dak.)
 - Cretaceous limestones of the Western Interior (M. A. Arthur, Columbia, S. C.)
 - Depositional history and petroleum geology, Minnelusa Formation (R. T. Ryder, D)
 - Devonian and Mississippian, Overthrust Belt and Great Basin (C. A. Sandberg, D)
 - Frontier Tertiary and Mesozoic hydrocarbon basins (T. D. Fouch, D)
 - Geology and petroleum potential, Western Overthrust Belt (R. B. Powers, D)
 - Reservoir petrology of low-permeability reservoirs (D. L. Goutier, D)
 - Source rocks of Permian age (E. K. Maughan, D)
- States:
 - Alaska, Petroleum assessment geology, North Slope provinces (K. J. Bird, M)
 - Arkansas, geologic framework, Ouachita Mountains (B. R. Haley, Little Rock)
 - California, Deposition and diagenesis, Monterey Formation, Santa Barbara and Santa Maria Basins (C. M. Isaacs, M)
 - Florida, geochemistry of carbonate rocks (J. G. Palacas, D)
 - Montana:
 - Oil and gas in overthrust terrains (W. J. Perry, Jr., D)
 - Reservoir studies, Disturbed belt (K. M. Nichols, D)
 - Oklahoma, Geologic framework, Ouachita Mountains (B. R. Haley, Little Rock)
 - South Dakota, depositional history and petroleum geology of the Minnelusa Formation (R. T. Ryder, NC)
 - Wyoming:
 - Depositional history and petroleum geology of the Minnelusa Formation (R. T. Ryder, NC)
 - Gas-bearing Mid-Cretaceous strata (E. A. Merewether, D)
- Wyoming-Montana-North Dakota-South Dakota, Williston Basin (C. A. Sandberg, D)

Petrology. *See* Geochemistry and petrology, field studies.

Phosphate:

Phosphoria Formation, stratigraphy and resources (R. A. Gulbrandsen, Great Falls, Montana)

States:

Idaho, Lower Valley quadrangle (P. Oberlindacher, c, M)

Nevada:

Loray quadrangle (S. T. Miller, c, M)

Montello Canyon quadrangle (S. T. Miller, c, M)

United States, Southeastern phosphate resources (J. B. Cathcart, D)

Placers:

Placers of Alaska (Warren Yeend, M)

Plant ecology:**Element availability:**

Soils (R. C. Severson, D)

Vegetation (L. P. Gough, D)

Western coal regions, geochemical survey of vegetation (J. A. Erdman, D)

See also Evapotranspiration; Geochronological investigations.

Platinum:

Montana, Stillwater complex (N. J. Page, M)

Platinum group elements from unconventional sources (R. R. Carlson, D)

Platinum—group metals resources (N. J. Page, M)

Primitive areas. *See* Mineral and fuel resources, compilations and topical studies.

Public and industrial water supplies. *See* Water quality, general.

Quality of water techniques and instrumentation:

Analytical technology transfer (M. J. Fishman, w, Arvada, Colo.)

Central Laboratories (W. W. Beetem, w, NC)

Field proficiency testing (D. E. Erdmann, w)

Geochemistry of shale leachates (T. R. Steinheimer, w, Arvada, Colo.)

Instrumentation, petrochemical (W. W. Beetem, w, NC)

Laboratory evaluation (V. J. Janzer, w, Arvada, Colo.)

Methods development (W. W. Beetem, w, NC)

National Water Quality Laboratory—Quality assurance support (Delora Boyle, w, Arvada, Colo.)

Organic chemistry of shale and sediment (W. E. Pereira, w, Arvada, Colo.)

Quality assurance (W. W. Beetem, w, NC)

Quality assurance (L. J. Schroder, w, Arvada, Colo.)

Quality assurance procedures (L. C. Friedman, w, Arvada, Colo.)

Standard reference water-sample program (V. J. Janzer, w, Arvada, Colo.)

States:

Arkansas (w, Little Rock):

Ouachita River model (E. E. Morris)

Stream water-quality modeling (C. T. Bryant)

California (w, Menlo Park):

Accuracy of suspended-sediment data (D. E. Burkham, Sacramento)

Colorado (w, Lakewood):

Suspended-sediment pumping samplers (W. F. Curtis, D)

Mississippi (w, Jackson):

Waste assimilation (G. A. Bednar)

South Dakota (w, Huron):

Geochemical survey, Big Sioux aquifer, South Dakota (N. F. Leibbrand)

Washington (w, Tacoma):

Columbia Basin demonstration project (P. R. Boucher)

Wyoming (w, Cheyenne):

Water quality of small streams, Wyoming (L. L. DeLong)

Quicksilver. *See* Mercury.

Radioactive waste disposal:

Geomechanics of radioactive waste storage (H. S. Swolfs, D)

Hard rock (Z. E. Peterman, D)

Magnetic and gravity studies, Basin and Range and Paradox Basin (T. G. Hildenbrand, D)

Properties of plutonic rocks, southeastern Piedmont (N. J. Trask, NC)

Rock-fluid interaction (I-Ming Chou, NC)

States:

Nevada (D):

Nevada Test Site (A. T. Fernald; E. C. Jenkins; G. L. Dixon)

Waste isolation geophysics (D. B. Hoover, D)

New Mexico, Delaware basin (R. P. Snyder, D)

Utah:

Paradox basin (J. D. Friedman, D)

Paradox salt dome (R. D. Watts, D)

Radioactivity:

Radiochemical network (R. J. Pickering, w, NC)

Reactor support (G. P. Kraker, w, D)

Transuranium research (J. M. Cleveland, w, D)

Tritium laboratory (T. A. Wyerman, w, NC)

Uranium mill tailings (E. R. Landa, w, D)

States:

Florida (w, Tallahassee):

Radionuclides in ground water (H. R. Sufcliffe, Sarasota)

Remote sensing:**Automated cartography:**

Computer system networking (K. P. Johnson, o, Technicolor Graphic Services, Inc., Sioux Falls, S. Dak.)

Data compression techniques for digital image data (R. J. Thompson, o, Sioux Falls, S. Dak.)

Datanap (O. Kays, o, NC)

Data reception and processing requirements for SPOT (R. J. Thompson, o, Sioux Falls, S. Dak.)

Geometric registration of multilevel image data sets (R. McKinney, o, Technicolor Graphic Services, Inc., Sioux Falls, S. Dak.)

High-resolution color film recorder investigation (J. Boyd, o, Technicolor Graphic Services, Inc., Sioux Falls, S. Dak.)

Large area digital mosaicing (R. McKinney, o, Technicolor Graphic Services, Inc., Sioux Falls, S. Dak.)

Media for digital products (R. McKinney, o, Technicolor Graphic Services, Inc., Sioux Falls, S. Dak.)

Multiple data base applications (D. T. Lauer, o, Sioux Falls, S. Dak.)

New techniques for storage of very large spatial data sets (D. Peuquet, o, NC)

Spatial data analysis software development (D. D. Greenlee, o, Sioux Falls, S. Dak.)

Technique development for digital analysis of multiple spatial data (S. K. Jenson, o, Technicolor Graphic Services, Inc., Sioux Falls, S. Dak.)

Techniques for processing digital line graph data (J. Thormodsgard, o, Sioux Falls, S. Dak.)

Transportable applications executive implementation (R. J. Thompson, o, Sioux Falls, S. Dak.)

Geologic applications:

Analysis of SIR-A data of China's deserts (A. Walker, o, NC)

Application of Landsat data to petroleum exploration in the Uinta Basin (G. B. Bailey, o, Sioux Falls, S. Dak.)

Bibliography and index of the geological literature of

Remote sensing—Continued

- Iceland: 1777-1980 (R. S. Williams, Jr., o, NC)
- Development of an automatic analog earthquake processor (J. P. Eaton, M)
- Electromagnetic research (F. C. Frischknecht, D)
- Evaluation of Alaska side-looking radar (J. W. Cady, D)
- Fraunhofer line discriminator luminescence studies (R. D. Watson, o, Flagstaff, Ariz.)
- Gamma-ray research (J. S. Duval, D)
- Geobotanical applications to mineral exploration (N. M. Milton, NC)
- Geochemical plant stress (F. C. Canney, D)
- Geologic mapping of the Wind River Range (C. S. Southworth, o, NC)
- Geometric and radiometric characteristics of Landsat-D (H. H. Kieffer, Flagstaff)
- Geothermal resources (Kenneth Watson, D)
- Heat Capacity Mapping Mission: Thermal-inertia mapping (Kenneth Watson, D)
- Hydrothermal alteration, desert lands (G. L. Raines, D)
- Illustrated geomorphic classification of volcanoes of Iceland (R. S. Williams, Jr., o, NC)
- Infrared surveillance of volcanoes (J. D. Friedman, D)
- Integrated interpretation of aeromagnetic and Landsat data, Interior Alaska (J. W. Cady, D)
- Interpretation of lineament gaps (J. W. Salisbury, o, NC)
- Land mass and plume characteristics of St. Augustine Volcano: 1974-1976 (A. McDade, o, NC)
- Microwave studies of vegetated terrain (M. D. Krohn, NC)
- Petroleum geology investigations in the People's Republic of China (G. B. Bailey, o, Sioux Falls, S. Dak.)
- Photogeologic map of a quadrangle of the Galilean Satellite Europa (A. S. Walker, o, NC)
- Photogrammetric structural studies (L. A. Soderblom, Flagstaff)
- Photo interpretation manual for surface mining inspectors (D. O. Ohlen, o, Technicolor Graphic Services, Inc., Sioux Falls, S. Dak.)
- Plume characteristics of Alaid Volcano, 1981 (A. McDade, o, NC)
- Radar and Landsat imagery of desert regions, hydrologic applications (G. G. Schaber, Flagstaff)
- Remote image processing stations (H. Wagner, Technicolor Graphics, Sioux Falls, S. Dak.)
- Remote sensing and mineral exploration (W. D. Carter; L. C. Rowan, NC)
- Remote-sensing geophysics (Kenneth Watson, D)
- Remote sensing of high-temperature geothermal area of Iceland (R. S. Williams, Jr., o, NC)
- Shuttle Multispectral Infrared Reflectance Radiometer (SMIRR) applications (L. C. Rowan, NC)
- Solar stimulated luminescence (W. Hemphill, o, NC)
- Sonar imaging, marine (P. S. Chavez, Jr., Flagstaff)
- Spectral reflectance of mineralized areas (L. C. Rowan, NC)
- Surficial geology of world deserts (J. F. McCauley, Flagstaff)
- Tectonic overlay for Landsat mosaic of U.S. (C. S. Southworth, o, NC)
- Testing of satellite uplinked remote surface weather stations in the Sierra Nevada (Donald Rottner, Bureau of Reclamation, Denver, Colo.)
- Visible and near-infrared spectra of soils (J. W. Salisbury, o, NC)
- Volcanic gas monitoring (Motoaki Sato, NC)
- Hydrologic applications:

Remote sensing—Continued

- Hydrologic information systems in Black Hills and Cheyenne River basin (L. G. Batten, o, Technicolor Graphic Services, Inc., Sioux Falls, S. Dak.)
- Irrigation potential, Lower Brule and Crow Creek Indian Reservations (P. M. Seevers, Technicolor Graphic Services, Inc., Sioux Falls, S. Dak.)
- Satellite image atlas of glaciers (R. S. Williams, Jr., and J. G. Ferrigno, o, NC)
- Sierra Cooperative Pilot Project:
- Satellite monitoring of cloud-top temperatures (O. H. Foehner, Bureau of Reclamation)
- Testing of satellite uplinked remote surface weather stations in the Sierra Nevada (Donald Rottner, Bureau of Reclamation, D)
- Land-resource applications:
- Analysis of urban vegetation from Landsat data (F. G. Sadowski, o, Technicolor Graphic Services, Inc., Sioux Falls, S. Dak.)
- Applications of Polar Orbiter data for estimation of wildfire fuels loading (W. A. Miller, o, Technicolor Graphic Services, Inc., Sioux Falls, S. Dak.)
- Colorado River natural resources and land use data inventory (H. D. Newkirk, Bureau of Reclamation, Denver, Colo.)
- Deserts and arid land reclamation in the People's Republic of China (A. S. Walkers, o, NC)
- Development of automatic techniques for land use mapping from remote-sensor data (J. R. Wray, o, NC)
- Evaluation of digital data base for classification and management of forested wetlands, Great Dismal Swamp (W. A. Miller, o, Technicolor Graphic Services, Inc., Sioux Falls, S. Dak.)
- Land resource analysis using airborne scanner data (R. L. Hanoen, Bureau of Reclamation, D)
- Landsat application for soil/vegetation inventory (R. H. Haas, o, Technicolor Graphic Services, Inc., Sioux Falls, S. Dak.)
- Reclamation land use analysis (R. L. Hansen, Bureau of Reclamation, D)
- Landsat experiments:
- Geological map of Cape Cod on a Landsat 3 RBV image base (R. N. Oldale, Woods Hole, Mass., and R. S. Williams, Jr., o, NC)
- Index map to optimum Landsat images of Antarctica (R. S. Williams, Jr.; J. G. Ferrigno; T. M. Kent, o; J. W. Schoonmaker, Jr., n, NC)
- Landsat D MSS/thematic mapper applications (J. Thormodsgard, o, Sioux Falls, S. Dak.)
- Landsat D Thematic Mapper near-infrared response (J. W. Salisbury o, NC)
- Landsat image maps for geoscience applications (R. S. Williams, Jr.; J. G. Ferrigno, o, NC)
- Landsat image maps of Cape Cod (R. S. Williams, Jr., o, NC)
- RBV radiometric response analysis and correction (D. Meyer, o, Technicolor Graphic Services, Inc., Sioux Falls, S. Dak.)
- Thematic mapper-simulator data evaluation (F. G. Sadowski, o, Technicolor Graphic Services, Inc., Sioux Falls, S. Dak.)
- Regional:
- Cascade Range (D. H. Knepper, Jr., D)
- San Juan Basin (D. H. Knepper, Jr., D)
- States:
- Alaska:

Remote sensing—Continued

Assessment of renewable resources of the Tanana River Basin (M. B. Shasby, o, Anchorage, Alaska)

Land cover and terrain data base for NPRA (D. M. Carneggie, o, Anchorage, Alaska)

Land cover mapping, Bristol Bay (D. M. Carneggie, o, Anchorage, Alaska)

Mineral resources in Bendeleben and Solomon quadrangles (J. York, o, Anchorage, Alaska)

Arizona, San Carlos Indian Reservation (D. H. Knepper, Jr., D)

Maine, Lewiston-Sherbrooke 2-degree quadrangle (H. A. Pohn, NC)

Minnesota, Lineament analysis of imagery of the Mesabi Range, Minnesota (A. S. Walker, o, NC)

Pennsylvania, Structure studies of the Allegheny Plateau (H. A. Pohn, NC)

Utah, Mineral assessment; uranium exploration applications (M. H. Podwysocki, NC)

Remote sensing, water:

COMSAT general pilot project (W. G. Shope, w, NC)

Ice modeling and remote sensing (W. J. Campbell, w, Tacoma, Wash.)

Satellite data relay project (W. G. Shope, w, NC)

Spatial data for hydrologic models (C. J. Robinove, w, NC)

States:

Hawaii (w, Honolulu):

GOES data platforms (B. L. Jones)

Kansas (w, Lawrence):

Mined-land hydrology, southeastern Kansas (A. M. Diaz)

Maine (w, Augusta):

COMSAT pilot project (D. J. Cowing)

Pennsylvania (w, Harrisburg):

COMSAT general pilot program, Pennsylvania (C. D. Kauffman)

Washington (w, Tacoma):

GOES telemetry (E. H. McGavock)

Wisconsin (w, Madison):

Hydrologic studies of ERTS-A imagery (J. H. Green)

Streamflow estimates using Landsat (G. J. Allord)

Wyoming (w, Cheyenne):

Radar imagery in hydrologic investigations (M. E. Cooley)

Reservoirs. See Evapotranspiration; Sediment.

Resource appraisal:

Energy research and development equipment acquisition (F. A. Kilpatrick, w, NC)

Our Nation's estuary (V. P. Carter, w, NC)

Southeast sand-aquifer study (H. B. Counts, w, Atlanta, Ga.)

Water-resources assessment (D. W. Moody, w, NC)

States:

Alaska (w, Anchorage):

Alaska coal-resources study (D. R. Scully)

Bristol Bay (L. L. Dearborn)

Chilkat Bald Eagle study (E. F. Bugliosi, Juneau)

Copper River water resources (P. A. Emery)

North Slope hydrology (C. E. Sloan)

North Star project (D. E. Wilcox, Fairbanks)

Northwest Alaska gas pipeline (C. E. Sloan)

Arizona (w, Tucson):

Verde Valley water resources (S. J. Owen-Joyce)

Water resources of the Papago Reservation, Arizona (K. J. Hollett)

Arkansas (w, Little Rock):

Arkansas Valley coal hydrology (C. T. Bryant)

Lignite hydrology (J. E. Terry)

Lignite water resources (J. E. Terry)

Resource appraisal—Continued

California (w, Menlo Park):

Borrego Valley ground-water study (W. R. Moyle, Laguna Niguel)

Delta isotope study (W. L. Bradford)

Ground-water appraisal, San Antonio Creek (Peter Martin, Laguna Niguel)

Mono Basin water study (P. A. Lipinski, Laguna Niguel)

Power plant desert basins cooling water (J. H. Koehler, Laguna Niguel)

Santa Ynez ground-water quality (S. N. Hamlin, Laguna Niguel)

Colorado (w, Lakewood):

Coal areas 54 and 61 (D. J. Lystrom, D)

Hydrology of El Paso County (J. L. Hughes, Pueblo)

Hydrology of Naval Oil Shale Reserve 1 (D. L. Collins, D)

Hydrology of Parachute-Roan Creek basin (D. B. Adams, Grand Junction)

Intensive monitoring, Raton, Colorado (D. P. Bauer, D)

Larimer-Weld hydrology (S. R. Blakely, D)

Regional monitoring (Gerhard Kuhn, D)

Regional monitoring, Raton Mesa, Colorado (A. P. Hall, Pueblo)

San Luis Valley, Colorado (J. L. Hughes, Pueblo)

Surface water, alluvial valleys, upper Rio Grande (G. A. Hearne, Pueblo)

Upper Arkansas River basin (D. L. Cain, Pueblo)

Warm-water sloughs (A. W. Burns, D)

Water monitoring—coal mining (L. K. Sakumoto, D)

White River basin, Colorado and Utah (D. P. Bauer, D)

Yampa River basin assessment (T. D. Steele, D)

Connecticut (w, Hartford):

Ground water of Southbury-Woodbury (D. L. Mazzaferro)

Ground-water quality in Connecticut (S. J. Grady)

Major Connecticut aquifers (J. W. Bingham)

Florida (w, Tallahassee):

Caloosahatchee River study (B. F. McPherson, Miami)

East Boundary area investigation (B. G. Waller, Miami)

Ground water in Citrus, Hernando, and Levy Counties (J. D. Fretwell, Tampa)

Hydrology, Leon, Jefferson, Wakulla Counties (B. J. Franks)

Hydrology, Manatee County (D. P. Brown, Sarasota)

Hydrology of lakes in southwestern Florida (S. E. Henderson, Tampa)

Loxahatchee River assessment (Benjamin McPherson, Miami)

Trend analysis, southeast Florida (W. L. Miller, Miami)

Water resource assessment, statewide (J. D. Simmons)

Water resources of Manasota Basin (D. P. Brown, Tampa)

Idaho (w, Boise):

Cottonwood geohydrology (T. K. Edwards)

Hydrologic evaluation of streamflow, upper Snake River (C. A. Thomas)

Illinois (w, Urbana):

Sangamon River assessment planning (J. K. Stamer)

Indiana (w, Indianapolis):

Cowles Bog wetland complex study (R. J. Shedlock)

Ground-water quality, southwestern Indiana (J. D. Martin)

Monitoring water resources Indiana Dunes National Lakeshore (R. J. Shedlock)

Water resources, Kokomo area (A. R. Martin)

Iowa (w, Iowa City):

Coal area 38 (M. G. Detroy)

Kansas (w, Lawrence):

Resource appraisal—Continued

- Coal area 40 (J. F. Kenny)
- Geohydrology of Arkansas River valley, southwestern Kansas (L. E. Dunlap, Garden City)
- Glacial deposits, Kansas (J. E. Denne)
- Kentucky (w, Louisville):
 - Somerset hydrology (R. W. Davis)
- Maryland (w, Towson):
 - Ground-water and surface-water quality, Frederick County (M. T. Duigon)
 - Ground-water and surface-water quality, northeastern Maryland (R. E. Willey)
- Massachusetts (w, Boston):
 - French-Quinebaug study (V. A. Eames)
 - Water resources, Chicopee River basin (B. E. Krejmas)
- Michigan (w, Lansing):
 - Water resources of Pictured Rocks, Michigan (A. H. Handy)
 - Water resources of Sleeping Bear Dunes, Michigan (A. H. Handy)
- Minnesota (w, St. Paul):
 - Ground-water development, Twin Cities (M. E. Schoenberg)
 - River basin summaries (G. W. Lindholm)
 - Sherburne Wildlife Refuge (B. M. Wrege)
 - Twin Cities ground-water study (D. C. Gillies)
- Mississippi (w, Jackson):
 - Salt-dome hydrology in Mississippi (P. A. Dooley)
- Missouri (w, Rolla):
 - Coal area 38 (John Skelton)
 - Irrigation water, Audrain County (L. F. Emmett)
 - Water in northwestern Missouri (John Skelton)
- Montana (w, Helena):
 - Coal area 49 (S. E. Slagle)
 - Hydrology of the Big Hole Basin, Montana (Julianne Levings)
 - Water monitoring—coal, Montana (R. R. Shields)
- Nebraska (w, Lincoln):
 - Hydrogeology of south-central Nebraska (J. M. Peckenpaugh)
- New Jersey (w, Trenton):
 - Sole-source aquifer system (E. F. Vowinkel)
 - Surface water-ground water relationship—KMR (G. M. Farlekas)
- New Mexico (w, Albuquerque):
 - Coal area 60 (S. D. Craig)
 - Southwest alluvial valleys (east) (D. W. Wilkins)
- New York (w, Albany):
 - Evaluation of Irondequoit Wetland (W. M. Kappel, Ithaca)
 - Ground-water resources, Montauk area (K. R. Prince, Syosset)
 - Water resources, South Fork Long Island (Bronius Nemickas, Syosset)
- North Dakota (w, Bismarck):
 - Coal area 47 (R. D. Butler)
 - Surface-water resources, North Dakota coal area (N. D. Haffield)
- Ohio (w, Columbus):
 - Water for coal conversion (A. C. Razem)
- Oklahoma (w, Oklahoma City):
 - Coal area 40 (M. V. Marcher)
 - Monitor, Oklahoma coal field (R. K. Corley)
- Pennsylvania (w, Harrisburg):
 - Oley Valley water resources (G. N. Paulachok, Malvern)
- Puerto Rico (w, San Juan):
 - St. Thomas water resources appraisal (A. L. Zack, Ft. Buchanan)

Resource appraisal—Continued

- Water resources of the Anasco Basin, Puerto Rico (J. R. Diaz)
- South Dakota (w, Huron):
 - Water resources, Aurora and Jerauld Counties (L. J. Hamilton)
 - Water resources, Brookings and Kingsbury Counties (L. J. Hamilton)
 - Water resources, Clark County (L. J. Hamilton)
 - Water resources, Davison and Hanson Counties (D. S. Hansen)
 - Water resources, Hughes County (S. D. McGarvie)
 - Water resources, Miner County (S. D. McGarvie)
 - Water resources, Moody County (D. S. Hansen)
 - Water resources, Yankton County (E. F. Bugliosi)
- Tennessee (w, Nashville):
 - Water resources of Sweetwater, Tennessee (R. D. Evaldi, Knoxville)
- Texas (w, Austin):
 - Edwards aquifer, Austin area (E. T. Baker)
 - Hydrology of lignite mining (E. T. Baker)
- Utah (w, Salt Lake City):
 - Coal areas 56 and 57 (G. C. Lines)
 - Ground water, Kaiparowitz area (P. J. Blanchard)
 - Hydrology, south Utah coal fields (G. C. Lines)
 - Navajo Sandstone, east-central Utah (J. W. Hood)
- Vermont (w, Montpelier):
 - Water quality, Black River, Vermont (K. W. Toppin, Concord, N.H.)
- Washington (w, Tacoma):
 - Quileute project (L. M. Nelson)
- Wisconsin (w, Madison):
 - Hydrogeology—Lower Fox River valley (J. T. Krohelski)
 - Hydrology of wetlands (R. P. Novitzki)
 - Wisconsin Indian Reservations (R. A. Lidwin)
- Wyoming (w, Cheyenne):
 - Coal area 50 (J. F. Wilson)
 - Coal area 52 (H. W. Lowham)
 - Quality of water coal data, Wyoming (D. A. Peterson)
 - Thrust-belt hydrology, Wyoming-Utah-Idaho (D. T. Hoxie)
 - Upper Colorado RASA, Wyoming (D. T. Hoxie)
 - Uranium hydrology reconnaissance, Wyoming (J. R. Marie)
- Resource planning analysis:**
 - Environmental conflict management and collaborative problem-solving activities (E. T. Smith, o, NC)
 - Long-range planning and future research studies (E. T. Smith, o, NC)
- Saline minerals:**
 - Continental evaporites (G. I. Smith, M)
 - Mineralogy (B. M. Madsen, M)
 - States:*
 - Colorado and Utah, Paradox Basin (O. B. Raup, D)
- Saline water:**
 - States:*
 - California (w, Menlo Park):
 - Salinity control, lower Palo Verde (J. G. Setmire, Laguna Niguel)
 - Colorado (w, Lakewood):
 - Colorado River salinity (D. L. Butler, Grand Junction)
 - Kentucky (w, Louisville):
 - Saline water investigations (D. S. Mull)
 - Ohio (w, Columbus):
 - Brine investigation (S. E. Norris)
 - Washington (w, Tacoma):
 - Quinault ground-water quality (B. W. Drost)

Saline water—Continued

West Virginia (w, Charleston):
 Saline ground water in West Virginia (J. B. Foster, Morgantown)

Saltwater encroachment:

States:

Florida (w, Tallahassee):
 Bay-aquifer interconnection (C. B. Hutchinson, Tampa)
 Fernandina saltwater intrusion investigation (D. P. Brown, Jacksonville)
 Long-term trend analysis, surface water, Florida (H. R. La Rose, Fort Myers)
 Saltwater interface, southwest Florida (K. W. Causseaux, Tampa)
 Saltwater intrusion, Cape Coral (D. J. Fitzpatrick, Fort Myers)
 Volusia County saltwater (A. T. Rutledge, Orlando)

Georgia (w, Doraville):
 Faults/salt water, Brunswick, Georgia (H. E. Gill)

Hawaii (w, Honolulu):
 Monitoring of critical ground-water areas, Hawaii (W. R. Souza)

Louisiana (w, Baton Rouge):
 Hydrologic conditions, Baton Rouge (C. D. Whiteman)

New Mexico (w, Albuquerque):
 Elephant Butte Irrigation District well-field evaluation (C. A. Wilson, Las Cruces)

Puerto Rico (w, San Juan):
 Freshening, Cano Tiburones area (A. L. Zack)
 Well monitoring (Eloy Colon-Dieppa)

South Carolina (w, Columbia):
 Cooper River environmental study (F. A. Johnson)

Washington (w, Tacoma):
 Saltwater intrusion (N. P. Dion)

Saltwater intrusion. See Water quality, general; Marine hydrology.

Sediment:

Bedload transport research (W. W. Emmett, w, D)
 Estuarine intertidal environments (J. L. Glenn, w, D)
 Estuary sedimentation and eutrophication (J. L. Glenn, w, D)
 Potomac estuary transport (James Bennett, w, NC)
 Sediment and solute transport modeling (W. W. Sayre, w, D)
 Sediment distribution (M. M. Wolman, w, Baltimore, Md.)
 Sediment impacts from coal mining (W. R. Osterkamp, w, NC)
 Sediment transport phenomena (D. W. Hubbell, w, D)

States:

Alabama (w, Tuscaloosa):
 Hydrology of Warrior coal field (Celso Puente)

Arizona (w, Tucson):
 Sediment—Paria River, Lees Ferry (W. B. Garrett)

California (w, Menlo Park):
 Los Padres Reservoir study (L. F. Trujillo)
 Ventura River sediment (C. E. McConaughy, Laguna Niguel)

Colorado (w, Lakewood):
 Sediment yield, Piceance Basin (J. E. Kircher, D)

Hawaii (w, Honolulu):
 Peak flow-sediment discharge relations (B. L. Jones)

Illinois (w, Urbana):
 Bay Creek long term sediment yields (T. R. Lazaro)
 Kankakee River sediment (T. R. Lazaro)

Indiana (w, Indianapolis):
 Analysis of sediment data base (L. J. Mansue)

Kansas (w, Lawrence):
 Fluvial sediment in Kansas (A. M. Diaz)

Kentucky (w, Louisville):

Sediment—Continued

Hydrology, Beaver Creek strip mine (J. A. McCabe)
 Sediment characteristics, Kentucky streams (R. F. Flint)

Minnesota (w, St. Paul):
 Quality of water, Coteau des Prairies (C. J. Smith)

Mississippi (w, Jackson):
 Tenn-Tom Divide, quality of water monitoring (D. J. Tomaszewski)

North Carolina (w, Raleigh):
 Sediment study (C. E. Simmons)

North Dakota (w, Bismarck):
 Water monitoring—coal mining, North Dakota (N. D. Haffield)

Ohio (w, Columbus):
 Highway 315 sediment study (D. R. Helsel)
 Surface mine sediment transport (D. R. Helsel)

Oklahoma (w, Oklahoma City):
 Sediment, mid-Arkansas and upper Red Rivers (Stephen Blumer)

Oregon (w, Portland):
 Estuary quality (S. W. McKenzie)
 Sediment in Cow Creek (D. A. Curtiss)
 Settling velocity (J. F. Rinella)
 Water quality of Bull Run watershed (M. V. Shulters)

Pennsylvania (w, Harrisburg):
 Highway construction effects on streams (J. F. Truhlar)
 Highway erosion control (L. A. Reed)
 Pennsylvania surface-mining models (L. A. Reed)
 Sediment control in mining areas (K. L. Wetzel)

South Dakota (w, Huron):
 James River basin sediment (L. D. Becker)

Tennessee (w, Nashville):
 Hydrologic study of coal mining, New River, Tennessee (W. P. Carey)

Quality of water of Big South Fork National River and Recreation Area (R. D. Livesay, Knoxville)

Washington (w, Tacoma):
 May Creek sediment study (W. L. Haushild)
 Sediment transport, Mount St. Helens (J. K. Culbertson, Vancouver)

West Virginia (w, Charleston):
 Coal River sediment (S. C. Downs)
 Gauley River basin (G. S. Runner)
 Sediment yield of Taylor Run (S. M. Ward, Morgantown)

Selenium. See Mineral and fuel resources.

Silver. See Lead, zinc, and silver.

Small watersheds

Precipitation chemistry (D. W. Fisher, w, NC)

States:

Alabama (w, Tuscaloosa):
 Small-stream studies (D. A. Olin)

Arizona (w, Tucson):
 Flood hydrology of Arizona (B. N. Aldridge, Tucson)

Colorado (w, Lakewood):
 Peak discharge and frequency—small watersheds, Colorado (D. R. Minges, D)

Florida (w, Tallahassee):
 Hydrology of urban areas, Tampa Bay region (M. A. Lopez, Tampa)
 Small stream flood frequencies (W. C. Bridges)

Kentucky (w, Louisville):
 Low-flow investigation (R. V. Swisshelm)

Minnesota (w, St. Paul):
 Small-streams program (K. T. Gunard)

Montana (w, Helena):

Small watersheds—Continued

- Peak flow, small drainage areas (R. J. Omang)
- Watershed model, Montana (L. E. Cary, Billings)
- North Carolina (w, Raleigh):
 - Channelization effects of Chicod Creek (C. E. Simmons)
- Ohio (w, Columbus):
 - Rural hydrology (E. E. Webber)
- Oklahoma (w, Oklahoma City):
 - Small-watershed studies (R. K. Corley)
- South Dakota (w, Huron):
 - Flood-frequency study, South Dakota (L. D. Becker)
 - Small streams flood frequency (L. D. Becker)
- West Virginia (w, Charleston):
 - Small drainage areas (G. S. Runner)
- Wisconsin (w, Madison):
 - Nonpoint source pollution (S. J. Field)

Socioeconomic:

Information in planning models (I. C. James, w, NC)

State:

Washington (w, Tacoma):

Rainier and Baker impacts (Martha Sabol)

Soil moisture. See also Evapotranspiration:

Modeling water relations in soils (R. F. Miller, w, D)

States:

Florida (w, Tallahassee):

Unsaturated zone, Biscayne aquifer (Howard Klein, Miami)

Nevada (w, Carson City):

Beatty disposal site investigation (H. H. Zehner)

New York (w, Albany):

Snow hydrology (W. N. Embree)

Specific aquifer:

Central Midwest RASA (D. G. Jorgensen, w)

EPA hazardous waste (Ren Jen Sun, w, NC)

Hydrology of the Madison aquifer (E. M. Cushing, w, D)

Northern Midwest regional aquifer study (W. L. Steinhilber, w, Madison, Wis.)

Southeast limestone aquifer study (R. H. Johnston, w, Atlanta, Ga.)

States:

California (w, Menlo Park):

City of Merced ground-water appraisal (C. J. Londquist, Sacramento)

Montara-El Granada geohydrology (K. S. Muir)

Colorado (w, Lakewood):

Ground water, Denver Basin (S. G. Robson, D)

High Plains aquifer study (R. G. Borman, D)

Potentiometric surface mapping (F. A. Welder, Meeker)

West slope aquifers (T. D. Brooks, Grand Junction)

Florida (w, Tallahassee):

Sand-gravel aquifer, Pensacola (L. J. Geiger)

Shallow aquifer, Palm Beach County (W. L. Miller, Miami)

Southeast limestone—northwestern Florida (G. L. Faulkner)

Southern Florida limestone aquifer study (F. W. Meyer, Miami)

Georgia (w, Doraville):

Southeast limestone aquifer study (R. E. Krause)

Hawaii (w, Honolulu):

Honolulu basal aquifer (R. H. Dale)

Topical studies, Hawaii (B. L. Jones)

Idaho (w, Boise):

Snake River Plain RASA (G. F. Lindholm)

Indiana (w, Indianapolis):

Ground-water model outwash aquifer, Indiana (B. S. Smith)

Regional aquifer study in Indiana (R. J. Shedlock)

Specific aquifer—Continued

Iowa (w, Iowa City):

Regional aquifer study in Iowa (M. R. Burkart)

Kansas (w, Lawrence):

Geohydrology, Cedar Hills (J. B. Gillespie)

Liquid waste, Arbuckle Group (J. E. Carr)

Lower Cretaceous aquifers, southwestern Kansas (K. R. Watts, Garden City)

Models, North and South Fork, Solomon River (R. D. Burnett)

Sandstone aquifer, southwestern Kansas (Jack Kume, Garden City)

Kentucky (w, Louisville):

Ground water, Ohio River valley (R. J. Faust)

Maine (w, Augusta):

Little Andy valley aquifer (D. J. Morrissey)

Maryland (w, Towson):

Hydrology of water-table aquifer (L. L. Bachman)

Massachusetts (w, Boston):

Connecticut River aquifer study (B. P. Hansen)

Ground water on Cape Cod, Massachusetts (D. R. LeBlanc)

Monitoring Cape Cod's ground water (B. J. Ryan)

Michigan (w, Lansing):

Hydrology of Sands Plain area, Michigan (N. G. Granemann)

Mississippi (w, Jackson):

Mississippi alluvial aquifer study (B. E. Wasson)

Missouri (w, Rolla):

Ground water in the Ozarks (E. J. Harvey)

Hydrogeology of southern Missouri (L. F. Emmett)

Regional aquifer system in Missouri (L. F. Emmett)

Water, southeast Missouri lowlands (R. R. Luckey)

Montana (w, Helena):

Geohydrologic maps, Madison aquifer (R. D. Feltis, Billings)

Nebraska (w, Lincoln):

Platte-Republican watershed (J. W. Goeke, North Platte)

Nevada (w, Carson City):

Kyle-Lee Canyons water resources (R. W. Plume)

Pumping effects on Devils Hole (R. L. Carson)

New Jersey (w, Trenton):

Geohydrology, east-central New Jersey (G. M. Farlekas)

New Mexico (w, Albuquerque):

Capitan limestone (W. L. Hiss)

Ground-water effects, San Juan mineral development (G. E. Welder)

Model study of Roswell Basin, New Mexico (P. A. Davis)

New York (w, Albany):

Aquifer model for Dale Valley (A. D. Randall)

Aquifer model, Binghamton area, New York (A. D. Randall)

Buried-channel aquifers, Albany (R. M. Waller)

Ground water in selected areas, Susquehanna River basin (R. J. Reynolds)

Ohio (w, Columbus):

Big Island aquifer test (S. E. Norris)

Ground-water occurrence in coal region (S. E. Norris)

Oklahoma (w, Oklahoma City):

Central Midwest RASA, Oklahoma (J. H. Irwin)

Pennsylvania (w, Harrisburg):

Hydrology of Gettysburg Formation (C. R. Wood)

Puerto Rico (w, San Juan):

Water resources of Rio Guanajibo Basin (Eloy Colon, Ft. Buchanan)

South Dakota (w, Huron):

Hydrology of the Madison Group (L. W. Howells)

Specific aquifer—Continued

- Tennessee (w, Nashville):
 Paleozoic rocks—Highland Rim (E. F. Hollyday)
- Texas (w, Austin):
 Salinity control, Brazos and Red River (Sergio Garza)
- Utah (w, Salt Lake City):
 Navajo Sandstone in San Juan County, Utah (C. F. Avery)
- Washington (w, Tacoma):
 Coarse-grid basalt model (D. B. Sapik)
 Special hydrologic problems (William Meyer)
 Spokane planners' summary (Dee Molenaar)
- West Virginia (w, Charleston):
 Hydrology of selected coal strata (W. A. Hobba, Morgantown)
- Wyoming (w, Cheyenne):
 Bighorn Basin aquifers (M. E. Cooley)
 High Plains aquifer study (C. F. Avery)
 Madison Limestone, Wyoming (C. L. Joy)
 Potentiometric map, Powder, Wyoming (C. L. Joy)

Springs:

- State:*
 Colorado (w, Lakewood):
 Spring hydraulics (R. L. Tobin, Meeker)

Stratigraphy and sedimentation:

- American stratigraphic code (S. S. Oriel, D)
 Antler flysch, Western United States (F. G. Poole, D)
 Carbonate and sedimentary diagenesis (E. A. Shinn, Miami)
 Middle and late Tertiary history, Northern Rocky Mountains and Great Plains (N. M. Denson, D)
 Pennsylvanian System stratotype section (K. J. Englund, NC)
 Permian, Western United States (E. K. Maughan, D)
 Phosphoria Formation, stratigraphy and resources (R. A. Gulbrandsen, M)
 Rocky Mountains and Great Basin, Devonian and Mississippian conodont biostratigraphy (C. A. Sandberg, D)
 Sedimentary structures, model studies (E. D. McKee, D)
 Soil and saprolite stratigraphy, Mid-Atlantic and eastern Gulf Coast (M. J. Pavich, NC)
 Soil correlation and dating, Western United States (M. N. Machette, D)
 Tight gas sands (D. D. Rice, D)
- States:*
 Alaska, Cretaceous (D. L. Jones, M)
 Arizona, Magnetic chronology, Colorado Plateau and environs (D. P. Elston, E. M. Shoemaker, Flagstaff)
 Arizona-New Mexico, Paleomagnetic correlation, Colorado Plateau (D. J. Strobell, Flagstaff)
 Louisiana, Continental Shelf (H. L. Berryhill, Jr., Corpus Christi, Tex.)
 Maryland, Cenozoic stratigraphy and structure, Tidewater area (W. L. Newell, NC)
- Montana:
 Quaternary chronology, Glacier National Park (P. E. Carrara, D)
 Ruby Range, Paleozoic rocks (E. T. Ruppel, D)
- Montana-North Dakota-South Dakota-Wyoming, Williston Basin (C. A. Sandberg, D)
- New Jersey, Glacial Lake Passaic (B. D. Stone, NC)
- New Mexico:
 North-central Tertiary stratigraphy (Kim Manley, D)
 Western and adjacent areas, Cretaceous stratigraphy (E. R. Landis, D)
- Oregon-California, Black Sands (M):
 Geologic investigations (H. E. Clifton)
 Hydrologic investigations (P. D. Snively, Jr.)

Stratigraphy and sedimentation—Continued

- Virginia, Cenozoic stratigraphy and structure, Tidewater area (W. L. Newell, NC)
- See also Paleontology, stratigraphic; specific areas under Geologic mapping.*
- Streamflow characteristics:**
- States:*
 Alabama (w, Tuscaloosa):
 Flow characteristics of streams (C. O. Ming, Montgomery)
 River-flow simulation, Alabama (R. A. Gardner, Montgomery)
- Arkansas (w, Little Rock):
 Flood investigations (T. E. Lamb)
- Colorado (w, Lakewood):
 Inventory of water resources on Ft. Carson (G. J. Leonard, D)
 Streamflow analysis, Piceance Basin (N. E. Spahr, D)
- Florida (w, Tallahassee):
 Basin-flow characteristics (J. W. Rabon, Ocala)
- Georgia (w, Doraville):
 Computation of dynamic streamflow (M. E. Blalock)
 Seasonal low flow (T. R. Dyar)
- Hawaii (w, Honolulu):
 Surface water data summary (Iwao Matsuoka)
- Illinois (w, Urbana):
 Low flows—Illinois streams (H. E. Allen, DeKalb)
- Indiana (w, Indianapolis):
 Streamflow characteristics (J. A. Stewart)
- Kansas (w, Lawrence):
 High-flow volume, Kansas (P. R. Jordan)
 Streamflow characteristics (P. R. Jordan)
- Louisiana (w, Baton Rouge):
 Low-flow investigations (G. J. Wiche)
- Maine (w, Augusta):
 Flow and quality of water characteristics, Maine streams (G. W. Parker)
- Maryland (w, Towson):
 Flow characteristics of Maryland streams (D. H. Carpenter)
 Low-flow studies in Maryland (R. W. James)
- Massachusetts (w, Boston):
 Gazetteer of Massachusetts streams (S. S. Wandle)
- Minnesota (w, St. Paul):
 Watershed water-quality appraisal (M. R. Have)
- Mississippi (w, Jackson):
 Flow characteristics, Tombigbee River (B. E. Colson)
- Missouri (w, Rolla):
 National eutrophication survey (John Skelton)
 Small-streams analysis (L. D. Hauth)
- Montana (w, Helena):
 Runoff characteristics, eastern Montana (R. J. Omang)
- New Jersey (w, Trenton):
 Trunk sewers and residual flow (E. G. Miller)
- New Mexico (w, Albuquerque):
 Miscellaneous, Pecos River (G. E. Welder)
- New York (w, Albany):
 Headwaters locations (B. B. Eissler)
 Surface-water inflow, Lake Ontario (E. C. Rhodehamel)
- North Carolina (w, Raleigh):
 Low-flow studies (H. G. Hinson)
 Requests for data (N. N. Jackson)
- North Dakota (w, Bismarck):
 Kinematic wave approximation (J. E. Miller)
- Ohio (w, Columbus):
 Cuyahoga River assessment (C. J. Childress)

Streamflow characteristics—Continued

- Floods versus channel geometry (E. E. Webber)
- Low-flow regionalization for Ohio (W. P. Bartlett)
- Oklahoma (w, Oklahoma City):
 - Effects of control on discharge (T. L. Huntzinger)
- Pennsylvania (w, Harrisburg):
 - Mean discharge, Pennsylvania (W. J. Herb)
 - Regionalization of streamflow data (J. M. Bettendorf)
 - Statistical analyses, Philadelphia streams (D. R. Glatfelter, Malvern)
- South Carolina (w, Columbia):
 - Nonpoint discharges, Reedy River (D. I. Cahal)
- Tennessee (w, Nashville):
 - Hydrologic data transfer (J. F. Lowery)
- Utah (w, Salt Lake City):
 - Mined lands rehabilitation (G. W. Sandberg, Cedar City)
- Virginia (w, Richmond):
 - Low flows (B. J. Prugh)
- Washington (w, Tacoma):
 - Flow of small streams (M. B. Miles)
 - Low flow of Washington streams (E. H. McGavock)
 - Small-stream surface water (J. R. Williams)
 - Streamflow statistics, southwest and east Washington (J. R. Williams)
- Wisconsin (w, Madison):
 - Low-flow study (B. K. Holmstrom)
 - Water-quality control (B. K. Holmstrom)
- Wyoming (w, Cheyenne):
 - Low flow, Powder Basin, Wyoming (G. W. Armentrout, Casper)
 - Streamflow in energy areas, Wyoming (H. W. Lowham)

Stream infiltration:

- Flow losses (R. F. Hadley, w, D)
- States:
 - Florida (w, Tallahassee):
 - Canal-aquifer interactions (L. J. Lefkoff, Miami)
 - St. Johns River deepening study (Roy Stone, Jacksonville)
 - Massachusetts (w, Boston):
 - PCB in river and ground water, Massachusetts (F. B. Gay)
 - New York (w, Albany):
 - Headwater Valley aquifers (A. D. Randall)

Structural geology and tectonics:

- Caribbean (J. E. Case, M)
- Central Appalachian tectonics (A. A. Drake, Jr., NC)
- Contemporary coastal deformation (R. O. Castle, M)
- Inner Coastal Plain tectonics, Mid-Atlantic States (R. B. Mixon, NC)
- Postglacial uplift, Northeastern United States (Carl Koteff, NC)
- Rock behavior at high temperature and pressure (E. C. Robertson, NC)
- Stratigraphy and tectonic framework, southern Rocky Mountains (E. H. Baltz, D)
- Structural studies, Basin and Range (F. G. Poole, D)
- States:
 - Arizona:
 - Southeastern tectonics (H. Drewes, D)
 - Tertiary rocks, eastern Mojave Desert (J. E. Pike, M)
 - Arkansas, northern (E. E. Glick, D)
 - California:
 - Providence and New York Mountains (D. M. Miller, M)
 - Tertiary rocks, eastern Mojave Desert (J. E. Pike, M)
 - California-Nevada, Transcurrent fault analysis, western Great Basin (R. E. Anderson, D)
 - Colorado, Southwestern tectonics (Ivo Lucchitta, Flagstaff)

Structural geology and tectonics—Continued

- Georgia coastal plain, stratigraphy and structure (Juergen Reinhardt, NC)
- Maine, Chain Lakes massif (Richard Goldsmith, NC)
- Nevada, Tertiary rocks, eastern Mojave Desert (J. E. Pike, M)
- New Mexico, Precambrian rock, Northern Sangre de Cristo Range (J. C. Reed, Jr., D)
- North Carolina-Tennessee, Age of the Greenbrier fault (D. J. Milton, NC)
- Virginia, Quaternary stratigraphy and bedrock structural framework, Giles County (R. C. McDowell, NC)

See also specific areas under Geologic mapping.

Subsidence:

- Mechanics of aquifer system (F. S. Riley, w, D)
- States:
 - Alabama (w, Tuscaloosa):
 - Solution subsidence and collapse (J. G. Newton)
 - Arizona (w, Tucson):
 - Land subsidence/earth fissures, Arizona (H. H. Schumann, Phoenix)
 - Subsidence/fissures, Tucson Basin, Arizona (S. R. Anderson)
 - California (w, Menlo Park):
 - Land-subsidence studies in California (R. L. Ireland, Sacramento)
 - New Jersey (w, Trenton):
 - Effects of land subsidence (William Kam)
 - Land subsidence in New Jersey (R. L. Walker)
 - Texas (w, Austin):
 - Texas coastal subsidence studies (R. K. Gabrysch, Houston)
 - Virginia (w, Richmond):
 - Coastal Plain land subsidence (H. T. Hopkins)

Surface water, general:

- Delaware River master activity (F. T. Schaefer, w, Milford, Pa.)
- 2-D finite element modeling (J. K. Lee, w, NSTL Station, Miss.)
- States:
 - Alabama (w, Tuscaloosa):
 - Drainage areas, Alabama (J. C. Scott, Montgomery)
 - Alaska (w, Anchorage):
 - Hydrologic techniques assessment (R. J. Madison)
 - Arkansas (w, Little Rock):
 - Arkansas-Oklahoma Compact (R. T. Sniegocki)
 - Colorado (w, Lakewood):
 - Rio Grande Compact Commission (J. F. Blakey, D)
 - Illinois (w, Urbana):
 - Surface-water network evaluation (D. M. Mades)
 - Maryland (w, Towson):
 - Acid rain in central Maryland (B. G. Katz)
 - Flow measurements in storm sewer (B. G. Katz)
 - Potomac Reservoir release routing (D. H. Carpenter)
 - Ohio (w, Columbus):
 - Comparison of reaeration methods (Janet Hren)
 - Reaeration (Janet Hren)
 - Puerto Rico (w, San Juan):
 - Contingent requests (E. D. Cobb)
 - Utah (w, Salt Lake City):
 - Canal loss studies (R. W. Cruff)
 - Wisconsin (w, Madison):
 - Automated dilution gaging (M. D. Duerk)
 - Regional reaeration (L. B. House)
 - Wyoming (w, Cheyenne):
 - Infiltration model, Wyoming (J. G. Rankl)

Surface-water principles and relations:

- China hydrology coop (Della Laura, w, NC)

Surface-water principles and relations—Continued

- Dams, weirs, and flumes (H. J. Tracy, w, Atlanta, Ga.)
- Hydrologic estimating techniques (D. G. Frickel, w, D)
- Isotope fractionation (T. B. Coplen, w, NC)
- Rating extensions (K. L. Wahl, w, NC)
- States:
- Colorado (w, Lakewood):
 - Reconnaissance of a strip-mine site (R. R. Williams, D)
- Connecticut (w, Hartford):
 - Remote sensing, Long Island (F. H. Ruggles)
- Kansas (w, Lawrence):
 - Flood volume-peak relations, western Kansas (C. A. Perry)
 - Soldier Creek (W. J. Carswell)
- New Mexico (w, Albuquerque):
 - Precipitation-runoff modeling (H. R. Hejl)
 - Runoff from channel geometry (J. P. Borland)
- New York (w, Albany):
 - Flood frequency for Rockland County streams (Richard Lumia)
- Oklahoma (w, Oklahoma City):
 - Coal-field hydrology, Oklahoma (R. L. Tortorelli)
- Pennsylvania (w, Harrisburg):
 - Coal hydrology, Greene County (D. R. Williams, Pittsburgh)
 - Low-flow regionalization, Pennsylvania (H. N. Flippo)
- South Carolina (w, Columbia):
 - Short-term planning studies (W. M. Bloxham)
- Surface-water supply and availability:**
- National assessment (S. M. Lang, w, Washington, D.C.)
- Technical transfer of hydrologic modeling (W. D. Harlan, w, D)
- Waterway treaty engineering studies (J. A. Bettendorf, w, NC)
- States:
- Arizona (w, Tucson):
 - Planning—Gila River basin (E. S. Davidson)
- Arkansas (w, Little Rock):
 - Arkansas Basin flows (G. G. Ducret)
 - Duration and frequency of streams (R. A. Hunrichs)
- California (w, Menlo Park):
 - Alameda Creek surface-water quality (L. E. Lopp)
- Colorado:
 - Arkansas River Compact (J. F. Blakey, D)
- Florida (w, Tallahassee):
 - Hillsborough River basin water supply (M. R. Fernandez, Tampa)
- Georgia (w, Doraville):
 - Storage requirements for Georgia streams (R. F. Carter)
- Hawaii (w, Honolulu):
 - Water-resources information: Trust Territory (D. A. Davis)
- Kansas (w, Lawrence):
 - Big Blue River Compact (E. E. Hedman)
 - Gains and losses—Neosho River, Kansas (W. J. Carswell)
 - Kansas-Oklahoma-Arkansas River Commission (E. E. Hedman)
 - Water yield, Kansas (W. J. Carswell)
- Mississippi (w, Jackson):
 - Information to the public (K. V. Wilson)
- New Mexico (w, Albuquerque):
 - Estimation of natural streamflow (J. P. Borland)
 - Mine discharge Kim-me-ni-oli Wash, New Mexico (Kim Ong)
 - Rio Grande Commission (P. L. Soule)
- North Dakota (w, Bismarck):
 - Boards and commissions (L. L. Moore)
- Ohio (w, Columbus):
 - Low-flow of Ohio streams (R. I. Mayo)
- Utah (w, Salt Lake City):

Surface-water supply and availability—Continued

- Bear River Commission (W. N. Jibson, Logan)
- Inflow to Great Salt Lake (J. C. Mundorff)
- Washington (w, Tacoma):
 - Okanogan River streamflow modeling (J. J. Vaccaro)
 - Unregulated flow at Union Gap (J. J. Vaccaro)
 - Water resources of the Hoh Indian Reservation (W. E. Lum)
- Wyoming (w, Cheyenne):
 - Water resources, Powder Basin (M. E. Lowry)
- Surface-water techniques and instrumentation:**
- Chemistry of sediment surfaces (M. C. Goldberg, w, D)
- Hydrologic instrumentation (G. E. Ghering, w, D)
- Instrumentation coordination (R. W. Paulson, w, NC)
- Instrument development lab (V. J. Latkovich, w, Bay St. Louis, Miss.)
- Interagency sedimentation project (J. V. Skinner, w, Minneapolis, Minn.)
- Sensor development (V. J. Latkovich, w, NSTL Station, Miss.)
- Suspended solids sensors (J. V. Skinner, w, Minneapolis, Minn.)
- States:
- Alabama (w, Tuscaloosa):
 - Remote sensing-data collection (J. G. Newton)
- Arizona (w, Tucson):
 - COMSAT general pilot program (F. C. Boner)
- California (w, Menlo Park):
 - AVM backup (J. G. Harmon, Sacramento)
 - Chippis Island acoustic flowmeter (S. H. Hoffard)
- Colorado (w, Lakewood):
 - COMSAT general pilot program, Colorado (L. L. Jones, D)
 - Remote video streamgaging (L. L. Jones, D)
- Florida (w, Tallahassee):
 - Telemetry evaluation program (W. M. Woodham, Tampa)
- Oregon (w, Portland):
 - AVM feasibility study (Antonius Laenen)
 - AVM progress report (Antonius Laenen)
- Wisconsin (w, Madison):
 - Automated dilution gaging (M. D. Duerk)
- Tantalum.** See Mineral and fuel resources, compilation, and topical studies.
- Temperature and thermal pollution:**
- Temperature modeling in natural streams (A. P. Jackman, w, Davis, Calif.)
- Thermal modeling (H. E. Jobson, w, NSTL Station, Miss.)
- Turbulent transport in open channel (Nobuhiro Yotsukura, w, NC)
- Water-temperature patterns (E. J. Pluhowski, w, NC)
- States:
- Delaware (w, Dover):
 - Thermal regimen, water-table aquifer (A. L. Hodges)
- Montana (w, Helena):
 - Thermal study—Madison River (A. J. Boettcher)
- New Jersey (w, Trenton):
 - New Jersey water temperatures (M. G. McDonald)
- Washington (w, Tacoma):
 - Yakima streamflow temperature (J. J. Vaccaro)
- Test drilling:**
- Paradox Basin hydrology (M. S. Whitfield, w, D)
- Water-resources activities (J. P. Monis, w, D)
- States:
- California (w, Menlo Park):
 - Nitrogen isotope study (Peter Martin, Laguna Niguel)
- Florida (w, Tallahassee):
 - Deeper zones in Floridan aquifer (D. P. Brown, Jacksonville)
 - Ground-water network evaluation (H. C. Rollins, Tampa)

Test drilling—Continued

Potentiometric surface, St. Petersburg-Tampa (R. M. Wolansky, Tampa)

Indiana (w, Indianapolis):

Landfill monitoring, Marion County (R. A. Pettijohn)

Kentucky (w, Louisville):

Maxey Flats investigation (R. J. Faust)

Maryland (w, Towson):

Definition of Maryland aquifers (E. G. Otton)

Missouri (w, Rolla):

Water development site studies (E. J. Harvey)

New Jersey (w, Trenton):

Geophysical logging (R. L. Walker)

New York (w, Albany):

Subsurface storage of chilled water (Julian Soren, Syosset)

Pennsylvania (w, Harrisburg):

Ground water—Delaware Gap (C. W. Poth)

Tennessee (w, Nashville):

Ground-water study for lignite (W. S. Parks, Memphis)

Utah (w, Salt Lake City):

Oil-shale hydrology, Utah (K. L. Lindskov)

Washington (w, Tacoma):

Water supply, Mt. Rainier (D. R. Cline)

Water supply, San Juan Island (D. R. Cline)

Thorium (D):

Analytical support (C. M. Bunker)

Investigations of thorium in igneous rocks (M. H. Staatz)

Resources appraisal (T. J. Armbrustmacher)

Time of travel:

States:

Arkansas (w, Little Rock):

Time-of-travel study (T. E. Lamb)

Maryland (w, Towson):

Time of travel, Jones Falls (R. W. James)

Time of travel, Potomac (K. R. Taylor)

North Carolina (w, Raleigh):

Time-of-travel studies (W. G. Stamper)

Ohio (w, Columbus):

Time of travel, Ohio streams (A. O. Westfall)

Pennsylvania (w, Harrisburg):

Time of travel, Lehigh River (C. D. Kauffman)

West Virginia (w, Charleston):

Time of travel on the New River (D. H. Appel)

Time of travel, South Branch Potomac (William Embree)

Titanium:

Rutile in porphyry copper deposits (E. R. Force, NC)

Trace elements:

Chemistry of hydrosolic metals (J. D. Hem, w, M)

Geochemistry, western coal region (G. L. Feder, w, D)

Geothermal trace element reactions (D. D. Nordstrom, w, M)

Sediment-water exchange of nutrients/metals (Edward Callender, w, NC)

Survey of Missouri waters (G. L. Feder, w, D)

Trace element availability in sediments (S. N. Luoma, w, M)

Trace element partitioning (D. K. Nordstrom, w, M)

Trace metals and nutrients (O. P. Bricker, w, NC)

Water quality analysis—Other Federal Agencies (J. P. Monis, w, D)

Water quality and health (G. L. Feder, w, D)

States:

Alaska (w, Anchorage):

Heavy trace metals (D. E. Wilcox, Fairbanks)

Colorado (w, Lakewood):

Sediment chemistry (J. T. Turk, D)

Storm-runoff quality, Denver (S. R. Ellis, D)

Trace elements—Continued

Florida (w, Tallahassee):

Bridge runoff, quality of water assessment (Donald McKenzie, Miami)

Illinois (w, Urbana):

American bottoms ground-water quality (J. K. Stamer)

Strip-mine hydrology (T. P. Brabets)

Indiana (w, Indianapolis):

Metals transport in mining areas (C. G. Crawford)

Mississippi (w, Jackson):

Background data in lignite area, Mississippi (J. P. Crout)

New York (w, Albany):

Sediment nutrient dynamics (J. T. Turk)

Ohio (w, Columbus):

Quality of water, abandoned mine land discharge (C. L. Pfaff)

Pennsylvania (w, Harrisburg):

Coal mining trace-metals transport (A. N. Ott)

Utah (w, Salt Lake City):

Trace-element transport (B. A. Kimball)

Uranium (D, except as otherwise noted):

Applied uranium geochemistry (J. N. Rosholt)

Distribution studies (R. A. Zielinski)

Exploration techniques:

Clays associated with uranium, mineralogy and geochemistry of (C. G. Whitney)

Geochemical patterns (Keith Robinson)

Geochemical techniques (R. A. Cadigan)

Geochemical techniques of halo uranium (J. K. Otton)

Morrison Formation (L. C. Craig)

Uranium in streams as an exploration technique (K. J. Wenrich)

Genesis of tabular uranium deposits on the Colorado Plateau (R. A. Brooks)

Geochronology (K. R. Ludwig)

Geophysics:

Borehole electrical techniques in uranium exploration (J. J. Daniels)

Borehole geophysical research in uranium exploration (J. H. Scott)

Gamma-ray spectrometry in uranium (J. S. Duval)

Gamma-ray spectroscopy for uranium exploration in crystalline terranes (J. A. Pitkin)

Geophysical studies relating to uranium deposits in crystalline terranes (D. L. Campbell)

Magnetic and mineralogic studies of uranium deposits (R. L. Reynolds)

Nonradiometric geophysical methods and uranium exploration (B. D. Smith)

Ore-forming processes (H. C. Granger)

Organic geochemistry (J. S. Leventhal)

Petrophysics (G. R. Olhoeft)

Powder River Basin (N. M. Denson)

Precambrian sedimentary and metasedimentary rocks (F. A. Hills)

Radium and other isotopic disintegration products in springs and subsurface water (J. K. Felmlee)

Remote sensing for uranium exploration (G. L. Raines)

United States:

Eastern:

Great Lakes Indian Lands (David Frishman)

Northeastern plutonic rocks (E. L. Boudette, NC)

Uranium vein deposits (R. I. Grauch)

Southwestern, basin analysis related to uranium potential in Permian rocks (J. A. Campbell)

Uranium—Continued**Western:**

Basin analysis of uranium-bearing Jurassic rocks (Fred Peterson)

Relation of diagenesis and uranium deposits (M. B. Goldhaber)

San Juan basin, remote sensing (D. H. Knepper, Jr.)

San Juan geophysics (L. E. Cordell)

Vein and disseminated deposits of uranium (J. T. Nash)

Uranium daughter products in modern decaying plant remains, in soils, and in stream sediments (K. J. Wenrich)

Volcanic source rocks (R. A. Zielinski)

States:**Alaska:**

Geophysics (J. W. Cady)

Sedimentary basin rocks (K. A. Dickinson)

Arizona:

Hualapai Indian Reservation (K. J. Wenrich)

Window Rock (R. E. Thaden)

Colorado:

Fossil Ridge (R. S. Zech)

Lake City (A. R. Kirk and R. I. Grauch)

Todilto-Pony Express Limestone (J. L. Ridgley)

Uranium-bearing Triassic rocks (R. D. Lupe)

New Mexico:

Crownpoint (J. F. Robertson)

Marfa Basin (C. T. Pierson)

North Church Rock (A. R. Kirk)

San Juan Basin (M. W. Green)

Sanostee (A. C. Huffman, Jr.)

Window Rock (R. E. Thaden)

Texas:

Tilden-Loma Alta area (K. A. Dickinson)

Uranium disequilibrium studies (F. E. Senftle, NC)

Utah, Remote-sensing applications (M. H. Podwysocski, NC)

Utah-Colorado, Uinta and Piceance Creek basin (L. C. Craig)

Wyoming:

Granite as a source rock of uranium (J. S. Stuckless)

Powder River Basin (E. S. Santos)

Stratigraphic analysis of Tertiary uranium basins of Wyoming (D. A. Seeland)

Stratigraphic analysis of Western Interior Cretaceous uranium basins (H. W. Dodge, Jr.)

Urban geology:**States:**

Alaska, Anchorage area (H. R. Schmoll, D)

California (M, except as otherwise noted):

Coastal geologic processes (K. R. Lajoie)

Flatlands materials and their land use significance (E. J. Helley)

Hillside materials and their land use significance (C. M. Wentworth, Jr.)

Pacific Palisades landslide area, Los Angeles (J. T. McGill, D)

Palo Alto, San Mateo, and Montara Mountain quadrangles (E. H. Pampeyan)

Quaternary framework for earthquake studies, Los Angeles Basin (J. C. Tinsley III)

Regional slope stability (T. H. Nilsen)

San Francisco Bay region, environment and resources planning study:

Bedrock geology (M. C. Blake)

Marine geology (D. S. McCulloch)

San Andreas fault:

Basement studies (D. C. Ross)

Urban geology—Continued

Basin studies (J. A. Bartow)

Regional framework (E. E. Brabb)

Tectonic framework (R. D. Brown)

Seismicity and ground motion (D. M. Boore)

Southern:

Eastern part (J. C. Matti, M)

Western part (R. F. Yerkes)

Georgia, Geochemical map of Savannah (H. A. Tourtelot, D)

Massachusetts, Boston and vicinity (C. A. Kaye, Boston)

New York, Engineering geology of New York City (C. A. Baskerville, NC)

Pennsylvania, Geochemistry of Pittsburgh urban area (H. A. Tourtelot, D)

Utah:

Salt Lake City and vicinity (Richard VanHorn, D)

Wasatch Front surficial geology (R. D. Miller, D)

Washington (D):

Engineering properties of unconsolidated materials in Port Townsend quadrangle (R. D. Miller)

Slope stability in Port Townsend quadrangle (R. D. Miller)

Urban hydrology:

Analysis of urban flood data in the United States (V. B. Sauer, Atlanta, Ga.)

Puget Sound urban area studies (B. L. Foxworthy, Tacoma, Wash.)

Urban runoff networks (H. H. Barnes, w, NC)

States:

Alaska (w, Anchorage):

Anchorage runoff study (T. P. Brabets)

Arizona (w, Tucson):

Tucson urban study (H. W. Hjalmarson)

California (w, Menlo Park):

Fresno urban runoff (R. N. Oltmann, Sacramento)

Colorado (w, Lakewood):

Urban runoff (S. R. Blakely, D)

Urban runoff (J. L. Blattner, D)

Connecticut (w, Hartford):

Connecticut valley urban pilot study (R. L. Melvin)

Urbanization effect, small streams (L. A. Weiss)

Florida (w, Tallahassee):

Assimilative capability, detention pond (P. S. Hampson, Jacksonville)

Hydrologic suitability study (L. V. Causey, Jacksonville)

Pollution control, Pinellas County (M. A. Lopez, Tampa)

Small streams flooding (R. D. Hayes, Tampa)

Streamwater contaminants—detention storage (R. A. Miller, Orlando)

Urban estuary quality in Tampa (W. M. Woodham, Tampa)

Urban hydrology, Bay Lake area (E. R. German, Orlando)

Urban hydrology, Leon County (M. A. Franklin)

Urban hydrology of Duval County, Florida (J. B. Largen, Jacksonville)

Illinois (w, Urbana):

Effects of detention ponds on quality of water (R. G. Striegl, DeKalb)

Kansas (w, Lawrence):

Urban flood-frequency (R. J. Hart)

Urban runoff, Wichita (C. A. Perry)

Kentucky (w, Louisville):

Northern Kentucky urban hydrology (R. W. Davis)

Maryland (w, Towson):

Baltimore urban hydrology (G. T. Fisher)

Minnesota (w, St. Paul):

Metro lakes study, Twin Cities (R. G. Brown)

Urban hydrology—Continued

Quality of runoff, Twin Cities area (M. A. Ayers)
 Surface-water quality of water assessment, Coon Creek watershed (A. D. Arntson)
 Twin Cities urban hydrology (M. A. Ayers)

Missouri (w, Rolla):

Hydrology of streams, St. Louis County (T. W. Alexander)
 Urban runoff in Kansas City (J. H. Barks)

New Mexico (w, Albuquerque):

Quality of water of Albuquerque urban runoff (Kim Ong)
 Urban flood-hydrology, Albuquerque (J. P. Borland)

New York (w, Albany):

Floods in urbanized basins, New York (Richard Lumia)
 Irondequoit urban runoff study (W. M. Kappel, Ithaca)
 Quality of water, urban construction (W. M. Kappel, Ithaca)
 Solid waste sites, Suffolk (G. E. Kimmel, Mineola)
 Urban data transfer (W. M. Kappel, Ithaca)
 Urban hydrology of Long Island (H. F. Ku, Syosset)

North Carolina (w, Raleigh):

Urban hydrology—Coastal Plain (H. C. Gunter)

Ohio (w, Columbus):

Urban hydrology (W. P. Bartlett)

Oklahoma (w, Oklahoma City):

Urban hydrology, Enid, Oklahoma (W. B. Mills)

Oregon (w, Portland):

Roseburg urban runoff (L. E. Hubbard)
 Salem storm-water quality (T. L. Miller)
 Salem urban runoff (Antonius Laenen)

Pennsylvania (w, Harrisburg):

Chester County urbanization (R. A. Sloto, Malvern)
 Stormwater measurements (T. G. Ross, Malvern)
 Urban hydrology, Philadelphia (T. G. Ross, Malvern)
 Urban hydrology, Warminster Township (R. A. Sloto, Malvern)

South Dakota (w, Huron):

Rapid City urban hydrology (K. E. Goddard, Rapid City)

Tennessee (w, Nashville):

Effects of urbanization on floods (C. H. Robbins)
 Memphis urban-flood frequency (B. L. Neely, Memphis)

Texas (w, Austin):

Dallas urban study (B. B. Hampton, Fort Worth)
 Effects, urban runoff on ground-water quality (F. L. Andrews)
 Houston urban study (Fred Liscum, Houston)
 San Antonio urban study (Roberto Perez, San Antonio)
 Urban hydrology of Austin (R. M. Slade)

Washington (w, Tacoma):

Bellevue urban runoff study (E. A. Prych)
 Urban hydrology of Washington (K. L. Walters)

Wisconsin (w, Madison):

Urban flood-frequency study (D. H. Conger)
 Urban nonpoint, southeast Wisconsin (P. E. Hughes)

Vegetation (D):**Element availability:**

Soils (R. C. Severson)
 Vegetation (L. P. Gough)

Plant geochemistry, urban areas (H. A. Tourtelot)

Western coal regions, geochemical survey of vegetation (J. A. Erdman)

See also Plant ecology.

Volcanic-terrane hydrology. See Artificial recharge.**Volcanology:**

Caldron and ash-flow studies (R. L. Smith, NC)
 Cascade volcano observations (D. W. Peterson, Vancouver, Wash.)

Volcanology—Continued

Recent volcanic processes (J. G. Moore, M)
 Regional volcanology (R. L. Smith, NC)
 Tephra hazards from Cascade Range volcanoes (D. R. Mullineaux, D)

Tephrochronology, Western United States (A. M. Sarna-Wojcicki, M)

Volcanic-ash chronology (R. E. Wilcox, D)

Volcanic hazards (D. R. Crandell, D)

Volcano hazards paleomagnetism (D. E. Champion, M)

States:

Alaska, Volcano hazards (T. P. Miller, Anchorage)

California:

Geology of the Lassen Volcanic National Park (L. J. P. Muffler, M)

Lassen Peak geophysics (R. C. Jachens, M)

Petrology, Clear Lake volcanics (D. C. Hearn, Jr., NC)

Volcanic hazards, Mono-Inyo Craters (C. D. Miller, D)

Hawaii (Hawaii National Park except as otherwise noted):

Eruptive history of Mauna Loa (J. P. Lockwood)

Eruptive processes (R. I. Tilling, NC)

Hawaiian Volcano Observatory (R. W. Decker)

Petrology of Hualalai Volcano (R. B. Moore)

Submarine volcanic rocks (J. G. Moore, M)

Subsurface magma mapping techniques, Kilauea (C. J. Zabolcki, NC)

Volcanism and planetary implications (R. W. Decker)

Idaho, Eastern Snake River Plain region (M. A. Kuntz, H. R. Covington, D)

Montana, Wolf Creek area, petrology (R. G. Schmidt, NC)

Oregon, Volcanic evolution of the Crater Lake region (C. R. Bacon, M)

Washington:

Mount St. Helens:

Depositional and thermoremanent magnetization (D. P. Elston, Flagstaff)

Monitoring (D. W. Peterson, Vancouver, Washington)

Pyroclastic flows and structural deformation (P. D. Rowley, D)

Waste disposal:

Migration of buried radionuclides (C. B. Yost, w, Idaho Falls, Idaho)

States:**Florida (w, Tallahassee):**

Subsurface waste storage, Florida (J. J. Hickey, Tampa)

Illinois (w, Urbana):

Mine reclamation hydrology (C. A. Peters)

Nevada (w, Carson City):

Lahontan Reservoir water quality (Kerry Garcia)

New York (w, Albany):

Basin recharge with sewage effluent (R. C. Prill, Syosset)

Waste disposal, nuclear:

Deep injection of tritiated water (E. V. Giusti, w, NC)

Favorable radioactive waste disposal area (M. S. Bedinger, w, D)

NTS paleohydrology (W. E. Wilson, w, D)

Radioactive waste coordination (A. M. LaSala, w, Columbus, Ohio)

Radiohydrology, Germantown coordination (G. D. DeBuchanne, w, NC)

States:**Illinois (w, Urbana):**

Sheffield site investigation (J. B. Foster)

Louisiana (w, Baton Rouge):

Hydrology of salt domes (G. N. Ryals, Alexandria)

Waste disposal, nuclear—Continued

South Carolina (w, Columbia):
Hydrology study of unsaturated zone (J. M. Cahill)

Water budget, vegetation effects:

Dendrochronology and hydrology (R. L. Phipps, w, NC)
Evapotranspiration (F. A. Branson, w, D)

States:

Kansas (w, Lawrence):
Natural recharge, Harvey County (C. A. Perry)
Natural recharge in the Kansas plains (Marios Sophocleous)

Montana (w, Helena):

Milk-St. Mary River apportionment, Montana (R. E. Thompson)

North Carolina (w, Raleigh):

North Carolina water atlas (G. L. Giese)

Utah (w, Salt Lake City):

Hydrologic reconnaissance, west-central Utah (J. S. Gates)

Waterpower classification:

States:

California (c, Sacramento):
Kings River basin, examination of pumped storage sites (W. T. Smith)

Mokelumne River basin, examination of pumped storage sites (D. E. Wilson)

Review of withdrawals:

Klamath River basin (D. E. Wilson)
North Fork Feather River basin (W. T. Smith)
Owens River basin Westside tributaries (R. D. Morgan)

Upper San Joaquin River basin, examination of pumped storage sites (W. T. Smith)

Westside tributaries (R. D. Morgan)

Idaho (c, Portland, Oreg.)

Pahsimeroi River, reservoir, and dam site (K. J. St. Mary)
Snake River basin, examination of pumped storage sites (H. Villalobos)

Oregon (c, Portland):

Review of withdrawals:

Clackamas River basin (L. O. Moe)
Nestucca River basin (K. J. St. Mary)
South Umpqua River basin (L. O. Moe)
Snake River basin, examination of pumped storage sites (H. Villalobos)

Washington (c, Portland, Oreg.):

Similkameem River basin, dam site investigation (H. Villalobos)

Water quality, general:

Analytical support for methods (A. W. Beetem, w, NC)
Arkansas River Compact (G. L. Selignan, w, D)
Energy research and development coordination (F. A. Kilpatrick, w, NC)

Foreign assistance, PL 80-402 (Della Laura, w, NC)

Foreign assistance, Section 607 (Della Laura, w, NC)

Geochemical kinetics studies (H. C. Claassen, w, D)

Geochemistry, oil field waters, Alaska (Y. K. Kharaka, w, M)

Improvement of quality of water data system (D. A. Goolsby, w, NC)

International organizations repayment (Della Laura, w, NC)

International organization training (Della Laura, w, NC)

Isotopes in hydrology (C. T. Rightmire, w, NC)

NAWDEX reimbursement: Federal (M. D. Edwards, w, NC)

NAWDEX reimbursement: Nonfederal (M. D. Edwards, w, NC)

Organic hydrogeochemistry (R. L. Malcolm, w, Arvada, Colo.)

Organic polyelectrolytes (R. L. Wershaw, w, Arvada, Colo.)

Other Federal agencies repay (Della Laura, w, NC)

Region unrestricted (J. D. Bredehoeft, w, M)

Water quality, general—Continued

Saudi Arabian Advisory Services (G. C. Tibbitts, w, NC)

Snow chemistry reconnaissance (H. R. Feltz, w, NC)

State Agency for International Development, miscellaneous (Della Laura, w, NC)

Subsurface waste coordination (L. A. Wood, w, NC)

States:

Arizona (w, Tucson):

Grand Canyon water resources (J. H. Eychaner)
Pecos River Commission (H. M. Babcock)

California (w, Menlo Park):

Ground-water quality inventory (J. P. Akers)

Colorado (w, Lakewood):

Energy development, stream quality (L. J. Britton, D)

Delaware (w, Dover):

Delaware-Potomac aquifer study (M. M. Martin)

Florida (w, Tallahassee):

Water atlas (D. E. Troutman)

Idaho (w, Boise):

Ground-water quality conditions (J. J. Yee)

Louisiana (w, Baton Rouge):

Quality of lower Mississippi River (C. R. Demas)

Maine (w, Augusta):

Phosphorus yields to Lovejoy Pond (W. J. Nichols)

Mississippi (w, Jackson):

Brine contamination (S. J. Kalkhoff)
Precipitation quality in Mississippi (P. E. Grantham)

Nevada (w, Carson City):

Geochemistry of Leviathan Mine (D. P. Hammermeister)

New York (w, Albany):

Acid precipitation bibliography (D. A. Wiltshire)
Chemical weathering model (N. E. Peters)
Precipitation network for New York (C. R. Barnes)

Ohio (w, Columbus):

Aquatic biology in Ohio coal fields (M. J. Engelke)

Oklahoma (w, Oklahoma City):

Surface-water suitability (J. D. Stoner)

Pennsylvania (w, Harrisburg):

Ohio River Valley Water Sanitation Compact (ORSANCO)
Commissioner duties (N. H. Beamer)
Pennsylvania Gazetteer of Streams, Part II (L. C. Shaw)

Texas (w, Austin):

Arkansas River Compact (Trigg Twichell)

Utah (w, Salt Lake City):

Jordan River quality study (R. C. Christensen)
Salt Lake County urban runoff study (R. C. Christensen)

Virginia (w, Richmond):

Acid deposition, Shenandoah Park (D. D. Lynch)

Washington (w, Tacoma):

Mount St. Helens lakes (S. S. Embrey)
Organic decay, Mount St. Helens (J. M. Klein)

Wisconsin (w, Madison):

Acid precipitation, northern Wisconsin (D. A. Wentz)
Acid precipitation, northwestern Wisconsin (D. A. Wentz)
Chemical loading to Lake Michigan (C. C. Harr)

Well interference:

Mechanics of ground-water flow (G. F. Pinder, w, NC)

States:

Arizona (w, Tucson):

Black Mesa monitoring program (G. W. Hill)

Indiana (w, Indianapolis):

St. Joseph basin study (J. G. Peters)

New York (w, Albany):

Bedrock well cluster study (A. D. Randall)

Puerto Rico (w, San Juan):

Well interference—Continued

Ground water in critical areas (Eloy Colon-Dieppa)

Utah (w, Salt Lake City):

Navajo Sandstone, southwestern Utah (R. M. Cordova)

Wilderness Program. *See* Primitive and Wilderness Areas under Mineral and fuel resources—compilations and topical studies, mineral-resource surveys.

Withdrawal and water use:

Effects of floods on vegetation (F. A. Branson, w, D)

Estimating drawdown, Ogallala/Landsat (John Bredehoeft, w, NC)

National Water Use Data Program (W. E. Mann, w, NC)

Water use in the U.S. (C. C. Murray, w, NC)

Water use in 1975 (C. C. Murray, w, NC)

States:

Alabama (w, Tuscaloosa):

Water use (J. R. Harkins, University)

Alaska (w, Anchorage):

Water use (Leslie Patrick)

Arkansas (w, Little Rock):

Water use (A. H. Ludwig)

California (w, Menlo Park):

Water use (J. R. Crippen)

Colorado (w, Lakewood):

Water use (R. R. Hurr, D)

Connecticut (w, Hartford):

Water use (F. P. Haeni)

Delaware (w, Dover):

Water use (A. L. Hodges)

Florida (w, Tallahassee):

Urban withdrawals, Jacksonville (R. M. Spechler, Jacksonville)

Water use (S. D. Leach)

Georgia (w, Doraville):

Water use (R. R. Pierce)

Hawaii (w, Honolulu):

Water use (R. H. Nakahara)

Idaho (w, Boise):

Water use (W. A. Harenberg)

Illinois (w, Urbana):

Water use (G. G. Curtis)

Indiana (w, Indianapolis):

Water use (Z. C. Bailey)

Iowa (w, Iowa City):

Water use (O. G. Lara)

Kansas (w, Lawrence):

Estimating ground-water withdrawals (C. H. Baker)

Water use (C. H. Baker)

Kentucky (w, Louisville):

Water use (D. S. Mull)

Louisiana (w, Baton Rouge):

Water use (W. H. Walter)

Maine (w, Augusta)

Water use (D. H. Tepper)

Maryland (w, Towson)

Water use (H. J. Frieberger)

Massachusetts (w, Boston)

Water use (R. A. Brackley)

Michigan (w, Lansing)

Water use (F. R. Twenter)

Withdrawal and water use—Continued

Minnesota (w, St. Paul):

Water-use data, Minnesota (E. L. Madsen)

Mississippi (w, Jackson):

Water use (J. A. Callahan)

Missouri (w, Rolla):

Water use (L. D. Hauth)

Montana (w, Helena):

Water use (Charles Parrett)

Nebraska (w, Lincoln):

Water use (D. R. Lawton)

Nevada (w, Carson City):

Water use (F. E. Artega)

New Jersey (w, Trenton):

Pumpage inventory (William Kam)

Water use (E. F. Vowinkel)

New Mexico (w, Albuquerque):

Water use (William Dein, Santa Fe)

New York (w, Albany):

Water use (D. S. Snively)

North Carolina (w, Raleigh):

Water use (M. N. Jackson)

Water-use data collection, North Carolina (R. C. Heath)

North Dakota (w, Bismarck):

Water use (M. L. Smith)

Ohio (w, Columbus):

Water use (R. R. Hathaway)

Oklahoma (w, Oklahoma City):

Water use (J. D. Stoner)

Oregon (w, Portland):

Water use (L. E. Hubbard)

Pennsylvania (w, Harrisburg):

Water use (K. L. Wetzel)

Puerto Rico (w, San Juan):

Water use (Fernando Gomez-Gomez, Ft. Buchanan)

Rhode Island (w, Providence):

Water use (H. E. Johnston)

South Carolina (w, Columbia):

Water Use (B. H. Whetstone)

South Dakota (w, Huron):

Water use (E. F. LeRoux)

Tennessee (w, Nashville):

Water use (L. G. Conn)

Texas (w, Austin):

Water use (L. F. Land)

Utah (w, Salt Lake City):

Water use (R. W. Cruff)

Vermont (w, Montpelier):

Water use (R. A. Brackley)

Virginia (w, Richmond):

Water use (H. T. Hopkins)

Washington (w, Tacoma):

Water use (E. H. McGavock)

Wisconsin (w, Madison):

Water use (C. L. Lawrence)

Wyoming (w, Cheyenne):

Water use (J. F. Wilson)

Zeolites:

California (southeastern), Oregon, and Arizona (R. A. Sheppard, D)

Zinc. *See* Lead, zinc, and silver.

SUBJECT INDEX

A

- absolute age** *see also* geochronology; isotopes
- absolute age—dates**
- bentonite*: K-Ar ages of bentonites in the Seabee Formation, northern Alaska 150-151
- biotite*: New evidence for strike-slip displacement on the Kaltag fault 78
- bones*: Gubik Formation, Alaskan North Slope 180
- calcium carbonate*: Thermoluminescence dating of pedogenic calcium carbonate 151-152
- foraminifers*: Italy 283-284
- galena*: Age and genetic constraints for the uranium deposit at Lilljuthatten 290
- gneisses*: Crystalline rocks near Frazier Mountain, western Transverse Ranges 70
- granite*: Geochemical, isotopic, and petrologic studies of an Archean granite, Owl Creek Mountains, Wyoming 144
— Two-mica granite geochronology, tectonic space, and uranium content 45
- granites*: Age of diorite-granodiorite gneisses 286
— Geochronology of granites and associated uranium occurrences, Olary Province, Australia 151
— Uranium-lead isotopic ages from Sierra Nevada batholith, California 143-144
- granodiorites*: Comagmatic granitoid sequence, Sierra Nevada 67
- gravel*: Pleistocene alluvial-gravel in eastern Idaho 63-64
- igneous rocks*: Lower Jurassic igneous rocks in the Culpeper basin, Northern Virginia 52-53
- lava*: Eruptive recurrence, Mauna Loa volcano, Hawaii 216-217
- lead*: Implications of common lead measurements 286-287
- peat*: Late Holocene eruptions, South Sister Volcano, Oregon 217
- plutonic rocks*: Age and strontium initial ratio of plutonic rocks 286
- pollen*: ²¹⁰Pb activity and pollen dating, Potomac estuary, Virginia 152
- sediments*: ²¹⁰Pb geochronology, Upper Klamath Lake, Oregon 152
- soils*: Dating landslides and other upper Pleistocene and Holocene features 221
— Soil chronosequences and ¹⁰Be isotopic dating in mid-Atlantic States 51-52
- tufa*: Lake Bonneville revisited 163-164
- uranium ores*: Geochronology of roll-type uranium ores of the Felder deposit, Texas 151
- volcanic ash*: Geochronology 223
- zircon*: Geochronology of a xenotime-monazite gneiss, southern New York 36
— Granitoid plutonic rocks of the Arabian Shield 287
— Radiometric ages of two-mica granites of northeastern Nevada 150
- acoustical surveys** *see under* geophysical surveys *under* California
- aerial photography** *see under* remote sensing
- aeromagnetic surveys** *see* magnetic surveys *under* geophysical surveys *under* Appalachians; Atlantic Coastal Plain; Atlantic Ocean; automatic data processing; California; Colorado; Egypt; Michigan; Nevada; North Carolina; North Dakota; Pacific Ocean; United States
- Africa** *see also* Botswana; Egypt; Lesotho; South Africa; Tanzania; Tunisia
- Africa—geophysical surveys**
- remote sensing*: Global Magsat anomaly signatures emphasizing West Africa and eastern South America 252-253
- Alabama—economic geology**
- coal*: Northern Black Warrior basin, Alabama 16
- Alabama—environmental geology**
- geologic hazards*: Flood frequency of urban streams in Alabama 235
- Alabama—hydrogeology**
- ground water*: Geochemistry of water from Cretaceous aquifers in the Southeastern United States; Mississippi, Alabama, Georgia, and South Carolina 146
- hydrology*: Mathematical model of the Alabama River 171
— Methodology for hydrologic evaluation of a potential surface mine, Tuscaloosa County, Alabama 224
— Watershed model for Warrior coal basin, Alabama 223-224
- surveys*: Southeastern Sand Aquifer Study 108
- Alabama—paleontology**
- Mammalia*: Hemphillian vertebrate fauna from Mobile County, Alabama 179
- Alabama—stratigraphy**
- Miocene*: Hemphillian vertebrate fauna from Mobile County, Alabama 179
- Pennsylvanian*: Northern Black Warrior basin, Alabama 16
- Alaska—areal geology**
- east-central Alaska*: East-central Alaska 77-78
- Kodiak A-6 Quadrangle*: Experimental 1:63,360-scale orthophotoquad of Kodiak A-6 quadrangle, Alaska 298
- northern Alaska*: Northern Alaska 76-77
- regional*: Alaska 75-81
- southern Alaska*: Southern Alaska 78-79
- southwestern Alaska*: Southeastern Alaska 79-81
- Southwestern Alaska 79
- Alaska—economic geology**
- copper ores*: Geochemical exploration by analyses of fecal material from herbivorous mammals 11
— Mineral resource assessment with digital geologic data bases 254-255
- fuel resources*: Hydrocarbon potential of Norton basin, Alaska 24
- gold ores*: Recycled gold in interior Alaska 77-78
— Recycled gold, interior Alaska 8-9
- metal ores*: New fossils from Taku terrane suggest permian metallogenic province 79-80

- mineral resources*: Alaska Mineral Resource Assessment Program 75
- Magnetic provinces, tectonostratigraphic terranes, and resource guides, Lake Clark quadrangle, Alaska 11
 - Regional geochemical exploration in Alaska 2-3
 - Statewide 75-76
- peat*: Peat in Maine and Alaska 1
- petroleum*: Alaska 24
- Maturity of upper Paleozoic surface rocks related to Cretaceous heating event 77
 - National Petroleum Reserve in Alaska 303-304
 - Time and degree of thermal maturity of rock units in NPRA 24
- uranium ores*: Uranium potential of the Kootznahoo Formation, Zerembo Island area, Alaska 40
- Alaska—engineering geology**
- permafrost*: Depth and temperature of permafrost on the Alaskan Arctic Slope 76
 - Permafrost, heat flow, and the geothermal regime at Prudhoe Bay 76
- Alaska—environmental geology**
- land use*: ANILCA activities 75
 - Land cover of the Arctic National Wildlife Refuge coastal area 304
 - Land use and land cover mapping in south-central Alaska 304
 - waste disposal*: Geochemistry of vegetation, soils, and spoil materials, Jarvis Creek, Alaska 198-199
- Alaska—geochemistry**
- isotopes*: Atmospheric carbon dioxide 150
 - properties*: Geochemistry of vegetation, soils, and spoil materials, Jarvis Creek, Alaska 198-199
- Alaska—geochronology**
- Cretaceous*: K-Ar ages of bentonites in the Seabee Formation, northern Alaska 150-151
- Alaska—geomorphology**
- glacial geology*: Desert conditions in northern Alaska during the last glaciation 76-77
 - Glacial studies in the Yukon-Tanana Upland 77
- Alaska—geophysical surveys**
- heat flow*: Permafrost, heat flow, and the geothermal regime at Prudhoe Bay 76
 - maps*: Mapping vegetation and land cover in Alaska with Landsat digital data 303-304
 - remote sensing*: Control extension using stereo radar strip imagery 305
 - Geologic applications of Landsat 3 RBV images 253-254
 - Land cover and terrain mapping for the Kenai National Wildlife Refuge using Landsat MSS data 258
 - Land cover of the Arctic National Wildlife Refuge coastal area 304
 - Land use and land cover mapping in south-central Alaska 304
 - Mineral resource assessment with digital geologic data bases 254-255
 - National Petroleum Reserve in Alaska 303-304
 - Prudhoe Bay region 304
 - Seasat altimeter 306
 - Side-looking airborne radar program 255
 - seismic surveys*: Hydrocarbon potential of Norton basin, Alaska 24
- Alaska—petrology**
- igneous rocks*: Granitic rocks and migmatites in the Coast plutonic complex near Petersburg 80-81
 - metamorphic rocks*: Mineral assemblages and compositional variations, Barrovian metamorphic sequence, near Juneau 80
- Alaska—sedimentary petrology**
- sedimentary rocks*: Burnt Island Conglomerate (Upper Triassic) on Screen Islands 79
 - The Kanayut Conglomerate: one of North America's most extensive ancient fluvial deposits 77
 - sedimentation*: Sediment transport in the Tanana River near Fairbanks, Alaska, 1977-79 162
- Alaska—seismology**
- earthquakes*: Southern Alaska seismicity during FY 81 207-208
- Alaska—soils**
- Paleosols*: The Kanayut Conglomerate: one of North America's most extensive ancient fluvial deposits 77
- Alaska—stratigraphy**
- Cambrian*: Middle Cambrian fossils in central Brooks Range, Alaska 180-181
 - Carboniferous*: Radiolaria indicate Carboniferous and Triassic ages for chert in the Circle Volcanics, Circle quadrangle 78
 - Cenozoic*: Evolution of sedimentary systems during the Mesozoic and Cenozoic Eras, southern Alaska 78-79
 - Devonian*: Tectonostratigraphic terrane studies 75-76
 - maps*: Pre-Carboniferous "basement" map of northern Alaska and northern Yukon 181
 - Mesozoic*: Evolution of sedimentary systems during the Mesozoic and Cenozoic Eras, southern Alaska 78-79
 - Miocene*: Asiatic mollusks in Miocene faunas of the Alaska Peninsula 178-179
 - Paleocene*: Limits to northward drift of the Paleocene Cantwell Basin, central Alaska 130
 - Paleozoic*: Maturity of upper Paleozoic surface rocks related to Cretaceous heating event 77
 - Pre-Carboniferous "basement" map of northern Alaska and northern Yukon 181
 - Permian*: New fossils from Taku terrane suggest permian metallogenic province 79-80
- Pleistocene*: Gubik Formation, Alaskan North Slope 180
 - Precambrian*: Pre-Carboniferous "basement" map of northern Alaska and northern Yukon 181
 - Quaternary*: Lacustrine sediment cores in south-central Alaska 163
 - Late Quaternary vegetation and climate history from western Alaska 162-163
 - Tertiary*: Tertiary Studies, Arctic Coastal Plain, Alaska 177-178
 - Uranium potential of the Kootznahoo Formation, Zerembo Island area, Alaska 40
 - Triassic*: Burnt Island Conglomerate (Upper Triassic) on Screen Islands 79
 - New fossils from Taku terrane suggest permian metallogenic province 79-80
 - Radiolaria indicate Carboniferous and Triassic ages for chert in the Circle Volcanics, Circle quadrangle 78
- Alaska—structural geology**
- faults*: New evidence for strike-slip displacement on the Kaltag fault 78
 - West-central Alaska 78
 - tectonics*: Evolution of sedimentary systems during the Mesozoic and Cenozoic Eras, southern Alaska 78-79
 - Tectonostratigraphic terrane studies 75-76
- Alaska—tectonophysics**
- plate tectonics*: Offset of Tertiary arcs on the Alaska Peninsula 79
- Alberta—hydrogeology**
- hydrology*: Joint United States-Canada study of flow of Milk River at the Montana-Alberta border 275-276
- algae—diatoms**
- Quaternary*: Late Quaternary vegetation and climate history from western Alaska 162-163
- Alps** *see also* the individual countries
- aluminum ores** *see also* *undereconomic geology under Appalachians*
- ammonites** *see* Mollusca
- ammonoids** *see under* mollusks
- Andes** *see also* the individual countries
- angiosperm flora** *see also* angiosperms
- angiosperm flora—biostratigraphy**
- Eocene*: Eocene montane floras 178
- angiosperms** *see also* angiosperm flora
- angiosperms—Dicotyledoneae**
- Holocene*: Computer model of wetlands forest 183
- Antarctica—geochemistry**
- isotopes*: Atmospheric carbon dioxide 150
- Antarctica—geophysical surveys**
- remote sensing*: Satellite glaciology 252
 - seismic surveys*: Antarctica 280
- Appalachians** *see also* the individual states and provinces
- Appalachians—areal geology**
- regional*: Appalachian Highlands and the coastal plains 49

- Appalachians—economic geology**
aluminum ores: Large hydrothermal systems studied in Carolina slate belt 6
natural gas: Potential gas resources of southern Blue Ridge province 30
- Appalachians—engineering geology**
geologic hazards: Large, old debris avalanches in the Appalachians 221
slope stability: Large, old debris avalanches in the Appalachians 221
 — Repetitive nature of Appalachian landslides 221
- Appalachians—geophysical surveys**
magnetic surveys: Correlation of aeromagnetic patterns with major lithotectonic units in the southern Appalachian Mountains 52
- Appalachians—petrology**
intrusions: Lower Jurassic igneous rocks in the Culpeper basin, Northern Virginia 52-53
- Appalachians—structural geology**
faults: Polydeformed rocks in the Lowndesville shear zone, South Carolina and Georgia 52
tectonics: A high Taconic slice in the Pennsylvania Piedmont 51
 — An Avalonian terrane in the Charlotte 2°-quadrangle, North and South Carolina Piedmont 50-51
 — Cambrian paleographic features of the central Virginia Piedmont 49-50
 — Correlation of aeromagnetic patterns with major lithotectonic units in the southern Appalachian Mountains 52
 — Exotic terranes in the New England Appalachians 48-49
 — Structures in the Roanoke recess area, Virginia and West Virginia 50
- aquifers** *see under* ground water
- Arabian Gulf** *see* Persian Gulf
- Arabian Peninsula** *see also* Saudi Arabia; Yemen
- Archean** *see also under* geochronology *under* Wyoming
- Arctic region** *see also* the individual countries; Greenland
- Argentina—seismology**
earthquakes: Aftershock investigations 202-203
- argon— isotopes**
Ar-40: Mexico 284-285
Ar-40/Ar-39: Age and strontium initial ratio of plutonic rocks 286
- arid regions** *see* deserts *under* glacial geology
- Arizona—economic geology**
copper ores: Studies of the root zone of the Ajo porphyry copper system 6
gold ores: Gold in the Gold basin # Lost basin districts, Mohave County, Arizona 5
mineral resources: Mineral resource potential of the Marble Platform, Coconino County, Arizona 3
uranium ores: Depositional cycles in the Chinle Formation 39
- Resistivity investigations of Tertiary basins of western Arizona 34
 — Volcano-tectonic evolution of the Date Creek basin uranium area in western Arizona 34
- Arizona—engineering geology**
land subsidence: Land subsidence and earth-fissure hazards in central Arizona 240
- Arizona—geophysical surveys**
electrical surveys: Resistivity investigations of Tertiary basins of western Arizona 34
heat flow: Heat flow from five wells in west-central Arizona 158-159
magnetotelluric surveys: Magnetotelluric soundings over the Colorado Plateau and Basin and Range provinces 134
remote sensing: Accuracy assessment of Landsat-derived Arizona wildland vegetation map 257
 — Contracted satellite data relay study 264
 — District satellite receive sites 264
 — Geologic mapping with HCMM data in the Powder River Basin, Wyoming and Cabeza Prieta, Arizona 261
 — Real-time data processing 263-264
well-logging: Schlumberger soundings in the Date Creek Basin, Arizona 134
- Arizona—hydrogeology**
ground water: Impact of ground-water pumpage for coal slurry, Navajo and Hopi Indian Reservations, Arizona 224
hydrology: Hydrologic regionalization by cluster analysis 172
- Arizona—petrology**
volcanism: Differentiation in the Springerville volcanic field, Arizona 142-143
- Arizona—stratigraphy**
Miocene: Age of Colorado Plateau margin, central Arizona 55-56
Tertiary: Tertiary stratigraphy, intrusion, and structure in the Mohave Mountains in west-central Arizona 65-66
Triassic: Depositional cycles in the Chinle Formation 39
- Arizona—structural geology**
faults: Reserve graben, southwestern New Mexico and eastern Arizona 61
folds: Origin of folding of Tertiary low-angle fault surfaces in southeastern California and western Arizona 66
tectonics: Tertiary stratigraphy, intrusion, and structure in the Mohave Mountains in west-central Arizona 65-66
- Arizona—tectonophysics**
crust: Geologic mapping with HCMM data in the Powder River Basin, Wyoming and Cabeza Prieta, Arizona 261
- Arkansas—hydrogeology**
ground water: Arkansas 90
 — Effects of 1980 drought on ground-water levels in the Mississippi alluvial plain 90
hydrology: Arkansas traveltime study 174-175
- Derivation of net photosynthetic production from community-metabolism analysis in Arkansas 194
 — Gas- and dye-tracer-estimation program in Arkansas 187-188
 — Modified version of one-dimensional, steady-state, stream water-quality model in Arkansas 187
 — New dissolved-oxygen probe in Arkansas 198
 — Sediment-oxygen-demand measurements by use of a laboratory respirometer in Arkansas 197
- Asia** *see also* Bangladesh; China; India; Indonesia; Japan; Malaysia; Philippine Islands; Thailand
- Asia—economic geology**
petroleum: CCOP 281
- Asia—oceanography**
marine geology: CCOP 281
- associations** *see also* survey organizations
- associations—general**
international cooperation: International commissions and representation 276-280
 — Summary of selected activities by country or region 280-291
International Geologic Correlation Program: International Geologic Correlation Program 275
International Standardization Organization: Activities related to other international organizations 279
symposia: Other international meetings and conferences 279-280
- Atlantic Coastal Plain—areal geology**
regional: Appalachian Highlands and the coastal plains 49
- Atlantic Coastal Plain—geochemistry**
Quaternary: Soil chronosequences and ¹⁰Be isotopic dating in mid-Atlantic States 51-52
- Atlantic Coastal Plain—geochronology**
Pleistocene: Amino-acid dating of fossil shells in the Atlantic Coastal Plain 53
- Atlantic Coastal Plain—geophysical surveys**
magnetic surveys: Geophysical studies, U.S. Atlantic Coastal Plain and continental margin 112-113
- Atlantic Coastal Plain—hydrogeology**
ground water: Analysis of fresh and saline ground water in the New Jersey Coastal Plain and Continental Shelf 109
 — Deep test well in Maryland 109
 — Freshwater beneath the Carolina Continental Shelf 113-114
 — Stressed flow system in the Tertiary limestone aquifer system 106
- Atlantic Coastal Plain—sedimentary petrology**
weathering: Studies of depth of weathering on Atlantic Coastal Plain formations 50
- Atlantic Coastal Plain—soils**
geochemistry: Soil chronosequences and ¹⁰Be isotopic dating in mid-Atlantic States 51-52

- Atlantic Coastal Plain—stratigraphy**
Cenozoic: Late Cenozoic sea levels 164
changes of level: Late Cenozoic sea levels 164
Cretaceous: Upper Cretaceous units in the southeastern Virginia Coastal Plain 108
Eocene: California Eocene Kellogg Shale correlated to Atlantic cores 178
Tertiary: Geology of Tertiary sediments near the Cooke fault, Charleston, South Carolina 53
- Atlantic Ocean** *see also* Gulf of Mexico
- Atlantic Ocean—economic geology**
petroleum: Petroleum geology of the U. S. Mid-Atlantic Slope 111
- Atlantic Ocean—engineering geology**
slope stability: Slope stabilities, Georges Bank and Baltimore Canyon areas, Atlantic continental margin 115-116
- Atlantic Ocean—geochemistry**
isotopes: Mineralogy and stable isotope geochemistry of hydrothermally altered rocks from the East Pacific Rise and the Mid-Atlantic Ridge 149
- Atlantic Ocean—geophysical surveys**
magnetic surveys: Geophysical studies, U.S. Atlantic Coastal Plain and continental margin 112-113
seismic surveys: Deposition sequences and stratigraphic gaps of the U.S. Atlantic margin 113
 — Geology and evolution of the Blake Escarpment 114
 — Multichannel seismic measurements in the Bahaman-Cuban collision zone 135
 — Offshore stratigraphy of Georges Bank Basin 113
- Atlantic Ocean—oceanography**
continental shelf: Geologic processes of the east coast Continental Shelf 116
 — Growth and development of the upper and middle Laurentian fan 110-111
continental slope: Mass movement, Atlantic Continental Slope off New England 116
ocean circulation: The Lydonia Canyon experiment; preliminary results 116-117
ocean floors: Geology and evolution of the Blake Escarpment 114
 — Submarine canyon dynamics 116
- Atlantic Ocean—paleontology**
foraminifera: Late Paleogene watermass fluctuations along east coast continental margin 114
- Atlantic Ocean—stratigraphy**
Mesozoic: Atlantic offshore stratigraphy-Georges Bank Basin and Blake Escarpment 177
Paleogene: Late Paleogene watermass fluctuations along east coast continental margin 114
- Atlantic Ocean Islands** *see also* Iceland
- Atlantic region** *see also* the individual countries
- Australia** *see also* Northern Territory
- Australia—economic geology**
uranium ores: Australia 280
 — Landsat studies of uranium settings, Australia and France 260
- Australia—geochronology**
Precambrian: Geochronology of granites and associated uranium occurrences, Olary Province, Australia 151
- Australia—geophysical surveys**
remote sensing: Australia 280
 — Landsat studies of uranium settings, Australia and France 260
- automatic data processing—economic geology**
coal: Computerization of the Nation's coal resources 15
copper ores: Mineral resource assessment with digital geologic data bases 254-255
mineral resources: Data collection and processing 12
petroleum: China 281-282
 — Malaysia 284
 — Probabilistic and statistical resource appraisal methodology 32-33
uranium ores: Application of genetic-geologic models for uranium resource estimates 41-42
- automatic data processing—engineering geology**
earthquakes: New computer codes for ground motion studies 212-213
geologic hazards: Mount St. Helens post-eruption flood hazards 229-230
methods: Engineering geologic mapping in New York City 219
underground installations: Geology of Nuclear Test Sites, Nevada Test Site 231
waste disposal: Evaluation of the Basin and Range province for possible nuclear waste disposal 233
- automatic data processing—environmental geology**
land use: Algorithms for generalization of land use and land cover map content 295
 — An assessment of the accuracy of land use and land cover maps 299
 — Applications software development for land use and land cover data 295
 — Computer graphics experiments and techniques 299-300
 — Geographic information system development 294
 — Identifying changes in land use and land cover 298-299
 — Indonesia 282-283
 — Land use and land cover statistics 299
- automatic data processing—general cartography**: Automated cartography 293-294
- computer programs**: Online Aerotriangulation Data Collection and Edit System 311
- computers**: Array processing 312-313
 — Computer resources and technology 312-313
- Teleconferencing and office automation 312
- data bases**: Data base development 292
- Fortran**: Application of linear algebra to computation of gridded data 297
- Generalized adjustment by least squares 297-298
- geography**: Geographic Names Information System 294-295
- information systems**: Information management technology 312
- maps**: The 1:2,000,000-scale data base 292
- microcomputers**: Microcomputers 312
- automatic data processing—geochemistry**
spectroscopy: Optimizing the selectivity of standard spectrofluorometers with computer control 198
- automatic data processing—geomorphology**
landform description: DEM editing using a polygon scan-conversion process 292-293
 — Map projections 295
 — Planimetric mapping of the planets 247-248
- automatic data processing—geophysical methods**
remote sensing: Analysis of return beam vidicon (RBV) radiometric response and development of correction techniques 251
 — Applications and techniques development for raster-formatted data 308-309
 — Computer system networking 249
 — Digital topographic data 250
 — Earth Resources Observation Systems Office 249
 — Geometric registration 250
 — Image generation using film recorder 251
 — Image processing laboratory developed to support uranium exploration 135
 — Innovative techniques for display of thematic maps 251-252
 — Inventory of computer software for spatial data handling 251
 — Mapsat 301-302
 — Multispatial data acquisition and processing 302
 — Multispectral classification procedures 251
 — Remote image processing station (RIPS) research, development, and technology transfer 249-250
 — Satellite surveying system 306-307
 — Spatial data analysis technique development 250
 — Spatial data handling capability assessment 249
 — Spatial data handling research and development 249-251
 — Techniques for the storage of very large spatial data sets 250-251
 — Techniques in processing digital data 251-252
- well-logging**: Development of a borehole radar system 233

— Hydraulic-conductivity logging 196-197

automatic data processing—geophysical surveys

magnetic surveys: Geomagnetic observatories 132

remote sensing: Contracted satellite data relay study 264

— Improved lithologic separation and data base application 255

— Land cover and terrain mapping for the Bristol Bay subregion using Landsat MSS data and digital terrain data 258

— Land cover and terrain mapping for the Kenai National Wildlife Refuge using Landsat MSS data 258

— Land cover mapping with merged Landsat RBV and MSS stereoscopic images 258

— Landsat studies of uranium settings, Australia and France 260

— Mapping forest fuels and predicting wildland fire behavior 257

— Mapping of irrigated cropland with Landsat digital data 303

— Mapping vegetation and land cover in Alaska with Landsat digital data 303-304

— Martian topography; a new method for rapid extraction 244

— National Petroleum Reserve in Alaska 303-304

— Real-time data processing 263-264

— Seasat altimeter 306

— Sioux Falls area geographic analysis 258-259

— Utility of a digital data base for improving Landsat classification results and managing a forested wetland 257

well-logging: Estimating radioisotope concentrations with gamma-radiation well logs 234

automatic data processing—hydrogeology

ground water: Automated conversion of geocoded water-withdrawal information for input to a two-dimensional ground-water model 168

— Ground-water hydrology 165

— Impact of ground-water pumpage for coal slurry, Navajo and Hopi Indian Reservations, Arizona 224

— Mathematical model of the Eagle Valley ground-water basin, west-central Nevada 166

— Model studies of surface storage and recovery of freshwater, southern Florida 168-169

— Numerical modeling of the hydrogeology of the principal artesian aquifer, Dougherty Plain, Georgia 168

— Numerical simulation of the alluvium and terrace aquifer along the North Canadian River from Canton Lake to Lake Overholser 167

— Projected effects of proposed salinity-control projects on fresh ground water in the upper Brazos and Wichita River basins, Texas 189

hydrology: An evaluation of Idaho stream-gaging networks 172-173

— Bias in standard deviation due to autocorrelation 172

— Data coordination, aquisition, and storage 99-101

— Data-network studies 172-173

— Development of a hydrologic data-acquisition system 197

— Development of a new microprocessor controller for National Urban Runoff data collection 195

— Dissolved-solids model of the Tongue River, Montana 188-189

— Effects of urbanization on flood peaks, Missoula, Montana 236

— Evaluation of selected one-dimensional stream water-quality models with field data 188

— Evaluation of streamflow-data networks 172

— Flow model of Saginaw River 171

— Geohydrology of stream-aquifer system, Finney and Kearny Counties, Kansas 191-192

— Hydrologic regionalization by cluster analysis 172

— Low-flow characteristics of Massachusetts streams 175-176

— Mathematical model of the Alabama River 171

— Microcomputer program for time-of-travel and dispersion characteristics of streams in Florida 188

— Model simulation of runoff hydrographs in the Coon Creek watershed, Anoka County, Minnesota 171

— National Stream Quality Accounting Network 104-105

— National water data exchange 100-101

— Potomac River Reservoir release routing 170-171

— Streamflow data network for Nevada 173

— Urban stormwater data management system 101-102

— Water-data storage system 101

— Water use 103-104

— Water use in Montana 104

— Watershed-model-evaluation study 171

automatic data processing—maps

cartography: Pass point marking system 310

data acquisition: Automated Map Symbol Placement System 310

microcomputers: Voice data entry system 310-311

automatic data processing—methods

cartography: Automated spatial data handling 292-295

automatic data processing—paleobotany

angiosperms: Computer model of wetlands forest 183

automatic data processing—seismology

earthquakes: Earthquake Early Alerting Service (EEAS) 202

— National earthquake data base 207

— Theoretical investigations 203-204

seismicity: Data and information 202

— Research and development 201

automatic data processing—techniques

models: Experimental 1:63,360-scale orthophotoquad of Kodiak A-6 quadrangle, Alaska 298

Azores *see also* Portugal

B

Baltic region *see also* the individual countries

Bangladesh—economic geology

energy sources: Bangladesh 281

Bangladesh—geophysical surveys

seismic surveys: Bangladesh 281

Barbados—stratigraphy

Miocene: Tropical Miocene silicoflagellates near Barbados 178

base metals *see also* under economic geology under California; New Mexico

Basin and Range Province—areal geology

regional: Basin and Range region 63-67

Basin and Range Province—economic geology

mineral resources: Mineral-resource studies 63

Basin and Range Province—engineering geology

waste disposal: Evaluation of the Basin and Range province for possible nuclear waste disposal 233

Basin and Range Province—petrology

igneous rocks: Igneous rocks 66-67

Basin and Range Province—stratigraphy

Phanerozoic: Stratigraphic and structural studies 63-66

Pleistocene: Distribution of pearlette family volcanic ash marker beds 56

Basin and Range Province—structural geology

tectonics: Stratigraphic and structural studies 63-66

batholiths *see under* intrusions

bentonite deposits *see also under* economic geology under Gulf Coastal Plain

Bering Sea—engineering geology

slope stability: Sea-floor hazards of the Navarin Basin, northern Bering Sea 118-119

Bering Sea—geophysical surveys

gravity surveys: Structure of the Navarin and Anadyr Basins, Bering Sea 112

remote sensing: Land cover and terrain mapping for the Bristol Bay subregion using Landsat MSS data and digital terrain data 258

Bering Sea—oceanography

ocean floors: Structure of the Navarin and Anadyr Basins, Bering Sea 112

Bering Sea—sedimentary petrology

sediments: Geotechnical properties and sedimentary processes of the Alaskan OCS 118

- Postglacial sediments of the northern Bering Sea 118
- beryllium—geochemistry**
- granites*: Baid al Jimalah tungsten deposit 287-288
- beryllium—isotopes**
- Be-10*: Dating landslides and other upper Pleistocene and Holocene features 221
- Soil chronosequences and ¹⁰Be isotopic dating in mid-Atlantic States 51-52
- biogeography—mollusks**
- Miocene*: Asiatic mollusks in Miocene faunas of the Alaska Peninsula 178-179
- Bivalvia** *see under* Mollusca
- boreholes** *see under* acoustical logging *under* well-logging; *see under* electrical logging *under* well-logging; *see under* methods *under* well-logging; *see under* radioactivity *under* well-logging
- Botswana—petrology**
- igneous rocks*: Pyroxene decomposition in kimberlites 138
- brachiopods—biostratigraphy**
- Cambrian*: Middle Cambrian fossils in central Brooks Range, Alaska 180-181
- British Columbia—economic geology**
- geothermal energy*: Geothermal systems of the Cascade Range 153-154
- bryophytes—occurrence**
- springs*: Uranium in spring water and bryophytes at Basin Creek in central Idaho 10

C

- California—areal geology**
- Inyo County*: Geologic and tectonic history of the southern Great Basin and Amargosa drainage system in southwestern Nevada 64-65
- regional*: California 67-71
- California—economic geology**
- base metals*: Anomalous electrical conductors as indicators of potential mineralization 11
- evaporite deposits*: Continental evaporites in Owens Lake, California 13
- fuel resources*: Conterminous United States offshore oil and gas resource assessments 32
- geothermal energy*: Gases of the Lassen geothermal system 155
- Geothermal systems of the Cascade Range 153-154
- Magnetotelluric study of the Cascade Range 46
- Stable isotope interpretation of the Lassen geothermal system 154-155
- The Lassen geothermal system 154
- manganese ores*: Origin of manganese deposits in Franciscan rocks of the Yolla Bolly Terrane, California 5
- mineral resources*: Geochemical mapping of the southern Coast Ranges of California 10
- Trace-element geochemistry of the West Shasta District, California 10
- California—engineering geology**
- earthquakes*: Attenuation of particle velocity in California 212
- Earthquake, new reverse fault, and crustal unloading near Lompoc, California 214
- Ground motion and ground failure hazards in the Los Angeles region, California 213
- Liquefaction studies in the Imperial Valley, California 219
- Mammoth Lake, California, earthquake studies 214-215
- Rates of slip on faults in the Los Angeles region, California 213
- Sediment failure of November 1980, Klamath River Delta, northern California 118
- Seismic monitoring, Oregon and California volcanoes 216
- Westmorland, California, earthquake studies 215
- 1906 earthquake fault offsets in northern San Mateo County, California 219
- geologic hazards*: Ground motion and ground failure hazards in the Los Angeles region, California 213
- Mammoth Lake, California, earthquake studies 214-215
- Rates of slip on faults in the Los Angeles region, California 213
- maps*: Historic and prehistoric landslides in coastal southern California 220
- slope stability*: Historic and prehistoric landslides in coastal southern California 220
- Landslide and flood disaster in the San Francisco Bay region 220
- Landslide hazards mapping in the San Francisco Bay region 220
- Landslide processes in the San Francisco Bay region 220
- California—geochemistry**
- isotopes*: Isotopic composition of uranium and thorium in crystalline rocks 148
- Neodymium and strontium isotopes in inclusions from the Sierra Nevada 147-148
- trace elements*: Trace-element geochemistry of the West Shasta District, California 10
- California—geochronology**
- Mesozoic*: Crystalline rocks near Frazier Mountain, western Transverse Ranges 70
- Uranium-lead isotopic ages from Sierra Nevada batholith, California 143-144
- thermoluminescence*: Thermoluminescence dating of silicic volcanic rocks 151
- California—geomorphology**
- fluvial features*: Late Quaternary tilting in the northeastern San Joaquin Valley, California 71
- glacial geology*: Glacially induced alluvial dams for Tulare Lake, California 71
- landform description*: Synthesis and analysis of accreted terranes in the Sierra Nevada 68
- shore features*: Pre-Flandrian sand sheet within Morro Bay, California 121
- California—geophysical surveys**
- acoustical surveys*: Inner shelf textural and bathymetric irregularities, Monterey Bay, California 121
- heat flow*: Heat flow in the east Brawley and Glamis areas of the Salton Trough, California 159
- Preliminary heat-flow investigations of the California Cascades 158
- magnetic surveys*: Geomagnetic observatories 132
- magnetotelluric surveys*: Tensor audio magnetotellurics 134
- remote sensing*: Estimating rangeland plant cover proportions with large-scale color-infrared aerial photographs 256
- Land cover mapping with merged Landsat RBV and MSS stereoscopic images 258
- seismic surveys*: Seismic refraction study of Mount Shasta and Medicine Lake region 157
- Seismic refraction survey of the Imperial Valley, California 157
- well-logging*: A new slim-hole gravity meter 136
- Schlumberger soundings at Medicine Lake, California 134
- California—hydrogeology**
- ground water*: Injection of treated wastewater for ground-water recharge in the Palo Alto, Baylands, California 169
- hydrology*: Bacterial denitrification in small streams in California 193-194
- Field experiment on in-stream uptake and regeneration of nitrate 192-193
- Late Cenozoic paleohydrology of California desert 164-165
- Riverine-estuarine process 122-123
- Water-quality assessment of the Merced River, California 186
- thermal waters*: Noble gases of the Lassen geothermal system 155
- California—oceanography**
- continental shelf*: Bottom stresses and sediment transport, central California continental shelf 117-118
- Inner shelf textural and bathymetric irregularities, Monterey Bay, California 121
- California—paleontology**
- Mammalia*: Elk Hills, California 180
- California—petrology**
- igneous rocks*: Comagmatic granitoid sequence, Sierra Nevada 67
- Emplacement of the andesite tuff and revised stratigraphy of the Medicine Lake Volcano, California 141
- Phenocrysts record magma mixing in Coso volcanic field, California 141
- inclusions*: Xenoliths from trachybasalt, Sierra Nevada 137
- California—seismology**
- earthquakes*: California seismicity studies for earthquake prediction 205

- Correlated changes in gravity, elevation and strain 206
- $\delta^{18}\text{O}$ and δD anomalies as earthquake precursors 150
- Seismic velocity measurements in the San Andreas fault zone 206
- Seismicity in the Cascades of Oregon and California 156
- Theoretical mechanics of earthquakes precursors 204
- seismicity*: Geodetic strain near Mammoth Lakes, California 206
- California—soils**
- pedogenesis*: Rapidly migrating sand ridges and pulses of foreshore accretion 121
- California—stratigraphy**
- Cenozoic*: Late Cenozoic paleohydrology of California desert 164-165
- Progress in correlation and age determination of late Cenozoic tephra 68-69
- Uplift of the San Bernardino Mountains, California 179-180
- Cretaceous*: Franciscan melange in central northern California 70
- Stratigraphy and sedimentology of the Hornbrook Formation 69
- Eocene*: California Eocene Kellogg Shale correlated to Atlantic cores 178
- Holocene*: Pre-Flandrian sand sheet within Morro Bay, California 121
- Jurassic*: Paleomagnetic evidence for structural rotation of the Klamath Mountains, California 131
- Mesozoic*: New ages for Franciscan rocks of Hull Mountain areas, northern California 69
- Permian*: Paleomagnetic evidence for structural rotation of the Klamath Mountains, California 131
- Quaternary*: Quaternary floodplain deposits of the lower San Joaquin River 71
- Quaternary reference core 162
- California—structural geology**
- faults*: Amount of offset of Salinian block remains equivocal 67
- Experimental studies of fault mechanics 204
- Geometry of a thrust fault in northern California 67
- Leveling surveys in southern California 212
- Surface evidence of fault activity in California 208-209
- The Yolla Bolly triple junction revisited 70
- Valley-margin faults of the western San Joaquin Valley 71
- faults*: Origin of folding of Tertiary low-angle fault surfaces in southeastern California and western Arizona 66
- neotectonics*: Deformation of the southern California uplift and the Colorado River delta 212
- Late Quaternary tilting in the northeastern San Joaquin Valley, California 71
- Quaternary deformation of the Sacramento Valley and northern Sierra 222
- Uplift of the San Bernardino Mountains, California 179-180
- tectonics*: Franciscan melange in central northern California 70
- Paleomagnetic evidence for structural rotation of the Klamath Mountains, California 131
- Permian and Triassic tectonic events in northern California and adjacent Nevada 63
- Structures in the offshore Eel River basin 67-68
- Synthesis and analysis of accreted terranes in the Sierra Nevada 68
- California—tectonophysics**
- plate tectonics*: The Yolla Bolly triple junction revisited 70
- California—volcanology**
- Mount Shasta*: Gravity monitoring, Mount Shasta and Lassen Peak, California 216
- research*: Seismic monitoring, Oregon and California volcanoes 216
- Cambrian** *see also under stratigraphy under Alaska; Virginia*
- Cambrian—stratigraphy**
- biostratigraphy*: Cambrian mollusk studies 182-183
- Canada** *see also Alberta; Appalachians; Atlantic Coastal Plain; British Columbia; Great Lakes; Great Lakes region; Great Plains; Rocky Mountains*
- Canada—engineering geology**
- waste disposal*: Canada 281
- Canada—hydrogeology**
- hydrology*: International commissions 279
- carbon—geochemistry**
- surface water*: Carbon transport from forested wetlands in a large Florida river basin 190
- uranium ores*: Uranium, carbon, and sulfur in roll-type uranium deposits in Wyoming 43
- carbon— isotopes**
- C-13/C-12*: Atmospheric carbon dioxide 150
- Calculations of global rate of burial of Cretaceous organic carbon and oceanic stable carbon as an aid to source-rock studies 31
- Comparative organic geochemistry of Middle Pennsylvanian shale and coal 29
- Geochemistry of oils from Pennsylvanian and Lower Permian Minnelusa Formation, Powder River Basin 25
- Mexico 284-285
- Mineralogy and stable isotope geochemistry of hydrothermally altered rocks from the East Pacific Rise and the Mid-Atlantic Ridge 149
- Origin of natural gases in San Juan basin 26
- Stable isotope systematics of copper-silver occurrences in the Belt Supergroup 148-149
- The origin of carbonate minerals in the Upper Freeport bed 22
- carbonates** *see under minerals*
- Carboniferous** *see also under stratigraphy under Alaska*
- Caribbean region** *see also the individual countries*
- Caribbean region—economic geology**
- coal*: Coal occurrences of North America and adjacent areas 15
- Caribbean region—stratigraphy**
- Tertiary*: Caribbean tectonostratigraphic terranes 115
- Caribbean region—tectonophysics**
- plate tectonics*: Caribbean tectonostratigraphic terranes 115
- Carpathians** *see also the individual countries*
- cartography** *see under maps*
- cement materials** *see construction materials under economic geology under North Carolina; South Carolina*
- Cenozoic** *see also under stratigraphy under Alaska; Atlantic Coastal Plain; California; Pacific Ocean*
- Cenozoic—stratigraphy**
- biostratigraphy*: Mesozoic and Cenozoic studies 177-180
- Central America** *see also Costa Rica; El Salvador; Nicaragua*
- Central America—economic geology**
- coal*: Coal occurrences of North America and adjacent areas 15
- chain silicates** *see under minerals*
- changes of level** *see also under stratigraphy under Atlantic Coastal Plain*
- chemical analysis** *see also spectroscopy*
- chemical analysis—methods**
- applications*: Analytical chemistry 198
- Analytical methods 198
- electron diffraction analysis*: Characterization of mineral precipitates by electron diffraction 139
- Electron-diffraction patterns of manganese oxides 138
- China—economic geology**
- petroleum*: China 281-282
- China—geophysical surveys**
- remote sensing*: Using principal components analysis to monitor arid land change 259
- China—petrology**
- meteorites*: The paradox of aqueous inclusions in a chondritic meteorite from Jilin, China 143
- chromite ores** *see also under economic geology under Montana*
- chromite ores—resources**
- ultramafics*: Low-grade chromite resources 1-2
- clastic rocks** *see under sedimentary rocks*
- clastic sediments** *see under sediments*
- clay** *see under composition under sediments*
- clay mineralogy—areal studies**
- Atlantic Coastal Plain*: Studies of depth of weathering on Atlantic Coastal Plain formations 50
- Colorado*: Mine studies, Lake City, Colorado 9-10
- Sedimentologic and diagenetic history of reservoirs in Niobrara Formation, Denver basin 25-26

- Great Plains*: Effect of clay on gas production data from Gammon Shale, Williston basin 25
- clays** *see also under economic geology under United States*
- climate, ancient** *see paleoclimatology*
- coal** *see also under economic geology under Alabama; automatic data processing; Caribbean region; Central America; Colorado; Costa Rica; Eastern U.S.; Florida; Great Britain; Greenland; Iceland; Kentucky; Montana; New Mexico; North America; North Carolina; North Dakota; Poland; United States; Utah; Virginia; Western U.S.; Wyoming; see also under organic residues under sedimentary rocks*
- coal—geochemistry**
- authigenic minerals*: Authigenic quartz in coal 22
- coalification*: Solid-state - ¹³C nuclear resonance studies of coalified logs 22
- experimental studies*: Coal geochemistry 21-24
- Mossbauer spectroscopy*: Use of Mossbauer spectroscopy to identify iron-sulfide minerals in coal 23-24
- coal—resources**
- development*: Hydrologic aspects of coal and mineral-resource development 223-229
- exploration*: Coal resources 15
- Coelenterata** *see also corals*
- Colorado—economic geology**
- coal*: Coal correlation in the Carbonate quadrangle, Colorado 17
- copper ores*: Copper and uranium in sediments shed from the ancestral Rocky Mountains 8
- gold ores*: Gold veins of the Granite District, Chaffee and Lake Counties, Colorado 7-8
- Mine studies, Lake City, Colorado 9-10
- mineral resources*: Ore genesis processes at Gilman-Leadville 7
- natural gas*: Origin of natural gases in San Juan basin 26
- petroleum*: Sedimentologic and diagenetic history of reservoirs in Niobrara Formation, Denver basin 25-26
- silver ores*: Mine studies, Lake City, Colorado 9-10
- uranium ores*: Copper and uranium in sediments shed from the ancestral Rocky Mountains 8
- Fossil Ridge, Colorado, uranium studies 41
- Mine studies, Lake City, Colorado 9-10
- Oligocene volcanic rock—a source of epigenetic uranium in central Colorado 35-36
- Ore emplacement in the Schwartzwalder mine, Jefferson County, Colorado 35
- Shifting margin of the Cretaceous sea in the San Juan basin 41
- Silver Plume Granite—a possible source of uranium, Tallahassee Creek deposits 37
- Studies of the Schwartzwalder mine, Jefferson County, Colorado 35
- The Middle Jurassic vanadium-uranium belt in western Colorado 40-41
- Uranium in granites, southwest Colorado 34
- vanadium ores*: The Middle Jurassic vanadium-uranium belt in western Colorado 40-41
- Colorado—engineering geology**
- waste disposal*: Geochemical characterization methods for potential radioactive-waste repository sites 233
- Colorado—environmental geology**
- geologic hazards*: Flood hydrology of foothill streams in Colorado 236
- pollution*: Toxicity of leachate from spent oil shale on a blue-green alga 224
- reclamation*: Composition of saltbush grown on oil-shale reclamation test plots, Colorado 198
- waste disposal*: Geochemical variability of soils and plants in the Piceance Basin, Colorado 199
- Colorado—geochemistry**
- isotopes*: Isotopic composition of uranium and thorium in crystalline rocks 148
- properties*: Composition of saltbush grown on oil-shale reclamation test plots, Colorado 198
- thorium*: Reversal of normal role of thorium in fractional crystallization 145-146
- Colorado—geomorphology**
- landform description*: DEM editing using a polygon scan-conversion process 292-293
- Colorado—geophysical surveys**
- magnetic surveys*: Geomagnetic observatories 132
- radioactivity surveys*: Interpretation of aerial radiometric data for Lake City caldera 135-136
- remote sensing*: Contracted satellite data relay study 264
- Improved lithologic separation and data base application 255
- Interpretation of aerial radiometric data for Lake City caldera 135-136
- Tectonic implication of lineaments in the northern Paradox Basin, Utah and Colorado 261-262
- Colorado—hydrogeology**
- ground water*: Colorado 93-94
- Elevated nitrate concentrations in the Widefield aquifer south of Colorado Springs, Colorado 187
- Ground water in Raton basin, Las Animas County 93-94
- hydrology*: Evaluation of selected one-dimensional stream water-quality models with field data 188
- Hydraulic geometry of stream channels in the Piceance basin area 175
- Preliminary analysis of historical streamflow and water-quality records for the San Juan River basin, New Mexico and Colorado 174
- Sensitivity to acidification of Flat Tops Wilderness Area lakes 192
- Streamflow changes in Platte River basin 174
- Toxicity of leachate from spent oil shale on a blue-green alga 224
- Colorado—soils**
- geochemistry*: Geochemical variability of soils and plants in the Piceance Basin, Colorado 199
- Colorado—stratigraphy**
- Cretaceous*: Coal correlation in the Carbonate quadrangle, Colorado 17
- Shifting margin of the Cretaceous sea in the San Juan basin 41
- Precambrian*: Precambrian rift filling beneath Colorado plains 57
- Tertiary*: Relation of Bishop Conglomerate to Browns Park Formation in eastern Uinta Mountains, Colorado and Utah 57-58
- Colorado—structural geology**
- faults*: Diffusion-equation model and degraded fault scarps, Colorado 209
- fractures*: Mechanics of joints in the Piceance Creek basin, Colorado 60-61
- tectonics*: Tectonic implication of lineaments in the northern Paradox Basin, Utah and Colorado 261-262
- Colorado Plateau** *see also the individual states*
- Colorado Plateau—geophysical surveys**
- remote sensing*: Analysis of Landsat linear feature data of southern Colorado Plateau 259
- Colorado Plateau—structural geology**
- tectonics*: Analysis of Landsat linear feature data of southern Colorado Plateau 259
- Columbia Plateau** *see also the individual states*
- conglomerate** *see also under clastic rocks under sedimentary rocks*
- congresses** *see symposia*
- Connecticut—economic geology**
- heavy mineral deposits*: Hydraulic concentration of heavy minerals in Pleistocene glacial lake delta sands 1
- Connecticut—environmental geology**
- land use*: Level III land use and land cover mapping in Connecticut 300
- maps*: Level III land use and land cover mapping in Connecticut 300
- Connecticut—geomorphology**
- glacial geology*: Glacial deposits of the Shetucket River basin, eastern Connecticut 47
- conodonts—biostratigraphy**
- Cambrian*: Middle Cambrian fossils in central Brooks Range, Alaska 180-181
- Devonian*: Age of vanadiferous shales in central Nevada 63
- Paleozoic*: Early Paleozoic Basin margin, Antelope Range, Nevada 181

D

- Permian*: New fossils from Taku terrane suggest permian metallogenic province 79-80
- conodonts—paleoecology**
Devonian: Conodont study as an aid to petroleum exploration of Upper Devonian Rocks 31
- conservation** *see also under* environmental geology *under* United States
- construction materials** *see also under* economic geology *under* North Carolina; South Carolina
- continental shelf** *see also under* oceanography *under* Atlantic Ocean; California; Eastern U.S.; Florida; Gulf of Mexico; North Carolina; Rhode Island; United States
- continental slope** *see also under* oceanography *under* Atlantic Ocean
- continental slope—economic geology**
petroleum: Sea-floor conditions and processes 115-119
- copper ores** *see also under* economic geology *under* Alaska; Arizona; automatic data processing; Colorado; Montana; Utah; Washington
- corals—biostratigraphy**
Mississippian: Mississippian coral zonation, western North America 183
- Costa Rica—economic geology**
coal: Costa Rica 282
- Cretaceous** *see also under* geochronology *under* Alaska; Nevada; *see also under* stratigraphy *under* Atlantic Coastal Plain; California; Colorado; Montana; New Mexico; Oregon; South Dakota; Utah; Virginia; Wyoming
- cross-bedding** *see under* planar bedding structures *under* sedimentary structures
- crust** *see also under* tectonophysics *under* Arizona; Hawaii; United States; Wyoming
- crust—evolution**
oceanic crust: Constraints on yield strength in the oceanic lithosphere 136
water: Role of water in crustal deformation 133
- crust—geochemistry**
isotopes: Evolution of continental crust as inferred from a hafnium isotope study 147
- crystal chemistry** *see also* minerals
- crystal chemistry—chain silicates**
bustamite: Stability of ferrobustamite 138-139
- crystal chemistry—framework silicates, silica minerals**
quartz: Silica solubilities in hydrothermal salt solutions 137
- crystal chemistry—oxides**
magnetite: Silicon-bearing magnetite 139
manganese oxides: Electron-diffraction patterns of manganese oxides 138
- crystal growth** *see also* crystal chemistry; minerals
- crystal structure** *see also* crystal chemistry; minerals
- crystallography** *see also* mineralogy

- dams** *see also under* engineering geology *under* Illinois
- dams—design**
floods: Effects of a flood-retarding dam 174
- deformation** *see also* geophysics; structural analysis
- deformation—theoretical studies**
yield strength: Constraints on yield strength in the oceanic lithosphere 136
- Delaware—hydrogeology**
ground water: Delaware 84
— Depth of supply well and efficiency of heat pumps 170
— Unconfined aquifer mapped in southeastern Sussex County 84
- deposition** *see under* sedimentation
- deposition of ores** *see* mineral deposits, genesis
- deuterium** *see also* hydrogen; tritium
- deuterium—geochemistry**
brines: Continental evaporites in Owens Lake, California 13
ground water: $\delta^{18}\text{O}$ and δD anomalies as earthquake precursors 150
thermal waters: Stable isotope interpretation of the Lassen geothermal system 154-155
- Devonian** *see also under* stratigraphy *under* Alaska
- diabase** *see under* igneous rocks
- diagenesis** *see also* sedimentation
- diagenesis—materials**
chalk: Sedimentologic and diagenetic history of reservoirs in Niobrara Formation, Denver basin 25-26
organic materials: The origin of primary pyrite in coal by bacterial diagenesis of organic sulfur 21-22
- diatoms** *see under* algae
- differentiation** *see under* magmas
- diorites** *see under* igneous rocks
- District of Columbia—hydrogeology**
hydrology: Potomac River Reservoir release routing 170-171
- domes** *see under* style *under* folds

E

- Earth—magnetic field**
solar cycle: Geomagnetic models and the solar cycle effect 132
- earthquakes** *see under* geologic hazards; seismology; *see also* engineering geology; seismology; *see also under* engineering geology *under* automatic data processing; California; Great Lakes; Nicaragua; South Carolina; United States; Washington; *see also under* seismology *under* Alaska; Argentina; automatic data processing; California; El Salvador; Hawaii; Japan; Mexico; New Mexico; Oregon; Peru; United States; Virginia; Washington
- earthquakes—causes**
deformation: Geodetic appraisal of earthquake potential 212
faults: Geologic appraisal of earthquake potential and fault activity 208-211
ground motion: Rupture processes of earthquakes 204-205
observations: National Earthquake Information Service 202
- earthquakes—effects**
experimental studies: Post-earthquake investigations 214-215
ground motion: Earthquake hazards studies 207-215
— Engineering seismology and ground motion research 212-213
— New computer codes for ground motion studies 212-213
seismic risk: Hazards and risks in urban regions 213-214
- earthquakes—observations**
causes: Earthquake studies 200-215
- earthquakes—prediction**
experimental studies: Earthquake mechanics and prediction studies 204-207
— Seismologic appraisal of earthquake potential 207-208
publications: Earthquake Early Alerting Service (EEAS) 202
- Eastern Hemisphere** *see also* Africa; Antarctica; Asia; Atlantic Ocean; USSR
- Eastern U.S.** *see also* Connecticut; Delaware; District of Columbia; Florida; Georgia; Maine; Maryland; Massachusetts; New England; New Hampshire; New Jersey; New York; North Carolina; Pennsylvania; Rhode Island; South Carolina; Vermont; Virginia; West Virginia
- Eastern U.S.—economic geology**
coal: Eastern coal 15
fuel resources: Eastern Overthrust Belt 30-31
natural gas: Regional metamorphism of organic matter in Devonian shale of Appalachian basin 30
petroleum: Atlantic continental shelf 30-31
— Evolution of humic substances in mid-Atlantic OCS and slope sediments 31
— Petroleum geology of the U. S. Mid-Atlantic Slope 111
— Thermal maturation study in Georges Bank basin, North Atlantic margin 30-31
- Eastern U.S.—engineering geology**
land subsidence: Active subsidence in carbonate terranes in the Eastern United States 240
— Inventory of active carbonate karst subsidence sites in Eastern U.S. 239
- Eastern U.S.—hydrogeology**
ground water: Potentiometric surface of the Tertiary limestone aquifer system, Southeastern United States 90
hydrology: Hydrology of Federal coal lands in eastern National Forest areas 125-126

- Multistate studies 91
 - Water quality of the Susquehanna, Potomac, and James Rivers 185
 - Eastern U.S.—oceanography**
 - continental shelf*: Atlantic continental shelf 30-31
 - Eastern U.S.—stratigraphy**
 - Mississippian*: Upper Mississippian invertebrate biostratigraphy, eastern Appalachians 182
 - ecology** *see also under* environmental geology *under* Florida
 - ecology—analysis**
 - forests*: Computer model of wetlands forest 183
 - ecology—environment**
 - estuarine environment*: The temporal scale of disturbance in estuarine benthic communities 122
 - ecology—Plantae**
 - coastal environment*: Patterns of vegetation in the Loxahatchee River estuary, Florida 183
 - Egypt—areal geology**
 - maps*: Egypt 282
 - Egypt—geomorphology**
 - erosion features*: Probable fluvial sources for dune sand on Mars 246
 - Egypt—geophysical surveys**
 - magnetic surveys*: Egypt 282
 - El Salvador—seismology**
 - earthquakes*: El Salvador seismic gap 206
 - electrical logging** *see under* well-logging
 - electrical surveys** *see under* geophysical surveys *under* Arizona; mineral exploration; Thailand; Utah
 - electromagnetic methods** *see under* geophysical methods
 - electron microscopy** *see also* chemical analysis; spectroscopy
 - emission spectroscopy** *see under* methods *under* spectroscopy
 - energy sources** *see also under* economic geology *under* Bangladesh; Philippine Islands
 - energy sources—exploration**
 - evaluation*: Mineral-fuel investigations 15-24
 - global*: Tropical resource studies 272-273
 - engineering geology** *see also* deformation; environmental geology; geodesy; ground water; impact statements; land subsidence; rock mechanics
 - engineering geology—field studies**
 - nuclear explosions*: Geology related to national security 231-232
 - engineering geology—methods**
 - cartography*: Engineering geologic mapping 218-219
 - Engineering geologic mapping in New York City 219
 - field studies*: Engineering geology 218-219
 - environmental geology** *see also* engineering geology; impact statements
 - environmental geology—experimental studies**
 - chemical analysis*: Environmental geochemistry 198-200
 - Eocene** *see also under* stratigraphy *under* Atlantic Coastal Plain; California; Mississippi; Rocky Mountains; Washington; Wyoming
 - erosion features** *see under* geomorphology
 - eruptive rocks** *see* igneous rocks
 - Europe** *see also* France; Great Britain; Iceland; Poland; Portugal; Sweden; United Kingdom
 - experimental studies** *see under* aquifers *under* ground water; *see under* changes *under* paleoclimatology; *see under* earthquakes *under* seismology; *see under* effects *under* environmental geology; fractures; geochemistry; geophysics; hydrogeology; hydrology; marine geology; mineralogy; paleomagnetism; paleontology; petrology; sedimentary petrology; *see under* geochemistry *under* coal; Western U.S.; *see under* methods *under* geochronology; *see under* plutonic rocks *under* igneous rocks; *see under* prediction *under* earthquakes; *see under* recharge *under* ground water; *see under* resources *under* fuel resources; geothermal energy; *see under* rivers and streams *under* hydrology; *see under* seismicity *under* seismology; *see under* tracers *under* isotopes; *see under* volcanic rocks *under* igneous rocks
 - explosions** *see also under* engineering geology *under* Nevada; *see also under* seismology *under* USSR
 - explosions—nuclear explosions**
 - effects*: Geology related to national security 231-232
 - S-waves*: Shear-wave velocity and changes in tuff due to shock loading 231
- F**
- Far East** *see also* the individual countries
 - faulting** *see* faults
 - faults** *see also* folds
 - faults—displacements**
 - normal faults*: Surface evidence of fault activity in California 208-209
 - reverse faults*: Earthquake, new reverse fault, and crustal unloading near Lompoc, California 214
 - Structures in the offshore Eel River basin 67-68
 - The Yolla Bolly triple junction revisited 70
 - Valley-margin faults of the western San Joaquin Valley 71
 - soils*: Soils chronology and fault history 210-211
 - strike-slip faults*: Inferred pre-Oligocene strike-slip fault zone in central Nevada 64
 - Mammoth Lake, California, earthquake studies 214-215
 - New evidence for strike-slip displacement on the Kaltag fault 78
 - thrust faults*: Complex thrusting in Snake River Range, Idaho 60
 - Geometry of a thrust fault in northern California 67
 - Libby thrust belt, northwestern Montana 60
 - Regional relations of Wah Wah-Frisco thrust fault in western Utah 64
 - Structural analysis; Valley and Appalachian Plateau, Pennsylvania 262-263
 - Thrust faults in the Highland Mountains, Montana 61
 - faults—distribution**
 - deformation*: The Pasayten fault, a major tectonic boundary in north-central Washington 75
 - dikes*: Evaluation of faulting near Monticello Reservoir, South California 211
 - displacements*: Young faulting, southwestern Wyoming and adjacent Utah 61-62
 - fault scarps*: Diffusion-equation model and degraded fault scarps, Colorado 209
 - fault zones*: Surface faulting in the Sonora, Mexico, earthquake of 1887 209
 - geodesy*: Leveling surveys in southern California 212
 - glacial pavement*: Analysis of faulted glacial pavement in southeastern New York 48
 - movement*: Recurrent movements on faults north of Boston 47
 - seismicity*: Fault definition and seismicity in the Ramapo seismic zone 49
 - Faults in Pleistocene sediments at trace of Ramapo fault 49
 - faults—effects**
 - gouge*: Experimental studies of fault mechanics 204
 - shear zones*: Polydeformed rocks in the Lowndesville shear zone, South Carolina and Georgia 52
 - slickensides*: Direction of post-Oligocene klippen movement, Markagunt Plateau, Utah 62
 - faults—orientation**
 - strike faults*: Tectonic implication of lineaments in the northern Paradox Basin, Utah and Colorado 261-262
 - faults—systems**
 - block structures*: Amount of offset of Salinan block remains equivocal 67
 - fault zones*: Juxtaposed terranes in northern New Hampshire: possible extension of Brevard zone 48
 - Quaternary faulting along the La Jencia fault, central New Mexico 210
 - grabens*: Early Tertiary crustal extension in northeastern Washington 71
 - Reserve graben, southwestern New Mexico and eastern Arizona 61
 - fission-track dating** *see under* geochronology
 - floods** *see under* geologic hazards
 - Florida—economic geology**
 - coal*: The origin of primary pyrite in coal by bacterial diagenesis of organic sulfur 21-22
 - fuel resources*: Gulf of Mexico and Florida 29-30

- peat*: Peat from Everglades: a study of the origin of coal and natural gas 21
 — Peat petrology and aspects of coal formation in the Everglades, Florida 20
petroleum: Petroleum source rocks found in South Florida basin 29-30
- Florida—engineering geology**
land subsidence: Sinkholes in west-central Florida 240
- Florida—environmental geology**
ecology: Patterns of vegetation in the Loxahatchee River estuary, Florida 183
waste disposal: Subsurface injection of highly treated sewage, St. Petersburg, Florida 169
- Florida—hydrogeology**
ground water: Florida 91
 — Hydrogeologic framework defined for the Sarasota-Port Charlotte area 91
 — Model studies of surface storage and recovery of freshwater, southern Florida 168-169
 — Modeling of well-field areas near Tampa, Florida 167
 — Saltwater movement in the coastal areas 123-124
 — Subsurface injection of highly treated sewage, St. Petersburg, Florida 169
 — Time-of-water sampling in tidal-affected chloride monitor well in west-central Florida 124
 — Time-of-water sampling in tidal-affected chloride monitor well in west-central Florida 170
hydrology: Carbon transport from forested wetlands in a large Florida river basin 190
 — Microcomputer program for time-of-travel and dispersion characteristics of streams in Florida 188
 — Nutrient and detritus transport in the Apalachicola River, Florida 190
- Florida—oceanography**
continental shelf: Destin Dome and the west Florida Shelf 111
 — Surface structures of the southwest Florida shelf 114-115
- Florida—paleontology**
bryozoans: Growth of estuarine-fouling organisms in Loxahatchee River estuary, Florida 124
- fluid inclusions** *see also* inclusions
- fluid inclusions—composition**
minerals: The paradox of aqueous inclusions in a chondritic meteorite from Jilin, China 143
- fluid inclusions—geochemistry**
analysis: Diurnal periodicity in NaCl precipitation in Permian salt basins 139
migration: Migration rates of brine inclusions in single crystals of NaCl 138
porphyry copper: Studies of the root zone of the Ajo porphyry copper system 6
uranium ores: Uraniferous opal, Virgin Valley, Nevada: conditions of formation 43
- fluorine—geochemistry**
granites: Baid al Jimalah tungsten deposit 287-288
- fluvial features** *see under* geomorphology
- folding** *see* folds
- folds** *see also* faults; foliation
- folds—mechanics**
denudation: Origin of folding of Tertiary low-angle fault surfaces in southeastern California and western Arizona 66
- folds—style**
domes: Newly recognized gneiss dome, northeastern Wisconsin 53-54
monoclines: Monocline southwest of Cedar Creek anticline, Montana 61
- foliation** *see also* folds; structural analysis
- foliation—style**
lineation: Deformation of Precambrian rocks along Jemez zone, New Mexico 60
- foraminifera—Fusulinidae**
Pennsylvanian: Fusulinids of the type Atokan Provincial Series, southern Oklahoma 181
- foraminifers** *see also* foraminifera
- fossils** *see* appropriate fossil group
- foundations** *see also* rock mechanics; *see also under* engineering geology *under* United States
- fractures—experimental studies**
cracks: Pressured fractures in hot rock 159
- fractures—style**
joints: Joints and ground-water flow in oil shale in Wyoming 229
 — Mechanics of joints in the Piceance Creek basin, Colorado 60-61
- France—economic geology**
uranium ores: Landsat studies of uranium settings, Australia and France 260
- France—geophysical surveys**
remote sensing: Landsat studies of uranium settings, Australia and France 260
- fuel resources** *see also under* economic geology *under* Alaska; California; Eastern U.S.; Florida; Great Plains; Gulf of Mexico; Rocky Mountains; United States; Wyoming
- fuel resources—resources**
distribution: Probabilistic and statistical resource appraisal methodology 32-33
experimental studies: Resource studies 32-33
exploration: Oil and gas resources 24-32
global: World oil and gas resources of small fields and unconventional deposits 32
- G**
- gas inclusions** *see* fluid inclusions
- genesis of ore deposits** *see* mineral deposits, genesis
- geochemistry—experimental studies**
chemical composition: Chemical composition of overburden rocks and sampling needs for reclamation of surface coal mines 200
- environmental geology*: Environmental geochemistry 198-200
 USGS: Experimental and theoretical geochemistry 136-138
 — Geochemistry, Mineralogy, and Petrology 136-152
water: Geochemistry of water and sediments 146-147
- geochemistry—processes**
absorption: Three-dimensional fluorescent spectra of humic acids 136-137
denitrification: Bacterial denitrification in small streams in California 193-194
diffusion: Temperature dependence of the gas-film coefficient 147
dilution: Liquid-waste disposal at the Idaho National Engineering Laboratory 233-234
ionization: Determination of chloride and bromide water 147
oxidation: Effects of chemical weathering on mine drainage in southwestern Virginia 229
- geochemistry—properties**
cation exchange capacity: Geochemistry and geohydrology of the Decker and Big Sky coal-mining areas, southeastern Montana 227
pH: Geochemistry of vegetation, soils, and spoil materials, Jarvis Creek, Alaska 198-199
 — Molybdenosis associated with uranium-bearing lignites in South Dakota 200
salinity: Composition of saltbush grown on oil-shale reclamation test plots, Colorado 198
 — Diurnal periodicity in NaCl precipitation in Permian salt basins 139
thermodynamic properties: National Center for the Thermodynamic Data of Minerals 137-138
 — Thermodynamic properties of minerals 137
- geochemistry—surveys**
Colorado: Geochemical characterization methods for potential radioactive-waste repository sites 233
Gulf of Mexico: Physical and chemical properties of fine-grained sediments 146-147
Wyoming: Changes in trace-element composition of sagebrush close to Bridger Powerplant, Wyoming 198
- geochronology** *see also* absolute age
- geochronology—fission-track dating**
clinker: Fission-track ages and structure in clinker 59
zircon: Volcanic ash on Missouri River - Yellowstone River drainage divide, Montana 60
- geochronology—methods**
experimental studies: Advances in geochronometry 150-152
- geochronology—racemization**
amino acids: Amino-acid dating of fossil shells in the Atlantic Coastal Plain 53

- geochronology—tephrochronology**
volcanic ash: Progress in correlation and age determination of late Cenozoic tephra 68-69
- geochronology—thermoluminescence**
sanidine: Thermoluminescence dating of silicic volcanic rocks 151
- geodesy—geodetic coordinates**
deformation: Geodetic appraisal of earthquake potential 212
- geodesy—surveys**
California: Correlated changes in gravity, elevation and strain 206
 — Geodetic strain near Mammoth Lakes, California 206
 — Leveling surveys in southern California 212
- geodetic coordinates** *see under* geodesy
- geologic hazards** *see also* land subsidence; *see also under* engineering geology *under* Appalachians; automatic data processing; California; Great Basin; Louisiana; Maryland; Mississippi; South Carolina; Tennessee; United States; Washington; Wyoming; *see also under* environmental geology *under* Alabama; Colorado; Montana; Nevada; Puerto Rico; Virginia
- geologic hazards—causes**
research: Reactor Hazards Research Program 222-223
seismic risk: Hazards and risks in urban regions 213-214
- geologic hazards—earthquakes**
effects: Earthquake hazards studies 207-215
- geologic hazards—floods**
observations: Floods 235-236
- geologic hazards—observations**
hydrology: Geology and hydrology applied to natural hazards 201-241
- geologic hazards—volcanoes**
damage: Volcanic hazards 215-218
field studies: Volcanic hazards assessment studies 216-218
monitoring: Volcano monitoring 215-216
- geologic time** *see* absolute age; geochronology
- geology—practice**
education: Participant training 272
international cooperation: Yugoslavia 274
- geology—research**
economic agreements: Scientific cooperation and research 273-276
 — Special Foreign Currency Program (SFCP) 273-274
 — Technical assistance 271-272
global: International activities in the earth sciences 267-291
international cooperation: Other 275-276
- geomorphology** *see also* glacial geology
- geomorphology—environment**
arid environment: Using principal components analysis to monitor arid land change 259
- geomorphology—erosion features**
inselbergs: Probable fluvial sources for dune sand on Mars 246
- geomorphology—fluvial features**
channel geometry: Morphologic changes in Platte River channels 161
drainage basins: Mount St. Helens mapping 296
 — Times of concentration and storage coefficients for Illinois streams 175
floodplains: Quaternary floodplain deposits of the lower San Joaquin River 71
rivers: Chemical characteristics of selected rivers, western Washington, 1961-1980 72
- terraces*: Effects of Pleistocene glaciation on development of New River terraces, Virginia 50
 — Late Quaternary tilting in the northeastern San Joaquin Valley, California 71
 — Scattered high-level terrace remnants along Nowood Creek, Bighorn basin, Wyoming 59-60
- geomorphology—impact features**
craters: Cratering rate of the Galilean satellites 243
 — Lunar crater studies 248
 — Measurement of cratering 247
- geomorphology—lacustrine features**
lakes: Australia 280
- geomorphology—landform description**
automatic data processing: DEM editing using a polygon scan-conversion process 292-293
cartography: Planimetric mapping of the planets 247-248
colluvium: Late Holocene geomorphic features near Cedar City, Utah 211
description: Map projections 295
scarps: The basal scarp of Olympus Mons 244-245
terraces: Synthesis and analysis of accreted terranes in the Sierra Nevada 68
valleys: Martian valleys and channels 244
- geomorphology—methods**
remote sensing: Accuracy assessment of Landsat-derived Arizona wildland vegetation map 257
 — Estimating rangeland plant cover proportions with large-scale color-infrared aerial photographs 256
 — Land cover and terrain mapping for the Bristol Bay subregion using Landsat MSS data and digital terrain data 258
 — Land cover and terrain mapping for the Kenai National Wildlife Refuge using Landsat MSS data 258
 — Land cover mapping with merged Landsat RBV and MSS stereoscopic images 258
 — Mapping forest fuels and predicting wildland fire behavior 257
 — Using aircraft and satellite acquired data to estimate food available to refuge waterfowl 256-257
 — Utility of a digital data base for improving Landsat classification results and managing a forested wetland 257
- geomorphology—shore features**
coastal dunes: Pre-Flandrian sand sheet within Morro Bay, California 121
foreshore accretion: Rapidly migrating sand ridges and pulses of foreshore accretion 121
- geomorphology—solution features**
karst: China 281-282
 — Inventory of active carbonate karst subsidence sites in Eastern U.S. 239
sinkholes: Active subsidence in carbonate terranes in the Eastern United States 240
 — Sinkholes in west-central Florida 240
- geomorphology—volcanic features**
stratovolcanoes: Morphometry of the volcanoes 247
- geophysical methods** *see under* automatic data processing
- geophysical methods—electromagnetic methods**
interpretation: Electromagnetic modeling and inversion of controlled source data 135
 — Time-domain electromagnetic sounding 134-135
- geophysical methods—gravity methods**
instruments: A new slim-hole gravity meter 136
- geophysical methods—magnetic methods**
magnetic anomalies: Effects of draping on aeromagnetic anomalies 133
- geophysical methods—methods**
instruments: New borehole geophysical tools for uranium exploration 136
radar methods: Radar studies 304-307
- geophysical surveys** *see under* Africa; Alaska; Antarctica; Appalachians; Arizona; Atlantic Coastal Plain; Atlantic Ocean; Australia; automatic data processing; Bangladesh; Bering Sea; California; China; Colorado; Colorado Plateau; Egypt; France; Great Britain; Great Lakes; Great Plains; Gulf of Mexico; Hawaii; Jupiter; Maine; Mars; Michigan; mineral exploration; Montana; Nebraska; Nevada; New England; New Hampshire; New Mexico; North Carolina; North Dakota; Oregon; Pacific Coast; Pacific Ocean; Pennsylvania; Persian Gulf; Rhode Island; Saturn; Saudi Arabia; South America; South Dakota; Texas; Thailand; Tunisia; United States; USSR; Utah; Venus; Vermont; Virginia; Washington; Wyoming; Yemen; *see* acoustical surveys *under* geophysical surveys *under* California; *see* electrical surveys *under* geophysical surveys *under* Arizona; mineral exploration; Thailand; Utah; *see* gravity surveys *under* geophysical surveys *under* Bering Sea; Maine; Nevada; New Hampshire; North Carolina; Saudi Arabia; United States; USSR; Vermont; *see* infrared surveys *under* geophysical surveys *under* Pacific Coast; Washington; *see* magnetic surveys *under* geophysical surveys *under* Appalachians; Atlantic Coastal Plain; Atlantic Ocean; automatic data processing; California; Colorado; Egypt; Michigan; Neva-

- da; North Carolina; North Dakota; Pacific Ocean; United States; *see* magnetotelluric surveys *under* geophysical surveys *under* Arizona; California; Nevada; Oregon; Utah; *see* radioactivity surveys *under* geophysical surveys *under* Colorado; *see* seismic surveys *under* geophysical surveys *under* Alaska; Antarctica; Atlantic Ocean; Bangladesh; California; Great Britain; Great Lakes; Gulf of Mexico; Hawaii; North Carolina; Oregon; Rhode Island; Saudi Arabia; United States; Washington; Wyoming
- geophysics** *see also* deformation; engineering geology
- geophysics—experimental studies**
applications: Applied geophysics 133-136
paleomagnetism: Rock magnetism 130-132
 USGS: Geophysics 130-133
- Georgia—hydrogeology**
ground water: Automated conversion of geocoded water-withdrawal information for input to a two-dimensional ground-water model 168
 — Geochemistry of water from Cretaceous aquifers in the Southeastern United States; Mississippi, Alabama, Georgia, and South Carolina 146
 — Ground-water-resource-management model of the Savannah, Georgia, area 167-168
 — Numerical modeling of the geohydrology of the principal artesian aquifer, Dougherty Plain, Georgia 168
 — Potentiometric surfaces and ground-water withdrawals from aquifers in southern Georgia 91
hydrology: Applications of draft-storage diagrams for Georgia streams 176
 — Errors due to time-sampling bias for streamflow statistic in Georgia 172
 — Evaluation of selected one-dimensional stream water-quality models with field data 188
 — Geologic and hydrologic effects of Late Cretaceous and Cenozoic faulting of the Coastal Plain near the Savannah River, Georgia and South Carolina 90
 — Georgia 91
 — Variability of average annual rainfall and average annual runoff 91
- Georgia—petrology**
metamorphic rocks: Geology of the Piedmont between the Brevard and Towaliga fault zones, central Georgia 49
- Georgia—stratigraphy**
Mississippian: The Mississippian-Pennsylvanian boundary 15-16
Pennsylvanian: The Mississippian-Pennsylvanian boundary 15-16
- Georgia—structural geology**
faults: Polydeformed rocks in the Lowndesville shear zone, South Carolina and Georgia 52
- geotechnics** *see* engineering geology
- geothermal energy** *see also* economic geology *under* British Columbia; California; Idaho; Mexico; Minnesota; Nevada; Oregon; Thailand; United States; Washington; Western U.S.; Wyoming
- geothermal energy—production**
fractures: Pressured fractures in hot rock 159
- geothermal energy—resources**
experimental studies: Geothermal resources 45-46
geothermal systems: Geothermal systems 152-159
- geothermal gradient** *see under* heat flow
- glacial geology** *see also* geomorphology
- glacial geology—glacial features**
alluvial dams: Glacially induced alluvial dams for Tulare Lake, California 71
glacial lakes: Faults in Pleistocene sediments at trace of Ramapo fault 49
 — Glacial deposits of the Shetucket River basin, eastern Connecticut 47
 — Glacial Lake Passaic 163
 — Lake Bonneville revisited 163-164
glacial pavement: Analysis of faulted glacial pavement in southeastern New York 48
kames: High kames trace fractures in late Wisconsinan ice in southeastern Massachusetts 47
moraines: Late Wisconsinan stratigraphy along the terminal moraine, northern New Jersey 47
outwash: Giant involutions in the upper Wisconsin drift of Nantucket Island 119
 — Outwash terraces along the Cowlitz River 72
 — Radionuclide transport in glacial outwash, Wood River Junction, Rhode Island 235
terraces: Glacial studies in the Yukon-Tanana Upland 77
till: Evidence for a major pre-Wisconsinan glacial event in New England 119
- glacial geology—glaciation**
deglaciation: Pinedale deglaciation in the North Fork of the Flathead Valley, Montana 59
deserts: Desert conditions in northern Alaska during the last glaciation 76-77
terraces: Effects of Pleistocene glaciation on development of New River terraces, Virginia 50
- glacial lakes** *see under* glacial features *under* glacial geology
- glaciation** *see under* glacial geology
- gold ores** *see also* *under* economic geology *under* Alaska; Arizona; Colorado; Saudi Arabia
- grabens** *see under* systems *under* faults
- granites** *see under* igneous rocks
- granodiorites** *see under* igneous rocks
- gravel** *see also* *under* clastic sediments *under* sediments
- gravity methods** *see under* geophysical methods
- gravity surveys** *see under* geophysical surveys *under* Bering Sea; Maine; Nevada; New Hampshire; North Carolina; Saudi Arabia; United States; USSR; Vermont
- Great Basin** *see also* the individual states
- Great Basin—engineering geology**
geologic hazards: Appraisal of methods for delineating flood-hazard areas in the Great Basin 236
- Great Britain—economic geology**
coal: Geophysical study of shallow coals 291
- Great Britain—geophysical surveys**
seismic surveys: Geophysical study of shallow coals 291
- Great Lakes—engineering geology**
earthquakes: Applied geophysics 222-223
- Great Lakes—geophysical surveys**
seismic surveys: Applied geophysics 222-223
- Great Lakes region** *see also* the individual states and provinces
- Great Lakes region—structural geology**
tectonics: Lake Superior basin geology and tectonics 54
- Great Plains** *see also* the individual states and provinces
- Great Plains—areal geology**
regional: Rocky Mountains and the Great Plains 54-62
- Great Plains—economic geology**
fuel resources: Great Plains and Rocky Mountain basins 24-26
mineral resources: Mineral resources 62
natural gas: Diagenesis and gas generation in Gammon Shale, northern Great Plains 24-25
 — Effect of clay on gas production data from Gammon Shale, Williston basin 25
reclamation: Chemical composition of overburden rocks and sampling needs for reclamation of surface coal mines 200
- Great Plains—environmental geology**
land use: A comparative study of change and disorganization in energy development communities of the Great Plains 266
- Great Plains—geomorphology**
surficial geology: Surficial geology 59-60
- Great Plains—geophysical surveys**
maps: Mapping of irrigated cropland with Landsat digital data 303
- Great Plains—hydrogeology**
ground water: High Plains aquifer study 107
 — Hydrochemistry of the Lower Cretaceous aquifers of the northern Great Plains, Montana, Wyoming, North Dakota, and South Dakota 93
hydrology: Central Region 92-93
 — Multistate studies 93
- Great Plains—petrology**
igneous rocks: Igneous rocks 54-55
- Great Plains—stratigraphy**
Phanerozoic: Stratigraphy 55-59
Pleistocene: Distribution of pearlette family volcanic ash marker beds 56
- Great Plains—structural geology**
tectonics: Structural geology 60-62
 — Tectonics 62

- Greenland—economic geology**
coal: Coal occurrences of North America and adjacent areas 15
ground water *see also* hydrogeology; hydrology
ground water—aquifers
data: Surface-water, quality-of-water, and ground-water-level records 314
experimental studies: Miscellaneous studies 169-170
models: Aquifer-model studies 166-169
water wells: Solutions to problems of well-test analysis 169
ground water—geochemistry
chloride ion: Determination of chloride and bromide water 147
water quality: Chemical and biological quality of ground water 186-187
ground water—models
interpretation: Relation between surface water and ground water 190-192
water quality: Ground-water quality models and processes 189
ground water—pollution
site exploration: Ground-water pollution 237-239
ground water—recharge
experimental studies: Recharge studies 169
ground water—surveys
Alabama: Geochemistry of water from Cretaceous aquifers in the Southeastern United States; Mississippi, Alabama, Georgia, and South Carolina 146
— Southeastern Sand Aquifer Study 108
Arizona: Impact of ground-water pumpage for coal slurry, Navajo and Hopi Indian Reservations, Arizona 224
Arkansas: Arkansas 90
— Effects of 1980 drought on ground-water levels in the Mississippi alluvial plain 90
Atlantic Coastal Plain: Analysis of fresh and saline ground water in the New Jersey Coastal Plain and Continental Shelf 109
— Deep test well in Maryland 109
— Freshwater beneath the Carolina Continental Shelf 113-114
— Stressed flow system in the Tertiary limestone aquifer system 106
Azores: Portugal 285
California: Injection of treated wastewater for ground-water recharge in the Palo Alto, Baylands, California 169
— Leveling surveys in southern California 212
Canada: Canada 281
Colorado: Colorado 93-94
— Ground water in Raton basin, Las Animas County 93-94
Delaware: Delaware 84
— Depth of supply well and efficiency of heat pumps 170
— Unconfined aquifer mapped in southeastern Sussex County 84
Eastern U.S.: Potentiometric surface of the Tertiary limestone aquifer system, Southeastern United States 90
Florida: Florida 91
— Hydrogeologic framework defined for the Sarasota - Port Charlotte area 91
— Model studies of surface storage and recovery of freshwater, southern Florida 168-169
— Modeling of well-field areas near Tampa, Florida 167
— Subsurface injection of highly treated sewage, St. Petersburg, Florida 169
— Time-of-water sampling in tidal-affected chloride monitor well in west-central Florida 124
— Time-of-water sampling in tidal-affected chloride monitor well in west-central Florida 170
Georgia: Automated conversion of geocoded water-withdrawal information for input to a two-dimensional ground-water model 168
— Geochemistry of water from Cretaceous aquifers in the Southeastern United States; Mississippi, Alabama, Georgia, and South Carolina 146
— Ground-water-resource-management model of the Savannah, Georgia, area 167-168
— Numerical modeling of the geohydrology of the principal artesian aquifer, Dougherty Plain, Georgia 168
— Potentiometric surfaces and ground-water withdrawals from aquifers in southern Georgia 91
Great Plains: High Plains aquifer study 107
— Hydrochemistry of the Lower Cretaceous aquifers of the northern Great Plains, Montana, Wyoming, North Dakota, and South Dakota 93
Idaho: Ground-water conditions in the Michaud Flats area, Fort Hall Indian Reservation 97-98
— Ground-water-quality assessment, southern Elmore and northern Owyhee Counties 98
— Ground-water trends 98
— Idaho 97-98
— Irrigation water use on the Snake River Plain in southern Idaho 104
— Liquid-waste disposal at the Idaho National Engineering Laboratory 233-234
— Model of the regional aquifer system underlying the Snake River Plain in southern Idaho and eastern Oregon 166
— Sealed monitoring wells for a radioactive environment 234
Illinois: Aquifer studies at a proposed coal strip mine near Industry, Illinois 225
— Ground-water flow to strip-mined lake from low-level radioactive-waste-disposal site near Sheffield, Illinois 234
— Piezometers in deep test well in northeast Illinois 108
— Radionuclide movement at a radioactive-waste burial site in Illinois 235
Indiana: Ground-water availability in the outwash aquifer, Marion County 85
— Ground-water resources of a glacial-outwash aquifer in Johnson and Morgan Counties 84
— Hydrologic and chemical evaluation of the ground-water resources of northwestern Elkhart County 84-85
— Indiana 84-85
Indonesia: Indonesia 282-283
Jordan: Jordan 284
Louisiana: Anomalous radioactivity levels in central Louisiana water well 186-187
— Regional geohydrology of the northern Louisiana salt-dome basin 91-92
Maryland: Deep test well in Maryland 109
— Ground-water chemistry of the Aquia aquifer in southern Maryland 146
— Hydrologic effects of underground coal mining, Garrett County, Maryland 226-227
— Maryland 85
— Newly discovered paleochannels on the Delmarva Peninsula 85
— Numerical-model evaluation of ground-water resources in the lower Susquehanna River basin 88
Massachusetts: Evaluation of the Mat-tapoisett aquifer 85-86
— Ground-water assessment in the Connecticut Valley lowlands 85
— Massachusetts 85-86
— No polychlorinated biphenyls in induced recharge from the Housatonic River, Massachusetts 238
— Treated-sewage plume in a sand and gravel aquifer, Cape Cod, Massachusetts 237-238
Michigan: Contamination delineated at Wurtsmith Air Force Base, Michigan 237
— Water quality of coal deposits and abandoned mines in Saginaw County, Michigan 227
Midwest: Central Midwest RASA Study 106-107
Minnesota: Appraisal of coal-tar derivatives in ground water in St. Louis Park, Minnesota 189
— Appraisal of surficial aquifers 86
— Appraisal of the surficial aquifers in the Pomme de Terre and Chippewa River valleys, western Minnesota 167
— Ground-water use in Minneapolis-St. Paul area, Minnesota 104
— Minnesota 86-87
— Northern Midwest (Minnesota) RASA Study 107
— Water-level changes in major aquifers of the Twin Cities metropolitan area 87
— Water-quality appraisal of sand-plain aquifers 86-87
Mississippi: Geochemistry of water from Cretaceous aquifers in the Southeastern United States; Mississippi, Alabama, Georgia, and South Carolina 146

- Missouri*: Ground-water flow patterns in northeastern Missouri 94
 — Missouri 94
Montana: Geochemistry and geohydrology of the Decker and Big Sky coal-mining areas, southeastern Montana 227
 — Ground water near wastewater-treatment facilities in Glacier National Park, Montana 238-239
 — Montana 94-95
 — Montana RASA Study 107-108
 — Potential impacts of coal mining in selected areas of eastern Montana 227-228
 — Water-resources investigations of the Lake Creek valley, northwestern Montana 94-95
Nebraska: Geohydrology of the High Plains aquifer system in Nebraska 95
 — Nebraska 95
 — Stream-aquifer interrelations in southeast Nebraska 190-191
Nevada: Ground water in Kyle and Lee Canyons, Spring Mountains, southern Nevada 98
 — Mathematical model of the Eagle Valley ground-water basin, west-central Nevada 166
 — Nevada 98
New Jersey: Analysis of fresh and saline ground water in the New Jersey Coastal Plain and Continental Shelf 109
New Mexico: Computing recharge to alluvial basins in New Mexico 169-170
 — Hydrologic testing of low-permeability zones in southeastern New Mexico at the Waste Isolation Pilot Plant 170
New York: Aldicarb pesticide contamination in ground-water in eastern Suffolk County, Long Island, New York 238
 — Evaluation of ground-water resources in the Montauk area, Long Island 87
 — Nassau County Recharge Project, Long Island, New York 169
 — New York 87-88
 — Potential supplement to New York City water supply 87
North Dakota: Extension of Spiritwood aquifer system through North Dakota into Canada 95
 — North Dakota 95
Oklahoma: Geohydrology of the Roubidoux aquifer, northeastern Oklahoma 95
 — Ground water in the Oklahoma coal field 228
 — Numerical simulation of the alluvium and terrace aquifer along the North Canadian River from Canton Lake to Lake Overholser 167
 — Oklahoma 95
 — Quality of water from coal-mine spoil, eastern Oklahoma 228
Oregon: Declining ground-water levels in northeastern Oregon 99
 — Model of the regional aquifer system underlying the Snake River Plain in southern Idaho and eastern Oregon 166
 — Oregon 98-99
Pennsylvania: Appraisal of aquifers 88
 — Numerical-model evaluation of ground-water resources in the lower Susquehanna River basin 88
 — Pennsylvania 88
Puerto Rico: Saltwater movement in the coastal areas 123-124
South Carolina: Geochemistry of water from Cretaceous aquifers in the Southeastern United States; Mississippi, Alabama, Georgia, and South Carolina 146
South Dakota: Aquifers in south-central South Dakota 96
 — Large yields from glacial aquifers in Aurora and Jerauld Counties 95
 — Outwash-channel aquifer in central South Dakota 95-96
 — South Dakota 95-96
Southwestern U.S.: Southwest Alluvial Basins RASA Study 108
Texas: Projected effects of proposed salinity-control projects on fresh ground water in the upper Brazos and Wichita River basins, Texas 189
United States: Ground-water hydrology 165
 — Northeastern region 83-88
 — Regional Aquifer-System Analysis Program 106-109
 — Summary appraisals of the Nation's ground-water resources 165-166
 — Temperature versus depth in deep drill holes in the U.S. 156
Utah: Response of ground water to rapid intrusion of magma 158
Vamoosa-Ada Aquifer: Possible sources of degradation of water quality of the Vamoosa-Ada aquifer, east-central Oklahoma 237
Virginia: Aquifer model of the Culpeper basin, Virginia 166-167
 — Hydrogeology of the Culpeper basin 92
Washington: Declining ground-water levels in east-central Washington 99
 — Occurrence and quality of ground water in selected islands, San Juan County 99
 — Washington 99
Widefield Aquifer: Elevated nitrate concentrations in the Widefield aquifer south of Colorado Springs, Colorado 187
Wisconsin: Deep test wells 88
 — Ground-water-level fluctuations 88
 — High sodium and sulfate in ground water in Brown County, Wisconsin 186
 — Water use in Wisconsin in 1979 104
 — Wisconsin 88
Wyoming: Joints and ground-water flow in oil shale in Wyoming 229
 — Solute transport of in-situ oil-shale retort water in Wyoming 229
Yemen: Yemen Arab Republic 291
Gulf Coastal Plain *see also* the individual states and countries

- Gulf Coastal Plain—economic geology**
 bentonite deposits: Bentonite in the Gulf Coastal Plain 13
 lignite: Chemical composition of gulf coast lignites 23
 — Gulf Coast lignite 17
Gulf of Mexico—economic geology
 fuel resources: Conterminous United States offshore oil and gas resource assessments 32
 — Gulf of Mexico and Florida 29-30
 — Oil and gas potential of the Gulf of Mexico Maritime Boundary region 115
 mineral resources: Petroleum potential of Maritime Boundary region, Gulf of Mexico 29
 petroleum: Detection of geopressured zones by seismic-reflection method 32
 — Petroleum potential of Maritime Boundary region, Gulf of Mexico 29
Gulf of Mexico—geochemistry
 isotopes: Radiometric studies of geopressured systems 147
Gulf of Mexico—geophysical surveys
 seismic surveys: Detection of geopressured zones by seismic-reflection method 32
Gulf of Mexico—oceanography
 continental shelf: Destin Dome and the west Florida Shelf 111
 sediments: Physical and chemical properties of fine-grained sediments 146-147
Gulf of Mexico—sedimentary petrology
 sedimentation: Importance of mass sediment transport in continental margin processes 117
 — Surface structures of the southwest Florida shelf 114-115

H

- hafnium— isotopes**
 Hf-177/Hf-176: Evolution of continental crust as inferred from a hafnium isotope study 147
Hawaii—geochemistry
 isotopes: Atmospheric carbon dioxide 150
Hawaii—geophysical surveys
 remote sensing: District satellite receive sites 264
 seismic surveys: Crustal structure of Mauna Loa Volcano, Hawaii 156
Hawaii—petrology
 inclusions: Depth of origin of olivine nodules, Loihi Seamount 140-141
Hawaii—seismology
 earthquakes: Hawaiian earthquakes 140
Hawaii—tectonophysics
 crust: Crustal structure of Mauna Loa Volcano, Hawaii 156
Hawaii—volcanology
 Kilauea: Eruption forecasting for Kilauea 140
 — The August 1981 intrusive event at Kilauea Volcano 140
 Mauna Loa: Eruptive recurrence, Mauna Loa volcano, Hawaii 216-217

- Mauna Loa Volcano 140
- regional*: Hawaiian volcano studies 140-141
- heat flow** *see also under* geophysical surveys *under* Alaska; Arizona; California
- heat flow—geothermal gradient**
- thermal conductivity*: Thermal convection in drill holes at high geothermal gradients 136
- heavy mineral deposits** *see also under* economic geology *under* Connecticut
- heavy minerals** *see under* composition *under* sediments; *see also* placers
- helium—geochemistry**
- sedimentary rocks*: Study of diurnal variations as an aid to helium-survey prospecting for small oil fields in Kansas 28-29
- soils*: Enhancement of data from helium soil gas surveys 42
- helium— isotopes**
- He-4/He-3*: Mexico 284-285
- Himalayas** *see also the* individual countries
- Holocene** *see also under* geochronology *under* Oregon; Virginia; Western U.S.; *see also under* stratigraphy *under* California; Virginia
- hot springs** *see* thermal waters *under* geochemistry *under* deuterium; tritium; *see* thermal waters *under* hydrogeology *under* California; Montana; United States; Washington; *see* thermal waters *under* hydrology *under* isotopes
- hydrogen** *see also* deuterium; tritium
- hydrogen—geochemistry**
- volcanoes*: Hydrogen monitoring, Cascade volcanoes 216
- hydrogen— isotopes**
- D/H*: Continental evaporites in Owens Lake, California 13
- $\delta^{18}\text{O}$ and δD anomalies as earthquake precursors 150
- tritium*: Radionuclide movement at a radioactive-waste burial site in Illinois 235
- hydrogeology** *see also* ground water; hydrology
- hydrogeology—experimental studies**
- applications*: Hydrologic applications 252
- hydrogeology—maps**
- U. S. Geological Survey*: State hydrologic unit maps 314
- hydrogeology—methods**
- principles*: Geologic and hydrologic principles, processes, and techniques 130-136
- remote sensing*: Applications to hydrologic studies 263-264
- hydrogeology—practice**
- publications*: State water-resources investigations folders 314-315
- hydrogeology—research**
- resources*: Special water-resource programs 99-109
- hydrology** *see also* ground water; hydrogeology
- hydrology—experimental studies**
- coastal environment*: Marine geology and coastal hydrology 110-124
- models*: Surface-water quality models and processes 187-189
- properties*: Chemical, physical, and biological characteristics of water 184-190
- water quality*: Chemical and biological quality of surface water 184-186
- hydrology—hydrologic cycle**
- interpretation*: Relation between surface water and ground water 190-192
- hydrology—methods**
- runoff*: Rainfall-runoff and runoff-quality model for urban watersheds 101
- suspension*: Trace-metal partitioning in suspended sediments from urban storm-water runoff 102
- hydrology—rivers and streams**
- effects*: Effects of a flood-retarding dam 174
- Hydrologic effects of volcanism 229-231
- estuarine environment*: Estuarine and coastal hydrology 122-124
- experimental studies*: Data-network studies 172-173
- Limnology and potamology 192-194
- Miscellaneous studies 173-176
- Surface-water hydrology 170-176
- Vertical velocity profiles in stratified open-channel flows 174
- models*: Model studies 170-171
- Ridge regression estimates of peak flow at ungaged sites 171-172
- Transport mechanisms of solutes sorbing onto sediment in pool-and-riffle streams 188
- pollution*: Surface-water pollution 236-237
- statistical analysis*: Statistical studies 171-172
- stochastic processes*: Bias in standard deviation due to autocorrelation 172
- water quality*: Areawide chemical loading 189-190
- Effects of pollutants on water quality 236-239
- watersheds*: Watershed-model-evaluation study 171
- hydrology—surveys**
- Alabama*: Methodology for hydrologic evaluation of a potential surface mine, Tuscaloosa County, Alabama 224
- Watershed model for Warrior coal basin, Alabama 223-224
- Alabama River*: Mathematical model of the Alabama River 171
- Alberta*: Joint United States-Canada study of flow of Milk River at the Montana-Alberta border 275-276
- Antarctica*: Satellite glaciology 252
- Apalachicola River*: Nutrient and detritus transport in the Apalachicola River, Florida 190
- Arizona*: Contracted satellite data relay study 264
- District satellite receive sites 264
- Hydrologic regionalization by cluster analysis 172
- Real-time data processing 263-264
- Arkansas*: Derivation of net photosynthetic production from community-metabolism analysis in Arkansas 194
- Gas- and dye-tracer-estimation program in Arkansas 187-188
- Modified version of one-dimensional, steady-state, stream water-quality model in Arkansas 187
- New dissolved-oxygen probe in Arkansas 198
- Sediment-oxygen-demand measurements by use of a laboratory respirometer in Arkansas 197
- Arkansas River*: Arkansas traveltime study 174-175
- Big Lost River*: Channel change in the Big Lost River, Idaho 160
- Big Marine Lake*: Hydrology of Big Marine Lake, Washington County, Minnesota 191
- California*: Bacterial denitrification in small streams in California 193-194
- Field experiment on in-stream uptake and regeneration of nitrate 192-193
- Late Cenozoic paleohydrology of California desert 164-165
- Riverine-estuarine process 122-123
- Canada*: International commissions 279
- Cape Fear River*: Water quality of the Cape Fear River, North Carolina 186
- China*: China 281-282
- Colorado*: Contracted satellite data relay study 264
- Evaluation of selected one-dimensional stream water-quality models with field data 188
- Flood hydrology of foothill streams in Colorado 236
- Hydraulic geometry of stream channels in the Piceance basin area 175
- Sensitivity to acidification of Flat Tops Wilderness Area lakes 192
- Toxicity of leachate from spent oil shale on a blue-green alga 224
- Eastern U.S.*: Hydrology of Federal coal lands in eastern National Forest areas 125-126
- Multistate studies 91
- Water quality of the Susquehanna, Potomac, and James Rivers 185
- Florida*: Carbon transport from forested wetlands in a large Florida river basin 190
- Microcomputer program for time-of-travel and dispersion characteristics of streams in Florida 188
- Saltwater movement in the coastal areas 123-124
- Georgia*: Applications of draft-storage diagrams for Georgia streams 176
- Errors due to time-sampling bias for streamflow statistic in Georgia 172
- Evaluation of selected one-dimensional stream water-quality models with field data 188
- Geologic and hydrologic effects of Late Cretaceous and Cenozoic faulting of the Coastal Plain near the Savannah River, Georgia and South Carolina 90
- Georgia 91

- Variability of average annual rainfall and average annual runoff 91
- Great Plains: Central Region* 92-93
- Mapping of irrigated cropland with Landsat digital data 303
- Multistate studies 93
- Hawaii: District satellite receive sites* 264
- Idaho: An evaluation of Idaho stream-gaging networks* 172-173
- Effects of irrigation-return flows on water quality in Marsh Creek, Rock Creek, and Cedar Draw in south-central Idaho 185
- Effects of volcanic ash on aquatic environments in northern Idaho 230
- Hydrologic evaluation of streamflow records at gaging stations in the Upper Columbia River basin and Bear River basin in Idaho 176
- Illinois: Effects of stormwater detention on water quality near Glen Ellyn, Illinois* 102
- Hydrology and water quality in coal areas of Illinois 225
- Long-term sediment yields from Bay Creek, Pike County, Illinois 160-161
- Mine-reclamation hydrology in Fulton County, Illinois 225
- Reach velocities in Illinois streams 176
- Runoff and sediment transport from an agricultural watershed in northern Illinois 162
- Times of concentration and storage coefficients for Illinois streams 175
- Illinois River: Stage-discharge relations at dams on the Illinois and Des Plaines Rivers in Illinois* 175
- Indiana: Chemical and biological characteristics of Indiana Dunes National Lakeshore streams* 184
- Comparison of metal and other trace-element concentrations on streambed sediments from forested, agricultural, and coal-mining areas of southwestern Indiana 225-226
- Preliminary biological assessment of streams in the coal-mining regions of southwestern Indiana, October-November 1979 225
- Indonesia: Indonesia* 282-283
- Kansas: Effects of abandoned lead and zinc mines on water quality in Kansas* 226
- Geohydrology of stream-aquifer system, Finney and Kearny Counties, Kansas 191-192
- Kentucky: Dynamic streamflow model and hysteretic stage-discharge relations* 171
- Lake Kocanusa: Primary productivity at Lake Kocanusa, Montana* 192
- Louisiana: Geohydrologic appraisal of potential surface lignite mines in northwestern Louisiana* 226
- Louisiana 91-92
- Saltwater movement in the coastal areas 123-124
- Maryland: Contamination of Jones Falls in Baltimore, Maryland* 102
- Massachusetts: Low-flow characteristics of Massachusetts streams* 175-176
- Merced River: Water-quality assessment of the Merced River, California* 186
- Milk River: Joint United States-Canada study of flow of Milk River at the Montana-Alberta border* 275-276
- Minnesota: Model simulation of runoff hydrographs in the Coon Creek watershed, Anoka County, Minnesota* 171
- Quality of runoff from watersheds in the Twin Cities metropolitan area, Minnesota 102-103
- Montana: Effects of urbanization on flood peaks, Missoula, Montana* 236
- Hydrology and potential effects of mining in the Cook Creek and Snider Creek areas, Montana 227
- Quality of streams in the Bull Mountains region, south-central Montana 227
- Surface-water quality in east-central Montana 185-186
- Water-quality of small reservoirs in northeastern Montana 192
- Water use in Montana 104
- Nebraska: Estimating water discharge for channel-width maintenance* 161
- Sediment transport and effective discharge 161
- Stream-aquifer interrelations in southeast Nebraska 190-191
- Nevada: Evaluation of streamflow-data networks* 172
- Nutrient loads to Lahontan Reservoir, west-central Nevada 193
- Streamflow data network for Nevada 173
- Water budget for Wahoe Valley near Reno, Nevada 98
- New England: Contracted satellite data relay study* 264
- New York: Bottom-sediment chemistry of the Saw Mill River, Westchester County, New York* 146
- Quality and quantity of urban stormwater runoff to recharge basins, Long Island, New York 103
- Synoptic study of snowpack chemistry 87-88
- North Carolina: Effects of channel excavation in North Carolina* 173
- Nueces River: Flow losses along the Nueces River, Cotulla to Simmons, Texas* 176
- Oklahoma: Suitability of surface-water of the Red River basin, Oklahoma, for water supply* 185
- Suspended sediment in the southern Oklahoma coal field 228
- Oregon: An evaluation of suspended sediment and turbidity in Cow Creek, Oregon* 160
- Background-water quality in Three sisters area 99
- Evaluation of selected one-dimensional stream water-quality models with field data 188
- Precipitation quality in Salem 98-99
- Pearl River: Hydraulic-model study of impact of Interstate route 10 crossing on backwater and flow distribution of lower Pearl River* 173
- Pennsylvania: Contracted satellite data relay study* 264
- Cost-effectiveness in stream gaging in Pennsylvania 173
- Effects of nonpoint sources to concentrations and loads of water-quality constituents in Pequea Creek basin, Pennsylvania 184
- Effects of scrubber sludge disposal on hydrology of Beaver County, Pennsylvania 236-237
- Evaluation of streamflow-data networks 172
- Hydrology of the Eastern Coal Province, Pennsylvania 228
- Sediment yields from areas affected by surface mining in Pennsylvania 161-162
- Temporal changes in chloride, sulfate, and sodium concentration in four eastern Pennsylvania streams 184
- Platte River: Large-scale bedforms in the Platte River, Nebraska* 161
- Streamflow changes in Platte River basin 174
- Potomac River: Potomac River Reservoir release routing* 170-171
- Rhode Island: Radionuclide transport in glacial outwash, Wood River Junction, Rhode Island* 235
- Saginaw River: Flow model of Saginaw River* 171
- San Juan River: Preliminary analysis of historical streamflow and water-quality records for the San Juan River basin, New Mexico and Colorado* 174
- Schuylkill River: Organochlorine pesticide and polychlorinated biphenyl residues at four tropic levels in the Schuylkill River, Pennsylvania* 237
- Snake River plain: Water-quality studies of the Snake River Plain in southern Idaho and eastern Oregon* 185
- South Carolina: Geologic and hydrologic effects of Late Cretaceous and Cenozoic faulting of the Coastal Plain near the Savannah River, Georgia and South Carolina* 90
- Hydrology of a low-level radioactive-waste burial site in South Carolina 235
- South Dakota: Determination of irrigation potential, Lower Brule and Crow Creek Indian reservations* 252
- Hydrologic information systems in Black Hills and Cheyenne River basin 252
- Susquehanna River: Water-quality loads of the Susquehanna River* 189
- Water-quality loads of the Susquehanna River at Harrisburg, Pennsylvania 189-190
- Tanana River: Sediment transport in the Tanana River near Fairbanks, Alaska, 1977-79* 162

- Texas*: Contracted satellite data relay study 264
- Tongue River*: Dissolved-solids model of the Tongue River, Montana 188-189
- United States*: Atmospheric Deposition Program 105-106
- Data coordination, acquisition, and storage 99-101
 - National Hydrologic Bench-Mark Network 105
 - National Stream Quality Accounting Network 104-105
 - National water data exchange 100-101
 - National water-quality programs 104-105
 - Southeastern region 89-90
 - Urban stormwater data management system 101-102
 - Urban Water Program 101-103
 - Water-data storage system 101
 - Water use 103-104
- Virginia*: Streamflow duration during low-flow periods in strip-mined areas of southwestern Virginia 229
- Virginia 92
- Washington*: Chemical characteristics of selected rivers, western Washington, 1961-1980 72
- District satellite receive sites 264
 - Effects of 1980 eruption of Mount St. Helens on selected lakes in Washington 230-231
 - Trophic classification of Washington lakes 193
- Western U.S.*: Western region 96-99
- Wisconsin*: Hydrology of Wisconsin lakes potentially affected by acid deposition 191
- Wyoming*: Bedload studies in Wyoming 160
- Channel-geometry relations for Wyoming streams 175
- Yemen*: Yemen Arab Republic 291
- hydrology—techniques**
- instruments*: Completion of Phase I of the Power System Study 195
 - Contracted development of electronic current-meter pickup systems 195
 - Development of a hydrologic data-acquisition system 197
 - Development of a new microprocessor controller for National Urban Runoff data collection 195
 - Evaluation of Helley-Smith bedload samplers 194
 - Feasibility study for developing a depth-integrating pumping sampler 195
 - Heat-pulse flowmeter 196
 - Measurement of water stage with ultrasonic-ranging instrumentation 194
 - Minimum standards for water-level sensing instruments 197
 - New continuous-flow sediment-concentration samples 194-195
 - New hydrologic instruments and techniques 194-198
 - New lightweight fiber wading tagline 194
 - New plastic pygmy-meter bucket wheels 194
 - New point-integrating and depth-integrating bag-type samplers 194
 - New stream-gaging equipment 195
 - Replacement for discontinued Pakron wading tagline reel 194
 - Retrofitting the Survey's battery-powered water-quality monitor 194
 - Water-use monitoring equipment 195
- hydrothermal alteration** *see under* processes *under* metasomatism
- hydrothermal processes** *see under* mineral resources *under* mineral deposits, genesis
- I**
- Iberian Peninsula** *see also* Portugal
- ice ages** *see* glacial geology
- Iceland—economic geology**
- coal*: Coal occurrences of North America and adjacent areas 15
- Idaho—economic geology**
- geothermal energy*: Geochemistry of thermal springs in the Idaho batholith region, Idaho 153
 - molybdenum ores*: Geochemistry and resource potential of the Selway-Bitterroot Wilderness 2
 - Molybdenum mineralization model for central Idaho 8
 - Molybdenum-silver anomalies, Ten Mile West RARE II Roadless Area, Idaho 2
 - silver ores*: Molybdenum-silver anomalies, Ten Mile West RARE II Roadless Area, Idaho 2
 - tin ores*: Geochemistry and resource potential of the Selway-Bitterroot Wilderness 2
 - uranium ores*: Central Idaho paleodrainage history and implications for uranium exploration 37-38
 - Proterozoic quartzite and conglomerate of central Idaho 37
 - Uranium in spring water and bryophytes at Basin Creek in central Idaho 10
- Idaho—engineering geology**
- waste disposal*: Liquid-waste disposal at the Idaho National Engineering Laboratory 233-234
 - Sealed monitoring wells for a radioactive environment 234
- Idaho—geochronology**
- Quaternary*: A new reversed polarity event within Brunhes epoch 152
- Idaho—hydrogeology**
- ground water*: Ground-water conditions in the Michaud Flats area, Fort Hall Indian Reservation 97-98
 - Ground-water-quality assessment, southern Elmore and northern Owyhee Counties 98
 - Ground-water trends 98
 - Idaho 97-98
 - Irrigation water use on the Snake River Plain in southern Idaho 104
 - Model of the regional aquifer system underlying the Snake River Plain in southern Idaho and eastern Oregon 166
- hydrology*: An evaluation of Idaho stream-gaging networks 172-173
- Effects of irrigation-return flows on water quality in Marsh Creek, Rock Creek, and Cedar Draw in south-central Idaho 185
 - Effects of volcanic ash on aquatic environments in northern Idaho 230
 - Hydrologic evaluation of streamflow records at gaging stations in the Upper Columbia River basin and Bear River basin in Idaho 176
 - Water-quality studies of the Snake River Plain in southern Idaho and eastern Oregon 185
- springs*: Geochemistry of thermal springs in the Idaho batholith region, Idaho 153
- Idaho—petrology**
- igneous rocks*: Geology of the Bitterroot lobe of the Idaho batholith 54-55
 - Miocene ash-flow tuffs, central Snake River Plain, Idaho 142
 - volcanism*: Eruption rates and lava compositions, Craters of the Moon lava field, Idaho 142
- Idaho—sedimentary petrology**
- sedimentation*: Channel change in the Big Lost River, Idaho 160
- Idaho—stratigraphy**
- sedimentation*: Pleistocene alluvial-gravel in eastern Idaho 63-64
 - Tertiary*: Geologic mapping on the Snake River Plain in southern Idaho 107
- Idaho—structural geology**
- faults*: Complex thrusting in Snake River Range, Idaho 60
- igneous rocks** *see also* fluid inclusions; inclusions; intrusions; lava; magmas; metamorphic rocks; metasomatism; phase equilibria
- igneous rocks—alkalic composition**
- petrology*: Petrology of alkaline intrusive rocks, western Montana 145
- igneous rocks—diabase**
- magnetic properties*: Lower Jurassic igneous rocks in the Culpeper basin, Northern Virginia 52-53
- igneous rocks—diorites**
- tonalite*: Geology of the Bitterroot lobe of the Idaho batholith 54-55
 - Granitic rocks and migmatites in the Coast plutonic complex near Petersburg 80-81
- igneous rocks—geochemistry**
- trace elements*: Geochemical characteristics of uranium-enriched volcanic rocks 33-34
- igneous rocks—granites**
- genesis*: Geochemical, isotopic, and petrologic studies of an Archean granite, Owl Creek Mountains, Wyoming 144

igneous rocks—granodiorites

- Cretaceous*: Molybdenum and tungsten mineralization in northern Washington 74
- petrology*: Geology of the Anaconda-Pintlar Wilderness Study Area, Montana 54
- Mapping at the eastern edge of the Idaho batholith, Montana 54
- plutons*: Comagmatic granitoid sequence, Sierra Nevada 67

igneous rocks—petrology

- Miocene*: Cogenetic volcanic and granitic rocks of Miocene age in the Questa caldera, northern New Mexico 143
- plutons*: Igneous rocks 66-67
- research*: Igneous rocks 54-55

igneous rocks—plutonic rocks

- cataclastic rocks*: Negative δO^{18} values in cataclastic plutonic rocks 149-150
- complexes*: Tectonic framework of Chief Joseph plutonic complex, southwest Montana 55
- experimental studies*: Plutonic rocks and magmatic processes 143-145
- granitic composition*: Granitoid plutonic rocks of the Arabian Shield 287

igneous rocks—pyroclastics

- andesite tuff*: Emplacement of the andesite tuff and revised stratigraphy of the Medicine Lake Volcano, California 141
- ash falls*: Redistribution of the Mount St. Helens ash with time 71-72
- ash-flow tuff*: Miocene ash-flow tuffs, central Snake River Plain, Idaho 142
- tuff*: Progress in correlation and age determination of late Cenozoic tephra 68-69
- Studies in Wheeler Peak, Latir Peak, and Columbine-Hondo area, New Mexico 55
- volcanic ash*: Postdepositional changes in Mount St. Helens ash 218
- Volcanic ash on Missouri River # Yellowstone River drainage divide, Montana 60

igneous rocks—ultramafics

- kimberlite*: Lake Ellen Kimberlite, Michigan; thermobarometry of mantle inclusions 145
- Pyroxene decomposition in kimberlites 138

igneous rocks—volcanic rocks

- experimental studies*: Volcanic rocks and processes 140-143
- observations*: Phenocrysts record magma mixing in Coso volcanic field, California 141
- olivine basalt*: Cenozoic volcanic rocks 287

Illinois—economic geology

- reclamation*: Mine-reclamation hydrology in Fulton County, Illinois 225

Illinois—engineering geology

- dams*: Stage-discharge relations at dams on the Illinois and Des Plaines Rivers in Illinois 175
- waste disposal*: Analysis of soil cores beneath radioactive-waste-disposal site, Sheffield, Illinois 234

Illinois—environmental geology

- isotopes*: Radionuclide movement at a radioactive-waste burial site in Illinois 235
- waste disposal*: Ground-water flow to strip-mined lake from low-level radioactive-waste-disposal site near Sheffield, Illinois 234

Illinois—geochemistry

- isotopes*: Isotopic composition of uranium and thorium in crystalline rocks 148

Illinois—geomorphology

- fluvial features*: Times of concentration and storage coefficients for Illinois streams 175

Illinois—hydrogeology

- ground water*: Aquifer studies at a proposed coal strip mine near Industry, Illinois 225
- Piezometers in deep test well in northeast Illinois 108
- hydrology*: Effects of stormwater detention on water quality near Glen Ellyn, Illinois 102
- Hydrology and water quality in coal areas of Illinois 225
- Mine-reclamation hydrology in Fulton County, Illinois 225
- Reach velocities in Illinois streams 176

Illinois—sedimentary petrology

- sedimentation*: Runoff and sediment transport from an agricultural watershed in northern Illinois 162
- sediments*: Long-term sediment yields from Bay Creek, Pike County, Illinois 160-161

impact features see under geomorphology**impact statements—land use**

- general*: Environmental impact studies 265-266

inclusions see also fluid inclusions**inclusions—mineral inclusions**

- olivine*: Depth of origin of olivine nodules, Loihi Seamount 140-141
- silicates*: The B chromite zone of the Stillwater Complex, Montana 6

inclusions—xenoliths

- kimberlite*: Lake Ellen Kimberlite, Michigan; thermobarometry of mantle inclusions 145
- pyroxenite*: Xenoliths from trachybasalt, Sierra Nevada 137
- trachyandesite*: Neodymium and strontium isotopes in inclusions from the Sierra Nevada 147-148

India—oceanography

- marine geology*: India 282

Indian Ocean see also Persian Gulf

- Indian Ocean Islands—economic geology**
- water resources*: British Indian Ocean Territory 281

Indiana—economic geology

- molybdenum ores*: Metals in black shales 12-13
- uranium ores*: Metals in black shales 12-13

Indiana—hydrogeology

- ground water*: Ground-water availability in the outwash aquifer, Marion County 85
- Ground-water resources of a glacial-outwash aquifer in Johnson and Morgan Counties 84
- Hydrologic and chemical evaluation of the ground-water resources of northwestern Elkhart County 84-85
- Indiana 84-85
- hydrology*: Chemical and biological characteristics of Indiana Dunes National Lakeshore streams 184
- Comparison of metal and other trace-element concentrations on streambed sediments from forested, agricultural, and coal-mining areas of southwestern Indiana 225-226
- Preliminary biological assessment of streams in the coal-mining regions of southwestern Indiana, October-November 1979 225

Indonesia—engineering geology

- slope stability*: Establishment of slope-movement monitoring stations in West Java, Indonesia 221-222
- Indonesia 282-283

Indonesia—environmental geology

- land use*: Indonesia 282-283

Indonesia—volcanology

- volcanoes*: Indonesia 282-283

industrial minerals see also under economic geology under New York**inert gases see noble gases****infrared surveys see under geophysical surveys under Pacific Coast; Washington****instruments see under cartography under maps; see under gravity methods under geophysical methods; see under methods under geophysical methods; see under mineral exploration under uranium ores; see under radioactivity under well-logging; see under techniques under hydrology; spectroscopy****intrusions see also igneous rocks; metamorphism; metasomatism****intrusions—batholiths**

- petrology*: Geology of the Bitterroot lobe of the Idaho batholith 54-55
- Mapping at the eastern edge of the Idaho batholith, Montana 54

intrusions—petrology

- allochthons*: Tertiary stratigraphy, intrusion, and structure in the Mohave Mountains in west-central Arizona 65-66

intrusions—plutons

- geochemistry*: Strontium-isotope composition of plutons in the southern Snake Range, Nevada 149
- Permian*: Permian plutons in north-central Nevada 66

intrusions—sills

- Virginia*: Lower Jurassic igneous rocks in the Culpeper basin, Northern Virginia 52-53

Invertebrata see also foraminifera; Mollusca**invertebrates see also brachiopods; conodonts; corals; mollusks; ostracods; radiolarians; trilobites**

- invertebrates—biostratigraphy**
Mississippian: Upper Mississippian invertebrate biostratigraphy, eastern Appalachians 182
- iridium—geochemistry**
sedimentary rocks: Cretaceous-Tertiary boundary iridium anomaly 177
 — Iridium anomaly at Cretaceous-Tertiary boundary, New Mexico 57
- iron—analysis**
Mossbauer spectroscopy: Use of Mossbauer spectroscopy to identify iron-sulfide minerals in coal 23-24
- isotope dating** *see* absolute age
- isotopes** *see also* absolute age; geochronology
- isotopes—analysis**
radioactive isotopes: Isotope and nuclear geochemistry 147-152
stable isotopes: Stable isotopes 148-150
- isotopes—beryllium**
Be-10: Dating landslides and other upper Pleistocene and Holocene features 221
 — Soil chronosequences and ¹⁰Be isotopic dating in mid-Atlantic States 51-52
- isotopes—carbon**
C-13/C-12: Atmospheric carbon dioxide 150
 — Calculations of global rate of burial of Cretaceous organic carbon and oceanic stable carbon as an aid to source-rock studies 31
 — Comparative organic geochemistry of Middle Pennsylvanian shale and coal 29
 — Mexico 284-285
 — Origin of natural gases in San Juan basin 26
 — The origin of carbonate minerals in the Upper Freeport bed 22
- isotopes—copper ores**
ratios: Stable isotope systematics of copper-silver occurrences in the Belt Supergroup 148-149
- isotopes—hafnium**
Hf-177/Hf-176: Evolution of continental crust as inferred from a hafnium isotope study 147
- isotopes—hydrogen**
D/H: Continental evaporites in Owens Lake, California 13
tritium: Radionuclide movement at a radioactive-waste burial site in Illinois 235
- isotopes—hydrology**
thermal waters: Geochemistry of thermal springs in the Idaho batholith region, Idaho 153
- isotopes—lead**
galena: Plumbic prospecting in the northern Rocky Mountains 148
Pb-207/Pb-206: Implications of common lead measurements 286-287
Pb-210: ²¹⁰Pb activity and pollen dating, Potomac estuary, Virginia 152
 — ²¹⁰Pb geochronology, Upper Klamath Lake, Oregon 152
ratios: Age and genetic constraints for the uranium deposit at Lilljuthatten 290
 — Origin of Kuroko ore deposits of Japan 9
 — Silver Plume Granite—a possible source of uranium, Tallahassee Creek deposits 37
- isotopes—metasomatic rocks**
rocks: Mineralogy and stable isotope geochemistry of hydrothermally altered rocks from the East Pacific Rise and the Mid-Atlantic Ridge 149
- isotopes—neodymium**
Nd-144/Nd-143: Neodymium and strontium isotopes in inclusions from the Sierra Nevada 147-148
- isotopes—oxygen**
O-18/O-16: $\delta^{18}\text{O}$ and δD anomalies as earthquake precursors 150
 — Negative δO^{18} values in cataclastic plutonic rocks 149-150
 — Stable isotope interpretation of the Lassen geothermal system 154-155
- isotopes—petroleum**
ratios: Geochemical prospecting over Bell Creek oil field, Powder River Basin 25
 — Geochemistry of oils from Pennsylvanian and Lower Permian Minnelusa Formation, Powder River Basin 25
- isotopes—radium**
Ra-228/Ra-226: Radiometric studies of geopressed systems 147
- isotopes—sedimentary rocks**
ratios: Sedimentologic and diagenetic history of reservoirs in Niobrara Formation, Denver basin 25-26
- isotopes—strontium**
Sr-87/Sr-86: Age and strontium initial ratio of plutonic rocks 286
 — Age of diorite-granodiorite gneisses 286
 — Strontium-isotope composition of plutons in the southern Snake Range, Nevada 149
- isotopes—tracers**
experimental studies: Isotope tracer studies 147-148
radioactive isotopes: Radionuclide transport in glacial outwash, Wood River Junction, Rhode Island 235
- isotopes—uranium**
U-235/Pb-204: Geochronology of roll-type uranium ores of the Felder deposit, Texas 151
U-238/U-234: Isotopic composition of uranium and thorium in crystalline rocks 148
 — Late Cenozoic sea levels 164
- isotopes—uranium ores**
stable isotopes: Ore emplacement in the Schwartzwalder mine, Jefferson County, Colorado 35
- Italy—geochronology**
Pleistocene: Italy 283-284
Pliocene: Italy 283-284
- J**
- Japan—economic geology**
lead-zinc deposits: Origin of Kuroko ore deposits of Japan 9
- Japan—engineering geology**
slope stability: Japan 284
- Japan—seismology**
earthquakes: Triggering of earthquakes by aseismic crustal movements 206-207
- joints** *see under* style *under* fractures
- Jordan—hydrogeology**
ground water: Jordan 284
- Jupiter—geomorphology**
impact features: Cratering rate of the Galilean satellites 243
- Jupiter—geophysical surveys**
remote sensing: Europa 242-243
 — Ganymede 243
 — Jupiter investigations 242-243
- Jupiter—volcanology**
volcanism: Volcanism on Io 242
- Jurassic** *see also under* geochronology *under* Nevada; *see also under* stratigraphy *under* California; New Mexico; Utah
- K**
- kames** *see under* glacial features *under* glacial geology
- Kansas—economic geology**
oil and gas fields: Study of diurnal variations as an aid to helium-survey prospecting for small oil fields in Kansas 28-29
- Kansas—hydrogeology**
hydrology: Effects of abandoned lead and zinc mines on water quality in Kansas 226
 — Geohydrology of stream-aquifer system, Finney and Kearny Counties, Kansas 191-192
- karst** *see under* solution features *under* geomorphology
- Kentucky—economic geology**
coal: Origin of the fire clay parting in eastern Kentucky 16-17
molybdenum ores: Metals in black shales 12-13
uranium ores: Metals in black shales 12-13
- Kentucky—hydrogeology**
hydrology: Dynamic streamflow model and hysteretic stage-discharge relations 171
- L**
- lacustrine features** *see under* geomorphology
- lakes** *see under* lacustrine features *under* geomorphology
- Lamellibranchiata** *see* Bivalvia *under* Mollusca
- land subsidence—causes**
effects: Land subsidence 239-240
- land subsidence—controls**
underground installations: Vertical displacements of a subsiding elastic layer 239

- land use** *see also* *under* environmental geology *under* Alaska; automatic data processing; Connecticut; Great Plains; Indonesia; Missouri; South Dakota; United States
- land use—effects**
impact statements: Land use and environmental impact 265-266
- land use—maps**
cartography: Geographic information system development 294
- land use—planning**
environmental geology: Computer graphics experiments and techniques 299-300
methods: Long range planning 265
natural resources: Algorithms for generalization of land use and land cover map content 295
 — Applications software development for land use and land cover data 295
- landform description** *see under* geomorphology
- landslides** *see under* slope stability
- lava** *see also* igneous rocks; magmas
- lava—petrology**
composition: Eruption rates and lava compositions, Craters of the Moon lava field, Idaho 142
models: Petrology of Loihi Seamount, Hawaii 110
- lead— isotopes**
galena: Plumbic prospecting in the northern Rocky Mountains 148
Pb-207/Pb-206: Implications of common lead measurements 286-287
Pb-210: ²¹⁰Pb activity and pollen dating, Potomac estuary, Virginia 152
 — ²¹⁰Pb geochronology, Upper Klamath Lake, Oregon 152
ratios: Age and genetic constraints for the uranium deposit at Lilljuthatten 290
 — Origin of Kuroko ore deposits of Japan 9
 — Silver Plume Granite—a possible source of uranium, Tallahassee Creek deposits 37
- Lesotho—petrology**
igneous rocks: Pyroxene decomposition in kimberlites 138
- lignite** *see also under* economic geology *under* Gulf Coastal Plain; Mississippi; Montana; Thailand
- lineation** *see also* foliation; structural analysis
- liquid inclusions** *see* fluid inclusions
- lithium—geochemistry**
granites: Baid al Jimalah tungsten deposit 287-288
- Louisiana—engineering geology**
geologic hazards: Hydraulic-model study of impact of Interstate route 10 crossing on backwater and flow distribution of lower Pearl River 173
- Louisiana—hydrogeology**
ground water: Anomalous radioactivity levels in central Louisiana water well 186-187
 — Regional hydrogeology of the northern Louisiana salt-dome basin 91-92
- Saltwater movement in the coastal areas 123-124
hydrology: Geohydrologic appraisal of potential surface lignite mines in northwestern Louisiana 226
 — Louisiana 91-92
- lunar studies** *see* Moon

M

magmas *see also* igneous rocks; intrusions; lava

magmas—differentiation
fractional crystallization: Reversal of normal role of thorium in fractional crystallization 145-146

magnetic field *see under* Earth

magnetic methods *see under* geophysical methods

magnetic surveys *see under* geophysical surveys *under* Appalachians; Atlantic Coastal Plain; Atlantic Ocean; automatic data processing; California; Colorado; Egypt; Michigan; Nevada; North Carolina; North Dakota; Pacific Ocean; United States

magnetism of rocks and minerals *see* paleomagnetism

magnetotelluric surveys *see under* geophysical surveys *under* Arizona; California; Nevada; Oregon; Utah

Maine—economic geology
peat: Peat in Maine and Alaska 1

Maine—geophysical surveys
gravity surveys: Geophysical studies in the Sherbrooke and Lewiston 1° × 2° quadrangles, Vermont, New Hampshire, and Maine 4

Malaysia—economic geology
petroleum: Malaysia 284

Mammalia—Rodentia
Cenozoic: Elk Hills, California 180

manganese ores—resources
sedimentary rocks: A new genetic model for sedimentary manganese deposits 1

mantle *see also under* tectonophysics *under* United States

maps *see also under* areal geology *under* Egypt; Pacific Ocean; *see also under* economic geology *under* Wyoming; *see also under* engineering geology *under* California; *see also under* environmental geology *under* Connecticut; Missouri; *see also under* general *under* automatic data processing; *see also under* geochemistry *under* New York; *see also under* geophysical surveys *under* Alaska; Great Plains; Michigan; Nevada; United States; *see also under* soils *under* United States; *see also under* stratigraphy *under* Alaska

maps—cartography
airborne methods: Associated activities 311
 — Testing and calibration of aerial cameras 311
automatic cartography: Application of linear algebra to computation of gridded data 297

- Automated cartographic lettering 307-308
 — Automated cartography 293-294
 — Automated Map Symbol Placement System 310
 — Automated spatial data handling 292-295
 — Data base development 292
 — DEM editing using a polygon scan-conversion process 292-293
 — Generalized adjustment by least squares 297-298
 — Geographic information system development 294
 — Geographic Names Information System 294-295
 — Map projections 295
 — The 1:2,000,000-scale data base 292
 — Voice data entry system 310-311
automatic data processing: Pass point marking system 310
computer programs: Online Aerotriangulation Data Collection and Edit System 311
engineering geology: Engineering geologic mapping 218-219
 — Engineering geologic mapping in New York City 219
geography: Cartographic and geographic studies 295-300
geologic maps: Experimental 1:63,360-scale orthophotoquad of Kodiak A-6 quadrangle, Alaska 298
geomorphologic maps: Mount St. Helens mapping 296
hydrologic maps: State hydrologic unit maps 314
imagery: Analysis of SLAR imagery for identification of base map categories 306
instruments: Map revision module for Kern PG2-AT stereoplottter 310
land use: Algorithms for generalization of land use and land cover map content 295
 — Cartographic and geographic research 292-300
methods: Landslide hazards mapping in the San Francisco Bay region 220
 — Screenless lithography 308
remote sensing: Aerial Profiling of Terrain System 308
 — Analysis of the image chain in the orthophoto production system 308
 — Applications and techniques development for raster-formatted data 308-309
 — Image map research 302-303
 — Landsat cartographic research 301
 — Screenless lithographic printing of 1:250,000-scale SLAR imagery 306
techniques: Systems and techniques research and development 307-310
topographic maps: Provisional map standards development 296-297
U. S. Geological Survey: Maps and charts 316
 — Maps and charts 317

- marine geology** *see also under* oceanography *under* Asia; India; Pacific Ocean; Puerto Rico
- marine geology—experimental studies**
coastal environment: Coastal marine geology 110-122
 — Marine geology and coastal hydrology 110-124
- Mars—areal geology**
cartography: Geologic mapping of Mars 245
- Mars—geomorphology**
erosion features: Probable fluvial sources for dune sand on Mars 246
landform description: Composite origin for martian outflow channels 245
 — Physical properties at the Viking landing sites 246
 — The basal scarp of Olympus Mons 244-245
volcanic features: Morphometry of the volcanoes 247
- Mars—geophysical surveys**
remote sensing: Geology of Valles Marineris 245
 — Mars highland volcanic province 245
 — Mars investigations 243-246
 — Martian topography; a new method for rapid extraction 244
- Mars—petrology**
lava: Lava-flow maps of Tharsis Montes 245
maps: Lava-flow maps of Tharsis Montes 245
- Mars—structural geology**
tectonics: Martian geology 243-244
- Maryland—engineering geology**
geologic hazards: Large, old debris avalanches in the Appalachians 221
- Maryland—hydrogeology**
ground water: Deep test well in Maryland 109
 — Ground-water chemistry of the Aquia aquifer in southern Maryland 146
 — Hydrologic effects of underground coal mining, Garrett County, Maryland 226-227
 — Maryland 85
 — Newly discovered paleochannels on the Delmarva Peninsula 85
 — Numerical-model evaluation of ground-water resources in the lower Susquehanna River basin 88
hydrology: Contamination of Jones Falls in Baltimore, Maryland 102
 — Potomac River Reservoir release routing 170-171
- Maryland—stratigraphy**
Miocene: Stratigraphy and structure of the Chesapeake Group in Virginia and Maryland 52
- Massachusetts—environmental geology**
pollution: No polychlorinated biphenyls in induced recharge from the Housatonic River, Massachusetts 238
 — Treated-sewage plume in a sand and gravel aquifer, Cape Cod, Massachusetts 237-238
- Massachusetts—geomorphology**
glacial geology: Evidence for a major pre-Wisconsin glacial event in New England 119
 — Giant involutions in the upper Wisconsin drift of Nantucket Island 119
 — High kames trace fractures in late Wisconsinan ice in southeastern Massachusetts 47
- Massachusetts—hydrogeology**
ground water: Evaluation of the Mattapoisett aquifer 85-86
 — Ground-water assessment in the Connecticut Valley lowlands 85
 — Massachusetts 85-86
hydrology: Low-flow characteristics of Massachusetts streams 175-176
- Massachusetts—structural geology**
faults: Recurrent movements on faults north of Boston 47
- mathematical geology** *see also* automatic data processing
- mathematical geology—methods**
Fourier analysis: Application of linear algebra to computation of gridded data 297
- Mediterranean region** *see also* the individual countries
- meetings** *see* symposia
- Mesozoic** *see also under* geochronology *under* California; *see also under* stratigraphy *under* Alaska; Atlantic Ocean; California; New Mexico
- metal ores** *see also* manganese ores; niobium ores; tantalum ores; *see also* undereconomic geology *under* Alaska; North Carolina; United States
- metals—geochemistry**
ground water: Geochemistry of the Bradys Hot Springs geothermal area, Churchill County, Nevada 153
sediments: Bottom-sediment chemistry of the Saw Mill River, Westchester County, New York 146
 — Comparison of metal and other trace-element concentrations on streambed sediments from forested, agricultural, and coal-mining areas of southwestern Indiana 225-226
water: Trace-metal partitioning in suspended sediments from urban storm-water runoff 102
- metamorphic rocks** *see also* igneous rocks; metamorphism; metasomatism
- metamorphic rocks—metasedimentary rocks**
gondite: Geology of the Piedmont between the Brevard and Towaliga fault zones, central Georgia 49
tourmaline: Tourmaline-rich rocks as possible indicators of massive sulfides 6
- metamorphic rocks—migmatites**
petrology: Granitic rocks and migmatites in the Coast plutonic complex near Petersburg 80-81
- metamorphic rocks—mineral assemblages**
research: Mineral assemblages and compositional variations, Barrovian metamorphic sequence, near Juneau 80
- metamorphic rocks—petrology**
processes: Metamorphic rocks and processes 145
- metamorphism** *see also* metamorphic rocks; metasomatism
- metamorphism—regional metamorphism**
shale: Regional metamorphism of organic matter in Devonian shale of Appalachian basin 30
- metasomatic rocks** *see also* igneous rocks; metamorphic rocks; metamorphism; metasomatism
- metasomatism** *see also* metamorphism
- metasomatism—processes**
hydrothermal alteration: Landsat hydrothermal alteration mapping of Richfield; CUSMAP 262
 — Large hydrothermal systems studied in Carolina slate belt 6
 — Mineralogy and stable isotope geochemistry of hydrothermally altered rocks from the East Pacific Rise and the Mid-Atlantic Ridge 149
 — Thematic mapper detection of hydrothermal alteration in Marysvale, Utah 260
- meteor craters** *see also* meteorites
- meteorites—composition**
chondrites: The paradox of aqueous inclusions in a chondritic meteorite from Jilin, China 143
- methods** *see under* cartography *under* maps; *see under* engineering geology *under* automatic data processing; New York; *see under* experimental studies *under* paleomagnetism; *see under* imagery *under* remote sensing; *see under* automatic data processing; chemical analysis; engineering geology; geochronology; geomorphology; geophysical methods; hydrogeology; hydrology; mathematical geology; mineral resources; remote sensing; spectroscopy; well-logging; *see under* mineral exploration *under* uranium ores; *see under* planning *under* land use
- Mexico** *see also* Gulf Coastal Plain
- Mexico—economic geology**
geothermal energy: Mexico 284-285
- Mexico—seismology**
earthquakes: Surface faulting in the Sonora, Mexico, earthquake of 1887 209
- Mexico—stratigraphy**
Paleozoic: Newly discovered Paleozoic section in central Sonora, Mexico 66
- Mexico—structural geology**
neotectonics: Deformation of the southern California uplift and the Colorado River delta 212
- Michigan—economic geology**
uranium ores: Electromagnetic geophysics of Jacobsville basin, northern Michigan 36-37
 — Uranium in Archean migmatites, northern Michigan 36

- water resources*: Michigan 86
 — Water in Van Buren County 86
 — Water resources in Sleeping Bear Dunes National Lakeshore 86
- Michigan—environmental geology**
pollution: Contamination delineated at Wurtsmith Air Force Base, Michigan 237
- Michigan—geophysical surveys**
magnetic surveys: Electromagnetic geophysics of Jacobsville basin, northern Michigan 36-37
 — Magnetic terranes of Iron River quadrangle 133
maps: Magnetic terranes of Iron River quadrangle 133
- Michigan—hydrogeology**
ground water: Water quality of coal deposits and abandoned mines in Saginaw County, Michigan 227
hydrology: Flow model of Saginaw River 171
- Michigan—petrology**
igneous rocks: Lake Ellen Kimberlite, Michigan; thermobarometry of mantle inclusions 145
- Middle East** *see also* Jordan
- Midwest** *see also* Illinois; Indiana; Kansas; Michigan; Minnesota; Missouri; Nebraska; North Dakota; Ohio; South Dakota; Wisconsin
- Midwest—areal geology**
regional: Central Region 53-54
- Midwest—hydrogeology**
ground water: Central Midwest RASA Study 106-107
- mineral deposits, genesis—manganese ores**
chert: Origin of manganese deposits in Franciscan rocks of the Yolla Bolly Terrane, California 5
sedimentary processes: A new genetic model for sedimentary manganese deposits 1
- mineral deposits, genesis—mineral resources**
hydrothermal processes: Ore genesis processes at Gilman-Leadville 7
- mineral deposits, genesis—uranium ores**
sedimentary processes: Origin of uranium deposits, Smith lake district, New Mexico 39
- mineral exploration—biogeochemical methods**
uranium ores: Geochemical exploration by analyses of fecal material from herbivorous mammals 11
- mineral exploration—geobotanical methods**
bryophytes: Uranium in spring water and bryophytes at Basin Creek in central Idaho 10
- mineral exploration—geochemical methods**
massive deposits: Trace-element geochemistry of the West Shasta District, California 10
mineral resources: Detailed study of Mohawk Mountain geochemical anomaly 4
 — Regional geochemical exploration in Alaska 2-3
monazite deposits: Probable monazite in South Carolina 10
resources: Geochemical and geophysical techniques in resource assessments 10-11
stream sediments: Geochemical mapping of the southern Coast Ranges of California 10
tin ores: Geochemical investigation of a molybdenum-tin anomaly in southwestern Utah 10
 — Geochemical investigation of a molybdenum-tin anomaly in southwestern Utah 10
- mineral exploration—geophysical surveys**
base metals: Anomalous electrical conductors as indicators of potential mineralization 11
electrical surveys: Crown Point uranium mineralization trend, New Mexico 11
mineral resources: Magnetic provinces, tectonostratigraphic terranes, and resource guides, Lake Clark quadrangle, Alaska 11
 — Magnetic provinces, tectonostratigraphic terranes, and resource guides, Lake Clark quadrangle, Alaska 11
- mineral inclusions** *see under* inclusions
- mineral prospecting** *see* mineral exploration
- mineral resources** *see also* the individual deposits; *see also under* economic geology *under* Alaska; Arizona; automatic data processing; Basin and Range Province; California; Colorado; Great Plains; Gulf of Mexico; Minnesota; Montana; Nevada; New Mexico; New York; Pacific Ocean; Rocky Mountains; United States
- mineral resources—exploration**
analysis: Mineral resource analysis 12
- mineral resources—methods**
automatic data processing: Data collection and processing 12
- mineral resources—resources**
development: Hydrologic aspects of coal- and mineral-resource development 223-229
evaluation: Mineral-resource assessments; land areas 2-5
 — United States and world mineral-resource assessments 1-2
exploration: Geochemical and geophysical techniques in resource assessments 10-11
mineral exploration: Geologic studies of mining districts and mineral-bearing regions 5-10
policy: Resource information systems and analysis 12
research: Mineral-resource investigations 1-13
sedimentary rocks: Sedimentary mineral resources 12-14
- mineralogy—experimental studies**
crystal chemistry: Mineralogic studies in crystal chemistry 138-140
- USGS*: Geochemistry, Mineralogy, and Petrology 136-152
- minerals** *see also* crystal chemistry
- minerals—carbonates**
genesis: The origin of carbonate minerals in the Upper Freeport bed 22
- minerals—chain silicates**
bustamite: Stability of ferrobustamite 138-139
- minerals—chain silicates, clin amphibole**
hornblende: Chemical compositions of igneous hornblende amphiboles 139-140
- minerals—chain silicates, pyroxene group**
decomposition: Pyroxene decomposition in kimberlites 138
- minerals—framework silicates, silica minerals**
quartz: Authigenic quartz in coal 22
 — Silica solubilities in hydrothermal salt solutions 137
- minerals—geochemistry**
electron diffraction analysis: Characterization of mineral precipitates by electron diffraction 139
- minerals—oxides**
magnetite: Silicon-bearing magnetite 139
manganese oxides: Electron-diffraction patterns of manganese oxides 138
- minerals—properties**
thermodynamic properties: National Center for the Thermodynamic Data of Minerals 137-138
 — Thermodynamic properties of minerals 137
- minerals—sheet silicates, chlorite group**
chlorite: Chlorite associated with Henry Mountains uranium deposits 139
- minerals—sulfates**
selenite: Hydrogeology of the Culpeper basin 92
- minerals—sulfides**
pyrite: Use of Mossbauer spectroscopy to identify iron-sulfide minerals in coal 23-24
- Minnesota—economic geology**
geothermal energy: Aquifer thermal-energy storage in the Franconia-Ironton-Galesville aquifer, St. Paul, Minnesota 152-153
mineral resources: Genesis of sulfide ores in the Duluth Complex 5
- Minnesota—hydrogeology**
ground water: Appraisal of coal-tar derivatives in ground water in St. Louis Park, Minnesota 86
 — Appraisal of surficial aquifers 86
 — Appraisal of the surficial aquifers in the Pomme de Terre and Chippewa River valleys, western Minnesota 167
 — Ground-water use in Minneapolis-St. Paul area, Minnesota 104
 — Minnesota 86-87
 — Northern Midwest (Minnesota) RASA Study 107
 — Water-quality appraisal of sand-plain aquifers 86-87

- hydrology*: Hydrology of Big Marine Lake, Washington County, Minnesota 191
 — Model simulation of runoff hydrographs in the Coon Creek watershed, Anoka County, Minnesota 171
 — Quality of runoff from watersheds in the Twin Cities metropolitan area, Minnesota 102-103
- Miocene** *see also under* geochronology *under* New Mexico; *see also under* stratigraphy *under* Alabama; Alaska; Arizona; Barbados; Maryland; Oregon; Virginia
- Miocene—stratigraphy**
biostratigraphy: Mesozoic and Cenozoic studies 177-180
- miospores** *see under* palynomorphs
- Mississippi—economic geology**
lignite: Stratigraphic framework and distribution of lignite along Wilcox outcrop belt, Mississippi 17
- Mississippi—engineering geology**
geologic hazards: Hydraulic-model study of impact of Interstate route 10 crossing on backwater and flow distribution of lower Pearl River 173
- Mississippi—hydrogeology**
ground water: Geochemistry of water from Cretaceous aquifers in the Southeastern United States; Mississippi, Alabama, Georgia, and South Carolina 146
- Mississippi—stratigraphy**
Eocene: Stratigraphic framework and distribution of lignite along Wilcox outcrop belt, Mississippi 17
Paleocene: Stratigraphic framework and distribution of lignite along Wilcox outcrop belt, Mississippi 17
- Mississippi Valley—structural geology**
tectonics: Tectonic history of the Mississippi Embayment 222
- Mississippian** *see also under* stratigraphy *under* Eastern U.S.; Georgia; North America; Western U.S.
- Missouri—environmental geology**
land use: Land use and land cover and environmental photographic interpretation keys; a guide for Missouri 300
maps: Land use and land cover and environmental photographic interpretation keys; a guide for Missouri 300
- Missouri—hydrogeology**
ground water: Ground-water flow patterns in northeastern Missouri 94
 — Missouri 94
- Mollusca—Ammonoidea**
Cretaceous: K-Ar ages of bentonites in the Seabee Formation, northern Alaska 150-151
- Mollusca—Bivalvia**
Cretaceous: K-Ar ages of bentonites in the Seabee Formation, northern Alaska 150-151
- mollusks—ammonoids**
Mississippian: Late Kinderhookian (Early Mississippian) ammonoids from the Western United States 181-182
- mollusks—biostratigraphy**
Cambrian: Cambrian mollusk studies 182-183
Mesozoic: New ages for Franciscan rocks of Hull Mountain areas, northern California 69
Miocene: Asiatic mollusks in Miocene faunas of the Alaska Peninsula 178-179
Permian: New fossils from Taku terrane suggest Permian metallogenic province 79-80
- molybdenum ores** *see also under* economic geology *under* Idaho; Indiana; Kentucky; Montana; Nevada; Tennessee; Utah; Washington
- monazite deposits** *see also under* economic geology *under* South Carolina
- Montana—economic geology**
chromite ores: The B chromite zone of the Stillwater Complex, Montana 6
coal: Coal-bed correlation in the Powder River basin, Montana 18
 — Coal in the northeastern part of the Crow Indian Reservation, Montana 19
 — Volcanic episodes in Montana coal bed 17-18
copper ores: Mineral resources of the Mt. Henry RARE II Study Area, Lincoln County, Montana 3
 — Stable isotope systematics of copper-silver occurrences in the Belt Supergroup 148-149
lignite: Lignite deposits in the Fort Peck Indian Reservation, Montana 19
mineral resources: Resource appraisal completed for Wallace 1° × 2° quadrangle, Montana and Idaho 4
molybdenum ores: Geochemistry and resource potential of the Selway-Bitterroot Wilderness 2
natural gas: Facies control of porosity in Mississippian gas reservoirs, northwestern Montana 27
petroleum: Geochemical prospecting over Bell Creek oil field, Powder River Basin 25
 — Interpretation of upper Paleozoic lineaments as an aid to petroleum exploration in southwestern Montana 27-28
 — New structural interpretation as an aid to petroleum exploration of Snowcrest Range area, southwestern Montana 27
silver ores: Mineral resources of the Mt. Henry RARE II Study Area, Lincoln County, Montana 3
 — Stable isotope systematics of copper-silver occurrences in the Belt Supergroup 148-149
tin ores: Geochemistry and resource potential of the Selway-Bitterroot Wilderness 2
uranium ores: Thrust fault uranium in overthrust and disturbed belts, Montana 40
- Montana—environmental geology**
geologic hazards: Effects of urbanization on flood peaks, Missoula, Montana 236
 — Flood estimation in Montana 236
pollution: Ground water near wastewater-treatment facilities in Glacier National Park, Montana 238-239
- Montana—geochronology**
Pleistocene: Fission-track ages and structure in clinker 59
 — Volcanic ash on Missouri River—Yellowstone River drainage divide, Montana 60
Pliocene: Fission-track ages and structure in clinker 59
- Montana—geomorphology**
glacial geology: Pinedale deglaciation in the North Fork of the Flathead Valley, Montana 59
- Montana—geophysical surveys**
remote sensing: Comparison of SLAR and DEM shaded relief imagery 304-305
 — Detection of forested wetlands and perennial snow or ice using SLAR imagery 305-306
 — Mapping forest fuels and predicting wildland fire behavior 257
 — Screenless lithographic printing of 1:250,000-scale SLAR imagery 306
- Montana—hydrogeology**
ground water: Geochemistry and hydrology of the Decker and Big Sky coal-mining areas, southeastern Montana 227
 — Montana 94-95
 — Montana RASA Study 107-108
 — Potential impacts of coal mining in selected areas of eastern Montana 227-228
 — Water-resources investigations of the Lake Creek valley, northwestern Montana 94-95
hydrology: Dissolved-solids model of the Tongue River, Montana 188-189
 — Hydrology and potential effects of mining in the Cook Creek and Snider Creek areas, Montana 227
 — Joint United States-Canada study of flow of Milk River at the Montana-Alberta border 275-276
 — Primary productivity at Lake Koocanusa, Montana 192
 — Quality of streams in the Bull Mountains region, south-central Montana 227
 — Surface-water quality in east-central Montana 185-186
 — Water-quality of small reservoirs in northeastern Montana 192
 — Water use in Montana 104
thermal waters: Hydrothermal systems in Montana 155-156
- Montana—mineralogy**
chain silicates, clin amphibole: Chemical compositions of igneous hornblende amphiboles 139-140
- Montana—petrology**
igneous rocks: Geology of the Anaconda-Pintlar Wilderness Study Area, Montana 54

- Geology of the Bitterroot lobe of the Idaho batholith 54-55
- Mapping at the eastern edge of the Idaho batholith, Montana 54
- Petrology of alkaline intrusive rocks, western Montana 145
- Tectonic framework of Chief Joseph plutonic complex, southwest Montana 55
- Montana—stratigraphy**
- Cretaceous*: Influence of storms and paleotectonism on shelf sedimentation in Montana, South Dakota, and Wyoming 56
- Precambrian*: Spokane Formation (Belt Supergroup), northwest Montana 58
- Stratigraphy of the Lower Belt Supergroup, Glacier National Park, Montana 59
- Tertiary*: Coal-bed correlation in the Powder River basin, Montana 18
- Montana—structural geology**
- faults*: Thrust faults in the Highland Mountains, Montana 61
- folds*: Monocline southwest of Cedar Creek anticline, Montana 61
- tectonics*: Interpretation of upper Paleozoic lineaments as an aid to petroleum exploration in southwestern Montana 27-28
- Libby thrust belt, northwestern Montana 60
- Tectonic framework of Chief Joseph plutonic complex, southwest Montana 55
- Moon—geomorphology**
- impact features*: Lunar crater studies 248
- Lunar geology 248
- volcanic features*: Morphometry of the volcanoes 247
- Moon—petrology**
- basalts*: Lunar geology 248
- Moon—theoretical studies**
- investigations*: Lunar investigations 248
- moraines** *see under* glacial features *under* glacial geology
- Mossbauer spectroscopy** *see under* analysis *under* iron; *see under* geochemistry *under* coal; *see under* methods *underspectroscopy*
- mud volcanoes** *see also* volcanology
- museums** *see also* associations; survey organizations

N

- natural gas** *see also under* economic geology *under* Appalachians; Colorado; Eastern U.S.; Great Plains; Montana; New Mexico; Virginia
- Nebraska—geomorphology**
- fluvial features*: Morphologic changes in Platte River channels 161
- Nebraska—geophysical surveys**
- remote sensing*: Using aircraft and satellite acquired data to estimate food available to refuge waterfowl 256-257

- Nebraska—hydrogeology**
- ground water*: Geohydrology of the High Plains aquifer system in Nebraska 95
- Nebraska 95
- Stream-aquifer interrelations in southeast Nebraska 190-191
- hydrology*: Large-scale bedforms in the Platte River, Nebraska 161
- Stream-aquifer interrelations in southeast Nebraska 190-191
- Streamflow changes in Platte River basin 174
- Nebraska—sedimentary petrology**
- sedimentation*: Sediment transport and effective discharge 161
- sediments*: Estimating water discharge for channel-width maintenance 161
- neodymium— isotopes**
- Nd-144/Nd-143*: Neodymium and strontium isotopes in inclusions from the Sierra Nevada 147-148
- neotectonics** *see also under* structural geology *under* California; Mexico; Utah
- Nevada—areal geology**
- Nye County*: Geologic and tectonic history of the southern Great Basin and Amargosa drainage system in southwestern Nevada 64-65
- Nevada—economic geology**
- cesium ores*: Cesium concentrations in caldera complex, Nevada and Oregon 10
- geothermal energy*: Geochemistry of the Bradys Hot Springs geothermal area, Churchill County, Nevada 153
- mineral resources*: Preliminary resource appraisal in the southern Snake Range, Nevada 3
- molybdenum ores*: Ages of mineralization at the Buckingham molybdenum deposit, Nevada 6-7
- uranium ores*: Redistributed uranium as indicator of incipient rock/water interaction 44
- Uraniferous opal, Virgin Valley, Nevada: conditions of formation 43
- Uranium occurrences with base and precious metals in Excelsior Mountains, Nevada 35
- vanadium ores*: Age of vanadiferous shales in central Nevada 63
- Nevada—engineering geology**
- explosions*: Geology of Nuclear Test Sites, Nevada Test Site 231
- nuclear facilities*: Investigation of a potential nuclear waste repository site, Nevada Test Site 232
- underground installations*: Geology of Nuclear Test Sites, Nevada Test Site 231
- waste disposal*: Investigation of a potential nuclear waste repository site, Nevada Test Site 232
- NTS radioactive waste isolation 132-133
- Nevada—environmental geology**
- geologic hazards*: Flood potential, Fortymile Wash and tributaries, southern Nevada 236

- Nevada—geochemistry**
- isotopes*: Negative δO^{18} values in cataclastic plutonic rocks 149-150
- Strontium-isotope composition of plutons in the southern Snake Range, Nevada 149
- trace elements*: Geochemistry of the Bradys Hot Springs geothermal area, Churchill County, Nevada 153
- Nevada—geochronology**
- Cretaceous*: Ages of mineralization at the Buckingham molybdenum deposit, Nevada 6-7
- Jurassic*: Radiometric ages of two-mica granites of northeastern Nevada 150
- Nevada—geophysical surveys**
- gravity surveys*: Comparison of Bouguer anomaly and isostatic residual maps of Nevada 63
- magnetic surveys*: Investigation of a potential nuclear waste repository site, Nevada Test Site 232
- magnetotelluric surveys*: Magnetotelluric soundings over the Colorado Plateau and Basin and Range provinces 134
- maps*: Comparison of Bouguer anomaly and isostatic residual maps of Nevada 63
- remote sensing*: Identification of altered minerals by using airborne spectral reflectance 259-260
- well-logging*: Interpretation of borehole geophysical data at NTS 132
- Nevada—hydrogeology**
- ground water*: Ground water in Kyle and Lee Canyons, Spring Mountains, southern Nevada 98
- Mathematical model of the Eagle Valley ground-water basin, west-central Nevada 166
- Nevada 98
- hydrology*: Evaluation of streamflow-data networks 172
- Nutrient loads to Lahontan Reservoir, west-central Nevada 193
- Streamflow data network for Nevada 173
- Water budget for Wahoe Valley near Reno, Nevada 98
- Nevada—petrology**
- igneous rocks*: Progress in correlation and age determination of late Cenozoic tephra 68-69
- intrusions*: Permian plutons in north-central Nevada 66
- Nevada—stratigraphy**
- Paleozoic*: Early Paleozoic Basin margin, Antelope Range, Nevada 181
- Nevada—structural geology**
- tectonics*: Inferred pre-Oligocene strike-slip fault zone in central Nevada 64
- Permian and Triassic tectonic events in northern California and adjacent Nevada 63
- New England—areal geology**
- regional*: New England 47-49

- New England—economic geology**
uranium ores: Two-mica granite geochronology, tectonic space, and uranium content 45
- New England—geochronology**
Precambrian: Two-mica granite geochronology, tectonic space, and uranium content 45
- New England—geophysical surveys**
remote sensing: Contracted satellite data relay study 264
- New England—structural geology**
tectonics: Exotic terranes in the New England Appalachians 48-49
- New Hampshire—economic geology**
tin ores: Geochemical anomalies of tin and tungsten in north-central New Hampshire 4
tungsten ores: Geochemical anomalies of tin and tungsten in north-central New Hampshire 4
- New Hampshire—geophysical surveys**
gravity surveys: Geophysical studies in the Sherbrooke and Lewiston 1° × 2° quadrangles, Vermont, New Hampshire, and Maine 4
- New Hampshire—structural geology**
faults: Juxtaposed terranes in northern New Hampshire: possible extension of Brevard zone 48
- New Jersey—economic geology**
uranium ores: Geochemical exploration by analyses of fecal material from herbivorous mammals 11
- New Jersey—geomorphology**
glacial geology: Faults in Pleistocene sediments at trace of Ramapo fault 49
 — Glacial Lake Passaic 163
- New Jersey—hydrogeology**
ground water: Analysis of fresh and saline ground water in the New Jersey Coastal Plain and Continental Shelf 109
- New Jersey—seismology**
seismicity: Seismo-tectonic model for Ramapo seismic zone, New York and New Jersey 49
- New Jersey—stratigraphy**
Pleistocene: Late Wisconsinan stratigraphy along the terminal moraine, northern New Jersey 47
- New Jersey—structural geology**
faults: Faults in Pleistocene sediments at trace of Ramapo fault 49
- New Mexico—economic geology**
base metals: Anomalous electrical conductors as indicators of potential mineralization 11
coal: Coal resources in the Alamo Band Navajo Indian Reservation, New Mexico 20
 — Coal resources in the Ramah Indian Reservation, New Mexico 20
 — Coal resources of the Canoncito Indian Reservation, New Mexico 21
 — Stratigraphic relations in Upper Cretaceous rocks of the Chaco area, New Mexico 19
- mineral resources*: Age of mineralization, Mogollon mining district, Catron County, New Mexico 9
 — Mineral resource potential, RARE II Study Areas, southwest New Mexico and east Arizona 4-5
natural gas: Origin of natural gases in San Juan basin 26
thorium ores: Thorium and rare-earth veins associated with alkalic rocks in New Mexico 37
uranium ores: Age of uranium mineralization of the Churchrock mine, New Mexico 43
 — Crown Point uranium mineralization trend, New Mexico 11
 — Geologic decision analysis in the San Juan basin, New Mexico 42
 — Origin of uranium deposits, Smith lake district, New Mexico 39
 — Petrographic investigations of primary uranium ore, Ambrosia Lake district, New Mexico 43
 — Reevaluation of Jurassic-Cretaceous contacts and uranium anomalies, Chama basin, New Mexico 40
 — San Juan basin drilling project, McKinley County, New Mexico 39
 — Uranium in the San Mateo Mountains, New Mexico 34
 — Westwater Canyon Sandstone Member of Morrison Formation 38-39
 — Westwater Canyon Sandstone Member of Morrison Formation 38-39
- New Mexico—engineering geology**
waste disposal: Hydrologic testing of low-permeability zones in southeastern New Mexico at the Waste Isolation Pilot Plant 170
- New Mexico—geochronology**
Miocene: Age of mineralization, Mogollon mining district, Catron County, New Mexico 9
thermoluminescence: Thermoluminescence dating of pedogenic calcium carbonate 151-152
- New Mexico—geophysical surveys**
remote sensing: Geologic applications of Landsat 3 RBV images 253-254
 — Paleoshorelines in the Point Lookout Sandstone, San Juan Basin, New Mexico 259
- New Mexico—hydrogeology**
ground water: Computing recharge to alluvial basins in New Mexico 169-170
hydrology: Preliminary analysis of historical streamflow and water-quality records for the San Juan River basin, New Mexico and Colorado 174
- New Mexico—petrology**
igneous rocks: Studies in Wheeler Peak, Latir Peak, and Columbine-Hondo area, New Mexico 55
volcanism: Cogenetic volcanic and granitic rocks of Miocene age in the Questa caldera, northern New Mexico 143
- New Mexico—seismology**
earthquakes: Quaternary faulting along the La Jencia fault, central New Mexico 210
- New Mexico—stratigraphy**
Cretaceous: Cretaceous-Tertiary boundary iridium anomaly 177
 — Iridium anomaly at Cretaceous-Tertiary boundary, New Mexico 57
 — Megafossil plant zonation, Raton Basin, New Mexico 178
 — Paleoshorelines in the Point Lookout Sandstone, San Juan Basin, New Mexico 259
 — Stratigraphic relations in Upper Cretaceous rocks of the Chaco area, New Mexico 19
Jurassic: Westwater Canyon Sandstone Member of Morrison Formation 38-39
Mesozoic: San Juan basin drilling project, McKinley County, New Mexico 39
paleomagnetism: Paleomagnetic evidence for structural development of the Latir volcanic field, New Mexico 130-131
Tertiary: Cretaceous-Tertiary boundary iridium anomaly 177
 — Iridium anomaly at Cretaceous-Tertiary boundary, New Mexico 57
Triassic: Details of Chinle stratigraphy in northwest New Mexico 56
- New Mexico—structural geology**
faults: Reserve graben, southwestern New Mexico and eastern Arizona 61
foliation: Deformation of Precambrian rocks along Jemez zone, New Mexico 60
- New York—economic geology**
industrial minerals: Tourmaline-rich rocks as possible indicators of massive sulfides 6
mineral resources: Detailed study of Mohawk Mountain geochemical anomaly 4
uranium ores: Geochemical exploration by analyses of fecal material from herbivorous mammals 11
 — Geochronology of a xenotime-monazite gneiss, southern New York 36
- New York—engineering geology**
methods: Engineering geologic mapping in New York City 219
- New York—environmental geology**
pollution: Aldicarb pesticide contamination in ground-water in eastern Suffolk County, Long Island, New York 238
 — Bottom-sediment chemistry of the Saw Mill River, Westchester County, New York 146
- New York—geochemistry**
maps: Detailed study of Mohawk Mountain geochemical anomaly 4
- New York—geochronology**
Precambrian: Geochronology of a xenotime-monazite gneiss, southern New York 36

- New York—geomorphology**
glacial geology: Analysis of faulted glacial pavement in southeastern New York 48
- New York—hydrogeology**
ground water: Evaluation of ground-water resources in the Montauk area, Long Island 87
 — Nassau County Recharge Project, Long Island, New York 169
 — New York 87-88
 — Potential supplement to New York City water supply 87
hydrology: Quality and quantity of urban stormwater runoff to recharge basins, Long Island, New York 103
 — Synoptic study of snowpack chemistry 87-88
- New York—seismology**
seismicity: Seismo-tectonic model for Ramapo seismic zone, New York and New Jersey 49
- New York—structural geology**
faults: Fault definition and seismicity in the Ramapo seismic zone 49
- Nicaragua—engineering geology**
earthquakes: Nicaragua 285
- niobium ores—resources**
economics: Niobium and tantalum world resource picture 1
- noble gases** *see also* argon; helium
- noble gases—geochemistry**
fumaroles: Noble gases of the Lassen geothermal system 155
- nodules—composition**
manganese composition: Geochemistry of sea-floor minerals and sediments 110
- North America** *see also* Appalachians; Atlantic Coastal Plain; Canada; Great Lakes; Great Lakes region; Great Plains; Gulf Coastal Plain; Mexico; Rocky Mountains; United States
- North America—economic geology**
coal: Coal occurrences of North America and adjacent areas 15
- North America—stratigraphy**
Mississippian: Mississippian coral zonation, western North America 183
- North Carolina—economic geology**
coal: Paleocology of a Mesozoic rift lake 16
construction materials: Mineral production from counties in the Charlotte 1° × 2° quadrangle, North and South Carolina 3
metal ores: Mineralization in North Carolina RARE II Areas 9
- North Carolina—engineering geology**
waterways: Effects of channel excavation in North Carolina 173
- North Carolina—geophysical surveys**
gravity surveys: Aeromagnetic and gravity data over the eastern overthrust 133-134
magnetic surveys: Aeromagnetic and gravity data over the eastern overthrust 133-134
- remote sensing*: Utility of a digital data base for improving Landsat classification results and managing a forested wetland 257
- seismic surveys*: Geologic history of Cape Hatteras 113
- North Carolina—hydrogeology**
hydrology: Water quality of the Cape Fear River, North Carolina 186
- North Carolina—oceanography**
continental shelf: Geologic history of Cape Hatteras 113
- North Carolina—paleobotany**
angiosperms: Computer model of wetlands forest 183
- North Carolina—structural geology**
tectonics: An Avalonian terrane in the Charlotte 2°-quadrangle, North and South Carolina Piedmont 50-51
- North Dakota—economic geology**
coal: Coal deposition in the southwestern Williston basin, North Dakota 17
- North Dakota—geophysical surveys**
magnetic surveys: Magnetic survey of eastern North Dakota 133
- North Dakota—hydrogeology**
ground water: Extension of Spiritwood aquifer system through North Dakota into Canada 95
 — North Dakota 95
- Northern Hemisphere** *see also* Africa; Asia; Atlantic Ocean; Central America; North America; Pacific Ocean; USSR
- Northern Territory—economic geology**
uranium ores: Geologic studies of the Ranger uranium deposits, Northern Territory, Australia 36
- nuclear explosions** *see under* explosions *under* seismology; *see under* explosions
- nuclear facilities** *see also under* engineering geology *under* Nevada; United States
- nuclear facilities—feasibility studies**
research: Reactor Hazards Research Program 222-223
- O**
- ocean circulation** *see also under* oceanography *under* Atlantic Ocean
- ocean floors** *see also under* oceanography *under* Atlantic Ocean; Bering Sea
- Ohio—engineering geology**
slope stability: Economics of landslide research 221
 — Landslides in the greater Cincinnati area 221
- oil and gas fields** *see also under* economic geology *under* Kansas; United States
- oil shale** *see also under* economic geology *under* United States; Utah
- oil shale—resources**
statistical analysis: Oil-shale resources 33
- Oklahoma—environmental geology**
pollution: Possible sources of degradation of water quality of the Vamoosa-Ada aquifer, east-central Oklahoma 237
- Oklahoma—hydrogeology**
ground water: Geohydrology of the Roubidoux aquifer, northeastern Oklahoma 95
 — Ground water in the Oklahoma coal field 228
 — Numerical simulation of the alluvium and terrace aquifer along the North Canadian River from Canton Lake to Lake Overholser 167
 — Oklahoma 95
 — Quality of water from coal-mine spoil, eastern Oklahoma 228
hydrology: Suitability of surface-water of the Red River basin, Oklahoma, for water supply 185
 — Suspended sediment in the southern Oklahoma coal field 228
- Oklahoma—paleontology**
foraminifera: Fusulinids of the type Atokan Provincial Series, southern Oklahoma 181
- Oklahoma—stratigraphy**
Pennsylvanian: Fusulinids of the type Atokan Provincial Series, southern Oklahoma 181
- Oregon—economic geology**
cesium ores: Cesium concentrations in caldera complex, Nevada and Oregon 10
geothermal energy: Geothermal drilling at Newberry Volcano, Oregon 46
 — Geothermal systems of the Cascade Range 153-154
 — Geothermal test drilling at Newberry Volcano, Oregon 153
 — Magnetotelluric study of the Cascade Range 46
- Oregon—geochronology**
Holocene: ²¹⁰Pb geochronology, Upper Klamath Lake, Oregon 152
- Oregon—geophysical surveys**
magnetotelluric surveys: Magnetotelluric study of the Cascade Range 46
seismic surveys: Seismic studies between Crater Lake and Mount Hood 157-158
- Oregon—hydrogeology**
ground water: Declining ground-water levels in northeastern Oregon 99
 — Model of the regional aquifer system underlying the Snake River Plain in southern Idaho and eastern Oregon 166
 — Oregon 98-99
hydrology: Background-water quality in Three sisters area 99
 — Evaluation of selected one-dimensional stream water-quality models with field data 188
 — Precipitation quality in Salem 98-99
 — Water-quality studies of the Snake River Plain in southern Idaho and eastern Oregon 185
- Oregon—sedimentary petrology**
sedimentation: An evaluation of suspended sediment and turbidity in Cow Creek, Oregon 160

- Oregon—seismology**
earthquakes: Seismicity in the Cascades of Oregon and California 156
- Oregon—stratigraphy**
Cretaceous: Stratigraphy and sedimentology of the Hornbrook Formation 69
Miocene: Paleointensity study of the Steens Mountain, Oregon polarity transition 130
- Oregon—volcanology**
Mount Mazama: Climactic eruption of Mount Mazama and formation of Crater Lake caldera, Oregon 141-142
research: Seismic monitoring, Oregon and California volcanoes 216
South Sister: Late Holocene eruptions, South Sister Volcano, Oregon 217
- organic materials—geochemistry**
coal: The origin of primary pyrite in coal by bacterial diagenesis of organic sulfur 21-22
nuclear magnetic resonance: Solid-state - \div C nuclear resonance studies of coalified logs 22
organic carbon: Calculations of global rate of burial of Cretaceous organic carbon and oceanic stable carbon as an aid to source-rock studies 31
peat: Peat from Everglades: a study of the origin of coal and natural gas 21
uranium ores: Uranium, carbon, and sulfur in roll-type uranium deposits in Wyoming 43
- organic materials—humic acids**
models: Three-dimensional fluorescent spectra of humic acids 136-137
- organic materials—kerogen**
humic acids: Evolution of humic substances in mid-Atlantic OCS and slope sediments 31
- Ostracoda** *see also* ostracods
- ostracods—biostratigraphy**
Cenozoic: Cenozoic Studies, Gulf of Alaska Tertiary province 180
- oxides** *see under* minerals
- oxygen— isotopes**
O-18/O-16: $\delta^{18}\text{O}$ and δD anomalies as earthquake precursors 150
 — Mineralogy and stable isotope geochemistry of hydrothermally altered rocks from the East Pacific Rise and the Mid-Atlantic Ridge 149
 — Negative δO^{18} values in cataclastic plutonic rocks 149-150
 — Stable isotope interpretation of the Lassen geothermal system 154-155
 — Stable isotope systematics of copper-silver occurrences in the Belt Supergroup 148-149
- P**
- Pacific Coast** *see also* the individual states and provinces
- Pacific Coast—areal geology**
regional: Pacific Coast region 67-75
- Pacific Coast—geophysical surveys**
infrared surveys: Thermal-infrared surveys, Cascades volcanoes 216
- Pacific Ocean** *see also* Bering Sea
- Pacific Ocean—areal geology**
maps: Circum-Pacific Map Project 274
- Pacific Ocean—economic geology**
mineral resources: Sea-floor mineral and water resources 110-111
petroleum: CCOP/SOPAC 281
polymetallic ores: Geology and mineral deposits of the Juan de Fuca Ridge off Oregon 110
- Pacific Ocean—engineering geology**
slope stability: Subaqueous avalanching, Carmel Canyon, California 117
- Pacific Ocean—environmental geology**
pollution: Simulations of seabird damage and recovery from oilspills in the northern Gulf of Alaska 265-266
- Pacific Ocean—geochemistry**
isotopes: Mineralogy and stable isotope geochemistry of hydrothermally altered rocks from the East Pacific Rise and the Mid-Atlantic Ridge 149
- Pacific Ocean—geophysical surveys**
magnetic surveys: Repeat magnetic surveys 132
- Pacific Ocean—oceanography**
marine geology: Aleutian Ridge tectonics, petrology, and sedimentation 111-112
 — CCOP/SOPAC 281
 — Geology and mineral deposits of the Juan de Fuca Ridge off Oregon 110
nodules: Geochemistry of sea-floor minerals and sediments 110
sediments: Geotechnical properties and sedimentary processes of the Alaskan OCS 118
 — Sediment deposition on the Pacific continental margin 118
- Pacific Ocean—petrology**
lava: Petrology of Loihi Seamount, Hawaii 110
- Pacific Ocean—stratigraphy**
Cenozoic: Cenozoic Studies, Gulf of Alaska Tertiary province 180
 — Pacific climatostratigraphy by oceanic silicoflagellates 179
- Pacific Ocean—tectonophysics**
plate tectonics: Decoupling within the Aleutian subduction zone 111
- Pacific region** *see also* the individual countries
- Paleocene** *see also under* stratigraphy *under* Alaska; Mississippi
- paleoclimatology—changes**
experimental studies: Climate 162-165
- paleoclimatology—Miocene**
Pacific Ocean: Pacific climatostratigraphy by oceanic silicoflagellates 179
- paleoclimatology—Pliocene**
Pacific Ocean: Pacific climatostratigraphy by oceanic silicoflagellates 179
- paleoclimatology—Quaternary**
Alaska: Late Quaternary vegetation and climate history from western Alaska 162-163
- California*: Quaternary reference core 162
- paleoecology—Mesozoic**
North Carolina: Paleoecology of a Mesozoic rift lake 16
- Paleogene** *see also under* stratigraphy *under* Atlantic Ocean
- paleogeography—Cambrian**
Virginia: Cambrian paleographic features of the central Virginia Piedmont 49-50
- paleogeography—Cretaceous**
Colorado: Shifting margin of the Cretaceous sea in the San Juan basin 41
- paleogeography—Tertiary**
Wyoming: Pre-Oligocene valleys as guides for uranium and hydrocarbon accumulation 38
- paleomagnetism—experimental studies**
ilmeneite: The origin of reverse thermoremanent magnetism in ilmenite-hematite 131
methods: Rock magnetism 130-132
petrophysics: Petrophysics 132-133
USGS: Geomagnetism 132
- paleomagnetism—Jurassic**
California: Paleomagnetic evidence for structural rotation of the Klamath Mountains, California 131
Virginia: Lower Jurassic igneous rocks in the Culpeper basin, Northern Virginia 52-53
- paleomagnetism—Miocene**
Oregon: Paleointensity study of the Steens Mountain, Oregon polarity transition 130
- paleomagnetism—Paleocene**
Alaska: Limits to northward drift of the Paleocene Cantwell Basin, central Alaska 130
- paleomagnetism—Pleistocene**
Montana: Fission-track ages and structure in clinker 59
- paleomagnetism—Quaternary**
Idaho: A new reversed polarity event within Brunhes epoch 152
Oregon: Volcanic correlation and dating using geomagnetic secular variation 131
- paleontology—experimental studies**
applications: Paleontology 176-183
- Paleosols** *see under* soils *under* Alaska
- Paleozoic** *see also under* stratigraphy *under* Alaska; Mexico; Nevada; Plantae; Rocky Mountains; Washington
- Paleozoic—stratigraphy**
biostratigraphy: Paleozoic studies 180-183
- paleozoogeography** *see* biogeography
- palynomorphs—miospores**
Holocene: ^{210}Pb activity and pollen dating, Potomac estuary, Virginia 152
- peat** *see also under* economic geology *under* Alaska; Florida; Maine; United States; *see also under* organic residues *undersediments*
- Pelecypoda** *see* Bivalvia *under* Mollusca

Pennsylvania—engineering geology
slope stability: Landslides caused by intense storms in Pennsylvania 220-221

Pennsylvania—environmental geology
pollution: Effects of scrubber sludge disposal on hydrology of Beaver County, Pennsylvania 236-237
 — Organochlorine pesticide and polychlorinated biphenyl residues at four tropic levels in the Schuylkill River, Pennsylvania 237

Pennsylvania—geophysical surveys
remote sensing: Contracted satellite data relay study 264
 — Structural analysis; Valley and Appalachian Plateau, Pennsylvania 262-263

Pennsylvania—hydrogeology
ground water: Appraisal of aquifers 88
 — Numerical-model evaluation of groundwater resources in the lower Susquehanna River basin 88
 — Pennsylvania 88
hydrology: Cost-effectiveness in stream gaging in Pennsylvania 173
 — Effects of nonpoint sources to concentrations and loads of water-quality constituents in Pequea Creek basin, Pennsylvania 184
 — Evaluation of streamflow-data networks 172
 — Hydrology of the Eastern Coal Province, Pennsylvania 228
 — Temporal changes in chloride, sulfate, and sodium concentration in four eastern Pennsylvania streams 184
 — Water-quality loads of the Susquehanna River 189
 — Water-quality loads of the Susquehanna River at Harrisburg, Pennsylvania 189-190

Pennsylvania—sedimentary petrology
sediments: Sediment yields from areas affected by surface mining in Pennsylvania 161-162

Pennsylvania—structural geology
tectonics: A high Taconic slice in the Pennsylvania Piedmont 51
 — Structural analysis; Valley and Appalachian Plateau, Pennsylvania 262-263

Pennsylvanian see also under stratigraphy under Alabama; Georgia; Oklahoma

Pennsylvanian—geochemistry
isotopes: The origin of carbonate minerals in the Upper Freeport bed 22

permafrost see also under engineering geology under Alaska

Permian see also under stratigraphy under Alaska; California

Persian Gulf—geophysical surveys
remote sensing: Geologic applications of Landsat 3 RBV images 253-254

Peru—seismology
earthquakes: Aftershock investigations 202-203

petroleum see also under economic geology under Alaska; Asia; Atlantic Ocean; automatic data processing; China; Colorado; continental slope; Eastern U.S.; Florida;

Gulf of Mexico; Malaysia; Montana; Pacific Ocean; Rocky Mountains; United States; Wyoming

petroleum—exploration
organic materials: Calculations of global rate of burial of Cretaceous organic carbon and oceanic stable carbon as an aid to source-rock studies 31
paleoecology: Conodont study as an aid to petroleum exploration of Upper Devonian Rocks 31
reservoir rocks: Carbonate submarine fans: better petroleum reservoirs than carbonate-debris aprons 32
techniques: New exploration techniques 31-32

petrology—experimental studies
 USGS: Geochemistry, Mineralogy, and Petrology 136-152

Phanerozoic see also under stratigraphy under Basin and Range Province; Great Plains; Rocky Mountains

phase equilibria—silicates
thermodynamic properties: Thermodynamic properties of minerals 137

Philippine Islands—economic geology
energy sources: Philippines 285

phosphate deposits see also under economic geology under Tunisia; United States

physical geography see geomorphology

placers—gold ores
 Alaska: Recycled gold in interior Alaska 77-78
 — Recycled gold, interior Alaska 8-9

planetology see also Jupiter; Mars; Moon; Saturn; Venus

planetology—theoretical studies
solar system: The solar system 247-248
techniques: Astrogeology 242-248
 — Planetary studies 242-248

Plantae see also algae; angiosperm flora; angiosperms; bryophytes; palynomorphs; Protista

Plantae—biostratigraphy
Paleocene: Megafossil plant zonation, Ra-ton Basin, New Mexico 178

Plantae—paleoecology
Holocene: Plant ecology 183

Plantae—stratigraphy
Paleozoic: The Kanayut Conglomerate: one of North America's most extensive ancient fluvial deposits 77

plate tectonics see also under tectonophysics under Alaska; California; Caribbean region; Pacific Ocean; Washington

Pleistocene see also under geochronology under Atlantic Coastal Plain; Italy; Montana; *see also under stratigraphy under* Alaska; Basin and Range Province; Great Plains; New Jersey; Rocky Mountains

Pliocene see also under geochronology under Italy; Montana

plutons see under intrusions

Poland—economic geology
coal: Poland 273-274
sulfur deposits: Poland 273-274

pollution see also under environmental geology under Colorado; Massachusetts; Michi-

gan; Montana; New York; Oklahoma; Pacific Ocean; Pennsylvania; South Dakota

pollution—ground water
site exploration: Ground-water pollution 237-239

pollution—pollutants
water quality: Effects of pollutants on water quality 236-239

pollution—water
surface water: Surface-water pollution 236-237

polymetallic ores see also under economic geology under Pacific Ocean

Polynesia see also Samoa

Portugal—economic geology
water resources: Portugal 285

potash see also under economic geology under Thailand

Precambrian see also under geochronology under Australia; New England; New York; Saudi Arabia; *see also under stratigraphy under* Alaska; Colorado; Montana

Proterozoic see also under geochronology under Saudi Arabia; *see also under stratigraphy under* Wisconsin

Protista—Silicoflagellata
Miocene: Tropical Miocene silicoflagellates near Barbados 178

Protozoa see Protista

Puerto Rico—environmental geology
geologic hazards: Resident time of flood sediment on insular shelf 119

Puerto Rico—hydrogeology
ground water: Saltwater movement in the coastal areas 123-124

Puerto Rico—oceanography
marine geology: Northwestern insular shelf, Puerto Rico 119

Pyrenees see also France

pyrite see under sulfides under minerals

pyroclastics see under igneous rocks

Q

quartz see under framework silicates, silica minerals under crystal chemistry; minerals

Quaternary see also under geochronology under Idaho; *see also under stratigraphy under* Alaska; California; Texas; Utah; Washington; Western U.S.

R

racemization see under geochronology

radar methods see under methods under geophysical methods

radioactive dating see absolute age

radioactivity surveys see under geophysical surveys under Colorado

radiocarbon dating see absolute age

radiolarians—biostratigraphy
Carboniferous: Radiolaria indicate Carboniferous and Triassic ages for chert in the Circle Volcanics, Circle quadrangle 78
Devonian: Tectonostratigraphic terrane studies 75-76

- radium— isotopes**
Ra-228/Ra-226: Radiometric studies of geopressed systems 147
- rare earths** *see also* neodymium
- rare earths—geochemistry**
veins: Thorium and rare-earth veins associated with alkalic rocks in New Mexico 37
- rare gases** *see* noble gases
- reclamation** *see also under* environmental geology *under* Colorado
- regional geology** *see* areal geology under the appropriate area term
- remote sensing** *see also under* geophysical surveys *under* Africa; Alaska; Antarctica; Arizona; Australia; automatic data processing; Bering Sea; California; China; Colorado; Colorado Plateau; France; Hawaii; Jupiter; Mars; Montana; Nebraska; Nevada; New England; New Mexico; North Carolina; Pennsylvania; Persian Gulf; Saturn; Saudi Arabia; South America; South Dakota; Texas; Thailand; Tunisia; United States; USSR; Utah; Venus; Virginia; Washington; Wyoming; Yemen
- remote sensing— aerial photography**
cartography: Aerial Profiling of Terrain System 308
- remote sensing— applications**
imagery: Applications to geologic studies 259-263
- remote sensing— imagery**
applications: Land resource applications 255-259
 — Multispatial data acquisition and processing 302
automatic data processing: Image generation using film recorder 251
cartography: Analysis of the image chain in the orthophoto production system 308
 — Applications and techniques development for raster-formatted data 308-309
geological methods: Geologic applications 252-255
hydrology: Applications to hydrologic studies 263-264
Landsat: Analysis of return beam vidicon (RBV) radiometric response and development of correction techniques 251
 — Combination of unlike data sets 302
 — Geometric registration 250
 — Hydrologic applications 252
 — Image map research 302-303
 — Image processing laboratory developed to support uranium exploration 135
 — Landsat cartographic research 301
 — Method to improve reproducibility of Landsat color images 260
 — Multispectral classification procedures 251
methods: Spatial data analysis technique development 250
models: Remote image processing station (RIPS) research, development, and technology transfer 249-250
satellite methods: Mapsat 301-302
- remote sensing— methods**
automatic data processing: Computer system networking 249
 — Digital topographic data 250
 — Earth Resources Observation Systems Office 249
 — Innovative techniques for display of thematic maps 251-252
 — Inventory of computer software for spatial data handling 251
 — Spatial data handling capability assessment 249
 — Spatial data handling research and development 249-251
 — Techniques for the storage of very large spatial data sets 250-251
 — Techniques in processing digital data 251-252
geophysical methods: Remote sensing and advanced techniques 249-264
imagery: Analysis of SLAR imagery for identification of base map categories 306
satellite methods: Remote sensing and space technology research 301-304
 — Satellite surveying system 306-307
- reservoir rocks** *see under* exploration *under* petroleum
- resistivity** *see under* electrical logging *under* well-logging
- Rhode Island— environmental geology**
waste disposal: Radionuclide transport in glacial outwash, Wood River Junction, Rhode Island 235
- Rhode Island— geophysical surveys**
seismic surveys: Modern sedimentary environments and geologic history, Rhode Island inner shelf 119-120
- Rhode Island— hydrogeology**
hydrology: Radionuclide transport in glacial outwash, Wood River Junction, Rhode Island 235
- Rhode Island— oceanography**
continental shelf: Modern sedimentary environments and geologic history, Rhode Island inner shelf 119-120
- rivers** *see under* fluvial features *under* geomorphology
- rock mechanics— deformation**
field studies: Quaternary deformation of the Sacramento Valley and northern Sierra 222
strength: Role of water in crustal deformation 133
- Rocky Mountains** *see also* the individual states and provinces
- Rocky Mountains— areal geology**
regional: Rocky Mountains and the Great Plains 54-62
- Rocky Mountains— economic geology**
fuel resources: Great Plains and Rocky Mountain basins 24-26
 — Oil and gas resources of western Overthrust belt 26
mineral resources: Mineral resources 62
petroleum: Middle Paleozoic history interpretation as an aid to western Overthrust belt petroleum exploration 26-27
 — Western Overthrust Belt 26-28
- Rocky Mountains— geochemistry**
isotopes: Plumbic prospecting in the northern Rocky Mountains 148
- Rocky Mountains— geomorphology**
surficial geology: Surficial geology 59-60
- Rocky Mountains— petrology**
igneous rocks: Igneous rocks 54-55
- Rocky Mountains— stratigraphy**
Eocene: Eocene montane floras 178
Paleozoic: Middle Paleozoic history interpretation as an aid to western Overthrust belt petroleum exploration 26-27
Phanerozoic: Stratigraphy 55-59
Pleistocene: Distribution of pearlette family volcanic ash marker beds 56
- Rocky Mountains— structural geology**
tectonics: Structural geology 60-62
 — Tectonics 62
- Russia** *see* USSR

S

- Sahara** *see also* the individual countries
- Samoa— geochemistry**
isotopes: Atmospheric carbon dioxide 150
- satellite methods** *see under* imagery *under* remote sensing; *see under* methods *under* remote sensing
- Saturn— geophysical surveys**
remote sensing: Saturn investigations 242
 — Voyager 2 encounter 242
- Saudi Arabia— areal geology**
Al'Awshaziyah Quadrangle: Reconnaissance geology of the Al'Awshaziyah quadrangle 285-286
geology: Saudi Arabia 285-290
Wadi Bidah region: Regional assessment of the Wadi Bidah district 287
- Saudi Arabia— economic geology**
gold ores: Mineralization at the Mahd adh Dhahab gold mine 288
tungsten ores: Baid al Jimalah tungsten deposit 287-288
water resources: Water resources advisory service 289-290
- Saudi Arabia— geochronology**
Precambrian: Age of diorite-granodiorite gneisses 286
 — Implications of common lead measurements 286-287
Proterozoic: Age and strontium initial ratio of plutonic rocks 286
- Saudi Arabia— geophysical surveys**
gravity surveys: Bouguer gravity of a part of the southern Arabian Shield 288-289
remote sensing: Geologic applications of Landsat 3 RBV images 253-254
seismic surveys: Interpretation of seismic deep-refraction line 289
 — The Geophysical Observatory 289
- Saudi Arabia— petrology**
igneous rocks: Cenozoic volcanic rocks 287
 — Granitoid plutonic rocks of the Arabian Shield 287

- Saudi Arabia—structural geology**
tectonics: Mineralization at the Mahd adh Dhahab gold mine 288
- sedimentary petrology—experimental studies**
sedimentary rocks: Sedimentology 159-162
- sedimentary rocks** *see also* sedimentary structures; sedimentation; sediments
- sedimentary rocks—clastic rocks**
conglomerate: Burnt Island Conglomerate (Upper Triassic) on Screen Islands 79
 — Stratigraphy and sedimentology of the Hornbrook Formation 69
 — The Kanayut Conglomerate: one of North America's most extensive ancient fluvial deposits 77
tonstein: Tonsteins in the C coal bed, Emery coal field, Utah 22-23
turbidite: Structures in the offshore Eel River basin 67-68
- sedimentary rocks—geochemistry**
trace elements: Cretaceous-Tertiary boundary iridium anomaly 177
 — Iridium anomaly at Cretaceous-Tertiary boundary, New Mexico 57
 — Metals in black shales 12-13
 — Supracrustal stratigraphy and geochemistry, northern Wisconsin 53
- sedimentary rocks—organic residues**
coal: Coal deposition in the southwestern Williston basin, North Dakota 17
 — The origin of carbonate minerals in the Upper Freeport bed 22
 — Volcanic episodes in Montana coal bed 17-18
lignite: Chemical composition of gulf coast lignites 23
virginite: Analyses of samples from the Vermillion Creek coal bed, Sweetwater County, Wyoming 23
- sedimentary rocks—properties**
physical properties: Physical properties evaluation of the Wasatch Formation near Sheridan, Wyoming 218
- sedimentary structures** *see also* sedimentary rocks; sediments
- sedimentary structures—planar bedding structures**
cross-bedding: Interpretation of compound crossbedding in the Navajo and Entrada Sandstones of southwestern Utah 65
- sedimentation—cyclic processes**
deposition: Depositional cycles in the Chinle Formation 39
- sedimentation—deposition**
basins: Thickness of Quaternary sediments, central Puget lowland 72
continental margin: Sediment deposition on the Pacific continental margin 118
evolution: Evolution of sedimentary systems during the Mesozoic and Cenozoic Eras, southern Alaska 78-79
gravel: Pleistocene alluvial-gravel in eastern Idaho 63-64
- sedimentation—environment**
estuarine environment: China 281-282
 — Estuarine and coastal hydrology 122-124
 — Growth of estuarine-fouling organisms in Loxahatchee River estuary, Florida 124
 — The temporal scale of disturbance in estuarine benthic communities 122
fluvial environment: The Kanayut Conglomerate: one of North America's most extensive ancient fluvial deposits 77
 — Vegetation distribution relative to stream-channel morphology and sediment size characteristics 183
glaciofluvial environment: Quaternary floodplain deposits of the lower San Joaquin River 71
lacustrine environment: Lacustrine sediment cores in south-central Alaska 163
shelf environment: Influence of storms and paleotectonism on shelf sedimentation in Montana, South Dakota, and Wyoming 56
- sedimentation—precipitation**
salt: Diurnal periodicity in NaCl precipitation in Permian salt basins 139
- sedimentation—processes**
transgression: Middle Paleozoic history interpretation as an aid to western Overthrust belt petroleum exploration 26-27
- sedimentation—transport**
marine transport: Bottom stresses and sediment transport, central California continental shelf 117-118
 — Importance of mass sediment transport in continental margin processes 117
stream transport: An evaluation of suspended sediment and turbidity in Cow Creek, Oregon 160
 — Bedload studies in Wyoming 160
 — Channel change in the Big Lost River, Idaho 160
 — Effects of a flood-retarding dam 174
 — Runoff and sediment transport from an agricultural watershed in northern Illinois 162
 — Sediment transport and effective discharge 161
 — Sediment transport in the Tanana River near Fairbanks, Alaska, 1977-79 162
- sediments** *see also* sedimentary rocks; sedimentary structures; sedimentation
- sediments—clastic sediments**
gravel: Pleistocene alluvial-gravel in eastern Idaho 63-64
- sediments—composition**
clay: Origin of the fire clay parting in eastern Kentucky 16-17
heavy minerals: Hydraulic concentration of heavy minerals in Pleistocene glacial lake delta sands 1
mineral composition: Mineralogy of volcaniclastic sands associated with Glacier Peak 72
- sediments—distribution**
size distribution: Estimating water discharge for channel-width maintenance 161
- sediments—environmental analysis**
postglacial environment: Postglacial sediments of the northern Bering Sea 118
sediment yield: Long-term sediment yields from Bay Creek, Pike County, Illinois 160-161
 — Sediment yields from areas affected by surface mining in Pennsylvania 161-162
- sediments—geochemistry**
metals: Bottom-sediment chemistry of the Saw Mill River, Westchester County, New York 146
salinity: Physical and chemical properties of fine-grained sediments 146-147
trace elements: Comparison of metal and other trace-element concentrations on streambed sediments from forested, agricultural, and coal-mining areas of southwestern Indiana 225-226
water: Geochemistry of water and sediments 146-147
- sediments—organic residues**
peat: Peat from Everglades: a study of the origin of coal and natural gas 21
 — Peat petrology and aspects of coal formation in the Everglades, Florida 20
- sediments—properties**
mechanical properties: Geotechnical properties and sedimentary processes of the Alaskan OCS 118
- seismic surveys** *see under* geophysical surveys
under Alaska; Antarctica; Atlantic Ocean; Bangladesh; California; Great Britain; Great Lakes; Gulf of Mexico; Hawaii; North Carolina; Oregon; Rhode Island; Saudi Arabia; United States; Washington; Wyoming
- seismology** *see also* engineering geology
- seismology—earthquakes**
aftershocks: Aftershock investigations 202-203
aseismic margins: Triggering of earthquakes by aseismic crustal movements 206-207
causes: Geologic appraisal of earthquake potential and fault activity 208-211
 — Probable causes of earthquakes in southwestern Virginia 208
deformation: Geodetic appraisal of earthquake potential 212
displacements: Rupture processes of earthquakes 204-205
effects: Earthquake hazards studies 207-215
experimental studies: Seismologic appraisal of earthquake potential 207-208
fault scarps: Diffusion-equation model and degraded fault scarps, Colorado 209
faults: Evaluation of faulting near Monticello Reservoir, South California 211
 — Experimental studies of fault mechanics 204

- Mammoth Lake, California, earthquake studies 214-215
- Quaternary faulting along the La Jencia fault, central New Mexico 210
- Surface evidence of fault activity in California 208-209
- Surface faulting in the Sonora, Mexico, earthquake of 1887 209
- Westmorland, California, earthquake studies 215
- focus*: Southern Alaska seismicity during FY 81 207-208
- geologic hazards*: Structural framework and earthquake hazards of the Mississippi embayment 209-210
- gravity surveys*: Correlated changes in gravity, elevation and strain 206
- mechanism*: Earthquake mechanics and prediction studies 204-207
- observations*: National Earthquake Information Service 202
- precursors*: $\delta^{18}\text{O}$ and δD anomalies as earthquake precursors 150
- Theoretical mechanics of earthquakes precursors 204
- prediction*: Earthquake Early Alerting Service (EEAS) 202
- publications*: United States earthquakes 202
- reverse faults*: Earthquake, new reverse fault, and crustal unloading near Lompoc, California 214
- seismic gaps*: El Salvador seismic gap 206
- seismic intensity*: Location and intensity of the 1872 Washington State earthquake 208
- soils*: Soils chronology and fault history 210-211
- theoretical studies*: Theoretical investigations 203-204
- U. S. Geological Survey*: Earthquake Information Bulletin 317
- Earthquake publications 315
- velocity*: Seismic velocity measurements in the San Andreas fault zone 206
- volcanic earthquakes*: Hawaiian earthquakes 140
- Volcanic tremor and hydrothermal wedging 159
- seismology—explosions**
 - nuclear explosions*: U.S.S.R. underground explosions 231-232
- seismology—microearthquakes**
 - focal mechanism*: Regional investigators 203
- seismology—observatories**
 - Saudi Arabia*: The Geophysical Observatory 289
 - seismograms*: Operations 201
 - U. S. Geological Survey*: Observatories 202
- seismology—seismicity**
 - arrays*: Networks 201
 - colluvium*: Late Holocene geomorphic features near Cedar City, Utah 211
 - deformation*: Geodetic strain near Mammoth Lakes, California 206
 - earthquakes*: Seismicity in the Cascades of Oregon and California 156
 - experimental studies*: Special investigations 202-204
 - faults*: Fault definition and seismicity in the Ramapo seismic zone 49
 - Seismo-tectonic model for Ramapo seismic zone, New York and New Jersey 49
 - leveling*: Leveling surveys in southern California 212
 - observations*: Data and information 202
 - Seismicity 201-204
 - P-waves*: Seismic investigations in geothermal areas 156
 - prediction*: California seismicity studies for earthquake prediction 205
 - reflection*: Geothermal energy in magma 158
 - seismographs*: Research and development 201
 - upper mantle*: Gravity evidence of crust and mantle structure and seismicity 211
- shear zones** *see under* effects *under* faults
- shore features** *see under* geomorphology
- shorelines** *see also under* engineering geology *under* Texas
- shorelines—hydraulics**
 - coastal environment*: Nearshore and coastal studies 119-122
- sills** *see under* intrusions
- silver ores** *see also under* economic geology *under* Colorado; Idaho; Montana
- slope stability** *see also* engineering geology; geomorphology; *see also under* engineering geology *under* Appalachians; Atlantic Ocean; Bering Sea; California; Indonesia; Japan; Ohio; Pacific Ocean; Pennsylvania; United States; Washington
- slope stability—landslides**
 - field studies*: Landslide hazards 219-222
 - soil mechanics*: Dating landslides and other upper Pleistocene and Holocene features 221
- soil mechanics** *see also* rock mechanics
- soils—geochemistry**
 - helium*: Enhancement of data from helium soil gas surveys 42
- soils—surveys**
 - Alaska*: Geochemistry of vegetation, soils, and spoil materials, Jarvis Creek, Alaska 198-199
 - Atlantic Coastal Plain*: Soil chronosequences and ^{10}Be isotopic dating in mid-Atlantic States 51-52
 - California*: Rapidly migrating sand ridges and pulses of foreshore accretion 121
 - Colorado*: Geochemical variability of soils and plants in the Piceance Basin, Colorado 199
 - Illinois*: Analysis of soil cores beneath radioactive-waste-disposal site, Sheffield, Illinois 234
 - Indonesia*: Indonesia 282-283
 - United States*: Landsat applications for soil-vegetation inventory 255-256
- Swelling clays map of the United States 218
- Western U.S.*: Element content of rehabilitation plant species and their relation to mine-soil geochemistry 199-200
- Soils chronology and fault history 210-211
- solar system** *see under* theoretical studies *under* planetology
- solution features** *see under* geomorphology
- South Africa—petrology**
 - igneous rocks*: Pyroxene decomposition in kimberlites 138
- South America** *see also* Argentina; Peru
- South America—geophysical surveys**
 - remote sensing*: Global Magsat anomaly signatures emphasizing West Africa and eastern South America 252-253
- South Carolina—economic geology**
 - construction materials*: Mineral production from counties in the Charlotte $1^\circ \times 2^\circ$ quadrangle, North and South Carolina 3
 - monazite deposits*: Probable monazite in South Carolina 10
- South Carolina—engineering geology**
 - earthquakes*: Hazards information and warnings 240-241
 - geologic hazards*: Hazards information and warnings 240-241
 - waste disposal*: Hydrology of a low-level radioactive-waste burial site in South Carolina 235
- South Carolina—hydrogeology**
 - ground water*: Geochemistry of water from Cretaceous aquifers in the Southeastern United States; Mississippi, Alabama, Georgia, and South Carolina 146
 - hydrology*: Geologic and hydrologic effects of Late Cretaceous and Cenozoic faulting of the Coastal Plain near the Savannah River, Georgia and South Carolina 90
- South Carolina—stratigraphy**
 - Tertiary*: Geology of Tertiary sediments near the Cooke fault, Charleston, South Carolina 53
- South Carolina—structural geology**
 - faults*: Evaluation of faulting near Monticello Reservoir, South California 211
 - Polydeformed rocks in the Lowndesville shear zone, South Carolina and Georgia 52
 - tectonics*: An Avalonian terrane in the Charlotte 2° -quadrangle, North and South Carolina Piedmont 50-51
- South Dakota—environmental geology**
 - land use*: Sioux Falls area geographic analysis 258-259
 - pollution*: Molybdenosis associated with uranium-bearing lignites in South Dakota 200
- South Dakota—geophysical surveys**
 - remote sensing*: Determination of irrigation potential, Lower Brule and Crow Creek Indian reservations 252
 - Hydrologic information systems in Black Hills and Cheyenne River basin 252

- Sioux Falls area geographic analysis
258-259
- South Dakota—hydrogeology**
ground water: Aquifers in south-central South Dakota 96
— Large yields from glacial aquifers in Aurora and Jerauld Counties 95
— Outwash-channel aquifer in central South Dakota 95-96
— South Dakota 95-96
- South Dakota—stratigraphy**
Cretaceous: Influence of storms and paleotectonism on shelf sedimentation in Montana, South Dakota, and Wyoming 56
- Southern Hemisphere** *see also* Africa; Antarctica; Atlantic Ocean; Pacific Ocean; South America
- Southern U.S.** *see also* Alabama; Arkansas; Kentucky; Louisiana; Mississippi; Tennessee
- Southwestern U.S.** *see also* Arizona; New Mexico; Oklahoma; Texas
- Southwestern U.S.—hydrogeology**
ground water: Southwest Alluvial Basins RASA Study 108
- Soviet Union** *see* USSR
- spectrometry** *see* spectroscopy
- spectroscopy** *see also* chemical analysis
- spectroscopy—methods**
emission spectroscopy: Three-dimensional fluorescent spectra of humic acids 136-137
Mossbauer spectroscopy: Use of Mossbauer spectroscopy to identify iron-sulfide minerals in coal 23-24
nuclear magnetic resonance: Solid-state - ν C nuclear resonance studies of coalified logs 22
- spectroscopy—techniques**
instruments: Optimizing the selectivity of standard spectrofluorometers with computer control 198
- springs** *see also* ground water; *see also under* hydrogeology *under* Idaho
- strontium— isotopes**
Sr-87/Sr-86: Age and strontium initial ratio of plutonic rocks 286
— Age of diorite-granodiorite gneisses 286
— Neodymium and strontium isotopes in inclusions from the Sierra Nevada 147-148
— Strontium-isotope composition of plutons in the southern Snake Range, Nevada 149
- structural analysis** *see also* folds; foliation
- structural analysis—folds**
fabric: Tectonics reflected in sediments of the Morrison Formation in south-central Utah 65
foliation: Tectonic framework of Chief Joseph plutonic complex, southwest Montana 55
shear zones: Polydeformed rocks in the Lowndesville shear zone, South Carolina and Georgia 52
- structural analysis—foliation**
lineation: Deformation of Precambrian rocks along Jemez zone, New Mexico 60
- structural petrology** *see* structural analysis
- sulfates** *see under* minerals
- sulfides** *see under* minerals
- sulfur—geochemistry**
coal: The origin of primary pyrite in coal by bacterial diagenesis of organic sulfur 21-22
uranium ores: Uranium, carbon, and sulfur in roll-type uranium deposits in Wyoming 43
- sulfur— isotopes**
S-34/S-32: Geochemistry of oils from Pennsylvanian and Lower Permian Minnelusa Formation, Powder River Basin 25
- sulfur deposits** *see also under* economic geology *under* Poland
- sulphur** *see* sulfur
- survey organizations** *see also* associations
- survey organizations—general**
U. S. Geological Survey: Book reports 316
— Book reports 316-317
— Books and maps 314
— By mail 316-317
— Earthquake Information Bulletin 317
— Earthquake publications 315
— How to obtain publications 316-317
— Maps and charts 316
— Maps and charts 317
— National Technical Information Service 317
— Open-file reports 315
— Over the counter 316
— Publications issued 315
— Publications program 314-315
— State hydrologic unit maps 314
— State list of publications on hydrology and geology 314
— State water-resources investigations folders 314-315
— Surface-water, quality-of-water, and ground-water-level records 314
— U.S. Geological Survey publications 314-317
- Sweden— areal geology**
regional: Sweden 290
- Sweden—economic geology**
uranium ores: Age and genetic constraints for the uranium deposit at Lilljuthatten 290
- symposia—hydrogeology**
hydrology: Office of Water Data Coordination 99-100
- T**
- tantalum ores—resources**
economics: Niobium and tantalum world resource picture 1
- Tanzania—petrology**
igneous rocks: Pyroxene decomposition in kimberlites 138
- techniques** *see under* cartography *under* maps; *see under* exploration *under* petroleum; *see under* automatic data processing; hydrology; spectroscopy; well-logging; *see under* theoretical studies *under* planetology
- tectonics** *see also* faults; folds; structural analysis; *see also under* structural geology *under* Alaska; Appalachians; Arizona; Basin and Range Province; California; Colorado; Colorado Plateau; Great Lakes region; Great Plains; Mars; Mississippi Valley; Montana; Nevada; New England; North Carolina; Pennsylvania; Rocky Mountains; Saudi Arabia; South Carolina; United States; Utah; Venus; Virginia; Washington; West Virginia
- tectonics—concepts**
research: Reactor Hazards Research Program 222-223
- tektites** *see also* meteorites
- Tennessee—economic geology**
molybdenum ores: Metals in black shales 12-13
uranium ores: Metals in black shales 12-13
- Tennessee—engineering geology**
geologic hazards: Large, old debris avalanches in the Appalachians 221
- tephrochronology** *see under* geochronology
- terraces** *see under* fluvial features *under* geomorphology; *see under* glacial features *under* glacial geology; *see under* glaciation *under* glacial geology
- Tertiary** *see also under* stratigraphy *under* Alaska; Arizona; Atlantic Coastal Plain; Caribbean region; Colorado; Idaho; Montana; New Mexico; South Carolina; Utah; Washington
- Texas—engineering geology**
land subsidence: Differential subsidence at Houston, Texas, oil fields 239
shorelines: Upper Quaternary stratigraphy of a south Texas barrier island complex 120-121
- Texas—geochemistry**
properties: Diurnal periodicity in NaCl precipitation in Permian salt basins 139
- Texas—geochronology**
absolute age: Geochronology of roll-type uranium ores of the Felder deposit, Texas 151
- Texas—geophysical surveys**
remote sensing: Contracted satellite data relay study 264
- Texas—hydrogeology**
ground water: Projected effects of proposed salinity-control projects on fresh ground water in the upper Brazos and Wichita River basins, Texas 189
hydrology: Flow losses along the Nueces River, Cotulla to Simmons, Texas 176
- Texas—stratigraphy**
Quaternary: Upper Quaternary stratigraphy of a south Texas barrier island complex 120-121

Thailand—economic geology
geothermal energy: Thailand 290-291
lignite: Thailand 290-291
potash: Thailand 290-291

Thailand—geophysical surveys
electrical surveys: Thailand 290-291
remote sensing: Thailand 290-291

theoretical studies *see under* earthquakes
under seismology; *see under* deformation;
Moon; planetology

thermal analysis *see also* chemical analysis;
spectroscopy

thermal waters *see also under* hydrogeology
under California; Montana; United States;
Washington

thermoluminescence *see under* geochronology

thorium—geochemistry
monazite: Reversal of normal role of thorium
in fractional crystallization 145-146

thorium—isotopes
Th-230: Isotopic composition of uranium
and thorium in crystalline rocks 148

thorium ores *see also under* economic geology
under New Mexico; United States

thorium ores—resources
development: Nuclear-fuel resources 33-45

thrust faults *see under* displacements *under*
faults

tin—geochemistry
granites: Baid al Jimalah tungsten deposit
287-288

tin ores *see also under* economic geology *under*
Idaho; Montana; New Hampshire; Utah

tourmaline *see under* metasedimentary rocks
under metamorphic rocks

trace elements *see under* geochemistry *under*
California; igneous rocks; Nevada; sedi-
mentary rocks; sediments; Wyoming

Triassic *see also under* stratigraphy *under*
Alaska; Arizona; New Mexico; Utah

trilobites—biostratigraphy
Cambrian: Middle Cambrian fossils in cen-
tral Brooks Range, Alaska 180-181
Paleozoic: Early Paleozoic Basin margin,
Antelope Range, Nevada 181

tritium *see also* deuterium; hydrogen

tritium—geochemistry
thermal waters: Geochemistry of thermal
springs in the Idaho batholith region,
Idaho 153
water: Hydrology of a low-level radioac-
tive-waste burial site in South Carolina
235

tungsten—geochemistry
granites: Baid al Jimalah tungsten deposit
287-288

tungsten ores *see also under* economic geology
under New Hampshire; Saudi Arabia;
Washington

Tunisia—economic geology
phosphate deposits: Tunisia 291

Tunisia—geophysical surveys
remote sensing: Tunisia 291

U

underground installations *see also under* engi-
neering geology *under* automatic data proc-
essing; Nevada

underground water *see* ground water

United Kingdom *see also* Great Britain

United Kingdom—areal geology
regional: United Kingdom 290

United States *see also* Alabama; Alaska;
Arizona; Arkansas; California; Colorado;
Connecticut; Delaware; District of Co-
lumbia; Eastern U.S.; Florida; Georgia; Ha-
waii; Idaho; Illinois; Indiana; Kansas; Ken-
tucky; Louisiana; Maine; Maryland; Mas-
sachusetts; Michigan; Midwest; Min-
nesota; Mississippi; Missouri; Montana;
Nebraska; Nevada; New England; New
Hampshire; New Jersey; New Mexico;
New York; North Carolina; North Dakota;
Ohio; Oklahoma; Oregon; Pacific Coast;
Pennsylvania; Rhode Island; South Caroli-
na; South Dakota; Southwestern U.S.;
Tennessee; Texas; Utah; Vermont; Vir-
ginia; Washington; West Virginia; Western
U.S.; Wisconsin; Wyoming

United States—areal geology
regional: Regional geologic investigations
47-54

United States—economic geology
clays: Swelling clays map of the United
States 218
coal: Computerization of the Nation's coal
resources 15
— Field investigations 15
— General coal lease sales for FY 1981
127
— Known Recoverable Coal Resource
Areas 126
— Paleobotany 20-21
— Photointerpretation manual for surface
mining inspectors 255
fuel resources: Comparative organic geo-
chemistry of Middle Pennsylvanian shale
and coal 29
— Conterminous United States offshore
oil and gas resource assessments 32
— Midcontinent 28-29
— Onshore oil and gas lease sales 128
— Outer Continental Shelf lease sales for
oil and gas 129
geothermal energy: Known Geothermal Re-
source Areas 126
— Low-temperature geothermal resources
in the United States—1981 45
metal ores: Landsat evaluation of mineral
production areas of the United States
254
mineral resources: Management of mineral
leases on Federal and Indian lands
127-128
— Onshore oil and gas lease sales 128
— Outer Continental Shelf lease sales for
oil and gas 129
oil and gas fields: Known geologic struc-
tures of producing oil and gas fields
126
oil shale: Known leasing areas for sodium
and oil shale 126
peat: Paleobotany 20-21

petroleum: Potential petroleum traps in
Pennsylvanian rocks, northeastern New
Mexico 62
phosphate deposits: Phosphate resources in
the U.S. 12
thorium ores: Uranium contents of igneous
zircons and granitic rocks 42
uranium ores: Uranium contents of igneous
zircons and granitic rocks 42
water resources: Waterpower classification;
preservation of resource sites 127

United States—engineering geology
earthquakes: National earthquake data
base 207
— Regional and national seismic risk as-
sessment 212
foundations: Reactor site reviews 223
geologic hazards: Ground Failure Hazards
Reduction Program 219
— Regional and national seismic risk as-
sessment 212
nuclear facilities: Reactor site reviews
223
slope stability: Ground Failure Hazards Re-
duction Program 219
— National landslide hazards assessment
219

United States—environmental geology
conservation: Cooperation with other Fed-
eral agencies 129
— Management of natural resources on
Federal and Indian lands 125-127
— Waterpower classification; preservation
of resource sites 127
fuel resources: Management of oil and gas
leases on the Outer Continental Shelf
128-129
land use: An assessment of the accuracy of
land use and land cover maps 299
— Classification and evaluation of mineral
lands 125
— Classified land 125-126
— General coal lease sales for FY 1981
127
— Identifying changes in land use and land
cover 298-299
— Known geologic structures of producing
oil and gas fields 126
— Known Geothermal Resource Areas
126
— Known leasing areas for sodium and oil
shale 126
— Known Recoverable Coal Resource
Areas 126
— Land use and land cover statistics
299
— Management of mineral leases on Fed-
eral and Indian lands 127-128
— Management of oil and gas leases on the
Outer Continental Shelf 128-129
— Onshore oil and gas lease sales 128
— Outer Continental Shelf lease sales for
oil and gas 129

United States—geophysical surveys
gravity surveys: Gravity evidence of crust
and mantle structure and seismicity
211

- magnetic surveys*: Repeat magnetic surveys 132
 — Total magnetic intensity map of the U.S. 132
maps: Total magnetic intensity map of the U.S. 132
remote sensing: An assessment of the accuracy of land use and land cover maps 299
 — Evaluation of data from new satellite imaging systems for geologic applications 254
 — Landsat applications for soil-vegetation inventory 255-256
 — Landsat evaluation of mineral production areas of the United States 254
 — Photointerpretation manual for surface mining inspectors 255
seismic surveys: Deposition sequences and stratigraphic gaps of the U.S. Atlantic margin 113
- United States—hydrogeology**
ground water: Ground-water hydrology 165
 — Northeastern region 83-88
 — Regional Aquifer-System Analysis Program 106-109
 — Summary appraisals of the Nation's ground-water resources 165-166
 — Water-level changes in major aquifers of the Twin Cities metropolitan area 87
hydrology: Atmospheric Deposition Program 105-106
 — Data coordination, acquisition, and storage 99-101
 — National Hydrologic Bench-Mark Network 105
 — National Stream Quality Accounting Network 104-105
 — National water data exchange 100-101
 — National water-quality programs 104-105
 — Southeastern region 89-90
 — Urban stormwater data management system 101-102
 — Urban Water Program 101-103
 — Water-data storage system 101
 — Water use 103-104
thermal waters: Temperature versus depth in deep drill holes in the U.S. 156
- United States—oceanography**
continental shelf: Management of oil and gas leases on the Outer Continental Shelf 128-129
 — Outer Continental Shelf lease sales for oil and gas 129
- United States—seismology**
earthquakes: Structural framework and earthquake hazards of the Mississippi embayment 209-210
 — United States earthquakes 202
microearthquakes: Regional investigators 203
- United States—soils**
maps: Swelling clays map of the United States 218
- United States—structural geology**
tectonics: Continental margin structural frameworks 111-119
 — Regional tectonics 222
- United States—tectonophysics**
crust: Gravity evidence of crust and mantle structure and seismicity 211
mantle: Gravity evidence of crust and mantle structure and seismicity 211
- uranium— isotopes**
U-235/Pb-204: Geochronology of roll-type uranium ores of the Felder deposit, Texas 151
U-238/U-234: Isotopic composition of uranium and thorium in crystalline rocks 148
 — Late Cenozoic sea levels 164
- uranium ores** *see also* *undereconomic geology*
under Alaska; Arizona; Australia; automatic data processing; Colorado; France; Idaho; Indiana; Kentucky; Michigan; Montana; Nevada; New England; New Jersey; New Mexico; New York; Northern Territory; Sweden; Tennessee; United States; Utah; Western U.S.; Wyoming
- uranium ores—genesis**
geochemistry: Quartz behavior in vanadium-uranium deposits 44
- uranium ores—geochemistry**
reduction: Vanadium reduction in vanadium-uranium deposits 44-45
- uranium ores—mineral exploration**
helium: Enhancement of data from helium soil gas surveys 42
instruments: New borehole geophysical tools for uranium exploration 136
methods: Image processing laboratory developed to support uranium exploration 135
- uranium ores—resources**
development: Nuclear-fuel resources 33-45
- USGS—geomorphology**
landform description: Martian valleys and channels 244
- USSR—geophysical surveys**
gravity surveys: Structure of the Navarin and Anadyr Basins, Bering Sea 112
remote sensing: Evaluation of data from new satellite imaging systems for geologic applications 254
- USSR—seismology**
explosions: U.S.S.R. underground explosions 231-232
- Utah—economic geology**
coal: Intertonguing of the Blackhawk Formation and Star Point Sandstone, Wasatch Plateau, Utah 20-21
copper ores: Developing regional setting, copper-uranium prospects, Uinta basin, Utah 40
evaporite deposits: Marine evaporites in southwestern Utah 14
molybdenum ores: Geochemical investigation of a molybdenum-tin anomaly in southwestern Utah 10
- oil shale*: Oil-shale core drilling in Uinta basin, Utah 33
tin ores: Geochemical investigation of a molybdenum-tin anomaly in southwestern Utah 10
uranium ores: Chlorite associated with Henry Mountains uranium deposits 139
 — Developing regional setting, copper-uranium prospects, Uinta basin, Utah 40
 — Formation of a tabular vanadium-uranium deposit at a solution interface 44
vanadium ores: Formation of a tabular vanadium-uranium deposit at a solution interface 44
- Utah—engineering geology**
waste disposal: Dc resistivity survey at Gibson Dome and Lockhart basin, San Juan County, Utah 232-233
 — Quaternary deformation in the Fisher Valley area, Utah 232
- Utah—geophysical surveys**
electrical surveys: Dc resistivity survey at Gibson Dome and Lockhart basin, San Juan County, Utah 232-233
magnetotelluric surveys: Magnetotelluric soundings over the Colorado Plateau and Basin and Range provinces 134
remote sensing: Improved lithologic separation and data base application 255
 — Landsat hydrothermal alteration mapping of Richfield; CUSMAP 262
 — Tectonic implication of lineaments in the northern Paradox Basin, Utah and Colorado 261-262
 — Thematic mapper detection of hydrothermal alteration in Marysvale, Utah 260
well-logging: Hole-to-surface resistivity mapping homogeneity in bedded salt 133
- Utah—hydrogeology**
ground water: Response of ground water to rapid intrusion of magma 158
- Utah—mineralogy**
sheet silicates, chlorite group: Chlorite associated with Henry Mountains uranium deposits 139
- Utah—sedimentary petrology**
sedimentary rocks: Tonsteins in the C coal bed, Emery coal field, Utah 22-23
sedimentary structures: Interpretation of compound crossbedding in the Navajo and Entrada Sandstones of southwestern Utah 65
- Utah—stratigraphy**
Cretaceous: Intertonguing of the Blackhawk Formation and Star Point Sandstone, Wasatch Plateau, Utah 20-21
 — Late Cretaceous orogenic pulses in north-central Utah 57
Jurassic: Stratigraphic relations of the Arapien Shale, central Utah 58
Quaternary: Quaternary deformation in the Fisher Valley area, Utah 232
Tertiary: Relation of Bishop Conglomerate to Browns Park Formation in eastern

- Uinta Mountains, Colorado and Utah 57-58
- Triassic*: Depositional cycles in the Chinle Formation 39
- Utah—structural geology**
- faults*: Regional relations of Wah Wah-Frisco thrust fault in western Utah 64
- Young faulting, southwestern Wyoming and adjacent Utah 61-62
- neotectonics*: Late Holocene geomorphic features near Cedar City, Utah 211
- Quaternary deformation in the Fisher Valley area, Utah 232
- tectonics*: Direction of post-Oligocene klippen movement, Markagunt Plateau, Utah 62
- Late Cretaceous orogenic pulses in north-central Utah 57
- Tectonic implication of lineaments in the northern Paradox Basin, Utah and Colorado 261-262
- Tectonics reflected in sediments of the Morrison Formation in south-central Utah 65
- V**
- valleys** *see under* landform description *under* geomorphology
- vanadium—geochemistry**
- uranium ores*: Vanadium reduction in vanadium-uranium deposits 44-45
- vanadium ores** *see also* undereconomic geology *under* Colorado; Nevada; Utah
- vanadium ores—genesis**
- geochemistry*: Quartz behavior in vanadium-uranium deposits 44
- vanadium ores—geochemistry**
- reduction*: Vanadium reduction in vanadium-uranium deposits 44-45
- varves** *see* lacustrine features *under* geomorphology
- Venus—geophysical surveys**
- remote sensing*: Venus investigations 246-247
- Venus—structural geology**
- tectonics*: Venus tectonics 246-247
- Vermont—geophysical surveys**
- gravity surveys*: Geophysical studies in the Sherbrooke and Lewiston 1° × 2° quadrangles, Vermont, New Hampshire, and Maine 4
- Vertebrata** *see also* Mammalia
- vertebrates—biostratigraphy**
- Miocene*: Hemphillian vertebrate fauna from Mobile County, Alabama 179
- Virginia—economic geology**
- coal*: Coal resources in Tazewell County, Virginia 17
- Paleocology of a Mesozoic rift lake 16
- The Mississippian-Pennsylvanian boundary 15-16
- natural gas*: Fracture-blanket reservoir with high gas potential in Pine Mountain thrust sheet, Virginia 30

- Virginia—environmental geology**
- geologic hazards*: Botanical evidence of historic floods on Passage Creek, Virginia 183
- Virginia—geochemistry**
- processes*: Effects of chemical weathering on mine drainage in southwestern Virginia 229
- Virginia—geochronology**
- Holocene*: ²¹⁰Pb activity and pollen dating, Potomac estuary, Virginia 152
- Virginia—geomorphology**
- fluvial features*: Effects of Pleistocene glaciation on development of New River terraces, Virginia 50
- Virginia—geophysical surveys**
- remote sensing*: Remote sensing in vegetated areas 260
- Utility of a digital data base for improving Landsat classification results and managing a forested wetland 257
- Virginia—hydrogeology**
- ground water*: Aquifer model of the Culpeper basin, Virginia 166-167
- Hydrogeology of the Culpeper basin 92
- hydrology*: Streamflow duration during low-flow periods in strip-mined areas of southwestern Virginia 229
- Virginia 92
- Virginia—paleobotany**
- angiosperms*: Computer model of wetlands forest 183
- Virginia—petrology**
- intrusions*: Lower Jurassic igneous rocks in the Culpeper basin, Northern Virginia 52-53
- Virginia—seismology**
- earthquakes*: Probable causes of earthquakes in southwestern Virginia 208
- Virginia—stratigraphy**
- Cambrian*: Cambrian paleogeographic features of the central Virginia Piedmont 49-50
- Cretaceous*: Upper Cretaceous units in the southeastern Virginia Coastal Plain 108
- Holocene*: Botanical evidence of historic floods on Passage Creek, Virginia 183
- Vegetation distribution relative to stream-channel morphology and sediment size characteristics 183
- Miocene*: Stratigraphy and structure of the Chesapeake Group in Virginia and Maryland 52
- Virginia—structural geology**
- tectonics*: Cambrian paleogeographic features of the central Virginia Piedmont 49-50
- Structures in the Roanoke recess area, Virginia and West Virginia 50
- volcanic features** *see under* geomorphology
- volcanic rocks** *see under* igneous rocks
- volcanism** *see under* volcanology
- volcanoes** *see under* volcanology
- volcanology—volcanism**
- Cenozoic*: Cenozoic volcanism in Western United States 141-143
- damage*: Volcanic hazards 215-218
- eruptions*: Eruption rates and lava compositions, Craters of the Moon lava field, Idaho 142

- field studies*: Volcanic hazards assessment studies 216-218
- hydrology*: Hydrologic effects of volcanism 229-231
- infrared surveys*: Thermal-infrared surveys, Cascades volcanoes 216
- monitoring*: Volcano monitoring 215-216
- observatories*: Cascades Volcano Observatory 215
- stratovolcanoes*: Morphometry of the volcanoes 247
- vents*: Differentiation in the Springerville volcanic field, Arizona 142-143
- volcanic rocks*: Cogenetic volcanic and granitic rocks of Miocene age in the Quessa caldera, northern New Mexico 143
- volcanology—volcanoes**
- California*: Seismic monitoring, Oregon and California volcanoes 216
- Glacier Peak Volcano*: Distal debris from Glacier Peak Volcano, Washington 217
- Hawaii*: Hawaiian volcano studies 140-141
- Kilauea*: Eruption forecasting for Kilauea 140
- The August 1981 intrusive event at Kilauea Volcano 140
- Mauna Loa*: Eruptive recurrence, Mauna Loa volcano, Hawaii 216-217
- Mauna Loa Volcano 140
- Mount Mazama*: Climactic eruption of Mount Mazama and formation of Crater Lake caldera, Oregon 141-142
- Mount Saint Helens*: Acoustics of the May 18, 1980, lateral blast, Mount St. Helens 217-218
- Debris-flow monitoring at Mount St. Helens 230
- Effects of 1980 eruption of Mount St. Helens on selected lakes in Washington 230-231
- Engineering studies, May 1980 eruption, Mount St. Helens 217
- Hydrogen monitoring, Cascade volcanoes 216
- Mount St. Helens activity 215-216
- Mount St. Helens mapping 296
- Mount St. Helens posteruption flood hazards 229-230
- Postdepositional changes in Mount St. Helens ash 218
- Pre-1980 eruptions of Mount St. Helens, Washington 217
- Redistribution of the Mount St. Helens ash with time 71-72
- Mount Shasta*: Gravity monitoring, Mount Shasta and Lassen Peak, California 216
- South Sister*: Late Holocene eruptions, South Sister Volcano, Oregon 217

W

- Washington—areal geology**
- regional*: Washington 71-75
- Washington—economic geology**
- copper ores*: Geologic and mineral-resource studies, Glacier Peak Wilderness Area, Washington 3

- geothermal energy*: Thermal energy yield of Mt. St. Helens 263
- molybdenum ores*: Geologic and mineral-resource studies, Glacier Peak Wilderness Area, Washington 3
- Molybdenum and tungsten mineralization in northern Washington 74
- tungsten ores*: Molybdenum and tungsten mineralization in northern Washington 74
- Washington—engineering geology**
- earthquakes*: Quaternary geology and earthquake hazards in the Puget Sound region, Washington 213-214
- geologic hazards*: Debris-flow monitoring at Mount St. Helens 230
- Engineering studies, May 1980 eruption, Mount St. Helens 217
- Mount St. Helens posteruption flood hazards 229-230
- slope stability*: Landslides in the White Bluffs, north of Pasco, Washington 220
- Washington—geomorphology**
- fluvial features*: Chemical characteristics of selected rivers, western Washington, 1961-1980 72
- glacial geology*: Outwash terraces along the Cowlitz River 72
- Washington—geophysical surveys**
- infrared surveys*: Aerial infrared surveys at Mount St. Helens, Washington 261
- remote sensing*: Detection of forested wetlands and perennial snow or ice using SLAR imagery 305-306
- District satellite receive sites 264
- Screenless lithographic printing of 1:250,000-scale SLAR imagery 306
- Thermal energy yield of Mt. St. Helens 263
- seismic surveys*: Seismic studies between Crater Lake and Mount Hood 157-158
- Washington—hydrogeology**
- ground water*: Declining ground-water levels in east-central Washington 99
- Occurrence and quality of ground water in selected islands, San Juan County 99
- Washington 99
- hydrology*: Effects of 1980 eruption of Mount St. Helens on selected lakes in Washington 230-231
- Trophic classification of Washington lakes 193
- thermal waters*: Fumarolic incrustation at Mount St. Helens 155
- Washington—petrology**
- igneous rocks*: Redistribution of the Mount St. Helens ash with time 71-72
- Washington—sedimentary petrology**
- sediments*: Mineralogy of volcanoclastic sands associated with Glacier Peak 72
- Washington—seismology**
- earthquakes*: Location and intensity of the 1872 Washington State earthquake 208
- Volcanic tremor and hydrothermal wedging 159
- Washington—stratigraphy**
- Eocene*: Eocene montane floras 178
- Paleozoic*: Tectonostratigraphic terranes in northeastern Washington 72-73
- Quaternary*: Quaternary geology and earthquake hazards in the Puget Sound region, Washington 213-214
- Thickness of Quaternary sediments, central Puget lowland 72
- Tertiary*: Stratigraphy of Tertiary volcanic rocks, Cascade Range 74
- Washington—structural geology**
- faults*: Early Tertiary crustal extension in northeastern Washington 71
- The Pasayten fault, a major tectonic boundary in north-central Washington 75
- tectonics*: Tectonostratigraphic terranes in northeastern Washington 72-73
- Timing and nature of tectonic events in northwest Olympic Peninsula 73
- Washington—tectonophysics**
- plate tectonics*: Tectonic framework, continental margin of southwestern Washington 112
- Washington—volcanology**
- Glacier Peak Volcano*: Distal debris from Glacier Peak Volcano, Washington 217
- Mount Saint Helens*: Acoustics of the May 18, 1980, lateral blast, Mount St. Helens 217-218
- Hydrogen monitoring, Cascade volcanoes 216
- Mount St. Helens activity 215-216
- Mount St. Helens mapping 296
- Postdepositional changes in Mount St. Helens ash 218
- Pre-1980 eruptions of Mount St. Helens, Washington 217
- waste disposal** *see also under* engineering geology *under* automatic data processing; Basin and Range Province; Canada; Colorado; Idaho; Illinois; Nevada; New Mexico; South Carolina; Utah; Wyoming; *see also under* environmental geology *under* Alaska; Colorado; Florida; Illinois; Rhode Island; Western U.S.; Wyoming
- waste disposal—radioactive waste**
- controls*: Water analysis of salt deposits being considered for radioactive waste depositories 233
- environment*: Relation of radioactive waste to the geologic environment 232-233
- site exploration*: Relation of radioactive waste to the hydrologic environment 233-235
- well-logging*: Development of a borehole radar system 233
- water** *see also* ground water; hydrogeology; hydrology
- water quality** *see under* experimental studies *under* hydrology; *see under* geochemistry *under* ground water; *see under* models *under* ground water; *see under* pollutants *under* pollution; *see under* rivers and streams *under* hydrology
- water resources** *see also under* economic geology *under* Indian Ocean Islands; Michigan; Portugal; Saudi Arabia; United States
- water resources—resources**
- development*: Hydrologic aspects of coal- and mineral-resource development 223-229
- programs*: Special water-resource programs 99-109
- research*: Water-resource investigations 82-109
- waterways** *see also under* engineering geology *under* North Carolina
- weathering** *see also under* sedimentary petrology *under* Atlantic Coastal Plain
- weathering—analysis**
- chemical weathering*: Effects of chemical weathering on mine drainage in southwestern Virginia 229
- weathering—minerals**
- gibbsite*: Studies of depth of weathering on Atlantic Coastal Plain formations 50
- well-logging—acoustical logging**
- boreholes*: Characterizing hydraulic properties of fractured rock bodies with borehole geophysics 197
- Improvements to borehole acoustic-televiwer logging system 196
- Theoretical methods for interpreting shear and head waves in fluid-filled boreholes 195-196
- well-logging—electrical logging**
- boreholes*: Correlating surface geophysical surveys with borehole data 196
- resistivity*: Hole-to-surface resistivity mapping homogeneity in bedded salt 133
- Interpretation of borehole geophysical data at NTS 132
- Schlumberger soundings at Medicine Lake, California 134
- Schlumberger soundings in the Data Creek Basin, Arizona 134
- well-logging—interpretation**
- petrophysics*: Petrophysics 132-133
- waste disposal*: NTS radioactive waste isolation 132-133
- well-logging—methods**
- boreholes*: A new slim-hole gravity meter 136
- Development of a borehole radar system 233
- Hydraulic-conductivity logging 196-197
- well-logging—radioactivity**
- boreholes*: Geophysical well logs detect fractures in granite 132
- instruments*: New borehole geophysical tools for uranium exploration 136
- monitoring*: Estimating radioisotope concentrations with gamma-radiation well logs 234
- neutron probe*: Prototype compensated neutron prosity probe 196
- well-logging—techniques**
- observations*: Solute transport of in-situ oil-shale retort water in Wyoming 229
- West Indies** *see also* Barbados; Puerto Rico
- West Virginia—structural geology**
- tectonics*: Structures in the Roanoke recess area, Virginia and West Virginia 50

- Western Hemisphere** *see also* Atlantic Ocean; Central America; North America; Pacific Ocean; South America
- Western U.S.** *see also* Alaska; California; Colorado; Hawaii; Idaho; Montana; Nevada; Oregon; Pacific Coast; Utah; Washington; Wyoming
- Western U.S.—economic geology**
coal: Indian reservations 19-20
 — Western coal 17-19
geothermal energy: Geothermal energy in magma 158
uranium ores: Application of genetic-geologic models for uranium resource estimates 41-42
 — Geochemical characteristics of uranium-enriched volcanic rocks 33-34
- Western U.S.—engineering geology**
land subsidence: Mining depth and geology affect coal mine subsidence hazards 239
- Western U.S.—environmental geology**
waste disposal: Element content of rehabilitation plant species and their relation to mine-soil geochemistry 199-200
- Western U.S.—geochemistry**
experimental studies: Chemical composition of overburden rocks and sampling needs for reclamation of surface coal mines 200
- Western U.S.—geochronology**
Holocene: Geochronology 223
- Western U.S.—geomorphology**
glacial geology: Lake Bonneville revisited 163-164
- Western U.S.—hydrogeology**
hydrology: Western region 96-99
- Western U.S.—paleontology**
Mollusca: Late Kinderhookian (Early Mississippian) ammonoids from the Western United States 181-182
- Western U.S.—petrology**
volcanism: Cenozoic volcanism in Western United States 141-143
- Western U.S.—seismology**
seismicity: Seismic investigations in geothermal areas 156
- Western U.S.—soils**
geochemistry: Element content of rehabilitation plant species and their relation to mine-soil geochemistry 199-200
pedogenesis: Soils chronology and fault history 210-211
- Western U.S.—stratigraphy**
Mississippian: Late Kinderhookian (Early Mississippian) ammonoids from the Western United States 181-182
Quaternary: Volcanic correlation and dating using geomagnetic secular variation 131
- Wisconsin—hydrogeology**
ground water: Deep test wells 88
 — Ground-water-level fluctuations 88
 — High sodium and sulfate in ground water in Brown County, Wisconsin 186
 — Water use in Wisconsin in 1979 104
 — Wisconsin 88
- hydrology*: Hydrology of Wisconsin lakes potentially affected by acid deposition 191
- Wisconsin—stratigraphy**
Proterozoic: Supracrustal stratigraphy and geochemistry, northern Wisconsin 53
- Wisconsin—structural geology**
folds: Newly recognized gneiss dome, northeastern Wisconsin 53-54
- Wyoming—economic geology**
coal: A thick coal deposit in the Powder River basin, Wyoming 18
 — Coal in the Cow Creek Butte area, Little Snake River field, Wyoming 18
 — Coal resource assessment of the Wind River Indian Reservation, Wyoming 19-20
fuel resources: Vertical seismic profiles help detect stratigraphic oil and gas traps 135
geothermal energy: Geologic mapping in Yellowstone National Park 156
maps: Geologic mapping in Yellowstone National Park 156
petroleum: Geochemistry of oils from Pennsylvanian and Lower Permian Minnelusa Formation, Powder River Basin 25
 — Interpretation of Cretaceous stratigraphy as an aid to petroleum exploration between Moxa arch and Overthrust belt, southwestern Wyoming 28
uranium ores: Pre-Oligocene valleys as guides for uranium and hydrocarbon accumulation 38
 — Tuffaceous sediments as source rocks for uranium: a case study in Wyoming 43-44
 — Uranium, carbon, and sulfur in roll-type uranium deposits in Wyoming 43
- Wyoming—engineering geology**
geologic hazards: Physical properties evaluation of the Wasatch Formation near Sheridan, Wyoming 218
land subsidence: Subsurface movements in abandoned coal mine 218-219
waste disposal: Estimating radioisotope concentrations with gamma-radiation well logs 234
- Wyoming—environmental geology**
waste disposal: Changes in trace-element composition of sagebrush close to Bridger Powerplant, Wyoming 198
- Wyoming—geochemistry**
isotopes: Isotopic composition of uranium and thorium in crystalline rocks 148
trace elements: Changes in trace-element composition of sagebrush close to Bridger Powerplant, Wyoming 198
- Wyoming—geochronology**
Archean: Geochemical, isotopic, and petrologic studies of an Archean granite, Owl Creek Mountains, Wyoming 144
- Wyoming—geomorphology**
fluvial features: Scattered high-level terrace remnants along Nowood Creek, Bighorn basin, Wyoming 59-60
- Wyoming—geophysical surveys**
remote sensing: Geologic applications of Landsat 3 RBV images 253-254
 — Geologic mapping with HCMM data in the Powder River Basin, Wyoming and Cabeza Prieta, Arizona 261
seismic surveys: Vertical seismic profiles help detect stratigraphic oil and gas traps 135
well-logging: Estimating radioisotope concentrations with gamma-radiation well logs 234
- Wyoming—hydrogeology**
ground water: Joints and ground-water flow in oil shale in Wyoming 229
 — Solute transport of in-situ oil-shale retort water in Wyoming 229
hydrology: Channel-geometry relations for Wyoming streams 175
 — Streamflow changes in Platte River basin 174
- Wyoming—sedimentary petrology**
sedimentary rocks: Analyses of samples from the Vermillion Creek coal bed, Sweetwater County, Wyoming 23
sedimentation: Bedload studies in Wyoming 160
- Wyoming—stratigraphy**
Cretaceous: Influence of storms and paleotectonism on shelf sedimentation in Montana, South Dakota, and Wyoming 56
 — Interpretation of Cretaceous stratigraphy as an aid to petroleum exploration between Moxa arch and Overthrust belt, southwestern Wyoming 28
Eocene: Physical properties evaluation of the Wasatch Formation near Sheridan, Wyoming 218
- Wyoming—structural geology**
faults: Young faulting, southwestern Wyoming and adjacent Utah 61-62
- Wyoming—tectonophysics**
crust: Geologic mapping with HCMM data in the Powder River Basin, Wyoming and Cabeza Prieta, Arizona 261

X

X-ray analysis *see also* chemical analysis; spectroscopy

xenoliths *see under* inclusions

Y

Yemen—geophysical surveys
remote sensing: Yemen Arab Republic 291

Yemen—hydrogeology
ground water: Yemen Arab Republic 291

Z

zoogeography *see* biogeography

INVESTIGATOR INDEX

A

Aburto, A.	206
Ager, T. A.	77, 162
Aleinikoff, J. N.	36
Algermissen, S. T.	202, 212, 223
Allredge, L. R.	132
Allen, H. E., Jr.	162
Allen, R. V.	87
Alley, W. M.	101
Altschuler, Z. S.	21
Anderson, B. M.	198
Anderson, L. A.	132
Anderson, T. W.	108
Anderson, W. H.	256
Anderson, W. L.	134, 135
Andrews, E. D.	279
Andrews, J. S.	223
Anima, R. J.	117, 121
Antweiler, J. C.	5
Applegate, A. W.	29
Applegate, L. H.	183
Argyropoulos, George	276
Armbrustmacher, Theodore J.	145
Armstrong, A. K.	66
Arndt, H. H.	19
Arnold, E. P.	223
Arntson, A. D.	171
Arteaga, F. E.	98, 166
Arthur, M. A.	25, 31
Arthur, Michael	114
Ascher, Uri	212
Ashe, S. J.	8
Atkins, R. L.	49
Atwater, B. F.	71, 72
Aubel, James	291
Aubele, J. C.	142
Avanzino, R. A.	188
Avanzino, R. J.	192
Ayers, M. A.	102
Ayuso, R. A.	6

B

Bachman, L. J.	85
Back, William	279, 281
Bacon, C. R.	131, 141, 153
Bailey, G. B.	255
Bailey, Z. C.	84
Bakun, W. H.	205
Balch, A. H.	135
Baldwin, Frank	207
Baldwin, M. J.	232
Ball, M. M.	111
Ball, Mahlon	272
Baltz, E. H.	62
Bamber, E. W.	183
Barclay, C. S. V.	18
Barker, J. B.	184
Barker, J. L.	237
Barker, R. M.	59
Barnes, C. R.	87

Barnes, H. H.	279
Barnes, I. K.	279
Bartsch-Winkler, S. B.	163
Baskerville, C. A.	219, 223
Bassari, M.	289
Bateman, P. C.	275
Bath, G. D.	232
Batten, L. G.	252
Beall, R. M.	291
Beauchemin, P. R.	221
Bedinger, M. S.	233, 279
Beeson, M. H.	156
Belkin, H. E.	143
Belknap, D. F.	53
Bell, Henry	10
Belt, E. S.	17
Bencala, K. E.	188
Bennett, M. J.	219
Bennetti, J. B., Jr.	218
Benton, L. L.	281
Berg, H. C.	79
Bergin, M. J.	272
Bernknopf, R. L.	221
Berryhill, H. L.	282
Bethel, John	72
Beverage, J. P.	194
Beyer, L. A.	136
Bigazzi, Giulio	283
Bigelow, B. B.	104
Billings, Patty	9
Billings, R. H.	197
Bingham, R. H.	235
Bisdorf, R. J.	134
Blackwelder, B. W.	53
Blair, W. N.	5
Blake, M. C., Jr.	5, 70
Blalock, M. E.	171
Blanchard, L. F.	20
Blome, Charles D.	69, 78
Blumer, S. P.	228
Bluntzer, R. L.	239
Boatwright, Jack	204
Bodenlos, Alfred	273
Bohor, B. F.	16, 22
Boje, R. R.	225
Bollinger, G. A.	208
Bonham, Selma	231
Bonner, K. G.	256
Bonner, W. J.	255
Booth, D. B.	74
Booth, J. S.	115
Borghese, J. V.	225
Bortleson, G. C.	99
Bosson, C. R.	223
Botbol, J. M.	281
Bothner, M. H.	116
Bothner, W. A.	4
Botinelly, Theodore	9
Boucher, Gary	112
Boudette, E. L.	45
Bowker, P. C.	113
Boyko, Christina	215
Brabb, Earl	284

Brabb, Earl E.	223
Bracken, R. E.	4
Bradbury, J. P.	162
Bradford, W. L.	105
Bradley, M. D.	54
Branson, F. A.	224
Bredehoeft, J. D.	285
Breed, C. S.	246
Breger, I. A.	21, 22
Brethauer, G. E.	231
Brew, D. A.	80
Brewer, M. C.	76
Bricker, O. P.	105
Briggs, J. P.	4
Briggs, N. D.	60
Brigham, Julie	177
Briskey, J. A.	275, 276
Britton, O. J.	201
Brockman, S. R.	223
Bromfield, C. S.	34
Brook, C. A.	159
Brooks, Rebekah	91
Brosge, W. P.	77, 181
Brouwers, E. M.	177, 180
Brown, A. E.	105
Brown, C. E.	6
Brown, D. E.	228
Brown, Louis	51, 221
Brown, P. E.	138
Brown, R. G.	102
Brown, T. L.	20
Bryant, Bruce	57
Bryant, Jack	251
Buckwalter, T. F.	236
Bukry, J. D.	178, 179
Buland, R. P.	203
Burford, R. D.	212
Burgan, R. R.	257
Burkham, D. E.	236
Burnett, W. C.	110
Burnley, Pam	133
Burrows, R. L.	162
Busacca, Alan	210
Bush, A. L.	3
Butler, H. M.	289
Butman, Bradford	116
Butt, K. A.	144
Bybell, L. M.	53
Byerlee, J. D.	204
Byrd, Ann	77

C

Cacchione, D. A.	117
Cahill, J. M.	235
Cain, D. L.	187
Calk, L. C.	137
Cameron, C. C.	1
Campbell, D. L.	133
Campbell, J. A.	40
Campbell, R. H.	221
Cannon, M. R.	227

Cannon, W. F. 1
 Cardinell, A. P. 115
 Carey, M. A. 15
 Cargill, Simon 282
 Carlson, M. A. 202
 Carlson, P. R. 118
 Carman, R. L. 193
 Carnese, M. J. 4
 Carr, M. H. 243, 244, 247
 Carr, W. J. 64
 Carrara, P. E. 59
 Carter, L. D. 76
 Carter, M. D. 15, 273
 Carter, R. F. 91, 172, 176
 Carter, W. D. 253, 254, 275
 Cartier, Kenn D. 175
 Casadevall, T. J. 155, 215
 Case, J. E. 11, 79, 115, 261, 276
 Cathcart, J. B. 12
 Cecil, C. B. 22, 23
 Champion, Duane E. 131, 142, 152
 Chandler, J. C. 21
 Chapelle, F. H. 146
 Chapman, Robert 75
 Charpentier, R. R. 32
 Chaves, Lisa 52
 Chavez, Pat 254
 Chen, H. H. 95
 Chen, J. H. 143
 Cheng, R. T. 122, 279
 Chidester, A. H. 273, 275, 276
 Chikao, Nishiwaki 274
 Chleboard, A. F. 218
 Choquette, A. F. 232
 Chou, I-Ming 138
 Choy, G. L. 203, 204
 Christenson, S. C. 167
 Christiansen, Robert. 272
 Cifuentes, I. L. 206
 Clague, David 110
 Clark, A. L. 281, 285
 Clark, M. M. 206, 214
 Clark, R. A. 276
 Clark, R. F. 8
 Clarke, A. L. 284
 Clarke, J. S. 91
 Clarke, S. H. 67
 Claypool, G. E. 24, 30
 Clayton, J. L. 25
 Cline, D. R. 99
 Cloern, J. E. 122
 Clow, G. D. 244, 247
 Clutson, F. G. 136
 Clynne, M. L. 154
 Coates, D. A. 59
 Cobb, E. D. 279
 Cobban, W. A. 28, 57, 150
 Cockerham, R. S. 205
 Coe, R. S. 130
 Coemaat, R. L. 228
 Coffin, J. E. 188
 Cole, J. C. 287
 Coleman, James M. 117
 Coleman, R. C. 287
 Collender, Edward 279
 Collier, J. D. 34
 Colman, S. M. 209, 232
 Colton, R. B. 60, 61
 Condit, Christopher 142

Coney, P. J. 75, 79
 Connor, C. W. 17
 Connor, J. J. 58
 Conrad, Gerry 204
 Conyac, Martin 3
 Cook, A. O. 156
 Cook, H. E. 32
 Cook, J. L. 281, 284, 285
 Cooley, R. L. 166
 Cooper, A. K. 112
 Cooper, J. A. 151
 Cooper, Roger 182
 Corchary, G. S. 231
 Cordes, E. H. 195
 Cormier, V. F. 203
 Corvalan, Jose 274
 Costa, J. E. 236
 Cox, D. P. 6
 Cox, L. J. 48
 Coxe, B. W. 2
 Cradock, Campbell 274
 Crawford, J. K. 186
 Crawford, T. J. 15
 Cressman, E. R. 4, 60
 Crone, A. J. 61, 209, 222
 Cronin, Thomas M. 120
 Crosby, Eleanor 272
 Crovelli, R. A. 32
 Crowe, B. M. 64
 Crowley, K. D. 161
 Crowley, S. S. 15
 Crumpler, L. S. 142
 Culbertson, W. C. 18
 Cummings, T. R. 86, 237
 Cunningham, C. G. 288
 Cunningham, K. I. 28
 Curtin, G. C. 2
 Curtiss, D. A. 160
 Curwick, P. B. 171
 Cushing, G. W. 78

D

Dalrymple, G. Brent 142, 151, 152
 Dalziel, Mary C. 25
 Daniel, R. G. 156
 Daniels, D. L. 133
 Daniels, Jeff J. 132, 133
 Daugherty, K. I. 276
 Davidson, D. F. 276
 Davies, P. A. 99
 Davies, W. E. 221
 Davis, D. A. 281
 Davis, J. O. 68
 Davis, M. E. 108
 Davis, P. A. 170, 291
 Davis, Philip 244
 Davis, R. E. 227
 Daws, T. A. 29
 Dean, Walter 199
 DeBuchanne, G. D. 281
 Dehnehy, K. F. 170
 Delaney, P. T. 158
 Delevaux, M. H. 9
 Delevaux, Maryse 148
 deLima, Virginia 85
 Dempsey, William J. 231
 DeNoyer, J. M. 276, 281
 Denver, J. M. 84

Desmarais, N. R. 55
 Dethier, D. P. 72, 217
 Detra, D. E. 2, 10
 Detterman, R. L. 2, 77, 79
 Devine, J. F. 223
 Dewey, J. D. 169
 Dewey, J. W. 207
 Dickey, D. D. 61, 223
 Dickey, J. W. 265
 Dickinson, K. A. 35, 40
 Dieterich, J. H. 204
 Dillon, W. P. 112, 114, 177
 Diment, W. H. 136
 Dingler, J. R. 117, 121
 Dion, N. P. 193, 230
 Dixon, G. L. 232
 Dodge, F. C. W. 137, 147
 Dodge, H. W., Jr. 40
 Doe, B. R. 9
 Doe, Bruce R. 148
 Doeblich, J. 288
 Domenick, M. A. 147
 Domenico, J. A. 4, 10
 Donnell, J. R. 17
 Donnelly-Nolan, J. M. 141
 Donovan, T. J. 25
 Douglass, R. C. 181
 Douth, Fred 274
 Doyel, W. W. 285
 Doyle, W. H., Jr. 171
 Doyle, W. Harry, Jr. 101
 Drake, D. E. 117
 Dressen, Roland 31
 Drummond, Kenneth 274
 Duff, J. H. 193
 Duffield, W. A. 153
 Duffield, Wendell 272
 Duigon, M. T. 226
 Dulong, F. T. 22, 23
 Dunlap, L. E. 191
 Dunrud, C. R. 239
 Dutro, J. T., Jr. 77, 181
 Duttweiler, K. A. 9
 Duttweiler, K. D. 2
 Duval, J. S. 135, 260
 Dwyer, J. L. 255

E

Earhart, R. L. 59
 Ebens, R. J. 288
 Eberl, D. D. 279
 Eckhardt, D. A. 88
 Edwards, B. D. 118
 Edwards, Brian D. 67
 Edwards, Lucy E. 53
 Edwards, T. K. 185
 Ege, J. E. 282
 Ege, J. R. 221, 239
 Ehrlich, G. G. 169
 Eidenshink, J. C. 252
 Elder, J. F. 190
 Ellefson, B. R. 104
 Ellen, Stephen 220
 Elliott, J. E. 287
 Elliott, J. G. 175
 Ellis, M. J. 190
 Ellis, Margaret 17
 Ellsworth, W. L. 205, 223

Ellwood, B. B. 52
 Embrey, S. S. 193, 230
 Emmett, W. W. 160, 162, 279
 Emmons, P. J. 88
 Endo, E. T. 215
 England, A. W. 260
 England, K. J. 273
 Englund, K. J. 15, 17
 Ensign, P. S. 36
 Eppinger, R. H. 4
 Erdman, J. A. 10, 200
 Eschner, T. R. 161
 Eskenasy, D. M. 119
 Espinosa, A. F. 212, 285
 Evans, B. J. 23
 Evans, D. H. 203
 Evans, J. R. 156
 Eychaner, J. H. 224, 279

F

Fabiano, E. B. 132
 Fairchild, R. W. 95
 Farmer, M. L. 187
 Fassett, J. E. 57
 Fates, D. G. 137
 Faye, R. E. 90, 91, 171
 Feder, G. L. 200
 Fehn, Udo 9
 Felmlee, J. K. 35
 Feng, M. S. 255
 Ferguson, H. M. 245
 Fernald, A. T. 231
 Ferreira, R. F. 94, 192
 Ferris, D. C. 54
 Festa, John 122
 Feuquay, J. W. 255
 Feuquay, Jay 250
 Ficken, J. H. 194, 195
 Field, M. E. 67, 118
 Field, M. W. 118
 Field, S. J. 174
 Finch, W. I. 41
 Fischer, J. A. 118
 Fischer, Lynn 150
 Fishel, D. K. 189
 Fisher, G. T. 102
 Fisher, M. A. 24
 Fishman, N. S. 39
 Flanders, A. F. 276
 Fleck, R. J. 3, 286
 Fleisig, S. W. 221
 Fleming, R. W. 221
 Flippo, H. N. 172, 173
 Flores, R. F. 20
 Flores, R. M. 17, 120
 Flynn, K. M. 171
 Flynn, M. E. 132
 Fonseca, E. L. 219
 Foose, M. P. 5
 Foote, R. Q. 29, 32, 115
 Force, E. R. 1
 Ford, A. B. 3, 80
 Foster, H. L. 77, 78
 Foster, J. B. 234
 Fournier, R. O. 137, 290
 Fox, K. F., Jr. 72
 Francica, J. R. 255
 Frank, D. 263

Frank, David 216, 261
 Freeman, V. L. 17
 Frenzel, S. A. 230
 Fretwell, J. D. 124, 170
 Frickel, D. G. 224
 Friedman, I. 13
 Friedman, Irving 149, 150
 Friedman, J. D. 261, 263
 Friedman, Jules 216
 Frischknecht, F. C. 134
 Frishman, David 36
 Frizzell, V. A. 74
 Frizzell, V. A., Jr. 70
 Froelich, D. C. 173
 Fuis, G. S. 157
 Fuller, T. D. 265
 Futrell, J. C. 194, 195
 Futrell, J. C., III 279

G

Gage, T. B. 4
 Galloway, D. L. 225
 Galloway, J. P. 76
 Garabedian, S. P. 166
 Garcia, K. T. 193
 Gardner, J. V. 67
 Gardner, J. W. 117
 Gardner, R. A. 171
 Garmenzy, Lawrence 54
 Garrison, L. E. 117
 Garza, Sergio 189
 Gautier, Donald L. 24, 25
 Gay, F. B. 238
 Geiger, L. J. H. 188
 Geissman, John W. 59
 Geldon, A. L. 93
 Gerhart, J. M. 88
 Gettings, M. E. 288, 289
 Gibbons, A. B. 61
 Gilbert, J. J. 173
 Gillespie, W. H. 15
 Gilmore, J. D. 212
 Gilmore, J. S. 57
 Gilroy, E. J. 172
 Gleason, J. D. 149
 Glick, Ernest E. 209, 222
 Glover, K. C. 229
 Goetz, C. L. 174
 Gohn, G. S. 53, 223
 Goldberg, M. C. 136, 198
 Goldhaber, Martin B. 44
 Goldsmith, Richard 50
 Gordon, D. W. 207
 Gordon, L. S. 221
 Gordon, Mackenzie, Jr. 181, 182
 Gori, P. L. 240
 Gough, L. P. 198, 199
 Gower, H. D. 213
 Graczyk, D. J. 174
 Graf, Julia B. 175, 176
 Graig, L. C. 40
 Granger, H. C. 40, 41, 44
 Grant, W. B. 117
 Grason, David 125
 Grauch, V. J. S. 133
 Gray, J. R. 162, 175
 Green, G. N. 63
 Green, H. G. 276

Green, M. W. 40
 Greene, H. G. 223
 Greene, M. R. 240
 Greenhaus, M. R. 134
 Greenlee, D. D. 250, 254, 255
 Greenwood, W. R. 54
 Gregory, R. 287
 Griffith, J. K. 17
 Griffiths, W. R. 9
 Grolier, M. J. 246, 291
 Gromme, C. S. 130, 131
 Groschen, G. E. 191
 Gross, R. S. 203
 Grout, M. A. 60
 Grove, K. A. 119
 Grow, J. D. 113
 Guffanti, Marianne 156
 Gulbrandsen, R. A. 12
 Gutschick, Raymond C. 26

H

Haas, J. L., Jr. 137
 Haas, R. H. 255
 Hackman, B. S. 17
 Hadley, D. G. 286
 Hadley, R. F. 161
 Haedy, S. B. 1
 Hagstrum, J. T. 130
 Hainly, R. A. 161
 Hait, M. H., Jr. 223
 Halkens, Gary 219
 Hall, L. M. 49
 Hall, R. E. 114
 Hall, W. E. 288
 Hallgarth, Walter 17
 Hamilton, L. J. 95
 Hamilton, R. M. 276
 Hamlin, S. N. 169
 Hammarstrom, Jane M. 139
 Hampson, J. C., Jr. 116
 Hampton, M. A. 118
 Handler, Philip 276
 Handy, A. H. 86, 227
 Hansen, B. P. 85
 Hansen, D. S. 96
 Hansen, V. L. 65
 Hansen, W. R. 57
 Hanshaw, B. B. 279
 Hansley, Paula 39
 Hardee, Jack 195
 Harden, Jennifer 210
 Hardie, J. K. 19
 Harding, S. T. 209
 Hardy, M. A. 184
 Harenberg, W. A. 172
 Harlow, D. H. 206
 Harmon, D. D. 122
 Harp, E. L. 219
 Harris, D. D. 99
 Harris, J. A., Jr. 219
 Harris, L. D. 30
 Harrison, J. E. 4, 60, 148
 Harsh, J. F. 108
 Hartzell, Steve 212
 Harvey, D. 204
 Harvey, Danny 203
 Harwood, D. S. 222
 Hasche, L. R. 18

Haselton, H. T. 137
 Hassemer, J. R. 4
 Hastings, D. A. 252, 255
 Hatch, Joseph R. 29
 Hatcher, P. G. 21, 22
 Havens, J. S. 107
 Hawkins, F. F. 232
 Hay, R. L. 64
 Hayes, L. R. 168
 Hayes, P. T. 272
 Hays, W. H. 220, 223
 Hazel, J. E. 53
 Healey, D. L. 231
 Healy, R. W. 234
 Hearn, B. C., Jr. 145
 Heaton, Tom 212
 Hedge, C. E. 144, 147
 Heffern, E. L. 59
 Hein, J. R. 275
 Helaby, A. M. 287
 Helenek, H. 49
 Helley, E. J. 222
 Hemingway, B. S. 137
 Henry, T. W. 15, 182, 273
 Herb, W. J. 228
 Herd, D. G. 209, 223
 Herzog, D. C. 132
 Hess, A. E. 196
 Hess, G. R. 118
 Hickey, J. J. 169
 Hickling, N. L. 19
 Higgins, M. W. 49
 Hildebrand, T. G. 211
 Hildenbrand, T. G. 63
 Hill, D. P. 156, 157
 Hillhouse, J. W. 64, 130
 Hills, F. A. 35, 37
 Himmelberg, G. R. 80
 Hine, Karl 112
 Hinkley, T. K. 200
 Hintze, L. F. 14
 Hirschaut, D. W. 117
 Hite, R. J. 290
 Hoblitt, R. P. 217
 Hodges, A. L., Jr. 170
 Hoffman, J. P. 201
 Hoffman, M. A. 36
 Holcomb, L. G. 201
 Holcomb, R. T. 215
 Holcombe, T. L. 115
 Holder, R. W. 71
 Hollett, K. J. 279
 Holmes, C. W. 114
 Holmes, M. L. 24
 Holmes, Mark 213
 Holt, C. L. R., Jr. 284
 Holtschlag, D. J. 171
 Holzer, T. L. 212, 239
 Honey, J. G. 18
 Hoover, D. B. 11
 Hoover, D. L. 64
 Hopkins, D. M. 76
 Hopper, M. G. 223
 Horn, M. A. 104
 Horowitz, A. J. 279
 Horton, J. W., Jr. 50
 Horvath, E. H. 255
 Hosterman, J. W. 13
 Hotchkiss, W. R. 107

Hovorka, D. S. 54
 Hubbell, D. W. 194
 Hubert, A. E. 10
 Huebner, J. S. 138
 Huffman, A. C. 39
 Hufschmidt, P. W. 229
 Hult, M. F. 189
 Hummer-Miller, Susanne. 261
 Hunt, C. 281
 Hunter, R. E. 65
 Hunter, R. E., Jr. 121
 Hupp, C. R. 183
 Hussein, Mir Amied. 287
 Huston, D. L. 2
 Hutchinson, C. B. 123, 167
 Hutchinson, D. H. 222
 Hutchison, N. E. 285
 Hutt, C. R. 201

I

Imbriogotta, T. E. 84
 Imes, J. L. 94
 Ireland, R. L. 284
 Irwin, W. P. 131
 Iyer, H. M. 64, 156, 216
 Izett, G. A. 56, 283

J

Jachens, R. C. 206, 216
 Jachens, Robert C. 67
 Jackman, A. P. 188
 Jacobson, N. D. 97
 Jacobson, R. L. 52
 Jacoby, J. M. 193
 Jahren, C. E. 232
 Jaksha, L. H. 203
 Janda, R. J. 279
 Janik, C. J. 154
 Janitzky, Peter 210
 Jarrett, R. D. 236
 Jayko, A. S. 5
 Jelinski, J. C. 195
 Jenkins, E. C. 231
 Jennings, M. E. 229
 Jennings, Paul 212
 Jensen, R. M. 284
 Jenson, S. K. 251, 252, 255
 John, D. A. 67
 Johnson, G. R. 263
 Johnson, J. G. 26
 Johnson, P. L. 15, 17
 Johnson, R. G. 23
 Johnson, T. V. 242
 Johnson, W. D. 2
 Johnston, D. A. 155
 Johnston, M. J. S. 206
 Jones, A. H. 59
 Jones, D. L. 63, 70, 75, 78, 79
 Julian, B. R. 203

K

Kanamori, Hiroo. 212
 Kane, M. F. 211, 275
 Kane, Martin F. 274
 Karl, H. A. 118

Karl, S. M. 79, 275
 Karlinger, M. R. 161, 174
 Kash, D. E. 276
 Katz, B. G. 102
 Keighin, C. W. 120
 Keith, T. E. C. 155
 Kennedy, V. C. 188, 192
 Kent, B. H. 18
 Kepferle, R. C. 12
 Keys, W. S. 196, 197
 Keys, W. Scott 281
 Kibler, J. E. 231
 Kidd, R. E. 223
 Kieffer, H. H. 261
 Kieffer, Hugh 216
 Kieffer, S. W. 217
 King, C. Y. 150
 King, E. R. 133
 King, H. D. 2
 Kipp, K. L. 235
 Kirby, J. R. 116
 Kirby, S. H. 133
 Kircher, J. E. 161, 174
 Kirk, A. R. 9, 39
 Kirschner, C. E. 78
 Kistler, R. W. 66, 147, 149
 Kjelstrom, L. C. 104
 Klau, Wolfgang 275
 Klein, Jeffrey 221
 Klein, T. L. 6
 Kleinkopf, M. D. 4
 Klise, D. A. 117
 Klitgord, K. D. 112
 Klusman, Ronald W. 199
 Knapp, David 156, 216
 Knapton, J. R. 227
 Knebel, H. J. 119
 Knepper, D. H., Jr. 259
 Knight, J. D. 57
 Knobel, L. L. 109
 Koesterer, M. E. 54
 Kohler, W. M. 157
 Kollman, Auriel 156, 216
 Konikow, L. F. 276, 279
 Kouvo, Olavi. 147
 Kraemer, T. F. 146, 147
 Krasnow, M. R. 21
 Krause, R. E. 106
 Kriausakul, Nivat 53
 Krinsley, D. B. 282
 Krohelski, J. T. 186
 Krohn, Dennis 260
 Krohn, K. K. 15
 Ku, H. F. H. 103
 Kuberry, R. W. 132
 Kulik, D. M. 27
 Kuntz, Mel A. 142, 152
 Kurnosov, Viktor B. 274
 Kvenvolden, K. A. 118

L

Labson, Victor 134
 Lachenbruch, A. H. 76, 158
 Laczniak, R. J. 166
 Lahr, J. C. 207
 Laird, Jo 78
 Lajoie, K. L. 208
 Lajoie, K. R. 68

- Lamb, George 179
Lamb, T. E. 174
Lambing, J. H. 94
Landing, Ed 182
Landis, E. R. 17, 272, 282
Landis, G. P. 1, 7
Lane, C. 113
Lane, M. E. 3, 4
Lang, D. J. 185
Langer, C. J. 202
Langford, R. H. 276, 279
Lanphere, M. A. 150
Larson, J. D. 229
Larson, Mark 40
LaSala, A. M., Jr. 281
Lauer, D. T. 258
Laura, D. 276
Laux, D. E. 252
Lawrence, C. L. 104
Lawrence, Viki 48
Lawson, C. A. 131
Lawver, L. A. 76
Lazaro, T. R. 160
Lazorchick, G. J. 88
Leach, D. L. 4
Leahy, P. P. 109
Leanderson, J. 288
Leaver, D. S. 157
Leavy, B. D. 52
LeBlanc, Denis 237
Lee, D. E. 66, 149, 150
Lee, H. J. 118
Lee, J. K. 173
Lee, M. W. 135
Lee, Roger W. 146
Lee, Russell 133
Lee, W. H. K. 207
Lefebvre, R. H. 142
Leinz, R. N. 10
Lemon, E. M. 53
Leo, G. W. 285
Lerch, H. E. 30
Lettis, William R. 71
Lettis, William Robert 71
Leventhal, Joel S. 12, 29, 39, 43
Levings, G. W. 94
Lewis, J. D. 172
Lewis, R. E. 98, 153
Lewis, R. S. 119
Liddicoat, J. C. 47, 53, 163
Lidke, D. J. 54
Lietman, P. L. 184
Lind, C. J. 138, 139
Linden, D. S. 257
Lindgren, R. J. 191
Lindh, A. G. 205
Lindholt, G. F. 107
Lindsey, D. A. 8
Linker, Mark 133
Lipin, B. R. 6
Lipman, P. W. 130, 143
Lipman, Peter W. 55
Liu, H. P. 206
Lockner, D. A. 204
Lockwood, J. P. 216, 282
Loferski, P. J. 6
Loney, R. A. 3
Long, C. L. 4
Lopez, D. A. 54
Lorens, J. A. 101
Love, A. H. 30
Low, W. H. 185
Lowham, H. W. 175
Lu Huan-Zhang 143
Lubeck, C. M. 30
Lucas, James 272
Lucchitta, B. K. 242, 243, 245
Ludwig, A. H. 90
Ludwig, K. R. 151
Lund, K. I. 54
Luoma, S. N. 279
Lupe, R. D. 39
Lyons, J. B. 45
Lyttle, P. T. 51
- M**
- Mabey, D. R. 63
Machette, M. M. 210
Machette, M. N. 151, 223
Maciel, G. E. 22
Mackey, G. W. 234
Mades, D. M. 175
Magoon, L. B. 24, 78
Malo, B. A. 105
Malone, S. D. 215
Malterer, T. J. 1
Manheim, F. T. 113, 146
Mankinen, E. A. 130, 131
Mapel, W. J. 20
Marchand, Denny 210
Marcher, M. V. 228
Marincovich, L. N. 177, 178
Markewich, H. W. 51
Marley, W. E. 20
Marlow, M. S. 112
Marshall, B. V. 76
Martin, Angel, Jr. 84
Martin, E. A. 152
Martin, R. A. 4
Martin, R. G. 29, 32, 115
Martinez, F. J. 136
Martinez, Fernando 219
Marvin, R. F. 149
Mase, C. W. 158, 159
Maslia, M. L. 168
Massey, B. C. 176
Masursky, Harold 242
Matalas, N. C. 276
Matheson, S. A. 68
Matson, Michael 254
Mattick, R. E. 30, 111
Matraw, H. C. 190
Matraw, H. C., Jr. 190
Maughan, E. K. 27
Mavko, G. M. 204
May, R. J. 151
May, S. R. 179, 180
Mays, R. E. 10
Mazor, Emanuel 155
McCallister, R. H. 138
McCammon, R. B. 41, 42, 281
McCartan, Lucy 52, 53, 164
McCarthy, R. P. 201
McCauley, J. F. 246
McClung, W. S. 109
McClymonds, N. E. 227
McCord, J. R. 276, 290
McCord, T. B. 242
McCoy, W. D. 163
McCutcheon, S. C. 174, 188
McDade, A. S. 254
McDougall, K. A. 177
McDowell, R. C. 50, 223
McEville, T. V. 205
McEwen, A. S. 242
McGee, E. S. 145
McGee, K. A. 216
McGill, J. T. 220
McGimsey, R. G. 59
McGregor, B. A. 115, 116
McKee, E. H. 5, 6
McKnight, D. M. 224
McLaughlin, R. J. 69, 70
McLellan, Marguerite 18
McMasters, C. R. 209
McNeal, J. M. 10
McNutt, M. K. 136
McPherson, B. F. 124, 183
Meade, R. H. 160
Meade, R. M. 279
Meade, Robert M. 281
Meeke, W. C. 168
Mehnert, H. H. 149
Meier, M. F. 276, 279, 281
Meisler, Harold 109
Meissner, C. R., Jr. 17
Menard, H. W. 136
Meng, A. A. 108
Mengis, R. C. 161
Merewether, E. A. 28
Merghelani, H. 289
Merritt, M. L. 168
Meyer, C. E. 68
Meyer, R. F. 32
Middleton, Roy 221
Miesch, A. T. 144
Miller, C. D. 282
Miller, F. K. 74
Miller, G. A. 40
Miller, G. H. 61
Miller, J. J. 135
Miller, J. William 75
Miller, R. E. 30, 31
Miller, R. F. 224
Miller, R. L. 272, 282
Miller, R. T. 152
Miller, T. L. 98
Miller, W. A. 255, 257
Miller, W. R. 10
Mills, H. H. 50
Milton, D. J. 50
Milton, Nancy 260
Minkin, J. A. 23
Mitterer, R. M. 53
Modreski, P. J. 139
Moench, A. F. 169
Moench, R. H. 48
Moffatt, R. L. 176
Molenaar, D. 99
Monfort, M. E. 64
Monfort, Mary 156
Moody, D. W. 265
Moody, J. A. 116
Mooney, W. D. 157, 289
Moore, D. G. 255
Moore, D. W. 60

Moore, G. W. 274
 Moore, H. J. 246
 Moore, J. C. 68
 Moore, J. G. 110, 143
 Moore, T. A. 23
 Moore, T. E. 77
 Moreland, J. A. 238
 Morris, Deutsch 285
 Morris, E. C. 244
 Morris, E. E. 187, 194, 197, 198
 Morris, H. T. 64
 Morris, R. H. 223
 Morrison, S. D. 68
 Morton, R. B. 237
 Moses, T. H., Jr. 76
 Mosher, J. A. 242
 Moss, M. E. 279
 Mostler, Helfried 275
 Moths, B. L. 205
 Motooka, J. M. 10
 Motzer, W. E. 54
 Moye, F. J. 71
 Muffler, L. J. P. 153, 154, 155, 156, 276
 Muldoon, W. J. 20
 Mullen, M. K. 1
 Muller, D. C. 231
 Mullineaux, D. R. 217
 Munroe, R. J. 158, 159
 Murchey, B. L. 78
 Murdock, J. N. 201
 Murphy, D. L. 249
 Myers, D. A. 62
 Myette, C. F. 86
 Myrick, R. M. 160
 Mytton, J. W. 19

N

Naeser, C. W. 283
 Nakata, J. K. 65
 Naqvi, Mohammed 287
 Narten, P. F. 282
 Nash, J. T. 5, 36
 Nathenson, Manuel 155, 156
 Needell, S. W. 119
 Needham, R. E. 203
 Nehring, N. L. 154, 155
 Nelson, A. E. 52
 Nelson, W. H. 3, 11
 Nestell, M. K. 181
 Newcomer, J. A. 255
 Newell, W. L. 52
 Newhall, C. G. 282
 Newmaun, A. C. 114
 Newton, G. D. 166
 Newton, J. G. 239, 240
 Nichols, D. A. 250
 Nichols, D. J. 27, 57
 Nichols, D. R. 284
 Nichols, F. H. 122
 Nichols, K. M. 27
 Nilsen, T. H. 69, 77
 Nishi, J. M. 2
 Nkomo, I. T. 144
 Noble, M. A. 116
 Nokleberg, W. J. 68
 Noland, K. M. 279
 Nord, G. L. 138
 Nord, G. L., Jr. 131

Nordin, C. F. 279
 Normark, W. R. 110
 Northrup, H. R. 44
 Northrup, Roy 139
 Novak, S. W. 141
 Nyman, D. J. 123

O

Oaksford, E. T. 169
 Obermeier, S. F. 209, 221
 Obradovich, J. D. 150, 283
 Offield, T. W. 261
 Ogata, Akio 169
 O'Hara, C. J. 119
 Ohlen, D. O. 252, 255
 Ohlin, H. N. 69
 Ohta, Eijun 6
 Okamura, A. T. 282
 Okubo, P. G. 204
 Oldale, R. N. 119
 O'Leary, D. W. 116, 209
 Olhoeft, G. R. 132, 263
 Olimpio, J. C. 85, 235
 Olin, D. A. 235
 Oliphant, J. 146
 Oliver, H. W. 63
 Olsen, H. W. 115
 Olsen, T. D. 193
 Olson, A. H. 212
 Olson, Annabel 21
 Omang, R. J. 236
 O'Neil, J. R. 149, 150
 O'Neill, J. M. 54, 61
 Oriel, S. S. 60
 Orr, D. G. 254
 Orth, C. J. 57, 177
 Osburn, J. C. 20
 Ossi, J. C. 17
 Osterkamp, W. R. 183
 Osterwald, F. W. 218
 Ostresh, L. M., Jr. 266
 Otton, J. K. 34
 Owen, D. E. 120
 Owens, J. P. 50, 53, 164

P

Page, R. A. 207
 Paillet, F. L. 279
 Paillet, Frederick L. 195, 197
 Palacas, J. G. 29
 Palmer, A. R. 180
 Pampeyan, D. H. 212
 Pampeyan, E. H. 219
 Pantea, M. P. 33
 Parfenov, Leonid 274
 Parks, Bruce 162
 Parliman, D. J. 98
 Parrett, Charles 104, 236
 Pasini, Giancarlo 283
 Patchett, P. J. 147
 Patterson, G. L. 88
 Patton, W. W., Jr. 24
 Paul, C. K. 114
 Pavich, M. J. 47, 51, 163, 221
 Pavlides, Louis 49
 Payne, G. A. 102

Peacock, B. S. 108
 Peddie, N. W. 132
 Peeler, D. 113
 Pendleton, A. F. 279
 Peper, J. D. 47
 Pereira, W. E. 224
 Perkins, D. M. 208, 223
 Perry, W. J., Jr. 27
 Person, Waverly J. 202
 Pessl, Fred, Jr. 72, 213
 Peter, K. D. 93
 Peterman, Z. E. 27
 Peters, C. A. 225
 Peters, N. E. 87, 105
 Peterson, D. H. 122
 Peterson, D. M. 220
 Peterson, Donald W. 215
 Peterson, Fred 65
 Peterson, J. R. 201
 Pettijohn, R. A. 95
 Peuquet, Donna 250
 Pfefferkorn, H. W. 15
 Phair, George 145
 Phillips, J. D. 133
 Phillips, R. Lawrence 121
 Phipps, R. L. 183
 Pickering, R. J. 105, 279
 Pickering, Thomas 276
 Pierce, Frances 18
 Pierce, K. L. 63
 Pierce, R. R. 168
 Pierson, C. T. 34, 40
 Pierson, T. C. 230
 Pike, J. E. 65
 Pike, R. J. 247, 248
 Pilkey, O. H. 119
 Pillmore, C. L. 57
 Piper, D. Z. 110
 Piper, David J. W. 110
 Pitkin, J. A. 135
 Pitt, A. M. 203
 Plume, R. W. 98
 Poag, C. W. 113, 177
 Podwysocki, M. 262
 Podwysocki, M. H. 260
 Pohn, H. A. 262
 Pojeta, John, Jr. 182
 Pollard, D. D. 159
 Pollastro, R. M. 25
 Pomeroy, J. S. 220
 Poole, F. G. 26, 63, 64, 66
 Popenoe, Peter 112, 113
 Post, G. J. 282
 Powell, J. D. 229
 Powell, R. E. 70
 Powers, R. B. 26, 29
 Prevot, Michel 130
 Prince, K. R. 87
 Prior, D. B. 117
 Prisley, S. P. 257
 Prowell, D. C. 90, 211
 Purdy, T. L. 262
 Pyke, A. R. 48

Q

Quillian, E. W. 172

R

- Raab, P. V. 134
 Rachlin, Jack..... 231
 Raines, G. L..... 260, 280
 Randich, P. G. 95
 Randolph, John..... 265
 Randolph, R. B. 167
 Rapp, D. H..... 197
 Ratcliffe, N. M. 48, 49
 Rathbun, R. E. 147
 Ratte, J. C. 4, 61
 Rawlinson, S. E. 1
 Raymond, C. A. 52
 Reagor, B. G. 202
 Reed, J. C., Jr. 55, 60
 Reed, L. A. 161
 Reed, M. J. 45
 Reed, T. E. 227
 Reeves, W. E. 176
 Reid, G. O. 220
 Reid, R. R. 54
 Reimer, G. E. 47, 163
 Reimer, G. M. 42
 Reinemund, J. A. 276
 Reiser, H. N..... 77
 Repenning, Charles A..... 179, 180
 Repetski, John E. 180, 181, 182
 Reynolds, R. D. 201
 Reynolds, R. L..... 39
 Reynolds, R. R., Jr. 266
 Rhea, B. S. 203
 Rice, C. A. 152
 Rice, D. D. 26, 56
 Rice, T. L. 115
 Richards, P. W..... 281
 Richmond, B. M. 121
 Richmond, W. C. 67
 Ridgley, J. L..... 40
 Riehle, J. R. 163
 Riggs, S. R. 113
 Rinehart, C. D. 71, 72
 Rinella, J. F. 102
 Rite, Alan 156, 216
 Ritter, J. R. 105
 Rivera, Jose..... 68
 Robb, J. M. 116
 Robbins, E. I. 16
 Robbins, S. L. 136
 Roberts, A. A. 28
 Roberts, C. W. 206
 Roberts, G. R. 219
 Robertson, J. F. 56
 Robertson, J. R. 55
 Robie, R. A. 137
 Robinson, A. C. 66, 67, 149
 Robinson, G. R. 137
 Robinson, Keith 11
 Robinson, L. N. 19
 Rodman, Wayne..... 195
 Roedder, Edwin 139, 143
 Roehler, H. W. 23
 Rogers, A. M. 64, 213
 Rogers, J. A. 207
 Rogers, R. J. 146
 Rohde, W. G. 257
 Rose, W. J. 191
 Rosenbaum, J. G. 232
 Rosenshein, J. S..... 276
 Rosholt, J. N. 148
 Ross, D. C. 67
 Rossman, D. L..... 282
 Rostad, C. E..... 224
 Rouillard, N. E. 132
 Rowan, L. C. 4, 259, 275
 Rowland, Stephen..... 182
 Rowley, P. D. 57
 Rubin, D. M..... 65
 Rubin, Meyer 163, 216
 Ruppert, L. F. 22
 Russ, D. P. 209
 Ryals, G. N. 91
 Ryan, B. J..... 235
 Ryder, R. T. 25, 27, 135
 Rye, R. O. 148, 288
 Rymer, M. J..... 163, 208

S

- Sable, E. G..... 62, 211
 Safioles, S. A. 72, 213, 217
 Sallenger, A. H., Jr. 121
 Saltus, R. W..... 63
 Sammel, E. A. 46, 153
 Sanchez, J. D..... 20
 Sandberg, C. A. 26, 31, 63
 Sando, W. J. 26, 183
 Sanford, R. F. 9
 Sanopter, Don..... 275
 Santos, E. S. 43
 Sanzolone, R. F. 10
 Sargent, K. A. 233
 Sarna-Wojcicki, A. M. 68
 Sarna-Wojcicki, Andre..... 223
 Sass, J. H. 76, 158, 159
 Sato, Moto 216
 Sauer, C. G. 191
 Savage, J. C..... 206
 Savostin, Leo..... 274
 Sawatzky, D. L. 135, 261
 Scanlon, K. M. 116
 Schaber, G. G. 246
 Schafer, C. S. 137
 Schafer, J. P. 47
 Schemel, L. E. 122
 Schimschal, Ulrich 196, 234
 Schlee, J. S. 112, 113
 Schmidt, R. G. 6
 Schmitt, L. J. 39
 Schneider, Robert..... 233
 Schneider, V. R. 229
 Schnepfe, M. M..... 21
 Schoenberg, M. E. 87
 Schoenthaler, D. R. 134
 Scholl, D. W. 111
 Scholle, P. A. 25, 31
 Schroeder, L. J..... 105
 Schroeder, R. A. 105
 Schultejan, P. A. 291
 Schultz, D. M. 31
 Schultz, K. J..... 53
 Schulz, K. J. 53
 Schumann, H. H. 240
 Schuster, R. L. 217, 218, 220
 Schweinfurth, S. P..... 16
 Scott, D. H. 245
 Scott, E. W..... 32
 Scott, J. H. 132, 136
 Scott, R. W., Jr. 33
 Scott, Southworth..... 254
 Scott, W. E. 63, 163, 217
 Secor, D. T., Jr. 211
 Seeland, D. A. 8, 37, 38
 Seevers, P. M..... 252
 Segal, D. 260, 262
 Segal, Don..... 260
 Senftle, F. E..... 23, 276
 Severson, R. C..... 198, 199
 Shacklette, H. T..... 10
 Shapiro, C. D. 221
 Sharp, R. V. 195, 208, 212, 215
 Shasby, M. B. 257
 Shasby, Mark 258
 Shaw, L. C. 228
 Shedlock, Kaye..... 209
 Sheldon, R. P..... 12
 Sherrill, M. G. 108
 Shew, Nora 79
 Shideler, G. L. 120
 Shinn, E. A. 114
 Shipley, Susan..... 71, 218
 Shoemaker, E. M..... 242, 243
 Shown, L. M. 224
 Shride, A. F. 47
 Shroba, R. R. 163, 210
 Siems, D. F. 3, 9, 10
 Signor, D. C..... 106
 Silber, C. C..... 20, 21
 Silberling, N. J..... 63, 75, 79
 Silver, L. T. 70
 Simmons, C. E. 173
 Simmons, D. L..... 103
 Simpson, R. W..... 211
 Simpson, S. L..... 261
 Sims, J. D. 163
 Sims, P. K. 53
 Sinclair, William C. 240
 Singer, Michael..... 210
 Sinnott, Allen 282
 Sipkin, S. A. 203
 Skinner, J. N. 194
 Skinner, J. V. 194
 Slack, L. J..... 228
 Slagle, S. E. 185
 Slate, J. L. 68
 Smigaj, M. J..... 226
 Smith, B. D. 11
 Smith, B. S. 85
 Smith, C. W. 287
 Smith, E. T..... 265
 Smith, G. I. 13, 280
 Smith, K. S. 200
 Smith, P. E..... 101, 229
 Smith, Robert 272
 Smoot, C. W. 186
 Snavelly, P. D., Jr. 73, 112
 Snider, J. L..... 226
 Soderblom, L. A. 242, 244
 Sohl, N. F..... 114
 Sonenshayn, L. P..... 274
 Sonnevil, R. A. 3
 Sonntag, W. H. 124
 Soren, Julian 238
 Sorenson, S. K. 186
 Soukup, W. G. 167
 Southworth, Scott..... 253, 254
 Sparkes, A. K..... 108

Spence, W. J. 202, 203
 Spencer, J. E. 66
 Spiker, E. C. 22, 31, 142
 Spruill, T. B. 226
 Spudich, Paul 212, 214
 Squires, R. R. 172, 236
 Staatz, M. H. 37
 Stacey, J. S. 150, 287, 288
 Stacey, John 286
 Stakes, D. S. 149
 Stanley, W. D. 46
 Stanton, R. W. 23
 Stark, J. R. 86, 237
 Starkey, H. C. 25
 Stauber, D. A. 156
 Steger, C. W. 265
 Stein, R. S. 206
 Steinkampf, W. C. 123
 Stelz, W. G. 238
 Stephens, C. D. 207
 Stevens, H. H., Jr. 194
 Stewart, J. H. 66
 Stewart, Roger 276
 Stiles, H. R. 91
 Stitt, James H. 182
 Stoesser, D. B. 287
 Stone, B. D. 1, 47, 163
 Stone, B. M. 49
 Stone, Claudia 158
 Stone, L. R. 200
 Stoner, J. D. 185
 Stover, C. W. 202
 Stover, Carl 212
 Striegl, R. G. 102
 Stuckless, J. S. 42, 144
 Sturdevant, J. A. 258
 Sumioka, S. S. 193
 Sundquist, E. T. 279
 Sutherland, P. K. 181
 Sutter, J. F. 52
 Sutton, A. J. 216
 Swadley, W. C. 64
 Swanson, Don A. 215
 Swanson, V. E. 272, 290
 Sweeney, R. E. 30
 Swint, T. R. 110
 Szabo, B. J. 53, 164
 Szajgin, John 257
 Szalona, J. J. 194
 Szeverenyi, N. M. 22

T

Tabor, R. W. 74
 Taggart, James 207
 Tai, D. Y. 147
 Tailleur, Irving 150
 Takahashi, K. I. 25
 Tanaka, K. L. 245
 Tarr, A. C. 203
 Tasker, G. D. 171, 172
 Tatsumoto, M. 147
 Tatsumoto, Mitsunobu 147
 Taylor, D. J. 32, 135
 Taylor, Emily 210
 Taylor, M. E. 181
 Teaford, N. K. 17
 Teleki, P. G. 276
 Tera, Fouad 221

Terman, M. J. 276, 281
 Terry, J. E. 187, 194, 197
 Thaden, R. E. 41
 Thatcher, Wayne 206
 Thenhaus, P. C. 223
 Theodore, T. G. 5, 6, 74
 Thomas, D. M. 276
 Thomas, R. E. 221
 Thomasson, Carol 207
 Thompson, B. W. 289
 Thompson, J. G. 266
 Thompson, J. M. 154
 Thompson, R. E. 275
 Threlkeld, C. N. 30
 Tibbitts, G. C., Jr. 291
 Tice, A. 146
 Tinsley, J. C. 213
 Todd, V. A. 75
 Todd, V. R. 72
 Todd, W. J. 258
 Tolbert, G. E. 276
 Toth, M. I. 54
 Trapp, Henry, Jr. 109
 Trautwein, C. M. 254, 272
 Triplehorn, D. M. 16, 22
 Tripp, R. B. 2
 Triska, F. J. 192, 193
 Trombley, Tom 170
 Troutman, D. E. 105
 Truesdell, A. H. 154, 155, 156
 Truesdell, Alfred 272
 Trumbull, J. V. A. 119
 Tschudy, R. H. 57, 177
 Tucker, J. D. 10
 Turk, J. T. 192
 Turner-Peterson, C. E. 38
 Tuttle, Michele 199
 Twenhofel, W. S. 231
 Twenter, F. R. 86, 237
 Tweto, Ogden 57
 Twichell, D. C. 116
 Tylor, H. E. 279

U

Ulrich, G. E. 55
 Urban, T. C. 136

V

Valentine, P. C. 114, 177
 Valentine, Page 113
 Vallier, T. L. 111
 Van Loenen, R. E. 3, 60
 Van Trump, George, Jr. 42
 Van Zee, C. J. 256
 Vaniman, D. T. 64
 Vedder, J. G. 32
 Verbeek, E. R. 59, 60
 Vincent, H. R. 91
 Vincent, R. L. 59
 Vogel, T. M. 118
 von Huene, Roland 111
 Vuke, Susan 61

W

Wadsworth, G. A. 3

Wagner, C. R. 279
 Wagner, H. C. 112
 Wagner, H. L. 249
 Walker, A. S. 259
 Walker, K. M. 255
 Wallace, A. K. 35
 Wallace, C. A. 54
 Walters, R. A. 122, 188
 Walton, A. H. 179
 Waltz, F. A. 249
 Walvatne, Gary 252
 Wandle, S. W., Jr. 175
 Wang, F. H. 276, 281
 Wangsness, D. J. 225
 Ward, D. E. 20
 Ward, J. R. 184
 Ward, P. L. 158
 Warlow, R. C. 19
 Warren, C. G. 44
 Warren, D. H. 203
 Warwick, P. 17
 Watkins, A. H. 276
 Watson, Kenneth 261
 Watts, R. D. 232, 233
 Weaver, C. S. 215
 Weber, F. R. 77, 78
 Webers, G. F. 182
 Webster, J. D. 43
 Wedow, Helmuth 275, 276
 Weems, R. E. 164
 Wehmiller, F. J. 164
 Wehmiller, J. F. 53
 Wehr, Wesley 178
 Weiner, E. R. 136, 198
 Welch, A. H. 153
 Wenner, D. B. 144
 Wenrich, K. J. 33
 Wentz, D. A. 174, 191
 Wershaw, R. L. 136
 Westphal, Jon 215
 Wheeler, R. L. 208
 Whelan, J. F. 148
 White, D. E. 154, 156
 White, Donald 272
 White, R. A. 206
 Whitehead, R. L. 107
 Whiteman, K. J. 99
 Whitlow, J. W. 9
 Whitmore, F. C. 179
 Whitney, C. G. 39, 44, 139
 Wiche, G. J. 173
 Wiczorek, G. F. 219, 220
 Wiczorek, Gerald 214
 Wilber, W. G. 225
 Wilcox, R. E. 56, 60
 Wilhelms, D. E. 248
 Wilinkson, K. P. 266
 Williams, A. S. 117
 Williams, D. F. 114
 Williams, D. R. 236
 Williams, J. H. 88
 Williams, P. L. 142
 Williams, R. P. 160
 Wilson, F. H. 79
 Wilson, J. M. 85
 Wilson, L. R. 132
 Windolph, J. E., Jr. 19
 Witkind, I. J. 58
 Wolansky, R. M. 91

Wolfe, J. A.....	178
Wolfe, R. F.	243
Wood, G. H., Jr.....	15
Wood, J. D.....	132, 289
Wood, S. H.	151
Wood, W. A.....	238
Woods, P. F.....	188, 192
Woodside, P. R.	272
Woodward, D. G.....	107
Woodward, M. J.	68
Worl, R. G.	288
Wray, J. R.	276
Wright, D. L.	233
Wynn, J. C.....	290

Y

Yeend, W. E.	77
Yeend, Warren	8
Yenne, Keith.....	272
Yerkes, R. F.....	214
Yochelson, E. L.....	182
York, J. E.....	254
Youd, T. L.	219
Young, H. W.	153
Young, J. C.	213
Young, R. J.	236
Yount, J. C.....	72

Z

Zack, A. L.	123
Zarske, S. E.	54
Zdzinski, A. J.....	19
Zech, R. S.	39, 41, 259
Zelibor, J. L.	21
Zellweger, G. W.	188
Zen, E-an.....	139
Zenone, Chester	92
Zielinski, R. A.	43, 44
Zimmerman, E. A.	229
Zimmerman, W. D.	284
Ziony, J. I.....	213
Zirbes, M. D.	203
Zohdy, A. A. R.	134
Zucca, J. J.	156, 157
Zuehls, E. E.....	225